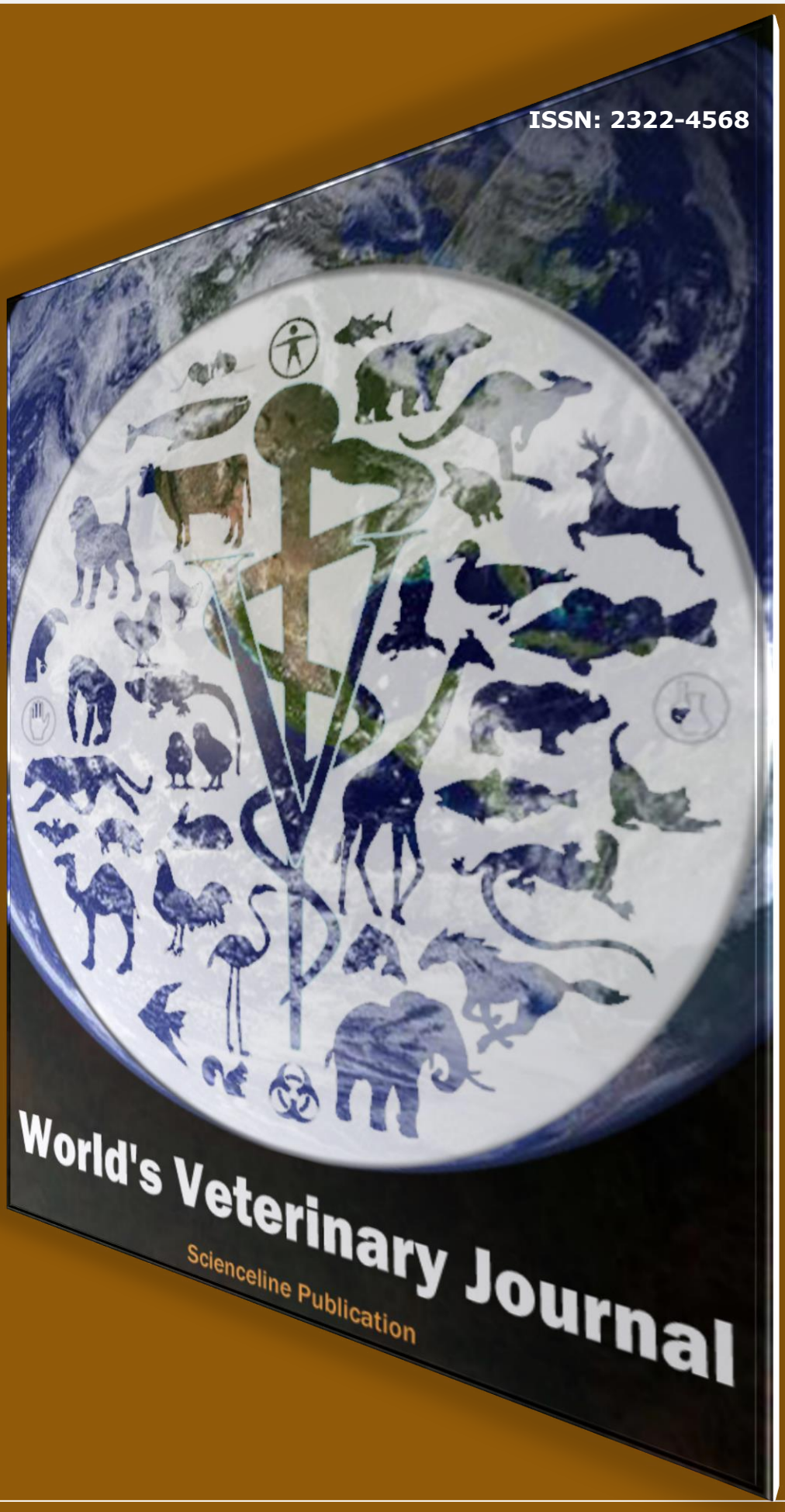
World's Veterinary Journal

BOOKLET



Volume 15, Issue 4, December 2025

2025, Scienceline Publication

World's Veterinary Journal

World Vet J, 15(4): 831-1148, December 2025

ISSN 2322-4568

Editors-in-Chief

Fikret Çelebi, PhD, Professor of Veterinary Physiology; Department of Veterinary, Atatürk University, **TÜRKIYE;** (Avesis; Scopus; ORCID; Email: fncelebi@atauni.edu.tr)

Daryoush Babazadeh, DVM, DVSc, PhD of Poultry Diseases, Shiraz University, Shiraz, **IRAN**; Head of Aria Veterinary Hospital, **IRAN**; (Scopus; ORCID; Researcher's ID; Full Member of WAME; Member of IAVE; Email: daryoush.babazadeh@shirazu.ac.ir)

Managing Editor

Alireza Sadeghi, DVM, Faculty of Veterinary Medicine, Tabriz Branch, Islamic Azad University, Tabriz, **IRAN**; Emails: alireza_sadeghi@science-line.com; alirezavet86@gmail.com

Associate Editors

Thandavan Arthanari Kannan, PhD, Full Professor, Centre for Stem Cell Research and Regenerative Medicine, Madras Veterinary College, Tamil Nadu Veterinary and Animal Sciences University, Chennai-600007, **INDIA**

Mykola Kukhtyn, Doctor of Veterinary Sciences, Microbiology of food raw materials, food products, disinfection, antibiotic resistance in microorganisms, microbial biofilms, Department of Food Biotechnology and Chemistry, Ternopil Ivan Puluj National Technical University, **UKRAINE**

Chaima Sabri, Laboratory of Natural Resources and Sustainable Development, Research Unit on Metabolism, Physiology, and Nutrition, Department of Biology, Faculty of Science, Ibn Tofail University, Kenitra, **MOROCCO**; ORCID

José Ramiro González Montaña, Faculty of Veterinary Medicine, University of Leon, **SPAIN**

Ahmed Readh CHAIB EDDOUR, Doctor of Agricultural Science, Agricultural and Food Development, Higher School of Agronomy, **ALGERIA**

Language Editors (Full time)

Atena Attaran; PhD in TEFL, Ferdowsi University of Mashhad, Mashhad, **IRAN**; ORCID

Statistical Editor

Daryoush Babazadeh, PhD, Shiraz University, Shiraz, **IRAN**

Technical Editor (Full time)

Pouria Ahmadi Simab, DVM, Faculty of Veterinary Medicine, Sanandaj Branch, Islamic Azad University, Sanandaj, **IRAN**; ORCID

Editorial Team

Gamil Sayed Gamil Zeedan, PhD, Professor of Microbiology and Virology at National Research Center, Ministry of High Education, Cairo, **EGYPT**; Researcher's ID, ORCID, Scopus

Kálmán IMRE, DVM, PhD, Dr. Habil Vice-Dean, Faculty of Veterinary Medicine Timișoara, Department of Animal Production and Veterinary Public Health, Banat University of Agricultural Sciences and Veterinary Medicine "King Michael I of Romania" from Timisoara, Calea Aradului no. 119, 300645 Timisoara, **ROMANIA**

Muhammad Saeed, PhD, Animal Nutrition and Feed Science, College of Animal Sciences and Feed Technology, Northwest A&F University, Yangling, 712100, **CHINA**; Researcher's ID, ORCID, Scopus

Shewangzaw Addisu Mekuria, BSc, MSc, Instructor, Department of Animal Production and Extension**,** University of Gondar, P. O. Box 196, Gondar, **ETHIOPIA**; Researcher's ID, ORCID, Scopus

Wafaa Abd El-Ghany, Professor and Head of Poultry and Rabbit Diseases Department, Faculty of Veterinary Medicine, Cairo University, **EGYPT**; ORCID

Yos Adi Prakoso, DVM, MSc, Biopathology, Pharmacology, Faculty of Veterinary Medicine, University of Wijaya Kusuma Surabaya, **INDONESIA**; Researcher's ID, ORCID, Scopus

RAJ PAL Diwakar, Assistant Professor, Department of Veterinary Microbiology, College of Veterinary Science and A. H., Acharya Narendra Deva University of Agriculture and Technology, Kumarganj. Ayodhya (UP)-224229, **INDIA**; ORCID

Rafael Ruiz de Gopegui, DVM, PhD, Professor of Veterinary Internal Medicine, Department of Animal Medicine and Surgery. Veterinary Faculty, Universitat Autónoma de Barcelona, **SPAIN**

Mulyoto Pangestu, PhD, Lecturer and Laboratory Manager, Education Program in Reproduction and Development (EPRD) Dept. Obstetrics and Gynaecology, Monash Clinical School, Monash University, Monash Medical, **AUSTRALIA**; Researcher's ID, ORCID, Scopus

Misael Chinchilla-Carmona, PhD, Parasitology, Department of basic research, Universidad de Ciencias Médicas (UCIMED), San José, **COSTA RICA**

Kuastros Mekonnen Belaynehe, Food and Agriculture Organization of the United Nations: Addis Ababa, **ETHIOPIA**; Antimicrobial Resistance (AMR) Expert (Emergency Center for Trans Boundary Animal Diseases-ECTAD); ORCID

Alvaro Faccini-Martinez, Ph.D., Tropical Medicine, University of Texas Medical Branch, Texas, **USA**

Alper Başa, Department of Surgery, Experimental Analysis,Faculty of Veterinary Medicine, Firat University, Elazig, **TÜRKIYE**; Researcher's ID, ORCID, Scopus

Abrham Ayele, DVM, MSc, Assistant Professor Department of Paraclinical Studies College of Veterinary Medicine and Animal Sciences University of Gondar, **ETHIOPIA**; ORCID, Scopus

Faezeh Modarresi-Ghazani; Drug Applied Research Center, Tabriz University of Medical Sciences, Tabriz, **IRAN**

Arman Moshaveri; DVM, Faculty of Veterinary Medicine, Karaj Branch, Islamic Azad University, Karaj, **IRAN**

Saghar Karimi, DVM, Resident of Veterinary Radiology, Department of Clinical Sciences, Faculty of Veterinary Medicine, Tehran University, **IRAN**; ORCID

Nadia Touil, PhD, Virology/Infectious diseases,cell culture, Université Mohammed V Souissi (UM5S), **MOROCCO**; ORCID

Baidaa Abdul Aziz Mohammed Salah Barwarei, PhD, Department of Biology and Zoology, College of Education for Pure Sciences, University of Mosul, Mosul, **IRAQ**; Researcher's ID, ORCID, Scopus

Olexandr L. Orobchenko, Head of the laboratory (veterinary pharmacology and toxicology), Ministry of Education and Science of **UKRAINE**

Sharina Omar, veterinary bacteriology, mycology, AMR, tuberculosis, Universiti Putra, **MALAYSIA**; ORCID, Scopus

Ayat ALaa ElDeen Fayed, Agricultural Sciences, livestock physiology, molecular biology, immunology, and meat quality, Assistant Professor of animal physiology, Faculty of Agriculture at Cairo University, **EGYPT**; ORCID

Felipp da Silveira Ferreira, Coordinator of the Specialization Course in Veterinary Cardiology, Patron of Veterinary Cardiology - Brazilian Association of Specialist Veterinary Doctors, **BRAZIL**; ORCID

André Prisca NDOUR, Veterinary epidemiology, PhD, Afrique One Aspire Sénégal, **SENEGAL**; Researcher's ID, ORCID

Walter Palomino Guerrera, Researcher of the National Institute of Agrarian Innovation (INIA), **PERU**; ORCID, Scopus

Anish Yadav, Ph.D., FNAVS (I), Professor and Head Ex-ICAR National Fellow, General Secretary, Indian Association For The Advancement of Veterinary Parasitology, Division of Veterinary Parasitology, Faculty of Veterinary Sciences and Animal Husbandry, University of

Agricultural Sciences and Technology of Jammu, Jammu and Kashmir, **INDIA**; Researcher's ID, ORCID, Scopus
Manal Hadi Ghaffoori Kanaan, Middle Technical University, Technica Institute of Suwaira, **IRAQ**; Researcher's ID, ORCID, Scopus
Sadiya Aziz Anah, University of AL-Qadisiyah, **IRAQ**
Daouia Keltoum BENMAAROUF, PhD Student, Ecole Nationale Supérieure Vétérinaire d'Alger, **ALGERIA**; Researcher's ID, ORCID, Scopus
Kholik Kholik, Department of Veterinary Public Health, Faculty of Veterinary Medicine, Universitas Pendidikan Mandalika, Mataram, **INDONESIA**; Researcher's ID, ORCID, Scopus
Niyonzima Nioyngabo Francois, University of Rwanda, **RWANDA**
Chencha Chebo, Animal Breeding & Genetics, Hawassa University, School of Animal & Range Sciences, **ETHIOPIA**; Researcher's ID, ORCID, Scopus
Nguyen Khanh Thuan, Veterinary Microbiology, Antibiotic resistance pathogens, College of Agriculture, Can Tho University, **VIETNAM**; Researcher's ID, ORCID, Scopus
Hadi Haghbin Nazarpak, Faculty of Veterinary Medicine, Department of Clinical Sciences, Garmsar Branch, Islamic Azad University, Garmsar, **IRAN**
Elizabeth Breininger, Reproducción Animal, Facultad de Ciencias Veterinarias, **ARGENTINA**; Researcher's ID, ORCID, Scopus
Ogechi Kadurumba, Department of Animal Science Technology, Federal University of Technology, **NIGERIA**; Researcher's ID, ORCID, Scopus
Laibané Dieudonné Dahourou, Department of animal breeding, Institute of Environmental Sciences and Rural Development, Daniel Ouezzin Coulibaly University, **BURKINA FASO**; Researcher's ID, ORCID, Scopus

Advisory Board

Alfonso J. Rodriguez-Morales, Hon.D.Sc., Tropical Medicine, Senior Researcher, Faculty of Medicine, Fundacion Universitaria Autonoma de las Americas, Pereira, Risaralda, **COLOMBIA**; ORCID

Mahendra Pal, PhD. Ex-Professor of Veterinary Public Health, College of Veterinary Medicine, Addis Ababa University, **ETHIOPIA**; ORCID

Zohreh Yousefi, PhD of Biology, Atatürk University, Erzurum, **TÜRKIYE**

Join WVJ Team

World's Veterinary Journal is always striving to add diversity to our editorial board and operations staff. Applicants who have previous experience relevant to the position they are applying for may be considered for more senior positions within WVJ. All other members must begin as section reviewer before progressing on to more senior roles. Editor and editorial board members do not receive any remuneration. These positions are voluntary.

If you are currently an undergraduate, MSc or PhD student at university and interested in working for WVJ, please fill out the application form below. Once your filled application form is submitted, the board will review your credentials and notify you within a week of an opportunity to membership in editorial board. If you are PhD, assistant, associate editors, distinguished professor, scholars or publisher of a reputed university, please rank the mentioned positions in order of your preference. Please send us a copy of your resume (CV) or your ORCID ID or briefly discuss any leadership positions and other experiences you have had that are relevant to applied poultry research, Researches or publications. This includes courses you have taken, editing, publishing, web design, layout design, and event planning. If you would like to represent the WVJ at your university, join our volunteer staff today! WVJ representatives assist students at their university to submit their work to the WVJ. You can also, registered as a member of journal for subsequent contacts by email and or invitation for a honorary reviewing articles.

Download WVJ Application Form

Contact us at editor [at] wvj.science-line.com

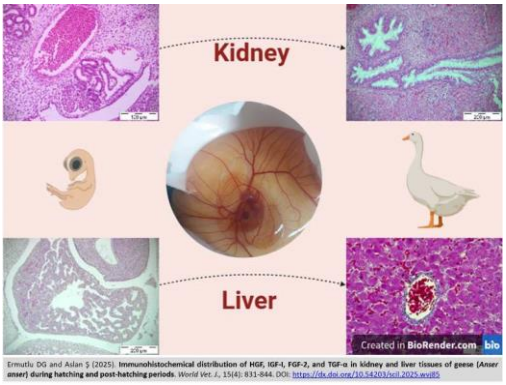
crossref metadata search

Volume 15 (4); December 2025 [EndNote XML for Agris]

Research Paper

Immunohistochemical distribution of HGF, IGF-I, FGF-2, and TGF-α in kidney and liver tissues of geese (*Anser anser*) during hatching and post-hatching periods

Ermutlu DG and Aslan Ş.
World Vet. J. 15(4): 831-844, 2025; pii:S232245682500085-15
DOI:https://dx.doi.org/10.54203/scil.2025.wvj85



ABSTRACT: Immunohistochemical studies during embryonic development of poultry are quite limited. The present study aimed to investigate the distribution of Hepatocyte growth factor (HGF), insulin-like growth factor-I (IGF-I), fibroblast growth factor-2 (FGF-2), and transforming growth factor-α (TGF-α) in the kidney and liver tissues of hatching and post-hatching geese via histologic and immunohistochemical methods. A total of 150 fertile goose eggs were used in the study. Throughout the incubation process (29 days), four eggs were used each day, starting from the sixth day, and the embryos were examined. The embryos were fixed in 10% formaldehyde solution. Geese at the 7, 15, 30, and 210 (adult) days after hatching were euthanized for a post-hatching evaluation. Routine histological procedures were performed on the kidney and liver tissues. For histological examinations were used Crossmonn's triple staining, Periodic Acid-Schiff (PAS), and Haematoxylin and Eosin (H&E) staining. HGF, IGF-I, FGF-2, and TGF-α immunoreactivities were investigated in the histological slides. An examination of kidney tissue development indicated that metanephric blastema formation started on day 10. The mesonephros was replaced by the metanephros, the permanent kidney, starting on the day 25. An examination of liver tissue development revealed that sinusoids began to narrow, hepatic plaques formed, and endothelial and Kupffer cells became distinguished as early as day 8. Upon general evaluation, FGF-2 was found to be the growth factor with the most intense immunoreactivity in the liver and kidney, while IGF-I had the least immunoreactivity. There is a paucity of studies on growth factors during the embryonic period in poultry. In the present study, all four growth factors were immunohistochemically investigated in the kidney and liver during the hatching and post-hatching periods. Because poultry have a shorter embryonic period than mammals, they need to utilize growth factors effectively and at high levels. The present study demonstrated that HGF, IGF-I, FGF-2, and TGF-α growth factors were effective in kidney and liver development during the incubation period in geese.

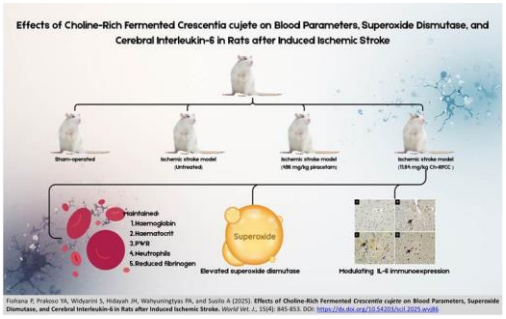
Keywords: Embryo, Goose, Growth factors, Kidney, Liver

[Full text-PDF] [Crossref Metadata] [Scopus] [Export from ePrint]

Research Paper

Effects of Choline-Rich Fermented *Crescentia cujete* on Blood Parameters, Superoxide Dismutase, and Cerebral Interleukin-6 in Rats after Induced Ischemic Stroke

Fiohana P, Prakoso YA, Widyarini S, Hidayah JH, Wahyuningtyas PA, and Susilo A.
World Vet. J. 15(4): 845-853, 2025; pii:S232245682500086-15
DOI:https://dx.doi.org/10.54203/scil.2025.wvj86



ABSTRACT: Ischaemic stroke is a major vascular disorder that profoundly impacts human health. Choline-rich fermented *Crescentia cujete* (Ch-RFCC) has emerged as a promising adjunctive therapy for ischemic stroke; however, its effects on hematological parameters, superoxide dismutase (SOD) activity, and interleukin-6 (IL-6) levels remain unexplored. The present study aimed to assess the impacts of Ch-RFCC on hematological parameters, SOD activity, and brain IL-6 levels in the rats' ischemic stroke model (ISM). A total of 40 three-month-old male rats, weighing 247.31 ± 4.95 g, were randomly assigned into four groups, including healthy rats with a skin incision as the control group (sham-operated, T1), ISM without treatment (T2), ISM treated with 496 mg/kg body weight of piracetam (T3), and ISM treated with 11.84 mg/kg body weight of Ch-RFCC (T4). Treatments using piracetam (T3) and Ch-RFCC (T4) were administered orally via gavage twice daily for 14 consecutive days. The current results demonstrated that Group T4 maintained haemoglobin and haematocrit levels, normalised the platelet-to-leucocyte ratio and neutrophil counts, reduced fibrinogen levels, elevated SOD activity, and enhanced IL-6 immunoreactivity compared to the untreated ISM group (T2). Furthermore, rats in Group T4 exhibited the least body weight loss compared to those in groups T2 and T3. These findings indicated that Ch-RFCC may alleviate ischemic stroke

in rats by enhancing antioxidant defenses, modulating IL-6 expression, and preserving hematological homeostasis.

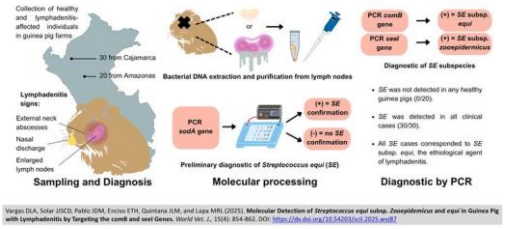
Keywords: Choline-rich fermented *Crescentia cujete*, Hematology, Interleukin-6, Ischemic stroke, Superoxide dismutase

[Full text-PDF] [Crossref Metadata] [Scopus] [Export from ePrint]

Research Paper

Molecular Detection of *Streptococcus equi* subsp. *Zooepidemicus* and *equi* in Guinea Pig with Lymphadenitis by Targeting the *comB* and *seeI* Genes

Vargas DLA, Solar JJSCD, Pablo JDM, Enciso ETH, Quintana JLM, and Lapa MRL.
World Vet. J. 15(4): 854-862, 2025; pii:S232245682500087-15
DOI: https://dx.doi.org/10.54203/scil.2025.wvj87



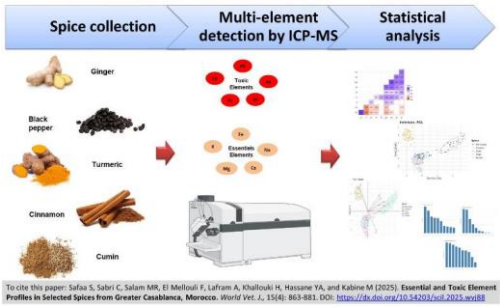
ABSTRACT: Despite the economic and sanitary relevance of cervical lymphadenitis in guinea pigs, little molecular information is available regarding the role of *Streptococcus* (*S.*) *equi* subspecies in cervical lymphadenitis in Peru. The present study aimed to identify the subspecies *S. equi* subsp. *zooepidemicus* (SEZ) and *S. equi* subsp. *equi* (SEE) in guinea pigs (*Cavia porcellus*), with and without cervical lymphadenitis, from the Amazonas and Cajamarca regions of Peru, using PCR amplification of the *sodA*, *comB,* and *seeI* genes. A total of 50 guinea pigs, aged 6-8 months, were evaluated, 30 from Cajamarca (mean weight 1210.1 grams; 22 Peruvian breed, 1 Inti, and 7 Brown) and 20 from Amazonas (mean weight 950 grams; 10 Peruvian breed and 10 Inti), comprising 30 animals with cervical lymphadenitis and 20 clinically healthy animals. The *sodA* gene was first employed as a preliminary diagnostic marker, which confirmed the presence of *S. equi* in all animals presenting lymphadenitis. Subsequent amplification of the *comB* gene confirmed the exclusive presence of SEZ in all clinical cases, with no detection in the 20 clinically healthy guinea pigs analyzed in both study regions. In contrast, the *seeI* gene, specific to SEE, indicated no amplification in any of the samples, indicating the absence of SEE in the study population. The prevalence of SEZ (positive *comB*) among guinea pigs with cervical lymphadenitis was 100% in Amazonas (10/10; 95% CI: 69.2-100%) and 100% in Cajamarca (20/20; 95% CI: 83.2-100%), with no significant difference between regions. The present findings established SEZ as the primary etiological agent of cervical lymphadenitis in guinea pigs from both regions, with no molecular evidence of SEE. The present study underscored the utility of *comB* and *seeI* as specific and reliable molecular markers for differentiating SEZ and SEE.
Keywords: *comB* gene, Guinea pig, *seeI* gene, *Streptococcus equi* subsp. *equi*, *Streptococcus equi* subsp. *zooepidemicus*

[Full text-PDF] [Crossref Metadata] [Scopus] [Export from ePrint]

Research Paper

Essential and Toxic Element Profiles in Selected Spices from Greater Casablanca, Morocco

Safaa S, Sabri C, Salam MR, El Mellouli F, Lafram A, Khallouki H, Hassane YA, and Kabine M.
World Vet. J. 15(4): 863-881, 2025; pii:S232245682500088-15
DOI: https://dx.doi.org/10.54203/scil.2025.wvj88



ABSTRACT: In Morocco, spices are an integral part of daily cuisine and serve as a vector of both nutritional and toxicological exposure. Monitoring elemental composition is essential to ensure consumer safety, animal health when used as feed additives, and compliance with international standards. The present study aimed to determine the concentrations of essential (potassium, calcium, magnesium, sodium, and iron) and toxic (lead, cadmium, arsenic, chromium, and nickel) elements in commonly consumed spices in Morocco, including cinnamon, cumin, ginger, black pepper, and turmeric. A total of 162 spice samples were obtained from markets in the Greater Casablanca, Morocco. Five essential elements, including potassium, calcium, magnesium, sodium, and iron, and five toxic trace metals, including lead, cadmium, arsenic, chromium, and nickel, were determined by inductively coupled plasma mass spectrometry (ICP-MS) after microwave-assisted digestion. Cumin indicated the highest levels of magnesium (6.86 ± 1.61 g/kg), sodium (3.98 ± 1.59 g/kg), calcium (11.13 ± 4.53 g/kg), and iron (753.71 ± 446.07 mg/kg). Turmeric had the highest levels of potassium (25.96 ± 13.51 g/kg). Cinnamon had elevated levels of lead (2.05 mg/kg) and cadmium (0.29 mg/kg), exceeding Moroccan and European regulatory limits. Additionally, cumin indicated the highest levels of arsenic (0.45 ± 0.30 mg/kg) and nickel (4.18 ± 2.85 mg/kg) compared to other spices. Principal component analysis (PCA) revealed distinct elemental patterns. The first component (PC1), driven by magnesium and sodium, clearly separated cumin due to its high macronutrient content. The second component (PC2), influenced by cadmium and lead, isolated cinnamon because of its toxic metal burden. The PC1 and PC2 accounted for 64.6% of the total variance. Turmeric and ginger formed a close cluster in the PCA plot, associated with higher levels of potassium, calcium, and nickel. Black pepper was positioned between these groups, reflecting intermediate composition. Pearson correlation analysis supported these findings, with a strong correlation between lead and cadmium, suggesting a shared

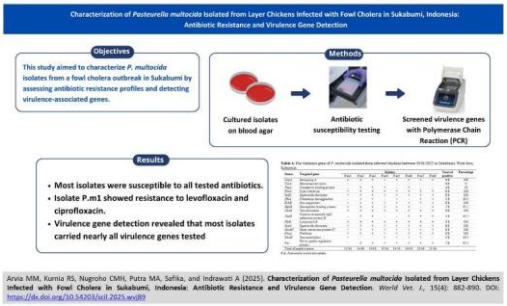
contamination source. These results emphasized the nutritional and toxicological roles of spices in Moroccan diets. Regular monitoring is essential to protect public health in both animals and humans.
Keywords: Food safety, Inductively coupled plasma mass spectrometry, Spices, Toxic metal

[Full text-PDF] [Crossref Metadata] [Scopus] [Export from ePrint]

Research Paper

Characterization of *Pasteurella multocida* Isolated from Layer Chickens Infected with Fowl Cholera in Sukabumi, Indonesia: Antibiotic Resistance and Virulence Gene Detection

Arvia MM, Kurnia RS, Nugroho CMH, Putra MA, Safika, and Indrawati A.
World Vet. J. 15(4): 882-890, 2025; pii:S232245682500089-15
DOI: https://dx.doi.org/10.54203/scil.2025.wvj89



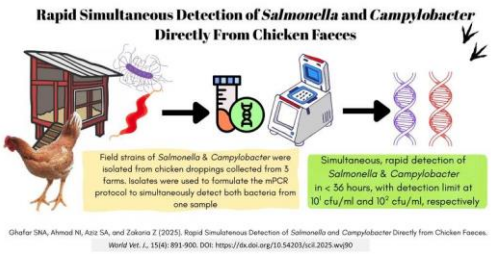
ABSTRACT: Fowl cholera is a contagious bacterial disease in poultry caused by *Pasteurella multocida* (*P. multocida*), which presents a significant threat to layer chicken farming due to its economic impact and potential antibiotic resistance. This study aimed to characterize *P. multocida* isolates from a fowl cholera outbreak in Sukabumi by assessing antibiotic resistance profiles and detecting virulence-associated genes. Eight *P. multocida* bacterial isolates from organ sample were cultured on blood agar and subjected to antibiotic susceptibility testing using the Sensititre™ GN4F system. Genomic DNA was extracted and analyzed for 16 virulence genes through conventional polymerase chain reaction (PCR). Results showed that all isolates were generally susceptible to the tested antibiotics, except for isolate P.m1, which was confirmed resistant to levofloxacin and ciprofloxacin. Virulence gene detection revealed that most isolates carried nearly all virulence genes tested, particularly those encoding capsule (*capA*), iron acquisition proteins (*exbB*, *hgbB*, *fur*), fimbriae and adhesins (*fim4*, *fimA*, *pfhA*, *tadD*), outer membrane proteins (*oma87*, *plpB*), sialidases (*nanB*, *nanH*), and superoxide dismutases (*sodA*, *sodC*). Notably, no isolates harbored the *toxA* gene. The presence of extensive virulence factors despite general antibiotic susceptibility underscored the pathogen's potential to persist and cause disease, and highlighted the need for targeted surveillance and comprehensive control strategies in Indonesia.
Keywords: Antibiotic resistance, Characterization, Fowl cholera, *Pasteurella multocida*, Virulence gene

[Full text-PDF] [Crossref Metadata] [Scopus] [Export from ePrint]

Research Paper

Rapid Simultaneous Detection of *Salmonella* and *Campylobacter* Bacteria Directly from Chicken Faeces

Ghafar SNA, Ahmad NI, Aziz SA, and Zakaria Z.
World Vet. J. 15(4): 891-900, 2025; pii:S232245682500090-15
DOI: https://dx.doi.org/10.54203/scil.2025.wvj90



ABSTRACT: *Campylobacter* and *Salmonella* are widely recognized as significant causes of foodborne diseases, with poultry and poultry products being the most frequent sources of infection in humans. Rapid, simultaneous detection of both pathogens can prevent contaminated food from entering the human food chain. The present study aimed to simultaneously detect *Salmonella* and *Campylobacter* spp. directly from faeces of broiler chickens aged 4 to 5 weeks by multiplex polymerase chain reaction (mPCR). The suitability of the PCR protocol using pairs of primers targeting the *invA* and *cadF* genes was evaluated to detect *Salmonella* and *Campylobacter* spp., respectively, from 15 samples. The specificity of the PCR assay was 100% for both pathogens, as no positive cross-reactions were detected with non-targeted bacteria. The limit of detection for pure culture of *Salmonella* was 1 CFU/mL, whereas for *Campylobacter* it was 10^1 CFU/mL. Incubation of spiked faeces in brain heart infusion broth for 24 to 48 hours maintained a detection limit of 1 CFU/mL for *Salmonella*; however, the sensitivity decreased, resulting in a detection limit of 10^2 CFU/mL for *Campylobacter*. Simultaneous detection from 15 chicken faecal samples revealed two samples co-carrying both *Salmonella* and *Campylobacter* spp., four samples positive for *Salmonella*, six samples positive for *Campylobacter*, and three samples were negative for both pathogens. The developed mPCR protocol in the present study was highly specific and sensitive for detecting *Salmonella* and *Campylobacter* spp. directly from chicken faeces, achieving results in under 36 hours compared to the conventional culture method. The mPCR protocol can benefit veterinary and public health authorities during epidemiological investigations and rapid diagnostic purposes, which require timely confirmation of the disease status in chickens during the grow period.
Keywords: *Campylobacter,* Faeces, Multiplex PCR, *Salmonella*, Simultaneous detection

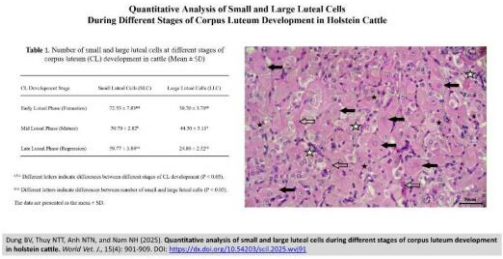
[Full text-PDF] [Crossref Metadata] [Scopus] [Export from ePrint]

Research Paper

Quantitative analysis of small and large luteal cells during different stages of corpus luteum development in holstein cattle

Dung BV, Thuy NTT, Anh NTN, and Nam NH.
World Vet. J. 15(2): 901-909, 2025; pii:S232245682500091-15

DOI: https://dx.doi.org/10.54203/scil.2025.wvj91



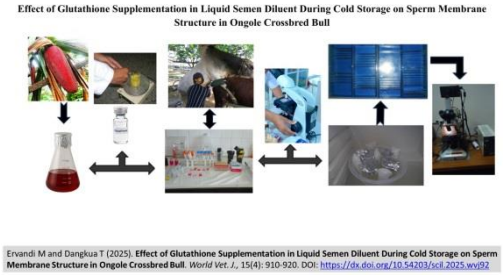
ABSTRACT: The bovine corpus luteum (CL) undergoes dynamic structural and functional changes throughout its lifespan, driven by distinct populations of steroidogenic cells, including small luteal cells (SLCs) and large luteal cells (LLCs). Although these cell types have been morphologically characterized, quantitative evaluations of their numerical abundance and relative distribution across different developmental phases of the CL in cows remain limited. This study sought to quantify the populations of small and large luteal cells across the early, mid, and late stages of corpus luteum development in Holstein cows. Histomorphometric analysis of hematoxylin and eosin–stained ovarian sections was performed to provide insights into their temporal roles in luteal function. Ovarian samples were obtained from 30 Holstein cows (30 pairs), immediately after slaughter, and categorized into early, mid, or late luteal phases according to ovarian morphology and the appearance of corpora lutea. A total of 30 CL samples (10 per stage) were selected for evaluation. Each CL was fixed, paraffin-embedded, and sectioned longitudinally (5 µm thick) for histological examination. Small (<20 µm) and large (> 35 µm) luteal cells were quantified in standardized microscopic fields at × 40 magnification using ImageJ software. The results revealed that SLC counts were highest during the early luteal phase (72.53 ± 7.83) and significantly exceeded LLC counts (30.70 ± 3.78). In the mid-luteal phase, SLCs decreased (50.70 ± 2.82) while LLCs increased (44.30 ± 3.11), with no significant difference between them. During the late luteal phase, SLCs increased slightly (59.77 ± 3.84), whereas LLCs declined markedly (24.80 ± 2.52). Overall, SLCs counted were highest during the early luteal phase and declined toward the mid phase, while LLCs increased markedly at the mid luteal phase and decreased again at the late phase.
Keywords: Corpus luteum, Histology, Large luteal cell, Small luteal cell

[Full text-PDF] [Crossref Metadata] [Scopus] [Export from ePrint]

Research Paper

Effect of Glutathione Supplementation in Liquid Semen Diluent During Cold Storage on Sperm Membrane Structure in Ongole Crossbred Bull

X Ervandi M and Dangkua T.
World Vet. J. 15(4): 910-920, 2025; pii:S232245682500092-15
DOI: https://dx.doi.org/10.54203/scil.2025.wvj92



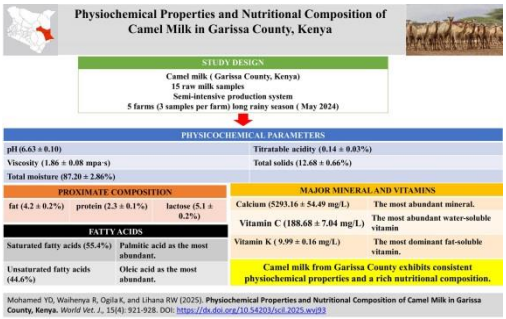
ABSTRACT: Damage to bovine spermatozoa membranes results from factors such as oxidative stress, high temperatures, extreme pH levels, and exposure to chemicals or infections. The present study aimed to explore the potential use of glutathione in liquid semen extenders during cold storage to protect the membrane structure of Peranakan Ongole (PO) crossbred bull semen. Semen samples were collected twice weekly from two PO crossbred bulls aged 2-3 years. Semen that met the quality standards was diluted with a red fruit (*Pandanus conoideus Lamk*) extract extender, supplemented with glutathione at various concentrations per 100 mL of the total volume extender. Sperm membrane evaluation included membrane integrity assessed by the hypoosmotic swelling test (HOST), sperm capacitation, and acrosome reaction assessed by chlortetracycline fluorescence staining. The treatments consisted of red fruit extract extender with 15% egg yolk (P0, control), red fruit extract extender with 15% egg yolk and 0.75 mM glutathione (P1), red fruit extract extender with 15% egg yolk and 1 mM glutathione (P2), and red fruit extract extender with 15% egg yolk plus 1.25 mM glutathione (P3). The present results indicated that Group P1 performed superior than other treatment groups. This was evidenced by higher spermatozoa membrane integrity and a higher proportion of non-capacitated spermatozoa, while the proportions of capacitated spermatozoa and acrosome reaction remained low. The extender formulation containing red fruit extract, 15% egg yolk, and 0.75 mM glutathione-maintained acrosome status above 50% after six days of cold storage. Therefore, the combination of red fruit extract, 15% egg yolk, and 0.75 mM glutathione was identified as the optimal formulation for liquid semen preservation, meeting the necessary conditions for practical use in artificial insemination programs in the field.
Keywords: Acrosome reaction, Glutathione, Membrane integrity, Red fruit extract

[Full text-PDF] [Crossref Metadata] [Scopus] [Export from ePrint]

Research Paper

Physiochemical Properties and Nutritional Composition of Camel Milk in Garissa County, Kenya

Mohamed YD, Waihenya R, Ogila K, and Lihana RW.
World Vet. J. 15(4): 921-928, 2025; pii:S232245682500093-15
DOI: https://dx.doi.org/10.54203/scil.2025.wvj93



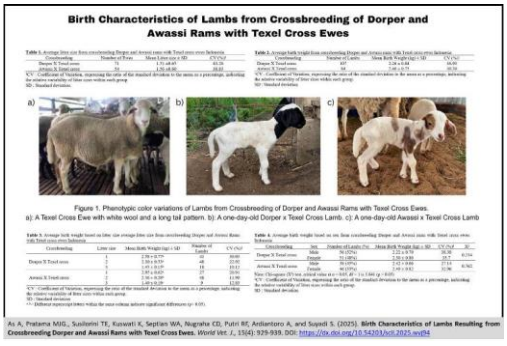
ABSTRACT: Camel milk is an important source of food, income, and livelihood for communities in arid and semi-arid regions. It contains essential macronutrients, minerals, vitamins, and bioactive compounds that contribute to human health. Despite Kenya's status as a prominent producer of camel milk, especially in Garissa County, comprehensive data regarding its physicochemical and nutritional composition remain scarce. The present study aimed to determine the physicochemical attributes and nutritional profile of camel milk sourced from Garissa County. Fifteen raw milk samples were collected in May 2024 during the long rainy season from randomly selected, clinically healthy lactating Somali dromedary camels reared under semi-intensive systems on five dairy farms in Garissa County, Kenya, under hygienic conditions (three samples per farm). Physicochemical parameters measured included pH, color, titratable acidity, viscosity, total solids, and moisture. Nutritional components analyzed were fat, protein, lactose, minerals, vitamins, and fatty acids using AOAC methods and gas chromatography–mass spectrometry. The camel milk samples exhibited a mean pH of 6.63 ± 0.10, 0.14 ± 0.03% titratable acidity, 1.86 ± 0.08 mPa·s viscosity, 12.68 ± 0.66% total solids, and 87.20 ± 2.86% moisture. Proximate composition indicated 4.2 ± 0.2% fat, 2.3 ± 0.1% protein, and 5.1 ± 0.2% lactose. Calcium (5293.16 ± 54.49mg/l) was the most abundant mineral. Among vitamins, vitamin C was the most abundant water-soluble vitamin, while vitamin K was the most dominant fat-soluble vitamin. Fatty acid analysis indicated that (55.4%) of the fatty acids were saturated and (44.6%) were unsaturated. Palmitic acid and oleic acid were the most abundant. The results indicated relatively uniform physicochemical and nutritional characteristics of camel milk produced under semi-intensive systems from selected farms in Garissa County, Kenya. The results of this study provided descriptive insight for future studies with larger sample sizes within this county, as well as comparative study across counties and different seasonal conditions.
Keywords: Camel milk, Fatty acid, Nutritional composition, Physicochemical characteristic

[Full text-PDF] [Crossref Metadata] [Scopus] [Export from ePrint]

Research Paper

Birth Characteristics of Lambs Resulting from Crossbreeding Dorper and Awassi Rams with Texel Cross Ewes

As A, Pratama MJG., Susilorini TE, Kuswati K, Septian WA, Nugraha CD, Putri RF, Ardiantoro A, and Suyadi S.
World Vet. J. 15(4): 929-939, 2025; pii:S232245682500094-15
DOI: https://dx.doi.org/10.54203/scil.2025.wvj94



ABSTRACT: Crossbreeding is an effective strategy to enhance sheep productivity under tropical conditions. This study evaluated the birth characteristics of lambs resulting from crossbreeding Dorper and Awassi rams with Texel cross ewes in Indonesia's tropical environment. The experiment was conducted from April to November 2023 at CV Kambing Burja, Malang Regency, East Java, Indonesia. A total of 125 Texel cross ewes aged 1.5 to over 3 years were naturally mated with 71 Dorper and 54 Awassi rams using a controlled colony mating system at a ram-to-ewe ratio of 1:25. The study employed complete enumeration, including all ewes that successfully lambed during the observation period. Sire groups comprising two to three rams per breed were rotated every 45 days to ensure equal mating opportunities and prevent exhaustion. Estrus synchronization followed a two-step hormonal protocol, including the administration of Conceptase ($PGF_{2\alpha}$, 2.5 mL/ewe) intramuscularly to induce luteolysis, followed 48 hours later by PG600 (1.5 mL/ewe) containing eCG and hCG to stimulate follicular development and ovulation. Mating behavior was observed daily, with successful copulation indicated by restlessness, vocalization, and receptivity. Measured parameters included birth weight, litter size, and sex ratio. Results showed no significant differences in mean litter size or birth weight between Dorper × Texel cross and Awassi × Texel cross lambs, although Awassi crosses exhibited more uniform birth weights. Birth weight decreased as litter size increased, and sex ratios remained balanced in both groups. These findings suggest that both Dorper and Awassi rams are suitable for enhancing the reproductive performance of Texel cross ewes under tropical management systems, highlighting the importance of integrating hormonal synchronization and controlled breeding for sustainable sheep production in Indonesia.
Keywords: Awassi sheep, Birth weight, Dorper sheep, Litter size, Sex ratio, Texel cross sheep

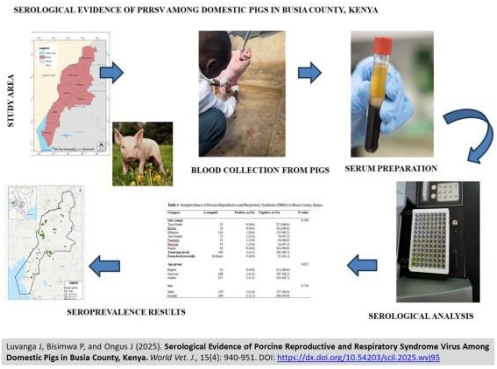
[Full text-PDF] [Crossref Metadata] [Scopus] [Export from ePrint]

Research Paper

Serological Evidence of Porcine Reproductive and Respiratory Syndrome Virus Among Domestic Pigs in Busia County, Kenya

Luvanga J, Bisimwa P, and Ongus J.

World Vet. J. 15(4): 940-951, 2025; pii:S232245682500095-15
DOI: https://dx.doi.org/10.54203/scil.2025.wvj95



Luvanga J, Bisimwa P, and Ongus J (2025). **Serological Evidence of Porcine Reproductive and Respiratory Syndrome Virus Among Domestic Pigs in Busia County, Kenya.** *World Vet. J.*, 15(4): 940-951. DOI: https://dx.doi.org/10.54203/scil.2025.wvj95

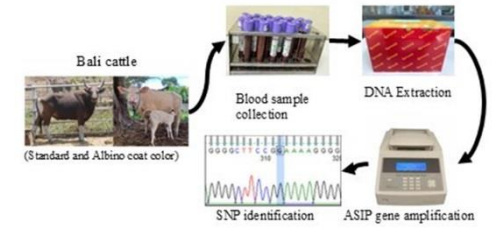
ABSTRACT: Porcine reproductive and respiratory syndrome virus (PRRSV) is a significant swine pathogen and one of the most damaging viruses affecting the global pig industry. Although clinical signs compatible with PRRS have been observed within Kenyan pig production systems, the virus has not yet been officially reported in the country. The present study sought to estimate the seroprevalence of PRRSV, describe farm characteristics, and identify risk factors associated with PRRSV infection among domestic pigs in Busia County, Kenya. Serum samples were collected from 398 pigs (52 piglets, 109 growers, and 237 adults) originating from 56 pig keeping farms/households and analyzed using a commercial indirect Enzyme Linked Immunosorbent Assay (ELISA). Farm characteristics, pig farming practices, pig husbandry, and biosecurity data were recorded via structured questionnaires. Pig-level seroprevalence was 1.3% (5/398), with positives detected in Matayos 0.8% (1/124), Nambale 2.0% (1/51), Teso South 2.8% (2/72), and Bunyala 2.9% (1/35) sub-counties, respectively. The farm-level seroprevalence was 8.9% (5/56). Seropositivity did not differ significantly by location, sex, or age category. Biosecurity uptake was generally low, with the use of dedicated clothing/aprons (14%), wearing of boots (32%), presence of footbaths (12.5%), quarantine of new pigs (11%), and handwashing after pig handling (16%). Not using separate clothing/aprons was the only risk factor significantly associated with farm seropositivity. The present findings provided evidence of PRRSV exposure in Kenyan pigs and reveal important gaps in farm-level biosecurity practices at the human-pig interface, underscoring the epidemiological relevance of these observations for pig industry in the region, although the small number of seropositive farms means that some degree of false positivity or false negativity may not be excluded.
Keywords: Biosecurity, Enzyme-linked immunosorbent assay, Porcine reproductive and respiratory syndrome virus, Seroprevalence

[Full text-PDF] [Crossref Metadata] [Scopus] [Export from ePrint]

Research Paper

Genetic Diversity of the *Agouti Signaling Protein* (ASIP) Gene in Determining Coat Color in Bali Cattle (*Bos javanicus*)

Kholijah K, Darwati S, Fakhrul Ulum M, Noor RR, and Jakaria J.
World Vet. J. 15(4): 952-959, 2025; pii:S232245682500096-15
DOI: https://dx.doi.org/10.54203/scil.2025.wvj96



Kholijah K, Darwati S, Fakhrul Ulum M, Noor RR, and Jakaria J (2025). **Genetic Diversity of the *Agouti Signaling Protein* (ASIP) Gene in Determining Coat Color in Bali Cattle (*Bos javanicus*).** *World Vet. J.*, 15(4): 952-959. DOI: https://dx.doi.org/10.54203/scil.2025.wvj96

ABSTRACT: Bali cattle, which are indigenous to Indonesia, display distinctive and unique coat color characteristics. The appearance of albinos has been observed as an abnormality. The present study aimed to explore the *agouti signaling protein* (*ASIP*) gene in Bali cattle and analyze its association with the occurrence of albinism and white-spotted coat colors in Bali cattle. A total of 68 blood samples from cattle were used, including standard Bali cattle (N = 39), Bali cattle with spotting (N = 9), and albino Bali cattle (N = 20). Standard and white-spotted Bali cattle samples were collected from the Bali Cattle Breeding Centre in Jembrana, Bali Province, and the Breeding Center Unit in Serading, West Nusa Tenggara, Indonesia. Albino cattle samples were obtained from Taro Village, Gianyar Regency, Bali. The DNA amplification was performed using polymerase chain reaction (PCR), single-nucleotide polymorphisms (SNPs) were determined through direct sequencing, and genotyping was performed using the PCR-RFLP method. The exon 1 and exon 2 regions of the *ASIP* gene were monomorphic or uniform. The coding region of exon 3 of the *ASIP* gene in Bali cattle exhibited polymorphisms, specifically regarding coat color. A novel SNP (g.498 A > G) was detected exclusively in Bali cattle; however, it has not yet been validated as a potential genetic marker for coat color in this breed. The findings of this study further revealed that the *ASIP* gene sequence does not distinguish between standard and albino coat colors in Bali cattle, despite the identification of this specific SNP.
Keywords: *Agouti signaling protein* gene, Bali cattle, Coat color, Polymerase chain reaction, Single nucleotide polymorphism

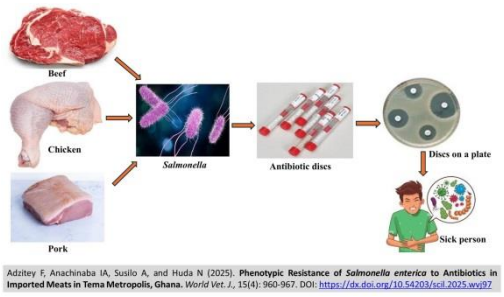
[Full text-PDF] [Crossref Metadata] [Scopus] [Export from ePrint]

Research Paper

Phenotypic Resistance of *Salmonella enterica* to Antibiotics in Imported Meats in Tema Metropolis, Ghana

Adzitey F, Anachinaba IA, Susilo A, and Huda N.
World Vet. J. 15(4): 960-967, 2025; pii:S232245682500097-15

DOI: https://dx.doi.org/10.54203/scil.2025.wvj97



ABSTRACT: *Salmonella enterica* (*S. enterica*) causes certain foodborne diseases and poses public health concerns when it becomes antibiotic-resistant. The present study aimed to determine the resistance of *S. enterica* to antibiotics from imported meats sold in the Tema Metropolis, Ghana. A total of 300 beef, chicken, and pork samples randomly selected from markets of the Metropolis were tested for *S. eneterica.* The disc diffusion method was used to determine the antibiotic resistance in 60 *S. enterica* isolates. The current results revealed that 40% of imported chicken, 38% of imported pork, and 29% of imported beef were positive for *S. enterica*. The S. enterica isolated from imported meat sources was 36.7% resistant to tetracycline but susceptible (≥ 68%) to imipenem, ciprofloxacin, tetracycline, chloramphenicol, trimethoprim, gentamicin, and ceftriaxone. The multiple antibiotic resistance (MAR) index fell within the range of 0.1 to 0.6, and 12 different patterns were observed. The present study revealed the contamination of *S. enterica* in some imported meat sold in Tema Metropolis, Ghana. Avoidance of cross-contamination and adequate thermal treatment of meats before eating is essential.
Keywords: Antibiotic resistance, Meat, Prevalence, *Salmonella enterica*

[Full text-PDF] [Crossref Metadata] [Scopus] [Export from ePrint]

Research Paper

Prevalence and Parasite Load of Helminths in Reintroduced Vicuñas (*Vicugna vicugna*) in High-Andean Communities, Huancavelica, Peru

Rojas E, Machuca ANG, and Bezada S.
World Vet. J. 15(4): 968-977, 2025; pii:S232245682500098-15

DOI: https://dx.doi.org/10.54203/scil.2025.wvj98



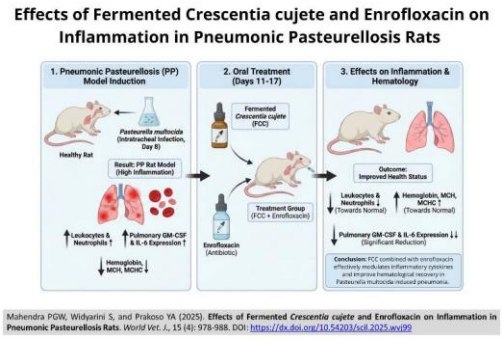
ABSTRACT: Gastrointestinal helminth infections represent a major threat to the health and conservation of vicuñas (*Vicugna vicugna*) in the Peruvian Andes, while epidemiological information on repopulated populations under community-based management remains limited. The present study aimed to determine the prevalence and parasite load of gastrointestinal helminths in reintroduced vicuñas from the high-Andean communities of Huancavelica, Peru. In the present study, 102 vicuñas from the communities of Atuna and Allarpo (Huancavelica), Peru, were evaluated during the 2023 *chaccu*, a traditional Andean practice in which wild vicuñas are collectively herded, captured, and shorn for fiber under community supervision. The sample consisted of 66 females and 36 males, of which 80 were classified as adults (>3 years old) and 22 as juveniles (1-3 years old). Rectal fecal samples were collected and analyzed to detect and quantify gastrointestinal helminth eggs, including strongyle-type eggs, *Nematodirus*, *Trichuris*, and *Fasciola hepatica* (*F. hepatica*). Samples were analyzed using flotation, modified McMaster, and sedimentation techniques to detect and quantify helminth eggs. Overall prevalence, including by community, sex, age, and parasite load (eggs per gram, EFG) as a geometric mean, was determined. The overall prevalence was 75.5%, with *F. hepatica* as the most frequent parasite, 79.2% in Allarpo and 60.9% in Atuna, followed by *Trichuris* spp. (11.6%) and *Nematodirus* spp. (10.2%), and Strongyle-type eggs 42.0% in Allarpo and 17.45% in Atuna. Juveniles had a higher prevalence of *F. hepatica* infection (90.9%) compared to adults (71.3%). The mean *F. hepatica* egg count was higher in Allarpo (34.4 EPG) than in Atuna (11.7 EPG), and this difference was statistically significant. When analyzed by sex, females indicated a higher mean egg count (24.6 EPG; 95% CI: 16.9-35.7) than males (17.4 EPG; 95% CI: 9.8-30.7). Regarding age, adults presented a higher mean EPG (23.6; 95% CI: 16.0-34.8) compared to juveniles (16.5; 95% CI: 8.8-31.1), although mentioned differences were not statistically significant. The findings of the present study indicated that helminth infections, particularly fascioliasis, are widespread, with higher risk in juveniles and environmentally favorable areas, highlighting the need for locally adapted monitoring and control strategies in reintroduced vicuña populations.
Keywords: *Fasciola hepatica*, Gastrointestinal helminth, Prevalence, *Vicugna vicugna*

[Full text-PDF] [Crossref Metadata] [Scopus] [Export from ePrint]

Research Paper

Effects of Fermented *Crescentia cujete* and Enrofloxacin on Inflammation in Pneumonic Pasteurellosis Rats

Mahendra PGW, Widyarini S, and Prakoso YA.
World Vet. J. 15(4): 978-988, 2025; pii:S232245682500099-15
DOI: https://dx.doi.org/10.54203/scil.2025.wvj99



Mahendra PGW, Widyarini S, and Prakoso YA (2025). **Effects of Fermented *Crescentia cujete* and Enrofloxacin on Inflammation in Pneumonic Pasteurellosis Rats**. *World Vet. J.*, 15 (4): 978-988. DOI: https://dx.doi.org/10.54203/scil.2025.wvj99

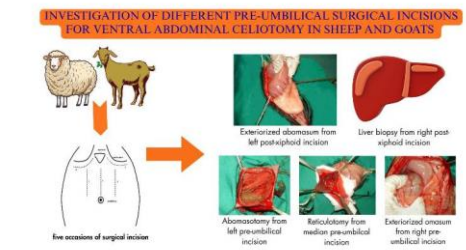
ABSTRACT: Pneumonic pasteurellosis (PP) is a respiratory disease caused by *Pasteurella multocida* (*P. multocida*) with broad host susceptibility and zoonotic potential. Pasteurellosis is classified as a strategic infectious animal disease and a neglected tropical disease in Indonesia, highlighting the need for effective supportive therapies. Fermented *Crescentia cujete* L. (FCC) contains bioactive compounds with anti-inflammatory and antioxidant activities. The present study aimed to evaluate the anti-inflammatory effects of FCC combined with enrofloxacin on hematological parameters and the immune expression of granulocyte-macrophage colony-stimulating factor (GM-CSF) and interleukin-6 (IL-6) in an induced PP rat model. Twenty male Sprague-Dawley rats, three months old and weighing 250-300 g, were divided into five groups, including healthy control (P1), untreated infected rats (P2), rats treated with 20 mg/kg body weight (BW) of enrofloxacin (P3), rats given 20 and 30 mg/kg BW of enrofloxacin and ibuprofen, respectively (P4), and rats administered 20 and 5.92 mg/kg BW of enrofloxacin and FCC (P5), respectively. After a 7-day acclimatization, rats were infected intratracheally with *P. multocida* on day 8, and treatments were administered orally for seven days starting on day 11. Hemoglobin, mean corpuscular hemoglobin (MCH), and mean corpuscular hemoglobin concentration (MCHC) decreased significantly in P2 compared to P1, with no difference between P2 and P3. Although hemoglobin, MCH, and MCHC improved in P4 and P5 toward control levels, most variables remained significantly different from P1. Leukocyte and neutrophil counts were significantly elevated in P2 compared to P1; however, P5 demonstrated a declining trend toward normal values and did not differ significantly from P1. Pulmonary GM-CSF and IL-6 immune expression increased markedly in P2 compared to P1. Groups P3 and P4 exhibited elevated cytokine expression compared to P1, without significant differences from P2. In contrast, P5 indicated a significant reduction in GM-CSF and IL-6 expression compared to P2, reaching levels comparable to those of P1. The FCC combined with enrofloxacin improved hematological status and modulated inflammatory cytokines in PP. The present findings indicated that FCC could be a potential supplementary treatment for managing inflammation and aiding hematological recovery in bacterial infection pneumonia.
Keywords: *Crescentia cujete*, Granulocyte Macrophage-Colony Stimulating Factor, Hematology, Interleukin-6, *Pasteurella multocida*

[Full text-PDF] [Crossref Metadata] [Scopus] [Export from ePrint]

Research Paper

Investigation of Different Pre-umbilical Surgical Incisions for Ventral Abdominal Celiotomy in Sheep and Goats

Abdullah Z, El-Hawari SF, Almubarak AI, Abdel-Raheem SM, Marzok M, and Abouelella AG.
World Vet. J. 15(4): 989-996, 2025; pii:S232245682500100-15
DOI: https://dx.doi.org/10.54203/scil.2025.wvj100



Abdullah Z, El-Hawari SF, Almubarak AI, Abdel-Raheem SM, Marzok M, and Abouelella AG. (2025). **Investigation of Different Pre-umbilical Surgical Incisions for Ventral Abdominal Celiotomy in Sheep and Goats**. *World Vet. J.*, 15(4): 989-996. DOI: https://dx.doi.org/10.54203/scil.2025.wvj100

ABSTRACT: Identifying the correct site for surgical incision and reducing unnecessary handling are crucial in veterinary surgical procedures. The current study aimed to evaluate surgical incisions in the pre-umbilical region in small ruminants with correlation to possible surgical operations in the abdominal organs. A randomized experimental study was conducted on 15 sheep (12 females and three males) and 15 goats (12 females and three males), with body weights of 44.9 ± 3.7 kilograms in sheep and 26.3 ± 4.6 kilograms in goats. Five different surgical exposures, including median, left paramedian, right paramedian, left post-xiphoid, and right post-xiphoid, were applied. The accessibility of abdominal viscera was evaluated for each incision site by documenting directly visible organs, organs that could be readily moved to the site of incision, and organs that could only be palpated. Access to the ventral ruminal sac and omentum was achieved through median, left, and right pre-umbilical celiotomy incisions. Furthermore, these surgical approaches allowed for reaching the abomasum and performing of abomasotomy. Abomasotomy and reticulotomy operations were performed through a median pre-umbilical incision. Omasum was palpable and easily examined via the right pre-umbilical celiotomy. The liver and gall bladder were exposed via a right post-xiphoid curved incision. In contrast, the reticulum was accessed for surgical intervention through a left post-xiphoid curved incision. The only recorded postoperative complication was tympany after gastrointestinal surgery. The present study indicated that choosing the appropriate pre-umbilical or post-xiphoid incision greatly improves access to targeted abdominal organs in small ruminants. Right and left pre-umbilical incisions were identified as the most effective approaches for abomasal

procedures, whereas post-xiphoid incisions provided the optimal exposure to the reticulum, liver, and gall bladder. Furthermore, access to abdominal organs may vary between sheep and goats when employing the same surgical approach.

Keywords: Abomasotomy, Incision, Laparotomy, Paramedian, Small ruminant

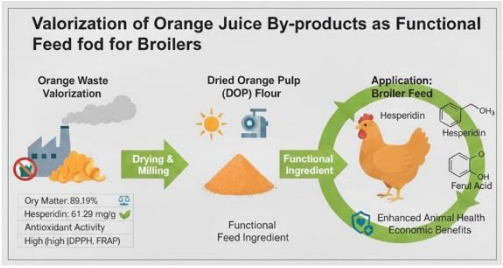
[Full text-PDF] [Crossref Metadata] [Scopus] [Export from ePrint]

Research Paper

Evaluation of the Chemical Composition and Antioxidant Capacity of Dried Orange Pulp

Chaib Eddour AR, Litim M, and Bouderoua K.
World Vet. J. 15(4): 997-1006, 2025; pii:S232245682500101-15
DOI: https://dx.doi.org/10.54203/scil.2025.wvj101

ABSTRACT: The disposal of orange juice by-products presents an environmental challenge due to their high volume and accumulation in landfills. Valorizing these residues supports the development of a circular economy within the agro-industrial sector, offering both environmental and economic benefits. This study aimed to valorize orange juice processing residues by producing a dried orange pulp (DOP) flour and characterizing its physicochemical and phytochemical properties to assess its potential suitability as a sustainable feed ingredient for broiler chickens. The physicochemical properties of the sun-dried and finely milled orange by-products (<1 mm) were analyzed using standard methods, including proximate composition analysis (moisture, ash, crude protein, crude cellulose), and spectrophotometric assays for phytochemicals (total phenolics, flavonoids, condensed tannins) and antioxidant activity [2,2-Diphenyl-1-picrylhydrazyl (DPPH), Ferric Reducing Antioxidant Power (FRAP)]. The DOP demonstrated high levels of dietary cellulose (89.19% Dry Matter), ash (3.81% Dry Matter), total phenolics (202.59 ± 15.93 mg Gallic Acids Equivalent/100 g DM), total flavonoids (430.70 ± 2.78 mg Quercetin Equivalent/100 g), and strong antioxidant activity (FRAP: 1158.8 ± 19.22 mg/g). Phenolic profiling via High-Performance Liquid Chromatography (HPLC) revealed flavanones as the dominant subclass, with hesperidin (61.29 mg/g) and ferulic acid (27.1 mg/g) as major constituents. These results highlight the nutritional and functional potential of DOP as a feed additive. The remarkable antioxidant capacity and high concentration of bioactive compounds like hesperidin position DOP not just as a filler, but as a functional feed additive that could enhance animal health.



Keywords: Ferulic acid, Hesperidin, Hydrocinnamic acid, Orange waste

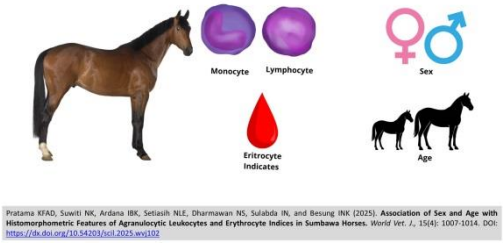
[Full text-PDF] [Crossref Metadata] [Scopus] [Export from ePrint]

Research Paper

Association of Sex and Age with Histomorphometric Features of Agranulocytic Leukocytes and Erythrocyte Indices in Sumbawa Horses

Pratama KFAD, Suwiti NK, Ardana IBK, Setiasih NLE, Dharmawan NS, Sulabda IN, and Besung INK.
World Vet. J. 15(4): 1007-1014, 2025; pii:S232245682500102-15
DOI: https://dx.doi.org/10.54203/scil.2025.wvj102

ABSTRACT: The Sumbawa horse, an indigenous Indonesian breed, plays important ecological and cultural roles in the region, such as participation in traditional ceremonies, local transportation, and horse-racing competitions; however, scientific data on its hematological and cellular characteristics remain limited, hindering accurate clinical evaluation and breed-specific health management. This study aimed to provide baseline histomorphometric and hematological data by examining 80 clinically healthy Sumbawa horses, grouped by sex (male and female) and age (young and adult). Peripheral blood smears were prepared immediately after venipuncture and stained using the modified Diff Quick method. Morphometric parameters of lymphocytes and monocytes, including cell diameter, perimeter, cell area, and nucleus to cytoplasm ratio, were measured using calibrated digital image analysis. Complete blood count parameters, including mean corpuscular hemoglobin (MCH), mean corpuscular hemoglobin concentration (MCHC), mean corpuscular volume (MCV), red cell distribution width coefficient of variation (RDW-CV), and red cell distribution width standard deviation (RDW-SD), were obtained using an automated hematology analyzer. Females exhibited larger lymphocyte dimensions (17.79 ± 5.89 µm² versus 16.57 ± 6.29 µm², whereas males showed larger monocyte size (18.44 ± 7.60 µm² versus 14.88 ± 5.46 µm²). Lymphocyte counts and percentages were higher in females, while monocyte values and RDW-CV were higher in males. Age significantly influenced lymphocyte morphometry and leukocyte profiles, whereas its effects on monocytes were limited, with only monocyte area showing a significant difference between age groups. These findings indicated *significant* age-related increases in lymphocyte perimeter, area, and diameter, whereas most monocyte and



erythrocyte indices remained relatively stable between age groups. Sex related differences were also evident, with females exhibiting significantly higher lymphocyte counts and percentages, and males showing significantly higher monocyte counts and greater erythrocyte variability. These reference values provide clear morphometric distinctions between groups of Sumbawa horses, with adults exhibiting larger lymphocyte dimensions and males showing higher monocyte counts and greater erythrocyte variability, thus offering a biologically calibrated basis for further physiological interpretation.

Keywords: Age, Agranulocytic leukocyte, Erythrocyte indice, Histomorphometry, Horse, Sex

[Full text-PDF] [Crossref Metadata] [Scopus] [Export from ePrint]

Research Paper

Risk Factors Associated with Conception Rate in Holstein and Lai Sind Crossbred Cows in Small Holding Farms in Vietnam

Thanh NV, Lanh DTK, Nam NH, and Dung BV.
World Vet. J. 15(4): 1015-1023, 2025;
pii:S232245682500103-15
DOI: https://dx.doi.org/10.54203/scil.2025.wvj103



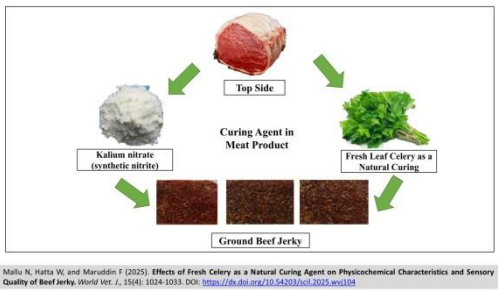
ABSTRACT: Reproductive efficiency is a critical factor in smallholder dairy systems, where management limitations often reduce fertility. Identifying factors influencing conception is essential to improving breeding performance in crossbred dairy cows raised in smallholder farms. The present study aimed to identify reproductive and management-related risk factors influencing conception rates in Holstein × Lai Sind crossbred cows at smallholder farms in Northern Vietnam. A retrospective analysis was conducted to evaluate the effects of ovarian disorders, estrus detection timing, age, parity, body condition score (BCS), calving-to-service interval, artificial insemination (AI) order, month of service, and age at first AI on conception rates in 433 cows. Farms were selected based on their willingness to participate, including a total of 40 smallholder farms in Northern Vietnam. Cows were included only if they had complete records on estrus detection, insemination, and pregnancy diagnosis; cows with missing or inconsistent data were excluded. Data was collected from the farm database and direct observation by trained personnel. Univariate analysis identified parity, age, age at first AI, month of AI, and BCS as significant factors influencing conception rates. The overall conception rate was 45.6%. Cows inseminated during December-January had a higher conception rate (52.9%) compared with those inseminated in September-October (37.7%). Heifers exhibited the highest conception rate (55.7%), while cows in parity 2 and parity 4-8 had significantly reduced fertility (37.6% and 42.0%, respectively). In the multivariate logistic regression model, parity and age at first AI were the most influential predictors of reproductive performance in Holstein crossbred cows. Cows first inseminated at 13-15 months, 16-17 months, and older than 17 months had significantly higher conception rates than those inseminated at 8-12 months. The present study demonstrated that both physiological factors (age, parity, and BCS) and seasonal management conditions (month of service) influence conception in Holstein × Lai Sind crossbred cows under smallholder conditions.
Keywords: Artificial insemination, Body condition, Month of service, Smallholder

[Full text-PDF] [Crossref Metadata] [Scopus] [Export from ePrint]

Research Paper

Effects of Fresh Celery as a Natural Curing Agent on Physicochemical Characteristics and Sensory Quality of Beef Jerky

Mallu N, Hatta W, and Maruddin F.
World Vet. J. 15(4): 1024-1033, 2025; pii:S232245682500104-15
DOI: https://dx.doi.org/10.54203/scil.2025.wvj104



ABSTRACT: Beef jerky is a processed meat product. Nitrite or nitrate salts are usually used as curing agents for beef jerky processing. However, excessive nitrite intake can pose health risks and raise public concern, so natural alternatives such as celery can be used. This study evaluated fresh celery as a natural curing agent for beef jerky based on its physicochemical and sensory qualities. The study was conducted in two stages. In the first stage, beef was treated with celery at three levels (2%, 4%, and 6%) and saltpeter as a control, combined with three incubation periods (1, 2, and 3 hours) to identify the optimal treatment for the subsequent stage based on color characteristics and nitrite residue. In the second stage, the selected curing treatments (saltpeter, 4% celery, and 6% celery) were applied to beef jerky and evaluated over different storage periods (0, 2, and 4 weeks). The parameters analyzed included color values, lightness (L*), redness (a*), yellowness (b*), nitrite content, and lipid oxidation, as well as sensory attributes. The results of the first stage showed that the use of saltpeter produced the highest nitrite content (0.54 mg/kg), while the highest b* value was obtained in the treatment of 4% and 6% celery. The

incubation length had no significant effect on all parameters, but there was a significant interaction between the type of curing material and the length of incubation on the value of a*. In the second stage, neither curing material treatment nor storage time had a significant impact on organoleptic characteristics, and Thiobarbituric acid reactive substances values were relatively low (< 0.5 mg MDA/kg) up to 4 weeks of storage. A 6% celery treatment yielded the highest L* value, while the highest a* value was indicated by saltpeter, followed by 6% and 4% celery. Overall, the 6% celery treatment showed comparable performance to saltpeter, especially in retaining redness, suppressing lipid oxidation, and maintaining the sensory qualities of ground beef jerky.
Keywords: Beef jerky, Celery leaf, Meat quality, Natural curing, Residual nitrite

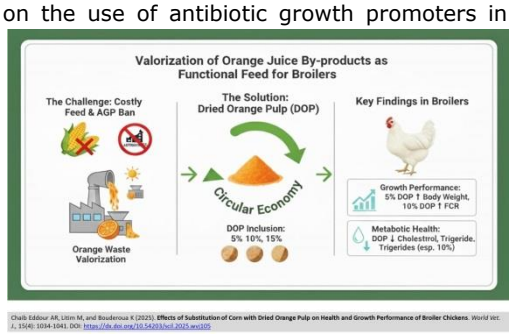
[Full text-PDF] [Crossref Metadata] [Scopus] [Export from ePrint]

Research Paper

Effects of Substitution of Corn with Dried Orange Pulp on Health and Growth Performance of Broiler Chickens

Chaib Eddour AR, Litim M, and Bouderoua K.
World Vet. J. 15(4): 1034-1041, 2025; pii:S232245682500105-15
DOI: https://dx.doi.org/10.54203/scil.2025.wvj105

ABSTRACT: The rising cost of cereal-based ingredients and restrictions on the use of antibiotic growth promoters in poultry have increased demand for sustainable alternatives. Agro-industrial by-products, particularly dried orange pulp (DOP), offer an economical, nutrient-rich solution with bioactive compounds that may improve broiler health and growth. The present study aimed to investigate the effects of incorporating different levels of dried orange pulp (*Citrus sinensis*) on growth performance and blood serum biochemical parameters in broiler chickens. A total of 200 one-day-old Arbor Acres chickens (45 ± 1.7 g) were randomly divided into four dietary groups. Each group consisted of 50 chickens, with five replicates of 10 chickens, and was reared for 49 days. The dietary groups included a control diet without DOP and three experimental diets in which DOP was partially replaced by corn at inclusion levels of 5% (50 g/kg of dry matter [DM]), 10% (100 g/kg of DM), and 15% (150 g/kg of DM). Growth performance was monitored throughout the entire rearing period. Blood samples were collected at 37 and 49 days of age to assess glucose, triglycerides, total cholesterol, high-density lipoprotein (HDL), and low-density lipoprotein (LDL). Broiler chickens fed DOP-substituted diets generally exhibited lower serum lipid levels, especially triglycerides and total cholesterol, compared to the control group at both sampling times. However, there was a slight increase in triglycerides in the 5% DOP group at 49 days compared to the control group. Glucose concentrations generally increased with higher levels of DOP inclusion, especially at 15%. Regarding growth performance, chickens fed the 5% DOP diet had the highest live weight, whereas those fed the 10% DOP diet demonstrated an improvement in feed conversion ratio compared to the control group. The dietary incorporation of DOP enhanced growth performance and positively influenced serum biochemical profiles in broiler chickens, with the 5% DOP level demonstrating the most significant improvements in performance and productivity parameters, while 10% DOP exerted the most beneficial effects on blood biochemical parameters.
Keywords: Cholesterol, HDL, LDL, Lipid fraction, Triglyceride



[Full text-PDF] [Crossref Metadata] [Scopus] [Export from ePrint]

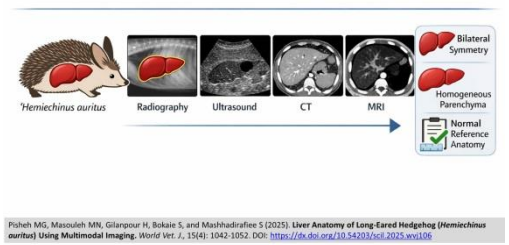
Research Paper

Liver Anatomy of Long-Eared Hedgehog (*Hemiechinus auritus*) Using Multimodal Imaging

Pisheh MG, Masouleh MN, Gilanpour H, Bokaie S, and Mashhadirafiee S.
World Vet. J. 15(4): 1042-1052, 2025; pii:S232245682500106-15

DOI: https://dx.doi.org/10.54203/scil.2025.wvj106

ABSTRACT: The long-eared hedgehog (*Hemiechinus auritus*), a small insectivorous species commonly encountered in exotic animal practice, lacks established imaging references for liver anatomy. The present study aimed to characterize the liver of clinically healthy adult animals using radiography, ultrasonography, computed tomography (CT), and magnetic resonance imaging (MRI). Seven clinically healthy adult one-year-old male hedgehogs with body weights of 320-410 grams were examined at the Diagnostic Imaging Unit of the Faculty of Veterinary Medicine, Islamic Azad University, Tehran, Iran. Radiography identified hepatic position and overall shape, while ultrasonography provided real-time assessment of parenchymal echotexture, gallbladder morphology, and major vascular landmarks. The CT and MRI provided detailed cross-sectional visualization, including morphometric measurements and evaluation of parenchymal and vascular architecture. Across all imaging techniques, the right and left hepatic lobes



exhibited comparable dimensions and tissue characteristics, with no statistically significant morphometric differences between lobes**.** The present study established a preliminary reference for liver anatomy in *Hemiechinus auritus* using multimodal imaging, thereby facilitating clinical diagnosis in this species.
Keywords: Hedgehog, Liver, MRI, Radiography, Ultrasonography

[Full text-PDF] [Crossref Metadata] [Scopus] [Export from ePrint]

Research Paper

Impacts of Tenebrio molitor Larval Meal on Zootechnical Performance, Biochemical Indices, and Intestinal Morphometry in Broiler Chickens

Nassi Guidi HI, Komi A, Komi A, Gnatepe MK, Vinakpon G, and Kokou T.
World Vet. J. 15(4): 1053-1062, 2025; pii:S232245682500107-15
DOI: https://dx.doi.org/10.54203/scil.2025.wvj107

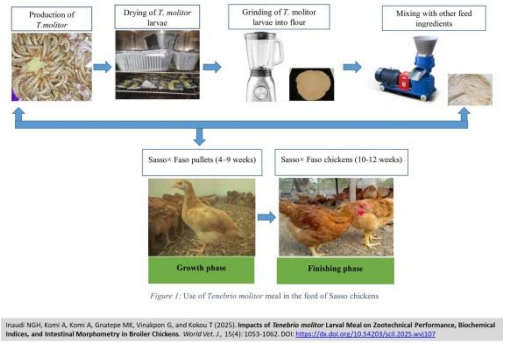


Figure 1: Use of *Tenebrio molitor* meal in the feed of Sasso chickens

Inaudi NGH, Komi A, Komi A, Gnatepe MK, Vinakpon G, and Kokou T (2025). **Impacts of *Tenebrio molitor* Larval Meal on Zootechnical Performance, Biochemical Indices, and Intestinal Morphometry in Broiler Chickens**. *World Vet. J.*, 15(4): 1053-1062. DOI: https://dx.doi.org/10.54203/scil.2025.wvj107

ABSTRACT: Protein resources availability is a major challenge for poultry farming in Sub-Saharan Africa. Insects such as *Tenebrio molitor* (*T. molitor*), known as yellow mealworm, which are rich in high-quality protein, offer a promising solution. The present study aimed to evaluate the effects of *T. molitor* larvae meal as an alternative protein source in broiler chicken diets. A total of 375 day-old hybrid broiler chickens (Crossbreeding of Sasso and Faso) were randomly assigned to five dietary treatments. Each treatment included five replicates with 15 chickens. During the 12-week study period, from hatching to the finishing phase, five dietary treatments were administered, including *T. molitor* larvae meal at 4% (TM4%), 6% (TM6%), 8% (TM8), black soldier fly larvae meal at 8% (BSF8), and as the control diet, fish meal at 8% (FM8). Biochemical parameters, including total protein, albumin, triglycerides, and cholesterol, as well as the small intestinal weight and length, and zootechnic performance such as feed intake, body weight gain, and feed conversion ratio (FCR), were measured. The current results indicated that feed consumption did not differ significantly among the treatments. However, the live weight of broiler chickens in TM8 was significantly higher in the finisher phase compared to other treatments, and their weight gain was higher in the grower and finisher phases. The FCR was significantly lower in the TM8 during the finisher phase than in other treatments. Carcass yield and gut length were significantly higher in the TM8. Total protein and albumin did not differ significantly among all groups. Cholesterol and triglyceride levels in TM6 were significantly higher than other groups. The incorporation of *T. molitor* meal at 8% inclusion level is recommended for broiler chicken feed.
Keywords: Biochemical parameter, Black soldier fly, Broiler chicken, Carcass yield, *Tenebrio molitor*, Weight gain

[Full text-PDF] [Crossref Metadata] [Scopus] [Export from ePrint]

Research Paper

Serodetection of Contagious Caprine Pleuropneumonia in Mosul City, Iraq

Al-lahibi MT and Al-Farwachi MI.
World Vet. J. 15(4): 1063-1069, 2025; pii:S232245682500108-15
DOI: https://dx.doi.org/10.54203/scil.2025.wvj108

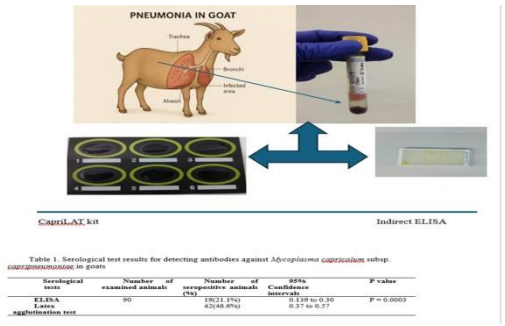


Table 1. Serological test results for detecting antibodies against *Mycoplasma capricolum* subsp. *capripneumoniae* in goats

Serological tests	Number of examined animals	Number of seropositive animals (%)	95% Confidence intervals	P value
ELISA Latex agglutination test	90	19(21.1%) 42(46.6%)	0.139 to 0.30 0.37 to 0.57	P = 0.0003

Al-lahibi MT and Al-Farwachi MI (2025). **Serodetection of Contagious Caprine Pleuropneumonia in Mosul City, Iraq.** *World Vet. J.*, 15(4): 1063-1069. DOI: https://dx.doi.org/10.54203/scil.2025.wvj108

ABSTRACT: Contagious caprine pleuropneumonia (CCPP) is a severe, highly transmissible respiratory disease in goats, resulting in significant economic losses. The precise antibody detection is critical for disease surveillance and control in suspected locations. The present study aimed to detect CCPP antibodies in goat sera using indirect enzyme-linked immunosorbent assay (ELISA) and latex agglutination tests (LAT) and to compare the diagnostic performance of these two serological methods. A cross-sectional study was conducted at the University of Mosul, Veterinary Teaching Hospital, Iraq. A total of 90 serum samples were collected from unvaccinated local goats (aged 1-7 years; 30 males, 60 females) exhibiting respiratory signs, including cough, nasal discharge, and dyspnea. The serum samples were analyzed for CCPP antibodies using both an indirect ELISA and LAT. The overall seropositivity rate was 21.1% for indirect ELISA and 46.6% for LAT. Among the latex-positive samples, 16.7% were weakly positive (+), 50% moderately positive (++), and 33.3% strongly positive (+++). The seroprevalence of CCPP was significantly higher in female goats than in males, as confirmed by both ELISA and LAT. Indirect ELISA revealed seroprevalence rates of 30.0% in females compared to 3.3% in males, while LAT results indicated a seroprevalence rate of 66.7% in females compared to 6.7% in males. The highest CCPP seroprevalence was found in the 2-3-year-old age group, with rates of 89.5% by ELISA and 92.9% by LAT. The LAT results demonstrated a sensitivity of 84.21%, a specificity of 63.38%, and an overall accuracy of 67.78%. Cohen's kappa coefficient (0.33) indicated fair agreement, while McNamara's test demonstrated a significant difference between the two tests. Based on receiver operating curve analysis, the indirect ELISA demonstrated an area under the curve of 0.83, with a suitable optical density limit of 0.15, resulting in 85% sensitivity and 70% specificity. Indirect ELISA offers greater reliability in detecting CCPP antibodies compared to LAT. The variability in LAT

results highlighted the need for ELISA, revealing higher seropositivity in older females, a distinct epidemiological feature of the population.

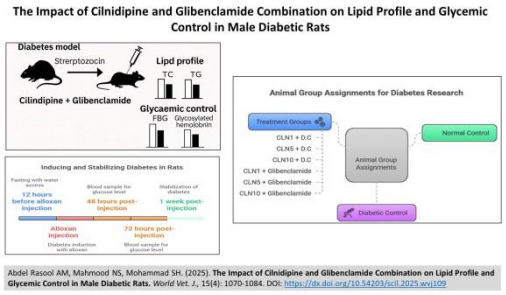
Keywords: Contagious caprine pleuropneumonia, Goat, Mycoplasma infection, Serodiagnosis

[Full text-PDF] [Crossref Metadata] [Scopus] [Export from ePrint]

Research Paper

Impacts of Cilnidipine and Glibenclamide Combination on Lipid Profile and Glycemic Control in Male Diabetic Rats

Abdel Rasool AM, Mahmood NS, and Mohammad SH.
World Vet. J. 15(4): 1070-1084, 2025; pii:S232245682500109-15
DOI: https://dx.doi.org/10.54203/scil.2025.wvj109



Abdel Rasool AM, Mahmood NS, Mohammad SH. (2025). **The Impact of Cilnidipine and Glibenclamide Combination on Lipid Profile and Glycemic Control in Male Diabetic Rats.** *World Vet. J.*, 15(4): 1070-1084. DOI: https://dx.doi.org/10.54203/scil.2025.wvj109

ABSTRACT: Current diabetes therapies frequently do not succeed in achieving target levels for hyperglycemia and dyslipidemia in a considerable number of patients. Glibenclamide is an oral hypoglycemic agent, whereas cilnidipine is a calcium channel blocker, which has been utilized for its additional metabolic benefits beyond its primary effect on blood pressure control. The presented study aimed to evaluate the synergistic effects of cilnidipine and glibenclamide on glycemic response, insulin sensitivity, and lipid profile in alloxan-induced diabetic rats. Forty-eight male rats were allocated into eight groups, each with six rats, including a normal control, a diabetic control, and six diabetic groups. Three groups were treated with oral cilnidipine alone at 1, 5, and 10 mg/kg, respectively, while the other three groups were treated with a combination of cilnidipine and glibenclamide at 2.5 mg/kg, orally. Diabetes was induced through the use of alloxan at a dosage of 100 mg/kg, intraperitoneally. Successful induction of diabetes was confirmed by an increase in blood glucose level over 200 mg/dl. Serum insulin, HOMA-IR, C-peptide, fasting plasma glucose (FPG), and the lipid markers were measured at the end of the treatment on day 28. In assessing the medicines' interactions, the combination index (CI) method was used. The present results indicated that a significant effect was observed with 10 mg/kg of cilnidipine combined with glibenclamide, which lowered glucose levels to 80.10 ± 5.80 mg/dL, increased insulin levels to 13 ± 0.64 mU/L, and raised C-peptide levels to 1.40 ± 0.09 ng/mL, while normalizing HOMA-IR to 2.56 ± 0.45, compared to the diabetic control group. The value of CI indicating a significant synergy was below 1 for FPG, insulin, and C-peptide. However, the combined medication therapy had an opposing effect (CI > 1) on all lipid parameters, including total, low- and high-density cholesterol, and triglycerides. Although it may be beneficial in enhancing glucose metabolism, it is insufficient to resolve the issues associated with diabetic dyslipidemia and should be considered as a part of a mixed treatment regime.
Keywords: Cilnidipine, Insulin sensitivity, Glibenclamide, HOMA-IR, Lipid profile

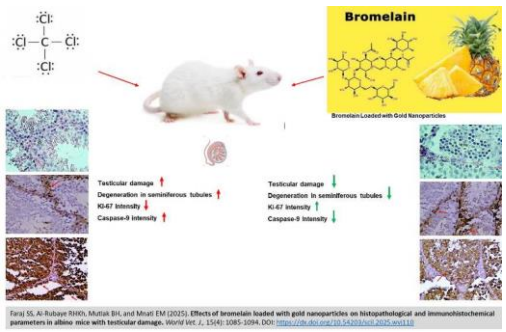
[Full text-PDF] [Crossref Metadata] [Scopus] [Export from ePrint]

Research Paper

Effects of Bromelain Loaded with Gold Nanoparticles on Histopathological and Immunohistochemical Parameters in Albino Mice with Testicular Damage

Faraj SS, Al-Rubaye RHKh, Mutlak BH, and Mnati EM.
World Vet. J. 15(4): 1085-1094, 2025; pii:S232245682500110-15

DOI: https://dx.doi.org/10.54203/scil.2025.wvj110



Faraj SS, Al-Rubaye RHKh, Mutlak BH, and Mnati EM (2025). **Effects of bromelain loaded with gold nanoparticles on histopathological and immunohistochemical parameters in albino mice with testicular damage.** *World Vet. J.*, 15(4): 1085-1094. DOI: https://dx.doi.org/10.54203/scil.2025.wvj110

ABSTRACT: Carbon tetrachloride (CCl4) has been demonstrated to induce testicular damage via oxidative stress. Bromelain (Br), a proteolytic enzyme known for its biological activities and pharmacological properties, exhibits limited absorption owing to its low solubility and bioavailability. The present study aimed to investigate the histological and immunohistochemical effects of bromelain conjugated with gold nanoparticles (AuNPs) on the testis histology of albino mice treated with CCl4. Thirty-five male albino mice (*Mus musculus*), with an average age of 9 weeks, were randomly divided into five groups, each containing seven mice. The experiment was prolonged for four weeks. The first group (G1) was the control group, the second group (G2) received weekly sub-peritoneal injections of CCl4 until the end of the experiment, and the third group (G3) received an oral dose of Au-NPs solution. The fourth group (G4) received injections of CCl4; one hour later, the mice were given an oral dose of 300 mg/kg bromelain. The fifth group (G5) received an injection of CCl4; subsequently, the mice received the same oral dosage of 300 mg/kg Au-NPs-bromelain after 60 minutes. The mice's testes were sampled to evaluate histopathological alterations and immunohistochemical markers, particularly Ki-67 and caspase-9. The present results indicated that mice treated with

CCl4 displayed a range of histological alterations, including testicular damage, degeneration in seminiferous tubules, vacuolation, and loss of germ cells. Furthermore, the immunohistochemistry study demonstrated that Ki-67 intensity decreased while caspase-9 intensity increased in groups G2 and G4 compared to the control group. Bromelain loaded with gold nanoparticles at a dosage of 300 mg/kg exhibited a notable reduction in the harmful effects of CCl4 on the testicular tissue of mice by restoring the histological structure, enhancing the Ki-67 proliferation protein, and suppressing the apoptotic cascade protein indicated by caspase 9.
Keywords: Bromelain, Carbon tetrachloride, Caspase, Gold nanoparticle

[Full text-PDF] [Crossref Metadata] [Scopus] [Export from ePrint]

Short Communication

Effects of Bitter Melon (*Momordica charantia*) Extract on Glucose Transporters 2 and 4 Levels in Streptozotocin-induced Hyperglycaemic Rats

Putri D, Utama IH, Suatha IK, Suartini IGAA, Suharsono H, Astawa INM, Kendran AAS, and Suarsana IN.
World Vet. J. 15(4): 1095-1100, 2025; pii:S232245682500111-15
DOI: https://dx.doi.org/10.54203/scil.2025.wvj111



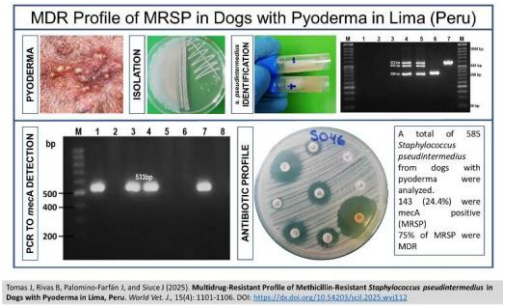
ABSTRACT: Glucose transporters (GLUTs) are essential for regulating glucose metabolism, with GLUT2 and GLUT4 serving as the primary transporters in muscle cells. In diabetic conditions, oxidative stress caused by free radicals damages glucose uptake into cells. Bioactive compounds in bitter melon, including triterpenoids, charantin, and conjugated linoleic acid, have been shown to have hypoglycaemic effects. Therefore, the present study aimed to evaluate the effect of bitter melon extract (*Momordica charantia*) on blood glucose, GLUT2, and GLUT4 in streptozotocin-induced hyperglycemic rats. The present study involved 15 male Wistar rats (white strain), 2 months old, with an average body weight of 130 grams. Diabetes was induced by administering streptozotocin at a dose of 60 mg/kg body weight. The animals were divided into three treatment groups, including the diabetic control group (P0), the diabetic group treated with 50% weight/volume (w/v) bitter melon extract (P1), and the diabetic group treated with 100% (w/v) bitter melon extract (P2). The extract was given orally at a dosage of 1 ml per rat for 14 days. Blood glucose concentrations were determined using a glucometer, whereas serum GLUT2 and GLUT4 levels were quantified with an ELISA kit. The results indicated that treatment P2 significantly lowered blood glucose levels compared to the diabetic control group, decreasing from 414.60 mg/dL (P0) to 223.60 mg/dL (P2). Serum GLUT2 concentrations declined from 21.51 (P0) to 16.50 (P2), and GLUT4 levels decreased from 19.94 (P0) to 17.60 (P2). These changes suggested an adaptive response intended to restore glucose homeostasis. Based on the present results, 100% w/v bitter melon extract concentration demonstrated a significant reduction in blood glucose, GLUT2, and GLUT4 levels in the serum of streptozotocin-induced diabetic rats.
Keywords: Bitter melon, Diabetes mellitus, Hyperglycemia, Glucose transporter

[Full text-PDF] [Crossref Metadata] [Scopus] [Export from ePrint]

Short Communication

Multidrug-Resistant Profile of Methicillin-Resistant *Staphylococcus pseudintermedius* in Dogs with Pyoderma in Lima, Peru

Tomas J, Rivas B, Palomino-Farfán J, and Siuce J.
World Vet. J. 15(4): 1101-1106, 2025; pii:S232245682500112-15
DOI: https://dx.doi.org/10.54203/scil.2025.wvj112



ABSTRACT: Methicillin resistance is a major global health concern, and recently, methicillin-resistant *Staphylococcus pseudintermedius* (MRSP) has emerged as a significant issue in veterinary medicine, with the potential to spread to humans. The present study aimed to analyze *Staphylococcus pseudintermedius* (*S. pseudintermedius*) strains isolated from 585 canine pyoderma samples from 2016 to 2024 at the Faculty of Veterinary Medicine, National University of San Marcos, Peru. The *mec*A gene was detected by conventional polymerase chain reaction, and antimicrobial susceptibility test included seven antibiotic families, including tetracyclines, sulfonamides, aminoglycosides, second-generation cephalosporins, penicillins, fluoroquinolones, and lincosamides. Out of 585 samples, 143 (24.4%) were positive for the *mecA* gene, confirming the presence of MRSP. Among these strains, 107 (74.8%) were multidrug resistant (MDR), and 119 (83.2%) exhibited phenotypic oxacillin resistance. The highest resistance rates of the *S. pseudintermedius* carrying the *mec*A gene were observed for lincosamides (86.0%), cephalosporins (78.3%), and sulfonamides (76.9%), whereas resistance to amoxicillin-clavulanate was the lowest (6.3%). In addition, two isolates were resistant to all the antibiotic

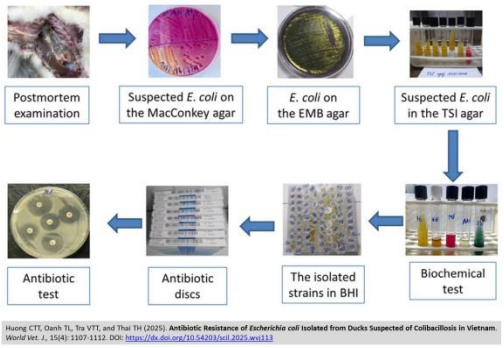
families evaluated. These findings underscored the increasing prevalence of MRSP and MDR *S. pseudintermedius*, highlighting the need for improved antibiotic protocols in veterinary medicine to mitigate resistance and ensure effective treatment strategies for canine pyoderma.
Keywords: Dog, Methicillin, Resistance, *Staphylococcus pseudintermedius*

[Full text-PDF] [Crossref Metadata] [Scopus] [Export from ePrint]

Short Communication

Antibiotic Resistance of Escherichia coli Isolated from Ducks Suspected of Colibacillosis in Vietnam

Huong CTT, Oanh TL, Tra VTT, and Thai TH.
World Vet. J. 15(4): 1107-1112, 2025; pii:S232245682500113-15
DOI: https://dx.doi.org/10.54203/scil.2025.wvj113



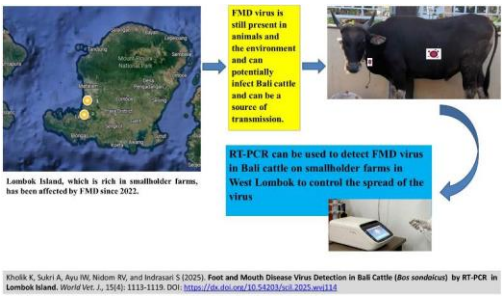
ABSTRACT: The extensive application of antibiotics within the livestock sector has led to a rise in bacterial resistance, especially against *Escherichia coli* (*E. coli*), complicating the treatment of bacterial infections in poultry. The present study aimed to determine the antibiotic resistance of the *E. coli* isolated from Cherry Valley ducks exhibiting signs of colibacillosis in northern Vietnam. From March to May 2025, 21 Cherry Valley duck flocks raised on 15 duck farms in Ha Nam Province, Vietnam, experienced disease outbreaks characterized by clinical signs such as anorexia, reduced mobility, abnormal movement, and respiratory distress, including sneezing, gasping, and nasal discharge, which were suspected of being caused by *E. coli* infection. A total of 63 ducks suspected of colibacillosis were necropsied for sampling and pathological observation. Heart, liver, and lung samples were collected simultaneously from all ducks for *E. coli* isolation. The isolated *E. coli* strains were examined for antibiotic susceptibility by the agar diffusion method. The *E. coli* strains demonstrated the highest susceptibility to levofloxacin (82.9%), followed by norfloxacin (78.0%), gentamicin (73.2%), and colistin (70.7%). The highest resistance rates were observed for ampicillin (75.6%) and tetracycline (73.2%), whereas resistance to ciprofloxacin, streptomycin, and doxycycline ranged from 31.7% to 48.8%. Of the 41 *E. coli* strains, 82.9% were resistant to at least one antibiotic; these strains exhibited 17 distinct antibiotic resistance patterns. Additionally, 63.4% isolated strains were identified as multi-drug resistant (MDR). The current results emphasized the high resistance of *E. coli* strains isolated from ducks to multiple antibiotics.
Keywords: Antibiotic resistance, Duck, Colibacillosis, Diffusion method

[Full text-PDF] [Crossref Metadata] [Scopus] [Export from ePrint]

Short Communication

Foot and Mouth Disease Virus Detection in Bali Cattle (*Bos sondaicus*) by RT-PCR in Lombok Island

Kholik K, Sukri A, Ayu IW, Nidom RV, and Indrasari S.
World Vet. J. 15(4): 1113-1119, 2025; pii:S232245682500114-15
DOI: https://dx.doi.org/10.54203/scil.2025.wvj114



ABSTRACT: Aphthovirus is responsible for foot-and-mouth disease (FMD) in cloven-hoofed animals, a highly infectious disease that has significant economic repercussions in various countries, including Indonesia. The present study aimed to use reverse transcription polymerase chain reaction (RT-PCR) to detect FMD in suspected Bali cattle in West Lombok, Indonesia. The current study was an observational, descriptive investigation conducted from July to August 2025, collecting 15 swab samples from male Bali cattle with an average weight of 210 kilograms and an average age of 2 years old. The samples were collected via purposive sampling from cattle demonstrating clinical signs of FMD, specifically from oral vesicular fluid. The samples were sourced from two smallholder farms in West Lombok; farm one, with 12 samples, and farm two, with three samples. The FMD was identified with a prevalence rate of 20% (3 out of 15), and a 328 bp DNA fragment was detected during gel electrophoresis. The current result indicated that the virus pathogen was detected in 20% of samples, and RT-PCR can be used as a high-sensitivity diagnostic method for this disease.
Keywords: Bali cattle, Foot-and-Mouth disease, PCR, Reverse transcription

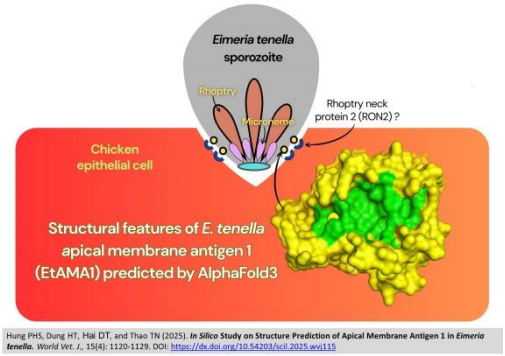
[Full text-PDF] [Crossref Metadata] [Scopus] [Export from ePrint]

Short Communication

In Silico Study on Structure Prediction of Apical Membrane Antigen 1 in *Eimeria tenella*

Hung PHS, Dung HT, Hai DT, and Thao TN.
World Vet. J. 15(4): 1120-1129, 2025; pii:S232245682500115-15

DOI: https://dx.doi.org/10.54203/scil.2025.wvj115



ABSTRACT: The micronemal apical membrane antigen 1 (AMA1) has been demonstrated to be critical for host cell invasion by apicomplexan parasites. The present study predicted the structure of *Eimeria tenella* AMA1 (EtAMA1) using AlphaFold3. The structural model ranked first by AlphaFold3 was selected for analysis after removing unreliable regions. Comparative structural analyses were performed between the resulting EtAMA1 model and the well-characterized *Plasmodium falciparum* AMA1 (PfAMA1) using PyMOL. The results indicated that domains I and II of EtAMA1 may adopt the PAN motif (a conserved structural fold consisting of a five-stranded β-sheet and an α-helix) stabilized by five disulfide bonds, similar to PfAMA1. In addition, aromatic residues within the ligand binding pocket of PfAMA1 are conserved in EtAMA1, except for the critical Y251. The Proline-rich DII loop at the corner of the conserved hydrophobic pocket in EtAMA1 is shorter than that of PfAMA1, which possibly makes the hydrophobic pocket wider. Notably, domain III of *Et*AMA1 is predicted to form a three-stranded β-sheet with no disordered loop and α-helix, which is different from *Plasmodium* AMA1 structures. The present study provided preliminary information on structural divergences of EtAMA1, based on AlphaFold3 prediction, underscoring the need for experimental validation and investigation of possible implications for the parasite invasion mechanism.
Keywords: Apical membrane antigen 1, Domain, Hydrophobic pocket, *Eimeria tenella*

[Full text-PDF] [Crossref Metadata] [Scopus] [Export from ePrint]

Review

Effects of Heat Stress on Growth Performance, Egg Production, Egg Quality, and Potential Controlling Strategies in Layer Chicken: A Review

Gobezie E, Timotiwos A, and Simeneh G.
World Vet. J. 15(4): 1130-1137, 2025; pii:S232245682500116-15

DOI: https://dx.doi.org/10.54203/scil.2025.wvj116



ABSTRACT: Egg production is a key indicator of laying hens' reproductive efficiency. High ambient temperatures cause heat stress in laying hens, which negatively impacts their health, behavior, blood chemistry, feed intake, egg production, and egg quality. The present study aimed to focus on the effects of heat stress on growth performance, egg production, egg quality, and potential controlling strategies for heat stress in layer chickens. Heat stress reduces body weight, feed efficiency, egg yield, and egg quality. Reduced feed intake is the main reason contributing to its negative impacts on production. The reduced feed intake and decreased nutrient digestibility have adverse effects on egg quality and production performance. Heat stress reduces egg production and impairs the behavior, welfare, and immunity of layer chickens, resulting in significant financial losses. Higher ambient temperatures (above 25°C) can lead to lower egg quality (soft shells or shell-less eggs), weakened skeletal integrity in hens, and fewer eggs. Poor hatchability results from reduced feed intake due to high temperatures, which adversely affects semen fertility and quality. Eggs produced under extreme heat stress had lower Haugh units, egg yolk color, and eggshell thickness and strength. Overcrowding, also known as high stocking density, adversely affects animal health by degrading their habitat and increasing competition for resources such as feed, which can ultimately lead to feather pecking and cannibalism. Due to a quicker metabolic rate, chickens produce more body heat and are more susceptible to heat stress. High stocking density and high ambient temperature increase the risk of heat stress. Reducing stocking density to prevent heat stress may limit the number of hens that can be raised in a given space. Heat stress significantly reduces egg production, egg quality, and egg weight in laying hens under hot conditions. The current findings highlighted the need for improved environmental management and methods to mitigate the harmful effects of heat stress in laying hens.
Keywords: Egg production, Egg quality, Egg weight, Heat stress, Laying chicken

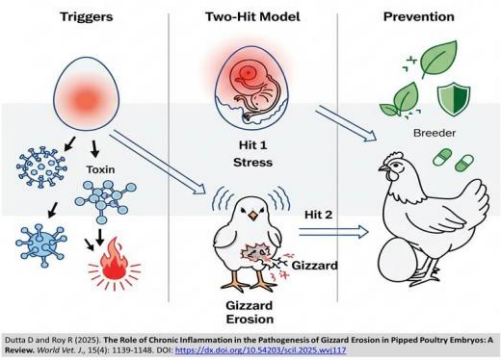
[Full text-PDF] [Crossref Metadata] [Scopus ID:] [Export from ePrint]

Review

The Role of Chronic Inflammation in the Pathogenesis of Gizzard Erosion in Pipped Poultry Embryos: A Review

Dutta D and Roy R.
World Vet. J. 15(4): 1139-1148, 2025; pii:S232245682500117-15
DOI: https://dx.doi.org/10.54203/scil.2025.wvj117

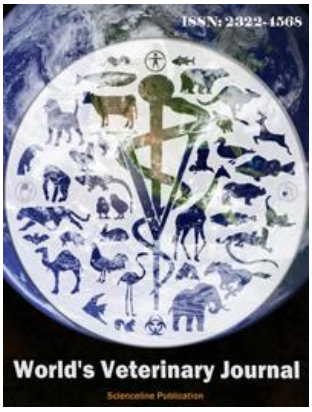
ABSTRACT: Gizzard erosion remains a recurrent issue in commercial broiler and layer embryos, leading to poor hatchability and early chick mortality, yet the mechanisms linking infectious, nutritional, and toxic factors remain poorly understood. The present review synthesized published pathological, immunological, and toxicological evidence to explore how these diverse factors may contribute to the development of gizzard erosion. A structured evaluation of experimental and field studies was performed to integrate the available findings. On the basis of this synthesis, the review proposed a two-hit inflammatory hypothesis to explain disease onset. In this hypothesis, the first hit involved chronic, low-grade inflammatory priming during embryogenesis driven by maternal mycotoxins, breeder immune stress, or vertically transmitted infections, whereas the second hit consisted of acute oxidative and metabolic stress during pipping and hatching that may precipitate visible epithelial injury in predisposed gizzards. The hypothesis is presented as a conceptual framework derived from existing literature rather than as an established mechanism, emphasizing that current evidence supports a plausible sequential inflammatory process. Understanding gizzard erosion through this exploratory framework underscores the need for preventive control of prenatal inflammatory triggers and identifies clear directions for future experimental validation at the embryonic level.
Keywords: Broiler, Chronic inflammation, Gizzard erosion, Immunology, Layer, Toxicology



[Full text-PDF] [Crossref Metadata] [Scopus] [Export from ePrint]

Previous issue| Next issue | Archive

This work is licensed under a Creative Commons Attribution 4.0 International License (CC BY 4.0).



World's Veterinary Journal

E-ISSN: 2322-4568

Frequency: Quarterly

DOI Prefix: 10.54203

Current Issue: 2025, Vol: 15, Issue: 4 (December)

Publisher: SCIENCELINE

www.wvj.science-line.com

World's Veterinary Journal (ISSN 2322-4568) is an international, English language, peer reviewed open access journal aims to publish the high quality material from veterinary scientists' studies ... View full aims and scope

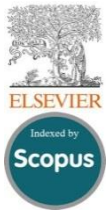
Editors-in-Chief:

Prof. Dr. Fikret Çelebi, Veterinary Physiology; Atatürk University, TURKEY;

Dr. Daryoush Babazadeh, DVM, DVSc (PhD) of Avian/Poultry Diseases, Shiraz University, Shiraz, IRAN

WVJ indexed/covered by SCOPUS (CiteScore=1.2), Embase, WoS MJL (BIOSIS), NLM Catalog, AGRIS, ScopeMed, NAAS (Score: 3.96), Ulrich's™/ProQuest, UBTIB, EBSCO, SHERPA/RoMEO, Genamic, INFOBASE ...full index information





- Open access full-text articles is available beginning with Volume 1, Issue 1.
- Digital Archiving: Journal Repository (eprints)
- Full texts and XML articles are available in Crossref and AGRIS.
- High visibility of articles over the Internet through Gold Open Access.
- This journal is in full compliance with Budapest Open Access Initiative and International Committee of Medical Journal Editors' Recommendations (ICMJE).
- This journal encourage the academic institutions in low-income countries to publish high quality scientific results, free of charges... view Review/Decisions/Processing/Policy
- Publisher Item Identifier ...details

Scienceline Publication, Ltd.
Editorial Office:
Ömer Nasuhi Bilmen Road, Dönmez Apart., G Block, No:1/6, Yakutiye, Erzurum/25100, Turkey
Homepage: www.science-line.com
Email: administrator@science-line.com
Phone: +90 538-7708824 (Turkey)

2025, Scienceline Publication
World's Veterinary Journal
World Vet J, 15(4): 831-844.
ISSN 2322-4568

DOI: https://dx.doi.org/10.54203/scil.2025.wvj85
PII: S232245682500085-15

Immunohistochemical distribution of HGF, IGF-I, FGF-2, and TGF-α in kidney and liver tissues of geese (*Anser anser*) during hatching and post-hatching periods

Dilem Gülece Ermutlu* and Şahin Aslan

Department of Histology and Embryology, Faculty of Veterinary Medicine, Kafkas University, Kars, Türkey

*Corresponding author's Email: dilemermutlu@gmail.com

ORIGINAL ARTICLE
Received: September 27, 2025
Revised: October 26, 2025
Accepted: November 27, 2025
Published: December 25, 2025

ABSTRACT

Immunohistochemical studies during embryonic development of poultry are quite limited. The present study aimed to investigate the distribution of Hepatocyte growth factor (HGF), insulin-like growth factor-I (IGF-I), fibroblast growth factor-2 (FGF-2), and transforming growth factor-α (TGF-α) in the kidney and liver tissues of hatching and post-hatching geese via histologic and immunohistochemical methods. A total of 150 fertile goose eggs were used in the study. Throughout the incubation process (29 days), four eggs were used each day, starting from the sixth day, and the embryos were examined. The embryos were fixed in 10% formaldehyde solution. Geese at the 7, 15, 30, and 210 (adult) days after hatching were euthanized for a post-hatching evaluation. Routine histological procedures were performed on the kidney and liver tissues. For histological examinations were used Crossmonn's triple staining, Periodic Acid-Schiff (PAS), and Haematoxylin and Eosin (H&E) staining. HGF, IGF-I, FGF-2, and TGF-α immunoreactivities were investigated in the histological slides. An examination of kidney tissue development indicated that metanephric blastema formation started on day 10. The mesonephros was replaced by the metanephros, the permanent kidney, starting on the day 25. An examination of liver tissue development revealed that sinusoids began to narrow, hepatic plaques formed, and endothelial and Kupffer cells became distinguished as early as day 8. Upon general evaluation, FGF-2 was found to be the growth factor with the most intense immunoreactivity in the liver and kidney, while IGF-I had the least immunoreactivity. There is a paucity of studies on growth factors during the embryonic period in poultry. In the present study, all four growth factors were immunohistochemically investigated in the kidney and liver during the hatching and post-hatching periods. Because poultry have a shorter embryonic period than mammals, they need to utilize growth factors effectively and at high levels. The present study demonstrated that HGF, IGF-I, FGF-2, and TGF-α growth factors were effective in kidney and liver development during the incubation period in geese.

Keywords: Embryo, Goose, Growth factors, Kidney, Liver

INTRODUCTION

Similar to mammals, poultry kidneys are the main excretory organs that play an important role in the process of removing waste products that can harm the body. However, they differ from the lobule structure of the mammalian kidney (Scanes and Dridi, 2021). Poultry kidneys consist of a pair of organs situated bilaterally within the os lumbosacrale (Aslan, 2018). The kidneys develop from the dorsal mesoderm in three stages, namely, pronephros, mesonephros, and metanephros (Hassa and Aştı, 1997; McGeady et al., 2006). The pronephros develops from the mesoderm and begins to differentiate on day 3 of embryonic development, where it is replaced by the mesonephros (Bolin and Burggren, 2013). Mesonephros development initiates on days 3-4, becomes functional between days 5 and 11, undergoes degeneration in chicken embryos by day 15, and is subsequently replaced by the metanephros (Neuhaus and Hollemann, 2009; Bolin and Burggren, 2013). The metanephros or permanent kidney develops from the metanephric blastema of the intermediate mesoderm (Hassa and Aştı, 1997) and initiates an active process of fluid absorption through the renal corpuscles and proximal convoluted tubules on embryonic day 12 in chickens (Bolin and Burggren, 2013).

In poultry, the liver is the largest gland in the body, located in the ventral hepatic peritoneal cavity, and consists of two or three lobes depending on the species (König et al., 2016). The liver's parenchyma has an endodermal origin, and the stroma has a mesodermal origin (McGeady et al., 2006). Following the onset of liver diverticulum formation, hematopoietic cells invade the embryonic liver, thereby establishing it as the primary hematopoietic organ (Hassa and Aştı, 1997; McGeady et al., 2006). Hematopoietic cells develop rapidly and begin to form hematoblasts and other cells of the liver (Yang et al., 2019).

To cite this paper: Ermutlu DG and Aslan Ş (2025). Immunohistochemical distribution of HGF, IGF-I, FGF-2, and TGF-α in kidney and liver tissues of geese (*Anser anser*) during hatching and post-hatching periods. *World Vet. J.*, 15(4): 831-844. DOI: https://dx.doi.org/10.54203/scil.2025.wvj85

Growth factors have different effects, including angiogenesis, chemotaxis, cell proliferation, fibroblast migration, wound healing, and collagen production, and are protein substances that affect cell activity both *in vivo* and *in vitro* (Tekinarslan et al., 2011). Insulin-like growth factors are synthesized predominantly in the liver but are also produced in many tissues, including the kidney (Le Roith, 1997; Le Roith et al., 2001). Insulin-like growth factors (IGFs) play important roles in various functions, including follicle growth and subsequent embryonic development (Choi et al., 2024). Although HGF is primarily associated with the liver, in a study in rats, HGF expression was four times greater in the kidney than in the liver (Liu, 2002). Studies on HGF in rats and mice have suggested that it plays an important role in kidney development, maintenance of normal kidney structure and function, and tubular repair (Matsumoto and Nakamura, 2001; Davies, 2001; Liu, 2002). In human embryos, FGF-2 plays an important role at various stages of embryonic development, including early liver development and stimulation of kidney tubules (Carlson, 2018).

Previous studies on rats have indicated that TGF-α serves as a potent mitogen for hepatocytes and is predominantly produced by hepatocytes undergoing DNA replication (Webber et al., 1994). Furthermore, high levels of TGF-α transcripts have been observed in certain structures, including the mesonephric tubules of the developing kidney (Derynck, 1992).

The functions of growth factors during the early and late embryonic periods attract a lot of interest in developmental biology. Although there is information about the effects of growth factors on cells in cell culture studies, immunohistochemical studies are quite limited. This study aimed to examine the development of the liver and kidney according to days during hatching and post-hatching periods and to determine the expression location of growth factors (HGF, IGF-I, FGF-2, and TGF-α) in these organs.

MATERIALS AND METHODS

Ethical approval

The required approval was obtained from the Local Ethics Committee of Kafkas University Animal Experiments (KAU-HADYEK/2021-171), Kars, Turkey, before the commencement of the study.

Materials

In the present study, eggs were collected daily from the sixth day of incubation (4 goose eggs per day) until the day 29. The kidney and liver tissues of the collected embryos were examined. On the day 29 of incubation, the geese hatched. This day (day 29) was considered day 0, and the liver and kidney tissues of the geese were examined on days 7, 15, 30, and 210 (adult stage; 4 geese per day). No specific euthanasia method was applied to geese during the incubation period. Euthanasia was performed by cervical dislocation on days 0, 7, 15, and 30. One hundred fifty fertilized goose eggs were obtained from the Kafkas University Veterinary Faculty Application and Research Farm, Kars, Türkiye. The eggs were sterilized via fumigation in a formaldehyde-potassium permanganate mixture (Tilki and Saatci, 2013) and placed in an incubator for 29 days (CIMUKA DF-103, Türkiye) within the goose unit, maintaining conditions of 37.5°C, 60% humidity, and rotation of 180° every 2 hours.

Methods

Starting from day 6 of incubation, four eggs were used each day, and the embryo was removed and fixed in 10% formaldehyde. The hatched geese were raised in cages in the goose unit. Water and feed were given *ad libitum*, lighting is 18 hours of light and 6 hours of darkness daily, temperature is 27-30°C (Tilki and Saatci, 2013). The hatching day was set to day 0. The geese at days 7, 15, 30, and 210 (adults) following hatching were euthanized on the indicated days for post-hatching evaluation, and their organs were fixed in 10% formaldehyde (Figure 1).

Tissue collection and preparation phase

Starting on day 6 of incubation, four embryos were removed daily and fixed in 10% formaldehyde. The heads of the embryos were removed, and the trunks were divided whole on days 6-10, in half crosswise on days 11-15, in thirds crosswise on days 16-20. And after day 20, the livers and kidneys were removed and embedded in paraffin. Routine histological procedures; Alcohol (70%, 80%, 90%, 96%, Absolute), Xylol (I, II, III), Xylol and paraffin and paraffin embedding) were performed on the tissues, and 5 µm thick sections were excised from these tissues.

Histochemical examination

Crossmonn's triple staining, Periodic Acid-Schiff (PAS), and Hematoxylin and Eosin (H&E) staining were performed for histological examinations. The histological slides were examined and photographed under a light microscope (Olympus BX51, Japan).

Immunohistochemical examination

The avidin-biotin-peroxidase complex technique (Hsu, 1981; Bingöl et al., 2024) was used to determine the immunohistochemical localization of HGF, IGF-I, FGF-2, and TGF-α antibodies in the kidney and liver tissues. Sections were incubated with anti-HGF (Santa-Cruz, sc-57193; 1:200), anti-IGF-I (Santa-Cruz, sc-74116; 1:25), anti-FGF-2

(Santa-Cruz, sc-74412; 1:100), and anti-TGF-α (Santa-Cruz, sc-374433; 1:100) for 12-16 hours at room temperature (20-22°C). Upon incubation, the sections were washed with phosphate-buffered saline (PBS), and the secondary antibodies (Biotinylated Goat Anti-Rabbit [Lab. Vision, 510.991.2800]) were added and maintained at room temperature for 30 minutes. Streptavidin horse-radish peroxidase was added to the sections, washed in PBS (3×5 minutes), and maintained for 30 minutes. Mayer's hematoxylin was used to stain the nuclei. Only the PBS solution was applied to the negative control group tissues (Figure 2). The preparations were examined under a light microscope (Olympus Bx51, Japan).

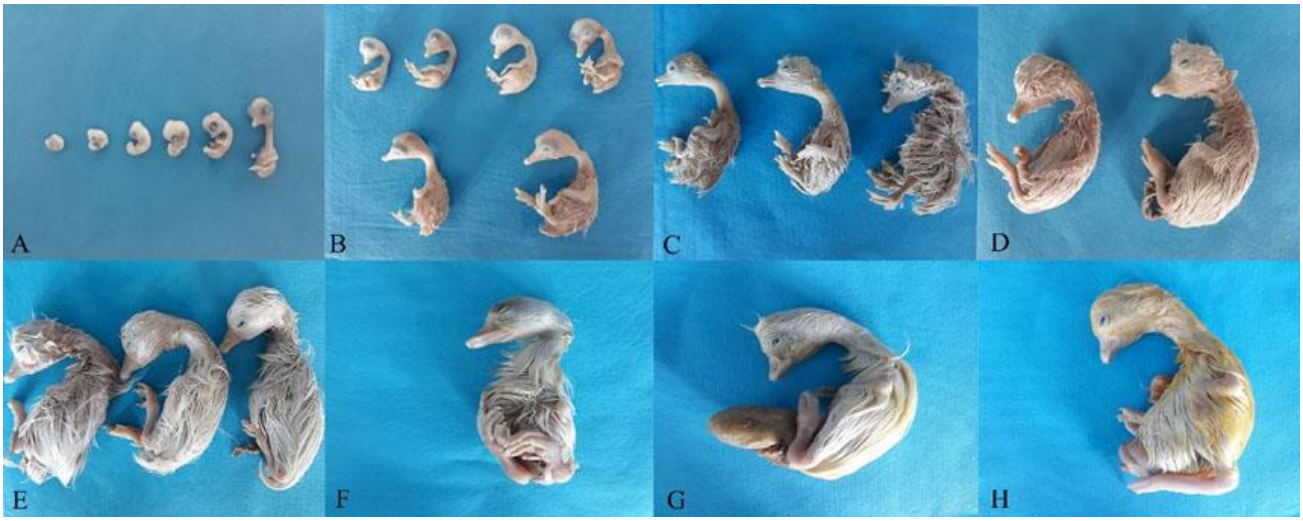


Figure 1. Geese (*Anser anser*) embryos in the hatching period (29 days). **A:** Days 6-11, **B:** Days 12-17, **C:** Days 18-20, **D:** Days 21-22, **E:** Days 23-25, **F:** Day 26, **G:** Day 27, **H:** Day 28

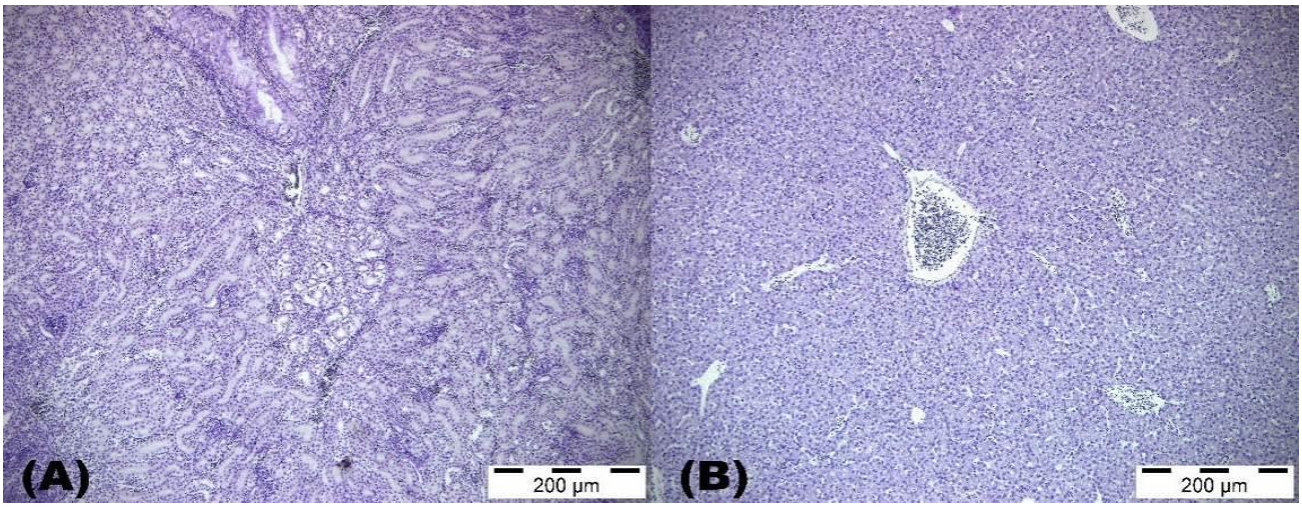


Figure 2. Negative control in kidney (**A**) and liver (**B**) tissues (Adult *Anser anser*), ×10 Avidin-biotin-peroxidase complex staining

RESULTS

Kidney

Tubule formation commenced by day 6 during the hatching period (Figure 3A). Mesonephric kidney was observed, along with the initiation of metanephric blastema formation on day 10 (Figure 3B). Degeneration of the mesonephric kidney began on days 16-17 (Figure 3C). By days 19-20, the cortex and medulla of the metanephric kidney began to differentiate (Figure 3D), with further distinction becoming more evident by day 25 (Figure 3E). In the post-hatching period, it was determined that the outer surface of the kidney is surrounded by a thin connective tissue capsule; this connective tissue sends extensions into the organ and shapes the lobules. There was a cortex and medulla in each lobe (Figure 3F). In the cortex, corpusculum renis, tubulus proximalis convoluta, tubulus distalis convoluta, perilobular ductus collectivus, and tubulus collectivus were seen (Figure 3F). In the medulla, thin and thick segments of Henle's loop, medullary ductus collectivus, and secondary branches of the ureter were seen (Figure 3G). It was determined that the corpusculum renis located in the cortex of the lobules belonged to the reptilian type nephron, and the corpusculum renis located close to the medulla belonged to the mammalian type nephron (Figure 3F, 3G, 3H). Hepatocyte growth factor (HGF) immunoreactivity was generally observed in the mesonephric tubules on hatching days 6-18, whereas in the metanephric kidney (pre-hatch and post-hatch, it was predominantly observed in the proximal tubules, with moderate expression in the ascending limb of the loop of Henle (Figure 4).

Insulin-like growth factor-I (IGF-I) immunoreactivity was generally observed in the mesonephric tubules on hatching

days 6-18, whereas it was mostly observed in the proximal tubules in the metanephric kidney (hatching and post-hatching periods (Figure 5). Fibroblast growth factor-2 (FGF-2) and transforming growth factor-α (TGF-α) immunoreactivity were generally observed in the mesonephric tubules and glomerulus on hatching days 6-18. In contrast, it was mostly observed in the proximal tubules, ascending limb of the loop of Henle, and secondary ureter sections in the metanephric kidney during hatching and post-hatching periods (Figures 6 and 7). There was no immunoreactivity associated with the four growth factors in the descending limb of the loop of Henle.

Liver

Areas formed by hematopoietic cells were observed in the liver at days 6-9 during the hatching period (Figure 8A). Hepatocytes, endothelial cells, and Kupffer cells were observed by day 6. The second lobe of the liver was more clearly distinguished from day 9 onward (Figure 8B). The radial arrangement of hepatocytes around the central vein was observed at day 10 (Figure 8C). The portal area and bile duct were observed on day 14 (Figure 8D). Fat storage started in the liver by post-hatching day 20, and this accumulation continued to decrease through post-hatching days 7 and 15 (Figure 8E, 8F).

It was determined that the histological structure of the liver was basically similar to the adult liver tissue starting from day 20 of hatching. It was observed that a thin connective tissue capsule surrounded the outer surface of the liver, and the lobule structure was not evident. In the portal area, the bile duct, hepatic artery, and interlobular vein were seen. It was determined that hepatocytes were polygonal in shape, most of them were dikaryotic, formed hepatic plaques in groups, and formed cords (Remark's cord) in groups of two, showing a radial arrangement around the central veins. It was observed that the sinusoids located between the Remark cords were covered by squamous endothelial cells, and there were Kupffer cells between these endothelial cells (Figure 5F). Additionally, in the present study, the PAS (+) reaction in hepatocytes, initially weak on day 13, became more prominent by day 15. In addition, the PAS (+) reaction was observed in Kupffer cells (Figure 9). Hepatocyte growth factor (HGF) immunoreactivity was observed in hepatocytes during the hatching and post-hatching periods, Kupffer cells on hatching days 6-14, and the bile duct by hatching day 22 (Figure 10). Insulin-like growth factor-I (IGF-I) immunoreactivity was observed in hepatocytes in the hatching and post-hatching periods, hematopoietic cells on hatching days 6-14, the bile duct, and the connective tissue in the portal area during the post-hatching period (Figure 11). Fibroblast growth factor-2 (FGF-2) and transforming growth factor-α (TGF-α) immunoreactivities were observed in hepatocytes in the hatching and post-hatching periods, hematopoietic cells on hatching days 6-14, Kupffer cells on hatching days 6-10, and connective tissue in the portal area from hatching day 22 (Figures 12 and 13).

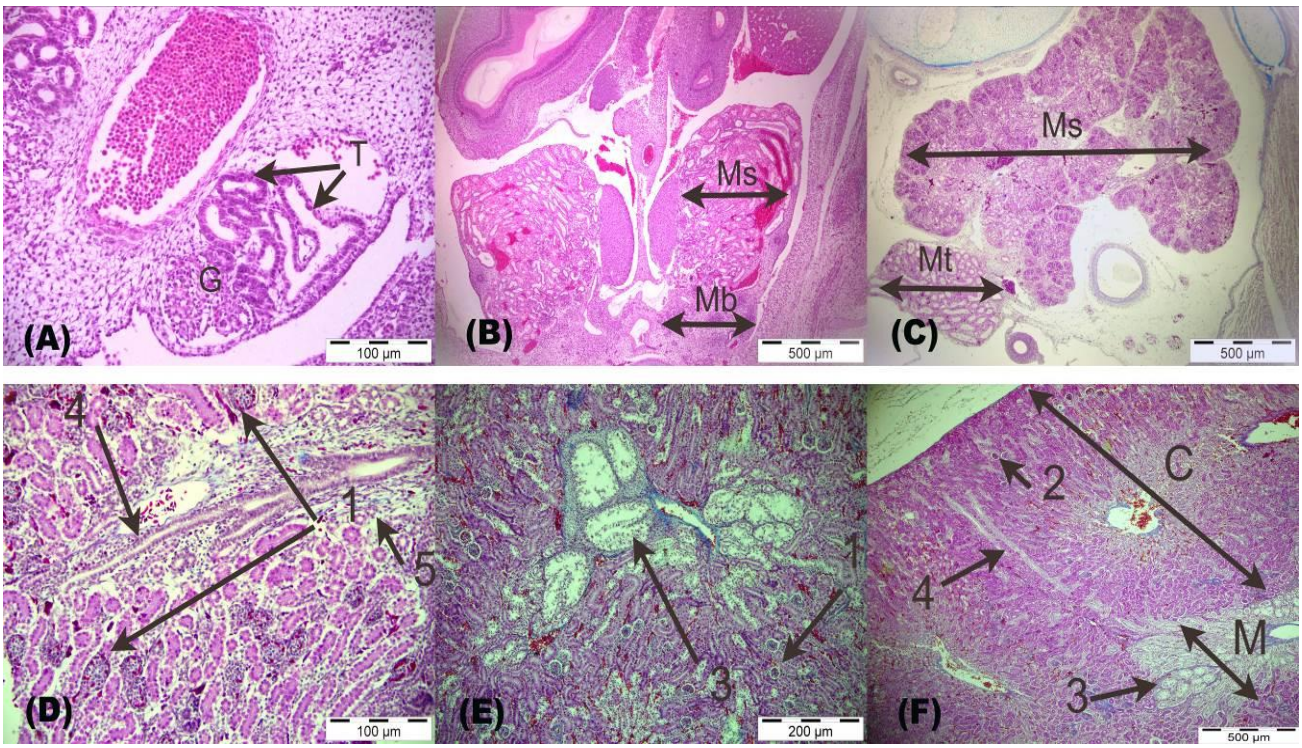


Figure 3. General view of the goose kidney in the pre-hatch (29 days) and post-hatch period. **A:** Day 6 (×20), **B:** Day 10 (×4), **C:** Day 17 (×4), **D:** Day 25 (×20), **E:** Post-hatching on day 15 (×10), **F:** Adult (×4), **G:** Glomerulus, **T:** Tubules, **Ms:** Mesonephros, **Mb:** Metanephric blastema, **Mt:** Metanephros, **M:** Medulla, **C:** Cortex, **1:** Mammalian type glomerulus, **2:** Reptilian type glomerulus, **3:** Medullary ductus collectivus, **4:** Peri-lobulary ductus collectivus, **5:** Ascending limb of loop of Henle. **A** and **B**: H&E staining, **C, D, E, F, G,** and H: Crossmonn's modified triple staining.

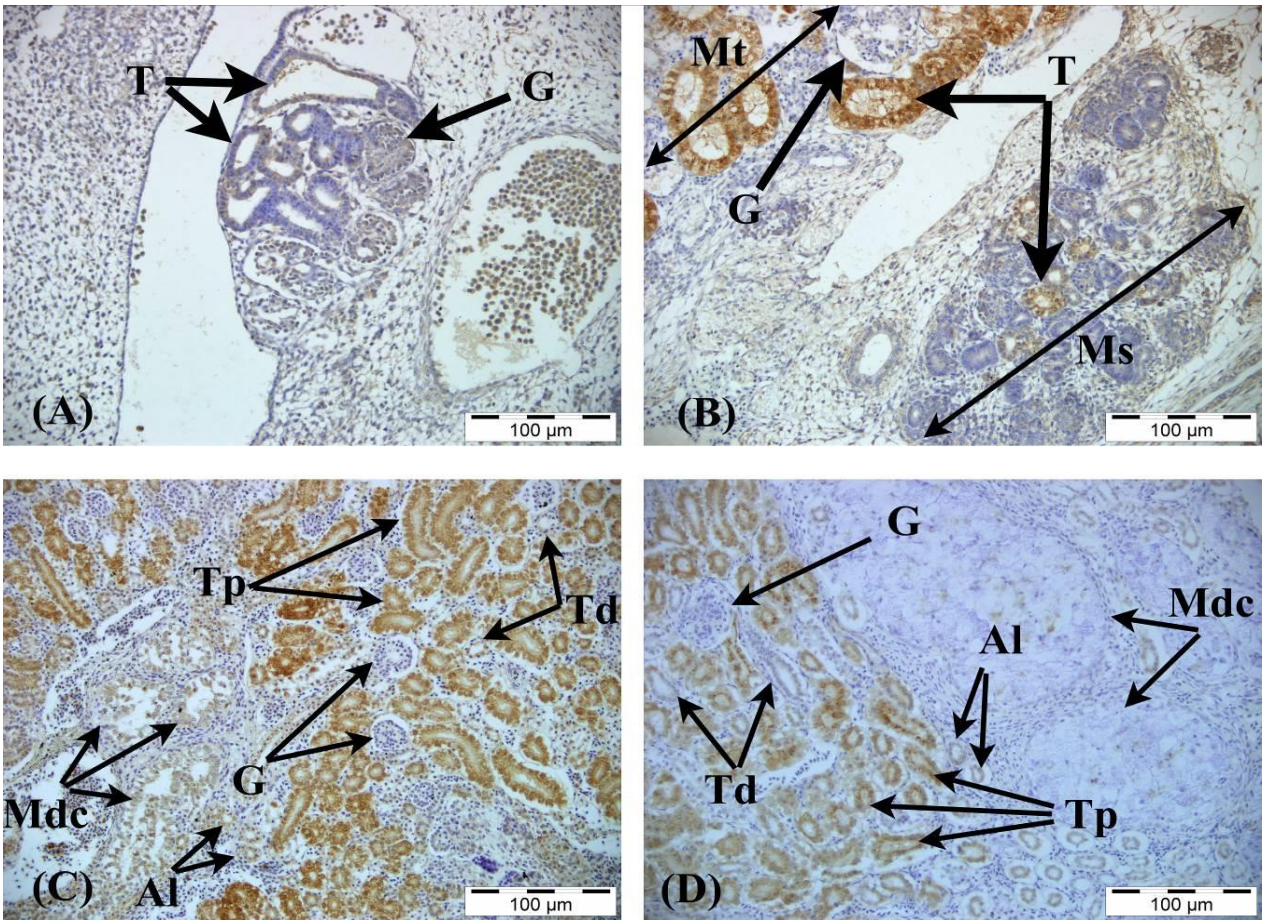


Figure 4. General view of HGF immunoreactivity in goose (*Anser anser*) kidney during incubation (29 days) and post-incubation period. **A:** Day 6, **B:** Day 14, **C:** Day 22, **D:** Adult, **G:** Glomerulus, **T:** Tubules, **Ms:** Mesonephros, **Mt:** Metanephros, **Tp:** Proximal tubules, **Td:** Distal tubules, **Al:** Ascending limb of loop of Henle. **Mdc:** Medullary ductus collectivus (×20).

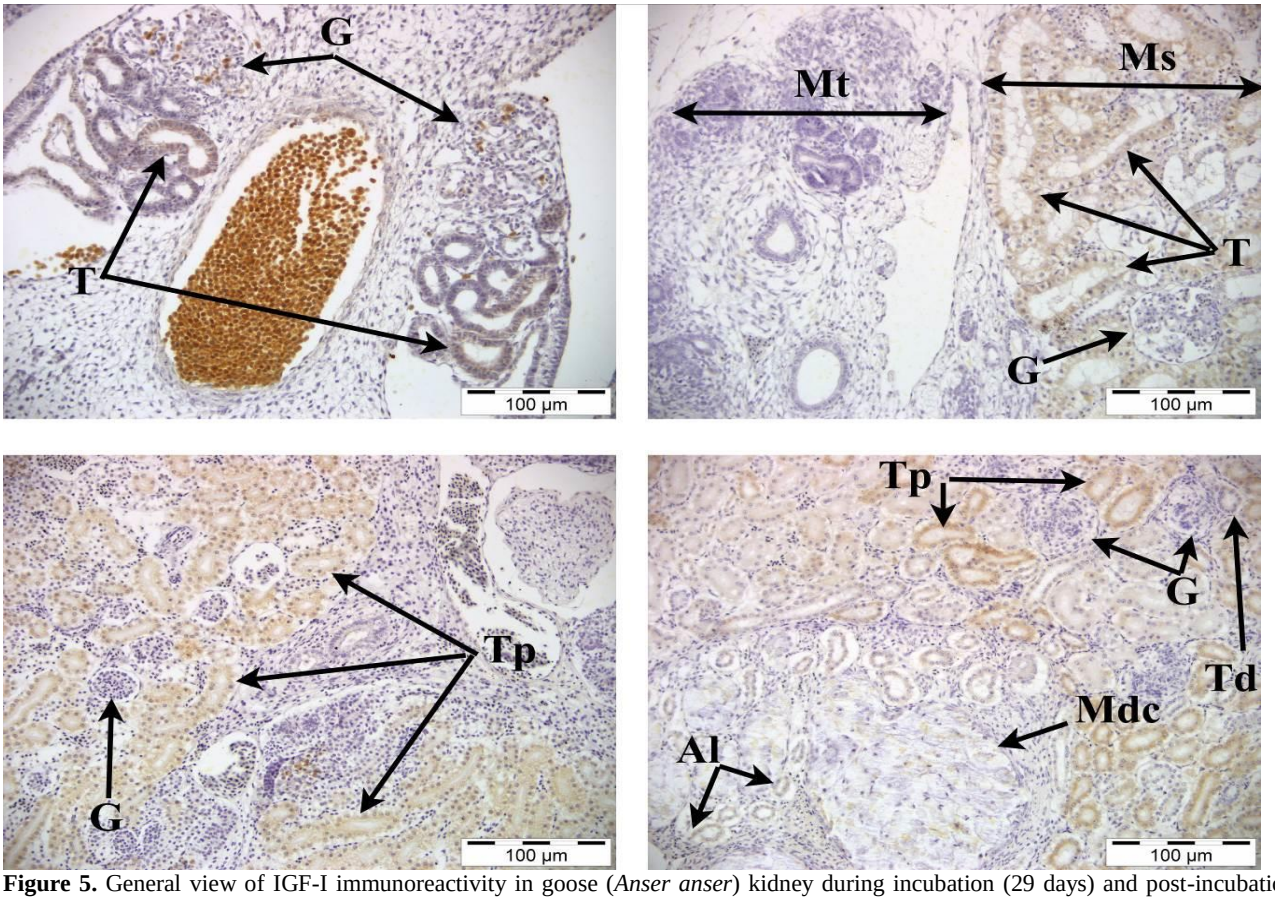


Figure 5. General view of IGF-I immunoreactivity in goose (*Anser anser*) kidney during incubation (29 days) and post-incubation period. **A:** Day 6, **B:** Day 14, **C:** Day 22, **D:** Adult, **G:** Glomerulus, **T:** Tubules, **Ms:** Mesonephros, **Mt:** Metanephros, **Tp:** Proximal tubules, **Td:** Distal tubules, **Al:** Ascending limb of loop of Henle. **Mdc:** Medullary ductus collectivus (×20).

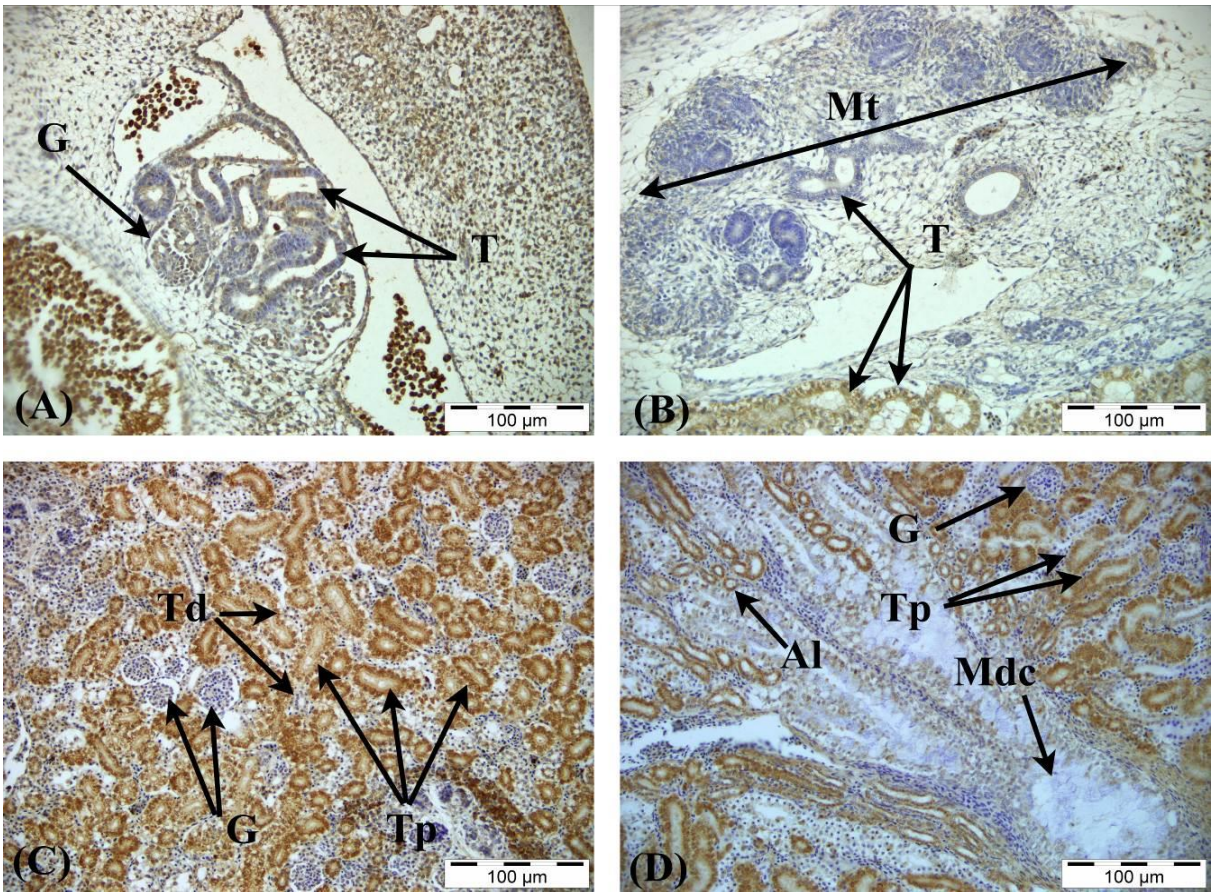


Figure 6. General view of FGF-2 immunoreactivity in goose (*Anser anser*) kidney during incubation (29 days) and post-incubation period. **A:** Day 6, **B:** Day 14, **C:** Day 22, **D:** Adult, **G:** Glomerulus, **T:** Tubules, **Mt:** Metanephros, **Tp:** Proximal tubules, **Td:** Distal tubules, **Al:** Ascending limb of loop of Henle. **Mdc:** Medullary ductus collectivus (×20).

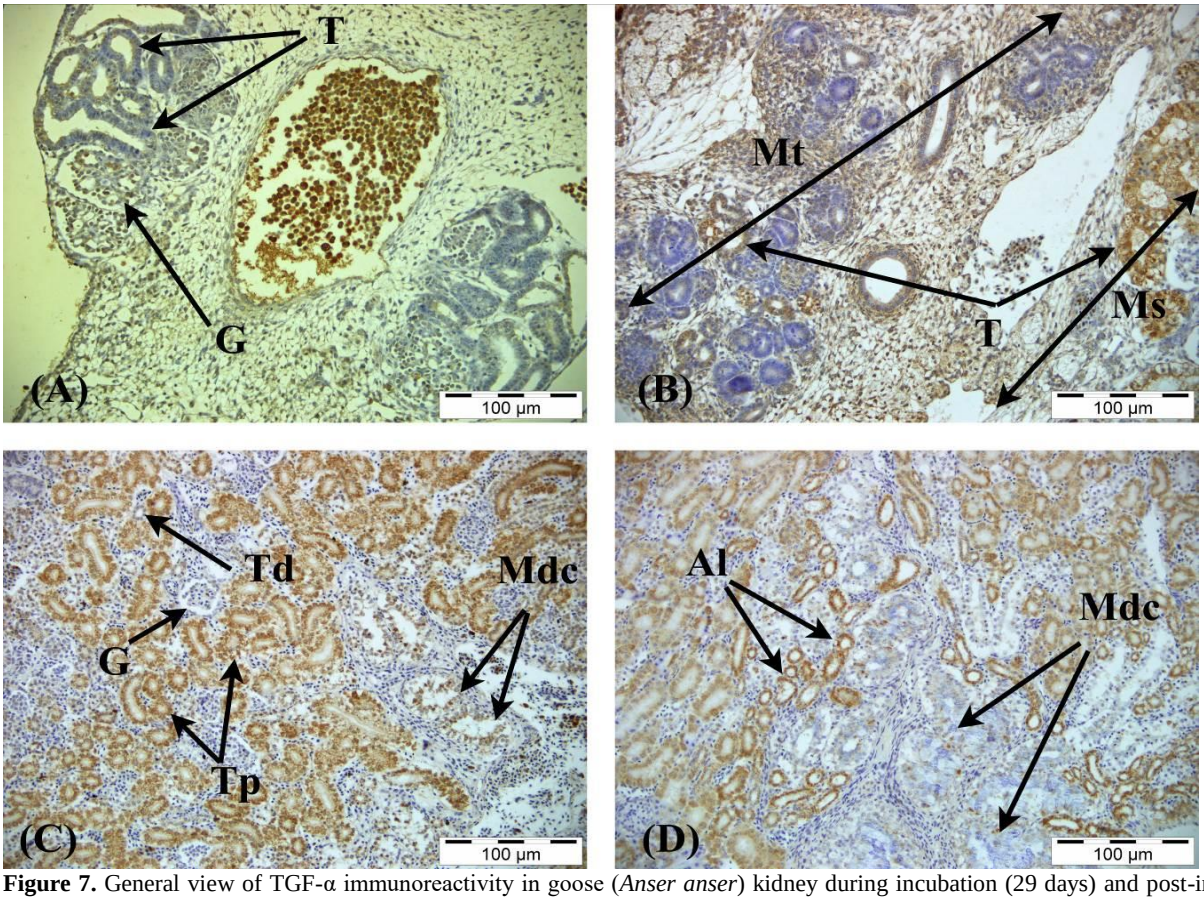


Figure 7. General view of TGF-α immunoreactivity in goose (*Anser anser*) kidney during incubation (29 days) and post-incubation period. **A:** Day 6, **B:** Day 14, **C:** Day 22, **D:** Adult, **G:** Glomerulus, **T:** Tubules, **Ms:** Mesonephros, **Mt:** Metanephros, **Tp:** Proximal tubules, **Td:** Distal tubules, **Al:** Ascending limb of loop of Henle. **Mdc:** Medullary ductus collectivus (×20).

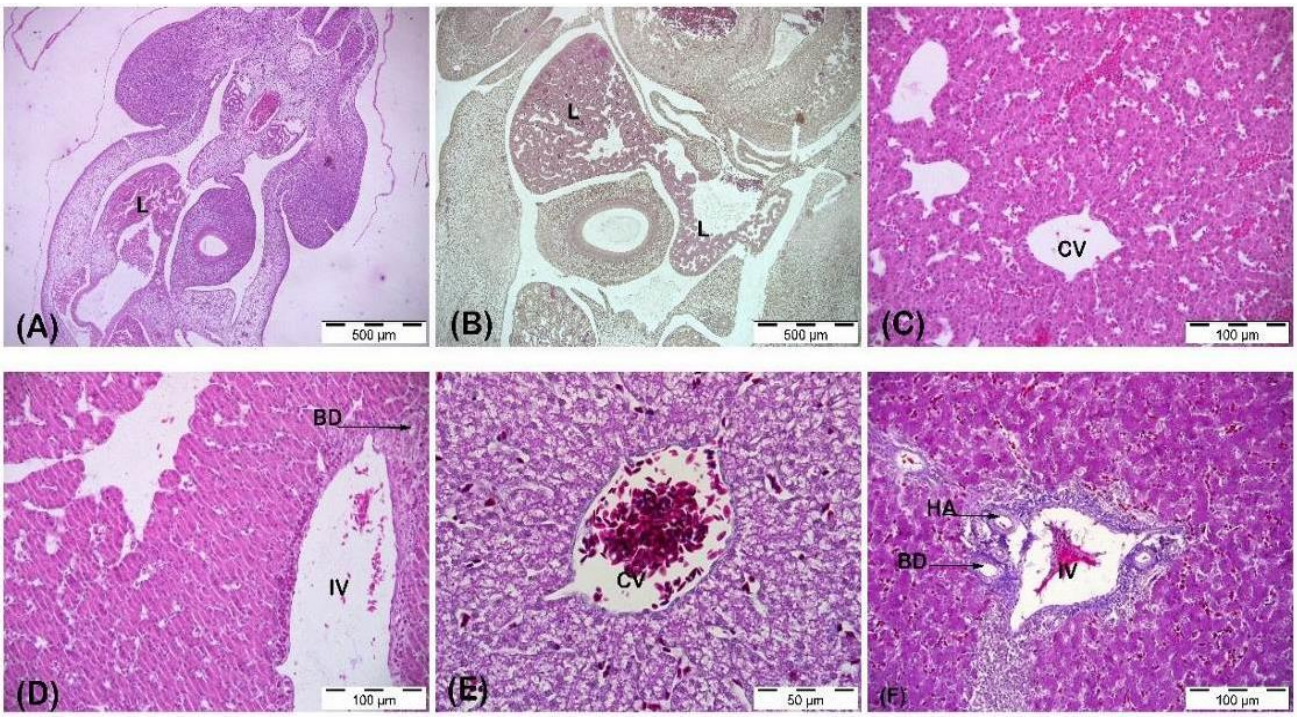


Figure 8. General view of the goose (*Anser anser*) liver in the pre-hatch (29 days) and post-hatch period. **A:** Day 6 (×4), **B:** Day 9 (×4), **C:** Day 10 (×20), **D:** Day 14 (×20), **E:** Day 23 (×40), **F:** Adult (×20). **L:** Liver, **CV:** Central vein, **IV:** Interlobular vein, **BD:** Bile duct, **HA:** Hepatic artery. **A, C,** and **D:** H&E staining, **B, E,** and **F:** Crossmonn's modified triple staining.

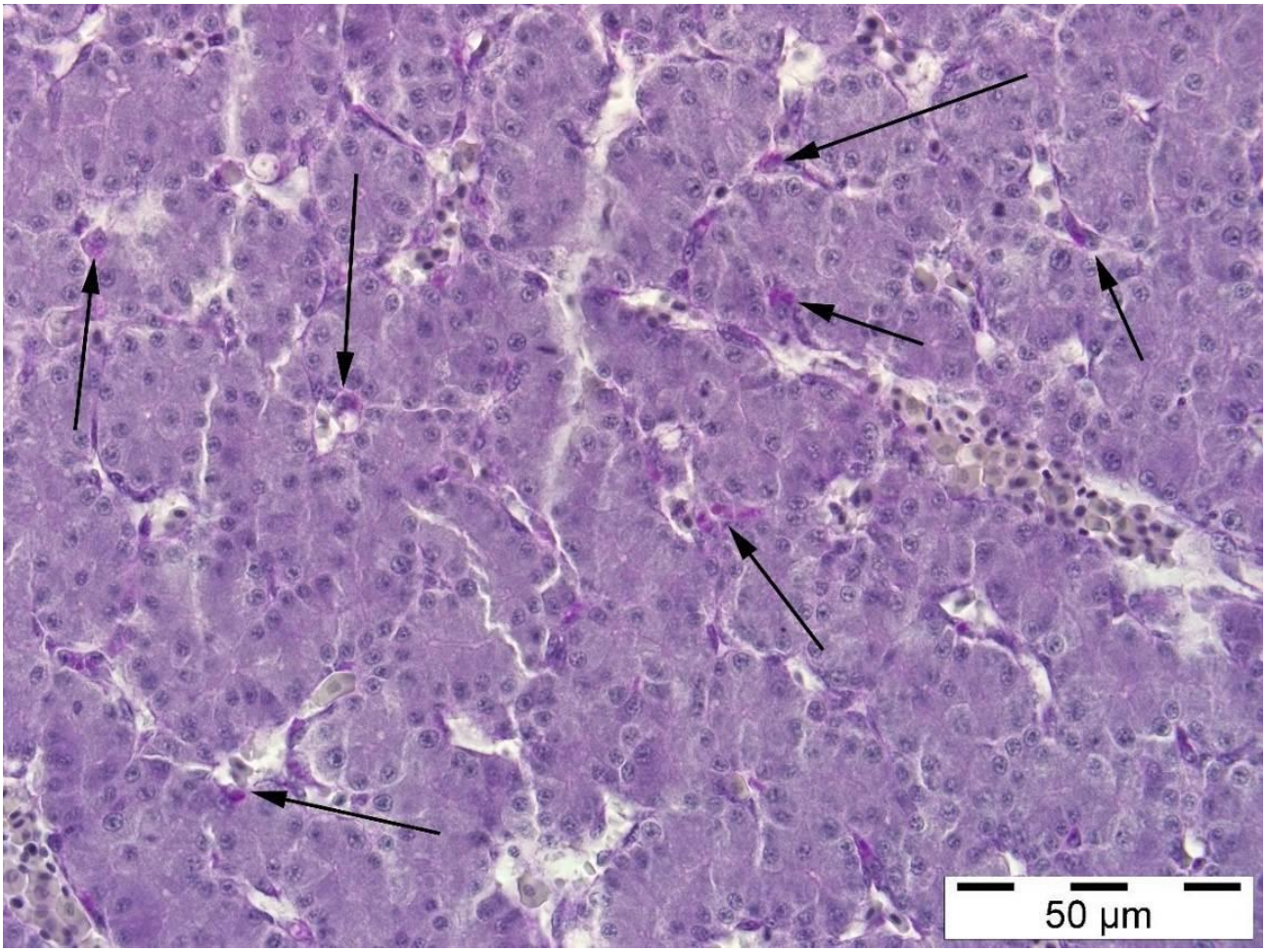


Figure 9. Periodic acid-Schiff (PAS) staining in geese (*Anser anser*), hatching day 15. Arrows: PAS (+) cells (×40).

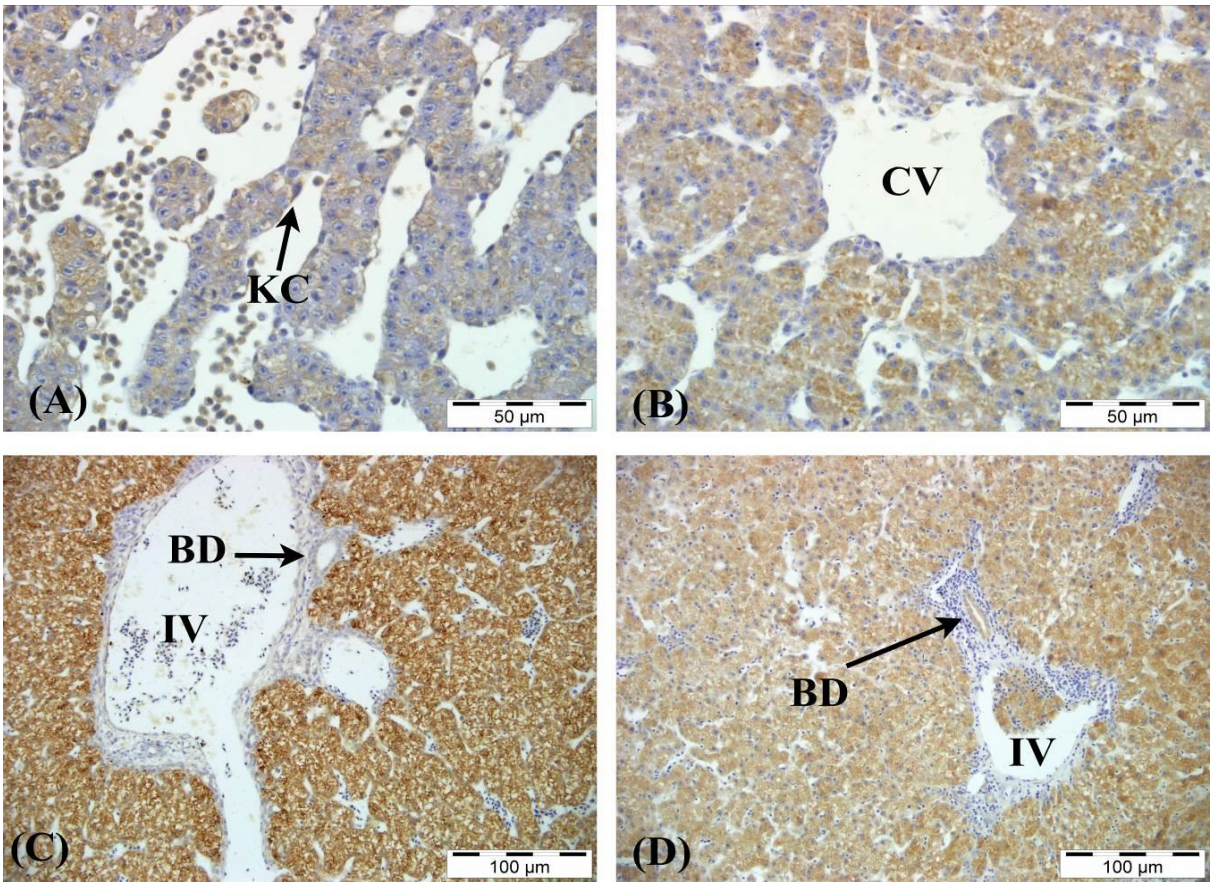


Figure 10. General view of HGF immunoreactivity in goose (*Anser anser*) liver during incubation (29 days) and post-incubation period. **A:** Day 6 (×40), **B:** Day 14 (×40), **C:** Day 22 (×20), **D:** Adult (×20), **KC:** Kupffer cells, **HC**: Hematopoietic cells, **CV:** Central vein, **IV:** Interlobular vein, **BD:** Bile duct, and **CT:** Connective tissue.

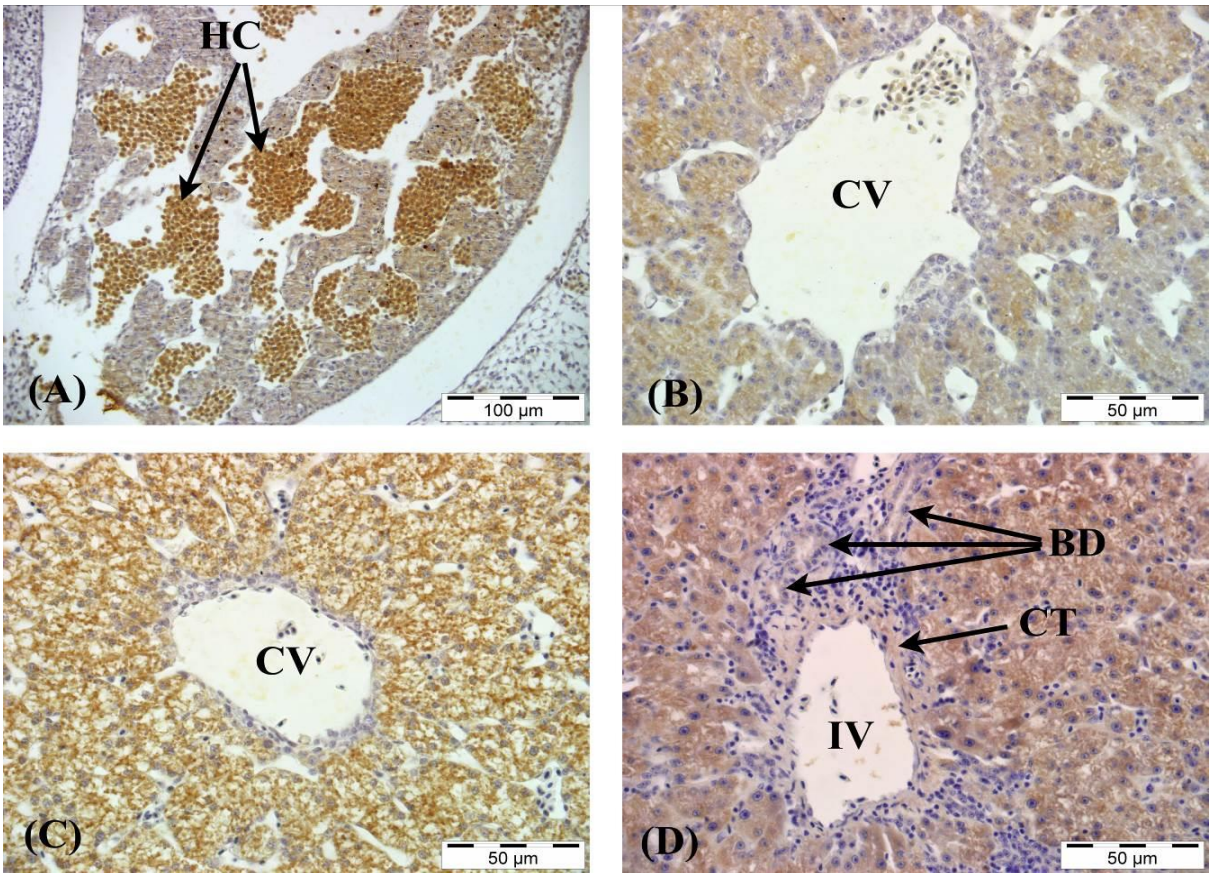


Figure 11. General view of IGF-I immunoreactivity in goose (*Anser anser*) liver during incubation (29 days) and post-incubation period. **A:** Day 6 (×20), **B:** Day 14 (×40), **C:** Day 22 (×40), **D:** Adult (×40), **KC:** Kupffer cells, **HC**: Hematopoietic cells, **CV:** Central vein, **IV:** Interlobular vein, **BD:** Bile duct, and **CT:** Connective tissue.

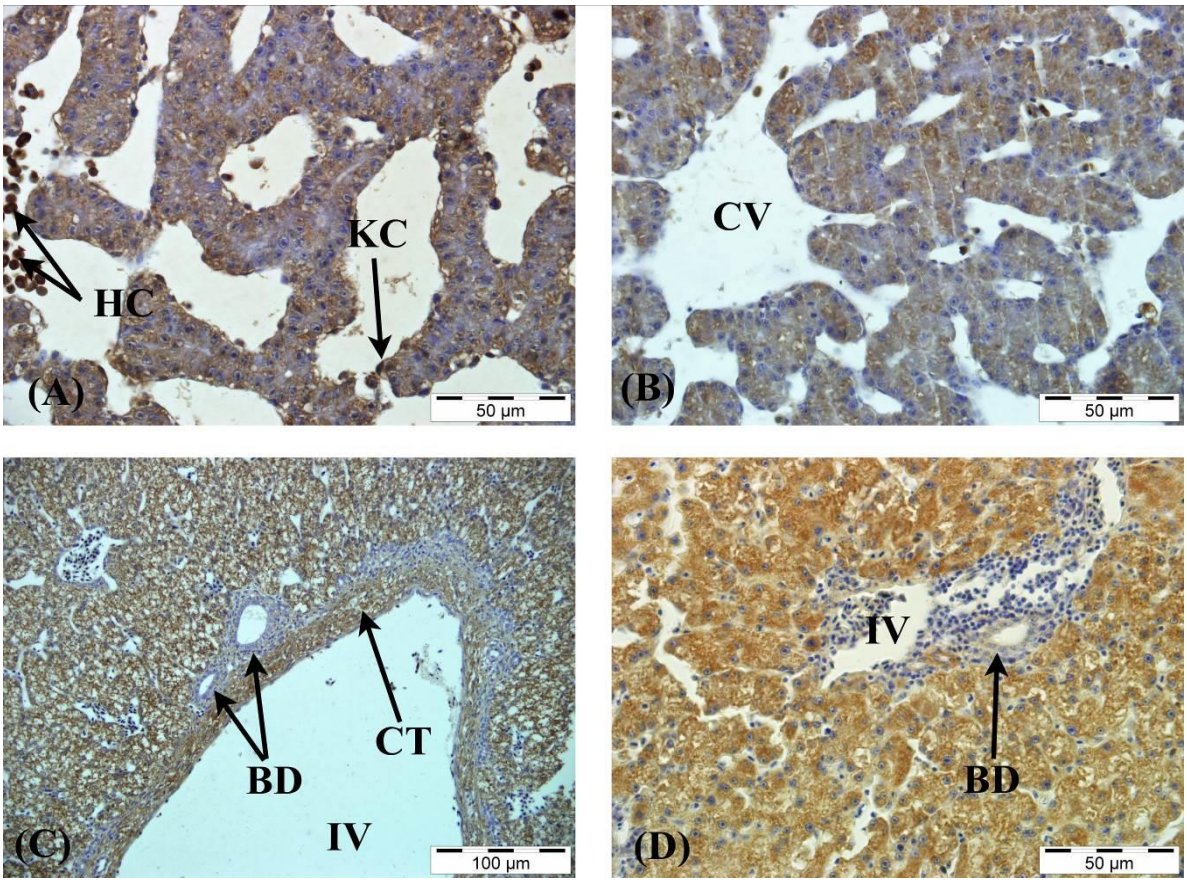


Figure 12. General view of FGF-2 immunoreactivity in goose (*Anser anser*) liver during incubation (29 days) and post-incubation period. **A:** Day 6 (×40), **B:** Day 14 (×40), **C:** Day 22 (×20), **D:** Adult (×40), **KC:** Kupffer cells, **HC**: Hematopoietic cells, **CV:** Central vein, **IV:** Interlobular vein, **BD:** Bile duct, and **CT:** Connective tissue.

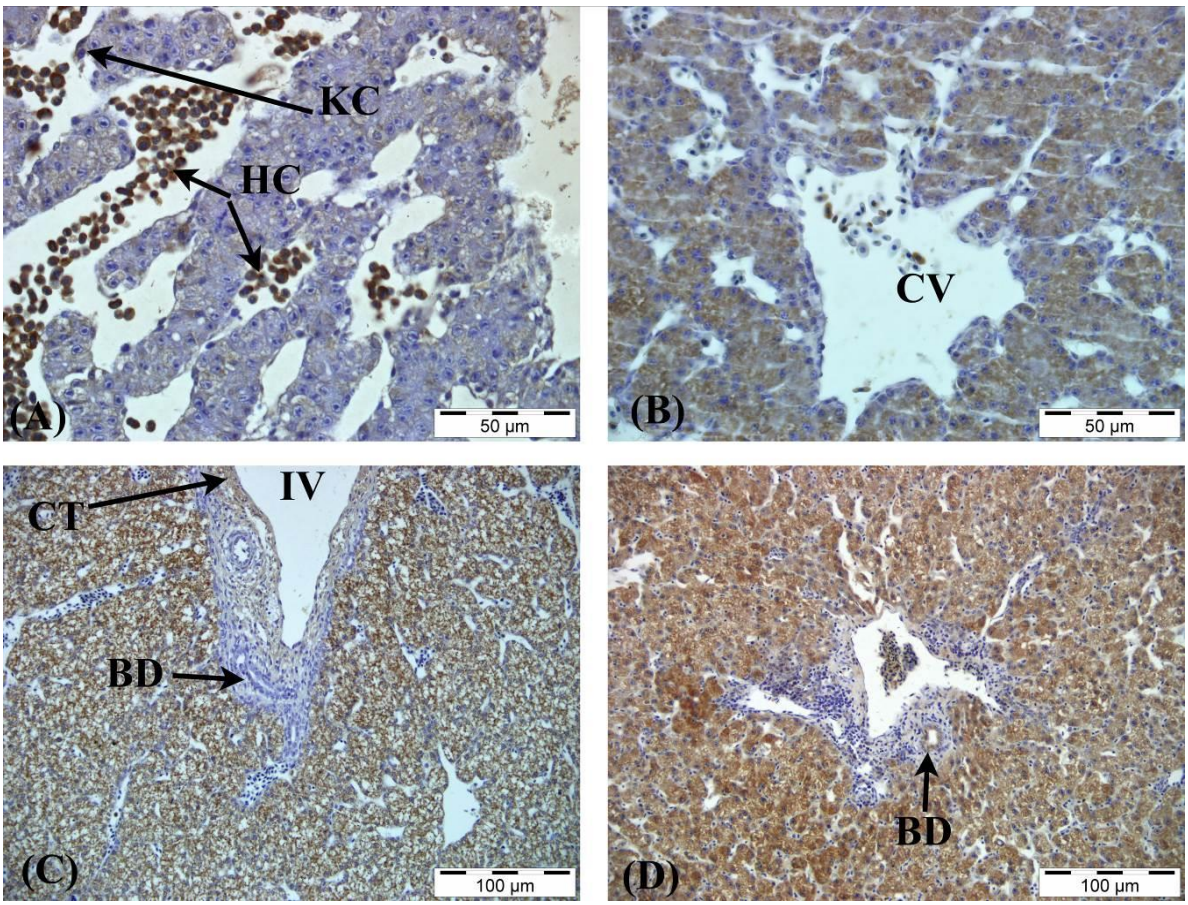


Figure 13. General view of TGF-α immunoreactivity in goose (*Anser anser*) liver during incubation (29 days) and post-incubation period. **A:** Day 6 (×40), **B:** Day 14 (×40), **C:** Day 22 (×20), **D:** Adult (×20), **KC:** Kupffer cells, **HC**: Hematopoietic cells, **CV:** Central vein, **IV:** Interlobular vein, **BD:** Bile duct, and **CT:** Connective tissue.

DISCUSSION

Kidney

The mesonephric kidney in chicken embryos morphologically formed on days 3-4, became functional on days 5-11, and degenerated into the metanephros on day 15 (Neuhaus and Hollemann, 2009; Bolin and Burggren, 2013). In the present study, the mesonephric kidney was observed on hatching day 6, and the metanephric blastema and the mesonephric kidney were formed on day 10. The general structure of the metanephric kidney began to fully form by day 14. The mesonephric kidney was observed on day 15 in chickens (Neuhaus and Hollemann, 2009; Bolin and Burggren, 2013) and on day 25 in geese. Histological studies have been conducted on the kidneys of poultry animals such as quail (Ahmad Alabdallah et al., 2021), goose (Taşçı et al., 2020), chicken, and duck (Abood et al., 2014). In these studies, cortex and medulla were identified in each lobe; corpusculum renis, proximal convoluta tubule, distal convoluta tubule, perilobular collectivus, and collectivus tubule in the cortex; thin and thick segments of Henle's loop, medullary collectivus ductus, and secondary branches of the ureter were identified in the medulla. In the present study, the histological structure of the kidney tissue of adult geese was consistent with that reported in previous studies (Abood et al., 2014; Taşçı et al., 2020; Ahmad Alabdallah et al., 2021).

HGF

Hepatocyte growth factor (HGF) immunoreactivity was reported in collecting tubules on day 17 of development in fetal rat kidneys (Defrances et al., 1992). HGF is produced in renal epithelial cells in mice kidney (Deprem et al., 2020) and plays an important role in cell growth and differentiation as well as embryogenesis (Davies, 2001; Matsumoto and Nakamura, 2001; Liu, 2002). In the present study, HGF immunoreactivity was observed in the mesonephric kidney tubules and the metanephric kidney; however, intense immunoreactivity was observed in the proximal tubules.

IGF-I

While serum IGF-I was detected in turkey (McMurtry et al., 1996) and chick embryos (Robcis et al., 1991), IGF-I was determined immunohistochemically in embryonic human and rat kidney (Coppola et al., 2009; Gurevich et al., 2021) and adult rat kidneys (Saltan and Aslan, 2017). IGF-I, produced in kidney tissue, plays a crucial role in bovine embryonic development, enhances cell proliferation (Makarevich and Markkula, 2002), and regulates the differentiation of germ layers in the early stages of embryogenesis as well as the organogenesis process (Mercola and Stiles, 1988). In the present study, IGF-I showed intense immunoreactivity in the hatching and post-hatching periods, especially in the proximal tubules.

FGF-2

Fibroblast growth factor-2 (FGF-2) was immunohistochemically detected in fetal (Cancilla et al., 1999) and adult rat kidneys (Floege et al., 1992). Fibroblast growth factor-2 was found to be expressed in various epithelial structures, such as the ureter, proximal tubules, and parietal epithelium of the glomerulus, in the fetal human kidney (Drummond et al., 1998). It was also suggested that FGF-2 stimulated the development of renal tubules and capillary growth in the embryonic process (Carlson, 2018), triggered the migration and proliferation of endothelial cells, and promoted the mitogenesis of smooth muscle cells and fibroblasts that induced the development of large vessels (Beenken and Mohammadi, 2009). In the present study, FGF-2 demonstrated intense immunoreactivity in the proximal tubules and ascending limb of the loop of Henle, as well as in sections of the secondary ureter.

TGF-α

Carev et al. (2008) reported that TGF-α immunoreactivity was observed in all mesonephric structures in the fetal human kidney at week 7 of gestation, but was more intense in the tubules. Intense TGF-α immunoreactivity in the proximal tubules of fetal human kidneys (Carev et al., 2008) was consistent with this study on geese. Previous studies on chick embryos (Diaz Ruiz et al., 1993) and adult chicken kidneys (Diaz Ruiz et al., 1996) reported TGF-α immunoreactivity in the distal tubules, with no observed immunoreactivity in glomeruli, proximal tubules, or the descending and ascending limbs of the loop of Henle. In the present study, TGF-α immunoreactivity was observed in all tubules and glomeruli in the mesonephric kidney. These results are consistent with the studies of Diaz Ruiz et al. (1993) and Diaz Ruiz et al. (1996) only in terms of distal tubules. Transforming growth factor-α has been reported to be present in self-renewing tissues, supporting new cell formation and development (Yetkin and Çelebi, 2001) and playing an important role in embryonic and fetal development (Burgess, 1989; Schultz et al., 1994). In the present study, intense immunoreactivity of TGF-α in renal tubules (especially in the proximal tubules and ascending limb of the loop of Henle) and in sections of the secondary ureter during the hatching and post-hatching periods suggests its crucial role in renal

development. Four growth factors examined in the hatching and post-hatching periods did not exhibit immunoreactivity in the descending limb of the loop of Henle.

Liver

Çöllü and Gürcü (2017) have indicated that the chicken liver forms in the cardio-hepatic region, with two lobes detected on hatching day 6 and the third lobe on day 7. Similar to chicks, the liver is located in the cardio-hepatic region in goose embryos. Unlike the chicken embryos, the second lobe could be distinguished on days 8-9, but the third lobe could not be observed. In the present study, the general histologic structure of the liver tissue of adult geese was similar to that reported in the Buteo buteo and Alectoris Chukar (Taşçı et al., 2018; Kara et al., 2019).

In poultry, fat synthesis is 20 times higher in hepatic tissue than in adipose tissue, unlike in mammals, leading to periodic fat accumulation in avian livers (Uni et al., 2012; Erhan and Ergün, 2018; Zaefarian et al., 2019). Consistent with previous studies, fat droplet formation in liver hepatocytes began around day 20 in the present study, peaking by days 25-28 (Uni et al., 2012; Erhan and Ergün, 2018; Zaefarian et al., 2019). In the present study, adiposity continued to decrease on post-hatching days 7, 15, and 30. In poultry, the embryo cannot obtain glucose from the maternal source and actively undergoes gluconeogenesis during developmental stages (Erhan and Ergün, 2018). As poultry store small amounts of carbohydrates in their livers, maintaining glucose concentration depends on gluconeogenesis (Erhan and Ergün, 2018). A study on partridge embryos (Hashemnia et al., 2015) reported PAS (+) reaction in hepatocytes cytoplasm on day 13 of development, whereas another study on chicken embryos (Doaa et al., 2013) reported PAS reactions beginning on day 5 and increasing by day 13. In the present study, the PAS (+) reaction in hepatocytes, initially weak on day 13, became more prominent by day 15. In addition, inconsistent with previous studies, PAS (+) reaction was observed in Kupffer cells and hepatocytes (Doaa et al., 2013; Hashemnia et al., 2015).

HGF

Iida et al. (2003) reported that HGF immunoreactivity was absent in fetal and neonatal rat livers but present in hepatocytes around the central vein during the post-hatching period. Wolf et al. (1991) reported that HGF immunoreactivity was moderate in Kupffer cells and the vascular endothelium in the rat liver, whereas there was no reaction in hepatocytes or bile ducts. It has been suggested that HGF played an important role in cell growth and differentiation as well as embryogenesis (Matsumoto and Nakamura, 2001; Davies, 2001; Liu, 2002) and that it was expressed in the liver by certain cells, including endothelial, Kupffer, and Ito cells (Yin et al., 2013; Thompson et al., 2015). In the present study, HGF immunoreactivity was observed in Kupffer cells during the initial days of the hatching period (days 6-14), in hepatocytes on all hatching and post-hatching days, and in epithelial cells of the bile duct on hatching day 22, indicating that HGF plays an important role in liver development.

IGF-I

Ralphs et al. (1990) observed similar immunohistochemical distribution of IGF in 13-day-old rat embryos and 20-28-day-old chick embryos, primarily in non-chondrogenic connective tissue, heart, smooth muscle, and peripheral and central nervous systems. Saltan and Aslan (2017) investigated IGF-I immunoreactivity in the livers of adult rats, reporting a reaction primarily in hepatocytes and the bile duct. Consistent with these findings, immunoreactivity was observed in hepatocytes and bile ducts in adult geese during the post-hatching period. IGF-I synthesis mainly occurs in the liver (Le Roith, 1997; Le Roith et al., 2001) and promotes increased mitotic activity during the post-hatching period (Owino et al., 2001). In the present study, IGF-I immunoreactivity was observed in hematopoietic cells early in the hatching period (days 6-14), hepatocytes in the hatching and post-hatching periods, and connective tissue in the portal area during the post-hatching period, highlighting its important role in liver development.

FGF-2

Gonzalez et al. (1990) examined 18-day-old rat fetuses and found lower FGF-2 immunoreactivity in the fetal liver compared with other tissues, and observed immunoreactivity only in the capsule and vessels but not in hepatocytes. It has been suggested that FGF-2 promotes liver development and stimulates capillary growth (Carlson, 2018), with FGF signaling playing an important role in liver differentiation (Zhang et al., 2004; Shin et al, 2007). In the present study, intense FGF-2 immunoreactivity was observed in liver hepatocytes during the hatching and post-hatching periods.

TGF-α

In an immunohistochemical study in adult rats, intense immunoreactivity of TGF-α was observed in the epithelium of newly formed bile ducts, with no immunoreactivity in hepatocytes (Alison et al., 1993). In the present study, different intensities of TGF-α immunoreactivity were observed in hepatocytes during hatching and post-hatching periods, whereas

no immunoreactivity was observed in the bile duct during the hatching period, contrary to the findings by Alison et al. (1993). It has been reported that TGF-α acts as a mitogen for hepatocytes and is primarily produced by hepatocytes undergoing DNA replication (Webber et al., 1994); supports new cell formation in the tissues where it is present (Yetkin and Çelebi, 2001); and directs the growth and differentiation processes of organogenesis (Mercola and Stiles, 1988). In the present study, intense TGF-α immunoreactivity was observed in liver hepatocytes during the hatching and post-hatching periods.

CONCLUSION

As a result of this study, the expressions of HGF, IGF-I, FGF-2, and TGF-α were assessed immunohistochemically in the goose kidney and liver during the hatching and post-hatching periods. Upon general evaluation, FGF-2 exhibited the most intense immunoreactivity in the liver and kidney, whereas IGF-I showed the least immunoreactivity. The concentration of the studied growth factors in the proximal tubules in the kidney and hepatocytes in the liver suggests that these organs are the main expression sites for HGF, IGF-I, FGF-2, and TGF-α. These findings highlight the significance of proximal tubules in reabsorption and the special metabolic tasks carried out by hepatocytes. It is thought that this study will contribute to the examination of the expression profiles of growth factors according to developmental periods using advanced molecular methods in embryonic development studies in various poultry species.

DECLARATIONS

Acknowledgments

The authors would like to thank Kafkas University Scientific Research Coordination Office for assistance during the study.

Authors' contributions

Şahin Aslan and Dilem Gülece Ermutlu designed the study. Dilem Gülece Ermutlu conducted the histological examination, interpretation, and preparation of the manuscript. All authors read and approved the final version of the manuscript to be published.

Conflict of interests

The authors have not declared any conflicts of interest.

Funding

This study was supported by Kafkas University, Kars, Türkiye, Scientific Research Coordination Office (Project No: 2022-TS-05).

Ethical considerations

The authors declare that this manuscript is original and is not being considered elsewhere for publication. Ethical issues, including consent to publish, misconduct, fabrication of data, and redundancy, have been checked by all authors. The authors did not use any AI applications for writing the full text of this article.

Availability of data and materials

The data that support the findings of this study are available from the corresponding author upon reasonable request.

REFERENCES

Abood DA, Reshag AF, Azhar SK, and Aziz M (2014). Comparative anatomical and histological features of the kidney in Harrier (*Circus auerоginosus*), chicken (*Gallus domesticus*) and Mallard duck (*Anas platyrhynchos*). The Iraqi Journal of Veterinary Medicine, 38(1): 107-113. DOI: https://www.doi.org/10.30539/iraqijvm.v38i1.262

Ahmad Alabdallah Z, Norezzine A, Anatolyevich Vatnikov Y, Alekseevich Nikishov A, Vladimirovich Kulikov E, Ravilievna Gurina R, Alexandrovna Krotova E, Il'yasovna Khairova N, Ivanovna Semenova V, Valerievna Magdeeva T et al. (2021). Influence of different genders of Japanese Quail on the functional state of kidneys. Archive of Razi Institute, 76(3): 667-680. DOI: https://www.doi.org/10.22092/ari.2021.355522.1694

Alison MR, Nasim MM, Anilkumar TV, and Sarraf CE (1993). Transforming growth factor-α immunoreactivity in a variety of epithelial tissues. Cell Proliferation, 26(5): 449-460. DOI: https://www.doi.org/10.1111/j.1365-2184.1993.tb00132.x

Aslan Ş (2018). Üriner sistem, In: Ş. Aslan (Editor), Kanatlı histolojisi [Poultry histology], Baskı, Dora Yayınevi, Bursa, pp. 85-99. Available at: https://dorayayincilik.com.tr/kitap-kanatli-histolojisi--439.html

Beenken A and Mohammadi M (2009). The FGF family: Biology, pathophysiology and therapy. Nature Reviews Drug Discovery, 8(3): 235-253. DOI: https://www.doi.org//10.1038/nrd2792

Bingöl SA, Deprem T, İlhan Aksu S, Koral Taşçı S, Ermutlu D, and Aslan Ş (2024). Immunohistochemical localization of leptin and ghrelin in kidney tissue of capsaicin administered diabetic and non-diabetic Rats. Kafkas University Faculty of Veterinary Medicine Journal, 30(3): 341-347. DOI: https://www.doi.org/10.9775/kvfd.2023.31202

Bolin G and Burggren WW (2013). Metanephric kidney development in the chicken embryo: Glomerular numbers, characteristics and perfusion. Comparative Biochemistry and Physiology, 166(2): 343-350. DOI: https://www.doi.org/10.1016/j.cbpa.2013.07.011

Burgess AW (1989). Epidermal growth factor and transforming growth factor α. British Medical Bulletin, 45(2): 401-424. DOI: https://www.doi.org/10.1093/oxfordjournals.bmb.a072331

Cancilla B, Ford-Perriss MD, and Bertram JF (1999). Expression and localization of fibroblast growth factors and fibroblast growth factor receptors in the developing rat kidney. Kidney International, 56(6): 2025-2039. DOI: https://www.doi.org/10.1046/j.1523-1755.1999.00781.x

Carev D, Saraga M, and Saraga-Babic M (2008). Expression of intermediate filaments, EGF and TGF-α in early human kidney development. Journal of Molecular Histology, 39(2): 227-235. DOI: https://www.doi.org/10.1007/s10735-007-9157-7

Carlson MB (2018). Human embryology and developmental biology, 6th Edition, Elsevier Health Science., USA, pp. 318-340, 358-372. Available at: https://books.google.com.tr/books?hl=tr&lr=&id=iyx6DwAAQBAJ&oi=fnd&pg=PP1&dq=human+embryology+carlson+2018&ots=ZDjAF_qX08&sig=_wLtGXaYQVFvddeFp8lC7W7LlU8&redir_esc=y#v=onepage&q=human%20embryology%20carlson%202018&f=false

Choi JW, Kim SW, Kim HS, Kang MJ, Kim SA, Han JY, Kim H, and Ku SY (2024). Effects of melatonin, GM-CSF, IGF-1, and LIF in culture media on embryonic development: Potential benefits of individualization. International Journal of Molecular Sciences, 25(2): 751. DOI: https://www.doi.org/10.3390/ijms25020751

Coppola D, Ouban A, and Gilbert-Barness E (2009). Expression of the insulin-like growth factor receptor 1 during human embryogenesis. Fetal and Pediatric Pathology, 28(2): 47-54. DOI: https://www.doi.org/10.1080/15513810802679498

Çöllü F and Gürcü B (2017). Development of embryonic chick liver and distribution of eNOS, iNOS, laminin α1. Celal Bayar University Journal of Science, 13(2): 311-318. DOI: https://www.doi.org/10.18466/cbayarfbe.305213

Davies J (2001). Intracellular and extracellular regulation of ureteric bud morphogenesis. Journal of Anatomy, 198(Pt 3): 257-264. DOI: https://www.doi.org/10.1046/j.1469-7580.2000.19830257.x

Deprem T, Aksu SI, Taşçi SK, Bingöl SA, Gülmez N, and Aslan Ş (2020). Immunohistochemical distributions of HGF and PCNA in the kidneys of diabetic and non-diabetic mice. Kafkas Üniversitesi Veteriner Fakültesi Dergisi, 26(3): 321-327. DOI: https://www.doi.org/10.9775/kvfd.2019.23002

Defrances MC, Wolf HK, Michalopoulos GK, and Zarnegar R (1992). The presence of hepatocyte growth factor in the developing rat. Development, 116(2): 387-395. DOI: https://www.doi.org/10.1242/dev.116.2.387

Derynck R (1992). The physiology of transforming growth factor-α. Advances in Cancer Research, 58: 27-52. DOI: https://www.doi.org/10.1016/s0065-230x(08)60289-420

Diaz Ruiz C, Asbert M, and Pérez-Tomás R (1996). Immunochemical study of a transforming growth factor-alpha-related protein in the chicken kidney. Kidney International, 49(4): 1053-1063. DOI: https://www.doi.org/10.1038/ki.1996.154

Diaz Ruiz C, Perez-Tomas R, Cullere X, and Domingo J (1993). Immunohistochemical localization of transforming growth factor and epidermal growth factor-receptor in the mesonephros and metanephros of the chicken. Cell and Tissue Research, 271(1): 3-8. DOI: https://www.doi.org/10.1007/BF00297536

Doaa MM, Enas AEH, Hassan AHS, and Fatma A (2013). Histogenesis of liver of Dandarawi chicken. American Journal of Life Science Research, 1(2): 47-58. Available at: https://www.semanticscholar.org/paper/Histogenesis-of-Liver-of-Dandarawi-Chicken-Doaa-Hassan/f94d9872316bd4735a21976032bee57e498a5b44

Drummond IA, Mukhopadhyay D, and Sukhatme VP (1998). Expression of fetal kidney growth factors in a kidney tumor line: role of FGF2 in kidney development. Experimental Nephrology, 6(6): 522-533. DOI: https://www.doi.org/10.1159/000020567

Erhan F and Ergün L (2018). Comparison of carbohydrate and fat metabolism in bird and mammal liver. Mehmet Akif Ersoy University Journal of Health Sciences Institute, 6(1): 33-42. DOI: https://www.doi.org/10.24998/maeusabed.356417

Floege J, Eng E, Lindner V, Alpers CE, Young BA, Reidy MA, and Johnson RJ (1992). Rat glomerular mesangial cells synthesize basic fibroblast growth factor. Release, upregulated synthesis, and mitogenicity in mesangial proliferative glomerulonephritis. The Journal of Clinical Investigation, 90(6): 2362-2369. DOI: https://www.doi.org/10.1172/JCI116126

Gonzalez AM, Buscaglia M, Ong M, and Baird A (1990). Distribution of basic fibroblast growth factor in the 18-day rat fetus: localization in the basement membranes of diverse tissues. The Journal of Cell Biology, 110(3): 753-765. DOI: https://www.doi.org/10.1083/jcb.110.3.753

Gurevich E, Segev Y, and Landau D (2021). Growth hormone and IGF1 actions in kidney development and function. Cells, 10(12): 3371. DOI: https://www.doi.org/10.3390/cells10123371

Hashemnia S, Shojaei B, and Razavi H (2015). Liver histogenesis in chukar partridge (*Alectoris chukar*) embryo. Anatomical Science, 12(3): 129-136. Available at: http://anatomyjournal.ir/article-1-117-en.html

Hassa O and Aştı RN (1997). Embriyoloji [Embryology], 3. Baskı, Yorum Basın Yayın, Ankara, pp. 117, 129-133.

Hsu SM, Raine L, and Fanger H (1981). Use of avidin-biotin-peroxidase complex (ABC) in immunoperoxidase techniques: A comparison between ABC and unlabeled antibody (PAP) procedures. The Journal of Histochemistry and Cytochemistry: Official Journal of the Histochemistry Society, 29(4): 577-580. DOI: https://www.doi.org/10.1177/29.4.6166661

Iida I, Johkura K, Teng R, Kubota S, Cui L, Zhao X, Ogiwara N, Okouchi Y, Asanuma K, Nakayama J et al. (2003). Immunohistochemical localization of hepatocyte growth factor activator (HGFA) in developing mouse liver tissues. Heterogeneous distribution of HGFA protein. The Journal of Histochemistry and Cytochemistry: Official Journal of the Histochemistry Society, 51(9): 1139-1149. DOI: https://www.doi.org/10.1177/002215540305100904

Kara H, Özüdoğru Z, Balkaya H, and Özdemir D (2019). Morphologic and histologic observation of Red-Legged Partridge's (*Alectoris chukar*) liver. Van Veterinary Journal, 30(3): 159-161. DOI: https://www.doi.org/10.36483/vanvetj.547719.

König HE, Korbel R, and Liebich HG (2016). Avian anatomy textbook and colour atlas, 2nd Edition, pp. 109-110.

Le Roith D (1997). Insulin-like growth factors. New England Journal of Medicine, 336(9): 633-640. DOI: https://www.doi.org/10.1056/NEJM199702273360907

Le Roith D, Bondy C, Yakar S, Liu J, and Butler A (2001). The somatomedin hypothesis. Endocrine Reviews, 22(1): 53-74. DOI: https://www.doi.org/10.1210/edrv.22.1.0419

Liu Y (2002). Hepatocyte growth factor and the kidney. Current opinion in Nephrology and Hypertension, 11(1): 23-30. DOI: https://www.doi.org/10.1097/00041552-200201000-00004

Makarevich AV and Markkula M (2002). Apoptosis and cell proliferation of bovine embryos stimulated with insulin-like growth factor-I during *in vitro* maturation and culture. Biology of Reproduction, 66(2): 386-392. DOI: https://www.doi.org/10.1095/biolreprod66.2.386

Matsumoto K and Nakamura T (2001). Hepatocyte growth factor: Renotropic role and potential therapeutics for renal diseases. Kidney International, 59(6): 2023-2038. DOI: https://www.doi.org/10.1046/j.1523-1755.2001.00717.x

McGeady TA, Quinn PJ, Fitzpatrick ES, and Ryan MT (2006). Veterinary embryology. John Wiley & Sons., USA, pp. 221-223, 243-252. Available at: https://books.google.com.tr/books?id=lNYtDwAAQBAJ

Mcmurtry JP, Richards MP, Brocht DM, Schoen T, and Waldbillig R (1996). Developmental changes in serum insulin-like growth factor-I and insulin-like growth factor binding proteins in the turkey embryo. Poultry Science, 75(4): 563-569. DOI: https://www.doi.org/10.3382/ps.0750563

Mercola M and Stiles CD (1988). Growth factor superfamilies and mammalian embryogenesis. Development, 102(3): 451-460. DOI: https://www.doi.org/10.1242/dev.102.3.451

Neuhaus H and Hollemann T (2009). Kidney specific expression of cTPTE during development of the chick embryo. Gene Expression Patterns, 9(8): 568-571. DOI: https://www.doi.org/10.1016/j.gep.2009.09.002

Owino V, Yang SY, and Goldspink G (2001). Age-related loss of skeletal muscle function and inability to express the autocrine form of insulin-like growth factor I (MGF) in response to mechanical overload. Federation of European Biochemical Societies Letters, 505(2): 259-263. DOI: https://www.doi.org/10.1016/s0014-5793(01)02825-3

Ralphs JR, Wylie L, and Hill DJ (1990). Distribution of insulin-like growth factor peptides in the developing chick embryo. Development, 109(1): 51-58. DOI: https://www.doi.org/10.1242/dev.109.1.51

Robcis H, Caldes LT, and De Pablo F (1991). Insulin-like growth factor-I serum levels show a midembryogenesis peak in chicken that is absent in growth-retarded embryos cultured *ex ovo*. Endocrinology, 128(4): 1895-1901. DOI: https://www.doi.org/10.1210/endo-128-4-1895

Saltan SK and Aslan Ş (2017). Immunohistochemical localization of ghrelin and IGF-I (insulin-like growth factor-I) in the liver and kidney tissues of melatonin-treated rats. Journal of Veterinary Science and Animal Husbandry, 5(4): 401. DOI: https://www.doi.org/10.15744/2348-9790.5.401

Scanes CG and Dridi S (2021). Sturkie's avian physiology, 7th Edition. Elsevier., Amsterdam, Netherlands, pp. 413-425. Available at: https://shop.elsevier.com/books/sturkies-avian-physiology/scanes/978-0-12-819770-7

Schultz G, Khaw PT, Oxford K, Macauley S, Setten GV, and Chegini N (1994). Growth factors and ocular wound healing, Eye, 8(2): 184-187. DOI: https://www.doi.org/10.1038/eye.1994.43

Shin D, Shin CH, Tucker J, Ober EA, Rentzsch F, Poss KD, Hammerschmidt M, Mullins MC, and Stainier DY (2007). Bmp and Fgf signaling are essential for liver specification in zebrafish. Development, 134(11): 2041-2050. DOI: https://www.doi.org/10.1242/dev.000281

Taşçı SK, Deprem T, Bingöl SA, and Akbulut Y (2018). The anatomical and histological structures of buzzard's (Buteo buteo) small intestine and liver, and immunohistochemical localization of catalase, Kafkas University Faculty of Veterinary Medicine Journal, 24(1): 69-74. DOI: https://www.doi.org/10.9775/kvfd.2017.18333

Taşçı SK, Gülmez N, Aslan Ş, Deprem T, and Bingöl SA (2020). Immunohistochemical localization of catalase in geese (*Anser anser*) kidney. Kafkas University Faculty of Veterinary Medicine Journal, 26(1): 41-46. DOI: https://www.doi.org/10.9775/kvfd.2019.22152

Tekinarslan İİ, Unur E, Ülger H, Ekinci N, Ertekin T, Hacıalioğulları M, and Arslan S (2011). Effects of FGF-9 on embryonic development *in vitro*. Balkan Medical Journal, 28: 18-22. DOI: https://www.doi.org/10.5174/tutfd.2009.02019.2

Thompson AI, Conroy KP, and Henderson NC (2015). Hepatic stellate cells: Central modulators of hepatic carcinogenesis. BMC Gastroenterol, 15: 63. DOI: https://www.doi.org/10.1186/s12876-015-0291-5

Tilki M and Saatçi M (2013). Her yönüyle kaz yetiştiriciliği [Goose breeding in all its aspects]. Salmat Basım Yayıncılık, Ankara, pp. 91-94.

Uni Z, Yadgary L, and Yair R (2012). Nutritional limitations during poultry embryonic development. The Journal of Applied Poultry Research, 21(1): 175-184. DOI: https://www.doi.org/10.3382/japr.2011-00478

Webber EM, Wu JC, Wang L, Merlino G, and Fausto N (1994). Overexpression of transforming growth factor-alpha causes liver enlargement and increased hepatocyte proliferation in transgenic mice. The American Journal of Pathology, 145(2): 398-408. Available at: https://pubmed.ncbi.nlm.nih.gov/8053497/

Wolf HK, Zarnegar R, and Michalopoulos GK (1991). Localization of hepatocyte growth factor in human and rat tissues: An immunohistochemical study. Hepatology, 14(3): 488-494. Available at: https://pubmed.ncbi.nlm.nih.gov/1831438/

Yang L, Li LC, Lamaoqiezhong, Wang X, Wang WH, Wang YC, and Xu CR (2019). The contributions of mesoderm-derived cells in liver development. Seminars in Cell and Developmental Biology, 92: 63-76. DOI: https://www.doi.org/10.1016/j.semcdb.2018.09.003

Yin C, Evason KJ, Asahina K, and Stainier DYR (2013). Hepatic stellate cells in liver development, regeneration, and cancer. The Journal of Clinical Investigation, 123(5): 1902-1910. DOI: https://www.doi.org/10.1172/JCI66369.

Yetkin G and Çelebi N (2001). Properties of transforming growth factor alpha, effects on cancer cells and ulcer wounds. FABAD Journal of Pharmaceutical Sciences, 26: 185-196. Available at: https://dergi.fabad.org.tr/en/2001-volume-26-issue-4/

Zaefarian F, Abdollahi MR, Cowieson A, and Ravindran V (2019). Avian Liver: The forgotten organ. Animals, 9(2): 63. DOI: https://www.doi.org/10.3390/ani9020063

Zhang W, Yatskievych TA, Baker RK, and Antin PB (2004). Regulation of *Hex* gene expression and initial stages of avian hepatogenesis by Bmp and Fgf signaling. Developmental Biology, 268(2): 312-326. DOI: https://www.doi.org/10.1016/j.ydbio.2004.01.019

Publisher's note: Scienceline Publication Ltd. remains neutral with regard to jurisdictional claims in published maps and institutional affiliations.

Open Access: This article is licensed under a Creative Commons Attribution 4.0 International License, which permits use, sharing, adaptation, distribution and reproduction in any medium or format, as long as you give appropriate credit to the original author(s) and the source, provide a link to the Creative Commons licence, and indicate if changes were made. The images or other third party material in this article are included in the article's Creative Commons licence, unless indicated otherwise in a credit line to the material. If material is not included in the article's Creative Commons licence and your intended use is not permitted by statutory regulation or exceeds the permitted use, you will need to obtain permission directly from the copyright holder. To view a copy of this licence, visit https://creativecommons.org/licenses/by/4.0/.
© The Author(s) 2025

2025, Scienceline Publication
World's Veterinary Journal
World Vet J, 15(4): 845-853.
ISSN 2322-4568

DOI: https://dx.doi.org/10.54203/scil.2025.wvj86
PII: S232245682500086-15

Effects of Choline-Rich Fermented *Crescentia cujete* on Blood Parameters, Superoxide Dismutase, and Cerebral Interleukin-6 in Rats after Induced Ischemic Stroke

Puput Fiohana[1]*, Yos Adi Prakoso[2], Sitarina Widyarini[3], Jasir Hakim Hidayah[2,4], Puput Ade Wahyuningtyas[2], and Achmadi Susilo[5]

[1]*RSI Siti Hajar Sidoarjo, Sidoarjo, East Java, 61234, Indonesia*
[2]*Department of Pharmacology, University of Wijaya Kusuma Surabaya, Surabaya, East Java, 60225, Indonesia*
[3]*Department of Pathology, University of Gadjah Mada, Yogyakarta, East Java, 55281, Indonesia*
[4]*D'Luna Vet Care, Jakarta Pusat, DKI Jakarta, 10460, Indonesia*
[5]*Agrotechnology Study Program, Faculty of Agriculture, University of Wijaya Kusuma Surabaya, Surabaya, 60225, Indonesia*

*Corresponding author's Email: fiohanap@gmail.com

ORIGINAL ARTICLE
Received: September 29, 2025
Revised: October 27, 2025
Accepted: November 30, 2025
Published: December 25, 2025

ABSTRACT

Ischaemic stroke is a major vascular disorder that profoundly impacts human health. Choline-rich fermented *Crescentia cujete* (Ch-RFCC) has emerged as a promising adjunctive therapy for ischemic stroke; however, its effects on hematological parameters, superoxide dismutase (SOD) activity, and interleukin-6 (IL-6) levels remain unexplored. The present study aimed to assess the impacts of Ch-RFCC on hematological parameters, SOD activity, and brain IL-6 levels in the rats' ischemic stroke model (ISM). A total of 40 three-month-old male rats, weighing 247.31 ± 4.95 g, were randomly assigned into four groups, including healthy rats with a skin incision as the control group (sham-operated, T1), ISM without treatment (T2), ISM treated with 496 mg/kg body weight of piracetam (T3), and ISM treated with 11.84 mg/kg body weight of Ch-RFCC (T4). Treatments using piracetam (T3) and Ch-RFCC (T4) were administered orally via gavage twice daily for 14 consecutive days. The current results demonstrated that Group T4 maintained haemoglobin and haematocrit levels, normalised the platelet-to-leucocyte ratio and neutrophil counts, reduced fibrinogen levels, elevated SOD activity, and enhanced IL-6 immunoreactivity compared to the untreated ISM group (T2). Furthermore, rats in Group T4 exhibited the least body weight loss compared to those in groups T2 and T3. These findings indicated that Ch-RFCC may alleviate ischemic stroke in rats by enhancing antioxidant defenses, modulating IL-6 expression, and preserving hematological homeostasis.

Keywords: Choline-rich fermented *Crescentia cujete*, Hematology, Interleukin-6, Ischemic stroke, Superoxide dismutase

INTRODUCTION

Ischemic stroke is a major vascular disorder that significantly impacts human health, greatly impairs the quality of life, and exerts a long-term financial burden on individuals and healthcare systems (Dhanasekara et al., 2024). The occlusion of cerebral arteries deprives brain tissue of oxygen and essential nutrients, resulting in infarction and neurological deficiencies such as paralysis (Lowry and Jin, 2020). The infarct area expands as cerebral blood flow decreases and neuronal cell death progresses (Zhao et al., 2022). Neuronal mortality is caused by deprivation of oxygen and nutrients, a condition that has the potential to upregulate the intracellular expression of interleukin-6 (IL-6, Ciryam et al., 2023). Feng et al. (2015) have indicated that IL-6 is essential for maintaining neuronal integrity. Additionally, IL-6 acts as a neurotrophic-like factor, promoting neuroplasticity, development, and regeneration during the progression of neuronal diseases (Erta et al., 2012). Elevated IL-6 levels in the brain may further support the development of dopaminergic neurons and regulate voltage-gated ion channels (Grebenciucova and VanHaerents, 2023).

During ischemic stroke pathogenesis, cerebral injury triggers systemic changes in blood composition. Circulating inflammatory cells increase; key biomarkers of this response include the platelet-to-leukocyte ratio (PLR; Amalia and Dalimonthe, 2020) and the neutrophil-to-lymphocyte ratio (NLR; Graça et al., 2024). Furthermore, the acute-phase response may also involve an increase in total plasma protein (TPP), reflecting a broader systemic inflammatory shift. Concurrently, erythrocyte count, hemoglobin (HGB) concentration, and haematocrit (HCT) often decline when nutritional intake is compromised by dysphagia (Brito et al., 2020. Furthermore, neuronal damage results in a significant reduction in plasma antioxidant defenses, particularly in superoxide dismutase (SOD) activity (Zhang et al., 2022). In humans, these hematological and biochemical changes are linked to the severity and prognosis of ischemic stroke,

To cite this paper: Fiohana P, Prakoso YA, Widyarini S, Hidayah JH, Wahyuningtyas PA, and Susilo A (2025). Effects of Choline-Rich Fermented *Crescentia cujete* on Blood Parameters, Superoxide Dismutase, and Cerebral Interleukin-6 in Rats after Induced Ischemic Stroke. *World Vet. J.,* 15(4): 845-853. DOI: https://dx.doi.org/10.54203/scil.2025.wvj86

highlighting the importance of comprehensive blood profiling during both the development and treatment stages (Liang et al., 2025).

Choline-rich fermented *Crescentia cujete* (Ch-RFCC) has emerged as a promising adjunctive therapy for ischemic stroke in animal models (Hidayah et al., 2023). This liquid fermentation product of *Crescentia cujete* is enriched in choline and has demonstrated immunostimulatory (Wijayanti et al., 2024), complementary effects on pneumonia (Prakoso et al., 2024a), and neuroprotective effects in preclinical models of stroke (Hidayah et al., 2023). A previous study reported that Ch-RFCC elevated brain levels of granulocyte-macrophage colony-stimulating factor (GM-CSF) and vascular endothelial growth factor (VEGF), thereby supporting cerebral angiogenesis and oxygenation (Prakoso et al., 2024b). However, its downstream effects on brain IL-6 expression and systemic hematological parameters have not yet been evaluated. The present study aimed to assess the impact of Ch-RFCC on hematological parameters, SOD activity, and brain IL-6 levels in the rats' ischemic stroke model (ISM).

MATERIALS AND METHODS

Ethical statement

The Animal Research Ethics Committee of the Faculty of Veterinary Medicine, University of Wijaya Kusuma Surabaya, Indonesia, approved the present study (Registration No. KKE-243/I/2025). The committee registered and observed all procedures, and the study was conducted in the Pharmacology Laboratory at the Faculty of Veterinary Medicine, University of Wijaya Kusuma Surabaya, from January to July 2025.

Preparation of fermented *Crescentia cujete*

The fruit of *Crescentia cujete* was collected from the garden of the University of Wijaya Kusuma Surabaya, Indonesia. A total of 400 g of fruit pulp was weighed and combined with 1000 mL of distilled water. The mixture was supplemented with 40 mL of pectinase (Pectinex Ultra AFP, United Kingdom) and 40 g of sugar, then fermented at 25°C for 30 days with stirring for 15 minutes once daily. The 1000 mL final fermentation product was referred to as Ch-RFCC. This procedure was adapted from the study conducted by Wilujeng et al. (2023). According to Prakoso et al. (2024a), each milliliter of the final product contained 114.12 mg of choline.

Animals

The present study comprised 40 male Sprague-Dawley rats, three months old, weighing 247.31 ± 4.95 g, obtained from the Laboratory of Pharmacology at the Faculty of Veterinary Medicine, University of Wijaya Kusuma Surabaya, Indonesia. Before the experiment, the animals were acclimated for seven days in cages (90 × 50 × 60 cm) maintained at 25°C. The cages were bedded with oven husk, and a commercial food (RatBio®, Indonesia) and water (Cleo®, Indonesia) were provided *ad libitum*. Relative humidity was kept at 60% using a Leka DH6628 dehumidifier (Indonesia). After the adaptation period, the rats were randomly divided into four groups. Each group consisted of 10 rats, including healthy rats with a skin incision without common carotid artery (CCA) ligation as the control group (sham-operated, T1), untreated ISM (T2), the ISM rats that received 496 mg/kg body weight of piracetam (T3; Bernofarm, Indonesia, Paliwal et al., 2018), and ISM rats that received 11.84 mg/kg body weight of Ch-RFCC (T4; Hidayah et al., 2023). Treatments using piracetam (T3) and Ch-RFCC (T4) were administered orally twice daily via gavage at 6:00 a.m. and 6:00 p.m. for 14 consecutive days.

Induction of ischemic stroke in rats

The rats in groups T1, T2, T3, and T4 were anesthetized with a combination of xylazine (Xylazil, Ilium, Australia) and Zoletil® (Virbac, India). Xylazine was administered intramuscularly at 4 mg/kg body weight (Bhatia et al., 2022). Fifteen minutes later, each rat received Zoletil® at 25 mg/kg body weight via intramuscular injection (Kosenko et al., 2020). Rats in Group T1 had their anterior necks shaved with surgical clippers. The skin was disinfected with isopropyl alcohol (Onemed, Indonesia), and a 2 cm midline incision was made. A skin incision was made in all groups. In Group T1, the incision was closed with simple interrupted sutures using 2-0 silk. In Groups T2, T3, and T4, the same incision was followed by ligation of the right common carotid artery (CCA) and its external and internal branches using the same suture material before closure. The ligations were removed to permit reperfusion after four hours of occlusion, following the method described by Prakoso et al. (2023).

Body weight and sample collection

The body weight of each rat was recorded on the day before induction (day 0), and the body weight was measured again on day 14 post-treatment. Percentage weight gain was calculated using the formula conducted by Beale et al. (2011).

W (%) = (WDx – WD0) / WD0 × 100 (Formula 1)

W (%) is the growth percentage, WDx is body weight on day x (g), and WD0 is body weight on day 0 (g).

After 14 days of treatment, rats were anesthetized with 25 mg/kg body weight Zoletil®. Blood was collected via the retro-orbital plexus using microhematocrit tubes. One aliquot was transferred into EDTA tubes (Onemed, Indonesia) for hematology analysis, and the residue into plain tubes for SOD analysis. Whole blood, plasma, and serum were stored at 4°C. Following blood collection, rats were euthanized by cervical dislocation. Brains were harvested and fixed in neutral-buffered formalin 10% (Leica, USA) for 24 hours.

Hematology test

Blood samples were analyzed against total red blood cells (RBC, 10^6 cells/mm^3), HGB (g/dL), HCT (%), mean corpuscular volume (MCV, fL), mean corpuscular hemoglobin (MCH, Pg), mean corpuscular hemoglobin concentration (MCHC, %), PLT, (10^5 cells/mm^3), PWR, white blood cells (WBC, 10^3 cells/mm^3), lymphocytes (LYM, 10^3 cells/mm^3), monocytes (MONO, 10^3 cells/mm^3), neutrophils (NEU, 10^3 cells/mm^3), eosinophils (EOS, 10^3 cells/mm^3), basophils (BAS, 10^3 cells/mm^3), and neutrophil per lymphocyte ratio (NLR) using a hematology analyzer (VetScan HM5, Zoetis, USA). Plasma was then assayed for fibrinogen (Schlimp et al., 2015) and TPP (Hunsaker et al., 2016). Superoxide dismutase activity was measured following the protocol described by Afrazeh et al. (2015).

Immunohistochemistry

The brains of rats from all groups, with ten brains per group, were subjected to routine histopathological examination as outlined by Ma et al. (2024). For the routine histopathology processes, the organ was dehydrated and cleared using graded alcohol (70%, 80%, 90%) and graded xylene (1 to 3). The brains were then embedded using liquid paraffin and blocked. The brain blocks were then sectioned using a microtome (Leica RM2125 RTS, USA). After sectioning, the slides were immunostained for the detection of IL-6 using an anti-IL-6 antibody (Santa Cruz, USA) at a 1:100 dilution. The immunohistochemistry protocol followed the manufacturer's instructions provided with the secondary antibody kit (Novocastra, Leica Biosystem, USA). Interleukin-6 immunoreactivity was visualized using diaminobenzidine (DAB; Leica, USA) at a 1:50 dilution. The IL-6 was then analyzed using ImageJ software (NIH Image, United States) and quantified as the percentage of positive staining area and the number of IL-6-positive cells.

Statistical analysis

The current data were analyzed using SPSS Statistics version 26 (IBM, United States). Body weight, hematology, TPP, fibrinogen, and SOD measurements were calculated by one-way ANOVA followed by Duncan's multiple range test. Immunohistochemistry data were analyzed using the Kruskal-Wallis test and the Mann-Whitney U test. Statistical significance was defined at the 95% significance level ($p \leq 0.05$).

RESULTS AND DISCUSSION

On the first day of induction, no significant differences in body weight were observed among the rats ($p \geq 0.05$), indicating that all groups had a similar weight, which suggested that the body weights of the rats were homogeneous on this day (Table 1). However, after 14 days of treatment using 11.89 mg/kg body weight of Ch-RFCC, significant divergences emerged between groups ($p \leq 0.05$). The Group T2 exhibited the lowest body weight (229.00 ± 10.73 g) compared to groups T1 (250.50 ± 5.32 g) and T4 (247.25 ± 3.40 g; $p \leq 0.05$), although it did not differ significantly from Group T3 (235.25 ± 6.84 g; $p \geq 0.05$). Group T4 was more effective at maintaining weight (247.25 ± 3.40 g) than groups T2 and T3 ($p \leq 0.05$), and its weights remained comparable to those of Group T1 (250.50 ± 5.32 g; $p \geq 0.05$). Furthermore, Group T1 experienced the most significant weight gain (over 1.83%) among all groups ($p \leq 0.05$), while Group T4 had the lowest percentage of weight loss compared to Groups T2 and T3 ($p \leq 0.05$; Table 1).

Table 1. Average body weight of ischemic stroke rats before and after 14 days of treatment

Parameter	Unit	T1	T2	T3	T4
Body weight before treatment	Gram	246.00 ± 5.35^a	247.00 ± 6.68^a	245.75 ± 5.73^a	250.50 ± 2.38^a
Body weight after treatment	Gram	250.50 ± 5.32^a	229.00 ± 10.73^b	235.25 ± 6.84^b	247.25 ± 3.40^a
Percentage of body weight loss	%	(+) 1.83 ± 0.87^a	(-) 7.31 ± 2.59^b	(-) 4.42 ± 3.15^c	(-) 1.29 ± 0.60^d

T1: Control group, T2: ISM without treatment, T3: ISM treated with 496 mg/kg body weight of piracetam, T4: ISM treated with 11.84 mg/kg body weight of Ch-RFCC, (+): Increase of body weight, (-): Decrease of body weight. $^{a,b,c, \text{ and } d}$ Different superscript letters indicate significant differences ($p \leq 0.05$).

After 14 days of treatment, there were no significant differences among groups T1, T2, T3, and T4 in the erythrocyte profile, MCV, MCHC, MONO, and EOS counts ($p \geq 0.05$). Group T2, however, indicated significant increases in HGB (12.59 ± 1.13 g/dL), PLT counts (1347.00 ± 97.59 × 10^5 cells/mm^3), PWR (134.63 ± 5.11), total leukocytes (10.20 ± 0.48 × 10^3 cells/mm^3), LYM (6.49 ± 0.50), and NLR (0.45 ± 0.09) compared to the other groups ($p \leq 0.05$). Group T2 exhibited a significant decrease in HCT (33.17 ± 3.10 %) and MCH (18.86 ± 2.06 Pg) compared to the other groups ($p \leq 0.05$; Table 2).

Furthermore, groups T3 and T4 restored several hematological parameters (RBC, HGB, HCT, MCV, MCH, MCHC, PWR, MONO, NEU, EOS, and NLR) to levels similar to those in Group T1 ($p \geq 0.05$), except for total PLT and LYM, which continued to exhibit significant differences ($p \leq 0.05$). After 14 days of treatment, groups T3 and T4 still exhibited significantly higher PLT (939.00 ± 13.54 and 864.50 ± 73.67 × 10^5 cells/mm^3, respectively) and LYM counts (5.46 ± 0.90 and 5.55 ± 0.71 × 10^3 cells/mm^3, respectively) than Group T1 (PLT: 647.75 ± 46.59 and LYM: 4.31 ± 0.39; $p \leq 0.05$), although their levels remained lower than those in Group T2 (PLT: 1374.00 ± 13.54 × 10^3 cells/mm^3 and LYM: 6.49 ± 0.50 × 10^3 cells/mm^3; $p \leq 0.05$). There were no significant differences between groups T3 and T4 for haematological parameters ($p \geq 0.05$; Table 2).

In Group T2, the TPP (8.40 ± 0.40 g/dL) and fibrinogen (440.25 ± 39.22 mg/dL) levels increased significantly compared to T1 (TPP: 6.77 ± 0.30 and fibrinogen: 225.00 ± 15.81 mg/dL; $p \leq 0.05$). In groups T3 and T4, both TPP (7.22 ± 0.33 and 7.55 ± 0.55 g/dL, respectively) and fibrinogen (323.25 ± 9.91 and 273.00 ± 23.07 mg/dL, respectively) decreased significantly compared to Group T2 ($p \leq 0.05$), yet remained higher than in Group T1 ($p \leq 0.05$). In contrast, the SOD activity dropped markedly in groups T2 (47.46 ± 6.68 U/mL) and T3 (49.08 ± 5.16 U/mL), whereas in Group T4 (60.21 ± 3.50 U/mL), SOD levels were not different from those of Group T1 (63.99 ± 6.68 U/mL; $p \geq 0.05$; Table 3). The percentage level of IL-6 immunoexpression did not differ significantly among groups T1 (17.49 ± 5.06 %), T2 (13.49 ± 2.43 %), and T3 (16.74 ± 2.32 %, $p \geq 0.05$), while Group T4 (22.96 ± 2.39 %) exhibited significantly higher expression than the other groups ($p \leq 0.05$). The quantity of IL-6-immunoreactive cells exhibited a pattern consistent with the percentage area measurements (Table 4). A representative qualitative evaluation of IL-6 is illustrated in Figure 1.

Table 2. Hematology profile of ischemic stroke rats after 14 days of treatment

Parameter	Unit	T1	T2	T3	T4
RBC	10^6 cells/mm^3	6.70 ± 0.38^a	6.69 ± 0.27^a	6.52 ± 0.25^a	6.68 ± 0.41^a
HGB	g/dL	14.31 ± 0.37^a	12.59 ± 1.13^b	14.13 ± 0.58^a	14.20 ± 0.36^a
HCT	%	40.07 ± 0.72^a	33.17 ± 3.10^b	39.07 ± 2.28^a	39.57 ± 3.40^a
MCV	fL	28.01 ± 1.24^a	26.48 ± 3.27^a	27.64 ± 0.66^a	27.86 ± 2.14^a
MCH	Pg	21.40 ± 1.52^a	18.86 ± 2.06^b	21.70 ± 1.57^a	21.31 ± 1.90^a
MCHC	%	35.74 ± 1.54^a	38.18 ± 4.68^a	36.19 ± 0.84^a	36.04 ± 2.62^a
PLT	10^5 cells/mm^3	647.75 ± 46.59^a	1374.00 ± 97.59^b	939.00 ± 13.54^c	864.50 ± 73.67^c
PWR	-	101.14 ± 9.87^a	134.63 ± 5.11^b	115.89 ± 13.30^a	103.50 ± 8.78^a
WBC	10^3 cells/mm^3	6.42 ± 0.41^a	10.20 ± 0.48^b	8.17 ± 0.84^c	8.39 ± 0.95^c
LYM	10^3 cells/mm^3	4.31 ± 0.39^a	6.49 ± 0.50^b	5.46 ± 0.90^b	5.55 ± 0.71^b
MONO	10^3 cells/mm^3	0.51 ± 0.24^a	0.53 ± 0.38^a	0.54 ± 0.30^a	0.55 ± 0.39^a
NEU	10^3 cells/mm^3	1.46 ± 0.20^a	2.91 ± 0.46^b	2.07 ± 0.51^a	2.15 ± 0.57^a
EOS	10^3 cells/mm^3	0.12 ± 0.04^a	0.25 ± 0.05^b	0.09 ± 0.07^a	0.12 ± 0.04^a
BAS	10^3 cells/mm^3	ND	ND	ND	ND
NLR	-	0.33 ± 0.04^a	0.45 ± 0.09^a	0.38 ± 0.12^a	0.39 ± 0.11^a

T1: Control group, T2: ISM without treatment, T3: ISM treated with 496 mg/kg body weight of piracetam, T4: ISM treated with 11.84 mg/kg body weight of Ch-RFCC, RBC: Total erythrocytes, HGB: Hemoglobin, HCT: Haematocrit, MCV: Mean corpuscular volume, MCH: Mean corpuscular hemoglobin, MCHC: Mean corpuscular hemoglobin concentration, PLT: Platelets, PWR: Platelet-to-leucocytes ratio, WBC: Leucocytes total, LYM: Lymphocytes, MONO: Monocytes, NEU: Neutrophils, EOS: Eosinophils, BAS: Basophils, NLR: Neutrophil per lymphocyte ratio, ND: Not detected. $^{a,b, \text{and } c}$ Different superscript letters indicate significant differences ($p \leq 0.05$).

Table 3. Level of total protein, fibrinogen, and superoxide dismutase in ischemic stroke rats after 14 days of treatment

Parameter	Unit	T1	T2	T3	T4
TPP	g/dL	6.77 ± 0.30^a	8.40 ± 0.40^b	7.22 ± 0.33^c	7.55 ± 0.55^c
FIB	mg/dL	225.00 ± 15.81^a	440.25 ± 39.22^b	323.25 ± 9.91^c	273.00 ± 23.07^d
SOD	U/mL	63.99 ± 4.31^a	47.46 ± 6.68^b	49.08 ± 5.16^b	60.21 ± 3.50^a

T1: Control group, T2: ISM without treatment, T3: ISM treated with 496 mg/kg body weight of piracetam, T4: ISM treated with 11.84 mg/kg body weight of Ch-RFCC, TPP: Total plasma protein, FIB: Fibrinogen, SOD: Superoxide dismutase. $^{a,b,c, \text{and } d}$ Different superscript letters indicate significant differences ($p \leq 0.05$).

Table 4. Immunohistochemistry of the brain's IL-6 in ischemic stroke rat models after 14 days of treatment

Parameter	Unit	T1	T2	T3	T4
Percentage area	%	17.49 ± 5.06[a]	13.49 ± 2.43[b]	16.74 ± 2.32[c]	22.96 ± 2.39[d]
Average number of immunoreactive cells	Cells	155.25 ± 30.34[a]	139.25 ± 27.41[b]	149.00 ± 19.54[c]	184.00 ± 20.14[d]

T1: Sham-operated, T2: ISM without treatment, T3: ISM treated with 496 mg/kg body weight of piracetam group, T4: ISM treated with 11.84 mg/kg body weight of Ch-RFCC group. [a,b,c, and d] Different superscript letters indicate significant differences ($p \leq 0.05$).

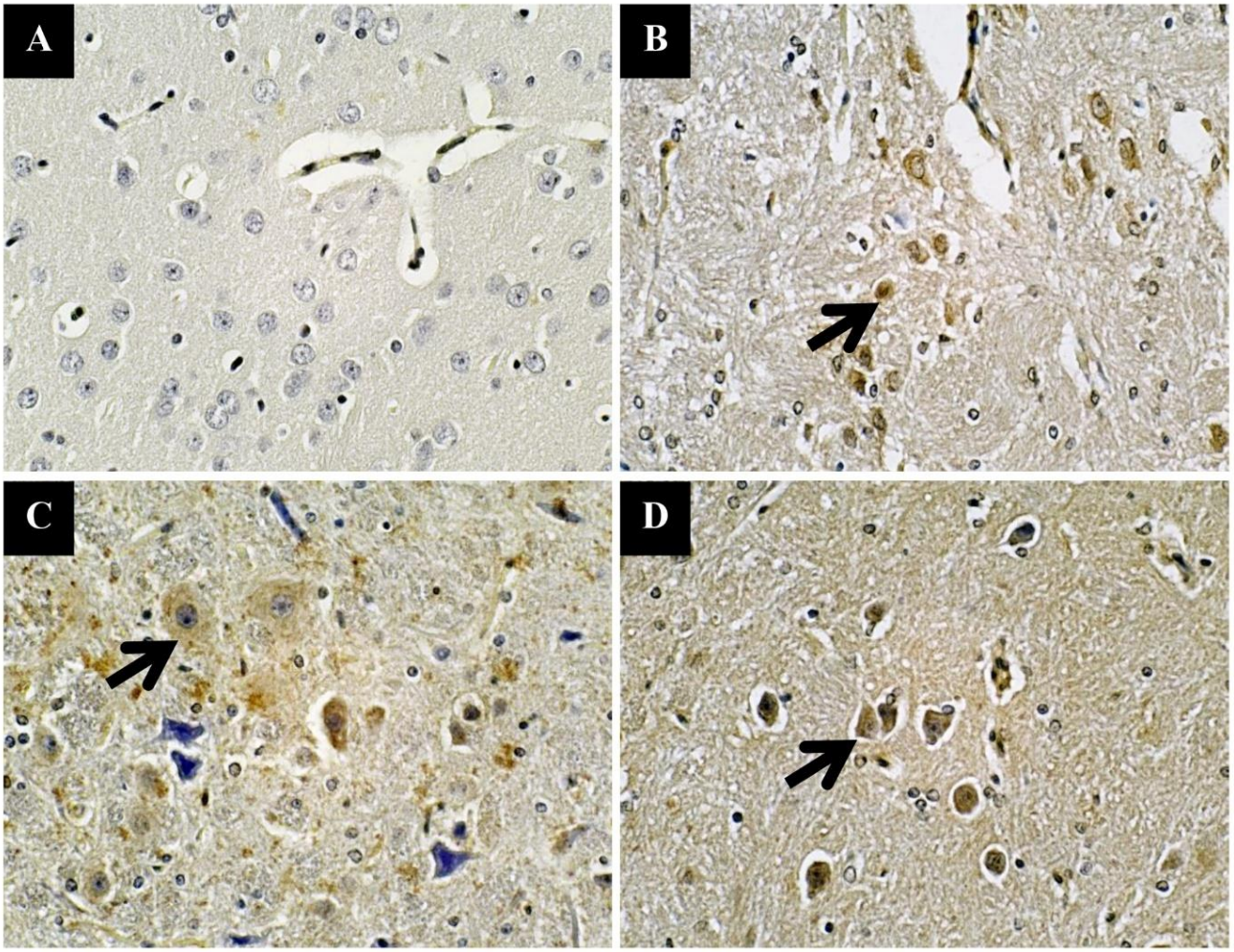


Figure 1. Immunohistochemical detection of IL-6 in brain sections from ischemic stroke rats after 14 days of treatment. **A**: The control group showing no IL-6 signal (400×), **B**: Group T2 treatment, IL-6 immunoreactivity evident (arrow; 100×), **C**: Group T3 treatment, IL-6 immunoreactivity evident (arrow; 400×), **D**: Group T4 treatment, IL-6 immunoreactivity evident (Arrow; 400×). Sections were incubated with anti-IL-6 antibody (1:100) and visualized using diaminobenzidine.

DISCUSSION

The present study demonstrated that cerebral infarction disrupted systemic circulation, evidenced by reductions in MCH and HCT levels, alongside increases in PLT count, PWR, total leukocytes, LYM, and NEU. The drop in MCH and HCT during ischemic stroke was associated with poor clinical outcomes (Kellert et al., 2012), mainly due to reduced delivery of nutrients, oxygen, and essential amino acids to the ischemic penumbra (Abuhulayqah et al., 2025).

Furthermore, damage to brain tissue increases the leukocytes and NEU levels as components of the inflammatory response (Jickling et al., 2015). Although NEU infiltration is essential for the removal of damaged tissue (Chen et al., 2021), it also increases local oxidative stress, consequently exacerbating neuronal injury (Mu et al., 2023). Oxidative stress within the ischemic region further promotes the release of prothrombotic factors that activate PLT (Amalia and Dalimonthe, 2020) and elevate the PWR (Prakoso et al., 2023). Concurrent inflammation increases TPP (Kalani et al., 2023) and fibrinogen levels (Prasad et al., 2023). Consequently, monitoring these hematological parameters provided a reliable way to evaluate the efficacy of interventions for ischemic stroke, as reported by Khandait and Barai (2019), who found that ischemic stroke leads to increased fibrinogen levels, which aligns with the present results. Similarly, Yang et

al. (2019) observed that elevated PLT counts are associated with poorer clinical outcomes in patients with ischemic stroke, which aligns with the present findings.

Piracetam is commonly used to treat ischemic stroke. As a nootropic agent, it facilitates the preservation of neuronal function and integrity (Chen et al., 2019) and protects the brain against further ischemic damage. In the current study, piracetam restored several blood parameters disrupted by stroke, including the normalization of HGB, HCT, PWR, and NEU counts, while reducing PLT and leukocyte counts as well as TPP and fibrinogen levels, compared to the untreated ISM group. However, these measures remained higher than in the control group and the Ch-RFCC treatment. Early administration of piracetam has been shown to improve blood flow to the infarcted area in the brain tissue (Winblad, 2005); however, Ricci et al. (2012) found no clinical benefit in over 1,000 patients. Ricci et al. (2012) concluded that piracetam should not be recommended as routine therapy for ischemic stroke. These conflicting findings highlighted the complexity of piracetam's efficacy and underscored the need for further evaluation of its study. Hence, an alternative therapy should be found, such as using Ch-RFCC. The choline inside the Ch-RFCC is a compound that contains phospholipid to promote brain recovery and neuroprotection. A study by Hidayah et al. (2023) indicated that Ch-RFCC promoted the clinical outcome of ischemic stroke via the histopathology and neurodeficits score analysis. Prakoso et al. (2024b) stated that Ch-RFCC improves brain oxygenation by activating VEGF and enhances the resolution of brain inflammation through microglia activation, thereby activating GM-CSF. The role of choline from Ch-RFCC has beneficial direct effects on neuronal cell survival through its capacity to act as a precursor for phosphatidylcholine (Zhong et al., 2021). The benefits of Ch-RFCC in the current study were demonstrated by the normalization of HGB, haematocrit, PWR, and NEU compared to the untreated ISM group, and indicated a reduction in PLT, leucocytes, and TPP, similar to the piracetam group. Additionally, the Ch-RFCC demonstrated a promising outcome in decreasing fibrinogen. As a previous study stated that fibrinogen is a key component of the inflammatory biomarker (Prasad et al., 2023).

Apart from hematological metrics, assessing antioxidant activity, particularly SOD, is essential for evaluating the success of ischemic stroke therapy (Anwar et al., 2025). An increase in SOD activity reflects enhanced detoxification of oxidative stress in the brain (Chidambaram et al., 2024) and supports functional neuronal recovery (Briones-Valdivieso et al., 2024). In the current study, the Ch-RFCC group exhibited a similar level of SOD activity comparable to that of the control group, indicating a promotion of brain tissue repair. The present findings align with those of Pawluk et al. (2024), who reported that reduced SOD activity is associated with worse neurological outcomes, larger infarct volumes, and a higher risk of poststroke cognitive impairment. Moreover, the meta-analysis conducted by Golenia and Olejnik (2025) concluded that heightened oxidative stress in cases of ischemic stroke, coupled with the depletion of catalase and SOD, undermines the integrity of the blood-brain barrier and results in neuronal damage and death. Adequate SOD activity is neuroprotective, protecting neurons from free radicals that cause cell death, inflammation, and blood-brain barrier breakdown (Haorah et al., 2011). Superoxide dismutase catalyzes the dismutation of superoxide radicals into hydrogen peroxide, which is then neutralized by other antioxidants such as glutathione peroxidase and catalase (Chidambaram et al., 2024). By this mechanism, SOD prevents the oxidative cascade that damages brain tissue. The brain's high metabolic rate, combined with limited antioxidant defenses, makes it especially susceptible to oxidative injury during ischemia (Zhang et al., 2022). Therefore, increasing SOD activity is important for supporting brain tissue remodeling after ischemic stroke.

The administration of Ch-RFCC resulted in a more effective increase in SOD levels compared to piracetam, and this increase suggests superior neuroprotective effects. This finding aligns with those of Jin et al. (2015), who described choline treatment as improving neurological outcome and reducing damage in the brain. The IL-6 expression induces a neuroprotective increase in SOD (Jung et al., 2011). Although IL-6 is generally considered an inflammatory marker, its elevation during ischemic stroke is associated with improved clinical outcomes (Tirandi et al., 2023). A study conducted by Feng et al. (2015) demonstrated that IL-6 mitigates inflammatory cell infiltration, prevents blood-brain barrier disruption by reducing Evans blue leakage, and downregulates matrix metalloproteinase-9 (MMP9) levels in ischemic brain tissue. The reduction of inflammatory cells, prevention of blood-brain barrier disruption, and decrease in MMP9 levels contribute to an improved prognosis following a stroke. These findings aligned with the current results, which indicated that the Ch-RFCC group exhibited higher increases in brain IL-6 and SOD levels compared to the piracetam-treated group.

Ultimately, improved prognosis after ischemic stroke in rat models can be evaluated by monitoring changes in body weight. Rats treated with piracetam or Ch-RFCC lost less weight compared to untreated controls. Notably, the Ch-RFCC group exhibited the least weight loss, even surpassing the weight loss of the piracetam group. The upward trend in body weight suggested that Ch-RFCC promoted neuronal recovery, which helped maintain feeding and drinking behaviors. Ciobanu et al. (2017) demonstrated that reduced weight loss is associated with promising outcomes in rat models of ischemic stroke.

CONCLUSION

The present study established that Ch-RFCC delivered superior recovery in rat models of ischemic stroke compared to piracetam. The advantages of Ch-RFCC were evidenced by its ability to sustain hemoglobin and hematocrit levels, normalize PWR and NEU counts, decrease fibrinogen levels, increase SOD activity, and improve IL-6 levels immunoreactivity. It is suggested that comprehensive toxicity and safety assessments should be conducted before considering Ch-RFCC for clinical evaluation in humans.

DECLARATIONS

Acknowledgments

The authors express their gratitude to Hibah Pasca Stroke Indonesia for their financial support towards the current study, provided under the grant number Hibah 01/18/PS/2022. Furthermore, all research assistants are duly acknowledged for their assistance.

Authors' contributions

Puput Fiohana, Yos Adi Prakoso, Jasir Hakim Hidayah, Sitarina Widyarini, Puput Ade Wahyuningtyas, and Achmadi Susilo performed the experiments. Yos Adi Prakoso supervised the study. Puput Fiohana formulated the Ch-RFCC compound. Yos Adi Prakoso, Jasir Hakim Hidayah, and Sitarina Widyarini collected specimens and carried out immunohistochemistry. Puput Fiohana and Puput Ade Wahyuningtyas conducted hematology and antioxidant analyses. Achmadi Susilo performed the statistical analysis. All authors contributed to the drafting, revising, and approval of the final manuscript.

Ethical considerations

This manuscript represents an original manuscript by the authors. Ethical issues, including plagiarism, consent to publish, misconduct, duplicate publication, data fabrication, and redundancy, have been reviewed and addressed. The authors did not use any AI application for preparing data, writing and revising the draft of this study.

Availability of data and materials

Data supporting the findings of the present study are available from the corresponding author upon reasonable request.

Funding

The present study was funded by Hibah Pasca Stroke Indonesia with funding number Hibah 34/12/PS/2024.

Competing interests

The authors declared no competing interests.

REFERENCES

Abuhulayqah S, Aldulijan FA, Turkistani AN, Almulhim AF, Almulhim CF, Bashir S, and Ali EN (2025). Impact of hemoglobin levels on acute ischemic stroke severity. Frontiers in Neurology, 16: 1534746. DOI: https://www.doi.org/10.3389/fneur.2025.1534746

Afrazeh M, Saedisar S, Khakzad MR, and Hojati M (2015). Measurement of serum superoxide dismutase and its relevance to disease intensity autistic children. Maedica, 10(4): 315-318. Available at: https://pubmed.ncbi.nlm.nih.gov/28465731/

Amalia L and Dalimonthe NZ (2020). Clinical significance of platelet-to-white blood cell ratio (PWR) and National Institute of Health Stroke Scale (NIHSS) in acute ischemic stroke. Heliyon, 6(10): e05033. DOI: https://www.doi.org/10.1016/j.heliyon.2020.e05033

Anwar S, Sarwar T, Khan AA, and Rahmani AH (2025). Therapeutic applications and mechanisms of superoxide dismutase (SOD) in different pathogenesis. Biomolecules, 15(8): 1130. DOI: https://www.doi.org/10.3390/biom15081130

Beale KE, Murphy KG, Harrison EK, Kerton AJ, Ghatei MA, Bloom SR, and Smith KL (2011). Accurate measurement of body weight and food intake in environmentally enriched male Wistar rats. Obesity, 19(8): 1715-1721. DOI: https://www.doi.org/10.1038/oby.2010.331

Bhatia A, Saikia PP, Dkhar B, and Pyngrope H (2022). Anesthesia protocol for ear surgery in Wistar rats (animal research). Animal Models and Experimental Medicine, 5(2): 183-188. DOI: https://www.doi.org/10.1002/ame2.12198

Briones-Valdivieso C, Briones F, Orellana-Urzúa S, Chichiarelli S, Saso L, and Rodrigo R (2024). Novel multi-antioxidant approach for ischemic stroke therapy targeting the role of oxidative stress. Biomedicines, 12(3): 501. DOI: https://www.doi.org/10.3390/biomedicines12030501

Brito M, Laranjo A, Nunes G, Oliveira C, Santos CA, and Fonseca J (2020). Anemia and hematopoietic factor deficiencies in patients after endoscopic gastrostomy: A nine-year and 472-patient study. Nutrients, 12(12): 3637. DOI: https://www.doi.org/10.3390/nu12123637

Chen R, Zhang X, Gu L, Zhu H, Zhong Y, Ye Y, Xiong X, and Jian Z (2021). New insight into neutrophils: A potential therapeutic target for cerebral ischemia. Frontiers in Immunology, 12: 692061. DOI: https://www.doi.org/10.3389/fimmu.2021.692061

Chen SY, Liu JW, Wang YH, Huang JY, Chen SC, Yang SF, and Wang PH (2019). The conditions under which piracetam is used and the factors that can improve national institute of health stroke scale score in ischemic stroke patients and the importance of previously unnoticed factors from a hospital-based observational study in Taiwan. Journal of Clinical Medicine, 8(1): 122. DOI: https://www.doi.org/10.3390/jcm8010122

Chidambaram SB, Anand N, Varma SR, Ramamurthy S, Vichitra C, Sharma A, Mahalakshmi AM, and Essa MM (2024). Superoxide dismutase and neurological disorders. IBRO Neuroscience Reports, 16: 373-394. DOI: https://www.doi.org/10.1016/j.ibneur.2023.11.007

Ciobanu O, Elena Sandu R, Tudor Balseanu A, Zavaleanu A, Gresita A, Petcu EB, Uzoni A, and Popa-Wagner A (2017). Caloric restriction stabilizes body weight and accelerates behavioral recovery in aged rats after focal ischemia. Aging Cell, 16(6): 1394-1403. DOI: https://www.doi.org/10.1111/acel.12678

Ciryam P, Gerzanich V, and Simard JM (2023). Interleukin-6 in traumatic brain injury: A janus-faced player in damage and repair. Journal of Neurotrauma, 40(21-22): 2249-2269. DOI: https://www.doi.org/10.1089/neu.2023.0135

Dhanasekara CS, Kahathuduwa CN, Quispe-Orozco D, Ota R, Duarte Celada WR, and Bushnaq S (2024). Effects of social determinants of health on acute stroke care among patients with acute ischemic stroke: A retrospective cohort study. Neurology, 103(9): e209951. DOI: https://www.doi.org/10.1212/WNL.0000000000209951

Erta M, Quintana A, and Hidalgo J (2012). Interleukin-6, a major cytokine in the central nervous system. International Journal of Biological Sciences, 8(9): 1254-1266. DOI: https://www.doi.org/10.7150/ijbs.4679

Feng Q, Wang YI, and Yang Y (2015). Neuroprotective effect of interleukin-6 in a rat model of cerebral ischemia. Experimental and Therapeutic Medicine, 9(5): 1695-1701. DOI: https://www.doi.org/10.3892/etm.2015.2363

Golenia A and Olejnik P (2025). The role of oxidative stress in ischaemic stroke and the influence of gut microbiota. Antioxidants, 14(5): 542. DOI: https://www.doi.org/10.3390/antiox14050542

Graça SC, Mosca T, Gagliardi VDB, Forte WCN, and Gagliardi RJ (2024). Prognostic impact of neutrophil-to-lymphocyte ratio in ischemic stroke. Journal of Personalized Medicine, 14(12): 1149. DOI: https://www.doi.org/10.3390/jpm14121149

Grebenciucova E and VanHaerents S (2023). Interleukin 6: At the interface of human health and disease. Frontiers in Immunology, 14: 1255533. DOI: https://www.doi.org/10.3389/fimmu.2023.1255533

Haorah J, Floreani NA, Knipe B, and Persidsky Y (2011). Stabilization of superoxide dismutase by acetyl-l-carnitine in human brain endothelium during alcohol exposure: novel protective approach. Free Radical Biology and Medicine, 51(8): 1601-1609. DOI: https://www.doi.org/10.1016/j.freeradbiomed.2011.06.020

Hidayah JH, Prakoso YA, and Widyarini S (2023). Brain histopathological changes after treatment using calabash fruit (*Crescentia cujete* L.) in rat model with artificially induced ischemic stroke. Advance in Animal and Veterinary Science, 11(12): 2003-2009. DOI: http://www.doi.org/10.17582/journal.aavs/2023/11.12.2003.2009

Hunsaker JJH, Wyness SP, Snow TM, and Genzen JR (2016). Clinical performance evaluation of total protein measurement by digital refractometry and characterization of non-protein solute interferences. Practical Laboratory Medicine, 6: 14-24. DOI: https://www.doi.org/10.1016/j.plabm.2016.08.001

Jickling GC, Liu D, Ander BP, Stamova B, Zhan X, and Sharp FR (2015). Targeting neutrophils in ischemic stroke: translational insights from experimental studies. Journal of Cerebral Blood Flow and Metabolism, 35(6): 888-901. DOI: https://www.doi.org/10.1038/jcbfm.2015.45

Jin X, Wang RH, Wang H, Long CL, and Wang H (2015). Brain protection against ischemic stroke using choline as a new molecular bypass treatment. Acta Pharmacologica Sinica, 36(12): 1416-1425. DOI: https://www.doi.org/10.1038/aps.2015.104

Jung JE, Kim GS, and Chan PH (2011). Neuroprotection by interleukin-6 is mediated by signal transducer and activator of transcription 3 and antioxidative signaling in ischemic stroke. Stroke, 42(12): 3574-3579. https://www.doi.org/10.1161/STROKEAHA.111.626648

Kalani R, Bartz TM, Psaty BM, Elkind MSV, Floyd JS, Gerszten RE, Shojaie A, Heckbert SR, Bis JC, Austin TR et al. (2023). Plasma proteomic associations with incident ischemic stroke in older adults: The cardiovascular health study. Neurology, 100(21): e2182-e2190. DOI: https://www.doi.org/10.1212/WNL.0000000000207242

Kellert L, Herweh C, Sykora M, Gussmann P, Martin E, Ringleb PA, Steiner T, and Bösel J (2012). Loss of penumbra by impaired oxygen supply? Decreasing hemoglobin levels predict infarct growth after acute ischemic stroke: Stroke: Relevant impact of hemoglobin, haematocrit and transfusion (STRAIGHT) - An observational study. Cerebrovascular Diseases Extra, 2(1): 99-107. DOI: https://www.doi.org/10.1159/000343731

Khandait V and Barai P (2019). Study of fibrinogen levels in patients of acute stroke. International Journal of Research in Medical Sciences, 7(1):20-24. DOI: http://www.doi.org/10.18203/2320-6012.ijrms20185356

Kosenko PO, Smolikov AB, Voynov VB, Shaposhnikov PD, Saevskiy AI, and Kiroy VN (2020). Effect of xylazine-tiletamine-zolazepam on the local field potential of the rat olfactory bulb. Comparative Medicine, 70(6): 492-498. https://www.doi.org/10.30802/AALAS-CM-20-990015

Liang Y, Chen J, Chen Y, Tong Y, Li L, Xu Y, and Wu S (2025). Advances in the detection of biomarkers for ischemic stroke. Frontiers in Neurology, 16: 1488726. DOI: https://www.doi.org/10.3389/fneur.2025.1488726

Lowry CA and Jin AY (2020). Improving the social relevance of experimental stroke models: social isolation, social defeat stress and stroke outcome in animals and humans. Frontiers in Neurology, 11: 427. DOI: https://www.doi.org/10.3389/fneur.2020.00427

Ma ZY, Zhang XF, Hu YZ, Zhu MD, Jin J, and Qian P (2024). Comparison of staining quality between rapid and routine hematoxylin and eosin staining of frozen breast tissue sections: An observational study. The Journal of International Medical Research, 52(6): 3000605241259682. DOI: https://www.doi.org/10.1177/03000605241259682

Mu C, Wang Y, Han C, Song H, Wu Q, Yang J, Guo N, Ma Y, Zhang C, Zhang J et al. (2023). Crosstalk between oxidative stress and neutrophil response in early ischemic stroke: a comprehensive transcriptome analysis. Frontiers in Immunology, 14: 1134956. DOI: https://www.doi.org/10.3389/fimmu.2023.1134956

Paliwal P, Dash D, and Krishnamurthy S (2018). Pharmacokinetic study of piracetam in focal cerebral ischemic rats. European Journal of Drug Metabolism and Pharmacokinetics, 43(2): 205-213. https://www.doi.org/10.1007/s13318-017-0435-9

Pawluk H, Tafelska-Kaczmarek A, Sopońska M, Porzych M, Modrzejewska M, Pawluk M, Kurhaluk N, Tkaczenko H, and Kołodziejska R (2024). The Influence of oxidative stress markers in patients with ischemic stroke. Biomolecules, 14(9): 1130. DOI: https://www.doi.org/10.3390/biom14091130

Prakoso YA, Susilo A, and Widyarini S (2024a). The standardization and efficacy of fermented *Crescentia cujete* (L.) in combination with enrofloxacin against artificially induced pneumonic pasteurellosis in rat models. Open Veterinary Journal, 14(12): 3404-3416. DOI: https://www.doi.org/10.5455/OVJ.2024.v14.i12.25

Prakoso YA, Hidayah JH, and Widyarini S (2024b). Fermented calabash fruit-derived choline (*Crescentia cujete* L.) against artificial-induced ischemic stroke in rat models: Analysis of N/LR, PWR, histopathology, GM-CSF, and VEGF. Journal of Applied Pharmaceutical Science. 14(11): 82-92. DOI: http://www.doi.org/10.7324/JAPS.2024.188046

Prakoso YA, Sigit M, and Aliviameita A (2023). Standardization of the simple methodology for experimentally induced ischemic stroke in rat models. World's Veterinary Journal, 13(4): 510-519. DOI: https://www.doi.org/10.54203/scil.2023.wvj54

Prasad MK, Marandi S, Mishra B, Guria RT, Kumar A, Birua H, Ray HN, Dungdung A, Kumar D, and Maitra S (2023). Association of fibrinogen with ischemic stroke: A systematic review and meta-analysis. Cureus, 15(1): e34335. DOI: https://www.doi.org/10.7759/cureus.34335

Ricci S, Celani MG, Cantisani TA, and Righetti E (2012). Piracetam for acute ischaemic stroke. The Cochrane Database of Systematic Reviews, 2012(9): CD000419. DOI: https://www.doi.org/10.1002/14651858.CD000419.pub3

Schlimp CJ, Khadem A, Klotz A, Solomon C, Hochleitner G, Ponschab M, Redl H, and Schöchl H (2015). Rapid measurement of fibrinogen concentration in whole blood using a steel ball coagulometer. The Journal of Trauma and Acute Care Surgery, 78(4): 830-836. DOI: https://www.doi.org/10.1097/TA.0000000000000546

Tirandi A, Sgura C, Carbone F, Montecucco F, and Liberale L (2023). Inflammatory biomarkers of ischemic stroke. Internal and Emergency Medicine, 18(3): 723-732. DOI: https://www.doi.org/10.1007/s11739-023-03201-2

Wijayanti AD, Prakoso YA, and Isla KJV (2024). Effects of fermented *Crescentia cujete* L. on the profile of hematology, clinical chemistry, and circulatory CD4+/CD8+ in Sprague Dawley rats. Open Veterinary Journal, 14(9): 2475-2483. DOI: https://www.doi.org/10.5455/OVJ.2024.v14.i9.36

Wilujeng S, Prakoso YA, and Wirjaatmadja R (2023). Effects of extraction, fermentation, and storage processes on the level of choline derived from calabash fruit (*Crescentia cujete* L.). Journal of Research in Pharmacy, 27(2): 620-626. DOI: http://www.doi.org/10.29228/jrp.3443

Winblad B (2005). Piracetam: A review of pharmacological properties and clinical uses. CNS Drug Reviews, 11(2): 169-182. DOI: https://www.doi.org/10.1111/j.1527-3458.2005.tb00268.x

Yang M, Pan Y, Li Z, Yan H, Zhao X, Liu L, Jing J, Meng X, Wang Y, and Wang Y (2019). Platelet count predicts adverse clinical outcomes after ischemic stroke or tia: subgroup analysis of CNSR II. Frontiers in Neurology, 10: 370. DOI: https://www.doi.org/10.3389/fneur.2019.00370

Zhang MS, Liang JH, Yang MJ, Ren YR, Cheng DH, Wu QH, He Y, and Yin J (2022). Low serum superoxide dismutase is associated with a high risk of cognitive impairment after mild acute ischemic stroke. Frontiers in Aging Neuroscience, 14: 834114. DOI: https://www.doi.org/10.3389/fnagi.2022.834114

Zhao Y, Zhang X, Chen X, and Wei Y (2022). Neuronal injuries in cerebral infarction and ischemic stroke: From mechanisms to treatment (Review). International Journal of Molecular Medicine, 49(2): 15. DOI: https://www.doi.org/10.3892/ijmm.2021.5070

Zhong C, Lu Z, Che B, Qian S, Zheng X, Wang A, Bu X, Zhang J, Ju Z, Xu T et al. (2021). Choline pathway nutrients and metabolites and cognitive impairment after acute ischemic stroke. Stroke, 52(3): 887-895. DOI: https://www.doi.org/10.1161/STROKEAHA.120.031903

Publisher's note: Scienceline Publication Ltd. remains neutral with regard to jurisdictional claims in published maps and institutional affiliations.

Open Access: This article is licensed under a Creative Commons Attribution 4.0 International License, which permits use, sharing, adaptation, distribution and reproduction in any medium or format, as long as you give appropriate credit to the original author(s) and the source, provide a link to the Creative Commons licence, and indicate if changes were made. The images or other third party material in this article are included in the article's Creative Commons licence, unless indicated otherwise in a credit line to the material. If material is not included in the article's Creative Commons licence and your intended use is not permitted by statutory regulation or exceeds the permitted use, you will need to obtain permission directly from the copyright holder. To view a copy of this licence, visit https://creativecommons.org/licenses/by/4.0/.
© The Author(s) 2025

2025, Scienceline Publication
World's Veterinary Journal
World Vet J, 15(4): 854-862.
ISSN 2322-4568

DOI: https://dx.doi.org/10.54203/scil.2025.wvj87
PII: S232245682500087-15

Molecular Detection of *Streptococcus equi* subsp. *Zooepidemicus* and *equi* in Guinea Pig with Lymphadenitis by Targeting the *comB* and *seeI* Genes

Diana Liseth Arista Vargas[1], Jakson Jacob Socrates Chuquimia Del Solar[1], Jhorsan David Mauri Pablo[1], Elthon Thomas Hinojosa Enciso[1], Jorge Luis Maicelo Quintana[2], and Marco Rainer Lopez Lapa[1]*

[1]*Molecular Physiology Laboratory, Institute of Livestock and Biotechnology Research, Faculty of Animal Science Engineering, Agribusiness and Biotechnology, Nacional Toribio Rodríguez de Mendoza de Amazonas University, Chachapoyas 01001, Peru*

[2]*Faculty of Animal Science Engineering, Agribusiness and Biotechnology, Nacional Toribio Rodríguez de Mendoza de Amazonas University, Chachapoyas 01001, Peru*

*Corresponding author's Email: rainer.lopez@untrm.edu.pe

ORIGINAL ARTICLE
Received: September 30, 2025
Revised: October 28, 2025
Accepted: November 29, 2025
Published: December 25, 2025

ABSTRACT

Despite the economic and sanitary relevance of cervical lymphadenitis in guinea pigs, little molecular information is available regarding the role of *Streptococcus* (*S.*) *equi* subspecies in cervical lymphadenitis in Peru. The present study aimed to identify the subspecies *S. equi* subsp. *zooepidemicus* (SEZ) and *S. equi* subsp. *equi* (SEE) in guinea pigs (*Cavia porcellus*), with and without cervical lymphadenitis, from the Amazonas and Cajamarca regions of Peru, using PCR amplification of the *sodA*, *comB*, and *seeI* genes. A total of 50 guinea pigs, aged 6-8 months, were evaluated, 30 from Cajamarca (mean weight 1210.1 grams; 22 Peruvian breed, 1 Inti, and 7 Brown) and 20 from Amazonas (mean weight 950 grams; 10 Peruvian breed and 10 Inti), comprising 30 animals with cervical lymphadenitis and 20 clinically healthy animals. The *sodA* gene was first employed as a preliminary diagnostic marker, which confirmed the presence of *S. equi* in all animals presenting lymphadenitis. Subsequent amplification of the *comB* gene confirmed the exclusive presence of SEZ in all clinical cases, with no detection in the 20 clinically healthy guinea pigs analyzed in both study regions. In contrast, the *seeI* gene, specific to SEE, indicated no amplification in any of the samples, indicating the absence of SEE in the study population. The prevalence of SEZ (positive *comB*) among guinea pigs with cervical lymphadenitis was 100% in Amazonas (10/10; 95% CI: 69.2-100%) and 100% in Cajamarca (20/20; 95% CI: 83.2-100%), with no significant difference between regions. The present findings established SEZ as the primary etiological agent of cervical lymphadenitis in guinea pigs from both regions, with no molecular evidence of SEE. The present study underscored the utility of *comB* and *seeI* as specific and reliable molecular markers for differentiating SEZ and SEE.

Keywords: *comB* gene, Guinea pig, *seeI* gene, *Streptococcus equi* subsp. *equi*, *Streptococcus equi* subsp. *zooepidemicus*

INTRODUCTION

Streptococcus (*S.*) *equi* subsp. *zooepidemicus* (SEZ) and *S. equi* subsp. *equi* (SEE) are Gram-positive cocci belonging to Lancefield group C (Bustos et al., 2017; Martínez et al., 2021). The SEZ is part of the upper respiratory tract microbiota of equids but can act as an opportunistic pathogen causing rhinitis, pneumonia, mastitis, and other infections in different hosts, including guinea pigs (Pelkonen et al., 2013; Quispe Avendaño, 2019). By contrast, SEE is responsible for strangles in horses, a transmissible condition that produces purulent swelling and abscess formation in the cervical and head lymph nodes (Alber et al., 2004; Bustos et al., 2017).

The biochemical differentiation of *S. equi* subspecies is generally based on sugar fermentation patterns. Typically, strains that ferment trehalose and lactose are classified as *zooepidemicus* subspecies, whereas those that ferment only salicin are identified as *equi* subspecies. However, atypical isolates exhibiting variable fermentation profiles have been documented, suggesting that these characteristics may not be uniformly exhibited across all strains (Abreu et al., 2016). However, due to the complexity of taxonomic differentiation between SEE and SEZ using conventional microbiological methods, molecular techniques such as polymerase chain reaction (PCR) targeting specific marker genes have been employed for more precise identification (Alber et al., 2004; Bustos et al., 2017). One of the most widely used molecular markers for preliminary detection of the genus *Streptococcus* and particularly *S. equi* is the *sodA* gene, which encodes a superoxide dismutase (Alber et al., 2004; 2005); however, *sodA* does not permit differentiation between the

To cite this paper: Vargas DLA, Solar JJSCD, Pablo JDM, Enciso ETH, Quintana JLM, and Lapa MRL (2025). Molecular Detection of *Streptococcus equi* subsp. *Zooepidemicus* and *equi* in Guinea Pig with Lymphadenitis by Targeting the comB and seeI Genes. *World Vet. J.*, 15(4): 854-862. DOI: https://dx.doi.org/10.54203/scil.2025.wvj87

zooepidemicus and *equi* subspecies (Alber et al., 2004). Therefore, in the present study, *sodA* was employed as a preliminary diagnostic tool to confirm the presence of *S. equi* in guinea pigs with cervical lymphadenitis.

Moreover, several molecular markers have been investigated in *S. equi* subspecies, including *seeI* (Alber et al., 2004), as well as others such as *seem*, *szeL*, and *szeM* (Alber et al., 2005), which encode superantigenic proteins but are not consistently present across strains. Additional targets, such as *SzP* (Anzai et al., 2002) and *comB* (Morris et al., 2023), have also been explored for diagnostic purposes. In the present study, *seeI* and *comB* were selected, following initial screening with *sodA*, due to their high specificity for each subspecies. The *seeI* gene encodes an exotoxin present only in SEE (Alber et al., 2004), whereas the *comB* gene is part of the genetic competence system of SEZ (Morris et al., 2023), which allows the simultaneous detection of both subspecies by PCR.

In guinea pigs (*Cavia porcellus*), *SEZ* is the primary causative agent of cervical lymphadenitis, a disease characterized by abscesses in the neck lymph nodes, and causes significant economic losses for small farmers (Quispe Avendaño, 2019; Jara et al., 2023). Recent studies in Peru have reported a high frequency of *Streptococcus* spp. associated with cervical abscesses in guinea pigs, with prevalence values exceeding 90% in Cusco, Peru (Angulo-Tisoc et al., 2021), while Vargas-Rocha et al. (2023) highlighted that cervical lymphadenitis remains one of the primary infectious diseases affecting guinea pig farming in the country. Despite its impact, there is limited molecular information on SEZ in guinea pig farming in Peru. Therefore, the present study aimed to confirm the presence of *SEZ* and to determine whether *SEE* is present in guinea pigs with and without cervical lymphadenitis from two regions of Northern Peru (Amazonas and Cajamarca), using PCR amplification of *sodA*, *seeI*, and *comB* marker genes.

MATERIALS AND METHODS

Ethical approval

The present study was approved by the Institutional Research Ethics Committee of the Toribio Rodríguez de Mendoza National University of Amazonas, Peru (CIEI-Nº0050). All animal procedures were carried out in accordance with animal welfare principles.

Animal selection, treatment, and sampling

Fifty domestic guinea pigs aged 6-8 months, from the provinces of Luya (Amazonas region) and Cajamarca (Cajamarca region), were selected. The animals from Cajamarca (n = 30) were all females, with a mean weight of 1210.1 g, and included 22 of the Peruvian breed, one Inti, and seven Brown. The animals from Amazonas (n = 20) comprised 13 females and seven males, with a mean weight of 950 g, and included 10 of the Peruvian breed and 10 Inti. A specialist in small animal health, who graduated from the National University Toribio Rodriguez de Mendoza, Peru, identified guinea pigs with signs compatible with cervical lymphadenitis, such as external neck abscess, enlarged lymph nodes, low weight, and nasal discharge, according to diagnostic criteria reported by Quispe Avendaño (2019) and Vargas-Rocha et al. (2023).

A total of 50 guinea pigs were evaluated, comprising four groups, including 20 with cervical lymphadenitis and 10 clinically healthy from Cajamarca (Table 1) and 10 with cervical lymphadenitis and 10 clinically healthy from Amazonas (Table 2).

Each animal was considered a biological replicate, and all PCR assays were performed in duplicate to confirm reproducibility. All selected animals were transported to the laboratory for processing. The guinea pigs had been raised under traditional farming conditions, at ambient temperatures ranging from 8 to 23°C and relative humidity of 60-70%. Their diet consisted of elephant grass (*Cenchrus purpureus*), alfalfa (*Medicago sativa*), and commercial concentrate (MESAJU, Peru), provided twice daily (morning and afternoon). Each animal received a daily total equivalent to approximately 5% of its live weight in concentrate and 30% of its live weight in fresh forage, with water available *ad libitum*. Feeding management was based on local practices described by Andrade-Yucailla et al. (2016). None of the guinea pigs had been vaccinated. The animals were housed in pens made of bricks (34.5 cm wide × 192 cm long × 15.8 cm deep) and were between 6 and 8 months of age at the time of sampling. The study was conducted in three months. Each guinea pig was administered an intraperitoneal anesthetic of ketamine (40 mg/kg; Ambavet, Ecuador) with xylazine (5 mg/kg; Ambavet, Ecuador); afterward, euthanasia was performed by an overdose of T-61 (Intervet International GmbH, Germany) at 0.5-2 mL per animal, depending on size through intrapulmonary injection for small rodents, as recommended by the manufacturer and following guidelines for the humane sacrifice of rodents (CONCEA, 2016).

Table 1. General characteristics of the guinea pigs selected from Cajamarca, Peru, according to the breed, weight, and sex.

Individual	Breed	Weight (g)	Sex
21C	Peru	1500	Female
22C	Peru	1000	Female
23C	Brown	1100	Female
24C	Peru	1400	Female
25C	Peru	1300	Female
26C	Peru	1500	Female
27C	Peru	1150	Female
28C	Peru	1500	Female
29C	Peru	1450	Female
30C	Brown	1550	Female
31C	Brown	1156	Female
32C	Brown	1157	Female
33C	Brown	1140	Female
34C	Peru	1150	Female
35C	Peru	1200	Female
36C	Peru	1050	Female
37C	Peru	1250	Female
38C	Peru	1300	Female
39C	Peru	1100	Female
40C	Peru	1550	Female
41C	Peru	1000	Female
42C	Peru	1100	Female
43C	Peru	950	Female
44C	Peru	1050	Female
45C	Peru	1250	Female
46C	Peru	1250	Female
47C	Brown	1150	Female
48C	Inti	1000	Female
49C	Brown	1050	Female
50C	Peru	1000	Female

Table 2. General characteristics of the guinea pigs selected from Amazonas, Peru, according to breed, weight, and sex

Individual	Breed	Weight (g)	Sex
1L	Peru	1500	Female
2L	Peru	1450	Female
3L	Peru	850	Male
4L	Peru	1200	Female
5L	Peru	650	Female
6L	Inti	1050	Female
7L	Inti	900	Female
8L	Inti	600	Female
9L	Inti	650	Female
10L	Inti	450	Male
11L	Inti	950	Male
12L	Inti	800	Female
13L	Inti	1050	Male
14L	Inti	1350	Male
15L	Inti	700	Female
16L	Peru	1200	Female
17L	Peru	800	Female
18L	Peru	1500	Female
19L	Peru	550	Male
20L	Peru	800	Male

Sample collection

Necropsies were conducted under sterile conditions, and the inflamed lymph nodes were collected from each guinea pig with cervical lymphadenitis. In the healthy guinea pigs, the corresponding healthy cervical lymph nodes were collected as control samples. No deaths occurred during the study. In total, samples were obtained from 50 guinea pigs; 20 with lymphadenitis and 10 clinically healthy animals from Cajamarca, and 10 with lymphadenitis and 10 clinically healthy animals from Amazonas. Each animal represented one independent sample. Sample collection and handling were performed under sterile conditions following general procedures for lymph node sampling in guinea pigs with lymphadenitis as described by Vargas-Rocha et al. (2023). The DNA extraction and downstream processing followed internal laboratory protocols routinely used for bacterial molecular analyses. The collection of cervical lymph nodes from guinea pigs with lymphadenitis and from clinically healthy animals was conducted within the microbiology laboratory inside a Class II biosafety cabinet (Biobase, USA). Upon excision, all tissues, including abscesses and/or lymph nodes, were initially rinsed with saline solution. Each sample was placed into a sterile 50 mL tube containing saline solution. For samples from animals with lymphadenitis, the tubes were treated with UV light for 15 minutes inside the biosafety cabinet to reduce excess purulent content. Approximately 50 mg of material was then collected from each sample using specific methods according to health status. In infected animals, purulent exudate was collected by sectioning the lymph node with a sterile scalpel, and in healthy guinea pigs, lymphatic tissue was homogenized into a fine powder using a mortar and pestle with liquid nitrogen. All resulting samples were transferred to 1.5 mL tubes and suspended in 160 µL of sterile PBS buffer (Thermo Fisher Scientific, USA). To prevent cross-contamination, all instruments were disinfected with 70% ethanol across samples. Samples were stored at 4°C until all animals were processed, with an average interval of approximately two hours between collection and genomic DNA extraction. This protocol minimized handling time and maintained the cold chain, thereby preventing DNA degradation and contamination. All samples were processed for extraction on the same day.

Target primers

Genomic DNA (gDNA) was then isolated using the ReliaPrep™ gDNA tissue miniprep system kit (Promega, USA), incorporating an additional lysozyme treatment (20 mg/mL) to enhance bacterial cell lysis, followed by the addition of 20 µL of proteinase K to ensure complete enzymatic digestion and release of genomic material. The resulting DNA was further purified with the genomic DNA clean and concentrator kit (Zymo Research Operations, USA). Quantification and purity assessment of gDNA was assessed with a NanoDrop One Spectrophotometer (Thermo Scientific, USA), and

To cite this paper: Vargas DLA, Solar JJSCD, Pablo JDM, Enciso ETH, Quintana JLM, and Lapa MRL (2025). Molecular Detection of *Streptococcus equi* subsp. *Zooepidemicus* and *equi* in Guinea Pig with Lymphadenitis by Targeting the comB and seeI Genes. *World Vet. J.*, 15(4): 854-862. DOI: https://dx.doi.org/10.54203/scil.2025.wvj87

only samples with a 260/280 ratio between 1.8 and 2.0 and a minimum concentration of 20 ng/µL were used for PCR analyses.

As an initial step in the molecular analysis, a preliminary diagnostic PCR was performed using the *sodA* gene as a universal marker for detecting *S. equi* (Alber et al., 2004; Mir et al., 2013). Primers described by Alber et al. (2004) were used, which amplified a conserved fragment of ~235 bp (Table 3). This PCR was designed to confirm the presence of *S. equi*, without discriminating between subspecies. The PCR program was based on the thermal profile described by Alber et al. (2004) with slight modifications. The reactions started with an initial denaturation at 94°C for two minutes, followed by 35 cycles consisting of denaturation at 94°C for 10 seconds, annealing at 56°C for 10 seconds, and extension at 72°C for 30 seconds. A final elongation step was performed at 72°C for five minutes.

Upon obtaining a positive confirmation with the *sodA* marker, specific amplification was performed for the molecular identification of SEZ and SEE, using the *comB* and *seeI* genes as targets, respectively. Specific primers according to Morris et al. (2023) were used for the *comB* primer (expected product ~450 bp) and a *seeI* primer (expected product 520 bp) according to Alber et al. (2004; Table 4). Each PCR assay was prepared in a final volume of 25 µL, which included 4 µL of genomic DNA template (≈100 ng), 12.5 µL of GoTaq® Green Master Mix 2X (Promega, USA), 1 µL of each primer (forward and reverse, 10 µM stock, final concentration 0.4 µM each), and 6.5 µL of nuclease-free water with standard ramp rates. Amplifications were performed in a thermocycler (Applied Biosystems SimpliAmp, USA). For the *comB* marker, the program started with denaturation at 95°C for two minutes, followed by 30 cycles of 95°C for 30 seconds, 55°C for 30 seconds, and 72°C for 15 seconds, and ended with a final extension at 72°C for five minutes. For the *seeI* marker, the program began with denaturation at 94°C for two minutes, then 35 cycles of 94°C for 10 seconds, 56°C for 10 seconds, and 72°C for 30 seconds, concluding with an extension at 72°C for five minutes. Each PCR run included a tube with no extracted gDNA and molecular-grade water as a negative control to rule out contamination. As positive controls, Kwik-Stik™ reference strains, including *Streptococcus equi* subsp. *equi* ATCC 33398 and *S. equi* subsp. *zooepidemicus* ATCC 700400, derived from the American type culture collection (ATCC, USA), were used. To minimize the risk of contamination, all PCR procedures were conducted following a unidirectional workflow, with physically separated areas designated for pre- and post-PCR operations. Reagent preparation was performed inside a Class II biosafety cabinet (Biobase, USA) using dedicated pipettes and aerosol-resistant filter tips. All reagents were aliquoted to prevent repeated freeze–thaw cycles. Work surfaces were routinely disinfected with sodium hypochlorite 10%, followed by ethanol 70% and UV light exposure before each use.

Table 3. Primers for amplification of the *sodA* gene for *Streptococcus equi* subsp. *zooepidemicus* and *Streptococcus equi subsp. equi*

Target gene	Primer	Sequence (5´-3´)	PCR product size (bp)	Reference
sodA	sodA equi/zooep-F	CAGCATTCCTGCTGACATTCGTCAGG	235	Alber et al. (2004)
	sodA equi/zooep-R	CTGACCAGCCTTATTATTCAACCAGCC		

Table 4. Primers for amplification of the *comB* gene for *Streptococcus equi* subsp. *zooepidemicus* and the *seeI* gene for *Streptococcus equi* subsp. *equi*

Target gene	Primer	Sequence	Expected product (pb)	Reference
comB	comB_F	GCTGGTTCAGGAGTGCAACA	450	Morris et al. (2023)
	comB_R	TTCGTGGAAAATCGTGCTGT		
seeI	seeI-F	GAAGGTCCGCCATTTTCAGGTAGTTTG	520	Alber et al. (2004)
	seeI-R	GCATACTCTCTCTGTCACCATGTCCTG		

Data analysis

The PCR products were analyzed by electrophoresis on agarose gels 2% in TAE buffer (Promega, USA), running at 100 V for 50 minutes. A 100 bp molecular weight marker (Promega and Novagen, USA) was used to compare and confirm the expected size of the amplified bands. The gels were visualized under UV transillumination and documented using a digital photodocumentation system (BIO-RAD, USA). For descriptive statistical analysis, the prevalence of SEZ (positive *comB*) in guinea pigs with cervical lymphadenitis was calculated for each region and overall. Exact binomial (Clopper-Pearson) 95% confidence intervals were estimated for each prevalence value, and Fisher's exact test at p = 1.00

was used to compare the proportions between regions (Amazonas compared to Cajamarca), which is appropriate for small and unequal sample sizes.

RESULTS

A total of 50 DNA samples from guinea pigs with cervical lymphadenitis and clinically healthy controls from the Amazonas and Cajamarca regions, Peru, were analyzed by conventional PCR. As the first step of the molecular analysis, amplification of the *sodA* was performed (Table 3). In Luya (Amazonas), 10 clinically healthy guinea pigs and 10 with cervical lymphadenitis were analyzed, and positive amplification of the *sodA* gene was observed in all the clinical cases (Figure 1). Meanwhile, in Cajamarca, 10 healthy guinea pigs and 20 with lymphadenitis were evaluated, and *sodA* gene amplification was detected in all clinical cases (Figure 2).

The prevalence of SEZ (positive *comB*) among guinea pigs with cervical lymphadenitis was 100% in Amazonas (10/10; 95% CI: 69.2-100%) and 100% in Cajamarca (20/20; 95% CI: 83.2-100%), with no significant difference between regions (Fisher's exact test, p = 1.00).

The amplification of the *comB* gene produced a specific amplicon of ~450 bp in all guinea pigs with cervical lymphadenitis sampled from both regions, whereas none of the healthy guinea pigs exhibited amplification of the *comB* gene (Figures 3 and 4). Notably, in the province of Luya (Amazonas), Peru, *comB* was found in all 10 guinea pigs with lymphadenitis and in none of the 10 healthy guinea pigs (Figure 3). Similarly, in the Cajamarca province, a positive *comB* amplification was observed in 20 out of 20 guinea pigs exhibiting lymphadenitis. In contrast, no positive results were observed in 10 healthy guinea pigs (Figure 4). The present results confirmed the presence of SEZ in all animals that presented cervical lymphadenitis, and the absence of SEZ in the clinically healthy guinea pigs examined. Additionally, the PCR tests for the *seeI* marker were negative in 100% of the samples. No amplification of *seeI* was detected in any guinea pig. The molecular detection by *seeI*/*comB* PCR demonstrated that the cases of cervical lymphadenitis in guinea pigs from the provinces of Luya and Cajamarca, Peru, were associated with SEZ, with no evidence of the involvement of SEE in these populations (Figures 5 and 6).

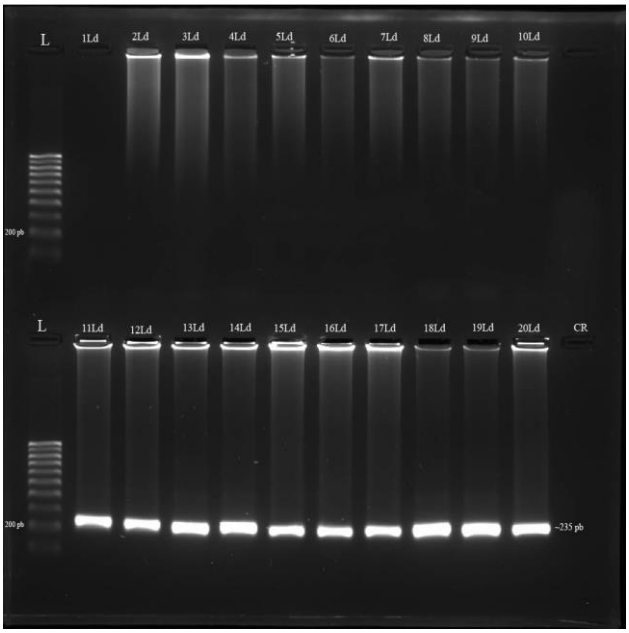


Figure 1. The PCR-amplified product of the *sodA* gene (~235 bp) for *Streptococcus equi* in guinea pigs aged 6-8 months with and without lymphadenitis from Amazonas, Peru. Lane L: 100 bp ladder, Lanes 1Ld-10Ld: Samples from healthy guinea pigs (negative for *S. equi*), Lanes 11Ld-20Ld: Samples from diseased guinea pigs (positive for *S. equi* at ~235 bp). Lane CR: Reagent control.

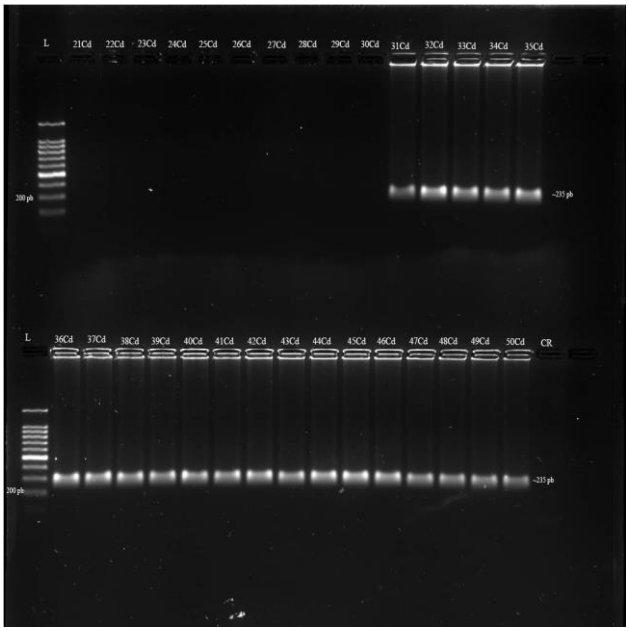


Figure 2. PCR-amplified product of the *sodA* gene (~235 bp) for *Streptococcus equi* in guinea pigs aged 6-8 months with and without lymphadenitis from Cajamarca, Peru. Lane L: 100 bp ladder, Lanes 21Cd-30Cd: Samples from healthy guinea pigs (negative for *S. equi*), Lanes 31Cc-50Cc: Samples from diseased guinea pigs (positive for *S. equi* at ~235 bp). Lane CR: Reagent control.

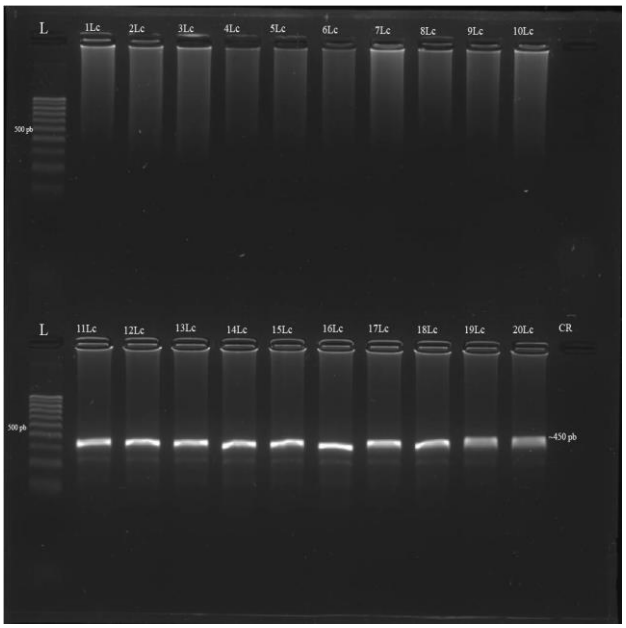


Figure 3. The PCR-amplified product of the *comB* gene (~450 bp) for *Streptococcus equi* subsp. *zooepidemicus* in guinea pigs aged 6-8 months without and with lymphadenitis from Amazonas, Peru. Lane L: 100 bp ladder (Novagen), Lanes 1Lc-10Lc: Samples from healthy guinea pigs (negative for *S. equi* subsp. *zooepidemicus*), Lanes 11Lc-20Lc: Samples from diseased guinea pigs (positive for *S. equi* subsp. *Zooepidemicus* at ~450 bp). Lane CR: Reagent control.

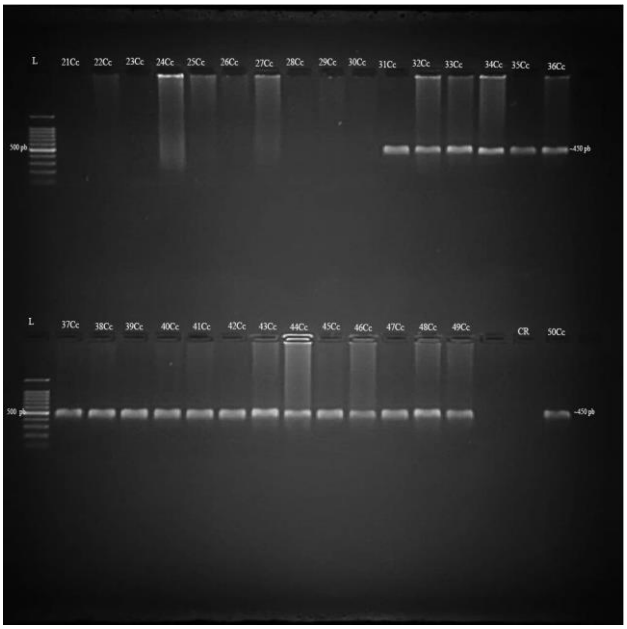


Figure 4. The PCR-amplified product of the *comB* gene (~450 bp) for *Streptococcus equi* subsp. *zooepidemicus* in guinea pigs aged 6-8 months without and with lymphadenitis from Cajamarca, Peru. Lane L: 100 bp ladder (Promega), Lanes 21Cc-30Cc: Samples from healthy guinea pigs (negative for *S. equi* subsp. *zooepidemicus*), Lanes 31Cc-50Cc: Samples from diseased guinea pigs (positive for *S. Equi* subsp. *Zooepidemicus* at ~450 bp), Lane CR: Reagent control.



Figure 5. The PCR-amplified product of the *seeI* gene (~520 bp) for *Streptococcus equi* subsp. *equi* in guinea pigs aged 6-8 months with and without lymphadenitis in Luya, Peru. Lane L: 100 bp ladder (Novagen), Lanes 1Ls-10Ls: Samples from healthy guinea pigs (negative for *S. equi* subsp. *equi*), Lanes 11Ls-20Ls: Samples from diseased guinea pigs (negative for *S. equi* subsp. *equi*), Lane CR: reagent control.

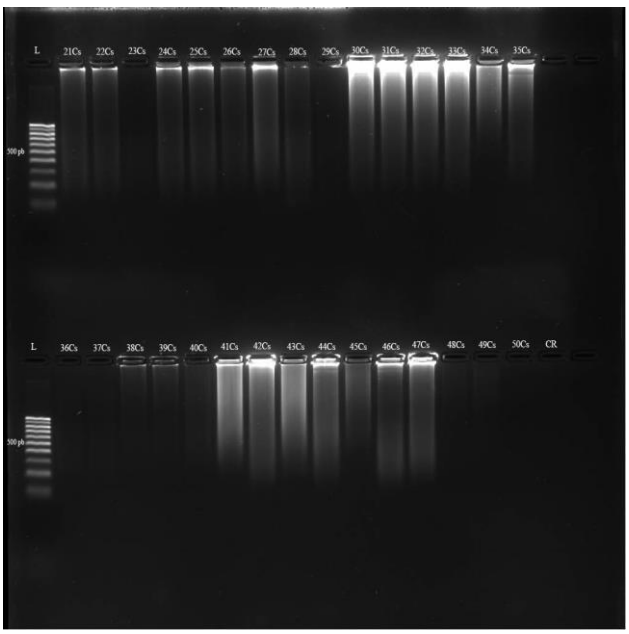


Figure 6. The PCR-amplified product of the *seeI* gene (~520 bp) for *Streptococcus equi* subsp. *equi* in guinea pigs aged 6-8 months with and without lymphadenitis in Cajamarca, Peru. Lane L: 100 bp ladder (Novagen), Lanes 21Cs-50Cs: Samples from healthy and diseased guinea pigs (negative for *S. equi* subsp. *equi*), Lane CR: Reagent control.

DISCUSSION

The detection of SEZ in guinea pigs with cervical lymphadenitis during the present study indicated its prevalence in the regions of Amazonas and Cajamarca in Peru. The SEZ was recognized as the leading cause of lymphadenitis in guinea pigs (Harkness et al., 2002). Additionally, severe outbreaks of cervical abscesses in Peruvian guinea pig farms have been attributed to SEZ (Jara et al., 2023). From a health and production perspective, early detection is crucial because SEZ is

an emerging zoonotic pathogen that can lead to severe infections in farm animals and humans (Jara et al., 2023). Since intensive guinea pig farming is an important economic activity in the Andean region of South America (Jara et al., 2023), an SEZ outbreak can result in substantial production losses due to mortality, growth retardation, or the culling of affected animals. The SEZ outbreaks are particularly relevant in some areas of the Amazonas and Cajamarca regions in Peru, where both large-scale and intensive production methods are employed, and where guinea pig farming serves as a primary source of livelihood income. Moreover, the zoonotic capability of SEZ poses risks to people who handle these animals, and human infection cases attributed to strains originating from guinea pigs have been documented (SHIC, 2021).

In the present study, SEZ was identified in guinea pigs with lymphadenitis from the provinces of Luya (Amazonas region) and Cajamarca, indicating that SEZ was present across different geographic regions of Northern Peru. In the Amazonas region, no previous studies have investigated lymphadenitis or the presence of SEZ, highlighting the importance of the present findings. In the case of Cajamarca, the presence of SEZ contrasted with the findings of Vargas-Rocha et al. (2023), who identified *Trueperella pyogenes* as the causative agent of cervical lymphadenitis in guinea pigs (*Cavia porcellus*) in Cajamarca, Peru, an uncommon pathogen associated with cervical abscesses in this species.

On the other hand, SEE was not detected in any of the sampled guinea pigs, which was consistent with its expected ecology, as SEE is a highly contagious pathogen of equids and is not part of the normal microbiota in rodents (SHIC, 2021). Therefore, the absence of SEE in guinea pigs, including those with cervical abscesses, indicated that SEE was not involved in the observed pathology. In addition, no evidence suggested that SEE was silently circulating in the facilities evaluated. Previous studies have not recorded the presence of SEE in guinea pigs, whereas SEZ has consistently been isolated as the causative agent of lymphadenitis in guinea pigs (Harkness et al., 2002; Jara et al., 2023), with documented outbreaks in guinea pig farms in the southern Peruvian Andes. This finding (absence of SEE in guinea pigs) during the present study confirmed that cervical abscesses in guinea pigs are almost always caused by SEZ rather than SEE. Therefore, the present findings reduce concerns about guinea pigs acting as a potential source of SEE or an equine-related zoonosis. According to previous reports, SEZ can act as an opportunistic pathogen in non-equine hosts, possibly entering through small oral lesions, whereas SEE requires horses as its natural host to persist and spread (SHIC, 2021). This distinction is consistent with the present findings, since SEZ was detected in guinea pigs with cervical abscesses, while SEE was absent in all samples.

Furthermore, the absence of SEZ in the clinically healthy guinea pigs analyzed in both regions indicated that, under the conditions studied, asymptomatic animals were not serving as silent carriers. The absence of SEZ in healthy guinea pigs is relevant because SEZ can be part of the commensal microbiota of the upper respiratory tract of different domestic animals, such as equines, swine, cattle, and dogs, and under certain conditions, SEZ may act as an opportunistic pathogen (Anzai et al., 2002). The current findings are consistent with those of Anzai et al. (2002), indicating that in guinea pigs, SEZ likely functions more as a pathogen than as part of normal microbiota. Although subclinical carriage of SEZ was not detected during the present study, its intermittent presence cannot be entirely excluded.

A notable aspect of the present study was indicating how the *comB* and *seeI* genes can effectively differentiate SEZ and SEE. The *equi* subspecies possesses exotoxin genes that are not found in *S. zooepidemicus*, a characteristic that has been previously exploited to specifically detect SEE by PCR in cases of strangles (Alber et al., 2004). In fact, amplification of the *seeI* gene has been successfully used to identify *S. equi* in equine samples, demonstrating greater sensitivity than traditional culture and enabling the detection of asymptomatic carriers following outbreaks of the disease (Alber et al., 2004). Meanwhile, the *comB* gene has emerged as a specific molecular target of SEZ, proposed in recently developed diagnostics to detect SEZ (Morris et al., 2023). The PCR assays targeting *comB* and *seeI* effectively differentiate between SEZ and SEE in the samples during the present study, which was essential considering their very close genetic relationship (98% DNA homology; SHIC, 2021). This molecular approach provided a rapid and reliable diagnosis, overcoming the limitations of conventional culture and biochemical identification methods, which can be slow or inconclusive when phenotypic traits overlap, as previously reported for detecting *S. equi* (Weese et al., 2023). Therefore, using specific PCR methods not only confirmed the pathogen responsible for cervical lymphadenitis in guinea pigs but also offered critical epidemiological insights to distinguish infections caused by SEZ from a potential introduction of SEE, aiding decision-making in animal health and guinea pig production in the Amazonas and Cajamarca regions of Peru (Jara et al., 2023).

The current study acknowledged several limitations. Firstly, its cross-sectional design restricts the ability to establish temporal or causal relationships between SEZ detection and disease onset (Setia, 2016). Additionally, while PCR is a sensitive method, it possesses an inherent detection limit and may produce false-negative results when the pathogen load is minimal. Therefore, negative findings in apparently healthy animals may not conclusively exclude the presence of low-level carriage.

CONCLUSION

Cervical lymphadenitis in guinea pigs from the Amazonas and Cajamarca regions in Peru was found to be exclusively associated with *Streptococcus equi* subsp. *zooepidemicus*. No evidence of *S. equi* subsp. *equi* was detected in the animals evaluated, which excludes the participation of *S. equi* subsp. *equi* in cervical lymphadenitis in guinea pigs. The *comB* (450 bp) and *seeI* (520 bp) genes proved to be effective molecular targets for differentiating *Streptococcus equi* subsp. *zooepidemicus* and *Streptococcus equi* subsp. *equi*. The use of these markers enabled a rapid and specific PCR-based diagnosis, overcoming the limitations of conventional culture or biochemical tests, and providing valuable epidemiological and health information for guinea pig farming in Peru. It would therefore be advisable to conduct studies with more sensitive molecular techniques, such as qPCR and longitudinal approaches, to achieve a more precise characterization of the health status of guinea pig populations.

DECLARATIONS

Authors' contributions

Diana Lizeth Arista Vargas was responsible for the conception and design of the study, acquired and analyzed the data, interpreted the findings, and drafted and critically revised the article. Jakson Jacob Socrates Chuquimia del Solar contributed to the study's design and the interpretation of the results, and critically revised the manuscript. Jhorsan David Mauri Pablo and Elthon Thomas Hinojosa Enciso were involved in analyzing the data, drafting the article, and critically revising its intellectual content. Jorge Luis Maicelo Quintana participated in the design of the study and critically revised the manuscript. Marco Rainer Lopez Lapa contributed to the conception of the study and critically revised the article. All authors have read and approved the final edition of the manuscript.

Ethical considerations

Ethical issues, including plagiarism, consent to publish, misconduct, data fabrication and/or falsification, double publication and/or submission, and redundancy, have been checked by all the authors. The authors confirmed that they have not assisted AI in conducting and preparing the present study.

Availability of data and materials

The data to support the present study's findings are available upon reasonable request to the corresponding author.

Funding

The present study was supported by project CUI N° 2254946, titled Creation of a Molecular Physiology Laboratory Service at the Faculty of Animal Science and Biotechnology at the National University Toribio Rodriguez de Mendoza, Peru, under the vice-rectorate for research at the National University Toribio Rodríguez de Mendoza, Amazonas, Peru, and contract PE501088227-2024-PROCIENCIA.

Competing interests

The authors declared no conflict of interest.

REFERENCES

Abreu MC, Do Monte LR, Moraes C, Leite FPL, and Nogueira CEW (2016). Biochemical identification of *streptococcus equi* strains isolated from equine guttural pouch washes. XVIII Scientific Initiation Congress, 2009, pp. 1-4. Available at: https://www2.ufpel.edu.br/cic/2009/cd/pdf/CA/CA_01403.pdf

Alber J, El-Sayed A, Estoepangestie S, Lämmler C, and Zschöck M (2005). Dissemination of the superantigen encoding genes *seeL*, *seeM*, *szeL*, and *szeM* in *Streptococcus equi* subsp. *equi* and *Streptococcus equi* subsp. *zooepidemicus*. Veterinary Microbiology, 109(1-2): 135-141. DOI: https://www.doi.org/10.1016/j.vetmic.2005.05.001

Alber J, El-Sayed A, Lämmler C, Hassan AA, Weiss R, and Zschöck M (2004). Multiplex polymerase chain reaction for identification and differentiation of *Streptococcus equi* subsp. *zooepidemicus* and *Streptococcus equi* subsp. *equi*. Journal of Veterinary Medicine, Series B, 51(10): 455-458. DOI: https://www.doi.org/10.1111/j.1439-0450.2004.00799.x

Andrade-Yucailla V, Fuentes I, Vargas-Burgos JC, Lima-Orozco R, and Jácome A (2016). Alimentación de cuyes en crecimiento-ceba a base de gramíneas tropicales adaptadas a la Región Amazónica [Feeding guinea pigs growing-fattening grass-based tropical adapted to the Amazon region]. Revista Electrónica de Veterinaria, 17(1): 1-7. Available at: https://redalyc.org/pdf/636/636460080003.pdf

Anzai T, Timoney JF, Kuwamoto Y, Wada R, Oikawa M, and Higuchi T (2002). Polymerase chain reaction-restriction fragment length polymorphism analysis of the SzP gene of Streptococcus *zooepidemicus* isolated from the respiratory tract of horses. American Journal of Veterinary Research, 63(9): 1298-1301. DOI: https://www.doi.org/10.2460/ajvr.2002.63.1298

Angulo-Tisoc J, Siuce J, and Jara LM (2021). Frequency of pathogens associated with cervical lymphadenitis in guinea pigs of family-commercial breeding centers in Cusco, Peru. Revista de Investigaciones Veterinarias del Perú, 32(1): e19505. DOI: https://www.doi.org/10.15381/rivep.v32i1.19505

Bustos CP, Guida N, Casamayor A, Muñoz AJ, Fernández-Garayzábal JF, and Vela Alonso AI (2017). First report of molecular characterization of Argentine isolates of *Streptococcus equi* subsp. equi by pulsed-field gel electrophoresis. Journal of Equine Veterinary Science, 53: 30-37. DOI: https://www.doi.org/10.1016/j.jevs.2017.01.007

National council for the control of animal experimentation (CONCEA) (2016). CONCEA regulations for the production, maintenance or use of animals in teaching or scientific research activities. Conselho Nacional de Controle de Experimentação Animal [National council for the control of animal experimentation], 3rd Edition, pp. 9-386. Available at: https://www.ceua.ufv.br/wp-content/uploads/2018/08/NORMATIVAS-DO-CONCEA-3%C2%AA-EDI%C3%87%C3%83O2.pdf

Harkness JE, Murray KA, and Wagner JE (2002). Biology and diseases of guinea pigs. Laboratory Animal Medicine, pp. 203-246. DOI: https://www.doi.org/10.1016/B978-012263951-7/50009-0

Jara LM, Angulo-Tisoc J, Giménez-Lirola LG, Li G, Andrade R, and Mamani J (2023). Outbreak of pathogenic *Streptococcus equi* subsp. *zooepidemicus* in guinea pigs farms of the Andean Region. Pathogens, 12(3): 445. DOI: https://www.doi.org/10.3390/pathogens12030445

Martínez D, Jorquera A, and Delpiano L (2021). Bacteremia by Streptococcus equi subspecie *zooepidemicus* in a young mother binomial. Revista Chilena de Infectología, 38(5): 702-706. DOI: https://www.doi.org/10.4067/s0716-10182021000500702

Mir IA, Kumar B, Taku A, Faridi F, Bhat MA, Baba NA, and Maqbool T (2013). Bacteriological and molecular detection of *Streptococcus equi* subsp. *equi* and *Streptococcus equi* subsp. *zooepidemicus* in equines of Northern India. Journal of Equine Science, 24(3): 53-55. DOI: https://www.doi.org/10.1294/jes.24.53

Morris ERA, Schroeder ME, Ferro PJ, Waller AS, McGlennon AA, Bustos CP, Gressler LT, Wu J, Lawhon SD, Boyle AG et al. (2023). Development of a novel real-time PCR multiplex assay for detection of *Streptococcus equi* subspecies equi and *Streptococcus equi* subspecies *zooepidemicus*. Veterinary Microbiology, 284: 109797. DOI: https://www.doi.org/10.1016/j.vetmic.2023.109797

Pelkonen S, Lindahl SB, Suomala P, Karhukorpi J, Vuorinen S, Koivula I, Väisänen T, Pentikäinen J, Autio T, and Tuuminen T (2013). Transmission of *Streptococcus equi* subspecies *zooepidemicus* Infection from horses to humans. Emerging Infectious Diseases, 19(7): 1041-1048. DOI: https://www.doi.org/10.3201/eid1907.121365

Quispe Avendaño MER (2019). Molecular sequencing of gen 16 S for the identification of the causal agent of lymphadenitis in cuyes (*Cavia porcellus*) Arequipa – 2017. Bachelor's Thesis, Universidad Catolica de Santa Maria, Peru. Available at: https://repositorio.ucsm.edu.pe/handle/20.500.12920/8993

Setia MS (2016). Methodology series module 3: Cross-sectional studies. Indian Journal of Dermatology, 61(3): 261-264. DOI: https://www.doi.org/10.4103/0019-5154.182410

Swine health information center (SHIC) (2021). *Streptococcus equi* subsp. *zooepidemicus* fact sheet. Available at: https://www.swinehealth.org/wp-content/uploads/2021/03/S.-Zoo-Fact-Sheet.pdf

Vargas-Rocha L, Malpartida-Aquino E, Medina-Sánchez W, Gómez-Sánchez J, Muñoz D, and Bustamante-Cabrera AM (2023). Isolation and sensitivity of cervical lymph node bacteria in cuyes (*Cavia porcellus*) with lymphadenitis in commercial family poultry farms in Cajamarca, Peru. Revista de Investigaciones Veterinarias del Perú, 34(1): e23026. DOI: https://www.doi.org/10.15381/rivep.v34i1.23026

Weese JS, Saab M, Moore A, Cai H, and McClure J (2023). Relationship between quantitative real-time PCR cycle threshold and culture for detection of Streptococcus equi subspecies equi. The Canadian Veterinary Journal, 64(6): 549-552. Available at: https://pmc.ncbi.nlm.nih.gov/articles/PMC10204887/

Publisher's note: Scienceline Publication Ltd. remains neutral with regard to jurisdictional claims in published maps and institutional affiliations.

Open Access: This article is licensed under a Creative Commons Attribution 4.0 International License, which permits use, sharing, adaptation, distribution and reproduction in any medium or format, as long as you give appropriate credit to the original author(s) and the source, provide a link to the Creative Commons licence, and indicate if changes were made. The images or other third party material in this article are included in the article's Creative Commons licence, unless indicated otherwise in a credit line to the material. If material is not included in the article's Creative Commons licence and your intended use is not permitted by statutory regulation or exceeds the permitted use, you will need to obtain permission directly from the copyright holder. To view a copy of this licence, visit https://creativecommons.org/licenses/by/4.0/.
© The Author(s) 2025

2025, Scienceline Publication
World's Veterinary Journal
World Vet J, 15(4): 863-881.
ISSN 2322-4568

DOI: https://dx.doi.org/10.54203/scil.2025.wvj88
PII: S232245682500088-15

Essential and Toxic Element Profiles in Selected Spices from Greater Casablanca, Morocco

Safaa Sabri[1], Chaima Sabri[2*], Mohamed Rida Salam[3], Fatiha El Mellouli[4], Asmaa Lafram[3], Hanane Khallouki[5], Yayé Abdou Hassane[6], and Mostafa Kabine[1]

[1]*Health and Environment Laboratory, Faculty of Sciences, Ain Chock, Hassan II University, Casablanca, Morocco*
[2]*Laboratory of Natural Resources and Sustainable Development, Research Unit on Metabolism, Physiology, and Nutrition, Department of Biology, Faculty of Science, Ibn Tofail University, Kenitra, Morocco*
[3]*Immunology and Biodiversity Laboratory, Faculty of Sciences, Ain Chock, Hassan II University, Casablanca, Morocco*
[4]*Regional Laboratory of Analysis and Research, National Office for Food Safety, Casablanca, Morocco*
[5]*Laboratory of Biochemistry, Environment and Agri-food, Faculty of Sciences and Technology of Mohammedia, Hassan II University, Casablanca, Morocco*
[6]*National Institute of Agricultural Research of Niger, Department of Animal Production, Niamey, Niger*

*Corresponding author's Email: sabri.chaima.2@gmail.com

ORIGINAL ARTICLE
Received: September 26, 2025
Revised: October 30, 2025
Accepted: November 28, 2025
Published: December 25, 2025

ABSTRACT

In Morocco, spices are an integral part of daily cuisine and serve as a vector of both nutritional and toxicological exposure. Monitoring elemental composition is essential to ensure consumer safety, animal health when used as feed additives, and compliance with international standards. The present study aimed to determine the concentrations of essential (potassium, calcium, magnesium, sodium, and iron) and toxic (lead, cadmium, arsenic, chromium, and nickel) elements in commonly consumed spices in Morocco, including cinnamon, cumin, ginger, black pepper, and turmeric. A total of 162 spice samples were obtained from markets in the Greater Casablanca, Morocco. Five essential elements, including potassium, calcium, magnesium, sodium, and iron, and five toxic trace metals, including lead, cadmium, arsenic, chromium, and nickel, were determined by inductively coupled plasma mass spectrometry (ICP-MS) after microwave-assisted digestion. Cumin indicated the highest levels of magnesium (6.86 ± 1.61 g/kg), sodium (3.98 ± 1.59 g/kg), calcium (11.13 ± 4.53 g/kg), and iron (753.71 ± 446.07 mg/kg). Turmeric had the highest levels of potassium (25.96 ± 13.51 g/kg). Cinnamon had elevated levels of lead (2.05 mg/kg) and cadmium (0.29 mg/kg), exceeding Moroccan and European regulatory limits. Additionally, cumin indicated the highest levels of arsenic (0.45 ± 0.30 mg/kg) and nickel (4.18 ± 2.85 mg/kg) compared to other spices. Principal component analysis (PCA) revealed distinct elemental patterns. The first component (PC1), driven by magnesium and sodium, clearly separated cumin due to its high macronutrient content. The second component (PC2), influenced by cadmium and lead, isolated cinnamon because of its toxic metal burden. The PC1 and PC2 accounted for 64.6% of the total variance. Turmeric and ginger formed a close cluster in the PCA plot, associated with higher levels of potassium, calcium, and nickel. Black pepper was positioned between these groups, reflecting intermediate composition. Pearson correlation analysis supported these findings, with a strong correlation between lead and cadmium, suggesting a shared contamination source. These results emphasized the nutritional and toxicological roles of spices in Moroccan diets. Regular monitoring is essential to protect public health in both animals and humans.

Keywords: Food safety, Inductively coupled plasma mass spectrometry, Spices, Toxic metal

INTRODUCTION

In many cultures, spices represent indispensable components of daily cooking, recognized for their sensory attributes as well as for their nutritional value and therapeutic potential (Peter, 2006; Embuscado, 2019). Spices provide bioactive compounds, dietary fiber, and micronutrients, particularly potassium (K), calcium (Ca), magnesium (Mg), sodium (Na), and iron (Fe), which play key roles in different physiological functions (Otunola et al., 2010). Cumin (*Cuminum cyminum* L.) is recognized for its richness in Fe and Mg (Bouhenni et al., 2019), while turmeric (*Curcuma longa* L.) is an essential source of K and antioxidant polyphenols (Saeed et al., 2021). Likewise, cinnamon provides high levels of Ca, Mg, and Fe (Gul and Safdar, 2009), ginger is rich in Ca and trace minerals such as Fe, copper (Cu), zinc (Zn), and manganese (Mn; Ayoade et al., 2023), and black pepper contains notable amounts of Ca, K, and essential trace elements (Ayoade et al., 2023).

Additionally, spices may be a potential dietary source of toxic metals such as lead (Pb), cadmium (Cd), arsenic (As), chromium (Cr), and nickel (Ni), which can adversely affect human health as shown by widespread contamination of spices with Pb, Cd, and As (Huff et al., 2025), and animal health even at minimal concentrations (Rahman and Singh, 2019). In animals, these elements can disrupt oxidative balance and damage key organs such as the liver, kidneys, and

To cite this paper: Safaa S, Sabri C, Salam MR, El Mellouli F, Lafram A, Khallouki H, Hassane YA, and Kabine M (2025). Essential and Toxic Element Profiles in Selected Spices from Greater Casablanca, Morocco. *World Vet. J.*, 15(4): 863-881. DOI: https://dx.doi.org/10.54203/scil.2025.wvj88

brain (Destro et al., 2025). Their presence in spices may result from soil contamination, the use of polluted irrigation water, atmospheric deposition, or inappropriate processing such as drying, grinding, or storage under unhygienic conditions (Osei-Safo et al., 2024). Several international surveys have demonstrated that spices marketed in both local and global markets may exceed the maximum limits of toxic trace metals set by national and international regulations. Moussa et al. (2024) reported that 50% of analyzed cinnamon samples from the Lebanese market exceeded the international safety limit for Pb, which was set at 0.3 mg/kg by Codex Alimentarius. In Pakistan, Olusola et al. (2025) documented elevated As concentrations in cumin, whereas in South Africa, Ezez et al. (2024) reported the occurrence of Cd in several spice varieties. These findings highlighted the need for strict monitoring of toxic trace metal concentrations in spices, particularly in developing countries where regulations may be less rigorously enforced (Akhtar et al., 2020).

Although spices are primarily associated with human nutrition, they are increasingly used in the formulation of natural additives and flavor enhancers in animal feed due to their antioxidant, antimicrobial, and growth-promoting properties (Windisch et al., 2008; Hashemi and Davoodi, 2011). However, their potential contamination with toxic trace elements raises concerns not only for human consumers but also for animal health and food safety within the livestock production chain (Jaishankar et al., 2014). Monitoring the elemental composition of spices is therefore essential to evaluate their safety and suitability for use in animal feed.

In Morocco, although a few studies have investigated the nutritional composition and metal contamination of certain spices (Bouzaid et al., 2024; Najem et al., 2024), data remain limited and do not cover all commonly consumed varieties. The Greater Casablanca region, the country's main urban and commercial center, constitutes a strategic market where spices from diverse geographic origins converge, potentially increasing the variability of elemental profiles and contamination levels (Boularbah et al., 2006). The present study aimed to determine the concentrations of essential (K, Ca, Mg, Na, Fe) and toxic (Pb, Cd, As, Cr, Ni) elements in five widely consumed spices in Morocco, including cinnamon, cumin, ginger, black pepper, and turmeric using inductively coupled plasma mass spectrometry (ICP-MS), and to assess potential risks to human and animal health through multivariate analysis and comparison with established limitations and existing data.

MATERIALS AND METHODS

Ethical approval

The present study was conducted *in vitro* according to the guidelines of the Faculty of Sciences, Ain Chock, Hassan II Casablanca University, Casablanca, Morocco.

Materials

Sample preparation was carried out in triplicate using a microwave digestion system (Milestone, Bergamo, Italy) equipped with temperature and pressure sensors. The system employed polytetrafluoroethylene (PTFE) vessels designed to withstand pressures up to 110 bar. An ICP-MS (Agilent Technologies, Santa Clara, CA, USA) was used for the spices analysis. The instrument was equipped with a standard Fassel-type plasma torch, featuring a 2.5 mm internal diameter. The ICP-MS operating conditions were specified with a forward power of 1.5 kW, a plasma gas flow of 15 L/min, an auxiliary gas flow of 0.8 L/min, a nebulizer gas flow of 1.06 L/min, and a spray chamber temperature maintained at 2°C. The ICP-MS was equipped with an off-axis ion lens, a quadrupole mass filter, and an electron multiplier detector, and it was further complemented by an ASX-520 autosampler (Cetac Technologies Inc., Omaha, NE, USA) and an integrated sample introduction system. High-purity argon (99.9998%) supplied by OXAIR (Morocco) was used. Before each experiment, the instrument was tuned for daily performance using 10 mL of the Elan 6100 DRC sensitivity detection limit solution (Perkin-Elmer Pure, USA).

Reagents

Concentrated analytical reagent grade nitric acid (HNO_3) 70% and hydrogen peroxide (H_2O_2) 30-32% were obtained from Merck (Darmstadt, Germany). Ultrapure deionized water with a resistivity of 18.2 MΩ·cm was obtained from a Milli-Q Plus water purification system (Millipore, Bedford, MA, USA). Stock standard solutions of Cr, Ni, As, Cd, and Pb (10 µg/mL in 2% HNO_3) and standard solutions of K, Ca, Na, Mg, and Fe (10,000 µg/mL in 5% HNO_3) were obtained from Agilent, Santa Clara, USA. Spinach leaves were used as a certified reference material because they were of plant origin, similar to spices. Standard reference material spinach leaves (SRM 1570a) was obtained from the National Institute of Standards and Technology, Gaithersburg, USA. Plastic and glass containers were soaked in 10% v/v HNO_3 for at least 24 hours and then thoroughly rinsed with Milli-Q water before use. All containers, polypropylene vials, pipette tips, and reagents that came into contact with samples or standard solutions were checked for potential contamination by analyzing reagent blanks under the same conditions.

Sample collection

A total of 137 bulk spice samples available on the market were collected from local markets across the greater Casablanca region, Morocco (Table 1). The samples were purchased at different times from February to June 2025. The spice samples were stored in clean, sealed containers at room temperature until further analysis, using the same analytical procedures and ICP-MS settings as for the samples.

Table 1. Distribution of spice samples sourced from greater Casablanca, Morocco, by type

Type of spice	Family	Part studied	Number of samples	Percentage (%)
Cumin	Apiaceae	Fruits	25	15.4
Cinnamon	Lauraceae	Bark	37	22.8
Turmeric	Zingiberaceae	Roots	25	15.4
Black pepper	Piperaceae	Fruits	25	15.4
Ginger	Zingiberaceae	Roots	25	15.4

Sample preparation and digestion

Exactly 1 g of each spice sample was weighed into a PTFE digestion vessel, followed by the addition of 5 mL of concentrated HNO_3 70% and 2 mL of H_2O_2 30-32%. The mixture was then digested using a microwave system, following a modified AOAC protocol (AOAC International, 2013). Microwave digestion started at 80°C for five minutes, followed by sequential heating to 120°C and 150°C, each for five minutes, then maintained at 180°C for 20 minutes before cooling to 40°C. Once cooled, the digests were brought to a final volume of 50 mL with ultrapure water, carefully labeled, and subsequently subjected to analysis. Control blanks were prepared in parallel using the identical procedure.

Quality assurance

For determining minor and trace elements in spices, the analytical assessment was validated by examining essential method performance parameters, including sensitivity, linearity, precision, accuracy, and recovery. The calibration process involved constructing curves based on the distinct concentrations of the standard solutions, including Na (0.5 mg/L), Mg (2.5 mg/L), K (5 mg/L), and Ca (50 mg/L), Fe (2, 10, 20, 100, and 200 µg/L), Cr (0.2 µg/L), Ni (1 µg/L), As (2 µg/L), Cd (10 µg/L), and Pb (20 µg/L). In addition, blanks were analyzed for each target element to verify linearity, and correlation coefficients (R^2) were subsequently calculated in accordance with the NF T90-210 standard (AFNOR, 2018).

Instrumental sensitivity was assessed by determining the detection limits for each of the analyzed elements, including Na, Mg, K, Ca, Fe, Cr, Ni, As, Cd, and Pb. The limits of detection (LOD) and limits of quantification (LOQ) were derived by dividing three and ten times the standard deviation of the blank, respectively, by the slope of the calibration curve. The calibration curves were designed to ensure that the concentrations of all analyte elements in the samples remained within the linear range and above the lower limit of linearity established for the method (Voica et al., 2021).

Method precision was verified through the analysis of an appropriate standard reference material (IAEA-407, International Atomic Energy Agency, Environment Laboratories, Monaco) to determine Na, Mg, K, Ca, Aluminium (Al), Mn, Fe, Cu, Zn, Cr, cobalt (Co), Ni, As, selenium (Se), Cd, and Pb. Precision was assessed by comparing the experimentally obtained concentrations of the elements with their certified reference values, and the results were expressed as percentage recovery. To ensure analytical quality control, spiking recovery tests were conducted following the general approach described by Mihaylova et al. (2013).

Statistical analysis

All statistical analyses were performed using R software (version 4.3.2, Posit Team, 2023). The raw multielement concentration data were first examined to detect potential outliers and missing values. The suitability of a factor analysis was initially assessed using the Kaiser-Meyer-Olkin (KMO) index (Kaiser, 1974) to measure sampling adequacy for studying inter-variable correlations. In parallel, Bartlett's test of sphericity (Bartlett, 1950) was applied to verify that the correlation matrix differed significantly from an identity matrix. A principal component analysis (PCA; Jolliffe and Cadima, 2016) was then conducted to reduce dimensionality and visually represent the variance gradients in the dataset. The first two principal components (PC1 and PC2) were used for graphical projection, enabling the potential clustering of samples based on their elemental profiles. To explore bivariate relationships between elements, Pearson correlation coefficients (r) were calculated (Pearson, 1895). Results were synthesized in a correlogram presented as a heatmap

(Friendly, 2002). Finally, a hierarchical cluster analysis (HCA) was performed using Ward's linkage method and Euclidean distance (Ward, 1963) to group samples or elements with similar concentration patterns. Statistical significance was considered at a p-value less than 5% ($p < 0.05$) for Bartlett's test and Pearson correlation coefficients.

RESULTS AND DISCUSSION

Validation of the analytical method

The ICP-MS method demonstrated strong performance in terms of reliability and robustness for the quantification of the target elements (Table 2). Linearity was excellent across all calibration curves, with correlation coefficients ranging from 0.9989 (Ca) to 0.9999 (Mg and Ni), significantly surpassing the standard acceptance limit of 0.995 for elemental quantification. The LOQ obtained was appropriate for trace and macro-elements. For trace elements (Cd, Pb, As, Cr, Ni, Fe), the LOQs were very low, ranging from 0.0030 µg/L (Cd) to 0.198 µg/L (Ni), thus enabling reliable detection at trace levels. In contrast, for macro-elements (K, Ca, Mg, Na), the LOQs were higher, ranging from 0.318 µg/L (Na) to 57.2 µg/L (K), which remains consistent with their naturally higher concentrations in food matrices (ICH, 2005).

The method demonstrated satisfactory precision, with relative standard deviations (RSD) ranging from 1.7% to 3.1%, well below the 5% acceptability criterion generally recommended for ICP-MS. Accuracy, evaluated through recovery rates, varied from 91.43% (K) to 105.12% (Pb), in compliance with international recommendations (80-120%). These results confirmed that the method of Food products-Determination of trace elements-Determination of arsenic, cadmium, mercury and lead by ICP-MS after pressure digestion (IMANOR, 2012) allowed reliable and reproducible quantification of both macro and trace elements, while maintaining a level of sensitivity appropriate for each element category.

Table 2. Linearity and precision of the analyzed elements, and validation through a standard reference material

Elements	R^2	LOQ (µg/L)	RSD	Recovery (%)
K	0.9992	57.2	1.7	91.43
Ca	0.9989	21.4	2.0	100.20
Mg	0.9999	0.350	1.8	98.65
Na	0.9996	0.318	1.8	91.49
Fe	0.9993	0.0793	2.5	99.25
Pb	0.9997	0.0250	3.1	105.12
Cd	0.9996	0.0030	2.5	102.22
As	0.9998	0.0078	2.2	92.65
Cr	0.9996	0.0522	2.0	97.74
Ni	0.9999	0.1980	2.9	99.24

R^2: Correlation coefficient, LOQ (µg/L): Limit of quantification, RSD: Relative standard deviation. Standard reference material: IAEA-407 established by the International Atomic Energy Agency, Environment Laboratories, Monaco.

Presence of multiple elements in spices

Toxic elements

The analysis of spice samples from the Greater Casablanca, Morocco, revealed measurable levels of five toxic elements, including Pb, Cd, As, Cr, and Ni across all spice types (Table 3). These concentrations were highly variable and, in many instances, exceeded international food safety thresholds. Lead was detected in all samples, with cinnamon exhibiting the highest concentration (2.05 ± 0.23 mg/kg), followed by black pepper (0.60 ± 0.24 mg/kg), cumin (0.3 ± 0.15 mg/kg), ginger (0.15 ± 0.09 mg/kg), and turmeric (0.14 ± 0.09 mg/kg). Under European regulation 2021/1317, the allowable limits for Pb depend on the spice category, comprising 2.00 mg/kg in bark-derived spices, 1.50 mg/kg in roots and rhizomes, 0.90 mg/kg in seeds, and 0.60 mg/kg in fruit spices. In the present results, the Pb concentration measured in cinnamon (2.05 ± 0.23 mg/kg), a bark-derived spice, exceeded the maximum level established by the European Union (EU). For black pepper (0.60 ± 0.24 mg/kg) and cumin (0.3 ± 0.15 mg/kg), classified as fruit and seed spices, respectively, the concentrations were within EU thresholds (0.60 mg/kg for fruit and 0.90 mg/kg for seed spices). Ginger (0.15 ± 0.09 mg/kg) and turmeric (0.14 ± 0.09 mg/kg), both considered root and rhizome spices, were well below the EU limit of 1.50 mg/kg.

Lead contamination in animal feed ingredients, including plant-based additives such as spices, is recognized as a major toxicological concern for domestic animals, including cattle, poultry, and pets (Aronson, 1971). Chronic Pb ingestion in livestock results in bioaccumulation in the liver, kidneys, and bones, leading to growth impairment, reproductive disorders, and neurological effects (Aronson, 1971). Analyses of feed materials have reported Pb concentrations as high as 3,600 mg/Kg, suggesting that even minor contamination from plant-derived additives can substantially increase total Pb intake in

animals (Fox and Boylen, 1978). Prolonged exposure has been associated with hematological and enzymatic dysfunctions, oxidative stress, and reproductive abnormalities in ruminants and poultry (Tesink, 1994).

Table 3. Minimum, maximum, mean, and standard deviation concentrations of trace elements in different spices

Element		Cr (mg/kg)	Ni (mg/kg)	Pb (mg/kg)	Cd (mg/kg)	As (mg/kg)
Cinnamon	Range	0.178-1.86	0.171-2.437	1.228-2.4	0.157-0.394	0.024-0.176
	Mean ± SD	0.96 ± 0.52	1.34 ± 0.73	2.05 ± 0.23	0.29 ± 0.07	0.09 ± 0.04
Cumin	Range	0.912-4.98	0.469-8.979	0.048-0.56	0.027-0.1	0.026-0.986
	Mean ± SD	2.64 ± 1.14	4.18 ± 2.85	0.30 ± 0.15	0.06 ± 0.02	0.45 ± 0.30
Ginger	Range	0.428-2.78	0.105-1.379	0.013-0.285	0.014-0.089	0.019-0.098
	Mean ± SD	1.79 ± 0.77	0.76 ± 0.39	0.15 ± 0.09	0.04 ± 0.02	0.06 ± 0.02
Black pepper	Range	0.899-6.583	0.648-0.952	0.818-0.96	0.006-0.049	0.401-0.493
	Mean ± SD	3.62 ± 2.13	0.45 ± 0.26	0.60 ± 0.24	0.03 ± 0.01	0.27 ± 0.14
Turmeric	Range	0.279-1.618	0.117-1.281	0.017-0.299	0.004-0.038	0.004-0.07
	Mean ± SD	0.81 ± 0.36	0.70 ± 0.37	0.14 ± 0.09	0.02 ± 0.01	0.04 ± 0.02

Cr: Chromium, Ni: Nickel, Pb: Lead, Cd: Cadmium, As: Arsenic, SD: Standard Deviation

The Pb level in cinnamon (2.05 mg/kg) approached or slightly exceeded the EU maximum permissible limit for bark spices (2.00 mg/kg; EU Commission, 2023) but remains within the Codex Alimentarius proposed limit (2.50 mg/kg). The Pb value in cinnamon was comparable to levels reported in Ecuador, where cinnamon samples averaged 0.36-0.80 mg/kg, with some exceeding the EU threshold (Yánez-Jácome et al., 2024), and to those detected in India, where Pb contamination has been documented in cinnamon and other common spices. Experimental studies using a catfish (*Clarias gariepinus*) model further highlighted that cinnamon exposed to Pb can accumulate the metal, with measurable toxicological consequences (Yousaf et al., 2025). In a Lebanese market survey, cinnamon exhibited the greatest mean Pb level (0.972 ± 0.893 mg/kg), remaining within the EU permissible range (Moussa et al., 2024). In the United States, a recent outbreak linked to cinnamon-containing applesauce resulted in widespread pediatric Pb poisoning, demonstrating that contaminated cinnamon can represent a significant public health risk (Troeschel, 2025).

In black pepper, the Pb content was 0.60 ± 0.24 mg/kg, matching exactly the EU regulatory limit for fruit spices. Beyond its contamination risk, black pepper has also been shown to improve growth performance, feed efficiency, blood parameters, and gut morphology in broiler chickens (El-Gogary et al., 2024). The Pb value in black pepper was consistent with concentrations reported in Libya, where black pepper and other spices contained Pb close to 0.60 mg/kg (Ziyaina et al., 2014). The Pb value in black pepper in the present study was comparable to Algeria, where remarkable mycological contamination and aflatoxin B_1 levels in common spices have been documented, although not specifically in black pepper (Azzoune et al., 2015). Similar ranges were reported in Europe, where Pb in black pepper was measured between 0.10 and 0.79 mg/kg (Blagojević et al., 2016), underscoring regional variability.

The Pb level in cumin (0.30 ± 0.15 mg/kg) falls well within the EU maximum (0.90 mg/kg for seed spices). Comparable results were found in Egypt, where cumin and other spices were reported to contain measurable concentrations of heavy metals such as Pb, Cd, and Cr (Abou-Arab and Abou Donia, 2000). In Iran, fungal contamination and related mycotoxins were detected in cumin samples, raising concerns about potential co-occurrence with heavy metals (Al-Harthi, 2024). The present findings highlighted how Pb levels in cumin and black pepper vary geographically, reflecting differences in soil composition, agricultural practices, and post-harvest handling.

Ginger in the present study exhibited a Pb concentration of 0.15 ± 0.09 mg/kg, well below the EU limit of 1.50 mg/kg for root and rhizome spices. Higher values have been found, with ginger samples containing up to 0.79 mg/kg Pb in European markets (Blagojević et al., 2016), while Moroccan spice surveys confirmed variability in composition and contamination profiles depending on geographic origin (Bouzaid et al., 2024). Comparable levels have been reported in India and European markets, where Pb contamination in ginger and other common spices was observed, with concentrations in some cases exceeding international safety thresholds (Blagojević et al., 2016).

Turmeric recorded the lowest Pb concentration at 0.14 ± 0.09 mg/kg, which was considerably lower than the Pb concentrations of 1.7 to 5.0 mg/kg reported in the study conducted by Vostrikova et al. (2021). In South Asia, although contamination levels are generally low to moderate, several market surveys have identified the use of Pb chromate as an adulterant in certain spice products (Forsyth et al., 2024). Studies from Bangladesh further highlighted turmeric as a potential source of chronic Pb exposure, especially for children (Gleason et al., 2014). The measured values were well below both EU and Codex limits, reflecting turmeric's relatively low natural uptake of Pb. However, the measured values highlighted potential risks from anthropogenic sources, including adulteration and inadequate post-harvest practices

Cadmium levels followed a similar trend, highest in cinnamon (0.29 ± 0.07 mg/kg), and notably present in cumin (0.06 ± 0.02 mg/kg), ginger (0.04 ± 0.02 mg/kg), black pepper (0.03 ± 0.01 mg/kg), and turmeric (0.02 ± 0.01 mg/kg). In cinnamon, the cadmium concentration was 0.29 mg/kg, which was similar to levels previously reported in South Asian spice markets (Baig et al., 2019). Similar studies have reported the presence of toxic trace elements such as Pb and Cd in spices and aromatic herbs collected in Tunisia and Italy (Potortì et al., 2020). Regulatory limits for Cd in spices are currently under development, with existing guidelines varying among different authorities. For example, the EU set a maximum level of 0.20 mg/kg for fresh herbs (Regulation EU 2021/1323), and this value might be adjusted for dried spices using a dehydration factor as recommended by the European spice association (EU Commission, 2021). Additionally, regulatory authorities such as the European Commission have set a maximum Cd level of 1.0 mg/kg for food supplements, a category that may include certain dried plant materials such as spices (EU Commission, 2021). However, the Alimentarius (1995) and Mayne (2023) have not yet established specific Cd limits for spices. In Lebanon, Cd was detected in over 8% of spice samples, with some exceeding the regulatory thresholds (Moussa et al., 2024). According to EU No 1275/2013 of 6 December 2013, amending Annex I to Directive 2002/32/EC on undesirable substances in animal feed, the maximum permissible level of Cd in complete animal feed was set at 0.5 mg/kg (at 12% moisture), with higher limits applying to certain categories, including 1 mg/kg for complete feed for cattle (except calves), sheep (except lambs), goats (except kids) and fish, and 2 mg/kg for complete feed for pet animals (Official Journal of the European Communities, 2002).

For ginger, the concentration of Cd, 0.04 mg/kg, was lower than the values reported in North African markets, where ginger and mixed spice samples contained Cd levels up to 0.36 mg/kg (Ziyaina et al., 2014). However, the level of Cd remained lower than that reported in Ethiopian ginger, where cadmium was detected in specific samples (Belay, 2014). The present results suggested that ginger contamination varies across regions but generally remains moderate.

The Cd concentration in the black pepper sample (0.03 mg/kg) was also lower than the range found in Indian markets, where heavy metal surveys reported Cd values between 0.12 and 0.20 mg/kg (Sharda et al., 2017), and was also lower than the Cd concentrations reported in black pepper samples, which ranged from 0.008 to 0.067 mg/kg (mean = 0.026 mg/kg; Tinggi, 2025). In the Cumin samples, the present value of 0.06 mg/kg was lower than the 0.16 mg/kg reported in Tunisian and well below the 0.21 mg/kg measured in Pakistan (Baig et al., 2019), suggesting comparatively reduced Cd contamination in cumin from the Casablanca region, Morocco.

The level of Cd in turmeric (0.02 mg/kg) was lower than that reported in Iranian markets, where turmeric and other spices indicated Cd values up to 0.13 mg/kg (Varmazyar and Sobhan, 2017). This level remains below that reported in North Africa, where turmeric sold in Libya was found to contain 0.36 mg/kg of Cd (Ziyaina et al., 2014). The EU Commission has set the maximum allowed Cd level in most spices at 0.20 mg/kg. In comparison, the average Cd concentration found in cinnamon samples (0.29 ± 0.07 mg/kg) in the present study was higher, which raised concern. No scientific data are currently available regarding the Cd content of turmeric when used in animal feed formulations. The nephrotoxic potential of Cd at low exposure levels was well documented, and chronic ingestion from dietary sources, including spices, has been highlighted in biomonitoring and exposure studies from Turkey (Sekeroglu et al., 2006), France (Arnich et al., 2012), and Morocco, where Cherkani-Hassani et al. (2020) reported Cd detection in breast milk, highlighting dietary exposure in humans. The present findings reinforced the importance of monitoring turmeric and other spices, even when average Cd levels appear relatively low.

Chronic ingestion of Cd-contaminated feed leads to its bioaccumulation in the liver and kidneys, resulting in nephrotoxicity, oxidative stress, and impaired reproductive and growth performance in livestock (Darmono, 1999; Hoogenboom et al., 2015). Studies have shown that even low Cd concentrations in feed (1-10 mg/kg) can exceed EU safety thresholds after prolonged exposure, particularly in pigs and ruminants (EFSA, 2004; Hoogenboom et al., 2015). The Cd exposure also interferes with the absorption of essential trace elements such as Zn and Cu, promoting metabolic disorders (Phillips and Prankel, 2011). Moreover, Cd residues in feed can accumulate in sheep tissues, particularly in the liver and kidneys, and may be transferred to animal-derived products such as meat and milk, posing an indirect risk to human health (Prankel et al., 2004; Penkov and Hristev, 2019).

Arsenic was highest in cumin (0.45 ± 0.30 mg/kg), followed by black pepper (0.27 ± 0.14 mg/kg), cinnamon (0.09 ± 0.04 mg/kg), ginger (0.06 ± 0.02 mg/kg), and turmeric (0.04 ± 0.02 mg/kg). The highest As level in cumin (0.45 mg/kg) substantially exceeded the values reported by Yücel et al. (2022), who found an average As concentration of 0.06 mg/kg in cumin samples from Turkey and Egypt, where spice blends including cumin indicated As levels up to 4.8 mg/kg (Abd El-Rahman, 2019). This concentration of As was also higher than that recorded in India, where cumin and black pepper samples contained As at levels of up to 0.17 mg/kg (Sharda et al., 2017), and in Pakistan, where As contamination of common spices reached 0.29 mg/kg (Baig et al., 2019). However, the EU and Codex Alimentarius do not presently establish maximum permissible levels for As in spices; As concentrations exceeding 0.2 mg/kg are often emphasized in risk assessments, based on benchmark levels derived from cereals and vegetables (EU Commission, 2021). In black pepper, the

As level of 0.27 ± 0.14 mg/kg aligned with published data, where concentrations up to 0.51 mg/kg were detected in pepper samples from European and North African markets (Blagojević et al., 2016).

The concentration of As in cinnamon was 0.09 ± 0.04 mg/kg, which was lower than the values recorded in Moroccan markets, where multi-element analysis confirmed the presence of measurable As and other toxic metals in cinnamon samples (El Youssfi et al., 2025). Ginger indicated an As concentration of 0.06 ± 0.02 mg/kg, which was lower than values reported in ginger powders, where As reached up to 0.51 mg/kg (Blagojević et al., 2016) and was also lower than findings from experimental studies in rats showing that ginger consumption can mitigate As toxicity (Adetutu et al., 2024). Lastly, turmeric presented the lowest As level at 0.04 ± 0.02 mg/kg, below average values reported in India, where As reached 0.14-0.18 mg/kg in turmeric and other spices (Sharda et al., 2017), and less than the levels detected in Egyptian spice samples, where As reached up to 4.8 mg/kg (Abd El-Rahman, 2019). According to the European Directive 2002/32/EC on undesirable substances in animal feed, the maximum permissible concentration of As is 2 mg/kg in complete feed and 4 mg/kg in complementary feed for all animal species (Official Journal of the European Communities, 2002). Later, Regulation EU No 744/2012 revised these limits for specific compound feeds, increasing the threshold to 10 mg/kg for particular categories of feed materials intended for bovine animals, sheep, goats, and horses (EU Commission, 2012).

Chromium content was highest in black pepper (3.62 ± 2.13 mg/kg), followed by cumin (2.64 ± 1.14 mg/kg), ginger (1.79 ± 0.77 mg/kg), cinnamon (0.96 ± 0.52 mg/kg), and turmeric (0.81 ± 0.36 mg/kg). The highest level of Cr was observed in black pepper (3.62 mg/kg), which was above the average range reported in Mediterranean markets, where Cr was detected in 95% of spice samples with values up to 1.42 mg/kg (Garcia et al., 2000), and higher than Egyptian values, where Cr concentrations in spices such as coriander reached 11.6 mg/kg (Abd El-Rahman, 2019). Comparable levels have been reported in Nigerian markets, where Cr in common spices such as ginger, turmeric, and black pepper varied widely, reflecting similar variability to Indian and Pakistani datasets (Olusola et al., 2025). Likewise, Ethiopian studies confirmed the occurrence of Cr in rhizomatous and seed spices, with measurable levels in ginger and cumin ranging from 0.013 to 0.034 mg/kg (Belay, 2014). There are currently no EU or Codex standards defining permissible levels of Cr in spices. However, dietary intake assessments rely on adequate intake (AI) references for trivalent chromium (Cr^{3+}), set at 35 µg/day for men and 25 µg/day for women, based on estimated average daily consumption (NASEM, 2022). Cumin contained 2.64 ± 1.14 mg/kg of Cr, which was comparable to levels reported in Moroccan markets, where multi-element ICP-MS analysis confirmed the presence of Cr in cumin samples (El Youssfi et al., 2025) and consistent with multi-country data confirming detectable Cr levels in cumin and other spices (Mir et al., 2024). Turmeric exhibited a concentration of Cr at 0.81 ± 0.36 mg/kg, lower than the international range where Cr was detected in 95% of spice samples from Mediterranean markets (Garcia et al., 2000) and below Egyptian data, where values reached up to 11.6 mg/kg in spice samples (Abd El-Rahman, 2019). The ginger sample contained 1.79 ± 0.77 mg/kg of Cr, which was within the range reported in Ethiopian ginger and cumin (0.013-0.034 mg/kg; Belay, 2014) and consistent with multi-country data from Saudi Arabia confirming detectable Cr in ginger, turmeric, cumin, and cinnamon (Seddigi et al., 2013). Finally, cinnamon indicated Cr concentration at 0.96 ± 0.52 mg/kg, which was within the range of values recorded for Moroccan and Saudi Arabian markets (Seddigi et al., 2013; El Youssfi et al., 2025), suggesting comparatively moderate Cr uptake in bark-based spices.

According to the National Research Council, the maximum tolerable concentration of Cr^{3+} in livestock feed is 3,000 mg/kg when supplied as chromium oxide (Cr_2O_3) and 1,000 mg/kg when supplied as chromium chloride ($CrCl_3$; NRC, 2001). At low doses, Cr improves metabolism, growth, and immune function in animals (Moreira et al., 2020). However, when exposure exceeds safe limits, Cr becomes toxic and can cause severe cellular damage, as demonstrated in studies using the mongoose as an environmental model (Andleeb et al., 2020).

Nickel levels were highest in cumin (4.18 ± 2.85 mg/kg), followed by cinnamon (1.34 ± 0.73 mg/kg), ginger (0.76 ± 0.39 mg/kg), turmeric (0.70 ± 0.37 mg/kg), and black pepper (0.45 ± 0.26 mg/kg). In cumin, the Ni concentration reached 4.18 mg/kg, which was lower than the levels previously reported in Algerian samples (7.61 mg/kg; Kachbi et al., 2022). Nickel contamination has also been reported in cumin and black pepper samples from Moroccan markets (El Youssfi et al., 2025).

Additionally, the concentration of Ni fell within the broader international range of 1.3 to 5.5 mg/kg reported in Iraqi samples and Nigerian markets, where Ni in spices was confirmed in multiple spice varieties (Gaya and Ikechukwu, 2016). Although there are currently no established EU or Codex limits for Ni in spices, dietary exposure assessments consider tolerable daily intake levels ranging from 2.8 to 12 µg/kg body weight/day, depending on population subgroup and risk model. No official or internationally recognized limit for Ni in animal feed has been established so far. In cinnamon, the Ni concentration was 1.34 ± 0.73 mg/kg, which was lower than values reported for Saudi Arabian samples, where Ni levels reached up to 2.6 µg/g (Seddigi et al., 2013) and in Moroccan markets, where ICP-MS analysis detected Ni among several toxic elements in cinnamon (El Youssfi et al., 2025). In Nigerian studies, black pepper contained Ni levels of 2.33 mg/kg in pepper blends (Iwegbue et al., 2013), with an average of 0.45 ± 0.26 mg/kg, which is lower than the data from the Rabat-Salé-Témara region in Morocco (El Youssfi et al., 2025). Turmeric contained 0.70 ± 0.37 mg/kg of Ni, lower than Saudi

Arabian findings, where Ni was consistently present in turmeric (Seddigi et al., 2013), and also higher than the levels reported in Iranian markets, where Ni was detected at 0.033 mg/kg in both packaged and unpackaged turmeric samples (Taghizadeh et al., 2024). Finally, ginger indicated 0.76 ± 0.39 mg/kg of Ni, which was lower than Moroccan values, in the results of Saudi Arabia, where ginger was confirmed as a Ni-accumulating spice (Seddigi et al., 2013), and where ginger samples contained detectable Ni (El Youssfi et al., 2025).

Macro-elements

The five spices analysed, cinnamon, cumin, ginger, black pepper, and turmeric, revealed remarkably diverse profiles for five key nutritionally relevant elements, including K, Ca, Mg, Na, and Fe (Table 4). These differences indicated distinct physiological uptake behaviors, soil conditions, and regional cultivation practices.

Table 4. Minimum, maximum, mean concentrations, and standard deviations of major elements in different spices

Element		K (g/kg)	Ca (g/kg)	Mg (g/kg)	Na (g/kg)	Fe (mg/kg)
Cinnamon	Range	0.676-6.151	1.798-8.894	0.327-2.358	0.102-0.647	81.013-398.146
	Mean ± SD	3.62 ± 1.75	5.01 ± 2.18	1.41 ± 0.64	0.41 ± 0.17	269.44 ± 95.61
Cumin	Range	20.034-22.985	2.45-18.972	3.672-9.897	1.512-6.06	100.801-1440.245
	Mean ± SD	21.64 ± 1.01	11.13 ± 4.53	6.86 ± 1.61	3.98 ± 1.59	753.71 ± 446.07
Ginger	Range	4.119-23.665	0.302-3.859	1.105-3.898	0.105-0.492	93.112-893.354
	Mean ± SD	13.97 ± 6.68	2.13 ± 1.13	2.64 ± 0.85	0.31 ± 0.14	423.11 ± 237.84
Black pepper	Range	16.754-17.893	3.802-6.952	1.895-2.97	0.269-0.269	39.002-488.474
	Mean ± SD	14.24 ± 2.06	4.81 ± 1.61	1.89 ± 0.61	0.17 ± 0.06	258.80 ± 164.07
Turmeric	Range	1.742-49.78	0.525-1.486	0.828-3.322	0.084-0.445	92.969-597.859
	Mean ± SD	25.96 ± 13.51	1.00 ± 0.32	1.90 ± 0.70	0.28 ± 0.11	335.18 ± 156.58

K: Potassium, Ca: Calcium, Mg: Magnesium, Na: Sodium, Fe: Iron, SD: Standard deviation.

Turmeric demonstrated a notably high K content, with a study conducted by Maghrabi (2014) reporting levels reaching 24.1 g/kg. Cumin maintained elevated values of K (~20 g/kg), reinforcing its nutritional potential as a dietary source of K. Cinnamon consistently recorded the lowest K, suggesting species-specific uptake limitations or cultivation on K-poor substrates. Potassium content of spices differed by species and region. In the present study, turmeric demonstrated exceptionally high K levels, often exceeding 25 g/kg and reaching nearly 50 g/kg. In the present study, the concentrations of K aligned closely with findings from Morocco, where turmeric recorded some of the highest K values among spices, with concentrations approaching 40 g/kg (El Youssfi et al., 2025). Similar high K levels for turmeric were reported in Uzbekistan, typically ranging from 30 to 45 g/kg, depending on the soil and region (Jabborova et al., 2021). The present results on cumin indicated K levels of around 20 g/kg, consistent with concentrations reported for Moroccan cumin samples, which ranged from 18 to 24 g/kg (El Youssfi et al., 2025). Additionally, Indian sources confirmed similar K concentrations in cumin, typically 16-22 g/kg. This was consistent with the value reported in Moroccan samples (16.72 g/kg; El Youssfi et al., 2025) and lower than that observed in Indonesian samples (33.84 mg/g; Ayustaningwarno et al., 2024), likely reflecting differences in soil characteristics and altitude. In contrast, cinnamon consistently exhibited the lowest K content in the present study (<1 g/kg), consistent with El Youssfi et al. (2025), who reported that Moroccan cinnamon contains less than 2 g/kg. Additionally, studies from India and New Zealand reported concentrations of K ranging from 0.5 to 1.5 g/kg (Cicero et al., 2022). These comparisons clearly indicated that turmeric consistently has the highest K concentration, followed by cumin and ginger, while cinnamon ranks lowest across all studies. Potassium levels in animal feed vary by species and source. In cats, commercial foods containing 0.32-0.34% dry matter are below the recommended minimum of 0.6% (Phillips, 1998). In dogs, K levels ranged from 0.44 to 1.03 g/MJ, aligning with recommended intakes of around 0.7-1 g/MJ (Bijsmans et al., 2021) and in ruminants, while typical needs are covered at 0.5% dry matter, local forages in North Africa can raise K content to 3.1% dry matter, far exceeding basic nutritional requirements (Ward, 1966; Bhanugopan et al., 2015).

In the present study, cumin displayed the highest Ca concentrations, ranging from 11.13 ± 4.53 g/kg, which was substantially higher than values reported for Jordanian sweet cumin in Jordan (~2.22 g/kg; 221.5 mg/100 g; Ereifej et al., 2015). Cinnamon ranked second (5.01 ± 2.18 g/kg), exceeding the 2.99 g/kg reported for Middle Eastern samples (Ereifej et al., 2015) and consistent with other reports of elevated Ca in cinnamon. Black pepper contained an average of 4.81 ± 1.61 g/kg of Ca, consistent with Indian data of 4.39 g/kg (Ayoade et al., 2023). Ginger contained 2.13 ± 1.13 g/kg, higher than the 0.67 g/kg reported in Jordanian samples. In contrast, turmeric recorded the lowest concentrations at 1.00

± 0.32 g/kg, well below the 0.13 g/kg observed in Jordan (Ereifej et al., 2015). These differences underlined the remarkable geographical variability in mineral composition, likely driven by soil properties, agronomic practices, and post-harvest handling.

In the present study, cumin recorded the highest Mg levels (6.86 ± 1.61 g/kg), which fall within the range previously reported for cumin seeds (0.81-36.6 g/kg; Mohammed et al., 2024). Ginger displayed moderate Mg concentrations (2.64 ± 0.85 g/kg), which aligns with literature values of 2-3 g/kg for ginger across African and Asian origins (Ajayi et al., 2013). Black pepper had Mg content of 1.89 ± 0.61 g/kg, comparable to 1.8-2.0 g/kg values reported in Indian and Indonesian samples (Cicero et al., 2022). Turmeric presented slightly lower values (1.90 ± 0.70 g/kg), overlapping with the 1.5-2.5 g/kg range reported in Indian studies (Jabborova et al., 2021). The lowest Mg concentrations was observed in cinnamon (1.41 ± 0.64 g/kg), in agreement with published data showing consistently low Mg levels in cinnamon, with reported levels around 1.40g/kg (Ereifej et al., 2015). The present results confirmed that cumin was the major dietary source of Mg among the tested spices, while cinnamon consistently ranked the lowest, reflecting similar trends reported in global datasets. Natural Mg concentrations measured in compound feeds vary by species. The level of 0.21% in poultry feed (Zang et al., 2014), compared to only 7-8 mg/kg in diets formulated for horses (Harrington, 1974).

Sodium content of spices in the present study indicated a wide variation between species, with cumin exhibiting the highest Na concentrations (3.98 ± 1.59 g/kg). Cinnamon presented intermediate values (0.41 ± 0.17 g/kg), consistent with 0.12 g/kg reported for cinnamon in Jordan (Ereifej et al., 2015). Ginger had low Na content (0.31 ± 0.14 g/kg). Although specific comparative studies are limited, broader mineral surveys have reported similar Na levels in ginger, with values of approximately 0.312 g/kg in Pakistan (Hussain et al., 2020) and 0.234 g/kg in Nigeria (Ayoade et al., 2023). Black pepper had Na content of 0.17 ± 0.06 g/kg, which was consistent with the value reported by El Youssfi et al. (2025) at 0.175 ± 0.006 g/kg in Rabat, Morocco. Turmeric contained 0.28 ± 0.11 g/kg of Na, in line with low Na content for spices found in nutrition references. For example, Zeiner et al. (2022) found Na concentrations in turmeric samples ranging from 0.05 to 0.50 g/kg. The present results confirmed that cumin was the primary dietary source of Na among the spices analyzed, while black pepper consistently indicated the lowest Na content across the present study. Commercial dry pet foods in Europe typically contain between 3,000 and 7,000 mg of Na per kilogram of dry matter, which remains within the EFSA's safe intake threshold of up to 9,000 mg/kg dry matter (Chandler, 2008). For dairy cows in tropical regions, Na-deficient rations may contain only 400 mg/kg, while the minimum recommended intake for lactating cows is approximately 1,200 mg/kg, requiring dietary supplementation (Thiangtum et al., 2011).

Iron content of the analyzed spices indicated noticeable variation among species. Cumin presented the highest concentrations, ranging from 753.71 ± 446.07 mg/kg, which was consistent with previous studies reporting Fe levels between 700 and 1500 mg/kg in cumin seeds from India and North Africa (Meena et al., 2024; El Youssfi et al., 2025). Turmeric exhibited a moderate level of Fe content (335.18 ± 156.58 mg/kg), aligning with reports conducted by Madhusankha et al. (2019), who indicated Fe levels between 320 and 380 mg/kg in Indian turmeric varieties. Ginger contained elevated levels of Fe (423.11 ± 237.84 mg/kg), comparable to levels reported in African samples, such as 578.2 mg/kg in Ethiopian ginger (Firisa et al., 2023) and in traditional leafy vegetables from South Africa (Odhav et al., 2007). Black pepper recorded Fe level of 258.80 ± 164.07 mg/kg, which falls within the 250-550 mg/kg range reported in previous studies conducted in India and Turkey (Yücel and Atasoy, 2019; Ayoade et al., 2023). Cinnamon indicated Fe values ranging from 269.44 ± 95.61 mg/kg, similar to the 250-350 mg/kg reported for Moroccan cinnamon (El Youssfi et al., 2025). The current findings confirmed that cumin was the main dietary source of Fe among the studied spices, while black pepper exhibited relatively low Fe concentrations. Commercial feeds for ruminants typically contain approximately 77 mg/kg of Fe, prior to any supplementation (Standish et al., 1969). In pigs, basal diets typically provide about 100 mg/kg of Fe, without added sources (Ullrey et al., 1960). To ensure safety, the EFSA recommended maximum Fe levels in complete feeds of 450 mg/kg for cattle and poultry, 500 mg/kg for sheep, and 600 mg/kg for pets, which generally aligns with the levels found in commercial products (EFSA Feedap Panel, 2016).

Correlation analysis between trace and macro-elements

As demonstrated in Figure 1, Strong inter-element correlations emerged from the Pearson matrix, notably between Pb and Cd (r = 0.87), indicating a high degree of association. While explicit r-values were not widely reported, the co-occurrence of Pb and Cd has been frequently noted in contaminated food matrices. Several studies have demonstrated a consistent co-occurrence of Pb and Cd in contaminated food matrices, such as Lebanese herbs and spices (Moussa et al., 2024), dark chocolate from the United States (Hands et al., 2024), and Turkish herbs and spices (Özden, 2021).

Other strong positive correlations were observed, particularly between Na and Mg (r = 0.76), Ca and As (r = 0.60), as well as Mg and Ca (r = 0.60). These associations may reflect shared geochemical origins linked to soil mineralogy or agricultural amendments. Similar patterns have been discussed in broader studies of heavy-metal contamination in soils and plants (Bouida et al., 2022) and confirmed in South African spice surveys (Oladeji et al., 2023).

Nickel exhibited a moderate correlation with Ca (r = 0.51) and a strong correlation with Na (r = 0.63), suggesting that these three elements may share a common geogenic origin. Similar association patterns were observed in groundwater studies, where Ni indicated a remarkable correlation with Mn (r = 0.766), likely reflecting geological inputs (Islam et al., 2025). Moderate positive correlations between Fe and other elements, specifically Fe and Ni (r = 0.38), Fe and Mg (r = 0.48), and Fe and Na (r = 0.47), implied shared soil-origin or organic matter inputs, consistent with crustal elemental co-distributions (Moore et al., 2022). By contrast, Cr exhibited only weak correlations with other elements, likely indicating distinct contamination sources or mechanisms, as environmental heavy-metal studies have noted differential behavior of Cr in geochemical and pollution contexts (Briffa et al., 2020). Notable negative correlations were found between Cd and K (r = -0.57) and between Pb and K (r = -0.62), suggesting that higher K levels were associated with lower accumulation of heavy metals in the samples. Although the present correlation data were specific to the selected spice samples, similar antagonistic dynamics between K and Cd uptake have been observed in controlled studies, particularly where K fertilization modulates Cd accumulation in crops (Wang et al., 2019).

Moderate inverse relationships were detected between Pb and Mg (r = -0.35) and between Cd and Mg (r = -0.30), indicating that higher Mg levels were associated with lower concentrations of these heavy metals. This inverse trend was consistent with observations in crops grown on calcareous soils, where elevated Mg and Ca contents contribute to reduced heavy-metal mobility and bioavailability (Zaragüeta et al., 2021). Negative but weak correlations between Pb and As (r = -0.15) and Cd and As (r = -0.16) confirmed the absence of strong relationships, although previous multivariate analyses of metals in spices reported a high positive correlation between Pb and As and moderate associations among other metals such as Cd and Zn (Shim et al., 2021).

Overall, the present study highlighted two main groups of elements. On one hand, Pb and Cd are strongly co-detected in spices, indicative of anthropogenic pollution reinforced by data from Lebanese spice markets (Moussa et al., 2024) and Turkish herb analyses (Özden, 2021). On the other hand, naturally interrelated elements such as Na, Mg, Ca, As, and Ni appeared largely of geological or agronomic origin, consistent with metal distribution studies in Moroccan soils (Barakat et al., 2022) and South African spice surveys (Oladeji et al., 2023). The inverse association between K and heavy metal concentrations, suggesting its potential role as an indirect indicator of less-contaminated areas, is supported by regional soil-metal interaction patterns observed in studies conducted on the Moroccan phosphate plateau (Barakat et al., 2022).

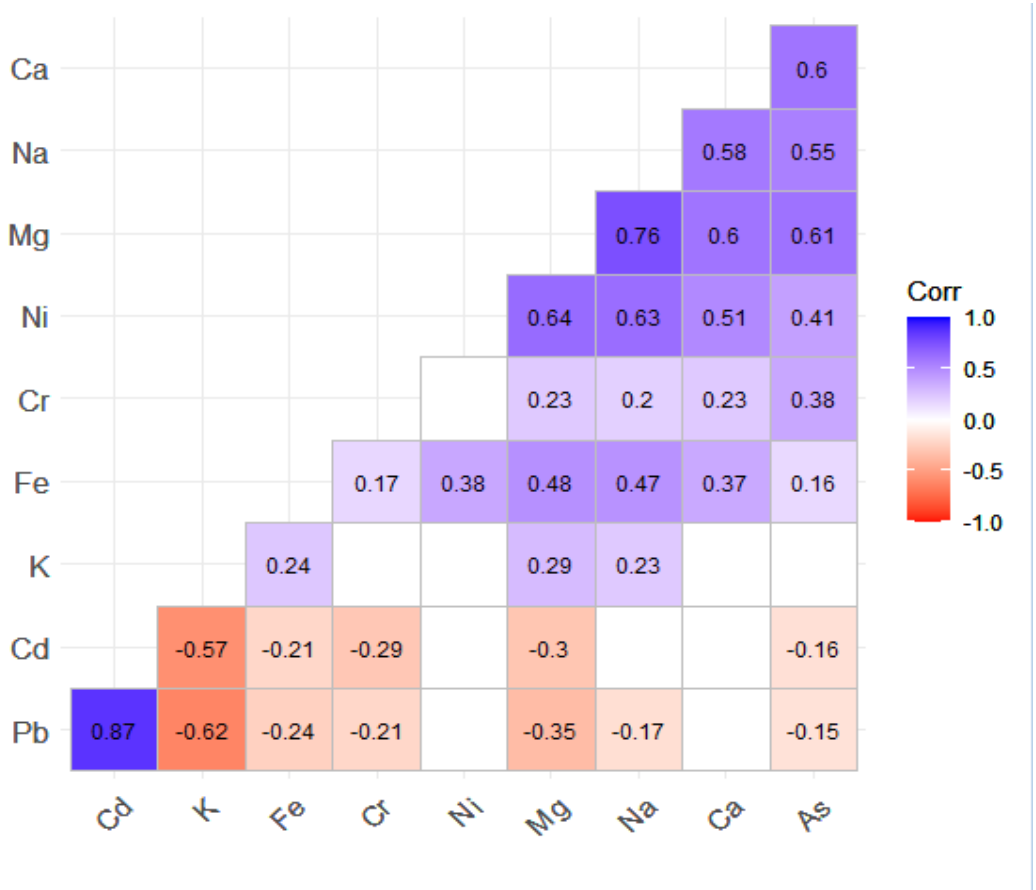


Figure 1. The linear relationships between major and trace elements analysed in the spice samples. K: Potassium, Ca: Calcium, Mg: Magnesium, Na: Sodium, Fe: Iron. Trace elements include Cr: Chromium, Ni: Nickel, Pb: Lead, Cd: Cadmium, and As: Arsenic.

Verification of data factorability

The factorability of the inter-correlation matrix was assessed using two statistical tests (Table 5), including the KMO measure of sampling adequacy and Bartlett's test of sphericity. The overall KMO value was 0.80, indicating a very adequate suitability of the dataset for factor analysis (Kaiser, 1974). Individual KMO values ranged from 0.67 (Pb) to 0.89 (Ni), corresponding to adequacies ranging from acceptable to excellent. Bartlett's test of sphericity confirmed that the correlation matrix was significantly different from an identity matrix ($\chi^2 = 153.42$, df = 45, $p < 0.001$), demonstrating that the observed correlations were sufficient to justify the application of PCA (Bartlett, 1950).

Table 5. Kaiser-Meyer-OLKIN and Bartlett test

KMO and Bartlett test		
Kaiser-Meyer-Olkin (KMO) test: Measure of sampling adequacy		0.797
Bartlett's Test of Sphericity	χ^2	153.42
	df	45
	p-value	0.001

KMO: Kaiser-Meyer-Olki, χ^2: Chi-square value, df: Degrees of freedom, p-value: Probability value

Factor structure and projection of variables

Figures 2 and 3 present the results of a PCA applied to the spice samples to visualize and compare their analytical profiles. The first two factorial axes, Dim 1 (41.2% of the explained variance) and Dim 2 (23.4%), together accounted for 64.6% of the total information, providing a synthetic yet faithful representation of the multivariate relationships among samples (Figure 2).

Examination of variable contributions to the first two principal components revealed marked associations between specific chemical elements and the differentiation of spices. For Dim 1 (41.2% of variance), the highest contributions were from Mg and Na, followed by As, Ni, and Ca. These variables were essential in distinguishing cumin, which was strongly positioned along the direction of these elements. For Dim 2 (23.4% of variance), the structure was dominated by Cd and Pb, each accounting for nearly one-third of the contribution, followed by K and Ca. These variables were particularly associated with cinnamon, which exhibited elevated Cd and Pb levels, and, to a lesser extent, with certain variations observed for turmeric and ginger. When both axes were considered (accounting for 64.6% of the total variance), Pb and Cd, along with Mg, Na, and Ca, emerged as the most discriminating elements (Figure 3). This pattern accounted for the distinct separation between cumin, marked by elevated concentrations of macro-elements (Mg, Na, Ca), and cinnamon, which was instead associated with higher levels of toxic trace metals (Cd, Pb). Other spices, such as turmeric and ginger, displayed intermediate profiles, influenced primarily by K, Ca, and Ni. This finding is consistent with studies from Morocco and Kenya, where cumin was also reported to have high levels of Mg, Na, Zn, and Fe (Chore et al., 2024; El Youssfi et al., 2025). In contrast, cinnamon exhibited concerning concentrations of heavy metals, particularly Pb and Cd, often exceeding regulatory limits. Multivariate analysis placed it as a distinct group, with a strong correlation between Pb and Cd (Mir et al., 2024; El Youssfi et al., 2025). Turmeric and ginger presented intermediate elemental profiles. Ginger, in particular, was rich in K and Mg, whereas turmeric, though slightly lower in concentration, remained a valuable source of nutrients (Savić et al., 2019; Chore et al., 2024).

The cumulative variance explained by the first two components in the present PCA (Dim 1 = 41.2%, Dim 2 = 23.4%, total = 64.6%) falls within the range generally observed for spice matrices profiled by ICP-MS or coupled plasma-optical emission spectroscopy (ICP-OES). For instance, in a multi-food dataset including spices analyzed by ICP-MS, PCA explained 56.85% of the variance on the first two axes (Voica et al., 2021). Similarly, for green, black, and white pepper as well as cayenne, multi-element profiling combined with PCA yielded a clear separation of groups along PC1-PC2. More recently, a comprehensive multi-analytical strategy combining stable isotope analysis, multi-element profiling, and Fourier transform infrared spectroscopy (FTIR) demonstrated clear discrimination among cinnamon samples, with excellent chemometric performance observed along the first principal components (Primožič et al., 2025). Reviews on food authentication using ICP-MS further highlighted that PC1-PC2 typically capture 40-60% of the total inertia, depending on the number of elements and batch diversity (Mazarakioti et al., 2022).

Overall, this PCA of the present study highlighted a clear structuring of the dataset. Some spices, such as cumin and cinnamon, displayed a well-defined and homogeneous analytical identity, while others, such as ginger and turmeric, presented broadly similar profiles. These similarities could reasonably be attributed to either convergent chemical compositions or common external influences, such as geographical origin, cultivation conditions, and processing practices. The ellipses reinforced these trends by depicting both the extent of internal variability and the potential overlaps between groups, which were key factors for interpreting sample variability and discriminability within analytical and traceability contexts.

The current PCA results revealed a clear structuring of the dataset with cumin and cinnamon displaying distinct and homogeneous elemental signatures, whereas ginger and turmeric demonstrated largely similar profiles along PC1-PC2. This pattern was consistent with multi-element ICP-MS/ICP-OES studies on spices and herbs, where PCA has been shown to clearly separate botanical families, with variance explained on the first two axes typically ranging between 40% and 60% (Tokalıoğlu et al., 2018; PavloviĆ et al., 2020). Comparable outcomes of the present study have been reported, including datasets from Sicily and Tunisia involving spices and aromatic herbs (Potortì et al., 2020), as well as in commercial foodstuffs containing spices (Voica et al., 2021).

Specifically, cumin in the present study formed a very compact cluster and was clearly distinguished from the other categories (Figure 4). Similar separations for seed spices have been observed in PCA analyses based on both major and trace elements, with seeds separating from bark or leaf spices already along PC1-PC2 (Potortì et al., 2020). Cinnamon, a bark spice, showed a stable and well-defined cluster in the present dataset. Similar, consistent, and distinctive mineral profiles for cinnamon have been described in multi-element analyses using chemometric tools (Voica et al., 2021) and further highlighted in broader reviews on elemental authentication (Mazarakioti et al., 2022).

For black pepper, the current results indicated partial overlap of ellipses. This proximity was anticipated, as multi-element profiles of typified pepper samples show that green and black pepper cluster closely together, whereas white pepper, due to its different processing, diverges more markedly along PC1-PC2 (Zeiner et al., 2023).

In Figure 4, each symbol and color correspond to a distinct spice, while ellipses drawn around the points represent 95% confidence intervals, illustrating intra-group dispersion and homogeneity. Examination of the relative positions highlighted several distinct configurations. Cumin (green squares) was strongly shifted towards positive Dim 1 values, standing out clearly from the other spices. Its tight distribution and small ellipse indicated a high degree of homogeneity in its measured characteristics. Cinnamon (yellow triangles), positioned in the upper left quadrant with positive Dim 2 and slightly negative Dim 1, also formed a compact cluster, reflecting a specific and stable chemical signature. Black pepper (red circles) was located in the central-left area of the factorial plane. The ellipse illustrated moderate dispersion, suggesting a characteristic but more variable chemical profile along PC1-PC2. Ginger (blur crosses) and turmeric (purple squares), positioned in the lower part of the plot, displayed substantial overlap of their point clouds. This overlap indicated that the two spices possess closely aligned analytical characteristics along the first two axes, implying that their effective discrimination would require the use of additional dimensions or discriminant variables.

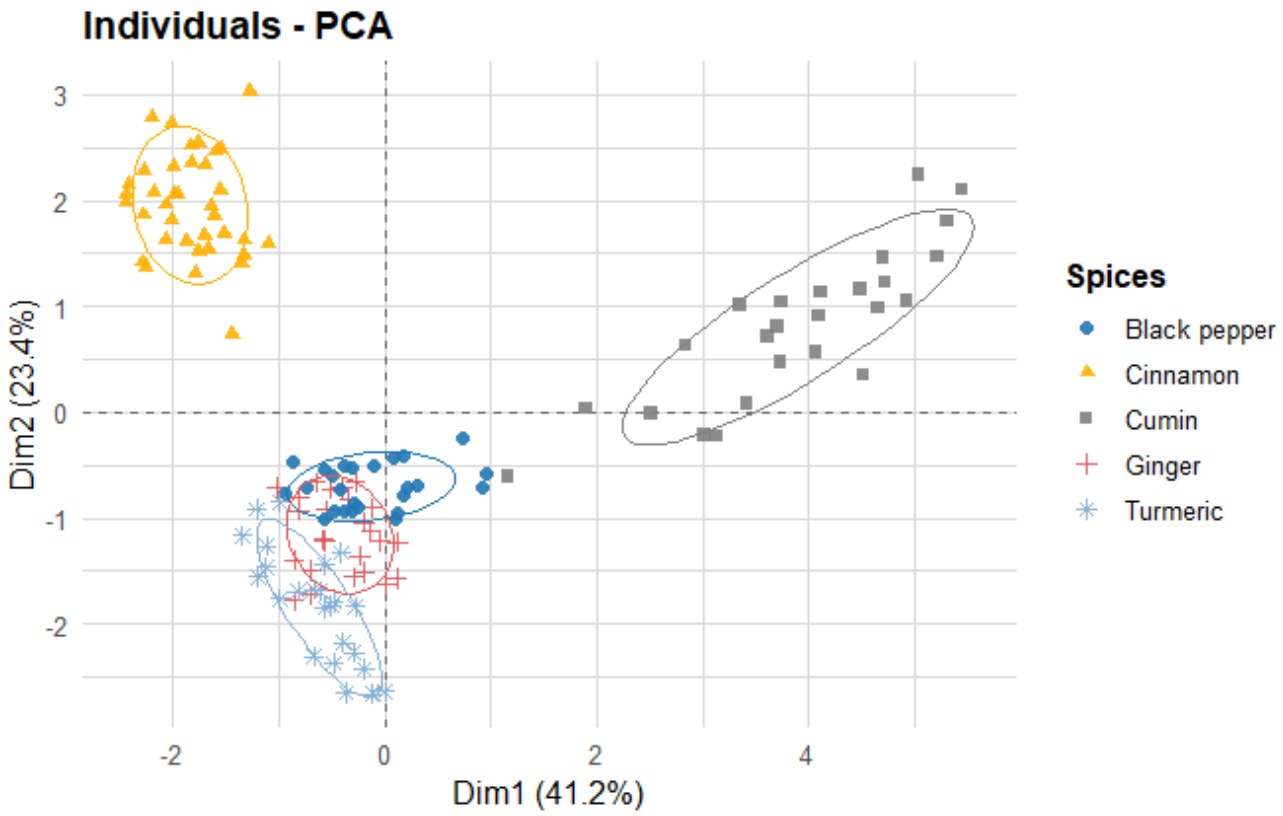


Figure 2. Multivariate separation of analytical spice profiles by principal component analysis. PCA: Principal component analysis, Dim 1: First principal component, Dim 2: Second principal component.

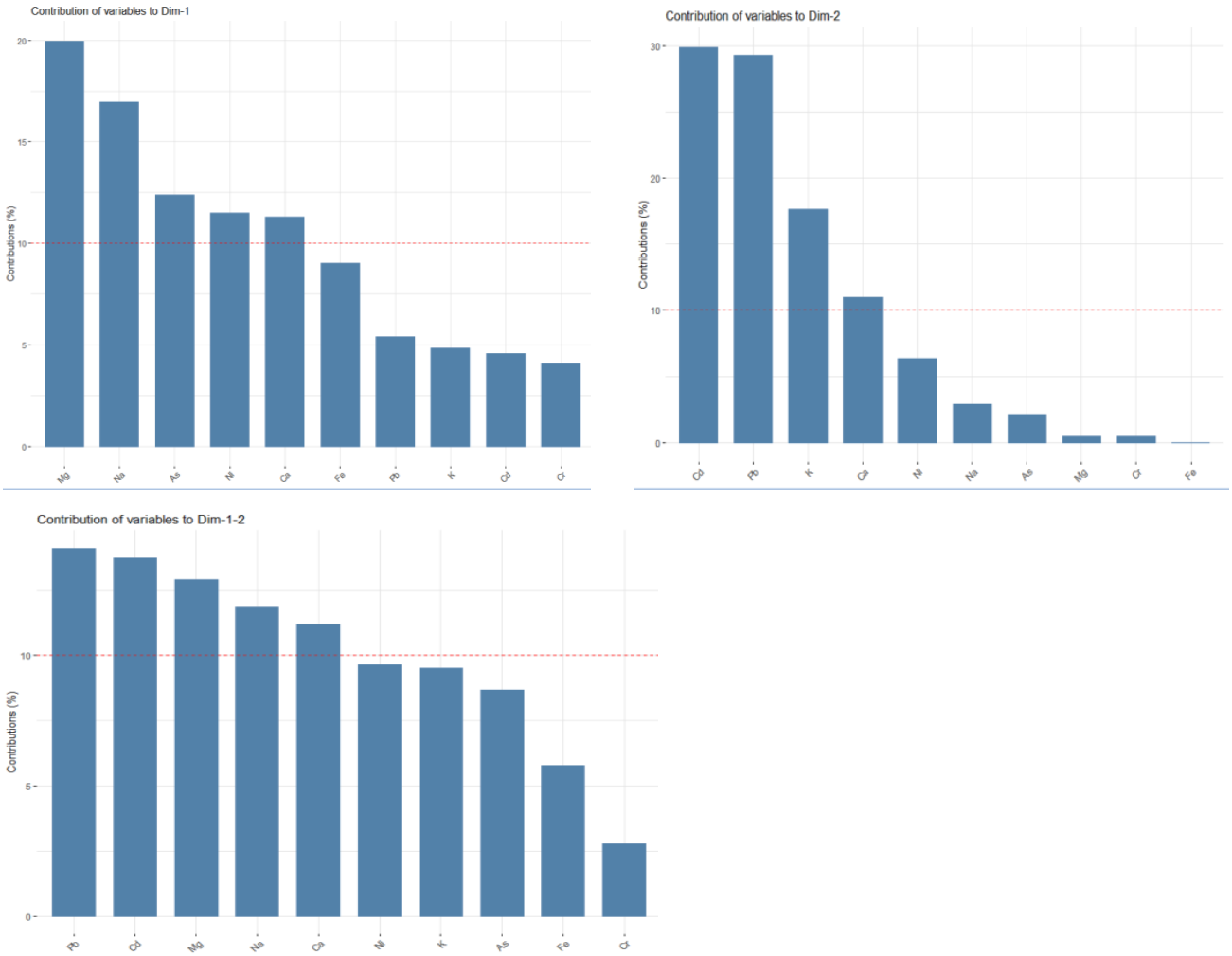


Figure 3. Contribution of macro-elements and trace metals to the differentiation of species in the first two main components of the principal component analysis. Dim 1/Dim 2: First and second principal components.

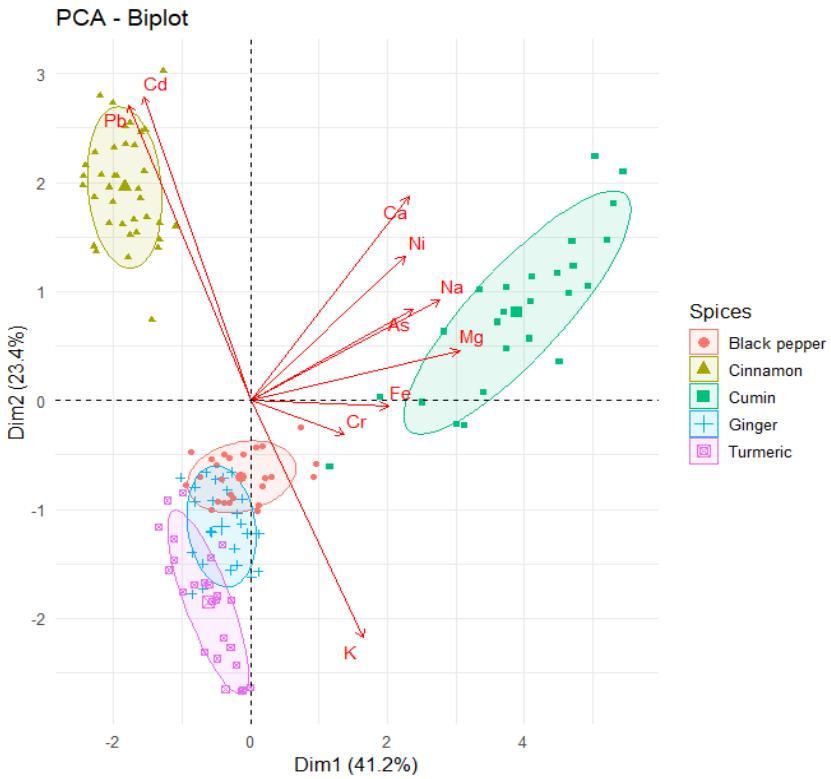


Figure 4. Principal component analysis biplot showing the separation of spice samples and correlation with chemical element contents. PCA: Principal component analysis, Dim 1/Dim 2: Principal components with explained variance (%).

CONCLUSION

The present study represented the first comprehensive multi-element analysis of spices marketed in the Greater Casablanca, Morocco, combining ICP-MS quantification with multivariate statistical approaches. The current results indicated that while some spices, such as turmeric and cumin, are distinguished by their high levels of essential elements such as K, Mg, Na, and Fe, notably cinnamon, display concerning concentrations of toxic metals, particularly Pb (2.05 ± 0.23 mg/kg) and Cd (0.29 ± 0.07 mg/kg), which frequently exceed regulatory limits. The PCA enabled the clear discrimination of spices based on their elemental profiles, revealing two main clusters with one dominated by macro-elements (Cumin, turmeric, ginger) and another characterized by elevated heavy metals (Cinnamon). Strong correlations between Pb and Cd suggested a common source of contamination, potentially linked to agricultural practices or processing methods. The present findings underscored the urgent need for strengthened quality control of spices on the Moroccan market, including systematic monitoring of toxic metals and the implementation of targeted corrective measures. Additionally, the results of the present study highlighted the value of integrated analytical approaches for differentiating products, tracing their origin, and assessing their safety, thereby contributing both to public health protection and to the valorization of local production. Future studies should investigate a larger set of spices across different Moroccan regions, exploring additional contaminants such as pesticides and mycotoxins, and examining the influence of agricultural practices, soil composition, and irrigation water on metal accumulation in spices.

DECLARATIONS

Acknowledgments

The authors would like to express their sincere gratitude to the Laboratory of Health and Environment, Department of Biology, Faculty of Sciences, Hassan II University of Casablanca, Morocco, for the scientific, technical, and logistical support provided during the completion of the present study.

Author's contributions

Safaa Sabri was responsible for the conceptualization of the study, initial drafting, collection of samples, scientific interpretations, data analysis, and coordination of the experimental process. Chaima Sabri supervised the study, the critical review of data, and the manuscript. Mohamed Rida Salam contributed to the interpretation of results, contributed to the literature review, and the scientific discussion. Fatiha El Mellouli contributed to the literature review and assisted in the statistical analysis of the data. Asmaa Lafram participated in laboratory experiments. Hanane Khallouki contributed to the statistical analysis and interpretation of results. Yayé Abdou Hassane contributed to the literature review and assisted in data organization. Mostafa Kabine provided general supervision, scientific guidance, and final approval of the manuscript. All authors checked and approved the findings of this study and the last edition of the submitted manuscript.

Funding

The present study was not supported financially and received no funding.

Competing interests

The authors declared that they have no competing interests.

Availability of data and materials

All data generated or analyzed during the present study are included in this published article.

Ethical considerations

Ethical issues, including plagiarism, consent to publish, misconduct, data fabrication and/or falsification, double publication and submission, and redundancy, have been checked by all authors. No artificial intelligence (AI) tools were used to assist in conducting, analyzing, or interpreting the present study.

REFERENCES

Abd El-Rahman MAM (2019). Microbiological quality and heavy metals content of some spices and herbs kinds. Journal of Food and Dairy Sciences, 10(7): 237-241. DOI: https://www.doi.org/10.21608/jfds.2019.53499

Abou-Arab AA and Abou Donia MA (2000). Heavy metals in Egyptian spices and medicinal plants and the effect of processing on their levels. Journal of Agricultural and Food Chemistry, 48(6): 2300-2304. Available at: https://pubs.acs.org/doi/10.1021/jf990508p

Adetutu A, Aborisade AB, Ogunsina FA, Adegbola PI, and Olaniyi TD (2024). Ginger mitigated the health risks associated with arsenic-contamination of rats feed via inflammatory and apoptosis regulation. Ecotoxicology and Environmental Safety, 269: 115768. DOI: https://www.doi.org/10.1016/j.ecoenv.2023.115768

Ajayi OB, Akomolafe SF, and Akinyemi FT (2013). Food value of two varieties of ginger (*Zingiber officinale*) commonly consumed in Nigeria. International Scholarly Research Notices, 2013(1): 359727. DOI: https://www.doi.org/10.5402/2013/359727

Akhtar S, Riaz M, Naeem I, Gong YY, Ismail A, Hussain M, and Akram K (2020). Risk assessment of aflatoxins and selected heavy metals through intake of branded and non-branded spices collected from the markets of Multan city of Pakistan. Food Control, 112: 107132. DOI: https://www.doi.org/10.1016/j.foodcont.2020.107132

Al-Harthi HF (2024). Mycobiota, total aflatoxins, and ochratoxin A of black and green cumin. Foodborne Pathogens and Disease, 22(5): 359-366. DOI: https://www.doi.org/10.1089/fpd.2024.0096

Alimentarius C (1995). General standard for contaminants and toxins in food and feed CXS 193-1995. Available at: https://www.fao.org/fao-who-codexalimentarius/codex-texts/list-standards

Andleeb S, Ahmad Z, Mahmood T, Bao S, Arif Saeed A, and Jha SK (2020). Evaluating toxicity impacts of environmental exposed chromium on small Indian mongoose (*Urva auropunctatus*) hematological, biochemical and histopathological functioning. Chemosphere, 259: 127485. DOI: https://www.doi.org/10.1016/j.chemosphere.2020.127485

AOAC International (2013). SMPR 2012.007: Standard method performance requirements for determination of heavy metals in a variety of foods and beverages. Available at: https://www.aoac.org/wp-content/uploads/2020/11/SMPR202012_007.pdf

Arnich N, Sirot V, Rivière G, Jean J, Noël L, Guérin T, and Leblanc JC (2012). Dietary exposure to trace elements and health risk assessment in the 2nd French total diet study. Food and Chemical Toxicology, 50(7): 2432-2449. DOI: https://www.doi.org/10.1016/j.fct.2012.04.016

Aronson AL (1971). Biologic effects of lead in domestic animals. Journal of the Washington Academy of Sciences, 61(2): 110-113. Available at: http://www.jstor.org/stable/24535474

Association française de normalisation (AFNOR) (2018). NF T 90-210: Qualité de l'eau — Protocole d'évaluation initiale des performances d'une méthode dans un laboratoire [Water quality — Initial evaluation protocol for the performance of a method in a laboratory]. AFNOR, Paris. Available at: https://www.boutique.afnor.org/fr-fr/norme/nf-t90210/qualite-de-leau-protocole-devaluation-initiale-des-performances-dune-method/fa190833/81632

Ayoade WG, Gbadamosi L, Ajayi MG, and Badmus MO (2023). Assessment of minerals and vitamin constituents of some commonly consumed spices. International Journal of Science Research Archive, 10(1): 53-61. DOI: https://www.doi.org/10.30574/ijsra.2023.10.1.0702

Ayustaningwarno F, Anjani G, Ayu AM, and Fogliano V (2024). A critical review of ginger's (*Zingiber officinale*) antioxidant, anti-inflammatory, and immunomodulatory activities. Frontiers in Nutrition, 11: 1364836. DOI: https://www.doi.org/10.3389/fnut.2024

Azzoune N, Mokrane S, Riba A, Bouras N, Verheecke C, Sabaou N, and Mathieu F (2015). Contamination of common spices by aflatoxigenic fungi and aflatoxin B1 in Algeria. Quality Assurance and Safety of Crops & Foods, 8(1): 137-144. DOI: https://www.doi.org/10.3920/QAS2014.0426

Baig J A, Bhatti S, Kazi TG, and Afridi HI (2019). Evaluation of arsenic, cadmium, nickel and lead in common spices in Pakistan. Biological Trace Element Research, 187(2): 586-595. DOI: https://www.doi.org/10.1007/s12011-018-1400-4

Barakat A, Khellouk R, Ennaji W, and Mosaid H (2022). Investigation of heavy metal contamination and ecological and health risks in farmland soils from southeastern phosphate plateaus of Khouribga (Morocco). Ecological Questions, 33(4): 61-75. DOI: https://www.doi.org/10.12775/EQ.2022.036

Bartlett MS (1950). Tests of significance in factor analysis. British Journal of Psychology, 3(2): 77-85. DOI: https://www.doi.org/10.1111/j.2044-8317.1950.tb00285.x

Belay K (2014). Analysis of lead (Pb), cadmium (Cd) and chromium (Cr) in Ethiopian spices after wet (acid) digestion using atomic absorption spectroscopy. Global Journal of Science Frontier Research, 14(4): 1-6. Available at: https://globaljournals.org/GJSFR_Volume14/1-Analysis-of-Lead-Pb-Cadmium-Cd.pdf

Bhanugopan MS, Fulkerson WJ, Hyde M, and Fraser DR (2015). Effect of dietary potassium supplementation on the calcium absorption capacity in the rumen and abomasum and fractional excretion of urinary minerals in sheep. Animal Production Science, 55(4): 508-514. DOI: https://www.doi.org/10.1071/AN12366

Bijsmans E, Quéau Y, and Biourge V (2021). Increasing dietary potassium chloride promotes urine dilution and decreases calcium oxalate relative supersaturation in healthy dogs and cats. Animals, 11(6): 1809. DOI: https://www.doi.org/10.3390/ani11061809

Blagojević SM, Blagojević SN, and Begović BM (2016). Lead, mercury and arsenic content in spices: Black, white and green pepper, black cumin and ginger. Facta Universitatis - Series: Physics, Chemistry and Technology, 13(3): 191-202. DOI: https://www.doi.org/10.2298/FUPCT1503191B

Bouhenni H, Doukani K, Şekeroğlu N, Gezici S, and Tabak S (2019). Comparative study on chemical composition and antibacterial activity of fenugreek (*Trigonella foenum graecum* L.) and cumin (*Cuminum cyminum* L.) seeds. Ukrainian Food Journal, 8(4): 755-767. DOI: https://www.doi.org/10.24263/2304-974X-2019-8-4-7

Bouida L, Rafatullah M, Kerrouche A, Qutob M, Alosaimi AM, Alorfi HS, and Hussein MA (2022). A review on cadmium and lead contamination: Sources, fate, mechanism, health effects and remediation methods. Water, 14(21): 3432. DOI: https://www.doi.org/10.3390/w14213432

Boularbah A, Schwartz C, Bitton G, Aboudrar W, Ouhammou A, and Morel JL (2006). Heavy metal contamination from mining sites in South Morocco: 2. Assessment of metal accumulation and toxicity in plants. Chemosphere, 63(5): 811-817. DOI: https://www.doi.org/10.1016/j.chemosphere.2005.07.076

Bouzaid H, Espírito Santo L, Ferreira DM, Machado S, Costa ASG, Dias MI, Calhelha RC, Barros L, Chater O, Rodi YK et al. (2024). Detailed phytochemical composition, cyto-/hepatotoxicity, and antioxidant/anti-inflammatory profile of Moroccan spices: A study on coriander, caraway, and mystical cumin. Molecules, 29(15): 3485. DOI: https://www.doi.org/10.3390/molecules29153485

Briffa J, Sinagra E, and Blundell R (2020). Heavy metal pollution in the environment and their toxicological effects on humans. Heliyon, 6(9): e04691. DOI: https://www.doi.org/10.1016/j.heliyon.2020.e04691

Chandler ML (2008). Pet food safety: Sodium in pet foods. Topics in Companion Animal Medicine, 23(3): 148-153. DOI: https://www.doi.org/10.1053/j.tcam.2008.04.008

Cherkani-Hassani A, Slaoui M, Ghanname I, Mojemmi B, Belhaj A, Kers B, Flayou M, and Mouane N (2020). Cadmium contamination in breast milk of Moroccan lactating women and the associated factors: Contamilk study. Biological Trace Element Research, 196(1): 47-59. DOI: https://www.doi.org/10.1007/s12011-019-01912-2

Chore E, Olale K, Mogwasi R, and Ogutu H (2024). Spicing up nutrition: Investigation of trace elements in some spices locally sold in two markets in Kisumu-Kenya. Environmental Monitoring and Assessment, 196(12): 1247. DOI: https://www.doi.org/10.1007/s10661-024-13429-w

Cicero N, Gervasi T, Durazzo A, Lucarini M, Macrì A, Nava V, Giarratana F, Tardugno R, Vadalà R, and Santini A (2022). Mineral and microbiological analysis of spices and aromatic herbs. Foods, 11(4): 548. DOI: https://www.doi.org/10.3390/foods11040548

Darmono D (1999). Cadmium (CD) in the environment and its effect on the animal health and productivity. Indonesian Center for Animal Research and Development, Wartazoa, 8(1): 28-32. Available at: https://wwwww.repository.pertanian.go.id/handle/123456789/4617

Destro A LF, Alves TS, Dias FR, Gonçalves RV, de Oliveira JM, de Oliveira LL, and Freitas MB (2025). Individual acute exposures to low concentrations of cadmium, chromium, lead, and nickel affect oxidative stress and pathological markers in fruit bats. ACS Omega, 10(19): 19797-19807. DOI: https://www.doi.org/10.1021/acsomega.5c00991

European commission (EU Commission) (2012). Commission regulation (EU) No. 744/2012 of 16 August 2012 amending Annex I to directive 2002/32/EC as regards maximum levels for arsenic, cadmium, lead, nitrites, volatile mustard oil and harmful botanical impurities in feed. Official Journal of the European Union, L 219: 5-12. Available at: https://eur-lex.europa.eu/legal-content/FR/ALL/?uri=CELEX:32012R0744

European commission (EU Commission) (2021). Commission regulation (EU) 2021/1323 of 10 August 2021 amending regulation (EC) No 1881/2006 as regards maximum levels of cadmium in certain foodstuffs. Official Journal of the European Union, L 288: 1-11. Available at: https://eur-lex.europa.eu/eli/reg/2021/1323/oj

EFSA feedap panel (2016). EFSA panel on additives and products or substances used in animal feed (EFSA feedap panel), Scientific opinion on the safety and efficacy of iron compounds (E1) as feed additives for all animal species: ferrous carbonate; ferric chloride, hexahydrate; ferrous fumarate; ferrous sulphate, heptahydrate; ferrous sulphate, monohydrate; ferrous chelate of amino acids, hydrate; ferrous chelate of glycine, hydrate, based on a dossier submitted by FEFANA asbl. EFSA Journal, 14(2): 4396. DOI: https://www.doi.org/10.2903/j.efsa.2016.4396

European food safety authority (EFSA) (2004). Opinion of the scientific panel on contaminants in the food chain on a request from the commission related to cadmium as undesirable substance in animal feed. European Food Safety Authority, 2(6): 72. DOI: https://www.doi.org/10.2903/j.efsa.2004.72

El-Gogary MR, Dorra TM, and El-Sayed IA (2024). Effects of black pepper (*Piper nigrum*) as feed additives on growth performance, carcass traits, some blood parameters and gut morphology in broiler chickens. Egyptian Poultry Science Journal, 44(4): 403-415. DOI: https://www.doi.org/10.21608/epsj.2024.401677

El Youssfi M, Flayou M, El Idrissi ZL, Ben Ali M, Bennani M, El Hamidi A, Ben Aakame R, Laghzizil A, Zinedine A, and Sifou A (2025). Multi-element analysis of spices by inductively coupled plasma mass spectrometry and human risk assessment in the Rabat-Salé-Témara area (Morocco). Journal of Food Composition and Analysis, 140: 107235. DOI: https://www.doi.org/10.1016/j.jfca.2025.107235

Embuscado ME (2019). Bioactives from culinary spices and herbs: A review. Journal of Food Bioactives, 6: 68-99. DOI: https://www.doi.org/10.31665/JFB.2019.6186

Ereifej KI, Feng H, Rababah TM, Tashtoush SH, Al-U'datt MH, Al-Rabadi GJ, Torley P, and Alkasrawi M (2015). Microbiological status and nutritional composition of spices used in food preparation. Food Nutrition Sciences, 6(12): 1134-1140. DOI: https://www.doi.org/10.4236/fns.2015.612118

European commission (Eu Commission) (2023). Commission regulation (EU) 2023/915 of 25 April 2023 on maximum levels for certain contaminants in food and repealing Regulation (EC) No 1881/2006. Official Journal of the European Union, L 119: 1-63. Available at: https://www.eur-lex.europa.eu/eli/reg/2023/915/oj

Ezez D, Birhanu H, Shamena S, and Engidaw S (2024). Bioaccumulation of heavy metals, assessment of carcinogenic and non-carcinogenic health risk in various spices. Journal of Hazardous Materials Advances, 15: 100441. DOI: https://www.doi.org/10.1016/j.hazadv.2024.100441

Firisa TG, Geletu AK, Wondimu KT, and Kedir WM (2023). Proximate composition, levels of heavy metals and their associated risk assessment in ginger (*Zingiber officinale* roscoe). International Journal of Sustainable Energy and Environmental Research, 12(2): 46-57. DOI: https://www.doi.org/10.18488/13.v12i2.3585

Forsyth JE, Mistree D, Nash E, Angrish M, and Luby SP (2024). Evidence of turmeric adulteration with lead chromate across South Asia. Science of the Total Environment, 949: 175003. DOI: https://www.doi.org/10.1016/j.scitotenv.2024.175003

Fox JG and Boylen GW (1978). Analysis of lead in animal feed ingredients. American Journal of Veterinary Research, 39(1): 167-169. DOI: https://www.doi.org/10.2460/ajvr.1978.39.01.167

Friendly M (2002). Corrgrams: Exploratory displays for correlation matrices. The American Statistician, 56(4): 316-324. DOI: https://www.doi.org/10.1198/000313002533

Garcia E, Cabrera C, Lorenzo ML, and López MC (2000). Chromium levels in spices and aromatic herbs. Science of the Total Environment, 247(1): 51-56. DOI: https://www.doi.org/10.1016/S0048-9697(99)00467-2

Gaya U and Ikechukwu S (2016). Heavy metal contamination of selected spices obtained from Nigeria. Journal of Applied Sciences Environmental Management, 20(3): 681-688. DOI: https://www.doi.org/10.4314/jasem.v20i3.23

Gleason K, Shine JP, Shobnam N, Rokoff LB, Suchanda HS, Ibne Hasan MOS, Mostofa G, Amarasiriwardena C, Quamruzzaman Q, Rahman M et al. (2014). Contaminated turmeric is a potential source of lead exposure for children in Rural Bangladesh. Journal of Environmental and Public Health, 2014(1): 730636. DOI: https://www.doi.org/10.1155/2014/730636

Gul S and Safdar M (2009). Proximate composition and mineral analysis of cinnamon. Pakistan Journal of Nutrition, 8(9): 1456-1460. DOI: https://www.doi.org/10.3923/pjn.2009.1456.146

Hands JM, Anderson ML, Cooperman T, Balsky JE, and Frame LA (2024). A multi-year heavy metal analysis of 72 dark chocolate and cocoa products in the USA. Frontiers in Nutrition, 11: 1366231. DOI: https://www.doi.org/10.3389/fnut.2024.1366231

Harrington DD (1974). Pathologic features of magnesium deficiency in young horses fed purified rations. American Journal of Veterinary Research, 35(4): 503-513. DOI: https://www.doi.org/10.2460/ajvr.1974.35.04.503

Hashemi SR and Davoodi H (2011). Herbal plants and their derivatives as growth and health promoters in animal nutrition. Veterinary Research Communications, 35(3): 169-180. DOI: https://www.doi.org/10.1007/s11259-010-9458-2

Hoogenboom RLAP, Hattink J, van Polanen A, van Oostrom S, Verbunt JT, Traag WA, Kan KA, van Eijkeren JCH, De Boeck G, and Zeilmaker MJ (2015). Carryover of cadmium from feed in growing pigs. Food Additives & Contaminants: Part A, 32(1): 68-79. DOI: https://www.doi.org/10.1080/19440049.2014.979370

Huff A, Lam H, Ghimirey A, Goldring J, Pimentel M, and Okatch H (2025). Heavy metals in spices from Lancaster, PA: Arsenic, cadmium, and lead exposure risks and the need for regulation. Environmental Monitoring and Assessment, 197(5): 608. DOI: https://www.doi.org/10.1007/s10661-025-14064-9

Hussain S, Zamir I, Javed M, Munawar KS, and Batool IJLGUJLS (2020). Phytochemical composition of ginger, its nutritional and pharmacological importance. LGU Journal of Life Sciences, 4(1): 17-31. DOI: https://www.doi.org/10.54692/lgujls.2019.040103

Institut Marocain de Normalisation [The Moroccan standards institute] (IMANOR) (2012). Produits alimentaires - Dosage des éléments traces - Dosage de l'arsenic, du cadmium, du mercure et du plomb par spectrométrie d'émission avec plasma induit par haute fréquence et spectromètre de

masse (ICP-MS) après digestion sous pression [Food products - Trace element analysis - Analysis of arsenic, cadmium, mercury and lead by inductively coupled plasma mass spectrometry (ICP-MS) after pressure digestion]. Institut Marocain de Normalisation (IMANOR). Available at: https://www.imanor.gov.ma/Norme/nm-en-15763/

Islam MS, Ahmed MK, Al Bakky A, Ismail Z, Ibrahim KA, and Idris AM (2025). Assessing chemical properties and heavy metals in groundwater resources in a developing country: A baseline study. Scientific Reports, 15(1): 29628. DOI: https://www.doi.org/10.1038/s41598-025-15128-z

Iwegbue CM, Nwozo SO, Overah CL, Bassey FI, and Nwajei GE (2013). Concentrations of selected metals in some ready-to-eat-foods consumed in Southern Nigeria: Estimation of dietary intakes and target hazard quotients. Turkish Journal of Agriculture - Food Science and Technology, 1(1): 1-7. DOI: https://www.doi.org/10.24925/turjaf.v1i1.1-7.1

Jabborova D, Choudhary R, Karunakaran R, Ercisli S, Ahlawat J, Sulaymanov K, Azimov A, and Jabbarov Z (2021). The chemical element composition of turmeric grown in soil–climate conditions of Tashkent Region, Uzbekistan. Plants, 10(7): 1426. DOI: https://www.doi.org/10.3390/plants10071426

Jaishankar M, Tseten T, Anbalagan N, Mathew BB, and Beeregowda KN (2014). Toxicity, mechanism and health effects of some heavy metals. Interdisciplinary Toxicology, 7(2): 60-72. DOI: https://www.doi.org/10.2478/intox-2014-0009

Jolliffe IT and Cadima J (2016). Principal component analysis: A review and recent developments. 374(2065): 20150202. DOI: https://www.doi.org/10.1098/rsta.2015.0202

Kachbi A, Arezoug D, Kara-Abdelfettah D, Benamor M, and Senhadji-Kebiche O (2022). Determination of metal contents in aromatic herbs and spices from Algeria: Chemometric approach. Journal of Chemometrics, 36(9): e3437. DOI: https://www.doi.org/10.1002/cem.3437

Kaiser HF (1974). An index of factorial simplicity. Psychometrika, 39(1): 31-36. DOI: https://www.doi.org/10.1007/BF02291575

Official journal of the European communities (2002). Directive 2002/32/EC of the European Parliament and of the Council of 7 May 2002 on undesirable substances in animal feed. Official Journal of the European Communities, (L 140): 10-21. Available at: https://eurlex.europa.eu/eli/dir/2002/32/oj/eng

Madhusankha GDMP, Thilakarathan RCN, Liyanage T, and Navaratne SB (2019). Compositional analysis of turmeric types cultivated in Sri Lanka and India. International Journal of Herbal Medicine, 7(1): 35-38. Available at: https://www.florajournal.com/archives/?year=2019&vol=7&issue=1&part=A&ArticleId=554

Maghrabi IA (2014). Determination of some mineral and heavy metals in Saudi Arabia popular herbal drugs using modern techniques. African Journal of Pharmacy and Pharmacology, 8(36): 893-898. DOI: https://www.doi.org/10.5897/AJPP12.1455

Mayne ST (2023). The FDA's action plan to reduce dietary exposure to arsenic, lead, cadmium, and mercury for infants and young children. The American Journal of Clinical Nutrition, 117(4): 647-648. DOI: https://www.doi.org/10.1016/j.ajcnut.2023.02.004

Mazarakioti EC, Zotos A, Thomatou AA, Kontogeorgos A, Patakas A, and Ladavos A (2022). Inductively coupled plasma-mass spectrometry (ICP-MS), a useful tool in authenticity of agricultural products' and foods' origin. Foods, 11(22): 3705. DOI: https://www.doi.org/10.3390/foods11223705

Meena SS, Sharma YK, Mahatma MK, Lal S, Meena MD, Meena RD, Chaudhary N, YR, and Bhardwaj V (2024). Cumin (*Cuminum cyminum* L.) an export-oriented Indian seed spice with inherent nutraceutical and therapeutic attributes: A review. International Journal of Seed Spices, 12(1): 1-12. DOI: https://www.doi.org/10.56093/IJSS.v12i1.1

Mihaylova V, Lyubomirova V, and Djingova R (2013). Optimization of sample preparation and ICP-MS analysis for determination of 60 elements for characterization of the plant ionome. International Journal of Environmental Analytical Chemistry, 93(13): 1441-1456. DOI: https://www.doi.org/10.1080/03067319.2012.736978

Mir MA, Ashraf MW, and Andrews K (2024). Assessment of heavy metals and fungi contamination of spices available in Saudi Arabian food cuisines. Food Chemistry Advances, 4: 100694. DOI: https://www.doi.org/10.1016/j.focha.2024.100694

Mohammed FS, Sevindik M, Uysal I, Cesko C, and Koraqi H (2024). Chemical composition, biological activities, uses, nutritional and mineral contents of cumin (*Cuminum cyminum*). Measurement: Food, 14: 100157. DOI: https://www.doi.org/10.1016/j.meafoo.2024

Moore EK, Martinez DL, Srivastava N, Morrison SM, and Spielman SJ (2022). Mineral element insiders and outliers play crucial roles in biological evolution. Life, 12(7): 951. DOI: https://www.doi.org/10.3390/life12070951

Moreira P, Palhari C, and Berber R (2020). Dietary chromium and growth performance animals: A review. Scientific Electronic Archives, 13(7): 59-66. DOI: https://www.doi.org/10.36560/13720201151

Moussa L, Hassan HF, Savvaidis IN, and Karam L (2024). Impact of source, packaging and presence of food safety management system on heavy metals levels in spices and herbs. PLoS One, 19(8): e0307884. DOI: https://www.doi.org/10.1371/journal.pone.0307884

Najem M, Bouiamrine EH, and Ibijbijen J (2024). Ras el hanout: A theriac of therapeutic plants and spices-qualitative and quantitative ethnobotanical investigation in the city of Meknes (Morocco). Ethnobotany Research Applications, 29: 1-32. Available at: https://www.ethnobotanyjournal.org/index.php/era/article/view/6462

National academies of sciences, engineering, and medicine (NASEM) (2022). Dietary reference intakes for chromium. Dietary reference intakes for vitamin A, vitamin K, Arsenic, Boron, Chromium, Copper, Iodine, Iron, Manganese, Molybdenum, Nickel, Silicon, Vanadium, and Zinc. The National Academies Press., Washington, pp.p.6. 241-265. https://www.ncbi.nlm.nih.gov/books/NBK222329/?utm_source=chatgpt.com

National research council (NRC) (2001). Nutrient requirements of dairy cattle, 7th Revised Edition. National Academies Press., Washington, DC. DOI: https://www.doi.org/10.17226/9825

Odhav B, Beekrum S, Akula U, and Baijnath H (2007). Preliminary assessment of nutritional value of traditional leafy vegetables in KwaZulu-Natal, South Africa. Journal of Food Composition and Analysis, 20(5): 430-435. DOI: https://www.doi.org/10.1016/j.jfca.2006.04.015

Oladeji OM, Aasa OA, Adelusi OA, and Mugivhisa LL (2023). Assessment of heavy metals and their human health risks in selected spices from South Africa. Toxicology Reports, 11: 216-220. DOI: https://www.doi.org/10.1016/j.toxrep.2023.09.008

Olusola J, Akintan O, and Osanyinlusi O (2025). Trace metals potential human health risks assessment through consuming common food spices in Ado Ekiti, Southwest, Nigeria. Journal of Trace Elements and Minerals, 11: 100208. DOI: https://www.doi.org/10.1016/j.jtemin.2024.100208

Osei-Safo I, Miezah K, Sackey LNA, Adusei-Gyamfi J, and Abdul AM (2024). Trace and heavy metals in locally and imported spices sold on markets in Accra Metropolis, Ghana. The Scientific World Journal, 2024(1): 3168279. DOI: https://www.doi.org/10.1155/2024/3168279

Otunola GA, Oloyede OB, Oladiji AT, and Afolayan AJ (2010). Comparative analysis of the chemical composition of three spices - *Allium sativum* L., *Zingiber officinale* Rosc. and *Capsicum frutescens* L. commonly consumed in Nigeria. African Journal of Biotechnology, 9(41): 6927-6931. DOI: https://www.doi.org/10.5897/AJB10.183

Özden H (2021). Assessment of toxic metals in commonly used herbs and spices in Turkey. İstanbul Journal of Pharmacy, 51(3): 392-397. DOI: https://www.doi.org/10.26650/IstanbulJPharm.2021.1000200

PavloviĆ AN, MrmoŠAnin JM, JovanoviĆ SČ, MitiĆ SS, ToŠIĆ SB, KrstiĆ JN, and StojanoviĆ GS (2020). Elemental analysis of culinary herbs and spices by Icp Oes: Classification by chemometrics. Studia Universitatis Babeș-Bolyai Chemia, 65(2): 69-83. DOI: https://www.doi.org/10.24193/subbchem.2020.2.06

Pearson K (1895). VII. Note on regression and inheritance in the case of two parents. The Royal Society, 58(347-352): 240-242. DOI: https://www.doi.org/10.1098/rspl.1895.0041

Penkov D and Hristev H (2019). Monitoring of some indicators of lead and cadmium spread along the trophic chain feed - animals - food in a region with an increased ecological Clarc. Bulgarian Journal of Agricultural Science, 25(1): 183-187. Available at: https://www.agrojournal.org/25/01-25.pdf

Peter KV (2006). Handbook of herbs and spices (Vol.3). Woodhead publishing in Food Science, Technology and Nutrition. Available at: https://www.sciencedirect.com/book/9781845690175/handbook-of-herbs-and-spices

Phillips CJC and Prankel SH (2011). Cadmium and the welfare of animals. In: J. Nriagu (Editor), Encyclopedia of environmental health, 2nd Edition. Elsevier., Oxford, pp. 470-474. DOI: https://www.doi.org/10.1016/B978-0-444-63951-6.00503-9

Phillips RW (1998). Questioning some of the CVMA pet food recommendations. Canadian Veterinary Journal, 39(6): 332-334. Available at: https://www.pubmed.ncbi.nlm.nih.gov/9635167/

Potortì AG, Bua GD, Lo Turco V, Ben Tekaya A, Beltifa A, Ben Mansour H, Dugo G, and Di Bella G (2020). Major, minor and trace element concentrations in spices and aromatic herbs from Sicily (Italy) and Mahdia (Tunisia) by ICP-MS and multivariate analysis. Food Chemistry, 313: 126094. DOI: https://www.doi.org/10.1016/j.foodchem.2019.126094

Prankel SH, Nixon RM, and Phillips CJC (2004). Meta-analysis of feeding trials investigating cadmium accumulation in the livers and kidneys of sheep. Environmental Research, 94(2): 171-183. DOI: https://www.doi.org/10.1016/S0013-9351(03)00084-7

Primožič S, Terro C, Strojnik L, Šegatin N, Poklar Ulrih N, and Ogrinc N (2025). Assessing the authenticity and quality of paprika (*Capsicum annuum*) and cinnamon (*Cinnamomum* spp.) in the Slovenian market: A multi-analytical and chemometric approach. Foods, 14(13): 2323. DOI: https://www.doi.org/10.3390/foods14132323

Rahman Z and Singh VP (2019). The relative impact of toxic heavy metals (THMs) (arsenic (As), cadmium (Cd), chromium (Cr)(VI), mercury (Hg), and lead (Pb)) on the total environment: An overview. Environmental Monitoring and Assessment, 191(7): 419. DOI: https://www.doi.org/10.1007/s10661-019-7528-7

Saeed MK, Nisa AU, Ahmad I, Hina S, Zahra N, and Kalim I (2021). Physico-chemical analysis, total polyphenolic content and antioxidant capacity of yellow dye extracted from curcuma longa: Antioxidant capacity of yellow dye. Biological Sciences, 64(1): 25-29. DOI: https://www.doi.org/10.52763/PJSIR.BIOL.SCI.64.1.2021.25.29

Savić S, Petrović S, Petronijević M, Cvetanović A, and Petronijević Ž (2019). Determination of the mineral content of spices by ICP-OES. Advanced Technologies, 8(1): 27-32. DOI: https://www.doi.org/10.5937/SavTeh1901027S

Seddigi ZS, Kandhro GA, Shah F, Danish E, and Soylak M (2013). Assessment of metal contents in spices and herbs from Saudi Arabia. Toxicology and Industrial Health, 32(2): 260-269. DOI: https://www.doi.org/10.1177/0748233713500822

Sekeroglu N, Ozkutlu F, Kara SM, and Ozguven M (2006). Determination of cadmium and selected micronutrients in commonly used and traded medicinal plants in Turkey. Journal of the Science of Food and Agriculture, 8(1): 86-90 DOI: https://www.doi.org/10.1002/jsfa.3048

Sharda N, Kumar D, and Srivastava S (2017). Analysis of trace element & heavy metals in common spices marketed in Gurgaon, Haryana, India. International Journal of Scientific Research in Science, Engineering and Technology, 3(3): 116-119. Available at: https://ijsrset.com/IJSRSET173319

Shim J, Cho Y, Lee K, An H, and Lee C (2021). Multivariate analysis of metals contents in spices commonly consumed in Republic of Korea. Food Additives & Contaminants: Part B, 14(3): 184-192. DOI: https://www.doi.org/10.1080/19393210.2021.1914196

Standish JF, Ammerman CB, Simpson CF, Neal FC, and Palmer AZ (1969). Influence of graded levels of dietary iron, as ferrous sulfate, on performance and tissue mineral composition of steers. Journal of Animal Science, 29(3): 496-503. DOI: https://www.doi.org/10.2527/jas1969.293496x

Taghizadeh SF, Giesy JP, Rezaee R, and Karimi G (2024). Non-carcinogenic and carcinogenic health risk assessment of pesticides and metals in spice samples from Iran. Journal of Food Composition and Analysis, 134: 106544. DOI: https://www.doi.org/10.1016/j.jfca.2024.106544

Tesink J (1994). Lead and health. Tijdschr Diergeneeskd, 119(7): 197-201. Available at: https://pubmed.ncbi.nlm.nih.gov/8160168/10.1289/ehp.94102s3331

The international council for harmonisation of technical requirements for pharmaceuticals for human use (ICH) (2005). Validation of analytical procedures: Text and methodology Q2(R1). European Medicines Agency. Available at: https://www.ema.europa.eu/en/documents/scientific-guideline/ich-q-2-r1-validation-analytical-procedures-text-methodology-step-5_en.pdf

Thiangtum W, Yawongsa A, Schonewille JT, Rukkwamsuk T, Yuangklang C, Verstegen MW, and Hendriks WH (2011). An attempt to define the sodium requirement of lactating dairy cows in a tropical environment. Journal of the Science of Food and Agriculture, 91(13): 2333-2337. DOI: https://www.doi.org/10.1002/jsfa.4462

Tinggi U, Farrell M, Porter J, Mitchell S, and Jurd S (2025). Heavy metal analysis in commercial spices and herbs by inductively coupled plasma mass spectrometry (ICP-MS) and estimated dietary exposure. Journal of Environmental Exposure Assessment, 4: 26. DOI: https://www.doi.org/10.20517/jeea.2025.10

Tokalıoğlu Ş, Çiçek B, İnanç N, Zararsız G, and Öztürk A (2018). Multivariate statistical analysis of data and ICP-MS determination of heavy metals in different brands of spices consumed in Kayseri, Turkey. Food Analytical Methods, 11(9): 2407-2418. DOI: https://www.doi.org/10.1007/s12161-018-1209-y

Troeschel AN, Buser MC, Winquist A, Ruckart P, Yeh M, Kuai D, Chang A, Pennington AF, Rumph JT, Smith MR et al. (2025). Investigation of lead and chromium exposure after consumption of contaminated cinnamon-containing applesauce—United States, November 2023-April 2024. Morbidity Mortality Weekly Report, 74(14): 239-244. DOI: https://www.doi.org/10.15585/mmwr.mm7414a2

Ullrey DE, Miller ER, Thompson OA, Ackermann IM, Schmidt DA, Hoefer JA, and Luecke RW (1960). The requirement of the baby pig for orally administered iron. The Journal of Nutrition, 70(2): 187-192. DOI: https://www.doi.org/10.1093/jn/70.2.187

Varmazyar L and Sobhan S (2017). The risk assessment of Pb and Cd through consuming spices. Journal of School of Public Health and Institute of Public Health Research, 15(2): 185-195. Available at: http://www.sjsph.tums.ac.ir/article-1-5529-en.html

Voica C, Nechita C, Iordache AM, Roba C, Zgavarogea R, and Ionete RE (2021). ICP-MS assessment of essential and toxic trace elements in foodstuffs with different geographic origins available in Romanian supermarkets. Molecules, 26(23): 7081. DOI: https://www.doi.org/10.3390/molecules26237081

Vostrikova N, Minaev M, and Chikovani K (2021). Determining the authenticity of turmeric. Food Systems, 4(1): 62-70. DOI: https://www.doi.org/10.21323/2618-9771-2021-4-1-62-70

Wang K, Fu G, Yu Y, Wan Y, Liu Z, Wang Q, Zhang J, and Li H (2019). Effects of different potassium fertilizers on cadmium uptake by three crops. Environmental Science and Pollution Research, 26(26): 27014-27022. DOI: https://www.doi.org/10.1007/s11356-019-05930-4

Ward GM (1966). Potassium metabolism of domestic ruminants—A review. Journal of Dairy Science, 49(3): 268-276. DOI: https://www.doi.org/10.3168/jds.S0022-0302(66)87848-7

Ward Jr JH (1963). Hierarchical grouping to optimize an objective function. Journal of the American Statistical Association, 58(301): 236-244. DOI: https://www.doi.org/10.1080/01621459.1963.10500845

Windisch W, Schedle K, Plitzner C, and Kroismayr A (2008). Use of phytogenic products as feed additives for swine and poultry. Journal of Animal Science, 86(suppl_14): E140-E148. DOI: https://www.doi.org/10.2527/jas.2007-0459

Yánez-Jácome GS, Romero-Estévez D, Rosero-Jácome AP, Cipriani-Avila I, Navarrete H, and Vélez-Terreros PY (2024). Lead content in cinnamon and its health risk assessment for Ecuadorian consumers. Food and Chemical Toxicology, 193: 115010. DOI: https://www.doi.org/10.1016/j.fct.2024.115010

Yousaf Z, Hussain SM, Ali S, Sarker K, and Al-Ghanim KA (2025). Recuperative effects of cinnamon (*Cinnamomum zeylanicum*) in Catla after sub-lethal exposure to lead. Biological Trace Element Research, 203(2): 1075-1084. DOI: https://www.doi.org/10.1007/s12011-024-04213-5

Yücel UM and Atasoy NJG (2019). Determination of Fe, Cu and Zn content in some spices sold without packaging in van. Gıda, 44(5): 889-897. DOI: https://www.doi.org/10.15237/gida.GD19032

Yücel, M, Özkan M, and Turhan E (2022). Determination of heavy metals in spices sold in Turkey. Turkish Journal of Agriculture - Food Science and Technology, 10(10): 1952-1956. DOI: https://www.doi.org/10.53424/balikesirsbd.1160866

Zang J, Chen J, Tian J, Wang A, Liu H, Hu S, Che X, Ma Y, Wang J, Wang C et al. (2014). Effects of magnesium on the performance of sows and their piglets. Journal of Animal Science and Biotechnology, 5(1): 39. DOI: https://www.doi.org/10.1186/2049-1891-5-39

Zaragüeta A, Enrique A, Virto I, Antón R, Urmeneta H, and Orcaray L (2021). Effect of the long-term application of sewage sludge to a calcareous soil on its total and bioavailable content in trace elements, and their transfer to the crop. Minerals, 11(4): 356. DOI: https://www.doi.org/10.3390/min11040356

Zeiner M, Fiedler H, Juranović Cindrić I, Nemet I, Toma D, and Habinovec I (2023). Preliminary study of pepper types based on multielement content combined with chemometrics. Foods, 12(16): 3132. DOI: https://www.doi.org/10.3390/foods12163132

Zeiner M, Šoltić M, Nemet I, and Juranović Cindrić I (2022). Multielement determination in turmeric (*Curcuma longa* L.) using different digestion methods. Molecules, 27(23): 8392. DOI: https://www.doi.org/10.3390/molecules27238392

Ziyaina M, Rajab A, Alkhweldi K, Algami W, Al-Toumi O, and Rasco B (2014). Lead and cadmium residue determination in spices available in Tripoli City markets (Libya). African Journal of Biochemistry Research, 8(7): 137-140. DOI: https://www.doi.org/10.5897/AJBR2014.0766

Publisher's note: Scienceline Publication Ltd. remains neutral with regard to jurisdictional claims in published maps and institutional affiliations.

Open Access: This article is licensed under a Creative Commons Attribution 4.0 International License, which permits use, sharing, adaptation, distribution and reproduction in any medium or format, as long as you give appropriate credit to the original author(s) and the source, provide a link to the Creative Commons licence, and indicate if changes were made. The images or other third party material in this article are included in the article's Creative Commons licence, unless indicated otherwise in a credit line to the material. If material is not included in the article's Creative Commons licence and your intended use is not permitted by statutory regulation or exceeds the permitted use, you will need to obtain permission directly from the copyright holder. To view a copy of this licence, visit https://creativecommons.org/licenses/by/4.0/.

© The Author(s) 2025

2025, Scienceline Publication
World's Veterinary Journal
World Vet J, 15(4): 882-890.
ISSN 2322-4568

DOI: https://dx.doi.org/10.54203/scil.2025.wvj89
PII: S232245682500089-15

Characterization of *Pasteurella multocida* Isolated from Layer Chickens Infected with Fowl Cholera in Sukabumi, Indonesia: Antibiotic Resistance and Virulence Gene Detection

Marsella Metta Arvia[1], Ryan Septa Kurnia[2], Christian Marco Hadi Nugroho[2], Muhammad Ade Putra[2], Safika[3], and Agustin Indrawati[3]*

[1]*School of Veterinary Medicine and Biomedical Sciences, IPB University, Bogor, 16680, Indonesia*
[2]*Indonesia Research and Diagnostic Unit, PT. Medika Satwa Laboratoris, Bogor, 16166, Indonesia*
[3]*Division of Medical Microbiology, School of Veterinary Medicine and Biomedical Sciences, IPB University, Bogor, 16680, Indonesia*

*Corresponding author's Email: indraseta@apps.ipb.ac.id

ORIGINAL ARTICLE
Received: September 30, 2025
Revised: October 27, 2025
Accepted: November 28, 2025
Published: December 25, 2025

ABSTRACT

Fowl cholera is a contagious bacterial disease in poultry caused by *Pasteurella multocida* (*P. multocida*), which presents a significant threat to layer chicken farming due to its economic impact and potential antibiotic resistance. This study aimed to characterize *P. multocida* isolates from a fowl cholera outbreak in Sukabumi by assessing antibiotic resistance profiles and detecting virulence-associated genes. Eight *P. multocida* bacterial isolates from organ sample were cultured on blood agar and subjected to antibiotic susceptibility testing using the Sensititre™ GN4F system. Genomic DNA was extracted and analyzed for 16 virulence genes through conventional polymerase chain reaction (PCR). Results showed that all isolates were generally susceptible to the tested antibiotics, except for isolate P.m1, which was confirmed resistant to levofloxacin and ciprofloxacin. Virulence gene detection revealed that most isolates carried nearly all virulence genes tested, particularly those encoding capsule (*capA*), iron acquisition proteins (*exbB*, *hgbB*, *fur*), fimbriae and adhesins (*fim4*, *fimA*, *pfhA*, *tadD*), outer membrane proteins (*oma87*, *plpB*), sialidases (*nanB*, *nanH*), and superoxide dismutases (*sodA*, *sodC*). Notably, no isolates harbored the *toxA* gene. The presence of extensive virulence factors despite general antibiotic susceptibility underscored the pathogen's potential to persist and cause disease, and highlighted the need for targeted surveillance and comprehensive control strategies in Indonesia.

Keywords: Antibiotic resistance, Characterization, Fowl cholera, *Pasteurella multocida*, Virulence gene

INTRODUCTION

The layer poultry farming sector has gained increased public attention due to the rising market demand for livestock products annually, driven by population growth and improved nutritional awareness (Maulana et al., 2017). However, the disease still represents a serious challenge in layer farms, causing economic impacts associated with lower egg yields and higher layer mortality (Faisal, 2019). One of the common diseases affecting layer farms is fowl cholera.

Fowl cholera is a contagious bacterial infection in avian species caused by *Pasteurella multocida* (*P. multocida*, Zainuddin, 2014). This gram-negative bacterium can colonize the mucosal surfaces of the upper respiratory tract, as well as the air sacs and lungs of chicken (Reuben et al., 2021). Transmission may occur through contact with infected layers, asymptomatic carriers, or contaminated equipment and environments. The clinical signs of fowl cholera include weakness, lethargy, anorexia, edema in the facial area, comb, and wattles (Zainuddin, 2014).

Treatment of *P. multocida* infections generally involves the use of antibiotics. Nonetheless, administration of antibiotics must be precise to prevent the emergence of antibiotic resistance (Furian et al., 2016). Antibiotic resistance poses a threat to animal health and well-being, increases production costs, and potentially facilitates the spread of resistance genes to other bacteria (Lobongona et al., 2019). Although antimicrobial resistance has been widely investigated in numerous poultry pathogens, information on the antibiotic resistance patterns of *P. multocida* in Asia remains limited (Sabsabi et al., 2021).

The pathogenesis of *P. multocida* infection arises from complex interactions between bacterial virulence genes and the host (Aski et al., 2016). Alongside comprehending pathogenesis, the identification of virulence genes advances the present understanding of the bacterium's epidemiology, immune evasion, and vaccine development. The identified virulence genes of *P. multocida* include capsule-based serotypes, iron metabolism proteins, toxins, fimbriae, adhesion factors, sialidase, and outer membrane proteins (Nguyen et al., 2023). Each virulence gene contributes a distinct role in enhancing the bacterium's ability to infect the host.

Understanding the antibiotic resistance profile of *P. multocida* is essential to ensure targeted and effective treatment while avoiding further resistance development. Likewise, identifying its virulence genes is important to determine the factors contributing to bacterial pathogenicity. These two parameters serve as a reference for developing appropriate control strategies for fowl cholera and preventing future outbreaks. The present study aimed to analyze the antibiotic

To cite this paper: Arvia MM, Kurnia RS, Nugroho CMH, Putra MA, Safika, and Indrawati A (2025). Characterization of *Pasteurella multocida* Isolated from Layer Chickens Infected with Fowl Cholera in Sukabumi, Indonesia: Antibiotic Resistance and Virulence Gene Detection. *World Vet. J.*, 15(4): 882-890. DOI: https://dx.doi.org/10.54203/scil.2025.wvj89

resistance and identify the virulence genes of *P. multocida* isolated from dead chickens in poultry during a fowl cholera outbreak in Sukabumi Regency, a major poultry production center in West Java Province, Indonesia.

MATERIALS AND METHODS

Ethical approval

Ethical approval for this study was obtained from the Animal Ethics Committee of the School of Veterinary Medicine and Biomedical Science, IPB University, Indonesia, under the approval number 121/SKE/X/2023.

Culture of *Pasteurella multocida* isolates

The *P. multocida* isolates used in this study were previously preserved as freeze-dried cultures and were revived prior to use. All eight isolates (P.m1–P.m8) originated from organ samples of dead chickens collected from poultry farms experiencing fowl cholera cases in Sukabumi between 2018 and 2022 (Table 1). The freeze-dried isolates were revived using 150 µL of Brain Heart Infusion (BHI) broth, streaked onto blood agar, and incubated overnight at 37°C. The isolates were tested biochemically for catalase, oxidase, and further verified by polymerase chain reaction (PCR; Mehmood et al., 2018).

Antibiotic resistance testing

Sensitivity to antibiotics assessed against 11 classes of antibiotics, including aminoglycosides, penicillins, β-lactamase inhibitor–penicillin combinations, carbapenems, fluoroquinolones, tetracyclines, cephalosporins, tigecycline, sulfonamides, monobactams, and nitrofurans. Antibiotic sensitivity was measured using the Minimum Inhibitory Concentration (MIC) method with the Sensititre™ GN4F system (Thermo Fisher, USA). Approximately 3–5 bacterial colonies were suspended in distilled water, and the bacterial concentration was adjusted to 0.5 McFarland standard, corresponding to an optical density (OD) of 0.08-0.1 at 600 nm, as measured using Genesys 10S UV-Vis spectrophotometer (Thermo Fisher, USA). Subsequently, 1 µL of the bacterial suspension was mixed with Mueller-Hinton Broth (MHB). A volume of 50 µL of the final suspension was dispensed into each well of the plate using a multichannel pipette. The plate was sealed and incubated at 34–36°C for 18–24 hours. The MIC results were manually interpreted by observing the presence or absence of bacterial growth, indicated by sediment at the bottom of each well. Genomic DNA from all *P. multocida* isolates was extracted using a modified boiling method as described by Sunartatie et al. (2024). Virulence gene detection was carried out through PCR. Each PCR reaction consisted of 5 µL of bacterial genomic DNA, 25 µL of MyTaq™ HS Red Mix master mix, 2 µL each of forward and reverse primers (Table 2) at a concentration of 10 µM, and 16 µL of nuclease-free water. The amplification was performed by SimpliAmp™ Thermal Cycler (Applied Biosystems, USA) under the following cycling conditions, including initial denaturation at 95°C for 15 seconds, annealing at 55°C for 15 seconds, and extension at 72°C for 10 seconds, repeated for 30 cycles. The PCR amplicons were analyzed by electrophoresis on a 1.5% agarose gel stained with 0.5 µg/mL ethidium bromide (EtBr). A 100 bp DNA ladder (VC 100 bp Plus DNA Ladder, Vivantis) was used as a molecular weight marker. The gel was electrophoresed at 120 V for 35 minutes (Indrawati et al., 2025).

Data analysis

Data obtained from the study were presented in tables and figures and analyzed descriptively. Antimicrobial susceptibility profiles were interpreted based on CLSI and EUCAST breakpoint criteria. The detection of virulence genes was reported as presence or absence for each isolate and displayed in a comparative table.

Table 1. *Pasteurella multocida* sample between 2018 and 2022 isolated from poultry farms in Sukabumi, West Java, Indonesia

No.	Isolate code	Date of isolation	Organ	Origin of the sample
1	P.m1	21/12/2018	Trachea	Cicurug, Sukabumi
2	P.m2	24/09/2019	Cardiac blood	Cicurug, Sukabumi
3	P.m3	25/09/2019	Liver	Cicurug, Sukabumi
4	P.m4	20/03/2020	Liver	Cicurug, Sukabumi
5	P.m5	23/12/2021	Tracheal	Cicurug, Sukabumi
6	P.m6	02/01/2022	Liver	Cicurug, Sukabumi
7	P.m7	01/08/2022	Lung	Cicurug, Sukabumi
8	P.m8	01/09/2022	Liver	Cicurug, Sukabumi

Table 2. Nucleotide sequence of *P. multocida* virulence gene primers

Genes	Targeted gene	Nucleotide Sequence (5'–3')	Amplicon size (bp)	Reference
CapA	*Serotyping A*	TGCCAAAATCGCAGTCAG TTGCCATCATTGTCAGTG	1044	Townsend et al. (2001)
ToxA	*Dermonecrotic toxin*	CTTAGATGAGCGACAAGG GAATGCCACACCTCTATAG	864	Tang et al. (2009)
TbpA	*Transferrin binding protein*	TGGTTGGAAACGGTAAAGC TAACGTGTACGGAAAAGCC	728	Townsend et al. (2001)
Fim4	*Type 4 fimbriae*	TGTGGAATTCAGCATTTTAGTGTGTC TCATGAATTCTTATGCGCAAAATCCTGCTGG	488	Tang et al. (2009)
SodC	*Superoxide dismutate*	AGTTAGTAGCGGGGTTGGCA TGGTGCTGGGTGATCATCATG	235	Ewers et al. (2006)
PfhA	*Filamentous hemagglutinin*	AGCTGATCAAGTGGTGAAC TGGTACATTGGTGAATGCTG	286	Atashpaz et al. (2009)
ExbB	*Iron acquisition*	TTGGCTTGTGATTGAACGC TGCAGGAATGGCGACTAAA	283	Tang et al. (2009)
HgbB	*Hemoglobin binding protein*	ACCGCGTTGGAATTATGATTG CATTGAGTACGGCTTGACAT	788	Ewers et al. (2006)
NanB	*Neuroaminidase*	GTCCTATAAAGTGACGCCGA ACAGCAAAGGAAGACTGTCC	554	Ewers et al. (2006)
TadD	*Putative non-spesific tight adherence protein D*	TCTACCCATTCTCAGCAAGGC ATCATTTCGGGCATTCACC	416	Tang et al. (2009)
PlpB	*Plasminogen-binding protein B*	TTTGGTGGTGCGTATGTCTTCT AGTCACTTTAGATTGTGCGTAG	282	Tang et al. (2009)
SodA	*Superoxide dismutate*	TACCAGAATTAGGCTACGC GAAACGGGTTGCTGCCGCT	361	Ewers et al. (2006)
Oma87	*Outer membrane protein 87*	ATGAAAAAACTTTTAATTGCGAGC TGACTTGCGCAGTTGCATAAC	948	Ewers et al. (2006)
FimA	*Fimbriae*	CCATCGGATCTAAACGACCTA AGTATTAGTTCCTGCGGGTG	866	Kim et al. (2019)
NanH	*Neuroaminidase*	GAATATTTGGGCGGCAACA TTCTCGCCCTGTCATCACT	360	Kim et al. (2019)
Fur	*Ferric uptake regulation protein*	GTTTACCGTGTATTAGACCA CATTACTACATTTGCCATAC	244	Kim et al. (2019)

RESULTS AND DISCUSSION

Antibiotic resistance

Antibiotics have been utilized in animal production for over five decades as therapeutic agents. Their ability to resist bacterial infections has contributed to increased average animal life expectancy, appropriate management of infectious diseases, reduced morbidity and mortality rates, and enhanced food safety. Their broad application in livestock health has also supported growth performance and productivity (Venkateswaran et al., 2023; Elbehiry and Marzouk, 2024). However, the misuse and overuse of antibiotics in these systems have accelerated the emergence of antimicrobial resistance, posing significant threats to both animal and public health (Alhassan et al., 2025). Antibiotic resistance denotes the ability of microorganisms to endure the inhibitory or bactericidal activity of antibiotic compounds (Abreu et al., 2023). Variations in Minimum Inhibitory Concentration (MIC) were observed among isolates for several antibiotics. The MIC is defined as the lowest concentration of an antibiotic compound, measured in µg/mL, that entirely inhibits the visible growth of a test microorganism *in vitro*. Analogous to the inhibition zone in qualitative methods, MIC values are used to determine the susceptibility or resistance category of a pathogen to a specific antibiotic. Elevated values correlate with an increased risk of treatment failure, regardless of the isolate's classification as susceptible to the tested antibiotic (Kowalska-Krochmal and Dudek-Wicher, 2021).

The antibiotic resistance profile of *P. multocida* isolates is presented in Table 3. Based on the analysis of sensitivity breakpoints for each antibiotic class, seven isolates were classified as sensitive to the tested antibiotics. Only one isolate, P.m1, exhibited resistance to two antibiotic classes (fluoroquinolones and tetracyclines). Fluoroquinolones are broad-spectrum antibiotics with high oral bioavailability and exert their bactericidal action by inhibiting bacterial topoisomerase II (gyrase) and topoisomerase IV (Redgrave et al., 2014; Hooper and Jacoby, 2015). Two fluoroquinolones, levofloxacin and ciprofloxacin, were evaluated in this study. According to EUCAST (2025), bacteria are considered susceptible to levofloxacin and ciprofloxacin if the MIC values are less than 2 µg/mL and less than 1 µg/mL, respectively. Isolate P.m1 was confirmed resistant to both levofloxacin and ciprofloxacin. Antibiotic resistance may arise from mutations in the target enzymes (Baggio and Ananda-Rajah, 2021).

Tetracyclines are broad-spectrum antibiotics that inhibit bacterial protein synthesis by binding to the 30S ribosomal subunit, preventing aminoacyl-tRNA from attaching to the A-site of the ribosome (Manoharan et al., 2023). Two

tetracyclines, tetracycline and minocycline, were tested in the present study. According to CLSI M45 (2015), bacteria are deemed susceptible to tetracycline if the MIC is less than 4 µg/mL. One isolate was verified resistant to tetracycline. Resistance to tetracycline is often facilitated by efflux pump mechanisms (Simanjuntak et al., 2022). Nevertheless, all isolates remained sensitive to minocycline.

In addition to its resistance phenotype, P.m1 carried fewer virulence-associated genes (11/16) compared to the other isolates, which possessed approximately 13–14 virulence genes. This difference suggests that P.m1 does not possess a unique virulence genotype that would confer a selective advantage over the fully susceptible isolates. The reduced virulence gene content may indicate a lower intrinsic virulence potential. Previous studies have demonstrated that the acquisition of antimicrobial resistance can impose a fitness cost on bacteria, sometimes affecting growth rate, virulence factor expression, or overall pathogenic potential (Hernando-Amado et al., 2017). Therefore, although P.m1 is resistant to multiple antibiotic classes, it is unlikely to be more pathogenic or epidemiologically successful than isolates with a broader virulence gene repertoire. These findings indicate that multidrug resistance alone does not necessarily translate into higher virulence or increased transmission potential in poultry infections.

Table 3. Results of *P. multocida* antibiotic resistance isolated from infected chicken between 2018-2022 in Sukabumi, West Java, Indonesia

Abs	Antibiotics	MIC (µg/mL)								Sensitivity standards
		P.m1	P.m2	P.m3	P.m4	P.m5	P.m6	P.m7	P.m8	
AMI	Amikacin	<8	<8	<8	<8	<8	<8	<8	16	≤16
P/T4	Piperacillin / tazobactam constant 4	<8/4	<8/4	<8/4	<8/4	<8/4	<8/4	<8/4	<8/4	≤16/8
TGC	Tigecycline	< 1	< 1	< 1	< 1	< 1	< 1	< 1	< 1	≤ 2
TIM2	Ticarcilin / clavulanic acid constant 2	< 8/2	< 8/2	< 8/2	< 8/2	< 8/2	< 8/2	< 8/2	<8/2	≤16/2
LEVO	Levofloxacin	2	< 1	< 1	< 1	< 1	< 1	< 1	< 1	< 2
NIT	Nitrofurantoin	< 32	< 32	< 32	< 32	< 32	< 32	< 32	< 32	≤ 32
TET	Tetracycline	➢	< 4	< 4	< 4	< 4	< 4	< 4	< 4	≤ 4
DOR	Doripenem	< 0.5	< 0.5	< 0.5	< 0.5	< 0.5	< 0.5	< 0.5	< 0.5	≤ 0.5
MIN	Minocycline	< 1	< 1	< 1	< 1	< 1	< 1	< 1	< 1	≤ 1
ETP	Ertapenem	< 0.25	< 0.25	< 0.25	< 0.25	< 0.25	< 0.25	< 0.25	< 0.25	≤ 0.5
SXT	Trimethoprim / sulfamethoxazole	< 2/38	< 2/38	< 2/38	< 2/38	< 2/38	< 2/38	< 2/38	< 2/38	≤ 2/38
IMI	Imipenem	1	< 0.5	< 0.5	1	< 0.5	< 0.5	< 0.5	< 0.5	≤ 1
PIP	Piperacillin	< 16	< 16	< 16	< 16	< 16	< 16	< 16	< 16	≤ 16
MERO	Meropenem	< 0.5	< 0.5	< 0.5	< 0.5	< 0.5	< 0.5	< 0.5	< 0.5	≤ 1
GEN	Gentamicin	< 2	< 2	< 2	< 2	< 2	< 2	4	< 2	≤ 4
FAZ	Cefazolin	< 1	< 1	< 1	< 1	< 1	< 1	< 1	< 1	≤ 2
TOB	Tobramycin	< 2	< 2	< 2	< 2	< 2	< 2	4	< 2	≤ 4
TAZ	Ceftazidime	< 1	< 1	< 1	< 1	< 1	< 1	< 1	< 1	≤ 4
A/S2	Ampicillin / sulbactam 2:1 ratio	< 4/2	< 4/2	< 4/2	< 4/2	< 4/2	< 4/2	< 4/2	< 4/2	≤ 8/4
AZT	Aztreonam	< 1	< 1	< 1	< 1	< 1	< 1	< 1	< 1	≤ 1
AMP	Ampicillin	< 8	< 8	< 8	< 8	< 8	< 8	< 8	< 8	≤ 8
FEP	Cefepime	< 4	< 4	< 4	< 4	< 4	< 4	< 4	< 4	≤ 4
CIP	Ciprofloxacin	2	< 0.5	< 0.5	< 0.5	< 0.5	< 0.5	< 0.5	< 0.5	≤ 1
AXO	Ceftriaxone	< 0.5	< 0.5	< 0.5	< 0.5	< 0.5	< 0.5	< 0.5	< 0.5	≤ 1
POS	Positive control	+++	+++	+++	+++	+++	+++	+++	+++	

Abs: Abbreviation; MIC: Minimum inhibitory concentration; P.m: *Pasteurella multocida* isolates refer to Table 1; +++: The appearance of a cell sediment indicates bacterial growth

Detection of virulence genes

The pathogenicity of *Pasteurella multocida* is largely determined by the assortment of virulence-associated genes and factors it carries (Effendi et al., 2022). Each gene group contributes a distinct role in enhancing the bacterium's ability to infect the host. In this study, 16 virulence genes were detected and classified into seven functional groups, including capsule, toxins, iron acquisition proteins, fimbriae and adhesins, sialidases, outer membrane proteins (OMPs), and superoxide dismutases (SODs). Genes involved in iron acquisition (*exbB, exbD, tonB*), OMPs (*ompA, oma87*), adhesins/fimbriae (*fimA*), heme-binding (*hgbA*), and sialidase (*nanB*) were present in over 90% of sheep isolates (Nguyen et al., 2023). Toxin gene *toxA*, however, was detected only in specific serotypes, such as serotype D in sheep, highlighting serotype-dependent variation (Nguyen et al., 2023). In rabbit-derived isolates, fimbrial and adhesin genes (*fimA, pfhA, ptfA*) and *toxA* were present, and superoxide dismutase gene *sodC* was detected in all strains; additionally, *pfhA* correlated with capsular type, indicating its role in bacterial persistence (D'Amico et al., 2024; Wang et al., 2024). Collectively, these virulence genes contribute to essential processes, including iron uptake, adhesion to host tissues,

immune evasion through capsule and OMPs, sialic acid modification, toxin-mediated damage, and protection against oxidative stress, supporting the infection and survival of *P. multocida* in the host.

Detection findings revealed that 100% of isolates harbored the genes *capA*, *fim4*, *sodC*, *exbB*, *nanB*, *plpB*, *sodA*, *oma87*, and *fim*A; 87.5% carried *hgbB* and *fur*; 62.5% were positive for *pfhA*, *tadD*, and *nanH*; and 50% for *tbpA*. The *toxA* gene was absent in all isolates (Table 4). Among the isolates, the antibiotic-resistant strain P.m1 exhibited a slightly lower number of positive virulence genes (11/16) compared with most other isolates (13-14/16). Notably, P.m1 lacked *pfhA, tadD, tbpA, hgbB, fur,* and *nanH,* which are associated with adhesion, iron acquisition, and sialidase activity. However, it retained all core genes (*capA, fim4, sodC, exbB, nanB, plpB, sodA, oma87,* and *fimA*) that are essential for bacterial survival, adhesion, immune evasion, and oxidative stress resistance. These findings suggest that although P.m1 carries antimicrobial resistance, it maintains the fundamental virulence determinants necessary for host infection. The combination of resistance and retained core virulence genes indicates that resistant isolates like P.m1 can still pose significant pathogenic threats, highlighting the importance of considering both resistance and virulence profiles in epidemiological and clinical assessments of *P. multocida*.

The capsule is a polysaccharide structure that contributes to desiccation resistance, anti-phagocytic activity, and interacts with the complement system. *Pasteurella multocida* is categorized into five capsular types (A, B, D, E, and F) according to the presence of distinct capsule antigens. The findings of this study align with those of Furian et al. (2014), who identified capsular type A as the most prevalent in avian cholera cases, detecting *capA* in 49 of 54 isolates via multiplex PCR. The result of this study aligns with Shivachandra et al. (2006), who reported that 92 out of 94 isolates carried the *capA* gene.

The *toxA* gene encodes a mitogenic toxin that stimulates cell proliferation by interacting with heterotrimeric G proteins and modifying the alpha subunit through deamidation. This mechanism leads to cytoskeletal rearrangement, cellular proliferation, differentiation, and survival (Kubatzky, 2022). In contrast with previous studies by Sahragard et al. (2012), which reported high *toxA* prevalence in isolates from nasal and tonsil swabs of sheep and goats this present study did not detect *toxA* in any isolate. This absence can be explained by the capsular type of the isolates analyzed, which all belong to capsular type A. Notably, *toxA* is primarily associated with serogroup D strains in ruminants, including sheep and goats, and is rarely found in type A isolates or poultry-derived strains (Harper et al., 2006). Therefore, the lack of *toxA* is consistent with known serotype-specific distribution patterns in *P. multocida*, because *toxA* is sparsely distributed and associated with a prophage in only some serogroup A and D strains (Siddaramappa et al., 2021). The absence of *toxA* in capsular type A isolates aligns with these observations. Importantly, even in the absence of *toxA*, other virulence determinants such as *oma87, plpB, exbB, sodA, sodC,* and *nanB* remain present and may drive infection in type A isolates, demonstrating that pathogenicity is not solely dependent on the toxin gene.

Iron plays a vital role in DNA and protein biosynthesis, biofilm formation, redox activity, and electron transport and is required for bacterial growth and metabolism. During host-pathogen interactions, iron facilitates bacterial proliferation, adhesion, and expression of virulence factors (Shen et al., 2025). These findings correspond with Ewers et al. (2006), who identified *tbpA* in 70% of ruminant isolates but not in those from poultry, felines, or canines. The absence of *tbpA* in some isolates may be due to its incompatibility with the iron sources present in the avian host. The high detection rate of *hgbB* suggests that heme serves as a primary iron source for *P. multocida*. Other iron acquisition and virulence genes, including *fur, tonB, exbB, exbD, hgbA,* and *hgbB1/2,* have been frequently identified in avian isolates, highlighting their importance in bacterial survival and pathogenicity (Farahani et al., 2019).

Fimbriae and adhesin genes are critical for the initial stages of pathogenesis by facilitating attachment to host surfaces and colonization of the upper respiratory tract (Gross 2006; Haghnazari et al., 2017). These findings are consistent with Tawor et al. (2024), who reported *pfhA* and *tadD* in 55% and 60% of isolates, respectively, obtained from lung samples and nasal swabs of cattle, sheep, goats, and pet birds with respiratory symptoms. D'Amico et al. (2024) similarly detected *pfhA, tadD, fim4, and fimA* in 76.27%, 59.32%, and 92.23% respectively, also 69.49% of isolates possessed *capA*. Despite variations in prevalence among studies, these adhesin-related genes are commonly distributed among *P. multocida* isolates from diverse host species, highlighting their potential role in colonization and pathogenesis.

Sialidases allow *P. multocida* to hydrolyze sialic acids for nutrient acquisition, enabling the bacterium to use sialic acid as a carbon source, facilitating its growth and persistence on mucosal surfaces (Mizan et al., 2000). In this study, the detection of *nanB* and *nanH* aligns with previous reports. Gharibi et al. (2017) documented the occurrence of *nanB* and *nanH* in 63.6% and 81.8% of isolates, respectively, obtained from nasopharyngeal and nasal swab samples collected from slaughtered cattle and buffaloes. Nugroho et al. (2022) further demonstrated the functional significance of *nanB*, showing its toxicity and hemolytic activity using chicken and rabbit red blood cells, while also reporting variable detection rates of these genes, although the causes of this variability remain ambiguous. Additional evidence across species has been reported. Lachowicz-Wolak et al. (2025) detected *nanH* in isolates recovered from deep nasal swabs

and lung/bronchi swabs of calves with respiratory disease, while Ziagham et al. (2024) identified both *nanB* and *nanH* in isolates obtained from the oral cavity of various cat breeds. Although detection rates vary among studies and host species, these findings collectively suggest that sialidase genes are widely distributed in *P. multocida* and may play an important role in host colonization and pathogenicity.

Outer membrane proteins function as selective barriers that inhibit the entry of toxic compounds and are crucial for nutritional uptake, molecular transport, and interactions with the host environment (Hatfaludi et al., 2010). In this study, all isolates carried *oma87*, consistent with Furian et al. (2016), who detected *oma87* in 100% of poultry isolates obtained from the liver or heart of chickens and turkeys and from the lung of pigs. Additional reports further support its prevalence. In goats from Sichuan, *oma87* was found in 100% of isolates (Li et al., 2025), and in a Vietnamese study on porcine *P. multocida*, *oma87* was also universally present (Vu-Khac et al., 2020). Aski et al. (2016) detected *oma87* in 100% of isolates obtained from several clinically healthy and diseased animals (bovine, sheep, goat, poultry, dog, and cat). The widespread distribution of *oma87* across diverse host species underscores its high conservation and likely essential role in the pathogenic potential of *P. multocida*.

In order to shield bacteria from oxidative stress, which may harm cellular components, including DNA, proteins, and lipids, superoxide dismutases catalyze the conversion of reactive oxygen species (ROS) generated by neutrophils and macrophages into hydrogen peroxide and oxygen (Verma et al., 2013). These genes are widely distributed among *P. multocida* isolates. Furian et al. (2016) reported that *sodA* and *sodC* were present in 96% of poultry isolates obtained from the liver or heart of chickens and turkeys and from the lungs of pigs. Similarly, Aski et al. (2016) detected both genes in 100% of isolates collected from nasal and lung swabs of clinically healthy and diseased bovine, sheep, goats, poultry, dogs, and cats. The consistently high detection rates across studies highlight the essential role of these oxidative-stress defense genes in the survival of *P. multocida* within the host environment.

Based on the 16 virulence gene detections, it is evident that all genes except *toxA* were present in the *P. multocida* isolates tested. The existence of these virulence genes supports the bacterium's ability to infect hosts and survive under host defense conditions, even when isolates remain susceptible to the majority of tested antibiotics.

Table 4. The virulence gene of *P. multocida* isolated from infected chickens between 2018-2022 in Sukabumi, West Java, Indonesia

Genes	Targeted gene	Isolates								Total of positive	Percentage
		P.m1	P.m2	P.m3	P.m4	P.m5	P.m6	P.m7	P.m8		
CapA	*Serotyping A*	+	+	+	+	+	+	+	+	8/8	100
ToxA	*Dermonecrotic toxin*	-	-	-	-	-	-	-	-	0/8	0
TbpA	*Transferrin binding protein*	-	+	+	+	-	+	-	-	4/8	50
Fim4	*Type 4 fimbriae*	+	+	+	+	+	+	+	+	8/8	100
SodC	*Superoxide dismutate*	+	+	+	+	+	+	+	+	8/8	100
PfhA	*Filametous hemagglutinin*	-	+	+	-	+	-	+	+	5/8	62.5
ExbB	*Iron acquisition*	+	+	+	+	+	+	+	+	8/8	100
HgbB	*Hemoglobin binding protein*	+	+	+	+	+	+	-	+	7/8	87.5
NanB	*Neuraminidase*	+	+	+	+	+	+	+	+	8/8	100
TadD	*Putative nonspesific tight adherence protein D*	-	+	+	-	-	+	+	+	5/8	62.5
PlpB	*Lipoprotein B*	+	+	+	+	+	+	+	+	8/8	100
SodA	*Superoxide dismutate*	+	+	+	+	+	+	+	+	8/8	100
Oma87	*Outer membrane protein 87*	+	+	+	+	+	+	+	+	8/8	100
FimA	*Fimbriae*	+	+	+	+	+	+	+	+	8/8	100
NanH	*Neuroaminidase*	+	-	-	+	+	+	+	-	5/8	62.5
Fur	*Ferric uptake regulation protein*	-	+	+	+	+	+	+	+	7/8	87.5
Total of positive genes		11/16	14/16	14/16	13/16	13/16	14/16	13/16	13/16		

P.m: *Pasteurella multocida* isolates

CONCLUSION

Antibiotic resistance investigations revealed that all *P. multocida* isolates were generally susceptible to the tested antibiotics, with the exception of isolate P.m1, which was confirmed to exhibit resistance to levofloxacin, ciprofloxacin, and tetracycline. Virulence gene detections showed that 100% of isolates were positive for *capA*, *fim4*, *sodC*, *exbB*, *nanB*, *plpB*, *sodA*, *oma87*, and *fimA*; 87.5% were positive for *hgbB* and *fur*; 62.5% for *pfhA*, *tadD*, and *nanH*; and 50% for *tbpA*. The *toxA* gene was not detected in any of the isolates. These findings indicated that, despite the isolates being mostly susceptible to antibiotics, the presence of multiple virulence genes suggests that *P. multocida* retains the potential to induce disease. Future studies should focus on monitoring virulence and resistance gene profiles in local isolates,

assessing vaccine efficacy under field conditions, and implementing effective preventive and management strategies to reduce the impact of fowl cholera in poultry farms.

DECLARATIONS

Acknowledgments

The authors acknowledge IPB University and PT Medika Satwa Laboratoris for their support and cooperation during the study. The authors would like to thank Lusianawati Widjaja for her valuable assistance in improving the clarity of the manuscript and for providing constructive input during the response-to-reviewers process.

Funding

This study received no specific grant from any funding agency in the public, commercial, or not-for-profit sectors.

Authors' contributions

Marsella Metta Arvia, Ryan Septa Kurnia, Christian Marco Hadi Nugroho, Muhammad Ade Putra, Safika, and Agustin Indrawati conceived, designed, collected and analyzed data, and wrote the manuscript. Ryan Septa Kurnia, Christian Marco Hadi Nugroho, and Agustin Indrawati designed, supervised the study, and reviewed the manuscript. All authors read and approved the final manuscript for publication.

Competing interests

The authors declared that there are no competing interests.

Ethical considerations

The authors declare that this manuscript is original and is not being considered elsewhere for publication. Other ethical issues, including consent to publish, misconduct, fabrication of data, and redundancy, have been checked by the authors. During the preparation of this manuscript, the authors used ChatGPT (OpenAI) solely to improve grammar, language clarity, and overall readability. The tool was not used to generate scientific content, perform data analysis, or contribute to the conclusions. All AI-assisted outputs were thoroughly reviewed, verified, and edited by the authors, who take full responsibility for the integrity and accuracy of the final manuscript.

Availability of data and materials

The additional data from the present study can be provided on request from the corresponding author.

REFERENCES

Abreu R, Semedo-Lemsaddek T, Cunha E, Tavares L, and Oliveira M (2023). Antimicrobial drug resistance in poultry production: current status and innovative strategies for bacterial control. Microorganisms, 11(4): 953. DOI: https://www.doi.org/10.3390/microorganisms11040953

Alhassan MY, Kabara MK, Ahmad AA, Abdulsalam J, and Habib HI (2025). Revisiting antibiotic stewardship: Veterinary contributions to combating antimicrobial resistance globally. Bulletin of the National Research Centre, 49(1): 25. DOI: https://www.doi.org/10.1186/s42269-025-01317-3

Atashpaz S, Shayegh J, and Hejazi MS (2009). Rapid virulence typing of *Pasteurella multocida* by multiplex PCR. Research in Veterinary Science, 87(3): 355-357. DOI: https://www.doi.org/10.1016/j.rvsc.2009.04.004

Aski HS and Tabatabaei M (2016). Occurence of virulence-associated genes in *Pasteurella multocida* isolates obtained from different hosts. Microbial Pathogenesis 96: 52-57. DOI: https://www.doi.org/10.1016/j.micpath.2016.04.008

Baggio D and Ananda-Rajah MR (2021). Fluoroquinolone antibiotics and adverse events. Australian Prescriber, 44(5): 161-164. DOI: https://www.doi.org/10.18773/austprescr.2021.035

D'Amico F, Messina D, Casalino G, Schiavitto M, Bove A, Romito D, D'onghia FP, Camarda A, and Circella E (2024). Characterisation of *Pasteurella multocida* strains from different lesions in rabbits. Animals, 14(11): 1569. DOI: https://www.doi.org/10.3390/ani14111569

Effendi MH, Faridah HD, Wibisono FM, Wibisono FJ, Nisa N, Fatimah, and Ugbo EN (2022). Detection of virulence factor encoding genes on *Escherichia coli* isolated from broiler chicken in Blitar District, Indonesia. Biodiversitas, 23(7): 3437. DOI: https://www.doi.org/10.13057/biodivd230716

Elbehiry A and Marzouk E (2025). From farm to fork: Antimicrobial-resistant bacterial pathogens in livestock production and the food chain. Veterinary Sciences, 12(9): 862. DOI: https://www.doi.org/10.3390/vetsci12090862

Ewers C, Lubke-Becker A, Bethe A, Kiebling S, Filter M, and Wieler LH (2006). Virulence genotype of *Pasteurella multocida* strains isolated from different hosts with various disease status. Veterinary Microbiology, 114(3-4): 304-317. DOI: https://www.doi.org/10.1016/j.vetmic.2005.12.012

Farahani MF, Esmaelizad M, and Jabbari AR (2019). Investigation of iron uptake and virulence gene factors (*fur, tonB, exbD, exbB, hgbA, hgbB1, hgbB2 and tbpA*) among isolates of *Pasteurella multocida* from Iran. Iranian Journal of Microbiology, 11(3): 191-197. DOI: https://www.doi.org/10.18502/ijm.v11i3.1314

Faisal ZA (2019). Web-based expert system for diagnosing layer chicken diseases using the case-based reasoning method. Jati, 3(2): 126-132. DOI: https://www.doi.org/10.36040/jati.v3i2.882

Furian TQ, Borges KA, Pilatti RM, Almeida C, Nascimento VP, Salle CTP, Moraes HL, and De S (2014). Identification of the capsule type of *Pasteurella multocida* isolates from cases of fowl cholera by multiplex PCR and comparison with phenotypic methods. Brazilian Journal of Poultry Science, 16(2): 31-36. DOI: https://www.doi.org/10.1590/1516-635z160231-36

Furian TQ, Borges KA, Laviniki V, Rocha SLDS, Almeida CND, Nascimento VPD, Salle CTP, and Moraes HLDS (2016). Virulence genes and

antimicrobial resistance of *Pasteurella multocida* isolated from poultry and swine. Brazilian Journal of Microbiology, 47(1): 210-216. DOI: https://www.doi.org/10.1016/j.bjm.2015.11.014

Gharibi D, Hajikolaei MRH, Ghorbanpour M, and Barzegar SK (2017). Virulence gene profiles of *Pasteurella multocida* strains isolated from cattle and buffalo. Veterinarski Arhiv, 87: 677-690. DOI: https://www.doi.org/10.24099/vet.arhiv.160727

Gross L (2006). Bacterial fimbriae designed to stay with the flow. PLoS Biology, 4(9): e314. DOI: https://www.doi.org/10.1371/journal.pbio.0040314

Haghnazari S, Jabbari A, and Tadayon K (2017). Prevalence of adhesion virulence factor genes, antibiogram, and pathogenicity of avian *Pasteurella multocida* isolate from Iran. Archives of Razi Institute, 72(2): 83-91. DOI: https://www.doi.org/10.22092/ari.2017.109843

Harper M, Boyce JD, and Adler B (2006). *Pasteurella multocida* pathogenesis: 125 after pasteur. FEMS Microbiology Letters, 265(1): 1-10. DOI: https://www.doi.org/10.1111/j.1574-6968.2006.00442.x

Hatfaludi T, Al-hasani K, Boyce JD, and Adler B (2010). Outer membrane proteins of *Pasteurella multocida*. Veterinary Microbiology, 144(1-2): 1-17. DOI: https://www.doi.org/10.1016/j.vetmic.2010.01.027

Hernando-Amado S, Sanz-García F, Blanco P, and Martínez JL (2017). Fitness costs associated with the acquisition of antibiotic resistance. Essays in Biochemistry, 61(1): 37-48. DOI: https://www.doi.org/10.1042/EBC20160057

Hooper DC and Jacoby GA (2015). Mechanisms of drug resistance: quinolone resistance. Annals of the New York Academy of Sciences, 1354(1): 12-31. DOI: https://www.doi.org/10.1111/nyas.12830

Indrawati A, Safika S, Nugroho CMH, Putra MA, Silaen OSM, Krisnamurti DGB, Sanam MUE, and Kurnia RS (2025). Development and evaluation of a bivalent oil-adjuvanted vaccine against necrotic enteritis and avian colibacillosis in poultry. Advances in Animal and Veterinary Sciences, 13(6): 1378-1386. DOI: https://www.doi.org/10.17582/journal.aavs/2025/13.6.1378.1386

Kim J, Kim JW, Oh SI, So BJ, Kim WI, and Kim HY (2019). Characterisation of *Pasteurella multocida* isolates from pigs with pneumonia in Korea. BMC Veterinary Research, 15:119. DOI: https://www.doi.org/10.1186/s12917-019-1861-5

Kowalska-Krochmal B, and Dudek-Wicher R (2021). The minimum inhibitory concentration of antibiotics: Methods, interpretation, clinical relevance. Pathogens, 10(2): 165. DOI: https://www.doi.org/10.3390/pathogens10020165

Kubatzky KF (2022). *Pasteurella multocida* toxin–lessons learned from a mitogenic toxin. Frontiers in Immunology, 13: 1058905. DOI: https://www.doi.org/10.3389/fimmu.2022.1058905

Lachowicz-Wolak A, Chmielina A, Przychodniak I, Karwańska M, Siedlecka M, Klimowicz-Bodys M, Dyba K, and Rypuła K (2025). Antimicrobial-resistance and virulence-associated genes of *Pasteurella multocida* and *Mannheimia haemolytica* isolated from Polish dairy calves with symptoms of bovine respiratory disease. Microorganisms, 13(3): 491. DOI: https://www.doi.org/10.3390/microorganisms13030491

Li S, Gu Q, Li B, Abi K, and Yang F (2025). High prevalence of virulence genes and multi-drug resistance in *Pasteurella multocida* from goats in Sichuan, China.The Veterinary Journal, 311: 106344. DOI: https://www.doi.org/10.1016/j.tvjl.2025.106344

Lobongona MLMNB, Afiff U, and Rotinsulu DA (2019). Antimicrobial effectiveness against *Pasteurella multocida* and *Mannheimia haemolytica* isolated from cattle suspected of having bovine respiratory disease complex. ARSHI Veteriner Letters, 3(2): 39-40. DOI: https://www.doi.org/10.29244/avl.3.2.39-40

Manoharan D, Srinivasan S, Vignesh NR, Senthilvel A (2023). Tetracyclines: The old, the new and the improved–A short review. Biomedical and Pharmacology Journal, 16(3): 1441-1450. DOI: https://www.doi.org/10.13005/bpj/2722

Maulana FH, Prasetyo E, and Sarenggat W (2017). Income analysis of layer chicken farming at Sumur Banger farm, Tersono Subdistrict, Batang Regency. Mediagro, 13(2): 1-12. DOI: https://www.doi.org/10.31942/mediagro.v13i2.2155

Mehmood MD, Zia S, Javed F, Gul M, Ashraf M, and Anwar H (2018). Physiochemical factors *in vitro* growth of *Pasteurella multocida*. African Journal of Microbiology Research, 12(11): 269-274. DOI: https://www.doi.org/10.5897/AJMR2017.8625

Mizan S, Henk L, Stallings A, Maier M, and Lee MD (2000). Coning and characterization of sialidases with 2-6 and 2-3 sialyl lactose specificity from *Pasteurella multocida*. Journal of Bacteriology, 182(24): 6874-6883. https://www.doi.org/10.1128/jb.182.24.6874-6883.2000

Nguyen PV, Le CT, Nguyen XH, Nguyen TM, and Nguyen KCT (2023). First study on capsular serotypes and virulence factors of *Pasteurella multocida* isolates from phan rang sheep in Vietnam. Veterinary World, 16(2): 281-290. DOI: https://www.doi.org/10.14202/vetworld.2023.281-290

Nugroho CMH, Kurnia RS, Tarigan S, Silaen OSM, Triwidyaningtyas S, Wibawan IWT, Natalia L, Takdir AK, and Soebandrio A (2022). Screening and purification of *nanB* sialidase from *Pasteurella multocida* with activity in hydrolyzing sialic acid Neu5Acα(2-6)Gal and Neu5Acα(2-3)Gal. Scientific Reports, 12: 9425. DOI: https://www.doi.org/10.1038/s41598-022-13635-x

Redgrave LS, Sutton SB, Webber MA, and Piddock LJV (2014). Fluoroquinolone resistance: Mechanisms, impact on bacteria, and role in evolutionary success. Trends in Microbiology, 22(8): 438-445. DOI: https://www.doi.org/10.1016/j.tim.2014.04.007

Reuben RC, Sarkar SL, Ibnat H, Setu MAA, Roy PC, and Jahid IK (2021). Novel multi-strain probiotics reduces *Pasteurella multocida* induced fowl cholera mortality in broilers. Scientific Reports, 11: 8885. DOI: https://www.doi.org/10.1038/s41598-021-88299-0

Sabsabi MA, Zakaria Z, Abu J, and Faiz NM (2021). Molecular characterisation and antibiotic sensitivity profile of *Pasteurella multocida* isolated from poultry farms in Malaysia. Austral Journal of Veterinary Sciences, 53(2). DOI: https://www.doi.org/10.4067/S0719-81322021000200121

Sahragard I, Tahamtan Y, Valadan M, Hyati M, Moazeni F, and Shirazi Z (2012). Development of rapid PCR method for simultaneous identification of species, specific capsular type, and toxigenicity of *Pasteurella* sp. isolates. Comparative Clinical Pathology, 21: 1333-1336. DOI: https://www.doi.org/10.1007/s00580-011-1291-7

Shen X, Guan L, Zhang J, Xue Y, Si L, and Zhao Z (2025). Study in the iron uptake mechanism of *Pasteurella multocida*. Veterinary Research, 56: 41. DOI: https://www.doi.org/10.1186/s13567-025-01469-0

Shivachandra SB, Kumar AA, Gautam R, Singh VP, Saxena MK, and Srivastava SK (2006). Identification of avian strains of *Pasteurella multocida* in India by conventional and PCR assays. The Veterinary Journal, 172(3): 561-564. https://www.doi.org/10.016/j.tvjl.2005.05.007

Siddaramappa S (2021). Comparative genomics of the *Pasteurella multocida* toxin. Genome, 64(7): 679-692. DOI: https://www.doi.org/10.1139/gen-2020-0176

Simanjuntak HA, Simanjuntak H, Maimunah S, Rahmiati R, and Situmorang TS (2022). Diameter zona hambat antibiotik amoxicillin dan tetracycline terhadap *Escherichia coli*. Herbal Medicine Journal, 5(2): 55-59. DOI: https://www.doi.org/10.58996/hmj.v5i2.52

Sunartatie T, Safika S, Abhirama HR, Kurnia RS, Putra MA, Nugroho CMH, Mayasari NLPI, and Indrawati A (2024). Identification and antibiotic resistance of *Pasteurella multocida* isolated from infected layer chickens in West Java, Indonesia. Journal of World's Poultry Research, 14(3):

282-290. DOI: https://www.doi.org/10.36380/jwpr.2024.29

Tang X, Zhao Z, Hu J, Wu B, Cai X, He Q, and Chen H (2009). Isolation, antimicrobial resistance, and virulence genes of *Pasteurella multocida* strains from swine in China. Journal of Clinical Microbiology, 47(4): 951-958. DOI: https://www.doi.org/10.1128/jcm.02029-08

Tawor AB, Erganis O, Balevi A, Kebabcioglu C, and Marangoz H (2024). The correlation between *ptfA*, *pfhA*, and *tadD* fimbriae genes and biofilm formation in *Pasteurella multocida* virulence and multidrug-resistant nature. The Microbe, 4: 100135. DOI: https://www.doi.org/10.1016/j.microb.2024.100135

Townsend KM, Boyce JD, Chung JY, Frost AJ, and Adler B (2001). Genetic organization of *Pasteurella multocida cap* loci and development of a multiplex capsular PCR typing system. Journal of Clinical Microbiology, 39(3): 924-929. DOI: https://www.doi.org/10.1128/JCM.39.3.924-929.2001

Venkateswaran N, Swetschinski LR, Fastl C, Bari CD, Criscuolo NG, Mulchandani R, Zhao C, Meštrović T, Ikuta KS, Martins SB et al. (2024). Using priorities between human and livestock bacterial antimicrobial resistance (AMR) to identify data gaps in livestock AMR surveillance. BMC Infectious Diseases, 24(1): 1027. DOI: https://www.doi.org/10.1186/s12879-024-09847-3

Verma S, Sharma M, Katoch S, Verma L, Kumar S, Dogra V, Chahota R, Dhar P, and Singh G (2013). Profiling of virulence associated genes of *Pasteurella multocida* isolated from cattle. Veterinary Research Communication, 37: 83-89. DOI: https://www.doi.org/10.1007/s11259-012-9539-5

Vu-Khac H, Trinh TTH, Nguyen TTG, Nguyen XT, and Nguyen TT (2020). Prevalence of virulence factor, antibiotic resistance, and serotype genes of *Pasteurella multocida* strains isolated from pigs in Vietnam. Veterinary World, 13(5): 896-904. DOI: https://www.doi.org/10.14202/vetworld.2020.896-904

Wang J, Sun S, Chen D, Gao C, Sang L, and Xie X (2024). Pathogenic and genomic characterization of rabbit-sourced *Pasteurella multocida* serogroup F isolates recovered from dead rabbits with respiratory disease. Microbiology Spectrum, 12(4): e03654-23. DOI: https://www.doi.org/10.1128/spectrum.03654-23

Zainuddin (2014). Pathological case study of fowl cholera in broiler chicken farming among local communities in Banda Aceh. Jurnal Medik Veteriner, 8(1): 5659. DOI: https://www.doi.org/10.21157/j.med.vet.v81.3337

Ziagham A, Gharibi D, Mosallanejad B, and Avizeh R (2024). Molecular characterization of *Pasteurella multocida* from cats and antibiotic sensitivity of the isolates. Veterinary Medicine and Science, 10(3): e1424. DOI: https://www.doi.org/10.1002/vms3.1424

Publisher's note: Scienceline Publication Ltd. remains neutral with regard to jurisdictional claims in published maps and institutional affiliations.

Open Access: This article is licensed under a Creative Commons Attribution 4.0 International License, which permits use, sharing, adaptation, distribution and reproduction in any medium or format, as long as you give appropriate credit to the original author(s) and the source, provide a link to the Creative Commons licence, and indicate if changes were made. The images or other third party material in this article are included in the article's Creative Commons licence, unless indicated otherwise in a credit line to the material. If material is not included in the article's Creative Commons licence and your intended use is not permitted by statutory regulation or exceeds the permitted use, you will need to obtain permission directly from the copyright holder. To view a copy of this licence, visit https://creativecommons.org/licenses/by/4.0/.

© The Author(s) 2025

2025, Scienceline Publication
World's Veterinary Journal
World Vet J, 15(4): 891-900.
ISSN 2322-4568

DOI: https://dx.doi.org/10.54203/scil.2025.wvj90
PII: S232245682500090-15

Rapid Simultaneous Detection of *Salmonella* and *Campylobacter* Bacteria Directly from Chicken Faeces

Sherryl Nurfarhanim Abd Ghafar[1], Nur Indah Ahmad[1]*, Saleha Abdul Aziz[2], and Zunita Zakaria[1]

[1]*Department of Veterinary Pathology and Microbiology, Faculty of Veterinary Medicine, Universiti Putra Malaysia, 43400 Serdang, Selangor, Malaysia*
[2]*Department of Veterinary Laboratory Diagnostics, Faculty of Veterinary Medicine, Universiti Putra Malaysia, 43400 Serdang, Selangor, Malaysia*

*Corresponding author's Email: nurindah@upm.edu.my

ORIGINAL ARTICLE
Received: October 02, 2025
Revised: October 28, 2025
Accepted: November 24, 2025
Published: December 25, 2025

ABSTRACT

Campylobacter and *Salmonella* are widely recognized as significant causes of foodborne diseases, with poultry and poultry products being the most frequent sources of infection in humans. Rapid, simultaneous detection of both pathogens can prevent contaminated food from entering the human food chain. The present study aimed to simultaneously detect *Salmonella* and *Campylobacter* spp. directly from faeces of broiler chickens aged 4 to 5 weeks by multiplex polymerase chain reaction (mPCR). The suitability of the PCR protocol using pairs of primers targeting the *invA* and *cadF* genes was evaluated to detect *Salmonella* and *Campylobacter* spp., respectively, from 15 samples. The specificity of the PCR assay was 100% for both pathogens, as no positive cross-reactions were detected with non-targeted bacteria. The limit of detection for pure culture of *Salmonella* was 1 CFU/mL, whereas for *Campylobacter* it was 10^1 CFU/mL. Incubation of spiked faeces in brain heart infusion broth for 24 to 48 hours maintained a detection limit of 1 CFU/mL for *Salmonella*; however, the sensitivity decreased, resulting in a detection limit of 10^2 CFU/mL for *Campylobacter*. Simultaneous detection from 15 chicken faecal samples revealed two samples co-carrying both *Salmonella* and *Campylobacter* spp., four samples positive for *Salmonella*, six samples positive for *Campylobacter*, and three samples were negative for both pathogens. The developed mPCR protocol in the present study was highly specific and sensitive for detecting *Salmonella* and *Campylobacter* spp. directly from chicken faeces, achieving results in under 36 hours compared to the conventional culture method. The mPCR protocol can benefit veterinary and public health authorities during epidemiological investigations and rapid diagnostic purposes, which require timely confirmation of the disease status in chickens during the grow period.

Keywords: *Campylobacter*, Faeces, Multiplex PCR, *Salmonella*, Simultaneous detection

INTRODUCTION

Campylobacter (*C.*) and *Salmonella* (*S.*) spp. are two of the top foodborne bacteria associated with diarrhoeal diseases in humans worldwide (WHO, 2015). Foodborne diseases pose a substantial threat to food safety and international trade (Gizaw, 2019; Tibebu et al., 2024). Although the poultry sector in Malaysia has exceeded local demand (Department of Veterinary Services Malaysia, 2017), efforts to increase the quality and safety of the food are necessary to sustain production in the long term.

In Malaysia, several studies have reported that *Campylobacter* and *Salmonella* spp. are prevalent in chicken farms (Osman et al., 2021; Wahab et al., 2021), as well as in chicken meat and retail outlets (Rejab et al., 2012). Sinulingga et al. (2020) found *Campylobacter* spp. in 50.9% of broiler chickens in farms and 26.6% of chicken meat in markets. *Salmonella* spp. was isolated from 46.3% of cloacal swabs collected from poultry farms (Osman et al., 2021) and in 35.0% of raw chicken meat sold in markets (Sukri et al., 2021).

Transmission of foodborne bacteria to humans most commonly occurs through consumption of contaminated food, including foods with animal origin (Rivera-Pérez et al., 2014; Heredia and García, 2018; Abebe et al., 2020), fruits and vegetables (Park et al., 2012; Abakpa et al., 2015; Nguyen et al., 2021), or from direct contact with animals (Ranjbar and Babazadeh, 2017; Sodagari et al., 2020; Babazadeh and Ranjbar, 2022), resulting in diarrhoea, abdominal pain, nausea, and fever. These transmission routes may reflect gaps in poultry husbandry practices, such as flock hygiene and biosecurity, as well as control measures throughout the poultry supply chain. Contamination of poultry products can occur during slaughtering and processing (Rivera-Pérez et al., 2014), as well as in markets and retail outlets (Sadek et al., 2023). Several studies have indicated higher rates of *Salmonella* spp. detected in retail markets compared to processing plants (Adeyanju and Ishola, 2014). Moreover, improper temperature control and inadequate hygiene practices at retail outlets can further promote bacterial growth and survival (Salama and Chennaoui, 2024).

The conventional method for identifying *Salmonella* and *Campylobacter* spp. involves bacterial isolation by a culture method, and biochemical tests for presumptive identification are time-consuming and laborious, requiring five to seven days to confirm the diagnosis (Strakova et al., 2021; Neyaz et al., 2024). Additionally, the inability to detect viable but non-culturable cells in the sample may result in false-negative outcomes. The development of rapid detection tests,

To cite this paper: Ghafar SNA, Ahmad NI, Aziz SA, and Zakaria Z (2025). Rapid Simultaneous Detection of *Salmonella* and *Campylobacter* Bacteria Directly from Chicken Faeces. *World Vet. J.*, 15(4): 891-900. DOI: https://dx.doi.org/10.54203/scil.2025.wvj90

such as multiplex polymerase chain reaction (mPCR), enables the simultaneous detection of multiple strains of pathogens (Settanni and Corsetti, 2007), allowing for early, rapid, responsive, and preventive measures to be taken. The direct detection of *Salmonella* and *Campylobacter* spp. as single organisms from faecal samples has been previously documented by Pathmanathan et al. (2003), Persson and Olsen (2005), and Al Amri et al. (2007); however, co-detection by mPCR directly from chicken faeces has yet to be established. Therefore, the present study aimed to simultaneously detect *Salmonella* and *Campylobacter* spp. directly from the faecal samples of 4- to 5-week-old broiler chickens in Malaysia, using mPCR.

MATERIALS AND METHODS

Ethical approval

The present study was approved by the Institutional Animal Care and Use Committee, Universiti Putra Malaysia, Malaysia (AUP no: UPM/IACUC/AUP-R089/2019).

Sample collection

To develop the protocol using field-isolated samples, 15 pooled chicken faecal samples were collected from three broiler farms in Selangor, Malaysia, by convenience sampling, following verbal consent from the farmers. The samples originated accidentally from physically healthy chickens aged four weeks, with no clinical signs of disease. Clean plastic sheets were placed on the floor in the chicken house for approximately 30 minutes to collect freshly voided faeces from live chickens. The faeces were then collected using a sterile spatula, with multiple droppings originating from different chickens piled together into a sterile 50 mL Falcon™ tube to ultimately collect five tubes of pooled faecal samples, and transported in an ice box to the laboratory. The samples were processed immediately upon arrival at the laboratory. To evaluate the developed protocol, all collected chicken faeces were analysed in parallel using both the conventional culture method and the mPCR assay.

Isolation and identification of *Salmonella* and *Campylobacter*

For isolation and identification of *Salmonella*, the method was conducted according to the terrestrial manual (WOAH, 2022). The faecal samples were placed in 10 mL of buffered peptone water broth (Oxoid, UK) and incubated for 18 to 24 hours at 37°C. Then, 1 mL of the overnight culture was inoculated into 9 mL of Rappaport-Vassiliadis (RV) enrichment broth (Oxoid, UK) and incubated for 18 to 24 hours at 42°C. A loopful of cultured RV broth was streaked onto selective media, which were xylose lysine deoxycholate (XLD) agar (Oxoid, UK) and brilliant green agar (BGA; Oxoid, UK), and incubated at 37°C for 24 hours. All presumptive colonies were identified from each plate, with the appearance of circular red colonies with a black center on XLD agar and pink with mucoid colonies on BGA agar (Figure 1A and B). The *Salmonella*-suspected colonies were subjected to a series of biochemical tests, namely oxidase (Remel Europe, UK), urease (Oxoid, UK), triple sugar iron (TSI; Oxoid, UK), citrate (Oxoid, UK), and further tested with slide agglutination using polyvalent O (A-G) and polyvalent H antisera (phase 1 and 2; Denka Seiken, Japan). The presumptive colonies were stored in glycerol at -40°C until further use.

For *Campylobacter*, the method was carried out based on ISO 10272-1:2017 (WOAH, 2018). The cotton swab containing the faecal sample was streaked directly onto modified charcoal cefoperazone deoxycholate agar (mCCDA; Oxoid, UK) and incubated under microaerophilic conditions at 42°C for 48 hours. Colony morphology was examined before Gram staining and the motility test. Presumptive colonies were sub-cultured onto Columbia blood agar (CBA; Oxoid, UK) agar containing 5% defibrinated horse blood and incubated in microaerophilic conditions for an additional 48 hours (Figure 1C and D). Then, the presumptive colonies were further identified by biochemical tests, including oxidase, catalase, urease, indoxyl acetate hydrolysis (Remel, USA), and hippurate hydrolysis (Sigma Aldrich, USA).

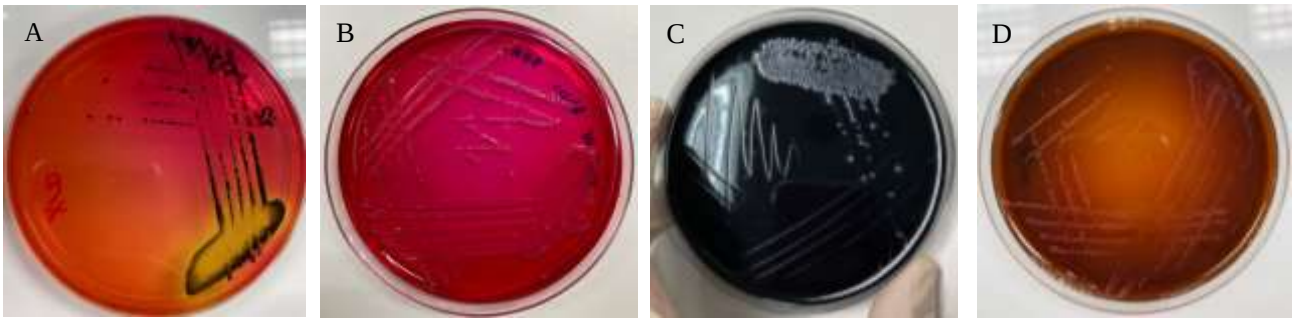


Figure 1. Presumptive isolates of Salmonella and Campylobacter spp. colonies on selective growth media agar plates. A: Presumptive growth with colony morphology typical of Salmonella on xylose lysine deoxycholate agar, B: Presumptive growth on brilliant green agar, C: Presumptive growth with colony morphology typical of Campylobacter spp. on modified charcoal cefoperazone deoxycholate agar, D: Presumptive growth on Columbia blood agar. Source: Authors of the present study.

Bacterial strain and DNA extraction

The reference bacterial strains used in the present study are listed in Table 1. The *S. typhimurium* ATCC 14028 and *C. jejuni* ATCC 29428 were cultured in brain heart infusion (BHI) broth (Oxoid, UK) at 37°C for 18 hours and 42°C, respectively. These strains served as positive controls for the development of mPCR. For direct detection of bacteria, the chicken faeces were placed in 20 mL of BHI and incubated for 24 hours at 37°C for *Salmonella* and in microaerophilic conditions at 42°C for *Campylobacter*. Then, 1 mL of the faecal mixture was transferred into a 1.5 mL microcentrifuge tube for DNA extraction. The DNA extraction was performed using a modified method described by Saeki et al. (2013). A 1 mL bacterial suspension was centrifuged for 10 minutes at 13,000 g, and the resulting pellet was resuspended in 200 µL of Triton X-100 2% lysis solution. After heating at 96°C for 10 minutes and cooling down on ice for two minutes, the mixture was centrifuged again at 13,000 g. The supernatant containing DNA was collected and stored at -20°C.

Table 1. The bacterial strains used for optimisation of the mPCR assay in the present study

Bacteria strains	Origin
Salmonella typhimurium ATCC 14028	Remel*
Salmonella enteritidis ATCC 13076	Remel*
Salmonella pullorum ATCC	Remel*
Escherichia coli ATCC 25922	Remel*
Klebsiella pneumonia ATCC 700603	Remel*
Campylobacter coli ATCC 33559	Remel*
Campylobacter jejuni ATCC 29428	Remel*
Pseudomonas spp.	FPV**
Staphylococcus spp.	FPV**
Enterococcus faecalis	FPV**
Enterobacter spp.	FPV**

Remel*: Strains manufactured by Remel Inc., USA, FPV**: Strains obtained from the Bacteriology Laboratory, Veterinary Laboratory Services Unit, Faculty of Veterinary Medicine, University of Putra Malaysia.

Multiplex PCR

The genus-specific genes, *invA* and *cadF*, were used for the development of mPCR to simultaneously detect *Salmonella* spp. and *Campylobacter* spp., respectively. The primer sequences are listed in Table 2. The final volume of the reaction mixture for the protocol was 50 µL, consisting of 8 µL RNAse-free water, 25 µL of REDiant PCR master mix 2X (1st BASE, Singapore), 3 µL each of the *invA* primer, 3 µL of each *cadF* primer, and 5 µL of the DNA template. The DNA amplification was performed using a lab cycler gradient (SensoQuest GmbH, Germany) under the following cycling conditions; Two minutes of initial denaturation at 95°C, 35 cycles of denaturation at 94°C for one minute, annealing for one minute at 52°C, one minute of extension at 72°C, and later finished by final extension for two minutes at 72°C. The finished PCR products were visualised on a 1.5% (w/v) agarose gel (1st BASE, Singapore). The product size was estimated by comparing with the positive control using the ExcelBand™ 100 DNA Ladder (Smobio, Taiwan).

Table 2. Primers used in mPCR for the simultaneous detection of the *Salmonella* and the *Campylobacte*r genus in broiler chicken

Species	Primer (Gene)	Sequence (5'-3')	Product size (bp)	Reference
Salmonella genus	*invA*	(F) AAA CGT TGA AAA ACT GAG GA (R) TCG TCA TTC CAT TAC CTA CC	119	Saeki et al. (2013)
Campylobacter genus	*cadF*	(F) TTG AAG GTA ATT TAG ATA TG (R) CTA ATA CCT AAA GTT GAA AC	400	Al Amri et al. (2007)

PCR specificity and sensitivity

The PCR specificity test was conducted using *Salmonella*, *Campylobacter* spp., and other bacterial species mentioned in Table 1. The specificity of PCR was assessed by determining the reactivity between genus-specific primers for *Salmonella* and *Campylobacter* and bacterial reference strains. The test was considered highly specific if the PCR protocol could accurately identify *Salmonella* and *Campylobacter* spp. The sensitivity of the PCR was evaluated by determining the ability of the protocol to detect *Salmonella* and *Campylobacter* DNA at the lowest dilution. The sensitivity of the mPCR assay was evaluated using a bacterial suspension containing 100 to 10^7 CFU of *Salmonella* and *Campylobacter* per mL of BHI broth (Saeki et al., 2013). The overnight bacterial suspensions were serially diluted in 9 mL of BHI broth at a 1:10 ratio. One mL of each dilution was extracted, and the DNA template was used to conduct the mPCR assay. The test was repeated three times to ascertain replicability. A PCR sensitivity test was conducted using DNA from *Salmonella* and *Campylobacter* spp., testing both species individually and in combination within a single reaction tube.

Spiked faeces experiment

The experiment was conducted using a modified method described by Alves et al. (2012). *Salmonella* and *Campylobacter*-negative chicken faeces samples were used in this experiment. One gram of chicken faeces was suspended in 20 mL of sterile BHI broth. The faecal suspension was inoculated with different concentrations of *Salmonella*, then incubated for 24 hours at 37°C. Additionally, *Campylobacter* was incubated at 42°C under microaerophilic conditions using CampyGen 2.5 L (Oxoid, UK) with oxygen levels maintained at 8-9% and carbon dioxide at 7-8%. For species detection, 1 mL of spiked faeces was transferred into a 1.5 mL microcentrifuge tube. For co-detection, 500 µL of *Campylobacter*-spiked faeces was mixed with 500 µL of *Salmonella*-spiked faeces in a 1.5 mL microcentrifuge tube. The spiked faecal mixture was spun at 13,000 g for 10 minutes. The pellet was washed twice with 900 µL of BHI broth, spun at 13,000 g for 10 minutes, and resuspended in 200 µL of Triton X-100 1%. The boiling method was conducted to extract DNA. The experiment was conducted in three independent replicates.

Data analysis

The diagnostic performance of the mPCR assay for detecting *Salmonella* and *Campylobacter* spp. in broiler faecal samples was evaluated using culture as the reference method. Sensitivity, specificity, positive predictive value, and negative predictive value were calculated using the data presented in Table 5, according to standard definitions and the following formulas (Parikh et al., 2008).

$$Sensitivity = \frac{100 \times True\ positive}{(True\ positive + False\ negative)}$$

$$Specificity = \frac{100 \times True\ negative}{(False\ positive + True\ negative)}$$

$$Positive\ predictive\ value = \frac{100 \times True\ Positive}{(True\ positive + False\ positive)}$$

$$Negative\ predictive\ value = \frac{100 \times True\ Negative}{(True\ negative + False\ negative)}$$

RESULTS AND DISCUSSION

A multiplex PCR protocol was developed for the co-detection of *Salmonella* and *Campylobacter* spp. directly from chicken faeces. In the present study, both genus-specific primers targeting the *invA* and *cadF* genes for *Salmonella* and *Campylobacter* spp., respectively, were included in the protocol. Before specificity and sensitivity tests, the PCR protocol was optimised to determine the most suitable primer concentrations and PCR cycling conditions. All *Salmonella* and *Campylobacter* strains tested were amplified and yielded 119 bp and 400 bp, respectively (Figure 2). Other non-targeted bacterial strains representing common gastrointestinal bacteria found in chicken indicated no amplification for both primer pairs. In alignment with prior studies conducted by Alves et al. (2012) and Saeki et al. (2013), the Styinva-JHO-2 primer pair demonstrated 100% specificity, supporting its reliability for detecting *Salmonella* serovars. The primer pair targeting the *invA* gene was a protein located in *Salmonella* pathogenicity island 1 (SPI-1) that plays a role in the invasion of host intestinal cells. The SPI-1 activates the Type III secretion system (T3SS) to assist *Salmonella* in invading epithelial cells and recruiting host immune cells (Singh et al., 2018). Amplification of the *invA* gene has been widely used in numerous studies to detect *Salmonella* from different types of samples, such as animal faeces (Deguenon et al., 2019), poultry meat (Shanmugasamy et al., 2011; Sharma, 2016), beef (Thung et al., 2018), and foods (Heymans et al., 2018).

Another virulence gene targeted in the present study was the *cadF* gene, which facilitates bacterial attachment to the host fibronectin matrix and subsequent invasion of epithelial cells during *Campylobacter* colonization (Ngobese et al., 2020). Casabonne et al. (2016) demonstrated high prevalence (100%) of *cadF*, *flaA*, and *cdtB* virulence genes compared to *ciaB* (50%), *docC* (23.3%), *wlaN* (20%), and *cgtB* (6.7%) genes when tested with different *Campylobacter* strains isolated from human stool samples. A high prevalence of the *cadF* gene was discovered in faecal samples from different livestock animals, including cattle, chickens, goats, sheep, and pigs (Ngobese et al., 2020), as well as in broiler chickens (Khoshbakht et al., 2013). Additionally, Reddy and Zishiri (2018) detected the *cadF* gene in 100% of broiler faeces and human clinical isolates, which could be suggestive of its pathogenic potential to humans. Additionally, Ayaz et al. (2016) reported 100% specificity for the detection of the *hipO* gene by PCR compared to the *ceuE* gene, which detected only 43.9% of 41 *C. jejuni* isolates. Although different genes were targeted to identify *Campylobacter* by PCR, *cadF* has a higher specificity rate compared to the other genes, such as *ciaB* and *ceuE*.

Serial dilution analysis demonstrated that the mPCR protocol could detect *Salmonella* spp. via the *invA* gene (119 bp) and *Campylobacter* spp. via the *cadF* gene (400 bp) in pure culture at concentrations as low as 1 CFU/mL and 10^1 CFU/mL, respectively. The assay proved effective for both the individual and simultaneous detection of the genes (Figures 3 and 4). After 24 hours of enrichment, both *Salmonella* (119 bp) and *Campylobacter* (400 bp) could be detected directly from chicken faeces at 1 CFU/mL and 10^2 CFU/mL, respectively (Figure 5). The mPCR assay presented in the present study was able to detect as low as 10^1 CFU/mL of *Salmonella* and *Campylobacter* spp. (Figure 6), which is more sensitive compared to the study reported by Alves et al. (2012). A pure culture of both *Salmonella* and *Campylobacter* spp. at 10^4 CFU/mL was detected during the study. The comparable sensitivity levels observed between the direct detection of spiked chicken rinses reported by Alves et al. (2012) and the present study, using chicken faecal

samples, highlighted the robustness of the mPCR assay, suggesting its suitability for reliable detection across different poultry matrices and potential application in broader food safety surveillance.

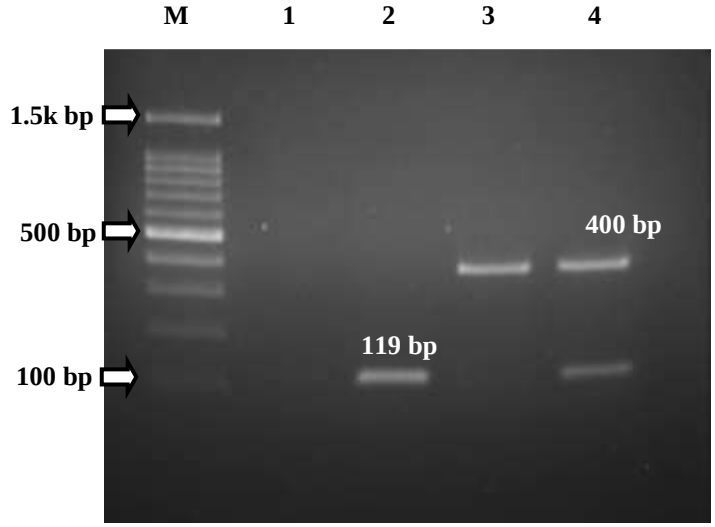


Figure 2. Multiplex PCR of positive controls used for the detection of *Salmonella* and *Campylobacter* spp. isolates from broiler chicken faeces. Lane M: Molecular size marker (100 bp). Lane 1: *Klebsiella pneumonia* ATCC 700603 (Negative control), Lane 2: *Salmonella* spp. (119 bp), Lane 3: *Campylobacter* spp. (400 bp), Lane 4: *Salmonella* spp. (119 bp) and *Campylobacter* spp. (400 bp).

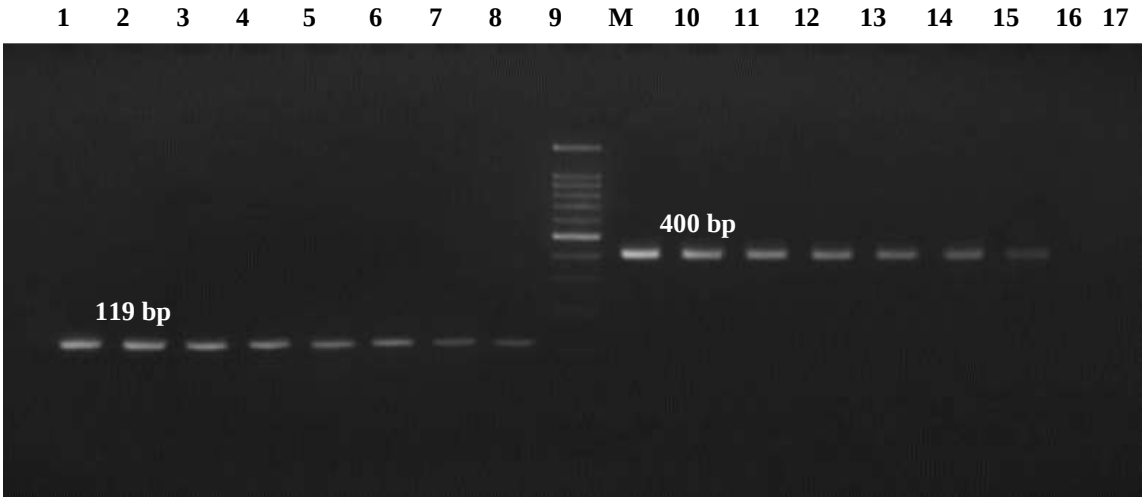


Figure 3. Sensitivity detection of *invA* and *cadF* genes from pure cultures of *Salmonella* and *Campylobacter* spp. from broiler chicken faeces by detecting each gene individually. Lane 1: *Klebsiella pneumonia* ATCC 700603, Lane 2-9: 10-fold serial dilution containing 10^7 to 1 CFU/mL of *Salmonella* (119 bp), M: molecular size marker (100 bp), Lane 10-17: 10-fold serial dilution containing 10^7 to 1 CFU/mL of *Campylobacter* spp. (400 bp).

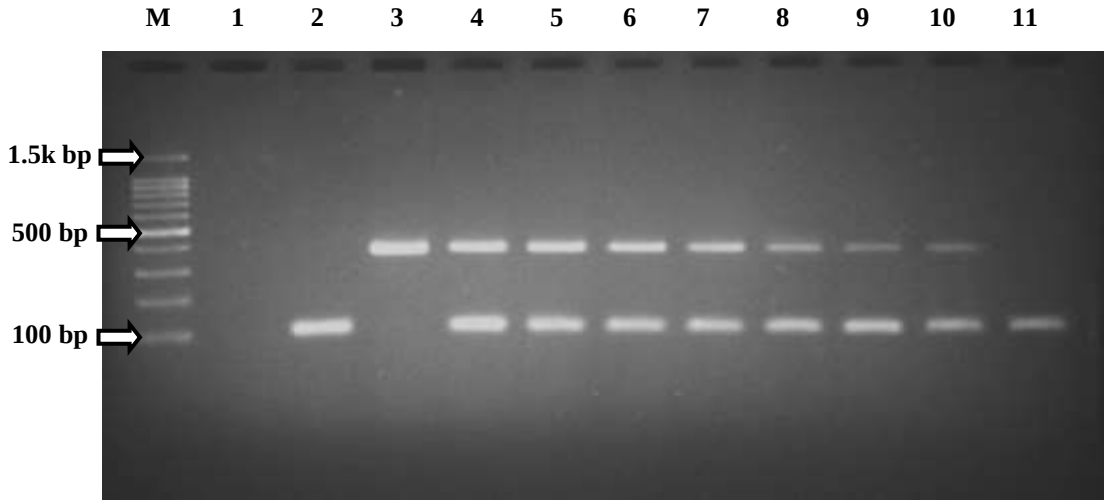


Figure 4. Sensitivity detection of the *invA* and *cadF* genes from pure cultures of *Salmonella* and *Campylobacter* spp. from broiler chicken faeces by detecting both genes simultaneously in one PCR tube. Lane M: Molecular size marker (100 bp), Lane 1: *Klebsiella pneumonia* ATCC 700603, Lane 2: *Salmonella* (119 bp), Lane 3: *Campylobacter* spp. (400 bp), Lane 4-11: 10-fold serial dilution of pure culture containing 10^7 to 1 CFU/mL of both *Salmonella* and *Campylobacter* spp.

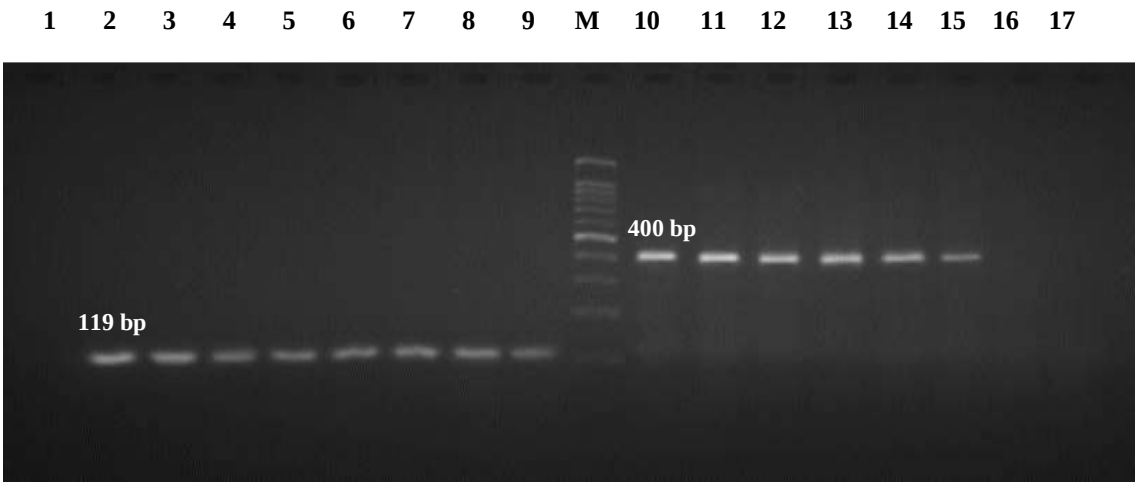


Figure 5. Sensitivity detection of *invA* and *cadF* genes from spiked broiler chicken faeces containing *Salmonella* and *Campylobacter* spp. after overnight incubation by detecting each gene individually. Lane 1: *Klebsiella pneumonia* ATCC 700603, Lane 2-9: 10-fold serial dilution containing 10^7 to 1 CFU/mL of *Salmonella* (119 bp), M: molecular size marker (100 bp), Lane 10-17: 10-fold serial dilution containing 10^7 to 1 CFU/mL of *Campylobacter* spp. (400 bp).

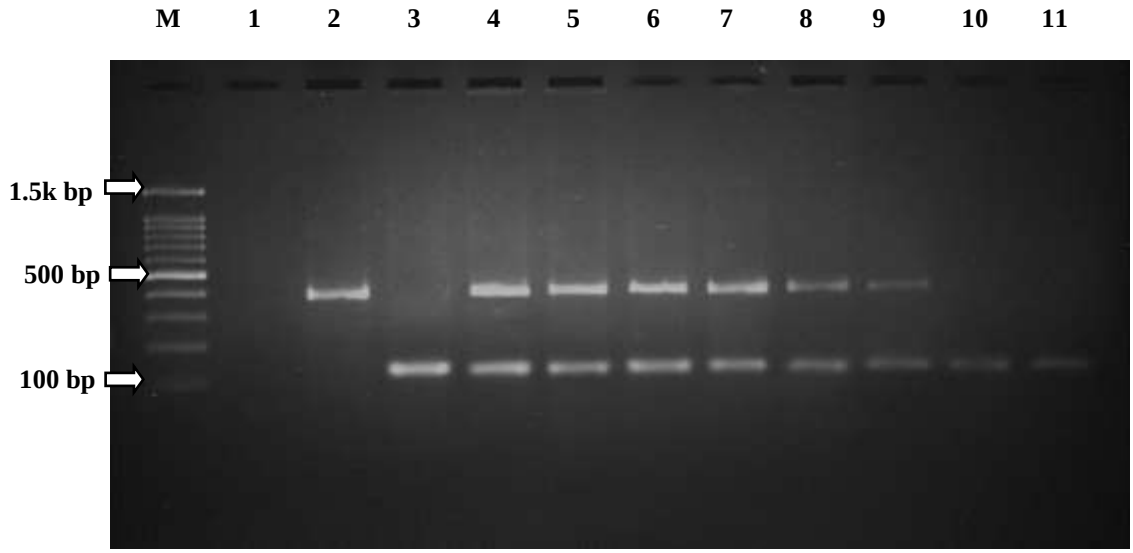


Figure 6. Detection of *invA* and *cadF* genes simultaneously from spiked broiler chicken faeces containing *Salmonella* and *Campylobacter* spp. in multiplex PCR in one PCR tube. Lane M: Molecular size marker (100 bp), Lane 1: *Klebsiella pneumonia* ATCC 700603, Lane 2: *Campylobacter* (400 bp), Lane 3: *Salmonella* (119 bp), Lane 4-11: 10-fold serial diluted spiked chicken faeces containing 10^7 to 1 CFU/mL of both *Salmonella* spp. and *Campylobacter* spp.

In the present study, the detection limit of the PCR for *Campylobacter* spp. in chicken faeces was 10^2 CFU/mL, indicating low analytical sensitivity compared to other studies. Lund et al. (2004) demonstrated a detection limit of 100 to 150 CFU/mL in chicken faecal suspension. The higher detection limit observed in the present study may be attributed to the nature of the faecal matrices that often contain PCR inhibitors such as bilirubin, bile salts, other organic and inorganic substances, which might interrupt the amplification of the targeted gene and, as a result, reduce the PCR sensitivity (Yan et al., 2020). Several studies suggested incorporating an enrichment step to supply essential nutrients, promote bacterial recovery and growth, and ultimately improve sensitivity and selectivity (Gwida and Al-Ashmawy, 2014; Lee et al., 2015). Additionally, Park and Ricke (2015) demonstrated that the optimized multiplex PCR and qPCR could detect approximately 2.2 CFU of *Salmonella* per gram following an 18-hour enrichment period in spiked chicken breast meat samples.

The mPCR protocol developed was compared to conventional culture methods using 15 pooled faecal samples from different broiler farms. The mPCR method detected more positive samples compared to the culture method, including some that the culture method failed to identify (Table 3). These results could be due to the higher sensitivity of mPCR, suggesting that conventional culture methods may underestimate the actual prevalence of the bacteria. In addition, this may reflect the ability of PCR to detect DNA from viable but non-culturable bacteria and samples with low bacterial loads. Among the culture-positive samples, *Salmonella* spp. was detected in 1/15 (6.7%) samples, *Campylobacter* in

6/15 (40%) samples, and co-detection of both bacteria was obtained in 2/15 (13.3%) samples. The mPCR assay detected *Salmonella* in 4/15 (26.7%) samples, *Campylobacter* in 6/15 (40.0%) samples, and both pathogens in 2/15 (13.3%) samples (Table 4). To determine the sensitivity, specificity, and predictive values, a two-by-two contingency table was constructed (Table 5). Table 5 indicates that the mPCR assay estimated sensitivity for classifying a sample as infected (Positive) was 100%. At the same time, 50% of samples were accurately identified as non-infected (Negative) by the mPCR. The mPCR approach had a 75% positive predictive value and a 100% negative predictive value. In the present study, some samples that were positive by mPCR but negative by culture were likely due to the presence of sub-lethally injured cells that fail to grow on selective media. This highlighted the greater sensitivity of PCR compared to conventional culture methods, rather than representing true false-positive results (Liang et al., 2018). Other comparative studies on detection methods using mPCR assay and conventional culture method to detect common diarrhoea causative bacteria, such as *Salmonella* spp., *Listeria monocytogenes*, *Campylobacter* spp., and *Escherichia coli* O157, indicated similar results to those in the present study (Gwida and Al-Ashmawy, 2014; Bonilauri et al., 2016; Huang et al., 2018).

The rapid identification of the common foodborne pathogens is beneficial for preventive and control measures, as it enables early intervention to reduce the dissemination of bacteria and potential contamination of poultry products (Zendrini et al., 2021). Comparable to the findings of Benlashehr et al. (2024), who demonstrated that pre-enrichment and selective enrichment were essential for the successful recovery of *Salmonella enteritidis* from poultry and murine faecal samples, the present study also indicated that a culture-based method with enrichment can detect *Salmonella* and *Campylobacter* spp. from the faecal samples. However, both culture and PCR approaches were able to identify the pathogens; culture required at least five days to obtain a result, whereas PCR yielded outcomes within a much shorter time frame. For *Campylobacter*, an additional 24 hours of incubation is required if no growth was observed on the plate, as recommended by ISO 10272-1:2017 (WOAH, 2018). This additional incubation period can delay reporting and the implementation of appropriate control measures, potentially allowing the foodborne pathogens to persist longer in the food production chain. In the current study, *Salmonella* and *Campylobacter* spp. were detected simultaneously directly from chicken faeces by reducing the detection time to less than 36 hours compared to the standard culture method as described in the terrestrial manual and ISO 10272-1:2017 (WOAH, 2018; 2022).

The values were used to calculate the sensitivity, specificity, positive predictive value, and negative predictive value of the mPCR assay in comparison to the culture method for detecting *Salmonella* and *Campylobacter* spp. in broiler faeces, using the formulas described by Parikh et al. (2008). The protocol developed in the present study successfully identified all (100%) true positive samples (sensitivity), with a positive predictive value of 75%, and 50% of the true negative samples (specificity), with a negative predictive value of 100%.

Table 3. Culture and mPCR assay results for detecting *Salmonella* and *Campylobacter* spp. from broiler chicken faeces

	Faeces samples (Number)	
	Culture	**mPCR**
Negative	6	3
Positive	9	12

mPCR: Multiplex polymerase chain reaction.

Table 4. Comparison of culture method and mPCR assay for detecting *Salmonella* and *Campylobacter* spp. from broiler chicken faeces

Targeted bacteria	Culture	mPCR
Salmonella spp.	1/15 (6.7%)	4/15 (26.7%)
Campylobacter spp.	6/15 (40.0%)	6/15 (40.0%)
Both *Salmonella* spp. and *Campylobacter* spp.	2/15 (13.3%)	2/15 (13.3%)

mPCR: Multiplex polymerase chain reaction.

Table 5. Two-by-two contingency table comparing the mPCR and culture results for *Salmonella* and *Campylobacter* spp. detection from broiler chicken faeces

		Culture		Total
		Positive	**Negative**	
mPCR	Positive	9	3	12
	Negative	0	3	3
Total		9	6	15

CONCLUSION

The use of cultivation techniques to isolate and detect pathogens may help explain the lack of surveillance data on *Salmonella* and *Campylobacter* infections in Malaysia. The mPCR protocol developed in the present study enabled the rapid, simultaneous detection of *Salmonella* and *Campylobacter* spp. directly from chicken faeces. The protocol developed allowed the detection of *Salmonella* and *Campylobacter* spp. simultaneously at the detection limit of 10^1

CFU/mL and 10^2 CFU/mL of spiked chicken faeces, respectively, after 24 hours of enrichment. Compared to conventional culture methods, this approach substantially reduced detection time by eliminating the need for bacterial isolation and separate confirmatory assays. The DNA extraction and multiplex amplification steps minimized labour and reagent use, while optimized primer sets maintained high sensitivity and specificity. These advantages make the protocol a practical tool for routine surveillance, enabling the detection of pathogens at an early stage of the food chain to prevent the spread and reduce the risk of transmission to humans. Since *Salmonella enteritidis*, *Salmonella typhimurium*, *C. jejuni*, and *C. coli* pose a public health threat, a simultaneous detection method for these species directly from chicken faeces is recommended for future studies.

DECLARATIONS

Acknowledgments

The authors wish to express their gratitude to all staff and lecturers at the Public Health Laboratory and Bacteriology Laboratory, Faculty of Veterinary Medicine, University of Putra Malaysia.

Authors' contributions

Sherryl Nurfarhanim Abd Ghafar has contributed to the sample collection, processing, and cultivation of the bacteria and the development of the mPCR protocol. Nur Indah Ahmad supervised and approved the final edition before submission. Saleha Abdul Aziz participated in the sample collection process and cultivation of the bacteria. Zunita Zakaria was involved in the molecular analysis. All authors read and approved the final manuscripts.

Funding

The present study was supported by Universiti Putra Malaysia (UPM) research grant (UPM/800-3/3/1/GP/2018/9617100).

Competing interests

The authors declared no conflict of interest.

Ethical considerations

This paper was originally written by the authors and has not been published elsewhere. All authors have verified the text of the article for plagiarism index and confirmed that the text of the article is written based on their original scientific results. The authors confirmed that no AI tools, including generative AI models, were used in the writing or preparation of the present study.

Availability data and materials

All datasets used in the current study are available from the corresponding author on reasonable request.

REFERENCES

Abakpa GO, Umoh VJ, Ameh JB, Yakubu SE, Kwaga, JKP, and Kamaruzaman S (2015). Diversity and antimicrobial resistance of *Salmonella* enterica isolated from fresh produce and environmental samples. Environmental Nanotechnology, Monitoring and Management, 3: 38-46. DOI: https://www.doi.org/10.1016/j.enmm.2014.11.004

Abebe E, Gugsa G, and Ahmed M (2020). Review on major foodborne zoonotic bacterial pathogens. Journal of Tropical Medicine, 2020: 46473235. DOI: https://www.doi.org/10.1155/2020/4674235

Adeyanju GT and Ishola O (2014). *Salmonella* and *Escherichia coli* contamination of poultry meat from a processing plant and retail markets in Ibadan, Oyo state, Nigeria. SpringerPlus, 3(1): 139. DOI: https://www.doi.org/10.1186/2193-1801-3-139

Al Amri A, Senok AC, Ismaeel AY, Al-Mahmeed AE, and Botta GA (2007). Multiplex PCR for direct identification of *Campylobacter* spp. in human and chicken stools. Journal of Medical Microbiology, 56(10): 1350-1355. DOI: https://www.doi.org/10.1099/jmm.0.47220-0

Alves J, Marques VV, Pereira LFP, Hirooka EY, and De Oliveira TCRM (2012). Multiplex PCR for the detection of *Campylobacter* spp. and *Salmonella* spp. in chicken meat. Journal of Food Safety, 32(3): 345-350. DOI: https://www.doi.org/10.1111/j.1745-4565.2012.00386.x

Ayaz N, Goncuoglu M, Cakmak O, and Erol I (2016). Comparison of *hipO* and *ceuE* gene based PCR assays for the detection of *Campylobacter jejuni*. Journal of Clinical Microbiology and Biochemical Technology, 2(1): 6-8. DOI: https://www.doi.org/10.17352/jcmbt.000008

Babazadeh D and Ranjbar R (2022). *Campylobacter* species in the Middle East. Journal of Veterinary Physiology and Pathology, 1(1): 1-9. DOI: https://www.doi.org/10.58803/jvpp.v1i1.3

Benlashehr I, Elmasry K, Kammon A, and Asheg A (2024). Evaluation of *Salmonella* Enteritidis isolated from layer hens and murine fecal pellets in poultry farms of Libya. Journal World Poultry Research, 14(2): 211-218. DOI: https://www.doi.org/10.36380/jwpr.2024.22

Bonilauri P, Bardasi L, Leonelli R, Ramini M, Luppi A, Giacometti F, and Merialdi G (2016). Detection of food hazards in foods: Comparison of real time polymerase chain reaction and cultural methods. Italian Journal of Food Safety, 5(1): 37-40.DOI: https://www.doi.org/10.4081/ijfs.2016.5641

Casabonne C, González A, Aquili V, Subils T, and Balagueá C (2016). Prevalence of seven virulence genes of *Campylobacter jejuni* isolated from patients with diarrhea in Rosario,Argentina. International Journal of Infection, 3(4): e37727. DOI: https://www.doi.org/10.17795/iji-37727

Deguenon E, Dougnon V, Lozes E, Maman N, Agbankpe J, Abdel-Massih RM, Djegui F, Baba-Moussa L, and Dougnon J (2019). Resistance and

virulence determinants of faecal *Salmonella* spp. isolated from slaughter animals in Benin. BMC Research Notes, 12(1): 317. DOI: https://www.doi.org/10.1186/s13104-019-4341-x

Department of Veterinary Services Malaysia (2017). Malaysia: Livestock population 2017-2018, pp. 1-15. Available at: https://www.dvs.gov.my/dvs/resources/user_1/2019/BP/Perangkaan%20Ternakan/3._Msia__Perangkaan_ternakan_M_Surat_1-15_.pdf

Gizaw Z (2019). Public health risks related to food safety issues in the food market: A systematic literature review. Environmental Health and Preventive Medicine, 24(1): 68. DOI: https://www.doi.org/10.1186/s12199-019-0825-5

Gwida MM and Al-Ashmawy MAM (2014). Culture versus PCR for *Salmonella* species identification in some dairy products and dairy handlers with special concern to its zoonotic importance. Veterinary Medicine International, 2014: 502370. DOI: https://www.doi.org/10.1155/2014/502370

Heredia N and García S (2018). Animals as sources of food-borne pathogens: A review. Animal Nutrition, 4(3): 250-255. DOI: https://www.doi.org/10.1016/j.aninu.2018.04.006

Heymans R, Vila A, van Heerwaarden CAM, Jansen CCC, Castelijn GAA, van der Voort M, and Biesta-Peters EG (2018). Rapid detection and differentiation of *Salmonella* species, *Salmonella Typhimurium* and *Salmonella* Enteritidis by multiplex quantitative PCR. PLoS ONE, 13(10): 10-15. DOI: https://www.doi.org/10.1371/journal.pone.0206316

Huang SH, Lin YF, Tsai MH, Yang S, Liao ML, Chao SW, and Hwang CC (2018). Detection of common diarrhea-causing pathogens in Northern Taiwan by multiplex polymerase chain reaction. Medicine, 97(23): e11006. DOI: https://www.doi.org/10.1097/MD.0000000000011006

Khoshbakht R, Tabatabaei M, Hosseinzadeh S, Shekarforoush SS, and Aski HS (2013). Distribution of nine virulence-associated genes in *Campylobacter jejuni* and *C. coli* isolated from broiler feces in Shiraz, Southern Iran. Foodborne Pathogens and Disease, 10(9): 764-770. DOI: https://www.doi.org/10.1089/fpd.2013.1489

Liang H, Wen Z, Li Y, Duan Y, Gu Y, and Zhang M (2018). Comparison of filtration culture and multple real-time PCR examination for *Campylobacter* spp. from stool specimens in diarrheal patients. Frontiers in Microbiology, 9(12): 2995. DOI: https://www.doi.org/10.3389/fmicb.2018.02995

Lee KM, Runyon M, Herrman TJ, Phillips R, and Hsieh J (2015). Review of *Salmonella* detection and identification methods: Aspects of rapid emergency response and food safety. Food Control, 47: 264-276. DOI: https://www.doi.org/10.1016/j.foodcont.2014.07.011

Lund M, Nordentoft S, Pedersen K, and Madsen M (2004). Detection of *Campylobacter* spp. in chicken fecal samples by real-time PCR. Journal of Clinical Microbiology, 42(11): 5125-5132. DOI: https://www.doi.org/10.1128/JCM.42.11.5125-5132.2004

Neyaz LA, Alghamdi HS, Alghashmari RM, Alswat SS, Almaghrabi RO, Bazaid FS, Albarakaty FM, Elbanna K, and Abulreesh HH (2024). A comprehensive review on the current status of culture media for routine standardized isolation of *Salmonella* and *Shigella* spp. from contaminated food. Journal of Umm Al-Qura University for Applied Sciences, 2024, pp. 1-14. DOI: https://www.doi.org/10.1007/s43994-024-00205-2

Ngobese B, Zishiri OT, and El Zowalaty ME (2020). Molecular detection of virulence genes in *Campylobacter* species isolated from livestock production systems in South Africa. Journal of Integrative Agriculture, 19(6): 1656-1670. DOI: https://www.doi.org/10.1016/S2095-3119(19)62844-3

Nguyen TK, Bui HT, Truong TA, Lam DN, Ikeuchi S, Ly LKT, Hara-Kudo Y, Taniguchi T, and Hayashidani H (2021). Retail fresh vegetables as a potential source of *Salmonella* infection in the Mekong Delta, Vietnam. International Journal of Food Microbiology, 341(1): 109049. DOI: https://www.doi.org/10.1016/j.ijfoodmicro.2021.109049

Osman AY, Elmi SA, Simons D, Elton L, Haider N, Azam Khan M, Othman I, Zumla A, McCoy D, and Kock R (2021). Antimicrobial resistance patterns and risk factors associated with *Salmonella* spp. isolates from poultry farms in the east coast of Peninsular Malaysia: A cross-sectional study. Pathogens, 10(9): 1160. DOI: https://www.doi.org/10.3390/pathogens10091160

Parikh R, Mathai A, Parikh S, Sekhar C, and Thomas R (2008). Understanding and using sensitivity, specificity and predictive values. Indian Journal of Ophthalmology, 56(4): 341. https://www.doi.org/10.4103/0301-4738.41424

Park SH and Ricke SC (2015). Development of multiplex PCR assay for simultaneous detection of *Salmonella* genus, *Salmonella* subspecies I, *Salmonella* Enteritidis, *Salmonella* heidelberg and *Salmonella* Typhimurium. Journal of Applied Microbiology, 118(1): 152-160. DOI: https://www.doi.org/10.1111/jam.12678

Park S, Szonyi B, Gautam R, Nightingale K, Anciso J, and Ivanek R (2012). Risk factors for microbial contamination in fruits and vegetables at the preharvest level: A systematic review. Journal of Food Protection, 75(11): 2055-2081. DOI: https://www.doi.org/10.4315/0362-028X.JFP-12-160

Pathmanathan SG, Cardona-Castro N, Sánchez-Jiménez MM, Correa-Ochoa MM, Puthucheary SD, and Thong KL (2003). Simple and rapid detection of *Salmonella* strains by direct PCR amplification of the *hilA* gene. Journal of Medical Microbiology, 52(9): 773-776. DOI: https://www.doi.org/10.1099/jmm.0.05188-0

Persson S and Olsen KEP (2005). Multiplex PCR for identification of *Campylobacter coli* and *Campylobacter jejuni* from pure cultures and directly on stool samples. Journal of Medical Microbiology, 54(11): 1043-1047. DOI: https://www.doi.org/10.1099/jmm.0.46203-0

Ranjbar R and Babazadeh D (2017). Contact with poultry and animals increases risk of *Campylobacter* infections in adults of Ardabil province, Iran. Universa Medicina, 36(1): 59-67. DOI: https://www.doi.org/10.18051/univmed.2017.v36.59-67

Reddy S and Zishiri OT (2018). Genetic characterisation of virulence genes associated with adherence, invasion and cytotoxicity in *Campylobacter* spp. isolated from commercial chickens and human clinical cases. Onderstepoort Journal of Veterinary Research, 85(1): a1507. DOI: https://www.doi.org/10.4102/ojvr.v85i1.1507

Rejab SBM, Zessin KH, Fries R, and Patchanee P (2012). Comparison of *Campylobacter* contamination levels on chicken carcasses between modern and traditional types of slaughtering facilities in Malaysia. Journal of Veterinary Medical Science, 74(1): 121-124. DOI: https://www.doi.org/10.1292/jvms.11-0145

Rivera-Pérez W, Barquero-Calvo E, and Zamora-Sanabria R (2014). *Salmonella* contamination risk points in broiler carcasses during slaughter line processing. Journal of Food Protection, 77(12): 2031-2034. DOI: https://www.doi.org/10.4315/0362-028X.JFP-14-052

Sadek SAS, Shaapan RM, and Barakat AMA (2023). *Campylobacteriosis* in poultry: A review. Journal of World's Poultry Research, 13(2): 168-179. DOI: https://www.doi.org/10.36380/jwpr.2023.19

Saeki EK, Alves J, Bonfante RC, Hirooka EY, and De Oliveira TCRM (2013). Multiplex PCR (mPCR) for the detection of *Salmonella* spp. and the differentiation of the *Typhimurium* and *Enteritidis* serovars in chicken meat. Journal of Food Safety, 33(1): 25-29. DOI: https://www.doi.org/10.1111/jfs.12019

Salama Y and Chennaoui M (2024). Understanding microbial contamination in meat and poultry production. Journal of Research in Agriculture and Food Sciences, 1(3): 87-107. DOI: https://www.doi.org/10.5455/jrafs.20240705062923

Shanmugasamy M, Velayutham T, and Rajeswar J (2011). *Inva* gene specific PCR for detection of *Salmonella* from broilers. Veterinary World, 4(12): 562-564. DOI: https://www.doi.org/10.5455/vetworld.2011.562-564

Sharma I (2016). Detection of *invA* gene in isolated *Salmonella* from marketed poultry meat by PCR Assay. Journal of Food Processing & Technology, 7(3). DOI: https://www.doi.org/10.4172/2157-7110.1000564

Singh Y, Saxena A, and Kumar RSM (2018). Virulence system of *Salmonella* with special reference to *Salmonella* enterica. In: M. T. Mascellino (Editor), Salmonella - A re-emerging pathogen. Intech, pp. 137-144. DOI: https://www.doi.org/10.5772/intechopen.77210

Sinulingga TS, Aziz SA, Bitrus AA, Zunita Z, and Abu J (2020). Occurrence of *Campylobacter* species from broiler chickens and chicken meat in Malaysia. Tropical Animal Health and Production, 52(1): 151-157. DOI: https://www.doi.org/10.1007/s11250-019-01995-y

Sodagari HR, Habib I, Shahabi MP, Dybing NA, Wang P, Bruce M (2020). A review of the public health challenges of *Salmonella* and turtles. Veterinary Sciences, 7(2): 56. DOI: https://www.doi.org/10.3390/VETSCI7020056

Strakova N, Korena K, Gelbicova T, Kulich P, and Karpiskova R (2021). A rapid culture method for the detection of *Campylobacter* from water environments. International Journal of Environmental Research and Public Health, 18(11): 6098. DOI: https://www.doi.org/10.3390/ijerph18116098

Sukri A, Zulfakar SS, Taib ISM, Omar NF, and Zin NM (2021). The high occurrence of multidrug-resistant *Salmonella* spp. isolated from raw chicken meat and contact surfaces at wet market in Malaysia. Sains Malaysiana, 50(12): 3765-3772. DOI: https://www.doi.org/10.17576/jsm-2021-5012-25

Thung TY, Radu S, Mahyudin NA, Rukayadi Y, Zakaria Z, Mazlan N, Tan BH, Lee E, Yeoh SL, Chin YZ, Tan CW, Kuan CH, Basri DF, and Wan MRCWJ (2018). Prevalence, virulence genes and antimicrobial resistance profiles of *Salmonella* serovars from retail beef in Selangor, Malaysia. Frontiers in Microbiology, 8(1): 02697. DOI: https://www.doi.org/10.3389/fmicb.2017.02697

Tibebu A, Tamrat H, and Bahiru A (2024). Review: Impact of food safety on global trade. Veterinary Medicine and Science, 10(5): e1585. DOI: https://www.doi.org/10.1002/vms3.1585

Wahab AM, Zeshan B, Ahmed N, Afzal M, and Naveed M (2021). Molecular survey of *Campylobacter jejuni* in broiler chicken farms in east coast of Peninsular, Malaysia. 53(4): 1555-1558. DOI: https://www.doi.org/10.17582/journal.pjz/20180702090700

World health organisation (WHO) (2015). WHO estimates of the global burden of foodborne diseases: Foodborne disease burden epidemiology reference group 2007-2015. Encyclopedia of Parasitology, 1-1. Available at: https://iris.who.int/bitstream/handle/10665/199350/9789241565165_eng.pdf

World organization for animal health (WOAH) (2018). Infection with *Campylobacter jejuni* and *C. coli*. Available at: https://www.woah.org/fileadmin/Home/eng/Health_standards/tahm/2.09.03_CAMPYLO.pdf

World organization for animal health (WOAH) (2022). Salmonellosis. 1-19. Available at: https://www.woah.org/fileadmin/Home/fr/Health_standards/tahm/3.10.03_SALMONELLOSIS.pdf

Yan L, Toohey-Kurth KL, Crossley BM, Bai J, Glaser AL, Tallmadge RL, and Goodman LB (2020). Inhibition monitoring in veterinary molecular testing. Inhibition monitoring in veterinary molecular testing. Journal of Veterinary Diagnostic Investigation, 32(6): 758-766. DOI: https://www.doi.org/10.1177/1040638719889315

Zendrini J, Carta V, Filipello V, Ragni L, Cosciani-cunico E, Arnaboldi S, Bertasi B, Franceschi N, Ajmone-marsan P, De Medici D, and Losio MN (2021). One-day molecular detection of *Salmonella* and *Campylobacter* in chicken meat: A pilot study, 10(5): 1-12. DOI: https://www.doi.org/10.3390/foods10051132

Publisher's note: Scienceline Publication Ltd. remains neutral with regard to jurisdictional claims in published maps and institutional affiliations.

Open Access: This article is licensed under a Creative Commons Attribution 4.0 International License, which permits use, sharing, adaptation, distribution and reproduction in any medium or format, as long as you give appropriate credit to the original author(s) and the source, provide a link to the Creative Commons licence, and indicate if changes were made. The images or other third party material in this article are included in the article's Creative Commons licence, unless indicated otherwise in a credit line to the material. If material is not included in the article's Creative Commons licence and your intended use is not permitted by statutory regulation or exceeds the permitted use, you will need to obtain permission directly from the copyright holder. To view a copy of this licence, visit https://creativecommons.org/licenses/by/4.0/.

© The Author(s) 2025

2025, Scienceline Publication
World's Veterinary Journal
World Vet J, 15(4): 901-909.
ISSN 2322-4568

DOI: https://dx.doi.org/10.54203/scil.2025.wvj91
PII: S2322456825000091-15

Quantitative Analysis of Small and Large Luteal Cells During Different Stages of Corpus Luteum Development in Holstein Cattle

Bui Van Dung*, Nguyen Thi Thanh Thuy, Nguyen Thi Ngoc Anh, and Nguyen Hoai Nam

Department of Animal Surgery and Theriogenology, Faculty of Veterinary Medicine, Vietnam National University of Agriculture, Trau Quy Town, Gia Lam District, Ha Noi, Viet Nam

*Corresponding author's Email: bvdung@vnua.edu.vn

ORIGINAL ARTICLE
Received: September 30, 2025
Revised: October 28, 2025
Accepted: November 26, 2025
Published: December 25, 2025

ABSTRACT

The bovine corpus luteum (CL) undergoes dynamic structural and functional changes throughout its lifespan, driven by distinct populations of steroidogenic cells, including small luteal cells (SLCs) and large luteal cells (LLCs). Although these cell types have been morphologically characterized, quantitative evaluations of their numerical abundance and relative distribution across different developmental phases of the CL in cows remain limited. This study sought to quantify the populations of small and large luteal cells across the early, mid, and late stages of corpus luteum development in Holstein cows. Histomorphometric analysis of hematoxylin and eosin–stained ovarian sections was performed to provide insights into their temporal roles in luteal function. Ovarian samples were obtained from 30 Holstein cows (30 pairs), immediately after slaughter, and categorized into early, mid, or late luteal phases according to ovarian morphology and the appearance of corpora lutea. A total of 30 CL samples (10 per stage) were selected for evaluation. Each CL was fixed, paraffin-embedded, and sectioned longitudinally (5 µm thick) for histological examination. Small (<20 µm) and large (> 35 µm) luteal cells were quantified in standardized microscopic fields at × 40 magnification using ImageJ software. The results revealed that SLC counts were highest during the early luteal phase (72.53 ± 7.83) and significantly exceeded LLC counts (30.70 ± 3.78). In the mid-luteal phase, SLCs decreased (50.70 ± 2.82) while LLCs increased (44.30 ± 3.11), with no significant difference between them. During the late luteal phase, SLCs increased slightly (59.77 ± 3.84), whereas LLCs declined markedly (24.80 ± 2.52). Overall, SLCs counted were highest during the early luteal phase and declined toward the mid phase, while LLCs increased markedly at the mid luteal phase and decreased again at the late phase.

Keywords: Corpus luteum, Histology, Large luteal cell, Small luteal cell

INTRODUCTION

The corpus luteum (CL) is a temporary endocrine structure that develops from the post-ovulatory follicle and is crucial for controlling the estrous cycle and supporting pregnancy by producing progesterone. During its lifespan, the CL undergoes dynamic morphological and functional changes characterized by intense tissue remodeling, including proliferation, differentiation, angiogenesis, and cell death (Neves et al., 2002). These processes are tightly regulated and critical for the establishment and maintenance of a functional luteal structure. The luteal tissue is composed of a heterogeneous population of cells, broadly classified into steroidogenic and non-steroidogenic types (Ponce-Barajas et al., 2023; Fernandez et al., 2024). Endothelial cells, fibroblasts, pericytes, macrophages, mast cells, and leukocytes represent the non-steroidogenic cell population. These cells contribute to structural stability, immune modulation, and vascular support within the tissue. In contrast, the steroidogenic compartment consists of two distinct cell types, including small luteal cells (SLCs) and large luteal cells (LLCs), which differ in their origin, size, morphology, hormone receptor expression, and capacity for steroidogenesis (Shimizu, 2016; Bishop et al., 2022; Fernandez et al., 2024).

Small luteal cells arise from the theca interna layer, are approximately 17 µm in diameter, and are characterized by their irregular nuclear shape, abundant smooth endoplasmic reticulum, and high density of luteinizing hormone (LH) receptors. Although their intrinsic progesterone output is low, SLCs respond acutely to LH stimulation and are involved in the dynamic regulation of luteal steroidogenesis (Ponce-Barajas et al., 2023; Fernandez et al., 2024). Large luteal cells (average ~38 µm), derived primarily from luteinized granulosa cells, are rich in organelles related to steroid production, and are responsible for the majority of progesterone and oxytocin secretion. However, these cells exhibit a weak response to LH because of their low expression of LH receptors (Bertan, 2006; Shimizu, 2016). These cells also store secretory granules containing oxytocin and relaxin and respond to prostaglandin F2α, playing a pivotal role in luteolysis (Skarzynski et al., 2008; Rękawiecki and Kotwica, 2008).

To cite this paper: Dung BV, Thuy NTT, Anh NTN, and Nam NH (2025). Quantitative analysis of small and large luteal cells during different stages of corpus luteum development in holstein cattle. *World Vet. J.*, 15(4): 901-909. DOI: https://dx.doi.org/10.54203/scil.2025.wvj91

Although the morphology and function of luteal cells are well characterized, quantitative changes in small and large luteal cell populations across the stages of corpus luteum development have not been fully elucidated. The relative abundance of SLCs and LLCs is known to fluctuate throughout the luteal lifespan, reflecting the gland's changing functional demands. However, previous studies have relied on qualitative or ultrastructural observations rather than direct quantitative comparisons of these cell types at defined stages (Pugliesi et al., 2023). Therefore, the present study provides new quantitative evidence on the relative proportions of SLCs and LLCs in Holstein cows during the early, mid, and late luteal phases, contributing to a clearer understanding of cellular remodeling associated with luteal development and regression. These changes in cellular composition are believed to underlie the shift from hormone-dependent to hormone-independent progesterone production and may influence the luteal lifespan and susceptibility to luteolysis (Basavaraja et al., 2021; Fernandez et al., 2024; Gecaj et al., 2024). Despite this, quantitative histological data on luteal cell populations at defined developmental stages remain limited, underscoring the need for more detailed analysis of luteal tissue organization and function.

Beyond steroidogenesis, luteal cells, particularly LLCs, exhibit significant secretory activity through cytoplasmic granules, which vary in size, density, and composition depending on the physiological stage. These secretory granules contain biologically active peptides, including oxytocin and relaxin, as well as proteins such as tissue inhibitors of metalloproteinases and apolipoproteins involved in extracellular matrix remodeling and lipid metabolism (Skarzynski et al., 2008; Shimizu, 2016; Bishop et al., 2022). The presence of these granules, particularly in LLCs, has been linked to high rates of protein synthesis and endocrine activity. Recent studies have expanded this view, demonstrating that luteal secretory activity is influenced by local immune signaling, angiogenic factors, and metabolic cues that modulate steroidogenesis and cell survival (Miyamoto et al., 2009; Shirasuna et al., 2012; Baddela et al., 2018). Moreover, progressive structural remodeling of the CL-characterized by connective tissue accumulation, altered extracellular matrix composition, and variable vascular density-occurs during luteal regression and advanced pregnancy, reflecting a coordinated balance between synthesis and degradation processes (Junqueira and Carneiro, 2008; Skarzynski et al., 2013).

Despite these advances, comprehensive quantitative data linking cellular composition with functional status remain scarce. The present study addresses this gap by providing quantitative evidence on the relative abundance of SLCs and LLCs across defined luteal phases in Holstein cows. This contributes to a more integrated understanding of how dynamic cellular remodeling supports the transition between active progesterone secretion and structural regression within the bovine corpus luteum (Miyamoto et al., 2009).

Previous studies have investigated the functional and morphological features of luteal cells in various physiological conditions (Xavier et al., 2012; Hryciuk et al., 2021; Ponce-Barajas et al., 2023), but quantitative comparisons of SLC and LLC populations across distinct phases of luteal development, namely early (formation), mid (mature), and late (regression) remain limited. Such data are critical for understanding the shifts in steroidogenic capacity, responsiveness to luteotropic and luteolytic signals, and the cellular mechanisms underlying luteal formation and regression.

Therefore, the objective of this study was to perform a quantitative analysis of small and large luteal cells in the bovine corpus lutea across three key stages of their lifecycle, including post-ovulation formation, functional maturity, and luteal regression. These data aimed to provide a morphological basis for understanding the endocrine functionality of the CL and contribute to the broader knowledge of bovine reproductive physiology.

MATERIALS AND METHODS

Ethical approval

This study involved the use of ovaries collected post-mortem from slaughtered Holstein cows and did not include any live animal handling or experimental intervention. All procedures, including sample collection and analysis, were conducted in accordance with the ethical guidelines for animal research established by the Vietnam National University of Agriculture.

Ovary collection and classification

Ovaries were collected from 30 multiparous Holstein cows (aged 45-90 months) within 30 minutes after routine slaughter at Phuxuyen slaughterhouse, Hanoi, Vietnam. Based on external morphological characteristics, CLs were categorized into three distinct phases (Figure 1) following the criteria described by Miyamoto et al. (2000). In the early luteal phase (formation stage), CLs exhibited a soft texture and a highly vascularized surface, consistent with post-ovulatory development. The mid-luteal phase (mature stage) was characterized by a firm texture and a reddish-yellow appearance, indicative of peak functional activity. In the late luteal phase (regression stage), CLs displayed a pale color and fibrous texture, reflecting structural and functional decline. The sample size was determined using an a priori power

analysis performed with G*Power version 3.1.9.7 (Heinrich-Heine-Universität Düsseldorf, Düsseldorf, Germany) for a one-way ANOVA (fixed effects, omnibus) design, assuming a significance level (α) of 0.05, a statistical power of 0.80, and an expected effect size (f) of 0.70. The analysis indicated that a minimum of 24 samples (8 per group) would provide sufficient power to detect significant differences among groups. To increase the robustness and reliability of the results, a total of 30 corpora lutea (10 per stage) were included in the study, exceeding the minimum requirement. Classification was conducted by a trained veterinarian using standardized morphological criteria to ensure consistency and minimize observer bias.

Table 1. Number of small and large luteal cells at different stages of corpus luteum (CL) development in cattle (Mean ± SD)

CL Development Stage	Small Luteal Cells (SLC)	Large Luteal Cells (LLC)
Early Luteal Phase (Formation)	72.53 ± 7.83^{am}	30.70 ± 3.78^{an}
Mid Luteal Phase (Mature)	50.70 ± 2.82^{b}	44.30 ± 3.11^{b}
Late Luteal Phase (Regression)	59.77 ± 3.84^{cm}	24.80 ± 2.52^{cn}

^{a,b,c} Different letters indicate differences between different stages of CL development ($p < 0.05$). ^{m,n} Different letters indicate differences between the number of small and large luteal cells ($p < 0.05$). CL: Corpus luteum. The data are presented as the mean ± SD.

Tissue fixation and processing

Following dissection, the CL was carefully separated from the ovary and immediately immersed in 10% neutral buffered formalin for a minimum of four hours to ensure pre-fixation as described by Mokhtar (2015). Subsequently, each CL was sectioned longitudinally into fragments approximately 0.5 cm thick, from the apex (top) to the base (bottom), to preserve the spatial orientation and zonal organization of the luteal tissue. The tissue fragments were then retained in the same fixative solution until further processing.

The tissue fragments underwent dehydration through a graded alcohol series, followed by clearing in xylene and embedding in paraffin using standard histological protocols. Serial sections with a thickness of 5 µm were cut using a rotary microtome (Microm HM 325, Thermo Scientific, Germany), and three representative slides were produced for each corpus luteum. These slides were stained with Hematoxylin and Eosin (H&E) to distinguish nuclear and cytoplasmic components, thereby enabling detailed histological assessment and cellular characterization.

Histological evaluation and cell counting

For quantitative histological analysis, paraffin-embedded sections of the CL were stained with H&E and examined under a light microscope (Japan) at ×40 magnification (Xavier et al., 2012). From each slide, three microscopic fields were randomly selected from different anatomical zones (peripheral, intermediate, and central), yielding a total of nine fields per CL to ensure representative sampling.

Steroid-producing luteal cells were recognized by their distinct morphological characteristics and cell diameters, which were measured using ocular and stage micrometers in accordance with the classification criteria outlined by Yoshioka et al. (2013). SLCs, derived from the theca interna, were characterized by a diameter of less than 20 µm, irregularly shaped nuclei, and dense cytoplasm. In contrast, LLCs, originating from granulosa cells, measured over 35 µm in diameter and exhibited a polygonal shape, abundant cytoplasm, centrally located round nuclei, and prominent nucleoli.

Cell counting was performed within a standardized area of 520 × 340 µm per field. Images were captured using Proview software (Optika Proview, version 4.12.24744, Optika, Ponteranica, Italy) on an Olympus CX31 (Japan) microscope, and the defined counting area was calibrated using an ocular micrometer (Japan). The acquired images were subsequently analyzed using the ImageJ Cell Counter plugin (NIH, USA) to ensure accurate identification and quantification. All counts were performed manually by the same trained observer to reduce inter-observer variability and ensure methodological consistency.

Statistical analysis

Descriptive statistics (mean ± SD) were calculated for each cell type across the three developmental stages. One-way ANOVA was applied to determine statistical differences in cell counts between stages for each cell type. Independent t-tests were used to compare SLC and LLC counts within each stage. Post-hoc analysis using Tukey's HSD test was performed when ANOVA revealed significant results. Statistical significance was set at $p < 0.05$. All analyses were conducted using IBM SPSS for Windows version 22 (IBM Corp., Armonk, New York, United States).

RESULTS AND DISCUSSION

The number of SLCs and LLCs varied significantly across the different stages of CL development (Table 1 and Figure 2). During the early luteal phase, the number of SLCs was highest (72.53 ± 7.83) and significantly greater than that of LLCs (30.70 ± 3.78; $p < 0.05$). In the mid-luteal phase, the number of SLCs decreased significantly compared with the early luteal phase (50.70 ± 2.82 versus 72.53 ± 7.83; $p < 0.05$), while the number of LLCs increased significantly compared with the early phase (44.30 ± 3.11 versus 30.70 ± 3.78; $p < 0.05$). As a result, there was no significant difference between SLCs and LLCs within this stage. This balanced proportion coincides with peak luteal function, characterized by maximal progesterone secretion. The shift toward increased LLCs aligns with previous reports by Shimizu (2016) and Bishop et al. (2022), who noted that LLCs, originating from granulosa cells, possess higher steroidogenic capacity and dominate during the mid-luteal stage when progesterone output is maximal.

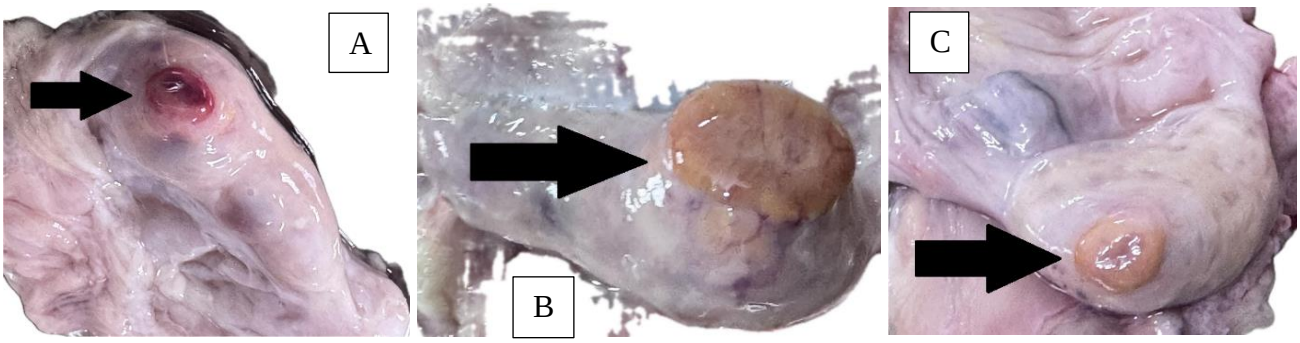
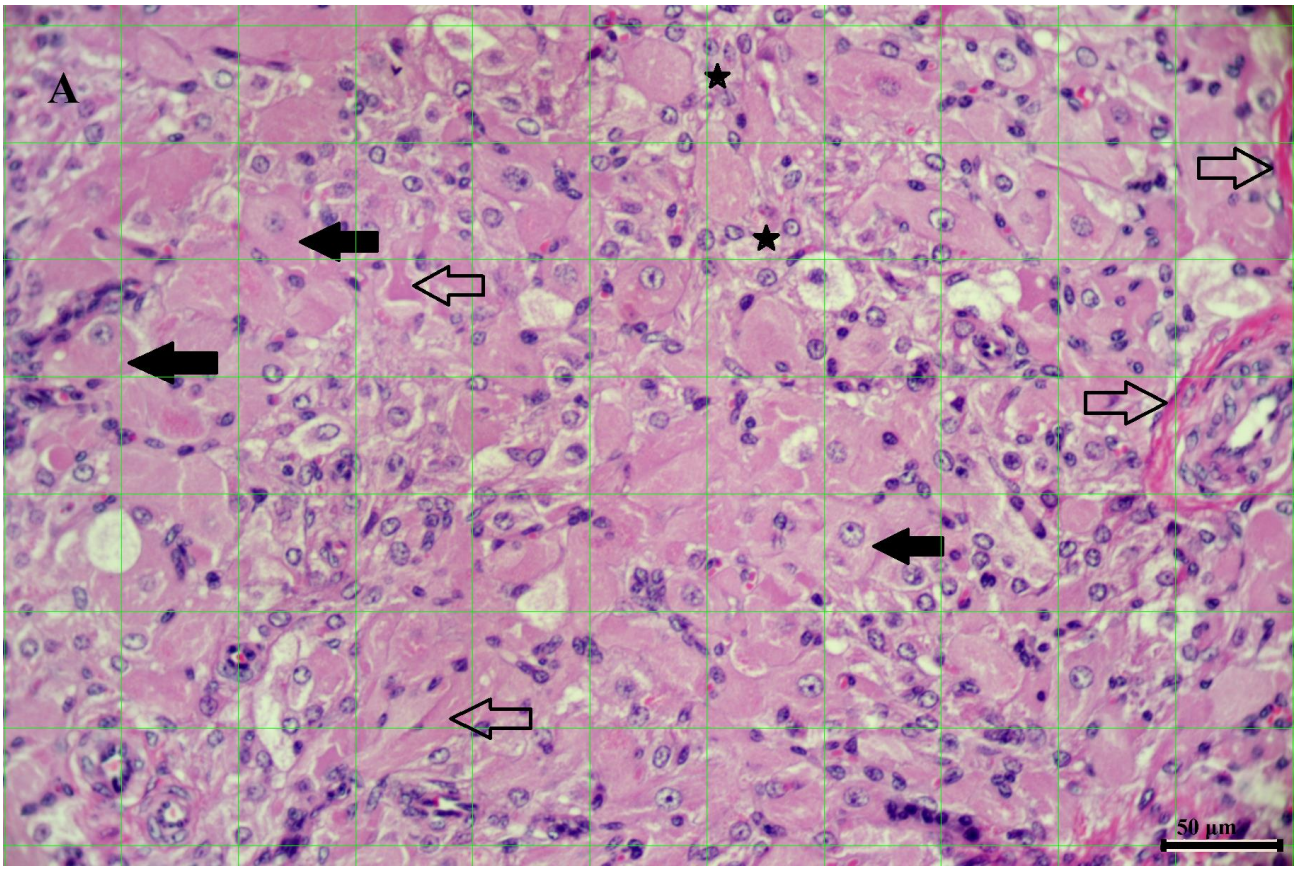


Figure 1. The appearance of bovine corpus luteum at three developmental stages. Representative images of the bovine corpus luteum (CL) at three distinct developmental stages, indicated by black arrows. **(A)** Early luteal phase-newly formed CL post-ovulation, with soft texture and highly vascularized surface; **(B)** Mid luteal phase-mature CL with firm consistency and reddish-yellow coloration; **(C)** Late luteal phase, regressing CL with reduced size, fibrotic appearance, and pale color (Source: Designed by authors).



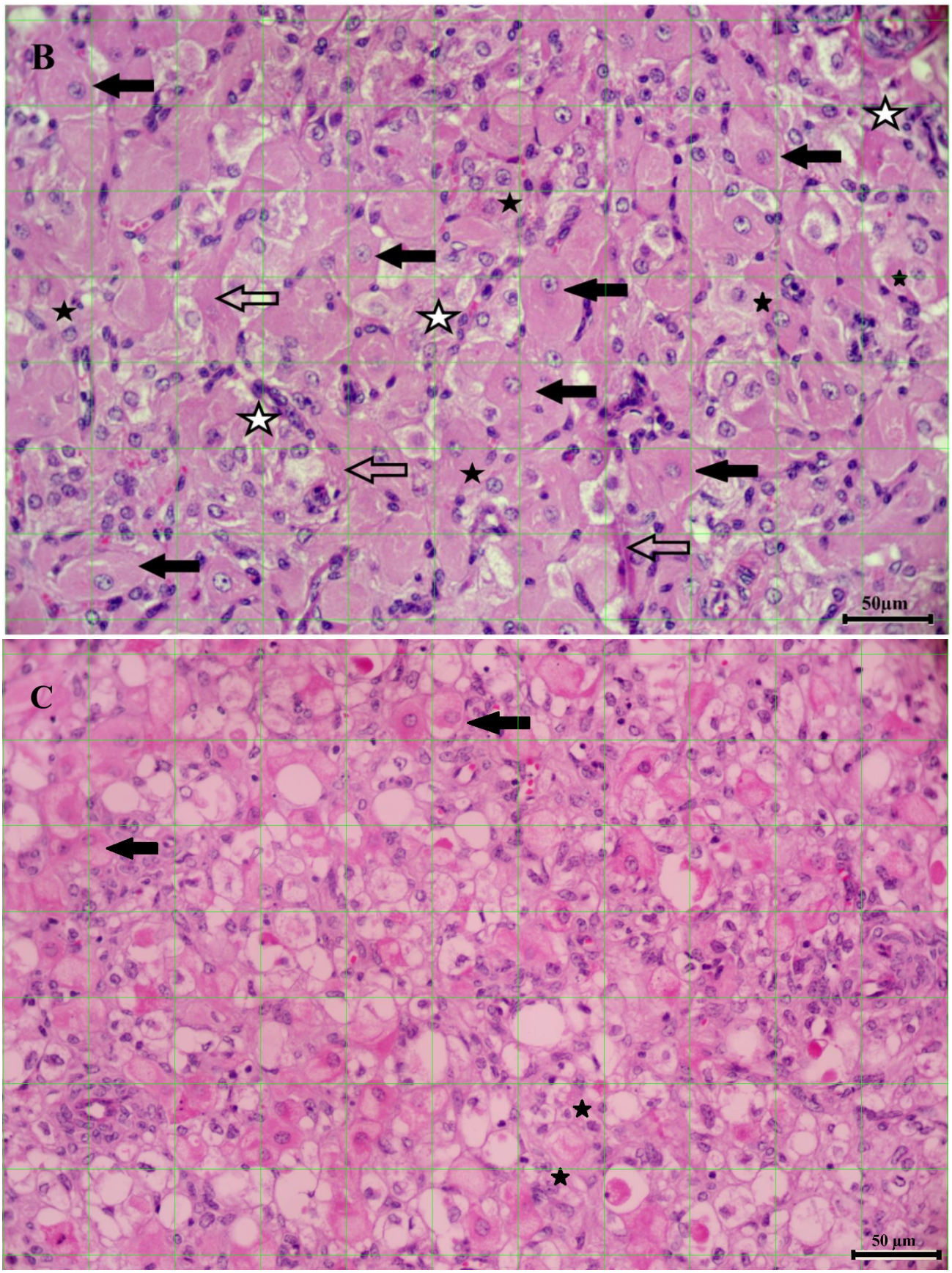


Figure 2. Histological features of the bovine corpus luteum at different luteal phases. (**A**) Early-luteal phase showing newly formed large luteal cells (black arrows) and small luteal cells (black stars) and developing vascular stroma (white arrow). (**B**) Mid-luteal phase showing fully differentiated large (black arrow) and small luteal cells (black star), with well-developed vascular stroma (white arrow) and interstitial fibroblasts (white star). (**C**) Late-luteal phase showing regressive luteal cells (black arrows and black stars), and reduced cellular density. H&E, 40×. The enumeration of large luteal cells and small luteal cells was facilitated using a grid system generated by the ImageJ program. (Source: Designed by authors).

In the late luteal phase, the number of SLCs increased slightly compared with the mid-luteal phase (59.77 ± 3.84 versus 50.70 ± 2.82; $p < 0.05$), whereas the number of LLCs declined markedly compared with the mid-luteal phase (24.80 ± 2.52 versus 44.30 ± 3.11; $p < 0.05$). The decline in LLCs is consistent with luteolytic regression, as LLCs are more sensitive to prostaglandin $F_2\alpha$–induced apoptosis (Shah et al., 2014; Basavaraja et al., 2021). Meanwhile, the relative persistence of SLCs may indicate greater resistance to luteolytic signals, a pattern also observed by Przygrodzka et al. (2021). Collectively, these patterns support the distinct temporal and functional roles of SLCs and LLCs in the cyclic remodeling of the bovine corpus luteum.

This study demonstrated that the number and distribution of SLCs and LLCs vary significantly across stages of CL development in Holstein cows. During the early luteal phase, SLCs predominated, suggesting their active proliferation and involvement in early CL formation, which is consistent with previous reports describing the rapid luteinization of theca-derived cells post-ovulation (Jiang et al., 2011; Ponce-Barajas et al., 2023). In contrast, the mid-luteal phase was characterized by a relatively balanced population of SLCs and LLCs, corresponding to the peak of luteal steroidogenic activity (Shimizu, 2016; Bishop et al., 2022; Fernandez et al., 2024). By the late luteal phase, a significant decline in LLCs was observed, accompanied by a modest increase in SLCs, potentially reflecting early luteolytic changes and the relative resistance of SLCs to apoptosis during CL regression (Przygrodzka et al., 2021). These dynamic changes in luteal cell composition highlight the distinct functional roles of SLCs and LLCs and the tightly regulated structural remodeling of the CL during its development and regression (Bishop et al., 2015; Bishop et al., 2022).

These findings provide new quantitative insights into the dynamic population shifts of small and large luteal cells during the bovine estrous cycle, emphasizing their complementary roles in CL development and function. The predominance of SLCs during the early and developing stages of CL formation indicates that these cells are essential for the initial establishment of the luteal structure and for sustaining early progesterone production before the CL reaches full maturity (Scully et al., 2021; Ponce-Barajas et al., 2023; Fernandez et al., 2024). As the CL progresses to the mid-luteal phase, the relative increase in LLCs, cells with greater steroidogenic capacity, suggests a cellular transition that supports the peak secretion of progesterone necessary for the maintenance of the luteal phase and establishment of early pregnancy (Shimizu, 2016; Bishop et al., 2022). These quantitative relationships between SLC and LLC populations therefore provide a cellular basis for understanding how the CL achieves and regulates its functional capacity throughout the estrous cycle (Bishop et al., 2015; Bishop et al., 2022). By linking morphological cell-type dynamics to physiological function, this study contributes to improving reproductive management and offers a foundation for exploring the cellular mechanisms underlying luteal insufficiency and subfertility in dairy cattle (Diskin and Morris, 2008; Bender et al., 2010; Basavaraja et al., 2021).

The results are consistent with previous findings by Yoshioka et al. (2013), who demonstrated that SLCs show substantial proliferative activity during the early and developing stages, as evidenced by strong Ki-67 expression and the upregulation of cell cycle-related genes such as *CCND2* and *CCNE1*. In contrast, LLCs exhibited minimal or no proliferative activity, supporting the notion that CL growth in the early phase is predominantly driven by SLC proliferation. The predominance of SLCs during early luteal development may be attributed to their origin from theca cells, which retain proliferative potential after ovulation. In contrast, LLCs are derived from granulosa cells that typically undergo terminal differentiation after the LH surge, resulting in cell cycle arrest (Regan et al., 2018; Abedel-Majed et al., 2019). This difference in cellular origin helps explain why SLCs are more numerous and proliferative in the early stages of CL development.

The transition from the developing to the mid-luteal stage is marked by a decline in SLC proliferation and a relative increase in LLC numbers. Yoshioka et al. (2013) demonstrated that LH plays a central role in this transition. LH treatment significantly reduced DNA synthesis and downregulated *CCND2* expression in SLCs derived from mid-stage CLs, but not in those from the developing stage. Concurrently, LH receptor mRNA expression increased at the mid-luteal stage, suggesting heightened LH sensitivity that may promote terminal differentiation and inhibit proliferation of SLCs. These results support the hypothesis that LH signaling mediates a shift from a proliferative to a differentiated state, contributing to the stabilization of luteal cell populations during the mid-luteal phase (Yoshioka et al., 2013). The mid-luteal phase also coincides with peak CL function and high progesterone output, largely due to the abundance and steroidogenic activity of LLCs. Large luteal cells originate from granulosa cells of the preovulatory follicle, and their numbers are closely linked to granulosa cell content. Studies have shown that aspiration of follicular granulosa cells or ovulation of small follicles results in smaller CLs and lower progesterone levels in cows and primates (Vasconcelos et al., 2001; Regan et al., 2018; Abedel-Majed et al., 2019). This indicates that the number of granulosa cells-and thus LLCs-is critical for CL size and steroidogenic capacity.

Molecular data from Hryciuk et al. (2025) further reinforce this relationship. In a controlled luteinized follicular cell culture model, the upregulation of *STAR*, *HSD3B1*, and *CYP11A1*, three essential genes for progesterone biosynthesis, was observed in luteinized granulosa-derived cells. These genes encode proteins involved in key steps of

steroidogenesis, including cholesterol transport (*STAR*), pregnenolone conversion (*CYP11A1*), and the transformation of pregnenolone into progesterone (*HSD3B1*). The observed upregulation in gene and protein expression, coupled with sustained progesterone secretion in culture, indicates that granulosa-derived LLCs can rapidly acquire a steroidogenically active phenotype upon luteinization. Additionally, the downregulation of *CYP17A1*, a key androgen-synthesizing enzyme, during early luteinization suggests a functional shift from androgen to progesterone production, consistent with the luteal phenotype (Magoffin, 2005).

In vivo, LLCs in the mid luteal phase exhibit structural features indicative of high steroidogenic activity, including abundant mitochondria, extensive smooth endoplasmic reticulum, and dense-core secretory granules containing oxytocin and relaxin (Rękawiecki and Kotwica, 2008; Shimizu, 2016; Bishop et al., 2022). These morphological characteristics correlate with increased basal progesterone secretion reported by Bishop et al. (2022) and Fernandez et al. (2024) during the mid-luteal phase, supporting the functional dominance of LLCs at this stage. In addition to LH-driven differentiation, angiogenic and growth factors, along with cell–cell interactions, are likely to support LLC function. Vascular endothelial growth factor (VEGF), which plays a central role in regulating luteal angiogenesis, exhibits elevated mRNA expression during the early and mid-luteal phases, followed by a marked decrease as the corpus luteum undergoes regression (Kisliouk et al., 2007). Additionally, interactions between large and small luteal cells through paracrine signaling have been reported to influence steroidogenic activity within the corpus luteum, as demonstrated in co-culture experiments (Bao et al., 2025).

In contrast, during the late luteal stage, a decline in LLC numbers was observed, coinciding with the initiation of luteolysis. Prostaglandin F2α (PGF2α), the primary luteolytic signal, targets LLCs and induces apoptosis and the release of secretory granules, ultimately leading to a reduction in progesterone secretion (Miyamoto et al., 2009). This selective sensitivity of LLCs to PGF2α is supported by their higher expression of PGF2α receptors compared to SLCs (Basavaraja et al., 2021), which likely accounts for the earlier onset of apoptosis in this cell type. Supporting this, Shah et al. (2014) reported that PGF2α treatment significantly reduces cytoplasmic electron-dense secretory granules in LLCs-but not in SLCs-indicating that degranulation serves as an early and selective indicator of luteolytic activity in LLCs. This persistence may reflect a delayed apoptotic response or reduced sensitivity to PGF2α. However, because of their lower steroidogenic capacity, SLCs contribute minimally to progesterone production during luteal regression (Shimizu, 2016; Bishop et al., 2022). Therefore, the selective loss of LLCs is a critical factor in the decline of luteal progesterone output and functional luteolysis.

Taken together, this data reinforces the model in which the structural and functional heterogeneity of the CL is orchestrated by distinct yet interconnected roles of SLCs and LLCs. These findings contribute to a more comprehensive understanding of luteal cell dynamics and the regulation of progesterone secretion throughout the estrous cycle. Elucidating these mechanisms provides important insight into how changes in luteal cell composition contribute to variations in circulating progesterone levels. Recent studies have highlighted the roles of lipid droplet-associated proteins such as *PLIN2* (Plewes et al., 2024), as well as transcriptional regulators like *STAR* (Zhao et al., 2025), in modulating steroidogenesis and luteal function. Further research should investigate how these molecular factors, particularly those responsive to luteotropic and luteolytic signals, influence luteal cell plasticity and progesterone production. In addition, trace elements such as zinc have been shown to modulate luteal function in a dose-dependent manner by influencing oxidative status and steroidogenic activity (Maruri et al., 2025). Exploring such metabolic and nutritional regulators alongside cellular mechanisms could help identify novel biomarkers or therapeutic strategies to improve reproductive efficiency in cattle.

CONCLUSION

These findings support the concept that the structural and functional heterogeneity of the corpus luteum is governed by the complementary roles of small and large luteal cells. The shifting proportions of SLCs and LLCs across the luteal phases reflect their coordinated contributions to CL development, maintenance, and regression. Future studies should focus on elucidating the molecular mechanisms underlying these cellular transitions, particularly the involvement of lipid droplet-associated proteins, steroidogenic regulators, and micronutrients such as zinc, which has been shown to modulate steroidogenesis and oxidative balance. Integrating cellular, molecular, and metabolic approaches may help identify new biomarkers or therapeutic strategies to enhance luteal function and reproductive efficiency in cattle.

DECLARATIONS

Acknowledgments
The authors would like to thank Nguyen Van Dai for his valuable assistance with sample collection.

Funding
This study was funded by Vietnam National University of Agriculture (Grant No. T2025-09-35).

Authors contributions
Bui Van Dung and Nguyen Hoai Nam conceptualized and designed the research. Data collection and statistical analyses were carried out by Bui Van Dung, Nguyen Thi Thanh Thuy, and Nguyen Thi Ngoc Anh. The initial draft of the manuscript was prepared by Bui Van Dung. All authors participated in data interpretation, provided critical revisions, and approved the final manuscript for publication.

Availability of data and materials
All data and materials supporting the present study are available upon reasonable request from the corresponding author.

Ethical considerations
The authors confirm that this manuscript is original, has not been published previously, and is not currently under review by any other journal. All authors have reviewed and approved the manuscript, ensuring compliance with ethical standards regarding authorship, research integrity, data accuracy, and publication consent. The authors did not use AI in any part of this study including, conducing the study, preparing data, statistical analysis, and writing the manuscript.

Competing of interests
The authors declared no conflict of interest.

REFERENCES

Abedel-Majed MA, Romereim SM, Davis JS, and Cupp AS (2019). Perturbations in lineage specification of granulosa and theca cells may alter corpus luteum formation and function. Frontiers in Endocrinology, 10: 832. DOI: https://www.doi.org/10.3389/fendo.2019.00832

Baddela VS, Koczan D, Viergutz T, Vernunft A, and Vanselow J (2018). Global gene expression analysis indicates that small luteal cells are involved in extracellular matrix modulation and immune cell recruitment in the bovine corpus luteum. Molecular and Cellular Endocrinology, 474: 201-213. DOI: https://www.doi.org/10.1016/j.mce.2018.03.011

Bao Y, Ma F, Huo C, Jia H, Li Y, Yang X, Liu J, Gu P, Shi C, Gu M et al. (2025). Single-nucleus RNA sequencing and spatial transcriptomics reveal cellular heterogeneity and intercellular communication networks in the hypothalamus-pituitary-ovarian axis of pregnant Mongolian cattle. Animals, 15(15): 2277. DOI: https://www.doi.org/10.3390/ani15152277

Basavaraja R, Drum JN, Sapuleni J, Bibi L, Friedlander G, Kumar S, Sartori R, and Meidan R (2021). Downregulated luteolytic pathways in the transcriptome of early pregnancy bovine corpus luteum are mimicked by interferon-tau *in vitro*. BMC Genomics, 22(1): 452. DOI: https://www.doi.org/10.1186/s12864-021-07747-3

Bender K, Walsh S, Evans AC, Fair T, and Brennan L (2010). Metabolite concentrations in follicular fluid may explain differences in fertility between heifers and lactating cows. Reproduction, 139(6): 1047-1055. DOI: https://www.doi.org/10.1530/REP-10-0068

Bertan CM, Cesar MC, Pugine SMP, Binelli M, Visintin JA, and Assumpção MEO (2006). Indução da ovulação em vacas com gonadotrofina coriônica humana (hCG) purificada por cromatografia de afinidade [Induction of ovulation in cows with affinity chromatography-purified Human Chorionic Gonadotropin (hCG)]. Brazilian Journal of Veterinary Research and Animal Science, 43(3): 379-386. DOI: https://www.doi.org/10.11606/ISSN.1678-4456.BJVRAS.2006.26486

Bishop CV, Selvaraj V, Townson DH, Pate JL, and Wiltbank MC (2022). History, insights, and future perspectives on studies into luteal function in cattle. Journal of animal science, 100(7): skac143. DOI: https://www.doi.org/10.1093/jas/skac143

Bishop CV, Xu F, Molskness TA, Stouffer RL, and Hennebold JD (2015). Dynamics of immune cell types within the macaque corpus luteum during the menstrual cycle: Role of progesterone. Biology of Reproduction, 93(5): 112. DOI: https://www.doi.org/10.1095/biolreprod.115.132753

Diskin MG and Morris DG (2008). Embryonic and early foetal losses in cattle and other ruminants. Reproduction in Domestic Animals, 43(2): 260-267. DOI: https://www.doi.org/10.1111/j.1439-0531.2008.01171.x

Fernandez J, Bruno-Galarraga MM, Cueto MI, Bonadeo N, Notaro U, Soto AT, de la Sota RL, Salvetti NR, Bianchi CP, Cristina C et al. (2024). Changes on corpus luteum structure and progesterone synthesis pathway after hCG or GnRH treatment during the early luteal phase in sheep. Animal Reproduction Science, 265: 107474. DOI: https://www.doi.org/10.1016/j.anireprosci.2024.107474

Gecaj RM, Behluli B, and Youngs CR (2024). Validation of selected microRNA transcriptome data in the bovine corpus luteum during early pregnancy by RT-qPCR. Current Issues in Molecular Biology, 46(7): 6620-6632. DOI: https://www.doi.org/10.3390/cimb46070394

Hryciuk MM, Jewgenow K, and Braun BC (2021). Luteinizing hormone effect on luteal cells is dependent on the corpus luteum stage in felids. Animals, 11(1): 179. DOI: https://www.doi.org/10.3390/ani11010179

Hryciuk MM, Schröter F, Claaßen S, Aurich C, Wauters J, Haße C, and Braun BC (2025). Development of a 3D *in vitro* model to study corpus luteum of felids based on luteinized cells from antral follicles. Cell and Tissue Research, 399(2): 211-229. DOI: https://www.doi.org/10.1007/s00441-024-03937-z

Jiang YF, Tsui KH, Wang PH, Lin CW, Wang JY, Hsu MC, Chen YC, and Chiu CH (2011). Hypoxia regulates cell proliferation and steroidogenesis through protein kinase A signaling in bovine corpus luteum. Animal Reproduction Science, 129(3-4): 152-161. DOI: https://www.doi.org/10.1016/j.anireprosci.2011.12.004

Kisliouk T, Friedman A, Klipper E, Zhou QY, Schams D, Alfaidy N, and Meidan R (2007). Expression pattern of prokineticin 1 and its receptors in bovine ovaries during the estrous cycle: Involvement in corpus luteum regression and follicular atresia. Biology of Reproduction, 76(5): 749-758. DOI: https://www.doi.org/10.1095/biolreprod.106.054734

Magoffin DA (2005). Ovarian theca cell. The International Journal of Biochemistry and Cell Biology, 37(7): 1344-1349. DOI: https://www.doi.org/10.1016/j.biocel.2005.01.016

Maruri A, Anchordoquy JP, Farnetano NA, Flaherti AL, Rosa DE, Balbi M, Lombardo D, Furnus CC, and Anchordoquy JM (2025). Effect of zinc supplementation on bovine luteal function: *In vivo* and *in vitro* findings. Theriogenology, 238: 117365. DOI: https://www.doi.org/10.1016/j.theriogenology.2025.117365

Miyamoto A, Shirasuna K, and Sasahara K (2009). Local regulation of corpus luteum development and regression in the cow: Impact of angiogenic and vasoactive factors. Domestic Animal Endocrinology, 37(3): 159-169. DOI: https://www.doi.org/10.1016/j.domaniend.2009.04.005

Miyamoto Y, Skarzynski DJ, and Okuda K (2000). Is tumor necrosis factor α a trigger for the initiation of endometrial prostaglandin F2α release at luteolysis in cattle?. Biology of Reproduction, 62(5): 1109-1115. DOI: https://www.doi.org/10.1095/biolreprod62.5.1109

Mokhtar DM (2015). Microscopic and histochemical characterization of the bovine uterine tube during the follicular and luteal phases of estrous cycle. Journal of Microscopy and Ultrastructure, 3(1): 44-52. DOI: https://www.doi.org/10.1016/j.jmau.2014.09.002

Neves MM, Marques Jr AP, Santana CV, Lima FPC, and Zambrano WJ (2002). Características de ovários de fêmeas zebu (Bos taurus indicus), colhidos em abatedouros [Characteristics of the ovaries of zebu cows (Bos taurus indicus) collected in slaughterhouses]. Arquivo Brasileiro de Medicina Veterinária e Zootecnia, 54(6): 651-654. DOI: https://www.doi.org/10.1590/S0102-09352002000600016

Plewes MR, Talbott HA, Schott MB, Wood JR, Cupp AS, and Davis JS (2024). Unraveling the role of lipid droplets and perilipin 2 in bovine luteal cells. The FASEB Journal, 38(11): e23710. DOI: https://www.doi.org/10.1096/fj.202400260RR

Ponce-Barajas P, Colazo MG, Behrouzi A, Ree TO, Kastelic JP, and Ambrose DJ (2023). Morphologic, steroidogenic, and transcriptomic assessment of the corpus luteum in Holstein cows after spontaneous or hormone-induced ovulation. Animals, 13(14): 2283. DOI: https://www.doi.org/10.3390/ani13142283

Przygrodzka E, Plewes MR, and Davis JS (2021). Luteinizing hormone regulation of inter-organelle communication and fate of the corpus luteum. International journal of molecular sciences, 22(18): 9972. DOI: https://www.doi.org/10.3390/ijms22189972

Pugliesi G, Guimarães da Silva A, Viana JHM, and Siqueira LGB (2023). Review: Current status of corpus luteum assessment by Doppler ultrasonography to diagnose non-pregnancy and select embryo recipients in cattle. Animal, 17(1): 100752. DOI: https://www.doi.org/10.1016/j.animal.2023.100752

Regan SLP, Knight PG, Yovich JL, Leung Y, Arfuso F, and Dharmarajan A (2018). Granulosa cell apoptosis in the ovarian follicle-A changing view. Frontiers in Endocrinology, 9: 61. DOI: https://www.doi.org/10.3389/fendo.2018.00061

Rękawiecki R and Kotwica J (2008). Involvement of progesterone, oxytocin, and noradrenaline in the molecular regulation of steroidogenesis in the corpus luteum of the cow. Bulletin of the Veterinary Institute in Pulawy, 52(4): 573-580. Available at: https://jvetres.piwet.pulawy.pl/files/archive/20084/20084573580.pdf

Scully DM, Campion D, McCartney F, Dulohery K, Reese S, and Kölle S (2021). Cystic ovary disease impairs transport speed, smooth muscle contraction, and epithelial ion transport in the bovine oviduct. Molecular Reproduction and Development, 88(8): 558-570. DOI: https://www.doi.org/10.1002/mrd.23521

Shah KB, Tripathy S, Suganthi H, and Rudraiah M (2014). Profiling of luteal transcriptome during prostaglandin F2-alpha treatment in buffalo cows: analysis of signaling pathways associated with luteolysis. PLoS One, 9(8): e104127. DOI: https://www.doi.org/10.1371/journal.pone.0104127

Shimizu T (2016). Molecular and cellular mechanisms for the regulation of ovarian follicular function in cows. Journal of Reproduction and Development, 62(4): 323-329. DOI: https://www.doi.org/10.1262/jrd.2016-044

Shirasuna K, Nitta A, Sineenard J, Shimizu T, Bollwein H, and Miyamoto A (2012). Vascular and immune regulation of corpus luteum development, maintenance, and regression in the cow. Domestic Animal Endocrinology, 43(2): 198-211. DOI: https://www.doi.org/10.1016/j.domaniend.2012.03.007

Skarzynski DJ, Ferreira-Dias G, and Okuda K (2008). Regulation of luteal function and corpus luteum regression in cows: hormonal control, immune mechanisms and intercellular communication. Reproduction in Domestic Animals, 43(2): 57-65. DOI: https://www.doi.org/10.1111/j.1439-0531.2008.01143.x

Skarzynski DJ, Piotrowska-Tomala KK, Lukasik K, Galvão A, Farberov S, Zalman Y, and Meidan R (2013). Growth and regression in bovine corpora lutea: regulation by local survival and death pathways. Reproduction in Domestic Animals, 48(1): 25-37. DOI: https://www.doi.org/10.1111/rda.12203

Vasconcelos JLM, Sartori R, Oliveira, HN, Guenther JG, and Wiltbank MC (2001). Reduction in size of the ovulatory follicle reduces subsequent luteal size and pregnancy rate. Theriogenology, 56(2): 307-314. DOI: https://www.doi.org/10.1016/s0093-691x(01)00565-9

Xavier PR, Leão RAC, Oliveira e Silva PVD, and Marques Júnior AP (2012). Histological characteristics of the corpus luteum of Nelore cows in the first, second and third trimester of pregnancy. Arquivo Brasileiro de Medicina Veterinária e Zootecnia, 64 (2): 505-509. DOI: https://www.doi.org/10.1590/S0102-09352012000200036

Yoshioka S, Abe H, Sakumoto R, and Okuda K (2013). Proliferation of luteal steroidogenic cells in cattle. PLoS One, 8(12): e84186. DOI: https://www.doi.org/10.1371/journal.pone.0084186

Zhao Z, Fei G, Miao T, Liu Y, Yang J, Liang Y, Chen H, and Chen S (2025). Structural analysis and core promoter prediction of STAR gene and its regulatory mechanism of progesterone synthesis in bovine luteal cells. Scientific Reports, 15(1): 7746. DOI: https://www.doi.org/10.1038/s41598-025-92446-2

Publisher's note: Scienceline Publication Ltd. remains neutral with regard to jurisdictional claims in published maps and institutional affiliations.

Open Access: This article is licensed under a Creative Commons Attribution 4.0 International License, which permits use, sharing, adaptation, distribution and reproduction in any medium or format, as long as you give appropriate credit to the original author(s) and the source, provide a link to the Creative Commons licence, and indicate if changes were made. The images or other third party material in this article are included in the article's Creative Commons licence, unless indicated otherwise in a credit line to the material. If material is not included in the article's Creative Commons licence and your intended use is not permitted by statutory regulation or exceeds the permitted use, you will need to obtain permission directly from the copyright holder. To view a copy of this licence, visit https://creativecommons.org/licenses/by/4.0/.

© The Author(s) 2025

2025, Scienceline Publication
World's Veterinary Journal
World Vet J, 15(4): 910-920.
ISSN 2322-4568

DOI: https://dx.doi.org/10.54203/scil.2025.wvj92
PII: S232245682500092-15

Effect of Glutathione Supplementation in Liquid Semen Diluent During Cold Storage on Sperm Membrane Structure in Ongole Crossbred Bull

Mohamad Ervandi* **and Talha Dangkua**

Department of Biological Resources Management, Muhammadiyah University of Gorontalo, Gorontalo, Indonesia

*Corresponding author's Email: m.ervandi@umgo.ac.id

ORIGINAL ARTICLE
Received: October 01, 2025
Revised: November 25, 2025
Accepted: December 16, 2025
Published: December 25, 2025

ABSTRACT

Damage to bovine spermatozoa membranes results from factors such as oxidative stress, high temperatures, extreme pH levels, and exposure to chemicals or infections. The present study aimed to explore the potential use of glutathione in liquid semen extenders during cold storage to protect the membrane structure of Peranakan Ongole (PO) crossbred bull semen. Semen samples were collected twice weekly from two PO crossbred bulls aged 2-3 years. Semen that met the quality standards was diluted with a red fruit (*Pandanus conoideus Lamk*) extract extender, supplemented with glutathione at various concentrations per 100 mL of the total volume extender. Sperm membrane evaluation included membrane integrity assessed by the hypoosmotic swelling test (HOST), sperm capacitation, and acrosome reaction assessed by chlortetracycline fluorescence staining. The treatments consisted of red fruit extract extender with 15% egg yolk (P0, control), red fruit extract extender with 15% egg yolk and 0.75 mM glutathione (P1), red fruit extract extender with 15% egg yolk and 1 mM glutathione (P2), and red fruit extract extender with 15% egg yolk plus 1.25 mM glutathione (P3). The present results indicated that Group P1 performed superior than other treatment groups. This was evidenced by higher spermatozoa membrane integrity and a higher proportion of non-capacitated spermatozoa, while the proportions of capacitated spermatozoa and acrosome reaction remained low. The extender formulation containing red fruit extract, 15% egg yolk, and 0.75 mM glutathione-maintained acrosome status above 50% after six days of cold storage. Therefore, the combination of red fruit extract, 15% egg yolk, and 0.75 mM glutathione was identified as the optimal formulation for liquid semen preservation, meeting the necessary conditions for practical use in artificial insemination programs in the field.

Keywords: Acrosome reaction, Glutathione, Membrane integrity, Red fruit extract

INTRODUCTION

Increasing the population and productivity of local cattle can be achieved through reproductive technologies, such as artificial insemination (AI). Artificial insemination is a reproductive technology introduced to commercial breeders to improve the genetic quality of livestock and increase beef production (Ervandi et al., 2020). The success of AI is influenced by the quality of semen produced by the cattle (Yekti et al., 2017). Semen quality can decrease during cryopreservation (preservation/storage) due to thermal cold shock, mechanical formation of intracellular ice crystals, chemical factors (diluent components), and osmotic stress (Khan et al., 2021). Semen diluents are essential for reducing the risk of decreased semen quality during processing and post-processing (Dzulqarnain et al., 2022). Commercial diluents are considered more practical as diluents (Ervandi et al., 2023). Previous studies have identified several diluents for liquid semen, using natural ingredients such as coconut water, carrot juice, tomato juice, egg yolk, honey, and guava filtrate (Sumadiasa et al., 2015; Malik et al., 2018; Astuti, 2018; Marawali et al., 2019). However, the resulting semen quality typically lasts for three to four days.

Based on previous studies, alternative natural liquid semen diluents, such as a combination of red fruit extract and coconut water, have not been able to maintain semen quality for long periods and are ineffective at protecting sperm membranes at low temperatures. Consequently, the quality and fertility of liquid semen decline with increasing storage time, partly due to the accumulation of excessive free radicals (Ervandi et al., 2023). Excessive free radicals can damage the sperm plasma membrane (Agung et al., 2023). During this process, spermatozoa undergo peroxidation, which generates free radicals, such as hydroxyl (-OH) and singlet oxygen ($^1O_2$; Bansal and Bilaspuri 2011; Park and Yu 2017). These radicals are highly reactive and potentially induce lipid peroxidation in the plasma and acrosome membranes (Douard et al., 2003). Lipid oxidation in the plasma membrane produces malondialdehyde (MDA), a marker of toxic free radicals, which reduces motility and causes DNA damage (Dutta et al., 2019). Wijayanti et al. (2023) indicated that the initial reactions of free radicals, if left uncontrolled, may initiate a continuous process that could potentially impair most

To cite this paper: Ervandi M and Dangkua T (2025). Effect of Glutathione Supplementation in Liquid Semen Diluent During Cold Storage on Sperm Membrane Structure in Ongole Crossbred Bull. *World Vet. J.,* 15(4): 910-920. DOI: https://dx.doi.org/10.54203/scil.2025.wvj92

or all of the spermatozoa plasma membrane. Therefore, the urgency of the present study highlighted the necessity of developing effective methods to preserve the quality of liquid semen at low temperatures by incorporating antioxidants into the semen extender, such as vitamin E, catalase enzyme, and glutathione, which have been identified to preserve semen quality (Telnoni et al., 2023). Although both compounds exhibited considerable antioxidant capacity, for instance, vitamin E has limited water solubility, resulting in uneven distribution within the semen extender. The catalase enzyme, being a large protein, is susceptible to denaturation at extreme temperatures during freezing and semen storage (Câmara et al., 2016; Ahmad et al., 2021; Wadhwa et al., 2024). As an alternative, glutathione, an endogenous antioxidant, exhibits promising potential for use in semen extenders (Ahmad et al., 2021). Glutathione is a primary antioxidant that prevents the formation of new free radicals (Ansari et al., 2021). Glutathione plays a crucial role in the cellular biochemical system as a primary antioxidant, detoxifying agent, and vital regulator of redox signaling. Its function is essential for maintaining cellular oxidation and reduction balance, supporting mitochondrial function, and preserving protein structural stability, particularly through the S-glutathionylation mechanism. The biological functions of glutathione are carried out by several specific enzymes, such as glutathione peroxidase, glutathione reductase, and glutaredoxin, which collectively contribute to the regulation of oxidation and reduction homeostasis and the response to oxidative stress (Carriço et al., 2023; Chai and Mieyal, 2023; Chen et al., 2024). Munsi et al. (2007) reported that glutathione added to semen extenders significantly increases sperm motility and reduces acrosomal damage in bull semen stored at low temperatures. Antioxidants are compounds that can slow or prevent damage to the spermatozoa plasma membrane caused by free radicals by counteracting free radical activity or breaking the chain of oxidation reactions caused by free radicals (Zou et al., 2021). Solihati et al. (2018) and Zou et al. (2021) suggested that the use of glutathione in dilution media is expected to reduce the emergence of free radicals that can damage the plasma membrane. Adding glutathione or enhancing related enzymatic activities in liquid semen extenders has been shown to improve sperm viability and motility after dilution, reduce oxidative damage to sperm membranes and DNA, and extend the shelf life of liquid semen (Zhu et al., 2023).

Damage to the bovine spermatozoa membrane can result from different factors, including oxidative stress, high temperature, extreme pH, and exposure to chemicals or infections (Younus et al., 2024). Membrane damage affects the integrity of the spermatozoa membrane, which can alter its ion system (Xue et al., 2025). Disruption of calcium ion transport across the cell membrane results in elevated intracellular calcium levels, which can induce capacitation and the acrosome reaction in spermatozoa (Maleki et al., 2023). Additionally, oxidative stress plays a crucial role in membrane damage by altering lipid components in the plasma membrane, altering membrane fluidity, and disrupting its functional integrity (Solihati et al., 2018). Xue et al. (2025) indicated that damage to the spermatozoa membrane may impair their ability to reach the oocyte, potentially leading to fertilization failure. Therefore, during the assessment of the quality of liquid semen from Peranakan Ongole (PO) crossbred bulls, the membrane structure parameter is an essential aspect to observe, as the membrane structure test can evaluate the permeability of the plasma membrane in maintaining spermatozoa physiology. Additionally, the intact acrosome membrane (IAM) cap test assesses the potential of spermatozoa to penetrate the zona pellucida during fertilization, through the acrosome reaction (Susilawati, 2011). Therefore, the present study aimed to determine the structure of the semen membrane of PO bulls after glutathione supplementation in liquid semen diluent during cold storage.

MATERIALS AND METHODS

Ethics approval

Ethics approval has been granted by the Ethics Committee of the Faculty of Science and Technology, Muhammadiyah University of Gorontalo, Gorontalo, Indonesia, in accordance with ethical guidelines regarding responsible behavior in the use of Ongole crossbred (PO) bulls in animal research. Ethics approval number is 081/FST-UMGO/V/2024.

Materials and equipment

The bovine semen was collected from two PO bulls aged approximately two to three years old at the Integrated Field Laboratory, Muhammadiyah University of Gorontalo, Indonesia. The semen used met the criteria of mass motility ≥++ and individual motility ≥ 70%, collected twice weekly using the artificial vagina method, and included ingredients, such as red fruit extract extender, egg yolk, glutathione, Diazabicyclooctane (DABCO) solution, Chlortetracycline (CTC) staining fixative solution, CTC staining dye solution, aluminum foil, fructose, penicillin, aqua bidestilata, 70% alcohol, 3% NaCl, and eosin-nigrosin. The equipment utilized included Olympus CX23 multimedia (Olympus corporation, Japan) microscope, epifluorescence microscope OPTIPHOT-2 using a UV-2A filter (Nikon Corporation, United Kingdom), centrifuge LC-8 C3100 (Benchmark Scientific Corporation, USA), cover slips, microscope slides,

thermometer, heater, pH indicator, water bath, magnetic stirrer, hemocytometer, refrigerator, Eppendorf tube, analytical balance, scissors, micropipettes, blue tips, yellow tips, Erlenmeyer flasks, test tubes, glass beakers, and glass stirrers.

Semen evaluation

The collected semen from a single male was subjected to both macroscopic and microscopic examinations. The macroscopic examination involved assessing volume, pH, consistency/viscosity, color, and odor. Sperm quality, including mass motility, individual motility, spermatozoa concentration, abnormalities, membrane integrity, and acrosome status, was evaluated microscopically using an Olympus CX23 microscope at 400× magnification (Susilawati 2011).

Liquid semen diluent with red fruit extract

The red fruit extract diluent was weighed (100 g), added to 300 mL of distilled water, blended for 5 minutes, and then left to settle for 2.5 hours. Afterward, the mixture was filtered using a filter cloth. This filtering process was repeated twice. The second filtering process used filter paper to obtain the red fruit extract. Then, fructose at 10 and 20 mg/mL, penicillin antibiotic at 1 mg/mL, sorbitol at 1000 µg/L, streptomycin sulfate at 1 mg/mL, and gentamicin at 0.05 µg/mL were added. After the red fruit extract diluent was prepared, egg yolk was added for subsequent use as a membrane protector. Egg yolk (15%) was added to the red fruit extract diluent (85%) to obtain a final extender concentration of 100%. The mixture was stirred for 30 minutes, then centrifuged at 1500 rpm for 30 minutes. Red fruit extract diluent supplemented with 15% egg yolk was stored at 3-5°C in a refrigerator. Subsequently, the mixture was prepared for use in the following stages of the study (Ervandi et al., 2023). For the test group, glutathione was added to the red fruit extract extender diluent at different concentrations according to treatments (Maleki et al., 2023).

Storage duration

Following dilution, semen samples were aliquoted into test tubes based on the assigned storage duration treatments. The tubes were placed in a test tube rack and stored at 5°C in a refrigerator. At each designated storage interval, semen samples were assessed for sperm motility, viability, abnormality, and membrane integrity (Syarifuddin et al., 2012).

Semen preservation process

Semen samples that were diluted with an extender and stored in a refrigerator at 5°C for several days were then evaluated for mass motility, individual motility, sperm concentration, abnormalities, membrane integrity, and acrosome status (Swarna et al., 2023).

Study design

The present study employed a randomized block design (RBD) with four replicates and 10 replications. Grouping was based on different semen collection times. The treatments included red fruit extract extender with 15% egg yolk (P0, control), red fruit extract extender with 15% egg yolk and 0.75 mM glutathione (P1), red fruit extract extender with 15% egg yolk and 1 mM glutathione (P2), and red fruit extract extender plus 15% egg yolk plus 1.25 mM glutathione (P3).

Sperm membrane integrity examination

Membrane integrity observation

Sperm cell membrane integrity was tested using the hypoosmotic swelling test (HOST). One milliliter of a hypoosmotic solution at 125 Osm/L, which was made from 0.31 g of sodium citrate and 0.565 g of fructose, dissolved in 50 mL of distilled water, was added to 100 µl of spermatozoa. The solution was then incubated at 37°C for 30 minutes. A smear was then prepared and observed under a light microscope (Olympus CX23 Multimedia, Japan) at ×400 magnification. Coiled or swollen tails characterized spermatozoa with IPM, while damaged ones exhibited straight tails (Susilawati 2011). Purnawan et al. (2023) stated that sperm quality analysis, including the assessment of plasma membrane integrity, was conducted by examining at least 200 cells per sample to ensure statistical reliability and a representative evaluation of the sperm population. Krishna et al. (2024) stated that the membrane integrity value of spermatozoa can be calculated using the following formula.

Membrane integrity (%) = (number of spermatozoa with intact plasma membranes / total number of spermatozoa observed) × 100

(Formula 1)

Observing sperm capacitation and the acrosome reaction

The capacitation of fresh spermatozoa can be observed using CTC staining. The CTC staining involves three final reagents, including DABCO solution, CTC fixative solution, and CTC dye solution. The procedure was performed

according to Susilawati (2011) with the following modifications. A total of 100 µL of semen (fresh and treated) was placed in an Eppendorf tube covered with aluminium foil, then 100 µL of CTC dye was added and vortexed for one minute. Then, 8 µL of CTC fixative was added, and the mixture was vortexed for one minute to homogenize. Then, 10 µL of the solution was taken and placed on a glass slide. Subsequently, 10 µL of DABCO was added, and the combination was carefully mixed. The slide was then covered with a coverslip, then covered with thick tissue paper and pressed carefully. The edges of the coverslip were sealed with nail polish, and the coverslip was placed in a water bath at 37°C. The mixture was left for approximately three minutes (Susilawati, 2011). Observations were conducted utilizing an Epifluorescence microscope OPTIPHOT-2 equipped with a UV-2A filter, examining 100 spermatozoa from a single field of view slide (Susilawati, 2011; Ervandi et al., 2013). The CTC staining results indicated that spermatozoa with completely bright-stained heads were non-capacitated. Conversely, bright staining on the upper part of the head indicated sperm capacitation (Krishna et al., 2024).

Statistical analysis

The current data were first transformed and subsequently analyzed using Analysis of Variance (ANOVA) to evaluate differences among treatments, followed by Duncan's post hoc test. A significance level of $p < 0.05$ was considered statistically significant, while $p < 0.01$ was regarded as highly significant (Sudarwati et al., 2019).

RESULTS AND DISCUSSIONS

Characteristics of fresh semen from Ongole crossbred

The fresh semen from Ongole crossbred bulls used in the present study had a motility of above 70%. The quality and macroscopic examination of the collected fresh semen samples are presented in Table 1.

Macroscopic examination of fresh semen is shown in Table 1. The average semen volume of Ongole crossbred bulls was 6.14 ± 1.16 mL, which was higher than the results of Yekti et al. (2017) and Mila et al. (2021), which were 4.17 ± 1.17 mL and 4.6 ± 1.51 mL, respectively. Suyadi et al. (2020) reported that the volume of semen in PO bulls in each ejaculation ranged from 5 to 10 mL, and the semen color was cream, which was regarded as an acceptable finding. Susilawati (2013) stated that normal semen is yellowish-white (cream) or milky-white, and the degree of turbidity depends on spermatozoa concentration. The degree of acidity (pH) in Ongole crossbred bulls' semen was 6.40 ± 0.10, lower than the findings of Yekti et al. (2017) and Dzulqarnain et al. (2022) at 6.63 ± 0.08 and 6.42 ± 0.23, respectively. The fresh semen from the Ongole crossbred bulls had a thick consistency. Ismaya (2014) indicated that semen consistency can be assessed by gently shaking the tube containing the semen, indicating a sperm concentration of 1,000 to 2,000 million/mL. The optimal pH of bovine semen ranges from 6.45 to 6.57, with a concentration of 1223.7 to 1961.8 million spermatozoa per milliliter, and the ideal individual motility is around 70%, along with a mass movement rating of 2+ (Arif et al., 2020; Wadhwa et al., 2024; Xue et al., 2025). The mass motility of Ongole crossbred bulls in the present study was 2+, while the individual motility was 76.40 ± 2.54. These findings are higher than those reported by Yekti et al. (2017) for Ongole bulls, with a value of 71.67 ± 2.58. The fresh Ongole bull semen demonstrated high quality, with both viability and abnormality percentages within the normal range. The current results align with the findings of Suyadi et al. (2014; 2020), who reported that fresh semen from Ongole bull can achieve up to 80% viability and maintain an average abnormality rate of 12-18% when stored under optimal conditions. The fresh semen samples from PO bulls exhibited characteristics that complied with the quality requirements for further processing.

Table 1. Fresh semen quality from Ongole crossbred bull

Parameters	Average ± Standard deviation
Macroscopic	
Volume (ml)	6.14 ± 1.16
pH	6.40 ± 0.10
Scent	Distinctives
Consistency	Thick
Color	Cream
Microscopic	
Individual motility (%)	76.40 ± 2.54
Viability (%)	92.10 ± 2.05
Abnormality (%)	2.81 ± 0.33
Sperm concentration (10^7/ml)	1351.09 ± 16.70
Mass motility	2+

Individual motility of Ongole crossbred semen

The average individual motility of PO bulls' semen after treatment is presented in Table 2. The individual motility of PO bulls demonstrated the highest durability in diluents P1 and P2, lasting up to six days with values of 44.21 ± 1.19% and 40.36 ± 1.32%, respectively, compared to P0 and P3. The present results indicated a significant difference ($p < 0.01$) in the individual motility of PO bulls on days six to eight of storage. The Least Duncan's post hoc test indicated that the P1 and P2 diluent treatments yielded the best results, with values of 44.21 ± 1.19% and 40.36 ± 1.32%, respectively, during the six days of storage. Red fruit extract diluent with 15% egg yolk supplemented with 0.75 mM glutathione (P1) demonstrated superior results compared to P0 (control), P2, and P3. This is attributable to the composition of P1, which maintains an optimal balance between antioxidant effects and sperm quality stability. Glutathione at 0.75 mM effectively improved protection of sperm cell membranes from oxidative damage without inducing osmotic stress or disrupting the redox equilibrium, concerns typically associated with higher glutathione concentrations, such as in 1 mM (P2) and 1.25 mM (P3).

Table 2. Mean motility of individual Ongole crossbred bulls with various levels of glutathione diluent during cold storage

Treatment	Mean motility (%) ± Standard deviation								
	D-1	D-2	D-3	D-4	D-5	D-6	D-7	D-8	D-9
P0 (RFE plus 15% EY)	70.31 ± 1.38^{a}	60.15± 1.29^{a}	58.76 ± 1.20^{a}	45.11 ± 0.19^{a}	40.14 ± 0.17^{a}	39.10 ± 0.15^{b}	35.16 ± 1.11^{b}	18.51 ± 1.10^{b}	14.20 ± 0.12^{a}
P1 (RFE plus 15% EY plus 0.75 mM GSH)	70.34 ± 1.14^{a}	69.16 ± 1.32^{a}	65.17 ± 1.24^{a}	60.57 ± 1.28^{a}	55.19 ± 1.20^{a}	44.21 ± 1.19^{a}	38.29 ± 1.11^{a}	23.41 ± 0.09^{a}	19.21± 0.00^{a}
P2 (RFE plus 15% EY plus 1 mM GSH)	66.13 ± 1.31^{a}	60.54 ± 1.56^{a}	50.32 ± 1.48^{a}	48.14 ± 1.33^{a}	45.26 ± 1.20^{a}	40.36 ± 1.32^{a}	24.78 ± 0.20^{b}	15.28 ± 0.10^{b}	08.32 ± 0.00^{b}
P3 (RFE plus 15% EY plus 1.25 mM GSH)	60.41 ± 1.31^{a}	50.12 ± 1.27^{a}	43.11 ± 1.24^{a}	40.61 ± 1.16^{a}	38.17 ± 1.17^{a}	30.28 ± 0.10^{c}	21.19 ± 0.08^{c}	09.51± 0.04^{c}	06.10± 0.00^{b}

P: Treatment, D: Storage days, ^{abcd} Means with different superscripts within the same column indicate highly significant differences ($p < 0.01$), (P0): Red fruit extract extender plus 15% egg yolk, (P1): Red fruit extract extender plus 15% egg yolk plus 0.75 mM glutathione, (P2): Red fruit extract extender plus 15% egg yolk plus 1 mM glutathione, (P3): Red fruit extract extender plus 15% egg yolk plus 1.25 mM glutathione.

The current results were similar to those of Agung et al. (2023), in which the addition of 0.75 mM and 1 mM glutathione resulted in higher responses in Limousin cattle. Fitri et al. (2025) indicated that adding glutathione at a concentration of 1 mM notably increased the progressive motility of spermatozoa during semen storage at 4°C. In comparison to the study conducted by Carriço et al. (2023), administering 1 mM glutathione exhibited a more considerable reduction in oxidative stress than 0.75 mM, suggesting potential advantages for improving liquid semen quality over a longer period. The differences in these results were likely attributable to several factors, including different cattle breeds that may influence physiological responses to glutathione supplementation, the composition of the semen extender, which affects membrane stability and enhances antioxidant efficacy, and semen storage conditions that can impact spermatozoa metabolism (Ansari et al., 2021; Agung et al., 2023). Red fruit extract functions as a natural source of antioxidants, egg yolk serves as both a physical protector and a nutrient provider that maintains spermatozoa membrane stability, while glutathione enhances the internal antioxidant defense system of spermatozoa and preserves mitochondrial function to support motility and viability (Ervandi et al., 2023; Chen et al., 2024). Carriço et al. (2023) reported that glutathione supplementation in diluents functions as an antioxidant, protecting cells from oxidative damage and supporting detoxification. Ogata et al. (2022) reported that adding glutathione reduces the level of lipid peroxidation and helps maintain the stability of semen membranes during storage of liquid semen at 4°C. This plays an important role in maintaining the morphological integrity of semen, especially during long-term liquid storage. Solihati et al. (2018) and Zou et al. (2021) suggested that the use of glutathione in dilution media is expected to reduce the emergence of free radicals that can damage the plasma membrane. Shah et al. (2017) indicated that glutathione helps sustain the survival of cattle spermatozoa by inhibiting apoptosis and cryocapitation pathways, thereby protecting spermatozoa from the adverse effects of cryopreservation on semen. In addition, Khan et al. (2021) demonstrated that glutathione supplementation in liquid bovine semen considerably reduced DNA fragmentation. Biological variations among cattle breeds, such as sperm cell size, enzyme levels, and sensitivity to oxidative stress and temperature changes, also affect the spermatozoa's ability to survive during storage. Berry et al. (2019) found that genetic variation among cattle breeds contributes to significant differences in semen quality, including volume and spermatozoa viability. Krishna et al. (2024) reported that antioxidant enzyme activities, such as superoxide dismutase and catalase, play a crucial role in maintaining semen quality; decreased activity of these enzymes leads to increased oxidative damage to spermatozoa.

The current results indicated that motility persisted until the five days of semen storage with P0 treatment, followed by P3 treatment. This was likely due to the toxic effects of excessive antioxidant accumulation in liquid semen storage media. The findings of Agung et al. (2023) indicated that glutathione concentrations higher than 1 mM may disrupt the spermatozoa reduction system, leading to decreased spermatozoa motility and viability in cattle. This imbalance can indirectly cause an increase in reactive oxygen species production and exacerbate spermatozoa damage. Carriço et al. (2023) reported that supplementation with glutathione at concentrations exceeding 2 mM results in a progressive decline in sperm motility, accompanied by increased spermatozoa mortality in cattle. The administration of glutathione at high concentrations has been demonstrated to induce morphological abnormalities in the head and tail regions of bovine spermatozoa (Zou et al., 2021). This effect is associated with alterations in the plasma membrane of spermatozoa resulting from an imbalance of glutathione in the semen storage environment. Semen quality supplemented with glutathione at concentrations above 1.5 mM exhibited reduced ability to penetrate oocytes, resulting in lower fertilization success rates in AI programs in cattle (Triwulaninngsih et al., 2003).

Sperm membrane integrity

The mean membrane integrity of PO bulls' spermatozoa after storage, measured on the first day and across six days at 50°C, is shown in Table 3. The present results indicated that the treatment of glutathione level supplementation in liquid semen diluent had a very significant effect ($p < 0.01$) on the percentage of membrane integrity of PO bulls' spermatozoa after six days of cold storage. The highest membrane integrity was observed in the P1 and P2 diluent treatments, with average values of 68.10 ± 0.02% and 60.12 ± 0.04%, respectively, compared to the P0 and P3 treatments. Additionally, the current results demonstrated a very significant difference ($p < 0.01$) in the membrane integrity of PO bulls on the sixth day of semen storage. Duncan's post hoc test demonstrated that the P1 and P2 diluent treatments produced the best results after six days of storage.

Table 3. Mean of sperm membrane integrity after preservation at 5°C

Treatment	Mean spermatozoa membrane integrity (%) ± Standard deviation		
	Fresh	D-1	D-6
P0 (RFE plus 15% EY)	88.16 ± 1.40^{a}	70.18 ± 1.13^{c}	49.16 ± 0.06^{c}
P1 (RFE plus 15% EY plus 0.75 mM GSH)	88.16 ± 1.40^{a}	85.02 ± 0.06^{a}	68.10 ± 0.02^{a}
P2 (RFE plus 15% EY plus 1 mM GSH)	88.16 ± 1.40^{a}	80.12 ± 1.08^{b}	60.12 ± 0.04^{b}
P3 (RFE plus 15% EY plus 1.25 mM GSH)	88.16 ± 1.40^{a}	63.13 ± 1.17^{d}	40.10 ± 0.07^{d}

P: Treatment, D: Storage days, ^{abcd} Means with different superscripts within the same column indicate highly significant differences ($p < 0.01$), (P0): Red fruit extract extender plus 15% egg yolk, (P1): Red fruit extract extender plus 15% egg yolk plus 0.75 mM glutathione, (P2): Red fruit extract extender plus 15% egg yolk plus 1 mM glutathione, (P3): Red fruit extract extender plus 15% egg yolk plus 1.25 mM glutathione.

The present results were similar to those of Fitri et al. (2025), who found that adding 0.75 mM glutathione to the cattle semen freezing medium had a significant positive effect on semen quality parameters, including motility, cell membrane integrity, and a decrease in the level of oxidative damage to spermatozoa. A dose of 0.75 mM can offer optimal protection for semen quality during cryopreservation (Zou et al., 2021), likely attributable to the glutathione antioxidant properties, which can mitigate or prevent damage to the sperm plasma membrane caused by free radicals. The combination of red fruit extract, abundant in natural antioxidants such as β-carotene and tocopherol, effectively scavenges free radicals. Egg yolk acts as a membrane protector owing to its rich phospholipid and lipoprotein composition, while glutathione plays a pivotal role in maintaining intracellular redox homeostasis and enhancing the endogenous antioxidant defense system (Solihati et al., 2018; Ervandi et al., 2023; Chen et al., 2024). The addition of 0.75 mM glutathione has been shown to reduce lipid peroxidation, preserve membrane integrity, and enhance the motility of bovine spermatozoa following storage (Ducha et al., 2024). A glutathione dose of 0.75 mM is generally considered optimal, as it provides adequate protection for semen without inducing adverse effects (Fitri et al., 2025). Using lower or higher doses might not achieve the expected membrane protection and semen motility improvements after refrigeration. Carriço et al. (2023) demonstrated that supplementation with 1 mM glutathione in bovine semen extenders can enhance sperm membrane integrity.

Red fruit extract contains α-tocopherol, β-carotene, oleic acid, linoleic acid, linolenic acid, vitamin C, calcium, phosphorus, and iron (Tethool et al., 2021). A formulation of red fruit extract with 15% egg yolk and 0.75 mM glutathione could maintain membrane integrity in PO bull's spermatozoa during six days of storage. This was likely attributable to the red fruit containing tocopherol and β-carotene, which protected spermatozoa cells from morphological damage, while glutathione functioned as an antioxidant capable of protecting the membrane of PO bull's spermatozoa. A combination of antioxidants, namely tocopherol and β-carotene, can complement each other in maintaining the oxidative status of spermatozoa. Tocopherol and β-carotene functioned as external antioxidants from the extender, whereas glutathione served as an internal antioxidant in the sperm cells. This combination of antioxidants could improve post-

thaw semen quality, including sperm motility and structural integrity, as well as enhance *in vitro* fertilization outcomes (Luo et al., 2022). Solihati et al. (2018) and Zou et al. (2021) applied glutathione in the dilution medium, which was expected to reduce the emergence of free radicals that could damage the plasma membrane. Antioxidants, such as glutathione, which can reduce oxidative damage, are crucial in preserving bovine semen (Fitri et al., 2025).

Sperm acrosome status

The average percentage of PO bulls' sperm acrosome status after storage for one to six days at a temperature of 5°C is shown in Table 4. The current results indicated that supplementing glutathione levels in semen diluent had a highly significant effect ($p < 0.01$) on the percentage of non-capacity of PO bulls' spermatozoa after six days of cold storage. The highest non-capacity was observed in the P1 and P2 treatments, with average values of 73.11 ± 0.05% and 65.19 ± 0.09%, respectively, compared to the P0 and P3 treatments. Additionally, the current results indicated a very significant difference ($p < 0.01$) in the non-capacity of PO bulls until the sixth day of semen storage. Duncan's post hoc test demonstrated the highest results for the P1 and P2 treatments after six days of storage.

Table 4. Mean of non-capacity after preservation at 5°C

Treatment	Mean of non-capacity (%) ± Standard deviation		
	Fresh	D-1	D-6
P0 (RFE plus 15% EY)	82.24 ± 1.30^{a}	70.30 ± 1.13^{c}	57.16 ± 0.15^{c}
P1 (RFE plus 15% EY plus 0.75 mM GSH)	82.24 ± 1.30^{a}	83.13 ± 1.03^{a}	73.11 ± 0.05^{a}
P2 (RFE plus 15% EY plus 1 mM GSH)	82.24 ± 1.30^{a}	73.20 ± 1.08^{b}	65.19 ± 0.09^{b}
P3 (RFE plus 15% EY plus 1.25 mM GSH)	82.24 ± 1.30^{a}	67.12 ± 1.20^{d}	51.20 ± 0.14^{d}

P: Treatment, D: Storage days, ^{abcd} Means with different superscripts within the same column indicate highly significant differences ($p < 0.01$), (P0): Red fruit extract extender plus 15% egg yolk, (P1): Red fruit extract extender plus 15% egg yolk plus 0.75 mM glutathione, (P2): Red fruit extract extender plus 15% egg yolk plus 1 mM glutathione, (P3): Red fruit extract extender plus 15% egg yolk plus 1.25 mM glutathione.

The current findings were similar to those of Fitri et al. (2025), who indicated that supplementing cattle semen freezing medium with 0.75 mM glutathione significantly improved semen quality, enhancing motility, cell membrane integrity, and reducing oxidative damage to spermatozoa. A dose of 0.75 mM provided optimal protection for semen quality during cryopreservation, with the best results observed for the P1 and P2 treatments, maintaining above 60% viability on the sixth day (Zou et al., 2021). These findings were likely due to the relatively high capacitation of PO bulls' spermatozoa, indicating that the spermatozoa had intact membranes, indicating that calcium ions were evenly distributed in the spermatozoa head. This condition was influenced by membrane cholesterol, indicating that the semen used in the present study was suitable for use in AI procedures in the field (Ervandi et al., 2020). Gualtieri et al. (2010) noted that reducing spermatozoa membrane cholesterol leads to increased permeability to calcium and bicarbonate, thereby helping to decrease spermatozoa that have not undergone capacitation. The contents of tocopherol, β-carotene, and ascorbic acid in red fruit extract, which also contains glucose, protein, fat, vitamin C, antioxidants, and glutathione, can strengthen the internal antioxidant defense system of spermatozoa and preserve mitochondrial function, thereby protecting the morphology of PO bulls' spermatozoa from damage (Suyadi et al., 2020; Ervandi et al., 2023). The content of red fruit, such as tocopherol, carotenoids, and β-carotene, can influence abnormalities that occur in spermatozoa (Tethool et al., 2021). The optimal dose of 0.75 mM glutathione improved sperm capacitation and fertilizing ability by enhancing motility and acrosome function (Fitri et al., 2025). Glutathione supplementation can help reduce oxidative damage to spermatozoa stored at low temperatures, such as 5°C, and improve semen quality after thawing (Izanloo et al., 2021).

The current findings indicated that the red fruit extract formulation with 15% egg yolk and 0.75 mM glutathione had a very significant effect ($p < 0.01$) on the percentage of PO bulls' spermatozoa capacitation after six days of cold storage, as shown in Table 5.

Table 5. Mean of capacitance after preservation at 5°C

Treatment	Mean of non-capacity (%) ± Standard deviation		
	Fresh	D-1	D-6
P0 (RFE plus 15% EY)	10.06 ± 1.31^{a}	11.52 ± 1.40^{c}	36.13 ± 0.23^{c}
P1 (RFE plus 15% EY plus 0.75 mM GSH)	10.06 ± 1.31^{a}	11.09 ± 1.10^{a}	13.10 ± 0.09^{a}
P2 (RFE plus 15% EY plus 1 mM GSH)	10.06 ± 1.31^{a}	11.17 ± 1.33^{b}	21.62 ± 0.10^{b}
P3 (RFE plus 15% EY plus 1.25 mM GSH)	10.06 ± 1.31^{a}	11.62 ± 1.52^{d}	55.10 ± 0.12^{d}

P: Treatment, D: Storage days, ^{abcd} Means with different superscripts within the same column indicate highly significant differences ($p < 0.01$), (P0): Red fruit extract extender lus 15% egg yolk, (P1): Red fruit extract extender plus 15% egg yolk plus 0.75 mM glutathione, (P2): Red fruit extract extender plus 15% egg yolk plus 1 mM glutathione, (P3): Red fruit extract extender plus 15% egg yolk plus 1.25 mM glutathione.

The Least Duncan's post hoc test indicated the best results for the P1 and P2 diluent treatments after a storage period of 6 days. The present results were similar to those of Fitri et al. (2025), who found that adding 0.75 mM glutathione to the cattle semen freezing medium had a significant positive effect on semen quality parameters, including motility, cell membrane integrity, and a decrease in oxidative damage to spermatozoa. A dose of 0.75 mM can provide optimal protection for semen quality during cryopreservation (Zou et al., 2021). Obtained the best observation results of P1 diluent treatment with a storage period of 6 days below 20%. The present results indicated that the red fruit extract with 15% egg yolk plus 0.75 mM glutathione (P1) was significantly different from the P0, P2, and P3 treatments. Consistent with the findings of Fitri et al. (2025), glutathione at 0.75 mM was shown to effectively protect spermatozoa from oxidative stress and enhance capacitation efficiency. Red fruit extract acts as a natural protector due to its antioxidant content, egg yolk supplies energy and helps maintain membrane stability in spermatozoa, and glutathione protects spermatozoa from oxidative stress (Ervandi et al., 2023). Zou et al. (2021) reported that glutathione at a concentration of 0.75 mM is effective in enhancing the quality of bovine semen during capacitation and in preventing oxidative damage to the sperm membrane. It was found that glutathione at a concentration of 0.75 mM can improve the quality parameters of bovine spermatozoa, including motility, viability, and membrane integrity (Fitri et al., 2025). Capacitation can be triggered by various factors, including changes in pH, calcium ion levels, and the formation of reactive oxygen species (Tethool et al., 2021). During the capacitation process, changes occur in the spermatozoon's plasma membrane, such as a decrease in plasma membrane proteins and changes in ionic permeability that enable the spermatozoon to undergo the acrosome reaction necessary to penetrate the ovum (Beltrán et al., 2016). Some of the key changes that occur during capacitation include alternation in spermatozoa membrane proteins, increased ionic permeability, and enzyme activation that enables the acrosome reaction to occur (Hitit et al., 2020).

The present findings demonstrated that the application of red fruit extract combined with 15% egg yolk and 0.75 mM glutathione had a very significant effect ($p < 0.01$) on the acrosome reaction variable in PO bulls during storage days one to six. The Least Duncan's post hoc test revealed that P1 treatment was significantly different from the P1, P2, and P3 treatments. This finding was probably attributable to the low percentage of acrosome reactions observed in each diluent treatment, suggesting that there was no significant spermatozoa damage exceeding 50%, which could adversely affect the fertility potential of PO bulls' semen. Hitit et al. (2020) indicated that spermatozoa lose their fertility when the acrosome is damaged by more than 50%. According to Muhammad et al. (2019), damage to the acrosomal membrane impairs its protective role, which is critical for spermatozoa function. The observed differences among treatments were likely due to their influence on the sperm plasma membrane, which protected the underlying acrosome. The integrity of this membrane in PO bull spermatozoa is highly dependent on its cholesterol content, which the treatments appeared to have modulated. The high cholesterol content in the membrane makes it more flexible, and when cholesterol is low in the membrane, it causes spermatozoa to be easily damaged (Muhammad et al., 2019). Adding glutathione at a concentration of 0.75 mM significantly improves spermatozoa quality, including accelerating the acrosome reaction (Ducha et al., 2024). Added glutathione to semen thinners plays an important role in maintaining the stability of spermatozoa membranes and improving acrosome function (Wadhwa et al., 2024). Glutathione can affect the acrosome reaction in cattle by increasing the ability of spermatozoa to penetrate the zona pellucida of oocytes (Ahmad et al., 2021).

CONCLUSION

Red fruit extract with 15% egg yolk and 0.75 mM glutathione diluent demonstrated superior results compared to other diluent treatments. These findings were indicated by spermatozoa that maintained membrane integrity and had not undergone capacitation, remaining elevated, while spermatozoa that had undergone capacitation and acrosome reaction remained low. The diluent formulation of red fruit extract with 15% egg yolk and 0.75 mM glutathione was able to maintain acrosome status above 50% after six days of cold storage. Therefore, the combination of red fruit extract, 15% egg yolk, and 0.75 mM glutathione was identified as the optimal formulation for liquid semen preservation, meeting the required standards for practical application in AI programs in the field. Furthermore, future studies should be conducted on fertility assessments related to semen quality utilizing AI technology.

DECLARATIONS

Authors' contributions

Mohamad Ervandi wrote the manuscript, designed the study, supervised the study, and reviewed the final version of the manuscript. Talha Dangkua collected and analyzed the data. All authors have read and approved the final edition of the manuscript.

Acknowledgements

The authors would like to extend their gratitude to the Directorate of Research, Technology, and Community Service (DRTPM), Jakarta, Indonesia, for their support of the present study.

Funding

The present study was funded by the Directorate of Research, Technology, and Community Service (DRTPM), Jakarta, Indonesia.

Ethical considerations

All authors have been screened for ethical issues, including plagiarism, consent for publication, ethical violations, data falsification, and multiple publications or submissions. AI was not used to generate data, perform statistical analyses, or interpret the research findings. All sections of the manuscript related to the methodology, results of the study, and conclusions were written entirely by the author based on the findings of the present study.

Availability of data and materials

The authors confirm that all data supporting the findings of this study are included within the manuscript.

Conflict of interests

The authors declared no conflicts of interest.

REFERENCES

Agung DS, Marawali A, Uly K, and Telupere FMS (2023). Effect of adding various levels of glutathione in coconut water–egg yolk extender on the semen quality of Angus bulls. Nucleus Journal of Animal Science, 10(1): 27-37. DOI: https://www.doi.org/10.35508/nukleus.v10i1.7948

Ahmad E, Naseer Z, and Aksoy M (2021). Glutathione supplementation in semen extender improves rabbit sperm attributes during refrigeration. World Rabbit Science, 29(2): 81-86. DOI: https://www.doi.org/10.4995/wrs.2021.14759

Ansari MS, Rakha BA, Akhter S, Akhter A, Blesbois E, and Santiago-Moreno J (2021). Effect of glutathione on pre and post-freezing sperm quality of Indian red jungle fowl (*Gallus gallus murghi*). Theriogenology, 172: 73-79. DOI: https://www.doi.org/10.1016/j.theriogenology.2021.06.008

Arif AA, Maulana T, Kaiin EM, Purwantara B, Arifiantini RI, and Memili E (2020). Comparative analysis of various step-dilution techniques on the quality of frozen Limousin bull semen. Veterinary World, 13(11): 2422-2428. DOI: https://www.doi.org/10.14202/vetworld.2020.2422-2428

Astuti ME (2018). Effect of tomato (*Solanum lycopersicum*) juice addition as a natural extender on the storage quality of Bali cattle (*Bos sondaicus*) spermatozoa. Bionature, 18(2): 129-139. DOI: https://www.doi.org/10.35580/bionature.v18i2.6144

Bansal AK and Bilaspuri G (2011). Impacts of oxidative stress and antioxidants on semen functions. Veterinary Medicine International, 2011: 686137. DOI: https://www.doi.org/10.4061/2011/686137

Beltrán C, Treviño CL, Mata-Martínez E, Chávez JC, Sánchez-Cárdenas C, Baker M, and Darszon A (2016). Role of ion channels in the sperm acrosome reaction. In: M. Buffone (Editor), Sperm acrosome biogenesis and function during fertilization. advances in anatomy, embryology and cell biology. Springer., Cham, pp. 35-69. DOI: https://www.doi.org/10.1007/978-3-319-30567-7_3

Berry DP, Eivers B, Dunne G, and McParland S (2019). Genetics of bull semen characteristics in a multi-breed cattle population. Theriogenology, 123: 202-208. DOI: https://www.doi.org/10.1016/j.theriogenology.2018.10.006

Câmara DR, Pinto LC, Pinto MM, Kastelic CM, Nunes JP, Barbosa JF, and Guerra MMP (2016). Influence of catalase and pre-freezing equilibration on post-thaw semen quality and conception rate in ewes laparoscopically inseminated. Animal Reproduction, 13(1): 21-27. DOI: http://www.doi.org/10.4322/1984-3143-AR729

Carriço C, Barbas JP, Pimenta J, and Simões J (2023). Effect of *in vitro* addition of melatonin and glutathione on seminal parameters of rams in diluted semen and after thawing. Veterinary Sciences, 10(7): 446. DOI: https://www.doi.org/10.3390/vetsci10070446

Chai YC and Mieyal JJ (2023). Glutathione and glutaredoxin-key players in cellular redox homeostasis and signaling. Antioxidants, 12(8): 1553. DOI: https://www.doi.org/10.3390/antiox12081553

Chen TH, Wang HC, Chang CJ, and Lee SY (2024). Mitochondrial glutathione in cellular redox homeostasis and disease manifestation. International Journal of Molecular Sciences, 25(2): 1314. DOI: https://www.doi.org/10.3390/ijms25021314

Douard V, Hermier D, Magistrini M, and Blesbois E (2003). Reproductive period affects lipid composition and quality of fresh and stored spermatozoa in Turkeys. Theriogenology, 59(3-4): 753-764. DOI: https://www.doi.org/10.1016/S0093-691X(02)01086-5

Ducha N, Isnawati I, Muhaimin FI, Prastyaningtias SD, Nafis FAD, and Fitri R (2024). Sperm quality profile of Bali bull as local Indonesian cattle in liquid storage in different diluents with the addition of synthetic antioxidants. BIO Web of Conferences, 162: 00012. DOI: https://www.doi.org/10.1051/bioconf/202516200012

Dutta S, Majzoub A, and Agarwal A (2019). Oxidative stress and sperm function: A systematic review on evaluation and management. Arab Journal of Urology, 17(2): 87-97. DOI: https://www.doi.org/10.1080/2090598X.2019.1599624

Dzulqarnain A, Saili T, and Rusdin M (2022). Bali cow spermatozoa quality after preservation using tris yellow egg and honey with different levels. Halu Oleo Animal Husbandry Scientific Journal, 4(3): 236-242. DOI: https://www.doi.org/10.56625/jipho.v4i3.27026

Ervandi M, Ihsan MN, Wahjuningsih S, and Susilawati T (2020). Pregnancy rate and reproductive disorders examination of inseminated brahman cross by rectal palpation and ultrasonography. American Journal of Animal and Veterinary Sciences, 15(1): 73-80. DOI: https://www.doi.org/10.3844/ajavsp.2020.73.80

Ervandi M, Mokoolang S, Ardiansyah W, and Ananda S (2023). Effectiveness of a combination of red fruit extract (*Pandanus conoideus lamk*) and green coconut water on the semen quality of Bali cattle during cold storage. Journal of Animal Science and Industry, 9(2): 161-176. DOI: https://www.doi.org/10.24252/jiip.v9i2.40465

Ervandi M, Susilawati T, and Wahjuningsih S (2013). Effect of different diluents on the quality of sperm sexing cows with a gradient albumin (egg white). Indonesian Journal of Animal and Veterinary Sciences, 18(3): 177-184. DOI: https://www.doi.org/10.14334/jitv.v18i3.319

Fitri R, Ducha N, and Retnowulan D (2025). Effects of adding glutathione to CEP diluent on post-thawing sperm quality of Bali cattle. LenteraBio: Scientific Journal of Biology, 14(1): 63-71. Available at: https://journal.unesa.ac.id/index.php/lenterabio/article/view/33904

Gualtieri R, Mallo V, Barbato V, and Talevi R (2010). Ability of sulfated glycoconjugates and disulfide-reductants to release bovine epididymal sperm bound to the oviductal epithelium *in vitro*. Theriogenology, 73(8): 1037-1043. DOI: https://www.doi.org/10.1016/j.theriogenology.2009.11.030

Hitit M, Ugur MR, Dinh TTN, Sajeev D, Kaya A, Topper E, Tan W, and Memili E (2020). Cellular and functional physiopathology of Bull sperm with altered sperm freezability. Frontiers in Veterinary Science, 7: 581137. DOI: https://www.doi.org/10.3389/fvets.2020.581137

Ismaya (2014). Biotechnology of artificial insemination in cattle and buffaloes. Gadjah Mada University Press., Yogyakarta. pp. 56-64. Available at: https://digitalpress.ugm.ac.id/book/79

Izanloo H, Soleimanzadeh A, Bucak MN, Imani M, and Zhandi M (2021). The effects of varying concentrations of glutathione and trehalose in improving microscopic and oxidative stress parameters in Turkey semen during liquid storage at 5°C. Cryobiology, 101: 12-19. DOI: https://www.doi.org/10.1016/j.cryobiol.2021.07.002

Khan IM, Cao Z, Liu H, Khan A, Rahman SU, Khan MZ, Sathanawongs A, and Zhang Y (2021). Impact of cryopreservation on spermatozoa freeze-thawed traits and relevance OMICS to assess sperm cryo-tolerance in Farm Animals. Frontiers in Veterinary Science, 8: 609180. DOI: https://www.doi.org/10.3389/fvets.2021.609180

Krishna VS, Singh LR, Ramana KV, Reddy KJM, Kumar DA, and Kumar ESA (2024). Influence of taurine on the integrity of the plasma membrane and acrosomes in eytc-diluted cattle bull semen. International Journal of Advanced Biochemistry Research, 8(12): 754-756. DOI: https://www.doi.org/10.33545/26174693.2024.v8.i12Sj.3195

Luo X, Wu D, Liang M, Huang S, Shi D, and Li X (2022). The effects of melatonin, glutathione and vitamin E on semen cryopreservation of Mediterranean buffalo. Theriogenology, 197: 94-100. DOI: https://www.doi.org/10.1016/j.theriogenology.2022.11.035

Maleki K, Ayen E, Khaki A, and Soleimanzadeh A (2023). Comparison of sperm characteristics and antioxidant and oxidant levels in bull semen frozen with four widely used extenders. Veterinary Research Forum, 14(7): 373-379. DOI: https://www.doi.org/10.30466%2Fvrf.2023.562594.3631

Malik A, Fauzi R, Zakir MI, and Sakiman S (2018). The substitution of glycerol by the pure honey in the cryopreservation of Bali bull semen on the post-thawing quality of spermatozoa. Acta Veterinaria Indonesian, 5(2): 98-104. Available at: https://journal.ipb.ac.id/actavetindones/article/view/23325

Marawali A, Abdullah MS, and Jalaludin J (2019). The effectiveness of guava filtrate supplementation in coconut water-egg yolk dilution on quality of liquid semen of Bali cattle. Indonesian Veterinary Journal, 20(1): 20-29. DOI: https://www.doi.org/10.19087/jveteriner.2019.20.1.20

Mila FNH, Kaka A, and Ina YT (2021). Characteristic and quality of Sumba Ongole bull semen in tris diluent supplemented with skim milk at a temperature of 3-5ºC. Journal of Animal Science and Technology, 3(1): 12-18. DOI: https://www.doi.org10.31605/jstp.v3i1.1201

Muhammad D, Isnaini N, Kuswati, Yekti APA, Aryogi, Lutfi M, Lukman HY, and Susilawati T (2019). Effect of various formulations of coconut water on the quality of PO (*Ongole crossbred*) bull sperm during cold storage. Indonesian Journal of Animal Sciences, 29(1): 1-8. Available at: https://jiip.ub.ac.id/index.php/jiip/article/view/486/pdf

Munsi MN, Bhuiyan MMU, Majumder S, and Alam MGS (2007). Effects of exogenous glutathione on the quality of chilled bull semen. Reproduction in Domestic Animals, 42(4): 358-362. DOI: https://www.doi.org/10.1111/j.1439-0531.2006.00789.x

Ogata K, Imai A, Sato S, Nishino K, Watana S, Sofmai T, Kobayasih E, and Takeda K (2022). Effects of reduced glutathione supplementation in semen freezing extender on frozen-thawed bull semen and *in vitro* fertilization. Journal of Reproduction and Development, 68(1): 53-61. DOI: https://www.doi.org/10.1262/jrd.2021-079

Park SH and Yu IJ (2017). Effect of antioxidant supplementation in freezing extender on porcine sperm viability, motility and reactive oxygen species. Journal of Embryo Transfer, 32(1): 9-15. DOI: https://www.doi.org/10.12750/JET.2017.32.1.9

Purnawan AB, Rimayanti R, Susilowati S, Mustofa I, Hernawati T, and Safitri E (2023). Evaluation of motility, viability, and integrity plasma membranes of frozen semen in Friesian Holstein with storage periods of 33, 30, 27, and 24 years. Journal of Veterinary Medicine, 6(2): 162-172. DOI: https://www.doi.org/10.20473/jmv.vol6.iss2.2023.162-172

Shah N, Singh V, Yadav HV, Verma M, Chauhan DS, Saxena A, Yadav S, and Swain DK (2017). Effect of reduced glutathione supplementation in semen extender on tyrosine phosphorylation and apoptosis like changes in frozen thawed Hariana bull spermatozoa. Journal Animal Reproduction Science, 182: 111-122. DOI: https://www.doi.org/10.1016/j.anireprosci.2017.05.006

Solihati N, Rasad SD, Setiawan R, Foziah EN, and Wigiyanti ET (2018). Semen quality of post-thawed local ram's in tris-egg yolk extender with different glutathione level. IOP Conference Series: Earth and Environmental Science, 119: 012034. Available at: https://iopscience.iop.org/article/10.1088/1755-1315/119/1/012034

Sudarwati H, Natsir MH, and Nurgiatiningsih, VMA (2019). Statistics and experimental design applications in animal science. Brawijaya University (UB Prees)., Malang, pp. 34-57. Available at: https://digilib.ub.ac.id/opac/detail-opac?id=79466

Sumadiasa IL, Susilawati T, Ciptadi G, and Isnaini N (2015). The potency of guava filtrate (*Psidium guajava linn*) for preservation of Bali bull spermatozoa. IOSR Journal of Agriculture and Veterinary Science, 8(5): 51-57. Available at: chrome-extension://efaidnbmnnnibpcajpcglclefindmkaj/https://www.iosrjournals.org/iosr-javs/papers/vol8-issue5/Version-1/L08515157.pdf

Susilawati T (2011). Spermatology. Brawijaya University (UB Prees)., Malang, pp. 76-80. Available at: https://bookstore.ub.ac.id/shop/peternakan/spermatology/

Susilawati T (2013). Artificial insemination reproductive technology. Brawijaya University (UB Prees)., Malang, pp. 23-38. Available at: https://digilib.ub.ac.id/opac/detail-opac?id=11915

Suyadi S, Purwantara B, Furqon A, Septian WA, Novianti I, Nursita IW, Nugraha CD, Putri RF, Ratiwi H, and Herwiyati E (2020). Influences of bull age and season on sperm motility, sperm concentration, and ejaculate volume of Ongole Grade cattle in Singosari National Artificial Insemination Center. Journal of the Indonesian Tropical Animal Agriculture, 45(4): 261-267. DOI: https://www.doi.org/10.14710/jitaa.45.4.261-267

Suyadi S., Hakim L, Wahjuningsih W, and Nugroho H (2014). Reproductive performance of Ongole crosbred (PO) and Limousin x PO crossbred (Limpo) cattle at different altitude areas in East Java, Indonesia. Journal of Applied Science and Agriculture, 9(11): 81-85. Available at: https://www.aensiweb.com/old/jasa/rjfh/Special%202%20ICABSE%202014/81-85.pdf

Swarna M, Biswas S, Biswas D, Saha N, and Paul A (2023). Impact of chilling duration on sperm quality of indigenous buck semen in the coastal area of Bangladesh. Bangladesh Journal of Veterinary Medicine, 21(1): 17-25. DOI: https://www.doi.org/10.33109/bjvmjj2023fam1

Syarifuddin A, Laksmi DNDI, and Bebas IW (2012). Effectiveness of adding various glutathione concentrations on viability and motility of post thawing Bali cattle spermatozoa. Indonesia Medicus Veterinus, 1(2): 173-185. Available at: https://ojs.unud.ac.id/index.php/imv/article/view/1806

Telnoni SP, Fahik M, and Baon GY (2023). Quality of Bali cattle (*Bos sondaicus*) spermatozoa in tris egg yolk extender with the addition of glutathione. Flobamora Biological Journal, 1(2): 8-15. Available at: https://ejurnal-unisap.ac.id/index.php/flobijo/article/view/69/47

Tethool AN, Ollong AR, and Koibur JF (2021). The effect of red fruit extract (*Pandanus conoideus Lam*) treatment on sperm abnormalities in local chickens. Journal of Tropical Animal and Veterinary Science, 11(2): 92-98. DOI: https://www.doi.org/10.46549/jipvet.v11i2.107

Triwulaninngsih E, Situmorang P, Sugiarti T, Sianturi RG, and Kusumaningrum DA (2003). The effect of glutathione addition in sperm diluent on the quality of bovine chilled semen. Indonesian Journal of Animal and Veterinary Sciences, 8(2): 91-97. DOI: https://www.doi.org/10.14334/jitv.v8i2.378

Wadhwa BS, Singh AK, Kumar A, Honparkhe M, Singh N, and Singh P (2024). Effect of glutathione supplementation in extender on quality and fertility of cryopreserved buffalo semen. Indian Journal of Animal Sciences, 94(9): 792-796. Available at: https://epubs.icar.org.in/index.php/IJAnS/article/view/148851/55732

Wijayanti A, Suprayogi TW, Prastiya RA, Hernawati T, Sardjito T, Saputro AL, Amaliya A, and Sulistyowati D (2023). Effect of green tea extract (*Camellia sinensis*) addition in tris egg yolk diluter on the quality of Bali cattle *(Bos sondaicus*) spermatozoa after freezing. Veterinary Medical Journal, 6(1): 66-74. DOI: https://www.doi.org/10.20473/jmv.vol6.iss1.2023.66-74

Xue SH, Xu BB, Yan XC, Zhang JX, and Su R (2025). Sperm membrane stability: in-depth analysis from structural basis to functional regulation. Veterinary Sciences, 12(7): 658 1-15. DOI: https://www.doi.org/10.3390/vetsci12070658

Yekti APA, Kusumawati ED, Kuswati K, Ridhowi A, Sudarwati H, Isnaini N, and Susilawati T (2017). Succesfull of artificial insemination by using chilled semen on Brahman cross cows. Advances in Health Sciences Research (AHSR), 5: 221-226. DOI: https://www.doi.org/10.2991/ICOH-17.2018.43

Younus AMD, Yamanaka T, and Shimada M (2024). The protective effects of antioxidants against endogenous and exogenous oxidative stress on bull sperm. In Vitro Cellular and Developmental Biology-Animal, 60: 969-982. DOI: https://www.doi.org/10.1007/s11626-024-00944-w

Zhu Z, Zhao H, Cui H, Adetunji AO, and Min L (2023). Resveratrol improves the frozen-thawed ram sperm quality. Animals, 13(24): 3887. DOI: https://www.doi.org/10.3390/ani13243887

Zou J, Wei L, Li D, Zhang Y, Wang G, Zhang L, Cao P, Yang S, and Li G (2021). Effect of glutathione on sperm quality in guanzhong dairy goat sperm during cryopreservation. Frontiers in Veterinary Science, 8: 771440. DOI: https://www.doi.org/10.3389/fvets.2021.771440

Publisher's note: Scienceline Publication Ltd. remains neutral with regard to jurisdictional claims in published maps and institutional affiliations.

Open Access: This article is licensed under a Creative Commons Attribution 4.0 International License, which permits use, sharing, adaptation, distribution and reproduction in any medium or format, as long as you give appropriate credit to the original author(s) and the source, provide a link to the Creative Commons licence, and indicate if changes were made. The images or other third party material in this article are included in the article's Creative Commons licence, unless indicated otherwise in a credit line to the material. If material is not included in the article's Creative Commons licence and your intended use is not permitted by statutory regulation or exceeds the permitted use, you will need to obtain permission directly from the copyright holder. To view a copy of this licence, visit https://creativecommons.org/licenses/by/4.0/.

© The Author(s) 2025

2025, Scienceline Publication
World's Veterinary Journal
World Vet J, 15(4): 921-928.
ISSN 2322-4568

DOI: https://dx.doi.org/10.54203/scil.2025.wvj93
PII: S232245682500093-15

Physiochemical Properties and Nutritional Composition of Camel Milk in Garissa County, Kenya

Yoonis Dayr Mohamed[1]*, Rebecca Waihenya[1,2], Kenneth Ogila[2], and Raphael W. Lihana[3]

[1]*Department of Molecular Biology and Biotechnology, Pan African University Institute for Basic Sciences Technology and Innovation (PAUSTI), Nairobi, Kenya*
[2]*Department of Zoology, School of Biological Sciences, Jomo Kenyatta University of Agriculture and Technology, Nairobi, Kenya*
[3]*Kenya Medical Research Institute Centre for Virus Research, Nairobi, Kenya*

*Corresponding author's Email: yoonisdayr@gmail.com

ORIGINAL ARTICLE
Received: October 03, 2025
Revised: November 13, 2025
Accepted: December 02, 2025
Published: December 25, 2025

ABSTRACT

Camel milk is an important source of food, income, and livelihood for communities in arid and semi-arid regions. It contains essential macronutrients, minerals, vitamins, and bioactive compounds that contribute to human health. Despite Kenya's status as a prominent producer of camel milk, especially in Garissa County, comprehensive data regarding its physicochemical and nutritional composition remain scarce. The present study aimed to determine the physicochemical attributes and nutritional profile of camel milk sourced from Garissa County. Fifteen raw milk samples were collected in May 2024 during the long rainy season from randomly selected, clinically healthy lactating Somali dromedary camels reared under semi-intensive systems on five dairy farms in Garissa County, Kenya, under hygienic conditions (three samples per farm). Physicochemical parameters measured included pH, color, titratable acidity, viscosity, total solids, and moisture. Nutritional components analyzed were fat, protein, lactose, minerals, vitamins, and fatty acids using AOAC methods and gas chromatography–mass spectrometry. The camel milk samples exhibited a mean pH of 6.63 ± 0.10, 0.14 ± 0.03% titratable acidity, 1.86 ± 0.08 mPa·s viscosity, 12.68 ± 0.66% total solids, and 87.20 ± 2.86% moisture. Proximate composition indicated 4.2 ± 0.2% fat, 2.3 ± 0.1% protein, and 5.1 ± 0.2% lactose. Calcium (5293.16 ± 54.49mg/l) was the most abundant mineral. Among vitamins, vitamin C was the most abundant water-soluble vitamin, while vitamin K was the most dominant fat-soluble vitamin. Fatty acid analysis indicated that (55.4%) of the fatty acids were saturated and (44.6%) were unsaturated. Palmitic acid and oleic acid were the most abundant. The results indicated relatively uniform physicochemical and nutritional characteristics of camel milk produced under semi-intensive systems from selected farms in Garissa County, Kenya. The results of this study provided descriptive insight for future studies with larger sample sizes within this county, as well as comparative study across counties and different seasonal conditions.

Keywords: Camel milk, Fatty acid, Nutritional composition, Physicochemical characteristic

INTRODUCTION

Camels are the most prevalent desert livestock animals in arid and semi-arid regions of Africa and Asia, particularly in the Horn of Africa, including Ethiopia, Djibouti, Somalia, and Kenya (Faye, 2020). The single-humped dromedary camel (*Camelus dromedarius*) is exceptionally adapted to hot and arid environments among domesticated animals (Faye, 2020). Current estimates are that there are more than 35 million camels in the world, of which the majority (~97%) are single-humped dromedaries (Camelus dromedarius), and less than 3% are two-humped Bactrian camels (*Camelus bactrianus*; Faye, 2020). Camels are famous for their resilience in desert environments, tolerating heat and limited availability of water (Faye, 2020). Although they need significantly less feed than other livestock due to their highly efficient metabolism and ability to utilize sparse desert vegetation. Camels can produce very high rates of milk, at times even higher than other livestock types in deserts such as cattle, goats, and sheep. In a lactation cycle between 8 and 18 months, a dromedary camel can deliver 1,000 to 2,000 liters of milk (Gebreyohanes and Assen, 2017). The global production of camel milk was reported to be 4.12 million metric tons (MMT) in 2022 (Ait El Alia et al., 2025). Kenya is the largest producer with (1.165 MMT) annually, followed by Somalia (0.958 MMT) and Mali (0.271 MMT; Oselu et al., 2022). The North-Eastern pastoralists in Kenya keep approximately 4.722 million camels, 80 % of the nation's camels (Oselu et al., 2022). Among these communities, such as the Somali, Gabbra, and Rendille, camels play a central role by providing milk, meat, hides, fiber, and transport services (Isako and Kimindu, 2019).

Camel milk is uniquely different from other ruminant milks in terms of nutritional composition and potential health benefits (Faye, 2020). Compared to bovine milk, camel milk contains higher concentrations of vitamin C, lacks β-lactoglobulin (a major allergen in cow milk), and has lower cholesterol levels (El-Agamy et al., 2009). It also contains special bioactive molecules such as immunoglobulins, lactoferrin, lactoperoxidase, and higher concentrations of vitamin

To cite this paper: Mohamed YD, Waihenya R, Ogila K, and Lihana RW (2025). Physiochemical Properties and Nutritional Composition of Camel Milk in Garissa County, Kenya. *World Vet. J.*, 15(4): 921-928. DOI: https://dx.doi.org/10.54203/scil.2025.wvj93

C than bovine milk (Alhassani, 2024). Moreover, the bioactive molecules in camel milk, particularly immunoglobulins, lactoferrin, and lactoperoxidase, have been reported to exhibit anti-diabetic, anti-allergic, antimicrobial, and immune-modulating effects (Seifu, 2023). The physicochemical characteristics of camel milk vary by geographic region, environmental context, breed, diet, and stage of lactation (Seifu, 2023). Northeastern Kenya is among the globe's biggest producers of camel milk, with Garissa County being among the top production hubs (Oselu et al., 2022). Despite the significance, there is a notable lack of detailed physicochemical and nutritional data on camel milk from Garissa County, Kenya. Addressing this gap is necessary because region-specific composition data can assist processors in setting product standards, support evidence-based nutritional guidance, facilitate product development within the camel milk value chain, and provide baseline values for future studies on factors influencing milk composition. Therefore, this study aimed to characterize the physicochemical properties and nutritional composition of camel milk produced under semi-intensive systems in Garissa County, Kenya.

MATERIALS AND METHODS

Study design and sampling

A cross-sectional descriptive study was conducted to characterize the physicochemical and nutritional composition of camel milk from Garissa County, Kenya. Fifteen samples of raw milk were collected in May 2024 (long-rainy season) from five dairy farms (three samples per farm). Clinically healthy, multiparous Somali dromedary camels (*Camelus dromedarius*) aged 5-12 years and in mid-lactation (3-7 months) were randomly selected. Udders and teats were wiped clean with 70% ethanol before sampling. Camels were reared under semi-intensive systems, grazing freely during the day and housed at night. Camels indicating signs of illness, udder health issues, abnormal lactation stages, or recent drug treatment (within 14 days) were excluded. Milking was performed in the early morning, and approximately 200 mL of milk was collected per camel**.** Samples were aseptically collected, placed on ice (4°C), and transported within 4 hours (Legesse et al., 2017) to the Food Fortification Laboratory, Jomo Kenyatta University of Agriculture and Technology (JKUAT), for analysis.

Physicochemical analysis

Physicochemical parameters were measured by employing the following standardized methods. The pH was measured using a calibrated pH meter (Model AD800, Hanna Instruments, Italy) calibrated with standard buffers pH 4.0, 7.0, and 10.0. Measurements were conducted at a controlled temperature of 25 ± 1°C (Legesse et al., 2017). The color of milk was measured using a Color Flex machine (HunterLab, Reston, VA, USA) with a CIELab system, D65 illuminant, 10° observer angle, and 45/0 measurement geometry. Samples were placed in transparent quartz cuvettes, and color was determined by measuring the light transmitted through the milk (El-Hatmi et al., 2023). The lactic acid content was determined according to the AOAC Official Method 947.05 (AOAC, 2016a) using a titrimetric procedure. Briefly, a known volume of camel milk was titrated with a standardized 0.1 N sodium hydroxide (NaOH) solution until the endpoint was reached, and the lactic acid percentage was calculated based on the volume of NaOH consumed.

The viscosity was measured using an Anton Paar Rheometer (RheolabQC, SN84508188, Anton Paar GmbH, Graz, Austria) with a CC27 concentric cylinder spindle. Before measurement, milk samples were gently homogenized to ensure homogeneity and were carefully put into the measurement cup to avoid air bubble formation. To obtain reliable viscosity values, samples were equilibrated at a controlled temperature of 30 ± 0.1°C for around 10 minutes before analysis. Viscosity measurements were taken at a constant shear rate of 50 s^{-1}, widely employed for low-viscosity dairy fluids. The dynamic viscosity was measured in mPa·s (Alhassani, 2024). Total solid and total moisture content were determined by a drying oven method according to AOAC 925.10 (AOAC, 2016b; AOAC International, Rockville, MD, USA), by placing approximately 5g of milk sample in a weighed crucible and keeping it in a drying oven (Memmert 100-800, Memmert) at 105°C approximately 3 hours or until constant weight was achieved, defined as the point at which repeated cycles of drying, cooling in a desiccator, and reweighing resulted in two consecutive weight measurements differing by less than 0.001 g, indicating complete removal of moisture (Abduku and Eshetu, 2024). Total moisture was determined on the basis of the loss of weight, because water evaporates, which was determined by an analytical balance (Model MS204TS, Mettler Toledo GmbH, Greifensee**,** Switzerland**),** with a precision of ± 0.0001 g. The total solid content was obtained using the weight of the dried sample (Abduku and Eshetu, 2024).

Nutritional composition analysis

Fat content was determined by the Rose–Gottlieb method (AOAC 989.05; AOAC International, Rockville, MD, USA) using approximately 10 g of milk, followed by solvent extraction with concentrated ammonium hydroxide, ethanol, diethyl ether, and petroleum ether in a Mojonnier fat-extraction flask (Gerber Instruments AG, Effretikon,

Switzerland). The extraction solvents were evaporated under vacuum at 60°C utilizing a rotary evaporator to slowly remove the solvents employed in extraction without decomposing the fat. Vacuum evaporation decreases the boiling points of the solvents, allowing them to evaporate at a moderate temperature successfully and leaving behind the crude fraction of fat (Model R-210, Büchi Labortechnik AG, Flawil, Switzerland). After vacuum, the extracted fat was dried at 102 ± 2°C for 30 minutes using a laboratory drying oven (Memmert GmbH and Co. KG, Schwabach, Germany) to eliminate residual moisture and then weighed using an analytical balance (Model MS204TS, Mettler Toledo GmbH, Greifensee, Switzerland; precision ± 0.0001 g; Bakry et al., 2021).

Crude protein content was determined using the Kjeldahl method according to AOAC Official Method 991.20 (AOAC International, Rockville, MD, USA), involving first sample digested with strong sulfuric acid, which converts organic nitrogen into ammonium sulfate. The solution is then made alkaline to release ammonia, which is distilled and collected in boric acid before being quantified by titration with a standard acid to estimate total nitrogen, which is then converted to crude protein using a factor of 6.38 (He et al., 2019).

Lactose content was determined by high-performance liquid chromatography (HPLC; Model LC-20AT, Shimadzu Corporation, Kyoto, Japan) on a carbohydrate analysis column (NH_2, 4.6 × 250 mm, 5 µm) using isocratic elution of acetonitrile water (75:25, v/v; HPLC-grade, Merck KGaA, Darmstadt, Germany) at 1 mL/min and refractive index detection. Quantitation was done using external lactose standards (Khaliq et al., 2024).

Mineral content (zinc, iron, magnesium, calcium, sodium, potassium, and phosphorus) was determined using an atomic absorption spectrophotometer (Model AA-7000, Shimadzu Corporation, Kyoto, Japan) with a graphite furnace. Milk samples were prepared by wet digestion: 5 mL of sample was mixed with 10 mL of concentrated nitric acid (HNO_3) and heated on a hot plate, followed by the addition of 2 mL of perchloric acid ($HClO_4$) until a clear solution was obtained. After cooling, the digest was diluted to 25 mL with deionized water and filtered through Whatman No. 42 filter paper (Cytiva, Buckinghamshire, UK). Mineral concentrations were measured at 213.9 nm for zinc, 248.3 nm for iron, 285.2 nm for magnesium, 422.7 nm for calcium, 589.0 nm for sodium, 766.5 nm for potassium, and 213.6 nm for phosphorus, using element-specific hollow cathode lamps operated at 10 mA. Calibration was performed using standard solutions prepared from certified stock standards (Abduku and Eshetu, 2024).

Vitamins were quantified using High-Performance Liquid Chromatography (HPLC; Model LC-2050C, Shimadzu Corporation, Kyoto, Japan). External standard calibration curves were prepared separately for each vitamin using certified pure standards, and vitamin concentrations were calculated by comparing sample peak areas against these calibration curves. All calibration curves indicated excellent linearity ($R^2 > 0.99$), confirming method validity. Fat soluble vitamins (A, E, K) were separated on a C18 column (4.6 × 250 mm, 5 µm) at 30°C using a gradient mobile phase of acetonitrile and water (0.1% formic acid), and detected at 280 nm with a UV-Vis detector (Faye et al., 2019). Water-soluble vitamins (vitamin C, B_1, B_2, B_3, B_6, B_9, and B_{12}) were separated on an amino column (4.6 × 250 mm, 5 µm) at 30°C using an isocratic mobile phase of water-acetonitrile containing 0.1% acetic acid and detected by fluorescence (excitation 340 nm, emission 450 nm; Faye et al., 2019).

Fatty acid analysis

The lipids were saponified and methylated, and the resulting fatty acid methyl esters (FAMEs) were quantified. The methylation reaction was carried out by combining 2 mL of 0.5 M potassium hydroxide (KOH) in methanol (Sigma-Aldrich, St. Louis, MO, USA) with 2 mL of 12% boron trifluoride (BF_3) in methanol (Sigma-Aldrich, St. Louis, MO, USA) for one hour at 100°C (Freije et al., 2024). The gas chromatograph-mass spectrometer (GC-MS; Agilent 7890B GC with 5977B MSD Detector, Agilent) was utilized to extract and identify the FAMEs. The DB-23 capillary column (30m, 0.25 mm, 0.25 µm) was utilized for this purpose. The parameters of injection included split injection with 1 µL of sample, 1 mL/min of helium carrier gas flow, injection temperature of 270°C, oven temperature program of 50°C for 1 minute, ramp to 240°C at the rate of 10°C per minute, hold at 240°C for 5 minutes, and detection by Mass Spectrometer Detector (Model 5977B MSD, Agilent Technologies Japan, Ltd., Tokyo, Japan). The compounds that were discovered were identified using the NIST 2017 library (Freije et al., 2024). Quantification of FAMEs was achieved using external standard calibration curves prepared from certified FAME standards at known concentrations. Sample peak areas were compared with those of the corresponding standards to calculate the concentrations of individual fatty acids. The results were expressed as the relative percentage of each fatty acid, calculated from its peak area relative to the total peak area of all identified FAMEs.

Statistical analysis

Data analysis was performed using SPSS software, version 26.0 (IBM Corp., Armonk, NY, USA). Descriptive statistics were applied to calculate the mean and standard deviation (SD) for each parameter per farm and for the overall samples.

RESULTS

Physicochemical properties

The physicochemical parameters of camel milk from five farms in Garissa County are summarized in Table 1. Descriptive analysis indicated that all measured traits, including pH, color, titratable acidity, viscosity, total solids, and moisture content, indicated close values among the five farms.

Proximate composition

Fat, protein, and lactose contents are presented in Table 2. Descriptive analysis indicated that the levels of fat, protein, and lactose were relatively similar across all farms, with only minor differences observed among samples.

Mineral composition

As presented in Table 3, descriptive analysis indicated that the levels of calcium, sodium, potassium, zinc, iron, magnesium, and phosphorus were relatively similar across farms, with only minor differences observed among samples.

Vitamin composition

Vitamin analysis results are summarized in Table 4. Descriptive analysis indicated that both water-soluble vitamins (C and B-group, including B_1, B_2, B_3, B_6, B_9, B_{12}) and fat-soluble vitamins (A, E, and K) were present, with only minor differences observed among samples across farms.

Fatty acid profile

The fatty acid distribution is presented in Table 5. Descriptive analysis indicated that saturated fatty acids accounted for a slightly higher proportion than unsaturated fatty acids, with only minor differences observed among samples across the farm.

Table 1. Physicochemical properties of camel milk from five farms in Garissa County, Kenya

Parameters	Farm 1 (Mean ± SD)	Farm 2 (Mean ± SD)	Farm 3 (Mean ± SD)	Farm 4 (Mean ± SD)	Farm 5 (Mean ± SD)	Total (Mean ± SD)
pH	6.67 ± 0.05	6.67 ± 0.12	6.70 ± 0.11	6.62 ± 0.06	6.50 ± 0.14	6.63 ± 0.10
Color (L*)	87.64 ± 2.06	88.19 ± 4.56	87.46 ± 2.18	87.31 ± 1.93	88.40 ± 1.53	87.80 ± 2.67
Titratable acidity lactic acid (%)	0.16 ± 0.03	0.14 ± 0.03	0.13 ± 0.03	0.16 ± 0.01	0.13 ± 0.02	0.14 ± 0.02
Viscosity (mPa·s)	1.86 ± 0.08	1.83 ± 0.10	1.85 ± 0.06	1.89 ± 0.09	1.89 ± 0.06	1.86 ± 0.08
Moisture content (%)	85.54 ± 1.16	87.80 ± 3.32	88.06 ± 1.34	88.03 ± 2.70	86.59 ± 4.44	87.20 ± 2.86
Total solid (%)	12.86 ± 0.44	12.16 ± 0.86	13.04 ± 0.77	12.60 ± 0.71	12.78 ± 0.43	12.68 ± 0.66

Note: Values are expressed as mean ± SD per farm (n = 3), with total mean ± SD representing the overall average (N = 15).

Table 2. Proximate composition of camel milk from five farms in Garissa County, Kenya

Parameters	Farm 1 (Mean ± SD)	Farm 2 (Mean ± SD)	Farm 3 (Mean ± SD)	Farm 4 (Mean ± SD)	Farm 5 (Mean ± SD)	Total (Mean ± SD)
Fat content (%)	4.34 ± 0.25	4.08 ± 0.19	4.36 ± 0.05	4.09 ± 0.19	4.17 ± 0.10	4.20 ± 0.17
Protein content (%)	2.40 ± 0.09	2.21 ± 0.18	2.37 ± 0.11	2.30 ± 0.04	2.34 ± 0.20	2.32 ± 0.13
Lactose content (%)	5.17 ± 0.23	5.15 ± 0.22	4.99 ± 0.11	5.00 ± 0.11	5.01 ± 0.18	5.06 ± 0.17

Note: Data are presented as mean ± SD for each farm (n = 3), and the total mean ± SD indicates the combined average for all samples (N = 15)

Table 3. Mineral composition of camel milk from five farms in Garissa County, Kenya

Parameters (mg/l)	Farm 1 (Mean ± SD)	Farm 2 (Mean ± SD)	Farm 3 (Mean ± SD)	Farm 4 (Mean ± SD)	Farm 5 (Mean ± SD)	Total (Mean ± SD)
Zinc (Zn)	3.94 ± 0.32	3.88 ± 0.27	3.89 ± 0.38	3.88 ± 0.27	3.86 ± 0.26	3.89 ± 0.30
Iron (Fe)	4.89 ± 0.15	4.88 ± 0.15	4.97 ± 0.36	4.94 ± 0.25	5.01 ± 0.28	4.93 ± 0.25
Magnesium (Mg)	51.42 ± 1.47	47.33 ± 0.90	48.51 ± 1.55	49.98 ± 1.10	51.38 ± 2.67	49.72 ± 1.65
Calcium (Ca)	5275.33 ± 65.28	5328.91 ± 34.50	5295.48 ± 46.86	5280.32 ± 83.40	5285.79 ± 58.73	5293.16 ± 54.49
Sodium (Na)	427.14 ± 5.09	426.18 ± 5.98	434.07 ± 1.61	423.49 ± 7.45	432.91 ± 1.81	428.75 ± 4.96
Potassium (K)	692.28 ± 3.67	685.64 ± 7.52	674.66 ± 3.41	680.68 ± 20.03	675.07 ± 14.62	681.66 ± 11.80
Phosphorus (P)	97.09 ± 3.86	96.09 ± 2.88	96.54 ± 1.64	97.09 ± 6.29	97.44 ± 2.70	96.85 ± 3.81

Note: Mineral concentrations are expressed as mean ± SD (mg/L) for each farm (n = 3), with total mean ± SD representing the overall average of all samples (N = 15).

Table 4. Vitamin composition of camel milk from five farms in Garissa County, Kenya

Parameters (mg/l)	Farm 1 (Mean ± SD)	Farm 2 (Mean ± SD)	Farm 3 (Mean ± SD)	Farm 4 (Mean ± SD)	Farm 5 (Mean ± SD)	Total (Mean ± SD)
Vitamin B1 (Thiamine)	3.66 ± 0.07	3.65 ± 0.12	3.70 ± 0.15	3.67 ± 0.13	3.73 ± 0.20	3.68 ± 0.14
Vitamin B2 (Riboflavin)	1.00 ± 0.12	1.01 ± 0.10	0.89 ± 0.10	1.00 ± 0.16	0.93 ± 0.09	0.96 ± 0.11
Vitamin B6 (Pyridoxine)	0.02 ± 0.00	0.02 ± 0.00	0.02 ± 0.00	0.02 ± 0.00	0.02 ± 0.00	0.02 ± 0.00
Vitamin B3 (Niacin)	3.74 ± 0.21	3.65 ± 0.10	3.66 ± 0.06	3.69 ± 0.08	3.79 ± 0.25	3.70 ± 0.15
Vitamin B9 (Folate)	0.03 ± 0.01	0.03 ± 0.00	0.03 ± 0.01	0.03 ± 0.01	0.04 ± 0.01	0.03 ± 0.01
Vitamin B12 (Cobalamin)	0.23 ± 0.06	0.22 ± 0.03	0.30 ± 0.14	0.27 ± 0.12	0.37 ± 0.08	0.27 ± 0.09
Vitamin C (Ascorbic acid)	188.11 ± 4.30	187.82 ± 1.94	190.70 ± 10.04	183.99 ± 11.16	192.79 ± 0.81	188.68 ± 7.04
Vitamin A (Retinol)	0.67 ± 0.06	0.71 ± 0.09	0.68 ± 0.06	0.66 ± 0.05	0.67 ± 0.04	0.67 ± 0.06
Vitamin E (Tocopherol)	5.81 ± 0.27	6.00 ± 0.15	6.26 ± 0.23	5.96 ± 0.16	5.99 ± 0.16	6.01 ± 0.20
Vitamin K (Phylloquinone)	10.05 ± 0.24	9.93 ± 0.17	9.89 ± 0.03	9.84 ± 0.18	10.24 ± 0.09	9.99 ± 0.16

Note: Vitamin levels are presented as mean ± SD (mg/L) for each farm (n = 3), and the total mean ± SD reflects the average concentration across all samples (N = 15).

Table 5. Fatty acid profile of camel milk from five farms in Garissa County, Kenya

Parameters (%)	Farm 1 (Mean ± SD)	Farm 2 (Mean ± SD)	Farm 3 (Mean ± SD)	Farm 4 (Mean ± SD)	Farm 5 (Mean ± SD)	Total (Mean ± SD
Palmitic acid (C16:0)	25.25 ± 2.12	24.91 ± 3.54	22.36 ± 2.05	24.77 ± 1.52	26.65 ± 2.83	24.78 ± 2.51
Stearic acid (C18:0)	10.95 ± 0.58	11.82 ± 0.73	11.29 ± 0.82	11.16 ± 0.81	11.22 ± 0.17	11.28± 0.66
Myristic acid (C14:0)	10.13 ± 0.32	10.36 ± 0.11	10.03 ± 0.56	10.34 ± 0.43	10.37 ± 0.24	10.24± 0.36
Margaric acid (C17:0)	3.70 ± 0.31	3.66 ± 0.10	3.47 ± 0.28	3.03 ± 0.05	3.57 ± 0.23	3.48 ± 0.21
Pentadecylic acid (C15:0)	3.43 ± 0.39	3.30 ± 0.26	3.26 ± 0.22	3.38 ± 0.28	3.18 ± 0.08	3.31 ± 0.26
Arachidic acid (C20:0)	0.89 ± 0.12	0.87 ± 0.08	0.83 ± 0.06	0.93 ± 0.19	0.88 ± 0.06	0.88 ± 0.11
Capric acid (C10:0)	0.22 ± 0.03	0.18 ± 0.01	0.16 ± 0.09	0.23 ± 0.05	0.26 ± 0.05	0.21 ± 0.05
Lauric acid (C12:0)	0.15 ± 0.04	0.17 ± 0.04	0.20 ± 0.07	0.24 ± 0.04	0.21 ± 0.06	0.19 ± 0.05
Nonadecanoic acid (C19:0)	0.47 ± 0.10	0.45 ± 0.15	0.52 ± 0.16	0.43 ± 0.01	0.43 ± 0.07	0.46 ± 0.11
Tridecanoic acid (C13:0)	0.10 ± 0.01	0.10 ± 0.02	0.10 ± 0.02	0.10 ± 0.03	0.09 ± 0.02	0.09 ± 0.02
Oleic acid (C18:1)	25.31 ± 2.27	27.79 ± 2.20	25.37 ± 1.97	26.46 ± 1.30	27.84 ± 2.37	26.55 ± 2.06
Palmitoleic acid (C16:1)	8.73 ± 0.46	8.56 ± 0.68	8.81 ± 0.18	8.60 ± 0.15	8.95 ± 0.21	8.73 ± 0.39
Linoleic acid (C18:2)	2.58 ± 0.01	2.72 ± 0.12	2.92 ± 0.29	2.63 ± 0.36	2.45 ± 0.16	2.66 ± 0.22
Trans-7-hexadecenoic Acid (C16:1 t7)	1.75 ± 0.20	1.51 ± 0.29	1.56 ± 0.26	1.68 ± 0.17	1.79 ± 0.19	1.65 ± 0.22
Trans-9-dodecenoic acid (C17:1 c10)	1.24 ± 0.10	1.30 ± 0.15	1.32 ± 0.10	1.32 ± 0.15	1.24 ± 0.13	1.28 ± 0.12
Eicosapentaenoic acid (EPA; C20:5 n-3)	0.63 ± 0.03	0.60 ± 0.06	0.71 ± 0.07	0.60 ± 0.12	0.63 ± 0.06	0.63 ± 0.07
Myristoleic acid (C14:1 n-5)	0.16 ± 0.06	0.24 ± 0.05	0.20 ± 0.06	0.24 ± 0.06	0.20 ± 0.01	0.20 ± 0.05
Gondoic acid (C20:1 n-9)	1.67 ± 0.02	1.67 ± 0.03	1.67 ± 0.15	1.71 ± 0.14	1.65 ± 0.04	1.67 ± 0.09

Note: Data are expressed as mean ± SD (% of total fatty acids) for each farm (n = 3), with the total mean ± SD representing all samples combined (N = 15).

DISCUSSION

The physicochemical and nutritional characteristics of camel milk from Garissa County, Kenya, were reported at the farm level, and the descriptive mean values indicated differences between farms. The mean pH (6.63 ± 0.10) was slightly higher than values reported in Ethiopia (6.13 ± 0.11), suggesting a lower acidity that may contribute to extended natural shelf-life by slowing microbial spoilage and delaying coagulation (Legesse et al., 2017). The pale appearance of the milk (L* = 87.8 ± 2.7) corresponded with previous observation in Ethiopia (Seifu, 2023). Titratable acidity (0.14 ± 0.03% lactic acid) was below Moroccan values (0.19%; Alaoui Ismaili et al., 2019), and viscosity (1.86 ± 0.08 mPa·s) was marginally higher than Ethiopian milk (1.78 ± 0.02 mPa·s; Habtegebriel et al., 2020), reflecting desirable consistency for consumer preference. Moisture (87.2 ± 2.9%) and total solids (12.7 ± 0.8%) were within the ranges previously reported in camel milk from the Somali Region of Ethiopia (Legesse et al., 2017), reinforcing the compositional camel milk stability. The differences observed across countries are consistent with those reported in the cited studies, where variation in lactation stage, feeding conditions, and production environment influenced physicochemical traits of camel milk.

Proximate composition demonstrated that Fat averaged (4.20 ± 0.17%), which is higher than the (3.28 ± 0.48) reported in Turkey (Karaman et al., 2022), which may reflect rich forage and mineral availability in Garissa rangelands. Protein averaged (2.3 ± 0.16%), which is lower than the (3.15 ± 0.15%) range described in Ethiopia (Legesse et al., 2017), while Lactose content was (5.1 ± 0.25%), closely matching the (4.81 - 5.02%) recorded in Ethiopia (Seifu, 2023). The observed levels of fat, protein, and lactose contribute to the recognized nutritional value of camel milk and provide baseline composition data that can be used to compare production systems, support quality monitoring, and inform value-addition efforts. The variation in fat and protein compared to Turkey and Ethiopia is consistent with the influence of local forage quality, feed availability, and production system differences described in those studies.

The mineral profile reaffirmed camel milk as an outstanding source of essential micronutrients. Calcium was the most abundant mineral, with a concentration (5293.17 ± 60.1 mg/L), exceeding the mean of 1052 mg/L reported for camel milk across seven regions of Iran (Mostafidi et al., 2016). The higher calcium levels observed in the present study may be attributed to differences in grazing ecology, mineral-rich forage availability, and water quality. The high calcium bioavailability in camel milk is particularly beneficial for bone development in children and maintaining skeletal health in pregnant and lactating women. Zinc and iron averaged 3.9 ± 0.3 mg/l and 4.9 ± 0.3 mg/l, respectively, which were comparable to the 3.99 ± 0.67 mg/l and slightly higher than the 3.77 ± 1.57 mg/l reported in camel milk from China (Yang et al., 2025). Zinc and iron fell within the international ranges for camel milk and are recognized for immunomodulatory and hematological roles, supporting nutritional resilience in arid and semi-arid communities (Yang et al., 2025).

Several other nutritionally important minerals were detected in Garissa camel milk, including Magnesium, sodium, potassium, and phosphorus were all present, supporting essential physiological roles including bone mineralization, electrolyte balance, muscle contraction, and energy metabolism (Mostafidi et al., 2016). Such differences in mineral content between regions have been associated with environmental mineral availability, soil characteristics, and water quality in the reference articles.

For water-soluble vitamins, vitamin C was abundant at 188.7 ± 7.05 mg/L, exceeding the 24-36 mg/l reported in Arabian dromedary camel milk from the United Arab Emirates (Wernery, 2006). The higher vitamin C concentration observed in the present study is likely due to methodological differences and better sample preservation, as vitamin C is highly unstable and rapidly degrades with heat, light exposure, and prolonged storage. The high vitamin C concentration in camel milk reflects camel physiology, where vitamin C supports thermoregulation and oxidative stress defense in hot climates and contributes significantly to daily dietary antioxidant intake. Vitamin B1 (Thiamine) was 3.7 ± 0.1 mg/l, which was markedly higher than the 0.33 - 0.60 mg/l reported in Arabian dromedary camel milk from the United Arab Emirates (Wernery, 2006), highlighting its contribution to energy metabolism. Other B-group vitamins detected included riboflavin (B2), niacin (B3), folate (B9), and cobalamin (B12), supporting energy metabolism, DNA synthesis, red blood cell formation, and neural health (Wernery, 2006). Vitamin B6 was also present, contributing to immune and amino acid metabolism. Among fat-soluble vitamins, vitamin A and vitamin K were found, which are important for immune function, vision, antioxidant activity, bone health, and blood clotting (Wernery, 2006).

The fatty acid profile indicated that palmitic acid (C16:0) was the most prevalent saturated fatty acid at 25.0 ± 2.6%. This was comparable to the 27.9% reported in camel milk from the farming system in Sudan (Mohamed and Mustafa, 2016), supporting energy supply and cell membrane structure.

Oleic acid (C18:1) was the most prevalent unsaturated fatty acid at 27.8 ± 2.7%, which is slightly higher than the 22.44% reported for Sudanese camel milk under farming systems (Mohamed and Mustafa, 2016), contributing to heart health and improved lipid metabolism. In addition, the detection of Long-chain polyunsaturated fatty acids (PUFAs) such as Eicosapentaenoic acid (EPA) averaged 0.6 ± 0.1%, which is considerably higher than the 0.12% reported in camel milk from Sudan under farming and pastoral systems (Mohamed and Mustafa, 2016), particularly in the farming system. Both Oleic acid and Eicosapentaenoic acid (EPA) are recognized for their anti-inflammatory and cardioprotective roles, reinforcing the functional food potential of camel milk (Alhassani, 2024). The fatty acid differences are consistent with previous reports where farming system and diet composition influenced the proportion of major fatty acids in camel milk.

In summary, the present results provide descriptive baseline information for camel milk produced in Garissa County and can support future studies on camel milk composition in Kenya.

CONCLUSION

The present study characterized the physicochemical and nutritional properties of camel milk produced under semi-intensive systems in Garissa County, Kenya. Revealing a consistent composition across farms and alignment with values reported in other camel-producing regions. The results of the present study highlighted the nutritional importance of

camel milk as a reliable food resource for communities in arid and semi-arid environments. The results provide essential baseline data for Kenyan camel milk and can inform nutritional profiling and value-addition initiatives in the dairy sector. However, given the limited number of farms and production systems assessed, further studies covering diverse regions, management practices, and seasonal variations are recommended to better understand the determinants of camel milk variability at a national scale.

DECLARATIONS

Acknowledgments

The authors sincerely thank the Pan African University Institute for Basic Sciences, Technology, and Innovation (PAUSTI), Kenya, and Jomo Kenyatta University of Agriculture and Technology (JKUAT), Kenya, for providing the opportunity, facilities, and institutional support to carry out this research.

Funding

The present study was financially supported by the African Union through the Pan African University Institute for Basic Sciences, Technology, and Innovation (PAUSTI), Kenya. The authors gratefully acknowledge this generous support, which made the successful completion of this study possible.

Author's contributions

Yoonis Dayr Mohamed conceived and designed the study, carried out the laboratory experiments, performed the data analysis, and drafted the manuscript. Prof. Rebecca Waihenya provided overall supervision, ensured the study followed its study objectives, and offered constructive feedback during the study process. Dr. Kenneth Ogila guided the methodological framework and assisted in refining the experimental design, while Dr. Raphael W. Lihana critically reviewed the manuscript and provided technical input for improvement. All authors read and approved the final edition of the manuscript.

Competing interests

The author declares no competing interests.

Ethical considerations

The present study was conducted in accordance with ethical study practices. The manuscript has been thoroughly reviewed to ensure originality, integrity, and compliance with standards, including avoidance of plagiarism, data fabrication, or duplicate submission. The authors confirm that no AI tools were used for data generation, analysis, or interpretation, and the study complies with ethical research and publication standards.

Availability of data and materials

All datasets generated and/or analyzed in this study are included in the manuscript. Additional information can be made available by the corresponding author upon reasonable request.

REFERENCES

Abduku H and Eshetu M (2024). Physico-chemical properties and processing characteristics of camel milk as compared with other dairy species: A review. Asian Journal of Dairy and Food Research, 43(1): 1-7. DOI: https://www.doi.org/10.18805/ajdfr.DRF-303

Ait El Alia O, Zine-Eddine Y, Chaji S, Boukrouh S, Boutoial K, and Faye B (2025). Global camel milk industry: A comprehensive overview of production, consumption trends, market evolution, and value chain efficiency. Small Ruminant Research, 243: 107441. DOI: https://www.doi.org/10.1016/j.smallrumres.2025.107441

Alaoui Ismaili M, Saidi B, Zahar M, Hamama A, and Ezzaier R (2019). Composition and microbial quality of raw camel milk produced in Morocco. Journal of the Saudi Society of Agricultural Sciences, 18(1): 17-21. DOI: https://www.doi.org/10.1016/j.jssas.2016.12.001

Alhassani WE (2024). Camel milk: Nutritional composition, therapeutic properties, and benefits for human health. Open Veterinary Journal, 14(12): 3164-3180. DOI: https://www.doi.org/10.5455/OVJ.2024.v14.i12.2

Association of official analytical collaboration (AOAC) (2016a). Official methods of analysis of AOAC international, 20th Edition. AOAC International, USA. Available at: https://aoac.org/official-methods-of-analysis/

Association of official analytical collaboration (AOAC) (2016b). Official methods of analysis of AOAC international, 20th Edition. AOAC International, USA. Available at: https://aoac.org/official-methods-of-analysis/

Bakry IA, Yang L, Farag MA, Korma SA, Khalifa I, Cacciotti I, Ziedan NI, Jin J, Jin Q, Wei W et al. (2021). A comprehensive review of the composition, nutritional value and functional properties of camel milk fat. Foods, 10(9): 2158. DOI: https://www.doi.org/10.3390/foods10092158

El-Agamy EI, Nawar M, Shamsia SM, Awad S, and Haenlein GFW (2009). Are camel milk proteins convenient to the nutrition of cow milk allergic children? Small Ruminant Research, 82(1): 1-6. DOI: https://www.doi.org/10.1016/j.smallrumres.2008.12.016

El-Hatmi H, Oussaief O, Hammadi I, Dbara M, Hammadi M, Khorchani T, and Jrad Z (2023). Relation between color and chemical composition of dromedary camel colostrum. Animals, 13(3): 442. DOI: https://www.doi.org/10.3390/ani13030442

Faye B (2020). How many large camelids in the world? A synthetic analysis of the world camel demographic changes. Pastoralism: Research, Policy and Practice, 10(25): 1-15. DOI: https://www.doi.org/10.1186/s13570-020-00176-z

Faye B, Konuspayeva G, and Bengoumi M (2019). Vitamins of camel milk: A comprehensive review. Journal of Camelid Science, 12: 17-32. Available at: https://hal.science/hal-05174776v1

Freije A, Abdulghafoor R, Abdulhussain H, Khonji A, Albasara J, Hussain H, Dhaif A, Aljar MA, and Perna S (2024). Analysis of the nutritional composition of Bahraini breed camel (*Camelus dromedarius*) milk: fatty acid, mineral, phenolic, and antioxidant content. Arab Journal of Basic and Applied Sciences, 31(1): 604-613. DOI: https://www.doi.org/10.1080/25765299.2024.2426294

Gebreyohanes MG and Assen AM (2017). Adaptation mechanisms of camels (*Camelus dromedarius*) for desert environment: A review. Journal of Veterinary Science and Technology, 8(6): 1000486. DOI: https://www.doi.org/10.4172/2157-7579.1000486

Habtegebriel H, Wawire M, Gaukel V, and Taboada ML (2020). Comparison of the viscosity of camel milk with model milk systems in relation to their atomization properties. Journal of Food Science, 85(10): 3459-3466. DOI: https://www.doi.org/10.1111/1750-3841.15451

He J, Xiao Y, Orgoldol K, Ming L, Yi L, and Ji R (2019). Effects of geographic region on the composition of bactrian camel milk in Mongolia. Animals, 9(11): 8901. DIO: https://www.doi.org/doi:10.3390/ani9110890

Isako T and Kimindu V (2019). Camel milk value chain in Kenya: A review. Journal of Marketing and Consumer Research, 58: 51- 64. DOI: https://doi.org/10.7176/JMCR/58-06

Karaman AD, Yildiz Akgül F, Öğüt S, Seçilmiş Canbay H, and Alvarez V (2022). Gross composition of raw camel's milk produced in Turkey. Food Science and Technology, 42: e59820. DOI: https://www.doi.org/10.1590/fst.59820

Khaliq A, Mishra AK, Niroula A, Baba WN, Shaukat MN, and Rabbani A (2024). An updated comprehensive review of camel milk: Composition, therapeutic properties, and industrial applications. Food Bioscience, 62: 105531. DOI: https://www.doi.org/10.1016/j.fbio.2024.105531

Konuspayeva G, Faye B, and Bengoumi M (2022). Mineral status in camel milk: A critical review. Animal Frontiers, 12(4): 52-60. DOI: https://www.doi.org/10.1093/af/vfac044

Legesse A, Adamu H, Alamirew N, and Feyera T (2017). A comparative study on the physicochemical parameters of milk of camel, cow and goat in Somali Regional State, Ethiopia. Chemical Sciences Journal, 8(4): 1000171. DOI: https://www.doi.org/10.4172/2150-3494.1000171

Mohamed E and Mustafa A (2016). Fatty acids content in milk of dromedary camel (*Camelus dromedarius*) from farming and pastoral systems in Sudan. International Journal of Science and Research, 5(6): 570-573. DOI: https://www.doi.org/10.21275/v5i6.nov164095

Mostafidi M, Moslehishad M, Piravivanak Z, and Pouretedal Z (2016). Evaluation of mineral content and heavy metals of dromedary camel milk in Iran. Food Science and Technology, 36(4): 717-723. https://www.doi.org//10.1590/1678-457X.16116

Oselu S, Ebere R, and Arimi JM (2022). Camels, camel milk, and camel milk product situation in Kenya in Relation to the World. International Journal of Food Science, 2022: 1237423. DOI: https://www.doi.org/10.1155/2022/1237423

Seifu E (2023). Camel milk products: Innovations, limitations and opportunities. Food Production, Processing and Nutrition, 5(1): 15. DOI: https://www.doi.org/10.1186/s43014-023-00130-7

Wernery U (2006). Camel milk: The white gold of the desert. Journal of Camel Practice and Research, 13(1): 15-26. Available at: https://camelsandcamelids.com

Yang Q, Xu L, Zheng W, Baisanbieke D, Zhu L, and Yimamu M (2025). Geographical variation in the mineral profiles of camel milk from Xinjiang: Implications for nutritional value and species identification. Agriculture, 15(20): 2120. DIO: https://www.doi.org//10.3390/agriculture15202120

Publisher's note: Scienceline Publication Ltd. remains neutral with regard to jurisdictional claims in published maps and institutional affiliations.

Open Access: This article is licensed under a Creative Commons Attribution 4.0 International License, which permits use, sharing, adaptation, distribution and reproduction in any medium or format, as long as you give appropriate credit to the original author(s) and the source, provide a link to the Creative Commons licence, and indicate if changes were made. The images or other third party material in this article are included in the article's Creative Commons licence, unless indicated otherwise in a credit line to the material. If material is not included in the article's Creative Commons licence and your intended use is not permitted by statutory regulation or exceeds the permitted use, you will need to obtain permission directly from the copyright holder. To view a copy of this licence, visit https://creativecommons.org/licenses/by/4.0/.

© The Author(s) 2025

2025, Scienceline Publication
World's Veterinary Journal
World Vet J, 15(4): 929-939.
ISSN 2322-4568

DOI: https://dx.doi.org/10.54203/scil.2025.wvj94
PII: S232245682500094-15

Birth Characteristics of Lambs from Crossbreeding of Dorper and Awassi Rams with Texel Cross Ewes

Asrullah As[1], Muhamad Jayfa Gilang Pratama[1], Tri Eko Susilorini[1], Kuswati Kuswati[1], Wike Andre Septian[1], Chairdin Dwi Nugraha[2], Rafika Febriani Putri[1], Ari Ardiantoro[1], and Suyadi Suyadi[1]*

[1]*Faculty of Animal Science, Brawijaya University, Malang 65145, Indonesia*
[2]*Research Center for Animal Husbandry, National Research and Innovation Agency, Republic of Indonesia (BRIN), Bogor, 16911, Indonesia*
*Corresponding author's Email: suyadi@ub.ac.id

ORIGINAL ARTICLE
Received: September 26, 2025
Revised: October 24, 2025
Accepted: November 30, 2025
Published: December 25, 2025

ABSTRACT

Crossbreeding is an effective strategy to enhance sheep productivity under tropical conditions. This study evaluated the birth characteristics of lambs resulting from crossbreeding Dorper and Awassi rams with Texel cross ewes in Indonesia's tropical environment. The experiment was conducted from April to November 2023 at CV Kambing Burja, Malang Regency, East Java, Indonesia. A total of 125 Texel cross ewes aged 1.5 to over 3 years were naturally mated with 71 Dorper and 54 Awassi rams using a controlled colony mating system at a ram-to-ewe ratio of 1:25. The study employed complete enumeration, including all ewes that successfully lambed during the observation period. Sire groups comprising two to three rams per breed were rotated every 45 days to ensure equal mating opportunities and prevent exhaustion. Estrus synchronization followed a two-step hormonal protocol, including the administration of Conceptase ($PGF_2\alpha$, 2.5 mL/ewe) intramuscularly to induce luteolysis, followed 48 hours later by PG600 (1.5 mL/ewe) containing eCG and hCG to stimulate follicular development and ovulation. Mating behavior was observed daily, with successful copulation indicated by restlessness, vocalization, and receptivity. Measured parameters included birth weight, litter size, and sex ratio. Results showed no significant differences in mean litter size or birth weight between Dorper × Texel cross and Awassi × Texel cross lambs, although Awassi crosses exhibited more uniform birth weights. Birth weight decreased as litter size increased, and sex ratios remained balanced in both groups. These findings suggest that both Dorper and Awassi rams are suitable for enhancing the reproductive performance of Texel cross ewes under tropical management systems, highlighting the importance of integrating hormonal synchronization and controlled breeding for sustainable sheep production in Indonesia.

Keywords: Awassi sheep, Birth weight, Dorper sheep, Litter size, Sex ratio, Texel cross sheep

INTRODUCTION

Sheep play an important role in supporting the livelihoods of smallholder farmers in Indonesia, particularly on the island of Java, which accounted for more than 92% of the national sheep population in both 2022 and 2023, with the majority raised under traditional smallholder farming systems (Badan Pusat Statistik, 2024). Domestic mutton consumption, as reflected by national production, reached 50,702.06 tons in 2021, 52,162.30 tons in 2022, and 52,998.80 tons in 2023, based on livestock slaughter data (Ditjen PKH, 2024). However, the national sheep population in Indonesia has experienced a notable decline, from 17.83 million head in 2019 to 15.62 million head in 2022, primarily due to genetic limitations, traditional management practices, and limited access to modern breeding technologies (Badan Pusat Statistik, 2023). This population decline highlights the urgent need for effective genetic improvement strategies to enhance sheep productivity in Indonesia, such as the implementation of systematic crossbreeding programs to improve genetic potential while maintaining adaptation to local environmental conditions.

Crossbreeding with exotic breeds, particularly Dorper and Awassi sheep, has emerged as a promising approach for genetic improvement in Indonesia. Dorper sheep, developed from Dorset Horn and Blackhead Persian crosses, are known for their superior growth rates and carcass quality. Adult Dorper rams can reach weights of up to 130 kg, while ewes typically weigh between 80 and 110 kg (Milne, 2000; Jannah et al., 2025). Their reproductive performance is notable, with single birth weights averaging around 3.54 ± 0.9 kg for Dorper lambs and 2.99 ± 0.9 kg for F1 Garut × Dorper crossbreds (Jannah et al., 2025). Similarly, Awassi sheep from the Middle East offer valuable multipurpose traits, producing an average of 91 liters of milk per 100-day lactation period even under challenging conditions (Haile et al., 2017). The breed's adaptability to tropical environments and ease of handling make Awassi sheep particularly suitable for crossbreeding programs (Üstüner and Oğan, 2013).

To cite this paper: As A, Pratama MJG., Susilorini TE, Kuswati K, Septian WA, Nugraha CD, Putri RF, Ardiantoro A, and Suyadi S. (2025). Birth Characteristics of Lambs Resulting from Crossbreeding Dorper and Awassi Rams with Texel Cross Ewes. *World Vet. J.*, 15(4): 929-939. DOI: https://dx.doi.org/10.54203/scil.2025.wvj94

Crossbreeding Dorper and Awassi rams with other sheep breeds has been shown to produce progeny with superior traits, including faster growth rates and improved feed efficiency (Wahyudi et al., 2023; Mudawamah, 2024). One of the key aspects of lambing characteristics is birth weight. Previous studies have indicated that lamb birth weight is influenced by genetic and environmental factors, including maternal nutrition during gestation (Boujenane et al., 2015; Magotra et al., 2022; As et al., 2025). Genetic factors such as breed group and heritability play important roles (Amarilho-Silveira et al., 2018; Hagan et al., 2022), while environmental factors such as season and birth type also have significant effects (Hagan et al., 2022). Maternal nutritional supplementation can enhance birth weight and postnatal productivity (Elnageeb and Abdelatif, 2013; McCoard et al., 2017). The birth characteristics of lambs resulting from Dorper rams crossed with Texel ewes demonstrate significant potential for enhancing sheep productivity in Indonesia. By harnessing the genetic advantages of both breeds, farmers can produce sheep with better adaptability and meat quality traits that are highly sought after in the Indonesian sheep industry (Wahyudi et al., 2023; Mudawamah, 2024).

In recent years, Indonesia has actively imported Dorper and Awassi sheep as part of crossbreeding programs aimed at improving the performance of local sheep breeds. In East Java, the majority of the sheep population consists of Local Texel and Texel cross types, which are currently being used in crossbreeding with Dorper or Awassi rams to produce offspring with enhanced productivity traits. Although the benefits of strategic crossbreeding have been well-documented in numerous studies (Getachew et al., 2016; Tesema et al., 2020), limited research has examined the specific interactions between dam age and reproductive parameters in Dorper and Awassi crosses under tropical conditions. For instance, recent field observations suggest differing sex ratio patterns among progeny, including Dorper crossbreeding tends to yield a male-biased ratio (58.5%), whereas Awassi crosses tend to produce more females (56.9%) when mated with Texel Cross ewes (Hudori et al., 2022). However, the combined effects of these genetic factors on key production traits such as birth weight, litter size, and sex ratio remain poorly understood, especially in tropical environments.

These initial observations underscore the complex interactions between genetic factors and physiological responses influenced by sire breed, highlighting the need for more comprehensive research to inform livestock production and management strategies. Therefore, the present study aimed to evaluate the effects of crossbreeding on lambing characteristics, specifically focusing on birth weight and litter size of Texel cross ewes mated with Dorper and Awassi rams under tropical conditions.

MATERIALS AND METHODS

Study location

The study was conducted at CV Kambing Burja, located in Bedali Village, Lawang Subdistrict, Malang Regency, East Java, Indonesia (7°50'20" S, 112°37'50" E). This location was purposefully chosen due to its active sheep breeding programs involving Texel cross ewes and purebred Dorper and Awassi rams. The study was carried out from April to June (dry season) for the mating period, and from September to November (rainy season) for the lambing period. The farm is situated at an altitude of approximately 550 meters above sea level, characterized by a tropical wet climate with an average temperature of 25-30°C and rainfall of 100-200mm per month.

Experimental animals

This study involved 125 crossbred Texel ewes obtained from the breeding flock at CV. Kambing Burja, a commercial sheep farm located in East Java, Indonesia. The sample size represented the entire population of ewes that successfully lambed during the observation period (September-November 2023) and met the inclusion criteria, thereby employing a complete enumeration approach. Due to the limited number of ewes that lambed within this period, random sampling was not applied; instead, all eligible individuals were included in the study. The ewes were between 1.5 and over 3 years of age and were stratified according to parity before being randomly allocated to treatment groups.

Two mature breeding rams were used, including a purebred Dorper ram (± 80 kg, > 2 years old) assigned to 71 ewes, and a purebred Awassi ram (± 80 kg, > 2 years old) assigned to 54 ewes. To maintain breeding efficiency and ensure ram welfare, multiple rams of the same breed were managed under a rotational colony system. Each breeding group comprised 2-3 rams of the same sire line with approximately 25 ewes per pen. Rams within each sire group were rotated every 45 days to provide adequate rest between breeding cycles, ensuring an effective ram-to-ewe ratio, minimizing fatigue, and maintaining high conception rates. Within each parity group, ewes were randomly allocated to either the Dorper or Awassi sire group before estrus synchronization.

Estrus synchronization followed a two-step hormonal protocol to coordinate breeding activity. Conceptase® (cloprostenol sodium, $PGF_2\alpha$; Agrovet Market, Peru) was administered intramuscularly at a dose of 50 µg or 2.5mL/ewe to induce luteolysis (Arroyo-Ledezma et al., 2015; Ramírez et al., 2018). After 48 hours, ewes received PG 600® (MSD Animal Health, USA), containing equine chorionic gonadotropin (eCG; 80 IU/mL) and human chorionic gonadotropin

(hCG; 40 IU/mL), at a dose of 1.5 mL/ewe, to stimulate follicular development and ovulation (Habeeb et al., 2019). This protocol promoted uniform estrus expression across the flock, enabling efficient natural mating within the 45-day breeding period. Mating behavior was monitored daily, and ewes exhibiting estrus signs (restlessness, vocalization, mounting behavior, and receptivity to the ram) were observed for successful copulation.

Management and feeding practices

The flock was managed intensively using a colony housing system with raised wooden floors designed for optimal ventilation and sanitation. The diet consisted of fresh Pakchong grass (Pennisetum purpureum cv. Thailand) offered at 10% of body weight per day, supplemented with a formulated concentrate feed containing 14% crude protein and approximately 3100 kcal/kg of metabolizable energy. The concentrate was composed of locally available ingredients such as cassava cobs, coffee husks, corn, kapok seeds, cassava peels, coconut meal, corn gluten feed (CGF), soybean meal (SBM), distillers dried grains (DDGS), soy sauce residue, iodized salt, lime, sheep premix, molasses, fermented mother liquor (FML), sodium bicarbonate, and pollard. Feed composition was adjusted according to sex and physiological status. Clean drinking water was provided *ad libitum*, and flock health was monitored biweekly.

The mating program followed standard farm procedures with a ram-to-ewe ratio of 1:25. Rams underwent a minimum seven-day conditioning period prior to mating. Both rams and ewes were groomed (hair and hoof trimming) before being placed in mating pens. To enhance reproductive performance, rams received nutritional supplementation with sprouts on day 7 and a traditional herbal mixture (*jamu*) on day 10 of the mating period. The herbal mixture (Indonesia) was formulated in-house by CV Kambing Burja (partner farm) using locally sourced ingredients, including palm sugar, native chicken eggs, garlic, honey, and vitamin E-selenium. Additionally, vitamin supplements were administered to both sexes every 10-14 days during the 45-day mating period. At the end of the mating period, rams were removed and returned to rest pens.

Pregnancy diagnosis was performed by transabdominal ultrasonography at 60- and 75-days post-mating. Confirmed pregnant ewes were transferred to lactation pens, while non-pregnant ewes were re-enrolled in the next breeding cycle. All breeding activities, including mating start and end dates, were systematically recorded.

Data collection

The reproductive traits were measured, including lamb birth weight, litter size, and sex ratio. Birth weights were obtained within 24 hours post-partum using a calibrated digital scale with 0.01 kg precision. Litter size was recorded for each ewe and classified into three categories include single, twin, or triplet births. Lamb sex was determined by visual examination immediately following birth. Meteorological data, including ambient temperature and relative humidity, were collected throughout the study period to evaluate potential environmental influences on reproductive parameters.

Statistical analysis

The observed variables included sex, litter size, and birth weight of lambs from Dorper × Texel cross and Awassi × Texel cross matings. Data were analyzed using Microsoft Excel and SPSS version 26. Descriptive statistics, including mean, standard deviation, and coefficient of variation, were calculated for all variables. Spearman correlation test and Analysis of Variance (ANOVA) with a significance level of $\alpha = 0.05$ were performed to examine the correlation and differences between birth weight and litter size, with differences between treatments further analyzed using the Games-Howell post-hoc test. Independent sample t-tests were conducted to analyze differences in lamb litter size from crossbreeding, birth weight from crossbreeding, and birth weight based on sex. Additionally, a chi-square test was used to evaluate sex ratio distribution among the crossbred progeny.

RESULTS AND DISCUSSION

Litter size

The phenotypes of the Dorper × Texel cross and Awassi × Texel cross progeny are shown in Figure 1. Statistical analysis (Table 1) indicated no significant difference in litter size between Dorper × Texel cross (1.51 ± 0.65) and Awassi × Texel cross (1.56 ± 0.60, $p > 0.05$). The high coefficients of variation were observed between crosses (43.26% and 38.83%, respectively)

Although not statistically significant, the slightly higher litter size observed in Awassi × Texel cross compared to Dorper × Texel cross may reflect breed-specific reproductive characteristics. Awassi sheep have demonstrated superior adaptability and reproductive performance in tropical environments (Haile et al., 2017), whereas Dorper sheep are primarily selected for growth rate and carcass traits rather than prolificacy (Milne, 2000). The litter sizes observed in both crossbreeds exceeded those reported for purebred Dorper (1.40 ± 0.05), Texel (1.25 ± 0.05), and Awassi (1.16 ±

0.01) sheep (Wolf et al., 2014; Gavojdian et al., 2015; Al-Najjar et al., 2022). Comparative studies on Dorper crossbreeding with Indonesian local sheep breeds have shown considerable variation in litter size, ranging from 1.35 to 2.1 across different genetic backgrounds and management systems. The highest litter sizes were observed in Garut sheep × Dorper crosses (1.7-2.1, Lusi et al., 2022) and Javanese local crossbreds (1.92, Hudori et al., 2022), while intermediate values were reported for thin-tailed sheep crosses in Sedan village (1.82, Najmuddin and Nasich, 2019) and West Java (1.79, Najmuddin and Nasich, 2019), fat-tailed sheep crosses (1.61, Sodiq et al., 2011), and Batur sheep crosses (1.55, Sodiq et al., 2011). Lower litter sizes of 1.44 and 1.35 have also been documented in some local sheep crosses (Hudori et al., 2022; Pratama and Siswoyo, 2024).

The average litter size of Texel cross in the current study was lower than that reported by Hakim et al. (2019) for Texel cross sheep in Wonosobo, Central Java, Indonesia (1.45), and by Talebi et al. (2023) for Texel × Moghani F1 sheep in Iran (1.42). It was also lower compared to the findings of Najafabadi et al. (2020) for Texel cross × Romney sheep in New Zealand, which ranged from 1.9 to 2.2. The high coefficients of variation may be influenced by several factors, including dam age, nutritional status, and the genetic potential of individuals within the studied population. Previous studies have reported that dam age and parity affect litter size, with younger ewes more likely to give birth to singletons, while older ewes have a greater likelihood of delivering twins or more (Gavojdian et al., 2013). In addition, environmental factors, such as feed availability and reproductive management, can also impact lambing outcomes (Tesema et al., 2020).



Figure 1. Phenotypic color variations in various sheep crossbreeds in Indonesia. **a:** A Texel cross ewe with white wool and a long tail pattern. **b:** A one-day-old Dorper x Texel cross lamb with a solid black or black-and-white pattern on its head, a pure white body, and a long tail similar to the Texel cross ewe. **c:** A one-day-old Awassi x Texel cross lamb with cream-colored wool, distinctive light brown patches on the head and face, and a long tail pattern resembling the Texel cross ewe (Designed by Authors).

Table 1. Average litter size from crossbreeding Dorper and Awassi rams with Texel cross ewes in Indonesia

Crossbreeding	Number of Ewes	Mean Litter size ± SD	CV (%)[1]
Dorper × Texel cross	71	1.51 ± 0.65	43.26
Awassi × Texel cross	54	1.56 ± 0.60	38.83

[1]CV: Coefficient of Variation, expressing the ratio of the standard deviation to the mean as a percentage, indicating the relative variability of litter sizes within each group. SD: Standard deviation

The crossbreeding program has influenced the genetic variation in reproductive traits, as indicated by the high coefficients of variation (CV) in litter size, ranging from 38.83% to 43.26%. The CV was calculated at the individual ewe level based on litter size per lambing. The reproductive physiology of sheep in tropical environments may differ from that in subtropical regions, potentially affecting hormone secretion patterns and ovulation rates independently of dam age (Notter, 2008; Abdoli et al., 2013). These findings suggest that, under optimal management conditions, the effect of maternal age on reproductive performance may be less pronounced than previously assumed. This highlights the importance of adopting a comprehensive approach in sheep breeding programs that integrates genetic, physiological, and environmental factors.

The high CV observed in this study might be attributed to several interacting factors, including dam age, nutritional status, and the inherent genetic potential of individuals within the population (Ptáček et al., 2017; Kuźnicka et al., 2020; Gaur et al., 2022). Previous studies have reported that parity influences maternal behavior, litter size, and lamb survival, with multiparous ewes exhibiting more nurturing behaviors that lead to better lamb survival rates. Previous studies have reported that dam age and parity significantly influence litter size, with younger ewes more likely to produce single lambs, while older ewes have a higher probability of multiple births (Gavojdian et al., 2013; Lv et al., 2016). Moreover, environmental conditions such as feed quality, reproductive management, and climate stress can further influence lambing outcomes (Safari et al., 2005; Tesema et al., 2020). Overall, the results indicate that crossbreeding Dorper and Awassi rams with Texel cross ewes produces comparable litter sizes but with a high degree of variability. Therefore,

strategic breeding design combined with optimized nutritional and reproductive management is essential to enhance reproductive efficiency and improve sheep production performance under tropical conditions in Indonesia. Birth weight. The statistical analysis (Table 2) showed no significant difference in overall birth weight between the two crossbreeding groups, Dorper × Texel and Awassi × Texel ($p > 0.05$). The high CV (36.93% and 30.39%) indicates considerable variability in birth weight within both crossbreeding types.

Table 2. Average birth weight from crossbreeding Dorper and Awassi rams with Texel cross ewes in Indonesia

Crossbreeding	Number of Lambs	Mean Birth Weight (kg) ± SD	CV (%)[1]
Dorper × Texel cross	107	2.26 ± 0.84	36.93
Awassi × Texel cross	84	2.46 ± 0.75	30.39

[1]CV: Coefficient of Variation, expressing the ratio of the standard deviation to the mean as a percentage, indicating the relative variability of litter sizes within each group. SD: Standard deviation

The comparison of average birth weights from crossbreeding Dorper and Awassi rams with Texel cross ewes provides insight into lamb growth performance. Studies by McGovern et al. (2020) and Abebe et al. (2023) revealed that lamb birth weight varies due to genetic factors, management practices, and climatic conditions. The study by Athifa et al. (2022) on post-weaning growth of lambs from Garut ewes crossed with Dorper rams indicated that Dorper genetics contribute positively to growth traits, reflected in both birth weight and average body weight (ABW). Environmental factors indeed influence growth traits in both Dorper and Awassi sheep. Studies have shown that factors such as year of birth, birth season, maternal effects, and management practices significantly affect growth performance in these breeds (Aljubouri et al., 2020; Besufkad et al., 2023; Jannah et al., 2025; Haddad et al., 2025). Getahun et al. (2019) and Kao et al. (2022) investigated the effects of heterosis in crossbred sheep, finding that hybrid vigor contributed to higher birth weights compared to weaning weights in various Awassi crossbreeding scenarios.

In the present study, lambs from Awassi crosses showed a higher birth weight (2.46 ± 0.75 kg) than those from Dorper crosses (2.26 ± 0.84 kg) when bred with Texel cross ewes (Table 2). This difference reflects the genetic characteristics of Awassi sheep, which exhibit superior maternal traits and enhanced fetal growth potential. Although Dorper sheep possess genetic advantages for post-natal growth and meat production, they tend to produce lower birth weights compared to Awassi sheep (Athifa et al., 2022), possibly due to breed-specific differences in placental development and maternal resource allocation (Özyürek, 2020; Daş et al., 2022).

The lower CV observed in Awassi crosses (30.39%) compared to Dorper crosses (36.93%) indicates more uniform birth weights in lambs from Awassi crosses. This greater uniformity reflects the consistent reproductive performance and enhanced maternal capacity of Awassi sheep under optimal management conditions (Alamer and Al-Hozab, 2004; Talafha and Ababneh, 2011).

Al-Thuwaini and Al-Hadi (2022) highlighted the critical role of maternal body condition in lamb growth, pointing to the need for further studies in sheep farming under tropical conditions. Several interconnected factors within the production system may explain the lack of statistically significant differences. Controlled feeding practices at the research site, regular provision of Pakchong grass (10% of body weight) and concentrate feed (14% crude protein) likely ensured equivalent nutritional status across all crossbred groups and age classes. These ideal nutritional conditions allowed younger ewes to overcome physical limitations, thereby supporting fetal development as effectively as older ewes.

The relatively high CV reflects the genetic diversity present in the Texel crossbred population. The controlled farming conditions, an elevation of 550 meters, ambient temperatures between 25-30°C, and carefully timed breeding (mating during the dry season from April to June, and lambing during the rainy season from September to November) provided an optimal environment for all ewes regardless of age. Under these favourable conditions, young ewes may compensate for their physical immaturity through more efficient nutrient utilization, better environmental adaptability, and optimal placental development, aligning with the findings of McGovern et al. (2020) regarding the interaction between environmental factors and maternal physiology.

Birth weight based on litter size

Based on the data presented in Table 3, single births produce the highest birth weight, followed by twin births and triplets. Additionally, there are differences in lamb birth weights based on litter size from crossbreeding Dorper and Awassi rams with Texel cross ewes. In the Dorper × Texel cross, birth weights of lambs with litter sizes 1 and 2 show no significant difference ($p > 0.05$), but both differ significantly from litter size 3, which has a lower birth weight ($p < 0.05$). A similar pattern was observed in the Awassi × Texel cross, where birth weights of lambs with litter size 1 differ significantly from both litter sizes 2 and 3 ($p < 0.05$).

Table 3. Average birth weight based on litter size, average litter size from crossbreeding Dorper and Awassi Rams with Texel cross ewes in Indonesia

Crossbreeding	Litter size	Mean birth weight (kg) ± SD	Number of lambs	CV (%)[1]
Dorper × Texel cross	1	2.58 ± 0.77[a]	41	30.03
	2	2.30 ± 0.53[a]	48	22.92
	3	1.45 ± 0.15[b]	18	10.12
Awassi × Texel cross	1	2.95 ± 0.62[a]	27	20.91
	2	2.36 ± 0.28[b]	48	11.90
	3	1.49 ± 0.19[c]	9	12.83

[1]CV: Coefficient of Variation, expressing the ratio of the standard deviation to the mean as a percentage, indicating the relative variability of litter sizes within each group. [a,b,c] Different superscript letters within the same column indicate significant differences ($p < 0.05$). SD: Standard deviation.

The coefficient of variation (CV), ranging from 10.12% to 30.03%, indicates moderate to high variability in the birth weight of lambs resulting from these crossbreeding programs. Birth weights based on litter size show a significant negative correlation in both Dorper × Texel cross and Awassi × Texel cross groups ($p < 0.05$). Birth weight demonstrates a decreasing trend with increasing litter size, where lambs from single births exhibit the highest average birth weight, followed by twins, and triplets showing the lowest birth weight. This inverse relationship, where single-born lambs are significantly heavier than twins and triplets, is consistent with the findings of Şahin et al. (2022), Al-Janabi et al. (2023), and Aksoy et al. (2023) ($p < 0.05$). This pattern is primarily attributed to intrauterine nutrient competition, as emphasized by Gaur et al. (2021). Single-born lambs benefit from greater placental resource allocation, resulting in higher birth weights. Studies conducted in various tropical regions consistently show an inverse relationship between litter size and birth weight. Pinheiro et al. (2020) in Brazil reported that single births resulted in higher birth weights compared to multiple births due to reduced competition for maternal resources. Furthermore, the relationship between litter size and birth weight has been widely studied, with findings indicating that as litter size increases, the average weight of individual lambs tends to decrease because of the shared maternal resources during gestation (Mellado et al., 2016).

The findings of the current study, which show a clear difference in birth weight between single and multiple births (2.58 ± 0.77 kg vs. 2.30 ± 0.53 kg in the Dorper cross), are in line with the study of Rather et al. (2020). That study demonstrated that lambs born as singletons had significantly higher birth weights compared to twins or triplets. In the present study, single and twin births differed significantly from triplet births in terms of birth weight ($p < 0.05$), reinforcing that litter size is a major factor influencing birth weight and early growth performance. In a comparative context, Prakash et al. (2017) noted that although the average litter size in their study was lower than in the present findings, they also observed a decrease in birth weight with increasing litter size, supporting the generalizability of this trend across different breeds and environments. Additionally, the study by Momoh et al. (2013) emphasized that birth type, whether single or multiple, significantly affects both birth weight and subsequent growth performance, which corroborates the results of the present study. Moreover, Chay-Canul et al. (2019) highlighted those environmental conditions and maternal health significantly influence birth outcomes.

The tropical climate plays a crucial role in birth weight patterns. Robertson and Friend (2022) demonstrated that high temperatures and heat stress can impair fetal development, reduce lamb birth weight, and increase perinatal lamb mortality. Heat stress above 32°C can significantly impact reproductive performance, including increased embryonic mortality and reduced birth weight. Gemiyo et al. (2014) and Oke et al. (2021) further noted that higher temperatures intensify the effects of intrauterine competition in multiple pregnancies, highlighting the critical relationship between climate and reproductive outcomes in tropical livestock production. Multiple factors influence lamb birth weight beyond litter size, including maternal nutrition, maternal characteristics, and environmental conditions. Boujenane and Diallo (2017) found that single lambs benefit from enhanced nutrient access throughout pre- and postnatal development. Habtegiorgis et al. (2022) identified additional factors, including ewe parity, management practices, and seasonal variations, noting increased litter sizes during dry seasons and higher birth weights during rainy seasons. Long-term selection programs have proven effective in improving both litter size and birth weight across generations (Habtegiorgis et al., 2022; Jimma et al., 2025), emphasizing the importance of proper management and adequate feeding, particularly for high-parity ewes and multiple births.

Birth weight based on sex

Based on the data in Table 4, the chi-square analysis of the sex ratio in crossbred lambs showed a χ^2 value of 0.234 ($p = 0.234$) for Dorper × Texel cross (52% male; 48% female) and χ^2 value of 0.762 ($p = 0.762$) for Awassi × Texel cross (45% male; 55% female). While these differences were not statistically significant ($p > 0.05$), the contrasting patterns between the two crossbreeds warrant further discussion. The Dorper crosses' tendency toward male offspring and Awassi crosses' inclination toward female offspring may be attributed to several underlying factors related to breed characteristics and physiological mechanisms.

Table 4. Average birth weight based on sex from crossbreeding Dorper and Awassi rams with Texel cross ewes in Indonesia

Crossbreeding	Sex	Number of lambs (%)	Mean birth weight (kg) ± SD	CV (%)[1]
Dorper × Texel cross	Male	56 (52%)	2.22 ± 0.79	38.38
	Female	51 (48%)	2.30 ± 0.88	35.7
Awassi × Texel cross	Male	38 (45%)	2.42 ± 0.66	27.14
	Female	46 (55%)	2.49 ± 0.82	32.96

CV: Coefficient of Variation, expressing the ratio of the standard deviation to the mean as a percentage, indicating the relative variability of litter sizes within each group. SD: Standard deviation.

In the Dorper crossbreeding program, the higher proportion of male offspring (52%) aligned with the findings of Zülkadir and Karabacak (2013), who reported a similar male-biased sex ratio in meat-type sheep breeds. This bias may be linked to the selection history of the Dorper breed for meat production traits, which could influence sex determination mechanisms (Zonabend König et al, 2017; Selala and Tyasi, 2022). The larger body size and higher muscle mass typical of Dorper rams may affect sperm motility patterns or the survivability of Y chromosome-bearing spermatozoa. Similar observations were reported by Al-Thuwaini and Al-Hadi (2022), who noted a correlation between ram breed type and offspring sex ratio in meat-focused breeding programs.

In contrast, the tendency for Awassi crossbreeding to produce a higher proportion of female offspring (55%) presents an interesting contrast that may be associated with its characteristics as a dairy breed. This pattern has been observed in other dairy sheep breeds as well, as reported by Boujenane and Diallo (2017), who found a slight female bias in crossbreeding programs oriented toward milk production. The physiological basis for this bias may involve differences in placental development, maternal recognition of pregnancy, or hormone profiles typical of dairy breeds. However, it is important to note that the differences in sex ratios observed in the present study were not statistically significant ($\chi^2 = 0.762$, $p > 0.05$), indicating that other factors may be influencing sex determination.

Variations in sex ratio distribution patterns may also be influenced by environmental and management factors (Gootwine, 2011; Casellas et al., 2023). Temperature, nutrition, and breeding season have been shown to affect the sex ratio in sheep, as documented by Thompson et al. (2021). The timing of mating during the dry season (April–June) may interact differently with the physiological characteristics of Dorper and Awassi rams, potentially affecting sex ratio outcomes. Additionally, factors such as ram age, semen quality, ejaculation frequency, and scrotal circumference may also contribute to these patterns, as suggested by Martínez-Velázquez et al. (2003).

A review of previous studies revealed inconsistent findings regarding breed-specific sex ratios in sheep. While some researchers have reported similar breed-based patterns (Al-Thuwaini and Al-Hadi, 2022), others have found no consistent relationship between breed type and offspring sex ratio (Casellas et al., 2023). This variability suggests that sex determination is a complex trait influenced by genetic, environmental, and management factors. Studies show low heritability for sex ratio in sheep breeds, indicating limited genetic influence (Kumar et al., 2021), though selecting sires with sex-specific tendencies may help skew ratios. Environmental conditions significantly impact sex ratios. Ewes fed diets high in omega-6 fatty acids have been shown to produce a higher proportion of female offspring, suggesting that dietary composition can directly influence lamb sex ratios (Laleva et al., 2022). In addition, seasonal variations have also been reported to affect these outcomes (Casellas et al., 2023). Future research should focus on larger sample sizes and multiple breeding seasons to better understand these mechanisms. The practical implications of these findings for breeding programs should be carefully considered. Although the observed differences in sex ratios were not statistically significant, understanding breed-specific tendencies may help farmers better plan their breeding strategies, especially when a specific sex ratio is desired for production or flock replacement purposes. However, further studies are needed to confirm whether these patterns can be consistently reproduced across different environments and management systems.

CONCLUSION

This study demonstrated that crossbreeding Dorper and Awassi rams with Texel cross ewes can enhance sheep productivity by optimizing birth weight and litter size. Although litter size did not differ significantly between the two crossbreeds, lambs from Awassi × Texel cross had higher and more uniform birth weights than those from Dorper × Texel Cross. A negative correlation was observed between litter size and birth weight, indicating that birth weight decreased as litter size increased. The sex ratio analysis showed contrasting tendencies, with Dorper producing more males and Awassi more females, though differences were not statistically significant. These findings highlight the need to optimize breeding strategies and management practices in Indonesia's smallholder systems to improve reproductive efficiency through selective mating and targeted nutrition for pregnant ewes. Future studies should investigate multi-generational performance, sex ratio mechanisms, economic viability, genotype and environment interactions, and nutritional interventions to enhance lamb survival and productivity.

DECLARATIONS

Funding

The funding was provided through the PMDSU (Pendidikan Magister menuju Doktor untuk Sarjana Unggul) scholarship under the Basic Research PMDSU scheme 2025.

Availability of data and materials

The data to support the present study's findings are available upon reasonable request to the corresponding author.

Ethical considerations

This study was prepared according to the guidelines of the WVJ journal and is free from plagiarism and has not been submitted to any other journal. The authors did not use any AI applications during conducting the study, performing the procedures and finally writing the manuscript.

Authors' contributions

Asrullah As, Suyadi, Tri Eko Susilorini, and Kuswati conceptualized the study, developed the methodology, provided resources, and supervised the study. Asrullah As, Ari Ardiantoro, Rafika Febriani Putri, and Muhamad Jayfa Gilang Pratama conducted the investigation and visualized the data. Asrullah As and Suyadi wrote the original manuscript. Wike Ande Septian and Chairdin Dwi Nugraha revised the manuscript. All authors agreed to the final version of the manuscript. No AI was used to conduct the current study.

Competing interests

The authors declare that there are no conflicts of interest regarding the publication of this article.

Acknowledgements

The authors gratefully acknowledge the members of the Animal Biotechnology Research Group Laboratory, Faculty of Animal Science, Brawijaya University. The authors would like to thank the Directorate General of Higher Education, the Ministry of Education, Culture, Research, and Technology, for providing funding through the Basic Research PMDSU scheme 2025, and CV. Kambing Burja for facilitating this research.

REFERENCES

Abdoli R, Zamani P, Deljou A, and Rezvan H (2013). Association of BMPR-1B and GDF9 genes polymorphisms and secondary protein structure changes with reproduction traits in Mehraban ewes. Gene, 524(2): 296-303. DOI: https://www.doi.org/10.1016/j.gene.2013.03.133

Abebe A, Berhane G, Getachew T, Gizaw S, and Haile A (2023). Reproductive performance and productivity of local and Dorper x local crossbred ewes under community-based management system, Ethiopia. Heliyon, 9(9): e19906. DOI: https://www.doi.org/10.1016/j.heliyon.2023.e19906

Aksoy Y, Şekeroğlu A, Duman M, and Çoban ÖB (2023). A study on the determination of some reproductive traits of ewes and the growth performance of Akkaraman lambs raised under farm conditions in Niğde Province. Turkish Journal of Agriculture–Food Science and Technology, 11(6): 1168-1175. DOI: https://www.doi.org/10.24925/turjaf.v11i6.1168-1175.5991

Aksoy Y, Ulutas Z, Sen U, Sirin E, and Sahin A (2023). Genetic parameters for direct and maternal effects on growth traits in lambs. Small Ruminant Research, 223: 106952. DOI: https://www.doi.org/10.1016/j.smallrumres.2023.106952

Alamer M and Al-Hozab A (2004). Effect of water deprivation and season on feed intake, body weight and thermoregulation in Awassi and Najdi sheep breeds in Saudi Arabia. Journal of Arid Environments, 59(1): 71-84. DOI: https://www.doi.org/10.1016/j.jaridenv.2004.01.003

Al-Janabi YAA, Habeeb HMH, and Al-Qasimi RH (2023). Effect of breed on some production traits and reproductive traits of local sheep. IOP Conference Series: Earth and Environmental Science, 1262(7): 072096. DOI: https://www.doi.org/10.1088/1755-1315/1262/7/072096

Aljubouri TRS, Al-Shuhaib MBS, and Javadmanesh A (2020). HMGA2 gene polymorphisms and their effects on main growth traits indices in Awassi and Karakul sheep. Agriculture and Natural Resources, 54(6): 587-594. DOI: https://www.doi.org/10.34044/j.anres.2020.54.6.03

Al-Najjar K, Al-Momani AQ, Al-Yacoub AN, Elnahas A, and Elsaid R (2022). Estimation of genetic parameters and non-genetic factors for milk yield and litter size at birth of Awassi sheep in Drylands. Egyptian Journal of Sheep and Goats Sciences, 17(1): 19-26. DOI: https://www.doi.org/10.21608/ejsgs.2022.266898

Al-Thuwaini TM and Al-Hadi ABA (2022). Association of lamb sex with body measurements in single and twin Awassi ewes. Advances in Animal and Veterinary Sciences, 10(8): 1849-1853. DOI: https://www.doi.org/10.17582/journal.aavs/2022/10.8.1849.1853

Amarilho-Silveira F, Dionello NJL, Mendonça GD, Motta JF, Fernandes TA, and Silva NDS (2018). Genetic components of birth weight of Texel sheep reared in extensive system. Acta Scientiarum. Animal Sciences, 40: e36481. DOI: https://www.doi.org/10.4025/actascianimsci.v40i1.36481

Arroyo-Ledezma J, Hernández-López J, Ávila-Serrano NY, and Camacho-Escobar MA (2015). Estrus response and hormonal profile in hair sheep synchronized with short prostaglandin protocols. Agrociencia, 49(5): 475-482. Available at: https://share.google/ZFEVtV65N5xDrdO6m

As A, Purwoagung AS, Susilorini TE, Septian WA, Nugraha CD, Putri RF, Ardiantoro A, and Suyadi S (2025). The effect of ewe age on birth weight and litter size of Texel cross sheep mated with Dorper and Awassi rams. Advances in Animal and Veterinary Sciences, 13(8): 1672-1680. DOI: https://www.doi.org/10.17582/journal.aavs/2025/13.8.1672.1680

Athifa IR, Aprilianna PZNLS, Budisatria I, Maharani D, Bintara S, Noor YG, and Hidayat R (2022). The pre-weaning growth of lambs from crossbreeding between Garut ewes and Dorper rams. Biodiversitas: Journal of Biological Diversity, 23(11): 5125-5132. DOI: https://www.doi.org/10.13057/biodiv/d231125

Badan pusat statistik (2023). Populasi Ternak Kambing, Domba, Babi Menurut Kabupaten/Kota dan Jenis Ternak di Provinsi Jawa Timur (Ekor), 2021 dan 2022 [Goat, sheep, and pig population by regency/city and livestock type in East Java Province (Heads), 2021 and 2022]. Available at: https://jatim.bps.go.id/id/statistics-table/1/MjYwMiMx/-populasi-ternak-kambing-domba-babi-menurut-kabupaten-kota-dan-jenis-ternak-di-provinsi-jawa-timur-ekor-2021-dan-2022.html

Badan pusat statistik (2024). Populasi Domba menurut Provinsi (Ekor), 2021-2023 [Sheep population by province (Heads), 2021-2023]. Available at: https://www.bps.go.id/id/statistics-table/2/NDczIzI=/populasi-domba-menurut-provinsi.html

Besufkad S, Goshme S, Abebe A, Bisrat A, Abebe A, Zewdie T, Areaya A, Mekonnen T, Eshete M, and Getachew T (2023). Genetic evaluation of growth rate and efficiency-related traits in Dorper sheep. Ecological Genetics and Genomics, 28: 100186. DOI: https://www.doi.org/10.1016/j.egg.2023.100186

Boujenane I and Diallo IT (2017). Estimates of genetic parameters and genetic trends for pre-weaning growth traits in Sardi sheep. Small Ruminant Research, 146: 61-68. DOI: https://www.doi.org/10.1016/j.smallrumres.2016.12.002

Boujenane I, Chikhi A, Ibnelbachyr M, and Mouh FZ (2015). Estimation of genetic parameters and maternal effects for body weight at different ages in D'man sheep. Small Ruminant Research, 130: 27-35. DOI: https://www.doi.org/10.1016/j.smallrumres.2015.07.025

Casellas J, Vázquez-Gómez M, Id-Lahoucine S, and de Hijas-Villalba MM (2023). Evidential segregation analysis for offspring sex ratio in rabbit and sheep populations. Livestock Science, 277: 105354. DOI: https://www.doi.org/10.1016/j.livsci.2023.105354

Chay-Canul AJ, Aguilar-Urquizo E, Parra-Bracamonte GM, Piñeiro-Vazquez ÁT, Sanginés-García JR, Magaña-Monforte JG, García-Herrera RA, and López-Villalobos N (2019). Ewe and lamb pre-weaning performance of Pelibuey and Katahdin hair sheep breeds under humid tropical conditions. Italian Journal of Animal Science, 18(1): 850-857. DOI: https://www.doi.org/10.1080/1828051x.2019.1599305

Daş A, Kahraman M, Güngören G, Daş B, and Boyraz M (2022). Yarı entansif şartlarda yetiştirilen ivesi ırkı koyunlarda süt verimi ve süt kalite özellikleri [Milk yield and milk quality characteristics of Awassi sheep raised under semi-intensive conditions]. Journal of Advances in VetBio Science and Techniques, 7(1): 62-71. DOI: https://www.doi.org/10.31797/vetbio.1000968

Direktorat Jenderal Peternakan dan Kesehatan Hewan (Ditjen PKH) (2024). Buku statistik peternakan dan kesehatan hewan 2023 [Livestock and animal health statistics book 2023]. Kementerian Pertanian, Direktorat Jenderal Peternakan dan Kesehatan Hewan, Jakarta [Ministry of Agriculture, Directorate General of Livestock and Animal Health, Jakarta], p. 128. Available at: https://satudata.pertanian.go.id/assets/docs/publikasi/Buku_Statistik_2023_ISSN.pdf

Elnageeb ME and Abdelatif AM (2013). Growth, thermoregulation, and hematological responses of lambs in relation to age and maternal nutritional supplementation. Journal of Biological Sciences, 13(5): 323-331. DOI: https://www.doi.org/10.3923/jbs.2013.323.331

Gaur P, Malik ZS, Bangar YC, Magotra A, and Yadav AS (2022). Genetic and non-genetic effects associated with ewe productivity in Harnali sheep. Zygote, 30(3): 386-390. DOI: https://www.doi.org/10.1017/S0967199421000897

Gaur P, Malik ZS, Bangar YC, Magotra A, Chauhan A, and Yadav DK (2021). Influence of maternal and additive genetic effects on lamb survival in Harnali sheep. Journal of Animal Breeding and Genetics, 139(2): 204-214. DOI: https://www.doi.org/10.1111/jbg.12655

Gavojdian D, Budai C, Cziszter LT, Csizmar N, Javor A, and Kusza S (2015). Reproduction efficiency and health traits in Dorper, White Dorper, and Tsigai sheep breeds under temperate European conditions. Asian-Australasian Journal of Animal Sciences, 28(4): 599-603. DOI: https://www.doi.org/10.5713/ajas.14.0659

Gavojdian D, Cziszter L, Păcală N, and Sauer M (2013). Productive and reproductive performance of Dorper and its crossbreds under a Romanian semi-intensive management system. South African Journal of Animal Science, 43(2): 219-228. DOI: https://www.doi.org/10.4314/sajas.v43i2.12

Gemiyo D, Abebe G, and Tegegne A (2014). Influences of non-genetic factors on early growth of Adilo lambs under smallholder management systems, southern Ethiopia. Tropical Animal Health and Production, 46(2): 323-329. DOI: https://www.doi.org/10.1007/s11250-013-0490-4

Getachew T, Haile A, Wurzinger M, Rischkowsky B, Gizaw S, Abebe A, and Sölkner J (2016). Review of sheep crossbreeding based on exotic sires and among indigenous breeds in the tropics: An Ethiopian perspective. African Journal of Agricultural Research, 11(11): 901-911. DOI: https://www.doi.org/10.5897/ajar2013.10626

Getahun D, Alemneh T, Akeberegn D, Getabalew M, and Zewdie D (2019). Importance of hybrid vigor or heterosis for animal breeding. Biochemistry and Biotechnology Research, 7(1): 1-4. Available at: https://www.netjournals.org/z_BBR_19_021.html

Gootwine E (2011). Husbandry of dairy animals: Sheep reproductive management. Encyclopedia of dairy sciences, 2nd Edition, pp. 887-892. DOI: https://www.doi.org/10.1016/B978-0-12-374407-4.00243-0

Habeeb HMH, Hazzard TM, Stormshak F, and Kutzler MA (2019). Effect of different dosages of PG-600 on ovulation and pregnancy rates in ewes during the breeding season. Translational Animal Science, 3(1): 429-432. DOI: https://www.doi.org/10.1093/tas/txy112

Habtegiorgis K, Haile A, Getachew T, Jimma A, and Gemiyo D (2022). Litter size, litter weight, and lamb survivability of Doyogena sheep managed under a community-based breeding program in Ethiopia. Heliyon, 8(11): e11576. DOI: https://www.doi.org/10.1016/j.heliyon.2022.e11576

Haddad NZ, Salim AH, and Al-Emarah M (2025). Effect of genetic group and sex on lamb growth characteristics in local and Turkish Awassi sheep in Iraq. IOP Conference Series: Earth and Environmental Science, 1487(1): 012171. DOI: https://www.doi.org/10.1088/1755-1315/1487/1/012171

Hagan BA, Salifu S, Asumah C, Yeboah ED, and Boa-Amponsem K (2022). Effects of genetic and non-genetic factors on body weight, pre-weaning growth, birth type and pre-weaning survivability of lambs in a sheep nucleus station. Department of Animal Production and Health, 34(4): 30. Available at: https://www.lrrd.cipav.org.co/lrrd34/4/3430bern.html

Haile A, Hilali M, Hassen H, Rekik M, Lobo RNB, Tibbo M, Mwacharo JM, and Rischkowsky B (2017). Evaluation of Awassi sheep genotypes for growth, milk production, and milk composition. Journal of Experimental Biology and Agricultural Sciences, 5(1): 68-75. DOI: http://www.doi.org/10.18006/2017.5(Spl-1-SAFSAW).S68.S75

Hakim FR, Arifin M, and Rianto E (2019). Growth pattern and productivity of female Wonosobo sheep in Wonosobo District, Central Java Province, Indonesia. IOP Conference Series: Earth and Environmental Science, 247(1): 012044. DOI: https://www.doi.org/10.1088/1755-1315/247/1/012044

Hudori HA, Pratama FEA, Andini P, Cnawp RP, and Chairina RL (2022). Produktivitas peternakan domba menggunakan sistem kawin alam di CV Gumukmas Multi Farm Kabupaten Jember [Productivity of sheep farming using natural mating system at CV Gumukmas Multi Farm, Jember Regency]. Conference of Applied Animal Science Proceeding Series, 3: 42-46. DOI: https://www.doi.org/10.25047/animpro.2022.335

Jannah ZN, Panjono P, Amrullah AHK, Atmoko BA, Aslimah S, Warman AT, Hudaya MF, Hikmah BTN, Sudarman A, and Ibrahim A (2025). Synergizing reproductive efficiency and growth performance: A large-scale evaluation of Dorper× Garut crossbreeding in Indonesian sheep. Veterinary World, 18(10): 2934-2944. DOI: https://www.doi.org/10.14202/vetworld.2025.2934-2944

Jimma A, Melesse A, Haile A, and Getachew T (2025). Exploring genetic parameters and correlations among growth, reproductive, and survival traits in Doyogena sheep. Advances in Agriculture, 2025(1): 6658918. DOI: https://www.doi.org/10.1155/aia/6658918

Kao MA, Van Wyk JB, Scholtz AJ, Cloete JJE, Matebesi PA, and Cloete SWP (2022). Breed and crossbreeding effects on growth, fitness and reproduction of commercial sheep in South Africa. Small Ruminant Research, 212: 106705. DOI: https://www.doi.org/10.1016/j.smallrumres.2022.106705

Kumar A, Misra, SS, Sharma, RC, and Gowane, GR (2021). Genetic parameters for sex ratio in an organised sheep farm. Indian Journal of Small Ruminants, 27(1): 31-36. DOI: https://www.doi.org/10.5958/0973-9718.2021.00014.3

Kuźnicka E, Kunowska-Slósarz M, and Gabryszuk M (2020). The ovulation rate, plasma leptin concentration, and litter size of a local ewe breed kept in a barn versus those kept under an overhead shelter. Agriculture, 10(9): 403. DOI: https://www.doi.org/10.3390/agriculture10090403

Laleva S, Slavova P, Ivanova T, Kalaydzhiev G, Popova Y, Slavova S, Ivanov N, and Metodiev N (2022). Study of the influence of some genetic and non-genetic factors on the productive performance of Ile de France ewes. Journal of Hygienic Engineering and Design, 39: 197-201. DOI: https://www.doi.org/10.13140/RG.2.2.10664.85763

Lusi D, Yurmiati H, and Ramdani D (2022). Pengaruh sistem pemeliharaan terhadap produktivitas induk domba Garut [Effect of rearing system on productivity of Garut ewes]. Journal of Applied Animal Production, 3(2): 73-79. DOI: https://www.doi.org/10.24198/jptt.v3i2.42288

Lv SJ, Yang Y, and Li FK (2016). Parity and litter size effects on maternal behavior of small Tail Han sheep in China. Animal Science Journal, 87(3): 361-369. DOI: https://www.doi.org/10.1111/asj.12441

Magotra A, Bangar YC, Chauhan A, Yadav AS, and Malik ZS (2022). Impact of mother genetic and resource environment on her offspring's growth features in Munjal sheep. Zygote, 30(4): 495-500. DOI: https://www.doi.org/10.1017/S096719942100085X

Martínez-Velázquez G, Gregory KE, Bennett GL, and Van Vleck LD (2003). Genetic relationships between scrotal circumference and female reproductive traits. Journal of Animal Science, 81(2): 395-401. DOI: https://www.doi.org/10.2527/2003.812395x

McCoard S A, Sales F A, and Sciascia, QL (2017). Invited review: Impact of specific nutrient interventions during mid-to-late gestation on physiological traits important for survival of multiple-born lambs. Animal, 11(10): 1727-1736. DOI: https://www.doi.org/10.1017/S1751731117000313

McGovern F M, McHugh N, Fitzmaurice S, Pabiou T, McDermott K, Wall E, and Fetherstone N (2020). Phenotypic factors associated with lamb live weight and carcass composition measurements in an Irish multi-breed sheep population. Translational Animal Science, 4(4): txaa206. DOI: https://www.doi.org/10.1093/tas/txaa206

Mellado M, Macías U, Avendaño L, Mellado J, and García J (2016). Growth and pre-weaning mortality of Katahdin lamb crosses. Revista Colombiana de Ciencias Pecuarias, 29(4): 288-295. DOI: https://www.doi.org/10.17533/udea.rccp.v29n4a06

Milne C (2000). The history of the Dorper sheep. Small Ruminant Research, 36(2): 99-102. DOI: https://www.doi.org/10.1016/S0921-4488(99)00154-6

Momoh OM, Rotimi EA, and Dim NI (2013). Breed effect and non-genetic factors affecting growth performance of sheep in a semi-arid region of Nigeria. Journal of Applied Biosciences, 67: 5302-5307. DOI: https://www.doi.org/10.4314/jab.v67i0.95053

Mudawamah M (2024). Profil dan estimasi ripitabilitas pertambahan bobot badan domba Texel sebagai dasar culling [Profile and repeatability estimation of body weight gain in Texel sheep as a basis for culling]. Jurnal Sains dan Teknologi Industri Peternakan, 4(2): 37-43. DOI: https://www.doi.org/10.55678/jstip.v4i2.1466

Najafabadi AH, Khansefid M, Mahmoud GG, Zhou H, and Hickford JG (2020). Identification of polymorphisms in the oocyte-derived growth differentiation factor 9 (GDF9) gene associated with litter size in New Zealand sheep (*Ovis aries*) breeds. Reproduction in Domestic Animals, 55(11): 1585-1591. DOI: https://www.doi.org/10.1111/rda.13813

Najmuddin M and Nasich M (2019). Produktivitas induk domba ekor tipis di desa Sedan kecamatan Sedan kabupaten Rembang [Productivity of thin-tailed ewes in Sedan Village, Sedan district, Rembang regency]. Journal of Tropical Animal Production, 20(1): 76-83. DOI: https://www.doi.org/10.21776/ub.jtapro.2019.020.01.10

Notter DR (2008). Genetic aspects of reproduction in sheep. Reproduction in Domestic Animals, 43(s2): 122-128. DOI: https://www.doi.org/10.1111/j.1439-0531.2008.01151.x

Oke OE, Uyanga VA, Iyasere OS, Oke FO, Majekodunmi BC, Logunleko MO, Abiona JA, Nwosu EU, Abioja MO, Daramola JO, and Onagbesan OM (2021). Environmental stress and livestock productivity in hot-humid tropics: Alleviation and future perspectives. Journal of Thermal Biology, 100: 103077. DOI: https://www.doi.org/10.1016/j.jtherbio.2021.103077

Özyürek S (2020). Investigation of relationship between udder morphology, lactation traits and milk components in Morkaraman and Awassi. Gümüşhane Üniversitesi Fen Bilimleri Enstitüsü Dergisi, 10(1): 268-274. DOI: https://www.doi.org/10.17714/gumusfenbil.630056

Pinheiro J, Eleutério P, Silva SP, Herbster CJL, de Oliveira VV, Cipriano JA, Cardoso SC, de Andrade DR, da Silva Barbosa AB, Gadelha CRF et al. (2020). Reproductive and productive characteristics of hair sheep raised in the tropical region grassland of Brazil. Research, Society and Development, 9(9): e331997287. DOI: https://www.doi.org/10.33448/rsd-v9i9.7287

Prakash V, Prince L, Sharma R, and Kumar A (2017). Growth and prolificacy performance of Garole sheep raised under semi-arid conditions. The Indian Journal of Animal Sciences, 87(10): 1264-1268 DOI: https://www.doi.org/10.56093/ijans.v87i10.75300

Pratama R and Siswoyo P (2024). Evaluasi hasil IB domba lokal terhadap bobot lahir, litter size, dan sex ratio [Evaluation of artificial insemination results in local sheep on birth weight, litter size, and sex ratio]. Jurnal Cakrawala Ilmiah, 3(9): 2407-2412. Available at: https://bajangjournal.com/index.php/JCI/article/view/7701

Ptáček M, Ducháček J, Stádník L, and Fantová M (2017). Effects of age and nutritional status at mating on the reproductive and productive traits in Suffolk sheep kept under permanent outdoor management system. Czech Journal of Animal Science, 62(5): 211-218. DOI: https://www.doi.org/10.17221/63/2016-CJAS

Ramírez AA, Villalvazo VMM, Arredondo ES, Ramírez HAR, and Sevilla HM (2018). D-Cloprostenol enhances estrus synchronization in tropical hair sheep. Tropical Animal Health and Production, 50(5): 991-996. DOI: https://www.doi.org/10.1007/s11250-018-1522-x

Rather MA, Shanaz S, Ganai NA, Hamadani A, Alam S, Khan NN, Baba A, Raja TA, and Bukhari S (2020). Genetic and non-genetic factors affecting growth and reproduction traits in Kashmir Merino sheep. The Indian Journal of Animal Sciences, 90(6): 950-953. DOI: https://www.doi.org/10.56093/ijans.v90i6.105014

Robertson S and Friend M (2022). Strategies to ameliorate heat stress effects on sheep reproduction. In: In: V. Sejian, S. S. Chauhan, C. Devaraj, P. K. Malik, R. Bhatta (Editors), Climate change and livestock production: Recent advances and future perspectives. Springer., Singapore, pp. 175-183. DOI: https://www.doi.org/10.1007/978-981-16-9836-1_15

Safari E, Fogarty NM, and Gilmour AR (2005). A review of genetic parameter estimates for wool, growth, meat and reproduction traits in sheep. Livestock Production Science, 92(3): 271-289. DOI: https://www.doi.org/10.1016/j.livprodsci.2004.09.003

Selala LJ and Tyasi TL (2022). Using morphological traits to predict body weight of Dorper sheep lambs. World's Veterinary Journal, 12(1): 66-73. DOI: https://www.doi.org/10.54203/scil.2022.wvj9

Sodiq A, Yuwono P, and Santosa SA (2011). Litter size and lamb survivability of Batur sheep in upland areas of Banjarnegara Regency, Indonesia. Animal Production, 13(3): 166-172. Available at: https://animalproduction.net/index.php/JAP/article/view/330

Talafha AQ and Ababneh MM (2011). Awassi sheep reproduction and milk production: Review. Tropical Animal Health and Production, 43(7): 1319-1326. DOI: https://www.doi.org/10.1007/s11250-011-9858-5

Talebi R, Ghaffari MR, Fabre S, Mardi M, and Kazemi Alamouti M (2023). Comparison of the growth performance between pure Moghani sheep and crosses with Texel or Booroola sheep carrying major genes contributing to muscularity and prolificacy. Animal Biotechnology, 34(8): 3495-3506. DOI: https://www.doi.org/10.1080/10495398.2023.2165933

Tesema Z, Deribe B, Kefale A, Lakew M, Tilahun M, Shibesh M, Belayneh N, Zegeye A, Worku G, and Yizengaw L (2020). Survival analysis and reproductive performance of Dorper × Tumele sheep. Heliyon, 6(4): e03840. DOI: https://www.doi.org/10.1016/j.heliyon.2020.e03840

Thompson AN, Bowen E, Keiller J, Pegler D, Kearney GA, and Rosales-Nieto CA (2021). The number of offspring weaned from ewe lambs is affected differently by live weight and age at breeding. Animals, 11(9): 2733. DOI: https://www.doi.org/10.3390/ani11092733

Üstüner H and Oğan M (2013). Main productive performance of Awassi sheep in the Central Anatolian Region of Turkey. Turkish Journal of Veterinary and Animal Sciences, 37(3): 271-276. DOI: https://www.doi.org/10.3906/vet-1205-13

Wahyudi F, Maylinda S, and Susilorini T (2023). Relationship between body linear measurements and body weight of Texel sheep and Awassi sheep. Jurnal Agripet, 23(1): 85-90. DOI: https://www.doi.org/10.17969/agripet.v23i1.24871

Wolf BT, McLean MBL, Davies OD, and Griffiths JB (2014). Performance of purebred Welsh Mountain and crossbred ewes in a hill environment. Livestock Science, 165(1): 181-188. DOI: https://www.doi.org/10.1016/j.livsci.2014.04.007

Zonabend König E, Ojango JMK, Audho J, Mirkena T, Strandberg E, Okeyo AM, and Philipsson J (2017). Live weight, conformation, carcass traits, and economic values of ram lambs of Red Maasai and Dorper sheep and their crosses. Tropical Animal Health and Production, 49(1): 121-129. DOI: https://www.doi.org/10.1007/s11250-016-1168-5

Zülkadir U and Karabacak A (2013). Distribution of birth within a day of Akkaraman and Awassi sheep. Journal of Animal Production Advances, 3(4): 120-125. Available at:https://journals.indexcopernicus.com/search/article?articleId=904528

Publisher's note: Scienceline Publication Ltd. remains neutral with regard to jurisdictional claims in published maps and institutional affiliations.

Open Access: This article is licensed under a Creative Commons Attribution 4.0 International License, which permits use, sharing, adaptation, distribution and reproduction in any medium or format, as long as you give appropriate credit to the original author(s) and the source, provide a link to the Creative Commons licence, and indicate if changes were made. The images or other third party material in this article are included in the article's Creative Commons licence, unless indicated otherwise in a credit line to the material. If material is not included in the article's Creative Commons licence and your intended use is not permitted by statutory regulation or exceeds the permitted use, you will need to obtain permission directly from the copyright holder. To view a copy of this licence, visit https://creativecommons.org/licenses/by/4.0/.

© The Author(s) 2025

2025, Scienceline Publication
World's Veterinary Journal
World Vet J, 15(4): 940-951.
ISSN 2322-4568

DOI: https://dx.doi.org/10.54203/scil.2025.wvj95
PII: S232245682500095-15

Serological Evidence of Porcine Reproductive and Respiratory Syndrome Virus Among Domestic Pigs in Busia County, Kenya

Julius Luvanga[1,2]*, Patrick Bisimwa[3,4], and Juliette Ongus[1,5]

[1]*Department of Molecular Biology and Biotechnology, Pan African University Institute for Basic Sciences, Technology and Innovation (PAUSTI), P.O. Box 62000-0200, Nairobi, Kenya*
[2]*Department of Veterinary Surgery and Theriogenology, College of Veterinary Medicine and Biomedical Sciences, Sokoine University of Agriculture (SUA), P.O. Box 3020, Morogoro, Tanzania*
[3]*Department of Animal Sciences and Production, Université Evangélique en Afrique, B.P. 3323, Bukavu, Democratic Republic of Congo*
[4]*Departement of Environnement, Institut Supérieur de Dévelopment Rural de Kaziba, Democratic Republic of Congo*
[5]*Department of Medical Laboratory Sciences, Jomo Kenyatta University of Agriculture and Technology (JKUAT), P.O. Box 62000-0200, Nairobi, Kenya*

*Corresponding author's Email: juliusluvanga@sua.ac.tz

ORIGINAL ARTICLE
Received: October 05, 2025
Revised: November 09, 2025
Accepted: December 03, 2025
Published: December 25, 2025

ABSTRACT

Porcine reproductive and respiratory syndrome virus (PRRSV) is a significant swine pathogen and one of the most damaging viruses affecting the global pig industry. Although clinical signs compatible with PRRS have been observed within Kenyan pig production systems, the virus has not yet been officially reported in the country. The present study sought to estimate the seroprevalence of PRRSV, describe farm characteristics, and identify risk factors associated with PRRSV infection among domestic pigs in Busia County, Kenya. Serum samples were collected from 398 pigs (52 piglets, 109 growers, and 237 adults) originating from 56 pig keeping farms/households and analyzed using a commercial indirect Enzyme Linked Immunosorbent Assay (ELISA). Farm characteristics, pig farming practices, pig husbandry, and biosecurity data were recorded via structured questionnaires. Pig-level seroprevalence was 1.3% (5/398), with positives detected in Matayos 0.8% (1/124), Nambale 2.0% (1/51), Teso South 2.8% (2/72), and Bunyala 2.9% (1/35) sub-counties, respectively. The farm-level seroprevalence was 8.9% (5/56). Seropositivity did not differ significantly by location, sex, or age category. Biosecurity uptake was generally low, with the use of dedicated clothing/aprons (14%), wearing of boots (32%), presence of footbaths (12.5%), quarantine of new pigs (11%), and handwashing after pig handling (16%). Not using separate clothing/aprons was the only risk factor significantly associated with farm seropositivity. The present findings provided evidence of PRRSV exposure in Kenyan pigs and reveal important gaps in farm-level biosecurity practices at the human-pig interface, underscoring the epidemiological relevance of these observations for pig industry in the region, although the small number of seropositive farms means that some degree of false positivity or false negativity may not be excluded.

Keywords: Biosecurity, Enzyme-linked immunosorbent assay, Porcine reproductive and respiratory syndrome virus, Seroprevalence

INTRODUCTION

Pig farming is becoming an increasingly vital component of rural and peri-urban livelihoods in low- and middle-income countries, including Kenya, where it serves as a dependable source of income, nutrition, and employment (Mutua et al., 2011; FAO, 2012). The pig population in Kenya has grown significantly, from an estimated 335,301 pigs in 2009 to approximately 860,160 in 2023 (Kenya National Bureau of Statistics, 2024). The majority of these pigs (73%) are reared under backyard systems characterized by low inputs, minimal veterinary oversight, and limited biosecurity (Mutua et al., 2011). According to Mbuthia et al. (2015), the expansion of pig production is largely driven by the rising demand for pork in both rural and urban markets, coupled with the species' high reproductive potential, rapid growth rate, and relatively low production costs. Collectively, these factors enable farmers to achieve quick and attractive economic returns from pig farming. However, the growth of pig farming in the country is hindered by different diseases (Mutua et al., 2011), with African swine fever, Cysticercosis, and Leptospirosis being identified as some of the predominant porcine diseases, which contribute to high morbidity, mortality, and economic losses (Thomas et al., 2016; Ngugi et al., 2019; Mwabonimana et al., 2020).

Growing evidence indicates that farmers and veterinarians in Kenya have increasingly reported reproductive problems (abortions, stillbirths, and weak piglets) and neonatal deaths in pigs, which are sometimes unexplained by known endemic diseases such as African swine fever and Leptospirosis (Ngugi et al., 2019; Akoko et al., 2020). These recurrent and unexplained reproductive and neonatal losses have raised suspicion of porcine reproductive and respiratory

To cite this paper: Luvanga J, Bisimwa P, and Ongus J (2025). Serological Evidence of Porcine Reproductive and Respiratory Syndrome Virus Among Domestic Pigs in Busia County, Kenya. *World Vet. J.,* 15(4): 940-951. DOI: https://dx.doi.org/10.54203/scil.2025.wvj95

syndrome (PRRS), a highly contagious viral disease that had not yet been investigated in Kenya. Porcine Reproductive and Respiratory Syndrome (PRRS) is caused by the porcine reproductive and respiratory syndrome virus (PRRSV), an enveloped, positive-sense, single-stranded RNA virus belonging to the genus *Arterivirus* and classified into two species, including PRRSV-1 (European) and PRRSV-2 (North American; Wensvoort et al., 1992; Nelsen et al., 1999; Walker et al., 2021). The virus spreads through both horizontal and vertical pathways, and infected pigs can remain persistent carriers (Cho and Dee, 2006). Clinical signs commonly include reduced appetite, elevated temperature, dullness, respiratory difficulty, blue or reddish ears and vulva, and edema affecting the limbs or subcutaneous tissues (Done et al., 1996; Cho and Dee, 2006). In breeding gilts and sows, infection is characterized by late-term abortions or preterm farrowing, frequent stillbirth, or mummified fetuses (Done et al., 1996; Cho and Dee, 2006). PRRS is regarded as among the economically damaging diseases of swine. Recent analyses estimate that PRRS causes losses of approximately US $1.2 billion annually in the United States pork industry, owing to both breeding herd and growing pig productivity declines (Osemeke et al., 2025). Since PRRSV emergence in North America in the late 1980s, PRRSV has spread widely across Europe and Asia, facilitated by global trade and poor farm biosecurity (Shi et al., 2010; Frossard et al., 2013). In Africa, the virus was first confirmed in South Africa in 2004, and more recently in Uganda and Namibia (Dione et al., 2018; Oba et al., 2022; Molini et al., 2024). Importantly, Uganda (Kenya's immediate neighbor) has reported reproductive and respiratory problems in pigs associated with PRRSV (Oba et al., 2022). The reported reproductive and respiratory failures in pigs of Uganda created a likelihood that the virus could spread into Kenya, particularly through cross-border trade of pigs and pig products in porous border regions such as Busia.

Busia County is among the major pig-producing areas in Western Kenya, where pigs are primarily managed in smallholder, free-range, or semi-intensive systems (Kagira et al., 2010). Frequent introduction of new pigs without quarantine, cross-border movements, sharing of equipment between farms, and absence of footbath are among factors that create a high-risk environment for the spread of infectious diseases (Pileri and Mateu, 2016). Moreover, factors such as limited knowledge of pig health, low adoption of vaccination, and minimal access to veterinary services further increase susceptibility. Risk factors related to pig demographics (age, sex, breed), management practices (housing, feeding, breeding), and biosecurity measures (quarantine, hygiene, movement control) are also well known to influence PRRSV transmission globally (Holtkamp et al., 2012; Frossard et al., 2013).

To date, there are no published reports on the occurrence, prevalence, or risk factors for PRRSV in Kenya. This lack of information leaves the pig sector vulnerable to undetected introduction and spread of the virus, with potentially severe economic and livelihood impacts. Busia County, given its pig population and strategic location along a porous international border, represents a critical hotspot for disease surveillance. Therefore, the present study aimed to indicate farm characteristics, estimate the seroprevalence of PRRSV, and identify risk factors associated with PRRSV infection in domestic pigs in Busia County, Kenya.

MATERIALS AND METHODS

Ethical approval

The ethical clearance for the present study was approved by the Jomo Kenyatta University of Agriculture and Technology, Kenya, Institutional Scientific and Ethical Review Committee (JKU/ISERC/02316/1725). In addition, a research permit was granted by the Kenyan National Commission for Science, Technology, and Innovation (NACOSTI) under license number NACOSTI/P/25/4173606. Authorization to carry out the research in Busia County was further provided by the County Veterinary Officer through a formal consent letter. Prior to data and sample collection, the objectives and procedures of the study were explained to all participating farmers, who were given the opportunity to ask questions and voluntarily decide whether or not to participate. Pigs were excluded if they had been presented with severe illnesses, physical injuries, or if owners declined participation.

Study area

The present study was carried out in Busia County, located in the Western region of Kenya. The county lies immediately east of the border town of Busia, Uganda, and is bordered by Lake Victoria to the southwest, Siaya County to the southeast, and Bungoma and Kakamega Counties to the east. The county consists of seven sub-counties, namely Teso North, Teso South, Nambale, Matayos, Butula, Samia, and Bunyala (Figure 1). The county lies about 500 km west of Nairobi at an average altitude of 1,227 meters (4,026 feet) above sea level and is located between coordinates 00°27'48.0"N and 34°06'19.0"E (Latitude: 0.463333; Longitude: 34.105278). The county experiences a warm, bimodal climate, with long rains occurring from late March to late May and short rains from August to October, receiving between 760 and 2,000 mm of rainfall annually. Temperatures remain relatively consistent throughout the county, with mean annual maximums ranging from 26°C to 30°C and mean annual minimums ranging from 14°C to 22°C (County

Government of Busia, 2024). Busia County was selected purposively because of its known popularity of pig rearing and previous reports of PRRS in the neighboring country, Uganda (Oba et al., 2022). The pig population in Busia County stood at 86,220 in 2023 against the national population of 860,220 (Kenya National Bureau of Statistics, 2024). The pig farming system in Busia County primarily consists of free-range and small-scale intensive systems, providing a representative sample of the diverse management practices in the area (Chege et al., 2023).

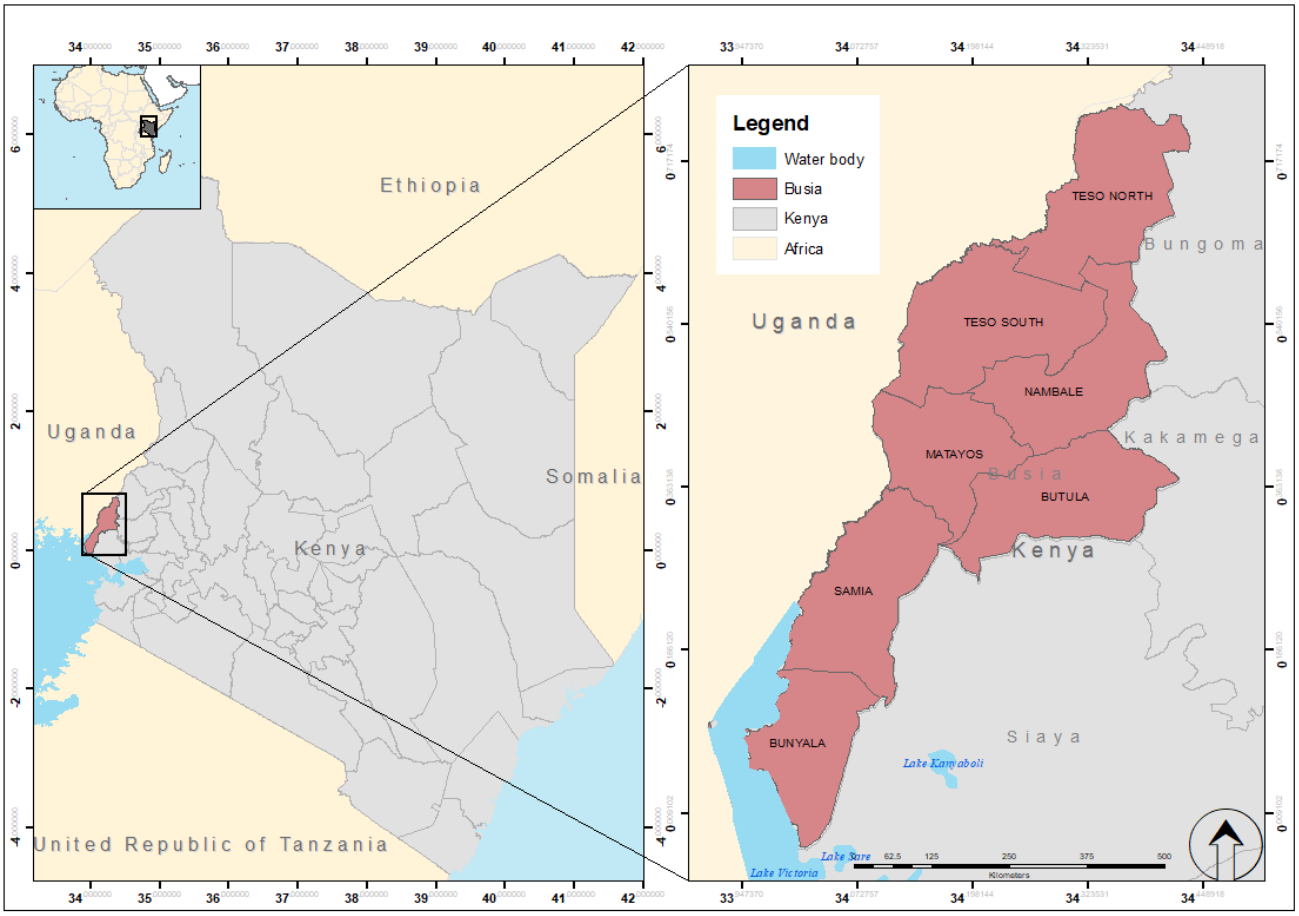


Figure 1. The study area in Busia County, Western Kenya, comprised seven sampled sub-counties. Map produced using ArcGIS Desktop 10.8 (Esri, Redlands, CA, USA)

Study design

The present study employed a cross-sectional design, and it was conducted between May and August 2025. The study population consisted of piglets, grower pigs, and adult pigs. A piglet was defined as a young pig from birth up to 8 weeks of age, a grower as a pig from just over 8 weeks to below 24 weeks of age, and an adult aged from 24 weeks of age (Ekesbo and Gunnarsson, 2018). Eligible herds were households keeping pigs across age categories (piglets, grower pigs, and adults). Pigs without a history of PRRS vaccination, including pregnant sows and gilts, were also eligible, because of ethical issues, pigs with severe illnesses (emaciation, lethargy, fever, and inappetence) and injuries were excluded after a physical examination by a veterinarian, and also any pigs whose owner declined participation were excluded.

Sampling

An initial sample size of 384 pigs was obtained using Cochran's formula for infinite populations (Cochran, 1977), based on a 95% confidence level, a 50% expected prevalence, and a 5% precision. To account for potential sample errors, the sample size was increased by 5% to 398 pigs, comprising 52 piglets, 109 growers, and 237 adults, guided by the relative availability and accessibility of animals within each category during field sampling, rather than strict proportional allocation. Sampling was structured to ensure representation across different management practices and pig breeds in the study area. A multistage sampling approach was applied. In the first stage, all seven sub-counties within Busia were purposely included to get a snapshot of the whole county. Within each sub-county, wards and villages were randomly chosen using random numbers, and pig-keeping households were identified. Households with pigs of different age groups were purposively included, and from each household, individual pigs were selected at random.

Surveys of households

Data were collected from the 56 sampled households using a structured questionnaire specifically designed based on study objectives to gather information on farm practices, husbandry, and biosecurity. The questionnaire was reviewed by two experienced researchers to ensure content validity, clarity, and relevance. Prior to the main survey, it was pre-tested on a small sample of 5 pig-keeping households to identify and correct any ambiguous or culturally inappropriate questions. The final questionnaire was printed and administered through face-to-face interviews with household heads or permanent adult residents of the respective farms. Although the questionnaire was written in English, interviews were conducted in Swahili, and questions were phrased to reflect local conditions. Global Positioning System (GPS) coordinates were recorded for each household to facilitate mapping. The questionnaire gathered information on farmers' demographic characteristics, pig farming practices, husbandry, and biosecurity measures. Biosecurity issues focused on the use of separate clothing when handling pigs, management of pig excreta, awareness of PRRS, isolation of sick pigs, quarantine of newly introduced pigs, fencing of pig units, handwashing practices, vaccination, and training in pig husbandry, among others. In addition, direct observations were made to validate responses and assess key practices, including the presence of footbaths, the wearing of boots, and control of access to pig units.

Blood sample collection

Before blood collection, biological information for each pig was recorded, including identification number, age, sex, breed, health status, and reproductive status (pregnant, lactating, or non-pregnant). Blood samples were collected by a veterinarian from the jugular vein of 398 pigs using sterile red-capped plain vacutainer tubes (without EDTA). The samples were transported in a cool box to the KEMRI Alupe Laboratory, Kenya, within 8 to 10 hours of blood collection, where blood was centrifuged at 3000 rpm for 10 minutes to obtain serum (Lee et al., 2024). The serum was harvested, aliquoted, and added to a 1.8 mL cryogenic vial and stored at -80°C before being transported on dry ice in Styrofoam boxes to the PAUSTI-JKUAT Laboratory, Kenya, for further analysis. To avoid adverse health effects, the volume of blood collected from each animal did not exceed 1% of its total blood volume at a single time point as recommended by Diehl et al. (2001).

Serological analysis

All serum samples were tested for IgG antibodies against PRRSV using a commercial indirect Enzyme Linked Immunosorbent Assay (I-ELISA) kit (INgezim® PRRS 2.0, Gold Standard Diagnostics, Spain) with a reported sensitivity of 99.3% and specificity of 98.2% for European strains, and 91% sensitivity with 96.5% specificity for North American strains, following the manufacturer's instructions. Optical densities (OD) were measured at 450nm using a microplate reader (BioTek Instruments, Inc®100 Tigan Street, Winooski, USA), and results were expressed as sample to positive (S/P) ratios. Samples with an S/P ratio of ≥ 0.40 were classified as positive for PRRSV antibodies, whereas those with an S/P ratio of < 0.40 were considered negative. A herd/farm was defined as positive if at least one pig tested seropositive. The test was considered valid when the OD_{450} of the positive control minus the OD_{450} of the negative control was higher than 0.35, and the negative control OD_{450} was lower than 0.35.

Statistical analysis

Data collected from questionnaires and laboratory assays were entered, checked for consistency, and cleaned in Microsoft Excel. Subsequent analyses were conducted using IBM SPSS Statistics version 27 (IBM Corp., Armonk, NY, USA). Descriptive statistics were used to summarize household and respondent characteristics, pig demographics, and the overall seroprevalence of antibodies to porcine reproductive and respiratory syndrome virus (PRRSV). At the farm level, the outcome was PRRS seropositivity, defined as having ≥1 sampled pig Ab-ELISA positive. For each binary farm-level risk factor (coded 1=Yes, 2=No), 2×2 contingency tables of the risk factor versus farm PRRS status were constructed, and associations were tested using Fisher's exact test (two-sided). For each risk factor, the odds ratio (OR) was computed with a 95% exact confidence interval (CI), oriented as No versus Yes, so that OR > 1 indicates higher odds of PRRS positivity among non-adopting farms. Statistical significance was set at $\alpha = 0.05$.

RESULTS

Characteristics of the sampled pigs

Of the 398 pigs sampled, 52 (13%) were piglets, 109 (27%) were growers, and 237 (60%) were adults. By sex, 129 (32%) were males, and 269 (68%) were females (Table 1). By breed, 139 (35%) were Large White, 117 (30%) Crossbreeds, 97 (24%) Local breed, 28 (7%) Duroc, and 17 (4%) Landrace (Table 1).

Table 1. Distribution of sampled pigs by age category, breed, and sex in Busia County, Kenya, collected between May and August 2025.

Category	Sampled (%)	Female (n; %)	Male (n; %)
Age category			
Piglets	52 (13)	35 (67)	17 (33)
Growers	109 (27)	61 (56)	48 (44)
Adults	237 (60)	173 (73)	64 (27)
Total	398 (100)	269 (68)	129 (32)
Breed			
Large white	139 (35)	98 (71)	41 (29)
Cross breeds	117 (30)	81 (69)	36 (31)
Local breed	97 (24)	64 (66)	33 (34)
Duroc	28 (7)	15 (54)	13 (46)
Landrace	17 (4)	11 (65)	6 (35)
Total	398 (100)	269 (68)	129 (32)

Seroprevalence of PRRSV

Out of 398 pigs sampled across the seven sub-counties of Busia, five pigs (1.3%) tested seropositive for PRRSV antibodies (Table 2). Positivity was detected in Matayos (0.8%), Teso South (2.8%), Nambale (2.0%), and Bunyala (2.9%) sub-counties (Table 2). There was no significant difference in PRRS seroprevalence among pigs from the different sub-counties ($p > 0.05$). The distribution of PRRSV seroprevalence by sex indicated 0.5% seropositivity in males and 0.8% in females. There was no significant association between sex ($p > 0.05$) and PRRS seroprevalence. Seropositivity to PRRSV was detected only among grower and adult pigs, with 2 out of 109 growers (1.8%) and 3 out of 237 adults (1.3%) testing positive, while none of the 52 piglets were seropositive. Although all seropositive pigs were within the grower and adult age groups, the difference in seroprevalence among age categories was not statistically significant ($p > 0.05$). At the farm level, 56 pig farms were sampled, and the five positive pigs originated from five different farms, giving an overall farm-level seroprevalence of 8.9%. The positive farms were not clustered in one area but were distributed across multiple sub-counties, located near the Kenya-Uganda border, particularly in Teso South and Matayos sub-counties (Table 2 and Figure 2).

Table 2. A seroprevalence of porcine reproductive and respiratory syndrome in Busia County, Kenya, was conducted between May and August 2025.

Category	Sampled (n)	Positive (n; %)	Negative (n; %)	P-value
Sub-county				0.790
Teso North	52	0 (0.0)	52 (100.0)	
Butula	28	0 (0.0)	28 (100.0)	
Matayos	124	1 (0.8)	123 (99.2)	
Teso South	72	2 (2.8)	70 (97.2)	
Nambale	51	1 (2.0)	50 (98.0)	
Bunyala	35	1 (2.9)	34 (97.1)	
Samia	36	0 (0.0)	36 (100.0)	
Total (pig-level)	398	5 (1.3)	393 (98.7)	
Farm-level (overall)	56 farms	5 (8.9)	51 (91.1)	
Age group				0.622
Piglet	52	0 (0.0)	52 (100.0)	
Grower	109	2 (1.8)	107 (98.2)	
Adult	237	3 (1.3)	234 (98.7)	
Sex				0.716
Male	129	2 (1.6)	127 (98.4)	
Female	269	3 (1.1)	266 (98.9)	

Note: P-values are for the overall association within each block. Farm-level seroprevalence is defined as ≥ 1 positive pig in a farm/household.

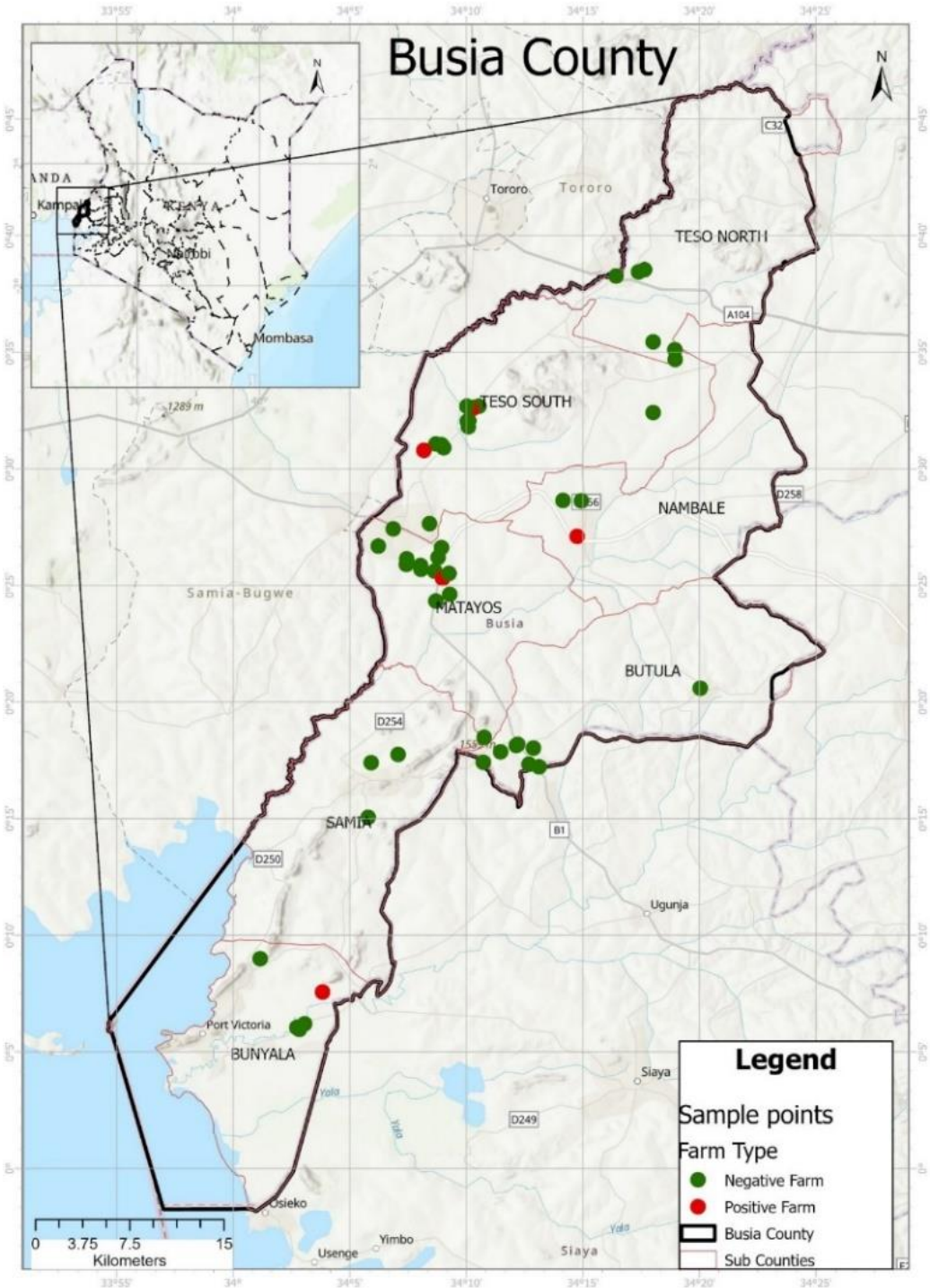


Figure 2. Distribution of sampled households/farms by PRRS serostatus in Busia County, Kenya. Red dots indicate seropositive and green dots indicate seronegative farms (Map produced using ArcGIS Desktop 10.8 Esri, Redlands, CA, USA).

Questionnaire survey results

Farmer demographics and farming practices

Among the 56 farmers surveyed, 66% were men, and most were above 50 years (37%), followed by 31-40 years (29%) and 41-50 years (25%). Education levels among respondents varied, with 45% having attained university or college education, 30% having completed secondary school (up to Form Four), 16% having completed primary education (up to Standard Eight), 5% having completed high school (Form Five and Six), and 4% having no formal education. Livelihoods were predominantly mixed crop-livestock farming (77%), with 21% employed and 2% in business (Table 3). Regarding pig farming practices, semi-intensive systems (37%) were most common, followed by backyard/scavenging (29%). Herds were generally small (5-10 pigs, 43%; 11-20 pigs 25%), and pig keeping was mainly commercial (95%). The breeds kept were exotic 46%, local 34%, and crossbreeds 20%. Experience in pig husbandry was typically 1-5 years (50%), with 41% having more than 5 years and 9% less than a year (Table 3).

Table 3. Demographics of 56 farmers and farming practices in Busia County, Kenya, between May and August 2025

Section	Characteristic	Category	N	%
Demographics	Sex	Male	37	66
		Female	19	34
	Age	Below 20	0	0
		20-30	5	9
		31-40	14	25
		41-50	16	29
		Above 50	21	37
	Education	No formal education	2	4
		Primary	9	16
		Secondary	17	30
		High school	3	5
		University/college	25	45
	Primary occupation	Farming (livestock and crops)	43	77
		Formal employment (public and private sector)	12	21
		Business	1	2
Farming practices	Pig farming system	Backyard/scavenging	16	29
		Semi-intensive	21	37
		Intensive-small scale	13	23
		Intensive-large scale	6	11
	Herd size	5-10	24	43
		11-20	14	25
		21-30	6	11
		31-40	3	5
		41-50	1	2
		≥ 50	8	14
	Main purpose	Commercial (income generation)	53	95
		Home consumption	2	3
		Breeding purpose	1	2
	Breeds kept	Exotic	26	46
		Local	19	34
		Crossbreeds	11	20
	Experience	< 1 year	5	9
		1-5 years	28	50
		≥ 5 years	23	41

Biosecurity, management practices, and PRRS awareness

Among the 56 farmers surveyed, biosecurity uptake was low; only 14% used separate clothing/aprons and 32% wore boots, 25% shared equipment between farms, and 12.5% had footbaths. About half of the farmers (50%) controlled farm entry, 30% isolated sick pigs, and 11% quarantined newly introduced pigs. While 52% of farms had fencing, only 16% of farmers reported washing their hands after handling pigs, despite 96% being aware that diseases can spread between pigs and farms (Table 4). Management practices indicated very low vaccination (5%), breeding relied on natural mating (96%), with stock sourced mainly from neighboring farmers (86%). Manure was mainly used on crop farms (94.6%), and when pigs were sick, 78.6% called a vet/animal health worker (10.7% used over-the-counter drugs and 10.7% sold/slaughtered the pigs). Feed was primarily commercial (69.6%), only 25% had received husbandry or disease prevention training, and barriers to veterinary access included cost (32.1%), lack of services (16.1%), and distance (14.3%; Table 4). PRRS awareness was very low (7%), reported clinical problems included respiratory issues (66% of farms) and reproductive losses (abortions 32%, stillbirths 46%, weak piglets 43%) while other signs (each ≤ 20%) included pneumonia, fever, diarrhea, coughing, sudden deaths, stunted growth, erythema, anorexia, mange, emaciation, hypersalivation, and congenital defects (Table 4).

Table 4. Biosecurity, management practices, and PRRS awareness among pig farmers in Busia County, Kenya, between May and August 2025

Section	Characteristic	Category	N	%
Biosecurity	Use of separate clothing/apron when handling pigs	Yes	8	14
		No	48	86
	Wearing of boots	Yes	18	32
		No	38	68
	Share equipment between farms	Yes	14	25
		No	42	75
	Presence of disinfectant/footbath at entrance	Yes	7	12.5
		No	49	87.5
	Control entry (visitors/buyers/vehicles)	Yes	28	50
		No	28	50
	Isolate sick pigs	Yes	17	30
		No	39	70
	Quarantine new pigs	Yes	6	11
		No	50	89
	Quarantine location	Near (< 25 m)	5	9
		Far (> 25 m)	1	2
	Fencing present	Yes	29	52
		No	27	48
	Aware diseases spread pig-to-pig/farm-to-farm	Yes	54	96
		No	2	4
	Handwashing after handling pigs	Yes	9	16
		No	47	84
Management	Manage pig excreta	Use on crops	53	94.6
		Sell	2	3.6
		Other uses	1	1.8
	When pigs are sick	Call a vet	44	78.6
		Over-the-counter drugs	6	10.7
		Sell or slaughter	6	10.7
	Source of breeding pigs	Neighboring farmers	48	86
		Breeding farms	8	14
	Method of breeding	Natural mating	54	96
		Both (natural + AI)	2	4
	Any vaccination?	Yes	3	5
		No	53	95
	If vaccinated, against which disease	Brucellosis	2	3.6
		Parvovirus	1	1.8
	Main feed source	Commercial feed	39	69.6
		Pasture/grazing	7	12.5
		Kitchen leftovers	6	10.7
		Crop residues	2	3.6
		Swill feed	2	3.6
	Any training received on husbandry/disease prevention	Yes	14	25
		No	42	75
	Challenges in accessing vet services	None	19	33.9
		High cost	18	32.1
		No services	9	16.1
		Long distance	8	14.3
		No awareness	1	1.8
		Other challenges	1	1.8
	Contact with an animal health worker	Yes	52	93
		No	4	7
PRRS awareness	Heard of PRRS	Yes	4	7
		No	52	93
	Reproductive problems	Abortions	18	32
		Stillbirths	26	46
		Born weak piglets	24	43
	Respiratory problems (any)	Yes	37	66
		No	19	33
	Other signs (in the past 6 months)	Pneumonia	11	20
		Fever	10	18
		Diarrhea	10	18
		Coughing	8	14
		Sudden death	8	14
		Stunted growth	8	14
		Erythema	7	13
		Loss of appetite	7	13
		Dullness	6	11
		Mange	5	9
		Emaciation	4	7
		Hypersalivation	2	4
		Congenital defect	1	2
		Experienced none	8	14

Note: Yes or No responses indicate the number of farms practicing or not practicing the respective activity, and do not represent the number of PRRSV-positive farms within each category.

Risk factors associated with farm-level PRRS seropositivity

Not using separate clothing/apron was the only factor that was significantly associated with PRRS farm seropositivity (OR = 13.89, 95% CI 1.84-100, $p < 0.05$). All other risk factors (wearing boots, sharing equipment, presence of footbath, controlling visitors, isolation, quarantine, fencing, handwashing, vaccination, and training) had $p > 0.05$, indicating no statistically significant evidence of association (Table 5).

Table 5. Association between farm-level practices and PRRS farm seropositivity in Busia County, Kenya, between May and August 2025

Predictor	Yes (n)	No (n)	OR (PRRS+, No versus Yes)	95% CI	P-value
Use of separate clothing /Apron while dealing with pigs	8	48	13.889	1.842 - 100	**0.017***
Wearing boots	18	38	1.459	0.221 - 9.615	0.652
Sharing of equipment between farms	14	42	0.235	0.012 - 4.520	0.316
Presence of disinfectants/footbath at the entrance	7	49	1.877	0.179 - 19	0.501
Do you control who enters your pig unit?	28	28	4.505	0.469 - 43	0.352
Isolation of sick pigs?	17	39	1.600	0.242 - 10	0.634
Quarantine of new pigs before introducing them into the farm?	6	50	2.299	0.213 - 25	0.445
Fencing of piggery units/farms?	29	27	4.167	0.435 - 40	0.353
Washing of hands after dealing with pigs	9	47	4.184	0.591 - 29	0.178
Have you ever vaccinated your pigs?	3	53	6.135	0.451 - 83	0.249
Have you ever received any training on husbandry?	14	42	2.163	0.323 - 14	0.590

Note: *Significant Fisher's exact test ($p < 0.05$).

DISCUSSION

Kenya's smallholder pig systems create conditions conducive to PRRSV transmission, yet detection may be limited by subclinical infection and sparse surveillance. The low pig-level and farm-level seroprevalence of 1.3% and 8.9% respectively, in the present study fits a pattern seen in other African settings where detection of PRRSV has tended to cluster in smallholder herds while larger and biosecure herds test negative against PRRSV (Dione et al., 2018; Molini et al., 2024). Within the region, the neighboring Uganda has also reported a low PRRSV seroprevalence of 1.55% (Dione et al., 2018). Another study in Uganda reported a prevalence of 24.65% and 2.73% for PRRSV-1 and PRRSV-2, respectively, by real-time PCR (Oba et al., 2022), highlighting heterogeneity across methods, time, and production systems. In Namibia, PRRSV was found only on three epidemiologically linked rural farms with a pig-level prevalence of 4.76% and a within-farm prevalence of 14 to 30% as detected by RT-PCR, while all industrial herds remained negative, underscoring the role of basic biosecurity in preventing introduction (Molini et al., 2024). On the contrary, higher seroprevalence has been reported in southwest Nigeria and in some parts of Nepal, where they reported a seroprevalence of 53.8% and 20% respectively, detected using ELISA assays (Aiki-Raji et al., 2017; Prajapati et al., 2023).

The present study found no significant differences in PRRSV seroprevalence by sub-county or sex, and the positive pigs in the present study were between 4 to 6 months of age. Although this may suggest possible age-related exposure dynamics, the observation is based on a small number of positive cases and should therefore be interpreted with caution. This finding agrees with other reports of no significant sex effect (Prajapati et al., 2023). However, other studies observed significant geographic heterogeneity by district and topography, and a strong age gradient with the highest prevalence in pigs of more than 18 months, contrary to the 4 to 6-month-old positive pigs in the present study (Kim et al., 2002; Ferrara et al., 2023; Prajapati et al., 2023). Regionally, a study in Uganda showed similarly low overall prevalence but district-level differences (Masaka 1.3% versus Lira 1.7%), underscoring that locality can matter even when absolute prevalence is low (Dione et al., 2018).

The farm characteristics and biosecurity profiles in the present study indicated a low uptake on the use of separate clothing while dealing with pigs (14%), footbaths (12.5%), handwashing after pig handling (16%), and quarantine (11%), the findings which were consistent with prior descriptions of pig farmers in western Kenya, Uganda and comparable country like Nepal (Kagira et al., 2010; Ekakoro et al., 2023; Prajapati et al., 2023). In Busia's smallholder

free-range systems, tethering, minimal housing, locally sourced feeds, and disease or feeding constraints have long been documented (Kagira et al., 2010), aligning with the low-input profile observed in the present study. Similar patterns of weak biosecurity and limited PRRS knowledge have been noted by a study in Nepal, where 40% had footbaths, 25% used separate boots, and 43% were aware of PRRS, reinforcing that awareness does not automatically translate into practice without supportive systems (Prajapati et al., 2023).

Mechanistic work and field observations emphasize that contaminated clothing, tools, and vehicles can mechanically carry PRRSV between pens and farms, the pathway targeted by measures such as dedicated use of aprons/boots, visitor control, and disinfection points (Pitkin et al., 2009; Prajapati et al., 2023). Against this backdrop, the finding that not using separate clothing/aprons was significantly associated with PRRS farm seropositivity is biologically and operationally plausible, as dedicated clothing directly interrupts fomite transmission at the human-pig interface (Fablet et al., 2016; Prajapati et al., 2023). Several other practices in the present study, such as not washing hands after pig handling, not controlling visitors, and a lack of fencing/footbaths, indicated elevated odds but were not statistically significant. These directions are consistent with the known role of hygiene and perimeter control in reducing between-pen and between-farm spread, even if the present study was underpowered to confirm those associations definitively. The relatively high (but non-significant) odds ratios observed for some of these practices suggest that they may represent true risk factors, and future studies with larger numbers of positive farms or longitudinal follow-up will be important to clarify their potential contribution to PRRSV introduction and spread.

Management practices also align with recognized risk pathways. Most farms sourced breeding stock locally and relied on natural service, a pattern that can connect otherwise separate herds (Kagira et al., 2010). In Namibia, rapid local spread was plausibly linked to sharing boars for breeding, a practice discouraged in favor of certified semen for artificial insemination (Molini et al., 2024). Reported vaccination coverage in the present study was very low, comparable to broader African contexts where vaccine access and uptake for swine pathogens are limited outside commercial systems, underscoring the importance of non-vaccine biosecurity in smallholder herds.

CONCLUSION

Based on the findings of the present study, this study provided the first serological evidence of PRRSV exposure among pigs in Kenya, with an overall pig-level seroprevalence of 1.3% and farm-level seroprevalence of 8.9%. Although the infection was detected at low levels and showed no significant differences by age, sex, or sub-county, it highlights the presence of PRRSV in the region and the need for improved farm-level disease prevention measures. It is recommended that the farmers be advised to focus on simple and high-yield biosecurity measures such as dedicated clothing, use of boots, visitor control, quarantine of newly introduced pigs, use of foot baths, fencing, and hand hygiene, also expanding surveillance programs beyond the commonly known diseases to include PRRSV and other respiratory and reproductive pathogens. However, the cross-sectional design, the small number of positive farms, and the use of ELISA limit causal inference and could fail to detect very recent infections, and the potential for false positives or false negatives due to limited test specificity may also be considered. Seropositivity could also reflect past infection since no farms used PRRS vaccines. Future studies should use larger samples, longitudinal designs, and include molecular detection and typing to define transmission pathways and PRRSV species at the Kenya and Uganda border.

DECLARATIONS

Acknowledgements

The authors would like to thank the county veterinary officers, village livestock officers, and the pig farmers in the visited sub-counties for their cooperation and support. The authors are also grateful to Dr. Steven Odhiambo (Field Assistant), Mr. Ezra Wanyama (Field Assistant), Mr. Peter Onyango (Field Assistant), Mr. Martin Samante (Field Assistant), Ms. Olpha Migosi (Laboratory Assistant, KEMRI-Alupe Laboratory), and Mr. Patrick Koech (Laboratory Assistant, PAUSTI Laboratory) for their invaluable assistance.

Authors' contributions

Julius Luvanga, Patrick Bisimwa, and Juliette Ongus made substantial contributions to the conception and design of this study. Julius Luvanga was also involved in the acquisition of data, laboratory work, data analysis, and interpretation of data. All authors have been involved in preparing the manuscript and revising it critically for important intellectual content. All authors gave final approval for the manuscript to be published.

Availability of data and materials

The original data presented in the study are available in the article.

Competing interests

The authors declare no competing interests.

Funding

This study was supported by the African Union Commission through the Pan African University Institute for Basic Sciences, Technology and Innovation (PAUSTI), Kenya. The funder had no role in study design, data collection and analysis, decision to publish, or preparation of the paper.

Ethical considerations

All authors affirmed that the study adheres to the highest ethical standards. Issues related to plagiarism, publication consent, research misconduct, data fabrication, duplicate submission, and redundant publications have been thoroughly addressed. No Artificial Intelligence (AI) tools were used to generate text or figures.

REFERENCES

Aiki-Raji CO, Adebiyi AI, Abiola JO, and Oluwayelu DO (2018). Prevalence of porcine reproductive and respiratory syndrome virus and porcine parvovirus antibodies in commercial pigs, Southwest Nigeria. Beni-Suef University Journal of Basic and Applied Sciences, 7(1): 80-83. DOI: https://www.doi.org/10.1016/j.bjbas.2017.07.006

Akoko J, Pelle R, Kivali V, Schelling E, Shirima G, Machuka EM, Mathew C, Fèvre EM, Kyallo V, Falzon LC et al. (2020). Serological and molecular evidence of Brucella species in the rapidly growing pig sector in Kenya. BMC Veterinary Research, 16(1): 133. DOI: https://www.doi.org/10.1186/s12917-020-02346-y

Chege B, Ndambuki G, Owiny M, Kiyong'a A, Fèvre EM, and Cook EAJ (2023). Improved latrine coverage may reduce porcine cysticercosis: A comparative cross-sectional study, Busia County, Kenya 2021. Frontiers in Veterinary Science, 10: 1155467. DOI: https://www.doi.org/10.3389/fvets.2023.1155467

Cho JG and Dee SA (2006). Porcine reproductive and respiratory syndrome virus. Theriogenology, 66(3): 655-662. DOI: https://www.doi.org/10.1016/j.theriogenology.2006.04.024

Cochran WG (1977). The estimation of sample size. Sampling techniques, 3rd Edition. John Wiley and Sons., New York, pp. 72-83. Available at: https://archive.org/details/cochran-1977-sampling-techniques/page/72/mode/2up

County government of Busia (2024). Busia county integrated development plan of 2023-2027. County government of Busia, pp. 1-2. Available at: https://busiacounty.go.ke/assets/documents/uploads/COUNTY%20INTEGRATED%20DEVELOPMENT%20PLAN%20-%202023%20-%202027-zBMPm.pdf

Diehl KH, Hull R, Morton D, Pfister R, Rabemampianina Y, Smith D, Vidal JM, and van de Vorstenbosch C (2001). European Federation of Pharmaceutical Industries Association and European Centre for the validation of alternative methods. A good practice guide to the administration of substances and removal of blood, including routes and volumes. Journal of Applied Toxicology, 21(1): 15-23. DOI: https://www.doi.org/10.1002/jat.727

Dione M, Masembe C, Akol J, Amia W, Kungu J, Lee HS, and Wieland B (2018). The importance of on-farm biosecurity: Sero-prevalence and risk factors of bacterial and viral pathogens in smallholder pig systems in Uganda. Acta Tropica, 187: 214-221. DOI: https://www.doi.org/10.1016/j.actatropica.2018.06.025

Done SH, Paton DJ, and White ME (1996). Porcine reproductive and respiratory syndrome (PRRS): A review, with emphasis on pathological, virological and diagnostic aspects. British Veterinary Journal, 152(2): 153-174. DOI: https://www.doi.org/10.1016/s0007-1935(96)80071-6

Ekakoro JE, Nawatti M, Singler DF, Ochoa K, Kizza R, Ndoboli D, Ndumu DB, Wampande EM, and Havas KA (2023). A survey of biosecurity practices of pig farmers in selected districts affected by African swine fever in Uganda. Frontiers in Veterinary Science, 10: 1245754. DOI: https://www.doi.org/10.3389/fvets.2023.1245754

Ekesbo I and Gunnarsson S (2018). Characteristics for assessment of health and welfare. Farm animal behavior. 2nd Edition. CAB International Wallingford., United Kingdom, pp. 27-66. DOI: https://www.doi.org/10.1079/9781786391391.0027

Fablet C, Marois-Créhan C, Grasland B, Simon G, and Rose N (2016). Factors associated with herd-level PRRSV infection and age-time to seroconversion in farrow-to-finish herds. Veterinary Microbiology, 192: 10-20. DOI: https://www.doi.org/10.1016/j.vetmic.2016.06.006

Food and Agriculture Organization (FAO) (2012). Pig sector Kenya. FAO Animal Production and Health Livestock Country Reviews. No. 3. Rome, pp. 3-8. Available at: https://fao.org/4/i2566e/i2566e00.pdf

Ferrara G, D'Anza E, Rossi A, Improda E, Iovane V, Pagnini U, Iovane G, and Montagnaro S (2023). A serological investigation of porcine reproductive and respiratory syndrome and three coronaviruses in the Campania Region, Southern Italy. Viruses, 15(2): 300. DOI: https://www.doi.org/10.3390/v15020300

Frossard JP, Hughes GJ, Westcott DG, Naidu B, Williamson S, Woodger NGA, Steinbach F, and Drew TW (2013). Porcine reproductive and respiratory syndrome virus: genetic diversity of recent British isolates. Veterinary Microbiology, 162(2-4): 507-518. DOI: https://www.doi.org/10.1016/j.vetmic.2012.11.011

Holtkamp DJ, Kliebenstein JB, Zimmerman JJ, Neumann E, Rotto H, Yoder TK, Wang C, Yeske P, Mowrer CL, and Haley C (2012). Economic impact of porcine reproductive and respiratory syndrome virus on United States pork producers. Journal of Swine Health and Production, 21(2): 72-84. DOI: https://www.doi.org/10.31274/ans_air-180814-28

Kagira JM, Kanyari PW, Maingi N, Githigia SM, Ng'ang'a JC, and Karuga JW (2010). Characteristics of the smallholder free-range pig production system in Western Kenya. Tropical Animal Health and Production, 42(5): 865-873. DOI: https://www.doi.org/10.1007/s11250-009-9500-y

Kenya National Bureau of Statistics (2024). National agriculture production report of 2024, pp. 82-83. Available at: https://www.knbs.or.ke/wp-content/uploads/2025/01/National-Agriculture-Production-Report-2024.pdf

Kim SM, Han TU, Kang SY, Shin KS, Kim CJ, Kim JT, and Kim HS (2002). Seroprevalence of antibody to porcine reproductive and respiratory syndrome virus in diagnostic submissions. Journal of Veterinary Science, 3(3): 159-161. DOI: https://www.doi.org/10.4142/jvs.2002.3.3.159

Lee YB, Kim JW, Jo W, Kang TK, Sung M, Kim K, Park NH, and Lee GH (2024). Assessment of PRRSV and PCV2 seroprevalence and antigen prevalence in minipigs at laboratory-animal production facilities. Journal of Advanced Veterinary and Animal Research, 11(4): 1017-1022. DOI: https://www.doi.org/10.5455/javar.2024.k852

Mbuthia JM, Rewe TO, and Kahi AK (2015). Analysis of pig breeding management and trait preferences in smallholder production systems in Kenya. Animal Genetic Resources, 56: 111-117. DOI: https://www.doi.org/10.1017/S207863361400054X

Molini U, Coetzee LM, Hemberger MY, Chiwome B, Khaiseb S, Dundon WG, and Franzo G (2024). First detection and molecular characterization of porcine reproductive and respiratory syndrome virus in Namibia, Africa. Frontiers in Veterinary Science, 10: 1323974. DOI: https://www.doi.org/10.3389/fvets.2023.1323974

Mutua FK, Dewey CE, Arimi SM, Ogara WO, Githigia SM, Levy M, and Schelling E (2011). Indigenous pig management practices in rural villages of Western Kenya. Livestock Research for Rural Development, 23(7): 144. Available at: https://lrrd.org/lrrd23/7/mutu23144.htm

Mwabonimana MF, King'ori AM, Inyagwa CM, Shakala EK, and Bebe BO (2020). Prevalence of porcine cysticercosis among scavenging pigs in Western Kenya. African Journal of Infectious Diseases, 14(2): 30-35. DOI: https://www.doi.org/10.21010/ajid. v14i2.5

Nelsen CJ, Murtaugh MP, and Faaberg KS (1999). Porcine reproductive and respiratory syndrome virus comparison: Divergent evolution on two continents. Journal of Virology, 73(1): 270-280. DOI: https://www.doi.org/10.1128/JVI.73.1.270-280.1999

Ngugi JN, Fèvre EM, Mgode GF, Obonyo M, Mhamphi GG, Otieno CA, and Cook EAJ (2019). Seroprevalence and associated risk factors of leptospirosis in slaughter pigs; A neglected public health risk, Western Kenya. BMC Veterinary Research, 15(1): 403. DOI: https://www.doi.org/10.1186/s12917-019-2159-3

Oba P, Dione MM, Erume J, Wieland B, Mutisya C, Ochieng L, Cook EAJ, and Mwiine FN (2022). Molecular characterization of porcine reproductive and respiratory syndrome virus (PRRSv) identified from slaughtered pigs in Northern Uganda. BMC Veterinary Research, 18(1): 176. DOI: https://www.doi.org/10.1186/s12917-022-03272-x

Osemeke O, Silva GS, Corzo CA, Kikuti M, Vadnais S, Yue X, Linhares D, and Holtkamp D (2025). Economic impact of productivity losses attributable to porcine reproductive and respiratory syndrome virus in United States pork production, 2016-2020. Preventive Veterinary Medicine, 244: 106627. DOI: https://www.doi.org/10.1016/j.prevetmed.2025.106627

Pileri E and Mateu E (2016). Review on the transmission porcine reproductive and respiratory syndrome virus between pigs and farms and impact on vaccination. BMC Veterinary Research, 47(1): 108. DOI: https://www.doi.org/10.1186/s13567-016-0391-4

Pitkin A, Deen J, and Dee S (2009). Further assessment of fomites and personnel as vehicles for the mechanical transport and transmission of porcine reproductive and respiratory syndrome virus. Canadian Journal of Veterinary Research, 73(4): 298-302. Available at: https://pmc.ncbi.nlm.nih.gov/articles/PMC2757711/

Prajapati M, Acharya MP, Yadav P, and Frossard JP (2023). Farm characteristics and sero-prevalence of porcine reproductive and respiratory syndrome virus (PRRSV) antibodies in pigs of Nepal. Veterinary Medicine and Science, 9(1): 174-180. DOI: https://www.doi.org/10.1002/vms3.1011

Shi M, Lam TT, Hon CC, Hui RK, Faaberg KS, Wennblom T, Murtaugh MP, Stadejek T, and Leung FC (2010). Molecular epidemiology of PRRSV: A phylogenetic perspective. Virus Research, 154(1-2): 7-17. DOI: https://www.doi.org/10.1016/j.virusres.2010.08.014

Thomas LF, Bishop RP, Onzere C, Mcintosh MT, Lemire KA, de Glanville WA, Cook EA, and Fèvre EM (2016). Evidence for the presence of African swine fever virus in an endemic region of Western Kenya in the absence of any reported outbreak. BMC Veterinary Research, 12(1): 192. DOI: https://www.doi.org/10.1186/s12917-016-0830-5

Walker PJ, Siddell SG, Lefkowitz EJ, Mushegian AR, Adriaenssens EM, Alfenas-Zerbini P, Davison AJ, Dempsey DM, Dutilh BE, García ML et al. (2021). Changes to virus taxonomy and to the International Code of Virus Classification and Nomenclature ratified by the International Committee on Taxonomy of Viruses. Archives of Virology, 166(9): 2633-2648. DOI: https://www.doi.org/10.1007/s00705-021-05156-1

Wensvoort G, de Kluyver EP, Luijtze EA, den Besten A, Harris L, Collins JE, Christianson WT, and Chladek D (1992). Antigenic comparison of Lelystad virus and swine infertility and respiratory syndrome (SIRS) virus. Journal of Veterinary Diagnostic Investigation, 4(2): 134-138. DOI: https://www.doi.org/10.1177/104063879200400203

Publisher's note: Scienceline Publication Ltd. remains neutral with regard to jurisdictional claims in published maps and institutional affiliations.

Open Access: This article is licensed under a Creative Commons Attribution 4.0 International License, which permits use, sharing, adaptation, distribution and reproduction in any medium or format, as long as you give appropriate credit to the original author(s) and the source, provide a link to the Creative Commons licence, and indicate if changes were made. The images or other third-party material in this article are included in the article's Creative Commons licence, unless indicated otherwise in a credit line to the material. If material is not included in the article's Creative Commons licence and your intended use is not permitted by statutory regulation or exceeds the permitted use, you will need to obtain permission directly from the copyright holder. To view a copy of this licence, visit https://creativecommons.org/licenses/by/4.0/.

© The Author(s) 2025

2025, Scienceline Publication
World's Veterinary Journal
World Vet J, 15(4): 952-959.
ISSN 2322-4568

DOI: https://dx.doi.org/10.54203/scil.2025.wvj96
PII: S232245682500096-15

Genetic Diversity of the *Agouti Signaling Protein* (*ASIP*) Gene in Determining Coat Color in Bali Cattle (*Bos javanicus*)

Kholijah Kholijah[1], Sri Darwati[2], Muhammad Fakhrul Ulum[3], Ronny Rachman Noor[2], and Jakaria Jakaria[2]*

[1]*Graduate School of Animal Production and Technology, Faculty of Animal Science, IPB University (Bogor Agricultural University), Indonesia*
[2]*Department of Animal Production and Technology, Faculty of Animal Science, IPB University (Bogor Agricultural University), Bogor 16680, Indonesia*
[3]*Division of Reproduction and Obstetrics, School of Veterinary Medicine and Biomedical Sciences, IPB University (Bogor Agricultural University), Bogor 16680, Indonesia*

*Corresponding author's Email: jakaria@apps.ipb.ac.id

ORIGINAL ARTICLE
Received: October 05, 2025
Revised: November 07, 2025
Accepted: December 03, 2025
Published: December 25, 2025

ABSTRACT

Bali cattle, which are indigenous to Indonesia, display distinctive and unique coat color characteristics. The appearance of albinos has been observed as an abnormality. The present study aimed to explore the *agouti signaling protein* (*ASIP*) gene in Bali cattle and analyze its association with the occurrence of albinism and white-spotted coat colors in Bali cattle. A total of 68 blood samples from cattle were used, including standard Bali cattle (N = 39), Bali cattle with spotting (N = 9), and albino Bali cattle (N = 20). Standard and white-spotted Bali cattle samples were collected from the Bali Cattle Breeding Centre in Jembrana, Bali Province, and the Breeding Center Unit in Serading, West Nusa Tenggara, Indonesia. Albino cattle samples were obtained from Taro Village, Gianyar Regency, Bali. The DNA amplification was performed using polymerase chain reaction (PCR), single-nucleotide polymorphisms (SNPs) were determined through direct sequencing, and genotyping was performed using the PCR-RFLP method. The exon 1 and exon 2 regions of the *ASIP* gene were monomorphic or uniform. The coding region of exon 3 of the *ASIP* gene in Bali cattle exhibited polymorphisms, specifically regarding coat color. A novel SNP (g.498 A > G) was detected exclusively in Bali cattle; however, it has not yet been validated as a potential genetic marker for coat color in this breed. The findings of this study further revealed that the *ASIP* gene sequence does not distinguish between standard and albino coat colors in Bali cattle, despite the identification of this specific SNP.

Keywords: *Agouti signaling protein* gene, Bali cattle, Coat color, Polymerase chain reaction, Single nucleotide polymorphism

INTRODUCTION

Bali cattle (*Bos Javanicus*) are a native Indonesian breed distinguished by their unique coat color characteristics. The coat is black in adult males, whereas females exhibit a brick-red hue. The lower part of the legs displays a white coloration resembling socks, and a crescent-shaped white patch is present on the buttocks. However, recent studies have identified coat colors that deviate from the usual characteristics, giving rise to albino Bali cattle (Reza et al., 2024). Albinism results from a lack of melanin in the skin, eyes, and hair (Ma and Wang, 2024). Albinism in mammals is an autosomal recessive condition that leads to abnormalities in eye, hair, and skin pigmentation (Zhao et al., 2015).

A 7.63% albino case rate in the Kupang region of Indonesia, while albino Bali cattle cases found in their native breeding area (Bali Province) amounted to 0.33% (Heryani et al., 2018). The discovery of albino Bali cattle is crucial, as it may impede the purification efforts of Bali cattle as a native Indonesian breed. Additionally, the emergence of albino Bali cattle poses a challenge in Bali cattle breeding, particularly in maintaining the purity of superior breeding males that will be distributed to the community (Purwantara et al., 2012). The uncontrolled increase in the population of albino Bali cattle can also lead to the extinction of pure Bali cattle breeds in Indonesia (Septian et al., 2015). Therefore, to preserve and maintain the genetic purity of Bali cattle, it is important to conduct studies that analyze the causes of albinism in this breed. Such studies can take advantage of advanced molecular genetic technologies, particularly marker-assisted selection (MAS), which allows for the identification of gene polymorphisms associated with albino traits. In general, coat color is determined by genetic factors (Gao et al., 2017).

Various genes, including *melanocortin 1 receptor* (*MC1R*), *receptor tyrosine kinase* (*KIT*; dominant white), *TYRP1* (brown), *KITLG* (roan), *MITF* (white-spotted), *TYR* (albinism), and *Agouti Signaling Protein* (*ASIP*; agouti), have been identified as influencing coat color in cattle (Schmutz, 2012). Analysis revealed the presence of Single Nucleotide

To cite this paper: Kholijah K, Darwati S, Fakhrul Ulum M, Noor RR, and Jakaria J (2025). Genetic Diversity of the *Agouti Signaling Protein* (*ASIP*) Gene in Determining Coat Color in Bali Cattle (*Bos javanicus*). *World Vet. J.*, 15(4): 952-959. DOI: https://dx.doi.org/10.54203/scil.2025.wvj96

Polymorphisms (SNPs) in the partial intron 2 and exon 3 regions of the *KIT* gene in Bali cattle (Jakaria et al., 2023). However, these SNPs cannot be used as standardized markers for coat color, white spotting, or albinism in Bali cattle. In addition, the MC1R gene was monomorphic. Some cattle exhibit primary pigmentation in red and black (Angus cattle; He et al., 2022), whereas others display a white coat (Charolais cattle; Gutiérrez-Gil et al., 2007). Colors such as spotting, dilution, roan, and brindle are influenced by various genes. Pigmentation in coat color is a crucial factor in livestock breeding, as it impacts productivity and adaptability to the environment (Goud et al., 2021).

The *ASIP* gene has been extensively studied in various cattle breeds and other animals, including French Brown Cattle (Royo et al., 2005), Australian Merino (Norris et al., 2008), Tibetan Sheep (Han et al., 2015), Chinese Simmental steers (Liu et al., 2019), and Nellore Cattle (Trigo et al., 2021). There has not been a study documenting the identification of the *ASIP* gene in Bali cattle. The current study aimed to explore the *ASIP* gene in Bali cattle and investigate its association with the occurrence of albinism and white-spotted coat color using direct sequencing.

MATERIALS AND METHODS

Ethical approval

The Animal Ethics Committee of Udayana University in Denpasar, Indonesia (Code ID: B/210/UN14.2.9/PT.01.04/2023) approved this study.

Study period and location

This study was conducted from June to November 2023. The study was conducted at several locations. Including Genetic analysis was carried out at the Molecular Genetics Laboratory, Division of Animal Breeding and Genetics, Department of Animal Production and Technology, Faculty of Animal Science, IPB University. Blood samples were collected from Bali cattle with standard (normal brown) and albino coat colors in Taro Village and the Livestock Center in the Sobangan Region, Bali Province.

Sample collection

A total of 68 blood samples from cattle were collected based on convenience and used in the current study, comprising standard Bali cattle (N = 39), Bali cattle with spotting (N = 9), and albino Bali cattle (N = 20; Figure 1). Samples of standard and white-spotted Bali cattle were collected from the Bali Cattle Breeding Centre, Jembrana (Bali Province), and Breeding Center Unit, Serading (West Nusa Tenggara). Albino cattle were sampled from Taro Village, Gianyar Regency, Bali, Indonesia. Approximately 5 mL of blood was obtained via jugular venipuncture using a venoject needle and Ethylenediaminetetraacetic acid (EDTA) vacutainer. The samples were stored at refrigeration temperature (-4°C) for a maximum of 3-4 days post-collection and subsequently processed for DNA extraction following Geneaid protocol (Geneaid Biotech Ltd., New Taipei City, Taiwan).



Figure 1. Standard coat color (**a**) and albino (**b**) in Bali cattle from the Bali Cattle, Indonesia.

Polymerase chain reaction amplification

To investigate the *ASIP* gene, primers were designed to cover exons 1-3 and the 3′UTR region (Table 1). Polymerase chain reaction (PCR) was carried out on an AB System thermocycler (Applied Biosystems, USA), manufactured in the United States of America. Each 25 µL reaction was prepared by combining 0.3 µL of both primers, 12.5 µL MyTaq HS RedMix, 9.9 µL of nuclease-free water, and 2 µL of DNA template. The cycling profile consisted of an initial denaturation step (95°C, 5 minutes), followed by 35 cycles of denaturation (95°C, 10 seconds), annealing (60°C, 20 seconds), and extension (72°C, 30 seconds), with a final elongation at 72°C for 5 minutes. Polymerase Chain Reaction (PCR) amplicons were analyzed by agarose gel electrophoresis, in which 3 µL of product was loaded on a 1.5% gel prepared with 0.5 × Tris-Borate-EDTA (TBE) buffer and stained with PeqGreen. Electrophoresis was performed at 100 V for approximately 30–35 minutes, and DNA fragments were visualized using UV transillumination. The sequencing of PCR products was performed using the Sanger sequencing method at the First Base Laboratory (Selangor, Malaysia) in collaboration with PT. Genetika Science, Indonesia.

Polymerase chain reaction products were distributed into 0.5 mL Eppendorf tubes with a volume of 5 µL. The PCR product was then combined with a mixture comprising 2 µL, consisting of 0.3 µL of the restriction enzyme, 0.7 µL of 10x buffer R, and 1 µL of nuclease-free water (NFW) in a 1.5 mL tube. Based on the results of the enzyme determination using NEB cutter, the restriction enzyme used was BspEl. The reaction mixture was incubated at 55°C for 2 hours. Following digestion with the restriction enzyme, DNA fragments were separated by electrophoresis on a 2% agarose gel at 100 V for 40 minutes, a standard condition for this fragment size range that produced clear bands without noticeable smearing, and visualized using a UV transilluminator in molecular biology labs, which is Bio-Rad (USA). The observed banding patterns were compared with a molecular size marker to estimate the fragment length, and genotypes were identified based on the resulting band sizes.

Table 1. Nucleotide sequences used as primers in PCR for the identification of *ASIP* genes

***ASIP* Gene Targeted**	**Primer sequence (5' to 3')**	**Amplicon Length (bp)**	**Annealing Temperature (°C)**	**Reference**
Exon-1	F:5'-TCAGAGTACCAGCCCAAAGA-3'			
	R:5'-TATCGGCTTGGGGAGTGTTT-3'	355		
Exon-2	F:5'-TTCATCCTCTCCCCAACCCT-3'		60	Manual design using Primer3 and PrimerStat websites
	R:5'-TCAGTGCTTGAGGTCAGGAC-3'	317		
Exon-3	F:5'-GAGTGGGGAGGACGTAGATG-3'			
	R:5'-GGGACTAGGCGAAGGGAAAA-3'	462		

F: Forward, R: Reverse, PCR: Polymerase chain reaction, *ASIP: Agouti Signaling Protein* gene.

Sequencing single-nucleotide polymorphisms identification and statistical analysis

The *ASIP* gene sequences were analyzed using FinchTV and BioEdit version 7.2 (Hall, 1999). Single-nucleotide polymorphisms (SNPs) were detected by aligning the sequences with Clustal W implemented in MEGA version 10 (Tamura et al., 2013). Population genetic parameters, including genotype and allele frequencies, observed and expected heterozygosity, and Hardy–Weinberg equilibrium (HWE), were calculated using POPGEN version 1.32 (Yeh et al., 2000). Hardy-Weinberg equilibrium (HWE) was analyzed using the chi-square test (2) to determine the HWE value in a population. The Hardy–Weinberg equilibrium test showed a $p > 0.05$, indicating no significant deviation from equilibrium, and $p \leq 0.05$ indicating significance.

RESULTS AND DISCUSSION

The coding regions (exon-1, exon-2, and exon-3) of the *ASIP* gene were successfully amplified with consecutive PCR product lengths of 355 bp, 317 bp, and 462 bp at an annealing temperature of 60°C, as shown in Figure 2. The success of the amplification process is crucial for obtaining reliable sequencing results. Several factors determining the success of gene amplification can be attributed to the design of the primers used (Housley et al., 2006). A well-designed primer can be identified by the percentage of guanine and cytosine content, typically ranging between 50% and 60%, a melting temperature (50-65°C), and a temperature difference between the forward and reverse primers of less than 5°C (Siswanto et al., 2022).

Figure 2 illustrates the sequence of the coding region of the *ASIP* gene, which was successfully sequenced and aligned. The alignment results revealed that the *ASIP* gene's exon-1 and exon-2 regions exhibited monomorphic characteristics, whereas exon-3 in Bali cattle displayed polymorphism or diversity. However, the diversity in the *ASIP* gene cannot be further analyzed to determine coat color markers in Bali cattle. This is due to the non-specific nature of

the identified SNP or mutations, preventing the differentiation of standard, albino, and white-spotted Bali cattle coat colors (Jakaria et al., 2023). Analysis of exon-3 of the *ASIP* gene revealed polymorphisms that did not correlate with coat color in Bali cattle. This lack of correlation may be due to the presence of silent (synonymous) mutations, which do not alter the amino acid sequence of the protein and are thus unlikely to affect its function (Royo et al., 2005; Girardot et al., 2006). Nevertheless, a novel aspect of this study is the discovery of a new SNP, g. 498 A > G was exclusively found in Bali cattle sequences. Consequently, this newly identified SNP has the potential to serve as a genetic marker, particularly for the coat color of Bali cattle. The g.498 A > G SNP in exon-3 of the *ASIP* gene has been implicated in coat color variation by modulating *ASIP* protein function (Zhang et al., 2017). This alteration affects melanogenesis pathways, potentially influencing pigmentation (Guo et al., 2019; Lei et al., 2021). These genetic variations are critical for understanding the molecular mechanisms underlying coat color diversity in mammals.

Figure 4 depicts the results of translating nucleotide base sequences into amino acids in the Bali cattle. The involvement of *ASIP* with other genes that control coat color is shown in Figure 5. The *ASIP* gene plays a significant role in regulating coat color formation. The alignment results of the amino acids in Bali cattle and other cattle breeds are shown in Figure 4. Figure 4 indicates the differences in the amino acids of valine and serine in Bali cattle compared to the Bos mutus grunniens breed. The uniformity of a livestock population is influenced by several factors, including inbreeding (Visscher, 2001), selection, migration, and genetic drift (Yeaman and Whitlock, 2011). Table 1 shows the genotype and allele frequency results for Bali cattle. The highest genotype frequency was observed in white-spotted Bali cattle with the GG genotype (0.67), making allele G the most prevalent in white-spotted Bali cattle. Additionally, in the population diversity of Bali cattle analyzed, white-spotted Bali cattle did not have the genotype AA (0.00), resulting in the lowest allele frequency of A compared to other herds.

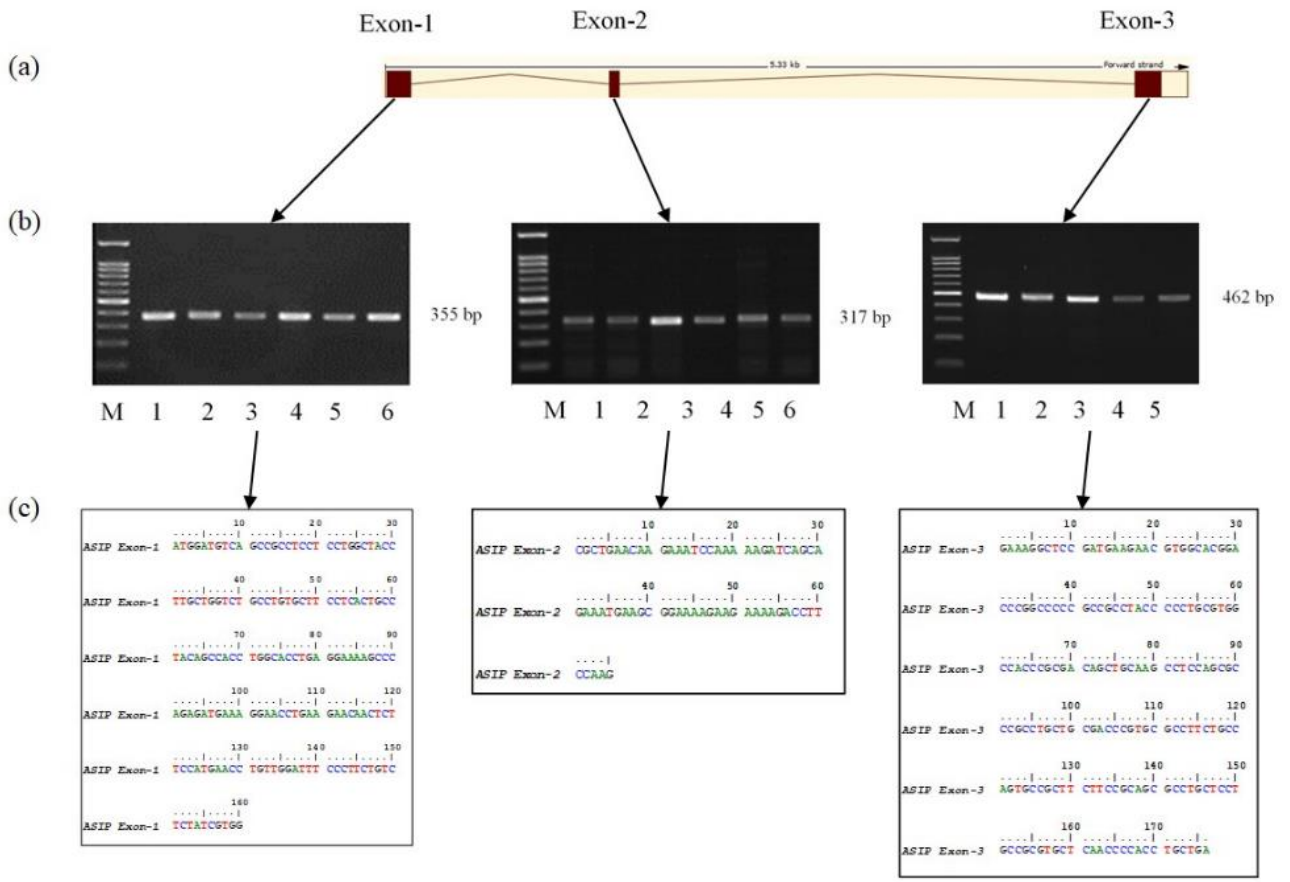


Figure 2. *ASIP* gene structure (**a**), PCR product (**b**), and coding region sequence of the *ASIP* Gene (**c**) in Bali Cattle, Indonesia.

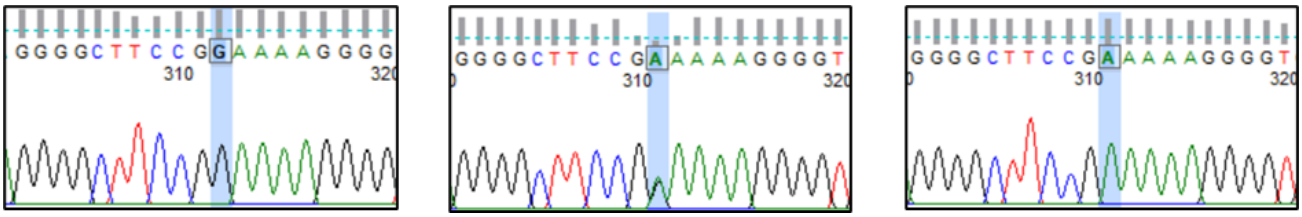
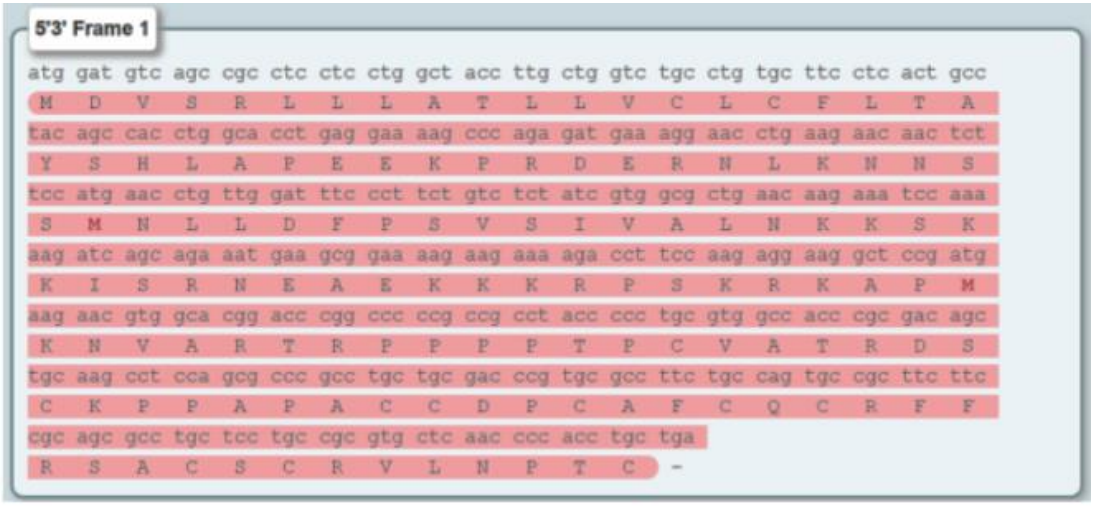


Figure 3. New SNP g.498 A > G in the exon-3 3'UTR region of the *ASIP* gene in Bali cattle, Indonesia.

(a)



(b)

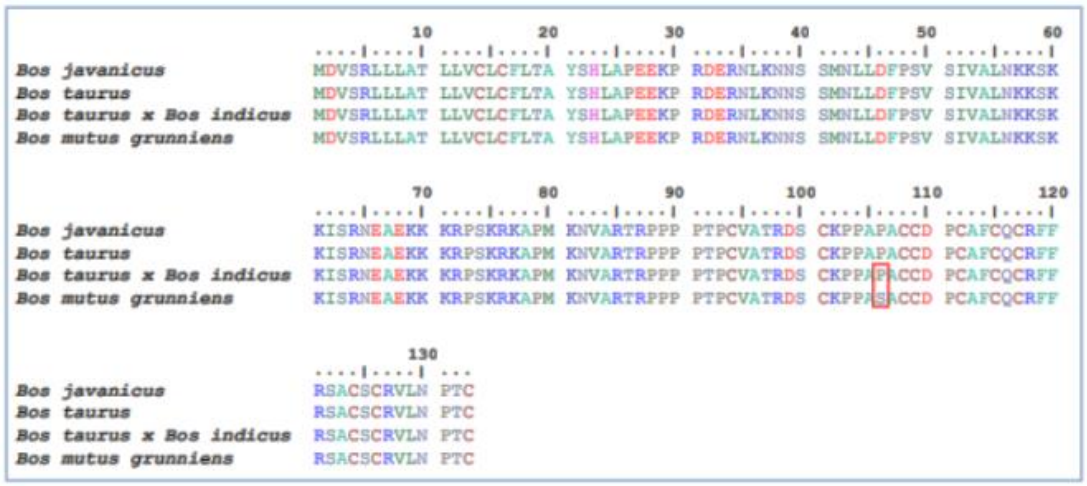


Figure 4. The nucleotide sequence of the *ASIP* gene was translated into amino acids with Expasy (**a**), and amino acid alignment of Bali cattle (*Bos javanicus*) against other breeds was conducted using MEGA (**b**).

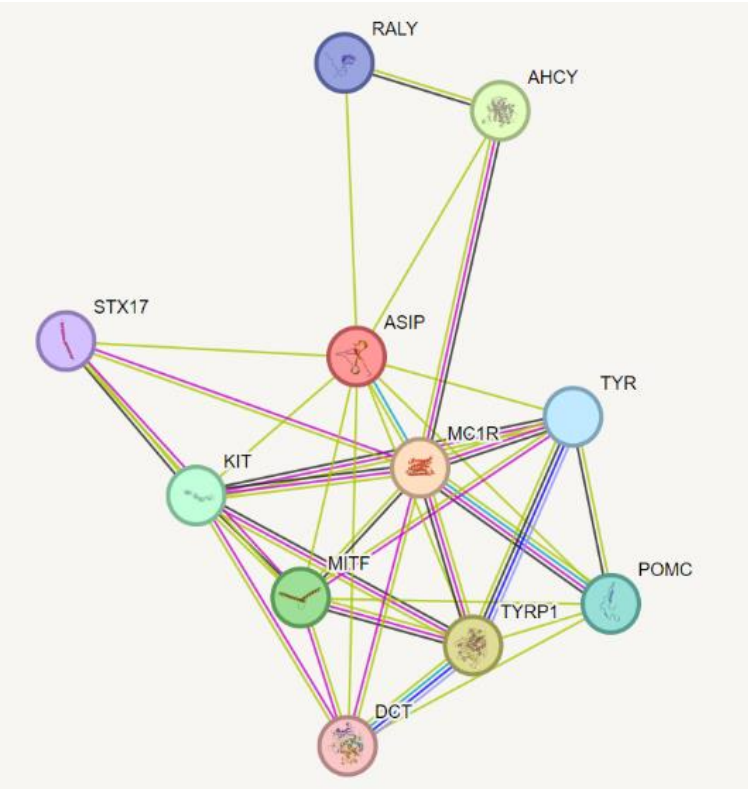


Figure 5. Involvement of the *ASIP* gene and other genes in controlling coat color in cattle (Source: www.string-db.org/).

Table 2 shows that all populations of standard, albino, and white-spotted Bali cattle have non-significant ($p > 0.05$), indicating that all these Bali cattle populations are in the Hardy-Weinberg equilibrium status. Although all Bali cattle populations (standard, albino, and white-spotted) showed non-significant χ^2 values ($p > 0.05$), these results should be interpreted with caution. Non-significant χ^2 values do not necessarily indicate Hardy–Weinberg equilibrium (HWE), particularly when statistical power is low. Bosco et al. (2012) showed that χ^2 tests may fail to detect deviations from HWE in randomly mating populations with low power, leading to false negatives, whereas non-random mating populations may produce false positives. Furthermore, genotyping errors can reduce the power of χ^2 tests, especially with rare allele frequencies (Wang and Shete, 2012). Therefore, conclusions regarding equilibrium status should consider both statistical power and data quality rather than relying solely on non-significant χ^2 values. Although all Bali cattle populations (standard, albino, and white-spotted) showed non-significant χ^2 values ($p > 0.05$), these findings should be interpreted carefully. A non-significant result does not automatically indicate Hardy–Weinberg equilibrium, particularly under conditions of low statistical power, such as small sample sizes or limited genetic diversity.

Table 2. Evaluation of SNP g.498 A > G in Bali cattle by RFLP-PCR

Phenotype	Number	Genotype frequency			Allele frequency		H_o	H_e	χ^2 test
		GG	AA	GA	A	G			
Albino	20	0.45	0.10	0.45	0.32	0.68	0.45	0.44	Ns
Standard	36	0.44	0.17	0.39	0.36	0.64	0.39	0.47	Ns
White-spotted	9	0.67	0.00	0.33	0.17	0.83	0.33	0.29	Ns

SNP: Single nucleotide polymorphism, N: Simple size, H_o: Observed heterozygosity, H_e: Expected heterozygosity, RFLP-PCR: Restriction fragment length polymorphism polymerase chain reaction Ns: Not significant ($p > 0.05$)

A study related to the *ASIP* gene in cattle has been previously conducted, which reported that the coding region of the *ASIP* gene in Spanish and French Brown cattle did not significantly influence the coat color formation process (Royo et al., 2005). Similarly, while exon-1 and exon-2 of the *ASIP* gene were monomorphic in Bali cattle, this observation is consistent with the findings in Brown cattle, suggesting that these regions have little effect on coat color (Royo et al., 2005). A polymorphism in intron 2 of the *ASIP* gene was observed in Hanwoo cattle (Suk Kim et al., 2007); however, it lacked conservation in the population. In addition to regulating coat color, the *ASIP* gene has other general roles, such as controlling the milk metabolism process, as reported by Xie et al. (2022). A study has been conducted on other livestock breeds, such as the Modense breed (Bertolini et al., 2022). However, no results have been reported on the *ASIP* gene and its relationship with coat color (standard, albino, and white-spotted) in Bali cattle.

CONCLUSION

Analysis of the *ASIP* gene showed that the exon-1 and exon-2 regions were monomorphic, indicating uniformity among Bali cattle. In contrast, exon-3 displayed polymorphism, and a novel SNP (g.498 A > G) was identified, suggesting potential genetic variation that may contribute to coat color diversity in this breed. This newly discovered SNP is unique to Bali cattle. However, it was non-specific, and a mutation in the *ASIP* gene was identified in albino, standard, and white-spotted Bali cattle. Consequently, this SNP cannot be considered a candidate genetic marker for coat color in Bali cattle, particularly in albino and white-spotted individuals. Amino acid alignment results of Bali cattle (*Bos javanicus*) with other cattle breeds showed consistent outcomes. Future studies should focus on exploring other candidate genes, regulatory regions, and gene–environment interactions to better understand the genetic basis of coat color variation in Bali cattle. Additionally, expanding the sample size and applying whole-genome sequencing approaches may provide more comprehensive insights into the molecular mechanisms underlying albinism and white-spotted phenotypes.

DECLARATIONS

Funding

This study was supported by the Ministry of Education, Culture, Research, and Technology for funding this research through a scheme of Penelitian Dasar Kompetitif Nasional (PDKN) under the contract number 15852/IT3.D10/PT.01.02/P/T/2023.

Acknowledgments

The authors gratefully acknowledge the support of the Ministry of Education, Culture, Research, and Technology of Indonesia, which funded this study through the National Competitive Basic Research scheme (Contract No. 15852/IT3.D10/PT.01.02/P/T/2023.

Availability of data and materials

All data and information analyzed in this review were obtained from publicly accessible articles that are properly cited in the manuscript. More information is available upon reasonable request from the corresponding author.

Authors' contributions

Kholijah Kholijah, Sri Darwati, Muhammad Fakhrul Ulum, Ronny Rachman Noor, Jakaria Jakaria. Kholijah Kholijah and Jakaria Jakaria collected the data and provided the original draft of the manuscript, while Sri Darwati, Muhammad Fakhrul Ulum, Ronny Rachman Noor, and Jakaria Jakaria reviewed it. All authors considered and agreed on the final version of the manuscript for publication in this journal.

Ethical considerations

All authors have checked for ethical issues, including plagiarism, consent to publish, misconduct, data fabrication and/or falsification, double publication and/or submission, and redundancy. The authors used ChatGPT (OpenAI) and Grammarly solely for language editing purposes; no AI tools were used for data analysis or manuscript content generation.

Competing interests

The authors declare no conflicts of interest.

REFERENCES

Bosco F, Castro D, and Briones MRS (2012). Neutral and stable equilibria of genetic systems and the Hardy-Weinberg principle: Limitations of the chi-square test and advantages of auto-correlation functions of allele frequencies. Frontiers in Genetics, 3: 276. DOI: https://www.doi.org/10.3389/fgene.2012.00276

Bertolini F, Moscatelli G, Schiavo G, Bovo S, Ribani A, Ballan M, Bonacini M, Prandi M, Dall'Olio S, and Fontanesi L (2022). Signatures of selection are present in the genome of two close autochthonous cattle breeds raised in the North of Italy and mainly distinguished for their coat colours. Journal of Animal Breeding and Genetics, 139(3): 307-319. DOI: https://www.doi.org/10.1111/jbg.12659

Dairoh, Ulum MF, Jakaria, Ishak ABL, and Sumantri C (2023). A novel SNPs of the SREBF1 and SCARB1 genes and the association with fatty acid profile in bali cattle. Tropical Animal Science Journal, 46(4): 428-438. DOI: https://www.doi.org/10.5398/tasj.2023.46.4.428

Guo J, Zhong J, Li L, Zhong T, Wang L, Song T, and Zhang H (2019). Comparative genome analyses reveal the unique genetic composition and selection signals underlying the phenotypic characteristics of three Chinese domestic goat breeds. Genetics Selection Evolution, 51(1): 70. DOI: https://www.doi.org/10.1186/s12711-019-0512-4

Gao Y, Gautier M, Ding X, Zhang H, Wang Y, Wang X, Omar Faruque MD, Li J, Ye S, Gou X et al. (2017). Species composition and environmental adaptation of indigenous Chinese cattle. Scientific Reports, 7(1): 16196. DOI: https://www.doi.org/10.1038/s41598-017-16438-7

Goud TS, Upadhyay RC, Pichili VBR, Onteru SK, and Chadipiralla K (2021). Molecular characterization of coat color gene in Sahiwal versus Karan Fries bovine. Journal of Genetic Engineering and Biotechnology, 19(1): 22. DOI: https://www.doi.org/10.1186/s43141-021-00117-2

Gutiérrez-Gil B, Wiener P, and Williams JL (2007). Genetic effects on coat colour in cattle: Dilution of eumelanin and phaeomelanin pigments in an F2-Backcross Charolais × Holstein population. BMC Genetics, 8(1): 56. DOI: https://www.doi.org/10.1186/1471-2156-8-56

Girardot M, Vaiman D, and Iannuccelli N (2006). The insertion of a full-length bos taurus line element is responsible for a transcriptional deregulation of the *normande agouti* gene. Pigment Cell Research, 19(4): 346-355. DOI: https://www.doi.org/10.1111/j.1600-0749.2006.00312.x

Hall T (1999). BioEdit: A user-friendly biological sequence alignment editor and analysis program for Windows 95/98/NT. Nucleic Acids Symposium Series, 41: 95-98.

Han JL, Yang M, Yue YJ, Guo TT, Liu JB, Niu CE, and Yang BH (2015). Analysis of *agouti signaling protein* (*ASIP*) gene polymorphisms and association with coat color in Tibetan sheep (*Ovis aries*). Genetics and Molecular Research, 14(1): 1200-1209. DOI: https://www.doi.org/10.4238/2015.February.6.22

He Y, Huang Y, Wang S, Zhang L, Gao H, Zhao Y, and Guangxin E (2022). Hereditary basis of coat color and excellent feed conversion rate of Red Angus cattle by next-generation sequencing data. Animals, 12(12): 1509. DOI: https://www.doi.org/10.3390/ani12121509

Heryani LGS, Susari NNW, and Gunawan IWNF (2018). The main component variables in the morphometrics of Taro white cattle based on body measurements. Buletin Veteriner Udayana, 10(1): 93-99. DOI: https://www.doi.org/10.24843/bulvet.2018.v10.i01.p15

Housley DJE, Zalewski ZA, Beckett SE, and Venta PJ (2006). Design factors that influence PCR amplification success of cross-species primers among 1147 mammalian primer pairs. BMC Genomics, 7: 253. DOI: https://www.doi.org/10.1186/1471-2164-7-253

Jakaria J, Kholijah K, Darwati S, Rahman Q, Daulay WL, Suhendro I, Londra IM, Ulum MF, and Noor RR (2023). Lack of association between coat color abnormalities in Bali cattle (*Bos javanicus*) and the coding regions of the MC1R and KIT genes. Veterinary World, 16(6): 1312-1318. DOI: https://www.doi.org/10.14202/vetworld.2023.1312-1318

Lei Z, Sun W, Guo T, Li J, Zhu S, Lu Z, Qiao G, Han M, Zhao H, Yang B et al. (2021). Genome-wide selective signatures reveal candidate genes associated with hair follicle development and wool shedding in sheep. Genes, 12(12): 1924. https://www.doi.org/10.3390/genes12121924

Liu Y, Fang X, Zhao Z, Li J, Albrecht E, Schering L, Maak S, and Yang R (2019). Polymorphisms of the *ASIP* gene and the haplotype are associated with fat deposition traits and fatty acid composition in Chinese Simmental steers. Archives Animal Breeding, 62(1): 135-142. DOI: https://www.doi.org/10.5194/aab-62-135-2019

Royo LJ, Alvarez I, Fernandez I, Arranz JJ, Gomez E, and Goyache F (2005). The coding sequence of the ASIP gene is identical in nine wild-type coloured cattle breeds. Journal of Animal Breeding and Genetics, 122(5): 357-360. DOI: https://www.doi.org/10.1111/j.1439-0388.2005.00541.x

Ma Q and Wang W (2024). Genotypic and phenotypic analysis of an oculocutaneous albinism patient: A case report and review of the literature. Journal of Medical Case Reports, 18: 624. DOI: https://www.doi.org/10.1186/s13256-024-04991-5

Norris BJ and Whan VA (2008). A gene duplication affecting expression of the ovine *ASIP* gene is responsible for white and black sheep. Genome Research, 18(8): 1282-1293. DOI: https://www.doi.org/10.1101/gr.072090.107

Purwantara B, Noor RR, Andersson G, and Rodriguez-Martinez H (2012). Banteng and Bali cattle in Indonesia: Status and forecasts. Reproduction in Domestic Animals, 47(Suppl. 1): 2-6. DOI: https://www.doi.org/10.1111/j.1439-0531.2011.01956.x

Reza MA, Noor RR, Jakaria, and Margawati ET (2024). Detection of the TYR gene as a candidate casual mutation for albinism in taro cattle. Journal Ilmu-Ilmu Peternakan, 34(2): 210-218. DOI: https://www.doi.org/10.21776/ub.jiip.2024.034.02.12

Royo LJ, Álvarez I, Fernández I, Arranz JJ, Gómez E, and Goyache F (2005). The coding sequence of the *ASIP* gene is identical in nine wild-type-coloured cattle breeds. Journal of Animal Breeding and Genetics, 122(5): 357-360. DOI: https://www.doi.org/10.1111/j.1439-0388.2005.00541.x

Schmutz SM (2012). Genetics of coat color in cattle. In: J. E. Womack (Editor), Bovine genomics. John Wiley & Sons, pp. 20-33. DOI: https://www.doi.org/10.1002/9781118301739.ch3

Septian WA, Jakaria, and Sumantri C (2015). Genetic diversity of Bali cattle based on microsatellite marker in Indonesian breeding centre. Media Peternakan, 38(1): 12-17. DOI: https://www.doi.org/10.5398/medpet.2015.38.1.12

Siswanto T, Sianipar NF, Warnars HLHS, and Prabowo H (2022). Algorithm model determination of DNA primer design for the success PCR process. International Journal of Emerging Technology and Advanced Engineering, 12(7): 101-107. DOI: https://www.doi.org/10.46338/ijetae0722_11

Suk Kim K, Do KT, Shin HY, Lee JH, Kim NS, Park EW, Yoon DH, and Kim KS (2007). Investigation of coat color candidate genes in Korean cattle (Hanwoo). Journal of Animal Science and Technology, 49(6): 711-718. DOI: https://www.doi.org/10.5187/JAST.2007.49.6.711

Tamura K, Stecher G, Peterson D, Filipski A, and Kumar S (2013). MEGA6: Molecular evolutionary genetics analysis version 6.0. Molecular Biology and Evolution, 30(12): 2725-2729. DOI: https://www.doi.org/10.1093/molbev/mst197

Trigo BB, Utsunomiya ATH, Fortunato AAAD, Milanesi M, Torrecilha RBP, Lamb H, Nguyen L, Ross EM, Hayes B, Padula RCM et al. (2021). Variants at the *ASIP* locus contribute to coat color darkening in Nellore cattle. Genetics Selection Evolution, 53(1): 40. DOI: https://www.doi.org/10.1186/s12711-021-00633-2

Visscher PM, Smith D, Hall SJG, and Wiliams JL (2001). A viable herd of genetically uniform cattle. Nature, 75: 14. DOI: https://www.doi.org/10.1038/35053160

Wang L and Shete S (2012). Testing departure from Hardy–Weinberg proportions. In: R. Elston, J. Satagopan, and S. Sun (Editors), Statistical human genetics; Methods in molecular biology. Springer, pp. 77-102. DOI: https://www.doi.org/10.1007/978-1-61779-555-8_6

Xie T, Liu Y, Lu H, Iqbal A, Ruan M, Jiang P, Yu H, Meng J, and Zhao Z (2022). The knockout of the *ASIP* gene altered the lipid composition in bovine mammary epithelial cells via the expression of genes in the lipid metabolism pathway. Animals, 12(11): 1389. DOI: https://www.doi.org/10.3390/ani12111389

Yeaman S and Whitlock MC (2011). The genetic architecture of adaptation under migration–selection balance. Evolution, 65(7): 1897-1911. DOI: https://www.doi.org/10.1111/j.1558-5646.2011.01269.x

Zhang X, Li W, Liu C, Peng X, Lin J, He S, Li X, Han B, Zhang N, Wu Y et al. (2017). Alteration of sheep coat color pattern by disruption of *ASIP* gene via CRISPR Cas9. Scientific Reports, 7: 8149. DOI: https://www.doi.org/10.1038/s41598-017-08636-0

Zhao H, Chen M, and Yang H (2015). Albinism. Developments in Aquaculture and Fisheries Science, 39: 211-228. DOI: https://www.doi.org/10.1016/B978-0-12-799953-1.00012-X

Publisher's note: Scienceline Publication Ltd. remains neutral with regard to jurisdictional claims in published maps and institutional affiliations.

Open Access: This article is licensed under a Creative Commons Attribution 4.0 International License, which permits use, sharing, adaptation, distribution and reproduction in any medium or format, as long as you give appropriate credit to the original author(s) and the source, provide a link to the Creative Commons licence, and indicate if changes were made. The images or other third party material in this article are included in the article's Creative Commons licence, unless indicated otherwise in a credit line to the material. If material is not included in the article's Creative Commons licence and your intended use is not permitted by statutory regulation or exceeds the permitted use, you will need to obtain permission directly from the copyright holder. To view a copy of this licence, visit https://creativecommons.org/licenses/by/4.0/.
© The Author(s) 2025

2025, Scienceline Publication
World's Veterinary Journal
World Vet J, 15(4): 960-967.
ISSN 2322-4568

DOI: https://dx.doi.org/10.54203/scil.2025.wvj97
PII: S232245682500097-15

Phenotypic Resistance of *Salmonella enterica* to Antibiotics in Imported Meats in Tema Metropolis, Ghana

Frederick Adzitey[1,2]*, Innocent Allan Anachinaba[1], Agus Susilo[3], and Nurul Huda[4]

[1]*Department of Animal Science, Faculty of Agriculture, Food and Consumer Sciences, University for Development Studies, Nyankpala Campus, Ghana*
[2]*Drylands Research Institute, University for Development Studies, Tamale, Ghana*
[3] *Department of Animal Science, Faculty of Animal Science, University of Brawijaya, Malang 65145, East Java, Indonesia*
[4]*Postgraduate School, University of Brawijaya, Malang 65145, East Java, Indonesia*

*Corresponding author's Email: adzitey@yahoo.co.uk

ORIGINAL ARTICLE
Received: September 21, 2025
Revised: October 24, 2025
Accepted: November 26, 2025
Published: December 25, 2025

ABSTRACT

Salmonella enterica (*S. enterica*) causes certain foodborne diseases and poses public health concerns when it becomes antibiotic-resistant. The present study aimed to determine the resistance of *S. enterica* to antibiotics from imported meats sold in the Tema Metropolis, Ghana. A total of 300 beef, chicken, and pork samples randomly selected from markets of the Metropolis were tested for *S. eneterica.* The disc diffusion method was used to determine the antibiotic resistance in 60 *S. enterica* isolates. The current results revealed that 40% of imported chicken, 38% of imported pork, and 29% of imported beef were positive for *S. enterica*. The S. enterica isolated from imported meat sources was 36.7% resistant to tetracycline but susceptible (≥ 68%) to imipenem, ciprofloxacin, tetracycline, chloramphenicol, trimethoprim, gentamicin, and ceftriaxone. The multiple antibiotic resistance (MAR) index fell within the range of 0.1 to 0.6, and 12 different patterns were observed. The present study revealed the contamination of *S. enterica* in some imported meat sold in Tema Metropolis, Ghana. Avoidance of cross-contamination and adequate thermal treatment of meats before eating is essential.

Keywords: Antibiotic resistance, Meat, Prevalence, *Salmonella enterica*

INTRODUCTION

Worldwide, meat is an essential source of protein for human populations. According to Ahmad et al. (2018), meat also contains some minerals, such as zinc, selenium, iron, and phosphorus, and vitamins, including vitamins A and B-complex. Ghana's meat production gross value reached approximately 150.88 million dollars, a net decrease of -53,266,00 USD (-26.09%) during previous years (Divercitytimes, 2022). Approximately 48,047 tonnes of bovine meat and 287,930 tonnes of poultry meat were imported into Ghana in 2020 (Knoema, 2021). Furthermore, importing edible meat offal in 2019 was recorded to be 78.4 million dollars, corresponding to about 484 million cedis (Sasu, 2012). Meat is an important part of the daily diet of most Ghanaians (Nkegbe et al., 2013). Nkegbe et al. (2013) added that chicken is the most consumed, followed by beef, chevon, grasscutter, pork, and mutton.

Despite the high nutrient composition of meats and their consumption, they serve as potential sources of microbial contaminants (El Hanafi et al., 2023; Adzitey et al., 2024; Monten et al., 2024). In particular, *Salmonella enterica* (*S. enterica*) has been found in chicken, pork, and beef (Zhao et al., 2001; Meyer et al., 2010; Ekli et al., 2020). Additionally, *S. enterica* has been reported to cause foodborne diseases in humans (CDC, 2021), causing 273 hospitalizations, 1,135 disease, and two deaths in people who consumed the animal meats (CDC, 2021).

Antibiotics, including tetracycline and amoxicillin, are sometimes used for the treatment of diseased animals, as prophylactics, and as growth promoters (Chattopadhyay, 2014). Antibiotics are also used for treating infections in humans that might be caused by consuming meat contaminated by bacteria such as *S. enterica* (CDC, 2021). The development of resistance by bacteria to antibiotics is partly due to the use of antibiotics in human treatments and animal production (Katakweba et al., 2012). Bacteria can develop resistance to three or more antibiotics (Yang et al., 2019), a phenomenon described as multidrug resistance. Bacteria that are resistant to multiple medicines are difficult to treat when they cause infections (Adzitey et al., 2020). *Salmonella enterica* isolated from meat sources have been reported to be resistant to antibiotics, such as gentamicin, tetracycline, chloramphenicol, amoxicillin, and ceftriaxone (Thai et al., 2012; Ejo et al., 2016).

Tema Metropolis in Ghana is one of the country's busiest urban centers, with a population from different countries and parts of Ghana. Therefore, active marketing and consuming meat are unavoidable. However, limited studies are

To cite this paper: Adzitey F, Anachinaba IA, Susilo A, and Huda N (2025). Phenotypic Resistance of *Salmonella enterica* to Antibiotics in Imported Meats in Tema Metropolis, Ghana. *World Vet. J.,* 15(4): 960-967. DOI: https://dx.doi.org/10.54203/scil.2025.wvj97

available on the existence of bacteria in sellable meat in Ghana. Therefore, the present study aimed to investigate the prevalence of *S. enterica* and their resistance to antibiotics in imported meats sold at Tema's markets, Ghana.

MATERIALS AND METHODS

Ethical approval

The study was conducted in accordance with the approved ethical procedures of the University for Development Studies ethics committee, as referenced by the UDS/RB/099/22.

Study area

The present study was carried out in Tema Metropolis, which lies within latitude 5°38'32' north and longitude 0°0'9' west (Tema Metropolitan Assembly [TMA], 2021). The Metropolis is known as Harbor City because the largest seaport and numerous industries are located there (TMA, 2021), and has a size of 565 km^2 (Ghana Administrative Division, 2021). Maps of Ghana and Tema Metropolis are shown in Figure 1.

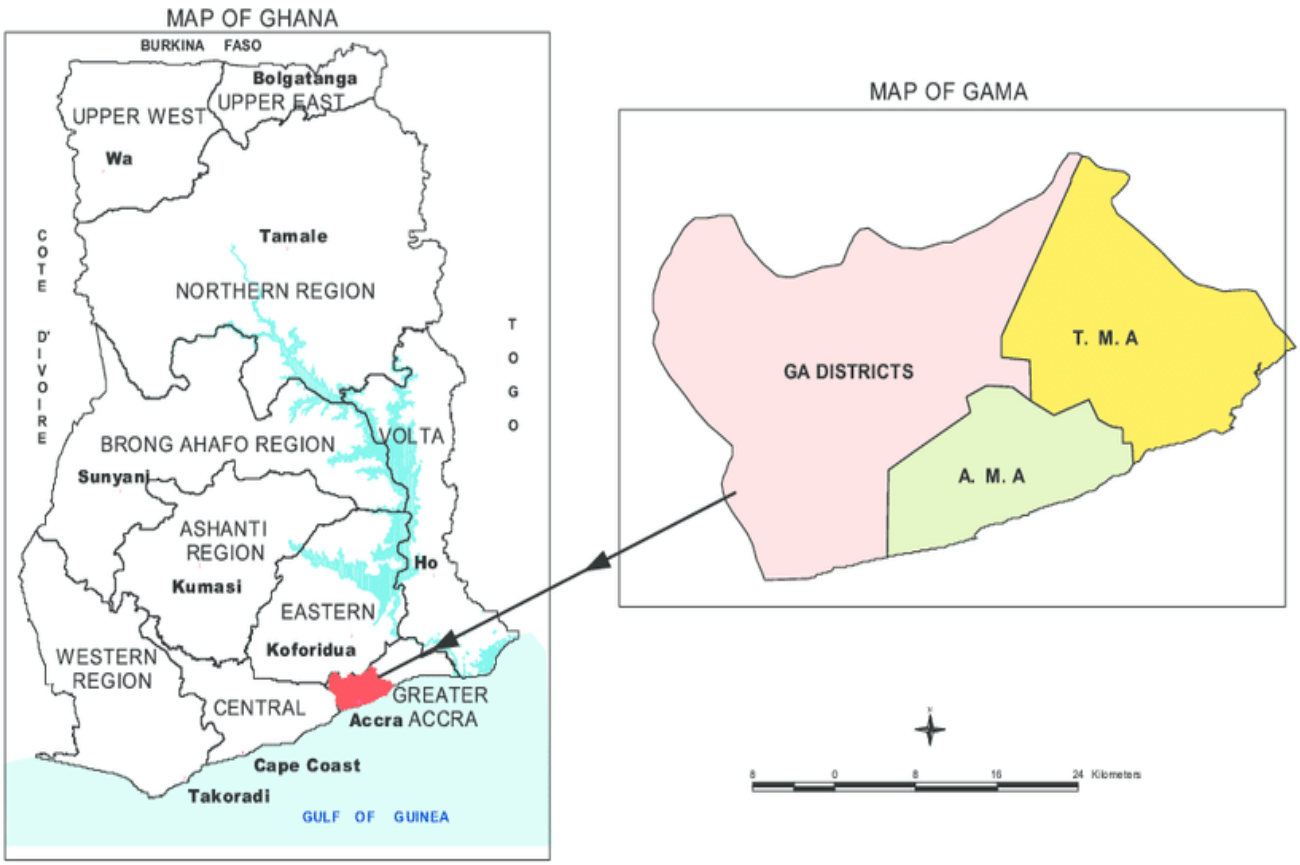


Figure 1. The map of Ghana, the Greater Accra region, and the Tema Metropolis (T.M.A). Source: TMA (2021)

Sample collection

Three hundred samples of imported chicken, pork, and beef (100 each) were randomly collected from markets in Tema Metropolis and analyzed for *S. enterica*. Sampling was carried out from April 2022 to September 2022. Fifty samples were collected each month from five different vendors. Ten samples were collected from each vendor. Collected samples were transported on ice to the Spanish Laboratory of the University for Development Studies for microbiological analysis.

Salmonella enterica microbiological analysis

The analysis for *S. enterica* was performed according to Wallace and Hammack (2013). The samples (10 g) were transferred into 90 mL buffered peptone water and incubated overnight at 37°C. Thereafter, the mixture was transferred into 10 mL of selenite cysteine and incubated at 37°C for 24 hours. In parallel, 0.1 mL was transferred into 10 mL of Rappaport-Vassiliadis broth (Oxoid Limited, UK) and incubated at 41°C for 48 hours. Incubated samples were plated onto brilliant green and xylose, lysine, and deoxycholate agars (Oxoid Limited, UK), and incubated overnight at 37°C.

Potential *S. enterica* isolates were streaked on trypticase soy agar (Oxoid Limited, UK) and incubated overnight at 37°C for purification. The isolates were then identified using Gram stain, growth on Simon citrate agar, triple sugar iron, lysine iron, and *Salmonella* latex agglutination test kit (Oxoid Limited, UK).

Confirmation of *Salmonella* using the polymerase chain reaction

The polymerase chain reaction (PCR) was carried out using the method of Upadhyay et al. (2010). Firstly, DNA was extracted from *Salmonella* cultures by lysing at 99°C for 10 minutes using 30 µl RNase/DNase-free water in a universal thermal cycler (VWR Prelab, UK). The 20 µl PCR reaction was made up of 10 µM each of primers (invA-F GTGAAATTATCGCCACGTTCGGGCAA and invA-R TCATCGCACCGTCAAAGGAACC), 22 mM NH_4Cl, 20 mM Tris-HCl (pH 8.9 at 25°C), 0.2 mM dNTPs, 0.25U One Taq® DNA polymerase (New England Biolabs® Inc), 1.8 mM $MgCl_2$, 0.06% IGEPAL® CA-630, 5% glycerol, 0.05% Tween-20, xylene Cyanol FF, and Tartrazine, and 2 µl lysate as template. The temperature cycles used were 94°C for five minutes, 40 cycles of 94°C for 40 seconds, 64°C for 30 seconds, 72°C for 30 seconds, and a final extension at 72°C for seven minutes.

The PCR products were separated using 2% agarose and stained with 2.5 µl ethidium bromide. The PCR products (7 µl) were mixed with the loading dye (1 µl), and the mixture was subjected to gel electrophoresis for 30 minutes at 80V. The gel was then viewed under a UV transilluminator from Cleaver Scientific Company, UK.

Antibiotic susceptibility of S*almonella enterica*

The antibiotic susceptibility test was carried out according to the Bauer et al. (1966) method against nine antibiotics, including ceftriaxone 30 µg (Cro), amoxicillin 30 µg (A), tetracycline 30 µg (T), chloramphenicol 30 µg (C), azithromycin 15 µg (Ath), gentamicin 10 µg (Gm), imipenem 10 µg (Imi), ciprofloxacin 5 µg (Cip), and trimethoprim 2.5 µg (Tm), purchased from MAST Group Limited, UK. *Salmonella enterica* colonies were transferred into trypticase soy (TS) broth (Oxoid Limited, UK) and incubated for 15 hours at 37°C. Sterile TS broth was used to adjust the turbidity to 0.5 McFarland Standard solution and transferred into Muller-Hinton (MH) agar (Oxoid Limited, UK). Four or five antibiotic discs were placed on MH agar and incubated for 24 hours at 37°C. Inhibition zones were measured, and the results were compared to the values of Clinical and Laboratory Standard Institute (CLSI, 2017). The multiple antibiotic resistance (MAR) index was calculated using the formula a/b, where a represents the number of antibiotics to which a particular isolate was resistant and b the total number of antibiotics examined (Krumperman, 1983).

Statistical analysis

Data on the prevalence of *S. enterica* were statistically computed using a generalized linear model of the Statistical Package for the Social Sciences version 20. Significant differences were recorded at 5% using the Wald chi-square.

RESULTS AND DISCUSSION

Prevalence of *Salmonella enterica*

Figure 2 depicts the prevalence of *S. enterica* in the imported chicken, beef, and pork samples collected from Tema Metropolis, Ghana. *Salmonella enterica* was isolated from 40.0% of the imported chicken, 38.0% of the pork, and 29.0% of the beef samples. Significant differences were not observed among the chicken, beef, and pork samples ($p > 0.05$). *Salmonella enterica* isolates were confirmed using PCR (Upadhyay et al., 2010). The bacteria yielded a band size of approximately 284 bp, confirming that the isolates were *S. enterica* (Figure 3).

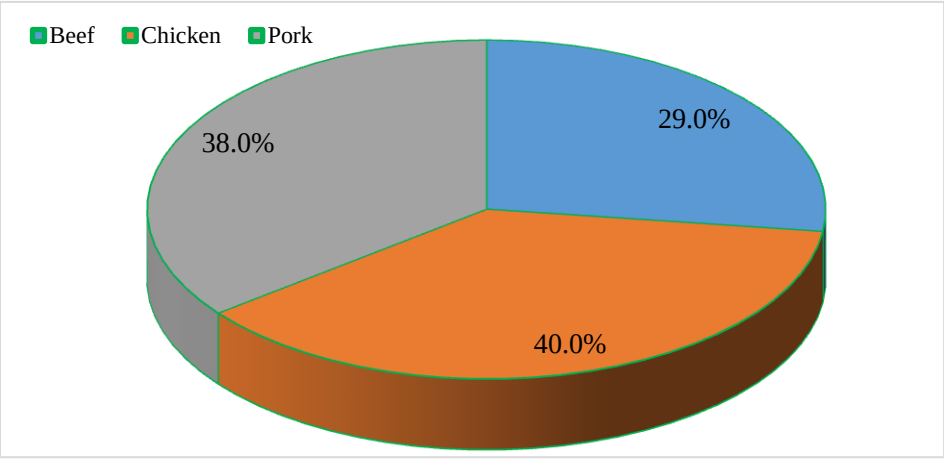


Figure 2. Prevalence of *Salmonella enterica* in imported beef, chicken, and pork samples obtained from Tema Metropolis, Ghana

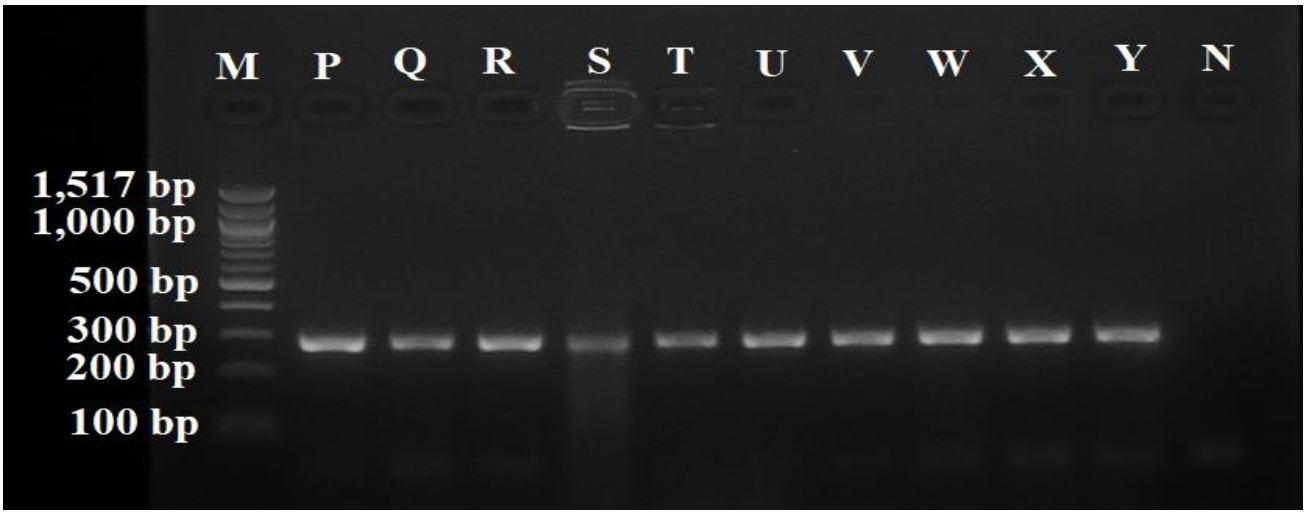


Figure 3. The bands of *Salmonella enterica* isolated from imported meats obtained from Tema Metropolis, Ghana. M: 100bp DNA ladder (New England Biolabs), P: Positive control (*Salmonella enterica ATCC 14028*), Q to Y: *Salmonella enterica* isolates (~284 bp), and N: Negative control (No DNA/Template).

In the present study, *S. enterica* were found in the imported chicken, pork, and beef samples obtained from the Tema Metropolis, Ghana. The contamination of the meat could be from the origin country, since not all meat samples were tested microbiologically at the ports of Ghana before being allowed into the country or during handling in Ghana. The contamination of different types of meat in different countries has been reported. In Southern Germany, Vidas' system for *Salmonella* identification found 1.8% of pork and 0.6% of beef to be positive for *Salmonella*, while the culture method found 1.1% of pork and 0.1% of beef to be positive for *Salmonella* (Meyer et al., 2010). The higher prevalence of *Salmonella* in pork samples compared to beef samples aligns with the present results. The presence of *S. enterica* in beef and pork during the present study was higher than that of Meyer et al. (2010). Poultry meat (29.3%) and beef (16.0%) samples from butcher shops and delicatessens in Bolu, Western Turkey, were found to be positive for *Salmonella* species using the cultural method (Arslan and Eyi, 2010). Additionally, the prevalence of *S. enterica* in beef samples was higher in the current study than that of Arslan and Eyi (2010). However, the prevalence of *S. enterica* in chicken meat was lower than that reported by Arslan and Eyi (2010). In the USA, 4.2% of chicken, 3.3% of pork, and 1.9% of beef meat were identified to be contaminated with *Salmonella* using the cultural method (Zhao et al., 2001), which were all lower than the findings of the present study. In Gondar, Ethiopia, Ejo et al. (2016) examined 50 raw meats using the cultural method and found 12.0% of the samples to be positive for *Salmonella*. While Yang et al. (2019) reported a higher prevalence in pork (37.3%) than in beef (16.1%) in China, the present study found a lower overall prevalence in pork but not in beef. Differences in the rate of contamination of meats could be attributed to the differences in the country or city of isolation, observance of standard and hygienic practices in animal and meat handling, the type of analyzed meat, and the isolation method employed (Zhao et al., 2001; Meyer et al., 2010).

Resistance of *Salmonella enterica* isolates

The resistance of *S. enterica* isolated from meat samples is presented in Table 1. The *S. enterica* isolates were 36.7% resistant to azithromycin and 20.0% resistant to amoxicillin. The *S. enterica* isolates were highly susceptible to imipenem (100.0%), ciprofloxacin (96.7%), tetracycline (96.7%), chloramphenicol (95.0%), trimethoprim (81.7%), gentamicin (70.0%), and ceftriaxone (68.3%). Furthermore, *S. enterica* exhibited relatively higher intermediate resistance to amoxicillin (48.3%) and azithromycin (36.7%).

Table 1. Resistance of *Salmonella enterica* isolated from imported chicken, beef, and pork meats in Tema, Ghana

Antibiotics	Susceptibility (%)	Intermediate resistance (%)	Resistant (%)
Amoxicillin 30µg (A)	31.7	48.3	20.0
Azithromycin 15µg (Ath)	26.7	36.7	36.7
Ceftriaxone 30µg (Cro)	68.3	26.7	5.0
Chloramphenicol 30µg (C)	95.0	0.0	5.0
Ciprofloxacin 5µg (Cip)	96.7	3.3	0.0
Gentamicin 10µg (Gm)	70.0	13.3	16.7
Imipenem 10µg (Imi)	100.0	0.0	0.0
Tetracycline 30µg (T)	96.7	0.0	3.3
Trimethoprim 2.5µg (Tm)	81.7	15.0	3.3
Overall	74.1	15.9	10.0

Multiple antibiotic resistance index and antibiotic resistance profile

The MAR index and antibiotic resistance profile of each *S. enterica* from the chicken, beef, and pork samples are shown in Table 2. The MAR index was in the range of 0.1 to 0.6, and 12 different resistance patterns occurred. Resistance to azithromycin alone was the most common pattern, which was observed in 12 isolates. The resistance to five, four, and three different antibiotics were 3.0%, 3.0% and 12.7%, respectively. Furthermore, 27 *S. enterica* isolates were not resistant to any of the antibiotics tested.

Table 2. Multiple antibiotic resistance index and antibiotic resistance pattern of individual *Salmonella enterica* isolated from imported chicken, beef, and pork meats in Tema, Ghana

Source	Code	Number of antibiotics	Antibiotic-resistant profile	MAR index
Foreign Beef	BLB4	5	Cro-A-C-Tm-T	0.6
Foreign Beef	CB4	4	A-C-Gm-T	0.4
Foreign Pork	BP5	3	Tm-Gm-Ath	0.3
Foreign Beef	BLB4	3	Cro-A-Ath	0.3
Foreign Chicken	CC5	3	A-Gm-Ath	0.3
Foreign Beef	UB1	3	A-C-Ath	0.3
Foreign Beef	CB10	2	Cro-Ath	0.2
Foreign Chicken	BC3	2	A-Gm	0.2
Foreign Chicken	UC8	2	A-Gm	0.2
Foreign Beef	BB4	2	A-Ath	0.2
Foreign Chicken	CC8	2	A-Ath	0.2
Foreign Pork	UP7	2	A-Ath	0.2
Foreign Beef	UB6	1	Gm	0.1
Foreign Chicken	BC7	1	Gm	0.1
Foreign Chicken	BLC6	1	Gm	0.1
Foreign Pork	UP2	1	Gm	0.1
Foreign Pork	UP9	1	Gm	0.1
Foreign Beef	BB2	1	Ath	0.1
Foreign Beef	BB5	1	Ath	0.1
Foreign Beef	BLB6	1	Ath	0.1
Foreign Chicken	BC1	1	Ath	0.1
Foreign Chicken	BC6	1	Ath	0.1
Foreign Chicken	CC9	1	Ath	0.1
Foreign Chicken	UC1	1	Ath	0.1
Foreign Chicken	UC10	1	Ath	0.1
Foreign Pork	BP10	1	Ath	0.1
Foreign Pork	BP8	1	Ath	0.1
Foreign Pork	CP2	1	Ath	0.1
Foreign Pork	CP3	1	Ath	0.1
Foreign Pork	CP4	1	Ath	0.1
Foreign Pork	NP5	1	Ath	0.1
Foreign Beef	CB7	1	A	0.1
Foreign Chicken	BC10	1	A	0.1

MAR: Multiple antibiotic resistance, Ceftriaxone 30µg (Cro), Tetracycline 30µg (T), Azithromycin 15µg (Ath), Chloramphenicol 30µg (C), Amoxicillin 30µg (A), Ciprofloxacin 5µg (Cip), Imipenem 10µg (Imi), Gentamicin 10µg (Gm), Trimethoprim 2.5 µg (Tm).

Using antibiotics in animal production and non-adherence to withdrawal periods before slaughtering the animals are the main factors driving the deposition of antibiotic residues in meat (Thai et al., 2012; Adzitey et al., 2013). Several studies have shown that *Salmonella* from different meat sources exhibited some level of resistance to commonly used antibiotics (Ejo et al., 2016; Yang et al., 2019; Aduah et al., 2023). Outbreaks resulting from antibiotic-resistant bacteria, including *Salmonella* species, are of public health concern, especially when consumed via meat (CDC, 2021). In contrast to the high resistance rates reported in US meat samples to tetracycline (80%), ceftriaxone (16%), and chloramphenicol (16%; White et al., 2001), the isolates in the current study exhibited lower resistance to these antibiotics. Resistance to gentamicin, however, was higher than the 4% previously reported. However, the current findings on ciprofloxacin and those of White et al. (2001) were similar. In China, Yang et al. (2019) examined meat samples for *Salmonella* and

reported resistance, intermediate resistance and susceptibility to ceftriaxone (5.5%, 0.9% and 93.6%), chloramphenicol (30.3%, 7.8% and 61.9%), ciprofloxacin (16.1%, 34.9% and 49.1%), gentamicin (15.1%, 5.0% and 9.8%), imipenem (0.9%, 2.8% and 96.3%) and tetracycline (65.6%, 5.5% and 28.9%), respectively, which were comparable to the present results. In contrast to the study conducted by Ejo et al. (2016) in Ethiopia, who reported 100% resistance to tetracycline and 33.3% to gentamicin with no resistance to amoxicillin or ceftriaxone, the present study found a distinct profile, with lower resistance to tetracycline and gentamicin, coupled with emerging resistance to amoxicillin and ceftriaxone. While Thai et al. (2012) documented considerable resistance to tetracycline (58.5%), chloramphenicol (37.3%), and trimethoprim (34.0%) in Vietnam, the resistance levels for these antibiotics were low during the present study. The present findings confirmed that *Salmonella* resistance to one or more antibiotics, including multidrug resistance, is a persistent global issue, as reported in several studies (Arslan and Eyi, 2010; Thai et al., 2012; Ejo et al., 2016; Yang et al., 2019).

CONCLUSION

Salmonella enterica was detected in imported beef, poultry, and pork samples from the Tema Metropolis, Ghana, with imported chicken being the most frequently contaminated source. *Salmonella* isolates demonstrated antimicrobial resistance, most notably to azithromycin and amoxicillin. One *Salmonella enterica* isolated from imported beef was resistant to five different antibiotics. Thus, imported meats sold at Tema Metropolis can be a potential source for transferring *S. enterica* resistant to some antibiotics. Further studies on the genetic diversity between *S. enterica* isolates from imported and local meats are recommended.

DECLARATIONS

Acknowledgments

The authors acknowledge the support provided by the University for Development Studies and the Visiting Lecture Programme of the University of Brawijaya for this study.

Authors' contributions

Frederick Adzitey conceived the idea, provided funds, was involved in data collection, and wrote the first draft. Innocent Allan Anachinaba was involved in data collection, provided funds, and data analysis. Agus Susilo conceived the idea, was involved in funding, and proofreading. Nurul Huda also conceived the idea, secured funding, and reviewed. All authors have reviewed and approved the final edition of the manuscript for publication.

Competing interests

The authors declared that they have no conflicts of interest.

Ethical considerations

Ethical issues, including plagiarism, consent to publish, misconduct, data fabrication and/or falsification, double publication and/or submission, and redundancy, have been checked by all the authors. The authors explicitly and transparently disclose that no AI tool was used in the whole of the article.

Availability of data and materials

The data obtained in the present study are available from the corresponding author upon reasonable request.

Funding

The present study was not supported by any external funding sources. Publication fee will be supported by the University of Brawijaya, East Java, Indonesia.

REFERENCES

Aduah M, Adzitey F, Ekli R, Teye AG, and Huda N (2023). Phenotypic antimicrobial resistance of *Salmonella enterica* isolated from meats, humans and working tools. Journal of Food: Microbiology, Safety & Hygiene, 8(7): 248. Available at: https://www.longdom.org/open-access-pdfs/phenotypic-antimicrobial-resistance-of-emsalmonella-entericaem-isolated-from-meats-humans-and-working-tools.pdf

Adzitey F, Anachinaba IA, Brown CAQ, Huda N, and Rambli M (2024). Prevalence of resistant *Escherichia coli* isolated from local meats sold in Tema Metropolis, Ghana. ASEAN Journal on Science and Technology for Development, 40(2): 118-122. DOI: https://www.doi.org/10.61931/2224-9028.1534

Adzitey F, Teye GA, and Amoako DG (2020). Prevalence, phylogenomic insights, and phenotypic characterization of *Salmonella enterica* isolated from meats in the Tamale Metropolis of Ghana. Food Science and Nutrition, 8: 3647-3655. DOI: https://www.doi.org/10.1002/fsn3.1647

Adzitey F, Rusul G, Huda N, Cogan T, and Corry J (2013). Prevalence, antibiotic resistance and genetic diversity of *Listeria monocytogenes* isolated from ducks, their rearing and processing environments in Penang, Malaysia. Food Control, 32(2): 607-614. DOI: https://www.doi.org/10.1016/j.foodcont.2012.12.016

Ahmad RS, Imran A, and Hussain MB (2018). Nutritional composition of meat. In: M. S. Arshad (Editor), Meat science and nutrition. IntechOpen, pp. 61-75. DOI: https://www.doi.org/10.5772/intechopen.77045

Arslan S and Eyi A (2010). Occurrence and antimicrobial resistance profiles of *Salmonella* species in retail meat products. Journal of Food Protection, 73(9): 1613-1617. DOI: https://www.doi.org/10.4315/0362-028x-73.9.1613

Bauer AW (1966). Antibiotic susceptibility testing by a standardized single disc method. The American Journal of Clinical Pathology, 45(4): 149-58. Available at: https://pubmed.ncbi.nlm.nih.gov/5325707/

Centers for disease prevention and control (CDC) (2021). *Salmonella* outbreaks linked to backyard poultry. Available at: https://www.cdc.gov/salmonella/backyardpoultry-05-21/index.html

Chattopadhyay MK (2014). Use of antibiotics as feed additives: A burning question. Frontiers in Microbiology, 5: 334. DOI: https://www.doi.org/10.3389/fmicb.2014.00334

Clinical and laboratory standard institute (CLSI) (2017). Document M31-A3. Performance standards for antimicrobial disk and dilution susceptibility tests for bacteria isolated from animals, approved standard, third edition. CLSI, 940 West Valley Road, Suite 1400, Wayne, Pennsylvania 19087-1898, USA. Available at: https://www.dbt.univr.it/documenti/OccorrenzaIns/matdid/matdid485539.pdf

Divercitytimes (2022). Ghana gross value of meat production. Available at: https://divercitytimes.com/agriculture/country/ghana-gross-value-meat accessed on 22/10/2025

Ejo M, Garedew L, Alebachew Z, and Worku W (2016). Prevalence and antimicrobial resistance of *Salmonella* isolated from animal-origin food items in Gondar, Ethiopia. Biomed Research International, 2016(1): 4290506. DOI: https://www.doi.org/10.1155/2016/4290506

Ekli R, Adzitey F, and Agbolosu AA (2020). Farmers' knowledge in antibiotic usage, antibiotic residues, and susceptibility of *Salmonella enterica* in beef samples from the Wa Municipality, Ghana. Bulletin of Animal Health and Production in Africa, 68(2): 89-101. Available at: https://www.scirp.org/reference/referencespapers?referenceid=3635330

El Hanafi M, Nourredine B, Saadia N, and Hakim K (2023). Occurrence of antibiotic resistance in *Salmonella* serotypes isolated from environment, humans, animals, and animal products in Morocco: A systematic review. World's Veterinary Journal, 13(1): 32-44. DOI: https://www.doi.org/10.54203/scil.2023.wvj4

Ghana administrative division (2021). Regions and districts. Available at: https://en.wikipedia.org/wiki/Tema_Metropolitan_District#cite_note-1

Katakweba AAS, Mtambo MMA, Olsen JE, and Muhairwa AP (2012). Awareness of human health risks associated with the use of antibiotics among livestock keepers and factors that contribute to selection of antibiotic resistance bacteria within livestock in Tanzania. Livestock Research for Rural Development, 24(10): 170. Available at: https://www.lrrd.org/lrrd24/10/kata24170.htm

Knoema (2021). Ghana - Meat imports quantity. Available at: https://knoema.com/atlas/Ghana/topics/Agriculture/Trade-Import-Quantity/Meat-imports-quantity

Krumperman PH (1983). Multiple antibiotic resistance indexing of *Escherichia coli* to identify high-risk sources of fecal contamination of foods. Applied and Environmental Microbiology, 46(1): 165-170. DOI: https://www.doi.org/10.1128/aem.46.1.165-170.1983

Meyer C, Thiel S, Ullrich U, and Stolle A (2010). *Salmonella* in raw meat and by-products from pork and beef. Journal of Food Protection, 73(10): 780-1784. DOI: https://www.doi.org/10.4315/0362-028x-73.10.1780

Monten SKK, Adzitey F, Bawah J, Depison, and Nurul H (2024). Investigation of the contamination rate of guinea fowl meats and its related samples by *Escherichia coli* using one health approach. Indonesian Food Science and Technology Journal, 8(1): 126-137. DOI: https://www.doi.org/ 10.22437/ifstj.v8i1.32101

Nkegbe E, Assuming-Bediako N, Aikins-Wilson S, and Hagan A (2013). Meat consumption trends in some selected households in Accra Ghana. Asian Journal of Agriculture and Food Sciences, 1(4): 151-157. Available at: https://ajouronline.com/index.php/AJAFS/article/view/443

Sasu DD (2021). Value of meat imported into Ghana from 2014 to 2019, pp. 1-129. Available at: https://mofa.gov.gh/site/images/pdf/2019%20AGRICULTURE%20FACT%20AND%20FIGURES.pdf

Tema metropolitan assembly (TMA) (2021). History of Tema. Available at: https://www.temametro.org/about-the-tema-city

Thai TH, Hirai T, Lan NT, and Yamaguchi R (2012). Antibiotic resistance profiles of *Salmonella* serovars isolated from retail pork and chicken meat in North Vietnam. International Journal of Food Microbiology, 156(2): 147-151. DOI: https://www.doi.org/10.1016/j.ijfoodmicro.2012.03.016

Upadhyay BP, Utrarachkij F, Thongshoob J, Mahakunkijcharoen Y, Wongchinda N, Suthienkul O, and Khusmith S (2010). Detection of *Salmonella invA* gene in shrimp enrichment culture by polymerase chain reaction. Southeast Asian Journal of Tropical Medicine and Public Health, 41(2): 426-435. Available at: https://pubmed.ncbi.nlm.nih.gov/20578527/

Wallace HA and Hammack TS (2013). *Salmonella* in bacteriological analytical manual. Available at: https://www.fda.gov/media/166699/download accessed on 22/10/2025

White DG, Zhao S, Sudler R, Ayers S, Friedman S, Chen S, McDermott PF, McDermott S, Wagner D, and Meng J (2001). The isolation of antibiotic-resistant *Salmonella* from retail ground meats. New England Journal of Medicine, 345(16): 1147-1154. DOI: https://www.doi.org/10.1056/NEJMoa010315

Yang X, Wu Q, Zhang J, Huang J, Chen L, Wu S, Zeng H, Wang J, Chen M, Wu H et al. (2019). Prevalence, bacterial load, and antimicrobial resistance of *Salmonella* serovars isolated from retail meat and meat products in China. Frontiers in Microbiology, 10: 2121. DOI: https://www.doi.org/10.3389/fmicb.2019.02121

Zhao C, Ge B, De Villena J, Sudler R, Yeh E, Zhao S, White DG, Wagner D, and Meng J (2001). Prevalence of *Campylobacter* spp., *Escherichia coli*, and *Salmonella* serovars in retail chicken, turkey, pork, and beef from the Greater Washington, D.C., area. Applied and Environmental Microbiology, 67(12): 5431-5436. DOI: https://www.doi.org/10.1128/AEM.67.12.5431-5436.2001

Publisher's note: Scienceline Publication Ltd. remains neutral with regard to jurisdictional claims in published maps and institutional affiliations.

Open Access: This article is licensed under a Creative Commons Attribution 4.0 International License, which permits use, sharing, adaptation, distribution and reproduction in any medium or format, as long as you give appropriate credit to the original author(s) and the source, provide a link to the Creative Commons licence, and indicate if changes were made. The images or other third party material in this article are included in the article's Creative Commons licence, unless indicated otherwise in a credit line to the material. If material is not included in the article's Creative Commons licence and your intended use is not permitted by statutory regulation or exceeds the permitted use, you will need to obtain permission directly from the copyright holder. To view a copy of this licence, visit https://creativecommons.org/licenses/by/4.0/.

© The Author(s) 2025

2025, Scienceline Publication
World's Veterinary Journal
World Vet J, 15(4): 968-977.
ISSN 2322-4568

DOI: https://dx.doi.org/10.54203/scil.2025.wvj98
PII: S232245682500098-15

Prevalence and Parasite Load of Helminths in Reintroduced Vicuñas (*Vicugna vicugna*) in High-Andean Communities, Huancavelica, Peru

Erick Rojas[1]*, Alberto Najarro[2], Gumercindo Machuca[3], and Sandra Bezada[4]

[1] *IVITA Research Center, Faculty of Veterinary Medicine, National University of San Marcos, Jr. 28 de Julio s/n, Km 34, Left Bank of the Central Highway, El Mantaro, Jauja – Junín, Peru*
[2] *IVITA Research Center, Faculty of Veterinary Medicine, National University of San Marcos*
[3] *Rural Agricultural Productive Development Program (AGRORURAL), Ministry of Agrarian Development and Irrigation (MIDAGRI), 653 Parra del Riego St., El Tambo, Huancayo, Peru*
[4] *Laboratory of Biochemistry, Animal Nutrition and Feed, Faculty of Veterinary Medicine, National University of San Marcos; 28 Circunvalación Ave., San Borja, Lima, Peru*

*Corresponding author's Email: erojasro@unmsm.edu.pe

ORIGINAL ARTICLE
Received: October 07, 2025
Revised: November 04, 2025
Accepted: December 05, 2025
Published: December 25, 2025

ABSTRACT

Gastrointestinal helminth infections represent a major threat to the health and conservation of vicuñas (*Vicugna vicugna*) in the Peruvian Andes, while epidemiological information on repopulated populations under community-based management remains limited. The present study aimed to determine the prevalence and parasite load of gastrointestinal helminths in reintroduced vicuñas from the high-Andean communities of Huancavelica, Peru. In the present study, 102 vicuñas from the communities of Atuna and Allarpo (Huancavelica), Peru, were evaluated during the 2023 *chaccu*, a traditional Andean practice in which wild vicuñas are collectively herded, captured, and shorn for fiber under community supervision. The sample consisted of 66 females and 36 males, of which 80 were classified as adults (>3 years old) and 22 as juveniles (1-3 years old). Rectal fecal samples were collected and analyzed to detect and quantify gastrointestinal helminth eggs, including strongyle-type eggs, *Nematodirus*, *Trichuris*, and *Fasciola hepatica* (*F. hepatica*). Samples were analyzed using flotation, modified McMaster, and sedimentation techniques to detect and quantify helminth eggs. Overall prevalence, including by community, sex, age, and parasite load (eggs per gram, EFG) as a geometric mean, was determined. The overall prevalence was 75.5%, with *F. hepatica* as the most frequent parasite, 79.2% in Allarpo and 60.9% in Atuna, followed by *Trichuris* spp. (11.6%) and *Nematodirus* spp. (10.2%), and Strongyle-type eggs 42.0% in Allarpo and 17.45% in Atuna. Juveniles had a higher prevalence of *F. hepatica* infection (90.9%) compared to adults (71.3%). The mean *F. hepatica* egg count was higher in Allarpo (34.4 EPG) than in Atuna (11.7 EPG), and this difference was statistically significant. When analyzed by sex, females indicated a higher mean egg count (24.6 EPG; 95% CI: 16.9-35.7) than males (17.4 EPG; 95% CI: 9.8-30.7). Regarding age, adults presented a higher mean EPG (23.6; 95% CI: 16.0-34.8) compared to juveniles (16.5; 95% CI: 8.8-31.1), although mentioned differences were not statistically significant. The findings of the present study indicated that helminth infections, particularly fascioliasis, are widespread, with higher risk in juveniles and environmentally favorable areas, highlighting the need for locally adapted monitoring and control strategies in reintroduced vicuña populations.

Keywords: *Fasciola hepatica*, Gastrointestinal helminth, Prevalence, *Vicugna vicugna*

INTRODUCTION

South American camelids play a fundamental role in the livelihoods of high-Andean populations, representing a genetic resource of high economic, social, cultural, and scientific value (González et al., 2019; Vilá and Arzamendia, 2022). Among them, the vicuña (*Vicugna vicugna*) is a wild species highly prized for the exceptional quality of its fiber, considered one of the most valuable natural fibers worldwide. However, gastrointestinal helminthiasis can negatively affect body condition, metabolism, and consequently fiber production and quality, thereby reducing the economic benefits derived from community-based management programs such as the chaccu. Understanding the epidemiology of these infections is therefore essential to ensure both animal health and the sustainable use of this valuable resource. Peru is the leading exporter of this fiber, which can reach prices of up to USD 400/kg in the international market, mainly destined for the luxury fashion industry (Quispe et al., 2009). Due to conservation programs and sustainable management, populations that had been decimated by overexploitation have recovered significantly. In several high-Andean regions, this process has included repopulation initiatives, involving the reintroduction of vicuñas into areas where their presence was scarce or absent (Wheeler and Hoces 1997; Lichtenstein 2009). vicuñas are translocated from zones with stable wild populations to high-Andean areas where the species had previously declined. The translocation is coordinated by the National Forest and Wildlife Service (SERFOR) and implemented by local communities under

To cite this paper: Rojas E, Machuca ANG, and Bezada S (2025). Prevalence and Parasite Load of Helminths in Reintroduced Vicuñas (*Vicugna vicugna*) in High-Andean Communities, Huancavelica, Peru. *World Vet. J.*, 15(4): 968-977. DOI: https://dx.doi.org/10.54203/scil.2025.wvj98

sustainable management programs. Once established, these populations are managed through annual chaccu events-traditional roundups organized for health monitoring and fiber shearing under official supervision. While these actions have strengthened species conservation and generated local economic benefits, they also pose health challenges, as management conditions, contact with domestic livestock, and adaptation to new environments can increase exposure to pathogens, particularly gastrointestinal helminths (Pérez et al., 2014; Angulo, 2021).

Gastrointestinal helminths infections negatively affect body condition, survival of young vicuñas, and fiber quality. Previous studies in wild and semi-captive vicuñas have reported prevalences of up to 80% for different genera of nematodes and trematodes (Marcoppido et al., 2016; Morsy et al., 2020), with *Fasciola hepatica* (*F. hepatica*) being one of the most important veterinary and zoonotic species in the Andean region of Peru. Transmission is influenced by environmental factors such as altitude, humidity, and the presence of intermediate hosts; by management practices including mixed grazing with domestic livestock, and by host-related factors such as age and immune status (Londoñe et al., 2009; Ibrahim, 2017). In high-Andean communities such as Allarpo-Chillama and Atuna-Quihuay in the Huancavelica region, Peru, the high prevalence of gastrointestinal helminths may be exacerbated by the inadequate use of anthelmintics, close contact with domestic livestock, and the effects of climate change, which can also contribute to the development of resistance to conventional treatments (Cafrune et al., 1996; Kelley et al., 2016; Chugá and Martínez, 2024).

Given the limited epidemiological information available for repopulated vicuñas under community-based management, this study aimed to determine the prevalence and parasite load of gastrointestinal helminth infections in vicuñas from the rural communities of Allarpo-Chillama and Atuna-Quihuay (Huancavelica, Peru).

MATERIALS AND METHODS

Ethical approval

Sample collection was carried out exclusively on vicuñas captured as part of the routine chaccu process, authorized and supervised by the National Forest and Wildlife Service (SERFOR). No additional capture or handling was performed for experimental purposes beyond the procedures established by the competent authorities. All activities complied with the animal welfare principles established by Peruvian Law No. 30407 on Animal Protection and Welfare.

Study area

The study was conducted in the rural communities of Allarpo-Chillama and Atuna-Quihuay, located in the Huancavelica region, Peru. These communities are located in the district of Seclla, Angaraes Province, in the Huancavelica region of Peru (approximately -13.05° S, -74.48° W). They are situated about 26 km east-southeast of the regional capital city of Huancavelica (-12.79° S, -74.98° W). The study sites are located at altitudes of 4,100 and 4,200 m above sea level, respectively, with a mean annual temperature of 10.7°C and an average relative humidity of approximately 65%. Local economic activities included livestock farming, subsistence agriculture, and vicuña management for fiber production. The study area covered approximately 60 km² and included vicuña repopulation zones selected for conservation programs of the species. The geographical location of the sampling sites, along with their spatial distribution within the Secclla district, is illustrated in Figure 1.



Figure 1. Location of the vicuña sampling sites in the communities of Allarpo **(A)** and Atuna **(B)**, Secclla district, Angaraes province, Huancavelica, Peru. Markers (red) indicate the approximate capture areas where fecal samples were collected during the chaccu. The inset map showed the position of the Huancavelica region within Peru.

Study design and animals

Sampling strategy and sample size were determined by the legal and operational constraints of working with protected wildlife. Because vicuñas are a protected species and captures are strictly restricted to the annual chaccu authorized by SERFOR, no a priori sample size calculation was performed. Instead, all individuals safely captured during the roundup were sampled, yielding a pragmatic census of the captured subset (n = 102). The resulting sex ratio reflects the natural social structure of vicuña family groups and the operational constraints of the capture, so equal numbers by sex could not be enforced. Vicuñas were classified as adults (> 3 years) or juveniles (1-3 years) based on field estimates of body size, dentition, and general morphology, since individual age records were not available. The age-based classification method is commonly applied during chaccu events, where handling time is limited, and animals are released immediately after sampling. The evaluated individuals originated from an original population translocated from the district of Pilpichaca, Huaytará, Huancavelica. Capture and handling were carried out as part of the official management authorized by the Servicio Nacional Forestal y de Fauna Silvestre (SERFOR), a public agency under the Ministry of Agrarian Development and Irrigation (MIDAGRI) of Peru.

Sample collection and parasitological analysis

Fecal samples were obtained directly from the rectum of each vicuña, between 11:00 a.m. and 14:00 p.m., using new sterile disposable latex gloves for each individual to avoid cross-contamination and ensure biosafety. Each sample was placed in a hermetically sealed bag labeled with individual animal data, including age, sex, community of origin, and sampling date. A minimum of 15 g of feces was collected per animal for laboratory analysis. Samples were kept at 4 °C in polystyrene containers for transport to the Microbiology and Parasitology Laboratory, Parasitology Section, Faculty of Veterinary Medicine, National University of San Marcos (UNMSM), in San Borja, Lima, Peru, following recommended procedures for fecal sample collection and transport in parasitological study (Taylor et al., 2007).

Parasitological analysis methods

Qualitative flotation technique with a supersaturated sugar solution)

A 1-2 g fecal sample was homogenized in 20 mL of water, filtered, and allowed to sediment. The sediment was resuspended in sugar solution to form a meniscus, covered with a coverslip, allowed to stand for 10 min, and examined under a microscope (10X; Leica Microsystems DM 750, Germany) to identify parasitic forms. This flotation method, based on differences in specific gravity, enables the recovery of light nematode and cestode eggs from fecal suspensions (Ministerio de Salud, 2002; Taylor et al., 2007).

Modified McMaster quantitative technique

The modified McMaster technique was used to detect and quantify oocysts, nematode eggs, and cestode eggs present in fecal samples. Approximately 3 g of feces were weighed, disaggregated in a mortar, and diluted with 42 mL of water. The mixture was filtered through a fine mesh sieve of 200 µm aperture into a test tube and allowed to stand for 30 minutes, or alternatively centrifuged at 1,500 rpm for 3 minutes. After discarding the supernatant, the sediment was homogenized with saturated saline solution to a final volume of 10 mL (Taylor et al., 2007; Bondarenko et al., 2009). Using a Pasteur pipette, both chambers of the McMaster slide (total volume of 1 mL) were filled, and the preparation was examined under a microscope (10X; Leica Microsystems DM 750, Germany) for parasite counting. The calculation of parasite load, expressed as eggs per gram (EPG), was based on the total volume of the fecal suspension examined under the microscope. When only two grids of the McMaster chamber (equivalent to 0.3 mL) were observed, the following formula was applied, EPG = A × 50. When the entire chamber (1 mL) was read, the following formula was used; EPG = A × 15 (A represents the number of parasitic forms counted). This volume-based adjustment ensures that the estimated EPG accurately reflects the proportion of eggs observed in relation to the examined volume. The methodological parameters were standardized according to previously validated protocols and adapted field guidelines (University of Rhode Island, 2018).

Dennis sedimentation method

The sedimentation method was performed according to the procedures described by Rojas-Moncada et al. (2024). This technique is used to concentrate and observe parasite eggs present in fecal samples. The procedure involved weighing between 3 and 6 g of feces, placing them in a mortar (Cole-Parmer, USA), and mixing with a 1% detergent solution. The sample is filtered into a 250 mL sedimentation cup, allowed to settle for 10-12 minutes, and the supernatant is decanted. The resuspension-sedimentation procedure using a 1% detergent solution was repeated two additional times. The process of resuspension and sedimentation with 1% detergent solution was repeated two additional

times to improve sediment cleaning. Subsequently, 4 to 6 drops of Lugol's iodine (Sigma-Aldrich, Merck, Germany) are added and allowed to act for 5 minutes to stain the sediment material.

The stained sediment is emulsified with running water and divided into several test tubes, which are centrifuged (Hettich, Germany) 1,500 rpm for 3 minutes. The resulting sediments are combined into a single tube and centrifuged again under the same conditions. Finally, the sediment is resuspended in 10 mL of water, and using a gridded Petri dish, the eggs present in the entire volume are counted. To express the parasite load as eggs per gram of feces (EPG), the total number of eggs recovered in the Petri dish was divided by the exact weight of feces used in the assay, following the standard formula, EPG = Total eggs counted / grams of feces processed. The Dennis sedimentation method allowed for clearer and more precise observation of parasites by concentrating and staining them, thereby facilitating their identification and quantification.

The three complementary parasitological techniques were employed to maximize the detection of a broad spectrum of helminth eggs and protozoan oocysts. The flotation method allowed for the qualitative identification of light nematode and cestode eggs, the modified McMaster technique provided a quantitative estimation of infection intensity, and the sedimentation method enables the detection of heavy trematode eggs such as *Fasciola hepatica* (Foreyt, 2001; Taylor et al., 2007).

Justification of quantitative indicators

The prevalence of helminth infections was calculated as a percentage, differentiating results by community of origin, sex, and age group of the evaluated vicuñas. Parasite load, EPG, indicated an asymmetric distribution with dispersed values. Therefore, the geometric mean (GM) was used as the measure of central tendency. The use of geometric mean provided a more accurate representation of parasitological data, as counts obtained through the McMaster and Dennis techniques typically indicate skewed distributions, with most values in the lower range and a few extremely high counts. Such irregularity can distort the arithmetic mean, overestimating the actual value. The GM, in contrast, offers a more representative estimate of the overall infection level in the evaluated population by minimizing the influence of extreme values (Ojja et al., 2018).

Statistical analysis

Data were organized and processed using R statistical software version 4.4.3 (R Core Team, 2025). To assess the relationship between the presence or absence of helminths and categorical variables such as sex, age, and community, the Chi-square test was applied. To compare parasite load between groups (males versus females, juveniles versus adults), the Mann-Whitney U test was used, as it is a non-parametric method suitable for non-normally distributed data (Nahm, 2016). A significance level of $p < 0.05$ was considered for all analyses, with p-values obtained from Chi-square tests (for prevalence comparisons) and Mann-Whitney U tests (for comparisons of parasite load).

RESULTS

The consolidated analysis of helminthiasis in vicuñas (*Vicugna vicugna*) from the communities of Allarpo and Atuna, Huancavelica, Peru, revealed a high overall infection frequency of 75.5% (Table 1). When results were disaggregated by sex, males indicated a slightly higher infection frequency (80.6%) compared to females (72.7%). Although the numbers of males and females examined were not equivalent, the comparison remains statistically sound because prevalence differences were evaluated with a Chi-square test, which accommodates unequal group sizes. The calculated odds ratio (OR = 1.55) indicated a higher likelihood of infection in males; however, this association was not statistically significant ($p > 0.05$; 95% CI: 0.58-4.17).

Regarding the age groups, juveniles (1-3 years) showed a markedly higher infection frequency (90.9%) compared with adults (> 3 years; 71.3%). However, because the juvenile group was smaller in size, this difference should be interpreted as an epidemiological trend rather than a statistically confirmed effect. Although the odds ratio indicated lower odds of infection in adults (OR = 0.25), the association did not reach statistical significance ($p > 0.05$; 95% CI: 0.054-1.15). The overall frequency of helminths in the sampled vicuñas was 69.2% in Atuna (Table 2) and 82.0% in Allarpo (Table 3). In Atuna, juveniles showed a higher infection frequency (91.7%) than adults (62.5%), corresponding to an odds ratio of 6.60. This OR indicates that juveniles were more likely to be infected; however, the association was not statistically significant ($p > 0.05$), and therefore represents an epidemiological trend rather than a confirmed difference. The unequal distribution of vicuñas across age classes reflects the natural demographic structure observed during the chaccu, and because all safely captured animals were sampled, the resulting dataset still provides a reliable epidemiological baseline. In Allarpo, a similar pattern was observed, with juveniles presenting a higher infection frequency (90.0%) than adults (80.0%), although this association was again not statistically significant (OR = 2.25; $p > 0.05$).

Table 1. Frequency of helminths in vicuñas by sex and age from Allarpo and Atuna districts in Huancavelica, Peru

Variable	Number of vicuñas	N	%	OR	P value	CI
Sex						
Female	66	48	72.7	0.65	-	-
Male	36	29	80.6	1.55	0.47	0.58 - 4.17
Age (years)						
Adults (> 3)	80	57	71.3	0.25	0.091	0.054 - 1.15
Juveniles (1-3)	22	20	90.9	4.00	-	-
Total	102	77	75.5			

Note: N: Positive cases, OR: Odds ratio, P: Statistical significance level, CI: Confidence interval

Table 2. Frequency of helminths in vicuñas by sex and age in Atuna, Huancavelica, Peru

Variable	Number of vicuñas	N	%	OR	P value	CI
Sex						
Female	35	23	65.7	0.59	-	-
Male	17	13	76.5	1.70	0.532	0.45 - 6.35
Age (years)						
Adults (> 3)	40	25	62.5	0.15	0.078	0.018 - 1.29
Juveniles (1-3)	12	11	91.7	6.60	-	
Total	52	36	69.2			

Note: N: Positive cases, OR: Odds ratio, P: Statistical significance level, CI: Confidence interval

Table 3. Frequency of helminths in vicuñas by sex and age in Allarpo, Huancavelica, Peru

Variable	Number of vicuñas	N	%	OR	P value	CI
Sex						
Female	31	25	80.6	-	-	-
Male	19	16	84.2	0.78	0.9	0.17 - 3.58
Age (years)						
Adults (> 3)	40	32	80.0	-	0.665	0.05 - 4.04
Juveniles (1-3)	10	09	90.0	2.25	-	-
Total	50	41	82.0	-	-	-

Note: N: Positive cases, OR: Odds ratio, P: Statistical significance level, CI: Confidence interval

In Atuna, Strongyle-type eggs (STE) were the most prevalent (17.45%), followed by *Trichuris* spp. (11.6%) and *Nematodirus* spp. (10.2%; Table 4). When comparing parasite species between adults and juveniles, the highest frequency was recorded for *F. hepatica* (60.9%) in Atuna. Within this community, prevalence was significantly higher in juveniles (91.7%) than in adults (50.0%; $p < 0.05$). In Allarpo, the frequency of STE was higher (42.0%), while *F. hepatica* reached 79.2%. Juveniles indicated a higher prevalence (90.0%) than adults (75.0%); however, no statistically significant difference was observed (Table 5).

In Table 6, the GM of the STE load was higher in Allarpo (69.5 EPG; 95% CI: 54.7-88.3) than in Atuna (50.2 EPG; 95% CI: 49.9-50.6), although the difference was not statistically significant ($p > 0.05$). The GM was used because it is less sensitive to extreme values compared to the arithmetic mean. For *F. hepatica*, the GM egg count was significantly higher in Allarpo (34.4 EPG; 95% CI: 22.5-52.6) than in Atuna (11.7 EPG; 95% CI: 7.5-18.2; $p < 0.05$). At the overall study level, females showed a higher *Fasciola hepatica* egg load (24.6 EPG; 95% CI: 16.9-35.7) compared with males (17.4 EPG; 95% CI: 9.8-30.7), although this difference was not statistically significant ($p > 0.05$). The GM of STE in males was 64.0 EPG (95% CI: 44.4-92.3), slightly higher than in females, 58.4 EPG (95% CI: 49.8-68.5). These values represent egg counts per gram (EPG), not percentages. According to age, adults indicated a higher *Fasciola hepatica* egg load 23.6 EPG (95% CI: 16.0-34.8) than juveniles 16.5 EPG (95% CI: 8.8-31.1); however, this difference was not statistically significant ($p > 0.05$). As indicated in Table 6, no superscript letters appear in this comparison, confirming the absence of statistical significance between age groups.

For *Nematodirus* spp. and *Trichuris* spp., the geometric mean (GM) and 95% CI appear as 50.0 (50.0-50.0) in several categories. This uniform value reflects the minimum detection threshold of the modified McMaster technique used in this study (1 egg = 50 EPG), and indicates that all positive animals for these parasites had counts at or near this lower detection limit rather than identical biological loads. Skrjabinema spp. was not included in the geometric mean (GM) analysis because the number of positive animals was insufficient to calculate a reliable GM value using the McMaster method.

No significant differences in STE load were observed between males and females ($p > 0.05$) or between adults and juveniles ($p > 0.05$). The same pattern was found for the other parasites. The only statistically significant difference corresponded to *Fasciola hepatica*, whose load was higher in Allarpo than in Atuna ($p < 0.05$).

Table 4. Prevalence of helminth eggs in vicuñas by sex and age in Atuna district, Huancavelica, Peru

Variable	Number of vicuñas	Strongyle-type eggs (%)	*Nematodirus* (%)	*Trichuris* (%)	*Skrjabinema* (%)	*F. hepatica* (%)
Sex						
Female	35	11.4 ^{b}	8.6^{b}	5.7^{b}	2.9^{b}	57.1^{a}
Male	17	23.5 ^{b}	11.8^{b}	17.6^{b}	5.8^{b}	64.7 ^{a}
Age (years)						
Adults (> 3)	40	12.5 ^{b,B}	10.0 ^{b,B}	7.5 ^{b,B}	2.5 ^{b,B}	50.0 ^{a,B}
Juveniles (1-3)	12	25.0 ^{b,B}	8.3 ^{b,B}	16.7 ^{b,B}	8.3 ^{b,B}	91.7 ^{a,A}
Total	52	17.5	10.2	11.6	4.3	60.9

Note: Different superscript lowercase letters (^{a,b}) within each row indicate a statistically significant difference ($p < 0.05$). Different superscript uppercase letters (^{A,B}) within each column indicate a statistically significant difference ($p < 0.05$).

Table 5. Prevalence of helminth eggs in vicuñas by sex and age in Allarpo district, Huancavelica, Peru

Variable	Number of vicuñas	Strongyle-type eggs (%)	*Nematodirus* (%)	*Trichuris* (%)	*Skrjabinema* (%)	*F. hepatica* (%)
Sex						
Female	31	41.9 ^{b}	19.4 ^{b}	6.5 ^{c}	3.2 ^{c}	74.2 ^{a}
Male	19	42.1 ^{b}	21.1 ^{b}	15.8^{b}	0	84.2 ^{a}
Age (years)						
Adults (> 3)	40	42.5 ^{b,B}	20.0 ^{c,B}	5.0 ^{d,B}	2.5 ^{d}	75.0 ^{a,B}
Juveniles (1-3)	10	40.0 ^{b,B}	20.0 ^{b,B}	30.0 ^{b,A}	0	90.0 ^{a,B}
Total	50	42.0	20.3	11.2	3.2	79.2

Note: Different superscript lowercase letters (^{a,b}) within each row indicate a statistically significant difference ($p < 0.05$). Different superscript uppercase letters (^{A,B}) within each column indicate a statistically significant difference ($p < 0.05$).

Table 6. Geometric mean of parasite load of Strongyle-type eggs, Nematodirus spp., *Trichuris* spp., and *Fasciola hepatica* spp. present in positive vicuñas from Atuna and Allarpo districts in Huancavelica, Peru

Variable	Strongyle-type eggs (STE)	Nematodirus	*Trichuris*	*F. hepatica*
	GM (CI)	GM (CI)	GM (CI)	GM (CI)
Sex				
Female	58.4 (49.8-68.5)	50.0 (50.0-50.0)	50.75 (50.3-51.2)	24.6 (16.9-35.7)
Male	64.0 (44.4-92.3)	50.0 (50.0-50.0)	57.2 (45.7-71.4)	17.4 (9.8-30.7)
Age (years)				
Adults (>3)	64.1 (44.5-92.4)	50.0 (50.0-50.0)	58.2 (44.5-76.3)	23.6 (16.0-34.8)
Juveniles (1-3)	61.3 (47.6-78.9)	50.0 (50.0-50.0)	50.6 (50.1-51.1)	16.5 (8.8-31.1)
Origin				
Atuna	50.2 (49.9-50.6)	50.0 (50.0-50.0)	50.8 (50.4-51.2)	11.7 (7.5-18.2)
Allarpo	69.5 (54.7-88.3)	50.0 (50.0-50.0)	58.0 (44.2-76.1)	34.4^{a} (22.5-52.6)
Total (CI 95%)	63.6 (53.1-76.1)	50.0 (50.0-50.0)	54.3 (47.4-62.2)	21.3 (15.3-29.7)

Note: 95% CI; ^{a} $p = 0.04$ (Mann–Whitney U test), CI: confidence interval.

DISCUSSION

The present study revealed a high overall prevalence of gastrointestinal helminths (75.5%) in vicuñas evaluated during the 2023 Chaccu in the communities of Allarpo and Atuna, confirming the persistent presence of gastrointestinal parasites in semi-captive management systems. The observed pattern is consistent with other reports from high Andean areas, where predisposing factors such as communal grazing, lack of systematic sanitary control, and favorable

ecological conditions contribute to helminth transmission (Marcoppido et al., 2016; Curay et al., 2022). In the present study, parasite detection was based on coprological examination, a method widely used in field surveys to estimate infection levels and describe general patterns of helminth occurrence. While this approach allows reliable assessment of prevalence and parasite burden in wildlife populations, more detailed identification would require additional laboratory techniques. Similar levels of gastrointestinal helminth infections have been described in other high-Andean camelid populations, such as alpacas from Macusani, Puno, where high prevalences were observed even during the dry season (Contreras et al., 2014). The results support the idea that helminth circulation remains consistently high in communal pastoral systems across the puna.

Among all the parasites detected, *Fasciola hepatica* clearly stood out. Its prevalence was higher in both communities and particularly marked in Allarpo (79.2%). The environmental conditions in this area—greater humidity, wetlands, and waterlogged soils, likely favor the presence and survival of Lymnaea spp., the intermediate host essential for the parasite's life cycle (Mas-Coma et al., 2009). Other environmental drivers such as altitude, temperature, vegetation structure, and water availability have been widely linked to fascioliasis transmission in Andean landscapes (Flores et al., 2014; Charlier et al., 2020). The significantly higher egg load recorded in Allarpo reinforces the idea that local ecological conditions shape infection intensity. The presence of domestic livestock, especially sheep and cattle, may add an additional layer of risk by increasing environmental contamination with infective stages (Julón et al., 2020; Angulo et al., 2021).

The overall prevalence of helminths was 69.2% in Atuna and 82.0% in Allarpo, similar to the 81.3% ± 5.3% reported in Cajamarca (Curay et al., 2022). This difference may be explained by variations in altitude, climatic conditions, and the level of interaction with other livestock species that serve as parasite reservoirs. Altitude and climatic conditions are known to significantly influence the epidemiology of helminth infections (Aguirre and Cafrune, 2007; Mas-Coma et al., 2009). Higher altitude and lower temperatures can affect the development and survival of larval stages in the environment. Temperatures around 15°C and a minimum monthly precipitation of 50 mm are ideal for the survival of many helminth larvae (Charlier et al., 2020). Additionally, some parasite eggs have been observed to withstand freezing temperatures as low as -16°C for extended periods, allowing their development in high altitude environments.

Increases in temperature can enhance parasite reproduction rates, altering helminth transmission dynamics (Rodríguez et al., 2013; Samamé et al., 2016; Chugá and Martínez, 2024). Previous studies in South American camelids have reported variations in helminth prevalence depending on water availability and pasture type (Issia, 2009), finding that vicuñas with greater access to water bodies have higher infections by trematodes such as *F. hepatica.* This is consistent with the present findings, where Allarpo, a more humid community, indicated a significantly higher prevalence of *F. hepatica*. Interaction with domestic livestock also plays a key role in helminth transmission to vicuñas. A study in llama and alpaca populations (Angulo et al., 2021), found that those sharing grazing areas with sheep and cattle had higher parasite loads, particularly gastrointestinal nematodes. The coexistence of vicuñas with domestic livestock in Allarpo could be facilitating helminth transmission in this region.

The high prevalence of *F. hepatica* is consistent with previous studies in the Andean region (Neyra et al., 2002; Samamé et al., 2016), where the presence of intermediate hosts and humid conditions favors its life cycle. In this regard, the higher prevalence of *F. hepatica* in Allarpo (79.2%) compared to Atuna (60.9%) could be related to environmental and management factors specific to each community. The presence of humid areas, such as wetlands and stagnant water bodies, promotes the proliferation of snails of the genus Lymnaea, essential intermediate hosts in the *F. hepatica* life cycle. Additionally, overgrazing in these areas can increase pasture contamination with infective metacercariae, raising the infection risk for vicuñas (Chacma, 2018). The *F. hepatica* infection in vicuñas has significant implications for their health and conservation. Liver damage associated with *Fasciola hepatica* infection can manifest as weight loss, anemia, and reduced body condition, affecting survival and productivity (Londoñe et al., 2009).

Juveniles showed higher infection frequencies than adults in both communities (90.9% versus 71.3%), a pattern commonly described in camelids and other ruminants (Valenzuela et al., 1998; Stevenson et al., 2022). Younger animals generally have less developed immune responses and often engage in more exploratory grazing, increasing their contact with contaminated vegetation. Although the differences observed in the present study were not statistically significant, the consistency of the trend suggests that juveniles represent a group requiring particular attention in monitoring and management plans. The greater susceptibility of juveniles to parasitic infections has also been attributed to their limited experience in selecting safe pastures and water sources. Thus, juveniles tend to consume vegetation in areas more exposed to fecal contamination, increasing their risk of helminth infection (Aguirre and Cafrune, 2007). The observed behavioral pattern, together with the consistently higher infection frequencies observed in juveniles, provides a basis for prioritizing targeted parasite control strategies in younger animals, which represent the highest-risk group within the management system (Silva-Díaz et al., 2015; Stevenson et al., 2022). The increased susceptibility observed in younger animals is consistent with broader evidence showing that helminths modulate and suppress key components of the host

immune response, making immunologically immature individuals more vulnerable to infection (Gazzinelli-Guimarães and Nutman, 2018).

Several aspects should be considered when interpreting these results. Age classification was based on field estimation rather than recorded birth data, which may affect the precision of age-related comparisons. In addition, the geometric mean (GM) values of 50.0 (50.0-50.0) reported for *Nematodirus* and *Trichuris* correspond to the minimum detection limit of the modified McMaster method (1 egg = 50 EPG). This does not indicate identical parasite burdens but rather infections at the lower threshold of detection. Unequal distributions across sex and age groups reflect natural chaccu capture patterns and can reduce statistical power in certain comparisons. Finally, the use of bivariate tests limits the ability to evaluate interactions among host, environmental, and management factors. More robust multivariate approaches would help clarify these relationships in future work.

The predominance of *F. hepatica* and the higher parasite load observed in Allarpo underscore the need for local, community-adapted control strategies. Efforts should focus on wetland areas and places with high snail density, as well as on coordinated parasite control for domestic livestock sharing the same grazing areas. Given that domestic livestock such as cattle and sheep share grazing grounds with vicuñas and act as reservoirs for multiple helminths, coordinated control actions between wildlife authorities and local herders are essential. Joint deworming schedules, improved livestock management near communal pastures, and proper handling of contaminated water sources may reduce cross-species transmission. Establishing clear community agreements that integrate livestock and wildlife health could enhance overall ecosystem resilience. Juveniles, given their consistently higher infection frequencies, should also receive priority in monitoring programs. Because fascioliasis may compromise body condition and productivity, potentially affecting fiber yield, a valuable resource for Andean communities (Londoñe et al., 2009), regular parasite surveillance should be incorporated into vicuña management and conservation efforts to ensure healthier populations and sustainable fiber production.

The close interaction between vicuñas and domestic livestock, especially sheep and cattle, may also contribute to parasite transmission, as interspecies contact can increase environmental contamination and facilitate shared infection cycles (Samamé et al., 2016). Community-based management strategies that include coordinated deworming of livestock, improved grazing rotation, and reduced access to wet areas during high-risk periods could help mitigate infection pressure in reintroduced vicuña populations

CONCLUSION

The frequency of gastrointestinal helminths in reintroduced vicuñas varied between the two communities studied, with a higher prevalence in Allarpo (82.0%) than in Atuna (69.2%). *F. hepatica* was the most prevalent parasite in both locations (60.9% in Atuna and 79.2% in Allarpo), followed by Strongyle-type eggs (STE), which were also more common in Allarpo (42.0%) than in Atuna (17.45%). Parasite load, expressed as the geometric mean (GM) of eggs per gram (EPG), was likewise significantly higher in Allarpo than in Atuna, reinforcing the notion that local environmental and management conditions strongly influence helminth transmission dynamics. Parasite identification in this study relied exclusively on coprological methods. Although these techniques provide dependable estimates of prevalence and parasite burden under field conditions, they do not allow species-level differentiation. Future studies incorporating larval culture, molecular diagnostics, or necropsy-based confirmation would improve taxonomic resolution and broaden our understanding of helminth diversity in reintroduced vicuña populations. Overall, the present findings emphasize the need to integrate continuous health surveillance and parasite control into vicuña reintroduction and conservation programs. Tailored management strategies—particularly in wetter areas that favor fascioliasis transmission and in zones where vicuñas coexist with domestic livestock—are essential to prevent the establishment of new infection reservoirs and to support the long-term sustainability of vicuña populations and fiber production in the Andean region.

DECLARATIONS

Availability of data and materials

The datasets generated and analyzed during the current study are available from the corresponding author on reasonable request.

Acknowledgments

The authors gratefully acknowledge the Regional Directorate of South American Camelids (DIRCAMS), Huancavelica, Peru, for the valuable technical and administrative support during the development of the present study.

Authors' contributions

All authors approved the final version of the article before publication in the journal. Formal analysis, Erick Rojas, Alberto Najarro, Gumercindo Machuca and Sandra Bezada; investigation, Erick Rojas and Sandra Bezada; acquisition of financing, Erick Rojas, Gumercindo Machuca and Sandra Bezada; research, Erick Rojas, Alberto Najarro and Sandra Bezada; methodology, Erick Rojas and Sandra Bezada; project management, Erick Rojas; resources, Erick Rojas, Sandra Bezada, Gumercindo Machuca; supervision, Erick Rojas; drafting: original draft, Erick Rojas, Sandra Bezada and Gumercindo Machuca; Writing: proofreading and editing, Erick Rojas, Sandra Bezada and Gumercindo Machuca. All authors have read and agreed to the published version of the manuscript.

Ethical considerations

Ethical issues (including plagiarism, consent to publish, misconduct, data fabrication and/or falsification, double publication and/or submission, and redundancy) have been checked by all the authors carefully. The authors confirm that no AI-generated content was used in the writing of the manuscript. The study design, data collection, analysis, and interpretation were entirely conducted by the authors.

Funding

The present research did not receive external financial support. Field sampling was authorized and facilitated by DIRCAMS and supervised by SERFOR as part of the official chaccu activities. All laboratory analyses, transportation, and field expenses were covered directly by the authors

Competing interests

The authors declare no conflict of interest.

REFERENCES

Aguirre DH and Cafrune MM (2007). Parásitos de los Camélidos Sudamericanos [Parasites of South American Camelids]. In: V. H. Suárez, F. V. Olaechea, J. R. Romero, C. E. Rossanigo (Editors), Enfermedades parasitarias de los ovinos y otros rumiantes menores en el Cono Sur de América [Parasitic diseases of sheep and other small ruminants in the Southern Cone of South America]. INTA EEA Anguil Ediciones., Argentina, pp. 281-296. DOI: https://www.doi.org/10.36610/j.jsaas.2023.100200116x

Angulo J, Pacheco J, Vélez V, García W, Castelo H, and Gomez-Puerta L (2021). Situación actual de la sarna e infecciones parasitarias en vicuñas (*Vicugna vicugna*) de la Región Cusco, Perú [Current situation of mange and parasitic infections in vicuñas from the Cusco region, Peru]. Revista de Investigaciones Veterinarias del Perú, 32(3): e20405. DOI: https://www.doi.org/10.15381/rivep.v32i3.20405

Bondarenko IG, Kinčeková J, Várady M, Kőnigová A, Kuchta M, and Koňáková G (2009). Use of modified McMaster method for the diagnosis of intestinal helminth infections and estimating parasitic egg load in human faecal samples in non-endemic areas. Helminthologia, 46(1): 62-64. DOI: https://www.doi.org/10.2478/s11687-009-0012-0

Cafrune MM, Rebuffi GE, Gaido AB, and Aguirre DH (1996). *Fasciola hepatica* in semi-captive vicuñas (*Vicugna vicugna*) in North West Argentina. VetRecord, 139(4): 97. DOI: https://www.doi.org/10.1136/vr.139.4.97-a

Chacma HH (2018). Determinación de la carga parasitaria de huevo de *Fasciola hepatica* en alpacas (*Lama pacos)* en la comunidad de Chillihua – Pampachiri – Andahuaylas – Apurímac [Determination of Fasciola hepatica egg load in alpacas]. Bachelor's Thesis, Universidad Nacional de San Antonio Abad del Cusco, Cusco, Perú. Available at: https://repositorio.unsaac.edu.pe

Charlier J, Höglund J, Morgan ER, Gledhof P, Vercruysse J, and Claerebout E (2020). Biology and epidemiology of gastrointestinal nematodes in cattle. Veterinary Clinics of North America: Food Animal Practice, 36(1): 1-15. DOI: https://www.doi.org/10.1016/j.cvfa.2019.11.001

Chugá Bastidas WS and Martínez Chugá RD (2024). Presencia de caracoles *Lymnaeidae* (Mollusca: Gastropoda), infectados con estadios larvarios de *Fasciola hepatica* (Linnaeus, 1758) en zonas ganaderas de la provincia de Carchi [Presence of *Lymnaeidae snails* infected with larval stages of *Fasciola hepatica*]. RECIENA, 4(3): 33-39. DOI: https://www.doi.org/10.47187/e42mnc67

Contreras N, Chávez A, Pinedo R, Leyva V, and Suárez F (2014). Helmintiasis en alpacas (*Vicugna pacos*) de dos comunidades de Macusani, Puno, durante la época seca [Helminthiasis in alpacas during the dry season in Macusani, Puno]. Revista de Investigaciones Veterinarias del Perú, 25(2): 268-275. Available at: http://www.scielo.org.pe/scielo.php?script=sci_arttext&pid=S1609-91172014000200014&lng=es&tlng=es

Curay J, Chávez A, Pinedo R, Falcón N (2022). Helmintiasis en vicuñas (*Vicugna vicugna*) en el distrito de Contumaza (Cajamarca, Perú) [Helminthiasis in vicuñas from Contumazá district (Cajamarca, Perú)]. Revista de Investigaciones Veterinarias del Perú, 33: e22629. DOI: https://www.doi.org/10.15381/rivep.v33i2.22629.

Flores B, Pinedo R, Suárez F, Angelats R, and Chávez A (2014). Prevalencia de fasciolosis en llamas y alpacas en dos comunidades rurales de Jauja, Perú [Prevalence of fascioliasis in camelids from Jauja]. Revista de Investigaciones Veterinarias del Perú, 25(2): 284-292. Available at: http://www.scielo.org.pe/pdf/rivep/v25n2/a16v25n2.pdf

Foreyt WJ (2001). Veterinary parasitology reference manual, 5th Edition. Wiley-Blackwell, pp. 115-117. Available at: https://www.wiley.com/en-us/Veterinary+Parasitology+Reference+Manual%2C+5th+Edition-p-9780813824192

Gazzinelli-Guimarães PH and Nutman TB (2018). Helminth parasites and immune regulation. F1000Research, 7(F1000 Faculty Rev): 1685. DOI: https://www.doi.org/10.12688/f1000research.15596.1

González B, Vásquez J, Gómez-Uchida D, Cortés J, Rivera R, Aravena N, Chero A, Agapito AM, Varas V, Wheleer J et al. (2019). Phylogeography and population genetics of *Vicugna vicugna*: Evolution in the Arid Andean High Plateau. Frontiers in Genetics, 10: 445. DOI: https://www.doi.org/10.3389/fgene.2019.00445

Ibrahim N (2017). Fasciolasis: Systematic review. Advances in Biological Research, 11(5): 278-285. DOI: https://www.doi.org/10.5829/idosi.abr.2017.278.285

Issia L, Pietrokovsky S, Sousa-Figueiredo J, Russell J, and Wisnivesky C (2009). *Fasciola hepatica* infections in livestock flock, guanacos and coypus in two wildlife reserves in Argentina. Veterinary Parasitology, 165: 341-344. DOI: https://www.doi.org/10.1016/j.vetpar.2009.07.011

Julón D, Puicón V, Chávez A, Bardales W, Gonzales J, Vásquez H, and Maicelo J (2020). Prevalencia de *Fasciola 977epática* y parásitos gastrointestinales en bovinos de la Región Amazonas, Perú [Prevalence of *Fasciola hepatica* in cattle from Amazonas]. Revista de Investigaciones Veterinarias del Perú, 31(1): e17560. DOI: https://www.doi.org/10.15381/rivep.v31i1.17560

Kelley JM, Elliott TP, Beddoe T, and Anderson G (2016). Current threat of triclabendazole resistance in *Fasciola hepatica*. Trends in parasitology, 32(6): 458-469. DOI: https://www.doi.org/10.1016/j.pt.2016.03.002

Lichtenstein G (2010). Vicuña conservation and poverty alleviation? Andean communities and international fibre markets. International Journal of the Commons, 4(1): 100-121. DOI: https://www.doi.org/10.18352/ijc.139

Londoñe P, Chávez A, Li O, Suárez A, and Pezo D (2009). Presencia de caracoles *Lymnaeidae* con formas larvarias de *Fasciola hepatica* en altitudes sobre los 4000 msnm en la sierra sur del Perú [Presence of *Lymnaeidae* snails with larval stages of *Fasciola hepatica* at altitudes above 4000 masl in the southern Peruvian highlands.]. Revista de Investigaciones Veterinarias del Perú, 20(1): 58-65. DOI: https://www.doi.org/10.15381/rivep.v20i1.533.

Marcoppido G, Schapiro J, Morici G, Arzamendia Y, and Vilá B (2016). Coproparasitological evaluation of nematodes and coccidia in wild vicuña (*Vicugna vicugna*) population in the Argentinean Andean Altiplano. Journal of Camelid Science, 9: 23-34. Available at: https://isocard.info/images/journal_camelid/FILEd935663619fa366.pdf

Mas-Coma S, Valero MA, and Bargues MD (2009). Climate change effects on trematodiases, with emphasis on zoonotic fascioliasis and schistosomiasis. Veterinary Parasitology, 163: 264-280. DOI: https://www.doi.org/10.1016/j.vetpar.2009.03.024

Ministerio de Salud (MINSA) (2002). Manual de procedimientos: Serie de normas técnicas N.° 37—Salud Pública. MINSA: Lima, Perú [Procedures manual: Technical standards series No. 37—Public health], pp. 19-21. Available at: https://repositorio.ins.gob.pe/server/api/core/bitstreams/b47fe475-130d-496e-9f08-43f9f1f7e09f/content

Morsy K, Yehia S, Ahmed M, El Ganainy S, Fol M, and Adel A (2020). Morphological characterization of *Moniezia expansa* Rudolphi, 1810 (*F: Anoplocephalidae*) isolated from the intestine of the domestic sheep, *Ovis aries* (Bovidae) by light microscopy. Egyptian Academic Journal of Biological Sciences, E. Medical Entomology & Parasitology, 12(1): 77-84. Available at: https://www.eajbse.journals.ekb.eg

Nahm FS (2016). Nonparametric statistical tests for the continuous data: The basic concept and the practical use. Korean Journal of Anesthesiology, 69(1): 8-14. DOI: https://www.doi.org/10.4097/kjae.2016.69.1.8

Neyra V, Chavarry E, and Espinoza JR (2002). Cysteine proteinases Fas1 and Fas2 are diagnostic markers for *Fasciola hepatica* infection in alpacas (*Lama pacos*). Veterinary Parasitology, 105(1): 21-32. DOI: https://www.doi.org/10.1016/s0304-4017(02)00002-x

Ojja S, Kisaka S, Ediau M, Tuhebwe D, Kisakye AN, Halage AA, Mugambe RK, and Mutyoba JN (2018). Prevalence, intensity and factors associated with soil-transmitted helminths infections among preschool-age children in Hoima district, rural western Uganda. BMC Infectious Diseases, 18(1): 408. DOI: https://wwwdoi.org/10.1186/s12879-018-3289-0

Pérez H, Chávez A, Pinedo R, and Leyva V (2014). Helmintiasis y eimeriasis en alpacas de dos comunidades de Cusco, Perú [Helminthiasis and eimeriasis in alpacas from Cusco]. Revista de Investigaciones Veterinarias del Perú, 25(2): 245-253. Available at: http://www.scielo.org.pe/pdf/rivep/v25n2/a12v25n2.pdf

Quispe EC, Rodríguez TC, Iñiguez LR, and Mueller JP (2009). Producción y manejo de la fibra de vicuña en el altiplano andino [Production and management of vicuña fiber in the Andean highlands]. Animal Genetic Resources Information, 45: 1-14. Available at: https://www.fao.org/4/i1102t/i1102t02.pdf

Rodríguez DJG, Olivares JL, Sánchez Castilleja Y, Alemán Y, and Arece J (2013). Cambios climáticos y su efecto sobre algunos grupos de parásitos [Climate change and its effect on parasite groups]. Revista de Salud Animal, 35(3): 145. Available at: https://revistas.censa.edu.cu/index.php/RSA/article/view/328

Rojas-Moncada J, Torrel-Pajares T, and Vargas-Rocha L (2024). Validation of the natural sedimentation technique in the diagnosis of chronic fasciolosis. Parasitology International, 101: 102889. DOI: https://www.doi.org/ 10.1016/j.parint.2024.102889

Samamé L, Chávez A, and Pinedo R (2016). Fasciolosis en vicuñas (*Vicugna vicugna*) de la Sierra Central del Perú [Fasciolosis in vicuñas from the central highlands]. Revista de Investigaciones Veterinarias del Perú, 27(1): 137-144. DOI: https://www.doi.org/10.15381/rivep.v27i1.11459

Silva-Díaz H, Hobán-Vergara C, Cruz-Cerna R, Solana H, and Ortiz-Oblitas P (2015). Inmunidad celular en ganado vacuno lechero naturalmente infectado con *Fasciola hepatica* en Cajamarca, Perú [Cellular immunity in dairy cattle naturally infected with *F. hepatica*]. Revista de Investigaciones Veterinarias del Perú, 26(4): 637-647. DOI: https://www.doi.org/10.15381/rivep.v26i4.11210

Stevenson MM, Valanparambil RM, and Tam M (2022). Myeloid-derived suppressor cells: The expanding world of helminth modulation of the immune system. Frontiers in immunology, 13: 874308. DOI: https://www.doi.org/10.3389/fimmu.2022.874308

Taylor M, Coop R, and Wall R (2007). The laboratory diagnosis of parasitism. In: M. A. Taylor, R. L. Coop, and R. L. Wall (Editors), Veterinary parasitology, 3rd Edition. Blackwell Publishing: Oxford, UK, Chapter 15, pp. 798-813. Available at: https://download.e-bookshelf.de/download/0003/7447/63/L-G-0003744763-0002367748.pdf

University of Rhode Island (2018). McMaster test: A guide to fecal egg counting in livestock. University of Rhode Island: Kingston, RI, USA, pp. 1-6. Available at: https://web.uri.edu/wp-content/uploads/sites/241/McMaster-Test_Final3.pdf

Valenzuela G, Leiva M, and Quintana I (1998). Estudio epidemiológico de larvas de nemátodos gastrointestinales en praderas pastoreadas por alpacas (*Lama pacos*) en Valdivia, Chile [Cellular immunity in dairy cattle naturally infected with *F. hepatica*]. Archivos de Medicina Veterinaria, 30: 79-90. DOI: https://www.doi.org/10.4067/S0301-732X1998000200008

Vilá B and Arzamendia Y (2022). Weaving a vicuña shawl. Pastoralism, 12(1): 46. DOI: https://www.doi.org/10.1186/s13570-022-00260-6

Wheeler JC and Hoces D (1997). Community participation, sustainable use, and vicuña conservation in Peru. Mountain Research and Development, 17(2): 123-126. DOI: https://www.doi.org/10.2307/3673855

Publisher's note: Scienceline Publication Ltd. remains neutral with regard to jurisdictional claims in published maps and institutional affiliations.

Open Access: This article is licensed under a Creative Commons Attribution 4.0 International License, which permits use, sharing, adaptation, distribution and reproduction in any medium or format, as long as you give appropriate credit to the original author(s) and the source, provide a link to the Creative Commons licence, and indicate if changes were made. The images or other third party material in this article are included in the article's Creative Commons licence, unless indicated otherwise in a credit line to the material. If material is not included in the article's Creative Commons licence and your intended use is not permitted by statutory regulation or exceeds the permitted use, you will need to obtain permission directly from the copyright holder. To view a copy of this licence, visit https://creativecommons.org/licenses/by/4.0/.
© The Author(s) 2025

2025, Scienceline Publication
World's Veterinary Journal
World Vet J, 15(4): 978-988.
ISSN 2322-4568

DOI: https://dx.doi.org/10.54203/scil.2025.wvj99
PII: S232245682500099-15

Effects of Fermented *Crescentia cujete* and Enrofloxacin on Inflammation in Pneumonic Pasteurellosis Rats

Paskalis Guntur Widya Mahendra[1], Sitarina Widyarini[2]*, and Yos Adi Prakoso[3]

[1]*Master Program in Veterinary Sciences, Faculty of Veterinary Medicine, University Gadjah Mada, Yogyakarta, 55281, Indonesia*
[2]*Department of Pathology, Faculty of Veterinary Medicine, University Gadjah Mada, Yogyakarta, 55281, Indonesia*
[3]*Department of Pharmacology, Faculty of Veterinary Medicine, Wijaya Kusuma Surabaya University, Surabaya 60225, Indonesia*

*Corresponding author's Email: w.sitarina@gmail.com

ORIGINAL ARTICLE
Received: October 18, 2025
Revised: November 21, 2025
Accepted: December 09, 2025
Published: December 25, 2025

ABSTRACT

Pneumonic pasteurellosis (PP) is a respiratory disease caused by *Pasteurella multocida* (*P. multocida*) with broad host susceptibility and zoonotic potential. Pasteurellosis is classified as a strategic infectious animal disease and a neglected tropical disease in Indonesia, highlighting the need for effective supportive therapies. Fermented *Crescentia cujete* L. (FCC) contains bioactive compounds with anti-inflammatory and antioxidant activities. The present study aimed to evaluate the anti-inflammatory effects of FCC combined with enrofloxacin on hematological parameters and the immune expression of granulocyte-macrophage colony-stimulating factor (GM-CSF) and interleukin-6 (IL-6) in an induced PP rat model. Twenty male Sprague-Dawley rats, three months old and weighing 250-300 g, were divided into five groups, including healthy control (P1), untreated infected rats (P2), rats treated with 20 mg/kg body weight (BW) of enrofloxacin (P3), rats given 20 and 30 mg/kg BW of enrofloxacin and ibuprofen, respectively (P4), and rats administered 20 and 5.92 mg/kg BW of enrofloxacin and FCC (P5), respectively. After a 7-day acclimatization, rats were infected intratracheally with *P. multocida* on day 8, and treatments were administered orally for seven days starting on day 11. Hemoglobin, mean corpuscular hemoglobin (MCH), and mean corpuscular hemoglobin concentration (MCHC) decreased significantly in P2 compared to P1, with no difference between P2 and P3. Although hemoglobin, MCH, and MCHC improved in P4 and P5 toward control levels, most variables remained significantly different from P1. Leukocyte and neutrophil counts were significantly elevated in P2 compared to P1; however, P5 demonstrated a declining trend toward normal values and did not differ significantly from P1. Pulmonary GM-CSF and IL-6 immune expression increased markedly in P2 compared to P1. Groups P3 and P4 exhibited elevated cytokine expression compared to P1, without significant differences from P2. In contrast, P5 indicated a significant reduction in GM-CSF and IL-6 expression compared to P2, reaching levels comparable to those of P1. The FCC combined with enrofloxacin improved hematological status and modulated inflammatory cytokines in PP. The present findings indicated that FCC could be a potential supplementary treatment for managing inflammation and aiding hematological recovery in bacterial infection pneumonia.

Keywords: *Crescentia cujete*, Granulocyte Macrophage-Colony Stimulating Factor, Hematology, Interleukin-6, *Pasteurella multocida*

INTRODUCTION

Pneumonic pasteurellosis (PP) is pneumonia caused by *Pasteurella multocida* (*P. multocida*), a Gram-negative facultative anaerobic bacterium (Wilson and Ho, 2013). Pneumonic pasteurellosis can infect different animals and livestock, causing fowl cholera and lower respiratory tract infections in cattle and pigs, which are potentially zoonotic. Transmission to humans occurs through bites or scratches from cats or dogs (Guan et al., 2020). In Indonesia, Pasteurellosis is classified as a strategic animal infectious disease under the Ministry of Agriculture Regulation No. 4026/Kpts/OT. 140/4/2013a and is also listed as a neglected tropical disease (Ministry of Health of the Republic of Indonesia, 2020).

Pasteurellosis targets erythrocytes and leukocytes, particularly monocytes, neutrophils, and macrophages (Kubatzky, 2012), leading to excessive inflammation and tissue damage (Yang et al., 2022). Pneumonic pasteurellosis increases expression of granulocyte-macrophage colony-stimulating factor (GM-CSF) in the type II pneumocyte, macrophages, and granulocyte cells, triggering inflammation (Wilkie et al., 2012). Inflammation is further characterized by the release of pro-inflammatory cytokines, specifically interleukin-6 (IL-6; Aliyu et al., 2022). Elevated IL-6 expression can exacerbate pneumonia (Yang et al., 2022).

The World Health Organization recommended treating PP with antibiotics combined with anti-inflammatory medicines such as ibuprofen, particularly for acute respiratory syndromes associated with severe inflammation and pneumonia (WHO, 2022). However, these combinations have side effects such as antibiotic resistance (Bindu et al., 2020), oxidative stress (Maigoda, 2021), impaired bacterial elimination (Peternel, 2013), lung tissue damage, leading to

To cite this paper: Mahendra PGW, Widyarini S, and Prakoso YA (2025). Effects of Fermented *Crescentia cujete* and Enrofloxacin on Inflammation in Pneumonic Pasteurellosis Rats. *World Vet. J.*, 15 (4): 978-988. DOI: https://dx.doi.org/10.54203/scil.2025.wvj99

the development of infections (Abbasifard and Khorramdelazad, 2020), and increased risk of hospitalization costs (MacLeod et al., 2021). The mentioned limitations highlighted the need for alternative therapies. Alternative treatments, such as herbal remedies, are necessary to reduce the side effects of medicines.

One herbal alternative is the berenuk fruit (calabash, *Crescentia cujete L.*). The calabash fruit is widely recognized as a medicinal plant with different uses, including anti-inflammatory and antioxidant properties (Gonzales et al., 2023). Calabash contains alkaloids, flavonoids, saponins, tannins, and polyphenols (Atmodjo, 2019). One procedure to increase the bioactive compounds in herbs is fermentation. The fermented *Crescentia cujete* (FCC) contains several bioactive compounds, including antioxidants, choline, phytonadione, alpha-tocopherol, and retinol (Prakoso et al., 2024). Therefore, the present study aimed to analyze the anti-inflammatory effects of FCC on hematology and immune expression of GM-CSF and IL-6 in the lungs of induced PP rats.

MATERIALS AND METHODS

Ethical approval

The present study was approved by the Ethical Committee for Research on Animals, Faculty of Dentistry, University Airlangga, Surabaya, Indonesia, with the ethical approval registration number of 0511/HRECC.FODM/IV/2025.

Herbal preparation

Crescentia cujete fruit was obtained from the garden of Wijaya Kusuma University, Surabaya, Indonesia. The fruit was washed, cleaned, and peeled. The fermentation of calabash fruit was carried out using a mixture of water, fruit, sugar, and pectinase (Pectinex Ultra AF-P, Novozymes, London, England). The components were combined at a ratio of 1,000 mL of water, 400 grams of fruit pulp, 40 grams of sugar, and 40 mL of pectinase. The mixture was stored at 25°C for 30 days, stirred manually every 24 hours, and, after fermentation was complete, stored at 4°C (Wilujeng et al., 2023).

Study design and animals

A total of 20 male Sprague-Dawley rats, 3 months old and weighing 250-300 g, were randomly divided into five groups, with four rats per group. The treatment groups included control healthy rats (P1) and infected rats with PP, which did not receive any treatments (P2). The third group included the PP rats that were treated with 20 mg/kg body weight (BW) of enrofloxacin (P3), the fourth group consisted of PP rats that were given 20 mg/kg BW of enrofloxacin and 30 mg/kg BW of ibuprofen (P4), and the fifth group was the PP rats that received 20 mg/kg BW of enrofloxacin and 5.92 mg/kg BW of FCC (P5; Prakoso et al., 2024). The rats were acclimated to the environment for seven days at 20-30°C, with a light cycle, and were fed BR-1 (Japfa Comfeed, Indonesia) food and water *ad libitum*. *Pasteurella multocida* was induced intratracheally on day eight post-adaptation (PA). Treatment was administered orally using an oral tube from days 11 to 18 PA.

Infection induced by *Pasteurella multocida*

The *P. multocida* used was derived from a collection of clinical isolates kept at the Laboratory of Microbiology, Faculty of Health, University of Muhammadiyah Sidoarjo, Indonesia. Induction using a *P. multocida* suspension was equated to a 0.5 McFarland standard (Himedia R092, Indonesia) with a density of 10^8 CFU. Inoculation of *P. multocida* was performed intratracheally with 100 µl (Duplessis et al., 2021). The procedure was performed once on day eight PA, with a severe acute infection degree reached on day 11 PA. The successful establishment of PP was characterized by signs of acute fever, severe fibrinous-fibrinopurulent bronchopneumonia, fibrinous pleurisy, and septicemia (Abdullah et al., 2014).

Blood sample examination

On day 19 PA, the rats were anesthetized using ketamine at a dose of 40 mg/kg BW (Ket-A-100®; Struck et al., 2011), and blood samples were collected by using a microhematocrit through the retroorbital plexus of rats and placed in a container containing ethylene diamine tetraacetic acid (EDTA). Blood was stored in a refrigerator at 4°C for up to 24 hours for further analysis. Blood was analyzed for total erythrocytes, total leukocytes, hemoglobin, packed cell volume (PCV), mean corpuscular volume (MCV), mean corpuscular hemoglobin (MCH), mean corpuscular hemoglobin concentration (MCHC), leukocyte differential, and platelets. Hematology profile analysis was performed using a vet automatic hemoanalyzer (Wheisman AC310, Indonesia).

Lung sample examination

Lung samples were collected on day 19 after treatment. Before lung collection, the rats were euthanized using cervical dislocation.

Immunohistochemistry

The lung sample slides were dehydrated using graded alcohols, xylene, and phosphate-buffered saline, and then blocked with skim milk 1% in PBS (Prakoso et al., 2021). For antigen retrieval, the slides were incubated in Bond Epitope Retrieval Solution (RE7119, Leica Biosystems, USA) at 98°C for 20 minutes, immediately followed by a rinse with cold water. Next, endogenous peroxidase activity was quenched by incubating the slides with hydrogen peroxide 4% (Peroxidase Block, RE7101, Leica Biosystems, USA) for five minutes, followed by rinsing with PBS. This step was followed by a protein-blocking stage, where the slides were treated with 0.4% casein in PBS (Protein Block, RE7102, Leica Biosystems, USA) for five minutes, then rinsed with PBS. The slides were then incubated with the primary antibodies, anti-GM-CSF (sc-32753, Santa Cruz Biotechnology Inc, USA) and anti-IL-6 (z03034, Santa Cruz Biotechnology Inc, USA), for 30 minutes, followed by a PBS rinse. The anti-IL-6 antibody was diluted 1:100, while the anti-GM-CSF antibody was diluted 1:250 in primary antibody diluent (AR9352, Leica Biosystems, USA). After the primary antibody step, Rabbit anti-mouse IgG, which was diluted in 10% animal serum (Post Primary Antibody, RE7111, Leica Biosystems, USA), was applied for 30 minutes, and the slides were rinsed with PBS. Subsequently, the slides were incubated with anti-rabbit poly-HRP IgG containing 10% animal serum (Novolink Polymer, RE7112, Leica Biosystems, USA) for 30 minutes, followed by rinsing with PBS. For signal visualization, the slides were treated with diaminobenzidine (DAB) chromogen for 5 minutes, rinsed with tap water, and then counterstained using hematoxylin (RE7107, Leica Biosystems, USA) for 30 seconds. Finally, the slides were rinsed with tap water for five minutes, after which they were dehydrated, cleared, and mounted (Prakoso et al. 2020). The slides were stained with mouse antibodies, anti-IL-6 (Cat. No. z03034; Santa Cruz Biotechnology Inc., USA) and anti-GM-CSF (Cat. No. sc-32753; Santa Cruz Biotechnology Inc., USA), following the staining protocol outlined by Prakoso et al. (2020). The anti-IL-6 antibody was diluted 1:100, and the anti-GM-CSF antibody was diluted 1:250 in the primary antibody diluent (Cat. No. AR9352; Leica Biosystems, USA).

The immune expression of GM-CSF and IL-6 was photographed by the pathologist from the Laboratory of Pathology, Faculty of Veterinary Medicine, University of Gadjah Mada. The image was captured five times in different fields at 400X magnification. The image was analyzed using Image J software (NIH, USA) and reported as a percentage of immunoreactive area.

Enzyme-linked immunosorbent assays

The GM-CSF and IL-6 levels were quantified using commercial enzyme-linked immunosorbent assay (ELISA) kits with the product catalog numbers of MBS3808110 for GM-CSF and MBS2021530 for IL-6 (MyBiosource, USA). The wells were coated with a capture antibody and incubated overnight at 4°C, then washed and blocked with BSA. The antigen was then added to bind the capture antibody and incubated at 37°C. After washing, a primary detection antibody and an enzyme-conjugated secondary antibody were sequentially added, each followed by incubation and washing. Finally, a substrate was introduced to produce a measurable color change, indicating that antigen-antibody binding had occurred, as per the manufacturer's standard procedure.

Data analysis

Normally distributed and homogeneous data were analyzed using SPSS software version 26. For normally distributed data, the Duncan post hoc test was applied. Data that were not normally distributed and/or not homogeneous were analyzed using the Kruskal-Wallis test and the Mann-Whitney U test. The Kruskal-Wallis test was used at a 95% confidence level.

RESULTS

Hemoglobin levels showed a significant decrease in P2 compared to P1 ($p < 0.05$), but there was no difference was observed when compared to P3 ($p > 0.05$). Groups P4 and P5 indicated an increase in hemoglobin levels, approaching the values observed in P1; however, it was statistically different from the control group ($p < 0.05$; Table 1). The MCH level in P2 decreased significantly compared to P1 ($p < 0.05$), but did not differ significantly compared to P3 ($p > 0.05$). Groups P4 and P5 demonstrated MCH levels within the range of P1, yet still showed a significant difference compared to P1 ($p < 0.05$; Table 1). The MCHC level in P2 decreased significantly compared to P1 ($p < 0.05$), but no significant difference was observed compared to P3 ($p > 0.05$). Groups P4 and P5 exhibited increasing MCHC levels, approaching the range observed in P1. Specifically, P4 indicated no significant difference compared to P1 ($p > 0.05$), whereas P5 remained significantly different in comparison to P1 ($p < 0.05$; Table 1). The leukocyte level in P2 was significantly higher than in P1 ($p < 0.05$), but did not differ significantly from P3 and P4 ($p > 0.05$). Group P5 demonstrated a decreasing trend in leukocyte levels compared to P2 and did not exhibit a statistically significant difference compared to

P1. ($p > 0.05$; Table 1). The neutrophil value in P2 was significantly higher than that in P1 ($p < 0.05$), but did not differ significantly compared to P3 ($p > 0.05$). Although groups P4 and P5 demonstrated a decreasing trend in neutrophil levels, they differed significantly compared to P1 ($p < 0.05$; Table 1).

Table 1. Mean and standard deviation of hematological results of Sprague Dawley rats on day 19 of the study

Parameter	P1	P2	P3	P4	P5
RBC ($\times 10^6$ cells/mm^3)	5.72 ± 0.19^a	5.77 ± 0.33^a	5.90 ± 0.21^a	5.71 ± 0.18^a	5.89 ± 0.30^a
Hemoglobin (g/dL)	14.43 ± 0.60^a	10.91 ± 1.47^b	10.50 ± 0.55^b	13.21 ± 0.45^c	12.40 ± 2.17^c
PCV (%)	42.18 ± 1.09^a	41.81 ± 1.19^a	41.23 ± 0.82^a	42.94 ± 1.72^a	42.00 ± 1.45^a
MCV (fL)	73.71 ± 3.17^a	72.56 ± 4.95^a	69.92 ± 2.40^a	75.25 ± 3.47^a	71.49 ± 5.01^a
MCH (Pg)	25.22 ± 1.39^a	18.86 ± 1.89^b	17.81 ± 1.06^b	23.14 ± 0.66^c	21.12 ± 4.14^c
MCHC (%)	34.25 ± 2.13^a	26.09 ± 3.33^b	25.50 ± 1.82^b	30.82 ± 2.03^a	29.64 ± 5.90^a
Platelets (cell/mm^3)	5.10 ± 0.27^a	5.19 ± 0.09^a	5.20 ± 0.25^a	4.95 ± 0.20^a	5.17 ± 0.28^a
Leukocyte ($\times 10^3$ cell/mm^3)	6.10 ± 0.38^a	7.25 ± 0.38^b	7.16 ± 0.42^b	6.76 ± 0.23^b	6.57 ± 0.41^a
Neutrophils ($\times 10^3$ cell/mm^3)	1.67 ± 0.18^a	2.60 ± 0.17^b	2.42 ± 0.13^b	2.01 ± 0.21^c	1.95 ± 0.16^c
Eosinophils ($\times 10^3$ cell/mm^3)	0.15 ± 0.07^a	0.12 ± 0.06^a	0.10 ± 0.04^a	0.11 ± 0.06^a	0.08 ± 0.06^a
Basophils ($\times 10^3$ cell/mm^3)	0.03 ± 0.03^a	0.00 ± 0.00^a	0.05 ± 0.03^a	0.06 ± 0.05^a	0.01 ± 0.03^a
Lymphocytes ($\times 10^3$ cell/mm^3)	3.93 ± 0.37^a	4.29 ± 0.29^a	4.36 ± 0.29^a	4.31 ± 0.21^a	4.29 ± 0.24^a
Monocytes ($\times 10^3$ cell/mm^3)	0.30 ± 0.07^a	0.21 ± 0.12^a	0.19 ± 0.06^a	0.25 ± 0.11^a	0.23 ± 0.05^a

Note: P1: Control, P2: Induced PP without therapy, P3: Induced PP with enrofloxacin 20 mg/kgBB, P4: Induced PP with enrofloxacin 20 mg/kgBB and ibuprofen 30 mg/kgBB, P5: Induced PP with enrofloxacin 20 mg/kgBB and FCC 5.92 mg/kgBB, PCV: Packed cell volume, MCV: Mean corpuscular volume, MCH: Mean corpuscular hemoglobin, MCHC: Mean corpuscular hemoglobin concentration. [a, b, and c] different superscript letters indicate significant differences in a row ($p \leq 0.05$).

The present study indicated that GM-CSF immune expression was localized in type II pneumocytes in the lung interstitium of rats in the control and PP-infected groups (Figure 1A). The expression level in P1 appeared relatively low compared to P2, P3, P4, and P5. Group P2 demonstrated an increase in GM-CSF immune expression compared to the control group (Figure 1B). Groups P3 and P4 indicated a reduction in GM-CSF immune expression compared to P2, but with a qualitatively higher intensity than in P1 (Figures 1C and D). The GM-CSF immune expression in P5 was relatively low compared to P2, P3, and P4, and was qualitatively lower than the control group (Figure 1E). The treatment exerted a significant effect on the pulmonary GM-CSF immune expression after PP induction (Table 2). Group P2 indicated a significant increase after induction compared to the control group ($p < 0.05$). Groups P3 and P4 exhibited a significant increase in GM-CSF immune expression after treatment compared to P1 ($p < 0.05$), but did not differ significantly compared to P2 ($p > 0.05$). Although the expression level in P5 did not significantly differ from the control group ($p > 0.05$), it was significantly lower than in P2.

The present results indicated that the immune expression of IL-6 was localized in inflammatory cells in bronchial-associated lymphoid tissue (BALT) and the lung interstitium in the PP groups (Figure 2). Qualitatively, the level of IL-6 immune expression in P2 was higher than in P3, P4, and P5 (Figure 2B). Group P3 indicated multifocal immune expression of IL-6 in the interalveolar septa, which was lower than P2 (Figure 2C). Groups P4 and P5 demonstrated a gradual decrease of IL-6 immune expression compared to P2 and P3, as illustrated qualitatively in Figures 2D and 2E. The treatment affected the IL-6 immune expression in the lungs following PP induction (Table 2). Group P2 indicated a significant increase post-induction compared to the control group ($p < 0.05$; Table 2). Groups P3 and P4 demonstrated a significant increase after therapy compared to P1 ($p < 0.05$), and there was no significant difference compared to P2 ($p > 0.05$; Table 2). The result of the IL-6 immune expression level in P5 did not differ significantly compared to the control group ($p > 0.05$), but there was a significant difference compared to P2 ($p < 0.05$; Table 2).

Table 2. Mean and standard deviation of immunohistochemistry results of Sprague Dawley rats on day 19 of the study

Parameter	P1	P2	P3	P4	P5
GM-CSF	7.57 ± 5.88^a	17.62 ± 2.24^b	13.14 ± 2.94^b	8.39 ± 3.59^c	5.84 ± 1.87^a
IL-6	6.68 ± 1.51^a	19.53 ± 2.02^b	17.92 ± 2.49^b	11.27 ± 2.62^c	8.50 ± 3.32^a

Note: P1: Control, P2: Induced PP without therapy, P3: Induced PP with enrofloxacin 20 mg/kgBB, P4: Induced PP with enrofloxacin 20 mg/kgBB and ibuprofen 30 mg/kgBB, P5: Induced PP with enrofloxacin 20 mg/kgBB and FCC 5.92 mg/kgBB, GM-CSF: Granulocyte macrophage-colony stimulating factor, IL-6: Interleukin-6. [a, b, and c] different superscript letters indicate significant differences in a row ($p \leq 0.05$).

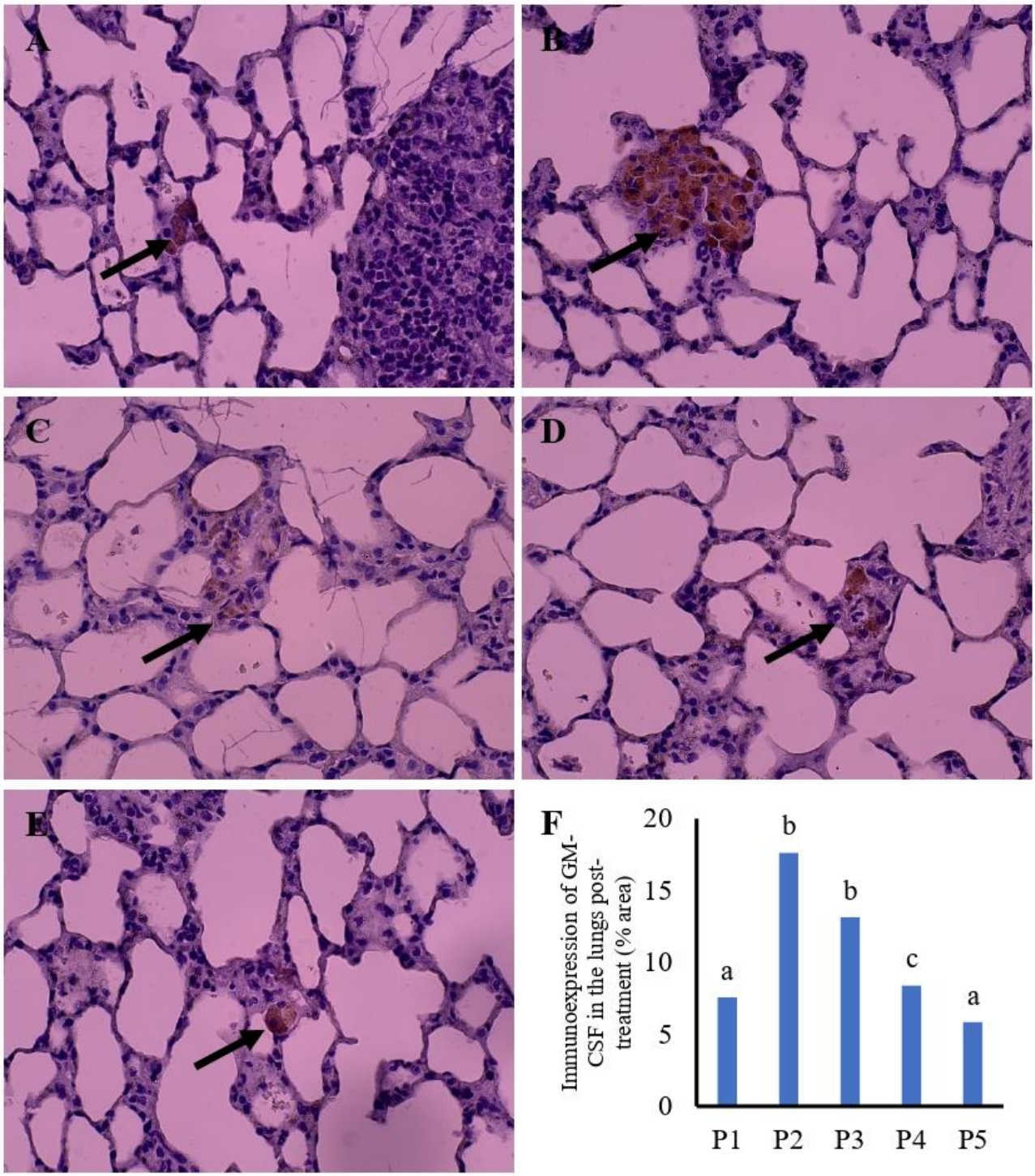


Figure 1. Granulocyte macrophage-colony stimulating factor (GM-CSF) immune expression in 3-month-old male rats with pneumonic pasteurellosis, post-treatment. **A**: GM-CSF immune expression in the lungs was localized to type II pneumocytes in the lung interstitium of group control (P1), **B**: untreated Group (P2), **C**: enrofloxacin Group (P3), **D**: enrofloxacin and ibuprofen Group (P4), **E**: enrofloxacin and FCC Group (P5), **F**: Mean pattern of GM-CSF immune expression post-treatment. IHC anti-GM-CSF antibody, DAB, 400× (A-E).

The ELISA results indicated that the treatment affected GM-CSF and IL-6 levels in the lungs after PP induction ($p < 0.05$; Figure 1A and B). The results indicated that the GM-CSF levels in P2 increased significantly compared to the control group ($p < 0.05$). Groups P3 and P4 exhibited a significant increase in GM-CSF expression compared to the control group ($p < 0.05$) and were not significantly different compared to P2 ($p > 0.05$). Group P5 did not differ significantly from the control group ($p > 0.05$), but exhibited a significantly lower value than P2 ($p < 0.05$), indicative of a successful reversion to near-normal levels. The level of IL-6 in the lungs after treatment indicated that IL-6 levels in P2 were significantly higher than in the control group ($p < 0.05$, Figure 1B). Group P3 indicated a significant increase

compared to P2 and the control group ($p < 0.05$). Group P4 indicated a significant decrease compared to the P2 ($p < 0.05$) and was not significantly different from the control group ($p > 0.05$). Group P5 did not differ significantly from the control group ($p > 0.05$) and was significantly lower than P2 ($p < 0.05$), indicating a successful restoration of IL-6 levels to near-normal values.

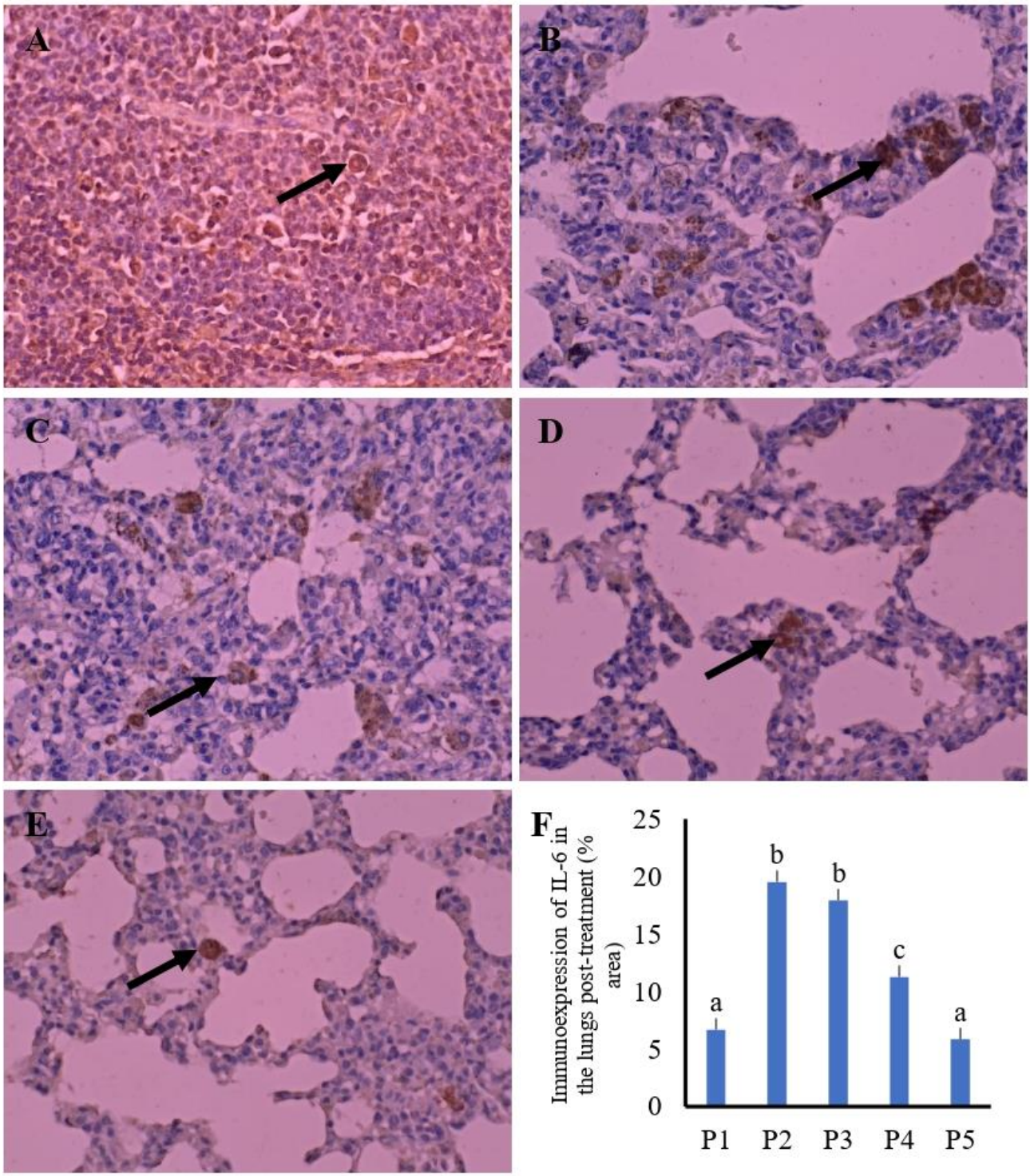


Figure 2. Interleukin-6 (IL-6) immune expression in 3-month-old male rats with pneumonic pasteurellosis, post-treatment. **A**: IL-6 immunoexpression in the lungs was localized to inflammatory cells in the bronchial associated lymphoid tissue (BALT) and in the lung interstitium of group P2, **B**: IL-6 immune expression in type II pneumocytes in the interalveolar septa of untreated group (P2), **C**: enrofloxacin Group (P3), **D**: enrofloxacin and ibuprofen Group (P4), **E**: enrofloxacin and FCC Group (P5), and figure **F**: Mean pattern of IL-6 immune expression post-treatment. IHC anti-IL-6 antibody, DAB, 400× (A-E).

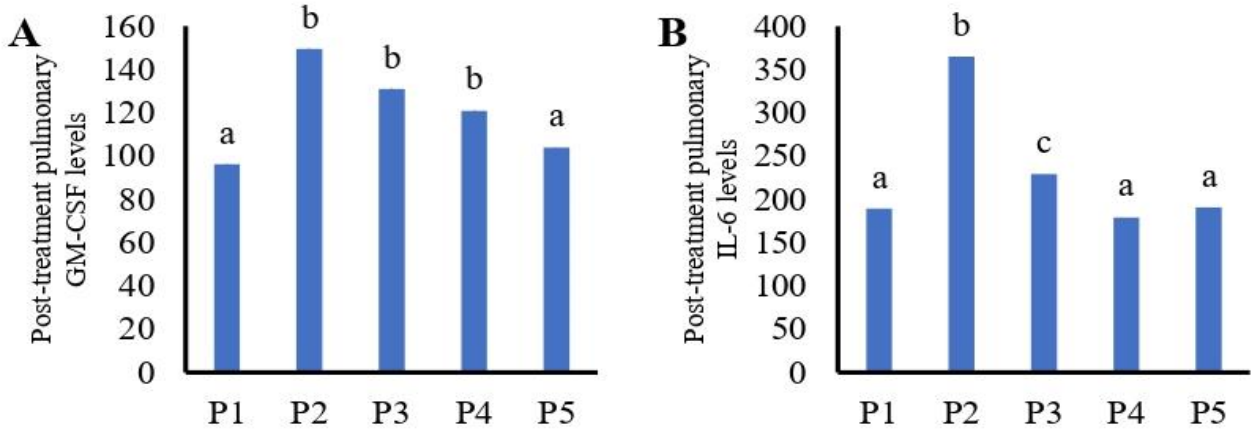


Diagram 1. Mean pattern of immune expression in 3-month-old male rats with pneumonic pasteurellosis model, post-treatment. **A**: Granulocyte macrophage-colony stimulating factor (GM-CSF), **B**: Interleukin-6 (IL-6).

DISCUSSION

Enrofloxacin acts by inhibiting DNA gyrase and topoisomerase IV and exhibits strong bactericidal activity against *Pasteurella* spp. (Hooper and Jacoby, 2016). However, its clinical efficacy in PP may be decreased due to increasing bacterial resistance and impaired drug distribution within the heavily infected lungs (Li et al., 2023). Adding ibuprofen can improve clinical outcomes by reducing inflammation. However, long-term use may decrease antibody production and pro-inflammatory cytokines such as IL-6 (Mihara et al., 2011). Inflammation can suppress protective immune responses, particularly in lungs that depend heavily on the balance between inflammation and local defense, which may lead to immunocompromised states or depletion of pulmonary immune function (Huemer, 2015). As an alternative, FCC has been shown to have potential as a natural anti-inflammatory and immunomodulatory agent capable of suppressing excessive inflammation (Prakoso et al., 2024).

Alterations in the hematological profile were observed, indicating a restorative effect on hemoglobin, MCH, MCHC, leukocytes, and neutrophils, along with decreased GM-CSF and IL-6 immune expression in male rats treated with enrofloxacin and FCC. The hematological changes might be due to FCC components, including choline, alpha-tocopherol, phytonadione, and retinol (Prakoso et al., 2024). Hemoglobin indicates the total amount of hemoglobin in the blood volume, while MCH and MCHC describe the distribution and concentration of hemoglobin at the cellular level (Yao et al., 2023); therefore, changes in hemoglobin levels would directly affect MCH and MCHC. Hemoglobin decreased considerably in rats treated with enrofloxacin and FCC (P5), consistent with the findings of Santos et al. (2003), who reported that choline alters red blood cell membrane properties, which can influence hemoglobin levels. Choline can enhance the stability and structure of hemoglobin by influencing hemostasis and erythropoiesis cell function (Huang et al., 2018). Alpha-tocopherol prevents the development of erythrocytopenia and helps maintain hemoglobin levels under oxidative stress conditions (Ivanova et al., 2011). Alpha-tocopherol protects red blood cell membranes from oxidative damage, thereby reducing hemolysis and increasing haptoglobin levels by binding free hemoglobin released due to hemolysis (Sovira et al., 2020). Phytonadione acts as an essential cofactor, enabling clotting factors to bind calcium and participate in blood clotting (Beaty, 2016). Retinol plays a crucial role in increasing hemoglobin levels by enhancing iron absorption and mobilization, supporting erythrocyte formation, and reducing inflammation (Sun et al., 2010).

The total leucocyte count in group P5 was similar to that in the control group, consistent with the findings of Daş et al. (2021), who reported that choline administration increased the number and function of leukocytes and reduced excessive inflammatory responses. Choline plays a vital role in maintaining leukocyte function and health by reducing oxidative stress and lowering leukocyte inflammatory activation (Mehta et al., 2009). It has been established that alpha-tocopherol can attenuate systemic inflammation and restore leukocyte counts elevated by excessive inflammatory responses. This observation aligns with the present findings, which revealed normalization in leukocyte parameters following alpha-tocopherol treatment (Moreira et al., 2022). The present findings align with previous studies, demonstrating that alpha-tocopherol stabilizes leukocyte counts under stress and inflammatory conditions (Sahakyan, 2024). Phytonadione has been reported to suppress the production of pro-inflammatory cytokines, thereby attenuating inflammatory responses. These anti-inflammatory effects can consequently reduce the occurrence of reactive leukocytosis, or leukocyte elevation, which typically increases during acute or chronic inflammatory conditions (Dahlberg et al., 2021). Previous studies have shown that retinol is essential for the differentiation of hematopoietic stem

cells into different leukocyte lineages. This finding agrees with the present study, indicating that retinol regulates leukocyte development and maintains hematological balance (Cañete et al., 2017).

The total neutrophils in P5 were close to the level in the control group, consistent with Zhou et al. (2018), who found that under severe inflammatory conditions, choline can reduce the number of neutrophils migrating to the site of inflammation systemically. Choline supplementation can reduce the expression of genes responsive to inflammation, modulate neutrophil activation, and reduce inflammation (Lopreiato et al., 2019). Alpha-tocopherol acts as an antioxidant, reducing oxidative stress that triggers neutrophil activation and suppressing the production of inflammatory cytokines that can trigger neutrophil recruitment (Hernandez et al., 2013; Wallert et al., 2019). Retinol has been reported to enhance neutrophil differentiation and bactericidal activity, improving host defense while limiting excessive neutrophil proliferation. The current results are consistent with previous findings demonstrating that retinol contributes to immune balance by stabilizing leukocyte responses under inflammatory conditions (Stream et al., 2024).

Immune expression of GM-CSF in rats with FCC therapy was reduced during the present study. Type II pneumocytes synthesize GM-CSF in response to inflammation; however, excessive production can lead to granulocyte and macrophage activation and proliferation, resulting in tissue damage and chronic inflammation (Ingelfinger et al., 2021). Choline in FCC could have suppressed the GM-CSF-mediated immune responses. This finding aligned with that of Mehta et al. (2009), indicating that choline reduced oxidative stress and inhibited the NF-κB pathway, which might indirectly modulate GM-CSF-mediated immune responses. Alpha-tocopherol has been shown to suppress NF-κB activation, thereby reducing the synthesis of pro-inflammatory cytokines (Li et al., 2012). Alpha-tocopherol can modulate immune responses across different cell types and suppress local and systemic inflammatory responses (Hu et al., 2022). Phytonadione can reduce oxidative stress, inhibit NF-κB and NLRP3 activation, and downregulate the expression of different pro-inflammatory cytokines. These mechanisms provide a plausible biological basis for the indirect effects of vitamin K in attenuating neutrophil activation and migration, as well as reducing GM-CSF levels under inflammatory conditions (Dosumu et al., 2021). Retinol can help modulate excessive immune responses and reduce the activation of inflammatory cells during severe inflammatory conditions (Spinas et al., 2015).

The immune expression of IL-6 in rats treated with enrofloxacin and FCC exhibited a reduction in IL-6 levels, nearing those of the control group. The BALT and the pulmonary interstitium synthesize pro-inflammatory cytokines, such as IL-6, in response to inflammation (Liska et al., 2013). Elevated IL-6 levels can trigger different physiological responses that may exacerbate inflammatory conditions and tissue damage (Kang and Kishimoto, 2021). Choline in FCC can suppress IL-6 immune expression, consistent with the findings of Baker et al. (2023), who reported that choline plays a crucial role in modulating the immune response through anti-inflammatory mechanisms by reducing IL-6 expression under inflammatory conditions. Choline acts as a precursor to acetylcholine, which can inhibit NF-κB activation, the primary transcription factor for pro-inflammatory cytokine genes, including IL-6 (Xia et al., 2022). Choline can reduce oxidative stress and inhibit the cholinergic inflammatory pathway (Yang et al., 2021). Alpha-tocopherol plays a crucial role in maintaining cellular membrane stability, preventing free radical damage, and reducing oxidative stress (Lemaire et al., 2010).

Alpha-tocopherol possesses antioxidant and anti-inflammatory activities that contribute to the reduction of IL-6 expression under inflammatory conditions. Alpha-tocopherol inhibited the formation of free radicals, which trigger activation of proinflammatory signaling pathways, particularly NF-κB, thereby reducing IL-6 gene transcription in immune cells such as macrophages, lymphocytes, and endothelial cells (Sharma and Vinayak, 2011). Retinol plays an important role in maintaining the integrity of the mucosal epithelium and reducing the infiltration of pro-inflammatory immune cells by inhibiting the release of pro-inflammatory cytokines such as IL-6, TNF, and macrophage inflammatory proteins (Wojtal et al., 2013). Retinol supports the regeneration of the mucosal surface and epithelium, which is vital for maintaining the structural integrity of the epithelium (Druilhe et al., 2008). Phytonadione exhibits anti-inflammatory effects by inhibiting NF-κB activation (Ohsaki et al., 2010), and its administration has been demonstrated to decrease oxidative stress. While there is no direct evidence linking this reduction to decreased IL-6 transcription or secretion in immune cells, it is biologically plausible, as oxidative stress can activate pro-inflammatory pathways such as NF-κB (Li et al., 2003).

CONCLUSION

The present study indicated that FCC improved hematological profiles, particularly hemoglobin, MCH, MCHC, leukocytes, and neutrophils, which reflected recovery responses in rats following treatment. Additionally, reduced immune expression of GM-CSF and IL-6 was observed in rats with induced PP. Future studies should be conducted to analyze the potential of FCC as an anti-inflammatory agent and its possible toxicity to ensure safety on a larger scale samples.

DECLARATIONS

Acknowledgments

The authors acknowledged the University Gadjah Mada for providing the financial support for the present study through the Final Project Recognition Program. Moreover, the laboratory technicians from Integrated Laboratory, University of Wijaya Kusuma Surabaya, Indonesia, were acknowledged for their support in conducting the present study.

Authors' contributions

Paskalis Guntur Widya Mahendra and Sitarina Widyarini designed the study. Paskalis Guntur Widya Mahendra, Yos Adi Prakoso, and Sitarina Widyarini performed the animal experimentation. Paskalis Guntur Widya Mahendra formulated, prepared, and preserved the tested compound. Paskalis Guntur Widya Mahendra and Yos Adi Prakoso performed data analysis and interpretation. Paskalis Guntur Widya Mahendra, Yos Adi Prakoso, and Sitarina Widyarini equally contributed to drafting, revising, and finalizing the submitted paper. All the authors approved the last edition of the manuscript.

Funding

The present study was supported and funded by Kemdikbudristek, the Republic of Indonesia, with Decree number 0070/C3/AL.04/2025, National grand number: 128/C3/DT.05.00/PL/2025, derivative grand number: 007/LL7/DT.05.00/PL/2025, 193/PL/LPPM/UWKS/V/2025.

Competing interests

The authors have not declared any conflict of interest.

Ethical considerations

The present manuscript is original, conducted solely by the authors, and it has not been published elsewhere. The authors confirmed that no AI tools, including generative AI models, were used in the writing, editing, or preparation of this manuscript.

Availability of data and materials

The data supporting the findings of the present study are available from the corresponding author upon reasonable request.

REFERENCES

Abbasifard M and Khorramdelazad H (2020). The bio-mission of interleukin-6 in the pathogenesis of COVID-19: A brief look at potential therapeutic tactics. Life Sciences, 257: 118097. Available at: https://pubmed.ncbi.nlm.nih.gov/32679148/

Abdullah JFF, Tijjani A, Adamu L, Teik Chung EL, Abba Y, Mohammed K, Saharee AA, Haron AW, Sadiq MA, and Mohd AML (2014). Pneumonic pasteurellosis in a goat. Iran Journal of Veterinary Medicine, 8(4): 293-296. DOI: https://www.doi.org/10.22059/ijvm.2015.52490

Aliyu M, Zohora FT, Anka AU, Ali K, Maleknia S, Saffarioun M, and Azizi G (2022). Interleukin-6 cytokine: An overview of the immune regulation, immune dysregulation, and therapeutic approach. International Immunopharmacology, 111: 109130. DOI: https://www.doi.org/10.1016/j.intimp.2022.109130

Atmodjo PK (2019). Diversity and utilization of the berenuk (*Crescentia cujete* L.) in the special region of Yogyakarta. Biota, 4(3): 116-123. DOI: https://www.doi.org/10.24002/biota.v4i3.2518

Baker JA, Breit KR, Bodnar TS, Weinberg J, and Thomas JD (2022). Choline supplementation modifies the effects of developmental alcohol exposure on immune responses in adult rats. Nutrients, 14(14): 2868. DOI: https://www.doi.org/10.3390/nu14142868

Beaty RS (2016). Hemostatic agents used to stop bleeding. In: J. Teruya (Editor), Management of bleeding patients. Springer., Cham, pp. 321-336. DOI: https://www.doi.org/10.1007/978-3-319-30726-8_34

Bindu S, Mazumder S, and Bandyopadhyay U (2020). Non-steroidal anti-inflammatory drugs (NSAIDs) and organ damage: A current perspective. Biochemical Pharmacology, 180: 114147. DOI: https://www.doi.org/10.1016/j.bcp.2020.114147

Cañete A, Cano E, Muñoz-Chápuli R, and Carmona R (2017). Role of vitamin A/retinoic acid in regulation of embryonic and adult hematopoiesis. Nutrients, 9(2): 159. DOI: https://www.doi.org/10.3390/nu9020159

Dahlberg S, Schött U, Eriksson EÄ, Tahirsylaj Y, Schurgers L, and Kander T (2021). Intravenous vitamin K1 for the correction of prolonged prothrombin times in non-bleeding critically ill patients: A prospective observational study. Nutrients, 13(8): 2580. DOI: https://www.doi.org/10.3390/nu13082580

Daş T, Buğra A, Arslan MN, Ziyade N, and Buyuk Y (2021). Evaluation of postmortem pathological changes in the lung in SARS-CoV-2 RT-PCR positive cases. Journal of Surgery and Medicine, 5(11): 1113-1120. DOI: https://www.doi.org/10.28982/josam.997381

Dosumu OA, Rotimi SO, Adeleye OO, Akamo AJ, Osinuga KT, Taiwo OA, Omotosho OO, and Sani LO (2021). Vitamin K protects against 7, 12-dimethylbenz (A) anthracene induced hepatotoxicity in Wistar rats. Environmental Toxicology, 36(3): 362-373. DOI: https://www.doi.org/10.1002/tox.23042

Druilhe A, Zahm JM, Benayoun L, El Mehdi D, Grandsaigne M, Dombret MC, Mosnier I, Feger B, Depondt J, Aubier M, and Pretolani M (2008). Epithelium expression and function of retinoid receptors in asthma. American Journal of Respiratory Cell and Molecular Biology, 38(3): 276-282. DOI: https://www.doi.org/10.1165/rcmb.2006-0453OC

Duplessis C, Warawa JM, Lawrenz MB, Henry M, and Biswas B (2021). Successful intratracheal treatment of phage and antibiotic combination therapy of a multi-drug resistant Pseudomonas aeruginosa murine model. Antibiotics, 10(8): 946. DOI:

https://www.doi.org/10.3390/antibiotics10080946

Gonzales AL, Huang SKH, Sevilla UTA, Hsieh CY, and Tsai PW (2023). In silico analysis of anti-inflammatory and antioxidant properties of bioactive compounds from *Crescentia cujete* L. Molecules, 28(8): 3547. DOI: https://www.doi.org/10.3390/molecules28083547

Guan L, Zhang L, Xue Y, Yang J, and Zhao Z (2020). Molecular pathogenesis of the hyaluronic acid capsule of Pasteurella multocida. Microbial Pathogenesis, 149: 104380. DOI: https://www.doi.org/10.1016/j.micpath.2020.104380

Hernandez ML, Wagner JG, Kala A, Mills K, Wells HB, Alexis NE, Lay JC, Jiang Q, Zhang H, Zhou H, and Peden DB (2013). Vitamin E, γ-tocopherol, reduces airway neutrophil recruitment after inhaled endotoxin challenge in rats and in healthy volunteers. Free Radical Biology and Medicine, 60: 56-62. DOI: https://www.doi.org/10.1016/j.freeradbiomed.2013.02.001

Hooper DC and Jacoby GA (2016). Topoisomerase inhibitors: Fluoroquinolone mechanisms of action and resistance. Cold Spring Harbor Perspectives in Medicine, 6(9): a025320. DOI: https://www.doi.org/10.1101/cshperspect.a025320

Huang NJ, Lin YC, Lin CY, Pishesha N, Lewis CA, Freinkman E, Farquharson C, Millán JL, and Lodish H (2018). Enhanced phosphocholine metabolism is essential for terminal erythropoiesis. Blood, The Journal of the American Society of Hematology, 131(26): 2955-2966. DOI: https://www.doi.org/10.1182/blood-2018-03-838516

Huemer HP (2015). Possible immunosuppressive effects of drug exposure and environmental and nutritional effects on infection and vaccination. Mediators of Inflammation, 2015: 349176. DOI: https://www.doi.org/10.1155/2015/349176

Hu M, Yang J, and Xu Y (2022). Effect of α-tocopherol in alleviating the lipopolysaccharide-induced acute lung injury via inhibiting nuclear factor kappa-B signaling pathways. Bioengineered, 13(2): 3958-3968. DOI: https://www.doi.org/10.1080/21655979.2022.2031399

Ingelfinger F, De Feo D, and Becher B (2021). GM-CSF: Master regulator of the T cell-phagocyte interface during inflammation. Seminars in Immunology, 54: 101518. DOI: https://www.doi.org/10.1016/j.smim.2021.101518

Ivanova AS, Sitnikova OG, and Nazarov SB (2011). Changes in the red blood cell system and in the activity of free radical processes in rats during chronic nitrite intoxication and alpha-tocopherol administration. Gigiena Sanitariia, 3: 78-80. Available at: https://pubmed.ncbi.nlm.nih.gov/21842742/

Kang S and Kishimoto T (2021). Interplay between interleukin-6 signaling and the vascular endothelium in cytokine storms. Experimental & Molecular Medicine, 53(7): 1116-1123. DOI: https://www.doi.org/10.1038/s12276-021-00649-0

Kubatzky KF (2012). Pasteurella multocida and Immune Cells. In: K. Aktories, J. Orth, and B. Adler (Editors), Pasteurella multocida. Current Topics in Microbiology and Immunology, vol 361. Springer., Berlin, Heidelberg, pp. 53-72. DOI: https://www.doi.org/10.1007/82_2012_204

Lemaire-Ewing S, Desrumaux C, Néel D, and Lagrost L (2010). Vitamin E transport, membrane incorporation and cell metabolism: Is α-tocopherol in lipid rafts an oar in the lifeboat?. Molecular Nutrition & Food Research, 54(5): 631-640. DOI: https://www.doi.org/10.1002/mnfr.200900445

Li CJ, Li RW, Kahl S, and Elsasser TH (2012). Alpha-tocopherol alters transcription activities that modulates tumor necrosis factor alpha (TNF-α) induced inflammatory response in bovine cells1. Gene Regulation and Systems Biology, 6: GRSB-S8303. DOI: https://www.doi.org/10.4137/GRSB.S8303

Li J, Lin JC, Wang H, Peterson JW, Furie BC, Furie B, Booth SL, Volpe JJ, and Rosenberg PA (2003). Novel role of vitamin k in preventing oxidative injury to developing oligodendrocytes and neurons. Journal of Neuroscience, 23(13): 5816-5826. DOI: https://www.doi.org/10.1523/JNEUROSCI.23-13-05816.2003

Li XS, Qi Y, Xue JZ, Xu GY, Xu YX, Li XY, Muhammad I, Kong LC, and Ma HX (2023). Transcriptomic Changes and satP Gene Function Analysis in Pasteurella multocida with Different Levels of Resistance to Enrofloxacin. Veterinary Sciences, 10(4): 257. DOI: https://www.doi.org/10.3390/vetsci10040257

Liska V, Glanc D, Vycital O, Bruha J, Pitule P, Kopalova J, Palek R, and Treska V (2013). Interleukin-6 inhibitors as novel generation of treatment strategies. Proteomics Research Journal, 4(3): 151. Available at: https://primo.qatar-weill.cornell.edu/permalink/974WCMCIQ_INST/oqaqc3/cdi_proquest_journals_1752112472

Lopreiato V, Vailati-Riboni M, Bellingeri A, Khan I, Farina G, Parys C, and Loor JJ (2019). Inflammation and oxidative stress transcription profiles due to in vitro supply of methionine with or without choline in unstimulated blood polymorphonuclear leukocytes from lactating Holstein cows. Journal of Dairy Science, 102(11): 10395-10410. DOI: https://www.doi.org/10.3168/jds.2019-16413

MacLeod M, Papi A, Contoli M, Beghé B, Celli BR, Wedzicha JA, and Fabbri LM (2021). Chronic obstructive pulmonary disease exacerbation fundamentals: diagnosis, treatment, prevention and disease impact. Respirology, 26(6): 532-551. DOI: https://www.doi.org/10.1111/resp.14041

Maigoda TC (2021). Tepung buah naga merah (*Hylocereus polyrhizus*) dan olahraga renang: Dampaknya terhadap penanda inflamasi, stres oksidatif, dan kebugaran dengan obesitas [Red dragon fruit (*Hylocereus polyrhizus*) flour and swimming exercise: Impact on inflammatory markers, oxidative stress, and fitness in obesity]. Indonesia: NEM. Available at: https://penerbitnem.com/2021/07/tepung-buah-naga-merah-hylocereus.html

Mehta AK, Arora N, Gaur SN, and Singh BP (2009). Choline supplementation reduces oxidative stress in mouse model of allergic airway disease. European Journal of Clinical Investigation, 39(10): 934-941. DOI: https://www.doi.org/10.1111/j.1365-2362.2009.02190.x Mihara M, Ohsugi Y, and Kishimoto T (2011). Tocilizumab, a humanized anti-interleukin-6 receptor antibody, for treatment of rheumatoid arthritis. Open Access Rheumatology: Research and Reviews, 3: 19-29. DOI: https://www.doi.org/10.2147/OARRR.S17118

Ministry of Health of the Republic of Indonesia (2020). Peraturan Menteri Kesehatan Republik Indonesia Nomor 21 Tahun 2020 Tentang Rencana Strategis Kementerian Kesehatan Tahun 2020-2024 [Regulation of the Minister of Health of the Republic of Indonesia Number 21 of 2020 concerning the strategic plan of the Ministry of Health for 2020-2024]. Available at: https://peraturan.bpk.go.id/Details/152564/permenkes-no-21-tahun-2020

Moreira LS, Chagas AC, Ames-Sibin AP, Pateis VO, Gonçalves OH, Silva-Comar FMS, and Comar JF (2022). Alpha-tocopherol-loaded polycaprolactone nanoparticles improve the inflammation and systemic oxidative stress of arthritic rats. Journal of Traditional and Complementary Medicine, 12(4): 414-425. DOI: https://www.doi.org/10.1016/j.jtcme.2021.12.003

Ohsaki Y, Shirakawa H, Miura A, Giriwono PE, Sato S, Ohashi A, Iribe M, Goto T, and Komai M (2010). Vitamin K suppresses the lipopolysaccharide-induced expression of inflammatory cytokines in cultured macrophage-like cells via the inhibition of the activation of nuclear factor κB through the repression of IKKα/β phosphorylation. The Journal of Nutritional Biochemistry, 21(11): 1120-1126. DOI: https://www.doi.org/10.1016/j.jnutbio.2009.09.011

Peternel Š (2013). Bacterial cell disruption: A crucial step in protein production. New biotechnology, 30(2): 250-254. DOI: https://www.doi.org/10.1016/j.nbt.2011.09.005

Prakoso YA, Hidayah N, Rini CS, and Kurniasih K (2021). Dynamic change of blood profile in rat models with acute skin injury artificially infected with methicillin-resistant Staphylococcus aureus. Veterinary World: 14(8): 2085-2090. DOI: http://www.doi.org/10.14202/vetworld.2021.2085-2090

Prakoso YA, Rini CS, Rahayu A, Sigit M, and Widhowati D (2020). Celery (Apium graveolens) as a potential antibacterial agent and its effect on cytokeratin-17 and other healing promoters in skin wounds infected with methicillinresistant Staphylococcus aureus. Veterinary World, 13(5): 865-871. DOI: https://www.doi.org/10.14202/vetworld.2020.865-871

Prakoso YA, Susilo A, and Widyarini S (2024). The standardization and efficacy of fermented *Crescentia cujete* (L.) in combination with enrofloxacin against artificially induced pneumonic pasteurellosis in rat models. Open Veterinary Journal, 14(12): 3404-3404. Available at: https://www.doi.org/10.5455/OVJ.2024.v14.i12.25

Sahakyan SG (2024). Hematological profile of alpha-tocopherol pre-treated rabbits at repeated hypoxic exposure. Proceedings of the YSU B: Chemical and Biological Sciences, 58(2): 264. DOI: https://www.doi.org/10.46991/PYSU:B.2024.58.2.133

Sharma R and Vinayak M (2011). α-Tocopherol attenuates NF-κB activation and pro-inflammatory cytokine IL-6 secretion in cancer-bearing mice. Bioscience Reports, 31(5): 421-428. DOI: https://www.doi.org/10.1042/BSR20100137

Santos T, Mesquita R, Martins e Silva J, and Saldanha C (2003). Effects of choline on hemorheological properties and NO metabolism of human erythrocytes. Clinical hemorheology and microcirculation, 29(1): 41-51. Available at: https://pubmed.ncbi.nlm.nih.gov/14561903/

Sovira N, Lubis M, Wahidiyat PA, Suyatna FD, Gatot D, Bardosono S, and Sadikin M (2020). Effects of α-tocopherol on hemolysis and oxidative stress markers on red blood cells in β-thalassemia major. Clinical and experimental pediatrics, 63(8): 314-320. DOI: https://www.doi.org/10.3345/cep.2019.00542

Spinas E, Saggini A, Kritas SK, Cerulli G, Caraffa A, Antinolfi P, Pantalone A, Frydas A, Tei M, Speziali A et al. (2015). Can vitamin a mediate immunity and inflammation?. Journal of Biology Regulator Homeostatic Agents, 29(1): 1-6. Available at: https://pubmed.ncbi.nlm.nih.gov/25864736/

Stream A, Corriden R, Döhrmann S, Gallo RL, Nizet V, and Anderson EL (2024). The effect of retinoic acid on neutrophil innate immune interactions with cutaneous bacterial pathogens. Infectious Microbes & Diseases, 6(2): 65-73. DOI: https://www.doi.org/ 10.1097/IM9.0000000000000145

Struck MB, Andrutis KA, Ramirez HE, and Battles AH (2011). Effect of a short-term fast on ketamine–xylazine anesthesia in rats. Journal of the American Association for Laboratory Animal Science, 50(3): 344-348. Available at: https://pubmed.ncbi.nlm.nih.gov/21640029/

Sun YY, Ma AG, Yang F, Zhang FZ, Luo YB, Jiang DC, Han XX, and Liang H (2010). A combination of iron and retinol supplementation benefits iron status, IL-2 level and lymphocyte proliferation in anemic pregnant women. Asia Pacific Journal of Clinical Nutrition, 19(4): 513-519. Available at: https://pubmed.ncbi.nlm.nih.gov/21147712/

Wallert M, Ziegler M, Wang X, Maluenda A, Xu X, Yap ML, Witt R, Giles C, Kluge S, Hortmann M et al. (2019). α-Tocopherol preserves cardiac function by reducing oxidative stress and inflammation in ischemia/reperfusion injury. Redox Biology, 26: 101292. DOI: https://www.doi.org/10.1016/j.redox.2019.101292

World health organization (WHO) (2022). The WHO aware (Access, Watch, Reserve) antibiotic book. World Health Organization. Licence, Geneva, CC BY-NC-SA 3.0 IGO. Available at: https://www.who.int/publications/i/item/9789240062382

Wilkie IW, Harper M, Boyce JD, and Adler B (2012). Pasteurella multocida: Diseases and pathogenesis. In: K. Aktories, J, Orth, and B. Adler (Editors), Current topics in microbiology and immunology. Springer., Berlin, Heidelberg, pp. 1-22. DOI: https://www.doi.org/10.1007/82_2012_216

Wilson BA and Ho M (2013). Pasteurella multocida: from zoonosis to cellular microbiology. Clinical Microbiology Reviews, 26(3): 631-655. DOI: https://www.doi.org/10.1128/cmr.00024-13

Wilujeng S, Wirjaatmadja R, and Prakoso YA (2023). Effects of extraction, fermentation, and storage processes on the levels of choline derived from calabash fruit (*Crescentia cujete* L.). Journal of Research in Pharmacy, 27(2): 620-626. Available at: https://dergipark.org.tr/en/download/article-file/4834601

Wojtal KA, Wolfram L, Frey-Wagner I, Lang S, Scharl M, Vavricka SR, and Rogler G (2013). The effects of vitamin A on cells of innate immunity *in vitro*. Toxicology in Vitro, 27(5): 1525-1532. DOI: https://www.doi.org/10.1016/j.tiv.2013.03.013

Xia Y, Wu Q, Mak S, Liu EY, Zheng BZ, Dong TT, Pi R, and Tsim KW (2022). Regulation of acetylcholinesterase during the lipopolysaccharide-induced inflammatory responses in microglial cells. The FASEB Journal, 36(3): 22189. DOI: https://www.doi.org/10.1096/fj.202101302RR

Yang M, Kuang M, Wang G, Ali I, Tang Y, Yang C, Li Y, and Li L (2021). Choline attenuates heat stress-induced oxidative injury and apoptosis in bovine mammary epithelial cells by modulating PERK/Nrf-2 signaling pathway. Molecular Immunology, 135: 388-397. DOI: https://www.doi.org/10.1016/j.molimm.2021.05.002

Yang W, Li M, Zhang C, Zhang X, Guo M, and Wu Y (2022). Pathogenicity, colonization, and innate immune response to Pasteurella multocida in rabbits. BMC Veterinary Research, 18(1): 416. DOI: https://www.doi.org/10.1186/s12917-022-03517-9

Yao QC, Zhai HL, and Wang HC (2023). Ratio of hemoglobin to mean corpuscular volume: A new index for discriminating between iron deficiency anemia and thalassemia trait. World Journal of Clinical Cases, 11(35): 8270. Available at: https://www.doi.org/10.12998/wjcc.v11.i35.8270

Zhou Z, Ferdous F, Montagner P, Luchini DN, Corrêa MN, and Loor JJ (2018). Methionine and choline supply during the peripartal period alter polymorphonuclear leukocyte immune response and immunometabolic gene expression in Holstein cows. Journal of dairy science, 101(11): 10374-10382. DOI: https://www.doi.org/10.3168/jds.2018-14972

Publisher's note: Scienceline Publication Ltd. remains neutral with regard to jurisdictional claims in published maps and institutional affiliations.

Open Access: This article is licensed under a Creative Commons Attribution 4.0 International License, which permits use, sharing, adaptation, distribution and reproduction in any medium or format, as long as you give appropriate credit to the original author(s) and the source, provide a link to the Creative Commons licence, and indicate if changes were made. The images or other third party material in this article are included in the article's Creative Commons licence, unless indicated otherwise in a credit line to the material. If material is not included in the article's Creative Commons licence and your intended use is not permitted by statutory regulation or exceeds the permitted use, you will need to obtain permission directly from the copyright holder. To view a copy of this licence, visit https://creativecommons.org/licenses/by/4.0/.
© The Author(s) 2025

2025, Scienceline Publication
World's Veterinary Journal
World Vet J, 15(4): 989-996.
ISSN 2322-4568

DOI: https://dx.doi.org/10.54203/scil.2025.wvj100
PII: S232245682500100-15

Investigation of Different Pre-umbilical Surgical Incisions for Ventral Abdominal Celiotomy in Sheep and Goats

Zakaria Abdullah[1], Sayed Fathi El-Hawari[1]*, Adel Ibrahim Almubarak[1], Sherief Mohamed Abdel-Raheem[2], Mohamed Marzok[1], and Amal Galal Abouelella[3]

[1]*Department of Clinical Sciences, College of Veterinary Medicine, King Faisal University, Al-Ahsa, 31982, Saudi Arabia*
[2]*Department of Public Health, College of Veterinary Medicine, King Faisal University, Al-Ahsa, 31982, Saudi Arabia*
[3]*Department of Surgery, Faculty of Veterinary Medicine, Sadat City University, Menofia, 32897, Egypt*

*Corresponding author's Email: selhawari@kfu.edu.sa

ORIGINAL ARTICLE
Received: October 04, 2025
Revised: November 07, 2025
Accepted: December 03, 2025
Published: December 25, 2025

ABSTRACT

Identifying the correct site for surgical incision and reducing unnecessary handling are crucial in veterinary surgical procedures. The current study aimed to evaluate surgical incisions in the pre-umbilical region in small ruminants with correlation to possible surgical operations in the abdominal organs. A randomized experimental study was conducted on 15 sheep (12 females and three males) and 15 goats (12 females and three males), with body weights of 44.9 ± 3.7 kilograms in sheep and 26.3 ± 4.6 kilograms in goats. Five different surgical exposures, including median, left paramedian, right paramedian, left post-xiphoid, and right post-xiphoid, were applied. The accessibility of abdominal viscera was evaluated for each incision site by documenting directly visible organs, organs that could be readily moved to the site of incision, and organs that could only be palpated. Access to the ventral ruminal sac and omentum was achieved through median, left, and right pre-umbilical celiotomy incisions. Furthermore, these surgical approaches allowed for reaching the abomasum and performing of abomasotomy. Abomasotomy and reticulutomy operations were performed through a median pre-umbilical incision. Omasum was palpable and easily examined via the right pre-umbilical celiotomy. The liver and gall bladder were exposed via a right post-xiphoid curved incision. In contrast, the reticulum was accessed for surgical intervention through a left post-xiphoid curved incision. The only recorded postoperative complication was tympany after gastrointestinal surgery. The present study indicated that choosing the appropriate pre-umbilical or post-xiphoid incision greatly improves access to targeted abdominal organs in small ruminants. Right and left pre-umbilical incisions were identified as the most effective approaches for abomasal procedures, whereas post-xiphoid incisions provided the optimal exposure to the reticulum, liver, and gall bladder. Furthermore, access to abdominal organs may vary between sheep and goats when employing the same surgical approach.

Keywords: Abomasotomy, Incision, Laparotomy, Paramedian, Small ruminant

INTRODUCTION

Sheep and goats are valuable ruminant species in both temperate and tropical agricultural regions. Sheep and goats serve as key sources of wool, meat, leather, and milk. Compared to cattle, the small ruminants are more suited to arid tropical environments, likely due to their more efficient utilization of water and nitrogen. Kidneys of small ruminants can concentrate urine to reduce water loss. Small ruminants can recycle urea into the rumen, allowing them to maintain nitrogen balance and protein synthesis even on low-quality forage (Field and Taylor, 2016; Lu Christopher, 2023).

In ruminants, many digestive issues can be treated with a laparotomy, including traumatic reticulitis, ruminal impaction, omasal impaction, ruminal distension, bezoar formation, abomasal displacement, correction of gastrointestinal displacement, vagal indigestion, and abomasal ulcers (Aubry, 2005; Fubini and Ducharme, 2016; Bayne and Edmondson, 2021). The primary reasons for ventral abdominal laparotomy incisions included abomaso- and omentopexy, bladder surgery, cesarean sections, exploratory laparotomies, intestinal surgeries, and exposure of non-pregnant genitalia, such as removing ovarian tumors, suturing a ruptured uterus, and performing ovariohysterectomies operations. Laparotomy in ruminants is typically conducted under local infiltration anesthesia following the administration of a tranquilizer (Abubakar et al., 2014; Fubini and Ducharme, 2016; Matthewes, 2016).

Ventral abdominal celiotomy is a surgical approach that necessitates restraint or sedation of animals in the dorsal recumbent position. Its utilization has become increasingly prevalent due to advancements in anesthesia, as contemporary and more sophisticated surgical procedures necessitate improved visibility and access to abdominal organs (Matthewes, 2016; Cowley et al., 2023).

To cite this paper: Abdullah Z, El-Hawari SF, Almubarak AI, Abdel-Raheem SM, Marzok M, and Abouelella AG. (2025). Investigation of Different Pre-umbilical Surgical Incisions for Ventral Abdominal Celiotomy in Sheep and Goats. *World Vet. J.*, 15(4): 989-996. DOI: https://dx.doi.org/10.54203/scil.2025.wvj100

Median and paramedian incisions were mentioned in the studies of Abubakar et al. (2014) and Bhattacharyya et al. (2020) for treatment of dystocia. In large ruminants, a paramedian incision provides effective access to the right-sided stomachs and can be extended if required. Some surgeons also prefer a paramedian incision due to its stronger incision closure compared to a midline incision. The disadvantages associated with the paramedian incision included wound dehiscence, edema in the ventral abdominal incision, and the formation of seromas or hematomas (Adugna et al., 2022).

The midline incision offers two key advantages, including that it can be easily enlarged to improve surgical access, and it typically resulted in less ventral edema than a paramedian incision. However, extending a midline incision can be challenging, particularly in male animals due to the presence of the penis and prepuce. Wound closure may be compromised, and there is an increased risk of oedema at the site of the pendulous umbilicus in cattle postoperatively (Adugna et al., 2022).

In laparotomy and laparoscopy procedures, selecting an appropriate approach for each abdominal organ via precise incision sites and minimizing traumatic injuries is considered the gold standard for surgeons. According to the current literature, no specific incision sites for approaching individual abdominal organs in sheep and goats have been described. The present study aimed to comprehensively evaluate pre-umbilical abdominal incisions in sheep and goats to define the optimal approach based on surgical access, operative efficiency, and postoperative complication rates.

MATERIALS AND METHODS

Ethical approval

The present study was approved by the institutional approval number is KFU-REC-2025-ETHICS 3519, and all animal handling follows the guidelines of ARRIVE for experimental animal research. All the experimental surgical procedures were performed according to the guidelines of King Faisal University, Saudi Arabia.

Animals

The present study was conducted on 30 small ruminants, including 15 sheep and 15 goats, which were kept for research purposes in King Faisal University, Saudi Arabia. There were six males and 24 females randomly selected for experimental abdominal operations. The ages of the animals were between 2 and 4 years old, with an average body weight of 44.9 ± 3.7 kg in sheep and 26.3 ± 4.6 kg in goats. The selected animals were examined to be clinically normal based on standard body temperature, heart rate, respiratory rate, complete blood count, and blood biochemical parameters analysis. The animals were randomly selected to undergo different ventral pre-umbilical celiotomy procedures with differing laparotomy incisions targeting multiple organs.

Pre-operative preparations and anesthesia

All operations were performed in recumbent position, and all operated animals were sedated before the operation by intramuscular injection of xylazine HCl 2% (Adwia company- xylaject- Egypt) at a dose of 0.2 mg/Kg in sheep (Mekonnen et al., 2023) and 0.02 mg/Kg in goats (Biobaku et al., 2016). Linear infiltration anesthesia was achieved using lidocaine HCL 1% at the dose of 1 mL for each cm of the incision site, and the maximum dose was not exceeded than 30 mL (Vesal et al., 2012). All operated animals were aseptically prepared for the operations and were fasted 24 hours prior to operations (Lussier et al., 2025).

Study design and evaluation criteria

Five experimental surgical incisions were performed in the pre-umbilical region (Figure 1), including a median pre-umbilical celiotomy. The incision site started at the midline, 3 cm caudal to the xiphoid process, and extended caudally toward the umbilicus, with a total length of 15 cm. This procedure was performed on three female sheep and three female goats while the animals were restrained in dorsal recumbency (Abubakar et al., 2014; Dieudoné et al., 2021).

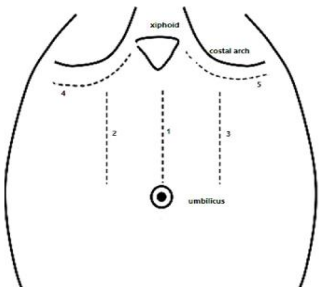


Figure 1. The sites of experimental incision at the pre-umbilical region in small ruminants. Number 1 is the median pre-umbilical incision, number 2 is the right pre-umbilical incision, number 3 is the left pre-umbilical incision, number 4 is the right post-xiphoid incision, and number 5 is the left post-xiphoid incision.

The second incision site was the left pre-umbilical celiotomy; the site of incision started 3 cm lateral to the midline and 3 cm caudal to the costal arch, with a total length of 15 cm to reach up to the level of the umbilicus. This incision was applied on three female sheep and three female goats while the animals were in dorsal recumbency (Haig et al., 2020; Dieudoné et al., 2021). The third incision site was the right pre-umbilical celiotomy; the site of incision started 3 cm lateral to the midline and 3 cm caudal to the costal arch with a total length of 15 cm. This incision was applied on three female sheep and three female goats while the animals were in dorsal recumbency (Haig et al., 2020; Dieudoné et al., 2021).

The fourth incision site was the right post-xiphoid incision; the incision was performed in a curved pattern parallel to the right ventral costal arch with a length of 10 cm in goats and 15 cm in sheep. This incision was applied to three female sheep and three female goats, and the animals were in semi-dorsal recumbency.

The fifth incision site was the left post-xiphoid incision; the incision was performed in a curved pattern parallel to the left ventral costal arch with a length of 10 cm in goats and 15 cm in sheep. This incision was applied on three male sheep and three male goats, and the animals were in semi-dorsal recumbency (Ghanshyam et al., 2020). To minimize operator-related variability and ensure consistent procedures, all surgeries were performed by the same surgeon. After opening the abdominal cavity, the surgeon assessed which organs were visible and could be surgically manipulated through the incision site, which organs could be grasped and exteriorized, and which organs could be examined by palpation but could not be exteriorized. Through each laparotomy technique, one organ was selected for surgical intervention to justify the feasibility of this exposure for such a procedure. The suture material used for closure of internal organs and abdominal muscles was catgut No. zero in goats and No.1 (Orion suture, India) in sheep with a round atraumatic needle. The skin was closed using silk No.1 or zero in all animals with a sharp needle. The follow-up period was extended up to six weeks, and all postoperative complications, such as seroma, wound dehiscence, wound infection, subcutaneous emphysema, herniation, and bloat, were recorded. Stitches were removed 12 days postoperatively in all animals.

RESULTS

In the median pre-umbilical celiotomy, the ventral sac of the rumen and the omentum were the first organs visible upon entering the abdominal cavity in both sheep and goats. The organs that were accessible via a median pre-umbilical celiotomy incision included the diaphragm in the cranial direction, the liver located cranially and to the right, and the omasum and spleen positioned cranially and to the left. Abomasotomy and reticulotomy (Figure 2A) were conducted without any complications, except for tympany observed in one goat immediately following the procedure. The condition was not well clarified in the subsequent assessment of the sheep. The organs that can be exteriorized in both sheep and goats were the abomasum, pylorus from the right aspect of the incision site (Figure 2B), and reticulum from the left side of the incision site (Tables 1 and 2).

In left pre-umbilical celiotomy, organs observed at the incision site in sheep and goats included the omentum and ventral sac of the rumen. Organs that could be exteriorized through this incision in both animals included the reticulum from the cranial aspect of the incision site and the abomasum from the lateral aspect of the incision site, especially the fundus body. The diaphragm could be examined and recognized in both animals, while the cranial part of the spleen was cranioventrally located to the right side, the omasum was located to the right side, and the liver was cranioventrally located to the right side. Abomasotomy operation was performed with proper closure of the abomasal incision in a double row of inverting suture (Figure 2C). The only postoperative complication noticed just after the operation was tympany in the left side, which was more obvious in goats than in sheep.

In the right pre-umbilical celiotomy immediately upon entering the abdominal cavity in goats, the ventral sac of the rumen, omentum, and part of the abomasum were revealed. In sheep, only the omentum covering the ventral ruminal sac was visible at the incision site. In sheep, only the abomasum and pylorus could be exteriorized through the incision site (Figure 2D). The organs in goats that were pulled out included the abomasum from the cranial side of the incision and, to some degree, the omasum from the medial side of the incision site. However, this site is the closest site to access the omasum (Figure 2E). Using this approach, surgeons could examine the diaphragm and liver cranially and the intestinal loops caudally in both sheep and goats. The Abomasotomy was successfully carried out at this site without complications, allowing excellent visualization and examination of the pylorus. The abomasal wall was then closed using a double layer of inverting sutures. The only postoperative complication observed was tympany on the left side of the abdomen, which was more distinctly noticeable in goats than in sheep.

In the right post-xiphoid celiotomy, the organs that were revealed at the site of incision included the ventral margin of the parietal surface of the liver, abomasum, and omentum. Organs that could be exteriorized through right post-xiphoid incision included part of the abomasum from the craniomedial aspect of the incision site, the gall bladder, and

the liver adherent to the costal arch. (Figure 2F). The examined and identified organs included the omasum (located cranially and toward the midline), the diaphragm cranially, and the rumen caudally. In addition, the surgeon obtained a liver biopsy without any observed postoperative complications.

In the left post-xiphoid celiotomy, the organs that were revealed at the incision site included the ventral sac of the rumen, reticulum, and omentum. Organs that could be exteriorized included the reticulum from the craniomedial aspect of the incision and the abomasum from the medial aspect of the incision. Organs which could be examined were the diaphragm cranially, the spleen ventrally, and the omasum medially. The Reticulotomy operation was performed without any postoperative complications.

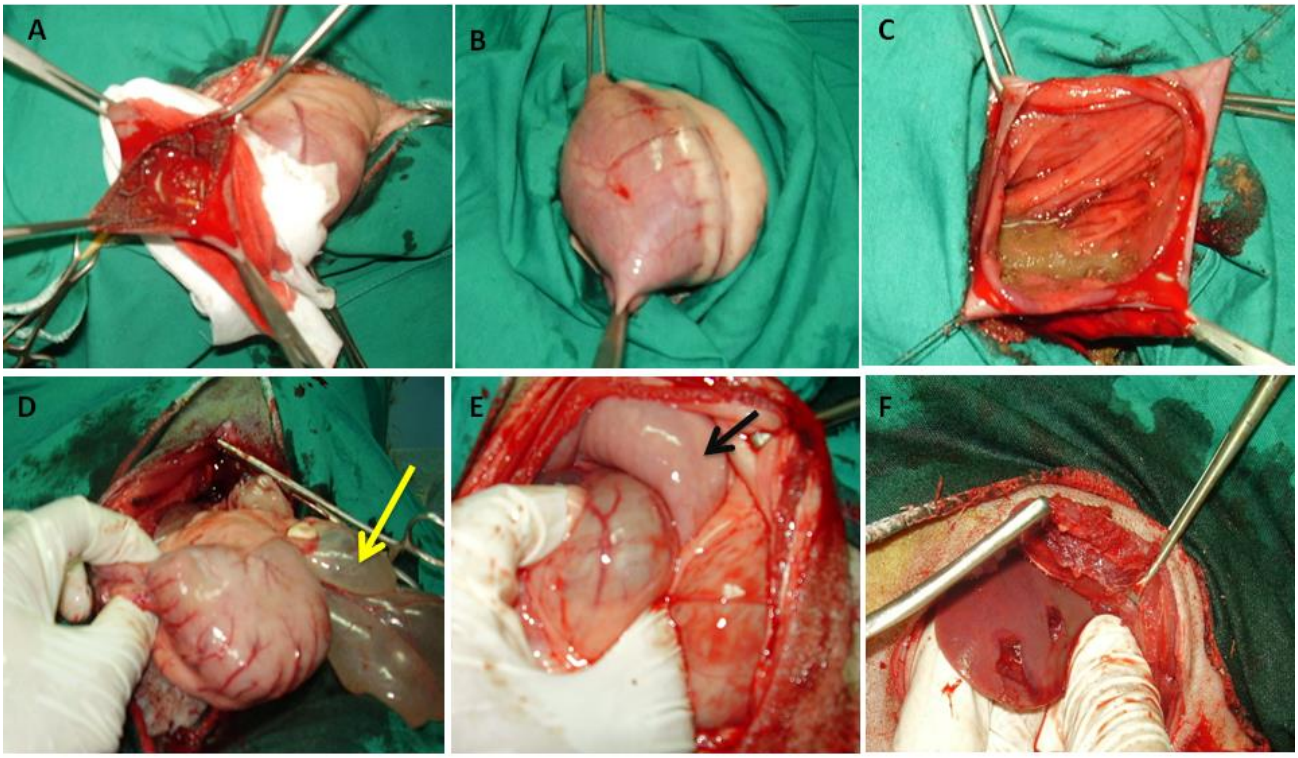


Figure 2. The different ventral pre-umbilical celiotomy incisions in small ruminants. **A**: The reticulotomy at the median pre-umbilical incision in a goat; **B**: The exposure of the abomasum at the median pre-umbilical incision in a sheep; **C**: the abomasotomy operation through a left pre-umbilical incision in a sheep; **D**: the exteriorized abomasum through a right pre-umbilical incision in sheep with multiple cysts (yellow arrow) attached to the omentum; **E**: the abomasum (black arrow) and catched omasum in a right pre-umbilical incision in a goat and **F**: the exposure of the liver through the right post-xiphoid incision in a goat.

Table 1. Ventral pre-umbilical incision sites and organs handled through incisions in goats

Type of incision	Organs seen at the site of incision	Exteriorized organs	Examined organs	Applied operation
Right pre-umbilical incision	Rumen, omentum, and a small part of abomasums	Abomasum and omasum	Part of the intestines, the diaphragm, and the liver	Abomasotomy (pylorus)
Median pre-umbilical incision	Omentum and rumen	Abomasum, pylorus, and reticulum	diaphragm, liver, omasum, and spleen	Abomasotomy and reticulotomy
Left pre-umbilical incision	Omentum and rumen	Abomasum and reticulum	Liver, spleen, omasum, and diaphragm	Abomasotomy (fundus and body)
Right post-xiphoid incision	Omentum, liver, and abomasums	Abomasum, gall bladder, and liver	Omasum, rumen, and diaphragm	Liver biopsy
Left post-xiphoid incision	Rumen, reticulum, and omentum	Reticulum and abomasum	Diaphragm, spleen, and omasum	Reticulotomy

Organs seen at the site of incision mean those organs directly exposed after opening the peritoneal cavity. Exteriorized organs mean organs that were easily pulled out and exposed from the incision site. Examined organs mean organs that were only palpated through the incision site.

Table 2. Ventral pre-umbilical incision sites observed organs, exteriorized, and examined through incisions in sheep

Type of incision	Organs seen at the site of incision	Exteriorized organs	Examined organs	Applied operation
Right pre-umbilical incision	Rumen and omentum	Abomasum	Part of the intestines, diaphragm, and liver	Abomasotomy (pylorus)
Median pre-umbilical incision	Omentum and rumen	Abomasum, pylorusand reticulum	diaphragm, liver, omasum, and spleen	Abomasotomy and reticulotomy
Left pre-umbilical incision	Omentum and rumen	Abomasum and reticulum	Liver, spleen, omasum, and diaphram	Abomasotomy (fundus)
Right post-xiphoid incision	Omentum, liver, and abomasum	Abomasum, gall bladder, and liver	Omasum, rumen, and diaphram	Liver biopsy
Left post-xiphoid incision	Rumen, reticulum, and omentum	Reticulum and abomasums	Diaphragm, spleen, and omasum	Reticulotomy

Organs seen at the incision site mean those organs directly exposed after opening the peritoneal cavity. Exteriorized organs mean organs that were pulled out and exposed from the incision site. Examined organs mean organs that were palpated through the incision site.

DISCUSSION

In the present study, all laparotomy operations were performed in the recumbent position under the effect of local analgesia and pre-anesthetic sedation. Typically, in small ruminants, abdominal surgery was done in the recumbent position, and general anesthesia was rarely indicated for abdominal surgery (El-Hawari et al., 2020; Al-Ali et al., 2023). The present study was conducted using five pre-umbilical incisions. Three of these were common and widely used in veterinary surgical practice, one was a median incision (Abubakar et al., 2014; Dieudoné et al., 2021), two were paramedian incisions (Haig et al., 2020; Dieudoné et al., 2021), and two were post-xiphoid incisions (right and left). The left post-xiphoid incision was previously described by Ghanshyam et al. (2020) for the treatment of diaphragmatic hernia in buffaloes and the removal of Extrareticular abscesses. The right post-xiphoid incision was performed as a mirror reflection of the left post-xiphoid incision to evaluate its accessibility to abdominal organs.

Many digestive, intestinal, obstetrical, and urinary tract issues can be treated with laparotomy or laparoscopy. Moreover, experimental studies of the rumen, spleen, intestine, urinary bladder, liver, and kidney were also performed via laparotomy (Newman and Anderson, 2005; Seif et al., 2005; Fubini and Ducharme, 2017).

The median ventral pre-umbilical celiotomy was performed in the present study with application of abomasotomy and reticulotomy operations. The abomasotomy operation through this site was previously described by Fubini and Ducharme (2017) for excision of ulcerative patches or removal of phytobezoars, impacted feed, or sand. The recommended approach was the right paramedian in the patient with lateral or dorsal recumbency. However, in the case of performing an abomasotomy in standing cattle from the left flank region, only a small part of the abomasum could be visualized (Trent, 1990). At the median ventral pre-umbilical incision site, the pylorus can be more extensively exteriorized compared to the right pre-umbilical celiotomy approach. In the current study, during the median ventral pre-umbilical celiotomy, the reticulum was located at the incision site just cranial to the abomasum, enabling a reticulum operation to be performed subsequently. This finding aligns with the anatomical description of Dyce et al. (2010), who reported that the reticulum of small ruminants is relatively larger than the reticulum of cattle, and it extends farther caudally within the abdominal cavity.

The right ventral pre-umbilical incision was made, and the abomasotomy was performed through an incision starting post-xiphoid and extending to the level of the umbilicus (Haig et al., 2020; Dieudoné et al., 2021; Tsukano et al., 2021). The present study revealed that this site of approach is an ideal site for reaching the pyloric region of the abomasum, which aligns with the findings of Aubry (2005). However, Tsukano et al. (2021) noted that the right paramedian incision for right paramedian abomasopexy in cattle was made 10 cm caudal to the sternum and 10 cm lateral to the right of the midline. Furthermore, the right ventral pre-umbilical incision offered superior visualization of the pyloric region of the abomasum in comparison to the median pre-umbilical incision (Fubini and Ducharme, 2017).

Concerning the location of the right ventral preumbilical incision in the current study, it was optimally positioned 3-4 cm lateral to the midline, with careful attention to preventing injury to the cranial epigastric vessels. In this type of approach, goats were observed to differ from sheep in the organs that were visible and could be exteriorized at the incision site. Rumen, omentum, and a small part of the abomasum were visualized in the goat at the site of incision, while in the sheep, rumen and omentum were the only organs visualized. This may be attributed to anatomical

differences between sheep and goats, as the topographical anatomy of the abdominal organs differs slightly between sheep and goats. In goats, the abomasum, especially its pyloric part, extends more cranially and slightly to the right side of the ventral abdominal wall compared to sheep. This positional difference results in the visibility of the abomasum during the right ventral pre-umbilical incision in goats. In contrast, in sheep, the rumen and omentum occupy a greater extent of the ventral abdominal cavity, thereby restricting direct access to the abomasum (Dyce et al., 2010). The present study revealed that in right ventral pre-umbilical celiotomy, the omasum was more easily accessible and handled through the right paramedian incision than other approaches. The omasum in small ruminants is predominantly located on the right side of the abdominal cavity, positioned between the liver cranially and the abomasum caudally, and is attached to the lesser curvature of the abomasum. Due to the right-sided and slightly ventral orientation, a right ventral or right paramedian pre-umbilical incision offers more direct access and facilitates easier manipulation of the omasum in comparison to median or left-sided approaches. Access to omasum through this site of incision could reduce the need for excessive tissue retraction and minimize interference from abdominal organs (Dyce et al., 2010; Fubini and Ducharme, 2017).

The left ventral pre-umbilical celiotomy was performed lateral and to the left of the midline until reaching the level of the umbilicus. Through this approach, the rumen and omentum were observed at the incision site in both sheep and goats, while the reticulum and abomasum (fundus and body) were exteriorized through the incision site. Moreover, liver, spleen, omasum, and diaphragm could be palpated through the left paramedian pre-umbilical incision in both sheep and goats (Dyce et al., 2010). In both sheep and goats, the rumen occupies most of the left side of the abdominal cavity. Consequently, when the left ventral pre-umbilical incision was performed, the rumen and its covering omentum were the initial structures encountered upon entering the abdominal cavity. The reticulum is positioned cranially to the rumen and slightly to the left. The fundus and body of the abomasum are placed on the ventral abdominal floor, curving toward the left side, thereby allowing for exteriorization through a left paramedian incision. Through the left paramedian pre-umbilical incision, the liver was palpable cranially and slightly to the right, while the spleen, attached to the dorsal sac of the rumen, was accessible along the left cranial abdomen wall. The omasum and diaphragm were palpated using this approach, although they are not typically exteriorized due to their fixed attachments and proximity to the cranial abdominal wall (Dyce et al., 2010; Fubini and Ducharme, 2017; Konig and Liebich, 2020). However, the current study elucidates that in small ruminants, abomasotomy targeting the body and fundus regions was most effectively performed via the left pre-umbilical paramedian incision, which offered direct access and facilitated exteriorization of the abomasum. The current results regarding the abomasum align with the findings of Silva et al. (2023), who found that a 12 cm paracostal incision in the abdominal wall was not suitable for accessing the greater curvature of the abomasum in goats, while a 15 cm paramedian incision caudal and lateral to the xiphoid provided easy access to the abomasum.

The right and left post-xiphoid crescent incisions were rarely mentioned in the literature. However, the current study demonstrated that the right post-xiphoid incision provided superior visualization of the liver compared to other incision sites, and liver biopsies were obtained by this approach. The liver in sheep and goats is located on the right side, caudal to the diaphragm, and extends from 8 to 12 intercostal spaces, with only a small part crossing the midline to the left. Due to this position, a right post-xiphoid (cranial pre-umbilical) incision just below the xiphoid process and slightly to the right of the midline provides direct, unobstructed access to the diaphragmatic and visceral surfaces of the liver (Dyce et al., 2010; Fubini and Ducharme, 2017). The left post-xiphoid incision in the current study demonstrated the presence of the rumen, reticulum, and omentum at the site of incision in both sheep and goats. Additionally, the abomasum and reticulum were mobilized to the site of incision in both species, with adequate access to the reticulum. Consistent with the current findings, Ghanshyam et al. (2020) and Sangwan and Kumar (2025) also indicated the left post-xiphoid pre-umbilical celiotomy as a feasible surgical approach to the reticulum for the repair of diaphragmatic hernias and the excision of extra-reticular abscesses in buffaloes. The current findings demonstrated that access to the reticulum and the performing reticulotomy operation can be accomplished via median and left post-xiphoid incisions. However, the left post-xiphoid incision was considered the ideal site for approaching the reticulum because no organ retraction was required, and the reticulum appeared spontaneously at the site of the left post-xiphoid incision. In contrast, minor abomasal retraction was required in the median incision to access the reticulum in both sheep and goats.

During the current study, the tympany that appeared after the abomasum and reticulum surgeries might be caused by long dorsal recumbency, which results in occlusion of the cardiac opening with ruminal content and subsequently traps gases inside the rumen. Gas escape from the reticulum or abomasum into the peritoneal cavity caused tympany; however, its presentation was not distinct in sheep. This may be attributed to variations in ruminal capacity, faster progression of the condition, or the presence of an extensive wool layer covering the left flank abdominal wall, thereby concealing the presence of slight tympany. However, the occurrence of postoperative tympany in the current study was likely related to the gastrointestinal nature of the surgery rather than the incision site performed in ruminants (Constable et al., 2017; Fubini and Ducharme, 2017). In the current study, none of the performed incision sites required elongation,

and no postoperative complications such as seroma, edema, abscessation, suture dehiscence, or herniation were observed. The current findings demonstrated that precise incision planning, adherence to aseptic techniques, and secure closure of the abdominal wall align with surgical observations in small ruminants (Fubini and Ducharme, 2017).

CONCLUSION

The present study indicated that using a precise pre-umbilical incision type could provide significantly superior exposure to the targeted abdominal organ without postoperative complications. Ventral ruminal sac and omentum were accessed through median pre-umbilical, left pre-umbilical, and right pre-umbilical celiotomy incisions. Abomasum was reached through median, left, and right pre-umbilical celiotomy incisions. Choosing the incision type to access the abomasum depends on the specific region of the abomasum to be operated upon. The body and fundus were reached through left pre-umbilical celiotomy incision, while the pyloric part was reached through the right or median pre-umbilical celiotomy incisions. The most suitable incision site for omasum examination was the right pre-umbilical celiotomy. The exposure to the liver and gall bladder was performed through a right post-xiphoid curved incision without any evidence of postoperative complications. A left post-xiphoid curved incision was employed to access the reticulum for surgical intervention. Further investigations are necessary to examine the blind approach through small incision (1-3cm) from all previously mentioned sites of incision via laparoscopy and to describe its related access to abdominal organs.

DECLARATIONS

Acknowledgments

The present study was supported by the Deanship of Scientific Research, Vice Presidency for Graduate Studies and Scientific Research, King Faisal University, Saudi Arabia, Grant No. (KFU254016).

Availability of data and materials

All data and materials are available upon reasonable request from the corresponding author.

Authors' contributions

El-Hawari and Almubarak contributed to the conceptualization of the study. Abdel-Raheem conducted the formal analysis. Abdullah was responsible for writing the original draft of the manuscript. El-Hawari and Marzok handled the investigation and validation of the research data. Abouelella provided supervision and methodology support. Abdullah and Abdel-Raheem were involved in data curation and funding acquisition. All authors read and approved the final edition of the manuscript for publication.

Funding

This work was supported by the Deanship of Scientific Research, Vice Presidency for Graduate Studies and Scientific Research, King Faisal University, Saudi Arabia (Grant No. KFU 254016).

Competing interests

The authors declared that there is no conflict of interest.

Ethical considerations

The authors have checked the publication ethical issues, including plagiarism, consent to publish, misconduct, double publication and/or submission, and redundancy, before submission of the article. The authors declare that no AI use for writing this article.

REFERENCES

Abubakar AA, Andeshi RA, Yakubu AS, Lawal FM, and Adamu U (2014). Comparative evaluation of midventral and flank laparotomy approaches in goat. Journal of Veterinary Medicine, 2014: 920191. DOI: https://www.doi.org/10.1155/2014/920191

Adugna SA, Kitessa JD, Feyissa CT, and Adem SA (2022). Review on a cesarean section in the cow: Its incision approaches, relative advantage, and disadvantages. Veterinary Medicine and Science, 8(4): 1626-1631. DOI: https://www.doi.org/10.1002/vms3.808

Al-Ali FT, Almubarak AI, Marzok M, El-Deeb WM, and El-Hawari SF (2023). Evaluation of the anti-nociceptive effect of lidocaine-tramadol and lidocaine-medetomidine lumbosacral epidural anesthesia: A cross-over comparative study in goats. German Journal of Veterinary Research, 3(4): 20-24. DOI: https://www.doi.org/10.51585/gjvr.2023.4.0066

Aubry P (2005). Routine surgical procedures in dairy cattle under field conditions: Abomasal surgery, dehorning, and tail docking. Veterinary Clinics of North America: Food Animal Practice, 21(1): 55-72. DOI: https://www.doi.org/10.1016/j.cvfa.2004.11.002

Bayne JE and Edmondson MA (2021). Diseases of the gastrointestinal system. Sheep, goat, and cervid medicine, 3rd Edition, pp. 63-96. DOI: https://www.doi.org/10.1016/B978-0-323-62463-3.00014-1

Bhattacharyya HK, Fazili MUR, Bhat F A, and Buchoo BA (2015). Prevalence of Dystocia in Sheep and Goats: A Study of 70 Cases (2004-2011). Journal of Advanced Veterinary Research, 5(1): 14-20. Available at: https://advetresearch.com/index.php/AVR/article/view/40

Biobaku KT, Agaie BM, Onifade KI, Odetokun IA, Okediran BS, Ameen SA, Ismaila MS, Adam M, and Raji LO (2016). Effects of xylazine on physiological and biochemical parameters of Sahel bucks exposed to twenty-eight hours road transportation. Sokoto Journal of Veterinary Sciences, 14(2): 43-52 DOI: http://www.doi.org/10.4314/sokjvs.v14i2.6

Constable PD, Hinchcliff KW, Done SH, and Grünberg W (2017). Veterinary medicine: A textbook of the diseases of cattle, horses, sheep, pigs and goats, 11th Edition. Elsevier. pp. 437-520. Available at: https://books.google.com.sa/books?hl=en&lr=&id=mx5uDQAAQBAJ&oi=fnd&pg=PP1&dq=Constable,+P.+D.,+Hinchcliff,+K.+W.,+Done,+S.+H.,+and+Gr%C3%BCnberg,+W.+(2017).+Veterinary+Medicine:+A+Textbook+of+the+Diseases+of+Cattle,+Horses,+Sheep,+Pigs+and+Goats+(11th+ed.).+Elsevier&ots=PeO4QXdnfK&sig=8n8VehfY82jEBm5KZnelTPGsgDU&redir_esc=y#v=onepage&q&f=false

Cowley J, Stockler J, and Maxwell H (2023). A review of small ruminant Cesarean section: case selection, surgical techniques, care of the neonates, and postoperative care of the dam. Clinical Theriogenology, 15: 70-81. DOI: https://www.doi.org/10.58292/ct.v.9620

Dieudoné K, Adamou S, Assani B, Kadja M, and Kondi A (2021). Surgical anatomy and approach to the abdominal wall of domestic animals. Asian Journal of Medicine and Health, 19(5): 11-21. DOI: https://www.doi.org/10.9734/ajmah/2021/v19i530325

Dyce KM, Sack WO, and Wensing CJG (2010). Textbook of veterinary anatomy, 4th edition. Elsevier., St. Louis Saunders, pp. 680-694. Available at: https://books.google.com.sa/books?hl=ar&lr=&id=Hb1BXjgb0McC&oi=fnd&pg=PP1&dq=Dyce+KM,+Sack+WO,+and+Wensing+CJG+(2010).+Textbook+of+Veterinary+Anatomy.+4th+edition.+St.+Louis:+Saunders+Elsevier.&ots=an8c5nax37&sig=l88EEogRndAa2AO1aM08w3andHk&redir_esc=y#v=onepage&q&f=false

El-Hawari SF, Ali S, and Abedellaah BEA (2020). Evaluation of intravenous regional anesthesia of lidocaine, medetomidine and lidocaine-medetomidine in the hind limb of goats. Journal of Advanced Veterinary Research, 10(2): 56-60. Available at: https://www.advetresearch.com/index.php/avr/article/view/425

Field TG and Taylor RE (2016). Scientific farm animal production. An introduction to animal science, 11th Edition. Pearson Prentice Hall, pp. 38-42. Available at: https://www.pearsonhighered.com/assets/preface/0/1/3/3/0133767205.pdf

Fubini SL and Ducharme NG (2017). Farm animal surgery, 2nd Edition. Elsevier., St. Louis, pp. 561-583. Available at: https://books.google.com.sa/books?hl=en&lr=&id=XOSxCwAAQBAJ&oi=fnd&pg=PP1&dq=Fubini,+S.+L.,+and+Ducharme,+N.+G.+(2017).Farm+Animal+Surgery+(2nd+ed.).+St.+Louis:+Elsevier.&ots=M46OmAXbEC&sig=c6aR9ky4r7FK1Mfv-XUBFXnvVKo&redir_esc=y#v=onepage&q&f=false

Ghanshyam PG, Vinayak SR, and Hiroji UA (2020). Comparative evaluation of single stage and double stage diaphragmatic Herniorrhaphr for repair of diaphragmatic hernia in buffaloes. Buffalo Bulletin, 39(4): 473-482. Available at: https://kukr.lib.ku.ac.th/kukr_es/kukr/search_detail/dowload_digital_file/406483/152701

Haig F, Baird A, Hawkins J, and Moore G (2020). Caudal paramedian approach to cryptorchidectomy in 29 small ruminants (2011-2019). Veterinary Surgery, 50(1): 170-176. DOI: https://www.doi.org/10.1111/vsu.13546

Konig HE and Liebich HG (2020). Veterinary anatomy of domestic mammals: Textbook and colour atlas, 7th Edition. Thieme., Stuttgart, pp. 319-360. Available at: https://vetbooks.ir/veterinary-anatomy-of-domestic-animals-textbook-and-colour-atlas-7th-edition/

Lu Christopher D (2023). The role of goats in the world: Society, science, and sustainability. Small Ruminant Research, 227: 107065. DOI: https://www.doi.org/10.1016/j.smallrumres.2023.107056

Lussier B, Behr L, Borenstein N, Brants I, Garabedian C, Ghesquiere L, Le Duc K, Sharma D, Storme L, Touzot-Jourde G et al. (2025). Sheep models in translational surgery. European Surgical Research, 66(1): 39-45. DOI: https://www.doi.org/10.1159/000546157

Matthews J (2016). Diseases of the goat, 4th Edition. John Wiley & Sons Limited, pp. 365-380. Available at: https://books.google.com.sa/books?hl=ar&lr=&id=f1FVDwAAQBAJ&oi=fnd&pg=PP10&dq=Matthews+J+(2016).+Diseases+of+the+goat,+Fourth+edition.+&ots=QME4YFXt4U&sig=RpQnJlqgu6ySpqqL-8rkQ6b26ts&redir_esc=y#v=onepage&q=Matthews%20J%20(2016).%20Diseases%20of%20the%20goat%2C%20Fourth%20edition.&f=false

Mekonnen A, Abderehman K, and Seyaka F (2023). Review on commonly used veterinary anesthetic drugs in small ruminants. Veterinary Sciences: Research and Reviews, 9(2): 103-113. DOI | https://www.doi.org/10.17582/journal.vsrr/2023/9.2.103.113.

Newman KD and Anderson DE (2005). Cesarean section in cows. Veterinary Clinics of North America: Food Animal Practice, 21(1): 73-100. DOI: https://www.doi.org/10.1016/j.cvfa.2004.12.001

Sangwan V and Kumar A (2025). An updated review on the diaphragmatic hernia in bovines. Indian Journal of Animal Research, B-5324: 1-11. available at: https://arccjournals.com/journal/indian-journal-of-animal-research/B-5324

Seif MM, Shalaby AA, and El-Nesr KA (2005). Hydronephrosis in goats: An experimental study, 8th Scientific Congress. Egyptian Society for Cattle Diseases, Assiut, Egypt.

Silva JRB, Alonso JM, Mendonça APA, Mendes LH, Hussni CA, Alves ALG, Watanabe MJ, and Rodrigues CA (2023). Abomasal impaction in a goat-surgical approach. Acta Scientiae Veterinariae, 51(Suppl 1): 872. DOI: https://www.doi.org/10.22456/1679-9216.122298

Trent AM (1990). Surgery of the bovine abomasum. Veterinary Clinics of North America: Food Animal Practice, 6(2): 399-348. DOI: https://www.doi.org/10.1016/S0749-0720(15)30868-9 Tsukano K, Nishi Y, Sasaki N, and Suzuki K (2021). Retrospective study on the outcomes and risk factors of right paramedian abomasopexy for right abomasal disorders in 47 dairy cows. Journal of Veterinary Medical Science, 83(10): 1521-1525. DOI: https://www.doi.org/10.1292/jvms.21-0123

Vesal N, Jahromi AR, and Oryan A (2012). Lidocaine containing high concentrations of a vasoconstrictor: Is it safe for infiltration anesthesia?. Comparative Clinical Pathology, 21: 1703-1706. DOI: https://www.doi.org/10.1007/s00580-011-1352-y

Publisher's note: Scienceline Publication Ltd. remains neutral with regard to jurisdictional claims in published maps and institutional affiliations.

Open Access: This article is licensed under a Creative Commons Attribution 4.0 International License, which permits use, sharing, adaptation, distribution and reproduction in any medium or format, as long as you give appropriate credit to the original author(s) and the source, provide a link to the Creative Commons licence, and indicate if changes were made. The images or other third party material in this article are included in the article's Creative Commons licence, unless indicated otherwise in a credit line to the material. If material is not included in the article's Creative Commons licence and your intended use is not permitted by statutory regulation or exceeds the permitted use, you will need to obtain permission directly from the copyright holder. To view a copy of this licence, visit https://creativecommons.org/licenses/by/4.0/.
© The Author(s) 2025

2025, Scienceline Publication
World's Veterinary Journal
World Vet J, 15(4): 997-1006.
ISSN 2322-4568

DOI: https://dx.doi.org/10.54203/scil.2025.wvj101
PII: S232245682500101-15

Evaluation of the Chemical Composition and Antioxidant Capacity of Dried Orange Pulp

Ahmed Readh Chaib Eddour[1]*, Miloud Litim[1], and Kaddour Bouderoua[2]

[1]*Laboratory of "Applied Biotechnology for Agriculture and Environmental Preservation," Higher School of Agronomy, Mostaganem, 27000, Algeria*
[2]*Laboratory of Food Technology and Nutrition, Abdelhamid Ibn Badis University, Mostaganem,27000, Algeria*

*Corresponding author's Email: a.chaibeddour@esa-mosta.dz

ORIGINAL ARTICLE
Received: September 27, 2025
Revised: October 30, 2025
Accepted: November 24, 2025
Published: December 31, 2025

ABSTRACT

The disposal of orange juice by-products presents an environmental challenge due to their high volume and accumulation in landfills. Valorizing these residues supports the development of a circular economy within the agro-industrial sector, offering both environmental and economic benefits. This study aimed to valorize orange juice processing residues by producing a dried orange pulp (DOP) flour and characterizing its physicochemical and phytochemical properties to assess its potential suitability as a sustainable feed ingredient for broiler chickens. The physicochemical properties of the sun-dried and finely milled orange by-products (<1 mm) were analyzed using standard methods, including proximate composition analysis (moisture, ash, crude protein, crude cellulose), and spectrophotometric assays for phytochemicals (total phenolics, flavonoids, condensed tannins) and antioxidant activity [2,2-Diphenyl-1-picrylhydrazyl (DPPH), Ferric Reducing Antioxidant Power (FRAP)]. The DOP demonstrated high levels of dietary cellulose (89.19% Dry Matter), ash (3.81% Dry Matter), total phenolics (202.59 ± 15.93 mg Gallic Acids Equivalent/100 g DM), total flavonoids (430.70 ± 2.78 mg Quercetin Equivalent/100 g), and strong antioxidant activity (FRAP: 1158.8 ± 19.22 mg/g). Phenolic profiling via High-Performance Liquid Chromatography (HPLC) revealed flavanones as the dominant subclass, with hesperidin (61.29 mg/g) and ferulic acid (27.1 mg/g) as major constituents. These results highlight the nutritional and functional potential of DOP as a feed additive. The remarkable antioxidant capacity and high concentration of bioactive compounds like hesperidin position DOP not just as a filler, but as a functional feed additive that could enhance animal health.

Keywords: Ferulic acid, Hesperidin, Hydrocinnamic acid, Orange waste

INTRODUCTION

Fruits and vegetables represent the highest food waste category globally, with estimated losses reaching approximately 45% of total production (Caldeira et al., 2019; Ortiz-Sanchez et al., 2024). Among these, citrus fruits stand out as one of the most cultivated and processed fruit groups worldwide, with an annual output exceeding 122.5 million tons, a significant portion of which is dedicated to juice production (Jiang et al., 2014). During processing, considerable quantities of citrus by-products are generated—particularly peel (flavedo) and rag (albedo)—which account for 45–60% of the whole fruit mass (Berk, 2016; Camacho et al., 2023).

Citrus processing generates substantial quantities of by-products, including peels, pulps, and seeds, which are typically discarded despite their richness in nutrients, dietary fiber, and bioactive phytochemicals. The accumulation of these residues poses environmental and economic challenges for the agro-industrial sector. Nevertheless, the valorization of citrus by-products has recently attracted significant interest within the framework of circular economy strategies, aiming to transform waste materials into value-added resources. Several studies have demonstrated that orange by-products contain higher concentrations of functional compounds than the edible portions of the fruit, particularly polyphenols and flavonoids known for their potent antioxidant properties. Quantitative analyses have shown considerable variation in the total phenolic content (TPC) of orange by-products. For instance, Castro et al. (2020) reported a value of 534 ± 30 mg gallic acid equivalents (GAE)/100 g dry matter (DM), while Escobedo-Avellaneda et al. (2014) found 650 ± 90 mg GAE/100 g DM in lyophilized whole orange samples (juice, flavedo, and albedo). Conversely, Danesi et al. (2018) recorded a lower TPC of 450 ± 30 mg GAE/100 g DM in orange albedo. Based on these findings, the orange by-product flour (OBPF) evaluated in the present study exhibited a higher phenolic content than that reported for flours derived from other fruit peels, underscoring its potential as a natural source of antioxidants for applications in feed and food formulations. Moreover, the antioxidant potential of the orange by-product flour (OBPF), evaluated using the FRAP and ORAC assays, was found to be 93 ± 5 µmol TE/100 g DM and 11,728 ± 541 µmol TE/100 g DM, respectively. The antioxidant activity showed a strong relationship with the TPC, indicating that higher

To cite this paper: Chaib Eddour AR, Litim M, and Bouderoua K (2026). Evaluation of the Chemical Composition and Antioxidant Capacity of Dried Orange Pulp. *World Vet. J.,* 15(4): 997-1006. DOI: https://dx.doi.org/10.54203/scil.2025.wvj101

concentrations of phenolic compounds contributed to greater antioxidant capacity in the flour. Comparable findings were reported for orange by-product (albedo) obtained from juice production, which exhibited a FRAP value of 49.7 ± 0.3 µmol TE/g DM (Castro et al., 2020). Similarly, Escobedo-Avellaneda et al. (2014) determined an ORAC value of 11,953 ± 538 µmol TE/100 g DM in their study assessing the phytochemical composition and antioxidant potential of various orange parts. These results confirm that the phenolic richness of OBPF plays a crucial role in its reducing and radical-scavenging capacities, reinforcing its suitability as a natural antioxidant source.

In this context, transforming citrus byproducts into functional ingredients is considered a viable approach to addressing the dual challenges of waste management and sustainable nutrition. Despite being rich in nutrients, dietary fiber, and bioactive compounds, these residues are frequently treated as waste, posing significant environmental burdens for the industry. The disposal of citrus waste, primarily through landfilling and uncontrolled dumping, leads to the generation of greenhouse gases, particularly methane, due to the anaerobic decomposition of its high organic load. Furthermore, the high moisture content (around 80-90%) and biodegradability of this waste result in leachate production, which can contaminate soil and groundwater with organic acids and other phytotoxic compounds (Zema et al., 2022).

Different studies have shown that orange juice residues can be utilized in animal feed (Bampidis and Robinson, 2006). Moreover, in a recent feeding trial, the effects of replacing yellow corn with orange peel by-product (OP) in broiler diets were demonstrated that chicks receiving the control and OP15 diets exhibited superior final body weights and feed conversion ratios compared with those fed higher inclusion levels. Additionally, the OP20 group showed a reduction in total serum cholesterol relative to the control, and all experimental treatments enhanced economic efficiency. Collectively, these findings indicate that orange peel by-product can replace up to 15% of yellow corn in broiler diets without compromising growth performance, highlighting its potential as a nutritionally viable and cost-effective feed ingredient (Dilek et al., 2025). Research indicated that various forms of orange waste, including dried pulp (Agu et al., 2010) and peel extracts (Pourhossein et al., 2015; Seidavi et al., 2015), can be effectively incorporated into poultry diets. Studies on broilers and laying hens showed that appropriate inclusion levels up to 15-20% for pulp (Agu et al., 2010), and 1000 mg/L for extract (Pourhossein et al., 2015; Seidavi et al., 2015) can improve performance metrics such as body weight and feed conversion ratio (Seidavi et al., 2015; Ciftci et al., 2016). Furthermore, these by-products positively influence carcass quality by reducing abdominal fat and liver weight (Ebrahimi et al., 2014; Abbasi et al., 2015), enhance immune response by increasing immunoglobulin and white blood cell counts (Pourhossein et al., 2015), and improve blood lipid profiles by lowering cholesterol and triglycerides (Nazok et al., 2010; Ciftci et al., 2016). These by-products positively influence carcass quality by reducing abdominal fat and liver weight, enhancing immune response by increasing immunoglobulin and white blood cell counts, and improving blood lipid profiles by lowering cholesterol and triglycerides. Moreover, these byproducts were used in the production of essential oils (Sahraoui et al., 2011). However, the objective of this study was to develop and characterize a flour derived from dried orange juice by-products, and to evaluate its potential inclusion in broiler chicken diets as a cost-effective and functional feed additive.

MATERIALS AND METHODS

Ethical approval

The work was conducted under the general institutional biosafety authorization ESA/GLP-2021/-03 issued by the Higher School of Agronomy, Mostaganem, Algeria.

Preparation

Orange juice co-products (peels, pulp, and seeds) from *Citrus sinensis* (sweet orange) were collected fresh from a local citrus juice processing facility located in Chelf, Algeria. The materials were dried in a passive solar greenhouse dryer at 35-45 °C for 48-72 hours, until the moisture content decreased below 10%, verified by weight monitoring and oven-drying at 105 °C (Özcan et al., 2021). Adequate ventilation was ensured using natural airflow and solar-powered fans to prevent microbial growth. The dried material was subsequently milled, passed through a 1 mm sieve, and stored in airtight, light-resistant polyethylene bags at 20–25 °C in a clean and ventilated environment (Readh et al., 2023).

Proximate composition analysis

The proximate composition of the powdered orange juice co-products was determined through standard procedures to quantify dry matter, moisture content, and ash content. Moisture determination was conducted by oven-drying the samples at 105 °C for 24 hours (Özcan et al., 2021). The dry matter and moisture content were calculated using the following equations (AOAC, 2005).

Dry Matter (%) = Mass (Dry Matter) (g)/Mass (sample) (g) × 100 (Formula 1)

Water content (g. $100g_{-1}$Sample) = 100 - Dry Matter (%) (Formula 2)

To determine ash content (mineral matter), the previously dehydrated samples were incinerated in a muffle furnace at 550 °C for 3 hours until a constant white ash was obtained (Ebouel et al., 2023). The content of mineral matter (MM) was calculated using the following formula.

Mineral Matter (MM %) = (M2 - M0) / (M1 - M2) × 10 (Formula 3)

The mineral matter (MM) content of the samples was determined using a gravimetric method (AOAC, 2005). The mass of the empty crucible was recorded as M_0 (g), followed by the mass of the crucible containing the test sample, denoted as M_1 (g). After incineration and cooling, the mass of the crucible and the remaining raw minerals was measured as M_2 (g). The mineral matter content was then calculated and expressed as grams per 100 grams of the sample (g/100 g).

Crude cellulose content

Crude cellulose content was analyzed using the Weende method (Ebouel et al., 2023). The sample was sequentially digested with hot acid and alkali, isolating cellulose. This residue was incinerated to remove organic matter. Cellulose was calculated by using Formula 4 (AOAC, 2005).

Cellulose content = (P1- P2) / P0 ×100/Dry Matter (Formula 4)

where P_0 represents the weight of the test sample (g), P_1 is the weight of the crucible with the residue before incineration (g), and P_2 is the weight of the crucible with the residue after incineration (g). DM denotes the dry matter content (%).

Protein content

Protein content in the powdered orange juice co-products was determined using the Lowry method, as outlined by Satpathy et al. (2020). A sample aliquot was homogenized in 25 mL of chilled physiological saline, filtered, and diluted. From the prepared dilution, 1 mL of the sample was mixed with the Lowry reagent and allowed to react for 10 minutes. Afterward, a diluted Folin–Ciocalteu reagent (Sigma-Aldrich, USA) was added, followed by vortexing. The reaction mixture was then kept at 4 °C in the dark for 30 minutes to complete color development. The absorbance was recorded at 700 nm using a UV–Visible spectrophotometer (SPECORD 210, Germany). Protein concentration was determined using a bovine serum albumin (BSA) standard curve and expressed as a percentage of dry matter.

Extraction of bioactive compounds

A 20 g powdered sample was mixed with 200 mL of methanol and agitated on an orbital shaker (Edmund Bühler GmbH, KS-15, Hechingen, Germany) at 450 rpm for 24 hours at 23 ± 1 °C in darkness to prevent photodegradation. The extract was filtered and stored in amber flasks. The extract was used for antioxidant assays (2,2-diphenyl-1-picrylhydrazyl (DPPH), 2,2′-Azino-bis (3-ethylbenzothiazoline-6-sulfonic acid (ABTS) and for quantifying total phenolics, flavonoids, and condensed tannins via validated spectrophotometric methods (Gargouri et al., 2013).

Quantification of phenolic compounds

Total phenolic content

The TPC was determined using the Folin–Ciocalteu colorimetric assay as described by Jaradat et al. (2015). In brief, 1 mL of the sample extract was combined with diluted Folin–Ciocalteu reagent (Sigma-Aldrich, USA) and 4 mL of sodium carbonate solution (75 g/L; Sigma-Aldrich, USA). The reaction mixture was incubated at room temperature for 1 hour, after which the absorbance was measured at 765 nm using a spectrophotometer. Total phenolic concentration was calculated from a gallic acid calibration curve (10-100 µg/mL) and expressed as milligrams of gallic acid equivalents per gram of dry extract (mg Gallic Acid Equivalent /g Dry Extract).

Total flavonoid content

The aluminum chloride colorimetric method was used to indicate total flavonoid content (Pertiwi et al., 2020). Equal volumes of extract and 2% $AlCl_3 \cdot 6H_2O$ (Sigma Aldrich, United States) were incubated for 10 minutes at room temperature, and absorbance was read at 430 nm. Results were expressed in mg quercetin equivalent per gram of dry extract (mg QE/g DE), after the use of quercetin standard curve (0-60mg/L).

Condensed tannins

Condensed tannin content was determined using the vanillin assay as described by Agbo et al. (2015). Briefly, 1.5 mL of concentrated sulfuric acid (Sigma-Aldrich, USA) and 3 mL of 4% vanillin solution prepared in methanol were added to 50 mL of the diluted extract. The mixture was incubated for 15 min at room temperature in the dark, after which absorbance was measured at 500 nm. The results were expressed as milligrams of catechin equivalents per 100 grams of dry matter (mg Catechin Equivalent/100 g Dry Matter), using a catechin calibration curve ranging from 0 to 400 µg/mL ($R^2 = 0.999$).

Antioxidant activity and phenolic compound characterization

Free radical scavenging assay by 2,2-diphenyl-1-picrylhydrazyl (DPPH)

The antioxidant activity of the orange by-product extract was assessed using the DPPH radical scavenging assay, following the reported method of Mohamadi et al. (2023). The DPPH radical scavenging activity was determined following the standard procedure. Briefly, 0.1 mL of the methanolic extract (31.25-500 µg/mL) was mixed with 2 mL of 0.4% DPPH solution prepared in ethanol. The mixture was vigorously shaken and incubated in the dark at 30 °C for 30 min. The absorbance was then measured at 517 nm, and the percentage of inhibition was calculated relative to the control. The percentage of radical inhibition was calculated using Formula 5 (Chewchinda et al., 2021).

IP (%) = (Ac-As)/Ac×100 (Formula 5)

(IP): Inhibition percentage, (Ac) is the absorbance of the control, and (As) is the absorbance of the sample.

Radical scavenging assay by 2,2'-Azino-bis-3-ethylbenzothiazoline-6-sulfonic acid (ABTS)

The ABTS radical scavenging capacity was determined following the procedure described and modified by Mohamadi et al. (2023). The $ABTS^{\bullet+}$ radical cation was generated by combining 7 mM ABTS solution with 2.45 mM potassium persulfate (Sigma-Aldrich, United States) and allowing the mixture to stand in the dark at 25 °C for 12-16 h. The resulting stock solution was then diluted with ethanol until its absorbance reached 0.70 ± 0.02 at 734 nm. Subsequently, 20 µL of the sample extract or Trolox standard was added to 2 mL of the $ABTS^{\bullet+}$ working solution. After incubation for 6 min at 30 °C, the absorbance was recorded at 734 nm. The antioxidant potential was expressed as Trolox Equivalent Antioxidant Capacity (TEAC), and measurements were performed at three different concentrations.

Identification and quantification of phenolic compounds

The phenolic composition of the orange by-product extract was determined through high-performance liquid chromatography coupled with diode array detection (HPLC-DAD/UV), as described by Maalej et al. (2022) with minor modifications. The analysis was performed using an Agilent 1260 system (Germany) equipped with an Eclipse DB C18 column (4.6 × 250 mm, 5 µm particle size). The mobile phase consisted of 0.1% acetic acid in water (solvent A) and acetonitrile (solvent B), applied under a gradient program as follows: 10% B for 0-22 min, 50% B for 22-32 min, 100% B for 32-44 min, followed by a return to 10% B at 44-50 min. The flow rate was maintained at 0.5 mL/min, with an injection volume of 5 µL, and the column temperature was set at 40 °C. UV-Vis spectra were monitored from 190 to 400 nm, while detection was carried out at 254, 280, and 330 nm to identify distinct groups of phenolic compounds.

Statistical analysis

The experiment was independently repeated five times on separate days using freshly prepared materials to obtain five biological replicates (n = 5). This approach accounts for the expected biological and procedural variability inherent in the experimental process. All analyses were subsequently performed on these five independent samples. Results are expressed as mean ± standard deviation (SD). Descriptive statistical methods were applied to evaluate data consistency and variability. Where applicable, statistical significance between groups was determined using a one-way analysis of variance (ANOVA) followed by a post-hoc Tukey test for multiple comparisons. All statistical analyses were performed using IBM SPSS Statistics version 26, and a p-value of less than 0.05 was considered statistically significant.

RESULTS AND DISCUSSION

Biochemical composition of dried orange pulp

The proximate biochemical composition of dried orange juice by-products is summarized in Table 1. These by-products contained low levels of fat and protein, moderate amounts of dietary cellulose, and a pH of approximately 6.10. Such characteristics suggest that this material can be incorporated as a fibrous and mildly acidic feed ingredient that supports normal digestive function in poultry. Moderate fiber levels enhance gut motility, while a slightly acidic environment promotes enzymatic activity and nutrient absorption. Moreover, the acidic nature of the material may contribute to improved intestinal microbiota balance by reducing populations of *Enterobacteriaceae*, *Escherichia coli*, and *Staphylococcus spp*, while increasing beneficial *Lactobacillus spp*. in the small intestine of broilers (Vlaicu et al., 2020).

The orange pulp analyzed in the present study contained 89.19% dry matter, 2.10% crude fat, 3.81% ash, and 5.50% crude protein. The crude protein content of the dried orange by-products analyzed in the present study is relatively low compared to conventional protein sources such as soybean meal or even cereal grains. This finding is consistent with the values previously reported by Castro et al. (2020), confirming that orange by-products are poor in nitrogenous compounds. Consequently, their incorporation into poultry diets should not aim to supply protein but rather to provide an

alternative energy and fiber source. Aside from being used as an alternative feed ingredient to replace energy sources, fruit peel meal as a feed ingredient in broiler rations is often used as a functional feed ingredient (Sugiharto et al., 2018). This is related to the presence of various active ingredients in fruit peel meal, such as antimicrobial, antioxidant, anti-inflammatory, immunomodulatory, and other components. Despite their modest protein content, dried orange pulp is characterized by a high concentration of readily fermentable carbohydrates, pectin, and bioactive compounds such as flavonoids and limonene, which can promote intestinal health, antioxidant status, and overall performance in broiler chickens. These values were higher than those reported by El-Beltagi et al. (2022) for crude fat and protein contents. Furthermore, the ash concentration was markedly elevated compared with the findings of Castro et al. (2020), while the protein level remained relatively comparable. The moisture content of the oven-dried orange peel powder was 11.35%, which is in close agreement with the results reported by Özcan et al. (2021) and consistent with the observations of the current study, 10.81.

Table 1. Chemical composition of dried orange by-products (g.100g^{-1}DM)

Parameter	Dried orange pulp
pH	6.10 ± 0.01
Aw (g.100g^{-1}DM)	10.81 ± 1.44
Dry Matter (g.100g^{-1}DM)	89.19 ± 1.44
Ash (g.100g^{-1}DM)	3.81 ± 0.09
Dietary Cellulose (g.100g^{-1}DM)	22.03 ± 1.89
Total fat (g.100g^{-1}DM)	2.10 ± 0.05
Crude Proteins (g.100g^{-1}DM)	5.50 ± 0.05

aw: Water activity. The results are expressed as means ± standard deviation

Phytochemical content and antioxidant capacity of dried orange pulp

The quantified levels of total polyphenols, flavonoids, and condensed tannins, together with antioxidant activities determined through DPPH and ABTS assays, are summarized in Table 2. These bioactive compounds are known to exert beneficial effects on animal performance and health by enhancing the secretion of endogenous digestive enzymes, saliva, bile, and mucus, thereby improving nutrient digestion and assimilation. In addition, their antioxidant and anti-inflammatory properties help to modulate gut morphology and reduce the population of pathogenic bacteria, while promoting beneficial microbiota balance (Juhari et al., 2021; Saleem et al., 2022). Several studies have further reported that higher growth rates and improved feed conversion ratios in poultry fed phenolic-rich diets result from increased intestinal surface area and enhanced digestive enzyme activity, which collectively facilitate better nutrient absorption (Ani and Abel, 2018; Maheshwari et al., 2022). Moreover, the bioactive compounds contributed to potential health-promoting properties (Diarra et al., 2018).

The results of this study revealed that dried orange pulp (DOP) contained a TPC of 202.59 mg Gallic Acid Equivalent/g Dry Extract and a total flavonoid content of 430.70 mg Quercetin Equivalent/g Dry Extract, confirming its richness in bioactive phytochemicals. Regarding flavonoid content, the results of the present study were comparable to those reported by Abou-Arab et al. (2016), who observed values ranging from 437.50 to 453.33 mg QE/100 g in microwave-dried mandarins, *Citrus valencia*, and *Citrus balady* pulp.

The TPC of the dried orange pulp obtained in this study was comparatively higher than that of orange and mandarin peels, which ranged from 169.54 to 178.90 mg GAE/100 g, and also exceeded the values reported for orange pulp (104.98–123.02 mg GAE/100 g) by Al-Juhaimi (2014). However, it remained below the 534 mg GAE/100 g reported by Castro et al. (2020).

The antioxidant capacity determined by the DPPH and ABTS assays reached 270.68 ascorbic acid /g Dry Extract and 1158.80 Trolox Equivalent Antioxidant Capacity/g dry Extract, respectively. The reducing power refers to the ability of DOP constituents to donate electrons to neutralize free radicals, thereby converting them into more stable and less reactive species. This strong electron-donating capacity highlights the potential of DOP as a natural antioxidant and functional feed additive in poultry nutrition. Moreover, the antioxidant activity (ABTS and DPPH assays) indicated a positive correlation with phenolic content, consistent with the findings of Barreca et al. (2014) and Papoutsis et al. (2016). The HPLC-DAD analysis identified a total of nineteen phenolic compounds in DOP, encompassing four flavonoids and spanning three main classes, including phenolic acids, flavanone glycosides, and flavanol glycosides (Figure 1 and Table 3). Furthermore, notable levels of quercetin (10.6 mg/g), rutin (0.4 mg/g), and epicatechin (7 mg/g)—members of the flavanol group—contributed significantly to the overall antioxidant potential of the extract. The chemical diversity and richness in both flavonoids and phenolic acids highlighted the nutritional value and functional bioactivity of dried orange pulp, supporting its application as a promising natural source of antioxidants.

Table 2. Phenolic compounds and antioxidant activity of the studied by-products (*Citrus Siensis*)

Parameter	Dried orange pulp
Phenolic compounds (mg GAE/g)	202.59 ± 15.93
Flavonoids (mg QE/g)	430.70 ± 2.78
Tannins (mg CE/g)	150.00 ± 18.03
ABTS (mg/g)	1158.8 ± 19.22
DPPH (mg/g)	270.68 ± 5.95

DPPH: 2,2-Diphenyl-1-picrylhydrazyl, ABTS: 2,2′-Azino-bis-3-ethylbenzothiazoline-6-sulfonic acid. The results are expressed as means ± standard deviations.

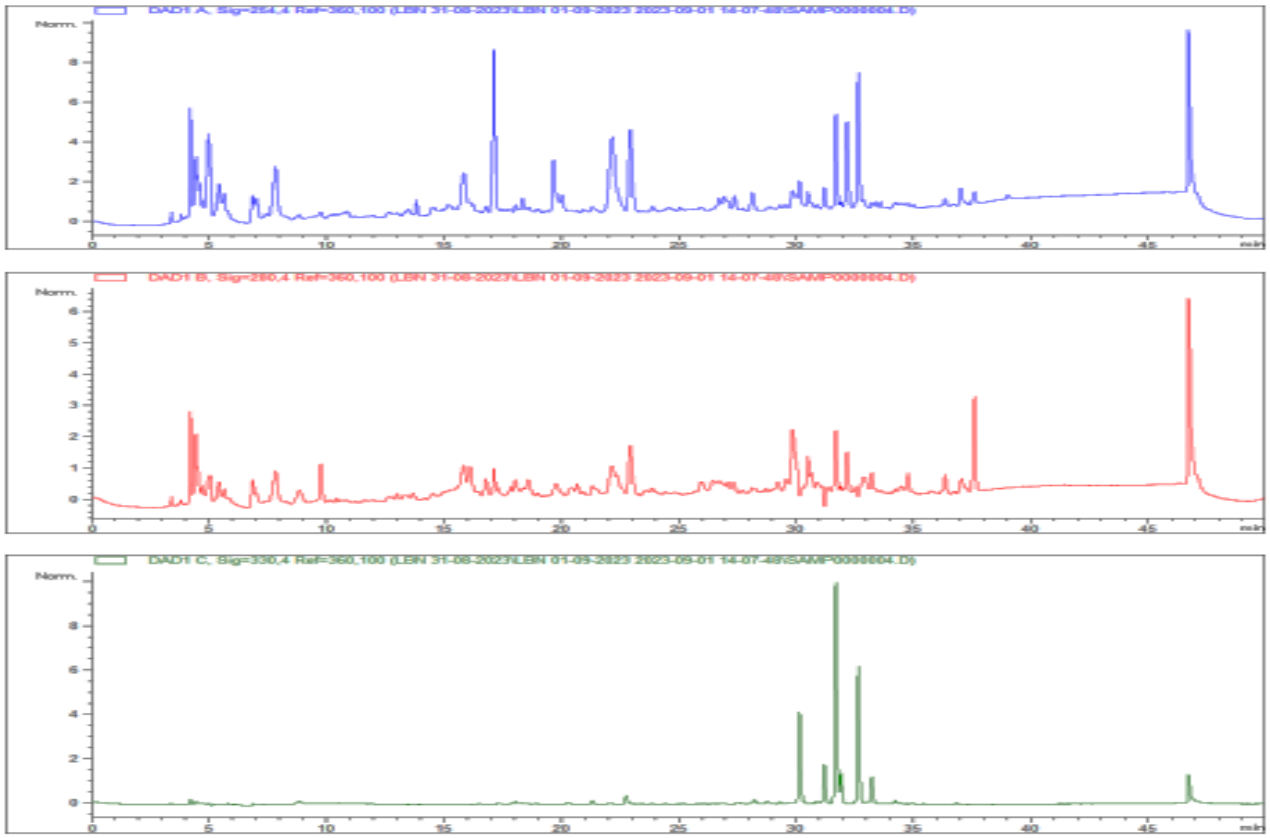


Figure 1. HPLC-DAD chromatograms of orange juice by-products recorded at 254, 280, and 330 nm

Table 3. Phenolic compounds in orange pulp

	RT	Component	mg/g	Λ nm	Subclasses of Compounds
1	8.92	Caffeic acid	1.00	330	Hydrocinnamic acids
2	17.12	Ferulic acid	27.1	280	
3	19.83	p-Coumaric acid	0.3	280	
4	7.03	p-Hydroxybenzoic acid	1.31	254	Hydrobenzoic acids
5	14.45	Vanillic acid	0.1	254	
6	23.86	Dydimine	0.61	330	Flavonones
7	20.91	Naringenin	0.2	280	
8	23.09	Naritunine	1.76	280	
9	32.77	Hesperidin	61.29	330	
10	42.72	Hesperetin	0.3	280	
11	22.74	Luteolin	0.8	330	Flavones
12	25.96	Apigenin	0.8	254	
13	15.15	Rutin	0.4	330	Flavanols
14	22.92	Quercetin	10.6	254	
15	13.66	Epicatechin	7	280	
16	22.51	Quercitrin	4.2	254	
17	10.40	Protocatechuic acid	Trace	280	Phenolic acids
18	7.89	Chlorogenic acid	2.7	254	
19	4.48	Ascorbic acid	3.2	280	
T			123.67		

RT: Retention time; C: Concentration (mg/mL); λ nm: Wavelength; T: Total

The phenolic profiling of the dried orange by-product revealed that hesperidin, a predominant flavanone, was the most abundant compound (61.29 mg/g), followed by ferulic acid (27.10 mg/g), underscoring the notable presence of flavonoids and phenolic acids.

This high concentration of hesperidin is particularly relevant, as previous research on *Arbor Acres* broilers demonstrated that dietary supplementation with flavonoids, specifically genistein and hesperidin at inclusion levels of 5 mg/kg, 20 mg/kg, and a 1:4 mixture, significantly enhanced the chicken's antioxidant defense system. Supplemented broilers exhibited elevated serum total antioxidant capacity (T-AOC) and superoxide dismutase (SOD) activity, along with reduced malondialdehyde (MDA) concentrations, indicating improved oxidative stability. Additionally, hesperidin supplementation favorably influenced lipid metabolism, resulting in decreased total cholesterol (TC), low-density lipoprotein cholesterol (LDL-C), and triglyceride (TG) levels, as well as an enhanced polyunsaturated fatty acid (PUFA) profile and an optimized n-6/n-3 fatty acid ratio in breast muscle. Therefore, the high hesperidin content identified in the orange by-product suggests its potential contribution to similar antioxidant and hypolipidemic effects when incorporated into broiler diets (Kamboh et al., 2013).

The dehydrated orange pulp analyzed in the present study exhibited higher concentrations of caffeic acid (1.00 mg/g), ferulic acid (27.10 mg/g), and p-coumaric acid (0.30 mg/g) than those reported for kinnow peel by Rafiq et al. (2019). However, the concentrations of quercetin (10.6 mg/g), caffeic acid (1.00 mg/g), naringin (0.20 mg/g), and rutin (0.40 mg/g) were lower than the levels reported by Omoba et al. (2015) in orange peel extracts. The identification of hydroxycinnamic acids, namely caffeic, ferulic, and p-coumaric acids, corroborates the findings of De Ancos et al. (2017) and Ferreira et al. (2018), who reported similar phenolic profiles in orange pulp and mandarin peel methanolic extracts, respectively. The presence of naringenin, hesperidin, narirutin, and didymin in the analyzed orange pulp is consistent with the findings of De Ancos et al. (2017). Notably, the hesperidin content in the samples exceeded the concentrations reported by Chen et al. (2017) for two varieties of orange peel, which were 26.81 mg/g and 20.99 mg/g. Furthermore, the detected concentrations of hesperidin and naringin were in agreement with those reported in *Citrus reticulata* peel, ranging from 50.13 to 100.52 mg/g (Liu et al., 2013). Hesperidin was identified as the predominant compound, with levels surpassing those documented by Molina-Calle et al. (2015).

Related research indicated that incorporating an appropriate amount of ferulic acid into broiler feed can significantly improve growth performance (Shu et al., 2022). The beneficial effects of phenolic compounds such as quercetin, rutin, and hesperidin on broiler performance and health have been well established. Quercetin improves performance efficiency by modulating intestinal morphology and nutrient absorption (Samuel et al., 2017), while rutin supplementation enhances body weight gain and feed conversion ratio through its positive impact on gut structure and digestive functionality (Viveros et al., 2011). Similarly, hesperidin at 20 mg/kg diet was reported to promote intestinal health and stimulate immune responses in poultry (Hong et al., 2012). Beyond these physiological effects, citrus flavanones, including hesperetin and naringin, display notable antimicrobial activity against pathogens such as *Helicobacter pylori*, *Aeromonas hydrophila*, and *Staphylococcus aureus*, thereby contributing to improved feed efficiency and meat oxidative stability (Bakar et al., 2012; Goliomytis et al., 2015; Agus et al., 2017; Chen et al., 2018).

Flavones such as luteolin and apigenin, commonly found in glycosylated forms, are hydrolyzed by intestinal Lactobacillus species (e.g., *L. agilis*) to produce aglycones and metabolites with enhanced bioavailability (Panche et al., 2016). These compounds and their derivatives exert positive effects on gut integrity and performance, as evidenced by improved growth efficiency in chickens fed alfalfa-derived flavones (Changxing et al., 2018). Furthermore, luteolin exhibits strong antibacterial activity against antibiotic-resistant *Escherichia coli* strains (Ouyang et al., 2013), highlighting the multifunctional role of flavones in maintaining intestinal health and productivity in poultry.

In poultry, dietary phenolics such as ferulic and caffeic acids have been associated with enhanced growth performance, reduced lipid peroxidation, and improved gut health, thereby supporting overall animal welfare and productivity.

CONCLUSION

The chemical composition of orange waste demonstrates its promise as a valuable bioresource for diverse industrial and nutritional applications, although validation through *in vivo* studies remains necessary. Extraction using methanol resulted in the highest recovery of bioactive compounds, underscoring their efficiency compared to other solvents. The key findings demonstrated that DOP is rich in dietary fiber (22.03% DM) and possesses a remarkable phytochemical profile, including high levels of total phenolics (202.59 mg GAE/g), total flavonoids (430.70 mg QE/g), and potent antioxidant activity (FRAP: 1158.8 mg TE/g). The elevated phenolic content highlights the antioxidant potential of this material, with hesperidin identified as the major active compound. The HPLC analysis identified flavonoids as the dominant subclass, with hesperidin (61.29 mg/g) and ferulic acid (27.10 mg/g) as the major constituents. Further studies are recommended to explore large-scale extraction processes, evaluate bioavailability in animal and human systems, and

assess the synergistic effects of these compounds when incorporated into feed and food formulations within circular economy models.

DECLARATIONS

Funding

This research was funded by the Laboratory of Biotechnology Applied to Agriculture and Environmental Preservation, Higher School of Agronomy, Mostaganem, Algeria, with grant number HSA-MEBAM-AGR-2021-14.

Availability of data and materials

The data supporting the findings of this study are available from the corresponding author upon reasonable request.

Acknowledgments

The authors would like to acknowledge the support of the Higher School of Agronomy "Mohamed El Amjed Ben Abdelmalek" for their valuable contributions to this research. The assistance provided in the form of technical support, funding, or intellectual input is gratefully appreciated.

Authors' contributions

Ahmed Readh Chaib Eddour contributed to Conceptualization, experimental design, data collection, statistical analysis, data interpretation, manuscript drafting, preparation of figures and tables, and final manuscript revision. Miloud Litim assisted in the experimental setup and contributed to data interpretation and manuscript review. Kaddour Bouderoua supervised the experimental procedures and ethical compliance, verification of analytical accuracy, and critical revision of the manuscript. The authors read and approved the last edition of the manuscript for publication.

Competing interests

The authors declare that there are no competing interests or conflicts of interest related to this work.

Ethical considerations

All ethical considerations related to this study, including but not limited to plagiarism, consent for publication, research misconduct, data fabrication or falsification, redundant publication, and simultaneous submission, have been thoroughly reviewed and addressed by all authors. The research was conducted in accordance with ethical standards and institutional guidelines. The authors confirm that no artificial intelligence (AI) tools were used in the conduct, analysis, or writing of this study.

REFERENCES

Abbasi H, Seidavi A, Liu W, and Asadpour L (2015). Investigation on the effect of different levels of dried sweet orange (*Citrus sinensis*) pulp on performance, carcass characteristics and physiological and biochemical parameters in broiler chicken. Saudi Journal of Biological Sciences, 22(2): 139-146. DOI: https://www.doi.org/10.1016/j.sjbs.2014.09.006

Abou-Arab AA, Mahmoud MH, and Abu-Salem FM (2016) Bioactive compounds content citrus peel as affected by drying processes. International Journal of Nutrition and Food Engineering, 10(4): 240-243. Available at: https://www.jalexu.journals.ekb.eg/article_161928

Agus S, Achmadi SS, and Mubarik NR (2017). Antibacterial activity of naringenin-rich fraction of pigeon pea leaves toward Salmonella thypi. Asian Pacific Journal of Tropical Biomedicine, 7(8): 725-728. DOI: https://www.doi.org/10.1016/j.apjtb.2017.07.019

Agbo MO, Uzor PF, Nneji UNA, Odurukwe CUE, Ogbatue UB, and Mbaoji EC (2015). Antioxidant, total phenolic and flavonoid content of selected Nigerian medicinal plants. Dhaka University Journal of Pharmaceutical Sciences, 14(1): 35-41. DOI: https://www.doi.org/10.3329/dujps.v14i1.23733

Al-Juhaimi FY (2014). Citrus fruits by-products as sources of bioactive compounds with antioxidant potential. Pakistan Journal of Botany, 46(4): 1459-1462. Available at: https://mail.pakbs.org/pjbot/PDFs/46(4)/38.pdf

Ani PN and Abel HC (2018). Nutrient, phytochemical, and antinutrient composition of *Citrus maxima* fruit juice and peel extract. Food Science & Nutrition, 6(3): 653-658. DOI: https://www.doi.org/10.1002/fsn3.604

Association of official analytical chemists (AOAC) (2005). Official method of analysis, 18th Edition. Washington, DC: Association of Officiating Analytical Chemists, method 935.14 and 992.24. Available at: https://www.studocu.vn/official-methods-of-analysis-of-aoac-international-18th-ed-2005/138442576

Bakar NS, Zin NM, and Basri DF (2012). Synergy of flavone with vancomycin and oxacillin against vancomycin-intermediate *Staphylococcus aureus*. Pakistan Journal of Pharmaceutical Science, 25(3): 633-638. Available at: https://pubmed.ncbi.nlm.nih.gov/22713953

Bampidis VA and Robinson PH (2006). Citrus by-products as ruminant feeds: A review. Animal Feed. Science and Technology, 128(3-4): 175-217. DOI: https://www.doi.org/10.1016/j.anifeedsci.2005.12.002

Barreca D, Bellocco E, Leuzzi U, and Gattuso G (2014). First evidence of C- and O-glycosyl flavone in blood orange (*Citrus sinensis (L.) Osbeck*) juice and their influence on antioxidant properties. Food Chemistry, 149: 244-252. DOI: https://www.doi.org/10.1016/j.foodchem.2013.10.096

Berk Z (2016). Citrus fruit processing. Chapter 10, pp. 219-233. DOI: https://www.doi.org/10.1016/b978-0-12-803133-9.00010-2

Camacho MDM, Martínez-Lahuerta JJ, Ustero I, García-Martínez E, and Martínez-Navarrete N (2023). Composition of powdered freeze-dried orange juice co-product as related to glucose absorption *in vitro*. Foods, 12(6): 1127. DOI: https://www.doi.org/10.3390/foods12061127

Caldeira C, De Laurentiis V, Corrado S, Van Holsteijn F, and Sala S (2019). Quantification of food waste per product group along the food supply chain in the European Union: A mass flow analysis. Resources, Conservation and Recycling, 149: 479-488. DOI: https://www.doi.org/10.1016/j.resconrec.2019.06.011

Castro LAD, Lizi JM, Chagas EGLD, Carvalho RAD, and Vanin FM (2020). From orange juice by-product in the food industry to a functional

ingredient: Application in the circular economy. Foods, 9(5): 593. DOI: https://www.doi.org/10.3390/foods9050593

Changxing L, Chenling M, Alagawany M, Jianhua L, Dongfang D, Gaichao W, Wenyin Z, Syed S, Arain M, and Saeed M (2018). Health benefits and potential applications of anthocyanins in poultry feed industry. World's Poultry Science Journal, 74(2): 251-264. DOI: https://www.doi.org/10.1017/S0043933918000053

Chen XM, Tait AR, and Kitts DD (2017). Flavonoid composition of orange peel and its association with antioxidant and anti-inflammatory activities. Food Chemistry, 218: 15-21. DOI: https://www.doi.org/10.1016/j.foodchem.2016.09.016

Chen L, Cao H, and Xiao J (2018). Polyphenols: Absorption, bioavailability, and metabolomics. Polyphenols: Properties, recovery, and applications. Chapter 2, pp. 45-67. DOI: https://www.doi.org/10.1016/B978-0-12-813572-3.00002-6

Chewchinda S, Suriyaphan O, Kanchanadumkerng P, Sato H, and Sato VH (2021). Comparison of antioxidant and α-glucosidase inhibitory activities in different cultivars of five mango (*Mangifera indica L.*) leaf extracts. Chiang Mai University Journal of Natural Sciences, 20: e2021014. DOI: https://www.doi.org/10.12982/CMUJNS.2021.014

Ciftci M, Şimşek ÜG, Dalkilic B, Azman MA, Yilmaz Ö, Mutlu Sİ, and Bahşi M (2016). Effect of dietary orange peel extract on physiological, biochemical, and metabolic responses of Japanese quail reared under low ambient temperature. Turkish Journal of Veterinary & Animal Sciences, 40(3): 288-297. DOI: https://www.doi.org/10.3906/vet-1504-11

De Ancos B, Cilla A, Barberá R, Sánchez-Moreno C, and Cano MP (2017). Influence of orange cultivar and mandarin postharvest storage on polyphenols, ascorbic acid and antioxidant activity during gastrointestinal digestion. Food Chemistry, 225: 114-124. DOI: https://www.doi.org/10.1016/j.foodchem.2016.12.098

Dilek FB, Barampouti EM, Mai S, Moustakas K, Malamis D, Martin DS, and Yetis U (2025). Orange peel waste valorization: An integrated assessment of environmental and economic sustainability in animal feed production. Waste and Biomass Valorization, 16: 3873-3894. DOI: https://www.doi.org/10.1007/s12649-025-03044-2

Danesi, EDG, Granato D, Iwassa IJ, Pinzon C, and Bolanho BC (2018). Effects of industrial by-products from orange, peach palm and soybean on the quality traits and antioxidant activity of flours: A response surface approach. International Food Research Journal, 25(3): 1219-1227. Available at: https://openurl.ebsco.com/EPDB%3Agcd%3A6%3A12797270/detailv2?sid=ebsco%3Aplink%3Ascholar&id=ebsco%3Agcd%3A131191335&crl=c&link_origin=scholar.google.com

Diarra SS (2018). Peel meals as feed ingredients in poultry diets: Chemical composition, dietary recommendations and prospects. Journal of Animal Physiology and Animal Nutrition, 102(5): 1284-1295. DOI: https://www.doi.org/10.1111/jpn.12954

Ebouel FLE, Medjo KE, Mandeng KFP, Tchuenkam JOT, Woumdi F, and Ntentie R (2023). Nutritional properties of the pulp of cola lateritia fruit: A common native fruit in Cameroon (Sub-Saharan Africa). World Journal of Nutrition and Food Science, 2(1): 1007. Available at: https://www.medtextpublications.com/open-access/nutritional-properties-of-the-pulp-of-cola-lateritia-fruit-a-1469.pdf

El-Beltagi HS, Eshak NS, Mohamed HI, Bendary ES, and Danial AW (2022). Physical characteristics, mineral content, and antioxidant and antibacterial activities of *Punica granatum* or *Citrus sinensis* Peel extracts and their applications to improve cake quality. Plants, 11(13): 1740. DOI: https://www.doi.org/10.3390/plants11131740

Escobedo-Avellaneda Z, Gutiérrez-Uribe J, Valdez-Fragoso A, Torres JA, and Welti-Chanes J (2014). Phytochemicals and antioxidant activity of juice, flavedo, albedo and comminuted orange. Journal of Functional, 6: 470-481. DOI: https://www.doi.org/10.1016/j.jff.2013.11.013

Ferreira SS, Silva AM, and Nunes FM (2018). *Citrus reticulata Blanco* peels as a source of antioxidant and anti-proliferative phenolic compounds. Industrial Crops and Products, 111: 141-148. DOI: https://www.doi.org/10.1016/j.indcrop.2017.10.009

Gargouri OD, Gargouri B, Trabelsi SK, Bouaziz M, and Abdelhédi R (2013). Synthesis of 3-O-methylgallic acid a powerful antioxidant by electrochemical conversion of syringic acid. Biochimica et Biophysica Acta (BBA)-General Subjects, 1830(6): 3643-3649. DOI: https://www.doi.org/10.1016/j.bbagen.2013.02.012

Goliomytis M, Kartsonas N, Charismiadou MA, Symeon GK, Simitzis PE, and Deligeorgis SG (2015). The influence of naringin or hesperidin dietary supplementation on broiler meat quality and oxidative stability. PLoS ONE, 10(10): e0141652. DOI: https://www.doi.org/10.1371/journal.pone.0141652

Hong JC, Steiner T, Aufy A, and Lien TF (2012). Effects of supplemental essential oil on growth performance, lipid metabolites and immunity, intestinal characteristics, microbiota and carcass traits in broilers. Livestock Science, 144(3): 253-262. DOI: https://www.doi.org/10.1016/j.livsci.2011.12.008

Jaradat NA, Hussen FM, and Al Ali A (2015). Preliminary phytochemical screening, quantitative estimation of total flavonoids, total phenols and antioxidant activity of Ephedra alata Decne, Journal of Materials and Environmental Science, 6(6): 1771-1778. DOI: https://www.doi.org/208-JMES-1662-2015-Jaradat.

Jiang J, Shan L, Chen Z, Xu H, Wang J, Liu Y, and Xiong Y (2014). Evaluation of antioxidant-associated efficacy of flavonoid extracts from a traditional Chinese medicine Hua Ju Hong (peels of *Citrus grandis* (L.) *Osbeck*). Journal of Ethnopharmacology, 158: 325-330. DOI: https://www.doi.org/10.1016/j.jep.2014.10.039

Juhari NKK, Wahid NBA, and Ramli S (2021). A review: Antimicrobial activity and toxicity analysis of the peel of banana, pomegranate, papaya, and citrus fruits (lemon and orange). Malaysian Journal of Microbiology, 17(4): 459-470. DOI: http://www.doi.org/10.21161/mjm.201076

Kamboh AA and Zhu WY (2013). Effect of increasing levels of bioflavonoids in broiler feed on plasma anti-oxidative potential, lipid metabolites, and fatty acid composition of meat. Poultry Science, 92(2): 454-461. DOI: https://www.doi.org/10.3382/ps.2012-02584

Liu EH, Zhao P, Duan L, Zheng GD, Guo L, Yang H, and Li P (2013). Simultaneous determination of six bioactive flavonoids in *Citri Reticulatae Pericarpium* by rapid resolution liquid chromatography coupled with triple quadrupole electrospray tandem mass spectrometry. Food Chemistry, 141(4): 3977-3983. DOI: https://www.doi.org/10.1016/j.foodchem.2013.06.077

Maalej A, Dahmen-Ben Moussa I, Karray F, Chamkha M, and Sayadi S (2022). Olive oil by product's contribution to the recovery of phenolic compounds from microalgal biomass: Biochemical characterization, anti-melanogenesis potential, and neuroprotective effect. Biomass Conversion and Biorefinery, 14: 4299-4311. DOI: https://www.doi.org/10.1007/s13399-022-02640-9

Maheshwari S, Kumar V, Bhadauria G, and Mishra A (2022). Immunomodulatory potential of phytochemicals and other bioactive compounds of fruits: A review. Food Frontiers, 3(2): 221-238. DOI: https://www.doi.org/10.1002/fft2.129

Mohamadi N, Meraghni M, Meradci F, Necib A, El Arbi M, Elhadef K, and Bouaziz M (2023). Investigation and quantification of the potential antioxidant, inflammatory, and antibacterial bioactive molecules of the extracts of Algerian black and green table olive brine. Quality Assurance and Safety of Crops & Foods, 15(1): 92-106. DOI: https://www.doi.org/10.15586/qas.v15i1.1250

Molina-Calle M, Priego-Capote F, and Luque de Castro MD (2015). Development and application of a quantitative method for determination of

flavonoids in orange peel: Influence of sample pretreatment on composition. Talanta, 144: 349-355. DOI: https://www.doi.org/10.1016/j.talanta.2015.05.054

Nazok A, Rezaei M, and Sayyahzadeh H (2010). Effect of different levels of dried citrus pulp on performance, egg quality, and blood parameters of laying hens in early phase of production. Tropical Animal Health and Production, 42(4): 737-742. DOI: www.doi.org/10.1007/s11250-009-9481-x

Omoba OS, Obafaye RO, Salawu SO, Boligon AA, and Athayde ML (2015). HPLC-DAD phenolic characterization and antioxidant activities of ripe and unripe sweet orange peels. Antioxidants, 4(3): 498-512. DOI: https://www.doi.org/10.3390/antiox4030498

Ortiz-Sanchez M, Cardona Alzate C A, and Solarte-Toro JC (2024). Orange peel waste as a source of bioactive compounds and valuable products: insights based on chemical composition and biorefining. Biomass, 4(1): 107-131. DOI: https://www.doi.org/10.3390/biomass4010006

Ouyang K, Xiong X, Wang W, Hu Y, Zhou P, and Liu D (2013). Effects of alfalfa flavones on growth performance and carcass quality of female Chongren chickens. Acta Prataculturae Sinica, 22(4): 340-345. Available at: https://www.cabidigitallibrary.org/doi/full/10.5555/20133350733

Özcan MM, Ghafoor K, Al Juhaimi F, Uslu N, Babiker EE, Mohamed Ahmed IA, and Almusallam IA (2021). Influence of drying techniques on bioactive properties, phenolic compounds and fatty acid compositions of dried lemon and orange peel powders. Journal of Food Science and Technology, 58: 147-158. DOI: https://www.doi.org/10.1007/s13197-020-04524-0

Panche AN, Diwan AD, and Chandra SR (2016). Flavonoids: An overview. Journal of Nutritional Science, 5: e47. DOI: https://www.doi.org/10.1017/jns.2016.41

Papoutsis K, Pristijono P, Golding JB, Stathopoulos CE, Bowyer MC, Scarlett CJ, and Vuong QV (2016). Optimisation of aqueous extraction conditions for the recovery of phenolic compounds and antioxidants from lemon pomace. International Journal of Food Science and Technology, 51(9): 2009-2018. DOI: https://www.doi.org/10.1111/ijfs.13168

Pertiwi RD, Suwaldi MR, and Setyowati EP (2020). Radical scavenging activity and quercetin content of *Muntingia calabura L.* leaves extracted by various ethanol concentration. Journal of Food and Pharmaceutical Sciences, 8(1): 174-184. DOI: https://www.doi.org/10.22146/jfps.581

Pourhossein Z, Qotbi AAA, Seidavi A, Laudadio V, Centoducati G, and Tufarelli V (2015). Effect of different levels of dietary sweet orange (*Citrus sinensis*) peel extract on humoral immune system responses in broiler chickens. Animal Science Journal, 86(1): 105-110. DOI: https://www.doi.org/10.1111/asj.12250

Rafiq S, Singh B, and Gat Y (2019). Effect of different drying techniques on chemical composition, color and antioxidant properties of kinnow (*Citrus reticulata*) peel. Journal of Food Science and Technology, 56: 2458-2466. DOI: https://www.doi.org/10.1007/s13197-019-03722-9

Readh CEA, Miloud L, Abdelkarim L, Kaddour B, and Chaima B (2023). Effect of graded levels of dried orange (*Citrus sinensis*) byproducts on production efficiency, blood parameters and antioxidant status of broiler chickens. Asian Journal of Dairy and Food Research, 42(3): 314-319. DOI: https://www.doi.org/10.18805/ajdfr.DRF-307

Sahraoui N, Abert M, El M, Boutekedjiret C, and Chemat F (2011). Valorization of citrus by-products using Microwave Steam Distillation (MSD). Innovative Food Science and Emerging Technologies, 12(2): 163-170. DOI: https://www.doi.org/10.1016/j.ifset.2011.02.002

Saleem A, Akhtar MF, Sharif A, Akhtar B, Siddique R, Ashraf GM, and Alharthy SA (2022). Anticancer, cardio-protective and anti-inflammatory potential of natural-sources-derived phenolic acids. Molecules, 27(21): 7286. DOI: https://www.doi.org/10.3390/molecules27217286

Samuel KG, Wang J, Yue HY, Wu SG, Zhang HJ, Duan ZY, and Qi GH (2017). Effects of dietary gallic acid supplementation on performance, antioxidant status, and jejunum intestinal morphology in broiler chicks. Poultry Science, 96(8): 2768-2775. DOI: https://www.doi.org/10.3382/ps/pex091

Shu G, Tang Z, Du H, Zheng Y, Chang L, Li H, and Lin J (2022). Effects of dietary ferulic acid supplementation on hepatic injuries in tianfu broilers challenged with lipopolysaccharide. Toxins, 14(3): 227. DOI: https://www.doi.org/10.3390/toxins14030227

Satpathy L, Dash D, Sahoo P, Anwar TS, and Parida SP (2020). Quantitation of total protein content in some common edible food sources by Lowry protein assay. Letters in Applied Nano Bio Science, 9(3): 1275-1283. DOI: https://www.doi.org/10.33263/LIANBS93.12751283

Seidavi A, Zaker-Esteghamati H, and Salem AZ (2020). A review on practical applications of *Citrus sinensis* by-products and waste in poultry feeding. Agroforestry Systems, 94(4): 1581-1589. https://www.doi.org/10.1007/s10457-018-0319-2

Seidavi A, Ebrahimi ABBAS, Qotbi AAA, and Nieto JG (2015). Effect of different levels of *Citrus sinensis* peel extract on broiler performance, blood parameters, thyroid gland activity and bone ash. Indian Journal of Animal Sciences, 85(11): 1225-1228. DOI: https://www.doi.org/10.56093/ijans.v85i11.53282

Sugiharto S, Yudiarti T, Isroli I, and Widiastuti E (2018). The potential of tropical agro-industrial by-products as a functional feed for poultry. Iranian Journal of Applied Animal Science, 8(3): 375-385. Available at: https://www.cabidigitallibrary.org/doi/pdf/10.5555/20183337346

Vlaicu PA, Untea AE, Panaite, TD, and Turcu RP (2020). Effect of dietary orange and grapefruit peel on growth performance, health status, meat quality and intestinal microflora of broiler chickens. Italian Journal of Animal Science, 19(1): 1394-1405. DOI: https://www.doi.org/10.1111/jpn.12954

Viveros A, Chamorro S, Pizarro M, Arija I, Centeno C, and Brenes A (2011). Effects of dietary polyphenol-rich grape products on intestinal microflora and gut morphology in broiler chicks. Poultry Science, 90(3): 566-578. DOI: https://www.doi.org/10.3382/ps.2010-00889

Zema DA, Calabro PS, Folino A, Tamburino V, and Zappia G (2022). Valorization of orange peel waste in a biorefinery loop. Waste Management & Research, 40(6): 734-744. DOI: https://www.doi.org/10.1016/j.jenvman.2022.115924

Publisher's note: Scienceline Publication Ltd. remains neutral with regard to jurisdictional claims in published maps and institutional affiliations.

Open Access: This article is licensed under a Creative Commons Attribution 4.0 International License, which permits use, sharing, adaptation, distribution and reproduction in any medium or format, as long as you give appropriate credit to the original author(s) and the source, provide a link to the Creative Commons licence, and indicate if changes were made. The images or other third party material in this article are included in the article's Creative Commons licence, unless indicated otherwise in a credit line to the material. If material is not included in the article's Creative Commons licence and your intended use is not permitted by statutory regulation or exceeds the permitted use, you will need to obtain permission directly from the copyright holder. To view a copy of this licence, visit https://creativecommons.org/licenses/by/4.0/.
© The Author(s) 2025

2025, Scienceline Publication
World's Veterinary Journal
World Vet J, 15(4): 1007-1014.
ISSN 2322-4568

DOI: https://dx.doi.org/10.54203/scil.2025.wvj102
PII: S232245682500102-15

Association of Sex and Age with Histomorphometric Features of Agranulocytic Leukocytes and Erythrocyte Indices in Sumbawa Horses

Kadek Ferdy Agastia Dwi Pratama[1]*, Ni Ketut Suwiti[2], Ida Bagus Komang Ardana[2], Ni Luh Eka Setiasih[2], Nyoman Sadra Dharmawan[2], I Nyoman Sulabda[2], and I Nengah Kerta Besung[3]

[1]*Master's Program in Veterinary Medicine, Udayana University, Denpasar 80234, Bali, Indonesia*
[2]*Department of Veterinary Basic Science, Faculty of Veterinary Medicine, Udayana University, Denpasar 80234, Bali, Indonesia*
[3]*Department of Veterinary Medicine, Faculty of Veterinary Medicine, Udayana University, Denpasar 80234, Bali, Indonesia*

*Corresponding author's Email: ferdyagastia@student.unud.ac.id

ORIGINAL ARTICLE
Received: October 11, 2025
Revised: November 12, 2025
Accepted: December 09, 2025
Published: December 31, 2025

ABSTRACT

The Sumbawa horse, an indigenous Indonesian breed, plays important ecological and cultural roles in the region, such as participation in traditional ceremonies, local transportation, and horse-racing competitions; however, scientific data on its hematological and cellular characteristics remain limited, hindering accurate clinical evaluation and breed-specific health management. This study aimed to provide baseline histomorphometric and hematological data by examining 80 clinically healthy Sumbawa horses, grouped by sex (male and female) and age (young and adult). Peripheral blood smears were prepared immediately after venipuncture and stained using the modified Diff Quick method. Morphometric parameters of lymphocytes and monocytes, including cell diameter, perimeter, cell area, and nucleus to cytoplasm ratio, were measured using calibrated digital image analysis. Complete blood count parameters, including mean corpuscular hemoglobin (MCH), mean corpuscular hemoglobin concentration (MCHC), mean corpuscular volume (MCV), red cell distribution width coefficient of variation (RDW-CV), and red cell distribution width standard deviation (RDW-SD), were obtained using an automated hematology analyzer. Females exhibited larger lymphocyte dimensions (17.79 ± 5.89 µm² versus 16.57 ± 6.29 µm², whereas males showed larger monocyte size (18.44 ± 7.60 µm² versus 14.88 ± 5.46 µm²). Lymphocyte counts and percentages were higher in females, while monocyte values and RDW-CV were higher in males. Age significantly influenced lymphocyte morphometry and leukocyte profiles, whereas its effects on monocytes were limited, with only monocyte area showing a significant difference between age groups. These findings indicated significant age-related increases in lymphocyte perimeter, area, and diameter, whereas most monocyte and erythrocyte indices remained relatively stable between age groups. Sex related differences were also evident, with females exhibiting significantly higher lymphocyte counts and percentages, and males showing significantly higher monocyte counts and greater erythrocyte variability. These reference values provide clear morphometric distinctions between groups of Sumbawa horses, with adults exhibiting larger lymphocyte dimensions and males showing higher monocyte counts and greater erythrocyte variability, thus offering a biologically calibrated basis for further physiological interpretation.

Keywords: Age, Agranulocytic leukocyte, Erythrocyte indice, Histomorphometry, Horse, Sex

INTRODUCTION

The Sumbawa horse is an indigenous Indonesian breed that plays an important role in transportation, agriculture, and cultural activities on Sumbawa Island. Despite its socioeconomic significance, scientific information on physiological and hematological characteristics specific to this breed remains limited (Sukri et al., 2022). Hematological parameters such as leukocyte profiles and erythrocyte indices are essential indicators of immune competence, metabolic adaptation, and overall health (de Siqueira and Fernandes, 2024). Because these values vary across equine breeds, establishing breed-specific reference ranges is necessary to support accurate clinical diagnosis and herd health monitoring (de Vega et al., 2024).

Age and sex are known intrinsic factors that influence hematological characteristics in horses. Age-related changes in leukocyte morphology and immune cell dynamics have been reported and are associated with maturation and immunosenescence (DeNotta and McFarlane, 2023). Likewise, sex-related variations in immune responses occur due to hormonal differences, in which estrogen enhances lymphocyte-mediated immunity while androgens modulate monocyte activity and innate immune function (Sciarra et al., 2023). Previous studies have also shown that erythrocyte indices such as mean corpuscular hemoglobin (MCH), mean corpuscular hemoglobin concentration (MCHC), and red cell distribution width (RDW) differ according to age, metabolic demands, and sex-specific physiological influences in ponies (Gaina et al., 2020). These intrinsic variations demonstrate that age and sex must be considered when interpreting hematological data in equine clinical practice (Silva et al., 2023).

To cite this paper: Pratama KFAD, Suwiti NK, Ardana IBK, Setiasih NLE, Dharmawan NS, Sulabda IN, and Besung INK (2025). Association of Sex and Age with Histomorphometric Features of Agranulocytic Leukocytes and Erythrocyte Indices in Sumbawa Horses. *World Vet. J.,* 15(4): 1007-1014. DOI: https://dx.doi.org/10.54203/scil.2025.wvj102

Histomorphometric assessment provides additional insight into the structural characteristics of blood cells that may not be detected through routine hematology (Walton and Lawson, 2021). Measurements such as cell diameter, perimeter, area, and the nucleus-to-cytoplasm ratio provide valuable insights into subtle morphological adaptations. Although previous studies have compared hematological variables among various horse breeds (Schaefer et al., 2024). Research focusing on the histomorphometry of agranulocytic leukocytes, particularly lymphocytes and monocytes, remains scarce. Furthermore, no published reference values exist for Indonesian indigenous horses, including the Sumbawa breed.

Given the unique genetic background, management systems, and environmental conditions in which Sumbawa horses are raised, generating specific physiological reference data is essential. The novelty of the present study lies in its combined analysis of leukocyte histomorphometry and erythrocyte indices in relation to age and sex, addressing the current lack of breed-specific data in Sumbawa horses and highlighting its importance for clinical diagnosis and health management, representing the first comprehensive baseline dataset for Sumbawa horses. Therefore, this study aimed to evaluate the histomorphometric features of agranulocytic leukocytes and erythrocyte indices in clinically healthy Sumbawa horses based on sex and age to enhance clinical interpretation and strengthen equine health management in this indigenous population.

MATERIALS AND METHODS

Ethical approval

The present study was approved by the Research Ethics Committee of the Faculty of Veterinary Medicine, Udayana University, Indonesia, under approval letter number B/211/UN.14.2.9/PT.01.04/2024. The authors considered the farmers' ethical concerns and obtained their consent before conducting the present study.

Study design

This observational cross-sectional study was conducted on Sumbawa Island, West Nusa Tenggara Province, Indonesia. A geographical map of the study area has been added as Figure 1. The sampled horses were managed under a semi-extensive system in which they grazed freely during the day and were confined to simple shelters or holding areas at night. The main plant species available in the grazing areas included Napier grass (*Pennisetum purpureum*), Setaria grass (*Setaria sphacelata*), signal grass (*Brachiaria decumbens*), and native savanna grasses such as *Digitaria* spp., *Chloris* spp., and *Panicum maximum*. Their diet consisted primarily of fresh rangeland grasses, supplemented with cut forage and rice bran provided once daily. All horses received the same feeding regimen regardless of age or sex, ensuring comparable nutritional conditions throughout the study.



Figure 1. The location of the study, Sumbawa Island, Indonesia

All horses included in this study were confirmed to be clinically healthy based on a veterinary physical examination conducted prior to blood collection. The assessment included evaluation of body condition, mucous membrane color, capillary refill time, rectal temperature, heart and respiratory rates, and the absence of gastrointestinal or respiratory abnormalities. A visual body condition assessment following the principles of the Henneke Body Condition Scoring

system (Henneke et al., 1983) was performed, and all horses showed normal body condition without signs of emaciation or obesity. In addition to the clinical evaluation, a fecal egg count was performed using the McMaster method to assess gastrointestinal parasite status (Lejeune et al., 2023; Mohammedsalih et al., 2025). Only horses with negative fecal egg counts were included in the study, ensuring that all sampled individuals met the criteria for being classified as healthy (Nielsen, 2021)**.** Physiological parameters recorded at examination were within normal ranges, including body temperature (37.2-38.3°C), heart rate (28-48 beats/min), respiratory rate (8-14 breaths/min), and capillary refill time (< 2 seconds). A total of 80 clinically healthy Sumbawa horses were selected using availability-based sampling consistent with previously published hematological studies. The animals were grouped by sex (male and female) and age (young and adult), forming four groups of 20 horses each, including young females, young males, adult females, and adult males.

Blood collection and sample preparation

Blood was collected from each horse (8 mL) through jugular venipuncture using sterile Venoject® needles and EDTA-coated vacuum tubes of the same volume. After collection, the tubes were labeled with the horse identification code and inverted 8–10 times to ensure proper anticoagulant mixing. Fresh blood was immediately used to prepare peripheral blood smears, while remaining samples were stored in a portable cooler at 4 ± 1°C and transported to the laboratory within two hours to prevent hemolysis (Rhodes et al., 2024). Peripheral blood smears were air-dried, fixed in absolute methanol for three minutes, and stained using the Modified Diff-Quik method (IndoReagen®, Indonesia; Catalog No. 710623-MD, manufacturer's protocol provided in the References). Microscopic examinations were performed using an OLYMPUS CX33 light microscope (Olympus Corporation, Tokyo, Japan) at 400× and 1000× magnifications.

Agranulocyte histomorphometry

Morphological identification of lymphocytes and monocytes was based on nuclear shape, cytoplasmic features, and overall cell structure. Histomorphometric measurements, including cell diameter, cell perimeter, cell area, and nucleus-to-cytoplasm ratio, were performed using EP View software Version 4.0. For each horse, 50 lymphocytes and 30 monocytes were examined to obtain representative morphometric values. Microscopic examination was carried out using an OLYMPUS CX33 light microscope at 400× and 1000× magnifications. Morphological identification and histomorphometric measurements were performed on lymphocytes and monocytes, considering nuclear shape, cytoplasmic structure, and cell size. Digital morphometric evaluation was conducted using EP View software (version 1.4, Poland), which allowed accurate and standardized measurement of cellular dimensions (Maśko et al., 2021).

Automated hematological analysis

EDTA blood samples were analyzed using the VetScan HM5 automated hematology analyzer (Abaxis, Union City, California, USA). Leukocyte parameters measured included total white blood cell counts, along with lymphocyte and monocyte counts and their respective percentages. Erythrocyte indices obtained included mean corpuscular hemoglobin (MCH), mean corpuscular hemoglobin concentration (MCHC), mean corpuscular volume (MCV), red cell distribution width–coefficient of variation (RDW-CV), and red cell distribution width–standard deviation (RDW-SD). The analyzer was calibrated and quality-controlled before each analytical session according to manufacturer guidelines.

Statistical analysis

Descriptive statistics were used to summarize leukocyte differentials and histomorphometric measurements. Differences in hematological and morphometric parameters according to age and sex were analyzed using two-way analysis of variance (two-way ANOVA). Tukey's post-hoc test was applied when significant effects were detected. Statistical analyses were conducted using IBM SPSS Statistics Version 29.0 (IBM Corp., Armonk, NY, USA). A p-value less than 0.05 was considered statistically significant.

RESULTS

Histological observations of Sumbawa horses based on sex (male and female) and age groups (young and adult) revealed no distinct morphological differences in the characteristics of lymphocytes and monocytes ($p > 0.05$). In general, lymphocytes (Figure 2) exhibited large, darkly stained, round to oval nuclei with slight indentations. The chromatin appeared coarse and prominent, while the cytoplasm formed a thin, light-blue rim surrounding the nucleus. Some large lymphocytes contained azurophilic granules within the cytoplasm. Meanwhile, monocytes (Figure 3) showed nuclei that were round to kidney-shaped or ovoid with noticeable indentations. The chromatin appeared less condensed, finely

textured, and paler compared to lymphocytes. The cytoplasm was wide, light blue, and occasionally contained fine vacuoles or azurophilic granules. Morphometric measurements demonstrated variations between age and sex groups, both in terms of mean values and statistical significance across certain parameters.

The histomorphometric analysis of agranulocytic leukocytes in Sumbawa horses based on sex revealed significant differences between females and males ($p < 0.05$; Table 1). The mean lymphocyte perimeter, area, and diameter were significantly higher in females compared to males ($p < 0.05$). Conversely, monocyte morphometric parameters were greater in males than in females, with a perimeter of 14.98 ± 3.43 µm, an area of 18.44 ± 7.60 µm², and a diameter of 4.80 ± 1.18 µm, all showing significant differences ($p < 0.05$). These findings suggest a sex-related variation in agranulocyte cell size, where lymphocytes tend to be larger in females, whereas monocytes are larger in males.

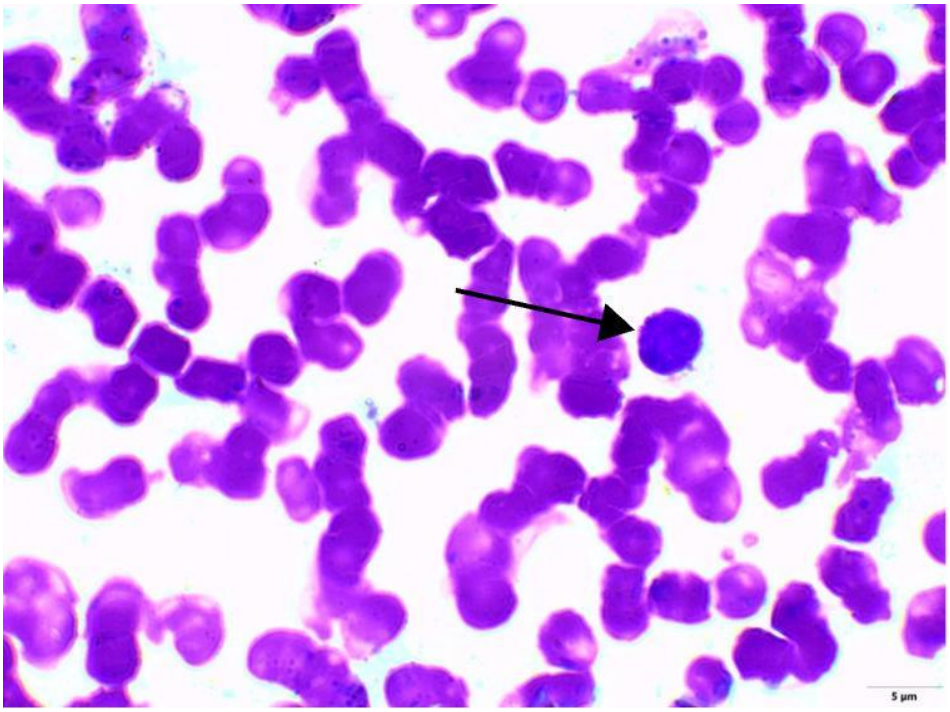


Figure 2. Representative lymphocyte in a peripheral blood smear of a Sumbawa horse (arrow). The lymphocyte shows a round, densely stained nucleus with a thin rim of cytoplasm.

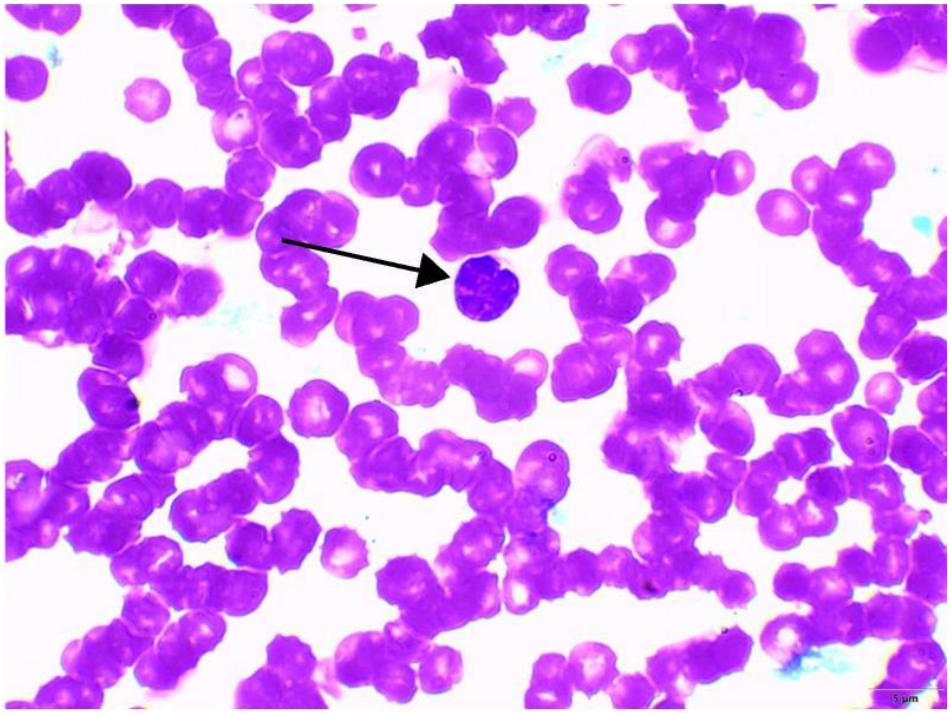


Figure 3. Representative monocyte in a peripheral blood smear of a Sumbawa horse (arrow). The monocyte shows a large kidney-shaped or horseshoe-shaped nucleus with lacy and fine chromatin.

Table 1. Histomorphometric values of agranulocytic leukocytes (lymphocytes and monocytes) in Sumbawa horses based on sex in West Nusa Tenggara, Indonesia.

Indicator	Female (Mean ± SD)	Male (Mean ± SD)
Lymphocyte perimeter (µm)	14.74 ± 2.48 [a]	14.19 ± 2.65[b]
Lymphocyte area (µm²)	17.79 ± 5.89[a]	16.57 ± 6.29[b]
Lymphocyte diameter (µm)	4.69 ± 0.79[a]	4.50 ± 0.84[b]
Monocyte perimeter (µm)	13.44 ± 2.43[a]	14.98 ± 3.43[b]
Monocyte area (µm²)	14.88 ± 5.46[a]	18.44 ± 7.60[b]
Monocyte diameter (µm)	4.28 ± 0.77[a]	4.80 ±1.18[b]

[a,b] Different superscript letters in the same row indicate significant differences ($p < 0.05$)

The histomorphometric analysis of agranulocytic leukocytes in Sumbawa horses based on age variation showed significant differences in most lymphocyte morphometric parameters but not in monocytes ($p < 0.05$; Table 2). The perimeter, area, and diameter of lymphocytes in adult horses (15.37 ± 2.20 µm; 19.20 ± 5.49 µm²; and 4.89 ± 0.69 µm) were significantly higher than those in young horses (13.56 ± 2.62 µm; 15.16 ± 6.06 µm²; and 4.31 ± 0.84 µm, $p < 0.05$). In contrast, monocytes in adult horses showed slightly higher mean values (14.41 ± 3.10 µm; 17.33 ± 7.71 µm²; and 4.59 ± 0.98 µm) than in young horses (14.01 ± 3.02 µm; 15.99 ± 5.79 µm²; and 4.50 ± 1.08 µm), though the differences were not statistically significant ($p > 0.05$). These results indicated that aging influences an increase in lymphocyte morphometric size but did not significantly affect monocyte dimensions in Sumbawa horses.

The leukocyte parameters and erythrocyte indices of Sumbawa horses according to sex are presented in Table 3. Female horses exhibited higher mean values of lymphocyte count (5.32 ± 2.08 ×10⁹/L), lymphocyte percentage (51.12 ± 16.04%), and mean corpuscular hemoglobin (MCH; 14.85 ± 3.15 pg) compared to males, with statistically significant differences ($p < 0.05$). Conversely, male horses showed higher monocyte count (0.33 ± 0.24 ×10⁹/L), monocyte percentage (3.87), and red cell distribution width (RDW-CV; 27.96) than females, also with significant differences ($p < 0.05$). No significant differences were observed in total white blood cell count (WBC#), mean corpuscular hemoglobin concentration (MCHC), and RDW-SD between sexes ($p > 0.05$). These findings indicated that sex variation influenced several leukocyte and erythrocyte parameters in Sumbawa horses.

Table 2. Histomorphometric values of agranulocytic leukocytes (lymphocytes and monocytes) in Sumbawa horses based on age in West Nusa Tenggara, Indonesia.

Indicator	Young (Mean ± SD)	Adult (Mean ± SD)
Lymphocyte perimeter (µm)	13.56 ±2.62[a]	15.37 ± 2.20[b]
Lymphocyte area (µm²)	15.16 ± 6.06 [a]	19.20 ± 5.49[b]
Lymphocyte diameter (µm)	4.31 ± 0.84[a]	4.89 ± 0.69[b]
Monocyte perimeter (µm)	14.01 ± 3.02[a]	14.41 ± 3.10[a]
Monocyte area (µm²)	15.99 ± 5.79[a]	17.33 ± 7.71[b]
Monocyte diameter (µm)	4.50 ± 1.08[a]	4.59 ± 0.98[a]

[a,b] Different superscript letters in the same row indicate significant differences ($p < 0.05$)

Table 3. Leukocyte parameters and erythrocyte indices of Sumbawa horses according to sex in West Nusa Tenggara, Indonesia.

Indicator	Female	Male
WBC# (×10⁹/L)	10.26 ± 2.40[a]	9.40 ± 2.35[a]
Lymphocyte# (×10⁹/L)	5.32 ± 2.08 [a]	3.96 ± 1.78[b]
Monocyte# (×10⁹/L)	0.23 ± 0.15[a]	0.33 ± 0.24[b]
Lymphocyte (%)	51.12[a]	41.55[b]
Monocyte (%)	2.38[a]	3.87[b]
MCH (pg)	14.85 ± 3.15[a]	12.89 ± 2.76[b]
MCHC (g/dL)	33.40 ± 5.15[a]	33.16 ± 4.58[a]
MCV (fL)	44.62 ± 7.11[a]	39.10 ± 7.27[b]
RDW-CV (%)	25.78[a]	27.96[b]
RDW-SD (fL)	39.94 ± 2.54[a]	40.64 ± 2.51[a]

WBC: White blood cell count, Lym: Lymphocyte count, Mon: Monocyte count, Lym: Lymphocyte percentage, Mon: Monocyte percentage, MCH: Mean corpuscular hemoglobin, MCHC: Mean corpuscular hemoglobin concentration, MCV: Mean corpuscular volume, RDW-CV: Red cell distribution width–coefficient of variation, RDW-SD: Red cell distribution width–standard deviation; [a,b] Different superscript letters in the same row indicate significant differences ($p < 0.05$); Data are expressed as Mean ± SD

The leukocyte parameters and erythrocyte indices of Sumbawa horses according to age are presented in Table 4. Young horses exhibited significantly higher total white blood cell count (WBC; 10.59 ± 2.79 ×10⁹/L), lymphocyte count (6.11 ± 1.20 ×10⁹/L), and lymphocyte percentage (58.34 ± 10.79%) compared to adults ($p < 0.05$). In contrast, adult horses showed significantly higher monocyte count (0.36 ± 0.23 ×10⁹/L) and monocyte percentage (4.16%) than younger horses ($p < 0.05$). The red cell distribution width (RDW-CV) was also significantly higher in young horses (27.76%) than in adults (25.98%, $p < 0.05$). Meanwhile, there were no significant differences in MCH, MCHC, MCV, and RDW-SD between the two age groups ($p > 0.05$). These results indicated that leukocyte profiles were more affected by age variation than erythrocyte indices in Sumbawa horses.

Table 4. Leukocyte parameters and erythrocyte indices of Sumbawa horses according to age.

Indicator	Young (Mean ± SD)	Adult (Mean ± SD)
WBC (×10⁹/L)	10.59 ± 2.79[a]	9.08 ±2.40[b]
Lymphocyte (×10⁹/L)	6.11 ± 1.20[a]	3.16 ± 1.59[b]
Monocyte (×10⁹/L)	0.22 ± 0.16[a]	0.36 ± 0.23[b]
Lymphocyte (%)	58.34[a]	34.33[b]
Monocyte (%)	2.08[a]	4.16[b]
MCH (pg)	13.66 ± 2.46[a]	14.08 ± 3.66[a]
MCHC (g/dL)	32.99 ± 4.07[a]	33.57 ± 5.54[a]
MCV (fL)	41.90 ± 8.58[a]	41.82 ± 6.74[a]
RDW-CV (%)	27.76[a]	25.98[b]
RDW-SD (fL)	40.69 ± 2.59[a]	39.89 ± 2.44[a]

WBC: White blood cell count, Lym: Lymphocyte count, Mon: Monocyte count, Lym: Lymphocyte percentage, Mon: Monocyte percentage, MCH: Mean corpuscular hemoglobin, MCHC: Mean corpuscular hemoglobin concentration, MCV: Mean corpuscular volume, RDW-CV: Red cell distribution width–coefficient of variation, RDW-SD: Red cell distribution width–standard deviation; [a,b] Different superscript letters in the same column indicate significant differences ($p < 0.05$); Data are expressed as Mean ± SD

DISCUSSION

Histological observations of lymphocytes and monocytes in Sumbawa horses showed that sex and age did not produce major morphological differences, although minor variations in morphometric measurements were apparent, such as slightly larger lymphocyte area and diameter in females and greater monocyte size in males. Lymphocytes in horses typically had large, dark-staining nuclei that were round to oval, surrounded by a thin cytoplasmic rim, while monocytes exhibited larger, kidney-shaped or ovoid nuclei with paler cytoplasm (Brooks et al., 2022). Similar leukocyte morphology and minor breed-related variations have also been reported in other indigenous horse populations (Lester et al., 2015). Occasional azurophilic granules within the cytoplasm denote the presence of primary lysosomes containing hydrolytic enzymes such as myeloperoxidase, which participate in normal phagocytic function. In horses, the appearance of these granules at low frequency is considered a normal component of monocyte maturation and immune surveillance. Thus, their presence reflects physiological cellular activation rather than an indication of inflammation, infection, or pathological hematological alterations (Maśko et al., 2021; Walton and Lawson, 2021).

Sex influenced leukocyte morphometry in this study, with females exhibiting larger lymphocyte perimeter, area, and diameter, whereas males had larger monocytes. This pattern in horses may be associated with hormonally driven immune modulation, where estrogens have been reported to support lymphocyte enlargement, and androgens may contribute to monocyte maturation in equine species (Benashour et al., 2024). Age also affected leukocyte dimensions in horses, as adult horses showed larger lymphocytes than juveniles, while monocyte size remained relatively stable. This suggests that lymphocyte enlargement is associated with age-related immune maturation and increased antigenic exposure, whereas monocytes appear to maintain more consistent structural characteristics across age groups (Miller et al., 2021).

Hematological findings paralleled the morphometric observations. Females had higher lymphocyte counts, lymphocyte percentages, and MCH in this study, a pattern consistent with reports in mares, where estrogen enhances adaptive lymphocyte activity (Jaworska et al., 2022). Conversely, males exhibited higher monocyte values and RDW-CV, which aligns with earlier studies reporting greater innate immune activation and erythrocyte size variability in stallions (Benashour et al., 2024). No significant sex differences were observed in total WBC, MCHC, or RDW-SD in horses, suggesting that these core hematological parameters are largely regulated by physiological mechanisms that are not strongly influenced by sex-related hormonal differences. This stability indicates that baseline leukocyte and

erythrocyte characteristics remain consistent between males and females, even though other immune traits may vary (Candrianisa et al., 2024; Rate et al., 2025).

These results highlight that sex and age selectively influence leukocyte and erythrocyte characteristics in Sumbawa horses. The minor variations observed in lymphocyte and monocyte morphology, as well as in erythrocyte indices, likely represent normal adaptive physiological mechanisms rather than pathological changes. This stability is clinically important because it helps establish reliable reference expectations for Sumbawa horses, allowing veterinarians to distinguish normal biological variation from early indicators of disease during routine hematological evaluation. Considering sex and age is crucial for interpreting hematological and immunological profiles, as these intrinsic factors influence baseline values that support clinical assessment, disease surveillance, and herd management in horses (Gaina et al., 2020; Rate et al., 2025). These findings also provide useful reference information for evaluating the health status of Sumbawa horses under field conditions.

CONCLUSION

Sex and age influence both the morphometry of agranulocytic leukocytes and hematological profiles in Sumbawa horses. Female horses exhibited larger lymphocyte dimensions and higher lymphocyte counts, percentages, and mean corpuscular hemoglobin, whereas males showed larger monocyte dimensions, higher monocyte counts, percentages, and RDW-CV. Age primarily affected lymphocyte size, with adults showed increased morphometric values compared to juveniles, while monocyte morphology remains relatively stable. These findings highlight the importance of considering sex and age when interpreting hematological and immunological parameters in Sumbawa horses. Future research may incorporate additional physiological, nutritional, and environmental variables to further refine the understanding of sex- and age-related hematological and morphometric patterns in Sumbawa horses.

DECLARATIONS

Authors' contributions

Kadek Ferdy Agastia Dwi Pratama conceptualized the study, designed the experiments, and conducted data collection and analysis. Ni Ketut Suwiti, Ida Bagus Komang Ardana, Nengah Kerta Besung, Ni Luh Eka Setiasih, Nyoman Sadra Dharmawan, and I Nyoman Sulabda contributed to blood sample preparation, laboratory management, statistical analyses, and drafting of the manuscript. All authors have read and approved the final version of the manuscript.

Acknowledgments

The authors express their sincere appreciation to the Faculty of Veterinary Medicine, Universitas Udayana, for providing research facilities and institutional support throughout this study. The authors also gratefully acknowledge the cooperation of horse farmers across Sumbawa Island, who willingly allowed their animals to be included in this research.

Funding

This research was supported by the Institute for Research and Community Service, Udayana University, Indonesia, through the Udayana Excellence Research Grant (Contract No. B/211/UN.14.2.9/PT.01.04/2024).

Competing interests

The authors declare no competing interests.

Availability of data and materials

All data supporting the findings of this study are available from the corresponding authors upon reasonable request.

Ethical considerations

This study was conducted using original data and did not involve any duplication, copy or plagiarism of previously published studies. The authors did not use AI to write the text of this article.

REFERENCES

Benashour F, Shmela M, Salheen S, Alnagar F, and Al-Zlitni R (2024). Effect of age on the biochemical and hematological blood profile in the Arabian horses raised in Libya. AlQalam Journal of Medical Applied Sciences, 7(3): 698-708. DOI: https://www.doi.org/10.54361/ajmas.247335

Brooks MB, Harr KE, Seelig DM, Wardrop KJ, and Weiss DJ (2022). Schalm's veterinary hematology, 7th Edition. Wiley Blackwell, pp. 385-401. DOI: https://www.doi.org/10.1002/9781119500537

Candrianisa ARP, Suwiti NK, Nindhia TS, Setiasih NLE, Kendran AAS, and Suatha IK (2024). Histologic features and granulocyte white blood cell counts of young and adult sumbawa horses reared under the lar system. Buletin Veteriner Udayana, 16(4): 1148-1158. DOI: https://www.doi.org/10.24843/bulvet.2024.v16.i04.p21

de Siqueira RF and Fernandes WR (2024). Dynamic hematological responses in endurance horses: Unraveling blood physiological markers of exercise stress and recovery. International Journal of Equine Science, 3(2): 74-81. DOI: https://www.doi.org/10.64292/ijes.116

de Vega CVM, de Meeûs d'Argenteuil C, Boshuizen B, De Mare L, Gansemans Y, Van Nieuwerburgh F, Deforce D, Goethals K, De Spiegelaere W, and Leybaert L (2024). Baselining physiological parameters in three muscles across three equine breeds. What can we learn from the horse?. Frontiers in Physiology, 15: 1291151. DOI: https://www.doi.org/10.3389/fphys.2024.1291151

DeNotta S and McFarlane D (2023). Immunosenescence and inflammaging in the aged horse. Immunity Ageing, 20(1): 2. DOI: https://www.doi.org/10.1186/s12979-022-00325-5

Gaina CD, Widi A, and Saputra A (2020). Age-sex related in hematological values of sandalwood pony horses (*Equus caballus*) in East Sumba, NTT. Journal of Veterinary and Animal Sciences, 3(2): 103-109. DOI: https://www.doi.org/10.24843/JVAS.2020.v03.i02.p06

Henneke D, Potter G, Kreider J, and Yeates B (1983). Relationship between condition score, physical measurements and body fat percentage in mares. Equine Veterinary Journal, 15(4): 371-372. DOI: https://www.doi.org/10.1111/j.2042-3306.1983.tb01826.x.

Jaworska J, de Mestre AM, Wiśniewska J, Wagner B, Nowicki A, Kowalczyk-Zięba I, and Wocławek-Potocka I (2022). Populations of NK cells and regulatory T cells in the endometrium of cycling mares- A preliminary study. Animals, 12(23): 3373. DOI: https://www.doi.org/10.3390/ani12233373

Lejeune M, Mann S, White H, Maguire D, Hazard J, Young R, Stone C, Antczak D, and Bowman D (2023). Evaluation of fecal egg count tests for effective control of equine intestinal strongyles. Pathogens, 12(11): 1283. DOI: https://www.doi.org/10.3390/pathogens12111283

Lester SJ, Mollat WH, and Bryant JE (2015). Overview of clinical pathology and the horse. Veterinary Clinics: Equine Practice, 31(2): 247-268. DOI: https://www.doi.org/10.1016/j.cveq.2015.04.004

Maśko M, Domino M, Jasiński T, and Witkowska-Piłaszewicz O (2021). The physical activity-dependent hematological and biochemical changes in school horses in comparison to blood profiles in endurance and race horses. Animals, 11(4): 1128. DOI: https://www.doi.org/10.3390/ani11041128

Miller AB, Loynachan AT, Barker VD, and Adams AA (2021). Investigation of innate immune function in adult and geriatric horses. Veterinary immunology immunopathology, 235: 110207. DOI: https://www.doi.org/10.1016/j.vetimm.2021.110207

Mohammedsalih KM, Hassan SA, Juma FR, Saeed SI, Bashar A, von Samson-Himmelstjerna G, Krücken J, and Vectors (2025). Comparative assessment of mini-FLOTAC, McMaster and semi-quantitative flotation for helminth egg examination in camel faeces. Parasites Vectors, 18(5): 1-18. DOI: https://www.doi.org/10.1186/s13071-024-06637-3

Nielsen MK (2021). What makes a good fecal egg count technique?. Veterinary Parasitology, 296: 109509. DOI: https://www.doi.org/10.1016/j.vetpar.2021.109509

Rate IMB, Suwiti NK, Suardana IBK, and Besung INK (2025). Effects of gender and age on immunoglobulin M profile of sumbawa horses raised in the traditional grazing system. Farm Animal Health Nutrition, 4(1): 1-5. DOI: https://www.doi.org/10.58803/fahn.v4i1.65

Rhodes AD, Wilkins PA, and McCoy AM (2024). Comparison of plasma l-lactate between jugular and cephalic veins in healthy and systemically ill horses using a point-of-care device. Journal of Veterinary Emergency Critical Care, 34(2): 131-134. DOI: https://www.doi.org/10.1111/vec.13364

Schaefer E, Edman J, and Magdesian K (2024). Comparison of hematologic variables among Warmbloods, Thoroughbreds, and Western stock horse breeds. Veterinary Clinical Pathology, 53(2): 179-185. DOI: https://www.doi.org/10.1111/vcp.13343

Sciarra F, Campolo F, Franceschini E, Carlomagno F, and Venneri MA (2023). Gender-specific impact of sex hormones on the immune system. International Journal of Molecular Sciences, 24(7): 6302. DOI: https://www.doi.org/10.3390/ijms24076302

Silva G, Queiroga F, Ferreira M, Andrade D, and Silvestre-Ferreira AC (2023). Establishment of reference intervals of hematological parameters and evaluation of sex and age effect in the Miranda donkey. Animals, 13(14): 2331. DOI: https://www.doi.org/10.3390/ani13142331

Sukri A, Dewi IN, Primawati SN, Wangiyana I, Muttaqin Z, and Winaya A (2022). Revealing the genetic diversity of Sumbawa endemic horse using microsatellite-based DNA fingerprint. Biodiversitas, 23(8): 4152-4158. DOI: https://www.doi.org/10.13057/biodiv/d230837

Walton RM and Lawson CA (2021). Equine hematology. In: R. L. Cowell (Editor), Equine hematology, cytology, and clinical chemistry, 2nd Edition. Wiley Online Library, pp. 9-26. DOI: https://www.doi.org/10.1002/9781119500186.ch2

Publisher's note: Scienceline Publication Ltd. remains neutral with regard to jurisdictional claims in published maps and institutional affiliations.

Open Access: This article is licensed under a Creative Commons Attribution 4.0 International License, which permits use, sharing, adaptation, distribution and reproduction in any medium or format, as long as you give appropriate credit to the original author(s) and the source, provide a link to the Creative Commons licence, and indicate if changes were made. The images or other third party material in this article are included in the article's Creative Commons licence, unless indicated otherwise in a credit line to the material. If material is not included in the article's Creative Commons licence and your intended use is not permitted by statutory regulation or exceeds the permitted use, you will need to obtain permission directly from the copyright holder. To view a copy of this licence, visit https://creativecommons.org/licenses/by/4.0/.
© The Author(s) 2025

2025, Scienceline Publication
World's Veterinary Journal
World Vet J, 15(4): 1015-1023.
ISSN 2322-4568

DOI: https://dx.doi.org/10.54203/scil.2025.wvj103
PII: S232245682500103-15

Risk Factors Associated with Conception Rate in Holstein and Lai Sind Crossbred Cows in Small Holding Farms in Vietnam

Nguyen Van Thanh, Do Thi Kim Lanh, Nguyen Hoai Nam, and Bui Van Dung*

Department of Animal Surgery and Theriogenology, Faculty of Veterinary Medicine, Vietnam National University of Agriculture, Trau Quy Town, Gia Lam District, Ha Noi, Viet Nam

*Corresponding author's Email: bvdung@vnua.edu.vn

ORIGINAL ARTICLE
Received: October 08, 2025
Revised: November 10, 2025
Accepted: December 05, 2025
Published: December 31, 2025

ABSTRACT

Reproductive efficiency is a critical factor in smallholder dairy systems, where management limitations often reduce fertility. Identifying factors influencing conception is essential to improving breeding performance in crossbred dairy cows raised in smallholder farms. The present study aimed to identify reproductive and management-related risk factors influencing conception rates in Holstein × Lai Sind crossbred cows at smallholder farms in Northern Vietnam. A retrospective analysis was conducted to evaluate the effects of ovarian disorders, estrus detection timing, age, parity, body condition score (BCS), calving-to-service interval, artificial insemination (AI) order, month of service, and age at first AI on conception rates in 433 cows. Farms were selected based on their willingness to participate, including a total of 40 smallholder farms in Northern Vietnam. Cows were included only if they had complete records on estrus detection, insemination, and pregnancy diagnosis; cows with missing or inconsistent data were excluded. Data was collected from the farm database and direct observation by trained personnel. Univariate analysis identified parity, age, age at first AI, month of AI, and BCS as significant factors influencing conception rates. The overall conception rate was 45.6%. Cows inseminated during December-January had a higher conception rate (52.9%) compared with those inseminated in September-October (37.7%). Heifers exhibited the highest conception rate (55.7%), while cows in parity 2 and parity 4-8 had significantly reduced fertility (37.6% and 42.0%, respectively). In the multivariate logistic regression model, parity and age at first AI were the most influential predictors of reproductive performance in Holstein crossbred cows. Cows first inseminated at 13-15 months, 16-17 months, and older than 17 months had significantly higher conception rates than those inseminated at 8-12 months. The present study demonstrated that both physiological factors (age, parity, and BCS) and seasonal management conditions (month of service) influence conception in Holstein × Lai Sind crossbred cows under smallholder conditions.

Keywords: Artificial insemination, Body condition, Month of service, Smallholder

INTRODUCTION

Reproductive performance is a fundamental factor of economic efficiency in dairy farming. Among several reproductive metrics, conception rate is a critical parameter influencing the number of calves born, the calving interval, and overall milk production, thereby affecting farm profitability (Ehsanollah et al., 2021; Ukita et al., 2022). Globally, dairy herds have experienced a decline in conception rates due to multifactorial influences, including increased metabolic stress associated with high milk production, suboptimal estrus detection, nutritional deficiencies, heat stress, and reproductive tract disorders (Lucy, 2007; Huang et al., 2009; Lee et al., 2024). Despite progress in reproductive management, achieving optimal conception rates is difficult because bovine fertility involves many factors (Kim and Jeong, 2018; Souames and Berrama, 2020). In Vietnam, fertility in dairy cows is strongly affected by smallholder production systems with limited access to advanced reproductive technologies such as estrus synchronization, sexed semen, and embryo transfer. Furthermore, dependence on visual estrus detection, inconsistent feeding practices, and seasonal heat stress substantially undermine reproductive efficiency (Nguyen-Kien et al., 2017). Understanding how these regional management conditions interact with genetic and physiological factors is therefore essential for improving reproductive outcomes in Vietnamese dairy herds.

To cite this paper: Thanh NV, Lanh DTK, Nam NH, and Dung BV (2025). Risk Factors Associated with Conception Rate in Holstein and Lai Sind Crossbred Cows in Small Holding Farms in Vietnam. *World Vet. J.*, 15(4): 1015-1023. DOI: https://dx.doi.org/10.54203/scil.2025.wvj103

Fertility in dairy cows is highly sensitive to seasonal conditions, particularly in regions where ambient temperatures regularly exceed optimal thresholds (Tep et al., 2020; Ruelle et al., 2021; Otava et al., 2021). Heat stress disrupts the hypothalamic-pituitary-adrenal axis, leading to increased fetal cortisol release, reduced conception rate, higher embryonic loss, delayed ovulation, and impaired reproductive efficiency (O'Sullivan et al., 2020; Ferag et al., 2024). Additionally, high temperatures can compromise placental function and fetal development, intensifying reproductive losses (Davidson et al., 2021). Moreover, heat stress in dairy cows delays follicle selection, weakens dominant follicle development, and reduces progesterone concentrations, leading to abnormal oocyte maturation, implantation failure, and increased risk of early embryonic death (Khodaei-Motlagh et al., 2011). These findings highlighted the importance of considering environmental heat stress when assessing fertility limitations in Vietnamese dairy herds.

Parity is another crucial factor affecting conception rate, as higher parity cows often exhibit reduced fertility due to accumulated physiological stress and reproductive tract changes (Vieira-Neto et al., 2017; Senbeta et al., 2024). Several studies have indicated that parity significantly affects different reproductive parameters, including calving interval, days open, services per conception, and milk production (Kim et al., 2009; Senbeta et al., 2024). Moreover, cow age plays a pivotal role in reproductive efficiency, with younger cows experiencing shorter postpartum anestrus and a faster resumption of ovarian cyclicity than older cows (Hossain et al., 2021). Additionally, body condition score (BCS) and nutritional status, including energy balance, protein intake, and micronutrient adequacy, directly influence gonadotropin secretion, luteal function, and follicular development, thereby significantly impacting reproductive performance (Horn et al., 2022; McCarthy et al., 2022; Briano et al., 2024; Claramunt et al., 2024). These factors emphasize the need for integrated management strategies that balance nutrition, parity structure, and reproductive physiology to optimize fertility in dairy herds.

Although extensive studies have been conducted globally on factors affecting conception rate in dairy cattle, studies focusing on Holstein × Lai Sind crossbred cows in tropical areas remain limited. In tropical regions such as Vietnam, declining conception rate in dairy cattle is influenced by ovarian disorders, environmental factors, and hormonal fluctuations (Long et al., 2022; Thanh et al., 2023). Cows with inactive ovaries have a lower pregnancy chance. Housing conditions, such as ventilation, stocking density, and bedding quality and mineral supplementation (selenium, zinc), can improve estrus expression, ovarian function, and conception rate (Long et al., 2022). In addition, semen quality and artificial insemination (AI) protocols are critical contributors to conception success. Recent evidence has shown that improving the post-thaw quality of cryopreserved bull sperm through extender optimization and antioxidant supplementation can enhance motility, reduce oxidative damage, and significantly increase *in vivo* fertility (Khaki et al., 2018; Borah et al., 2021; Afsar et al., 2024). These findings emphasized that both female reproductive status and semen characteristics should be considered when evaluating fertility outcomes.

This retrospective study aimed to investigate the effects of factors, including ovarian disorders, estrus detection timing, age, parity, BCS, calving-to-service interval (CSI), AI order, month of service, and age at first AI, on conception rate in Holstein × Lai Sind crossbred cows in Northern Vietnam.

MATERIALS AND METHODS

Ethical approval

This retrospective study was based on existing farm production and reproductive records from smallholder dairy farms in Northern Vietnam. No direct interventions, experimental procedures, or animal handling were performed during the present study. All procedures were conducted in accordance with the ethical guidelines for animal research established by the Vietnam National University of Agriculture (Approval No. CARE-2023/06).

Animals and sample size

The required sample size was calculated using G*Power version 3.1.9.7 (Heinrich-Heine-Universität Düsseldorf, Düsseldorf, Germany) for a linear multiple regression model (fixed model, R^2 deviation from zero, Faul et al., 2009). An effect size of 0.06 was selected as the minimum detectable effect size. With a significance level of $\alpha = 0.05$, a desired statistical power of 0.95, and eight predictors in the model, the analysis indicated that a minimum of 387 animals were required (Faul et al., 2009). A total of 433 Holstein × Lai Sind crossbred cows with complete reproductive records from smallholder farms in Bavi, Vietnam, were included in the present study. Cows with incomplete or inconsistent records were excluded. Housing was provided in well-ventilated barns, either in individual or group sections. A total mixed ration consisting of grass silage, rice straw, and concentrate was provided to all cows, formulated to supply approximately 18% of crude protein and 2,550 kcal/kg of metabolizable energy (NRC, 2001), with *ad libitum* access to mineral blocks and clean drinking water. Estrus detection was performed by farm personnel based on the primary sign (standing to be mounted) and secondary signs such as increased activity, mounting, transparent vaginal discharge,

sniffing, licking, or chin-resting (Michaelis et al., 2014). Insemination with frozen-thawed semen was performed according to the a.m./p.m. guideline; cows identified as being in estrus in the morning were inseminated that evening, whereas cows first detected in the evening were inseminated the following morning (Trimberger and Davis, 1943). This method ensures insemination occurs approximately 12 hours after the onset of estrus, optimizing fertility. Pregnancy examination was carried out on day 45 post-insemination using either an ultrasound fitted with a linear probe emitting 7.5 MHz (KX-5200; China) or rectal palpation.

Study design and data collection

Data collection was performed by trained personnel through direct observation and manual recording from farmers' record books. The collected information included cow identification, date of birth, time of estrus detection, cow age, parity, BCS, CSI, AI order (first, second, or ≥ third insemination), month of service (month of AI), and age at first insemination. The study used a purposive sampling approach to include all cows meeting the inclusion criteria, with the final sample size determined by the availability of complete records. The data collection period spanned from November 2023 to April 2024.

The investigated reproductive factors were classified into different categories before analysis. The time of estrus detection was categorized as morning or afternoon. Cow age was divided into three groups, including < 3 years, 3-6 years, and > 6 years. Parity was classified into five groups, including heifer, parity 1, parity 2, parity 3, and parity 4-8. The BCS was categorized into three groups, including ≤ 2.5, 2.75-3, and > 3 (Randall et al., 2015). The CSI was classified into four groups, including < 2 months, 2-3 months, 4-5 months, and >5 months. The AI order was classified into three groups, including first service, second service, and third service onward. The month of service was divided into three categories, including September-October, November, and December-January. Age at first insemination was grouped into four categories, including 8-12 months, 13-15 months, 16-17 months, and >17 months.

Statistical analysis

Logistic regression was performed to examine the potential risk factors for conception rate. At first, univariate analysis was performed to identify the association between different single potential risk factors and conception rate. The independent risk factors included time of estrus detection, age of the cows, parity, BCS, CSI, AI order, month of service, and age at first service. Second, a multivariate logistic regression analysis was conducted to build the final multivariable model that best explained the variation of conception rate. All statistical analyses were performed using IBM SPSS Statistics for Windows, Version 22.0 (IBM Corp., Armonk, NY, 2013). For all analyses, including one-way ANOVA and Student's t-test, a P-value of less than or equal to 0.05 was considered statistically significant.

RESULTS

The overall conception rate was 45.6%. The present results revealed that parity, age, age at first AI, month of AI, and BCS had significant effects on conception rate ($p < 0.05$; Table 1). Conception rates were higher in heifers and cows with a BCS ≤ 2.5 and those inseminated from December to January. However, lower conception rates were observed in cows with parity 2 and 4-8, those older than 6 years, and those inseminated from September to October. Parity and age at first AI had significant effects on conception rate ($p < 0.05$). Fertility significantly declined from the second parity compared to the heifers and first-parity cows ($p < 0.05$). Cows inseminated at older ages (≥ 13 months) exhibited higher conception rates (43.8%) than those inseminated at 8-12 months (24.4%; Table 1). Additionally, age was a contributing factor, with cows over six years of age showing significantly lower fertility than younger cows ($p < 0.05$). The BCS indicated a significant relationship with fertility ($p < 0.05$). Cows having a BCS ≤ 2.5 achieved the highest conception rate (54.3%). In contrast, cows with a moderate BCS (2.75-3.0) demonstrated reduced fertility compared to those having either a lower (≤ 2.5) or higher (> 3.0) BCS. The month of service had a significant impact on conception rate ($p < 0.05$), with cows inseminated from December to January (52.9%) exhibiting markedly higher conception rates than those inseminated in September-October (37.7%). Other variables, including time of estrus detection, CSI, and AI order, did not demonstrate a significant association with conception rate in the univariate analysis ($p > 0.05$).

The multivariate analysis indicated that parity and age at first AI were the most significant factors associated with conception rate ($p < 0.05$; Table 2). Heifers exhibited the highest conception rate (55.7%, 59/106). In comparison to heifers, conception rates were significantly lower in parity 2 (OR = 0.45, $p < 0.05$) and parity 4-8 cows (OR = 0.50, $p < 0.05$). No significant differences in conception rate were observed between parity 1 and parity 3 ($p > 0.05$). Cows inseminated at 13-15 months, 16-17 months, and >17 months had significantly higher conception rates than those inseminated at 8-12 months ($p < 0.05$).

Table 1. The potential risk factors for conception rate in Holstein crossbred cows raised in Northern Vietnam, 2024

Factors	Conception rate	OR (95%CI)	P-value
Time of estrus detection			
Morning	49.8 (137/275)	1	
Afternoon	46.2 (73/158)	0.865(0.59-1.18)	0.469
Age			
<3 years	53.1 (102/192)	1	
3-6 years	48.2 (93/193)	0.821 (0.55-1.22)	0.333
>6 years	32.6 (15/46)	0.43(0.22-0.84)	0.014*
Parity			
Heifer	55.7 (59/106)	1	
Parity 1	46.7 (42/90)	0.70 (0.40-1.23)	0.21
Parity 2	37.6 (35/93)	0.48 (0.27-0.85)	0.012*
Parity 3	60.0 (45/75)	1.20 (0.66-2.18)	0.561
Parity 4-8	42.0 (29/69)	0.58 (0.31-1.07)	0.079
Body condition score			
≤2.5	54.3 (119/219)	1	
2.75-3	40.9 (76/186)	0.58 (0.39-0.86)	0.007*
>3	53.6 (15/29)	0.97 (0.44-2.13)	0.939
Calving to service			
<2 months	48.5 (16/33)	1	
2-3 months	43.2 (38/98)	0.81 (0.36-1.80)	0.602
4-5 months	47.4 (54/114)	0.96 (0.44-2.08)	0.91
>5 months	46.2 (43/93)	0.91 (0.41-2.02)	0.824
AI order			
First service	51.2 (85/166)	1	
Second service	49.3 (75/152)	0.93 (0.60-1.44)	0.74
From the 3rd service onward	43.5 (50/115)	0.73 (0.45-1.18)	0.203
Month of service			
September-October	37.7 (40/106)	1	
November	47.2 (25/53)	1.47 (0.76-2.87)	0.255
December-January	52.9 (145/274)	1.86 (1.17-2.93)	0.008*
Age at first AI			
8-12 months	24.4 (10/41)	1	
13-15 months	43.8 (63/144)	2.41 (1.10-5.29)	0.028*
16-17 months	55.6 (89/160)	3.89 (1.79-8.46)	0.001*
>17 months	54.5 (48/88)	3.72 (1.63-8.51)	0.002*

* Significant difference at the level of $p \leq 0.05$. OR: Odds ratio, CI: Confidence interval

Table 2. The multivariate analysis of potential risk factors for conception rate in Holstein crossbred cows raised in Northern Vietnam, 2024

Factors	OR (95%CI)	P value
Parity		
Heifer	1	
Parity 1	0.69 (0.40-1.24)	0.217
Parity 2	0.45 (0.25-0.81)	0.008*
Parity 3	1.19 (0.64-2.22)	0.575
Parity 4-8	0.5 (0.27-0.94)	0.031*
Age at first AI		
8-12 months	1	
13-15 months	2.41 (1.10-5.29)	0.028*
16-17 months	3.89 (1.79-8.46)	0.001*
>17 months	3.72 (1.63-8.51)	0.002*

* Significant difference at the level of $p \leq 0.05$. OR: Odds ratio, CI: Confidence interval

DISCUSSION

The present investigation noted a marked reduction in conception rates in cows over six years of age, suggesting an age-associated decline in reproductive efficiency. These findings are consistent with several studies conducted by Shorten et al. (2015), Samkange et al. (2019), and Otava et al. (2021). Shorten et al. (2015) reported a notable quadratic effect of cow age on pregnancy rate, with fertility increasing during the early reproductive years and declining as age progressed beyond physiological maturity. Similarly, a decline in conception rates among older dams has been documented in beef cattle by Samkange et al. (2019), as well as in dairy buffalo (Otava et al., 2021). Reproductive efficiency declines more starkly in multiparous cows compared to heifers or primiparous cows, a trend likely attributable to cumulative reproductive stress, heightened metabolic demands, and previously experienced calving-related challenges (Otava et al., 2021). Moreover, age-related reproductive issues have been reported by Hossain et al. (2021), including longer CSI in older cows, further compromising reproductive performance. Beyond physiological aging, genetic background interacts with reproductive performance. In crossbred Holsteins, breed composition and heat-stress adaptability can modify estrous expression and ovarian activity, thereby affecting conception probability. Nutritional interventions, including general supplementation with antioxidants or methyl donors, have been demonstrated to improve thermotolerance and sperm quality in bulls under heat stress (Ijab et al., 2022). These trends are probably driven by biological factors such as decreased oocyte quality (Walters et al., 2002), changes in the uterine environment (Thurmond et al., 2005; López-Gatius, 2012; Figueiredo et al., 2023), accumulating metabolic stresses (Lean et al., 2023), and physiological stresses (López-Helguera et al., 2016), with a notable increase in parity chance. Structural and functional changes in the uterine environment, including reduced uterine tone, increased uterine size, and delayed involution, have become more noticeable with higher parity (López-Helguera et al, 2016), where maternal age is a key factor linked to pregnancy loss (Thurmond et al., 2005; López-Gatius, 2012). These findings are consistent with those of Iwata et al. (2016), who attribute reduced conception rates in cows older than six years to declining oocyte quality.

The current results indicated that parity remarkably affected conception rate, with cows in parities 2-8 having a lower conception chance than heifers and first-parity cows. This pattern suggested that parity affects fertility by altering physiological maturity, metabolic status, and reproductive tract condition throughout the cow's productive lifespan. Jayawardana et al. (2022) reported that first-parity cows, such as Holstein-Friesian × Jersey crossbred, exhibited lower fertility metrics and conception rates. In contrast, third-parity cows demonstrated the highest fertility and conception rates under tropical and subtropical production systems. While the first and third parity groups did not exhibit considerable deviations from heifers, notable reductions were observed in the second and 4-8 parity groups, suggesting a threshold effect. Similarly, conception rates did not increase steadily with higher parity. However, Bhagat and Gokhale (2016) demonstrated that conception rates peaked around the third lactation and then gradually declined in later parities, thereby indicating a physiological threshold effect. The threshold effect describes the point where increasing parity initially enhances fertility up to an optimal level, after which further increases in parity result in a decline (Bhagat and Gokhale, 2016). This pattern supports the present finding that fertility is not linearly related to parity and may peak at intermediate parities. These findings underscored the complex relationship between parity and fertility. Heifers and young cows may require nutritional and hormonal support to achieve optimal reproductive readiness, while older cows may benefit from enhanced monitoring for uterine health, metabolic disorders, and improved estrous detection efficiency.

The present results highlighted the substantial impact of BCS on conception rate in dairy cows raised within smallholder farms in Northern Vietnam, where feeding strategies, heat load, and housing conditions vary considerably among households. The decreased performance in cows with higher BCS might be attributed to metabolic factors such as impaired insulin sensitivity, increased adipose-derived inflammation, and reduced estrous expression, all of which have been associated with diminished reproductive efficiency in dairy cows (Qiao et al., 2024). Since this pattern differs from findings in temperate regions, the present results should be interpreted with caution. Cows with moderate to high BCS might be more susceptible to the adverse effects of environmental conditions, such as heat stress, which could negatively influence ovarian function and estrous expression (Ettema and Santos, 2004). Heat stress might explain the differences observed, as cows with greater body fat tend to dissipate heat less effectively and have higher temperatures in tropical settings (Becker et al., 2020). In tropical or subtropical environments such as Northern Vietnam, cows with lower BCS may experience less thermal changes and maintain more proper metabolic and endocrine conditions (Jayawardana et al., 2022), thereby facilitating timely ovulation and successful fertilization. The present findings contrast with those of Kim and Jeong (2018) in non-tropical regions, where a BCS below 3.0 was associated with lower conception rates. These differences highlighted the critical influence of the regional environment, indicating that the current BCS threshold might not be directly suitable for tropical environmental settings.

The current results demonstrated that the month of service considerably influenced conception rates, with higher success observed in December-January compared to September-October. This seasonal variation suggested that environmental factors, such as temperature and humidity, could affect reproductive physiology (Becker et al., 2020). Supporting this finding, Nguyen-Kien et al. (2017) indicated that conception rates in cows in Vietnam were significantly higher during the cooler months (December–January), when the temperature-humidity index (THI) was at its lowest (76.6-78.6), and substantially lower in September-October, when THI remained elevated (approximately 81.3). The reduced heat stress during December to January might have enhanced estrus expression, improved sperm survival within the female reproductive tract, and promoted optimal uterine conditions. Specifically, a lower THI helps adequate blood flow to the uterus, stabilizes uterine pH, and maintains the endometrium activity, thereby promoting early embryo development and implantation. Previous studies have provided strong evidence supporting the impacts of seasonal factors on fertility. Higher conception rates are correlated with later months in the breeding season, a relationship driven by improved weather conditions (Fenlon et al., 2017). Similarly, high temperature and humidity during warmer months increase THI, leading to decreased estrous expression and impaired oocyte quality (Ferreira et al., 2011). Additionally, conception rates differ notably across seasons, highlighting the vital role of climatic conditions in reproductive performance (Ettema and Santos, 2004; Kuhn et al., 2006). These findings highlighted that environmental stress, especially heat load indicated by THI, can influence reproductive efficiency.

The present findings indicated that cows aged 8-12 months at first AI had lower conception rates, likely due to insufficient uterine and endocrine maturity. Delaying the first AI until at least 16 months might enhance reproductive success. This approach provided economic benefits by reducing the number of inseminations, lowering breeding costs, and ensuring heifers gain adequate body size for the recommended age at first calving. These findings align with those reported by Wathes et al. (2008), Cooke et al. (2013), and Zavadilová and Stípková (2013), suggesting that the optimal age for first calving is 24-25 months. This corresponds to a first AI at approximately 15-16 months, thereby ensuring maximal reproductive efficiency through proper heifer development. Consistent with the present findings, Boulton et al. (2017) reported that first calving before 24 months has been shown to support fertility, reduce rearing costs, and shorten the generation interval. Exposure to multiple estrous cycles before the first AI has been linked to higher estrus expression and improved conception rates (Galvão et al., 2004; Pereira et al., 2014). Ooi et al. (2023) demonstrated that high fertility was associated with improved reproductive performance, including increased submission rates, higher conception to first service, and earlier calving, thereby supporting genetic selection for improved fertility.

CONCLUSION

The present study demonstrated that parity and age at first AI are the most influential factors affecting conception rates in Holstein × Lai Sind crossbred cows under smallholder conditions in Northern Vietnam. Heifers exhibited the highest fertility, while cows in parity 2, parity 4-8, and those older than six years had reduced conception rates. Delaying the first AI to 16 months or later significantly improved fertility, emphasizing the importance of reproductive maturity before breeding. The current results highlighted that optimizing parity management and age at the first AI can enhance reproductive performance in tropical dairy systems. Implementing this approach in Northern Vietnam could boost fertility rates and enhance herd productivity, emphasizing the value of structured heifer breeding programs. However, these findings are based on smallholder conditions in Northern Vietnam and should be validated under different management systems and regions before broader application.

DECLARATIONS

Ethical considerations

The authors declared that this manuscript is original, has not been published elsewhere, and is not under consideration by any other journal. All authors have read and approved the manuscript, confirming adherence to ethical standards concerning authorship, research integrity, data accuracy, and publication consent. No artificial intelligence was used for preparing and writing the current study.

Authors' contributions

Bui Van Dung, Nguyen Van Thanh, and Nguyen Hoai Nam conceived and designed the study. Data collection and statistical analyses were conducted by Bui Van Dung, Nguyen Van Thanh, Do Thi Kim Lanh, and Nguyen Hoai Nam. The first draft of the manuscript was written by Bui Van Dung. All authors contributed to data interpretation, critically revised the manuscript, and approved the final edition for publication.

Availability of data and materials

All data and materials supporting the present study are available from the corresponding author upon reasonable request.

Fundings

The present study was funded by Vietnam National University of Agriculture (Grant No. SV2024-06-36).

Competing interests

The author declared no conflict of interest.

REFERENCES

Afsar M, Soleimanzadeh A, Khaki A, and Ayen E (2024). Improvement of post-thaw quality and *in vivo* fertility of Simmental bull Spermatozoa using ferulic acid. Veterinary Medicine and Science, 10(6): e70064. DOI: https://www.doi.org/10.1002/vms3.70064

Becker CA, Collier RJ, and Stone AE (2020). Invited review: Physiological and behavioral effects of heat stress in dairy cows. Journal of Dairy Science, 103(8): 6751-6770. DOI: http://www.doi.org/10.3168/jds.2019-17929

Bhagat RL and Gokhale SB (2016). Studies on factors influencing conception rate in rural cattle. Indian Journal of Animal Sciences, 86(5): 550-552. DOI: https://www.doi.org/10.56093/ijans.v86i5.58489

Borah B, Deka B, Biswas R, Chakravarty P, Sinha S, Ahmed K, and Deori S (2021). Antioxidants improve semen quality following cryopreservation in Indian yak bulls. Indian Journal of Animal Science, 91(8): 623-627. DOI: https://www.doi.org/10.56093/ijans.v91i8.115918

Boulton AC, Rushton J, and Wathes DC (2017). An empirical analysis of the cost of rearing dairy heifers from birth to first calving and the time taken to repay these costs. Animal, 11(8): 1372-1380. DOI: https://www.doi.org/10.1017/S1751731117000064

Briano C, Meikle A, Velazco JI, and Quintans G (2024). Metabolic and hormonal profiles and productive performance in primiparous and multiparous cows grazing different forage allowance in late gestation. Theriogenology, 227: 68-76. DOI: https://www.doi.org/10.1016/j.theriogenology.2024.07.007

Claramunt M, Meikle A, and Soca P (2024). Direct and carry-over effect of grassland herbage allowance on metabolic hormones and reproduction in primiparous beef cows undergoing temporary weaning and flushing. Animal, 18(9): 101261. DOI: https://www.doi.org/10.1016/j.animal.2024.101261

Cooke JS, Cheng Z, Bourne NE, and Wathes DC (2013). Association between growth rates, age at first calving and subsequent fertility, milk production and survival in Holstein-Friesian heifers. Open Journal of Animal Science, 3(1): 1-12. DOI: http://www.doi.org/10.4236/ojas.2013.31001

Davidson BD, Dado-Senn B, Padilla NR, Fabris TF, Casarotto LT, Ouellet V, Toledo IM, Dahl GE, and Laporta J (2021). Late-gestation heat stress abatement in dairy heifers promotes thermoregulation and improves productivity. Journal of Dairy Science, 104(2): 2357-2368. DOI: https://www.doi.org/10.3168/jds.2020-18998

Ehsanollah S, Pouya R, Risco CA, and Hernandez JA (2021). Observed and expected combined effects of metritis and other postpartum diseases on time to conception and rate of conception failure in first lactation cows in Iran. Theriogenology, 164: 36-41. DOI: https://www.doi.org/10.1016/j.theriogenology.2021.01.016

Ettema JF and Santos JEP (2004). Impact of age at calving on lactation, reproduction, health, and income in first-parity Holsteins on commercial farms. Journal of Dairy Science, 87(8): 2730-2742. DOI: https://www.doi.org/10.3168/jds.S0022-0302(04)73400-1

Faul F, Erfelder E, Buchner A, and Lang AG (2009). Statistical power analysis using GPower 3.1: Tests for correlation and regression analyses. Behavior Research Methods, 41(4): 1149-1160. DOI: https://www.doi.org/10.3758/BRM.41.4.1149

Fenlon C, O'Grady L, Butler S, Doherty ML, and Dunnion J (2017). The creation and evaluation of a model to simulate the probability of conception in seasonal-calving pasture-based dairy heifers. Irish Veterinary Journal, 70: 32. DOI: https://www.doi.org/10.1186/s13620-017-0110-0

Ferag A, Gherissi DE, Khenenou T, Boughanem A, Moussa HH, Kechroud AA, and Fares MA (2024). Heat stress effect on fertility of two imported dairy cattle breeds from different Algerian agro-ecological areas. International Journal of Biometeorology, 68(12): 2515-2529. DOI: https://www.doi.org/10.1007/s00484-024-02761-y

Ferreira RM, Ayres H, Chiaratti MR, Ferraz ML, Araújo AB, Rodrigues CA, Watanabe YF, Vireque AA, Joaquim DC, Smith LC et al. (2011). The low fertility of repeat-breeder cows during summer heat stress is related to a low oocyte competence to develop into blastocysts. Journal of Dairy Science, 94(5): 2383-2392. DOI: https://www.doi.org/10.3168/jds.2010-3904

Figueiredo CC, Balzano-Nogueira L, Bisinotto DZ, Ruiz AR, Duarte GA, Conesa A, Galvão KN, and Bisinotto RS (2023). Differences in uterine and serum metabolome associated with metritis in dairy cows. Journal of Dairy Science, 106(5): 3525-3536. DOI: https://www.doi.org/10.3168/jds.2022-22552

Galvão KN, Santos JEP, Juchem SO, Cerri RLA, Coscioni AC, and Villaseñor M (2004). Effect of addition of a progesterone intravaginal insert to a timed insemination protocol using estradiol cypionate on ovulation rate, pregnancy rate, and late embryonic loss in lactating dairy cows. Journal of Animal Science, 82: 3508-3517. DOI: https://www.doi.org/10.2527/2004.82123508x

Horn EJ, Read CC, Edwards JL, Schrick FN, Rhinehart JD, Payton RR, Campagna SR, Klabnik JL, Clark HM, and Myer PR (2022). Preovulatory follicular fluid and serum metabolome profiles in lactating beef cows with thin, moderate, and obese body condition. Journal of Animal Science, 100(7): skac152. DOI: https://www.doi.org/10.1093/jas/skac152

Hossain MS, Rahman MA, Bari FY, and Bhuiyan MMU (2021). Factors affecting calving to service interval in crossbred Friesian cows in a large dairy farm. Bangladesh Veterinarian, 38(1-2): 33-41. DOI: https://www.doi.org/10.3329/bvet.v38i1-2.63675

Huang C, Tsuruta S, Bertrand JK, Misztal I, Lawlor TJ, and Clay JS (2009). Trends for conception rate of Holsteins over time in the southeastern United States. Journal of Dairy Science, 92(9): 4641-4647. DOI: https://www.doi.org/10.3168/jds.2008-1982

Ijab R, Ayen E, Khaki A, and Soleimanzadeh A (2022). Evaluation of dietary betaine on post-thawed semen quality in mature bulls during summer heat stress. Veterinary Research Forum, 13(1): 61-70. DOI: https://www.doi.org/10.30466/vrf.2020.124845.2927

Iwata H (2016). Age-associated events in bovine oocytes and possible countermeasures. Reproductive Medicine and Biology, 15(3): 155-164. DOI: https://www.doi.org/10.1007/s12522-015-0233-5

Jayawardana JMDR, Lopez-Villalobos N, McNaughton LR, and Hickson RE (2022). Fertility of dairy cows milked once daily or twice daily in New Zealand. Journal of Dairy Science, 105(11): 8911-8923. DOI: https://www.doi.org/10.3168/jds.2021-20946

Khaki A, Araghi A, Nourian A, and Lotfi M (2018). Evaluating the potential relationship between semen quality parameters and serum catalase, superoxide dismutase, and glutathione peroxidase in bulls. Caspian Journal of Reproductive Medicine, 4(2): 1-9. Available at: http://caspjrm.ir/article-1-141-en.html

Khodaei-Motlagh M, Shahneh AZ, Masoumi R, and Derensis F (2011). Alterations in reproductive hormones during heat stress in dairy cattle. African Journal of Biotechnology, 10(29): 5552-5558. Available at: https://www.academicjournals.org/AJB

Kim BH, Lee SK, Kim IH, and Kang HG (2009). The effect of parity and calving seasons on the reproductive performance of Korean native cows. Journal of Embryo Transfer, 24(2): 127-130. Available at: https://koreascience.kr/article/JAKO200926158875125.pdf

Kim IH and Jeong JK (2018). Risk factors limiting first service conception rate in dairy cows and their economic impact. Asian-Australasian Journal of Animal Sciences, 32(4): 519-526. DOI: https://www.doi.org/10.5713/ajas.18.0296

Kuhn MT, Hutchison JL, and Wiggans GR (2006). Characterization of Holstein heifer fertility in the United States. Journal of Dairy Science, 89(12): 4907-4920. DOI: https://www.doi.org/10.3168/jds.S0022-0302(06)72541-3

Lean IJ, LeBlanc SJ, Sheedy DB, Duffield T, Santos JEP, and Golder HM (2023). Associations of parity with health disorders and blood metabolite concentrations in Holstein cows in different production systems. Journal of Dairy Science, 106(1): 500-518. DOI: https://www.doi.org/10.3168/jds.2021-21673

Lee JG, Seo J, Alam M, Song H, Lee S, Cho J, Dang CG, and Lee J (2024). Estimation of genetic parameters for reproductive traits in Korean dairy cattle. Animal Bioscience, 38(1): 33-40. DOI: https://www.doi.org/10.5713/ab.24.0455

Long ST, Toan NC, Gioi PV, and Hang PT (2022). Factors associated with the odds of pregnancy for dairy cattle after treatment of ovarian disorders in Northern Vietnam. Tropical Animal Science Journal, 45(3): 277-283. DOI: https://www.doi.org/10.5398/tasj.2022.45.3.277

López-Gatius F (2012). Factors of a noninfectious nature affecting fertility after artificial insemination in lactating dairy cows: A review. Theriogenology, 77(6): 1029-1041. DOI: https://www.doi.org/10.1016/j.theriogenology.2011.10.014

López-Helguera I, Colazo MG, Garcia-Ispierto I, and López-Gatius F (2016). Factors associated with ovarian structures and intrauterine fluid in the postpartum period in dairy cows. Journal of Dairy Science, 99(5): 3925-3933. DOI: https://www.doi.org/10.3168/jds.2015-10615

Lucy MC (2007). Fertility in high-producing dairy cows: Reasons for decline and corrective strategies for sustainable improvement. Society for Reproduction and Fertility Supplement, 64: 237-254. DOI: https://www.doi.org/10.5661/rdr-vi-237

McCarthy MC, Mee JF, McAloon CG, and O'Grady L (2022). A comparison of the age at first calving of contract-reared versus home-reared replacement dairy heifers. Theriogenology, 181: 105-112. DOI: https://www.doi.org/10.1016/j.theriogenology.2022.01.018

Michaelis I, Burfeind O, and Heuwieser W (2014). Evaluation of oestrous detection in dairy cattle comparing an automated activity monitoring system to visual observation. Reproduction in Domestic Animals, 49(4): 621-628. DOI: https://www.doi.org/10.1111/rda.12337

National research council (NRC) (2001). Nutrient requirements of dairy cattle, 7th Revised Edition. National Academy Press, Washington, D. C., USA. Available at: https://guelphdhmcp.ca/wp-content/uploads/2018/03/NRC-2001.pdf

Nguyen-Kien C, Van Khanh N, and Hanzen C (2017). Study on reproductive performance of Holstein x Lai Sind crossbred dairy heifers and cows at smallholdings in Ho Chi Minh City, Vietnam. Tropical Animal Health and Production, 49: 483-489. DOI: https://www.doi.org/10.1007/s11250-016-1217-0

Ooi E, Stevenson MA, Goddard ME, Beggs DS, Mansell PD, Pryce JE, and Pyman MF (2023). Validating the female fertility estimated breeding value in Australian commercial dairy herds. Journal of Dairy Science, 106(5): 3376-3396. DOI: https://www.doi.org/10.3168/jds.2022-21955

O'Sullivan M, Butler ST, Pierce KM, Crowe MA, O'Sullivan K, Fitzgerald R, and Buckley F (2020). Reproductive efficiency and survival of Holstein-Friesian cows of divergent Economic Breeding Index, evaluated under seasonal calving pasture-based management. Journal of Dairy Science, 103(2): 1685-1700. DOI: https://www.doi.org/10.3168/jds.2019-17374

Otava G, Squicciarini S, Marc S, Suici T, William Onan G, Hutu I, Torda I, and Mircu C (2021). Effects of age and season on conception rate of Mediterranean Italian Dairy Buffalo (*Bubalus bubalis*) following oestrus synchronization and fixed-time artificial insemination. Reproduction in Domestic Animals, 56(12): 1511-1518. DOI: https://www.doi.org/10.1111/rda.14013

Pereira MHC, Rodrigues ADP, De Carvalho RJ, Wiltbank MC, and Vasconcelos JLM (2014). Increasing the length of an estradiol and progesterone timed artificial insemination protocol decreases pregnancy losses in lactating dairy cows. Journal of Dairy Science, 97(3): 1454-1464. DOI: https://www.doi.org/10.3168/jds.2013-7287

Qiao K, Jiang R, Contreras GA, Xie L, Pascottini OB, Opsomer G, and Dong Q (2024). The complex interplay of insulin resistance and metabolic inflammation in transition dairy cows. Animals, 14(6): 832. DOI: https://www.doi.org/10.3390/ani14060832

Randall LV, Green MJ, Chagunda MGG, Mason C, Archer SC, Green LE, and Huxley JN (2015). Low body condition predisposes cattle to lameness: An 8-year study of one dairy herd. Journal of Dairy Science, 98(6): 3766-3777. DOI: https://www.doi.org/10.3168/jds.2014-8863

Ruelle E, Shalloo L, and Butler ST (2021). Economic impact of different strategies to use sex-sorted sperm for reproductive management in seasonal-calving, pasture-based dairy herds. Journal of Dairy Science, 104(11): 11747-11758. DOI: https://www.doi.org/10.3168/jds.2021-20150

Samkange A, Kandiwa E, Mushonga B, Bishi A, Muradzikwa E, and Madzingira O (2019). Conception rates and calving intervals of different beef breeds at a farm in the semi-arid region of Namibia. Tropical Animal Health and Production, 51: 1829-1837. DOI: https://www.doi.org/10.1007/s11250-019-01876-4

Senbeta EK, Abebe AS, and Gibe AW (2024). Effect of parity on service per conception, gestation length, milk yield, calving interval, and calf birth weight of crossbred dairy cows. Archives of Veterinary Science, 29(2): 1-7. DOI: https://www.doi.org/10.5380/avs.v29i2.94325

Shorten PR, Morris CA, and Cullen NG (2015). The effects of age, weight, and sire on pregnancy rate in cattle. Journal of Animal Science, 93(4): 1535-1545. DOI: https://www.doi.org/10.2527/jas.2014-8490

Souames S and Berrama Z (2020). Factors affecting conception rate after the first artificial insemination in a private dairy cattle farm in North Algeria. Veterinary World, 13(12): 2608-2611. DOI: https://www.doi.org/10.14202/vetworld.2020.2608-2611

Tep B, Morita Y, Matsuyama S, Ohkura S, Inoue N, Tsukamura H, Uenoyama Y, and Pheng V (2020). Seasonal changes in the reproductive performance in local cows receiving artificial insemination in the Pursat province of Cambodia. Asian-Australasian Journal of Animal Sciences, 33(12): 1922-1929. DOI: https://www.doi.org/10.5713/ajas.19.0893

Thanh NV, Hang PT, Gioi PV, Toan NC, and Long ST (2023). The relationship between plasma progesterone concentration on day 6 after artificial insemination and pregnancy rate of dairy cows in Vietnam. Tropical Animal Science Journal, 46(2): 146-150. DOI: https://www.doi.org/10.5398/tasj.2023.46.2.146

Thurmond MC, Branscum AJ, Johnson WO, Bedrick EJ, and Hanson TE (2005). Predicting the probability of abortion in dairy cows: a hierarchical Bayesian logistic-survival model using sequential pregnancy data. Preventive Veterinary Medicine, 68(2-4): 223-239. DOI: https://www.doi.org/10.1016/j.prevetmed.2005.01.008

Trimberger GW and Davis H (1943). Conception rate in dairy cattle by artificial insemination at various stages of estrus. Historical Research Bulletins, Nebraska Agricultural Experiment Station, 47: 1-14. Available at: https://core.ac.uk/download/pdf/188111066.pdf

Ukita H, Yamazaki T, Yamaguchi S, Abe H, Baba T, Bai H, Takahashi M, and Kawahara M (2022). Environmental factors affecting the conception rates of nulliparous and primiparous dairy cattle. Journal of Dairy Science, 105(8): 6947-6955. DOI: https://www.doi.org/10.3168/jds.2022-21948

Vieira-Neto A, Galvão KN, Thatcher WW, and Santos JEP (2017). Association among gestation length and health, production, and reproduction in Holstein cows and implications for their offspring. Journal of Dairy Science, 100(4): 3166-3181. DOI: https://www.doi.org/10.3168/jds.2016-11867

Walters AH, Bailey TL, Pearson RE, and Gwazdauskas FC (2002). Parity-related changes in bovine follicle and oocyte populations, oocyte quality, and hormones to 90 days postpartum. Journal of Dairy Science, 85(4): 824-832. DOI: https://www.doi.org/10.3168/jds.S0022-0302(02)74142-8

Wathes DC, Brickell JS, Bourne NE, Swali A, and Cheng Z (2008). Factors influencing heifer survival and fertility on commercial dairy farms. Animal, 2(8): 1135-1143. DOI: https://www.doi.org/10.1017/S1751731108002322

Zavadilová L and Stípková M (2013). Effect of age at first calving on longevity and fertility traits for Holstein cattle. Czech Journal of Animal Science, 58(2): 47-57. DOI: http://www.doi.org/10.17221/6614-CJAS

Publisher's note: Scienceline Publication Ltd. remains neutral with regard to jurisdictional claims in published maps and institutional affiliations.

Open Access: This article is licensed under a Creative Commons Attribution 4.0 International License, which permits use, sharing, adaptation, distribution and reproduction in any medium or format, as long as you give appropriate credit to the original author(s) and the source, provide a link to the Creative Commons licence, and indicate if changes were made. The images or other third party material in this article are included in the article's Creative Commons licence, unless indicated otherwise in a credit line to the material. If material is not included in the article's Creative Commons licence and your intended use is not permitted by statutory regulation or exceeds the permitted use, you will need to obtain permission directly from the copyright holder. To view a copy of this licence, visit https://creativecommons.org/licenses/by/4.0/.
© The Author(s) 2025

2025, Scienceline Publication
World's Veterinary Journal
World Vet J, 15(4): 1024-1033.
ISSN 2322-4568

DOI: https://dx.doi.org/10.54203/scil.2025.wvj104
PII: S232245682500104-15

Effects of Fresh Celery as a Natural Curing Agent on Physicochemical Characteristics and Sensory Quality of Beef Jerky

Nurafni Mallu[1], Wahniyathi Hatta[2]*, and Fatma Maruddin[2]

[1]*Graduate Student of Animal Science and Technology, Faculty of Animal Science, Hasanuddin University, Makassar, 90245, Indonesia*
[2]*Department of Animal Productions, Faculty of Animal Science, Hasanuddin University, Makassar, 90245, Indonesia*

*Corresponding author's Email: wahnihatta@gmail.com

ORIGINAL ARTICLE
Received: September 20, 2025
Revised: October 23, 2025
Accepted: November 19, 2025
Published: December 31, 2025

ABSTRACT

Beef jerky is a processed meat product. Nitrite or nitrate salts are usually used as curing agents for beef jerky processing. However, excessive nitrite intake can pose health risks and raise public concern, so natural alternatives such as celery can be used. This study evaluated fresh celery as a natural curing agent for beef jerky based on its physicochemical and sensory qualities. The study was conducted in two stages. In the first stage, beef was treated with celery at three levels (2%, 4%, and 6%) and saltpeter as a control, combined with three incubation periods (1, 2, and 3 hours) to identify the optimal treatment for the subsequent stage based on color characteristics and nitrite residue. In the second stage, the selected curing treatments (saltpeter, 4% celery, and 6% celery) were applied to beef jerky and evaluated over different storage periods (0, 2, and 4 weeks). The parameters analyzed included color values, lightness (L*), redness (a*), yellowness (b*), nitrite content, and lipid oxidation, as well as sensory attributes. The results of the first stage showed that the use of saltpeter produced the highest nitrite content (0.54 mg/kg), while the highest b* value was obtained in the treatment of 4% and 6% celery. The incubation length had no significant effect on all parameters, but there was a significant interaction between the type of curing material and the length of incubation on the value of a*. In the second stage, neither curing material treatment nor storage time had a significant impact on organoleptic characteristics, and Thiobarbituric acid reactive substances values were relatively low (< 0.5 mg MDA/kg) up to 4 weeks of storage. A 6% celery treatment yielded the highest L* value, while the highest a* value was indicated by saltpeter, followed by 6% and 4% celery. Overall, the 6% celery treatment showed comparable performance to saltpeter, especially in retaining redness, suppressing lipid oxidation, and maintaining the sensory qualities of ground beef jerky.

Keywords: Beef jerky, Celery leaf, Meat quality, Natural curing, Residual nitrite

INTRODUCTION

Beef jerky is one of the oldest processed meat products that is traditionally processed through a preservation process. The curing process usually uses synthetic nitrites from sodium nitrite or potassium nitrate (commonly called saltpeter), which plays a role in forming a simple, antibacterial, red color and produces the distinctive taste and aroma of preserved meat products (Kim et al., 2014). However, excessive nitrite intake has been reported to negatively affect human health due to the formation of carcinogenic N-nitroso compounds (Ferysiuk and Wójciak, 2020). These health concerns, along with growing consumer demand for clean-labeled meat products, have encouraged researchers to investigate natural alternatives to synthetic nitrites. Several natural ingredients have shown potential as nitrite substitutes in meat products, including celery (Li et al., 2011), parsley (Riel et al., 2017), cranberry (Karwowska et al., 2017), and beet root (Sucu and Turp, 2018).

Celery is one of the alternative natural ingredients to replace synthetic nitrites because of its high nitrate content, especially in the leaves. The nitrate content in celery can be converted to nitrite through controlled incubation (Sebranek, 2007; Saputro, 2017). Celery powder and juice have been reported to improve the redness of processed meat without compromising overall consumer acceptability compared to conventionally cured products (Ramachandraiah and Chin, 2022).

Despite being of natural origin, the use of celery as a curing agent also presents challenges, including the potential formation of nitrosamines, especially in meat products processed at high temperatures, such as beef jerky (Oral et al., 2024). During storage, lipid oxidation in beef jerky can produce Malondialdehyde (MDA), a major secondary oxidation product of polyunsaturated fatty acids. MDA is widely used as an indicator of lipid oxidation in meat because even at low concentrations, it can lead to rancid odor development (Domínguez et al., 2019). The antioxidant properties of celery may help mitigate such oxidative degradation (Hassanen et al., 2015).

To cite this paper: Mallu N, Hatta W, and Maruddin F (2025). Effects of Fresh Celery as a Natural Curing Agent on Physicochemical Characteristics and Sensory Quality of Beef Jerky. *World Vet. J.*, 15(4): 1024-1033. DOI: https://dx.doi.org/10.54203/scil.2025.wvj104

Several previous studies have used celery as a curing ingredient in various processed meat products, such as ham slices, pork patties, pork sausage, and cold-smoked sausage (Horch et al., 2014; Sucu et al., 2018; Eisinaitė et al., 2020). Specific investigations on the use of fresh celery leaves in ground beef jerky remain limited. Beef jerky has unique processing characteristics and oxidative susceptibility during storage, thus requiring further study. Therefore, the present study aimed to evaluate the potential of fresh celery leaves (*Apium graveolens*) as a natural source of nitrite to replace synthetic nitrites in ground beef jerky, and to assess their effects on physicochemical properties (color, nitrite residue, lipid oxidation) and sensory attributes as indicators of animal product quality.

MATERIALS AND METHODS

Ethical approval

This study involved sensory evaluation by human panelists who assessed non-edible attributes of beef jerky samples. No tasting or ingestion was performed. All panelists participated voluntarily after being informed about the procedure. This study did not involve live animals; beef samples were obtained from halal-certified Antang slaughterhouses in Makassar, South Sulawesi, Indonesia. This study has been carried out in accordance with the applicable ethical guidelines at Hasanuddin University, Indonesia.

Time and place of study

This study was conducted from July to September 2024. Nitrite residue testing was carried out at the Health Laboratory Center in Makassar in August 2024, Makassar, Indonesia. Color testing (L,a,b*), Thiobarbituric acid reactive substances (TBARS) value analysis, and organoleptic evaluation were conducted from July to September 2024 at the Meat and Egg Product Processing Laboratory, Faculty of Animal Science, Hasanuddin University, Makassar, Indonesia.

Study design

The study was conducted in two phases**.** Phase 1 focused on optimizing the celery leaf level and incubation time to determine the optimal concentration of celery leaves and the incubation time required to generate sufficient nitrite levels and achieve the desired meat color prior to jerky processing. The study employed a complete randomized design (CRD) in a factorial arrangement consisting of two factors. The first factor, the curing ingredient, consists of four treatment groups, including control (C0) with 0.03% saltpeter and celery leaves at 2% (C1), 4% (C2), and 6% (C3). The second factor was incubation time, consisting of 1, 2, and 3 hours. Each treatment combination was replicated three times, yielding a total of 36 experimental units. The parameters observed at this stage included color (Fadlilah et al., 2022) and nitrite content (SNI, 1992).

Phase 2 focused on evaluating the quality of ground beef jerky during storage. This phase assessed the effects of celery leaf application, under the optimal conditions determined in Phase 1, on the quality and stability of ground beef jerky during storage. A completely randomized design (CRD) in a factorial arrangement with two factors was employed. The first factor was the curing ingredient, consisting of three treatment groups, including Control (C0), 4% celery (C2), and 6% celery (C3), selected based on the result of phase 1. The second factor was storage duration, consisting of 0, 2, and 4 weeks. Each combination was replicated three times, resulting in a total of 27 experimental units. The parameters observed in this phase included color (Fadlilah et al., 2022), lipid oxidation (Apriyantono et al., 1989), and sensory attributes (Sugiarto and Marfuah, 2023).

Celery leaf preparation and incubation

The preparation of celery leaves as a curing agent is carried out based on the method of Saputro et al. (2016a) with several modifications. Fresh celery leaves (Apium graveolens) are obtained from Pasar Daya, Makassar, Indonesia, and are selected based on their ripeness level and uniform quality. Celery leaves are then washed using running water to remove dirt and dust, drained, and then weighed according to the predetermined treatment levels (2%, 4%, and 6%). Weighing was carried out by the ratio of celery weight to beef weight (weight/weight [w/w]). The weighed celery leaves are added with clean water in a ratio of 5:1, then mashed using a blender (Cosmos, Indonesia) until a homogeneous paste is formed.

The celery paste is applied evenly to the surface of the beef according to the treatment. Four treatments were used in this stage, namely control with saltpeter (potassium nitrate; brand Koepoe-Koepoe sourced from the local supermarket) and three celery treatments (2%, 4%, and 6%). All samples were then incubated at room temperature (± 32°C) for 1, 2, or 3 hours, depending on the treatment group. The incubation process aims to activate the natural nitrate reductase enzyme contained in celery, thereby facilitating the conversion of nitrate into nitrite through microbial activity.

Jerky preparation

The production of beef jerky in this study refers to the modified method of Saputro et al. (2016b), with the formulation of ingredients following the study of Suryati et al. (2014) as shown in Table 1. The beef that has been cut to a uniform size is treated with curing ingredients (0%, 4%, and 6%), and each treatment is made three times to produce 9 sample units, then incubated for 2 hours at room temperature (± 32°C). After incubation, the meat is ground using a food processor (Cosmos, India) with spices until a homogeneous dough is obtained. The dough is then shaped into sheets with a thickness of about 2.2 mm and dried using a food dehydrator (Getra, China) at 75 °C for 4 hours on each side.

Table 1. Formulation of ground beef jerky

Treatment / Ingredient	C0		C1		C2		C3	
	(%)	Weight (g)	(%)	Weight (g)	(%)	Weight (g)	(%)	Weight (g)
Beef		1000		1000		1000		1000
Salt	2.5	25	2.5	25	2.5	25	2.5	25
Galangal	8.5	85	8.5	85	8.5	85	8.5	85
Coriander	2.0	10	2.0	10	2.0	10	2.0	10
sGarlic	10	50	10	50	10	50	10	50
Palm sugar	16.5	165	16.5	165	16.5	165	16.5	165
White sugar	16.5	165	16.5	165	16.5	165	16.5	165
Tamarind	0.3	3	0.3	3	0.3	3	0.3	3
Pepper	0.3	3	0.3	3	0.3	3	0.3	3
Saltpeter	0.03	0.3	-	-	-	-	-	-
Celery leaves	-	-	2	20	4	40	6	60

C0: 0.03% saltpeter, C1: 2% celery leaves, C2: 4% celery leaves, C3: 6% celery leaves.

Physicochemical analysis

Nitrite content

Nitrite content analysis was conducted at the Central Public Health Laboratory (BBLK), Makassar, in August 2024, following the Indonesian National Standard method for nitrite determination in food products (SNI 01-2894-1992). Samples were extracted using hot water, followed by protein precipitation, after which the nitrite was reacted with sulfanilamide and the reagent N-1-naphthyl ethylenediamine dihydrochloride (NED) to form a pink azo dye, and the absorbance was measured spectrophotometrically to quantify nitrite concentration using a standard calibration curve as specified in the SNI method.

Lipid oxidation

Lipid oxidation in the samples was assessed by measuring malondialdehyde (MDA) levels using the (thiobarbituric acid) TBA assay, as described by Apriyantono et al. (1989). For this analysis, 10 g of homogenized ground beef jerky sample was transferred into a 300 mL Kjeldahl flask, the pH was adjusted, and the mixture was distilled. An aliquot of the distillate was reacted with TBA reagent and heated in a water bath (Memmert, Germany) at 75°C for 35 minutes to form a red chromogen. The absorbance was measured at 528 nm using a spectrophotometer UV-1800 (Shimadzu, Japan) against a blank. The TBA value was expressed as milligrams of malondialdehyde per kilogram of sample (mg MDA/kg).

Color measurement

Color measurements were performed objectively using a color meter (TES 135, Taiwan) based on the International Commission on Illumination (CIE) Lab* color space system (Fadlilah et al., 2022).

Sensory evaluation

Sensory evaluation was conducted using a modified method based on Sugiarto and Marfuah (2023). Fifteen semi-trained panelists participated in three separate sessions to assess the color, aroma, tenderness, texture, and overall acceptability of the jerky samples. All attributes were assessed using a 5 point hedonic scale, in which color ranged from 1 (very brown) to 5 (reddish brown), aroma from 1 (no meat aroma), tenderness from 1 (very fragile) to 5 (very hard), texture from 1 (very smooth) to 5 (very coarse) and overall acceptability from 1 (dislike very much) to 5 (like very much).

Statistical analysis

All data were subjected to one-way analysis of variance (ANOVA) to evaluate the significance of differences among treatment groups. When significant differences were detected ($p < 0.05$), Duncan's multiple range test was conducted for post hoc comparisons of means. Results are presented as mean ± standard deviation (SD). Statistical analyses were performed using SPSS software, version 16.0 (IBM Corp., Armonk, NY, USA).

RESULT AND DISCUSSION

Optimization of celery concentration and incubation time (Phase 1)

Nitrite content

One of the main objectives of this study is to evaluate the ability of fresh celery leaves to produce sufficient nitrite levels for natural preservation. Curing material has a significant effect on the nitrite content in beef, as shown in Table 2 the highest nitrite concentration was observed in the burp treatment (C0) with an average nitrite content of 0.54 mg/kg, while the celery concentration (C1-C3) resulted in a much lower average nitrite content value of 0.11-0.13 mg/kg ($p < 0.05$). However, these levels are still within an acceptable range and are functionally comparable for preservation purposes. According to Indonesian Food and Drug Authority (BPOM, 2019), the limit for nitrite use in beef is 30mg/kg, while according to the Joint Expert Committee of the Food and Agriculture Organization (JEFCA) and the World Health Organization (WHO), the acceptable daily intake is 0.07 mg nitrite per kg of body weight (Shakil et al., 2022). This confirms that celery can be used as an alternative source of natural nitrites. These findings are in line with previous research that showed that celery powder can effectively replace synthetic nitrites without compromising product quality (Meawad Ahmed et al., 2022).

Although incubation time did not significantly affect nitrite concentration ($p > 0.05$), there was a tendency for nitrite levels to increase with longer incubation periods. Incubation for 1 hour yielded nitrite levels of 0.12 mg/kg, then increased to 0.24 mg/kg at 2-hour incubation, and continued to increase to 0.29 mg/kg at 3-hour incubation. This trend may be attributed to the activity of endogenous nitrate reductase enzymes present in celery, which facilitate the conversion of nitrate to nitrite during incubation (Saputro et al., 2016a).

Color attributes

In addition to its role as a preservative, nitrite also plays a crucial role in producing the characteristic and appealing color of cured meat products (Sorour et al., 2023). The measurements of color parameters L* (lightness) and b* (yellowness) in this study are presented in Table 3. The results for a* values (redness) are presented separately in Figure 1, as this parameter exhibited a significant interaction between curing agent treatments and incubation duration ($p < 0.05$).

Table 2. Nitrite content of beef samples (mg/kg) in the present study

Curing agent (%) \ Incubation time (hours)	1	2	3	Mean ± SD
C0	0.16±0.15	0.63±0.74	0.84±0.31	0.54±0.40[b]
C1	0.11±0.05	0.11±0.03	0.10±0.04	0.11±0.04[a]
C2	0.08±0.06	0.08±0.06	0.09±0.06	0.08±0.06[a]
C3	0.12±0.02	0.13±0.01	0.13±0.02	0.13±0.02[a]
Average	0.12±0.07	0.24±0.21	0.29±0.11	

Note: C0: 0.03% saltpeter; C1: 2% celery leaves; C2: 4% celery leaves; C3: 6% celery leaves. [a,b] Different superscript letters in the same column indicate significant differences ($p < 0.05$).

Table 3. L* (lightness) and b* values (yellowness) of beef samples treated with different curing agents and incubation time

Color	Curing agent (%)	Incubation time (hours)			Mean ± SD
		1	2	3	
L	C0	39.64±7.83	40.63±4.12	39.75 ±5.30	40.01±5.75
	C1	39.96±3.44	40.32 ±6.55	39.88±6.64	40.05±5.54
	C2	38.93±6.55	40.43±3.37	38.35±3.26	39.24±4.39
	C3	44.06±5.34	37.91±5.00	41.88±5.94	41.28±5.43
	Average	40.65±5.79	39.82±4.76	39.97± 5.29	
b	C0	4.68±0.07	6.19±0.82	6.34±2.43	5.73±1.11[a]
	C1	7.56±0.53	5.81±0.89	7.60±1.51	6.99±0.98[ab]
	C2	8.01±1.93	8.41±2.26	6.50±1.83	7.64±2.01[b]
	C3	9.37±1.33	8.09±2.71	8.56±1.30	8.67±1.78[b]
	Average	7.405±0.97	7.125±1.67	7.25±1.77	

Note: C0: 0.03% saltpeter; C1: 2% celery leaves; C2: 4% celery leaves; C3: 6% celery leaves. [ab] Different superscript letters in the same column indicate significant differences ($p < 0.05$).

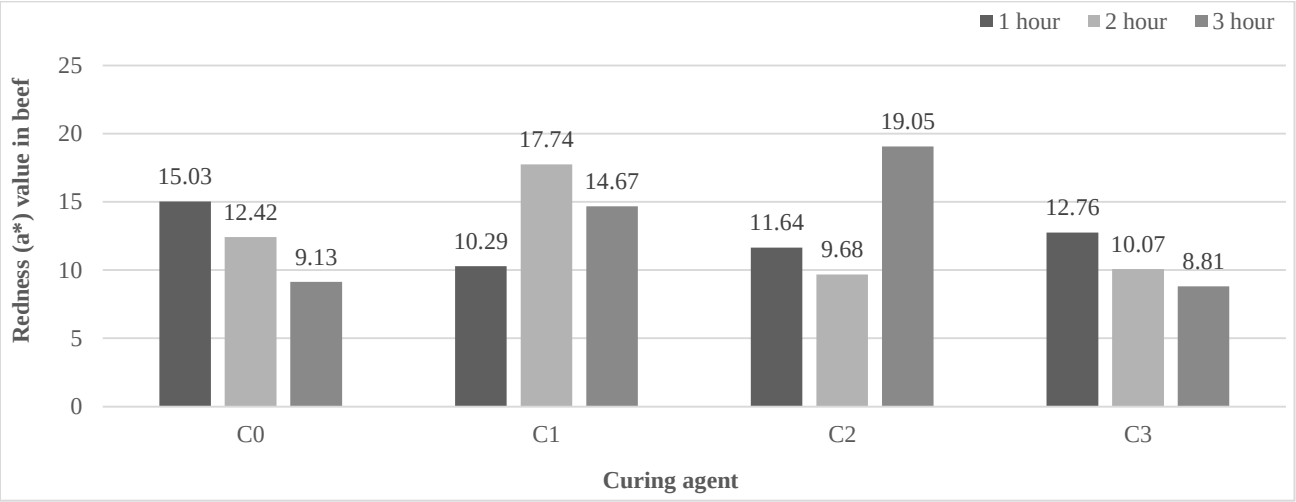


Figure 1. The a* value (redness) of beef as affected by different curing agents (C0: 0.03% saltpeter; C1: 2% celery leaves; C2: 4% celery leaves; C3: 6% celery leaves) and incubation times (1, 2, and 3 hours)

L* value in Beef

The curing agents, incubation time, and their interaction did not significantly affect the brightness value (L*) in beef jerky, as shown in Table 3 ($p > 0.05$). Interestingly, the highest L* value was found in the treatment with 6% celery (C3), which indicates that natural curing using celery can achieve a level of brightness comparable to or even better than conventional curing methods. These findings were in agreement with Policarpio (2024), who reported that celery juice powder acts as an effective natural color stabilizer in meat products.

b* value in Beef

The concentration of celery had a significant effect on b* values ($p < 0.05$), with higher concentrations (4% and 6%) resulting in increased yellowness compared to the saltpeter treatment, as shown in Table 3. This increase may be attributed to the presence of natural pigments and antioxidant compounds in celery, such as flavonoids (Horsch et al., 2014). In contrast, incubation time did not significantly affect b* values ($p > 0.05$). The observed increase in yellowness is likely associated with pigment interactions during the curing process, including the formation of nitrosomyoglobin and the reduction of oxymyoglobin facilitated by nitrite activity (Keszler et al., 2008).

a* value in Beef

A significant interaction between the curing agent and incubation time on the a* value of beef was observed ($p < 0.05$), as presented in Figure 2. The highest a* value was recorded in the treatment with 4% celery and 3 hours of incubation (19.05), followed by 2% celery with 2 hours of incubation (17.74), both of which were significantly higher than all treatments using 0.03% saltpeter ($p < 0.05$). This increase in redness indicated that the nitrate present in celery was successfully converted into nitrite during incubation, which then reacted with myoglobin in the meat to form the characteristic cured meat color. These findings further demonstrate that successful nitrate to nitrite conversion under optimal conditions allows active nitrite to preserve or improve a* value in beef. This finding was consistent with the report of Sindelar and Milkowski (2012), who emphasized nitrite's dual role in both color stabilization and microbial inhibition. The results confirmed that celery, when properly applied, can replicate the color development effects of synthetic nitrite. Based on the best results of Phase 1 of the present study, treatment C2 (4% celery) and C3 (6% celery), demonstrated strong potential as natural curing agents. Both treatments produce redness (value a*) comparable to or higher than C0 (synthetic nitrites), while resulting in substantially lower nitrite residues. The selection of the 2-hour incubation period was supported by the study results, as the a* value obtained at 2 hours did not differ significantly from that at 3 hours, whereas the L* value (lightness) was higher at 2 hours. The higher L* value contributes positively to the visual appearance of jerky products, while also offering improved time efficiency.

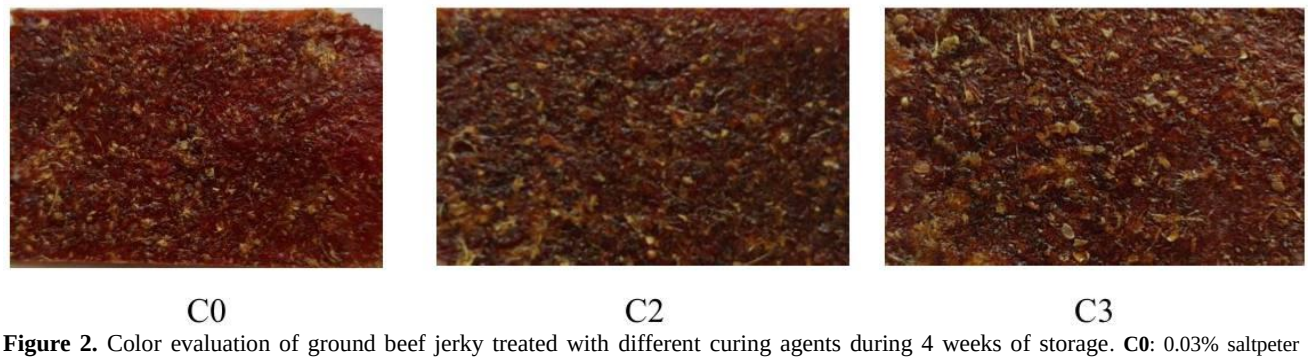


Figure 2. Color evaluation of ground beef jerky treated with different curing agents during 4 weeks of storage. **C0**: 0.03% saltpeter (synthetic nitrite); **C2**: 4% celery leaves; **C3**: 6% celery.

Storage stability – Lipid oxidation (TBA values, Phase 2)

Lipid oxidation

As shown in Table 4, the thiobarbituric acid reactive substances (TBARS) analysis revealed no significant differences in lipid oxidation levels between curing agents or across storage durations ($p > 0.05$). All TBARS values remained low (< 0.5 mg MDA/kg), indicating that lipid oxidation was effectively controlled throughout the 4-week storage period. The presence of nitrite from both saltpeter and celery likely contributed to this oxidative stability, as nitrite is known to function as an antioxidant. According to Jo et al. (2020), nitrite could neutralize reactive oxygen species such as hydroxyl radicals, thereby delaying lipid oxidation.

In this study, the antioxidant compounds present in celery also contributed to inhibiting lipid oxidation during storage. Wulandari et al. (2015) reported that celery contains flavonoids, saponins, and essential oils, all of which contribute to the preservation of meat quality during storage. This is in line with the findings of Kisworo et al. (2020), who stated that celery leaf powder can be used as a source of antioxidants that can prevent and inhibit fat breakdown in sausages. These findings are consistent with the previous study of Bolognesi et al. (2015), who noted that significant lipid oxidation in commercial jerky products typically occurs after 120 days of storage, substantially longer than the duration of this study.

Table 4. Thiobarbituric acid reactive substances values in ground beef jerky

Storage period (week) / Curing agent (%)	1	2	3	Mean ± SD
C0	0.29±0.08	0.38±0.39	0.26±0.41	0.31±0.29
C2	0.23±0.13	0.39±0.23	0.33±0.35	0.32±0.23
C3	0.32±0.14	0.33±0.25	0.44±0.67	0.36±0.37
Average	0.28±0.11	0.37±0.26	0.34±0.44	

Note: C0: 0.03% saltpeter; C2: 4% celery leaves; C3: 6% celery leaves

Color stability during storage

Color is a key quality attribute in processed meat products, as it directly influences consumer perception and marketability (Sorour et al., 2023). In cured meats, long-term color stability is primarily affected by pigment development and oxidative processes. The results of the effects of celery leaf and storage duration on the lightness (L*), redness (a*), and yellowness (b*) of ground beef jerky, presented in Figure 2.

Color values in beef jerky

Lightness in beef jerky

The lightness (L*) is one of the main visual attributes in processed meat products (do Santos et al., 2019). As presented in Table 5, the storage time had no significant effect on the L* value ($p > 0.05$) in beef jerky, while the type of curing material had a significant effect on the brightness level ($p < 0.05$) of jerky. The C3 treatment produced the highest L* value, while the C0 and C2 treatments produced lower L* did not differ significantly between the two. This indicates that C3 can increase the brightness level in beef jerky compared to other treatments.

Overall, L* values ranged from 30.22 to 34.40, reflecting relatively dark surface tones. This darkness may be attributed to Maillard browning reactions during the drying process (Hosry et al., 2025). According to Han et al. (2024), the interaction between reducing sugars and amino acids at elevated temperatures promotes the formation of melanoidins, contributing to the characteristic brown color of jerky products. These findings are consistent with those reported by Saputro et al. (2016b), who observed no significant changes in L* values in naturally cured meat stored for up to 28 days, which suggests that pigment stability can be maintained using plant-based curing agents such as celery

Redness values in beef jerky

One of the objectives of this study was to evaluate the effect of curing agent concentration, particularly celery, and storage duration on the redness (a*) of beef jerky. As shown in Table 5, curing ingredients, both from synthetic nitrites and celery, had a very significant influence on the value of a* ($p < 0.01$) on beef jerky, while storage time had a significant influence on beef jerky ($p < 0.05$).

The highest redness value was observed in the synthetic nitrite treatment (C0), followed by 6% celery (C3) and 4% celery (C2). While the 6% celery treatment produced results comparable to synthetic nitrite, lower concentrations may have yielded insufficient nitrite for optimal pigment formation and stabilization. Despite slight fluctuations during storage, all treatments consistently maintained the characteristic cured red color of meat for up to 4 weeks. This finding is in agreement with Govari and Pexara (2015), who reported that nitrite compounds are able to stabilize red color by participating in color fixation processes, through interactions with heme proteins and scavenging free radicals, thereby preventing pigment oxidation during storage.

Yellowness values in beef jerky

The results of the analysis showed that variations in curing ingredients and storage duration did not have a significant effect on the b* value of beef jerky ($p > 0.05$), with values ranging from 8 to 12.46. According to the CIE Lab* color system, the b* parameter represents yellowness. As shown in Table 5, storage for up to 4 weeks did not affect the b* value of beef jerky. These findings are consistent with the study of Salim et al. (2019), who reported that the b* values were not influenced by storage time or muscle type.

Sensory attribute

Organoleptic test results are presented in Table 6. Based on the analysis of variance, the type of curing agent, either synthetic nitrite (saltpeter) or natural (celery leaf), had no significant effect on any of the sensory parameters during the storage period ($p > 0.05$). These findings indicated that the use of celery leaves as a natural source of nitrite did not negatively impact the sensory quality of ground beef jerky. Furthermore, its performance in terms of consumer perception, specifically color, meat aroma, chewiness, texture, and overall acceptability, was comparable to that of synthetic nitrite. These results aligned with the findings of Pennisi et al. (2020), who reported that vegetable-derived nitrates, whether in powder or juice form, exhibit high potential as natural alternatives to synthetic nitrates and nitrites in processed meat products, providing a high nitrite source without leaving residues. In particular, celery powder provides a pleasant, mild aroma without negatively affecting the product's appearance.

Table 5. Color values (L, a, b*) of beef jerky

Color	Curing Agent (%)	Storage Period (week)			Mean ± SD
		0	2	4	
L	C0	31,07±1,54	31,55±1,11	31,49±0,07	31,37±0,98[a]
	C2	30,22±0,93	32,91±1,55	32,68±0,50	31,94±1,60[a]
	C3	33,90±3,50	33,89±3,50	34,40±2,19	34,06±2,49[b]
	Average	31,73±2,58	32,78±1,96	32,86±1,69	
a	C0	12,44±0,40	12,90±0,23	11,81±0,57	12,38±0,60[c]
	C2	8,84±0,38	10,86±1,13	9,46±0,64	9,72±1,12[a]
	C3	10,49±1,06	11,39±1,04	11,75±0,93	11,21±1,04[b]
	Average	10,59±1,67[a]	11,71±1,20[b]	11,01±1,32 [ab]	
b	C0	9,72±4,38	9,96±2,57	10,83±1,16	10,17±2,66
	C2	8,00±0,79	10,80±1,42	10,76±0,25	9,85±1,61
	C3	12,46±3,83	11,57±2,75	12,65±2,13	12,23±2,63
	Average	10,06±3,52	10,78±2,13	11,41±1,53	

Note**:** Color parameters (L*, a*, b*) of beef jerky treated with different curing agents (C0: 0.03% saltpeter; C2: 4% celery leaves; C3: 6% celery leaves) during storage. [a, b] Different superscript letters in the same column indicate significant differences ($p < 0.05$), while different superscripts in the same row indicate highly significant differences ($p < 0.01$), where applicable.

Table 6. Sensory evaluation results of ground beef jerky

Parameter	Curing Agent (%)	Storage Period (week)			Mean ± SD
		0	2	4	
Color	C0	3.44±0.67	2.67±0.22	3.06±0.69	3.06±0.60
	C2	2.31±0.13	2.810.82	2.72±0.17	2.61±0.48
	C3	3.17±0.29	3.11±0.69	2.53±0.13	2.94±0.49
	Average	2.97±0.63	2.86±0.58	2.77±0.43	
Aroma	C0	3.06±0.10	3.08±0.22	3.14±0.55	3.09±0.30
	C2	3.42±0.14	2.92±0.17	3.11±0.34	3.15±0.30
	C3	2.94±0.19	2.83±0.50	2.94±0.39	2.91±0.34
	Average	3.14±0.25	2.94±0.31	3.06±0.39	
Tenderness	C0	3.00±0.29	3.08±0.44	3.06±0.29	3.05±0.30
	C2	3.50±0.17	3.11±0.27	3.17±0.44	3.26±0.33
	C3	2.64±0.17	3.14±0.29	3.08±0.22	2.95±0.31
	Average	3.05±0.42	3.11±0.30	3.10±0.29	
Texture	C0	3.03±0.49	3.39±0.13	3.36±0.17	3.26±0.32
	C2	3.69±0.27	3.22±0.13	3.25±0.08	3.39±0.28
	C3	3.25±0.30	3.00±0.44	3.28±0.32	3.18±0.34
	Average	3.22±0.43	3.20±0.29	3.30±0.19	
Overall acceptability	C0	3.11±0.19	3.14±0.55	3.11±0.55	3.12±0.40
	C2	2.81±0.13	3.11±0.34	3.14±0.32	3.02±0.29
	C3	3.19±0.38	2.94±0.39	3.17±0.30	3.10±0.33
	Average	3.04±0.28	3.06±0.39	3.14±0.35	

CONCLUSION

Treatment with 4% and 6% celery combined with 2 hours of incubation successfully produced safe nitrite levels, maintained the color of the preserved meat, and maintained oxidative stability during 4 weeks of storage. Among such treatments, 6% celery showed comparable performance to saltpeter, especially in retaining redness, minimizing lipid oxidation, and not negatively impacting the sensory qualities of ground beef jerky. These findings confirmed the potential of fresh celery leaves as a natural preservative agent in processed meat products and reduce reliance on synthetic additives. This study has not evaluated the taste aspects of beef jerky, so further study is needed to optimize the potential of fresh celery as a natural curing ingredient. In addition, further study is also needed to validate its effectiveness in terms of food safety to ensure its feasibility for application in commercial meat processing

DECLARATIONS

Acknowledgments

The authors would like to thank the panelists who were willing to spend time on this research, as well as the Meat and Egg Laboratory, the Faculty of Animal Husbandry, Hasanuddin University, Indonesia.

Funding

The present study did not receive any financial support.

Ethical considerations

This article was originally written by the author and is not being considered or published elsewhere. The authors have checked the text of the article and confirmed that this article was written based on the results of their original research. The authors declare that no AI was used for conducting current study.

Authors' contributions

Nurafni Mallu performed formal analysis, investigation, writing, and data curation. Wahniyathi Hatta contributed to conceptualization, methodology, resources, supervision, validation, and review. Fatma Maruddin contributed to methodology, resources, supervision, validation, and review. All authors approved the edition of the article before submission to the journal.

Competing interests

The authors have stated that they have no conflicts of interest

Availability of data and materials

The data that support the findings of this study are available from the corresponding author upon reasonable request.

REFERENCES

Apriyantono A, Fardiaz D, Puspitasari NL, Sudarnawati, and Budjijanto S (1989). Petunjuk laboratorium analisis pangan [Laboratory manual for food analysis]. IPB Press., Bogor. Available at: https://books.google.co.id/books/about/Analisis_pangan.html?id=TY4unQAACAAJ

Bolognesi JV, Roberto do Rego Monteiro de Carvalho P, Maria Ferreira de Castro Ville G, Lúcia Masson M, Mara Woranovicz Barreira S, and Eduardo Rocha Garcia C (2015). Nitrite, oxidation, and color during shelf life of jerked beef. African Journal of Pharmacy and Pharmacology, 9(34): 856-860. DOI: https://www.doi.org/10.5897/AJPP2015

Domínguez R, Pateiro M, Gagaoua M, Barba FJ, Zhang W, and Lorenzo JM (2019). A comprehensive review on lipid oxidation in meat and meat products. Antioxidants, 8(10): 429. DOI: https://www.doi.org/10.3390/antiox8100429

do Santos TC, Gates RS, de Fatima Souza C, Tinôco ID, Cândido MGL, da Silva Ramos Freitas LC (2019). Meat quality parameters and the effects of stress: A review. Journal of Agricultural Science and Technology, 9(5): 305-315. DOI: https://www.doi.org/10.17265/2161-6264/2019.05.001

Eisinaitė V, Tamkutė L, Vinauskienė R, and Leskauskaitė D (2020). Freeze-dried celery as an indirect nitrate source in cold-smoked sausages: Effect on safety and color formation. LWT-Food Science and Technology, 129: 1-9. DOI: https://www.doi.org/10.1016/j.lwt.2020.109586

Fadlilah A, Rosyidi D, and Susilo A (2022). Karakteristik warna L* a* b* dan tekstur dendeng daging kelinci yang difermentasi dengan Lactobacillus plantarum [Characteristics of L* a* b* color and texture of rabbit meat jerky fermented with *Lactobacillus plantarum*]. Wahana Peternakan, 6(1): 30-37. DOI: https://www.doi.org/10.37090/jwputb.v6i1.533

Ferysiuk K and Wójciak KM (2020). Reduction of nitrite in meat products through the application of various plant-based ingredients. Antioxidants, 9(8): 711. DOI: https://www.doi.org/10.3390/antiox9080711

Govari M and Pexara A (2015). Nitrates and nitrites in meat products. Journal of the Hellenic Veterinary Medical Society, 66(3): 127-140. DOI: https://www.doi.10.12681/jhvms.15856

Han J, Wang Y, Wang Y, Hao S, Zhang K, Tian J, and Jin Y (2024). Effect of changes in the structure of myoglobin on the color of meat products. Food Materials Research, 4: 1-9. DOI: https://www.doi.org/10.48130/fmr-0024-0003

Hassanen NH, Eissa FAM, Hafez MEBA, and Mosa MEA (2015). Antioxidant and antimicrobial activity of celery (*Apium graveolens*) and coriander (*Coriandrum sativum*) herb and seed essential oils. International Journal of Current Microbiology and Applied Sciences, 4(3): 284-296. Available at: https://www.ijcmas.com

Horsch A, Sebranek JG, Dickson JS, Niebuhr SE, Larson EM, Lavieri NA, Ruther BL, and Wilson LA (2014). The effect of pH and nitrite concentration on the antimicrobial impact of celery juice concentrate compared with conventional sodium nitrite on *Listeria monocytogenes*. Meat Science, 96: 400-407. DOI: https://www.doi.org/10.1016/j.meatsci.2013.07.036

Hosry EL, Elias V, Chamoun V, Halawi M, Cayot P, Nehme A, and Bou-Maroun E (2025). Maillard reaction: Mechanism, influencing parameters, advantages, disadvantages, and food industrial applications: A review. Foods, 14(11): 1-43. DOI: https://www.doi.org/10.3390/foods14111881

Indonesian food and drug authority (BPOM) (2019). Peraturan kepala badan pengwas obat dan makanan Indonesia nomor 36 tentang batas maksimum penggunaan bahan tambahan pangan pengawet [Regulation of the head of the Indonesian food and drug supervisory agency number 36 concerning the maximum limit for the use of preservative food additives]. Available at: https://jdih.pom.go.id

Jo K, Lee S, Yong HI, Choi YS, and Jung S (2020). Nitrite sources for cured meat products. Food Science and Technology, 129: 109583. DOI: https://www.doi.org/10.1016/j.lwt.2020.109583

Karwowska M and Dolatowski ZJ (2017). Effect of acid whey and freeze-dried cranberries on lipid oxidation and fatty acid composition of nitrite-/nitrate-free fermented sausage made from deer meat. Asian-Australian Journal of Animal Science, 30(1): 85-93. DOI: https://www.doi.org/10.5713/ajas.16.0023

Keszler A, Piknova B, Schechter AN, and Hogg N (2008). The reaction between nitrite and oxyhemoglobin: A mechanistic study. Journal of Biological Chemistry, 283(15): 9615-9622. DOI: https://www.doi.org/10.1074/jbc.M705630200

Kisworo D, Yasin M, Wulandani B, Chotimah CM, and Fudholi A. (2020). Beef sousage traits enhanced with celery leaf powder (*Apium graveolens* L.). Journal of Critical Reviews, 7(19): 4488-4497. DOI: https://www.doi:10.31838/jcr.07.19.526

Li N, Mandrean L, and Tita O (2011). Celery as a natural alternative to chemical nitrite added to meat products. Bulletin UASVM Agriculture, 68(2): 317-320. Available at: https://www.cabidigitallibrary.org/doi/full/10.5555/20123003869

Meawad Ahmed A, Alkazzaz ASRM, Abdelrahman HA, Ahmed AM, Helal IM, and Ahmed NI (2022). Effect of replacing sodium nitrite with celery on sensory and chemical quality of popular dry sausage. Journal of Advanced Veterinary Research, 12(4): 404-408. Available at: https://www.advetresearch.com/index.php/AVR/article/view/1026/567

Oral ZFY, Kaya M, and Kaban G (2024). Using celery powder in a semi-dry fermented sausage 'heat-treated sucuk': Nitrosamine formation, lipid oxidation, and volatile compounds. Foods, 13(20): 3306. DOI: https://www.doi.org/10.3390/foods13203306

Pennisi L, Verrocchi E, Paludi D, and Vergara A (2020). Effects of vegetable powders as nitrite alternative in Italian dry fermented sausage. Italian Journal of Food Safety, 9(2): 132-136. DOI: https://www.doi.org/10.4081/ijfs.2020.8422

Policarpio JKJ (2024). Evaluation of celery juice powder as a natural curing agent for tocino. American Journal of Food Science and Technology, 3(2): 30-35. DOI: https://www.doi.org/10.54536/ajfst.v3i2.3087

Ramachandraiah K and Chin KB (2021). Antioxidant, antimicrobial, and curing potentials of micronized celery powders added to pork sausages. Food Science of Animal Resources, 41(1): 110-121. DOI: https://www.doi.org/10.5851/KOSFA.2020.E86

Riel G, Boulaaba A, Popp J, and Klein G (2017). Effects of parsley extract powder as an alternative for the direct addition of sodium Nitrite in the production of mortadella-type sausages–impact on microbiological, physicochemical and sensory aspects. Meat Science, 131: 166-175. DOI: https://www.doi.org/10.1016/j.meatsci.2017.05.007

Salim APAA, Suman SP, Canto ACVCS, Costa-Lima BRC, Viana FM, Monteiro MLG, Silva TJP, and Conte-Junior CA (2019). Muscle-specific color stability in fresh beef from grain-finished Bos indicus cattle. Asian-Australian Journal of Animal Sciences, 32(7): 1036-1043. DOI: https://www.doi.org/10.5713/ajas.18.0531

Saputro VP, Bintoro, and Pramono YB (2016a). Agen kyuring alami pengganti natrium nitrit sintesis pada kyuring daging sapi [Natural curing agent to replace synthetic sodium nitrite in meat curing]. Jurnal Ilmu Pertanian, 12(1): 65-75. Available at: https://download.garuda.kemdikbud.go.id/article.php?article=2936913&val=25919&title=AGEN%20KYURING%20ALAMI%20PENGGANTI%20NATRIUM%20NITRIT%20SINTETIS%20PADA%20KYURING%20DAGING%20SAPI

Saputro VP, Bintoro, and Pramono YB (2016b). Color, pigment, and residual nitrite of dendeng sapi naturally cured at various levels of celery leaves and incubation temperatures. Journal of the Indonesian Tropical Animal Agriculture, 41(2): 99-105. DOI: https://www.doi.org/10.14710/jitaa.41.2.99-105

Saputro E (2017). Pemanfaatan kyuring alami pada produk daging sapi [The use of natural curing on beef products]. Wartazoa, 26(4): 183-190. DOI: https://www.doi.org/10.14334/wartazoa.v26i4.1399

Sebranek JG and Bacus JN (2007). Cured meat products without direct addition of nitrate or nitrite: What are the issues?. Meat Science, 77(1): 136-147. DOI: https://www.doi.org/10.1016/j.meatsci.2007.03.025

Shakil M H, Trisha AT, Rahman M, Talukdar S, Kobun R, Huda N, and Zzaman W (2022). Nitrites in cured meats, health risk issues, alternatives to nitrites: A review. Foods, 11(21): 3355. DOI: https://www.doi.org/10.3390/foods11213355

Sindelar JJ and Milkowski AL (2012). Human safety controversies surrounding nitrate and nitrite in the diet. Nitric Oxide - Biology and Chemistry, 26(4): 259-266. DOI: https://www.doi.org/10.1016/j.niox.2012.03.011

Standar nasional Indonesia (SNI) (1992). Standar nasional Indonesia dengan nomor series 01-2894-1992 tentang cara uji bahan pengawet makanan dan bahan tambahan yang dilarang untuk makanan [Indonesian national standard with series number 01-2894-1992 regarding testing methods for food preservatives and prohibited food additives]. Dewan Standarisasi Nasional. Available at: https://pesta.bsn.go.id

Sorour MA, Mehanni AHE, Mahmoud ESA, and El-Hawashy RM (2023). Nitrate, nitrite, and N-nitrosamine in meat products. Journal of Sohag Agriscience, 8(1): 121-135. Available at: https://jsasj.journals.ekb.eg

Sucu C and Turp GY (2018). The investigation of the use of beetroot powder in Turkish fermented beef sausage (sucuk) as nitrite alternative. Meat Science, 140: 158-166. DOI: https://www.doi.org/10.1016/j.meatsci.2018.03.012

Sugiarto and Marfuah N (2023). Kualitas kimia dan organoleptik dendeng sapi dengan kemasan ukuran rongga udara yang berbeda [Chemical and organoleptic quality of beef jerky with different air cavity size packaging]. Prosiding Seminar Nasional Pembangunan dan Pendidikan Vokasi Pertanian, 4(1): 350-362. DOI: https://www.doi.org/10.47687/snppvp.v4i1.658

Suryati T, Astawan M, Lioe HN, Wresdiyati T, and Usmiati S (2014). Nitrite residue and malonaldehyde reduction in dendeng Indonesian dried meat influenced by spices, curing methods, and precooking preparation. Meat Science, 96(3): 1403-1408. DOI: https://www.doi.org/10.1016/j.meatsci.2013.11.023

Wulandari P, Herdini, and Yumita A (2015). Uji aktivitas antioksidan DPPH dan aktivitas terhadap Artemia salina Leach ekstrak etanol 96% daun seledri (*Apium graveolens L*) [DPPH antioxidant activity and activity against Artemia salina Leach using 96% ethanol extract of celery leaves (*Apium graveolens L*). Sainstech Farma, 8(2): 6-13. Available at: https://journal.istn.ac.id/index.php/saintechfarma/article/view/381

Publisher's note: Scienceline Publication Ltd. remains neutral with regard to jurisdictional claims in published maps and institutional affiliations.

Open Access: This article is licensed under a Creative Commons Attribution 4.0 International License, which permits use, sharing, adaptation, distribution and reproduction in any medium or format, as long as you give appropriate credit to the original author(s) and the source, provide a link to the Creative Commons licence, and indicate if changes were made. The images or other third party material in this article are included in the article's Creative Commons licence, unless indicated otherwise in a credit line to the material. If material is not included in the article's Creative Commons licence and your intended use is not permitted by statutory regulation or exceeds the permitted use, you will need to obtain permission directly from the copyright holder. To view a copy of this licence, visit https://creativecommons.org/licenses/by/4.0/.
© The Author(s) 2025

2025, Scienceline Publication
World's Veterinary Journal
World Vet J, 15(4): 1034-1041.
ISSN 2322-4568

DOI: https://dx.doi.org/10.54203/scil.2025.wvj105
PII: S232245682500105-15

Effects of Substitution of Corn with Dried Orange Pulp on Health and Growth Performance of Broiler Chickens

Ahmed Readh Chaib Eddour[1]*, Miloud Litim[1], and Kaddour Bouderoua[2]

[1]*Laboratory of "Applied Biotechnology for Agriculture and Environmental Preservation, Higher School of Agronomy'Mohamed El Amjed Ben Abdelmalek, Mostaganem, 27000, Algeria*
[2]*Laboratory of Food Technology and Nutrition, Abdelhamid Ibn Badis University, Mostaganem,27000, Algeria*

*Corresponding author's Email: a.chaibeddour@esa-mosta.dz

ORIGINAL ARTICLE
Received: September 26, 2025
Revised: October 25, 2025
Accepted: November 25, 2025
Published: December 31, 2025

ABSTRACT

The rising cost of cereal-based ingredients and restrictions on the use of antibiotic growth promoters in poultry have increased demand for sustainable alternatives. Agro-industrial by-products, particularly dried orange pulp (DOP), offer an economical, nutrient-rich solution with bioactive compounds that may improve broiler health and growth. The present study aimed to investigate the effects of incorporating different levels of dried orange pulp (*Citrus sinensis*) on growth performance and blood serum biochemical parameters in broiler chickens. A total of 200 one-day-old Arbor Acres chickens (45 ± 1.7 g) were randomly divided into four dietary groups. Each group consisted of 50 chickens, with five replicates of 10 chickens, and was reared for 49 days. The dietary groups included a control diet without DOP and three experimental diets in which DOP was partially replaced by corn at inclusion levels of 5% (50 g/kg of dry matter [DM]), 10% (100 g/kg of DM), and 15% (150 g/kg of DM). Growth performance was monitored throughout the entire rearing period. Blood samples were collected at 37 and 49 days of age to assess glucose, triglycerides, total cholesterol, high-density lipoprotein (HDL), and low-density lipoprotein (LDL). Broiler chickens fed DOP-substituted diets generally exhibited lower serum lipid levels, especially triglycerides and total cholesterol, compared to the control group at both sampling times. However, there was a slight increase in triglycerides in the 5% DOP group at 49 days compared to the control group. Glucose concentrations generally increased with higher levels of DOP inclusion, especially at 15%. Regarding growth performance, chickens fed the 5% DOP diet had the highest live weight, whereas those fed the 10% DOP diet demonstrated an improvement in feed conversion ratio compared to the control group. The dietary incorporation of DOP enhanced growth performance and positively influenced serum biochemical profiles in broiler chickens, with the 5% DOP level demonstrating the most significant improvements in performance and productivity parameters, while 10% DOP exerted the most beneficial effects on blood biochemical parameters.

Keywords: Cholesterol, HDL, LDL, Lipid fraction, Triglyceride

INTRODUCTION

In 2022, global poultry meat production reached 141 million tons, representing a 1.9% increase from the previous year. In 2021, chicken meat demonstrated the highest absolute and relative growth since 2000 (+107%, or 63 million tons), and remained the most produced type of meat (Ortiz-Sanchez et al., 2024). In recent years, there has been a steady rise in the costs of livestock production, mainly due to increasing prices of feedstuffs such as soybean products and cereal grains (Lawrence et al., 2008). Implementing a resilient feeding strategy enhances production efficiency, reduces costs, and ensures the delivery of high-quality products to consumers (Ebrahimi et al., 2013).

Simultaneously, the use of synthetic growth promoters and antibiotics has been investigated due to their association with antimicrobial resistance, risks to human health, and consumer demand for residue-free, organic poultry products (Nhung et al., 2017). In response, natural feed additives such as probiotics, prebiotics, essential oils, organic acids, and plant-derived by-products rich in polyphenols and flavonoids have emerged as promising alternatives to antibiotics (Imran, 2022; Saeed et al., 2024). Among these, phytobiotics, plant-derived compounds with antioxidant, antimicrobial, and anti-inflammatory properties, have shown potential in improving gut health, enhancing immunity, and regulating lipid metabolism, including the mitigation of hypercholesterolemia in quail (Tufan et al., 2023). Large amounts of orange processing waste (OPW) are produced worldwide, totaling 24 million tons (Bouaita et al., 2022). To mitigate environmental damage and promote a circular economy, new methods are being explored to valorize OPW within the citrus value chain. Dried orange byproducts (*Citrus sinensis*) could be a potential source of valuable nutrients, such as carbohydrates, lipids and fatty acids, vitamins, minerals, phenolic compounds and flavonoids, and organic acids, serving as a natural source of antioxidants for poultry feed (Ebrahimi et al., 2013; 2014; 2015). Orange peels contain high concentrations of phenols, flavonoids (Wang et al., 2015), and vitamins, especially vitamin C (Manthey et al., 2004).

To cite this paper: Chaib Eddour AR, Litim M, and Bouderoua K (2025). Effects of Substitution of Corn with Dried Orange Pulp on Health and Growth Performance of Broiler Chickens. *World Vet. J.,* 15(4): 1034-1041. DOI: https://dx.doi.org/10.54203/scil.2025.wvj105

Finally, dried citrus pulp (DCP) contains high levels of fermentable carbohydrates and sugars, making it a valuable energy source in poultry nutrition (Bampidis et al., 2006) with antibacterial, antioxidant properties, and immune-stimulating activities (Ebrahimi et al., 2015; Pourhossein et al., 2015). Therefore, the present study aimed to evaluate the effects of replacing dried orange pulp (DOP) with maize in broiler diets on growth performance, blood biochemical parameters, and production efficiency over a 49-day rearing period.

MATERIALS AND METHODS

Ethical approval

All experimental procedures involving animals were conducted in accordance with the guidelines for the care and use of experimental animals established by the National Committee for Ethics in Animal Experimentation (Algeria). The experimental protocol was reviewed and approved by the Institutional Animal Ethics Committee of the Higher School of Agronomy, Mostaganem, Algeria (ESAM-PA-2023-011).

Dried orange pulp preparation

Fresh Citrus sinensis pulp residues were collected from a local juice processing facility and spread onto thin layers (2-3 cm) of clean, food-grade plastic sheets. The pulp was sun-dried under greenhouse conditions with proper ventilation for 2-4 days, depending on ambient humidity and temperature, until moisture content dropped below 10%. Moisture content was determined by oven-drying 5 g of the sample at 105°C for 24 hours to stabilize the weight, and expressed as percentage loss in weight relative to the initial sample mass (AOAC, 2005). Manual turning was performed twice daily to ensure uniform drying and avoid microbial contamination. The dried material was then ground using a hammer mill, sieved through a 1 mm mesh, and stored in airtight containers at room temperature (Fernández-López et al., 2009).

Animals and experimental design

A total of 200 one-day-old unsexed Arbor Acres broiler chickens, weighing 45 ± 1.7 g, were used for the present study. During the first 15 days, all chickens were fed a standard starter diet containing 3035 kcal/kg of metabolizable energy (ME) and 22% crude protein formulated according to the nutritional requirements established by the Algerian West Poultry Group (ORAVIO) for chickens. From day 16 onward, chickens were randomly assigned to four dietary treatments, each comprising five replicates with ten chickens, including a control group without DOP and three experimental diets in which DOP was replaced by corn at 5%, 10%, or 15%. The experimental diets were formulated to be isonitrogenous and isocaloric and were balanced according to the nutrient recommendations of the nutrient requirements of poultry (NRC, 1994). Diet formulation was performed using linear programming (least-cost formulation) with feed formulation software (Win Feed/Feed soft or equivalent), entering the analyzed nutrient values of local raw materials. Dried orange pulp replaced corn at 5, 10, and 15% (w/w) on a grower-finisher basis (15-49 days). Diets were supplemented with DL-methionine and L-lysine HCl to ensure they met or exceeded NRC targets for amino-acid requirements in grower-finisher broiler chickens (lysine ≈ 0.9 -1.1% total diet; methionine ± cystine ≈ 0.45-0.55% total diet). The ME values were calculated from ingredient tables and confirmed by proximate analysis according to the nutritional requirements established by the Algerian West Poultry Group (ORAVIO) for chickens. All diets included a commercial vitamin-mineral premix containing vitamins A, D3, E, K, and B-complex, and trace minerals, provided per kg of diet to meet the micronutrient requirements listed in Table 1.

Table 1. Ingredients and nutrient composition of different diets in broiler chickens' feed

Diets (16 to 49 days of age) / Ingredients (%)	Control	DOP 5%	DOP 10%	DOP 15%
Corn grains	67.00	62.00	57.00	52.00
Soybean meal	27.00	27.00	27.00	27.00
Wheat bran	4.00	4.00	4.00	4.00
Dicalcium phosphate	1.00	1.00	1.00	1.00
Vit-Min Premix *	1.00	1.00	1.00	1.00
Dried orange pulp	0	5.00	10.00	15.00
Chemical analysis				
Metabolizable energy	3121.49	3140.41	3162.50	3187.45
Proteins content	21.77 ± 0.12	20.60 ± 0.78	20.43 ± 0.51	20.22 ± 0.89
Ash	3.07 ± 2.28	3.20 ± 0.98	3.51 ± 2.73	3.82 ± 1.99
Fat content	4,36 ± 0,41	3,65 ± 0,48	3,21 ± 0,13	3,16 ± 0,8
Crude cellulose	5.09 ± 0.68	6.43 ± 0.54	6.59 ± 0.34	6.68 ± 0.79

*Vitamin-mineral premix: Provided (in mg kg of diet), Vitamin E: 6, Vitamin K3: 0.80, Vitamin B1: 1, Vitamin B2: 3, Pantothenate of Ca: 6, Vitamin B6: 1.5, Vitamin B12: 0.006, Folic acid: 0.2, Nicotinic acid: 12, Copper: 5, Cobalt: 0.65, Manganese: 65, Zinc: 65, Selenium: 0.25, Iron: 50, Iode: 0.8, Magnesium: 100, C: Control diet, CP: Calcium + Phosphore, DOP 5,10, and 15%: Dried orange pulp at 5, 10, and 15%.

Housing

The feeding trial was conducted in a thoroughly fumigated, washed, and disinfected poultry facility with a surface area of 20 m², following the Arbor Acres management guidelines (2018). Broiler chickens were randomly distributed into pens measuring 5 m² (10 birds/m²), equipped with wood-shaving litter, a feeder, and a drinker. Environmental conditions were maintained according to standard broiler rearing protocols. The brooding temperature was initially set at 34°C during the first week and gradually reduced to 24°C by the fourth week, while relative humidity was maintained between 60-70%. The lighting schedule consisted of 23 hours of light and 1 hour of darkness during the first three days, and was subsequently adjusted to 22 hours of light and 2 hours of darkness from Day 21 until Day 49. Feed and water were supplied *ad libitum* throughout the experimental period. Ventilation was regulated using a thermostat-controlled cross-ventilation system.

Vaccination

All chickens were vaccinated following a standardized protocol. At hatch, chickens received vaccination against Marek's disease (HVT strain, 2000 PFU, Cevac® Rispens, Ceva Santé Animale, France), Newcastle (LaSota strain, Zoetis, USA), and infectious bronchitis (Massachusetts strain, Bronhivit®, Spain) on Days 7 and 21 via drinking water. Vaccination against infectious bursal disease (Intermediate strain, Cevac® IBD L, Ceva Santé Animale, France) was administered on Days 14 and 28. The vaccination program was identical for all experimental groups (Wegner et al., 2024).

Zootechnical parameters

Growth performance parameters, including body weight and feed conversion ratio (FCR), were measured and recorded weekly. Feed intake was determined by recording the quantity of feed offered and the residues remaining at the end of the rearing period. Body weight was measured individually at the beginning of the experiment and at the end of the rearing period. The FCR was calculated as the ratio of feed intake to body weight gain for each replicate group over the entire 49-day rearing period. Mortality, if it occurred, was recorded daily and used to adjust feed intake and performance data.

Sampling

Blood samples were collected on days 37 and 49 by randomly selecting two chickens from each pen, yielding a total of 10 chickens per treatment group. Approximately 3 mL of blood per chicken was drawn from the brachial vein using sterile syringes and collected into plain vacutainer tubes without anticoagulant. Sampling and serum preparation followed the protocol of Readh et al. (2023). Samples were centrifuged at 8000 × g for 8 minutes to obtain serum, which was subsequently stored at -20°C until further analysis. Biochemical analyses included measurements of glucose, triglycerides, total cholesterol, HDL-cholesterol, and LDL-cholesterol using commercial diagnostic kits (BIOLABO SAS, France) and quantified with a SPECORD® 210 spectrophotometer (Analytik Jena GmbH, Germany). All analyses were performed at the Laboratory of Applied Biotechnology, Mostaganem, Algeria.

Statistical analysis

All data were analyzed using IBM SPSS Statistics version 26.0. A one-way analysis of variance (ANOVA) was structured to detect significant differences in body weight, FCR, and serum biochemical parameters with 80% statistical power and a significance level (α) of 0.05. Data normality was verified using the Shapiro-Wilk test, and homogeneity of variances was confirmed before ANOVA. When significant differences were found ($p < 0.05$), Tukey's HSD post hoc test was used for pairwise comparisons, with Bonferroni adjustments where appropriate. Results were expressed as Mean ± Standard Deviation (SD).

RESULTS

The effects of different levels of DOP on growth performance, body weight, and FCR in broiler chickens during the whole rearing period are presented in Table 2. At day 49 of rearing, dietary inclusion with DOP significantly affected body weight ($p < 0.05$). Broiler chickens fed the DOP 5% diet exhibited the most significant improvement, with an increased average body weight of 14.4% compared to the control group. The DOP 10% and 15% diets increased final body weight by 6.0% and 2.9%, respectively, compared to the control group. These findings showed that moderate levels of DOP, especially at 5%, had a strong positive impact on growth performance. Higher levels of DOP (10-15%) improved growth performance, but to a smaller degree. The dose-dependent trend indicated that DOP can effectively replace corn in broiler diets, with the best results at lower substitution levels.

Feed conversion ratio was not significantly affected by dietary inclusion of DOP ($p > 0.5$). The control group recorded the highest FCR, whereas the 5%, 10%, and 15% of DOP demonstrated numerical improvements at approximately 6.1%, 9.7%, and 4.0%, respectively. Although these differences were not statistically significant, the trend suggested a potential improvement in feed efficiency with moderate levels of DOP substitution, particularly at DOP 10%.

Table 2. Effect of dried orange pulp on the performance of broiler chickens aged 49 days (Mean ± SD)

Item \ Treatments	Control	DOP 5%	DOP 10%	DOP 15%	SE	p value
Whole rearing period 1st–49st day						
Weight (g/chick/duration)	$2994^{a} \pm 163$	$3424^{c} \pm 126$	$3174^{bc} \pm 117$	$3081^{b} \pm 102$	28.91	0.01
Feed conversion ratio	$2.47^{a} \pm 0.13$	$2.32^{a} \pm 0.11$	$2.23^{a} \pm 0.17$	$2.37^{a} \pm 0.14$	0.25	0.19

DOP: Dried orange pulp, SE: Standard deviation, each least squares mean represents 12 replicated pens. Means within each row of dietary treatments with no common superscript differ significantly at $p < 0.05$. $^{a–c}$ Means in each row with no common superscript letter differ significantly at ($p < 0.05$).

Table 3 presents the results regarding the impact of DOP on different blood parameters, including glucose, cholesterol, triglycerides, high-density lipoprotein (HDL), and low-density lipoprotein (LDL) in broiler chickens, measured at two distinct time points, 37 and 49-days post-hatch. The inclusion of DOP in broiler diets significantly influenced serum glucose and lipid levels, with responses depending on diet and age. At day 37, glucose concentrations were significantly increased in the DOP 10% (+26%) and DOP 15% (+39%) compared to the control group ($p < 0.05$). However, glucose concentrations in DOP 5% did not differ from those in the control group. Triglyceride and total cholesterol concentrations were significantly reduced in the DOP 10% by 37% and 48%, respectively ($p < 0.05$).

On day 49, glucose levels steadily increased with higher DOP inclusion, reaching a peak in DOP 15% (68%) compared to the control group ($p < 0.05$). For lipid levels, total cholesterol and LDL were significantly decreased in all DOP-fed groups ($p < 0.05$), while HDL concentrations were significantly elevated, particularly in the DOP 10% (5%) compared to the control group ($p < 0.05$). Chickens fed the DOP 5% diet exhibited a moderate decrease in cholesterol of approximately 32% compared to the control group, whereas the DOP 10% and 15% diets markedly reduced cholesterol levels by 48% and 35%, respectively. These results suggested that increasing dietary inclusion of DOP exerted a hypocholesterolemic effect, particularly at 10% substitution, which produced the most pronounced reduction.

Triglyceride levels tended to decrease in DOP-fed groups; however, this effect was less consistent and was not statistically significant ($p < 0.05$).

Table 3. The impact of dried orange pulp diets on serum glucose and lipid fractions at 37 and 49 days of rearing

SAMP	Diets	GLU (mg/dl)	TRIG (mg/dl)	CHOL (mg/dl)	HDL (mg/dl)	LDL (mg/dl)
37d (S1)	Control	127.07^{a}	121.08^{c}	137.16^{c}	74.67^{ab}	36.56^{a}
	DOP 5%	120.84^{a}	92.94^{b}	117.44^{b}	74.67^{ab}	32.89^{a}
	DOP 10%	160.47^{b}	67.33^{a}	71.82^{a}	78.00^{b}	32.56^{a}
	DOP 15%	177.39^{c}	76.61^{ab}	105.07^{b}	68.44^{a}	32.40^{a}
49d (S2)	Control	175^{a}	137.15^{c}	212.23^{c}	98.67^{a}	51.00^{b}
	DOP 5%	163^{a}	143.70^{c}	140.71^{b}	98.00^{a}	47.24^{ab}
	DOP 10%	209^{b}	71.82^{a}	101.98^{a}	102.44^{a}	45.71^{ab}
	DOP 15%	252.50^{c}	112.73^{b}	137.21^{b}	89.73^{a}	40.71^{a}
S1	**P value**	$p < 0.01$	$p < 0.01$	$p < 0.01$	$p < 0.01$	$p > 0.05$
S2		$p < 0.01$	$p < 0.01$	$p < 0.01$	$p > 0.05$	$p < 0.01$
Age		$P < 0.01$	$P < 0.01$	$P < 0.01$	$p < 0.01$	$p < 0.01$
Diet*Age		$p < 0.01$	$p < 0.01$	$p < 0.01$	$p > 0.05$	$p < 0.01$

Glu: Glucose; Trig: Triglycerides; Chol: Cholesterol; HDL: High density lipoprotein, and LDL: Low density lipoprotein. For each group, n = 10. SAMP: Samples; S1: First sample; S2: Second sample. Diet × Age: Represents the interaction effect between the type of diet and the age of the chickens. $^{a–c}$ Means in each row with no common superscript letter differ significantly at ($p < 0.05$). The results are expressed as the mean.

The global analysis confirmed that diet, age, and their interaction significantly affected glucose and lipid metabolism ($p < 0.05$). The current results demonstrated that DOP supplementation induced a beneficial hypolipidemic effect, reducing total cholesterol, triglycerides, and LDL while enhancing HDL, with the most consistent improvements observed at the DOP 10% dietary group.

The serum glucose and lipid profiles revealed that dietary DOP had a significant and age-dependent impact (Table 3). Importantly, DOP incorporation had a dual effect; it regularly decreased lipid levels, notably triglycerides and total cholesterol, while also causing a dose-dependent rise in serum glucose. This glycemic effect was significantly more pronounced in the older cohort (S2). Statistical analysis confirmed significant interactions between diet and age for glucose, triglycerides, and cholesterol ($p < 0.01$), underscoring that the host's age is a crucial factor in the metabolic response to DOP.

DISCUSSION

The present findings are consistent with those reported by Parobali et al. (2024), who demonstrated that supplementing broiler diets with *Citrus sinensis* seed at inclusion levels of 0.25%, 0.5%, and 0.75% considerably improved body weight gain and FCR at 49 days of rearing period compared to the control group. Similarly, the current results align with those of Abu Al-Makarem et al. (2024), who reported that supplementing a basal corn-soybean meal diet with 1% and 2% DOP enhanced FCR in broiler chickens.

The current results indicated age-related increases in serum glucose levels, reflecting metabolic development. Similar trends were reported by Tůmová et al. (2019).

Ahmad et al. (2024) suggested that the positive effect of orange peel inclusion on broiler weight gain might be related to the citric acid content, which helps modulate gut microbial balance by inhibiting pathogenic bacteria. This antimicrobial activity can improve digestive efficiency, thereby enhancing nutrient absorption and overall growth performance. The low pH of these acids inhibits pathogenic gastrointestinal microbes, thereby reducing the toxicity of bacterial products, improving protein digestibility and energy utilization, and ultimately enhancing weight gain. Additionally, Jiang et al. (2020) demonstrated that naringin content in DOP improved performance parameters and reduced FCR in the naringin-treated group.

Similarly, Nazok et al. (2010) reported that the inclusion of citrus by-products enhanced growth performance. Mehmet and Simsek (2016) observed elevated glucose levels in broilers fed *Citrus sinensis* essential oil, likely due to impaired glucose uptake. This response may be attributed to the action of citrus flavonoids such as hesperidin, naringin, and narirutin, which are known to modulate carbohydrate metabolism and glucose transport (Chen et al., 2017). Flavonoids can influence glucose homeostasis by affecting the expression or activity of key enzymes involved in glycolysis and gluconeogenesis, such as hexokinase, glucose-6-phosphatase, and phosphoenolpyruvate carboxykinase. Moreover, flavonoids may alter insulin signaling pathways and the translocation of glucose transporter proteins in cell membranes, thereby reducing cellular glucose uptake and contributing to increasing the blood glucose levels.

Triglyceride levels fell within the Arbor Acres strain's typical range, varying from 0.17 to 1.61 g/l. Moreover, serum cholesterol concentrations ranged from 0.20 to 1.50 g/L, aligning with the reference range for *Arbor Acres* broiler chickens (Arzour-Lakehal and Boudebza, 2021), except for a deviation observed in the control group during the second sampling.

In the present study, triglyceride and cholesterol levels increased with age, which was consistent with the findings of Almeida et al. (2006), who reported that elevated lipid levels in older chickens were associated with higher energy demands during the finishing phase. As reported by Silva et al. (2007), the elevation of cholesterol and triglyceride levels during the rearing period is also linked to reduced mobility and increased synthesis of these lipids within the body.

Incorporating DOP into chicken diets effectively modulated serum lipid metabolism by reducing cholesterol, triglyceride, and LDL levels, while promoting higher glucose concentrations, particularly at higher inclusion levels (10–15% DOP). Similar findings were reported when orange peel or pulp was incorporated into chicken diets by Alefzadeh et al. (2016), Akpe et al. (2019), Abd El Latif et al. (2023), and Hussein et al. (2023). Moreover, the lipid analysis in the present study was consistent with that reported by Younis et al. (2025), who observed that dietary supplementation with dried pomegranate reduced serum cholesterol and triglyceride levels. The current findings corroborated the results reported by Abbasi et al. (2015) and Alefzadeh et al. (2016), who demonstrated that dietary DOP and orange pulp reduced blood cholesterol and triglycerides. This effect might be attributed to the hypocholesterolemic properties of citrus fruits. The flavonoids have been shown to inhibit cholesterol synthesis in the liver by inhibiting the hepatic enzyme 3-hydroxy-3-methylglutaryl-CoA reductase (Gilani et al., 2018).

Moreover, supplementation with DOP and citrus waste in broiler diets decreased blood cholesterol, triglyceride, and LDL levels (Abu Al-Makarem et al., 2024). In 37 days, broiler chickens fed DOP 10% had the highest HDL levels compared to the control group, indicating an improved lipid profile. Additionally, the supplementation of polyphenols from green tea at 50 and 100 mg/kg of body weight for 20 days has been shown to reduce serum lipid levels in chickens (*Gallus gallus domesticus*) by inhibiting fatty acid synthesis and promoting lipolysis (Huang et al., 2013). Although

Huang et al. (2013) used green tea polyphenols, DOP also has a high content of polyphenolic compounds, which are recognized for their similar lipid-lowering and antioxidant properties.

CONCLUSION

The inclusion of DOP in broiler diets demonstrated positive effects on both growth performance and serum biochemical parameters. The DOP 5% exhibited the highest live weight, showing an improvement of approximately 15% compared to the control group, while the DOP 10% recorded the FCR. In terms of biochemical responses, increasing DOP inclusion level reduced serum cholesterol and triglyceride concentrations, particularly in DOP 10% and 15%, and increased HDL levels, indicating a healthier lipid profile. These findings confirmed that DOP, rich in polyphenols and natural antioxidants, can effectively replace part of the corn in broiler diets without compromising performance or metabolic health. Further studies are recommended to investigate the long-term effects of DOP on meat quality, immune response, and gut microbiota composition, and to evaluate its optimal inclusion level across different rearing and environmental conditions.

DECLARATIONS

Funding

The present study was funded by the Laboratory of Biotechnology Applied to Agriculture and Environmental Preservation, Higher School of Agronomy, Mostaganem, Algeria.

Availability of data and materials

The data supporting the findings of this study are available from the corresponding author upon reasonable request.

Acknowledgments

The authors would like to acknowledge the support of the Higher School of Agronomy "Mohamed El Amjed Ben Abdelmalek" for their valuable contributions to this study. The assistance provided in the form of technical support, funding, or intellectual input is gratefully appreciated.

Authors' contributions

Ahmed Readh Chaib Eddour contributed to conceptualization, experimental design, data collection, statistical analysis, data interpretation, manuscript drafting, figure and table preparation, and final manuscript revision. Miloud Litim assisted in the experimental setup and contributed to data interpretation and manuscript review. Kaddour Bouderoua supervised the experimental procedures and ethical compliance, verification of analytical accuracy, and critical revision of the manuscript. All authors read and approved the final edition of the manuscript.

Competing interests

The authors declared no competing interests in the present study.

Ethical considerations

All ethical considerations related to this study, including but not limited to plagiarism, consent for publication, research misconduct, data fabrication or falsification, redundant publication, and simultaneous submission, have been thoroughly reviewed and addressed by all authors. The research was conducted in accordance with ethical standards and institutional guidelines. The authors confirm that no AI tools were used to generate, manipulate, or fabricate any data in this study. All data were obtained through standard experimental procedures and analyzed by the research team

REFERENCES

Abd El Latif MA, Abdel-Wareth AA, Daley M, and Lohakare J (2023). Effect of dietary orange peel meal and multi-enzymes on productive, physiological and nutritional responses of broiler chickens. Animals, 13(15): 2473. DOI: https://www.doi.org/10.3390/ani13152473

Abu Al-Makarem MA, Younis M, and Abdo SG (2024). Growth performance, carcass characteristics, blood parameters, health status and economic efficiency of broiler chicks fed diets supplemented with dried orange peel powder. Egyptian Journal of Veterinary Sciences, pp. 1-12. DOI: https://www.doi.org/10.21608/ejvs.2024.306144.2267

Ahmad F, Sultan A, Khan S, Ali M, Ali I, Abdullah H, Suliman GM, and Swelum AA (2024). Effect of citrus peeling (*Citrus sinensis*) on production performance, humoral immunity, nutrients, and energy utilization of broiler quails. Poultry Science, 103(1): 103207. DOI: https://www.doi.org/10.3390/ani10071209

Akpe ME, Oluremi, OIA, and Tuleun CDT (2019). Haematological and serum biochemical indices of broiler chickens fed diets containing graded

levels of biodegraded sweet orange (*Citrus sinensis*) Peel. IOSR Journal of Agriculture and Veterinary Science, 12(8): 54-59. DOI: https://www.doi.org/10.9790/2380-1208025459

Alefzadeh T, Bouyeh M, den Hoven RV, Seidavi A, Laudadio V, and Tufarelli V (2016). Effect of dietary dried orange (*Citrus sinensis*) peel powder and exogenous multi-enzymes on growth and carcass traits and ileal microflora of broiler chickens. Pakistan Journal of Zoology, 48(6). DOI: https://www.doi.org/10.5555/20173330486

Almeida JG, Vieira SL, Gallo BB, Conde ORA, and Olmos AR (2006). Period of incubation and post hatching holding time influence on broiler performance. Brazilian Journal of Poultry Science, 8(3): 153158. DOI: https://www.doi.org/10.1590/S1516-635X2006000300003

Association of official analytical chemists (AOAC) (2005). Official method of analysis, 18th Edition. Washington, DC: Association of Officiating Analytical Chemists, method 935.14 and 992.24. Available at: https://www.studocu.vn/official-methods-of-analysis-of-aoac-international-18th-ed-2005/138442576

Arzour-Lakehal N and Boudebza A (2021). Biochemical reference intervals in broiler chickens according to age and strain. Agricultural Science & Technology, 13(4): 357-364. DOI: https://www.doi.org/10.15547/ast.2021.04.058

Bampidis VA and Robinson PH (2006). Citrus by-products as ruminant feeds: A review. Animal Feed Science and Technology, 128(3-4): 175-217. DOI: https://www.doi.org/10.1016/j.anifeedsci.2005.12.002

Bouaita R, Derbal K, Panico A, Iasimone F, Pontoni L, Fabbricino M, and Pirozzi F (2022). Methane production from anaerobic co-digestion of orange peel waste and organic fraction of municipal solid waste in batch and semi-continuous reactors. Biomass Bioenergy, 160: 106421. DOI: https://www.doi.org/10.1016/j.biombioe.2022.106421

Chen XM, Tait AR, and Kitts DD (2017). Flavonoid composition of orange peel and its association with antioxidant and anti-inflammatory activities. Food Chemistry, 218: 15-21. DOI: https://www.doi.org/10.1016/j.foodchem.2016.09.016

Ebrahimi A, Santini A, Alise M, Pourhossein Z, Miraalami N, and Seidavi A (2015). Effect of dried *Citrus sinensis* peel on gastrointestinal microbiota and immune system traits of broiler chickens. Italian Journal of Animal Science, 14(4): 4194. DOI: https://www.doi.org/10.4081/ijas.2015.4194

Ebrahimi A, Qotbi AAA, Seidavi A, and Bahar B (2014). The effects of dietary supplementation of *Citrus sinensis* peel extract on production and quality parameters of broiler chicken. Journal of Applied Animal Research, 42(4): 445-450. DOI: https://www.doi.org/10.1080/09712119.2013.875916

Ebrahimi A, Qotbi AA, Seidavi A, Laudadio V, and Tufarelli V (2013). Effect of different levels of dried sweet orange (*Citrus sinensis*) peel on broiler chickens growth performance. Archiv Tierzucht, 56(2): 11-17. DOI: https://www.doi.org/10.7482/0003-9438-56-002

Fernández-López J, Sendra-Nadal E, Navarro C, Sayas E, Viuda-Martos M, and Alvarez JAP (2009). Storage stability of a high dietary fibre powder from orange by-products. International Journal of Food Science and Technology, 44(4): 748-756. DOI: https://www.doi.org/10.1111/j.1365-2621.2008.01892.x

Gilani, Zehra S, Faiz-ul-Hassan, Galani S, and Ashraf A (2018). Effect of natural growth promoters on immunity and biochemical and haematological parameters of broiler chickens. Tropical Journal of Pharmaceutical Research.17(4): 627-633. DOI: https://www.doi.org/10.4314/tjpr.v17i4.9

Huang J, Zhang Y, Zhou Y, Zhang Z, Xie Z, Zhang J, and Wan X (2013). Green tea polyphenols alleviate obesity in broiler chickens through the regulation of lipid-metabolism-related genes and transcription factor expression. Journal of Agricultural and Food Chemistry, 61(36): 8565-8572. DOI: https://www.doi.org/10.1021/jf402004x

Hussein E, Alhotan RA, Ebrahim A, and Selim S (2023). Unraveling the potential of orange pulp for improving laying rate, egg quality, oxidative stability, fatty acids composition, and reproductive tract morphology of laying hens. Animals, 13(13): 2199. DOI: https://www.doi.org/10.3390/ani13132199

Imran A and Alsayeqh A (2022). Anticoccidial efficacy of citrus sinensis essential oil in broiler chicken. Pakistan Veterinary Journal, 42(4): 461-466. DOI: https://www.doi.org/10.29261/pakvetj/2022.082

Jiang XR, Zhang HJ, Wang J, Wu SG, Yue HY, Lü HY, Cui H, Bontempo V, and Qi GH (2016). Effect of dried tangerine peel extract supplementation on the growth performance and antioxidant status of broiler chicks. Italian Journal of Animal Science, 15: 642-648. DOI: https://www.doi.org/10.1080/1828051X.2016.1222246

Lawrence JD, Mintert JR, Anderson JD, and Anderson DP (2008). Feed grains and livestock: Impacts on meat supplies and prices. Choices, 23(2): 11-15. Available at: https://www.choicesmagazine.org/UserFiles/file/article_25.pdf

Manthey JA (2004). Fractionation of orange peel phenols in ultrafiltered molasses and mass balance studies of their antioxidant levels. Journal of Agricultural and Food Chemistry, 52(25): 7586-7592. DOI: https://www.doi.org/10.1021/jf049083j

Mehmet C and Simsek UG (2016). Effect of dietary orange peel extract on physiological, biochemical, and metabolic responses of Japanese quail reared under low ambient temperature. Turkish Journal of Veterinary & Animal Sciences 40(3): 288-297. DOI: https://www.doi.org/ 10.3906/vet-1504-11

Nazok A, Rezaei M, and Sayyahzadeh H (2010). Effect of different levels of dried citrus pulp on performance, egg quality, and blood parameters of laying hens in early phase of production. Tropical Animal Health and Production, 42(4): 737-742. DOI: https://www.doi.org/ 10.1007/s11250-009-9481-x

Nhung NT, Chansiripornchai N, and Carrique-Mas JJ (2017). Antimicrobial resistance in bacterial poultry pathogens: A review. Frontiers in Veterinary Science, 4: 126. DOI: https://www.doi.org/10.3389/fvets.2017.00126

National research council and subcommittee on poultry nutrition (NRC) (1994). Nutrient requirements of poultry: 1994. National Academies Press. https://www.agropustaka.id

Ortiz-Sanchez M, Cardona Alzate, CA, and Solarte-Toro JC (2024). Orange peel waste as a source of bioactive compounds and valuable products: insights based on chemical composition and biorefining. Biomass, 4(1): 107-131. DOI: https://www.doi.org/10.3390/biomass4010006

Pourhossein Z, Qotbi AAA, Seidavi A, Laudadio V, Centoducati G, and Tufarelli V (2015). Effect of different levels of dietary sweet orange (*Citrus sinensis*) peel extract on humoral immune system responses in broiler chickens. Animal Science Journal, 86(1): 105-110. DOI: https://www.doi.org/10.1111/asj.12250

Parobali T, Adjei-Mensah B, Songuine T, Yarkoa T, Karou SD, and Eklu-Gadegbeku K (2024). Influence of *Citrus Sinensis* seed powder on growth performance, morphological and histological development of the small intestine of broiler chickens. Journal of Applied Poultry Research, 33(2): 100395. DOI: https://www.doi.org/10.1016/j.japr.2023.100395

Readh CEA, Miloud L, Abdelkarim L, Kaddour B, and Chaima B (2023). Effect of graded levels of dried orange (*Citrus sinensis*) byproducts on production efficiency, blood parameters and antioxidant status of broiler chickens. Asian Journal of Dairy and Food Research, 42(3): 314-319. DOI: https://wwww.doi.org/ 10.18805/ajdfr.DRF-307

Saeed M, Kamboh AA, and Huayou C (2024). Promising future of citrus waste into fermented high-quality bio-feed in the poultry nutrition and safe environment. Poultry Science, 103: 103549. DOI: https://www.doi.org/10.1016/j.psj.2024.103549

Silva PRL, Freitas Neto OC, Laurentiz AC, Junqueira OM, and Fagliari JJ (2007). Blood serum components and serum protein test of Hybro-PG broilers of different ages. Brazilian Journal of Poultry Science, 9: 229-232. DOI: https://www.doi.org/10.1590/S1516-635X2007000400004

Tufan T, Bolacali M, İrak K, Arslan C, Ãzcan C, Kaplan O, and Irmak M (2023). Dietary fig seeds improve growth performance and antioxidant capacity of quail. South African Journal of Animal Science, 53: 302-314. DOI: http://www.doi.org/10.4314/sajas.v53i2.14

Tůmová E, Chodová D, Härtlová H, Fučiková A, and Ketta M (2019). Effect of feeding regime on the performance and blood parameters of male and female broiler chickens. South African Journal of Animal Science, 49(2): 244-252. DOI: https://www.doi.org/ 10.4314/sajas.v49i2.5

Wang D, Yan J, Chen J, Wu W, Zhu X, and Wang Y (2015). Naringin improves neuronal insulin signaling, brain mitochondrial function, and cognitive function in High-Fat Diet-induced obese mice. Cellular and Molecular Neurobiology, 35(7): 1061-1071. DOI: https://www.doi.org/10.1007/s10571-015-0201-y

Wegner M, Gesek M, Banaszak M, Adamski M, Wlaźlak S, and Biesek J (2024). Research Note: The infectious bursal disease (*Gumboro* disease) vaccination scheme affects the quantitative and qualitative carcass characteristics and the immune response of Ross 308 broiler chickens. Poultry Science, 103(12): 104344. https://www.doi.org/10.1016/j.psj.2024.104344

Younis M, Abdo SG, Elmakarem MAA, Mustafa FEZA, and Fawaz MA (2025). Evaluating dried pomegranate peel as a functional feed additive: effects on growth, carcass traits, and gut health in broilers. Tropical Animal Health and Production, 57(4): 221. DOI: https://www.doi.org/10.1007/s11250-025-04455-y

Publisher's note: Scienceline Publication Ltd. remains neutral with regard to jurisdictional claims in published maps and institutional affiliations.

Open Access: This article is licensed under a Creative Commons Attribution 4.0 International License, which permits use, sharing, adaptation, distribution and reproduction in any medium or format, as long as you give appropriate credit to the original author(s) and the source, provide a link to the Creative Commons licence, and indicate if changes were made. The images or other third party material in this article are included in the article's Creative Commons licence, unless indicated otherwise in a credit line to the material. If material is not included in the article's Creative Commons licence and your intended use is not permitted by statutory regulation or exceeds the permitted use, you will need to obtain permission directly from the copyright holder. To view a copy of this licence, visit https://creativecommons.org/licenses/by/4.0/.
© The Author(s) 2025

2025, Scienceline Publication
World's Veterinary Journal
World Vet J, 15(4): 1042-1052.
ISSN 2322-4568

DOI: https://dx.doi.org/10.54203/scil.2025.wvj106
PII: S232245682500106-15

Liver Anatomy of Long-Eared Hedgehog (*Hemiechinus auritus*) Using Multimodal Imaging

Mahdi Ghanaat Pisheh[1], Mohammad Nasrollahzadeh Masouleh[1]*, Hassan Gilanpour[2], Saied Bokaie[3], and Siamak Mashhadirafiee[1]

[1]*Department of Clinical Sciences, SR.C., Islamic Azad University, Tehran, Iran*
[2]*Department of Basic Sciences, SR.C., Islamic Azad University, Tehran, Iran*
[3]*Department of Epidemiology and Zoonosis, Faculty of Veterinary Medicine, University of Tehran, Tehran, Iran*

*Corresponding author's Email: 2594205443@iau.ir

ORIGINAL ARTICLE
Received: October 07, 2025
Revised: November 11, 2025
Accepted: December 10, 2025
Published: December 31, 2025

ABSTRACT

The long-eared hedgehog (*Hemiechinus auritus*), a small insectivorous species commonly encountered in exotic animal practice, lacks established imaging references for liver anatomy. The present study aimed to characterize the liver of clinically healthy adult animals using radiography, ultrasonography, computed tomography (CT), and magnetic resonance imaging (MRI). Seven clinically healthy adult one-year-old male hedgehogs with body weights of 320-410 grams were examined at the Diagnostic Imaging Unit of the Faculty of Veterinary Medicine, Islamic Azad University, Tehran, Iran. Radiography identified hepatic position and overall shape, while ultrasonography provided real-time assessment of parenchymal echotexture, gallbladder morphology, and major vascular landmarks. The CT and MRI provided detailed cross-sectional visualization, including morphometric measurements and evaluation of parenchymal and vascular architecture. Across all imaging techniques, the right and left hepatic lobes exhibited comparable dimensions and tissue characteristics, with no statistically significant morphometric differences between lobes. The present study established a preliminary reference for liver anatomy in *Hemiechinus auritus* using multimodal imaging, thereby facilitating clinical diagnosis in this species.

Keywords: Hedgehog, Liver, MRI, Radiography, Ultrasonography

INTRODUCTION

The long-eared hedgehog (*Hemiechinus auritus* [*H. auritus*]), a popular exotic companion animal, has attracted attention for its distinctive physiological characteristics, including a desert-adapted metabolic profile, seasonal hibernation behavior, and an insectivorous diet (Juan-Sallés and Garner, 2007). Similar to other small exotic mammals, hedgehogs are prone to hepatic disorders that may progress to systemic illness if not detected early (Ballard and Cheek, 2016). The most frequently reported hepatic abnormalities in hedgehogs included hepatic lipidosis, inflammatory hepatopathies, and metabolic hepatic dysfunction (Juan-Sallés and Garner, 2007). Considering the liver's vital functions in detoxification, metabolic regulation, and nutrient storage, accurate anatomical characterization is essential for effective clinical diagnosis and management (Capello and Lennox, 2013; Bexton, 2016).

Although the hepatic disease is clinically significant in hedgehogs, there are still limited species-specific anatomical studies for assessing the normal liver in the long-eared hedgehog. Most available information on hedgehog visceral anatomy is based on general veterinary literature or from pathological reports and imaging studies of other small mammals, such as African hedgehogs (*Atelerix albiventris*), rabbits, chinchillas, and ferrets (Juan-Sallés and Garner, 2007; Ballard and Cheek, 2016). Although comparative anatomical and imaging data derived from other small exotic mammals, including African hedgehogs, rabbits, chinchillas, and ferrets, provide proper context, anatomical variation between species limits their direct relevance to *H. auritus*, particularly for organs such as the liver, which is sensitive to metabolic and physiological differences.

Previous imaging and anatomical investigations in small exotic mammals have demonstrated that hepatic morphology, lobar proportions, and spatial relationships with adjacent organs may differ considerably among species and body conformations (Capello and Lennox, 2013; von Stade and Sadar, 2024). However, imaging-based descriptions of normal liver anatomy in *H. auratus* are lacking, and no comprehensive reference framework integrating radiography,

To cite this paper: Pisheh MG, Masouleh MN, Gilanpour H, Bokaie S, and Mashhadirafiee S (2025). Liver Anatomy of Long-Eared Hedgehog (*Hemiechinus auritus*) Using Multimodal Imaging. *World Vet. J.*, 15(4): 1042-1052. DOI: https://dx.doi.org/10.54203/scil.2025.wvj106

ultrasonography, computed tomography (CT), and magnetic resonance imaging (MRI) has been established for this species.

Advanced cross-sectional imaging techniques have improved the ability to illustrate hepatic lobar structure, vascular arrangements, and parenchymal features in different exotic mammals (Nabipour and Dehghani, 2012). Without baseline reference data for *H. auritus*, interpreting hepatic imaging results in clinical practice is difficult, especially when animals show nonspecific systemic signs. Defining standard, species-specific imaging features of the liver is crucial for enhancing diagnostic precision, informing clinical choices, and aiding comparative and translational investigation in exotic veterinary medicine. Therefore, the present study aimed to provide a comprehensive, descriptive multimodal imaging evaluation of liver anatomy in *H. auritus*, establishing essential reference data for clinical and study use.

MATERIALS AND METHODS

Ethical statement

The present study was conducted in accordance with national and international ethical standards for animal research and was approved by the Animal Ethics Committee of the Islamic Azad University, Science and Research Branch, Tehran, Iran (approval code: IR.IAU.SRB.REC.1403.338). All procedures were designed to minimize stress and avoid unnecessary harm. Only the sedation required for diagnostic imaging was performed; no invasive interventions were conducted. No animals were euthanized during or after the study, and all hedgehogs recovered fully following imaging. The study adhered to institutional, national, and international guidelines for the humane care and use of animals in research.

Animals

The study comprised seven clinically healthy, 1-year-old male *H. auritus* hedgehogs, with body weights ranging from 320 to 410 g. The hedgehogs were obtained from licensed wildlife rehabilitation centers located in the South Khorasan and Sistan-Baluchestan provinces of Iran, regions within the natural distribution of *H. auritus*. Each hedgehog underwent a complete physical examination, including visual inspection, palpation, and preliminary abdominal radiographic screening, to confirm the absence of systemic, gastrointestinal, or urinary abnormalities, in accordance with standard diagnostic guidelines for small exotic mammals (Capello and Lennox, 2013).

The animals were housed individually in stainless steel enclosures measuring 60 × 45 × 45 cm, maintained at a temperature of 20-25°C, with a relative humidity of 40-60%, and exposed to a 12-hour light/dark cycle. All hedgehogs were fed a commercially formulated insectivore/exotic-mammal diet (VetLife Exotic Diet, Italy), with *ad libitum* access to fresh water. Environmental enrichment was provided to reduce stress and encourage natural behaviors, including opaque shelters, nesting material, PVC tunnels, and a shallow digging substrate.

Ethical restrictions on anesthesia for advanced imaging and the limited availability of healthy adult *H. auritus* necessitated a sample size of seven animals for the present study. The sample size was considered appropriate for descriptive anatomical and diagnostic imaging investigations and was consistent with the guidelines of Animal Research Reporting of *in vivo* Experiments (ARRIVE) for establishing preliminary baseline morphologic reference data in rare or protected species.

Anesthesia procedure

To minimize stress and to ensure adequate immobilization during imaging, all hedgehogs were anesthetized using ketamine (20 mg kg^{-1}, intramuscular; Alfasan, Woerden, Netherlands) combined with diazepam (2 mg kg^{-1}, intramuscular; Caspian Tamin Pharmaceutical Co., Tehran, Iran). Physiological parameters, including heart rate, respiratory rate, peripheral oxygen saturation (SpO_2), mucous membrane color, and palpebral and pedal reflexes, were continuously monitored using a multiparameter veterinary monitor (CMS8000VET, Contec Medical Systems Co., Qinhuangdao, China). Normal physiologic ranges and anesthetic safety criteria were interpreted in accordance with established guidelines for hedgehog and small exotic mammal anesthesia (Bexton, 2016; Hawkins et al., 2020).

Supplemental anesthesia was administered only when necessary. Additional ketamine (5 mg kg^{-1}, intramuscular) was administered when clinical signs indicated inadequate anesthesia, such as partial return of withdrawal reflexes, reduced muscle relaxation, spontaneous limb movements, or purposeful reactions during imaging.

All hedgehogs were deprived of feed for 12 hours and water for 2 hours prior to anesthesia to mitigate the risk of regurgitation aspiration, following standard anesthetic safety recommendations for small exotic mammals. Following imaging, animals were moved to heated recovery enclosures and carefully monitored until they restored normal posture, coordinated movement, and full responsiveness. No adverse reactions or complications related to anesthesia were observed in any of the animals.

Radiography procedure

Radiographic evaluation was performed to assess the position and relative radiodensity of the liver within the abdomen. All imaging was conducted at the Diagnostic Imaging Unit of the Faculty of Veterinary Medicine, Science and Research Branch, Islamic Azad University, Tehran, Iran. Animals were positioned in dorsal recumbency for ventrodorsal projections and in right lateral recumbency for lateral projections.

Radiographs were obtained using a CR Fuji computed radiography system (Fujifilm Corporation, Tokyo, Japan). Exposure parameters were optimized for small exotic mammals, with mean exposure settings of 55 kVp and 3.5 mAs, consistent with published radiographic techniques for exotic companion mammals (Capello and Lennox, 2013). All radiographic studies were reviewed by a board-certified veterinary radiologist. Animals were excluded from further imaging upon detection of any abnormality potentially affecting liver assessment. The mentioned abnormalities included hepatomegaly, irregular or rounded hepatic margins, peritoneal effusion, abdominal mineralization, gastrointestinal issues, or thoracic abnormalities. Radiographs served as the baseline reference for evaluating liver location, structure, and radiodensity compared to the surrounding organs.

Ultrasound procedure

Ultrasonography was conducted in the Diagnostic Imaging Unit of the Faculty of Veterinary Medicine, Islamic Azad University (Tehran, Iran), using a Mindray S9 veterinary ultrasound system (Mindray Medical International Ltd., Shenzhen, China) equipped with a 7-12 MHz high-frequency linear transducer. The cranial abdominal region was clipped, and acoustic coupling gel was applied to optimize sound transmission and reduce surface artifacts. Scans were performed through the intercostal spaces and the subxiphoid window to obtain a comprehensive visualization of the liver parenchyma. Gain, depth, and focal settings were adjusted manually for each animal to optimize contrast resolution and delineation of hepatic and vascular structures. Animals were placed in dorsal and right-lateral recumbency to obtain standardized longitudinal and transverse images. A consistent morphometric protocol was applied. Hepatic length was measured in a longitudinal plane from the diaphragmatic surface to the caudal parenchymal margin. The caudal landmark for the right lobe was the cranial pole of the right kidney, while the caudal boundary of the left lobe was located near the lesser curvature of the stomach. Hepatic width was measured in the transverse plane at the level of the main portal vein bifurcation, using the maximal medial-to-lateral parenchymal dimension. All measurements were taken at end-expiration to minimize respiratory motion and were repeated three times by the same experienced examiner; the mean of the three measurements was used for analysis to minimize operator variability.

The gallbladder, intrahepatic vasculature, and major portal venous branches were qualitatively assessed for morphology, echogenicity, wall definition, and anatomical relationships. Hepatic margins, lobar echotexture patterns, and portal vein clarity were documented to establish baseline ultrasonographic characteristics of the healthy long-eared hedgehog.

Computed tomography procedure

Computed tomography was performed in the Diagnostic Imaging Unit of the Faculty of Veterinary Medicine, Islamic Azad University (Tehran, Iran), using a dual-detector CT scanner (Siemens Healthineers, Erlangen, Germany). Animals were positioned in dorsal and sternal recumbencies to achieve consistent abdominal cross-sectional images.

For contrast-enhanced studies, iohexol (Omnipaque™ 300 mg I/mL; GE Healthcare, Chicago, USA) was administered intravenously at a dosage of 600 mg iodine/kg body weight, equivalent to 2 mL/kg of this formulation. The dosing protocol aligned with published CT contrast studies in small exotic mammals, including chinchillas and ferrets, where non-ionic iodinated contrast media were used at similar volume-based doses (Karakurum et al., 2024; von Stade and Sadar, 2024). Scanning started about 25-30 seconds after the contrast was given, which was chosen to match the early portal venous phase. The timing helps ensure that the liver tissue and intrahepatic structures are properly highlighted vasculature. CT images were acquired at a slice thickness of 1.0 mm. High-frequency reconstruction algorithms optimized for soft-tissue evaluation were applied. The datasets were processed using Vitrea vital advanced visualization software (version 6.3.2160; Vital Images, Inc., Minnetonka, USA), which enabled three-dimensional (3D) reconstruction of the hepatic structures. The 3D reconstructions were used to evaluate overall hepatic morphology, delineate hepatic lobe boundaries, and assess spatial relationships between the liver and adjacent abdominal organs.

Magnetic resonance imaging procedure

Magnetic resonance imaging was performed in the Diagnostic Imaging Unit of the Faculty of Veterinary Medicine, Islamic Azad University (Tehran, Iran), using a 1.5-T MRI system (Philips Achieva; Philips Healthcare, Best, Netherlands). All animals were positioned in dorsal recumbency, and imaging was performed with a small-animal surface coil to maximize signal-to-noise ratio.

T2-weighted fast spin-echo (T2-W) images, which provide enhanced sensitivity to differences in tissue water content, were obtained in the axial plane with repetition time (TR) at 3027 ms, echo time (TE) at 100 ms, slice thickness at 2.0 mm, field of view (FOV) at 80 × 80 mm, matrix size at 256 × 256, number of excitations (NEX) at 3, bandwidth of 180 Hz/pixel, and slice spacing at 0 mm (contiguous slices). Additional T1-weighted and T2-weighted sequences were acquired in axial and coronal planes using TR at 597 ms, TE at 15 ms, slice thickness at 2.0 mm, FOV at 80 × 80 mm, matrix size at 256 × 256, NEX at 3, and bandwidth of 180 Hz/pixel. The acquired sequences provided complementary anatomical information and were used to characterize hepatic margins, delineate hepatic lobe boundaries, and visualize intrahepatic vascular structures. For contrast-enhanced MRI examinations, a gadolinium-based contrast agent (gadopentetate dimeglumine; Magnevist®, Bayer HealthCare, Berlin, Germany) was administered intravenously at a dose of 0.1 mmol/kg body weight. Contrast-enhanced T1-weighted images were acquired approximately 20-30 seconds after contrast administration to achieve early vascular and parenchymal enhancement. The contrast agent and dosage were chosen according to well-established, weight-based MRI protocols commonly used across mammalian species, since there are currently no MRI contrast studies specific to hedgehogs (Islam and Tsnobiladze, 2024).

MRI datasets were evaluated qualitatively based on hepatic parenchymal signal intensity relative to skeletal muscle and subcutaneous fat. Quantitative morphometric measurements, including hepatic lobe length and width, were obtained from isotopically reconstructed MRI volumes using standardized anatomical landmarks consistent with those applied in the CT analysis.

Image analysis

All CT and MRI datasets were reconstructed into 3D volumes and independently evaluated by two experienced veterinary radiologists, each with over five years of diagnostic imaging experience. Radiologists examined all CT and MRI datasets without separating the modalities, ensuring a consistent cross-modality approach. The CT datasets were analyzed using Vitrea Vital advanced visualization software (version 6.3.2160; Vital Images, Inc., Minnetonka, USA), which was also used for 3D reconstruction and quantitative morphometric measurements. MRI measurements were performed using the integrated measurement tools of the Philips Achieva workstation software (Philips Healthcare, Best, Netherlands). Quantitative variables included hepatic lobe dimensions and parenchymal attenuation values on CT, expressed in Hounsfield units. The MRI variables included qualitative signal intensity relative to skeletal muscle and subcutaneous fat. Additional qualitative assessments included intrahepatic vascular branching patterns, gallbladder position, hepatic capsule morphology, and lobar boundary definition. To assess measurement consistency, inter-observer reliability was quantified using a two-way random-effects intraclass correlation coefficient (ICC) with absolute agreement. The ICC values for hepatic lobe length and width were 0.87-0.94, indicating excellent agreement. Where measurements disagreed or discrepancies exceeded 10%, both radiologists reassessed the datasets to reach a consensus value, which was used in the final analysis.

Statistical analysis

Statistical analyses were conducted using SPSS software (version 26.0; IBM Corp., Chicago, USA). Results were reported as mean ± standard deviation (SD). Because of the small sample size (n = 7), data for each variable were first tested for normal distribution using the Shapiro-Wilk test to confirm whether parametric methods were appropriate. All measured variables met the normality assumptions, allowing paired-sample t-tests to compare the right and left hepatic lobes within each imaging modality. A p-value less than 5% ($p < 0.05$) was considered statistically significant. Given the exploratory nature of the study and limited sample size, statistical outcomes were interpreted cautiously. As a secondary confirmatory analysis, non-parametric Wilcoxon signed-rank tests were also performed. The mentioned tests produced results consistent with the findings of the paired t-test. To avoid overinterpretation, all statistical conclusions were evaluated in conjunction with qualitative and descriptive imaging findings.

RESULTS

Radiography

Radiographic imaging provided clear visualization of the liver and its anatomical connection to the nearby organs in the long-eared hedgehog. The liver was consistently observed in the cranial abdomen, extending caudally from the diaphragm toward the stomach. The right hepatic lobe was positioned near the caudal margin of the diaphragm, while the left hepatic lobe was located more ventrally, near the gastric curvature. Both ventrodorsal and right lateral projections demonstrated smooth, well-defined hepatic margins with sufficient contrast to distinguish the liver from neighboring soft-tissue organs, including the stomach, intestines, and diaphragm (Figure 1).

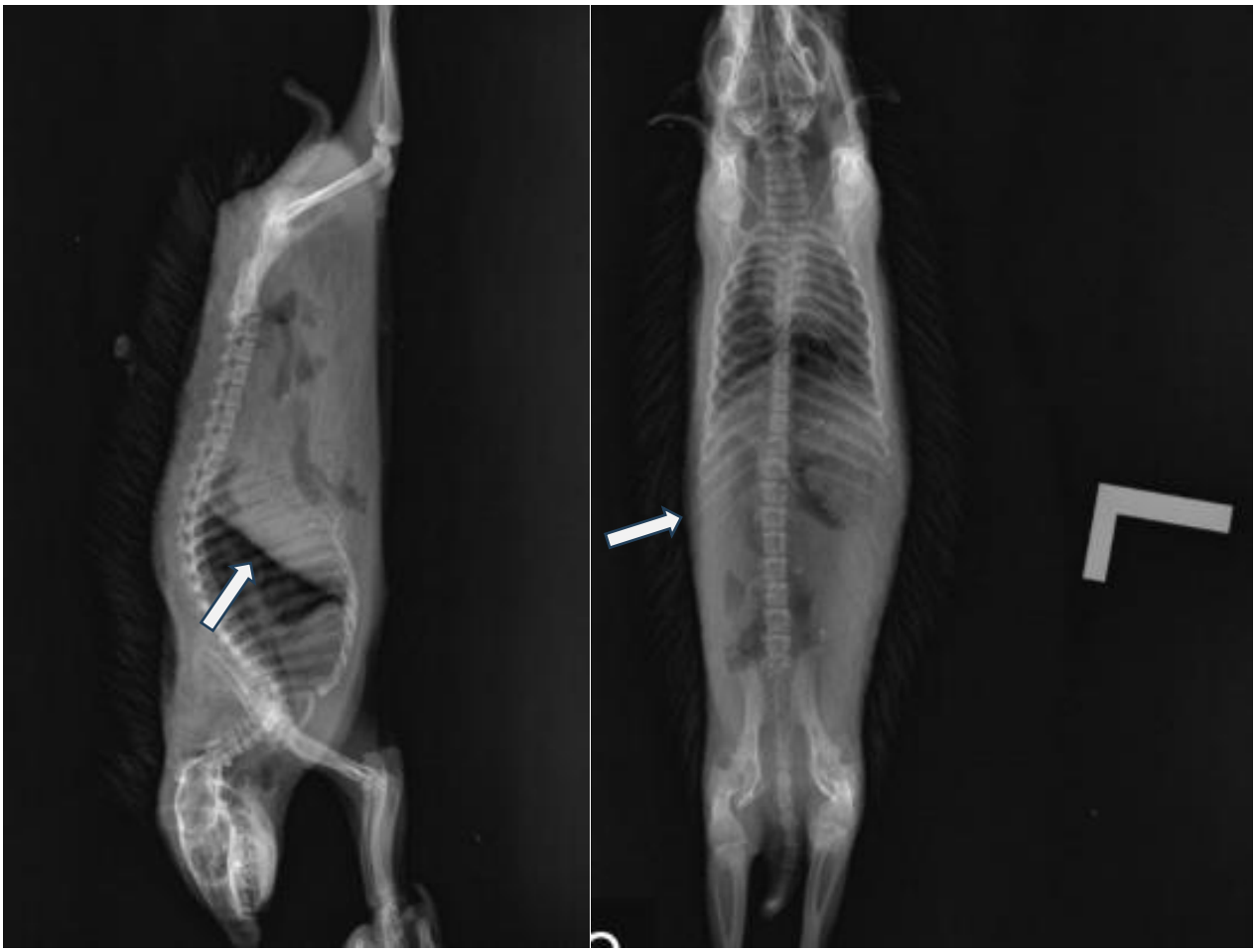


Figure 1. Right lateral (left) and ventrodorsal (right) radiographic views of an adult male long-eared hedgehog (*Hemiechinus auritus*; mean body weight 365 g). Arrows indicate the liver, visualized as a soft-tissue opacity in the cranial abdomen.

Ultrasonography

Ultrasonographic assessment produced high-resolution images with clearly delineated hepatic parenchymal structure. Overall, the hepatic parenchyma appeared homogeneous in both lobes. Quantitative ultrasonographic measurements of hepatic length and width for the right and left lobes are summarized in Table 1 and indicate no statistically significant differences between lobes ($p > 0.05$). Minor subjective echogenic variation was occasionally observed between lobes; however, the differences were subtle, inconsistent across individuals, and not associated with any measurable differences in shape or structure. The gallbladder was consistently visualized as an anechoic, thin-walled, fluid-filled sac situated along the visceral surface of the liver (Figure 2). Major vascular structures, including branches of the portal vein and hepatic veins, were easily identified and displayed typical anechoic lumens with well-defined echogenic walls (Figure 2). Hepatic margins were smooth and clearly defined, and no focal parenchymal abnormalities or biliary dilatation were observed.

Table 1. Morphometric measurements of the liver in long-eared hedgehogs (*Hemiechinus auritus*) across imaging techniques

Modality	Liver lobe	Length (cm)	Width (cm)	p-value (Length)	p-value (Width)
Radiography	Right	2.15 ± 0.22	1.28 ± 0.10	0.284	0.317
	Left	2.22 ± 0.25	1.31 ± 0.11		
Ultrasound	Right	2.20 ± 0.24	1.30 ± 0.12	0.301	0.355
	Left	2.27 ± 0.26	1.33 ± 0.13		
CT	Right	2.18 ± 0.20	1.29 ± 0.11	0.265	0.298
	Left	2.24 ± 0.22	1.32 ± 0.12		
MRI	Right	2.16 ± 0.21	1.27 ± 0.10	0.290	0.341
	Left	2.23 ± 0.23	1.30 ± 0.12		

Note: Values represent mean ± standard deviation (SD). Length and width measurements were obtained using standardized anatomical landmarks specific to each imaging modality. P-values indicate paired comparisons between right and left hepatic lobes within each modality.



Figure 2. Ultrasonographic image of the liver in an adult male long-eared hedgehog (*Hemiechinus auritus*; aged one year old). The arrow indicates the hepatic parenchyma, showing a homogeneous echotexture.

Computed tomography

Computed tomography provided detailed morphometric and volumetric information for the hepatic lobes of the long-eared hedgehog. The right hepatic lobe was consistently positioned near the caudate lobe, whereas the left hepatic lobe was situated closer to the spleen. Across all CT assessments, the right hepatic lobe measured 2.18 ± 0.20 cm in length and 1.29 ± 0.11 cm in width, while the left lobe measured 2.24 ± 0.22 cm in length and 1.32 ± 0.12 cm in width (Table 1). No statistically significant morphometric differences were observed between the right and left liver lobes in animals ($p > 0.05$), and measurements indicated substantial overlap between lobes in the present study. Contrast-enhanced CT scans provided sharp delineation of hepatic margins and excellent visualization of intrahepatic vascular structures, including central portal and hepatic venous branches. Non-contrast CT images illustrated homogeneous soft-tissue attenuation throughout the hepatic parenchyma, with density values intermediate between those of pulmonary tissue and bone. The 3D reconstructions enhanced anatomical understanding by illustrating vascular branching patterns and verifying the absence of focal lesions, abnormal structures, or asymmetry (Figures 3 and 4; Table 2).

Table 2. Liver volume and attenuation/signal intensity in Long-Eared Hedgehogs (*Hemiechinus auritus*) across imaging techniques

Modality	Liver lobe	Volume (mL; Mean ± SD)	Attenuation / Signal intensity	p-value (Volume)
CT (non-contrast)	Right	1.92 ± 0.20	Homogeneous parenchyma, 52.4 ± 4.8 HU	0.18
	Left	2.01 ± 0.22	Similar pattern, 53.9 ± 5.1 HU	-
CT (contrast)	Right	1.95 ± 0.21	Homogeneous parenchyma, 103.6 ± 9.7 HU	0.17
	Left	2.04 ± 0.23	Homogeneous parenchyma, 99.8 ± 8.9 HU	-
CT (3D)	Right	1.94 ± 0.19	Homogeneous parenchyma with clear intrahepatic vessels	0.19
	Left	2.03 ± 0.21	Homogeneous parenchyma; no focal hepatic lesions	-
MRI (non-contrast)	Right	1.96 ± 0.20	Intermediate signal relative to muscle; lower than subcutaneous fat	0.20
	Left	2.05 ± 0.22	Homogeneous parenchymal signal	-
MRI (contrast)	Right	1.98 ± 0.21	Homogeneous enhancement; intermediate relative to muscle; lower than fat	0.19
	Left	2.07 ± 0.23	Homogeneous enhancement with well-defined margins	-

Note: Volume values are presented as mean ± standard deviation (SD). CT attenuation values are expressed in Hounsfield units (HU). MRI signal intensity findings are qualitative and reported relative to adjacent tissues. A p-value represents paired comparisons between right and left hepatic lobes within each imaging modality (paired-sample t-tests). Statistical results are interpreted as exploratory due to the small sample size (n = 7).

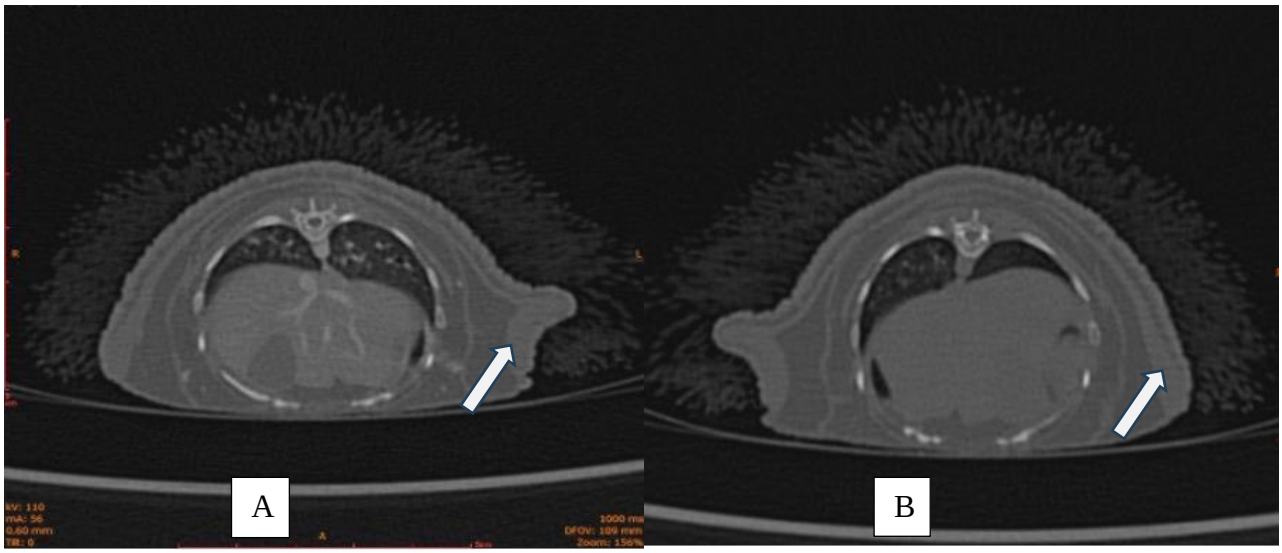


Figure 3. Transverse computed tomography (CT) images of the cranial abdomen in an adult male long-eared hedgehog (*Hemiechinus auritus*). **A:** A contrast-enhanced CT image, **B:** A non-contrast CT image. Arrows indicate the liver, visualized as a homogeneous soft-tissue structure in the cranial abdomen.

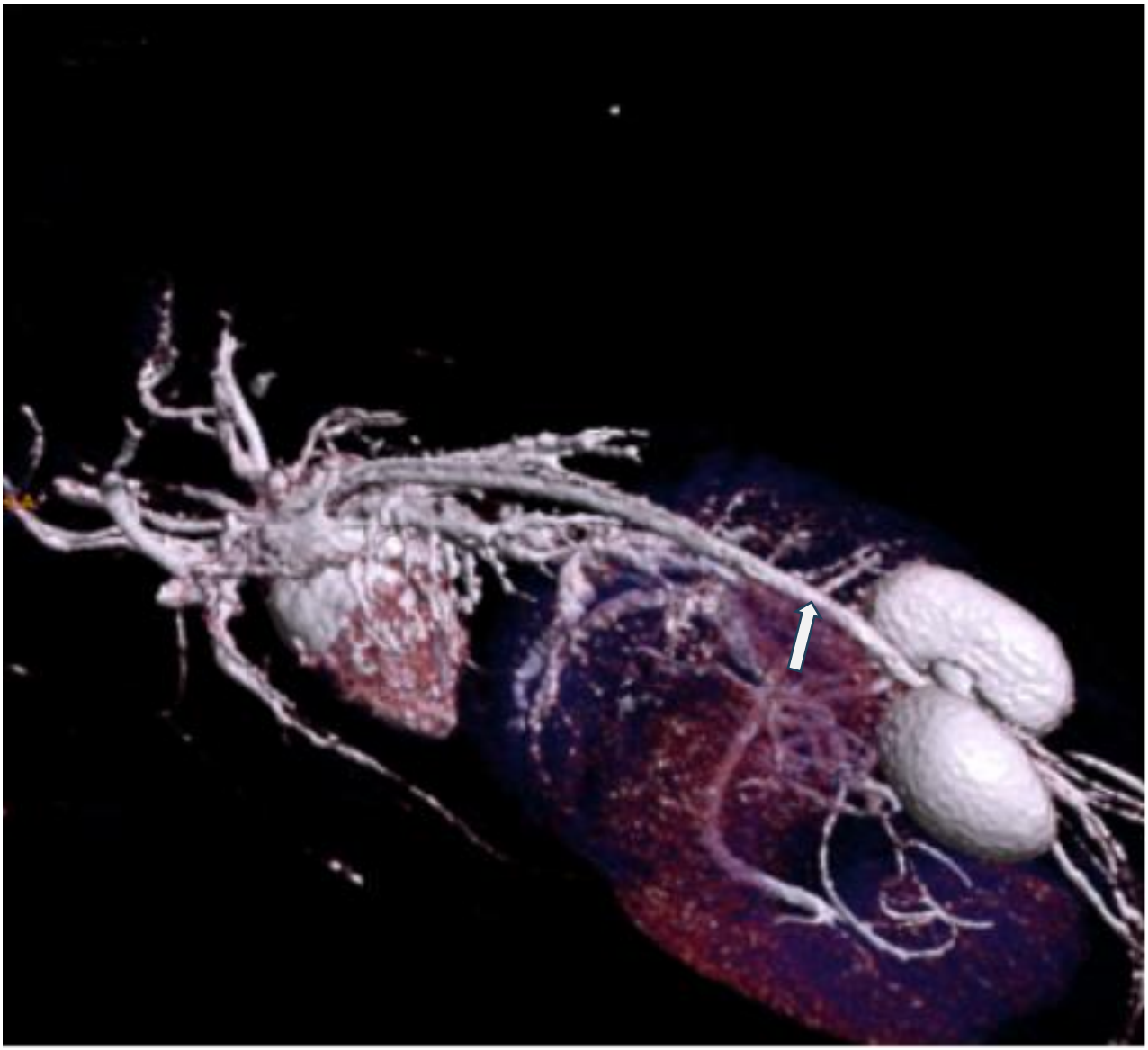


Figure 4. Three-dimensional contrast-enhanced computed tomography (CT) reconstruction of the cranial abdomen in an adult male long-eared hedgehog (*Hemiechinus auritus*). The arrow indicates the liver, showing its overall three-dimensional configuration and the intrahepatic vascular branches visualized after contrast administration.

Magnetic resonance imaging

Magnetic resonance imaging provided superior soft-tissue contrast compared to the other imaging techniques. On T2-weighted sequences, the hepatic parenchyma appeared hypointense relative to nearby soft tissues, whereas intrahepatic vascular and biliary structures demonstrated hyperintense luminal signals, making them more visible. On T1-weighted sequences, hepatic signal intensity was lower than that of the spleen, which facilitated accurate delineation of lobar margins and the hepatic capsule. Contrast-enhanced MRI sequences demonstrated uniform parenchymal development with signal intensity intermediate between that of skeletal muscle and subcutaneous fat. Hepatic borders were sharply defined, and the lobes exhibited consistent internal structures. Non-contrast MRI sequences illustrated similar morphological features, with no focal parenchymal lesions, vascular abnormalities, biliary dilation, or signal heterogeneity (Figure 5).

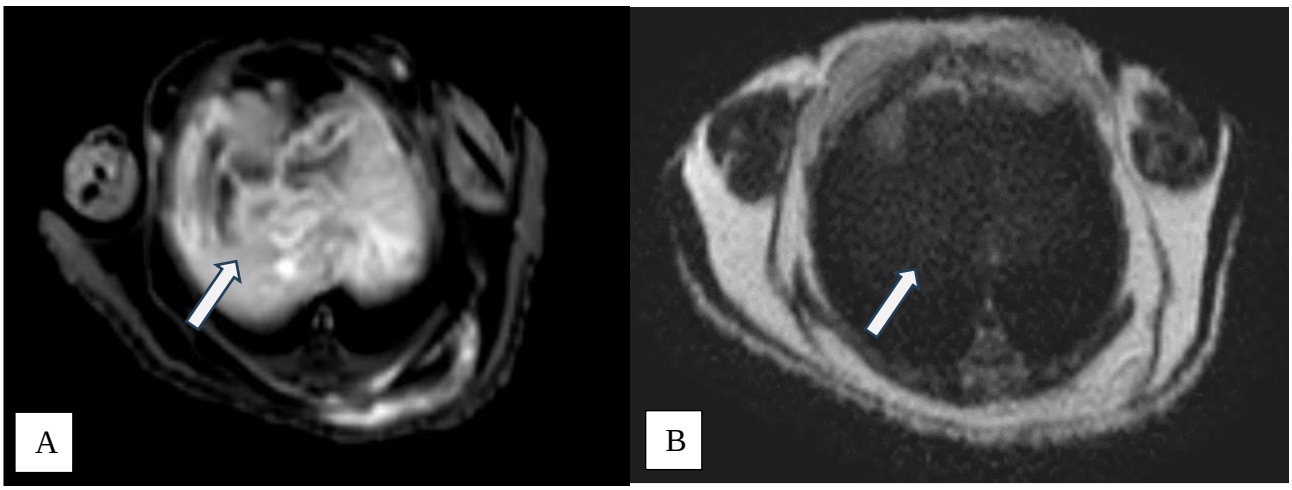


Figure 5. Transverse magnetic resonance imaging (MRI) images of the cranial abdomen in an adult male long-eared hedgehog (*Hemiechinus auritus*; aged one year old). **A**: A contrast-enhanced MRI image, **B**: A non-contrast MRI image. Arrows indicate the liver in both panels.

Comparative morphometric analysis

Morphometric evaluation across all imaging techniques indicated that the right and left hepatic lobes of *H. auritus* had closely similar dimensions, with only slight numerical differences in mean length and width (Table 1). The calculated length-to-width ratios for both lobes were nearly identical, demonstrating considerable overlap and indicating no measurable structural distinction between the two lobes. Quantitative measurements from CT and MRI consistently illustrated similar shapes, highlighting their morphological similarity rather than distinct differences in the lobes. Paired-sample statistical comparisons further supported these observations. No significant differences were detected between the right and left hepatic lobes in length, width, estimated volume, or CT/MRI-derived attenuation and signal characteristics ($p > 0.05$; Tables 1 and 2). Due to the small sample size, these analyses were interpreted as exploratory. Nonetheless, the lack of statistical significance was observed consistently across all techniques. The morphometric results indicated that the liver of the long-eared hedgehog has a mostly symmetrical lobar structure, with no measurable signs of asymmetry. The morphometric suggested there was no evidence of functional differences or species-specific specializations between the liver lobes, indicating a uniform liver structure.

DISCUSSION

The multimodal imaging approach used in the present study provided a coherent, detailed description of hepatic anatomy in the long-eared hedgehog. Radiography, ultrasonography, CT, and MRI each contributed complementary information, enabling visualization of hepatic margins, parenchymal features, and major vascular landmarks in clinically healthy adult animals.

The radiographic assessment confidently highlighted the hepatic structure in the cranial abdomen, showing a clear separation from neighboring organs. As with other small exotic mammals, radiography provided limited detail of parenchymal structure but remained helpful in assessing the liver's position and overall shape (Sarani et al., 2024). Ultrasonography provided superior resolution of internal hepatic structure, consistently demonstrating homogeneous parenchymal echotexture, visible gallbladder morphology, and well-defined portal and hepatic vasculature. The

ultrasonographic appearance of the hepatic parenchyma, gallbladder, and central vascular structures observed in the present study was consistent with findings reported in African hedgehogs and other small mammals, including rabbits and chinchillas (Taki-El-Deen, 2020; Taati et al., 2024).

The CT imaging further enhanced structural definition, allowing precise delineation of hepatic margins, lobar boundaries, and intrahepatic vascular branching. The observed CT-based anatomical features were consistent with prior findings in chinchillas, ferrets, and rabbits, where non-invasive cross-sectional imaging was highly effective for characterizing visceral morphology (Capello and Lennox, 2013; Karakurum et al., 2024). MRI provided the highest soft-tissue contrast among all imaging techniques, enabling more precise differentiation of lobar boundaries and parenchymal features, especially in areas impacted by partial-volume effects or diaphragm overlap seen on CT. Such advantages of MRI, particularly its superior soft-tissue contrast and reduced susceptibility to overlapping structures compared with CT, are well recognized in veterinary diagnostic imaging across domestic animals, exotic species, and wildlife, regardless of the organ (Zhang et al., 2013; Jones et al., 2020; Greco et al., 2023).

Across all imaging techniques, the right and left hepatic lobes demonstrated closely similar dimensions, volumes, and tissue characteristics. This bilateral symmetry was consistent with published anatomical observations in several small exotic mammals, including ferrets, chinchillas, and African hedgehogs (Capello and Lennox, 2013). The high numerical agreement among measurements was due to the use of standardized anatomical landmarks, repeated measurements, and strong inter-observer reliability, with ICC values between 0.87 and 0.94. These methodological strengths reduced variability and supported the internal consistency of the morphometric dataset.

The species-specific reference values established in the present study provided valuable baseline data for veterinarians assessing liver health in *H. auritus*. Given the limited availability of published imaging data for hedgehogs, which are frequently obtained from diseased cases rather than healthy populations, the current findings enhance the existing diagnostic framework by establishing reference data on normal hepatic dimensions, parenchymal appearance, and vascular patterns across several imaging techniques. The established reference parameters may help clinicians to distinguish normal anatomical variation from early manifestations of hepatic disease.

The present study has some limitations, including a small sample size, which reduced statistical power and might not represent the full biological variability within the species. Only healthy adult males were examined, so age-related, sex-related, or pathological differences could not be assessed. Some images might have been affected by minor motion artifacts, species-specific thoracoabdominal shapes, and varying inflation levels of gastrointestinal structures. Doppler ultrasonography and advanced MRI techniques can provide additional insights into hepatic vascular dynamics, as indicated by previous veterinary imaging studies on abdominal organ perfusion and vascular evaluation (Greco et al., 2023; Karakurum et al., 2024). Comparative studies involving African hedgehogs, chinchillas, rabbits, and ferrets could provide valuable context for understanding hepatic morphology across small exotic mammals, thereby improving the interpretive value of the current findings (Taati et al., 2024; von Stade and Sadar, 2024).

CONCLUSION

The present study demonstrated that the combined use of radiography, ultrasonography, CT, and MRI provided detailed and complementary evaluations of hepatic anatomy in the long-eared hedgehog (*H. auritus*). Radiography reliably identified the overall position and shape of the liver, ultrasonography allowed dynamic visualization of parenchymal echotexture, the gallbladder, and central vascular structures, CT enabled precise morphometric assessment and clear depiction of lobar boundaries and intrahepatic vasculature, and MRI provided the highest soft-tissue contrast, improving visualization of parenchymal signal patterns and capsular margins. Across all techniques, the right and left hepatic lobes indicated similar dimensions and imaging features, indicating a bilaterally symmetrical liver structure in healthy adult animals. The reference measurements and qualitative imaging features established in the present study provided initial normative data for *H. auritus*, offering a practical diagnostic framework for clinicians evaluating liver health in long-eared hedgehog species. Future studies should investigate larger sample sizes, incorporate diseased individuals, and employ functional imaging techniques such as Doppler ultrasonography or perfusion MRI. The mentioned suggestions would be necessary to expand these baseline observations and enhance diagnostic interpretation in exotic animal practice.

DECLARATIONS

Acknowledgements

The authors would like to express their gratitude to the staff of the Diagnostic Imaging Unit, Faculty of Veterinary Medicine, Islamic Azad University, Science and Research Branch, Tehran, Iran, for their technical assistance during

imaging procedures. They also acknowledge the wildlife rehabilitation centers in South Khorasan and Sistan-Baluchestan provinces, Iran, for their cooperation in facilitating access to the animals utilized in the present study.

Authors' contributions

Mohammad Nasrollahzade Masule conceived and designed the study and supervised the research. Mehdi Ghanaat Pisheh performed radiographic and ultrasonographic imaging. Hassan Gilanpour contributed to anatomical interpretation and manuscript revision. Saied Bokaie assisted with statistical analysis and data interpretation. Siamak Mashhadirafiee conducted CT and MRI imaging and prepared the figures. All authors read and approved the final edition of the manuscript.

Ethical considerations

All experimental procedures were approved by the Animal Ethics Committee of the Islamic Azad University, Science and Research Branch, Tehran, Iran (Approval Code: IR.IAU.SRB.REC.1403.338). The authors confirm that this manuscript is original, has not been published previously, and is not under consideration elsewhere. No artificial intelligence (AI) tools were used for generating or writing the scientific content of this manuscript. The authors of the present study used Grammarly only for language and grammar refinement after they had fully prepared the scientific content. After using Grammarly assistance, the authors reviewed and edited the manuscript as required and take full responsibility for the content of the manuscript.

Funding

The present study received no financial support.

Competing interests

The authors declared no conflict of interest.

Availability of data and materials

The data supporting the findings of the present study are included in the article and are available from the corresponding author upon reasonable request.

REFERENCES

Ballard B and Cheek R (2016). Introduction to exotic animal medicine. In: R. Cheek and B. Ballard (Editors), Exotic animal medicine for the veterinary technician. John Wiley & Sons., Hoboken, NJ, USA, pp. 1-2. Available at: https://www.wiley.com/en-us/Exotic+Animal+Medicine+for+the+Veterinary+Technician%2C+4th+Edition-p-9781119863144

Bexton S (2016). Hedgehogs. BSAVA manual of wildlife casualties. British Small Animal Veterinary Association, Gloucester, UK, pp. 117-136. DOI: https://www.doi.org/10.22233/9781910443316.12

Capello V and Lennox AM (2013). Clinical radiology of exotic companion mammals. John Wiley & Sons., Hoboken, NJ, USA, pp. 11-13. Available at: https://pmc.ncbi.nlm.nih.gov/articles/PMC2797350/

Greco A, Meomartino L, Gnudi G, Brunetti A, and Di Giancamillo M (2023). Imaging techniques in veterinary medicine. Part II: Computed tomography, magnetic resonance imaging, nuclear medicine. European Journal of Radiology Open, 10: 100467. DOI: https://www.doi.org/10.1016/j.ejro.2022.100467

Hawkins SJ, Doss GA, and Mans C (2020). Evaluation of subcutaneous administration of alfaxalone-midazolam and ketamine-midazolam as sedation protocols in African pygmy hedgehogs (*Atelerix albiventris*). Journal of the American Veterinary Medical Association, 257(8): 820-825. DOI: https://www.doi.org/10.2460/javma.257.8.820

Jones K, Van Asselt N, Mans C, Hetzel S, and Waller III KR (2020). Use of radiographs and computed tomography for measurement of kidney size in healthy chinchillas (*Chinchilla lanigera*). Journal of Exotic Pet Medicine, 35: 106-111. DOI: https://www.doi.org/10.1053/j.jepm.2020.04.011

Juan-Sallés C and Garner MM (2007). Cytologic diagnosis of diseases of hedgehogs. Veterinary Clinics of North America: Exotic Animal Practice, 10(1): 51-59. DOI: https://www.doi.org/10.1016/j.cvex.2006.10.003

Karakurum E, Dimitrov R, Stamatova-Yovcheva K, Ersen M, and Dilek OG (2024). Anatomical computed tomography and magnetic resonance imaging architecture of the kidneys in the chinchilla (*Chinchilla lanigera*). Indian Journal of Animal Research, 58(5): 785-790. DOI: https://www.doi.org/10.18805/IJAR.BF-1511

Islam MT and Tsnobiladze V (2024). The application, safety, and recent developments of commonly used gadolinium-based contrast agents in MRI: A scoping review. European Medical Journal, 9(3): 63-73. DOI: https://www.doi.org/10.33590/emj/ZRVN2069

Nabipour A and Dehghani H (2012). Light and electron microscopic features of the kidney in hedgehog (*Hemiechinus auritus*). Journal of Veterinary Anatomy, 5(1): 91-106. DOI: https://www.doi.org/10.21608/jva.2012.44887

Sarani S, Enferadi A, Hasani SJ, Sarani MY, Rahnama M, and Sarani F (2024). Identification of zoonotic pathogenic bacteria from blood and ticks obtained from hares and long-eared hedgehogs (*Hemiechinus megalofis*) in eastern Iran. Comparative Immunology, Microbiology and Infectious Diseases, 104: 102097. DOI: https://www.doi.org/10.1016/j.cimid.2023.102097

Taati M, Raisi A, Golmirzaei M, and Rashnoei N (2024). Electrocardiogram assessment in long-eared hedgehogs (*Hemiechinus auritus*) following administration of anesthetics. Veterinary and Animal Science, 26: 100400. DOI: https://www.doi.org/10.1016/j.vas.2024.100400

Taki-El-Deen F (2020). Comparative anatomical studies on the skull of three mammals in Egypt having different diets. The Egyptian Journal of Hospital Medicine, 80(1): 696-703. DOI: https://www.doi.org/10.21608/EJHM.2020.99345

von Stade L and Sadar MJ (2024). Advanced imaging of small mammals. Advances in Small Animal Care, 5(1): 51-65. DOI: https://www.doi.org/10.1016/j.yasa.2024.06.004

Zhang JL, Rusinek H, Chandarana H, and Lee VS (2013). Functional MRI of the kidneys. Journal of Magnetic Resonance Imaging, 37(2): 282-293. DOI: https://www.doi.org/10.1002/jmri.23805

Publisher's note: Scienceline Publication Ltd. remains neutral with regard to jurisdictional claims in published maps and institutional affiliations.

Open Access: This article is licensed under a Creative Commons Attribution 4.0 International License, which permits use, sharing, adaptation, distribution and reproduction in any medium or format, as long as you give appropriate credit to the original author(s) and the source, provide a link to the Creative Commons licence, and indicate if changes were made. The images or other third party material in this article are included in the article's Creative Commons licence, unless indicated otherwise in a credit line to the material. If material is not included in the article's Creative Commons licence and your intended use is not permitted by statutory regulation or exceeds the permitted use, you will need to obtain permission directly from the copyright holder. To view a copy of this licence, visit https://creativecommons.org/licenses/by/4.0/.
© The Author(s) 2025

2025, Scienceline Publication
World's Veterinary Journal
World Vet J, 15(4): 1053-1062.
ISSN 2322-4568

DOI: https://dx.doi.org/10.54203/scil.2025.wvj107
PII: S232245682500107-15

Impacts of *Tenebrio molitor* Larval Meal on Zootechnical Performance, Biochemical Indices, and Intestinal Morphometry in Broiler Chickens

Nassi Guidi Hoeness Inaudi[1,2]*, AgbokA Komi[2], Attivi Komi[1], Mlaga Kodjo Gnatepe[1], Guénnolé Vinakpon[1], and Tona Kokou[1]

[1]*Laboratory of Poultry Production Techniques, Regional Centre of Excellence on Poultry Sciences (CERSA) of the University of Lomé, Lomé, Togo*
[2]*Laboratory for Research on Agro Resources and Environmental Health (LARASE), Higher School of Agronomy of the University of Lomé, Lomé, Togo*

*Corresponding author's Email: hoenessnassiguidi@gmail.com

ORIGINAL ARTICLE
Received: September 19, 2025
Revised: October 25, 2025
Accepted: November 25, 2025
Published: December 31, 2025

ABSTRACT

Protein resources availability is a major challenge for poultry farming in Sub-Saharan Africa. Insects such as *Tenebrio molitor* (*T. molitor*), known as yellow mealworm, which are rich in high-quality protein, offer a promising solution. The present study aimed to evaluate the effects of *T. molitor* larvae meal as an alternative protein source in broiler chicken diets. A total of 375 day-old hybrid broiler chickens (Crossbreeding of Sasso and Faso) were randomly assigned to five dietary treatments. Each treatment included five replicates with 15 chickens. During the 12-week study period, from hatching to the finishing phase, five dietary treatments were administered, including *T. molitor* larvae meal at 4% (TM4%), 6% (TM6%), 8% (TM8), black soldier fly larvae meal at 8% (BSF8), and as the control diet, fish meal at 8% (FM8). Biochemical parameters, including total protein, albumin, triglycerides, and cholesterol, as well as the small intestinal weight and length, and zootechnic performance such as feed intake, body weight gain, and feed conversion ratio (FCR), were measured. The current results indicated that feed consumption did not differ significantly among the treatments. However, the live weight of broiler chickens in TM8 was significantly higher in the finisher phase compared to other treatments, and their weight gain was higher in the grower and finisher phases. The FCR was significantly lower in the TM8 during the finisher phase than in other treatments. Carcass yield and gut length were significantly higher in the TM8. Total protein and albumin did not differ significantly among all groups. Cholesterol and triglyceride levels in TM6 were significantly higher than other groups. The incorporation of *T. molitor* meal at 8% inclusion level is recommended for broiler chicken feed.

Keywords: Biochemical parameter, Black soldier fly, Broiler chicken, Carcass yield, *Tenebrio molitor*, Weight gain

INTRODUCTION

Proteins, such as amino acids, are the main components of poultry feed and the biologically active compounds in the body, which contribute to tissue synthesis, tissue renewal, and body growth (Shariat Zadeh et al., 2019; Kidd et al., 2021). Proteins exist in the form of enzymes and hormones, playing important roles in the physiological functioning of living organisms (Sleman et al., 2015). In poultry, proteins are mainly provided through feed. Thus, the protein sources used in poultry feed are from two origins, namely animal protein sources and plant-based protein (Pexas et al., 2023). Conventional protein sources, such as fish and soybean meal, not only compete for human consumption but also contribute to deforestation and threaten fishery resources through widespread production and the constant harvesting of seafood to feed poultry (Attivi et al., 2023). It is essential to find alternative protein sources that are not in competition with human consumption, economically viable, and can be used in poultry feed as replacements for soybeans and fishmeal (Heuel et al., 2021).

Several studies have identified insects as an economically viable source of animal-based protein that can be used in poultry feed with less negative impacts on the environment (Khusro et al., 2012; Veldkamp et al., 2012; Shumo et al., 2019). Insects such as termites, beetles, caterpillars, fleas, and ants have all been used as dietary supplements in poultry feed (Ravindran and Blair, 1993). According to Mushambanyi and Balezi (2002), the expensive animal protein source, which accounts for approximately 10% of poultry feed, can be effectively replaced with meal produced from cockroaches and termites. Other studies have indicated that silkworm pupae (by-product of the silk industry) or housefly larvae can totally or partially substitute fishmeal in the feed of laying hens and broiler chickens without negatively affecting their production performance. Moreover, housefly larvae are an excellent alternative source of protein in broiler

To cite this paper: Nassi Guidi H.I., Agboka K., Attivi K., Gnatep M.K., Vinakpon G., Tona K. (2025). Impacts of *Tenebrio molitor* Larval Meal on Zootechnical Performance, Biochemical Indices, and Intestinal Morphometry in Broiler Chickens. *World Vet. J.*, 15(4): 1053-1062. DOI: https://dx.doi.org/10.54203/scil.2025.wvj107

chicken feeds (Pieterse et al., 2014; Khan et al., 2016) and laying hens (Akpodiete et al., 1998; Agunbiade et al., 2007). Several studies have been carried out on the use of soldier fly maggots in the feed of broiler chickens and laying hens, with convincing results, particularly improvements in growth performance and egg production (Attivi et al., 2023).

Tenebrio molitor (*T. molitor*), known as yellow mealworm, is one of the most widely consumed insects in the world and recognized for its valuable nutritional content, digestibility of its nutrients and essential amino acids, especially in monogastrics such as poultry and pigs (Bovera et al., 2016; Benzertiha et al., 2020; Elahi et al., 2020). Most studies have reported positive effects of *T. molitor* meal in broiler diets, particularly on body weight gain (Bovera et al., 2016; Biasato et al., 2018). However, most existing studies have not investigated the impact of *T. molitor* meal on blood biochemical parameters in broiler chickens. It should be noted that most studies on the use of *T. molitor* larvae in poultry feed have not recommended an appropriate inclusion rate of *T. molitor* larvae in the diet of broiler chickens, especially for breeds that are improved and adapted to tropical climates. Intermediate-growing broiler chickens, in particular the chickens resulting from the Sasso hens and local Faso cocks crossbreeding, are more adapted to the tropical climate (Bilalissi et al., 2022). The present study aimed to evaluate the effects of adding *T. molitor* to broiler chicken feed on digestive, biochemical, and zootechnical parameters, which are sensitive indicators of feed quality in animals.

MATERIAL AND METHOD

Ethical approval

All experimental protocols were reviewed and approved by the Ethics Committee of the Regional Center of Excellence in Poultry Sciences (CERSA) at the University of Lomé, Lomé, Togo, a branch of the National Ethics Committee for the control and supervision of experiments on animals. All the authors complied with the ARRIVE guidelines.

Biological materials

Tenebrio molitor larvae

The *T. molitor* used for larval production originated from strains imported from the United States in 2021. These strains were subsequently multiplied and reared at the Research Laboratory on Agro Resources and Environmental Health of the University of Lomé, Togo. For larval production, the method of Aguilar-Miranda et al. (2002) was carried out for four months. For mating, 20 males and 30 females of *T. molitor*, aged 5-11 days, were selected and introduced into 25 boxes (Length = 6.5 cm and Width = 4.5 cm) containing a mixture of 50 g wheat bran and maize bran (Aguilar-Miranda et al., 2002). Eggs of *T. molitor* were collected after one week and incubated in rearing trays (a blue, round plastic tray with a diameter of 80 cm and a height of 5 cm). The eggs effectively hatched after three weeks of incubation. The hatched larvae were fed with 4 kg of wheat-maize bran/box for three months. A total of 50 g of orange slices was placed in each rearing tray to provide larvae with water and energy (Aguilar-Miranda et al., 2002). The larvae were collected at the early pre-chrysalid stage based on specific characteristics, including reduced mobility, pale body, and slight cuticle hardening, indicating the onset of pupation. The larvae collected were starved for 24 hours to allow emptying of the gastrointestinal tract (GIT), minimizing internal contents that could affect subsequent analyses, then oven dried (CL012N, Belgium) at 65°C for 72 hours. After drying, the larvae were left in the open air at the ambient temperature (28 ± 1°C) for 15-20 minutes. Larvae were then ground in a GRINDOMIX GM 300 mixer (Retsch GmbH, Germany) to obtain 1.2 kg/box of *T. molitor* larvae powder, which has been stored at 4°C for further experiments.

Black soldier fly larvae

The reference method of Attivi et al. (2023) was used for the production of black soldier fly (BSF; *Hermetia illucens*) larvae. Incubation boxes were used to collect freshly laid eggs, and first-stage larvae were obtained after three days. A medium containing a mixture of 50% palm kernel cake and 50% beer dregs, supplied by KSY POPO Group (Lomé, Maritime Region, Togo), was used to grow the young larvae. A relative humidity of 60-70% and a temperature of 28 ± 1°C with a photoperiod of 12:12 (Light: dark) were maintained in the rearing room. A total of 100 kg of fresh larvae aged 14 days were produced, collected, and killed (by freezing) at -20°C. The harvested larvae were washed and dried at 70°C for 72 hours in an autoclave dryer (CL012N, Belgium) at the production unit of the Regional Centre of Excellence in Avian Sciences at the University of Lomé, Togo. After drying, a total of 30 kg of BSF larvae meal was used in the present study, with an inclusion rate of 8% in the diet, based on the findings of Attivi et al. (2023). Table 1 shows the chemical and nutritional composition of the meal of *H. illucens* larvae.

For feed manufacturing, all ingredients, including corn, wheat bran, soybean meal, black soldier larvae, brewers' grains, oyster shells, common salt, *T. molitor* larvae meal, and essential amino acids, were first ground in a grinder, and homogeneous mixing was performed using a vertical mixer with a grinder.

Fishmeal

The fishmeal (30 kg) used in the present study was imported from Senegal Halieutics SA, Senegal. Fishmeal is widely used by West African poultry farmers (Attivi et al., 2023). Table 1 shows the chemical and nutritional composition of fishmeal.

Table 1. Chemical and nutritional composition of different protein sources, including fish meal, black soldier fly larvae meal, and *Tenebrio molitor* larvae meal, for the hybrid broiler chickens' diet

Parameters \ Protein sources	Fish meal	Black soldier fly	*Tenebrio molitor*
Dry matter (%)	94.4	91.3	85.3
Crude protein (%)	40	47.1	52.09
Fat (%)	10	25	37.44
Calcium (%)	4	6.5	1.45
Phosphorus (%)	2.5	1.05	3.5
Methionine + Cysteine (%)	1.54	1.42	4.63
Lysine (%)	2	4.90	1.6
Energy (kcal/kg)	2.800	3.102	2.36

Nutritional analysis of fishmeal, *Tenebrio molitor, and Hermetia illucens*

Nutritional value of insect meal (*T. molitor and H. illucens*) and fishmeal was analyzed at the Togolese Institute of Agronomic Research, Lomé, Togo. Nutritional analyses focused on dry matter content, crude protein, lipid levels, and calcium, phosphorus, methionine, lysine, cysteine, and energy values. The protein content was determined by the Kjeldahl method according to NF V18-100 (1977). The dry matter content was expressed as a percentage of the weight of the fish meal, *T. molitor*, and the BSF larvae sample. The fat was determined using a Soxhlet apparatus (C. Gerhardt GmbH & Co. KG, Germany) according to the AOAC 960.39 method (AOAC, 1999). Calcium and phosphorus contents were determined using the AOAC 935.13 and 965.17 methods, respectively (AOAC International, 2005). Calcium was released by acid digestion and quantified by titration with EDTA using a suitable indicator, while phosphorus was measured after digestion and determined spectrophotometrically (PG Instruments, United Kingdom) as phosphate. The methionine and lysine content was achieved in accordance with TS EN ISO 17180. Cysteine content was determined by spectrophotometry using L-cysteine tablets (Now Foods, Bloomingdale, IL, USA). Metabolizable energy (ME) was calculated as described by the University of Georgia Poultry Science Extension (2025).

Experimental diets

A total of five rations were designed, including diets with 4% of *T. molitor* (TM4), 6% of *T. molitor* (TM6), 8% of *T. molitor* meal (TM8), 8% of black soldier flies' maggots (BSF8), and 8% of fish meal (FM8), representing the control group (Mlaga et al., 2022; Attivi et al., 2023). These diets have been formulated to contain similar levels of energy and protein across the developmental stages, including the starter (3 weeks), grower (6 weeks), and finisher phases (3 weeks; Table 2). Based on the nutritional content of the ingredients and the dietary needs of chickens raised in tropical conditions, specifically 17-22% of crude protein and 2700-3000 kcal/kg of metabolizable energy, as reported by Kpomasse et al. (2020), the inclusion rates of these ingredients were calculated using a locally developed Excel software. Water and feed were provided *ad libitum* according to Chokakkar et al. (2024) during the 12-week experiment.

Experimental design

Unsexed, day-old broiler chickens from the crossbreeding of 35-week-old Sasso hens, imported from France, and a 35-week-old local Faso rooster, imported from Burkina Faso, were used for the present study. A total of 375 day-old crossbred broiler chickens were randomly divided into five treatment groups, with five replicates per treatment, each containing 15 chickens. The treatment groups were fed with 4% of *T. molitor* larvae meal (TM4), 6% of *T. molitor* larvae meal (TM6), 8% of T. *molitor* larvae meal (TM8), 8% of BSF larvae meal (BSF8), and 8% of fish meal (FM8). The chickens were raised for 12 weeks (from day one to 12 weeks of age) in a semi-closed building, at an ambient temperature ranging from 27 to 35°C and a relative humidity from 50 to 60%. Lighting was provided for 24 hours per day during the first week and adjusted to 18 hours per day thereafter. Chickens were reared at a density of 10 Chickens/m². Chickens were fed a diet with a metabolizable energy value ranging from 2,734 to 2,934 kcal/kg and a crude protein content varying from 17.35% to 20.84%.

Table 2. Composition of experimental diets formulated for hybrid broiler chickens from day 1 to 12 weeks of age, across starter, grower, and finisher phases

Ingredients	Starter phase					Grower phase					Finisher phase				
	FM8	BSF8	TM4	TM6	TM8	FM8	BSF8	TM4	TM6	TM8	FM8	BSF8	TM4	TM6	TM8
	Incorporation rate														
Togo-Benin maize (%)	43	58.5	55	54.65	53	49	57	53	52	53	50	56	54	53	53
Cubed bran/ wheat (%)	10.15	4	4.65	4	4.65	10.15	4	4.65	8.75	4.65	10.15	4.75	4.65	4	4
Roasted soybeans (%)	20	9.5	8	8	8	14	9.5	9	6	8	13	8.5	8	8	7
Soybean meal 45%	7	7.65	16	15	15	8	7.65	16	15	15	8	7.65	16	16.75	15.75
Beer spent grains (%)	8	5	5	5	4	7	6.5	6	5	4	7	6.5	6	5	5
Fishmeal 40%	8	0	0	0	0	8	0	0	0	0	8	0	0	0	0
Tenebrio molitor (%)	0	0	4	6	8	0	0	4	6	8	0	0	4	6	8
Black soldier fly maggots (%)	0	8	0	0	0	0	8	0	0	0	0	8	0	0	0
MMC 5%	100	5	5	5	5	1	5	5	5	5	1	1	5	5	5
Methionine (%)	0.1	0.1	0.1	0.1	0.1	0.1	0.1	0.1	0.1	0.1	0.1	0.1	0.1	0.1	0.1
Lysine (%)	0.2	0.2	0.2	0.2	0.2	0.2	0.2	0.2	0.2	0.2	0.2	0.2	0.2	0.2	0.2
Oyster shell (%)	2	1.5	1.5	1.5	1.5	2	1.5	1.5	1.4	1.5	2	2	1.5	1.4	1.4
NaCl (g)	0.3	0.3	0.3	0.3	0.3	0.3	0.3	0.3	0.3	0.3	0.3	0.3	0.3	0.3	0.3
Premix 2 (%)	0.25	0.25	0.25	0.25	0.25	0.25	0.25	0.25	0.25	0.25	0.25	5	0.25	0.25	0.25
Total (%)	100	100	100	100	100	100	100	100	100	100	100	100	100	100	100
Nutritional values															
Crude protein (%)	20.81	20.67	20.83	20.29	20.4	17.91	17.91	17.45	17.93	17.4	18.56	18.93	19.00	18.91	18.98
Crude fat (%)	7.68	6.11	6.2	6.89	7.53	6.6	6.16	6.4	6.55	7.53	6.43	5.81	6.23	6.38	7.36
Crude ash (%)	2.23	2.08	1.31	1.34	1.4	1.88	2.14	1.41	1.51	1.4	1.83	2.14	1.36	1.46	1.35
Crude fiber (%)	5.87	4.95	5.3	5.16	5	5.71	5.11	5.42	5.39	5	5.7	4.96	5.4	5.38	4.98
Lysine (%)	1.4	1.21	1.14	1.11	1.1	1.31	1.22	1.17	1.09	1.1	1.29	1.09	1.15	1.07	1.08
Methionine (%)	0.55	0.53	0.53	0.52	0.51	0.52	0.53	0.54	0.52	0.51	0.52	0.41	0.53	0.51	0.51
Meth. + Cysteine (%)	0.83	0.7	0.79	0.77	0.76	0.79	0.71	0.8	0.77	0.76	0.79	0.56	0.79	0.76	0.75
Tryptophan (%)	0.13	0.06	0.06	0.05	0.05	0.1	0.06	0.06	0.06	0.05	0.09	0.06	0.06	0.05	0.05
Threonine (%)	0.41	0.35	0.18	0.18	0.17	0.31	0.37	0.21	0.18	0.17	0.3	0.36	0.19	0.16	0.16
Calcium (%)	1.17	0.83	0.84	0.83	0.82	1.17	0.83	0.84	0.8	0.82	1.17	0.84	0.84	0.8	0.82
Phosphorus (%)	0.7	0.54	0.6	0.58	0.57	0.69	0.55	0.6	0.62	0.57	0.69	0.41	0.6	0.61	0.57
Metabolizable energy (kcal/kg)	2868.11	2897.45	2892.98	2927.79	2934.2	2759.01	2790.77	2788.88	2752.17	2734.2	2858.66	2849.27	288853	2851.82	2833.85

FM8: 8% of Fish meal, BSF8: 8% of black soldier fly larvae meal, TM4: 4% of *T. molitor* larvae meal, TM6: 6% of *T. molitor* larvae meal, TM8: 8% of *T. molitor* larvae meal, MMC: Meat meal concentrate 5%.

To cite this paper: Nassi Guidi H.I., Agboka K., Attivi K., Gnatep M.K., Vinakpon G., Tona K. (2025). Impacts of *Tenebrio molitor* Larval Meal on Zootechnical Performance, Biochemical Indices, and Intestinal Morphometry in Broiler Chickens. *World Vet. J.*, 15(4): 1053-1062. DOI: https://dx.doi.org/10.54203/scil.2025.wvj107

Vaccination program

The chickens underwent a prophylactic program adapted by CERSA, Togo, for Newcastle disease in accordance with the recommendations of Rauw et al. (2009). On days 5, 15, and 25 of age, they were vaccinated against Newcastle disease and infectious bronchitis with the AVINDHB1 vaccine (Laproved, Hungary) and the IB vaccine (Laproved, Hungary), respectively. On days 7, 14, and 21, they were vaccinated against Gumboro disease using the CEVAC IBD vaccine (Ceva Santé Animale, France). The antibiotic Alizeryl (Interchemie werken 'De Adelaar' B.V., Netherlands) was administered from days 16 to 20 and again from days 40 to 44. The anticoccidial Amprocox WS (Interchemie werken 'De Adelaar' B.V., Netherlands) was administered from days 30 to 34. Each treatment was accompanied by vitamin supplementation for two days.

Zootechnical performance

Throughout the duration of the experiment from August 15 to November 15, 2024, the Feed offered and leftovers per replicate were recorded weekly. Feed consumption was determined to be the difference between the food offered and the leftovers. Chickens were weighed at the end of each week, and weight gain was calculated as the difference between final weight and initial weight during the rearing period. Body weights and feed consumption were used to calculate the feed conversion ratio (FCR) according to the following formula (Attivi et al., 2023).

$$\text{Feed conversion ratio} = \frac{\text{Feed intake}}{\text{Weight gain}} \quad \text{(Formula 1)}$$

Biochemical parameters

At 12 weeks of age, blood samples (6 mL) were collected from 10 randomly selected chickens per treatment group into plain tubes without anticoagulant via the wing vein to evaluate the effect of different feed rations on the biochemical parameters of the chickens. The blood collected was centrifuged at 3000 rpm for 15 minutes by a Vacutainer brand centrifuge (Kouame et al., 2019). The serum obtained helped to analyze the biochemical parameters, including total proteins, albumin, cholesterol, and triglycerides, using the Synergy H1 microplate reader device (Agilent Technologies, United States). Different methods were used to perform the biochemical analyses of protein (Gomall et al., 1949), total cholesterol (Allain et al., 1974), and triglyceride concentrations (Fossati and Prencipe, 1982) in broiler chicken serum, respectively. The albumin concentration was determined according to the recommendations of Doumas et al. (1971) and the hydrolysis method of p-nitrophenyl phosphate at pH 10.4 (Krawczun et al., 2020).

Slaughtering

The methodology of Mlaga et al. (2020) was used for chicken culling. At 12 weeks of age, for slaughter, 10 chickens from each treatment were randomly selected and individually weighed using a digital weighing scale (ADVENTURER, Atlanticlabo, France) to ensure uniformity in live weights. Before slaughtering, chickens were fasted for 14 hours, but water was provided *ad libitum*. The selected chickens were first subjected to electrical stunning (Electric stunner VE memory, SOPRODA, France) and then were slaughtered by bleeding after an incision of the jugular vein. Once bled out, the slaughtered chickens were hung on hooks to allow the blood to flow completely. Afterwards, the carcasses were scalded in a hot water bath maintained at a temperature of 55 to 65°C. Defeathering was performed by mechanical plucking using an automatic plucking machine (Flexevi model, manufactured by BAYLE SA, France).

Carcass cutting

The carcasses were cut using the method described by Tougan et al. (2013). After the slaughter, plucking, evisceration, and cleaning, the following steps were employed. Initially, the legs were severed at the level of the Tibiotarsus-metatarsal joint, then the head was detached at the junction between the atlas and the occipital. After that, organs from the abdominal and thoracic cavities were extracted, along with the removal of abdominal fat. The weight of hot carcasses was measured, as well as the weight of viscera, including gizzard, liver, and intestines. The intestinal length was also measured using a flexible measuring tape after the intestine was laid flat without stretching. Finally, each carcass was cut to measure the weight of the different parts, namely the thigh, drumstick, wing, and keel, as well as the rest of the carcass.

Statistical analysis

All the data collected were subjected to a one-way analysis of variance (ANOVA) using the general linear model (GLM) procedure of GraphPad Prism Statistical Software, version 8.02. All comparisons between means were tested using the Tukey method at a p-value less than 5% ($p < 0.05$) significance level of acceptance.

RESULTS

Zootechnical performance

Table 3 presents the effects of *T. molitor* meal on the zootechnical performance in chickens. The results indicated that the feed consumption did not differ significantly ($p > 0.05$) among the different treatments (TM4, TM6, TM8, BSF8,

To cite this paper: Nassi Guidi H.I., Agboka K., Attivi K., Gnatep M.K., Vinakpon G., Tona K. (2025). Impacts of *Tenebrio molitor* Larval Meal on Zootechnical Performance, Biochemical Indices, and Intestinal Morphometry in Broiler Chickens. *World Vet. J.*, 15(4): 1053-1062. DOI: https://dx.doi.org/10.54203/scil.2025.wvj107

FM8) from the starter to the finisher phases. Similarly, live weight exhibited no significant difference ($p > 0.05$) among the different treatments (TM4, TM6, TM8, BSF8, FM8) in the starter and grower phases (0-9 weeks). However, in the finisher phase, live weight was significantly higher ($p < 0.05$) in TM8 (1385 g) and BSF8 (1325 g), compared to FM8 (1272 g), TM6 (1268 g), and TM4 (1213 g). Moreover, weight gain and FCR did not differ significantly ($p > 0.05$) among the different groups (TM4, TM6, TM8, BSF8, FM8) during the starter phase. However, the highest weight gain and the lowest FCR were observed in TM8 during the grower (15.79; 2.82) and finisher phases (20.66; 5.70).

Carcass characteristics

Table 4 illustrates carcass, drumstick, thigh, wing, and keel yields according to the different treatments. Among all diets, broiler chickens in TM8 and BSF8 indicated a significant difference in wing yield. However, the highest yields were observed in carcass (67.62%), thighs (9.91%), drumsticks (9.98%), and Keel yield (16.66%) in TM8. In contrast, the lowest yields in carcass (60.88%), thigh (7.94%), drumstick (7.70%), and Keel yield (12.12%) were observed in the FM8.

Length and relative weight of the small intestine

The relative weight of the intestine, gizzard, and liver indicated no significant differences ($p > 0.05$) among different groups (FM8, BSF8, TM4, TM6, and TM8). However, the length of the intestine was significantly higher ($p < 0.05$) in TM8 (167.8cm) compared to TM4 (159.5cm), TM6 (158.6cm), BSF8 (153.3cm), and FM8 (150.8cm; Table 5).

Table 3. Feed intake, average weight gain, and feed conversion ratio in hybrid broiler chickens during the starter, grower, and finisher phases

Parameters \ Treatments	FM8	BSF8	TM4	TM6	TM8	P value
Starter phase (0-3weeks)						
Live weight (g)	281.0 ± 3.48	297.7 ± 4.86	272.7 ± 11.02	277 ± 8.88	287.7 ± 3.06	0.1329
Feed intake (g/day)	16.96 ± 2.96	20.26 ± 1.6	17.85 ± 1.51	18.85 ± 1.51	19.78 ± 1.52	0.2292
Weight gain (g)	11.71 ± 0.17	12.51 ± 0.24	11.30 ± 0.53	11.52 ± 0.43	12.03 ± 0.15	0.1313
FCR	1.42 ± 0.29	1.60 ± 0.12	1.57 ± 0.12	1.62 ± 0.10	1.64 ± 0.07	0.3453
Grower phase (4-9 weeks)						
Live weight(g)	865.3 ± 15.72	911.3 ± 0.421	854.0 ± 32.58	873.3 ± 37.25	951.0 ± 20.09	0.1441
Feed intake (g/day)	44.33 ± 2.01	42.54 ± 2.02	41.11 ± 2.09	40.15 ± 1.86	44.45 ± 2.29	0.4888
Weight gain (g)	13.92 ± 0.45^{c}	14.61 ± 0.128^{b}	13.85 ± 0.51^{c}	14.21 ± 0.68^{bc}	15.79 ± 0.41^{a}	0.0448
FCR	3.20 ± 0.10^{a}	2.91 ± 0.06^{b}	2.97 ± 0.01^{b}	2.84 ± 0.07^{c}	2.82 ± 0.06^{c}	0.0061
Finisher phase (10-12 weeks)						
Live weight (g)	1272 ± 17.30^{b}	1325 ± 26.23^{a}	1213 ± 42.81^{b}	1268 ± 22.79^{b}	1385 ± 39.80^{a}	0.04097
Feed intake (g/day)	120.1 ± 6.03	118.8 ± 6.48	111.4 ± 6.82	113.7 ± 7.11	116.9 ± 6.31	0.8729
Weight gain (g)	19.39 ± 1.11^{b}	19.70 ± 1.27^{a}	17.08 ± 0.51^{b}	18.77 ± 0.69^{b}	20.66 ± 0.94^{a}	0.0026
FCR	6.28 ± 0.31^{ab}	6.03 ± 0.07^{b}	6.53 ± 0.08^{a}	6.08 ± 0.18^{b}	5.70 ± 0.24^{c}	0.0018

FM8: 8% of Fish meal, BSF8: 8% of black soldier fly larvae meal, TM4: 4% of *T. molitor* larvae meal, TM6: 6% of *T. molitor* larvae meal, TM8: 8% of *T. molitor* larvae meal, FCR: Feed conversion ratio. [a,b, and c] Means within the same row followed by different subscript letters differ significantly ($p < 0.05$).

Table 4. Carcass characteristics, thighs, drumstick, wing, and keel at 12 weeks of age in hybrid broiler chickens

Parameters \ Treatments	FM8	BSF8	TM4	TM6	TM8	P value
Carcass yield (%)	60.88 ± 1.28^{c}	63.89 ± 0.56^{b}	61.69 ± 0.58^{c}	63.38 ± 0.31^{b}	67.62 ± 0.77^{a}	< 0.0001
Thigh yield (%)	7.94 ± 0.95^{c}	9.58 ± 0.25^{a}	9.03 ± 0.14^{b}	9.56 ± 0.28^{a}	9.91 ± 0.26^{a}	0.0440
Drumstick yield (%)	7.70 ± 0.95^{c}	9.36 ± 0.18^{ab}	9.13 ± 0.35^{b}	9.78 ± 0.40^{ab}	9.98 ± 0.17^{a}	0.0185
Wing yield (%)	7.36 ± 0.74^{c}	8.81 ± 0.15^{ab}	8.53 ± 0.18^{b}	8.67 ± 0.11^{b}	9.17 ± 0.25^{a}	0.0222
Keel yield (%)	12.12 ± 1.26^{b}	15.57 ± 0.53^{a}	12.61 ± 1.60^{b}	15.82 ± 0.54^{a}	16.66 ± 0.70^{a}	0.0067

FM8: 8% of Fish meal, BSF8: 8% of black soldier fly larvae meal, TM4: 4% of *T. molitor* larvae meal, TM6: 6% of *T. molitor* larvae meal, TM8: 8% of *T. molitor* larvae meal. [a,b, and c] Means within the same row followed by different subscript letters differ significantly ($p < 0.05$).

Table 5. Length and relative weight of the small intestine, gizzard, and liver at 12 weeks of age in hybrid broiler chickens

Parameters \ Treatments	FM8	BSF8	TM4	TM6	TM8	P value
Relative intestinal weight (g/cm)	0.55 ± 0.04	0.62 ± 0.12	0.56 ± 0.04	0.57 ± 0.06	0.60 ± 0.04	0.9463
Intestinal length (cm)	150.8 ± 4.28^{b}	153.3 ± 3.64^{b}	159.5 ± 4.73^{b}	158.6 ± 3.97^{b}	167.8 ± 0.88^{a}	0.0215
Relative weight of gizzard (%)	1.812 ± 0.07	1.985 ± 0.08	2.069 ± 0.125	1.865 ± 0.09	1.742 ± 0.11	0.1481
Relative weight of the liver	1.867 ± 0.08	1.785 ± 1.00	1.977 ± 0.08	1.988 ± 0.12	1.684 ± 0.09	0.1353

FM8: 8% of Fish meal, BSF8: 8% of black soldier fly larvae meal, TM4: 4% of *T. molitor* larvae meal, TM6: 6% of *T. molitor* larvae meal, TM8: 8% of *T. molitor* larvae meal. $^{a \text{ and } b}$ Means within the same row followed by different subscript letters differ significantly ($p < 0.05$).

Biochemical parameters

Blood parameters, including total protein and albumin in the chickens, did not demonstrate significant differences ($p > 0.05$) among all groups. Triglyceride concentrations in the BSF8 (59.5 g/dL) and TM6 (59.75 g/dL) treatments were significantly higher compared to the FM8 treatment (38.75 g/dL), which recorded the lowest values. Total cholesterol concentration was higher in TM6 (140.5 g/dL) compared to the TM4 (130g/dL), FM8 (108.3 g/dL), and BSF8 (103.5 g/dL).

Table 6. Biochemical analysis at 12 weeks in hybrid broiler chickens fed different diets from day 1 to 12 weeks of age

Parameters \ Treatments	FM8	BSF8	TM4	TM6	TM8	P value	Normal range
Total protein (g/L)	47.43 ± 2.19	40.80 ± 1.30	44.50 ± 3.75	45.73 ± 2.29	45.88 ± 6.26	0.3630	30-60
Albumin (g/L)	16.60 ± 0.38	14.68 ± 0.56	16.70 ± 1.00	16.78 ± 0.76	15.00 ± 1.00	0.1993	10-30
Triglyceride (g/dL)	38.75 ± 1.28^{c}	59.5 ± 5.59^{a}	46.25 ± 4.26^{b}	59.75 ± 8.07^{a}	54. 75 ± 8.99^{ab}	0.0005	30-100
Cholesterol (g/dL)	108.3 ± 5.05^{c}	103.5 ± 5.45^{c}	130 ± 7.82^{ab}	140.5 ± 8.69^{a}	125.8 ± 5.54^{b}	0.0011	100-180

^{a,b,c} Means within the same row followed by different subscript letters differ significantly ($p < 0.05$). FM8: 8% of Fish meal, BSF8: 8% of black soldier fly larvae meal, TM4: 4% of *T. molitor* larvae meal, TM6: 6% of *T. molitor* larvae meal, TM8: 8% of *T. molitor* larvae meal

DISCUSSION

The current results indicated that *T. molitor* did not have a substantial effect on feed consumption in chickens across different treatment groups. This result could be due to the fact that *T. molitor* larvae have a palatability similar to that of BSF larvae and fishmeal, and they lack any adverse effects that could affect feed intake in poultry diets. The current findings are similar to those of Bovera et al. (2016), who included 29.65% of *T. molitor* larvae in poultry feed and observed no significant differences in feed consumption among different treatments. The present results demonstrated that during the starter phase (0-3 weeks), there were no notable differences in body weight, weight gain, and FCR. The current results suggested that short-term use of *T. molitor* at rates less than or equal to 8% did not affect the growth performance in broiler chickens. However, after six weeks, the inclusion of *T. molitor* at 8% in the diet resulted in higher weight gain and a lower FCR than other treatments. These improvements in weight gain and the reduction in FCR might be attributed to the nutritional quality of the larvae, which provided an optimal balance of energy, amino acids, vitamins, and mineral salts essential for superior growth in poultry. These findings are consistent with those of Benzertiha et al. (2020), who reported enhanced growth and efficiency FCR in broilers fed diets containing even very low levels of *T. molitor* (0.2% and 0.3%) as a functional additive. Similarly, Shariat Zadeh et al. (2019) observed an increase in body weight in quails when fishmeal was replaced with *T. molitor* meal at inclusion levels of 22.5 g and 30 g. Loponte et al. (2017) reported improved growth performance in partridges following the inclusion of *T. molitor* flour at 250-500 g in their feed ration.

The current findings indicated that an increase in carcass yield was associated with enhanced growth performance in chickens fed *T. molitor* at 8%, which might be due to higher nutrient availability in *T. molitor*, providing a balance between energy and protein utilization and thereby boosting growth. The current results are similar to those of Khatun et al. (2003), Hwangbo et al. (2009), and Ballitoc and Sun (2013), who reported improvements in carcass weight, compared to the weight of fillet muscle, and thigh, respectively, by adding silkworm pupae, house fly maggot, and *T. molitor* larvae in broiler feed. In poultry, intestinal development begins during embryonic life and reaches its peak between 6 and 10-days post-hatch (Noy and Sklan, 1998). Based on the present results, the total intestinal length increased in chickens fed insects, which led to longer feed retention in the digestive tract, improved digestion, and greater absorption. The extended contact between digesta and absorptive surfaces improves digestion and nutrient absorption; these factors are

essential for greater growth performance (Alyileili et al., 2020), as observed in the current experiments with broiler chickens fed *T. molitor* and BSF larvae diets.

The results of the blood parameters offered insights into the biochemical markers important for assessing the quality of *T. molitor* larvae. The present study found that total protein and albumin did not differ notably among treatments, suggesting that the proteins from *T. molitor* larvae were effectively metabolized and did not impair liver function in broiler chickens. These results are consistent with those of Jiang et al. (2024), who found no remarkable differences in biochemical parameters, including total protein and albumin, when *T. molitor* larvae diets at 3%, 5%, 7%, and 9% concentrations were incorporated into broiler feed. Sedgh-Gooya et al. (2021) found no notable effects on total protein and albumin when evaluating the impact of including *T. molitor* larval meal at 2.5% and 5% on growth performance, carcass characteristics, gut microbiota, and blood parameters in broiler chickens.

Kohout et al. (2013) stated that triglycerides originate from hepatic synthesis and dietary fats. Current findings on triglyceride changes suggested that appropriate inclusion levels of *T. molitor* larval meal in the diet may have promoted broiler growth by improving lipid metabolism. This finding is consistent with Jiang et al. (2024), who found elevated triglyceride concentrations in broiler chickens fed diets containing more than 3% of *T. molitor* larvae. However, the present results on increased triglyceride levels contradicted those of Kim et al. (2014), who found no significant differences in triglyceride concentrations in broiler chickens fed diets containing *T. molitor* larvae meal.

CONCLUSION

The inclusion of *T. molitor* larvae meal in broiler chickens' diets demonstrated promising effects on zootechnical performance, carcass traits, and selected biochemical parameters. Including *T. molitor* larvae meal at 8% improved weight gain and decreased FCR, but feed consumption remained unchanged in broiler chickens during the grower and finishing phases. Likewise, *T. molitor* at 8% enhanced carcass yield and intestinal length in broiler chickens. Although total protein and albumin levels remained stable across treatments, elevated triglyceride levels were observed in chickens fed black soldier fly larvae at 8% and *T. molitor* at 6%. Therefore, *T. molitor* larvae meal can be recommended at an inclusion rate of 8% in broiler diets. Future studies should examine the feed digestibility of *T. molitor* in chickens to determine its influence on production performance and to assess its effect on the nutritional quality of chicken meat.

DECLARATIONS

Availability of data and materials

All data generated or analyzed during the present study are available from the corresponding author upon reasonable request.

Acknowledgements

The authors express their sincere gratitude to the World Bank for funding support through the Regional Centre of Excellence in Avian Sciences (CERSA) at the University of Lomé, Togo. Special appreciation is extended to Mr. Essen Paulinus Ogbonnaya for his invaluable assistance with editing, language refinement, and comprehensive manuscript review, which greatly enhanced the clarity and presentation of the present study. The authors also acknowledge the contributions of all individuals and institutions who supported the present study directly or indirectly.

Authors' contributions

Nassi Guidi Hoeness Inaudi was responsible for experimental implementation, including project administration and methodology. Agboka Komi participates in the correction of the protocol, funding acquisition, and reading of the manuscript. Attivi Komi contributed to the revision of the study, participated in Funding acquisition, and reviewed the manuscript. Mlaga Kodjo Gnatépé participated in the experimental procedures and contributed to the manuscript review. Tona Kokou provided critical reading and revision of the manuscript. All authors have read and approved the final edition of the manuscript submitted for publication.

Ethical considerations

All ethical issues, including plagiarism, consent to publication, research misconduct, data fabrication or falsification, and duplicate publication or submission, were carefully considered and verified by all authors prior to submission. There was no use of artificial intelligence in preparing the study and writing this article.

Funding

The present study was supported by the World Bank Grant for International Development Association (IDA) 5424 through the Regional Centre of Excellence in Avian Sciences (CERSA) at the University of Lomé, Togo.

Competing interests

The authors declared no competing financial interests or personal relationships.

REFERENCES

Aguilar-Miranda ED, Mercedes G, Loâpez, Clara ES, Ana P, and de la Rosa B (2002). Characteristics of maize flour tortilla supplemented with ground *Tenebrio molitor* larvae. Journal of Agricultural and Food Chemistry, 50(1): 192-195. DOI: https://www.doi.org/10.1021/jf010691y

Agunbiade JA, Adeyemi OA, Ashiru OM, Awojobi HA, Taiwo AA, Oke DB, and Adekunmisi AA (2007). Replacement of fish meal with maggot meal in cassava-based layers' diets. The Journal of Poultry Science, 44(3): 278-282. DOI: https://www.doi.org/10.2141/jpsa.44.278

Akpodiete OJ, Ologhobo AD, and Onwade AA (1998). Maggot meal as a substitute for fish meal in laying chickens diet. Journal of Agricultural Science, 31(2): 137-142. DOI: https://www.doi.org/10.4314/gjas.v31i2.1932

Allain CC, Poon LS, Chan CS, Richmond WFPC, and Fu PC (1974). Enzymatic determination of total serum cholesterol. Clinical Chemistry, 20(4): 470-475. DOI: https://www.doi.org/10.1093/CLINCHEM/20.4.470

Alyileili SR, Al-Yousef YM, Al-Shammari AM, and Al-Shammari TH (2020). Intestinal development and histomorphometry of broiler chickens fed Trichoderma reesei degraded date seed diets. International Journal of Poultry Science. 19(2): 49-56. DOI: https://www.doi.org/10.3923/ijps.2020.49.56

French Association for Standardization (1977). Animal feeding stuffs Determination of nitrogen for the calculation of crude protein content (NF V 18-100). French Association for Standardization (AFNOR), Paris, France p. 8. Available at: https://www.boutique.afnor.org/fr-fr/norme/nf-v18100/aliments-des-animaux-dosage-de-lazote-en-vue-du-calcul-de-la-teneur-en-prot/fa011756/55406

Association of official analytical chemists (AOAC) (1999). Official methods of analysis, 16th Edition. Method 960.39 –Fat (Crude) or Ether extract in meat. AOAC International, Gaithersburg, MD, USA. pp. 17-19. Available at: Microsoft Word - Thesis - with OGS corrections 8-29 Round 1

Association of official analytical chemists (AOAC) International (2005). AOAC International official methods of analysis, 18th Edition. AOAC Int, Gaithersburg, MD (2005). Available at: https://pdfcoffee.com/aoac-2005-2-pdf-free.html

Attivi K, Agboka K, Mlaga KG, Dassidi N, Oke OE, Karou SD, Onagbesan O, Hai L, and Tona K (2023). Productive performance, follicular development, and reproductive hormone profiles of laying hens fed with black soldier fly (*Hermetia illucens*) larvae meal as a substitute for fish meal. European Poultry Science, 87: 1-17. DOI: https://www.doi.org/10.1399/eps.2023.368

Ballitoc DA and Sun S (2013). Ground yellow mealworms (*Tenebrio molitor* L.) feed supplementation improves growth performance and carcass yield characteristics in 336 broilers. Open Science Repository Agriculture, 18: e23050425. DOI: http://www.doi.org/10.7392/0penaccess.23050425

Benzertiha A, Kierończyk B, Kołodziejski P, Pruszyńska–Oszmałek E, Rawski M, Józefiak D, and Józefiak A (2020). *Tenebrio molitor* and *Zophobas morio* full-fat meals as functional feed additives affect broiler chickens' growth performance and immune system traits. Poultry Science, 99(1): 196-206. DOI: http://www.doi.org/10.1016/j.psj.2019.08.043

Biasato I, Gasco L, De Marco M, Renna M, Rotolo L, Dabbou S, Capucchio M, Biasibetti E, Tarantola M, Sterpone L et al. (2018). Yellow mealworm larvae (*Tenebrio molitor*) inclusion in diets for male broiler chickens: Effects on growth performance, gut morphology, and histological findings. Journal of Poultry Science and Biotechnology, 97(2): 540-548. DOI: http://www.doi.org/10.3382/ps/pex308

Bilalissi A, Lombo Y, Kossoga KA, Tona K, Batimsoga BB, Voemesse K, Tare TP, Vagan B, and Oke OE (2022). Influence of crossbreeding of Sasso and Faso chickens on some hatching events and post-hatch performances. International Journal of Food Science and Agriculture, 6(2): 228-236. DOI: https://www.doi.org/10.26855/ijfsa.2022.06.013

Bovera F, Loponte R, Marono S, Piccolo G, Parisi G, Iaconisi V, Gasco L, and Nizza A (2016). Use of *Tenebrio molitor* larvae meal as protein source in broiler diet: Effect on growth performance, nutrient digestibility, and carcass and meat traits. Journal of Animal Physiology and Animal Nutrition, 100(4): 748-756. DOI: https://www.doi.org/10.1111/jpn.12436

Chokakkar AA, Bhoyar AR, Virkar PN, and Koli SS (2024). Enhancing broiler chicken growth: The impact of dietary black soldier fly larvae (*Hermetia illucens*) on weight gain. International Journal of Veterinary Science and Animal Husbandry, 9(5): 563-566. DOI: https://www.doi.org/10.22271/veterinary.2024.v9.i5i.1766

Doumas BT, Watson W A, and Biggs HG (1971). Albumin standards and the measurement of serum albumin with bromcresol green. Clinica Chimica Acta, 31: 87-96. DOI: https://www.doi.org/10.1016/0009-8981(71)90365-2

Elahi U, Wang J, Ma Y, Wu S, Wu J, Qi G, and Zhang H (2020). Evaluation of yellow mealworm meal as a protein feedstuff in the diet of broiler chicks. Animals, 10(2): 224. DOI: https://www.doi.org/10.3390/ani10020224

Fossati PL and Prencipe (1982). Serum triglycerides determined colorimetrically with an enzyme that produces hydrogen peroxide Clinical Chemistry, 28(10): 2077-2080. DOI: https://www.doi.org/10.1093/CLINCHEM/28.10.2077

Gomall AG, Bardawill CS, and David MM (1949). Determination of serum proteins by means of the biuret reaction. Journal of Biological Chemistry, 177(2): 751-766. DOI: https://www.doi.org/10.1016/S0021- 9258(18)57021-6

Heuel M, Sandrock C, Leiber F, Mathys A, Gold M, Zurbrüegg C, Zurbrüegg C, Gangnat IDM, Kreuzer M, and Terranova M (2022). Black soldier fly larvae meal and fat as a replacement for soybeans in organic broiler diets: Effects on performance, body N retention, carcass and meat quality. British Poultry Science, 63(5): 650-661. DOI: https://www.doi.org/10.1080/00071668.2022.2053067

Kohout M, Kohoutova B, and Heimberg M (1971). The regulation of hepatic triglyceride metabolism by free fatty acids. Journal of Biological Chemistry, 246(16): 5067-5074. Available at: The Regulation of Hepatic Triglyceride Metabolism by Free Fatty Acids - Journal of Biological Chemistry

Hwangbo J, Hong EC, Jang A, Kang HK, Oh JS, Kim BW, and Park BS (2009). Utilization of house fly-maggots, a feed supplement in the production of broiler chickens. Journal of Environmental Biology, 30(4): 609-614. Available at: https://pubmed.ncbi.nlm.nih.gov/20120505/

Jiang T, Zhao X, Li H, Zhang L, Tang B, Ding Y, and Wu Y (2024). Effects of yellow mealworm (*Tenebrio molitor*) larvae meal on the growth performance, serum biochemical parameters and caecal metabolome in broiler chickens. Italian Journal of Animal Science, 23(1): 813-823. DOI: http://www.doi.org/10.1080/1828051X.2024.2350230

Khan SRU, Khan A, Sultan M, Khan SU, Hayat, and Shahid MS (2016). Evaluating the suitability of larvae meal as a partial substitute of soya bean on the productive traits, digestibility indices and organoleptic properties of broiler meat. Journal of Animal Physiology and Animal Nutrition, 100: 649-656. DOI: http://www.doi.org/10.1111/jpn.12535

Kidd MT, Maynard CW, and Mullenix GJ (2021). Progress of amino acid nutrition for diet protein reduction in poultry. Journal of Animal Science and Biotechnology, 12: 45. DOI: https://www.doi.org/10.1186/s40104-021-00568-0

Khatun R, Howlider Mar, Rahman MM, and Hasanuzzaman M (2003). Replacement of fish meal by silkworm pupae in broiler diets. Pakistan Journal of Biological Sciences, 6(11): 955-958. DOI: http://www.doi.org/10.3923/pjbs.2003.955.958

Kim SG, Kim JE, Oh HK, Kang SJ, Koo HY, Kim HJ, Choi HC, and Sun SS (2014). Feed supplementation of yellow mealworms (*Tenebrio molitor* L.) full-fat meals as functional feed additives affect broiler chickens' growth performance and immune system traits. Journal of Agricultural Science and Technology, 49: 9-18. DOI: http://www.doi/10.29335/tals.2014.49.9

Krawczun N, Bielawa M, Szemiako K, Łubkowska B, Sobczewski I, Zylicz-Stachula A, and Skowron PM (2020). Boosting toxic protein biosynthesis: transient in vivo inactivation of engineered bacterial alkaline phosphatase. Microbial Cell Factories, 19: 166. DOI: https://www.doi.org/10.1186/s12934-020-01424-y

Kouame YAE, Nideou D, Kouakou K, and Tona K (2019). Effect of guinea fowl egg storage duration on embryonic and physiological parameters, and keet juvenile growth. Poultry Science, 98(11): 6046-6052. DOI: http://www.doi/10.3382/ps/pez264

Kpomasse CC, Sodjinou B, Voemesse K, Houndonougbo FM, and Tona K (2020). Effect of sequential feeding with variations in energy and protein levels on performances of Sasso Broilers under hot and humid climate. International Journal of Poultry Science, 19(9): 416-423. DOI: http://www.doi.org/10.3923/ijps.2020.416.423

Khusro M, Andrew NR, and Nicholas A (2012). Insects as poultry feed: A scoping study for poultry production systems in Australia. World's Poultry Science Journal, 68(3): 435-446. DOI: https://www.doi.org/10.1017/S0043933912000554

Loponte R, Nizza S, Bovera F, De Riu N, Fliegerova K, Lombardi P, Vassalotti G, Mastellone V, Nizza A, and Moniello G (2017). Growth performance, blood profiles and carcass traits of Barbary partridge (*Alectoris barbara*) fed two different insect larvae meals (*Tenebrio molitor and Hermetia illucens*). Research in Veterinary Science, 115: 183-188. DOI: http://www.doi.org/10.1016/j.rvsc.2017.04.017

Mlaga GK, Agboka K, Attivi K, Oke O, Osseyi E, Ameyapoh Y, Teteh A, Adjrah Y, Onagbesan O, and Tona K (2020). The effects of feeding black soldier fly (*Hermetia illucens*) maggot meal as a substitute for fish meal on broiler meat quality. International Journal of Poultry Science, 19(4): 186-192. DOI: https://www.doi.org/10.3923/ijps.2020.186.192

Mlaga KG, Agboka K, Attivi K, Tona K, and Osseyi E (2022). Assessment of the chemical characteristics and nutritional quality of meat from broiler chicken fed black soldier fly (*Hermetia illucens*) larvae meal. Heliyon, 8(11): e11718. DOI: https://www.doi.org/10.1016/j.heliyon.2022.e11718

Mushambanyi TMB and Balezi N (2002). Use of cockroaches and termites as potential replacements for meat meal in broiler chicken diets in South Kivu, Democratic Republic of the Congo. Tropicultura, 20(1): 10-16. Available at: https://web.archive.org/web/20180424021127id_/http://www.tropicultura.org/text/v20n1/10.pdf

Noy Y and Sklan D (1998). Metabolic responses to early nutrition. Journal of Applied Poultry Research, 7(4): 437-451. DOI: http://www.doi.org/10.1093/japr/7.4.437

Pexas G, Doherty B, and Kyriazakis I (2023). The future of protein sources in livestock feeds: Implications for sustainability and food safety. Frontiers in Sustainable Food Systems, 7: 1188467. DOI: https://www.doi.org/10.3389/fsufs.2023.1188467

Pieterse E, Pretorius Q, Hoffman LC, and Drew DW (2014). The carcass quality, meat quality and sensory characteristics of broilers raised on diets containing either *Musca domestica* larvae meal, fish meal or soya bean meal as the main protein source. Animal Production Science, 54(5): 622-628. DOI: http://www.doi.org/10.1071/AN13073

Ravindran V and Blair R (1993). Feed resources for poultry production in Asia and the Pacifici. Animal protein sources. World's Poultry Science Journal, 49(3): 219-235. DOI: https://www.doi.org/10.1079/WPS19930020

Rauw F, GardinY, van den Berg T, and Lambrecht B (2009). Vaccination against Newcastle disease in chickens [*Gallus gallus*]. BASE. Biotechnology, Agronomy, Society and Environment, 13(4): 587-596. Available at: https://popups.uliege.be/1780-4507/index.php?id=17234&file=1&pid=4758

Sedgh-Gooya S, Torki M, Darbemamieh M, Khamisabadi H, Karimi Torshizi MA, and Abdolmohamadi A (2021). Yellow mealworm, *Tenebrio molitor* (Col: *Tenebrionidae*), larvae powder as dietary protein sources for broiler chickens: Effects on growth performance, carcass traits, selected intestinal microbiota and blood parameters. Journal of Animal Physiology and Animal Nutrition, 105(1): 119-128. DOI: https://www.doi.org/10.1111/jpn.13434

Shariat Zadeh Z, Kheiri F, and Faghani M (2019). Use of yellow mealworm (*Tenebrio molitor*) as a protein source on growth performance, carcass traits, meat quality and intestinal morphology of Japanese quails (*Coturnix japonica*). Veterinary and Animal Science, 8: 100066. DOI: https://www.doi.org/10.1016/j.vas.2019.100066

Shumo M, Osuga IM, Khamis FM, Tanga CM, Fiaboe KKM, Subramanian S, Ekesi S, van Huis A, and Borgemeister C (2019). The nutritive value of black soldier fly larvae reared on common organic waste streams in Kenya. Scientific Reports, 9: 10110. DOI: http://www.doi.org/10.1038/s41598-019-46603-z

Sleman S M B, Robert AS, and Paul AI (2015): Specialized protein products in broiler chickens nutrition: A review, Journal of Animal Nutrition, 1(2): 47-53. DOI: http://www.doi.org/10.1016/j.aninu.2015.05.005

Tougan UP, Dahouda M, Salifou C, Ahounou S, Kpodekon M, Mensah G, Kossou D, Amenou C, Kpogbeto C, Thewis A et al. (2013). Variability of carcass traits of local poultry populations of *Gallus gallus* species of Benin. International Journal of Poultry Science, 12(8): 473-483. DOI: https://www.doi.org//10.3923/ijps.2013.473.483

Veldkamp T, van Duinkerken G, van Huis A, Iakemond CMM, Ottevanger E, Bosch G, and Van Boekel T (2012). Insects as a sustainable feed ingredient in pig and poultry diets - A feasibility study. Wageningen UR, Livestock Research, Report No. 638, pp. 48-50. Available at: https://api.semanticscholar.org/CorpusID:115019139

Publisher's note: Scienceline Publication Ltd. remains neutral with regard to jurisdictional claims in published maps and institutional affiliations.

Open Access: This article is licensed under a Creative Commons Attribution 4.0 International License, which permits use, sharing, adaptation, distribution and reproduction in any medium or format, as long as you give appropriate credit to the original author(s) and the source, provide a link to the Creative Commons licence, and indicate if changes were made. The images or other third party material in this article are included in the article's Creative Commons licence, unless indicated otherwise in a credit line to the material. If material is not included in the article's Creative Commons licence and your intended use is not permitted by statutory regulation or exceeds the permitted use, you will need to obtain permission directly from the copyright holder. To view a copy of this licence, visit https://creativecommons.org/licenses/by/4.0/.
© The Author(s) 2025

2025, Scienceline Publication
World's Veterinary Journal
World Vet J, 15(4): 1063-1069.
ISSN 2322-4568

DOI: https://dx.doi.org/10.54203/scil.2025.wvj108
PII: S232245682500108-15

Serodetection of Contagious Caprine Pleuropneumonia in Mosul City, Iraq

Mahmood T Al-lahibi and Maab I. Al-Farwachi*

Department of Internal and Preventive Medicine, College of Veterinary Medicine, University of Mosul, Mosul, Iraq

*Corresponding author's Email: maabalfrwche@yahoo.com

ORIGINAL ARTICLE
Received: October 06, 2025
Revised: November 10, 2025
Accepted: December 14, 2025
Published: December 31, 2025

ABSTRACT

Contagious caprine pleuropneumonia (CCPP) is a severe, highly transmissible respiratory disease in goats, resulting in significant economic losses. The precise antibody detection is critical for disease surveillance and control in suspected locations. The present study aimed to detect CCPP antibodies in goat sera using indirect enzyme-linked immunosorbent assay (ELISA) and latex agglutination tests (LAT) and to compare the diagnostic performance of these two serological methods. A cross-sectional study was conducted at the University of Mosul, Veterinary Teaching Hospital, Iraq. A total of 90 serum samples were collected from unvaccinated local goats (aged 1-7 years; 30 males, 60 females) exhibiting respiratory signs, including cough, nasal discharge, and dyspnea. The serum samples were analyzed for CCPP antibodies using both an indirect ELISA and LAT. The overall seropositivity rate was 21.1% for indirect ELISA and 46.6% for LAT. Among the latex-positive samples, 16.7% were weakly positive (+), 50% moderately positive (++), and 33.3% strongly positive (+++). The seroprevalence of CCPP was significantly higher in female goats than in males, as confirmed by both ELISA and LAT. Indirect ELISA revealed seroprevalence rates of 30.0% in females compared to 3.3% in males, while LAT results indicated a seroprevalence rate of 66.7% in females compared to 6.7% in males. The highest CCPP seroprevalence was found in the 2-3-year-old age group, with rates of 89.5% by ELISA and 92.9% by LAT. The LAT results demonstrated a sensitivity of 84.21%, a specificity of 63.38%, and an overall accuracy of 67.78%. Cohen's kappa coefficient (0.33) indicated fair agreement, while McNamara's test demonstrated a significant difference between the two tests. Based on receiver operating curve analysis, the indirect ELISA demonstrated an area under the curve of 0.83, with a suitable optical density limit of 0.15, resulting in 85% sensitivity and 70% specificity. Indirect ELISA offers greater reliability in detecting CCPP antibodies compared to LAT. The variability in LAT results highlighted the need for ELISA, revealing higher seropositivity in older females, a distinct epidemiological feature of the population.

Keywords: Contagious caprine pleuropneumonia, Goat, Mycoplasma infection, Serodiagnosis

INTRODUCTION

Contagious caprine pleuropneumonia (CCPP) is caused by the F38 biotype of *Mycoplasma* (*M.*), which has recently been reclassified as *M. capricolum* subspecies *capri pneumoniae* (Ahaduzzaman, 2021; Ali et al., 2024). This specific infection is very contagious in housed goats, with high morbidity (100%), and mortality ranging from 60% to 100% (Yatoo et al., 2018; 2019; Ahmad et al., 2021). Only goats are naturally infected; clinical signs include anorexia, listlessness, pyrexia, cough, and dyspnea with accompanying grunting and wide-based forelimb stance (Elhassan and Salama, 2018; Tharwat et al., 2025). On necropsy, a fibrinous pleuritis and pleural effusion are generally found, with occasional pericarditis. The lung lobes (unilateral or bilateral) are enlarged, firm, and variegated with red, yellow, white, and gray foci (Yatoo et al., 2019; Kabir et al., 2021; Tharwat et al., 2025). While clinical signs and gross lesions may be strongly suggestive during outbreaks, they are not definitive for diagnosis and require confirmatory laboratory testing (Tharwat and Al-Sobayil, 2017). An accurate diagnostic procedure requires proper sample collection and transportation under aseptic and standardized conditions (WOAH, 2021). Isolating *M. capricolum* subspecies *capri pneumoniae* by culture and identifying it through biochemical and antigenic techniques has limitations, including low sensitivity due to contamination and cross-reactivity with other *Mycoplasma* species. Additionally, these conventional methods require specialized media, prolonged incubation, and skilled laboratory technicians, which makes them time-consuming and frequently unsuitable for controlling outbreaks (Rather et al., 2021; Khodakaram-Tafti et al., 2023).

Conventional polymerase chain reaction (conventional PCR), real-time PCR, sequencing, and isothermal methods have become routine for CCPP detection; however, their adoption is limited by technological and financial barriers (Le Grand et al., 2004; Yatoo et al., 2019).

Serology is widely used for herd surveillance and exposure detection of CCPP (Ali et al., 2024). The latex agglutination test (LAT) is rapid, simple, suitable for whole blood or serum, and recommended for diagnosis of CCPP in the field, and has a sensitivity of about 80% (March et al., 2000). Multiple reports indicate that the LAT is more sensitive

To cite this paper: Al-lahibi MT and Al-Farwachi MI (2025). Serodetection of Contagious Caprine Pleuropneumonia in Mosul City, Iraq. *World Vet. J.*, 15(4): 1063-1069. DOI: https://dx.doi.org/10.54203/scil.2025.wvj108

than the complement fixation test and simpler to perform than competitive enzyme-linked immunosorbent assays (ELISA; March et al., 2000; Wambugu, 2005; Soayfane et al., 2018).

Different forms of ELISA, including blocking ELISA, competitive ELISA, and indirect ELISA, offer enhanced specificity and sensitivity for detecting CCPP (Sharew et al., 2005; Jean de Dieu et al., 2019; Shaheen et al., 2024). Unlike complement fixation tests, which frequently cross-react with other *Mycoplasma* species, these ELISA techniques can distinguish CCPP from other respiratory infections, offering a more specific diagnostic alternative (Peyraud et al., 2014; Khan et al., 2025). Additionally, the CCPP was isolated and detected among sheep and goats in Iraq's neighboring countries, such as Saudi Arabia (El-Deeb et al., 2017), Turkey (Özdemir et al., 2018), and Iran (Khodakaram-Tafti et al., 2023).

In Iraq, CCPP is often misdiagnosed as other forms of caprine *Mycoplasma* pneumonia, leading to its underestimation as a distinct disease. Therefore, the present study aimed to identify CCPP seropositivity in symptomatic native goats in Mosul, Iraq, and to evaluate the diagnostic accuracy of the LAT compared to indirect ELISA.

MATERIALS AND METHODS

Ethical approval

The College of Veterinary Medicine Committee at the University of Mosul granted its approval for this study (Approval number: UM.VET. 2025.038) in August 2025.

Study area

Mosul is one of the largest cities in Iraq, situated in the Northern part of the country (Figure 1), just about 400 km (250 miles) north of Baghdad on the Tigris River. The area of the city is 32,308 km². This city experiences four distinct seasons, with variable rainfall periods in autumn, winter, and early spring. The temperatures in winter potentially range from 5°C to 25°C, and in summer from 25°C to 45°C. This zone is branded by diverse districts, such as rivers, fields, pastures, and agricultural lands with biological variety (Yaqoob et al., 2023).



Figure 1. Mosul city is located in the North-west of Iraq.

Study design and animals

A cross-sectional study was conducted in August 2025 at the University of Mosul, Veterinary Teaching Hospital in Iraq. Ninety serum samples were randomly collected from local goats (aged 1-7 years) presenting with respiratory symptoms such as cough, nasal discharge, and dyspnea. The cohort comprised 30 males and 60 females, distributed across age groups (≤ 1 year: 10 goats; 2–3 years: 78 goats; and ≥ 5 years: 2 goats). Blood samples (5 mL) were collected aseptically from the jugular vein into plain vacutainer tubes. Sera were separated by centrifugation at 3000 rpm for 10 minutes and stored at -20°C until further analysis. All sera were tested for antibodies against CCPP using two diagnostic methods, including commercial indirect ELISA and the LAT.

Anti-CCPP antibodies were detected using a commercially available indirect ELISA kit (ID SL0128Gt, Sunlong Biotech Co., Hangzhou, China) as the reference protocol, following the manufacturer's instructions. The optical density (OD) values were determined using an ELISA plate reader (Multiskan FC, Thermo Fisher Scientific, USA) at a wavelength of 450 nm. The effectiveness was measured by the average value of the positive control (≥ 1.00) and negative control (≤ 0.10). The significant value (CUT OFF) was determined as the average value of the negative control plus 0.15. Samples were considered negative for anti-CCPP antibodies if the optical density (OD) value was below the calculated cut-off. An OD value equal to or greater than the cut-off indicated a positive result.

Latex agglutination test

A commercial CapriLAT kit (Animal and Plant Health Agency, Surrey, UK) was used according to the manufacturer's recommendations, and positive reactions were classified into three levels, including fine agglutination (weak) as +, clear agglutination (moderate) as ++, and strong clumping as +++.

Statistical analysis

The present data was stored in a Microsoft Office Excel 2007 file. The diagnostic performance of the LAT was compared to ELISA, which was regarded as the reference standard. Sensitivity, specificity, positive predictive value (PPV), negative predictive value (NPV), and total accuracy were measured. Cohen's kappa coefficient (κ) was used to examine the agreement between the two tests and was interpreted as per usual standards. McNemar's test was used to determine the statistical significance differences between the two assays. Additionally, receiver operating characteristic (ROC) curve analysis was performed to determine the optimal ELISA cutoff. The distribution of positive and negative samples by age and sex was summarized using Chi-Square (χ^2), such as frequencies and percentages. Statistical significance was defined as a p-value less than 5% ($p < 0.05$). The diagnostic test evaluation was performed using MedCalc Software Ltd. (Dhamnetiya et al., 2021).

RESULTS AND DISCUSSION

Specific antibodies against *M. capricolum* subspecies *capripneumoniae* were detected in 21.1% of serum samples using indirect ELISA and in 46.6% using the LAT (Table 1). The higher seropositivity observed with LAT might be attributed to its lower specificity and potential cross-reactivity with other *Mycoplasma* species, as previously reported in similar studies (March et al., 2000; Chandio et al., 2019). The indirect ELISA, known for its high specificity and reproducibility in CCPP serodiagnosis, produced a more conservative seropositivity result. Among latex-positive samples, 16.7% were weakly positive (+), 50% moderately positive (++), and 33.3% strongly positive (+++; Table 2). Seropositivity for CCPP was significantly higher in females than in males in both ELISA and LAT. Using indirect ELISA, seropositivity was 30.0% in females compared to 3.3% in males, by LAT 66.7% and 6.7% in females and males, respectively. These differences were statistically significant ($P = 0.0036$ for ELISA; $P < 0.0001$ for LAT). Sex-related differences in seropositivity or immune response to CCPP might be attributed to management and physiological factors. Female goats are frequently kept in herds for breeding and milk production, which increases their cumulative exposure to pathogens. Conversely, males are usually fewer and more likely to be sold or culled, which limits their duration of contact with diseased animals in the herd. Hormonal or physiological stresses associated with pregnancy and lactation might increase susceptibility or stronger antibody responses in females.

Table 1. Serological results for detecting antibodies against *Mycoplasma capricolum* subsp. *Capripneumoniae* in goats from Mosul, Iraq, 2025

Serological tests	Number of examined animals	Number of seropositive animals (%)	P-value
Indirect ELISA	90	19(21.1%)	P = 0.0003
Latex agglutination test		42(46.6%)	

Table 2. Distribution of seropositive goats according to the strength of the latex agglutination test in goats from Mosul, Iraq, 2025

Serological reactions	Number of seropositive animals	P-value
Strong	14 (33.3%)	P=0.2983
moderate	21(50%)	P=0.0661
Weak	7 (16.7%)	

Table 3. Distribution of antibodies against *Mycoplasma capricolum* subspecies *capripneumoniae* by sex and age in goats from Mosul, Iraq, 2025

Variables	Number of animals	Seropositive animals by Indirect ELISA (%)	Seropositive animals by latex agglutination test (%)
Sex			
Male	30	1(3.3)	2(6.7)
Female	60	18(30.0)	40(66.7)
P value		P = 0.0036	P < 0.0001
Age (years)			
≤ 1	10	1(5.3)	2(4.8)
2-3	78	17(89.5)	39(92.9)
≥ 5	2	1(5.3)	1(14.2)

Table 4. Diagnostic values of the latex agglutination test using indirect ELISA as a reference standard for the detection of antibodies against *Mycoplasma capricolum* subspecies *capripneumoniae* in goats from Mosul, Iraq, 2025

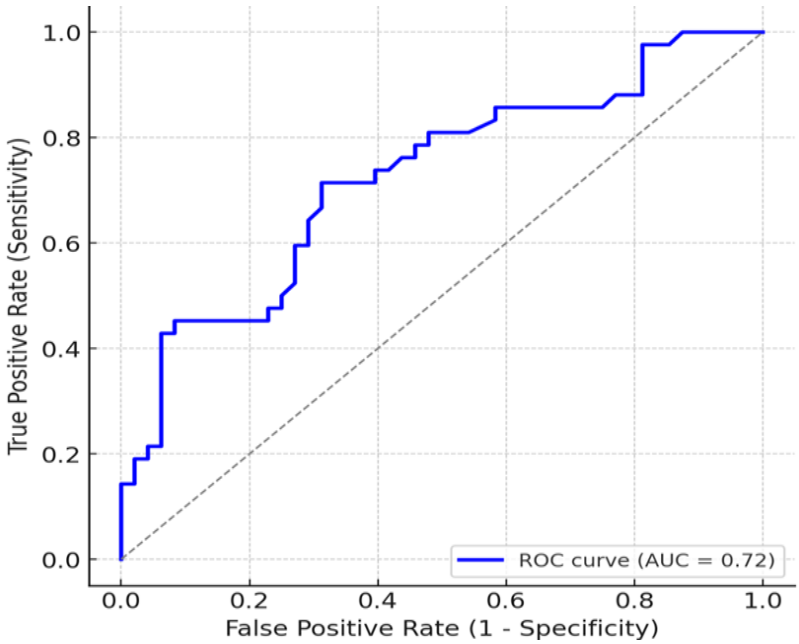
	Latex agglutination test			Total
Indirect ELISA (Reference standard)		16 (True positive)	3 (False negative)	19
		26 (False positive)	45 (False negative)	71
	Total	42	48	90
Test characteristic			Results	
Sensitivity (%)			84.21	
Specificity (%)			63.38	
Positive predictive value, PPV (%)			38.10	
Negative predictive value, NPV (%)			93.75	
Accuracy (%)			67.78	
Cohen's Kappa (κ)			0.33 (Fair agreement)	
McNemar's test (χ^2)			18.24, p < 0.0001	

Additionally, seropositivity varied by age group, with the highest percentages found in animals aged 2-3 years at 89.5% using ELISA and 92.9% using LAT. Lower seropositivity rates were observed in animals ≤ 1 year and ≥ 5 years old (Table 3). The highest seropositivity was recorded in animals aged 2-3 years, which are typically at peak productivity and most frequently in contact with the rest of the herd. Animals in this age group generally have repeated exposure to the infection, leading to higher antibody detection. In contrast, young animals (≤ 1 year) may have had limited exposure time or immature immune responses, resulting in lower positivity rates. Several factors might explain the reduced seropositivity in the oldest goats (≥ 5 years), including limited sample size, management practices that remove chronically affected animals, or natural declines in humoral immunity. The present findings aligned with previous reports suggesting that age and sex may influence exposure risk due to behavioral and physiological factors, such as prolonged herd contact and longer lifespan in breeding females (Teshome et al., 2020; Moti et al., 2024).

The LAT demonstrated a sensitivity of 84.21%, a specificity of 63.38%, and an overall accuracy of 67.78%, compared to ELISA. A sensitivity of 84.21% in the LAT test suggested the test effectively identified the majority of infected animals. McNemar's test revealed a statistically significant difference between ELISA and Latex results (Table 4). Table 4 reveals that the LAT had moderate diagnostic performance, but with a low specificity (63.38%), which resulted in a large number of false-positive results, compared to the indirect ELISA. The overall diagnosis accuracy was 67.78%, which indicated moderate agreement with the ELISA reference. The NPV was high (93.75%), whereas the PPV was low (38.1%). The low PPV (38.10%) demonstrated that many LAT-positive results were not confirmed by ELISA. On the other hand, the high NPV (93.75%) indicated that LAT was more reliable for excluding infection than confirming it. Cohen's kappa coefficient was 0.33, indicating a fair level of agreement between the LAT and ELISA. These findings confirmed that the LAT tends to overestimate seropositivity. Consequently, while the LAT is suitable for rapid field screening, ELISA remains necessary for confirmatory diagnosis and accurate serological assessment for *M. capricolum*

subsp. *capripneumoniae*. These results align with previous reports indicating that while LAT assays provide rapid and practical diagnostic advantages, they generally exhibit lower specificity and discordant results compared to ELISA, underscoring the importance of complementary testing in CCPP diagnosis (Jean de Dieu et al., 2019; Shaheen et al., 2024). Across clinical, pathological, and serological comparisons, ELISA was superior to LAT in accuracy, whereas PCR-based methods directly detect *M. capricolum* subsp. *capripneumoniae* DNA, providing a definitive diagnosis in early and subclinical infections (Tharwat and Al-Sobayil, 2017; Tharwat et al., 2025).

Receiver operating characteristic curve analysis was performed to assess the diagnostic performance of ELISA using the LAT as a reference. The area under the curve (AUC) was 0.72 (Graph 1), indicating the strong discriminative ability of ELISA, suggesting the ELISA is a reasonably accurate test for detecting CCPP, with an AUC above 0.7, typically interpreted as acceptable to strong performance in diagnostic evaluations (Aggarwal and Ranganathan, 2018). The current findings confirmed that ELISA provided reliable detection of CCPP antibodies compared to the LAT.



Graph 1. Receiver operating characteristic curve of ELISA using the latex agglutination test as the reference standard in goats

CONCLUSION

Indirect ELISA demonstrated superior reliability compared to LAT in the detection of CCPP antibodies. The greater intensity of LAT reactivity and higher seropositivity in females and goats aged 2–3 years suggest distinct epidemiological patterns within the study population. Future studies should assess the performance of LAT and ELISA in larger and more diverse goat populations, incorporating molecular diagnostic methods such as PCR for confirmation. Longitudinal antibody monitoring would help detection of infection frequency and the most effective time to conduct serological testing.

DECLARATIONS

Availability of data and materials

The data that support the findings of this study are available upon reasonable request from the corresponding author.

Acknowledgments

The authors would like to thank the Department of Internal and Preventive Medicine for providing the necessary assistance and facilities to conduct this study as a part of an MSc thesis accepted by the College of Veterinary Medicine at the University of Mosul, Iraq.

Authors' contributions

Maab AL-Farwachi performed methodology, investigation, data analysis, original draft writing, statistical data, and review. Mahmood Al-lahibi provided sampling, laboratory analysis, and data analysis. The authors confirmed the final edition of the manuscript.

Funding

The authors declared that this study has received no financial support.

Competing interests

The authors have not declared any conflict of interest.

Ethical considerations

Ethical issues, including plagiarism, consent to publish, misconduct, data fabrication and/or falsification, double publication and/or submission, and redundancy, have been checked by all the authors. The authors did not use AI for preparing any part of this study and writing this manuscript.

Availability of data and materials

The data to support the present study's findings are available upon reasonable request to the corresponding author.

REFERENCES

Ahaduzzaman M (2021). Contagious caprine pleuropneumonia (CCPP): A systematic review and meta-analysis of the prevalence in sheep and goats. Transboundary and Emerging Diseases, 68(3): 1332-1344. DOI: https://www.doi.org/10.1111/tbed.13794

Ahmad F, Khan H, Khan FA, Carson BD, Sadique U, Ahmad I, Saeed M, Rehman FU, and Rehman HU (2021). The first isolation and molecular characterization of *Mycoplasma capricolum* subsp. Capripneumoniae Pakistan strain: A causative agent of contagious caprine pleuropneumonia. Journal of Microbiology, Immunology and Infection, 54(4): 710-717. DOI: https://www.doi.org/10.1016/j.jmii.2020.06.002

Aggarwal R and Ranganathan P (2018). Understanding diagnostic tests - Part 3: Receiver operating characteristic curves. Perspectives in Clinical Research, 9(3): 145-148. DOI: https://www.doi.org/10.4103/picr.PICR_87_18

Ali H, El-Neweshy M, Al Mawly J, Heller M, Weber M, and Schnee C (2024). A molecular epidemiological investigation of contagious caprine pleuropneumonia in goats and captive Arabian sand gazelle (*Gazella marica*) in Oman. BMC Veterinary Research, 20: 155. DOI: https://www.doi.org/10.1186/s12917-024-03969-1

Chandio MA, Dildar HK, Shahid HA, Muhammad SK, Alexander K, Ghulam ML, Abdul Aziz S, Muhammad AN, and Akhtar AC (2019). Sero-epidemiological analysis of contagious caprine pleuropneumonia in goats. Journal of Animal and Plant Sciences, 29(5): 1279-1289. Available at: https://thejaps.org.pk/Volume/2019/29-05/abstract/08.php

Dhamnetiya D, Jha RP, Shalini S, and Bhattacharyya K (2021). How to Analyze the Diagnostic Performance of a New Test? Explained with Illustrations. Journal of Laboratory Physicians, 14(1): 90-98. DOI: https://www.doi.org/10.1055/s-0041-1734019

El-Deeb W, Almujalli AA, Eljalii I, Elmoslemany A, and Fayez M (2017). Contagious caprine pleuropneumonia: The first isolation and molecular characterization of *Mycoplasma capricolum* subsp. Capripneumoniae in the Kingdom of Saudi Arabia. Acta Tropica, 168: 74-79. DOI: https://www.doi.org/10.1016/j.actatropica.2017.01.017.

Elhassan MA and Salama AO (2018). Clinical and laboratory diagnosis of contagious caprine pleuropneumonia in Qassim region, Saudi Arabia: a comparative study. Tropical Biomedicine, 35(1): 67-75. Available at: 67-75 Elhassan MA Saeed.pmd

Jean de Dieu B, Charles BS, Nwankpa N, Chitsungo E, Moustapha Boukary CR, Maina N, Tefera TA, Nwankpa RV, Mwangi N, and Mathurin Koffi Y (2019). Development and evaluation of epitope-blocking ELISA for detection of antibodies against contagious caprine pleuropneumonia in goat sera. Veterinary Sciences, 6(4): 82. DOI: https://www.doi.org/10.3390/vetsci6040082

Kabir A, Mirani AH, Rasheed M, Bhuptani DK, Kaleri HA, Kumar R, Abro MB, Khatri M, Bozdar ZH, and Solangi AW (2021). A review on contagious caprine Pleuro-pneumonia disease in small ruminants; sheep and goats. Pure and Applied Biology, 11(2): 536-547. DOI: http://www.doi.org/10.19045/bspab.2022.110053

Khan H, Khan FA, Sadique U, Ahmad I, Ahmad F, Rahman H, and Saeed M (2025). Development and evaluation of inactivated whole-cell contagious caprine pleuropneumonia vaccine against *Mycoplasma capricolum* subsp. Capripneumoniae Pakistan Strain. Pakistan Journal of Zoology, 57(1): 19. DOI: https://www.doi.org/10.17582/journal.pjz/20240114191217

Khodakaram-Tafti A, Derakhshandeh A, Daee A, and Seyedin M (2023). Identification of *Mycoplasma capricolum* subspecies capripneumoniae and *Mycoplasma arginini* by culture, PCR, and histopathology in pneumonic lungs of slaughtered goats in Mashhad, Iran. Iranian Journal of Veterinary Research, 24(2): 96-101. DOI: https://www.doi.org/10.22099/IJVR.2023.45321.6655

Le Grand D, Saras E, Blond D, Solsona M, and Poumarat F (2004). Assessment of PCR for routine identification of species of the *Mycoplasma mycoides* cluster in ruminants. Veterinary Research, 35(6): 6359-649. DOI: https://www.doi.org/10.1051/vetres:2004037

March JB, Gammack C, and Nicholas R (2000). Rapid detection of contagious caprine pleuropneumonia using a *Mycoplasma capricolum* subsp. *Capripneumoniae capsular* polysaccharide-specific antigen detection latex agglutination test. Journal of Clinical Microbiology, 38(11): 4152-4159. DOI: https://www.doi.org/10.1128/jcm.38.11.4152-4159.2000

Moti TB, Bulbula A, Kinfe G, and Leliso S A (2024). Sero-epidemiological survey on contagious caprine pleuropneumonia (CCPP) in the Pastural Area of Borana Zone, South West Oromia, Ethiopia. European Journal of Clinical and Biomedical Sciences, 10(4): 51-56. DOI: https://www.doi.org/10.11648/j.ejcbs.20241004.11.

Özdemir Ü, Türkyilmaz MA, Sayi O, Erpek SH, and Nicholas RAJ (2018). Survey of contagious caprine pleuropneumonia in goat herds in the Thrace region of Turkey. Revue Scientifique et Technique, 37(3): 831-836. DOI: https://www.doi.org/10.20506/rst.37.3.2889

Peyraud A, Poumarat F, Tardy F, Manso-Silván L, Hamroev K, Tilloev T, Amirbekov M, Tounkara K, Bodjo C, and Wesonga H (2014). An international collaborative study to determine the prevalence of contagious caprine pleuropneumonia by monoclonal antibody-based cELISA. BMC Veterinary Research, 10(1): 48. DOI: https://www.doi.org/10.1186/1746-6148-10-48

Rather IUH, Parray OR, Ain QU, Bhat RA, Muheet M, Wani S, Mushtao M, Parrah JU, Muhff A, Dhamk K et al. (2021). A mini-review on diagnosis of contagious caprine pleuropneumonia. The Indian Journal of Animal Sciences, 91(9): 687-691. DOI: https://www.doi.org/10.56093/ijans.v91i9.116454.

Shaheen M, Bashir S, Hassan N, Akhoon ZA, and Muhee A (2024). Caprine respiratory mycoplasmosis (*Contagious caprine pleuropneumonia* CCPP)- A global perspective of the disease, epidemiology, diagnosis, chemotherapy and immunization: A review. Indian Journal of Animal Research. 58(5): 709-715. DOI: DOI: 10.18805/IJAR.B-4425

Sharew AD, Staak C, Thiaucourt F, and Roger F (2005). A serological investigation into contagious caprine pleuropneumonia (CCPP) in Ethiopia. Tropical Animal Health and Production, 37(1): 11-19. DOI: https://www.doi.org/10.1023/B:TROP.0000047921.19064.d9

Soayfane Z, Houshaymi B, and Nicholas RAJ (2018). *Mycoplasma capricolum* subsp. Capripneumoniae, the cause of contagious caprine pleuropneumonia, comprises two distinct biochemical groups. Open Veterinary Journal, 4(8): 393-400. DOI: https://www.doi.org/10.4314/ovj.v8i4.7

Tharwat M and Al-Sobayil F (2017). Ultrasonographic findings in goats with contagious caprine pleuropneumonia caused by *Mycoplasma capricolum* subsp. *capripneumoniae*. BMC Veterinary Research, 13(1): 263. DOI: https://www.doi.org/10.1186/s12917-017-1167-4

Tharwat M, Alkheraif AA, and Ali H (2025). Clinical cases of contagious caprine pleuropneumonia in sheep: Retrospective clinical, sonographic, and pathological investigations. Open Veterinary Journal, 15(5): 1947-1957. DOI: https://www.doi.org/10.5455/OVJ.2025.v15.i5.9

Teshome D, Sori T, Sacchini F, and Wieland B (2019). Epidemiological investigations of contagious caprine pleuropneumonia in selected districts of Borana zone, Southern Oromia, Ethiopia. Tropical Animal Health and Production, 51(3): 703-711. DOI: https://www.doi.org/10.1007/s11250-018-1744-y

Wambugu AN (2005). Development and evaluation of an improved assay for detecting specific antibodies post contagious caprine pleuropneumonia exposure. MSc Thesis submitted to Kenyatta University, Kenya. Available at: http://thesisbank.jhia.ac.ke/1746/

World organisation for animal health (WOAH) (2021). Manual of diagnostic tests and vaccines for terrestrial animals, 13th Edition. Contagious caprine pleuropneumonia, Chapter 3.8.4. World Organisation for Animal Health (WOAH), pp. 1-15. Available at: fmd with viaa test incl

Yaqoob MM, Somlyai I, Berta C, Bácsi I, Al-Tayawi AN, Al-Ahmady KK, Mohammed RH, Alalami O, and Grigorszky I (2023). The impacts of land use and seasonal effects on phytoplankton taxa and physical-chemical variables in the Tigris River within the City of Mosul. Water, 15(6): 1062. DOI: https://www.doi.org/10.3390/w15061062

Yatoo MI, Parray OR, Mir MS, Qureshi SQ, Kashoo ZA, Mir Nadeem M, Mujeeb-ur-Rehman Fazili MU, Tufani NA, Kanwar MS, Sandip Chakraborty SC et al. (2018). Mycoplasmoses in small ruminants in India: A review. Journal of Experimental Biology and Agricultural Sciences, 6(2): 264-281. DOI: http://www.doi.org/10.18006/2018.6(2).264.281

Yatoo MI, Parray OR, Tauseef Bashir S, Muheet, Ahmed Bhat R, Gopalakrishnan A, Karthik K, Dhama K, and Vir Singh S (2019). Contagious caprine pleuropneumonia - A comprehensive review. Veterinary Quarterly, 39(1): 1-25. DOI: https://www.doi.org/10.1080/01652176.2019.1580826

Publisher's note: Scienceline Publication Ltd. remains neutral with regard to jurisdictional claims in published maps and institutional affiliations.

Open Access: This article is licensed under a Creative Commons Attribution 4.0 International License, which permits use, sharing, adaptation, distribution and reproduction in any medium or format, as long as you give appropriate credit to the original author(s) and the source, provide a link to the Creative Commons licence, and indicate if changes were made. The images or other third party material in this article are included in the article's Creative Commons licence, unless indicated otherwise in a credit line to the material. If material is not included in the article's Creative Commons licence and your intended use is not permitted by statutory regulation or exceeds the permitted use, you will need to obtain permission directly from the copyright holder. To view a copy of this licence, visit https://creativecommons.org/licenses/by/4.0/.
© The Author(s) 2025

2025, Scienceline Publication
World's Veterinary Journal
World Vet J, 15(4): 1070-1084.
ISSN 2322-4568

DOI: https://dx.doi.org/10.54203/scil.2025.wvj109
PII: S232245682500109-15

Impacts of Cilnidipine and Glibenclamide Combination on Lipid Profile and Glycemic Control in Male Diabetic Rats

Abeer Mansour Abdel Rasool[1], Nada Satea Mahmood[2]*, and Shatha Hani Mohammad[2]

Pharmacology and Toxicology Department, College of Pharmacy, Nineveh University, Mosul, 41003, Iraq
Pharmacology Department, College of Medicine, University of Mosul, Mosul, 41002, Iraq

*Corresponding author's Email: nadasm79.nm@uomosul.edu.iq

ORIGINAL ARTICLE
Received: September 21, 2025
Revised: October 22, 2025
Accepted: November 29, 2025
Published: December 31, 2025

ABSTRACT

Current diabetes therapies frequently do not succeed in achieving target levels for hyperglycemia and dyslipidemia in a considerable number of patients. Glibenclamide is an oral hypoglycemic agent, whereas cilnidipine is a calcium channel blocker, which has been utilized for its additional metabolic benefits beyond its primary effect on blood pressure control. The presented study aimed to evaluate the synergistic effects of cilnidipine and glibenclamide on glycemic response, insulin sensitivity, and lipid profile in alloxan-induced diabetic rats. Forty-eight male rats were allocated into eight groups, each with six rats, including a normal control, a diabetic control, and six diabetic groups. Three groups were treated with oral cilnidipine alone at 1, 5, and 10 mg/kg, respectively, while the other three groups were treated with a combination of cilnidipine and glibenclamide at 2.5 mg/kg, orally. Diabetes was induced through the use of alloxan at a dosage of 100 mg/kg, intraperitoneally. Successful induction of diabetes was confirmed by an increase in blood glucose level over 200 mg/dl. Serum insulin, HOMA-IR, C-peptide, fasting plasma glucose (FPG), and the lipid markers were measured at the end of the treatment on day 28. In assessing the medicines' interactions, the combination index (CI) method was used. The present results indicated that a significant effect was observed with 10 mg/kg of cilnidipine combined with glibenclamide, which lowered glucose levels to 80.10 ± 5.80 mg/dL, increased insulin levels to 13 ± 0.64 mU/L, and raised C-peptide levels to 1.40 ± 0.09 ng/mL, while normalizing HOMA-IR to 2.56 ± 0.45, compared to the diabetic control group. The value of CI indicating a significant synergy was below 1 for FPG, insulin, and C-peptide. However, the combined medication therapy had an opposing effect (CI > 1) on all lipid parameters, including total, low- and high-density cholesterol, and triglycerides. Although it may be beneficial in enhancing glucose metabolism, it is insufficient to resolve the issues associated with diabetic dyslipidemia and should be considered as a part of a mixed treatment regime.

Keywords: Cilnidipine, Insulin sensitivity, Glibenclamide, HOMA-IR, Lipid profile

INTRODUCTION

Diabetes mellitus (DM) is a metabolic disorder characterized by persistent hyperglycemia resulting from deficiencies in insulin secretion, insulin action, or both. International statistics have indicated that the present adult population affected by diabetes was projected to increase to 783 million by the year 2045, compared to 537 million in 2021 (El-Kebbi, 2021; Taneera et al., 2025). Chronic hyperglycaemia may lead to complications such as neuropathy, cardiovascular diseases, nephropathy, and retinopathy if not treated. Cardiovascular issues remain the predominant cause of morbidity and mortality, often exacerbated by accompanying dyslipidemia characterized by elevated levels of total cholesterol, low-density lipoprotein, and triglycerides, along with decreased high-density lipoprotein (Shah et al., 2022).

Managing diabetes involves not only controlling hyperglycemia but also reducing cardiovascular diseases through improving lipid profiles. There are many oral hypoglycemic agents that are available for glycemic control, such as sulfonylureas, biguanides, and thiazolidinediones; Nonetheless, their impact on reducing dyslipidemia remains inconsistent and, to some extent, limited (Feingold, 2023). Glibenclamide, a second-generation sulfonylurea, stimulates the secretion of insulin from pancreatic *β*-cells (Aloke et al., 2022). Insulin secretion is achieved by the inhibition of K_{ATP} channels in β-cells via SUR1 binding. In addition, Glibenclamide improves insulin gene expression, increases mitochondrial ATP production and bioenergetics, endorsing sustained insulin secretion. In fact, in therapeutic doses, glibenclamide has been established to decrease glucotoxicity and preserve β-cell function (Alotaibi et al., 2019). On the other hand, cilnidipine has specific pharmacological properties. Unlike traditional calcium channel blockers (CCBs), cilnidipine functions by blocking both L-type channels in vascular smooth muscle and N-type channels on sympathetic nerve endings, which ultimately promotes vasodilation with decreased sympathetic activity, which helps control blood pressure without causing reflex tachycardia (Chakraborty et al., 2021).

To cite this paper: Abdel Rasool AM, Mahmood NS, and Mohammad SH (2025). Impacts of Cilnidipine and Glibenclamide Combination on Lipid Profile and Glycemic Control in Male Diabetic Rats. *World Vet. J.*, 15(4): 1070-1084. DOI: https://dx.doi.org/10.54203/scil.2025.wvj109

The dual L/N-type CCBs activity related to cilnidipine is also used to improve metabolic parameters in diabetic patients (Mehta et al., 2024). In a meta-analysis study, cilnidipine was found to lessen oxidative stress, advance endothelial function, and modify lipid profiles, which makes this agent a promising help to diabetes management (Kumari et al., 2023). The above-mentioned mechanisms are well documented to promote the regulation of lipid levels, improve insulin sensitivity, reduce oxidative stress, and enhance endothelial function (Li et al., 2024). Furthermore, cilnidipine is considered notably beneficial for patients with metabolic syndrome or diabetes (Mehta et al., 2024), as it improves the endothelial function.

The use of cilnidipine for renal protection is achieved by reducing proteinuria and preventing diabetic nephropathy progression (Mehta et al., 2024). The distinctive mechanism and diverse benefits of cilnidipine make it an appealing medicine for treating hypertension, diabetes, and related complications, providing an overall strategy to enhance patient outcomes (Fujita et al., 2007). Additionally, cilnidipine has been used in diabetes not only for its antihypertensive effects but also for its role in enhancing insulin sensitivity, mitigating oxidative stress, improving lipid profiles, and providing protection against renal and cardiovascular diseases (Nishida et al., 2013; Thrasher, 2017). The diverse benefits of cilnidipine suggest that it could serve as a potential therapeutic agent for diabetic patients, particularly those suffering from hypertension or other metabolic disorders (Nishida et al., 2013).

Combination therapy for diabetes addresses several pathophysiological processes, including insulin resistance, *β*-cell dysfunction, and impaired incretin action (Alotaibi et al., 2019). Effective combinations present automatic complementarity, pharmacokinetic compatibility, and safety synergy (Fujita et al., 2007). Combined therapy offers improved glycemic regulation and reduces cardiovascular risk factors (Xie et al., 2023). Cilnidipine and glibenclamide are a combination that addresses both the metabolic and cardiovascular aspects of type 2 diabetes mellitus, particularly in patients with related hypertension (Mehta et al., 2024). Both medicines have confounding effects on insulin signalling (via PI3K/Akt), AMPK activation, and calcium regulation response (Shaikh and Das, 2025). The combination of two medications may exhibit additive effects through the action of glibenclamide on insulin secretion. Although cilnidipine enhances insulin sensitivity and ameliorates dyslipidemia, factors that can further impact the pathophysiology of diabetes, including β-cell dysfunction and insulin resistance, these effects contribute to a comprehensive therapeutic approach to dyslipidemia.

Alloxan is a well-known chemical compound utilized in experimental diabetes studies. Alloxan is a diabetogenic agent that causes dysfunction of pancreatic β-cells. It generally induces an acute diabetic model by generating additional reactive oxygen species, a critical factor involved in the pathogenesis and progression of type 2 diabetes mellitus (Szkudelski, 2001).

The present study aimed to assess the effect of cilnidipine alone and in combination with glibenclamide on glycemic and lipid parameters in alloxan-induced diabetic rats by evaluating FPG, C-peptide, fasting serum insulin, homeostatic calculation model for insulin resistance (HOMA-IR), and lipid profile. Additionally, this study aimed to determine whether the combination therapy has synergistic effects on improving glycemic control and adjusting lipid disturbances associated with monotherapies.

MATERIALS AND METHODS

Ethical approval

The authors strictly complied with all applicable institutional and international ethical regulations during the conduct of the animal experiments. The study protocol received approval from the Institutional Animal Ethics Committee (IAEC) of the University of Mosul, Iraq, which was recognized by the National Institutes of Health Guide. The approval number was UOM/COM/MREC/24-25/NOV11, dated November 14, 2024.

Animals

In the current study, 48 healthy adult male Wistar rats, weighing between 180 and 220 g and aged 8 to 11 weeks, were utilized. Animals were allowed to acclimate to the laboratory conditions for one week before the experiment began, under the supervision of a licensed veterinarian to monitor their health and ensure suitability for the study. Rats were housed in rodent plastic cages measuring 30 × 20 × 17 cm, fitted with wire mesh covers, and bedding consisting of homogenized wood shavings. The animals were maintained under a temperature of 22 ± 2°C, relative humidity of 50-60%, and a 12-hour light/dark cycle (Sidhu and Sharma, 2014). The animals were provided with a standard pellet diet and water *ad libitum* (Pioneer/Iraq). Animals were divided into eight random groups, each consisting of 6 rats, including a normal control, a diabetic control, and six diabetic groups treated with cilnidipine alone or in combination with glibenclamide (treatment groups). Normal control rats were non-diabetic and untreated, while the diabetic control rats with alloxan-induced diabetes remained untreated. The rats in the third group were treated with 1mg of cilnidipine (CLN1 + D), in the fourth group were treated with 5 mg (CLN5 + D), and in the fifth group were treated with 10 mg of cilnidipine (CLN10 + D). The rats in the sixth group treated with 1 mg of cilnidipine, combined with 2.5 mg/kg of glibenclamide (CLN1 with glibenclamide), in the seventh group treated with 5 mg of cilnidipine, combined with 2.5

mg/kg of glibenclamide (CLN5 with glibenclamide), and in the eighth group treated with 10 mg of cilnidipine, combined with 2.5 mg/kg of glibenclamide (CLN10 with glibenclamide; Figure 1).

The selection of cilnidipine doses at 1, 5, and 10 mg/kg was based on previously published experimental studies that evaluated its pharmacological efficacy and safety in diabetic and hypertensive rat models (Toba et al., 2011; Ueno et al., 2013). The graded dosing employed in the present experiment permitted the evaluation of a potential dose-dependent response and facilitated the assessment of synergistic interactions when combined with glibenclamide at a dosage of 2.5 mg/kg, a well-established hypoglycemic agent extensively utilized in alloxan-induced diabetic rat models (Sidhu and Sharma, 2014). The administration of cilnidipine and glibenclamide was conducted daily and orally administered (gastric gavage) for 28 days.

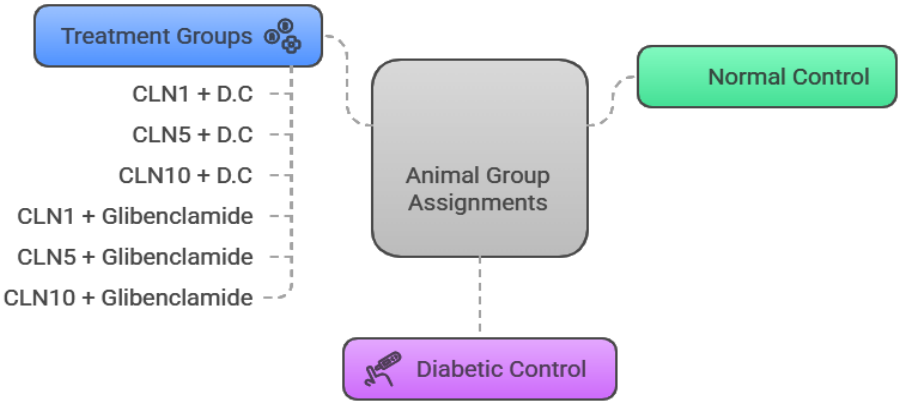


Figure 1. Animals grouping in the current study. Control: Not diabetic and untreated rats, diabetic control: Alloxan induced diabetes rats, CLN1 + D, CLN5 + D, CLD10 + D: Diabetic rats treated with cilnidipine at 1 mg/kg, 5 mg/kg and 10 mg/kg, respectively; CLN1, CLN5 and CLN 10 with glibenclamide: Diabetic rats treated with cilnidipine at 1 mg/kg, 5 mg/kg and 10 mg/kg with 2.5 mg/kg glibenclamide, respectively.

Induction of diabetes

A single alloxan injection (Sigma-Aldrich Chemical Co., St Louise, MO, USA) of 100 mg/kg was administered intraperitoneally (IP) to induce diabetes in rats, by mixing it with a freshly dissolved 5% distilled water solution at room temperature with a pH of 7 (Chougale et al., 2007). To prevent hypoglycemic shock and deaths caused by severe hypoglycemia, a 5% glucose solution in tap water was orally administered to the animals immediately following the injection and again after 24 hours. Animals were deprived of food for 12 hours before being given alloxan (Rasool and Mahmood, 2021), as shown in Figure 2, with free access to drinking water. A portable glucometer (Joycoo, Hamburg, Germany) was used to measure glucose levels in blood samples obtained from rats' tails, under light ether anaesthesia. Diabetes was confirmed by measuring FPG of 200 mg/dl (11.1 mmol/L) or more, at the 48 and 72 hours post-injection mark (Chougale et al., 2007; Saeedan et al., 2021).

Rats that were not diabetic or ill were not used and were excluded from the study (5 rats). After stabilizing diabetes for one week, the diabetic group was divided into seven subgroups (six rats each). Six groups were treated with cilnidipine, either alone or in combination with glibenclamide, by oral gavage for four weeks (Figure 1). It is essential to acknowledge that type 2 diabetes mellitus is a chronic and multifactorial disorder; one of the well-known implicated factors in its pathogenesis is oxidative stress imbalance and fractional β-cell dysfunction. Hence, alloxan was used to induce hyperglycemia (Szkudelski, 2001).

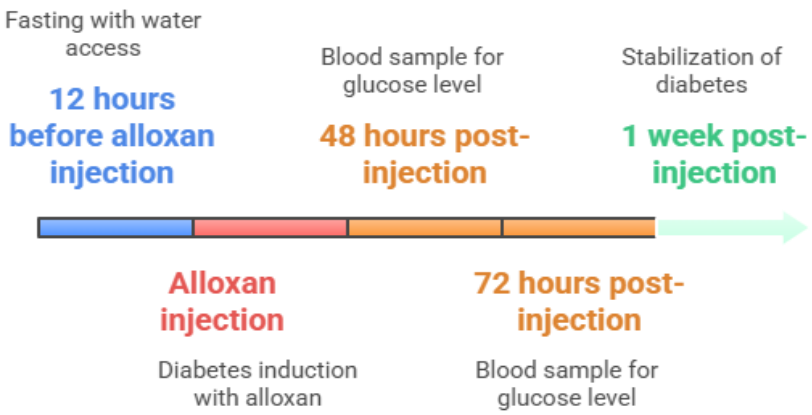


Figure 2. Induction of diabetes in the present study. Animals were starved, and alloxan was administered, after which serial blood glucose levels were measured at 48 h and 72 h post-injection to ensure that diabetes was induced. Hyperglycemia was stabilized in a period of one week.

Determination of fasting plasma glucose

The enzymatic glucose-oxidase-peroxidase technique was used to measure FPG, and this method is highly specific for D-glucose, utilizing a kit supplied by Randox Laboratories Ltd (England) (Mahmood and Mohammad, 2023). In the present method, the enzymatic oxidation of glucose, by glucose oxidase (GOD), was used to generate gluconic acid and hydrogen peroxide (H_2O_2), which in turn reacted with the 4-aminophenazone (4-AP) and phenol under the catalysis of the peroxidase (POD) to produce a pink quinonimine product. The color intensity of the resulting reaction mixture was directly proportional to the glucose concentration in the sample, as described by the following formula (Randox Laboratories Ltd, England).

Glucose + O_2 + H_2O → gluconic acid + H_2O_2

H_2O_2 +4-aminophenazone + phenol → quinoneimine + H_2O

A total of 10 µL of sample was added to 1,000 µL of working reagent (1:100 ratio) and incubated for 10 minutes at 37°C. Absorbance of test and standard samples was measured at a wavelength of 500 nm using a UV-Visible spectrophotometer (Shimadzu UV-1800, Japan). The glucose concentration was 99 mg/dL (5.55 mmol/L), which was utilized to calibrate the assay. Blood samples were collected from the tail vein at 48 and 72 hours after alloxan injection, whereas samples were obtained via cardiac puncture (under light anaesthesia) at the end of the experimental period (28 days). The blood samples were allowed to clot at room temperature for 20-30 minutes and subsequently centrifuged at 3,000 rpm for 10 minutes at 4°C. The supernatant was then separated and stored at -20°C until further analysis (Alotaibi et al., 2019).

Determination of rat serum insulin

The rat-specific Sandwich Enzyme-Linked Immunosorbent Assay (ELISA) kit (Elabscience 2466, USA; Cat. No. E-EL-R2466) was used to determine serum insulin levels according to the manufacturer's instructions. A total of 50 µl rat serum and 50 µl enzyme-conjugate reagent were put in wells, which had been coated with antibody and incubated at 37°C for 45 minutes. The incubation was followed by washing of the wells five times using the provided wash buffer to clear the free material from the incubate. A total of 90 µl of 3,3',5,5'-tetramethylbenzidine substrate solution (TMB) was then incubated in the dark for 15 minutes at 37°C to produce a colored product. Then, stop reagent was added to stop the reaction, and the absorbance was measured at 450 nm in a microplate reader (BioTek ® ELx800, USA). Serial dilutions of the insulin standard were used to construct a standard curve, and the results were reported in µIU/mL (Alotaibi et al., 2019).

Measurement of insulin resistance HOMA-IR

Homeostatic model assessment for insulin resistance (HOMA-IR) was calculated through the following formula.

HOMA-IR = F. serum insulin (µIU/ml) × F. serum glucose (mmol/l) /405

An HOMA-IR value equal to or higher than 2.6 would be considered indicative of insulin resistance (Alotaibi et al., 2019).

Measurement of serum lipid profile

Serum lipid profile that was measured in the current study included total cholesterol (TC), Triglycerides (TG), high-density lipoprotein cholesterol (HDL-C), and low-density lipoprotein cholesterol (LDL-C). The TC was measured by the enzymatic colorimetric method using the Cholesterol CHOD-PAP kit from Biolabo (France), serum TG was measured by the enzymatic colorimetric method using the triglycerides GOP kit manufactured by Biolabo (France), while the precipitation method was employed to measure serum HDL-C, using HDL-Cholesterol (PTA) and Cholesterol CHOD-PAP by Biolabo (France). The Friedewald formula was used to calculate LDL-C (LDL-C in mg/dl = TC - HDL - TG/5), whereas a derived equation from this formula was used to calculate VLDL-C (VLDL-C in mg/dl = TG/5; Corso et al., 2016). It is important to note that the validity of the Friedewald formula is contingent upon triglyceride levels, as its accuracy diminishes when TG exceeds 400 mg/dL.

Measurement of serum C-peptide

Serum C-Peptide was quantified utilizing the rat serum C-Peptide ELISA kit. The measurement of serum C-peptide was conducted through an immune enzymatic assay (IEA), employing the TOSHA/AIA analyzer (Tosoh Corporation, Japan), with adherence to appropriate sample handling, storage, and automated calculation protocols. The reference range for serum C-peptide within this assay system was established as 0.69-2.45 ng/ml (Alotaibi et al., 2019). The concentration of serum C-peptide was determined automatically according to the following formula used by the analyser system. C-peptide concentration (ng/ml) = [(Absorbance of sample -Absorbance of blank)/ (Absorbance of standard - Absorbance of blank)] × Concentration of standard (Alotaibi et al., 2019).

Gene expression analysis

The trizol reagent was used to extract the total RNA of rat skeletal muscle tissue following the instructions of the manufacturer (Invitrogen, USA). The purity and concentration of RNA were spectrophotometrically assessed at A260/A280 nm utilizing a NanoDrop analyzer (Thermo Fisher Scientific, USA), and the integrity of the RNA was evaluated through agarose gel electrophoresis. A synthesis of 1 µg of total RNA into complementary DNA (cDNA) was conducted utilizing a RevertAid First Strand cDNA Synthesis Kit (Thermo Fisher Scientific, USA). Quantitative real-time PCR was executed with SYBR Green Master Mix (Applied Biosystems, USA) on a Step One Plus Real-Time PCR System (Applied Biosystems, USA). The primers were gene-specific primers and included glucose transporter type 4 (GLUT4; as target gene), forward 5'-GGCTCTTCCTTTGGCTTTCT-3', while reverse 5'-GGAAGCACA GGCTTGTTCAT-3'. For the housekeeping gene, β-actin, the forward was 5'-AGAGCTACGAGCTGCCTGAC-3', while the Antisense was 5′-AGCACTGTGTTGGCGTACAG-3'. The thermal cycling conditions included initial denaturation at 95°C for five minutes, then 40 cycles of 95°C for 15 seconds, 60°C for 30 seconds, and 72°C for 30 seconds. The $2^{-}\Delta\Delta Ct$ method was employed to calculate relative mRNA expression, with GLUT4 as the target gene, and β-actin was the housekeeping gene. All of the reactions were conducted three times to achieve replicability.

Neural network-based predictive modelling

To achieve HbA1c value, glucose level, HOMA-IR, and systolic blood pressure following combined cilnidipine-glibenclamide therapy, a neural network was developed to construct a deep learning model to predict the aforementioned clinical outcomes (as a simulation or prospective plan, rather than validating predictive accuracy). The model architecture consisted of an input layer with 25 features, such as dosing factors, baseline glucose/HbA1c levels, and the treatment group. The model architecture included three hidden layers with 128, 64, and 32 neurons, respectively. All hidden layers used rectified linear unit (ReLU) activation along with Dropout regularization (30%, 20%, 10%) and batch normalization to enhance generalization and prevent overfitting. The output layer was linear and produced four continuous variables. The loss function employed was mean squared error (MSE), and the Adam optimizer (learning rate = 0.001) was used to train the model. Python 3.10 was used for training, along with TensorFlow 2.11. An 80/20 training-validation split of the preclinical dataset records was applied. Model performance was evaluated using the coefficient of determination (R^2), mean absolute error (MAE), and validation loss (Brigato and Iocchi, 2021).

Combination index analysis

Combination index analysis (CI) was conducted according to the Chou and Talalay method in 1984, to compare the effect of the combination (cilnidipine with glibenclamide) to the effect of cilnidipine alone at the same dose; where CI < 1 designates synergism (the combination effect is greater than the additive effect). CI = 1 indicates an additive effect (the effect is exactly as expected if the drugs are additive). CI > 1 indicates antagonism (the combination effect is less than anticipated from additive effects).

Statistical analysis

Statistical analysis was achieved with SPSS, version 23. Data preparation was carried out by Excel 2013. Normality was checked by Kolmogorov-Smirnov and Shapiro-Wilk tests ($p > 0.05$). Parametric tests followed a normal distribution. Descriptive stats are presented as mean ± standard error of the mean.

RESULTS

The present study demonstrated that cilnidipine alone and in combination with glibenclamide significantly enhances FPG in alloxan-diabetic rats ($p < 0.05$), which was significantly increased in 28 days in the diabetic control group (224.0 ± 5.52 mg/dL) compared to the healthy control group (81.25 ± 19.39 mg/dL). Cilnidipine monotherapy caused a dose-dependent decrease in FPG, with the highest dose (CLN10) reaching levels close to normal (86.50 ± 6.50 mg/dL). The combined administration of cilnidipine and glibenclamide produced hypoglycemic effects, which were observed in the CLN10 with glibenclamide (80.00 ± 5.80 mg/dL). The CLN10 with glibenclamide did not indicate a significant difference compared to the control group (Table 1 and Figure 3).

Serum insulin concentration was significantly reduced in the diabetic control group compared to the normal control group ($p<0.05$), which confirmed the initiation of insulin deficiency in the diabetic conditions. The low doses of cilnidipine in CLN1 and CLN5 indicated statistically equivalent insulin levels (8.90 and 9.17 mU/L, respectively) compared to the diabetic control (9.54 mU/L). In contrast, the high dose of cilnidipine in CLN10 restored insulin concentrations to levels comparable to the normal control group (14.34 mU/L). The combination therapy with glibenclamide exhibited a dose-dependent increase in insulin levels, particularly in the CLN10 with glibenclamide,

which showed an insulin concentration statistically similar to the control group (13.00 mU/L versus 14.34 mU/L, respectively; Table 2, Figure 4).

Table 1. Impact of different treatment groups on fasting plasma glucose (mg/dl) in rats on day 28

Groups	Mean fasting plasma glucose (mg/dl)	SEM
Control	81.22[a]	6.39
Diabetic control	224.20[c]	5.52
CLN1 + D	108.69[b]	9.17
CLN5 + D	96.01[b]	6.88-
CLN10 + D	86.51[a]	6.50
CLN1 with glibenclamide	95.30[b]	7.10
CLN5 with glibenclamide	85.10[a]	6.30
CLN10 with glibenclamide	80.10[a]	5.80
P- value	0.001	

[a, b, c] means different superscript letters in a column differ significantly ($p < 0.05$). Control: Not diabetic and untreated rats, diabetic control: Alloxan induced diabetes rats, CLN1+D, CLN5+D, CLD10+D: Diabetic rats treated with cilnidipine at 1 mg/kg, 5 mg/kg and 10 mg/kg, respectively; CLN1, CLN5 and CLN10 with glibenclamide: Diabetic rats treated with cilnidipine at 1 mg/k, 5 mg/kg and 10 mg/kg with 2.5 mg/kg glibenclamide, respectively.

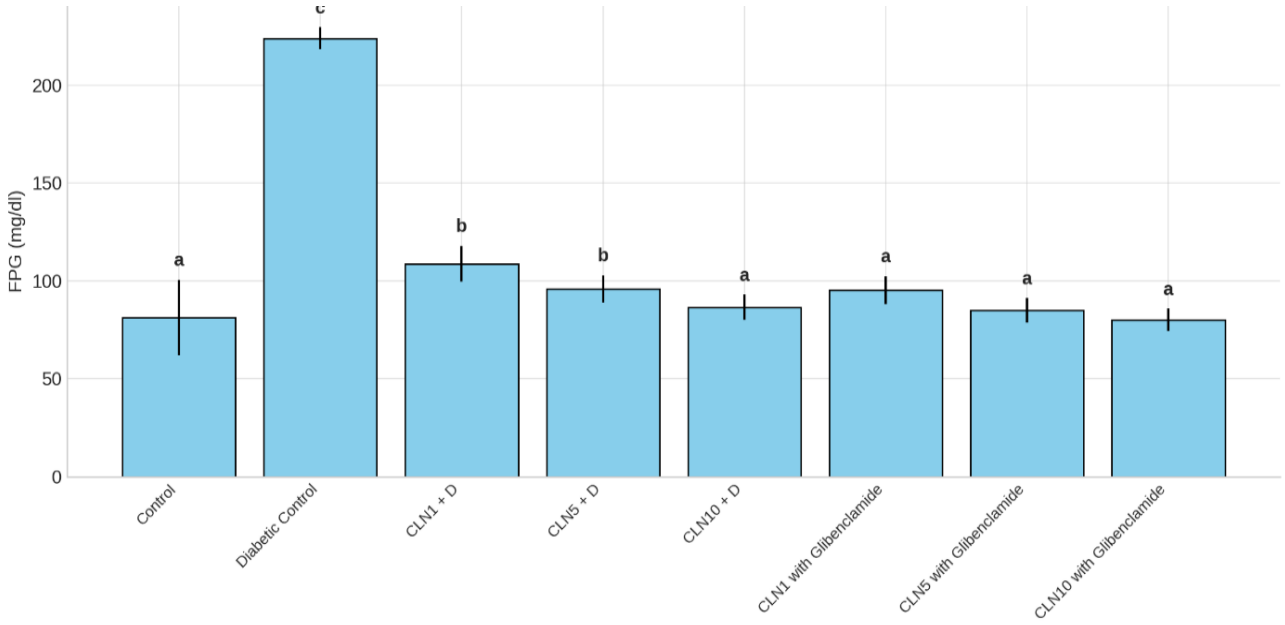


Figure 3. Impact of different treatment groups on fasting plasma glucose (mg/dl) in rats on day 28. Control: Not diabetic and untreated rats, diabetic control: Alloxan induced diabetes rats, CLN1+D, CLN5+D, CLN10+D: Diabetic rats treated with cilnidipine at 1 mg/kg, 5 mg/kg and 10 mg/kg, respectively, CLN1, CLN5 and CLN10 with glibenclamide: Diabetic rats treated with cilnidipine at 1 mg/kg, 5 mg/kg and 10 mg/kg with 2.5 mg/kg glibenclamide, respectively. [a, b, c] means different superscript letters differ significantly ($p < 0.05$).

Table 2. Impact of different treatment groups on mean serum insulin in rats on day 28.

Groups	Mean serum insulin (mU/L)	SEM
Control	14.34[a]	0.60
Diabetic control	9.54[c]	0.55
CLN1 + D	8.90[c]	0.69
CLN5 + D	9.17[c]	0.76
CLN10 + D	13.67[a]	0.64
CLN1 with glibenclamide	10.50[b]	0.70
CLN5 with glibenclamide	11.50[b]	0.75
CLN10 with glibenclamide	13.00[a]	0.64
P- Value	0.001	

[a, b, c] means different superscript letters in a column differ significantly ($p < 0.05$). Control: Not diabetic and untreated rats, diabetic control: Alloxan induced diabetes rats, CLN1+D, CLN5+D, CLN10+D: Diabetic rats treated with cilnidipine at 1 mg/kg, 5 mg/kg and 10 mg/kg, respectively, CLN1, CLN5 and CLN10 with glibenclamide: Diabetic rats treated with cilnidipine at 1 mg/kg, 5 mg/kg and 10 mg/kg with 2.5 mg/kg glibenclamide, respectively.

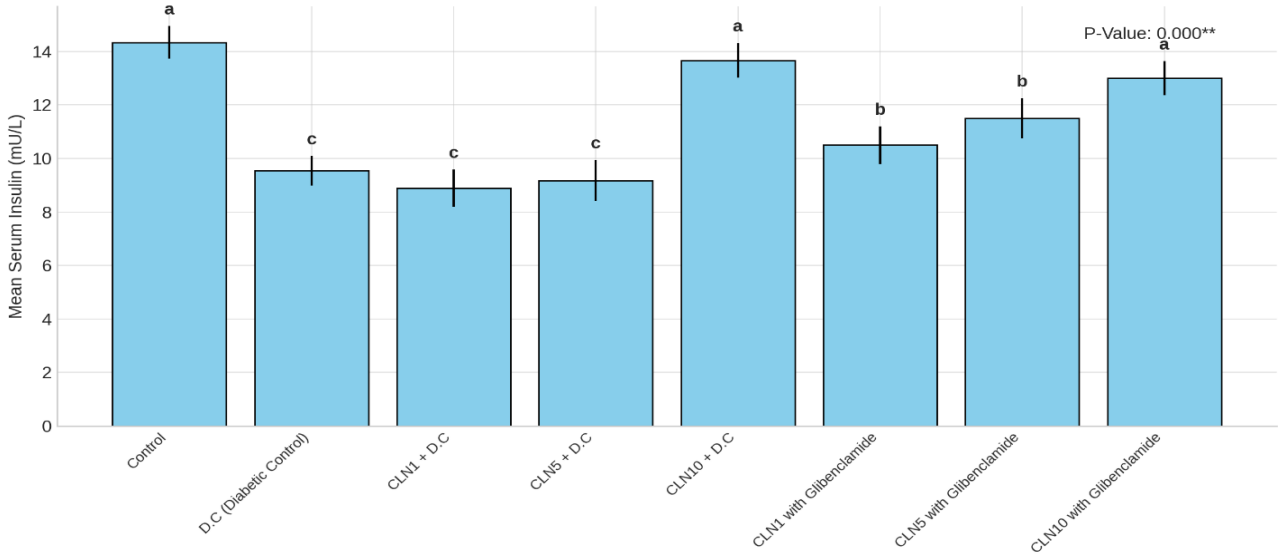


Figure 4. Impact of different treatment groups on mean serum insulin (mU/L) in rats on day 28. Control: Not diabetic and untreated rats, diabetic control: Alloxan induced diabetes rats, CLN1+D, CLN5+D, CLN10+D: Diabetic rats treated with cilnidipine at 1 mg/kg, 5 mg/kg and 10 mg/kg, respectively CLN1, CLN5 and CLN10 with glibenclamide: Diabetic rats treated with cilnidipine at 1 mg/kg, 5 mg/kg and 10 mg/kg with 2.5 mg/kg glibenclamide, respectively. [a, b, c] means different superscript letters differ significantly ($p < 0.05$).

Table 3. Impact of different treatment groups on HOMA-IR in rats on day 28.

Groups	HOMA-IR	SEM
Control	2.86[a]	1.35
Diabetic control (DC)	5.17[b]	0.58
CLN1 + D	2.40[a]	1.03
CLN5 + D	2.16[a]	0.75
CLN10 + D	2.60[a]	0.48
CLN1 with glibenclamide	2.45[a]	0.68
CLN5 with glibenclamide	2.43[a]	0.56
CLN10 with glibenclamide	2.56[a]	0.45
P- Value	0.001	

[a, b, c] means different superscript letters in a column differ significantly ($p < 0.05$). Control: Not diabetic and untreated rats; Diabetic control: Alloxan induced diabetes rats, CLN1+D, CLN5+D, CLN10+D: Diabetic rats treated with cilnidipine at 1 mg/kg, 5 mg/kg and 10 mg/kg, respectively, CLN1, CLN5 and CLN10 with glibenclamide: Diabetic rats treated with cilnidipine at 1 mg/kg, 5 mg/kg and 10 mg/kg with 2.5 mg/kg glibenclamide, respectively.

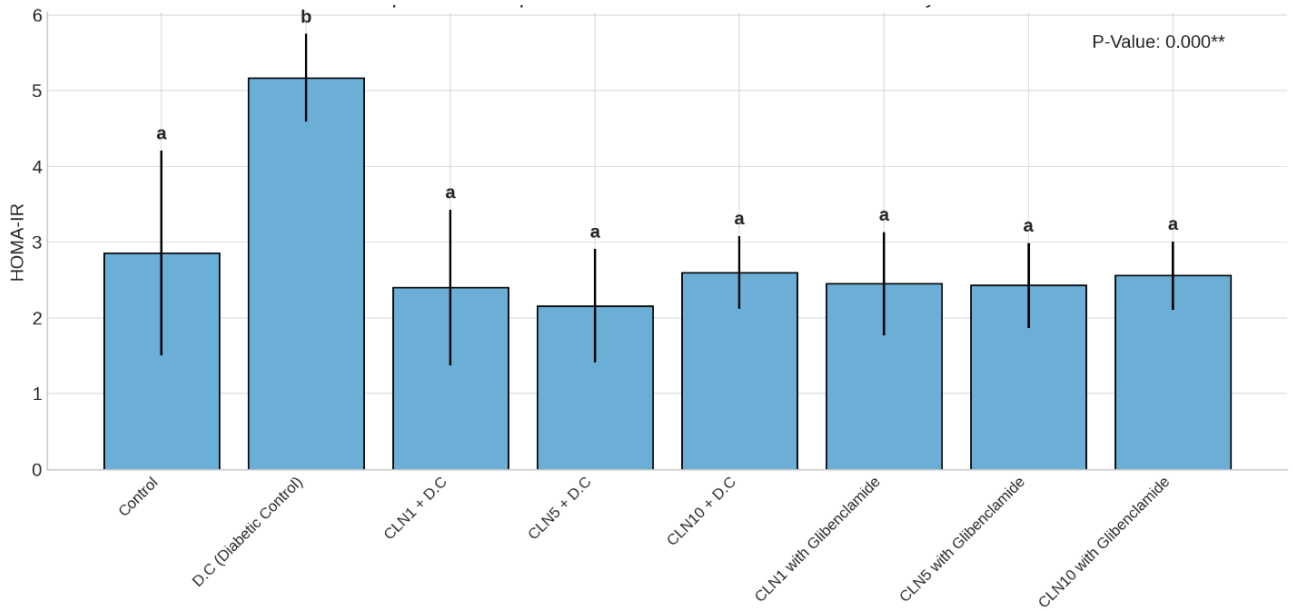


Figure 5. Impact of different treatment groups on HOMA-IR in rats on day 28. Control: Not diabetic and untreated rats, diabetic control: Alloxan induced diabetes rats; CLN1+D, CLN5+D, CLN10+D: Diabetic rats treated with cilnidipine at 1 mg/kg, 5 mg/kg and 10 mg/kg, respectively, CLN1, CLN5 and CLN10 with glibenclamide: Diabetic rats treated with cilnidipine at 1 mg/kg, 5 mg/kg and 10 mg/kg with 2.5 mg/kg glibenclamide, respectively. [a, b, c] means different superscript letters differ significantly ($p < 0.05$).

Table 4. Impact of different treatment groups on lipid parameters in rats on day 28

Group	Total cholesterol (mg/dL)	LDL-C (mg/dL)	HDL-C (mg/dL)	Triglycerides (mg/dL)
Control	180 ± 4.50^{a}	100 ± 5.01^{a}	50 ± 1.22^{b}	120 ± 6.01^{a}
Diabetic control	220 ± 5.20^{d}	150 ± 5.52^{d}	45 ± 1.32^{a}	180 ± 6.81^{d}
CLN1 + D	210 ± 4.80^{c}	140 ± 5.13^{c}	48 ± 1.42^{ab}	160 ± 6.32^{c}
CLN5 + D	200 ± 5.02^{ab}	130 ± 5.31^{b}	49 ± 1.51^{ab}	140 ± 6.50^{b}
CLN10 + D	185 ± 4.61^{a}	110 ± 5.02^{a}	52 ± 1.21^{bc}	130 ± 6.01^{ab}
CLN1 with glibenclamide	190 ± 4.70^{ab}	115 ± 5.12^{ab}	55 ± 1.31^{c}	135 ± 6.23^{ab}
CLN5 with glibenclamide	195 ± 5.03^{ab}	120 ± 5.30^{ab}	56 ± 1.50^{c}	125 ± 6.50^{a}
CLN10 with glibenclamide	180 ± 4.90^{a}	105 ± 5.22^{a}	60 ± 1.40^{d}	120 ± 6.32^{a}
P- Value	0.001	0.001	0.001	0.001

$^{a, b, c}$ means different superscript letters in a column differ significantly ($p < 0.05$). Control: Not diabetic and untreated rats; Diabetic control: Alloxan induced diabetes rats; CLN1+D, CLN5+D, CLN10+D: Diabetic rats treated with cilnidipine at 1 mg/kg, 5 mg/kg and 10 mg/kg, respectively; CLN1, CLN5 and CLN10 with glibenclamide: Diabetic rats treated with cilnidipine at 1 mg/kg, 5 mg/kg and 10 mg/kg with 2.5 mg/kg glibenclamide, respectively.

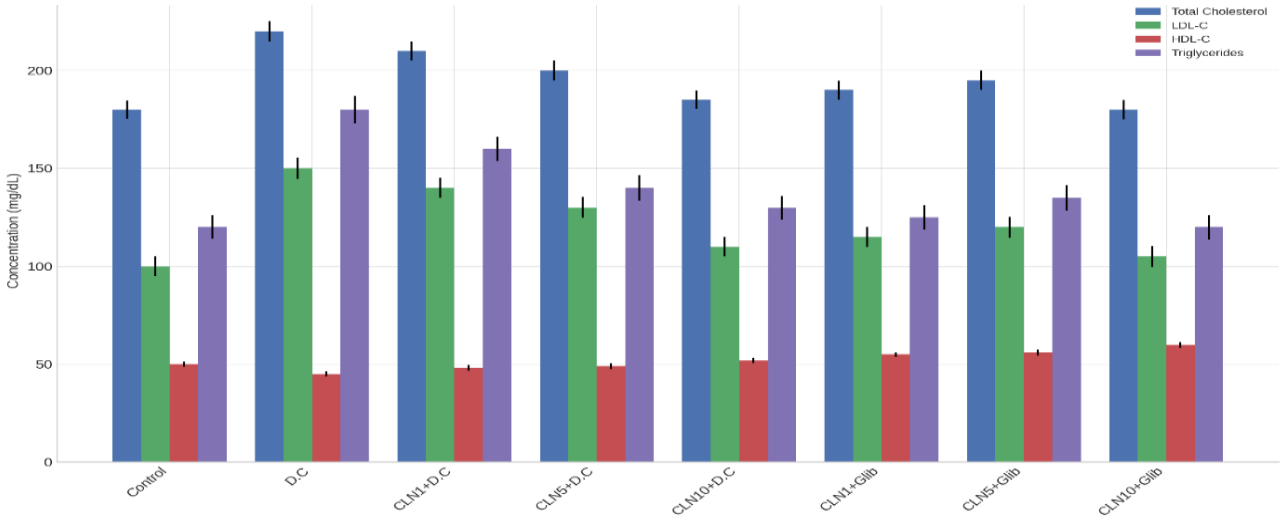


Figure 6. Impact of different treatment groups on lipid parameters in rats on day 28. Control: Not diabetic and untreated rats, diabetic control: Alloxan induced diabetes rats, CLN1+D, CLN5+D, CLN10+D: Diabetic rats treated with cilnidipine at 1 mg/kg, 5 mg/kg and 10 mg/kg, respectively; CLN1, CLN5 and CLN10 with glibenclamide: Diabetic rats treated with cilnidipine at 1 mg/kg, 5 mg/kg and 10 mg/kg with 2.5 mg/kg glibenclamide, respectively. $^{a, b, c}$ means different superscript letters differ significantly ($p < 0.05$).

The HOMA-IR scores were significantly elevated in the diabetic control group (5.17 ± 0.58), indicating enhanced insulin resistance compared to the normal control group (2.86 ± 1.35; $p < 0.05$). Treatment with cilnidipine alone or in combination with glibenclamide significantly reduced HOMA-IR across all treated groups compared to the diabetic control group ($p<0.05$). All treated groups, including CLN1+D with the lowest monotherapy dose, had HOMA-IR values that were as low as or lower than those of the normal control group (Table 3, Figure 5). The diabetic control group had significant dyslipidemia, increased total cholesterol, LDL-C, and triglycerides, and decreased HDL-C compared to the normal control group ($p < 0.01$). Single cilnidipine therapy improved lipid profile parameters in a dose-dependent manner. The initial results of the insulin and lipid parameters did not differ significantly ($p > 0.05$) in CLN10 alone and CLN10 with glibenclamide, implying that the effects of a higher dose of cilnidipine were similar to the lower doses (Table 4, Figure 6). The C-peptide was reduced significantly in the diabetic control group (0.30 ± 0.03 ng/mL) compared to the normal control group (1.50 ± 0.05 ng/mL), indicating *β-cell* dysfunction. The C-peptide was increased in parallel with the increase of cilnidipine dose, starting from 0.45 ± 0.04 ng/mL in the CLN1 group to 0.85 ± 0.06 ng/mL in the CLN10 group. Combination therapy with glibenclamide caused an additional increase in C-peptide concentration. The CLN10 with glibenclamide returned to C-peptide levels close to the normal level (1.40 ± 0.09 ng/mL), similar to the control group (1.50 ± 0.05 ng/mL). All these differences were statistically significant ($p < 0.01$), confirming the effectiveness of combination therapy in restoring pancreatic β-cell function (Table 5, Figure 7).

Table 5. Impact of different treatment groups on C-Peptide in rats on day 28.

Group	C-peptide (ng/mL; Mean ± S.E)
Control	1.50 ± 0.05^{a}
Diabetic control	0.30 ± 0.03^{d}
CLN1 + D	0.45 ± 0.04^{cd}
CLN5 + D	0.65 ± 0.05^{c}
CLN10 + D	0.85 ± 0.06^{bc}
CLN1 with glibenclamide	0.90 ± 0.07^{b}
CLN5 with glibenclamide	1.20 ± 0.08^{ab}
CLN10 with glibenclamide	1.40 ± 0.09^{a}

$^{a, b, c}$ means different superscript letters in a column differ significantly ($p < 0.05$). Control: Not diabetic and untreated rats, diabetic control: Alloxan induced diabetes rats, CLN1+D, CLN5+D, CLN10+D: Diabetic rats treated with cilnidipine at 1 mg/kg, 5 mg/kg and 10 mg/kg, respectively, CLN1, CLN5 and CLN10 with glibenclamide: Diabetic rats treated with cilnidipine at 1 mg/kg, 5 mg/kg and 10 mg/kg with 2.5 mg/kg glibenclamide, respectively.

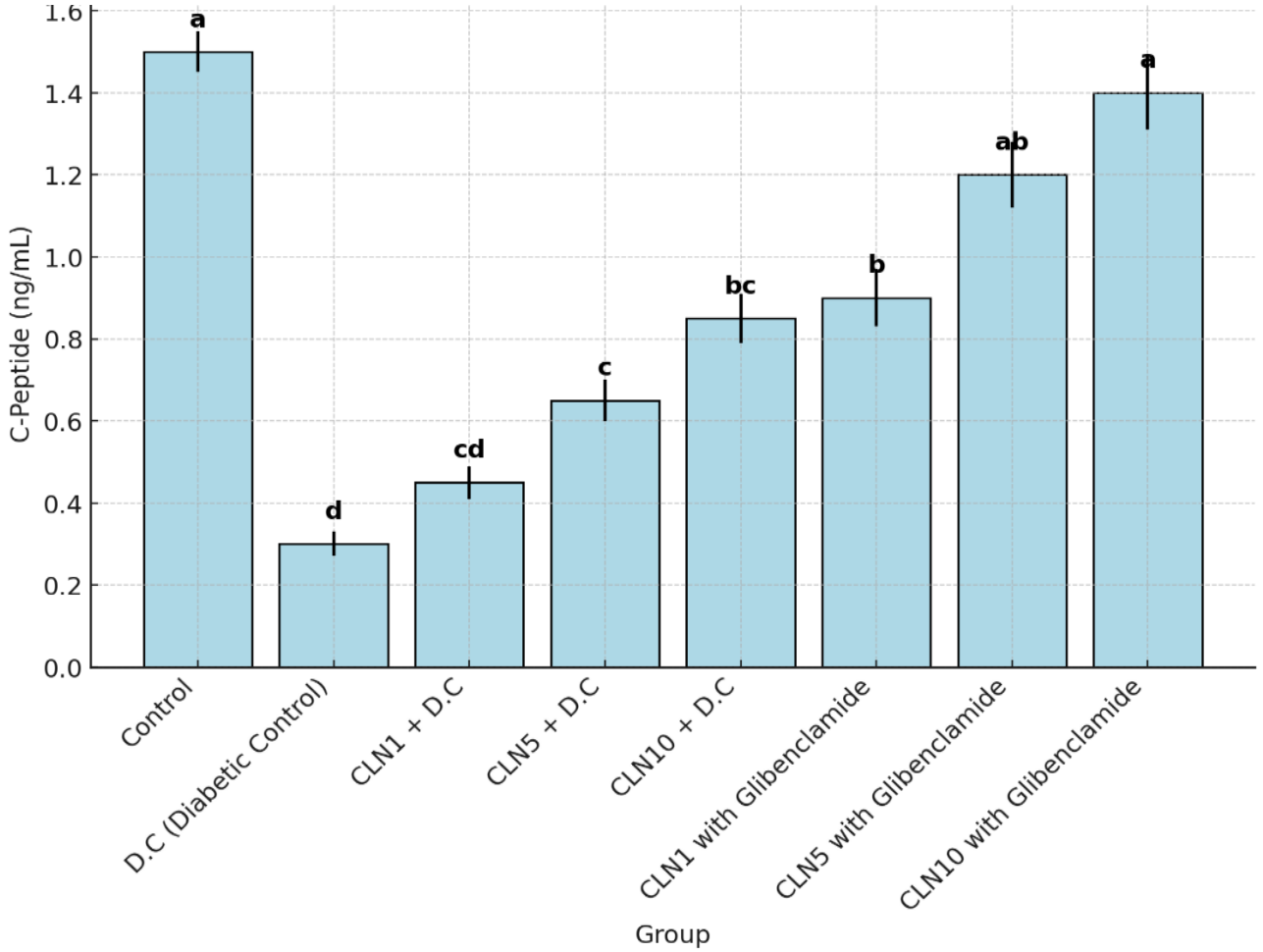


Figure 7. Impact of different treatment groups on C-Peptide (ng/mL) in rats on day 28. Control: Not diabetic and untreated rats, diabetic control: Alloxan induced diabetes rats; CLN1+D, CLN5+D, CLN10+D: Diabetic rats treated with cilnidipine at 1 mg/kg, 5 mg/kg and 10 mg/kg, respectively, CLN1, CLN5 and CLN10 with glibenclamide: Diabetic rats treated with cilnidipine at 1 mg/kg, 5 mg/kg and 10 mg/kg with 2.5 mg/kg glibenclamide, respectively. [a, b, c] means different superscript letters differ significantly ($p < 0.05$).

Combination index analysis of cilnidipine and glibenclamide co-administration on glycemic, insulin, and lipid parameters

As demonstrated in Table 6, the combination index (CI) analysis demonstrated different interactions between cilnidipine and glibenclamide concerning lipid and metabolic parameters, including fasting plasma glucose and serum insulin. Notably, the highest dose combination (CLN10 with glibenclamide) exhibited a synergistic effect (CI = 0.95), whereas lower doses indicated additive (CLN1) or antagonistic (CLN5) interactions. The C-peptide always exhibited synergy in all combinations of doses, with the lowest value of CI (0.25) at CLN1 with glibenclamide, reflecting enhanced β-cells secretory functions, as presented in Table 6. In contrast, lipid profile parameters such as total cholesterol, LDL-C, HDL-C, and triglycerides failed to achieve a perfect cure (CI > 1), implying that combination therapy was less effective in improving lipid profile when compared to its effectiveness on FPG. The lipid parameters results highlighted that the overall benefits of combination therapy were dose-dependent and optimally expressed on glucose metabolism and pancreatic function, while there were no beneficial therapeutic effects on lipid parameters.

The Chou–Talalay method equation was employed to determine the CI by comparing different doses of cilnidipine (1 mg/kg, 5 mg/kg, and 10 mg/kg) administered independently with these same doses of cilnidipine in combination with glibenclamide (2.5 mg/kg). In addition, the control dose column in Table 6 served only for illustrative purposes and comparison, and was not used for CI calculation.

Figure 8 indicates the fine-scale structure of the artificial neural network used to predict the synergistic treatment response. It illustrates data flow from 25 input features through three hidden layers to four clinical output targets.

Table 6. Comprehensive combination index analysis for different treatment groups on metabolic and lipid parameters in rats on day 28

Parameter	Control dose	Combination dose	CI value	Interpretation
Fasting plasma glucose (mg/dL)	81.25 (Control)	95.20 (CLN1 with glibenclamide)	1.10	Antagonism
	81.25 (Control)	85.00 (CLN5 with glibenclamide)	1.05	Additive
	81.25 (Control)	80.00 (CLN10 with glibenclamide)	0.95	Synergistic
Serum insulin (mU/L)	14.34 (Control)	10.50 (CLN1with glibenclamide)	1.10	Antagonism
	14.34 (Control)	11.50 (CLN5 with glibenclamide)	1.105	Additive
	14.34 (Control)	13.00 (CLN10 with glibenclamide)	0.95	Synergistic
Total cholesterol (mg/dL)	180 (Control)	190 (CLN1 with glibenclamide)	1.68	Antagonism
LDL-C (mg/dL)	100 (Control)	115 (CLN1 with glibenclamide)	1.43	Antagonism
HDL-C (mg/dL)	50 (Control)	55 (CLN1 with glibenclamide)	1.75	Antagonism
Triglycerides (mg/dL)	120 (Control)	125 (CLN10 with glibenclamide	1.36	Antagonism
C-peptide (ng/mL)	0.45 (CLN1 + D alone)	0.90 (CLN1 with glibenclamide)	0.25	Synergistic
	0.65 (CLN5 + D alone)	1.20 (CLN5 with glibenclamide)	0.39	Synergistic
	0.85 (CLN10 + D alone)	1.40 (CLN10 with glibenclamide)	0.50	Synergistic

Note: Control: Not diabetic and untreated rats; CLN1+D, CLN5+D, CLN10+D: Diabetic rats treated with cilnidipine at 1 mg/kg, 5 mg/kg and 10 mg/kg, respectively; CLN1, CLN5 and CLN10 with glibenclamide: Diabetic rats treated with cilnidipine at 1 mg/kg, 5 mg/kg and 10 mg/kg with 2.5 mg/kg glibenclamide, respectively.

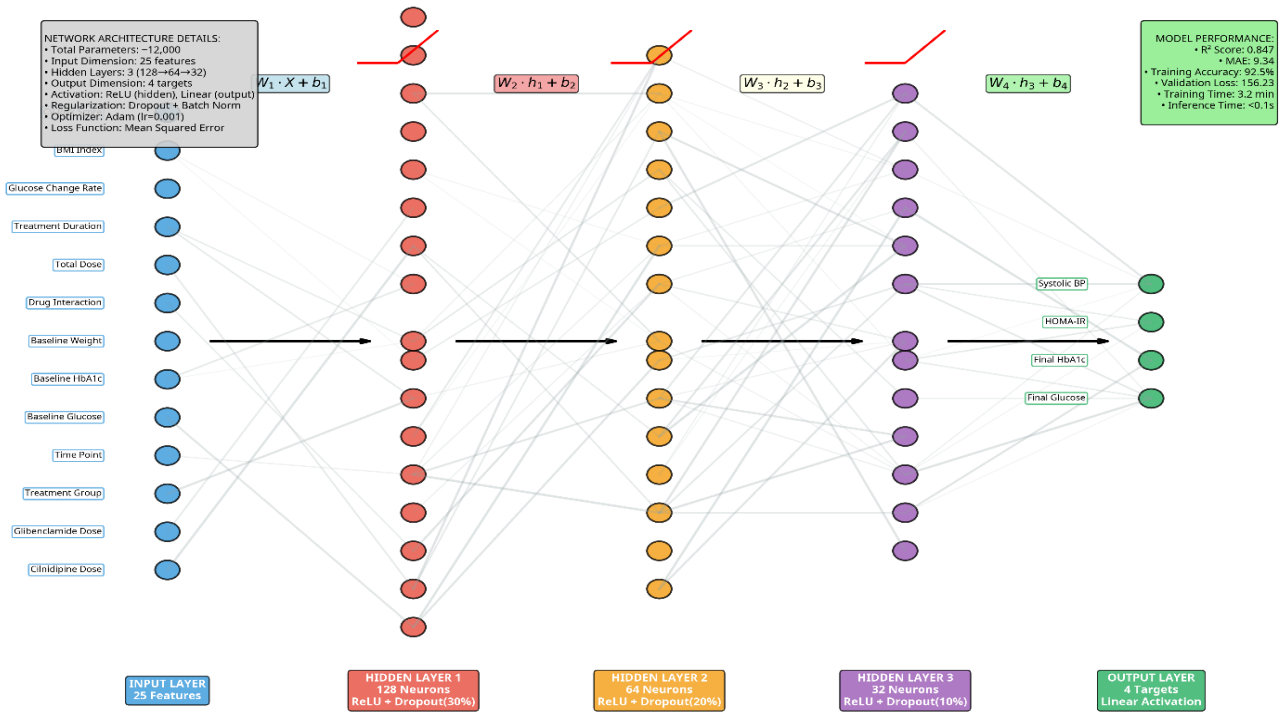


Figure 8. Deep neural network architecture used for predicting the effect of combined cilnidipine and glibenclamide treatment on glycemic and cardiovascular parameters in rats. The model deploys dropout, batch normalization, and ReLU activations for regularization and non-linearity.

Gene expression

The GLUT4 mRNA expression was highly suppressed ($p < 0.05$) between the diabetic control group (0.48 ± 0.06) and the normal control group (set as 1.00 ± 0.03; Table 7). Cilnidipine alone reinstated the GLUT4 expression in a dose-dependent manner, and its co-administration with glibenclamide further enhanced the expression. The group treated with CLN10 and glibenclamide exhibited the highest GLUT4 level (2.25 ± 0.18; $p < 0.05$) compared to the diabetic control group, demonstrating a synergistic antidiabetic effect.

Table 8 indicates that PI3K expression and p-AKT/AKT ratio were significantly reduced in the diabetic control group (0.46 and 0.39, respectively) and indicate deficient insulin signalling. Cilnidipine alone reactivated the pathway in a dose-dependent way. When combined with glibenclamide, there was a synergistic and significant increase, reaching its peak in the CLN10 with glibenclamide group of PI3K2 (2.22 ± 0.13), p-AKT/AKT (2.34 ± 0.14; $p < 0.05$), which confirmed a strong reactivation of the PI3K/AKT insulin signalling pathway compared to the diabetic control group.

Table 7. Glucose transporter type 4 gene expression by RT-qPCR in rats on day 28 of the study

Group	GLUT4 expression (fold change ± SD)	P-value versus diabetic control	Interpretation
Control	1.00 ± 0.03	-	Baseline normal expression
Diabetic control	0.48 ± 0.06	-	Downregulated due to diabetes
CLN1 + D	0.72 ± 0.08	0.03	Mild improvement
CLN5 + D	0.96 ± 0.10	0.01	Restored to near-normal
CLN10 + D	1.12 ± 0.09	0.002	Significant restoration
CLN1 with glibenclamide	1.45 ± 0.12	< 0.001	Synergistic increase
CLN5 with glibenclamide	2.08 ± 0.15	< 0.001	Strong synergy
CLN10 with glibenclamide	2.25 ± 0.18	< 0.001	Maximal GLUT4 upregulation observed

Significant: $p < 0.05$. Control: Not diabetic and untreated rats; diabetic control: Alloxan induced diabetes rats; CLN1+D, CLN5+D, CLN10+D: Diabetic rats treated with cilnidipine at 1 mg/kg, 5 mg/kg and 10 mg/kg, respectively; CLN1, CLN5 and CLN10 with glibenclamide: Diabetic rats treated with cilnidipine at 1 mg/kg, 5 mg/kg and 10 mg/kg with 2.5 mg/kg glibenclamide, respectively.

Table 8. Gene expressions of PI3K and p-AKT in rats on day 28 of the study

Group	PI3K (Rel. intensity ± SD)	p-AKT/AKT ratio ± SD	p-value versus diabetic control	Interpretation
Control	1.00 ± 0.00	1.00 ± 0.00	-	Normal activity
Diabetic control	0.46 ± 0.05	0.39 ± 0.04	-	Suppressed insulin signalling
CLN1 + D	0.69 ± 0.06	0.58 ± 0.06	0.04	Partial restoration
CLN5 + D	0.91 ± 0.07	0.81 ± 0.05	0.01	Near-complete restoration
CLN10 + D	1.07 ± 0.08	0.97 ± 0.04	0.003	Normalization of signalling
CLN1 with glibenclamide	1.42 ± 0.11	1.55 ± 0.09	< 0.001	Synergistic activation
CLN5 with glibenclamide	1.93 ± 0.14	2.11 ± 0.12	< 0.001	Strongest activation until now
CLN10 with glibenclamide	2.22 ± 0.13	2.34 ± 0.14	< 0.001	Maximal enhancement of PI3K/AKT signalling

Significant: $p < 0.05$. Control: Not diabetic and untreated rats, diabetic control: Alloxan induced diabetes rats, CLN1+D, CLN5+D, CLN10+D: Diabetic rats treated with cilnidipine at 1 mg/kg, 5 mg/kg and 10 mg/kg, respectively, CLN1, CLN5 and CLN10 with glibenclamide: Diabetic rats treated with cilnidipine at 1 mg/kg, 5 mg/kg and 10 mg/kg with 2.5 mg/kg glibenclamide, respectively.

DISCUSSION

Combined administration of cilnidipine and glibenclamide in the current investigation provided outstanding improvement in key metabolic markers in diabetic rats, including FPG, serum insulin, HOMA-IR, lipid profile, and C-peptide levels. While cilnidipine monotherapy demonstrated a dose-dependent improvement in some glycemic status, the CI analysis for all lipid parameters (Total-C, LDL-C, HDL-C, TG) indicated an antagonistic reaction (CI > 1). Competing metabolic pathways or drug-drug interactions, rather than cilnidipine alone, could be a potential explanation at the molecular level for these findings. Additionally, cilnidipine's blockage of N-type calcium channels could indirectly affect lipolysis in adipose tissues (Toba et al., 2011). Finally, enhancements in the lipid profile may necessitate additional time to become apparent.

Levels of FPG, remarkably increased in diabetic controls, were notably normalized following combination therapy, especially the maximal dose of cilnidipine (CLN10 with glibenclamide), which normalized glucose to values equalling healthy controls, and this reflected a potent hypoglycemic action potentially superior to monotherapy.

Cilnidipine, a dual L/N-type CCB, exerts its effects through mechanisms that are independent of blood pressure reduction. Cilnidipine modulates sympathetic overactivity, enhances endothelial function, and suppresses oxidative stress, all of which are recognized contributors to insulin resistance (Shete, 2016).

In the present study, the striking reduction of HOMA-IR values in all cilnidipine-treated groups (alone or in combination with glibenclamide) strongly indicated increased insulin sensitivity, particularly in combination with glibenclamide, and this result may be attributed to different pharmacologic effects of cilnidipine beyond calcium channel blockade. Both L-type and N-type calcium channels were blocked by cilnidipine. The inhibition in N-type channels has been demonstrated to decrease sympathetic nerve activity (Shete, 2016), which consequently results in an increase in catecholamine levels. Eventually, insulin resistance developed due to the increase in hepatic glucose output and impaired glucose uptake in peripheral tissues. Therefore, cilnidipine's autonomic modulatory effect, achieved through calcium channel blockade, normalized insulin signalling in the liver, skeletal muscle, and adipose tissue (Russo et al., 2021). Although the current evidence aligns with the hypothesis that the sympatho-inhibitory effect of cilnidipine may contribute to improved metabolic regulation, direct evidence for the relationship between autonomic modulation and enhanced insulin signalling remains limited and warrants further investigation.

Furthermore, it has been reported that cilnidipine has a protective role against oxidative stress and pro-inflammatory cytokine expression (TNF-α, IL-6; Fouda et al., 2018), which are directly involved in the pathogenesis of insulin resistance. By reducing oxidative stress, cilnidipine maintains the structural integrity of insulin receptors and facilitates insulin signal transduction through the PI3K/Akt pathway, an essential process for GLUT4 translocation and glucose uptake (Yinyan et al., 2025). This is evident in the present study, as cilnidipine (whether alone or in combination) restored the PI3K/AKT/GLUT4 pathway in a synergistic and highly notable up-regulation (Tables 7 and 8).

At the cellular level, cilnidipine has been reported to increase endothelial nitric oxide (NO) bioavailability. Endothelial nitric oxide plays an important role in insulin-mediated vasodilation and glucose disposal, especially in skeletal muscle. Increased NO availability increases microvascular perfusion, which facilitates insulin and glucose delivery to peripheral tissues (Chandra and Ramesh, 2013).

In addition, cilnidipine's action on pancreatic β-cells can indirectly support insulin sensitivity. The normalization of C-peptide and serum insulin levels indicated an improved β-cell function and endogenous insulin secretion, potentially decreasing the need for compensatory hyperinsulinemia, which is often linked to insulin resistance (Takeda et al., 1999; Ueno et al., 2013; Kumari et al., 2023).

Blocking calcium channels decreases sympathetic overactivity, which is notorious for insulin signalling impairment. Cilnidipine facilitates nitric oxide-mediated vasodilation in vascular smooth muscles, thereby improving microvascular perfusion and enhancing glucose uptake in peripheral tissues. Additionally, cilnidipine possesses anti-inflammatory and antioxidant effects that improve the signalling in insulin receptors. The observed decrease in the HOMA-IR score with cilnidipine therapy could be explained by the above-mentioned coordinated actions. All in all, these benefits not only enhanced insulin receptor sensitivity but also promoted glucose uptake and utilization, thereby increasing the potential of cilnidipine as a metabolically active antihypertensive agent in patients with diabetes.

The model's capacity to incorporate multiple inputs, such as medicine interaction, dosing, and physiological baselines, indicates the complexity level of pharmacodynamic interactions that traditional models cannot have independently, and these findings validate the utility of deep learning in pharmacological synergy studies, particularly in identifying optimal combination doses and predicting patient-specific outcomes. The molecular results suggested that cilnidipine and glibenclamide acted synergistically to enhance insulin signalling and glucose uptake by upregulating the PI3K/AKT/GLUT4 pathway, providing a mechanistic basis for their antidiabetic activity. The ability of this combination to exceed typical levels of expression further highlights its potential not only in reversing insulin resistance but also in optimizing clinical glycemic control (Simon-Szabó et al., 2024).

Certain limitations should be acknowledged in the current study. The experiment was conducted exclusively on male Wistar rats, and sex-specific responses were not examined, which could influence metabolic responses. The second limitation was that the study lasted only 28 days, and the long-term effects on β-cell preservation, cardiovascular risk, and renal function were not assessed. While the CI had provided insights into pharmacodynamic interactions, molecular mechanisms such as markers of oxidative stress, inflammatory cytokines, or insulin receptor signalling pathways (excluding the insulin receptor signalling pathway, PI3K/AKT) and their downstream target (GLUT4) were not examined. Furthermore, the experiment was limited to monotherapies and two-medicine combinations; the inclusion of additional antidiabetic or lipid-lowering agents could potentially enhance efficacy.

CONCLUSION

The present study demonstrated that high doses of cilnidipine and its combination with glibenclamide could be a more integrated approach to diabetes and its comorbidities. A significant effect was observed in the combination of cilnidipine 10 mg/kg with glibenclamide, which resulted in reduced fasting plasma glucose (FPG), an increase in insulin and C-peptide levels, and the normalization of HOMA-IR. Furthermore, they demonstrated the highest levels of GLUT4 and a

significant upregulation of PI3K/p-AKT expression. However, this combination therapy exerted an opposing effect on all lipid parameters. The findings necessitated the exploration of the present results in clinical trials to establish the translational potential in diabetic patients. Future studies need to address these gaps by using long-term models, including females in the studies, investigating specific mechanistic pathways, such as whether it directly impacts the insulin cascade, testing glibenclamide alone for comparison purposes, and exploring its potential for clinical application in humans with diabetes.

DECLARATIONS

Funding

The present study was not supported financially and received no funding.

Authors' contributions

Shatha Hani Mohammad designed and implemented the present study. Nada Satea Mahmood assisted in checking the manuscript, supervision, and ensuring necessary revisions and corrections. Abeer Mansour Abdel Rasool contributed to data analysis, interpretation, and writing the manuscript. All authors checked and approved the findings of the present study and the final edition of the submitted manuscript.

Competing interests

The authors have not declared any conflict of interest.

Ethical considerations

Ethical issues, including plagiarism, consent to publish, misconduct, data fabrication or falsification, double publication, and redundancy, have been checked by all the authors. No artificial intelligence (AI) or generation was used for writing or preparing the manuscript.

Availability of data and materials

The data supporting the findings of the present study are available from the corresponding author upon reasonable request.

REFERENCES

Alotaibi MR, Fatani AJ, Almnaizel AT, Ahmed MM, Abuohashish HM, and Al-Rejaie SS (2019). *In vivo* assessment of combined effects of glibenclamide and losartan in diabetic rats. Medical Principles and Practice, 28(2): 178-185. DOI: https://www.doi.org/10.1159/000496104

Aloke C, Egwu CO, Aja PM, Obasi NA, Chukwu J, Akumadu BO, Ogbu PN, and Achilonu I (2022). Current advances in the management of diabetes mellitus. Biomedicines, 10(10): 2436. DOI: https://www.doi.org/10.3390/biomedicines10102436

Brigato L and Iocchi L (2021). A close look at deep learning with small data. International Conference on Pattern Recognition (ICPR), pp. 2490-2497. DOI: https://www.doi.org/10.48550/arXiv.2003.12843

Chakraborty RN, Langade D, More S, Revandkar V, Birla A, Langade DG, and Revandlkar V (2021). Efficacy of cilnidipine (L/N-type calcium channel blocker) in treatment of hypertension: A Meta-analysis of randomized and non-randomized controlled trials. Cureus, 13(11): e19822. DOI: https://www.doi.org/10.7759/cureus.19822

Chandra KS and Ramesh G (2013). The fourth-generation calcium channel blocker: Cilnidipine. Indian Heart Journal, 65(6): 691-695. DOI: https://www.doi.org/10.1016/j.ihj.2013.11.001

Chougale AD, Panaskar SN, Gurao PM, and Arvindekar AU (2007). Optimization of alloxan dose is essential to induce stable diabetes for prolonged period. Asian Journal of Biochemistry, 2(6): 402-408. DOI: https://www.doi.org/10.3923/ajb.2007.402.408

Corso G, Papagni F, Gelzo M, Gallo M, Barone R, Graf M, Scarpato N, and Dello Russo A (2016). Development and validation of an enzymatic method for total cholesterol analysis using whole blood spot. Journal of Clinical Laboratory Analysis, 30(5): 517-523. DOI: https://www.doi.org/10.1002/jcla.21890

El-Kebbi IM, Bidikian NH, Hneiny L, and Nasrallah MP (2021). Epidemiology of type 2 diabetes in the Middle East and North Africa: Challenges and call for action. World Journal of Diabetes, 12(9): 1401-1425. DOI: https://www.doi.org/10.4239/wjd.v12.i9.1401

Feingold KR (2023). Dyslipidemia in patients with diabetes. In: K. R Feingold, B. Anawalt, A. Boyce, G Chrousos, E. Corpas, W. W. de Herder, K. Dhatariya, K. Dungan, J. Hofland, S. Kalra, G. Kaltsas, N. Kapoor, C. Koch, P. Kopp, M. Korbonits, C. S. Kovacs, W. Kuohung, B. Laferrère, M. Levy, E. A. McGee, R. McLachlan, R. Muzumdar, J. Purnell, R. Rey, R. Sahay, A. S. Shah, F. Singer, M. A. Sperling, C. A. Stratakis, D. L. Trence, and D. P. Wilson (Editors), Endotext. MDText.com, Inc., South Dartmouth, pp. 1-32. Available at: https://www.endotext.org/chapter/dyslipidemia-in-patients-with-diabetes/

Fujita T, Ando K, Nishimura H, Ideura T, Yasuda G, Isshiki M, and Takahashi K (2007). Antiproteinuric effect of the calcium channel blocker cilnidipine added to renin-angiotensin inhibition in hypertensive patients with chronic renal disease. Kidney International, 72(12): 1543-1549. DOI: https://www.doi.org/10.1038/sj.ki.5002623

Fouda AM, Youssef AR, and Sharaf Eldin O (2018). Comparative study of amlodipine vs. cilnidipine for the prevention of hepatic ischemia-reperfusion injury in rat model. Fundamental and Clinical Pharmacology, 32(2): 163-173. DOI: https://www.doi.org/10.1111/fcp.12335

Kumari K, Sinha R, Toppo MS, Mishra P, Alam S, and Majhee L (2023). Blood pressure reducing potential and renoprotective action of cilnidipine among hypertensive patients suffering from chronic kidney disease: A meta-analysis. Cureus, 15(4): e37774. DOI: https://www.doi.org/10.7759/cureus.37774

Li Z, Wei H, Li R, Wu B, Xu M, YangX, Zhang Y, and Liu Y (2024). The effects of antihypertensive drugs on glucose metabolism. Diabetes, Obesity and Metabolism, 26(11): 4820-4829. DOI: https://www.doi.org/10.1111/dom.15821

Mahmood M and Mohammad S (2023). The Effect of cilnidipine on insulin sensitivity. Iraqi Journal of Pharmacy, 20(Supplementary 1): 210-216. DOI: https://www.doi.org/10.33899/iphr.2023.143299.1060

Mehta KK, Tiwaskar M, and Kasture P (2024). Cilnidipine, a dual L/N-type Ca^{2+} channel blocker in hypertension management: A review. The Journal of the Association of Physicians of India, 72(4): 54-58. DOI: https://www.doi.org/10.59556/japi.72.0516

Nishida M, Ishikawa T, Saiki S, Sunggip C, Aritomi S, Harada E, Kuwahara K, Hirano K, Mori Y, and Kim-Mitsuyama S (2013). Voltage-dependent N-type Ca2+ channels in endothelial cells contribute to oxidative stress-related endothelial dysfunction induced by angiotensin II in mice. Biochemical and Biophysical Research Communications, 434(2): 210-216. DOI: https://www.doi.org/10.1016/j.bbrc.2013.03.040

Rasool AMA and Mahmood IH (2021). Impact of metformin on proinflammatory cytokines and histological evaluation of the liver iInduced diabetes on albino male rats. International Journal of Drug Delivery Technology, 11(4): 1307-1312. DOI: https://www.doi.org/ 10.25258/ijddt.11.4.31

Russo B, Menduni M, Borboni P, Picconi F, and Frontoni S (2021). Autonomic nervous system in obesity and insulin-resistance—the complex interplay between leptin and central nervous system. International Journal of Molecular Sciences, 22(10): 5187. DOI: https://www.doi.org/10.3390/ijms22105187

Saeedan AS, Soliman GA, Abdel-Rahman RF, Abd-Elsalam RM, Ogaly HA, Alharthy KM, and Abdel-Kader M S (2021). Possible synergistic antidiabetic effects of quantified artemisia judaica extract and glyburide in streptozotocin-induced diabetic rats via restoration of PPAR-α mRNA expression. Biology, 10(8): 796. DOI: https://www.doi.org/10.3390/biology10080796

Shah A, Isath A, and Aronow WS (2022). Cardiovascular complications of diabetes. Expert Review of Endocrinology and Metabolism, 17(5): 383-388. DOI: https://www.doi.org/10.1080/17446651.2022.2099838

Shaikh GB and Das KK (2025). Cilnidipine: An L-and N-Type blocker of calcium channels ameliorating renal damage in experimental hypertensive rats. Cureus, 17(3): e81404. DOI: https://www.doi.org/10.7759/cureus.81404

Shete MM (2016). Cilnidipine: Next generation calcium channel blocker. Journal of the Association of Physicians of India, 64(4): 95-99. Available at: https://pubmed.ncbi.nlm.nih.gov/27734656/

Sidhu MC and Sharma T (2014). Antihyperglycemic activity of petroleum ether leaf extract of *Ficus krishnae* L. on alloxan-induced diabetic rats. Indian Journal of Pharmaceutical Sciences, 76(4): 323-331. Available at: https://pubmed.ncbi.nlm.nih.gov/25284930/

Simon-Szabó L, Lizák B, Sturm G, Somogyi A, Takács I, and Németh Z (2024). Molecular aspects in the development of type 2 diabetes and possible preventive and complementary therapies. International Journal of Molecular Sciences, 25(16): 9113. DOI: https://www.doi.org/10.3390/ijms25169113

Szkudelski T (2001). The mechanism of alloxan and streptozotocin action in B cells of the rat pancreas. Physiological Research, 50(6): 537-546. DOI: http://www.doi:10.33549/physiolres.930111

Takeda S, Ueshiba H, Hattori Y, and Irie M (1999). Cilnidipine, the N- and L-type calcium channel antagonist, reduced on 24-h urinary catecholamines and C-peptide in hypertensive non-insulin-dependent diabetes mellitus. Diabetes Research and Clinical Practice, 44(3): 197-205. DOI: https://www.doi.org/10.1016/S0168-8227(99)00053-4

Taneera J, Bustanji Y, Alsukour H, Al-Khateeb, K, and Hassan T (2025). Mapping the landscape of diabetes research; an emirati perspective of trends, challenges, and opportunities. Advances in Biomedical and Health Sciences, 4(3): 99-156. DOI: https://www.doi.org/10.4103/abhs.abhs_38_25

Thrasher J (2017). Pharmacologic management of type 2 diabetes mellitus: Available therapies. The American Journal of Cardiology, 120(1): S4-S16. DOI: https://www.doi.org/10.1016/j.amjmed.2017.04.004

Toba H, Yoshida M, Tojo C, Nakano A, Oshima Y, Kojima Y, Noda K, Wang J, Kobara M, and Nakata T (2011). L/N-type calcium channel blocker cilnidipine ameliorates proteinuria and inhibits the renal renin–angiotensin–aldosterone system in deoxycorticosterone acetate-salt hypertensive rats. Hypertension Research, 34: 521-529. DOI: https://www.doi.org/10.1038/hr.2010.279

Ueno D, Masaki T, Gotoh K, Chiba S, Kakuma T, and Yoshimatsu H (2013). Cilnidipine regulates glucose metabolism and levels of high-molecular adiponectin in diet-induced obese mice. Hypertension Research, 36(3): 196-201. DOI: https://www.doi.org/10.1038/hr.2012.141

Xie X, Wu C, Hao Y, Wang T, Yang Y, Cai P, Zhang Y, Huang J, Deng K, and Yan D (2023). Benefits and risks of drug combination therapy for diabetes mellitus and its complications: a comprehensive review. Frontiers in Endocrinology, 14: 1301093. DOI: https://www.doi.org/10.3389/fendo.2023.1301093

Yinyan Li, Sizu Yang, Feng Jiang, Siqi Luo, Jinlong Liang, Linrui Jiang, Zhixuan Chen, Xin Chen, Jie Yang (2025). Cilnidipine exerts antiviral effects *in vitro* and *in vivo* by inhibiting the internalization and fusion of influenza A virus. BioMed Central Medicine, 23: 200. DOI: https://www.doi.org/10.1186/s12916-025-04022-0

Publisher's note: Scienceline Publication Ltd. remains neutral with regard to jurisdictional claims in published maps and institutional affiliations.

Open Access: This article is licensed under a Creative Commons Attribution 4.0 International License, which permits use, sharing, adaptation, distribution and reproduction in any medium or format, as long as you give appropriate credit to the original author(s) and the source, provide a link to the Creative Commons licence, and indicate if changes were made. The images or other third party material in this article are included in the article's Creative Commons licence, unless indicated otherwise in a credit line to the material. If material is not included in the article's Creative Commons licence and your intended use is not permitted by statutory regulation or exceeds the permitted use, you will need to obtain permission directly from the copyright holder. To view a copy of this licence, visit https://creativecommons.org/licenses/by/4.0/.

© The Author(s) 2025

2025, Scienceline Publication
World's Veterinary Journal
World Vet J, 15(4): 1085-1094.
ISSN 2322-4568

DOI: https://dx.doi.org/10.54203/scil.2025.wvj110
PII: S232245682500110-15

Effects of Bromelain Loaded with Gold Nanoparticles on Histopathological and Immunohistochemical Parameters in Albino Mice with Testicular Damage

Saddama Saed Faraj, Rana Hanan Khudhair Al-Rubaye*, Baydaa Hussain Mutlak, and Entidhar Mohammed Mnati

Department of Biology, College of Education for Pure Sciences/ Ibn Al-Haitham, University of Baghdad, Iraq

*Corresponding author's Email: rana.h.k@ihcoedu.uobaghdad.edu.iq

ORIGINAL ARTICLE
Received: September 20, 2025
Revised: October 25, 2025
Accepted: November 23, 2025
Published: December 31, 2025

ABSTRACT

Carbon tetrachloride (CCl4) has been demonstrated to induce testicular damage via oxidative stress. Bromelain (Br), a proteolytic enzyme known for its biological activities and pharmacological properties, exhibits limited absorption owing to its low solubility and bioavailability. The present study aimed to investigate the histological and immunohistochemical effects of bromelain conjugated with gold nanoparticles (AuNPs) on the testis histology of albino mice treated with CCl4. Thirty-five male albino mice (*Mus musculus*), with an average age of 9 weeks, were randomly divided into five groups, each containing seven mice. The experiment was prolonged for four weeks. The first group (G1) was the control group, the second group (G2) received weekly sub-peritoneal injections of CCl4 until the end of the experiment, and the third group (G3) received an oral dose of Au-NPs solution. The fourth group (G4) received injections of CCl4; one hour later, the mice were given an oral dose of 300 mg/kg bromelain. The fifth group (G5) received an injection of CCl4; subsequently, the mice received the same oral dosage of 300 mg/kg Au-NPs-bromelain after 60 minutes. The mice's testes were sampled to evaluate histopathological alterations and immunohistochemical markers, particularly Ki-67 and caspase-9. The present results indicated that mice treated with CCl4 displayed a range of histological alterations, including testicular damage, degeneration in seminiferous tubules, vacuolation, and loss of germ cells. Furthermore, the immunohistochemistry study demonstrated that Ki-67 intensity decreased while caspase-9 intensity increased in groups G2 and G4 compared to the control group. Bromelain loaded with gold nanoparticles at a dosage of 300 mg/kg exhibited a notable reduction in the harmful effects of CCl4 on the testicular tissue of mice by restoring the histological structure, enhancing the Ki-67 proliferation protein, and suppressing the apoptotic cascade protein indicated by caspase 9.

Keywords: Bromelain, Carbon tetrachloride, Caspase, Gold nanoparticle

INTRODUCTION

Carbon tetrachloride (CCl4) is a colorless chemical molecule that is volatile, stable, and rapidly absorbed by both people and animals. It is released into the environment by toxic gas emissions such as tetrachloromethane, polluting soil, water, and air (Sherry et al., 2018). These industrial pollutants can enter the body via multiple routes and are known to damage different organs by altering cellular and tissue structure and functions (Sönmez et al., 2014). Although the liver is the main site of CCl4 toxicity and carcinogenesis, it also adversely affects the structure and function of other body organs, including the brain, lung, kidney, and testis (Unsal et al., 2021). The CCl4 exposure is known to induce testicular toxicity by reducing testicular and seminal vesicle weight, quantity, and quality of semen, and hormone levels, such as testosterone, follicle-stimulating hormone, and luteinizing hormone, all of which are critical for spermatogenesis (Rahmouni et al., 2019). Bromelain is a complex mixture of proteolytic enzymes derived from plants of the Bromeliaceae family, mostly extracted from the pineapple (*Ananas comosus*), being the most common species in this family (Varilla et al., 2021). Bromelain can scavenge free radicals and prevent lipids from oxidizing due to its antioxidant properties (Kansakar et al., 2024). Numerous cellulases, phosphatases, β-glucosidases, peroxidases, thiol endopeptidases, glycoproteins, and protease inhibitors are found in bromelain (Ali et al., 2024).

To cite this paper: Faraj SS, Al-Rubaye RHKh, Mutlak BH, and Mnati EM (2025). Effects of Bromelain Loaded with Gold Nanoparticles on Histopathological and Immunohistochemical Parameters in Albino Mice with Testicular Damage. *World Vet. J.*, 15(4): 1085-1094. DOI: https://dx.doi.org/10.54203/scil.2025.wvj110

In recent years, gold nanoparticles (AuNPs) have become more prominent because of their improved and unique physical, chemical, and biological properties (Rajkumar et al., 2025). Conjugating proteins to nanoparticles can enhance their stability, protect them from enzymatic digestion, as well as increase solubility and permeability while decreasing toxicity (Brito et al., 2021). Bromelain's large size, proteolytic nature, and water-soluble properties hinder its cell penetration, but formulating it into nanoemulsions or nanoparticles can improve its intracellular delivery for therapeutic purposes by protecting the enzyme from inactivation and facilitating entry across cell membranes (Rohmah et al., 2021). Although the direct association between bromelain and the proliferation protein Ki-67 in the testis is not well established, it may have an indirect effect by altering oxidative stress, inflammation, and cell proliferation (Yakut et al., 2025). Ki-67 is a nuclear DNA-binding protein, expressed in all vertebrates, often used as a marker to evaluate cell proliferation due to its specific localization to actively cycling cells (Zhao et al., 2018). Consequently, Ki-67 expression levels in the testis are a typical marker of spermatogenic cell proliferation and can also be used to evaluate the proliferation of spermatogenic cells (Menon et al., 2019). Apoptosis serves as a fundamental quality control mechanism in the testis, regulating germ cell development from genital differentiation through fertilization. It ensures the proper function of male germ cells and maintains a healthy ratio between germ and Sertoli cells (Asadi et al., 2021). The cytoplasm possesses a cysteine protease called caspase, which is one of the first caspases. Caspase-9 is essential to the intrinsic apoptotic process, which can receive upstream apoptotic signals to activate downstream caspases (Yu et al., 2024). Given the antioxidant properties of bromelain and the drug delivery capabilities of AuNPs, the present study aimed to investigate the effect of bromelain-loaded AuNPs on testicular histology and bromelain bioavailability in albino mice injured by carbon tetrachloride.

MATERIALS AND METHODS

Ethical approval

The present study has been approved by the ethical committee of the biology department at the University of Baghdad, College of Education for Pure Sciences/ Ibn Al-Haitham in Baghdad, Iraq. On 19/1/2025, the authorization was acquired under reference number EC-84.

Materials and reagents

Carbon tetrachloride, trisodium citrate, bromelain (EC:3.4.22.32), and chloroauric trihydrate (HauCl4.3H2O). were supplied by Sigma-Aldrich (St. Louis, USA). Only analytical-grade reagents were used, as all materials mentioned had sufficient purity for quantitative chemical analysis. De-ionized water was utilized for all laboratory and reaction requirements.

AuNPs and Br-AuNPs preparation

A gold stock solution was prepared by boiling 0.1 mM of aqueous HAuCl4.3H2O, then 1% trisodium citrate was added, and the solution was left to develop the red nanoparticle solution (Abeed et al., 2023). Then bromelain was added to AuNPs at a ratio of 1:5 v/v, meaning that for every milliliter of bromelain, 5 mL of gold solution was added (Ali et al., 2024).

Preparation of the carbon tetrachloride solution

To produce the solution, 1 mL of concentrated pure CCl4 was diluted with 3 mL of olive oil in a glass beaker. The mixture was then thoroughly combined and was stored at room temperature until further utilization within two days (Abeed and Al-Shmgani, 2024).

Experimental design and animals

The study involved 35 male albino mice, *Mus musculus*, aged 8-10 weeks and weighing 26 ± 5 g, sourced from the Biotechnology Research Center at Al Nahrain University, Iraq. The animals were placed inside clean, sterilized breeding cages with a litter of sawdust in a well-ventilated room with a temperature ranging from 5 ± 25℃ and an average of 12 hours of light versus 12 hours of darkness. The mice were supplied with a standard diet, a commercially available rodent chow pellet providing approximately 3.9 kcal of metabolizable energy (ME) per gram and a crude protein (CP) content of 15%, in addition to drinking water. The cages (50×20×30) in the breeding room were cleaned and sterilized on a weekly schedule. The experiment was extended for four weeks. Animals were separated into five groups, seven in each. The first group (G1) was the control group, which received normal saline daily for 4 weeks. Mice in Group G2 were injected subperitoneally with 0.1 mL of CCl4 once a week at a concentration of 0.1 mL/100 g of body weight for four

weeks. Mice in Group G3 were given an oral dose of Au-NPs solution at 0.1 mL/100 g of body weight daily for four weeks. Group G4 received an injection of 0.1 mL of CCl4. After 60 minutes, the mice were given an oral dose of 300 mg/kg bromelain solution at a daily dose of 0.1 mL for four weeks, and mice in Group G5 were injected with 0.1 mL of CCl4. After 60 minutes, the mice received the oral dosage of 300 mg/kg Au-NPs bromelain for four weeks.

Histopathology and immunohistochemistry

The testis samples were fixed in formalin 10% for 48 hours and washed under running water. Several procedures for histological examinations were performed using the method of Stevens and Bancroft (2010). A MEIJI light microscope (Meiji Techno, Japan), equipped with a high-resolution digital camera (Canon), was utilized to capture images of the slides. Immunohistochemical staining for Ki-67 and Caspase-9 was conducted using immunohistochemical staining kits (DAKO, USA) in accordance with the manufacturer's instructions. Briefly, four mm-thick tissue sections were deparaffinized in xylene and hydrated through a graded ethanol series. Antigen retrieval was conducted using a high pH solution at 95°C in a water bath for 40 minutes. Endogenous peroxidase activity was inhibited by applying peroxide black and incubating for 10 minutes in a humid chamber. Subsequently, three drops of peroxide powder block were added and incubated for 10 minutes in a humid chamber. Following a 20-minute incubation with the primary antibody, the secondary antibody HRP was applied and incubated for a further 10 minutes. The slides were then counterstained with Mayer's hematoxylin for one minute, mounted with cover slides, and prepared for microscopic examination and scoring (Ali et al., 2024). Immunohistochemical changes in the testes were documented by staining intensity, which can be scored to identify changes in protein expression. These changes indicated how a substance (antigen) was distributed and its concentration within the tissue, categorized as no changes (0), mild (1), moderate (2), and severe (3). Grading was determined according to the following percentage ranges. Less than 30% changes from 0%, up to 30% changes (mild change), 30%-50% (moderate change), and more than 50% (severe change, Korany et al., 2019).

RESULTS

The paraffin section of the control testis exhibited normal-sized and well-structured seminiferous tubules, with intact basement membranes and a typical thickness of the epithelial germinal layer. The lumen was filled with spermatozoa, and the interstitial tissue appeared normal (Figure 1). Group G2, injected with CCl4, displayed vacuolation within the germinal epithelium lining the seminiferous tubules, along with mild cellular swelling of spermatogonia cells, and some figures of necrosis and vascular congestion were observed within the interstitial tissue (Figure 2). Additionally, Group G3 (animals injected with gold nanoparticles) exhibited marked hypertrophy of seminiferous tubules with normal testicular interstitium (Figure 3). The testis sample in the group treated with bromelain solution demonstrated hyperplasia of germinal epithelium (Figure 4). Group G5 treated with Au-NPs-Bromelain illustrated almost normal architecture with marked hypertrophy of seminiferous tubules associated with normal interstitial cells (Figure 5).

Immunohistochemical findings

Ki-67 immunohistochemical results

The immunodetection of the proliferation marker Ki-67 in the testis demonstrated intense (+3) staining, indicative of active spermatogenesis. However, a moderate level of Ki-67 staining (+2) was observed in the basal epithelium of seminiferous tubules in Group G2 treatment with CCl4. The expression of Ki-67 remained largely unchanged following exposure to AuNPs, with many cells continuing to exhibit strong Ki-67 staining, scored as +3. Group G4 had a weak score of +1. Ki-67 expression increased in the testicular germinal epithelium treated with AuNPs-Brom solution with a +2 score (Figure 6).

Caspase-9 immunohistochemical results

Immunohistochemical staining of caspase-9 in mice testes exhibited moderate positive staining results (+2) in the control group (G1), Group G3, and Group G5. In contrast, intense staining results (+3) were observed in Group G2 and Group G4 (Figure 7).

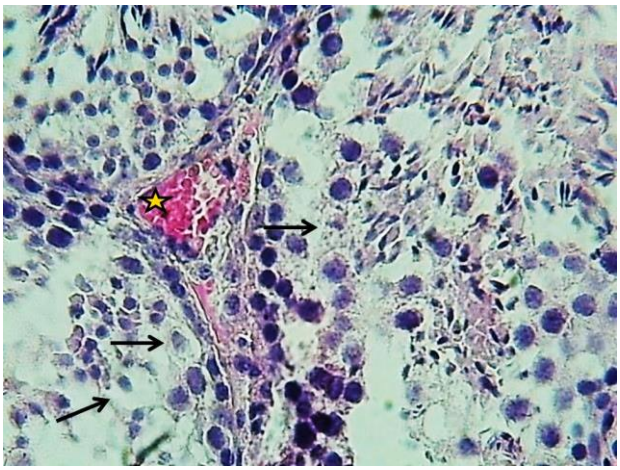


Figure 1. The testis section in male albino mice aged 8-10 weeks received normal saline. The control group with normal appearance of germinal epithelial cells (Asterisk) with normal testicular interstitial cells (Black arrow). H&E staining, 400x.

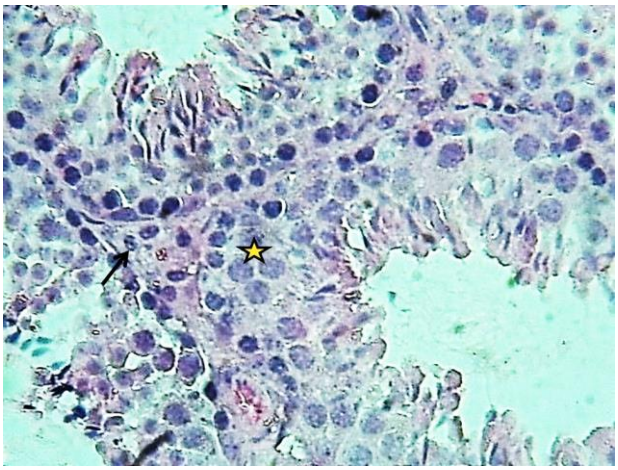


Figure 2. Testis section in male albino mice aged 8-10 weeks treated with Carbon tetrachloride. Group G2 with Mild cellular swelling of spermatogium cells with some figures of necrosis (Arrows) and vascular congestion of interstitial tissue (Asterisk). H&E staining, 400x.

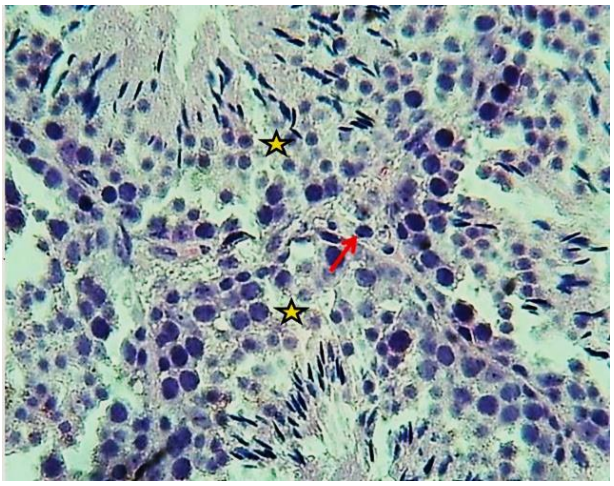


Figure 3. Testis section in male albino mice aged 8-10 weeks treated with gold nanoparticle solution for four weeks. Group G3 with normal appearance of germinal epithelial cells (Asterisks) with normal testicular interstitial cell (Arrow). H&E staining, 400x.

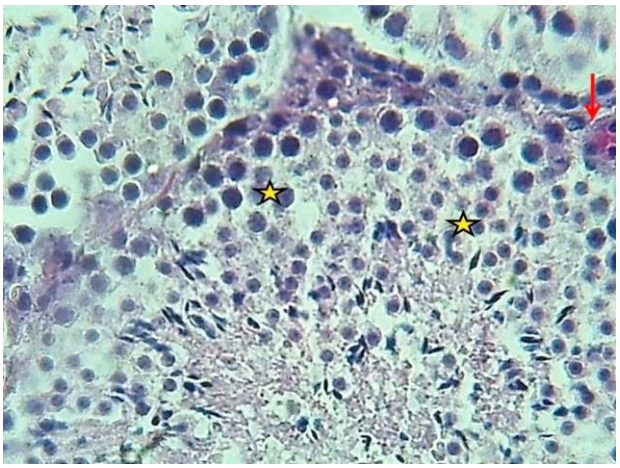


Figure 4. Testis section in male albino mice aged 8-10 weeks treated with Carbon tetrachloride. In group G4, after 60 minutes, the mice were given an oral dose of 300 mg/kg bromelain solution, marked hyperplasia of germinal epithelium (Asterisks) with congestion of interstitial blood vessels (Arrow). H&E staining, 400x.

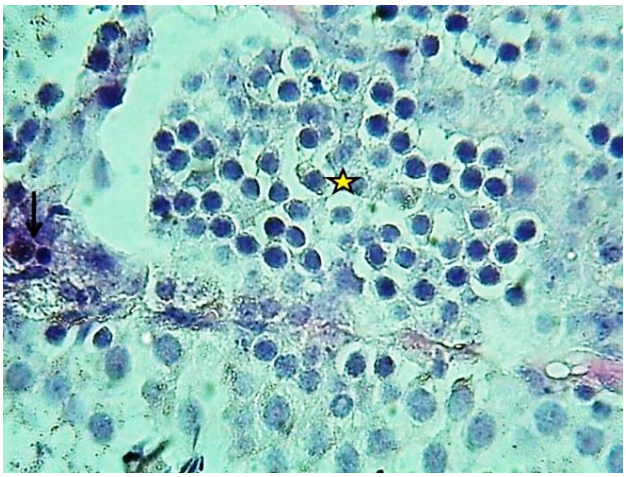


Figure 5. Testis section in adult mice treated with Carbon tetrachloride with marked hyperplasia of germinal epithelium (Asterisks). After 60 minutes, the mice received the oral dosage of 300 mg/kg gold nanoparticles bromelain for 4 weeks interstitial cells (Arrow). H&E staining, 400x.

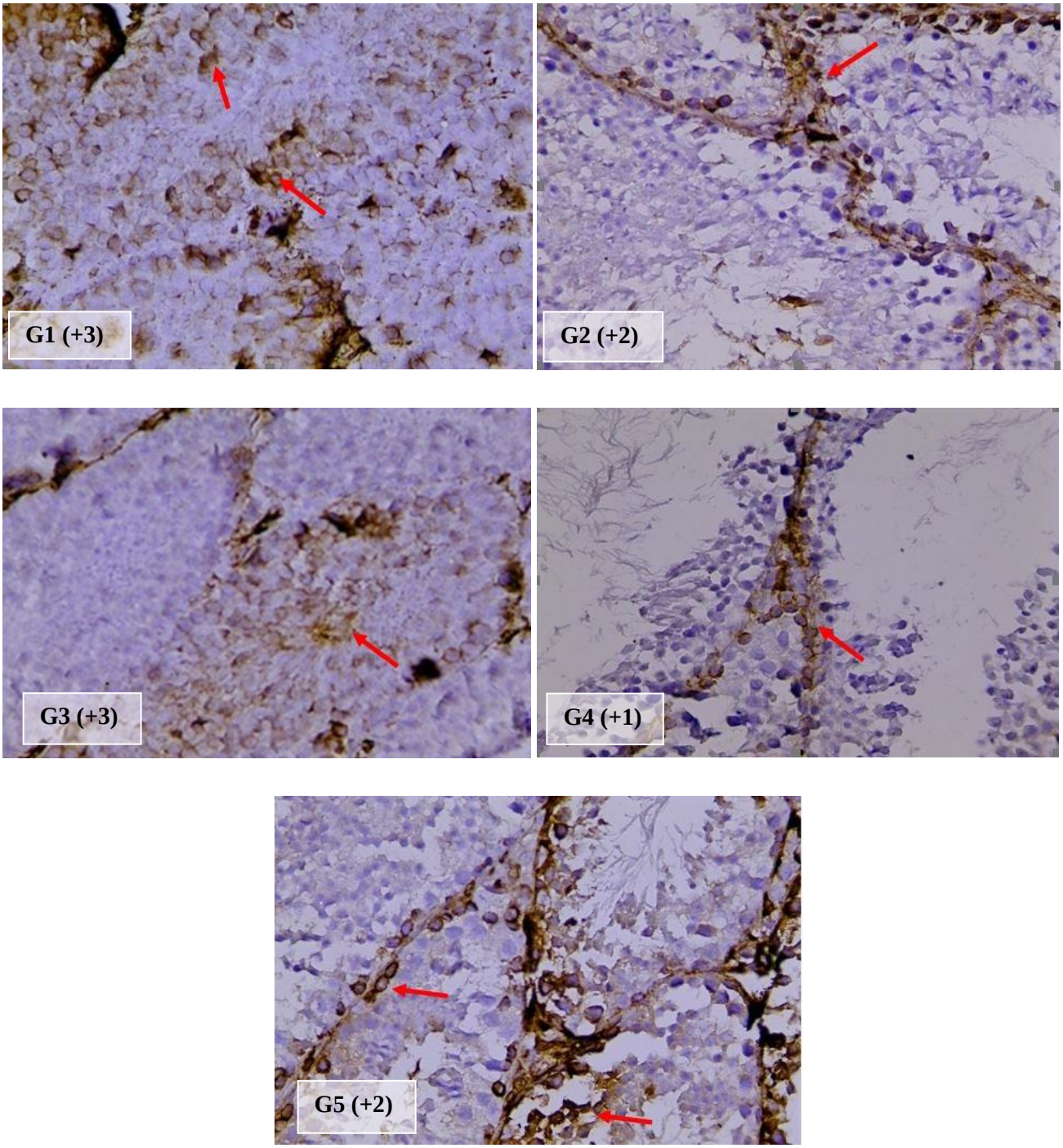


Figure 6. Adult mice (*Mus musculus*) testis scoring with immunohistochemistry staining. The control group (**G1)** illustrates a strongly positive expression of Ki-67 (+3, Red arrow), **G2** shows a slight positive expression of Ki-67 (+2, Red arrow), **G3** exhibits a severe positive expression of Ki-67 (+3, Red arrow), **G4** shows a weak positive expression of Ki-67 (+1, Red arrow), and **G5** exhibits a moderate positive expression of Ki-67 (+2, Red arrow, IHC, 40X).

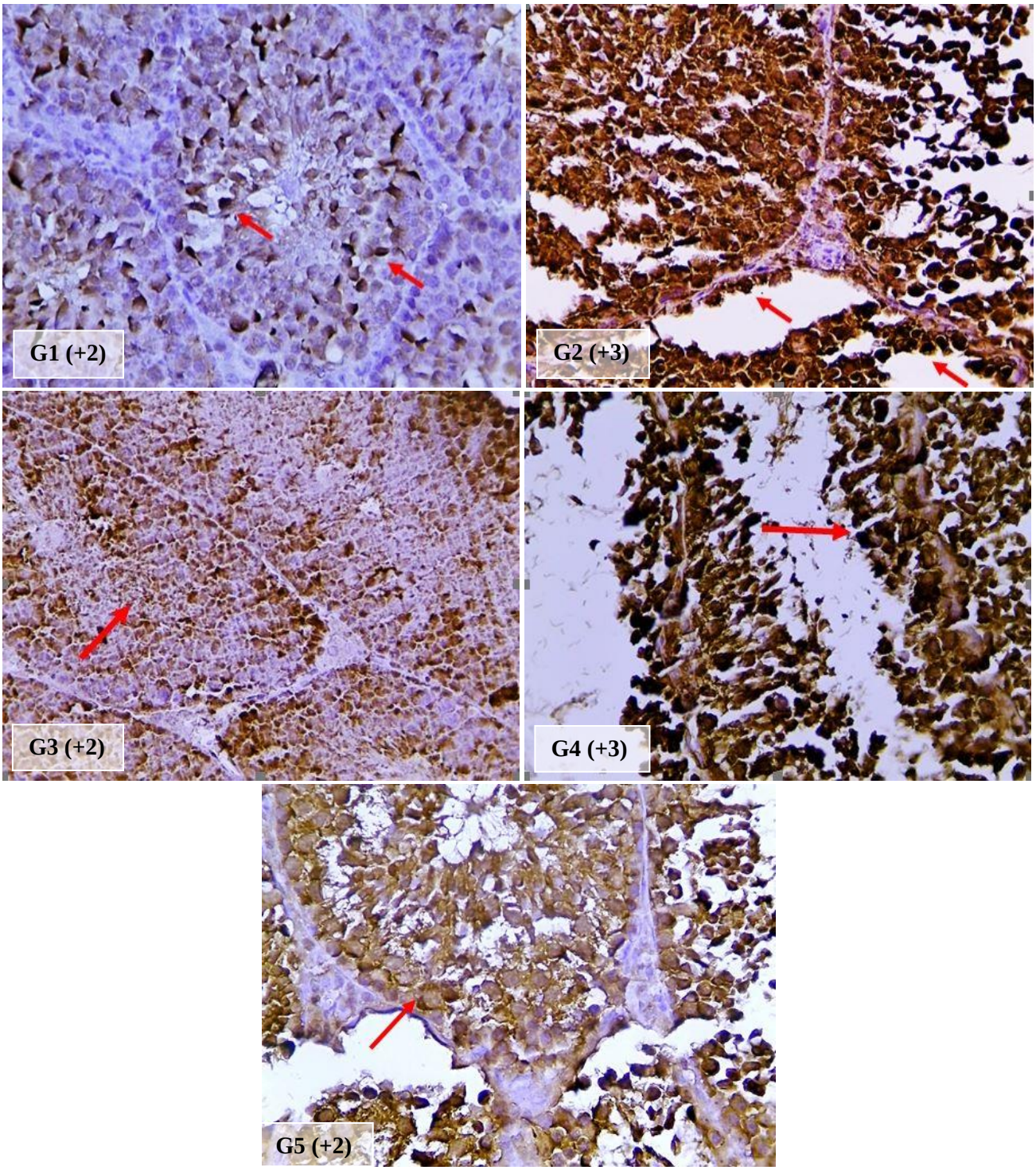


Figure 7. Adult mouse testis (*Mus musculus*) with immunohistochemistry staining. Control group (**G1)** shows a slight positive expression of expression of caspase-9 (+2, Red arrow), **G2** illustrates a strongly positive expression of caspase-9 (+3 Red arrow), **G3** exhibits a moderate positive expression caspase-9 (+2, Red arrow), **G4** shows a severe positive expression caspase-9 (+3 Red arrow), and **G5** illustrates a moderate positive expression of caspase-9 (+2, Red arrow, IHC, 40X).

DISCUSSION

Histological examination revealed abnormalities in the testicular structure of the CCl4 group. Mice treated with gold nanoparticles had no substantial protective effect, whereas animals treated with bromelain exhibited slight improvements in histological structure. Meanwhile, animals treated with bromelain loaded with gold nanoparticles demonstrated a more protective effect on testicular tissue, exhibiting regular seminiferous tubules, a normal interstitial space, occasional hemorrhages, and a germinal epithelium containing cells in the spermatogenesis stage that were similar to those in the control. According to the current results, CCl4 injection caused slight hyperplasia in the germinal epithelial cells and

congestion in the interstitial tissue. These findings are in agreement with a study of Gülhan et al. (2023), who demonstrated that CCl4 caused seminiferous tubule atrophy, degeneration, basal membrane separation, and an increase in interstitial space in rat testes. Another study reported that CCl4 reduced the number of spermatogonia, primordial spermatocytes, Sertoli cells, and interstitial cells (Eljaafari et al., 2024). The alterations in testicular histology during the present study indicated the toxic effects of CCl4. The CCl4 itself is not toxic but is metabolized by cytochrome P450 enzymes in the body into the free radical CCl3 and other metabolites (Cohen et al., 2023). Since CCl4 rapidly diffuses through tissues after absorption, especially tissues rich in lipids (Abu et al., 2022), it may negatively affect the testes, which contain high amounts of polyunsaturated fatty acids (Tran et al., 2017). Hashem (2021) found that free radicals produced by CCl4 may directly induce male infertility or indirectly cause reproductive failure by disrupting male hormone balance (Dutta et al., 2021). Another study conducted by Azouz et al. (2023) indicated that the testis is naturally vulnerable to oxidative stress due to its high content of unsaturated fatty acids, which are prone to damage and produce reactive oxygen species (ROS). Elevated ROS levels can impair testicular function and cause oxidative damage. The conjugation of bromelain with gold nanoparticles protected testicular tissue against CCl4 toxicity by integrating bromelain's antioxidant and anti-inflammatory properties with the unique conductivity of gold nanoparticles. This combination functioned synergistically to enhance cellular function by modulating ROS levels and restoring normal tissue structure (Abeed and Al-Shmgani, 2024; Hosseinpour et al., 2025). Additionally, bromelain can enhance the production of inflammatory mediators such as interleukin (IL)-1β, IL-6, interferon (IFN)-γ, and tumor necrosis factor (TNF)-α by immune cells, including mouse macrophages (Rathnavelu et al., 2016). Studies on the toxicological impact of AuNPs on male reproductive health have indicated contradictory results. A study of Li et al. (2012) found that intravenous or intraperitoneal injection of AuNPs did not affect sperm quality, spermatogenesis, or fertility. Conversely, another study suggested that AuNPs might reduce the ability of sperm to fertilize *in vitro* (Das et al., 2016). The current study found that AuNPs did not affect testicular structure. Animals treated only with bromelain showed minor improvements in testicular histology, whereas those treated with a conjugate of bromelain and gold nanoparticles exhibited a more notable protective effect against CCl4 toxicity.

The Ki-67 protein is a DNA-binding protein that is strongly associated with cellular proliferation. Its expression correlates with the rate of proliferation. It is expressed during all active phases of the cell cycle but is absent in resting cells. Therefore, levels of Ki-67 protein expression in the testis are conventionally utilized as a marker of spermatogenic cell proliferation and can be employed to evaluate the status of spermatogenesis (Zhao et al., 2018). In the current study, Ki-67 immunostaining revealed the expected pattern of cellular proliferation in the testes of the control group, but was remarkably decreased in the CCl4 group. It is well known that CCl4's harmful effects are the result of excessive ROS generation (Eljaafari et al., 2024). Increased ROS formation, resulting from both internal and external stimuli, can lead to oxidative stress, which alters the structure and function of phospholipids and proteins. The ROS attack DNA in the nucleus, fragmenting it and triggering apoptosis, which consequently alters gene and protein expression. Additionally, endogenous ROS can function as second messengers in regulating cell signaling pathways and transmitting signals crucial for controlling spermatogonia self-renewal and proliferation, which suggests a potential impact of ROS on the nuclear proliferation protein Ki-67 (Juárez-Rojas et al., 2022). The AuNPs solution did not cause notable changes in Ki-67 expression, while Ki-67 levels were lower in the group treated only with bromelain. This may be due to hypoplasia and degeneration of the germinal epithelium caused by CCl4. Regarding the conjugation of bromelain and AuNPs, immunohistochemistry results indicated an increase in Ki-67 expression. This increase may be attributed to bromelain’s protective properties and nanoparticles' tremendous advantages for absorbing medications (Chakraborty et al., 2021). Previous results have demonstrated that bromelain reduces the adverse effects of oxidative stress on the male reproductive system by increasing sperm count, normalizing sperm morphology, and elevating testosterone levels (Khazaeel et al., 2022), which may also influence Ki-67 expression. The immunohistochemistry analysis in the present study revealed different levels of positive caspase-9 expression in mouse testis tissue sections, with a score of +2 for the control group and scores ranging from +2 to +3 for the different treatment groups. Apoptosis, or programmed cell death, is an essential mechanism in the normal growth and function of the mouse testis, as it regulates the number of germ cells during spermatogenesis. During spermatogenesis, a significant number of germ cells undergo apoptosis. Several variables influence spermatogenesis, including hormonal balance, developmental stage, and specific stages within the spermatogenic cycle (Dunkel et al., 1997). Testis tissue sections in the group treated with CCL4 indicated increased Caspase-9 immunoexpression, reaching a score of +3. The CCL4 metabolization produces ROS, which can cause apoptosis, autophagy, inflammation, and other pathogenic phenomena, and the mitochondrial pathway plays a significant role in CCl4-induced apoptosis (Zhou et al., 2022). The ROS disrupts mitochondrial membrane potential and alters the interactions of pro- and anti-apoptotic proteins, leading to germ cell death (El-Wakf et al., 2020). In response to mitochondrial stress, cytochrome C is generated, which activates caspases-3 and -9, leading to apoptosis (Wang, 2015) and potentially affecting the immunohistochemical expression of caspase-9. The current study indicated that there were

no considerable differences in the expression of caspase-9 in mice that received an oral dose of Au-NP solution, compared to the control group. Several studies have investigated the correlation between bromelain and apoptosis; however, the results have been inconsistent. Scientists have demonstrated that bromelain induces apoptosis by activating caspase-dependent apoptotic pathways in cancer cells (Chang et al., 2019). The present study demonstrated that bromelain decreased caspase-9 expression by lowering its score, which was in accordance with the findings of Rathnavelu et al. (2016), who reported that bromelain reduced apoptosis and protected cells from damage. One potential explanation is that bromelain enhances the production of pro-apoptotic proteins, leading to the release of cytochrome C from the mitochondria and the activation of the mitochondrial apoptosis pathway (Rathnavelu et al., 2016). Alternatively, it inhibits the generation of inflammatory cytokines, which can lead to cell death and an inflammatory environment (Bahar et al., 2024). In a study, bromelain has been identified to activate caspases in some cases, but it may downregulate or inhibit caspase-9 in other situations (Bhui et al., 2009).

CONCLUSION

The current results suggested that conjugating bromelain with gold nanoparticles at a dosage of 300 mg/kg may effectively reduce CCl4 toxicity by repairing the natural antioxidant defense system, enhancing protein function, increasing cell proliferation, and preventing programmed cell death, as well as improving histological structure following pathological exposure. The efficacy of Au-NPs-Bromelain was more effective in the repair of testicular damage than the single administration of bromelain. Further studies are needed to fully understand the interaction between bromelain and caspase-9 in different cell types.

DECLARATIONS

Funding

The present study has not been supported financially.

Availability of data and materials

The data that support the findings of this study are available from the corresponding author upon reasonable request.

Acknowledgments

The authors wish to express their gratitude to the Department of Biology, College of Education for Pure Sciences/Ibn Al-Haitham, University of Baghdad, as well as to the staff of the Biotechnology Research Center at Al Nahrain University for providing facilities and their assistance throughout the present study.

Authors' contributions

Saddama Saed Faraj and Rana Hanan Khudhair Al-Rubaye conceived and planned the experiments. Baydaa Hussain Mutlak conducted the preparation of gold nanoparticles and the immunohistochemical study. Entidhar Mohammed Mnati reviewed and documented the histological results. All authors participated in the experiments and contributed to the interpretation of the results. Baydaa Hussain Mutlak assumed the lead in the manuscript preparation. All authors provided critical feedback, read, and approved the final edition of the manuscript.

Competing interests

The authors declared no conflict of interest concerning the publication of this manuscript.

Ethical considerations

All authors contributed to the preparation of this original paper. This article was originally written by the authors and has not been published elsewhere. All authors checked the text of the article and confirmed that the article is written based on their original scientific results and they never used the AI tools during this study.

REFERENCES

Abeed BS and Al-Shmgani HA (2024). Evaluation of the potential protective role of Galangin associated with gold nanoparticles in the histological and functional structure of testis of adult male albino mice administered with carbon tetrachloride. Baghdad Science Journal, 21(8): 17. DOI: https://www.doi.org/10.21123/bsj.2024.9086

Abeed BS, Al-Shmgani HS, Khalil KA, and Mohammed HA (2023). Histological and biochemical effects of Galangin conjugated gold nanoparticles

on the kidneys damage induced by carbon tetrachloride of adult male Albino mice. Ibn AL-Haitham Journal for Pure and Applied Sciences, 36(3): 72-84. Available at: https://jih.uobaghdad.edu.iq/index.php/j/article/view/3250

Abu OD, Iyare HE, and Ogboi KU (2022). Cardiac oxidative status in CCl4-exposed rats treated with extracts of *Dialium guineense* stem bark. Global Journal of Scientific Frontier Research, 22(B1): 37-42. Available at: https://journalofscience.org/index.php/GJSFR/article/view/102574

Ali HI, Mutlak BH, Alshareef SA, and Alhuwaymil Z (2024). Effect of CCl4 on renal tissues of male mice and prevented by pretreatment with bromelain loaded with gold nanoparticles: Histopathological and Caspase-9 expression alterations. Trends in Sciences, 21(12): 8358. DOI: https://www.doi.org/10.48048/tis.2024.8358

Asadi A, Ghahremani R, Abdolmaleki A, and Rajaei F (2021). Role of sperm apoptosis and oxidative stress in male infertility: A narrative review. International Journal of Reproductive Biomedicine, 19(6): 493-504. DOI: https://www.doi.org/10.18502/ijrm.v19i6.9371

Azouz RA, Korany RM, and Noshy PA (2023). Silica nanoparticle–induced reproductive toxicity in male albino rats via testicular apoptosis and oxidative stress. Biological Trace Element Research, 201(4): 1816-1824. DOI: https://www.doi.org/10.1007/s12011-022-03280-w

Bahar R, Chegeni MJ, Tahvildari A, Sani M, Khakpour Y, Hashemabady M, Sagharichi M, Balaghirad N, Taghizadeh M, Mehranpour M et al. (2024). Bromelain decreases oxidative stress and Neuroinflammation and improves motor function in adult male rats with cerebellar Ataxia induced by 3-acetylpyridine. Neuropeptides, 107: 102455. DOI: https://www.doi.org/10.1016/j.npep.2024.102455

Bhui K, Prasad S, George J, and Shukla Y (2009). Bromelain inhibits COX-2 expression by blocking the activation of MAPK regulated NF-kappa B against skin tumor-initiation triggering mitochondrial death pathway. Cancer Letters, 282(2): 167-176. https://www.doi.org/10.1016/j.canlet.2009.03.003

Brito AMM, Oliveira V, Icimoto MY, and Nantes-Cardoso IL (2021). Collagenase activity of bromelain immobilized at gold nanoparticle interfaces for therapeutic applications. Pharmaceutics, 13(8): 1143. DOI: https://www.doi.org/10.3390/pharmaceutics13081143

Chakraborty AJ, Mitra S, Tallei TE, Tareq AM, Nainu F, Cicia D, Dhama K, Emran TB, Simal-Gandara J, and Capasso R (2021). Bromelain a potential bioactive compound: A comprehensive overview from a pharmacological perspective. Life, 11(4): 317. DOI: https://www.doi.org/10.3390/life11040317

Chang TC, Wei PL, Makondi PT, Chen WT, Huang CY, and Chang YJ (2019). Bromelain inhibits the ability of colorectal cancer cells to proliferate via activation of ROS production and autophagy. PloS One, 14(1): e0210274-e0210292. DOI: https://www.doi.org/10.1371/journal.pone.0210274

Cohen SM, Bevan C, Gollapudi B, and Klaunig JE (2023). Evaluation of the carcinogenicity of carbon tetrachloride. Journal of Toxicology and Environmental Health, Part B, 26(6): 342-370. DOI: https://www.doi.org/10.1080/10937404.2023.2220147

Das J, Choi YJ, Song H, and Kim JH (2016). Potential toxicity of engineered nanoparticles in mammalian germ cells and developing embryos: Treatment strategies and anticipated applications of nanoparticles in gene delivery. Human Reproduction Update, 22(5): 588-619. DOI: https://www.doi.org/10.1093/humupd/dmw020

Dunkel L, Hirvonen V, and Erkkilä K (1997). Clinical aspects of male germ cell apoptosis during testis development and spermatogenesis. Cell Death & Differentiation, 4(3): 171-179. Available at: https://www.nature.com/articles/4400234

Dutta S, Sengupta P, Slama P, and Roychoudhury S (2021). Oxidative stress, testicular inflammatory pathways, and male reproduction. International Journal of Molecular Sciences, 22(18): 10043. DOI: https://www.doi.org/10.3390/ijms221810043

Eljaafari H, Mabrouk ZE, Mohamed F, Tunsi H, and Sasi SM (2024). Carbon tetrachloride-induced testicular toxicity and histopathological alteration in male Swiss Albino mice. AlQalam Journal of Medical and Applied Sciences, 7(1): 36-43. Available at: https://journal.utripoli.edu.ly/index.php/Alqalam/article/view/450

El-Wakf AM, El-Habibi ESM, Ali DA, Abd El-Ghany E, and Elmougy R (2020). Marjoram and sage oils protect against testicular apoptosis, suppressed Ki-67 expression and cell cycle arrest as a therapy for male infertility in the obese rats. Journal of Food Biochemistry, 44(1): e13080. DOI: https://www.doi.org/10.1111/jfbc.13080

Gülhan B, Taşlidere E, Vardi N, TAŞLIDERE A, and Elbe H (2023). Protective effects of caffeic acid phenethyl ester against carbon tetrachloride-induced testicular damage in rats: A histological study. Namık Kemal Medical Journal, 11(1): 17-21. DOI: https://www.doi.org/10.4274/nkmj.galenos.2023.82474

Hashem AS (2021). Defensive impact of propolis against CCl4 actuated rats' testicular damage. Journal of Advanced Veterinary and Animal Research, 8(1): 70-77. DOI: http://www.doi.org/10.5455/javar.2021.h487

Hosseinpour M, Dalband AM, Lajevardi Z, SoltanattarA, Tafazolimoghadam A, Karamian A, Abdollahifar MA, Abbaszadeh HA, Hodaeipour M, Charmchi A et al. (2025). The protective effect of bromelain on testicular dysfunction and oxidative stress induced by REM sleep deprivation in adult male rats. Tissue and Cell, 95: 102927. DOI: https://www.doi.org/10.1016/j.tice.2025.102927

Juárez-Rojas L, Casillas F, López A, Betancourt M, Ommati MM, and Retana-Márquez S (2022). Physiological role of reactive oxygen species in testis and epididymal spermatozoa. Andrologia, 54(4): e14367. DOI: https://www.doi.org/10.1111/and.14367

Kansakar U, Trimarco V, Manzi M V, Cervi E, Mone P, and Santulli G (2024). Exploring the therapeutic potential of bromelain: Applications, benefits, and mechanisms. Nutrients, 16(13): 2060-2079. DOI: https://www.doi.org/10.3390/nu16132060

Khazaeel K, Rad OR, Jamshidian J, Tabandeh MR, Mohammadi G, and Atashfaraz A (2022). Effect of bromelain on sperm quality, testicular oxidative stress and expression of oestrogen receptors in BISPHENOL-A treated male mice. Andrologia, 54(11): e14584. DOI: https://www.doi.org/10.1111/and.14584

Korany RM, Ahmed KS, Halawany HA, and Ahmed KA (2019). Effect of long-term arsenic exposure on female Albino rats with special reference to the protective role of Spirulina platensis. Exploratory Animal and Medical Research, 9(2): 125-136. Available at: https://doaj.org/article/4cde25e3d25d44bda753cb0365949e5d

Li WQ, Wang F, Liu ZM, Wang YC, Wang J, and Sun F (2012). Gold nanoparticles elevate plasma testosterone levels in male mice without affecting fertility. Small, 9(9-10): 1708-1714. DOI: https://www.doi.org/10.1002/smll.201201079

Menon SS, Guruvayoorappan C, Sakthivel KM, and Rasmi RR (2019). Ki-67 protein as a tumour proliferation marker. Clinica Chimica Acta, 491: 39-45. DOI: https://www.doi.org/10.1016/j.cca.2019.01.011

Rahmouni F, Daoud S, and Rebai T (2019). Teucrium polium attenuates carbon tetrachloride-induced toxicity in the male reproductive system of rats. Andrologia, 51(2): e13182. DOI: https://www.doi.org/10.1111/and.13182

Rajkumar M, Davis Presley SI, Thiyagarajulu N, Girigoswami K, Janani G, Kamaraj C, Madheswaran B, Prajapati B, Ali N, and Rashid Khan M (2025). Gelatin/PLA-loaded gold nanocomposites synthesis using Syzygium cumini fruit extract and their antioxidant, antibacterial, anti-inflammatory, antidiabetic and anti-Alzheimer's activities. Scientific Reports, 15(1): 2110. DOI: https://www.doi.org/10.1038/s41598-024-84098-5

Rathnavelu V, Alitheen NB, Sohila S, Kanagesan S, and Ramesh R (2016). Potential role of bromelain in clinical and therapeutic applications. Biomedical Reports, 5(3): 283-288. DOI: https://www.doi.org/10.3892/br.2016.720

Rohmah A, Prabowo H A, Setiasih S, Handayani S, Jufri M, and Hudiyono S (2021). The evaluation of activity and stability of isolated bromelain from pineapple cores (*Ananas comosus* [L.] Merr) and *in vitro* penetration test of nanoemulsion topical base. International Journal of Applied Pharmaceutics, 13(5): 336-342. DOI: https://www.doi.org/10.22159/ijap.2021v13i5.41769

Sherry D, McCulloch A, Liang Q, Reimann S, and Newman PA (2018). Current sources of carbon tetrachloride (CCl4) in our atmosphere. Environmental Research Letters, 13(2): 024004. DOI: https://www.doi.org/10.1088/1748-9326/aa9c87

Sönmez M, Türk G, Çeribaşı S, Çiftçi M, Yüce A, Güvenç M, Özer Kaya S, Çayand M, and Aksakal M (2014). Quercetin attenuates carbon tetrachloride-induced testicular damage in rats. Andrologia, 46(8): 848-858. DOI: https://www.doi.org/10.1111/and.12159

Stevens A and Bancroft JD (2010). Theory and practice of histological techniques. Churchill Livingston., London, pp. 174-176. Available at: https://www.google.iq/books/edition/Theory_and_Practice_of_Histological_Tech/Dhn2KispfdQC?hl=ar&gbpv=1&dq=Theory+and+Practice+of+Histological+Techniques&printsec=frontcover

Tran LV, Malla BA, Kumar S, and Tyagi AK (2017). Polyunsaturated fatty acids in male ruminant reproduction-a review. Asian-Australasian Journal of Animal Sciences, 30(5): 622-637. DOI: https://www.doi.org/10.5713/ajas.15.1034

Unsal V, Cicek M, and Sabancilar İ (2021). Toxicity of carbon tetrachloride, free radicals and role of antioxidants Reviews on Environmental Health, 36(2): 279-295. DOI: https://www.doi.org/10.1515/reveh-2020-0048

Varilla C, Marcone M, Paiva L, and Baptista J (2021). Bromelain, a group of pineapple proteolytic complex enzymes (*Ananas comosus*) and their possible therapeutic and clinical effects. A summary. Foods, 10(10): 2249. DOI: https://www.doi.org/10.3390/foods10102249

Wang K (2015). Autophagy and apoptosis in liver injury. Cell Cycle, 14(11): 1631-1642. DOI: https://www.doi.org/10.1080/15384101.2015.1038685

Yakut S, Karabulut M, Koca RH, Erbaş E, Özkanlar S, Gençer BT, Kara A, and Kumar KSJ (2025). Protective effects of bromelain in testicular torsion-detorsion: Reducing inflammation, oxidative stress, and apoptosis while enhancing sperm quality. Biomolecules, 15(2): 292. DOI: https://www.doi.org/10.3390/biom15020292

Yu W, Zhu H, Huang R, Yan B, Xu B, Shi Y, Mao J, Liu Z, and Wang J (2024). Roles of cyt-c/caspase-9/caspase-3/bax/bcl-2 pathway in cd-induced testicular injury in rats and the protective effect of quercetin. Toxicon, 237(3): 107561. DOI: https://www.doi.org/10.1016/j.toxicon.2023.107561

Zhao WP, Wang HW, Liu J, Tan PP, Luo XL, Zhu SQ, Chen XL, and Zhou BH (2018). Positive PCNA and Ki-67 expression in the testis correlates with spermatogenesis dysfunction in fluoride-treated rats. Biological Trace Element Research, 186(1): 489-497. DOI: https://www.doi.org/10.1007/s12011-018-1338-6

Zhou C, Liu A, Liu G, Yang C, Zhou Q, Li H, Yang H, Yang M, Li G, Si H et al. (2022). Protective effects of *Sophorae tonkinensis* Gagnep. (Fabaceae) Radix et Rhizoma water extract on carbon tetrachloride-induced acute liver injury. Molecules, 27(24): 8650. DOI: https://www.doi.org/10.3390/molecules27248650

Publisher's note: Scienceline Publication Ltd. remains neutral with regard to jurisdictional claims in published maps and institutional affiliations.

Open Access: This article is licensed under a Creative Commons Attribution 4.0 International License, which permits use, sharing, adaptation, distribution and reproduction in any medium or format, as long as you give appropriate credit to the original author(s) and the source, provide a link to the Creative Commons licence, and indicate if changes were made. The images or other third party material in this article are included in the article's Creative Commons licence, unless indicated otherwise in a credit line to the material. If material is not included in the article's Creative Commons licence and your intended use is not permitted by statutory regulation or exceeds the permitted use, you will need to obtain permission directly from the copyright holder. To view a copy of this licence, visit https://creativecommons.org/licenses/by/4.0/.
© The Author(s) 2025

2025, Scienceline Publication
World's Veterinary Journal
World Vet J, 15(4): 1095-1100.
ISSN 2322-4568
DOI: https://dx.doi.org/10.54203/scil.2025.wvj111
PII: S232245682500111-15

Effects of Bitter Melon (*Momordica charantia*) Extract on Glucose Transporters 2 and 4 Levels in Streptozotocin-induced Hyperglycaemic Rats

Dahlia Putri[1], Iwan Harjono Utama[2], I Ketut Suatha[3], I Gusti Ayu Agung Suartini[2], Hamong Suharsono[2], I Nyoman Mantik Astawa[4], Anak Agung Sagung Kendran[5], and I Nyoman Suarsana[2]*

[1]*Student of Faculty of Veterinary Medicine, Udayana University, Bali, 80234, Indonesia*
[2]*Department of Biochemistry, Faculty of Veterinary Medicine, Udayana University, Bali, 80234, Indonesia*
[3]*Department of Anatomy, Faculty of Veterinary Medicine, Udayana University, Bali, 80234, Indonesia*
[4]*Department of Immunology, Faculty of Veterinary Medicine, Udayana University, Bali, 80234, Indonesia*
[5]*Department of Clinical Diagnose, Clinical Pathology, and Radiology, Faculty of Veterinary Medicine, Udayana University, Bali, 80234, Indonesia*

*Corresponding author's Email: suarsana65@unud.ac.id

SHORT COMMUNICATION
Received: September 29, 2025
Revised: October 25, 2025
Accepted: November 28, 2025
Published: December 31, 2025

ABSTRACT

Glucose transporters (GLUTs) are essential for regulating glucose metabolism, with GLUT2 and GLUT4 serving as the primary transporters in muscle cells. In diabetic conditions, oxidative stress caused by free radicals damages glucose uptake into cells. Bioactive compounds in bitter melon, including triterpenoids, charantin, and conjugated linoleic acid, have been shown to have hypoglycaemic effects. Therefore, the present study aimed to evaluate the effect of bitter melon extract (*Momordica charantia*) on blood glucose, GLUT2, and GLUT4 in streptozotocin-induced hyperglycemic rats. The present study involved 15 male Wistar rats (white strain), 2 months old, with an average body weight of 130 grams. Diabetes was induced by administering streptozotocin at a dose of 60 mg/kg body weight. The animals were divided into three treatment groups, including the diabetic control group (P0), the diabetic group treated with 50% weight/volume (w/v) bitter melon extract (P1), and the diabetic group treated with 100% (w/v) bitter melon extract (P2). The extract was given orally at a dosage of 1 ml per rat for 14 days. Blood glucose concentrations were determined using a glucometer, whereas serum GLUT2 and GLUT4 levels were quantified with an ELISA kit. The results indicated that treatment P2 significantly lowered blood glucose levels compared to the diabetic control group, decreasing from 414.60 mg/dL (P0) to 223.60 mg/dL (P2). Serum GLUT2 concentrations declined from 21.51 (P0) to 16.50 (P2), and GLUT4 levels decreased from 19.94 (P0) to 17.60 (P2). These changes suggested an adaptive response intended to restore glucose homeostasis. Based on the present results, 100% w/v bitter melon extract concentration demonstrated a significant reduction in blood glucose, GLUT2, and GLUT4 levels in the serum of streptozotocin-induced diabetic rats.

Keywords: Bitter melon, Diabetes mellitus, Hyperglycemia, Glucose transporter

INTRODUCTION

The increasing prevalence of diabetes mellitus is a significant and alarming threat to global health. The IDF (2021) reported that the worldwide number of individuals with diabetes mellitus has reached 537 million and is expected to rise to 643 million by 2030. Diabetes mellitus is characterized by chronic hyperglycemia resulting from impaired insulin secretion, action, or both (Antar et al., 2023). Hyperglycemia increases the amount of glucose in the glycolytic pathway, leading to increased production of free radicals, which heightens oxidative stress in cells. Persistent free radicals within cells also damage cellular macromolecules, including nucleic acids, lipids, and proteins (Rochette et al., 2014).

Glucose is a primary energy source for cellular activity in living organisms. However, due to its hydrophilic property, glucose transport across the cell membrane requires a specific carrier protein. Glucose transporters (GLUTs) are transmembrane proteins that facilitate the movement of glucose across cell membranes (Wang et al., 2020). Elevation of blood glucose level stimulates GLUT2 to transport glucose into β cells and trigger insulin secretion. Increased insulin promotes glucose uptake into muscle and adipose tissues by regulating GLUT4 translocation to the plasma membrane (Leto and Saltiel, 2012). Therefore, GLUT2 and GLUT4 play crucial roles in the progression of diabetes mellitus.

Diabetes mellitus treatment mainly focuses on managing blood glucose levels to prevent complications. However, prolonged use of synthetic antidiabetic medicines poses risks of side effects and toxicity (Wang et al., 2019). Therefore, finding safe, affordable, and effective alternative treatments is essential. One potential plant as an alternative treatment is bitter melon (*Momordica charantia*). Bioactive compounds in bitter melon, including triterpenoids, charantin, and

To cite this paper: Putri D, Utama IH, Suatha IK, Suartini IGAA, Suharsono H, Astawa INM, Kendran AAS, and Suarsana IN (2025). Effects of Bitter Melon (*Momordica charantia*) Extract on Glucose Transporters 2 and 4 Levels in Streptozotocin-induced Hyperglycaemic Rats. *World Vet. J.,* 15(4): 1095-1100. DOI: https://dx.doi.org/10.54203/scil.2025.wvj111

conjugated linoleic acid, have been shown to have their hypoglycaemic and antioxidant effects that reduce oxidative stress (Mahmoud et al., 2017; Liu et al., 2021). The reduction in oxidative stress may improve GLUT2 and GLUT4 translocation and regulation, thereby enhancing glucose uptake and homeostasis (Çiçek, 2022).

A previous study by Poovitha and Parani (2017) demonstrated that several compounds in bitter melon enhance GLUT4 translocation through the AMP-activated protein kinase (AMPK) pathway in muscle cells. Furthermore, Malekshahi et al. (2019) reported that bitter melon reduces the expression of GLUT2, leading to decreased glucose reabsorption in the kidneys and increased urinary glucose excretion. Nevertheless, studies investigating the influence of bitter melon on serum GLUT2 and GLUT4 levels in streptozotocin (STZ)-induced diabetic rat models are still scarce. Therefore, the present study aimed to assess the effects of bitter melon *(Momordica charantia*) extract on blood glucose, as well as serum GLUT2 and GLUT4 levels, in STZ-induced hyperglycemic rats.

MATERIALS AND METHODS

Ethical approval

Ethical approval for the present study was granted by the animal ethics committee of the Faculty of Veterinary Medicine, Udayana University, Bali, Indonesia (No. B/M.145/UN14.2.9/PT.01.04/2024). All experimental procedures were carried out in strict accordance with animal welfare principles.

Extract preparation

The extraction process was performed traditionally with a blender, incorporating the method outlined by Jenie and Indraswari (2021) with some modifications. Bitter melon samples were sourced from the Jimbaran traditional market in Badung Regency, Bali, Indonesia. The procedure began by selecting fresh, green fruits, which were then washed and sliced into small pieces. A total of 100 g (wet weight) of bitter melon was blended, and the resulting extract was filtered using cheesecloth and transferred into a volumetric flask. Distilled water was added to increase the volume to 100 mL, resulting in a 100% w/v solution concentration. To prepare a 50% w/v concentration, 50 mL of the 100% extract was diluted with distilled water to a final volume of 100 mL. The extracts at both 50% and 100% w/v concentrations were stored in clean bottles and refrigerated at 4°C to preserve their stability.

Animals and treatments

Fifteen males white Wistar rats, approximately 2 months old, with an average body weight of 130 g, were used in the current experiment. Wistar rats were divided into three treatment groups, each consisting of five rats with five repetitions. The experimental animals were fasted for 12 hours before being induced intraperitoneally with STZ (Merck KGaA, Germany) at a dose of 60 mg/kg body weight (Gavaher et al., 2022). Bitter melon extract was administered after the rats exhibited blood glucose levels reached 200 mg/dL (Furman, 2021). The extract was administered on day 7 post-STZ induction, with every group receiving the same amount of 1 mL doses/day orally. In the control group, the rats were given water without the extract (P0). In the P1 treatment group, the rats were given bitter melon extract at a 50% w/v concentration. In the P2 treatment group, the rats were given bitter melon extract at a 100% w/v concentration every day for 14 days of treatment. Serum collection was performed on day 14 post-treatment, followed by the sandwich ELISA method (Kohrain Biotech, China) to analyze the levels of GLUT2 and GLUT4 in the rat serum.

Measurement of glucose transporter concentration

For the GLUT2 and GLUT4 level analysis methods, the procedures listed on the ELISA Kit were used. Rat serum samples were analyzed using the rat glucose transporter 2 (GLUT2 ELISA Kit, E1058Ra, Zhejiang, China) and rat glucose transporter 4 (GLUT4 ELISA Kit, E0499Ra, Zhejiang, China) from the bioassay technology laboratory.

Sample processing

The sample collection began 14 days after the treatment; every rat was fully anesthetized using ketamine-HCl doses of 50 mg/kg body weight (Wellington et al., 2013). The blood samples were obtained from the orbital vein using a capillary pipette and collected into 3 mL plain Vacutainer tubes. The rats were subsequently euthanized by the cervical dislocation method. The collected blood was then centrifuged at 2000 rpm for 20 minutes. The serum samples were thereafter delivered to the Biochemistry Laboratory, Faculty of Medicine, Udayana University, Bali, Indonesia, for further analysis. Blood glucose levels were measured on day 0 before injection as baseline data, 7 days after STZ induction, and at 14 days after the treatment (end of the treatment). Blood glucose levels of the experimental rats were measured using a glucometer (Allmedicus, South Korea). The rats were categorized as diabetic when the blood glucose level reached a minimum of 200 mg/dL after STZ induction (Furman, 2021).

Statistical analysis

Blood glucose and GLUT2 and GLUT4 levels were analyzed by analysis of variance (ANOVA) using data processing software SPSS Statistics 26.0 (IBM, USA). For the significant values, post-hoc Duncan tests were performed. The data were presented as means ± standard deviation, and a p-value less than 0.05 was considered statistically significant.

RESULTS

The average results of blood glucose, GLUT2, and GLUT4 levels are presented in Table 1. Blood glucose levels differed significantly among the treatment groups ($p < 0.05$). The control group (P0) indicated the highest level of blood glucose (414.60 ± 17.67 mg/dL), followed by P1 (370.80 ± 19.60 mg/dL) and P2 (223.60 ± 12.52 mg/dL). This difference indicated that the administration of bitter melon extract at a 100% concentration (P2) significantly reduced blood glucose levels compared to the 50% concentration group (P1) and the control group.

Analysis of GLUT2 levels demonstrated that administration of 100% bitter melon extract (P2) resulted in a value of 16.50 ± 3.65, which was lower and significantly different ($p < 0.05$) compared to the control group (P0, 21.51 ± 3.31), but not significantly different compared to the P1 group (19.11 ± 3.3, $p > 0.05$). Meanwhile, the GLUT4 level in P2 was 17.6 ± 1.25, lower and significantly different ($p < 0.05$) compared to the P0 (19.94 ± 1.1), but not significantly different compared to P1 (18.97 ± 1.16, $p > 0.05$).

Table 1. Blood glucose, Glucose transporters 2 and 4 levels in rats after 14 days of treatment

Treatment	Blood glucose	Glucose transporters 2 (GLUT2)	Glucose transporters 4 (GLUT4)
P0	414.60 ± 17.67^{c}	21.51 ± 3.31^{b}	19.94 ± 1.10^{b}
P1	370.80 ± 19.60^{b}	19.11 ± 0.96^{ab}	18.97 ± 1.16^{ab}
P2	223.60 ± 12.52^{a}	16.50 ± 3.65^{a}	17.60 ± 1.25^{a}

^{a,b,c} Different superscript letters differ significantly ($p < 0.05$), and the values are presented as means ± standard deviation. P0: Diabetes control group; P1: Diabetes group received bitter melon extract 50% w/v; P2: Diabetes group received bitter melon extract 100% w/v.

DISCUSSION

The current results demonstrate that the administration of bitter melon extract in diabetic mellitus rats significantly reduced blood glucose levels, with a statistically significant difference compared to the positive control group. However, the blood glucose levels did not reach normal values (50-130 mg/dL) as reported by Hidayaturrahman et al. (2020). This blood glucose-lowering effect may be due to the active compounds in bitter melon, namely phenols and flavonoids (Rezaeizadeh et al., 2011). Several studies stated that secondary metabolites in bitter melon, including charantin, polypeptides, alkaloids, momordicin, flavonoids, and cucurbitane-type triterpenoids, play crucial roles in reducing blood glucose levels (Pahlavani et al., 2019; Xu et al., 2022).

One of the main types of saponins in bitter melon is triterpenoids, which are divided into two main types, oleanane and cucurbitane. According to Çiçek (2022), eight types of cucurbitane triterpenoids promote GLUT4 translocation in L6 myotubes and 3T3-L1 adipocytes by activating the AMPK pathway, thereby improving fatty acid oxidation and glucose uptake. The AMPK is an energy-sensing protein kinase activated by the phosphorylation of Thr172 on its catalytic α-subunit. The AMPK facilitates glucose uptake into cells independently of insulin signalling and Akt activation (Chang et al., 2021). The AMPK activation can occur through multiple mechanisms, including the canonical pathway regulated by the adenine nucleotide ratio, the non-canonical pathway involving binding at the AdaM site, and the Ca2+-dependent pathway mediated by Ca2+/calmodulin-stimulated protein kinase beta (CaMKKβ). A study conducted by Iseli et al. (2013) noted that triterpenoid compounds in bitter melon activate AMPK via the CaMKKβ pathway.

The bioactive compounds found in bitter melon play vital roles in reducing blood glucose levels. Specifically, charantin, which inhibits the α-glucosidase and α-amylase enzymes (Ahamad et al., 2019), whereas alkaloid compounds act through an insulin-like mechanism (Mahwish et al., 2023). Furthermore, the conjugated linoleic acid present in bitter melon enhances insulin sensitivity by promoting adipogenesis via lipoprotein lipase activation (Gadang et al., 2011). Bitter melon contains two main types of polypeptides, including P-insulin and peroxidase. P-insulin is a carbohydrate-binding protein that can help lower blood glucose levels, facilitating cell recognition and mediating adhesion reactions (Richter et al., 2023). This protein mimics insulin activity by binding to Insulin (INS) receptors. Meanwhile, peroxidase contributes to reducing oxidative stress and detoxifying peroxides by converting them into non-toxic substances. Xu et

al. (2022) further demonstrated that bitter melon extract remarkably increases pancreatic β-cell populations by regenerating and restoring partially damaged β-cells in STZ-induced diabetic rats.

Oxidative stress is a redox imbalance characterized by increased production and accumulation of free radicals, accompanied by impaired antioxidant function in cells or tissues (An et al., 2023). Free radicals play important roles in intracellular signalling, cell activity regulation, apoptosis induction, and immune responses. Additionally, free radicals stimulate inflammatory responses through protein kinase activation, transcription factor regulation, and the expression of pro-inflammatory genes (Darenskaya et al., 2021). Free radical-induced cell damage can lead to the release of intracellular substances into the bloodstream (González et al., 2023), including GLUT.

The current findings indicated that diabetic mellitus rats treated with bitter melon extract had lower serum levels of GLUT2 and GLUT4 compared to the control group. This mechanism may be due to the phenolic, flavonol, and flavonoid components in bitter melon, which act as antioxidants that bind to free radicals, inhibiting chain reactions and preventing further cell damage (Tan et al., 2016). Furthermore, bitter melon possesses antiglycation properties that prevent the formation of advanced glycation end-products (AGEs), which are key contributors to diabetic complications (Aljohi et al., 2016). Under hyperglycemic conditions, the elevated production of AGEs triggers the generation of free radicals and pro-inflammatory molecules, thereby disturbing the homeostasis of endothelial cells (An et al., 2023).

During the present study, the control group exhibited the highest levels of GLUT2 and GLUT4, possibly due to STZ triggering oxidative stress and lipid peroxidation, which led to hyperglycemia (Soliman, 2016). β-cells are particularly vulnerable to oxidative stress because they contain low concentrations of endogenous antioxidant enzymes, including catalase and glutathione peroxidase (Rochette et al., 2014). However, in the group receiving the bitter melon extract at a 100% concentration, the blood glucose levels, GLUT2, and GLUT4 demonstrated considerable decreases compared to the control group. This effect might be due to the incomplete β-cell destruction caused by STZ, allowing the antioxidant compounds in bitter melon extract to prevent further chain reactions of free radicals and cellular damage. The present findings aligned with those of Bortolotti et al. (2019), who demonstrated that the antioxidant properties of bitter melon function by alleviating oxidative stress, neutralizing free radicals, and preventing lipid peroxidation. By preventing cellular damage, intracellular substances such as GLUT remain preserved within the cells.

The release of GLUT into the bloodstream can affect the amount of glucose entering cells. The GLUT2 is a transporter protein that not only facilitates passive glucose transport into pancreatic β-cells but also functions as a glucose homeostasis sensor (Kahraman et al., 2015). When blood glucose levels increase, GLUT2 triggers insulin secretion (Berger and Zdzieblo, 2020). Insulin is released into the bloodstream, then binds to its receptor and promotes the translocation of insulin-sensitive GLUT4 to the cell membrane surface. At the cell surface, GLUT4 binds and fuses to form a channel, allowing glucose to enter the cell. Conversely, when there is no insulin stimulation, GLUT4 returns to the cytosol (Wang et al., 2020). Disruptions in GLUT2 and GLUT4 expression and function can prevent glucose from entering cells, leading to prolonged hyperglycemia. This condition can progress to diabetes-related complications such as vascular endothelial damage, hepatic impairment, diabetic ketoacidosis, diabetic retinopathy, diabetic nephropathy, and diabetic neuropathy (Ofuegbe et al., 2020; An et al., 2023).

CONCLUSION

The administration of bitter melon extract at a more optimal concentration of 100% can reduce blood glucose, GLUT2, and GLUT4 levels in STZ-induced diabetic rats. It is recommended to evaluate the effects of bitter melon administration on GLUT2 and GLUT4 levels using multipolar solvents. Additionally, future studies should consider measuring GLUT levels in different organs, such as the liver, pancreas, muscles, intestines, and brain.

DECLARATIONS

Availability of data and materials

All data supporting this study's findings are included within the article's materials, and no additional supporting datasets are available.

Authors' contributions

Dahlia Putri contributed to conducting the experiments, analyzing the data, and drafting the manuscripts. I Gusti Ayu Agung Suartini contributed to supervision, revised the manuscript, and validated it. I Nyoman Mantik Astawa, Hamong Suharsono, and Anak Agung Sagung Kendran contributed to the supervision and validation of the experiment and manuscript. I Nyoman Suarsana contributed to designing the research project, supervised the study procedure, revised the manuscript, and validated the manuscript. All authors read and approved the final edition of the manuscript.

Acknowledgements

The present study was supported by the Institute for Research and Community Service, Udayana University, Bali, Indonesia.

Competing interests

The authors declared no conflict of interest.

Fundings

The present study is part of the Skim Group Research Grant 2024, funded by the Institute for Research and Community Service, Udayana University, Indonesia.

Ethical considerations

The manuscript is original, and it has not been published elsewhere. All authors reviewed the original content of the manuscript. No AI tools was used during the study and writing the manuscript.

REFERENCES

Ahamad J, Mir SR, and Amin S (2019). Antihyperglycemic activity of charantin isolated from fruits of *Momordica charantia* linn. International Research Journal of Pharmacy, 10(1): 61-64. Available at: https://journals.indexcopernicus.com/api/file/viewByFileId/1009684

Gavaher MA, Babazadeh D, Sadeghi A, Hejazi V, Sasani F, Moshavery A, and Ahmadi Simab P (2022). Comparative assessment of portulaca oleracea, omega-3 fatty acids, and combination of selenium plus vitamin E on histopathology of pancreas in diabetic rats. Journal of Veterinary Physiology and Pathology, 1(1): 17-23. DOI: https://www.doi.org/10.58803/jvpp.v1i1.6

Aljohi A, Matou-Nasri S, and Ahmed N (2016). Antiglycation and antioxidant properties of Momordica charantia. PLOS ONE, 11(8): e0159985. DOI: https://www.doi.org/10.1371/journal.pone.0159985

An Y, Xu B, Wan S, Ma X, Long Y, Xu Y, and Jiang Z (2023). The role of oxidative stress in diabetes mellitus-induced vascular endothelial dysfunction. Cardiovascular Diabetology, 22: 237. Available at: https://cardiab.biomedcentral.com/articles/10.1186/s12933-023-01965-7

Antar SA, Ashour NA, Sharaky M, Khattab M, Ashour NA, Zaid RT, Roh EJ, Elkamhawy A, and Al-Karmalawy AA (2023). Diabetes mellitus: Classification, mediators, and complications; A gate to identify potential targets for the development of new effective treatments. Biomedicine & Pharmacotherapy, 168: 115734. DOI: https://www.doi.org/10.1016/j.biopha.2023.115734

Berger C and Zdzieblo D (2020). Glucose transporters in pancreatic islets. Pflügers Archiv - European Journal of Physiology, 472(9): 1249-1272. Available at: https://pmc.ncbi.nlm.nih.gov/articles/PMC7462922/pdf/424_2020_Article_2383

Bortolotti M, Mercatelli D, and Polito L (2019). *Momordica charantia*, a nutraceutical approach for inflammatory-related disease. Frontiers in Pharmacology, 10: 486. DOI: https://www.doi.org/10.3389/fphar.2019.00486

Çiçek SS (2022). *Momordica charantia* L.—diabetes-related bioactivities, quality control, and safety considerations. Frontiers in Pharmacology, 13: 904643. DOI: https://www.doi.org/10.3389/fphar.2022.904643

Chang CI, Cheng SY, Nurlatifah AO, Sung WW, Tu JH, Lee LL, and Cheng HL (2021). Bitter melon extract yields multiple effects on intestinal epithelial cells and likely contributes to anti-diabetic functions. International Journal of Medical Sciences, 18(8): 1846-1856. DOI: https://www.doi.org/10.7150/ijms.55866

Darenskaya MA, Kolesnikova LI, and Kolesnikov SI (2021). Oxidative stress: Pathogenetic role in diabetes mellitus and its complications and therapeutic approaches to correction. Bulletin of Experimental Biology and Medicine, 171(2): 179-189. DOI: https://www.doi.org/10.1007/s10517-021-05191-7

Furman BL (2021). Streptozotocin-induced diabetic models in mice and rats. Current Protocols, 1: e78. DOI: https://www.doi.org/10.1002/cpz1.78

Gadang V, Gilbert W, Hettiararchchy N, Horax R, Katwa L, and Devareddy L (2011). Dietary bitter melon seed increases peroxisome proliferator-activated receptor-γ gene expression in adipose tissue, down-regulates the nuclear factor-κB expression, and alleviates the symptoms associated with metabolic syndrome. Journal of Medicinal Food, 14(1-2): 86-93. DOI: https://www.doi.org/10.1089/jmf.2010.0010

González P, Lozano P, Ros G, and Solano F (2023). Hyperglycemia and oxidative stress: An integral, updated and critical overview of their metabolic interconnections. International Journal of Molecular Sciences. 24(11): 9352. DOI: https://www.doi.org/10.3390/ijms24119352

Hidayaturrahman BSH, Aulia RR, and Kartikasari D (2020). Blood glucose level of white rats (*Rattus norvegicus*) after giving catfish biscuit (*Pangasius hypothalmus*). BIO Web of Conferences, 20(4): 04005. DOI: https://www.doi.org/10.1051/bioconf/20202004005

Internasional diabetes federation (IDF) (2021). The diabetes atlas. Available at: https://diabetesatlas.org/

Iseli TJ, Turner N, Zheng XY, Cooney GJ, Kraegen EW, Yao S, Ye Y, James DE, and Ye JM (2013). Activation of AMPK by bitter melon triterpenoids involves CaMMKβ. PLOS One, 8(4): e62309. DOI: https://www.doi.org/10.1371/journal.pone.0062309

Jenie IM and Indraswari RI (2021). Hypoglycaemic effects of Javanese ginseng (*Talinum paniculatum* (Jacq.) Gaertn.) root infusion on alloxan-induced diabetic rats. Jurnal Kedokteran Hewan, 15(3): 84-91. DOI: https://www.doi.org/10.21157/j.ked.hewan.v15i3.19568

Kahraman S, Aydin C, Elpek GO, Dirice E, and Sanlioglu AD (2015). Diabetes-resistant nor mice are more severely affected by streptozotocin compared to the diabetes-prone nod mice: Correlations with liver and kidney glut2 expressions. Journal of Diabetes Research, 2015: 450128. DOI: https://www.doi.org/10.1155/2015/450128

Leto D and Saltiel AR (2012). Regulation of glucose transport by insulin: Traffic control of GLUT4. Nature Reviews Molecular Cell Biology, 13(6): 383-396. DOI: https://www.doi.org/10.1038/nrm3351

Liu Z, Gong J, Huang W, Lu F, and Dong H (2021). The effect of *Momordica charantia* in the treatment of diabetes mellitus: A review. Evidence-Based Complementary and Alternative Medicine, 2021: 3796265. DOI: https://www.doi.org/10.1155/2021/3796265

Mahmoud MF, El Ashry FEZZ, El Maraghy NN, and Fahmy A (2017). Studies on the antidiabetic activities of *Momordica charantia* fruit juice in streptozotocin-induced diabetic rats. Pharmaceutical Biology, 55(1): 758-765. DOI: https://www.doi.org/10.1080/13880209.2016.1275026

Mahwish, Saeed F, Nosheen F, Ain QU, Niaz B, Afzaal M, Ehsan K, Hussain M, Imran M, and Al Jbawi E (2023). Bio-evaluation of alkaloids and saponins from bitter melon: Probing more desirable compound in treating hyperglycemia and hyperlipidemia. Cogent Food & Agriculture, 9(1): 2242634. DOI: https://www.doi.org/10.1080/23311932.2023.2242634

Malekshahi H, Bahrami G, Miraghaee S, Ahmadi SA, Sajadimajd S, Hatami R, Mohammadi B, and Keshavarzi S (2019). *Momordica charantia* reverses type II diabetes in rat. Journal of Food Biochemistry, 43(11): e13021. DOI: https://www.doi.org/10.1111/jfbc.13021

Ofuegbe SO, Oyagbemi AA, Omobowale TO, Adedapo AD, Ayodele AE, Yakubu MA, Oguntibeju OO, and Adedapo AA (2020). Methanol leaf extract of Momordica charantia protects alloxan-induced hepatopathy through modulation of caspase-9 and interleukin-1β signaling pathways in rats. Veterinary World, 13(8): 1528-1535. DOI: https://www.doi.org/10.14202/vetworld.2020.1528-1535

Pahlavani N, Roudi F, Zakerian M, Ferns GA, Navashenaq JG, Mashkouri A, Ghayour MM, and Rahimi H (2019). Possible molecular mechanisms of glucose-lowering activities of *Momordica charantia* (karela) in diabetes. Journal of Cellular Biochemistry, 120(7): 10921-10929. DOI: https://www.doi.org/10.1002/jcb.28483

Poovitha S and Parani M (2017). Protein extract from the fruit pulp of *Momordica charantia* potentiate glucose uptake by upregulating Glut4 and AMPK. Journal of Functional Foods, 37: 507-512. DOI: https://www.doi.org/10.1016/j.jff.2017.08.022

Rezaeizadeh A, Zakaria ZBAB, Abdollahi M, Meng GY, Mustapha NM, Hamid MB, and Ibrahim TABT (2011). Antioxidant and antihyperglycaemic effects of an aqueous extract from *Momordica charantia* fruit in a type II diabetic rat model. Journal of Medicinal Plants Research, 5(14): 2990-3001. Available at: https://academicjournals.org/journal/JMPR/article-full-text-pdf/00F209018729

Richter E, Geetha T, Burnnett D, Broderick TL, and Babu JR (2023). The effect of *Momordica charantia* on type 2 diabetes mellitus and alzheimer's disease. International Journal of Molecular Sciences, 24(5): 4643. DOI: https://www.doi.org/10.3390/ijms24054643

Rochette L, Zeller M, Cottin Y, and Vergely C (2014). Diabetes, oxidative stress and therapeutic strategies. Biochimica et Biophysica Acta, 1840(9): 2709-2729. DOI: https://www.doi.org/10.1016/j.bbagen.2014.05.017

Soliman AM (2016). Potential impact of *Paracentrotus lividus* extract on diabetic rat models induced by high-fat diet/streptozotocin. The Journal of Basic & Applied Zoology, 77: 8-20. DOI: https://www.doi.org/10.1016/j.jobaz.2016.01.001

Tan SP, Kha TC, Parks SE, and Roach PD (2016). Bitter melon (*Momordica charantia* L.) bioactive composition and health benefits: A review. Food Reviews International, 32(2): 181-202. DOI: https://www.doi.org/10.1080/87559129.2015.1057843

Wang Q, Wu X, Shi F, and Liu Y (2019). Comparison of antidiabetic effects of saponins and polysaccharides from Momordica charantia L. in STZ-induced type 2 diabetic mice. Biomedicine & Pharmacotherapy, 109: 744-750. DOI: https://www.doi.org/10.1016/j.biopha.2018.09.098

Wang T, Wang J, Hu X, Huang X, and Chen GX (2020). Current understanding of glucose transporter 4 expression and functional mechanisms. World Journal of Biological Chemistry, 11(3): 76-98. DOI: https://www.doi.org/10.4331/wjbc.v11.i3.76

Wellington D, Mikaelian I, and Singer L (2013). Comparison of ketamine–xylazine and ketamine–dexmedetomidine anesthesia and intraperitoneal tolerance in rats. Journal of the American Association for Laboratory Animal Science, 52(4): 481-487. Available at: https://pmc.ncbi.nlm.nih.gov/articles/PMC3725934/pdf/jaalas2013000481.pdf

Xu B, Li Z, Zeng T, Zhan J, Wang S, Ho CT, and Li S (2022). Bioactives of *Momordica charantia* as potential antidiabetic/hypoglycemic agents. Molecules, 27(7): 2175. DOI: https://www.doi.org/10.3390/molecules27072175

Publisher's note: Scienceline Publication Ltd. remains neutral with regard to jurisdictional claims in published maps and institutional affiliations.

Open Access: This article is licensed under a Creative Commons Attribution 4.0 International License, which permits use, sharing, adaptation, distribution and reproduction in any medium or format, as long as you give appropriate credit to the original author(s) and the source, provide a link to the Creative Commons licence, and indicate if changes were made. The images or other third party material in this article are included in the article's Creative Commons licence, unless indicated otherwise in a credit line to the material. If material is not included in the article's Creative Commons licence and your intended use is not permitted by statutory regulation or exceeds the permitted use, you will need to obtain permission directly from the copyright holder. To view a copy of this licence, visit https://creativecommons.org/licenses/by/4.0/.
© The Author(s) 2025

2025, Scienceline Publication
World's Veterinary Journal
World Vet J, 15(4): 1101-1106.
ISSN 2322-4568

DOI: https://dx.doi.org/10.54203/scil.2025.wvj112
PII: S232245682500112-15

Multidrug-Resistant Profile of Methicillin-Resistant *Staphylococcus pseudintermedius* in Dogs with Pyoderma in Lima, Peru

Juan Tomás, Brayan Rivas, Joel Palomino-Farfán, and Juan Siuce*

Laboratory of Veterinary Bacteriology and Mycology, Faculty of Veterinary Medicine, National University of San Marcos, Lima 15021, Peru

*Corresponding author's Email: jsiucem@unmsm.edu.pe

SHORT COMMUNICATION
Received: September 26, 2025
Revised: October 27, 2025
Accepted: November 22, 2025
Published: December 31, 2025

ABSTRACT

Methicillin resistance is a major global health concern, and recently, methicillin-resistant *Staphylococcus pseudintermedius* (MRSP) has emerged as a significant issue in veterinary medicine, with the potential to spread to humans. The present study aimed to analyze *Staphylococcus pseudintermedius* (*S. pseudintermedius*) strains isolated from 585 canine pyoderma samples from 2016 to 2024 at the Faculty of Veterinary Medicine, National University of San Marcos, Peru. The *mec*A gene was detected by conventional polymerase chain reaction, and antimicrobial susceptibility test included seven antibiotic families, including tetracyclines, sulfonamides, aminoglycosides, second-generation cephalosporins, penicillins, fluoroquinolones, and lincosamides. Out of 585 samples, 143 (24.4%) were positive for the *mecA* gene, confirming the presence of MRSP. Among these strains, 107 (74.8%) were multidrug resistant (MDR), and 119 (83.2%) exhibited phenotypic oxacillin resistance. The highest resistance rates of the *S. pseudintermedius* carrying the *mec*A gene were observed for lincosamides (86.0%), cephalosporins (78.3%), and sulfonamides (76.9%), whereas resistance to amoxicillin-clavulanate was the lowest (6.3%). In addition, two isolates were resistant to all the antibiotic families evaluated. These findings underscored the increasing prevalence of MRSP and MDR *S. pseudintermedius*, highlighting the need for improved antibiotic protocols in veterinary medicine to mitigate resistance and ensure effective treatment strategies for canine pyoderma.

Keywords: Dog, Methicillin, Resistance, *Staphylococcus pseudintermedius*

INTRODUCTION

Canine pyoderma, one of the most frequently diagnosed dermatological disorders in veterinary medicine, is commonly associated with *Staphylococcus pseudintermedius* (*S. pseudintermedius*), a coagulase-positive bacterium belonging to the *S. intermedius* group (Bannoehr and Guardabassi, 2012). *Staphylococcus pseudintermedius* is an opportunistic pathogen commonly implicated in canine skin infections. Several studies have reported that *S. pseudintermedius* represents 70-90% of bacterial isolates from dogs with pyoderma and other conditions, including otitis externa, otitis media, and postoperative or wound infections (Cheung et al., 2024). Additionally, *S. pseudintermedius* can occur in dogs with genetic, dermatological**,** or immunological factors that predispose certain breeds, including the West Highland White Terrier, Shar Pei, Boxer, English and French Bulldog, Labrador Retriever, Golden Retriever, Dachshund, and German Shepherd to skin disorders, creating an environment in which *S. pseudintermedius* can overgrow (Bannoehr and Guardabassi, 2012). In recent years, concerns about multidrug-resistant (MDR) strains, especially methicillin-resistant *S. pseudintermedius* (MRSP), have grown due to their resistance to first-line antimicrobials such as macrolides, tetracyclines, aminoglycosides, and fluoroquinolones. Limited treatment options are further constrained by co-resistance in MRSP, caused by the presence of multiple mobile genetic elements, such as *SCCmec* and *Tn5405*-like structures, which carry distinct resistance genes (Nocera and De Martino, 2024). In the Netherlands, the proportion of MRSP isolates increased from 0.9% in 2004 to 7% in 2013. Meanwhile, in Tennessee, USA, out of 6453 *S. pseudintermedius* isolates, 45.5% exhibited MDR, and 30.8% were methicillin-resistant (Lord et al., 2022; Nocera and De Martino, 2024) .

The emergence of MRSP is mainly driven by carrying the *mecA* gene, which encodes an alternative penicillin-binding protein (PBP2a) characterized by a reduced affinity for β-lactam antibiotics (Murakami et al., 1991). This resistance mechanism, first identified in *Staphylococcus aureus* (*S. aureus*) by Murakami et al. (1991), has since been acquired by coagulase-positive staphylococci of animal origin, contributing to the worldwide emergence of MRSP in veterinary clinical settings (Bannoehr and Guardabassi, 2012). The *mec*A-positive strains are often associated with resistance to multiple classes of antibiotics, such as macrolides, tetracyclines, aminoglycosides, and fluoroquinolones, making their management in veterinary practice a significant challenge (Nocera and De Martino, 2024).

To cite this paper: Tomas J, Rivas B, Palomino-Farfán J, and Siuce J (2025). Multidrug-Resistant Profile of Methicillin-Resistant *Staphylococcus pseudintermedius* in Dogs with Pyoderma in Lima, Peru. *World Vet. J.*, 15(4): 1101-1106. DOI: https://dx.doi.org/10.54203/scil.2025.wvj112

In Peru, veterinary studies on MDR staphylococcal infections remain limited. Reports on MRSP prevalence in canine pyoderma are especially rare, despite the critical implications for animal welfare, such as prolonged suffering, increased treatment failure, and the potential of zoonotic transmission. The present study aimed to evaluate the prevalence of MRSP among *S. pseudintermedius* isolates from dogs with canine pyodermas in Peru and assess their resistance profiles to seven commonly used families of antibiotics. Additionally, some of these affected dogs demonstrated mixed infections, with fungal agents identified and investigated to understand potential coinfections that could complicate treatment outcomes.

MATERIALS AND METHODS

Ethical approval

No approval from research ethics committees was required for the present study, as procedures were conducted using microbial culture collections from the Bacteriology and Mycology Lab at the School of Veterinary Medicine, National University of San Marcos, Peru. No animals were involved in the present study.

Study design

The present study was conducted as an observational study between January 2016 and December 2024 at the School of Veterinary Medicine, National University of San Marcos, Lima, Peru. Samples from dogs with pyoderma were collected by veterinarians using sterile swabs, which were then placed into tubes containing Stuart transport medium (Merck Millipore, Germany). Swabs were inoculated onto trypticase soy agar (Merck Millipore, Germany) and incubated at 37°C for 24-48 hours. Subsequently, biochemical characterization, including coagulase, catalase, and carbohydrate fermentation tests, were performed. Out of 585 canine pyoderma samples, *S. pseudintermedius* was identified in 86.92% of isolates using polymerase chain reaction-restriction fragment length polymorphism (PCR-RFLP), following the protocol described by Alvarez et al. (2020), in which the PCR amplicons were digested with the restriction enzyme MboI (5 U). These *S. pseudintermedius* isolates were then screened for the *mecA* gene using conventional PCR with primers described by Murakami et al. (1991). The isolates were stored at -20°C in 20% (v/v) glycerol (Merck Millipore, Germany) for long-term preservation (Miyamoto-Shinohara et al., 2008) during the study period at the Bacteriology and Mycology Lab of the Faculty of Veterinary Medicine at The National University of San Marcos, Peru. The mean age of the affected dogs was 5.36 years (ranged from 0.3 to 13.5). In terms of sex distribution, 51.1% (n = 299) of the dogs were male, and 48.9% were female (n = 286).

Conventional PCR was performed based on the method used by Murakami et al. (1991), with slight modifications to detect the *mecA* gene in 585 samples of *S. pseudintermedius* isolates using the primers previously reported by Murakami et al. (1991); forward 5'-AAA ATC GAT GGT AAA GGT TGG C-3' and reverse 5'-AGT TCT GCA GTA CCG GAT TTG C-3', at a concentration of 0.2 µM each. The PCR was carried out using the DreamTaq PCR Master Mix (Thermo Fisher Scientific, USA) in a total volume of 30 µL. The thermocycling conditions consisted of an initial denaturation at 94°C for five minutes, followed by 30 cycles of denaturation at 94°C for 60 seconds, hybridization at 50°C for 30 seconds, and elongation at 72°C for 60 seconds, with a final elongation at 72°C for five minutes. *Staphylococcus aureus* ATCC 43300 was used as a positive control, and the Negative control was *Escherichia coli* ATCC 8739. An electrophoresis gel with agarose 1.5% (Sigma-Aldrich, USA) in Tris-borate-EDTA buffer (Sigma-Aldrich, USA) was prepared to evaluate the PCR products (533 bp), which were visualized under a blue light transilluminator.

All *mecA*-positive *S. pseudintermedius* isolates, along with the MRSA control strain *S. aureus* ATCC 43300, were tested for oxacillin susceptibility using the Kirby–Bauer disk diffusion method in accordance with the Clinical and Laboratory Standards Institute guidelines (CLSI M100, 2025). For *S. pseudintermedius*, oxacillin disk diffusion was the recommended phenotypic method for detecting methicillin resistance, as specified in CLSI guidelines. In addition, seven families of antibiotics, including tetracycline (doxycycline and oxytetracycline), sulfonamide (sulfamethoxazole), aminoglycoside (gentamycin and neomycin), second-generation cephalosporin (cephalexin), penicillins (oxacillin and acid clavulanate amoxicillin), fluoroquinolone (enrofloxacin and ciprofloxacin), and lincosamide (clindamycin and/or lincomycin), were selected to determinate their resistance and classify as MDR those that exhibit resistance to three or more families of antibiotics (Magiorakos et al., 2012).

Fungal identification as a co-infection was determined in hair and scale samples from the affected skin area. Placing the collected material directly onto a fungal culture medium in a dermatophyte test medium (Merck Millipore, Germany) and sabouraud agar (Merck Millipore, Germany) at 25°C for 5-14 days. Macroscopic analysis, including colony morphology, colony color, growth rate, pigmentation, topography, and margin, and microscopic analysis (Zeiss, Germany) at 40× magnification was conducted using the Scotch tape impression technique, followed by staining with methylene blue (Merck Millipore, Germany). Hyphae, conidiophores or sporangiophores, conidia or spores, and

specialized structures, such as phialides, vesicles, chlamydospores, ascus/asci, and basidia, were identified to determine the genus and species of the fungus (Hayden et al, 2018).

Data analysis

Descriptive statistics were applied to report the proportion of *mecA*-positive samples and the distribution of antibiotic susceptibility and resistance rates.

RESULTS

The *mecA* gene, which indicates methicillin resistance, was identified in 143 out of 585 *S. pseudintermedius* isolates examined, resulting in a prevalence rate of 24.4%. All *mecA*-positive isolates were therefore classified as MRSP (Figure 1). Among these *mec*A-positive isolates, 83% (n = 119) exhibited phenotypic resistance to oxacillin, and ~75% (n = 107) were classified as MDR. These strains presented the highest resistance to lincosamides (86%), followed by cephalosporins (78.3%), sulfonamides (76.9%), fluoroquinolones (71.3%), aminoglycosides (55.2%), and tetracyclines (37.8%). The combination of amoxicillin and clavulanate resulted in the lowest resistance (6.3%). Notably, in the present study, two isolates exhibited resistance to all seven antimicrobial families, including Pandrug-resistant (PDR) strains.

A subset of 98 dogs with *mec*A-positive isolates had clinical suspicion of external mycoses. Among 98 dogs, six were positive for *Microsporum canis* (*M. canis*), and four were positive for *Malassezia pachydermatis* (*M. pachydermatis*).

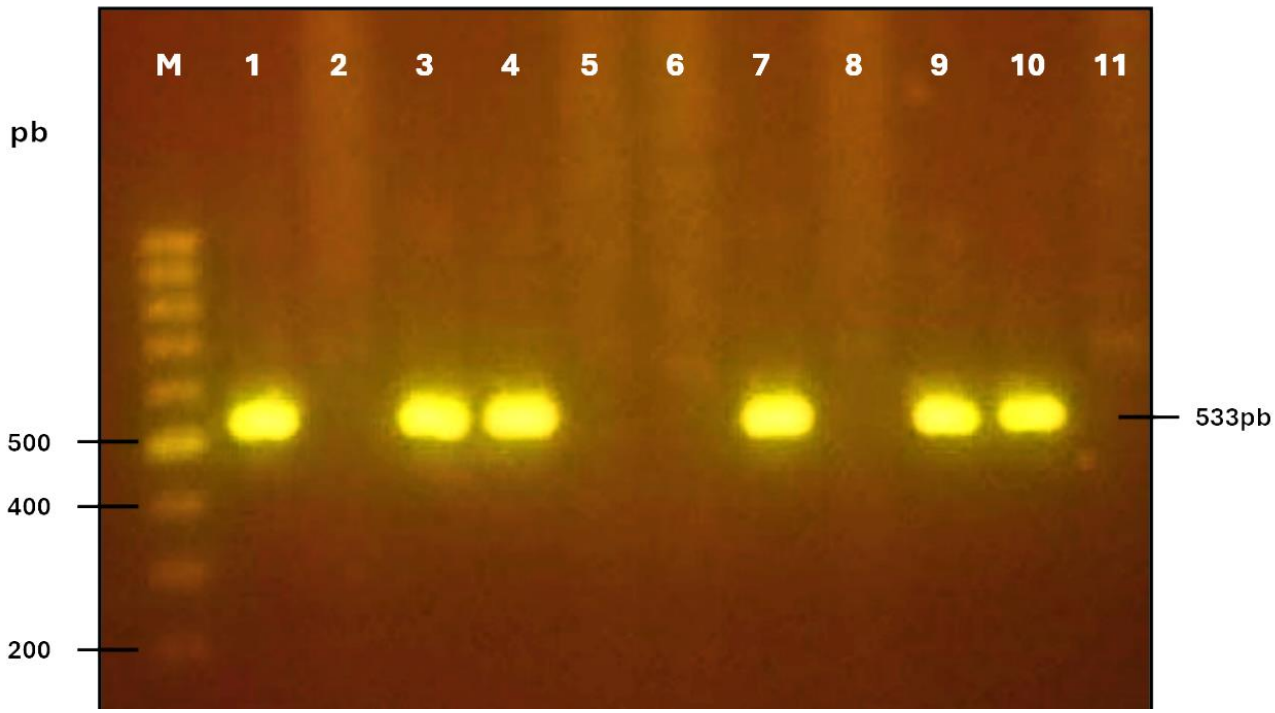


Figure 1. Agarose gel electrophoresis of the PCR products to detect the *mecA* gene in *Staphylococcus pseudintermedius* isolated from pyoderma in dogs. Lane M: Molecular weight marker 100 bp DNA ladder, Lane 1: Positive control, *Staphylococcus aureus* ATCC 43300, Lane 2: Negative control, *Escherichia coli* ATCC 8739, Lanes 3, 4, 7, 9, and 10: Positive samples at 533 bp, Lanes 5, 6, 8, and 11: Negative samples. The image was provided by the authors of the present study.

DISCUSSION

The detection of the *mec*A gene in 24.4% of isolates confirmed the presence of MRSP. This prevalence is higher than the 14.06% reported by Guimarães et al. (2023) in samples of pyoderma and otitis from dogs. Differences in sample origin may explain the lower rate observed in other studies, as *S. pseudintermedius* isolated from otitis cases often exhibited lower virulence and antimicrobial resistance profiles, with other *Staphylococcus* species, such as *S. schleiferi*, playing a more prominent role.

The current findings aligned with those of Ruzauskas et al. (2016), who reported a prevalence of 29%, and Lord et al. (2022), with a prevalence of 30.8% in dog samples. However, the prevalence of MRSP remains notably lower than

the 59% reported by Lynch and Helbig (2021), who recovered the isolates from dogs with chronic infections that had been previously diagnosed as pyoderma, having had major exposure to antimicrobials, which could explain the higher rate of resistance compared to the current study. Although humans are not the natural host of *S. pseudintermedius*, Guimarães et al. (2023) demonstrated that among nine MRSP strains isolated from canine pyoderma, two were closely related to strains found in their owners, highlighting potential zoonotic concerns.

The present findings emphasized the increasing threat posed by MRSP in veterinary medicine. Notably, ~75% of the *mecA*-positive isolates were MDR, exhibiting resistance to broad-spectrum antimicrobials such as macrolides, aminoglycosides, cephalosporins, fluoroquinolones, and lincosamides, medicines commonly used to treat severe or refractory infections (Nocera and De Martino, 2024). The present findings highlighted a crucial public health concern regarding the overuse of antibiotics in veterinary practice. This pattern aligns with the findings of Palomino-Farfán et al. (2021), who reported comparably higher rates of *mec*A-positive strains in South American canine populations. The role of MDR staphylococci in complicating routine veterinary treatments, as noted by Lynch and Helbig (2021), remains a considerable issue. Resistance to oxacillin was observed in 83.2% of the *mec*A-positive isolates, supporting its reliability as a phenotypic marker for MRSP detection, as outlined in the CLSI M100 guidelines (CLSI, 2025). In particular, two isolates demonstrated resistance to all seven antibiotic families tested, raising concerns about the limited treatment options available. The observed resistance patterns suggested potential clonal dissemination of highly resistant strains within veterinary hospital settings, a phenomenon previously reported in hospital-associated MRSP outbreaks (Lord et al., 2022).

Furthermore, concurrent mycoses were identified in ten dogs with *mec*A-positive isolates, with *M. canis* and *M. pachydermatis*. Mixed infections can amplify inflammatory responses, prolong wound healing, and increase the risk of developing chronic or recurrent dermatologic conditions. Dinkova and Rusenova (2025) highlighted the clinical relevance of co-infections involving *M. pachydermatis* and bacteria, noting that staphylococci are the bacterial pathogens most frequently associated with these skin disorders. Moreover, the administration of antibiotics without concurrent antifungal therapy in instances of mixed infection presents a risk of promoting microbial imbalance, which may facilitate fungal overgrowth and the development of multidrug-resistant bacteria such as MRSP. This finding highlighted the clinical necessity for effective topical agents with dual activity. Supporting these findings, Oliveira et al. (2018) demonstrated that a honey-based gel exhibited *in vitro* efficacy against primary canine pathogens, including *S. pseudintermedius* and *M. pachydermatis*, thereby indicating its potential as a single-agent therapeutic option for such cases.

The high MDR rate and the presence of PDR isolates in the present study highlighted the urgent need for enhanced responsible antibiotic use in veterinary practice in Peru. Empirical therapy for MRSP canine pyoderma should be guided by susceptibility testing, as demonstrated in the present study, to reduce the risk of promoting further antimicrobial resistance (Nocera and De Martino, 2024). Additionally, the detection of concurrent fungal infections necessitates a multidisciplinary approach to managing canine pyoderma, including the use of antifungal therapy when indicated.

CONCLUSION

The present study highlighted the significant presence of methicillin-resistant *Staphylococcus pseudintermedius* (MRSP) in canine isolates, with 24.4% of the canine isolates testing positive for the *mec*A gene and 75% of the canine isolates classified as multidrug resistant (MDR). The high MDR rate highlighted the growing concern regarding antibiotic overuse in veterinary medicine, particularly as two isolates of the 143 MRSP exhibited resistance to all seven antimicrobial families tested. The present findings underscore the urgent need for enhanced antibiotic protocols to prevent the spread of MRSP and MDR strains in Lima, Peru. Further studies are needed to investigate the molecular epidemiology of MRSP in Peru, including potential zoonotic transmission routes, given the close contact between dogs and humans in many households. In addition, surveillance programs aimed at monitoring antibiotic resistance trends in veterinary pathogens are essential for developing evidence-based treatment guidelines.

DECLARATIONS

Authors' contributions

All authors contributed to the conception, methodology, and design of the study. Material preparation and the original draft were carried out by Juan Tomás and Néstor Rivas. Writing, review, and editing were performed by Joel Palomino, Juan Siuce, and Luis Alvarez. Joel Palomino and Juan Siuce served as supervisors for the present study. All authors reviewed and approved the final edition of the manuscript.

Availability of data and materials

The data supporting the present findings are available upon reasonable request to the corresponding author.

Competing interests

The authors declared that there are no conflicts of interest.

Funding

The present study was supported by Universidad Nacional Mayor de San Marcos, RR N° 03556-R-19, Peru, and project number A19080891.

Ethical considerations

The present study was originally written by the authors and has not been published elsewhere. The authors checked the text of the article for plagiarism index and confirmed that the text of the article is written based on their original scientific results. The authors have not used AI in generating data and conducting the present study.

REFERENCES

Alvarez L, Siuce J, Palomino J, Gonzales S, Sedano A, and Calle S (2020). Detección molecular de *Staphylococcus pseudintermedius* en piodermas caninas. Revista de Investigaciones Veterinarias Del Perú, 31(3): e18734. DOI: https://www.doi.org/10.15381/rivep.v31i3.18734

Bannoehr J and Guardabassi L (2012). *Staphylococcus pseudintermedius* in the dog: Taxonomy, diagnostics, ecology, epidemiology and pathogenicity. Veterinary Dermatology, 23(4): 253-266. DOI: https://www.doi.org/10.1111/j.1365-3164.2012.01046.x

Cheung GYC, Lee JH, Liu R, Lawhon SD, Yang C, and Otto M (2024). Methicillin resistance elements in the canine pathogen *Staphylococcus pseudintermedius* and their association with the peptide toxin PSM-mec. Antibiotics, 13(2): 130. DOI: https://www.doi.org/10.3390/antibiotics13020130

Clinical and laboratory standards institute (CLSI) (2025). Performance standards for antimicrobial susceptibility testing, 35th Edition. CLSI supplement M100, pp. 95-96. Available at: https://www.iacld.com/UpFiles/Documents/9079a0e6-129e-4c3b-9e86-d47a9da251dc.pdf

Dinkova V and Rusenova N (2025). Prevalence of Malassezia pachydermatis yeasts in clinical infections in dogs: A single-center retrospective study at the University Veterinary Hospital, Stara Zagora, Bulgaria (2019-2023). Open Veterinary Journal, 15(9): 4354-4361. DOI: https://www.doi.org/10.5455/OVJ.2025.v15.i9.42

Guimarães L, Teixeira IM, da Silva IT, Antunes M, Pesset C, Fonseca C, Santos AL, Côrtes MF, and Penna B (2023). Epidemiologic case investigation on the zoonotic transmission of Methicillin-resistant *Staphylococcus pseudintermedius* among dogs and their owners. Journal of Infection and Public Health, 16(Suppl 1): 183-189. DOI: https://www.doi.org/10.1016/j.jiph.2023.10.041

Hayden RT, Larone DH, and Walsh TJ (2018). Medically important fungi: A guide to identification, 6th Edition. ASM Press., Washington, pp. 243-256. Available at: https://wiley.com/en-us/Larone's+Medically+Important+Fungi%3A+A+Guide+to+Identification%2C+6th+Edition-p-9781683670537

Lynch SA and Helbig KJ (2021). The complex diseases of *Staphylococcus pseudintermedius* in Canines: Where to next?. Veterinary Sciences, 8(1): 11. DOI: https://www.doi.org/10.3390/vetsci8010011

Magiorakos AP, Srinivasan A, Carey RB, Carmeli Y, Falagas ME, Giske CG, Harbarth S, Hindler JF, Kahlmeter G, Olsson-Liljequist B et al. (2012). Multidrug-resistant, extensively drug-resistant and pandrug-resistant bacteria: An international expert proposal for interim standard definitions for acquired resistance. Clinical Microbiology and Infection, 18(3): 268-281. DOI: https://www.doi.org/10.1111/j.1469-0691.2011.03570.x

Miyamoto-Shinohara Y, Sukenobe J, Imaizumi T, and Nakahara T (2008). Survival of freeze-dried bacteria. Journal of Pure and Applied Microbiology, 54(1): 9-24. DOI: https://www.doi.org/10.2323/jgam.54.9

Murakami K, Minamide W, Wada K, Nakamura E, Teraoka H, and Watanabe S (1991). Identification of methicillin-resistant strains of staphylococci by polymerase chain reaction. Journal of Clinical Microbiology, 29(10): 2240-2244. DOI: https://www.doi.org/10.1128/JCM.29.10.2240-2244.1991

Nocera FP and De Martino L (2024). Methicillin-resistant *Staphylococcus pseudintermedius*: epidemiological changes, antibiotic resistance, and alternative therapeutic strategies. Veterinary Research Communications, 48: 3505-3515. DOI: https://www.doi.org/10.1007/s11259-024-10508-8

Lord J, Millis N, Jones RD, Johnson B, Kania SA, and Odoi A (2022). Patterns of antimicrobial, multidrug and methicillin resistance among *Staphylococcus* spp. isolated from canine specimens submitted to a diagnostic laboratory in Tennessee, USA: A descriptive study. BMC Veterinary Research, 18: 91. DOI: https://www.doi.org/10.1186/s12917-022-03185-9

Oliveira A, Devesa J, and Hill P (2018). *In vitro* efficacy of a honey-based gel against canine clinical isolates of *Staphylococcus pseudintermedius* and *Malassezia pachydermatis*. Veterinary Dermatology, 29(3): 180-e65. DOI: https://www.doi.org/10.1111/vde.12533

Palomino-Farfán JA, Alvarez LG, Calle S, Gonzales S, and Siuce JJ (2021). Methicillin-resistant *Staphylococcus schleiferi* subspecies *coagulans* isolated from dogs with otitis externa and pyoderma in Peru. Open Veterinary Journal, 11(3): 364-369. DOI: https://www.doi:10.5455/OVJ.2021.v11.i3.5

Ruzauskas M, Couto N, Pavilonis A, Klimiene I, Siugzdiniene R, Virgailis M, Vaskeviciute L, Anskiene L, and Pomba C (2016). Characterization of *Staphylococcus pseudintermedius* isolated from diseased dogs in Lithuania. Polish Journal of Veterinary Sciences, 19(1): 7-14. DOI: https://www.doi.org/10.1515/pjvs-2016-0002

Publisher's note: Scienceline Publication Ltd. remains neutral with regard to jurisdictional claims in published maps and institutional affiliations.

Open Access: This article is licensed under a Creative Commons Attribution 4.0 International License, which permits use, sharing, adaptation, distribution and reproduction in any medium or format, as long as you give appropriate credit to the original author(s) and the source, provide a link to the Creative Commons licence, and indicate if changes were made. The images or other third party material in this article are included in the article's Creative Commons licence, unless indicated otherwise in a credit line to the material. If material is not included in the article's Creative Commons licence and your intended use is not permitted by statutory regulation or exceeds the permitted use, you will need to obtain permission directly from the copyright holder. To view a copy of this licence, visit https://creativecommons.org/licenses/by/4.0/.
© The Author(s) 2025

2025, Scienceline Publication
World's Veterinary Journal
World Vet J, 15(4): 1107-1112.
ISSN 2322-4568

DOI: https://dx.doi.org/10.54203/scil.2025.wvj113
PII: S232245682500113-15

Antibiotic Resistance of *Escherichia coli* Isolated from Ducks Suspected of Colibacillosis in Vietnam

Chu Thi Thanh Huong, Truong Lan Oanh, Vu Thi Thu Tra, and Truong Ha Thai*

Faculty of Veterinary Medicine, Vietnam National University of Agriculture, Gia Lam, Hanoi, Vietnam

*Corresponding author's Email: ththai@vnua.edu.vn

SHORT COMMUNICATION
Received: October 02, 2025
Revised: November 08, 2025
Accepted: December 05, 2025
Published: December 31, 2025

ABSTRACT

The extensive application of antibiotics within the livestock sector has led to a rise in bacterial resistance, especially against *Escherichia coli* (*E. coli*), complicating the treatment of bacterial infections in poultry. The present study aimed to determine the antibiotic resistance of the *E. coli* isolated from Cherry Valley ducks exhibiting signs of colibacillosis in northern Vietnam. From March to May 2025, 21 Cherry Valley duck flocks raised on 15 duck farms in Ha Nam Province, Vietnam, experienced disease outbreaks characterized by clinical signs such as anorexia, reduced mobility, abnormal movement, and respiratory distress, including sneezing, gasping, and nasal discharge, which were suspected of being caused by *E. coli* infection. A total of 63 ducks suspected of colibacillosis were necropsied for sampling and pathological observation. Heart, liver, and lung samples were collected simultaneously from all ducks for *E. coli* isolation. The isolated *E. coli* strains were examined for antibiotic susceptibility by the agar diffusion method. The *E. coli* strains demonstrated the highest susceptibility to levofloxacin (82.9%), followed by norfloxacin (78.0%), gentamicin (73.2%), and colistin (70.7%). The highest resistance rates were observed for ampicillin (75.6%) and tetracycline (73.2%), whereas resistance to ciprofloxacin, streptomycin, and doxycycline ranged from 31.7% to 48.8%. Of the 41 *E. coli* strains, 82.9% were resistant to at least one antibiotic; these strains exhibited 17 distinct antibiotic resistance patterns. Additionally, 63.4% isolated strains were identified as multi-drug resistant (MDR). The current results emphasized the high resistance of *E. coli* strains isolated from ducks to multiple antibiotics.

Keywords: Antibiotic resistance, Duck, Colibacillosis, Diffusion method

INTRODUCTION

Escherichia coli (E. coli) is a widely recognized bacterium within the *Enterobacteriaceae* family, commonly found in the intestinal tracts of poultry and other animal species (Darwish et al., 2015; Luo et al., 2023). Nevertheless, certain strains of *E. coli* carry virulence-associated genes that enable them to induce diarrhea and intestinal hemorrhage in poultry (Darwish et al., 2015).

As in other Asian countries, duck farming is highly popular in Vietnam. However, during the breeding process, some infectious diseases in ducks, such as pasterellosis, salmonellosis, riemerellosis, and colibacillosis, have been recorded in the Mekong Delta (Thuan and Khai, 2018; Thu et al., 2019) and northern Vietnam (Vui and Tiep, 2016). Ducks can be infected with *E. coli* at different ages, but the disease typically manifests in ducks between 2 and 6 weeks old. Infected ducks have a high mortality rate, reaching up to 43.5% (Roshdy et al., 2012). Since 1961, the pathogenic role of *E. coli* in poultry has been recognized; however, the disease has not gained much attention in many countries so far (Dziva and Stevens, 2008). Prevention and treatment of bacterial diseases in poultry still rely on using antibiotics. However, the frequent use of antibiotics results in continuous exposure of the intestinal microbiota, thereby developing antibiotic resistance (Kissinga et al., 2018; Yanestria et al., 2022).

Antibiotic resistance is a major public health threat and hinders the treatment of bacterial diseases in poultry. Nevertheless, the management of colibacillosis depends on antibiotics globally (Azam et al., 2019). The widespread use of antibiotics in animal livestock has increased the antibiotic resistance in pathogenic bacteria, including *E. coli*, and can cause public health problems (Magiorakos et al., 2013; Luo et al., 2023). Therefore, the present study aimed to examine the antibiotic resistance of *E. coli* strains isolated from ducks suspected of colibacillosis raised on duck farms in Ha Nam, Vietnam.

To cite this paper: Huong CTT, Oanh TL, Tra VTT, and Thai TH (2025). Antibiotic Resistance of *Escherichia coli* Isolated from Ducks Suspected of Colibacillosis in Vietnam. *World Vet. J.*, 15(4): 1107-1112. DOI: https://dx.doi.org/10.54203/scil.2025.wvj113

MATERIALS AND METHODS

Ethics approval

The present study was conducted by collecting samples in accordance with the guidelines outlined in the Helsinki declaration and the animal welfare and safety procedures of the Committee on Animal Research and Ethics (CARE), Faculty of Veterinary Medicine, Vietnam National University of Agriculture, Vietnam (Approval No. CARE-2025/02).

Sampling

The present study was conducted on 21 commercially-raised Cherry Valley duck flocks, aged 3-6 weeks, that experienced disease outbreaks on 15 farms in Ha Nam Province, Vietnam, from March to May 2025. Affected ducks exhibited clinical signs suggestive of colibacillosis, including anorexia, moodiness, reduced mobility, impaired movement, bloody diarrhoea, and lesions such as an inflamed pericardium, swollen liver, and pneumonia (Punnoose et al., 2021). Sixty-three ducks suspected of colibacillosis underwent postmortem examination and necropsy for sampling and pathological observations in accordance with the QCVN 01-83:2011/BNNPTNT guidelines of the Ministry of Agriculture and Rural Development (MARD, 2011). Several samples of heart, liver, and lung were collected simultaneously from each of sixty-three affected ducks. The samples were placed in sterile bags, put in a dry-ice container, and transported to the laboratory of the Faculty of Veterinary Medicine, Vietnam National University of Agriculture, for further analysis within 24 hours.

Escherichia coli isolation

Isolation of *E. coli* was carried out according to the protocol of Roshdy et al. (2012) with some modifications. Each sample was streaked onto MacConkey agar (Merck, Germany) and incubated at 37°C for 24 hours. Subsequently, the pink colonies from MacConkey agar were subculture onto eosin methylene blue agar (EMB; Merck, Germany) and incubated at 37°C for 24 hours. Then, a typical colony exhibiting the green metallic sheen on EMB agar was selected, streaked onto a triple sugar iron (TSI; Merck, Germany) agar tube, and incubated at 37°C for 24 hours. Colonies exhibiting a typical TSI profile, including glucose and lactose fermentation with gas production and no H2S, were identified as *E. coli* by Gram staining and biochemical tests, such as citrate utilization, indole production, the methyl red, and Voges-Proskauer reactions. All isolates were kept in brain heart infusion broth (BHI; Merck, Germany) supplemented with 50% glycerol at-20°C for subsequent experiments.

Antibiotic susceptibility testing

A total of 41 *E. coli* strains from positive ducks were selected for antibiotic susceptibility analysis, in accordance with the Clinical and Laboratory Standards Institute guidelines (CLSI, 2024). Antibiotic susceptibility was determined using the agar disc diffusion method on Mueller-Hinton agar (MHA; Merck, Germany), as described by Bauer et al. (1966). Twelve different antibiotics (Oxoid, UK) were tested, including ampicillin (10µg), amoxicillin/clavulanic acid (20/10µg), ciprofloxacin (5µg), colistin (10µg), doxycycline (30µg), florfenicol (30µg), gentamicin (10µg), kanamycin (30µg), levofloxacin (5µg), norfloxacin (10µg), streptomycin (10µg), and tetracycline (30µg). The *E. coli* ATCC 25922 strain was used for quality control. One *E. coli* strain was classified as a resistant isolate following the confirmation of resistance to at least one tested antibiotic. It was further designated as a multidrug-resistant (MDR) strain upon confirmation of resistance to at least one antibiotic from three different antibiotic classes (Magiorakos et al., 2012).

Data analysis

Isolation and antibiotic resistance rates of *E. coli* were compared using the Chi-Square test in EpiInfo version 7.2.3.1. The P-value was calculated and considered significantly less than 5% ($p < 0.05$).

RESULTS

The *E. coli* isolation rates for each type of sample are shown in Table 1. The *E. coli* was detected in 41 of the 63 duck samples (65.1%). Isolation rates ranged from 44.4% to 65.1% across different types of samples. The highest rate of *E. coli* isolation was observed in liver samples (65.1%), followed by heart (58.7%) and lung (44.4%).

The antibiotic susceptibility of the 41 *E. coli*-positive strains are presented in Table 2. The selected isolates demonstrated the highest susceptibility to levofloxacin (82.9%), followed by norfloxacin (78.0%), gentamicin (73.2%), and colistin (70.7%). Higher susceptibility (≥ 50%) was observed for florfenicol (68.3%), amoxicillin-clavulanate acid (65.9%), and kanamycin (61.0%). Meanwhile, 75.6% and 73.2% of the isolates were resistant to ampicillin and tetracycline, respectively. Resistance to ciprofloxacin, streptomycin, and doxycycline was lower, ranging from 31.7% to

48.8%. The antibiotic resistance patterns of the *E. coli* isolates are presented in Table 3. The *E. coli* strains exhibited 17 different antibiotic resistance patterns. The current results indicated that 34 of the 41 *E. coli* isolates (82.9%) were resistant to at least one antibiotic, of which 26 (63.4%) were MDR.

Table 1. Incidence of *Escherichia coli* isolated from Cherry Valley ducks suspected of colibacillosis collected from Northern Vietnam

Order	Kind of sample	Positive, n (%)
1	Heart	37 (58.7)
2	Liver	41 (65.1)
3	Lung	28 (44.4)

n: Number

Table 2. The antibiotic resistance rates of the *Escherichia coli* isolated from Cherry Valley ducks suspected of colibacillosis collected from Northern Vietnam

Kind of antibiotics	Susceptibility n (%)	Intermediate n (%)	Resistance n (%)
Ampicilin	6 (14.6)	4 (9.8)	31 (75.6)
Amoxicillin/clavunalic acid	27 (65.9)	3 (7.3)	11 (26.8)
Colistin	29 (70.7)	12 (29.3)	0 (0.0)
Doxycyline	19 (46.3)	2 (4.9)	20 (48.8)
Ciprofloxacin	18 (43.9)	10 (24.4)	13 (31.7)
Florfenicol	28 (68.3)	4 (9.8)	9 (22.0)
Gentamicin	30 (73.2)	2 (4.9)	9 (22.0)
Levofloxacin	34 (82.9)	7 (17.1)	0 (0.0)
Streptomycin	18 (43.9)	4 (9.8)	19 (46.3)
Tetracycline	11 (26.8)	0 (0.0)	30 (73.2)
Norfloxacin	32 (78.0)	4 (9.8)	5 (12.2)
Kanamycin	25 (61.0)	5 (12.2)	11 (26.8)

Table 3. The antibiotic resistance patterns of the *Escherichia coli* isolated from Cherry Valley ducks suspected of colibacillosis collected from Northern Vietnam

Order	Antibiotic resistance pattern	resistant antibiotics (Number)	n (%)
1	All susceptible	0	7 (17.1)
2	TET	1	3 (7.3)
3	AMP, STR	2	2 (4.9)
4	AMP, DOX, TET	3	3 (7.3)
5	AMP, FLO, TET	3	1 (2.4)
6	AMP, STR, TET	3	5 (12.2)
7	AMC, AMP, CIP, STR	4	2 (4.9)
8	AMP, DOX, CIP, TET	4	2 (4.9)
9	AMP, DOX, FLO, TET	4	3 (7.3)
10	AMP, DOX, CIP, FLO, TET	5	1 (2.4)
11	AMP, DOX, FLO, GEN, TET	5	1 (2.4)
12	AMC, AMP, DOX, STR, TET, KAN	6	1 (2.4)
13	AMC, AMP, GEN, STR, TET, KAN	6	1 (2.4)
14	AMP, DOX, CIP, FLO, TET, KAN	6	1 (2.4)
15	AMC, AMP, DOX, FLO, STR, TET, KAN	7	1 (2.4)
16	AMP, DOX, CIP, GEN, STR, TET, KAN	7	1 (2.4)
17	AMC, AMP, DOX, CIP, FLO, GEN, STR, TET, KAN	9	1 (2.4)
18	AMC, AMP, DOX, CIP, GEN, STR, TET, NOR, KAN	9	5 (12.2)

No: Number; AMP: Ampicillin; AMC: Amoxicillin/clavunalic axit; CIP: Ciprofloxacin; DOX: Doxycycline; FLO: Florfenicol; GEN: Gentamicin; KAN: Kanamycin; NOR: Norfloxacin; STR: Streptomycin, and TET: Tetracycline.

DISCUSSION

The prevalence of *E. coli* found during the present study (44.4-65.1%) aligns with findings of Majumder et al. (2017) in Bangladesh (43.33%) and Bariha et al. (2019) in India (55%). However, the isolation rates in the present study were lower than those reported by Thu et al. (2019) in the Mekong Delta, southern Vietnam, who reported an 78.3% isolation rate from liver and 71.8% from lung samples. The differences in isolation rates are likely due to factors such as farming practices, regions, duck ages, sampling, and isolation methods. Previous studies from Bangladesh (Singh et al., 2012) and Nepal (Kissinga et al., 2018) reported *E. coli* isolation rates of 100% and 91.0%, respectively. Postmortem findings, including fibrinous perihepatitis, pericarditis, enteritis, and pneumonia, confirmed systemic dissemination of *E. coli* to multiple organs, including the liver, lungs, and heart, which led to septicemia and subsequent death (Kabir, 2010).

High resistance of the *E. coli* strains to common antibiotics, such as ampicillin, tetracycline, and streptomycin, has been reported in previous studies in northern Vietnam (Vui and Tiep, 2016) and in the Mekong Delta in southern Vietnam (Trang et al., 2017; Sang et al., 2017; Thu et al., 2019). This pattern of resistance has been observed in many countries worldwide, including China (Dou et al., 2016; Afayibo et al., 2022), Malaysia (Adzitey et al., 2013), Tanzania (Kissinga et al., 2018), and Egypt (Reham et al., 2023). This is likely because these antibiotics have been used extensively in livestock farming in these countries for a long time (Thu et al., 2019; Afayibo et al., 2022). The doxycycline resistance rate among *E. coli* strains in the current study was 48.8%; a rate that fell within the wide range (20.3-77.14%) reported in earlier studies from southern Vietnam (Sang et al., 2017; Thuan and Khai, 2018; Thu et al., 2019). In contrast, amoxicillin resistance was markedly lower (26.0%) than the high rates documented in Egypt (66.7%; Reham et al., 2023) and China (90%; Luo et al., 2023). This discrepancy may be attributed to the widespread use of doxycycline and amoxicillin for disease prevention and treatment in poultry farming in China and Vietnam (Thu et al., 2019; Luo et al., 2023). Based on the present findings, gentamicin resistance was 22.0%, consistent with previous studies in Vietnam (Vui and Tiep, 2016; Thu et al., 2019). The florfenicol resistance rate among *E. coli* strains in the present study (22.0%) was higher than that reported in Mekong Delta provinces, Vietnam (16.5%; Thu et al., 2019), but lower than the 41.9% found in Dong Thap province (Sang et al., 2017). Additionally, quinolone-resistant *E. coli* strains were observed in the current study. The isolated *E. coli* strains exhibited ciprofloxacin resistance at 31.7%. This resistance may stem from the ready availability of ciprofloxacin in the retail market, despite its official prohibition for veterinary purposes in Vietnam. The observed norfloxacin resistance rate of 12.2% was consistent with previous reports on *E. coli* from southern Vietnam (Thu et al., 2019) and Egypt (Abdel Rahman et al., 2020). Colistin is a highly effective antibiotic against *E. coli* and has been widely used for the prevention and treatment of colibacillosis in animals. However, none of the E.coli strains were resistant to colistin in the present study. This may be due to the antibiotic's poor absorption in the poultry gastrointestinal tract after oral administration, making it rarely used in ducks for treatment and prevention (Thu et al., 2019).

In the current study, 63.4% of *E. coli* strains were identified as MDR. The prevalence of MDR *E. coli* in the present study was consistent with rates of 60.0-65.5% reported in southern Vietnam (Thuan and Khai, 2018) and similar to findings in Korea (Jeong et al., 2021). Notably, 100% of the *E. coli* isolates from China were found to be MDR (Afayibo et al., 2022). The emergence of MDR indicates that livestock facilities serve as critical hotspots for antibiotic resistance, and livestock themselves function as substantial reservoirs of antibiotic-resistant genes and microorganisms (Kissinga et al., 2018; Yanestria et al., 2022). A critical factor for the spread of antibiotic resistance in the environment is intensive animal husbandry (Karwowska, 2024). Moreover, the high rates of antibiotic resistance among *E. coli* strains isolated from affected ducks in the current study indicated that antibiotics were frequently used to prevent and treat infections on duck farms. This resulted in a very high rate of antibiotic resistance among bacterial strains isolated from duck farms in Vietnam.

CONCLUSION

The current study highlighted the high resistance of *E. coli* strains to multiple antibiotics isolated from ducks in the study area. The studied antibiotics are generally used in treating and preventing diseases in human and veterinary medicine. The presence of MDR *E. coli* in ducks highlighted a significant public health concern, as these strains can facilitate the spread of antibiotic resistance. Controlling antibiotic use in poultry is therefore essential to mitigate risks within the food chain.

DECLARATIONS

Funding

The present study received no external funding. The authors contributed to this study independently.

Acknowledgments

The authors of the current study would like to thank the students for sample transportation and the local veterinarian for their excellent technical assistance.

Authors' contributions

Chu Thi Thanh Huong designed the investigation and methodology and contributed to the manuscript. Vu Thi Thu Tra and Truong Lan Oanh participated in doing the experiments and analysing the data. Truong Ha Thai was responsible for supervision, methodological support, and primarily for writing the manuscript. All authors revised and approved the final edition of the manuscript.

Availability of data and materials

All data are included in the submitted paper and will be available upon reasonable requests from the corresponding author.

Ethical considerations

The authors considered farmers' ethical concerns and consent before conducting the study. This article was written originally without any copy from published articles and books. No AI was used to conduct the current study.

Competing interests

The authors declared no conflict of interest.

REFERENCES

Abdel Rahman MAA, Roshdy H, Samir AH, and Hamed EA (2020). Antibiotic resistance and extended-spectrum β-lactamase in *Escherichia coli* isolates from imported 1-day-old chicks, ducklings, and turkey poults. Veterinary World, 13(6): 1037-1044. DOI: https://www.doi.org/10.14202/vetworld.2020.1037-1044

Adzitey F, Ali GRR, Huda N, and Ting SL (2013). Antibiotic resistance and plasmid profile of *Escherichia coli* isolated from ducks in Penang, Malaysia. International Food Research Journal, 20: 1473-1478. Available at: https://www.cabidigitallibrary.org/doi/pdf/10.5555/20133249138

Afayibo DJA, Zhu H, Zhang B, Yao L, Abdelgawad HA, Tian M, Qi J, Liu Y, and Wang S (2022). Isolation, molecular characterization, and antibiotic resistance of Avian pathogenic *Escherichia coli* in Eastern China. Veterinary Sciences, 9(7): 319. DOI: https://www.doi.org/10.3390/vetsci9070319

Azam M, Mohsin M, Sajjad-Ur-Rahman, and Saleemi MK (2019). Virulence-associated genes and antimicrobial resistance among avian pathogenic *Escherichia coli* from colibacillosis affected broilers in Pakistan. Tropical Animal Health and Production, 51(5): 1259-1265. DOI: https://www.doi.org/10.1007/s11250-019-01823-3

Bariha UN, Mishra R, Kundu AK, Rath PK, Mishra C, Das S, and Soren N (2019). Microbial etiology of duck mortality in Odisha, India. International Journal of Current Microbiology and Applied Sciences, 8(8): 1577-1585. DOI: https://www.doi.org/10.20546/ijcmas.2019.808.186

Bauer AW, Kirby WM, Sherris JC, and Turck M (1966). Antibiotic susceptibility testing by a standardized single disk method. American Journal of Clinical Pathology, 45(4): 493-96. Available at: https://academic.oup.com/ajcp/article-abstract/45/4_ts/493/4821085?redirectedFrom=fulltext

Clinical and laboratory standards institute (CLSI) (2024). Performance standards for antimicrobial susceptibility testing, 34th Edition. CLSI supplement M100. Wayne, PA: Clinical and Laboratory Standards Institute, pp. 24-25. Available at:

https://pid-el.com/wp-content/uploads/2024/07/CLSI-M100.pdf

Darwish WS, Saad Eldin WF, and Eldesoky KI (2015). Prevalence, molecular characterization and antibiotic susceptibility of *Escherichia coli* isolated from duck meat and giblets. Journal of Food Safety, 35(3): 410-415. DOI: https://www.doi.org/10.1111/jfs.12189

Dou X, Gong J, Han X, Xua M, Shena H, Di Z, Zhuang l, Liu J, and Zou J (2016). Characterization of avian pathogenic *Escherichia coli* isolated in Eastern China. Genes, 576(1): 244-248. DOI: https://www.doi.org/10.1016/j.gene.2015.10.012

Dziva F and Stevens MP (2008). Colibacillosis in poultry: Unravelling the molecular basis of virulence of avian pathogenic *Escherichia coli* in their natural hosts. Avian Pathology, 37(4): 355-366. DOI: https://www.doi.org/10.1080/03079450802216652

Jeong J, Lee JY, Kang MS, Lee HJ, Kang SI, Lee OM, Kwon YK, and Kim JH (2021). Comparative characteristics and zoonotic potential of avian pathogenic *Escherichia coli* (APEC) isolates from chicken and duck in South Korea. Microorganisms, 9(5): 946. DOI: https://www.doi.org/10.3390/microorganisms9050946

Kabir S (2010). Avian colibacillosis and salmonellosis: A closer look at epidemiology, pathogenesis, diagnosis, control and public health concerns. International Journal of Environmental Research *and* Public Health, 7(1): 89-114. DOI: https://www.doi.org/10.3390/ijerph7010089

Karwowska E (2024). Antibiotic resistance in the farming environment. Applied Sciences, 14(13): 5776. DOI: https://www.doi.org/10.3390/app14135776

Kissinga HD, Mwombeki F, Said K, Katakweba AAS, Nonga HE, and Muhairwa AP (2018). Antibiotic susceptibilities of indicator bacteria *Escherichia coli* and *Enterococci* spp. isolated from ducks in Morogoro Municipality, Tanzania. BMC Research Notes, 11: 87. DOI: https://www.doi.org/10.1186/s13104-018-3201-4

Luo S, Liao C, Peng J, Tao S, Zhang T, Dai Y, Ding Y, and Ma Y (2023). Resistance and virulence gene analysis and molecular typing of *Escherichia coli* from duck farms in Zhanjiang, China. Frontiers in Cellular and Infection Microbiology, 13: 1202013. DOI: https://www.doi.org/10.3389/fcimb.2023.1202013

Magiorakos AP, Srinivasan A, Carey RB, Carmeli Y, Falagas ME, Giske CG, Harbarth S, Hindler JF, Kahlmeter G, Olsson-Liljequist B et al. (2012). Multidrug-resistant, extensively drug-resistant and pandrug-resistant bacteria: An international expert proposal for interim standard definitions for acquired resistance. Clinical Microbiology and Infection, 18(3): 268-281. DOI: https://www.doi.org/10.1111/j.1469-0691.2011.03570.x

Majumder S, Akter MM, Islam MM, Hussain K, Das S, Hasan I, Nazir KHMNH, and Rahman M (2017). Prevalence, isolation and detection of virulent gene in *Escherichia coli* from duck. Journal of Advances in Medicine and Medical Research, 20(2): 1-8. DOI: https://www.doi.org/10.9734/BJMMR/2017/32003

Ministry of agriculture and rural development (MARD) (2011). National technical regulation on Animal diseases - General requirements for sample collection, storage and shipment. QCVN 01-83: 2011/BNNPTNT. Available at: https://sgtvt.bacninh.gov.vn/documents/154127/14279228/QCVN+01-83-2011-BNNPTNT.pdf/2a692d85-15d0-445c-969e-8964f5dadcad

Punnoose P, Vineetha S, and Mahesh M (2021). Current scenario and pathology of duck diseases - A systematic review. Indian Journal of Veterinary Pathology, 45(4): 242-65. DOI: http://www.doi.org/10.5958/0973-970X.2021.00046.8

Reham ME, Al-Shaimaa TH, and Tamer MEF (2023). Virulence, resistance profile, antimicrobial resistance genes of ESBLs, XDR *Escherichia coli* isolated from ducks. Journal of Advanced Veterinary Research, 13(3): 425-430. Available at: https://advetresearch.com/index.php/AVR/article/view/1253/711

Roshdy H, Abd El-Aziz S, and Refai M (2012). Incidence of *E. coli* in chickens and ducks in different governorates in Egypt, 1st Conference Animal Health Research Institute Association, Cairo. pp. 420-426. Available at: http://scholar.cu.edu.eg/sites/default/files/hanem/files/incidence_of_e_coli_in_poultry.pdf

Sang NH, Thu HTV, and Khai LTL (2017). Study on the infection rate and antimicrobial resistance of *Escherichia coli* in ducks in Dong Thap province. Can Tho University Journal of Sciences, 50b: 59-66. DOI: https://www.doi.org/10.22144/ctu.jvn.2017.037

Singh A, Khan MSR, Saha S, Hassan J, and Roy U (2012). Isolation and detection of antibiotic sensitivity pattern of *Escherichia coli* from ducks in Bangladesh and Nepal. Microbes and Health, 1(1): 6-8. DOI: https://www.doi.org/10.3329/mh.v1i1.13704

Thuan C and Khai LTL (2018). Isolation and investigation of the antibiotic resistance of *Escherichia coli* bacteria in Vinh Long provinces. Can Tho University Journal of Sciences, 54(6): 63-71. DOI: https://www.doi.org/10.22144/ctu.jvn.2018.097

Thu HTV, Anh DT, and Dong LV (2019). *Escherichia coli* infection in ducks in the Mekong Delta: bacterial isolation, serogroup distribution and antibiotic resistance. Can Tho University Journal of Sciences, 11(1): 24-29. DOI: https://www.doi.org/10.22144/ctu.jen.2019.003

Trang LTT, Thu HTV, and Khai LTL (2017). Prevalence and antibiotic resistance of *Escherichia coli* strains injected in ducks in Hau Giang province. Can Tho University Journal of Sciences, 50b: 44-50. DOI: https://www.doi.org/10.22144/ctu.jvn.2017.035

Vui DT and Tiep NB (2016). Isolation and characterization of *Escherichia coli* in of Bau and Dom ducks at Dai Xuyen duck breeding and research center. Vietnam Journal of Agricultural Sciences, 14(12): 1894-1902. Available at: https://vjol.info.vn/index.php/hvnn/article/view/31135/26396

Yanestria SM, Dameanti FNAEP, Musayannah BG, Pratama JWA, Witaningrum AM, Effendi MH, and Ugbo EN (2022). Antibiotic resistance pattern of extended-spectrum β-Lactamase (ESBL) producing *Escherichia coli* isolated from a broiler farm environment in Pasuruan district, Indonesia. Biodiversitas, 23(9): 4460–4465. DOI: https://www.doi.org/10.13057/biodiv/d230911

Publisher's note: Scienceline Publication Ltd. remains neutral with regard to jurisdictional claims in published maps and institutional affiliations.

Open Access: This article is licensed under a Creative Commons Attribution 4.0 International License, which permits use, sharing, adaptation, distribution and reproduction in any medium or format, as long as you give appropriate credit to the original author(s) and the source, provide a link to the Creative Commons licence, and indicate if changes were made. The images or other third party material in this article are included in the article's Creative Commons licence, unless indicated otherwise in a credit line to the material. If material is not included in the article's Creative Commons licence and your intended use is not permitted by statutory regulation or exceeds the permitted use, you will need to obtain permission directly from the copyright holder. To view a copy of this licence, visit https://creativecommons.org/licenses/by/4.0/.
© The Author(s) 2025

2025, Scienceline Publication
World's Veterinary Journal
World Vet J, 15(4): 1113-1119.
ISSN 2322-4568

DOI: https://dx.doi.org/10.54203/scil.2025.wvj114
PII: S232245682500114-15

Foot and Mouth Disease Virus Detection in Bali Cattle (*Bos sondaicus*) by RT-PCR in Lombok Island

Kholik Kholik[1]*, Akhmad Sukri[2], Ieke Wulan Ayu[3], Reviany Vibrianita Nidom[4], and Setyarina Indrasari[4]

[1]*Department of Veterinary Public Health, Faculty of Veterinary Medicine, Universitas Pendidikan Mandalika, Mataram City, 83125, Indonesia*
[2] *Department of Biology Education, Faculty of Science and Engineering, Universitas Pendidikan Mandalika, Mataram City, 83125, Indonesia*
[3]*Department of Argotechnology, Faculty of Agriculture, Universitas Samawa, Sumbawa Besar City, 84316, Indonesia*
[4]*Professor of Nidom Foundation, Surabaya City, 60115, Indonesia*

*Corresponding author's Email: kholiqvet@gmail.com

SHORT COMMUTATION
Received: October 03, 2025
Revised: November 08, 2025
Accepted: December 05, 2025
Published: December 31, 2025

ABSTRACT

Aphthovirus is responsible for foot-and-mouth disease (FMD) in cloven-hoofed animals, a highly infectious disease that has significant economic repercussions in various countries, including Indonesia. The present study aimed to use reverse transcription polymerase chain reaction (RT-PCR) to detect FMD in suspected Bali cattle in West Lombok, Indonesia. The current study was an observational, descriptive investigation conducted from July to August 2025, collecting 15 swab samples from male Bali cattle with an average weight of 210 kilograms and an average age of 2 years old. The samples were collected via purposive sampling from cattle demonstrating clinical signs of FMD, specifically from oral vesicular fluid. The samples were sourced from two smallholder farms in West Lombok; farm one, with 12 samples, and farm two, with three samples. The FMD was identified with a prevalence rate of 20% (3 out of 15), and a 328 bp DNA fragment was detected during gel electrophoresis. The current result indicated that the virus pathogen was detected in 20% of samples, and RT-PCR can be used as a high-sensitivity diagnostic method for this disease.

Keywords: Bali cattle, Foot-and-Mouth disease, PCR, Reverse transcription

INTRODUCTION

Bali cattle (*Bos sondaicus*), known for their high productivity and genetic diversity, are among Indonesia's most valuable livestock (Saili, 2020; Hayanti et al., 2022). Bali cattle are essential to Indonesia's food security, offering villagers both income and a source of livestock protein. These cattle are distributed across Indonesia, notably on Lombok Island in West Nusa Tenggara. According to the Central Statistics Agency of West Nusa Tenggara Province, Indonesia, there were 1,219,784 Bali cattle recorded in the province in 2022 (BPS, 2020; 2024).

Lombok Island supplies beef to several regions in Indonesia through the 1,000 Cattle Village program. This program is a government policy to achieve food self-sufficiency, initiated by a pilot project in West Nusa Tenggara Province, which is one of the five largest beef cattle-producing provinces in Indonesia. Since 2013, Lombok Island has encompassed around 504 livestock farmer groups, of which 238 comprised novice and conventional farmers. Considering the potential of Bali cattle, which are beef-producing cattle in West Nusa Tenggara Province, the existence of Bali cattle farms is crucial for supporting the national food security (Ranta et al., 2022). Since 2022, Foot-and-Mouth Disease (FMD) has become a major problem on Lombok Island, especially in Central Lombok, where 28,612 cases have been reported out of a cattle population of 323,232 (Bani and Asruddin, 2022; Septiani et al., 2023).

Cattle farming is particularly economically affected by FMD. In non-endemic countries, the economic impact of FMD can exceed US$1.5 billion annually, while in endemic areas, losses can range from US$6.5 billion to US$21 billion (Knight-Jones and Rushton, 2013). There are seven serotypes of the RNA virus that cause FMD, including O, A, C, Asia 1, SAT 1, SAT 2, and SAT 3, which belong to the genus Aphthovirus within the Picornaviridae family (Grubman and Baxt, 2004). Indicators of Foot-and-Mouth Disease (FMD) in cattle encompass fever (40°C), diminished appetite, decreased rumen activity, excessive salivation, lowered milk yield, difficulty breathing, rapid breathing, and groaning. Additionally, there may be vesicular lesions, erosions, and ulcers observed in the oral cavity, interdigital spaces, as well as on the muzzle and teats (Mohebbi et al., 2017). The FMD in Indonesia is a disease that has reemerged, with historical records indicating its presence as early as 1887 (Zainuddin et al., 2022). The FMD spreads rapidly and has caused outbreaks in several regions worldwide, including Indonesia. The FMD virus circulating in Southeast Asia is serotype O, topotype ME-SA, which has been widely reported in Myanmar and Thailand (Bo et al., 2019;

To cite this paper: Kholik K, Sukri A, Ayu IW, Nidom RV, and Indrasari S (2025). Foot and Mouth Disease Virus Detection in Bali Cattle (*Bos sondaicus*) by RT-PCR in Lombok Island. *World Vet. J.*, 15(4): 1113-1119. DOI: https://dx.doi.org/10.54203/scil.2025.wvj114

Chanchaidechachai et al., 2021). The FMD outbreak in Indonesia occurred in May 2022 and was detected with serotype O/ME-SA/Ind-2001 (Susila et al., 2023).

The FMD virus particles can be detected using a sandwich enzyme-linked immunosorbent assay (ELISA) and reverse transcription polymerase chain reaction (RT-PCR). The main advantage of RT-PCR over ELISA for detecting FMD in cattle is its significantly higher sensitivity (Paixão et al., 2008). The reported sandwich ELISA for FMD virus targeting the VP1 protein achieved 100% specificity and 80% sensitivity, though positive results require verification by a neutralization test. Conversely, a multiplex PCR test exhibited 100% specificity but only minimal sensitivity (Sharma et al., 2015). In 2023, a study indicated that 58% of cattle in Lomongan and Surabaya, East Java, were infected with FMD as detected by RT-PCR (Dinana et al., 2023). Another study on the diagnosis of FMD in field conditions in Brazil, using RT-PCR, identified three positive samples out of 260 oral swabs, which were collected from cattle in areas with FMD outbreaks (Paixão et al., 2008).

Several initiatives have been undertaken on Lombok Island to overcome FMD. These strategies include educating livestock farmers through participatory methods that emphasize early detection, implementing biosafety and biosecurity vaccination programs, and addressing the impact of livestock movement and regulations (Kholik et al., 2024). Government and community efforts to combat FMD have been inadequate, resulting in an FMD outbreak in Lombok Island, potentially allowing the virus to remain in the environment, infecting susceptible animals, and becoming a source of FMD transmission. The virus can only survive long-term when it is repeatedly brought in from outside the herd (McLachlan et al., 2019). Theoretically, an alternative mechanism for the presence of the FMD virus in a region could be the carrier's ability to support its persistence (Guyver-Fletcher et al., 2022). Accurate detection of FMD virus in susceptible animals is essential as an initial step, supported by surveillance of carriers and the environment, and accompanied by increased public knowledge to overcome FMD disease. Humphreys et al. (2025) stated that critical knowledge gaps in FMD epidemiology hinder effective control of FMD.

According to Ministry of Agriculture Decree No. 708 of 2024, all regencies in Bali and West Nusa Tenggara, Indonesia, are affected by FMD (Denpasar Veterinary Center, 2025). Molecular-based investigations on FMD virus in smallholder livestock are essential for early detection and accurate diagnosis using RT-PCR to prevent transmission. Several studies have used RT-PCR to detect and perform initial screening for FMD virus in cattle. Given the large number of smallholder farms, especially in West Lombok, early detection of the FMD virus is critically important. This study would be a novel approach for practical field application, enabling fast, accurate diagnosis and early warning detection to help eradicate FMD virus transmission. The current study aimed to detect FMD virus in Bali cattle on smallholder farms in West Lombok, Indonesia, using RT-PCR based on clinical signs.

MATERIALS AND METHODS

Ethical approval

This study was conducted according to the guidelines of Mandalika University, Mataram, Indonesia. The Samples of vesicular fluid were collected for FMD virus analysis under the supervision of a veterinarian from the Faculty of Veterinary Medicine, Mandalika University of Education, Mataram, Indonesia, with 129/C3/DT.05.00/PL/2025 contract number.

Study design

The present observational descriptive study was conducted from July to August 2025, focusing on Bali cattle on two smallholder farms on Lombok Island, West Nusa Tenggara Province, Indonesia, bordering Bali Island. This border area has the potential for FMD transmission between different regions due to the presence of Lembar Port (a trade center). These farms were suspected of FMD infection and exhibited FMD-like signs. Purposive sampling was used to select animals exhibiting signs of FMD. The male Bali cattle, around 2 years old with an average weight of 210 kg, were observed for clinical signs of FMD, including nasal discharge, oral lesions, and muscle weakness. The sample size for the Bali cattle nasal vesicular fluid swab was determined using the Thrusfield formula for detecting disease in the population (Thrusfield, 2007).

Sample collection

Sampling was conducted from July to August 2025 following the protocol established by Edwards et al. (2024). A total of 15 nasal swab samples were collected from Bali cattle showing clinical signs of FMD on two smallholder farms in West Lombok, Indonesia. These farms were the Gerung People's Farm, located at latitude -8.686738° and longitude 116.0941378 (8°41'12.3"S 116°05'38.9" E; Farm 1), and the Lembar People's Farm, located at latitude -8.767573 and longitude 116.074415 (8°46'03.3"S 116°04'27.9"E; Farm 2; Figure 1). From the first farm, with a population of 50 Bali

cattle, 12 samples were collected, and from the second farm, with 10 Bali cattle, three samples were collected. The samples were collected by swabbing vesicular lesions and oral discharge directly from the cattle using a sterile swab. The collected samples were stored at -80°C in the laboratory of the Faculty of Veterinary Medicine at Mandalika University of Education, Mataram, Indonesia, until further analysis (Edwards et al., 2024). The samples were then transferred to the diagnostic laboratory at the Professor Nidom Foundation, Indonesia, in an ice box.



Figure 1. Sampling locations. Location marked with an asterisk, number 1 is the Gerung smallholder farm, Gerung City, Indonesia. Location marked with an asterisk, number 2 is Lembar smallholder farm, Lembar City, Indonesia (Source: Google Maps)

Extraction of RNA virus

Following the manufacturer's instructions, FMD viral RNA was extracted from samples using the QiAamp viral RNA mini kit (Qiagen, Hilden, Germany) and eluted in 50 µL of nuclease (DNase)-free water (Edwards et al., 2024).

RT-PCR procedure

Viral RNA was amplified by RT-PCR using universal primers, including the forward primer 5′-GCCTGGTCTTTCCAGGTCT-3′ and the reverse primer 5′-CCAGTCCCCTTCTCAGATC-3′ (Reid et al., 2000), resulting in an amplicon of 328 bp.The PCR reaction mixture was prepared by combining 4 µl of 5× first-strand buffer, 2 µl of acetylated bovine serum albumin (1 mg/ml), 1 µl of dNTPs (10 mM), 0.2 µl of dithiothreitol (DTT; 1 M), and 1 µl of Moloney murine leukemia virus reverse transcriptase (200 U/µl). The amplification protocol consisted of an initial pre-denaturation at 94 °C for 5 min, followed by denaturation at 94 °C for 20 s, annealing at 55 °C for 1 min, and extension at 72 °C for 2 min. A final extension step was performed at 72 °C for 7 min. The PCR was conducted for a total of 35 cycles (WOAH, 2022). According to the study by Dinana et al. (2023), the results of FMD viral amplification by RT-PCR were visualized on an agarose gel 2%.

RESULTS AND DISCUSSION

Bali cattle examined on two farms exhibited FMD-like clinical signs, including lesions on the snout, hypersalivation, fever, and hoof lesions (Figure 2). The RT-PCR results of the vesicular fluid swabs yielded a 20% FMD detection rate (3/15). One positive FMD sample out of 12 samples collected from smallholder Farm 1, and two positive FMD samples out of three samples collected from smallholder Farm 2. Additionally, the presence of the 328 bp DNA band on gel electrophoresis indicated a positive result for FMD virus infection in Bali cattle (Figures 3 and 4).

These current results, demonstrating a 20% detection rate for FMD, are consistent with those of Dinana et al. (2023) in Lamongan and Surabaya, Indonesia, who used RT-PCR with universal primers and detected the 328 bp FMD virus segment in symptomatic cattle. In Al-Qadisiyah Province, Iraq, FMD has been detected in 73 samples (75.3%) using RT-PCR with universal primers at 330 bp (Mansour et al., 2018). The differences between the present results and other studies using RT-PCR are likely due to genetic variation in the virus. Although universal primers are designed to detect all strains of FMD virus, differences in viral genetic sequences can prevent efficient primer annealing. Meanwhile, Sharma et al. (2015) indicated that the detection of FMD virus using the VP1 target region protein in a sandwich ELISA should be confirmed by a neutralization test, which is more time-consuming. To confirm a suspected FMD diagnosis based on clinical signs, RT-PCR was performed on persistently infected cattle under field conditions on a dairy farm in India following the natural FMD outbreak (Biswal et al., 2019).



Figure 2. The clinical signs of foot and mouth disease in Bali cattle in West Lombok Regency of West Nusa Tenggara Province, Indonesia. **a**: The erosions on the nose (arrow), **b**: Hypersalivation (arrow), **c:** The ulcers in the mouth (arrow), **d:** The erosive lesions on the foot (arrow); Source: Authors of the current study.

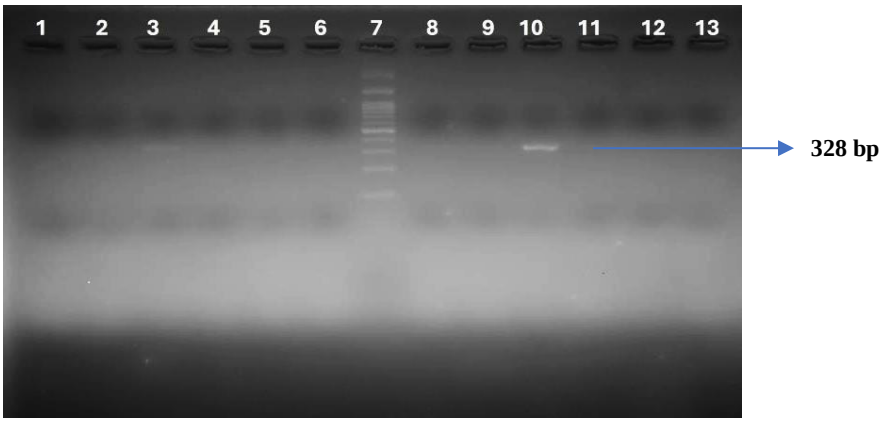


Figure 3. The RT-PCR product analysis using 2% agarose gel electrophoresis from Gerung smallholder farm in Gerung City, West Lombok Regency, West Nusa Tenggara, Indonesia (location 1). Lane 7: 100 bp marker ladder, lane 11: Positive bands of FMD at 328 bp, lanes 1,2,3,4,5,6,8,9,11,12,13: Negative bands of FMD.

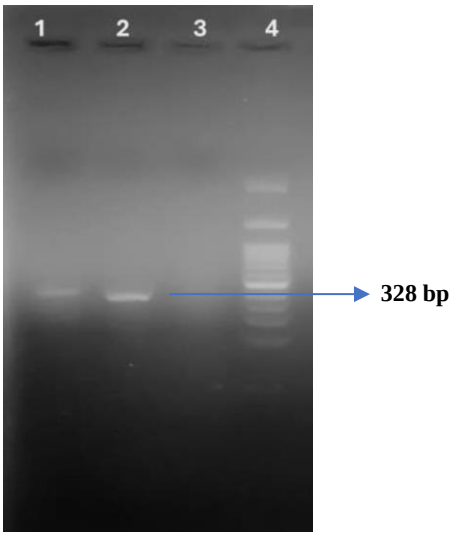


Figure 4. The RT-PCR product analysis using 2% agarose gel electrophoresis from Lembar smallholder farm in Lembar City, West Lombok Regency of West Nusa Tenggara Province, Indonesia (location 2). Lane 4: 100 bp marker ladder, lanes 1 and 2: Positive bands of FMD at 328 bp, lane 3: Negative bands of FMD

Detecting FMD virus from nasal vesicular swabs in Bali cattle with RT-PCR was quick and precise, and it was a non-invasive method that simplified data collection for field veterinary officers. This enabled a timely response, thereby helping to control the transmission of FMD. The RT-PCR method for early detection of FMD in cattle provides benefits over ELISA, as it is more precise in identifying small quantities of viral genetic sequences, such as RNA. The ELISA typically detects viral antibodies, which do not necessarily indicate active infection (Brahma et al., 2024). The laboratory

results indicated that RT-PCR can provide a definitive diagnosis in supernatant fluid from cell cultures inoculated at the first passage, and its sensitivity is greater than that of ELISA in vesicular epithelial suspensions and at least equivalent to virus isolation in cell cultures in FMD examinations (Reid et al., 2023). The RT-PCR is an effective method for detecting FMD in the field compared to virus isolation and ELISA (Paixão et al., 2008). In Brazil, RT-PCR was used as a diagnostic tool to verify FMD in the field. Out of 460 oral swabs taken from cattle in both affected and FMD-free regions, three samples from areas experiencing FMD outbreaks tested positive via RT-PCR, whereas only two samples were confirmed positive through virus isolation and ELISA (Paixão et al., 2008). In Iraq, RT-PCR was conducted using primers for VP1 serotype O as the initial diagnostic examination for FMD in cattle from local farms in Sulaimani province. Phylogenetic analysis indicated that the resulting isolates were Pakistani (KU365843) and Iranian (KY091283) strains, with sequence identities of 96.00% and 95.00%, respectively (Baba Sheikh et al., 2021).

In a study conducted by Reid et al. (2000), RT-PCR detected the virus in 85% of 28 epithelial suspension samples, whereas ELISA yielded a lower detection rate of 62%. A previous study in Punjab, Pakistan, employing RT-PCR with the universal VP1 primer pair P1/P2 on 250 tissue and 175 secretion samples, detected FMD in 72.8% of tissue samples and 52.6% of secretion samples from cattle, buffalo, and goats (Saeed et al., 2011).

A research was carried out in West Lombok Regency, located in the West Nusa Tenggara Province of Indonesia, which shares a border with Bali. Consequently, this closeness presented a risk of transmission, given that the FMD virus has demonstrated the ability to easily cross-national boundaries and trigger epidemics in regions that are free from the disease (Mansour et al., 2018). Additionally, the FMD virus can spread rapidly without proper and immediate control measures. This risk was heightened on Lombok Island, where smallholder farms used conventional practices with minimal biosecurity and inadequate disinfection. Furthermore, the presence of animals such as goats, sheep, and buffalo around the farm could pose a risk, as they may carry the FMD virus. A study on FMD risk factors in East Java, Indonesia, found that the absence of routine disinfection (OR = 3.98) and the sharing of equipment with infected animals (OR = 3.39) were considerably associated with disease outbreaks (Rehman et al., 2025). Detecting FMD virus in Bali cattle using RT-PCR facilitated accurate diagnosis from molecular-based field isolates, enabling identification of the virus type and informing vaccination strategies. Moreover, RT-PCR helped trace transmission sources and supported control of FMD outbreaks in regions.

CONCLUSION

The RT-PCR method determined a prevalence rate of 20% for the FMD virus in the 15 collected samples (3 positive out of 15), with a 328 bp DNA fragment. The current results provided a deeper understanding of FMD virus distribution in the study area, serving as critical information for mapping viral distribution and informing effective FMD control strategies on Lombok Island. Further analysis of PCR product sequencing is essential to identify FMD viruses associated with the Indonesian government's vaccination program. In addition, FMD virus surveillance and monitoring of vaccination results are very necessary to anticipate the emergence of new strains of the FMD virus.

DECLARATIONS

Funding

The present study was financially supported by Direktorat Jenderal Riset dan Pengembangan (Risbang), Kementerian Pendidikan Tinggi, Sains, and Teknologi through the Penelitian Fundamental Regular scheme for the 2025 fiscal year under contract numbers 129/C3/DT.05.00/PL/2025 and 2166/LL8/AL.04/2025.

Acknowledgments

The authors would like to express gratitude to the Direktorat Penelitian dan Pengabdian kepada Masyarakat (DPPM), Direktorat Jenderal Riset dan Pengembangan (Risbang), Kementerian Pendidikan Tinggi, Sains, dan Teknologi, Indonesia for funding this study through the Penelitian Fundamental Regular scheme for the 2025 fiscal year under contract numbers 129/C3/DT.05.00/PL/2025 and 2166/LL8/AL.04/2025. The authors would like to thank Mandalika University of Education and Professor Nidom Foundation for facilitating the implementation of the present study.

Authors' contributions

Kholik Kholik conceptualized and designed the study, collected samples, and prepared the manuscript. Akhmad Sukri designed the methodology and directed the study. Ieke Wulan Ayu assisted in the research process, edited, and checked the writing of the manuscript. Reviany Vibrianita Nidom and Setyarina Indrasari conducted sample examinations in the laboratory and data analysis. All authors read and approved the final edition of the manuscript for processing and publication in the present journal.

Availability of data and materials
All data and materials are available upon reasonable request from the corresponding author.

Competing interests
The authors declare no conflict of interest.

Ethical considerations
Ethical issues, including plagiarism, consent to publish, misconduct, data fabrication and/or falsification, double publication and/or submission, and redundancy, have been checked by all the authors. The authors confirmed that AI tools has not been used during this research.

REFERENCES

Baba Sheikh M, Rashid PA, Raheem Z, Marouf AS, and Amin KM (2021). Molecular characterization and phylogenetic analysis of foot and mouth disease virus isolates in Sulaimani province, Iraq. Veterinary Research Forum, 12(2): 247-251. DOI: https://www.doi.org/10.30466/vrf.2019.101755.2424

Bani AU and Asruddin A (2023). Detection of foot and mouth disease in cattle by applying the naive bayes method. Journal of Computer System and Informatics, 3(4): 264-268. DOI: https://www.doi.org/10.47065/josyc.v3i4.1934

Biswal JK, Ranjan R, Subramaniam S, Mohapatra JK, Patidar S, Sharma MK, Bertram MR, Brito B, Rodriguez LL, Pattnaik B et al. (2019). Genetic and antigenic variation of foot-and-mouth disease virus during persistent infection in naturally infected cattle and Asian buffalo in India. PloS One, 14(6): e0214832. DOI: https://www.doi.org/10.1371/journal.pone.0214832

Bo LL, Lwin KS, Ungvanijban S, Knowles NJ, Wadsworth J, King DP, Abila R, and Qiu Y (2019). Foot-and-mouth disease outbreaks due to an exotic serotype Asia 1 virus in Myanmar in 2017. Transboundary and Emerging Diseases, 66(2): 1067-1072. DOI: https://www.doi.org/10.1111/tbed.13112

Brahma D, Sharma K, Barman NN, Deka P, Borah B, Buragohain BM, Ahmed R, and Hazarika R (2024). Comparing typing methods for foot-and-mouth disease virus serotypes: Sandwich ELISA, multiplex PCR, RT-LAMP and SYBR green real-time PCR. Indian Journal of Animal Research, 1: 9. DOI: https://www.doi.org/10.18805/IJAR.B-5417

Chanchaidechachai T, de Jong MCM, and Fischer EAJ (2021). Spatial model of foot-and-mouth disease outbreak in an endemic area of Thailand. Preventive Veterinary Medicine, 195: 105468. DOI: https://www.doi.org/10.1016/j.prevetmed.2021.105468

Denpasar Veterinary Center (2025). Animal disease status map in the Denpasar Veterinary Center's work Area in 2024. Ministry of Agriculture, Directorate General of Animal Husbandry and Animal Health, Denpasar, pp. 7-9. Available at: https://bbvdps.ditjenpkh.pertanian.go.id/storage/master/file/D84yLeFS_Laporan_Peta_situasi_status_Penyakit_hewan_revisi.pdf

Dinana Z, Rantam FA, Suwarno S, Mustofa I, Rahmahani J, and Kusnoto K (2023). Detection of foot and mouth disease virus in cattle in Lamongan and Surabaya, Indonesia using RT-PCR Method. Jurnal Medik Veteriner, 6(2): 191-196. DOI: https://www.doi.org/10.20473/jmv.vol6.iss2.2023.191-196

Edwards N, Reboud J, Yan X, Guo X, Cooper JM, Wadsworth J, Waters R, Mioulet V, King DP, and Shaw AE (2024). Detection of foot-and-mouth disease virus RNA using a closed loop-mediated isothermal amplification system. Frontiers in Microbiology, 15: 1429288. DOI: https://www.doi.org/10.3389/fmicb.2024.1429288

Grubman MJ and Baxt B (2004). Foot-and-mouth disease. Clinical Microbiology Reviews, 17(2): 465-493. DOI: https://www.doi.org/10.1128/cmr.17.2.465-493.2004

Guyver-Fletcher G, Gorsich EE, and Tildesley MJ (2022). A model exploration of carrier and movement transmission as potential explanatory causes for the persistence of foot-and-mouth disease in endemic regions. Transboundary and Emerging Diseases, 69(5): 2712-2726. DOI: https://wwww.doi.org/10.1111/tbed.14423

Hayanti SY, Handiwirawan E, and Susilawati E (2022). Diversity of qualitative characteristics and their use to distinguish the origin of the Bali cattle population. Indian Journal of Animal Research, 56(8): 1041-1046. Available at: https://arccjournals.com/journal/indian-journal-of-animal-research/BF-1417

Humphreys JM, Stenfeldt C, King DP, Knight-Jones T, Perez AM, Vander Waal K, Sanderson MW, Di Nardo A, Jemberu WT, Pamornchainavakul N et al. (2025). Epidemiology and economics of foot-and-mouth disease: current understanding and knowledge gaps. Veterinary Research, 56(1): 141. DOI: https://www.doi.org/10.1186/s13567-025-01561-5

Kholik K, Pradana M, Al Haddar M, Nofisulastri N, Riwu KH, Dharmawibawa ID, and Sukri A (2024). Biosafety training and introduction to livestock diseases using participatory rural appraisal method in Pade Angen livestock group, East Lombok Regency. Jurnal Pengabdian UNDIKMA, 5(4): 526-533. DOI: https://www.doi.org/10.33394/jpu.v5i4.13220

Knight-Jones TJ and Rushton J (2013). The economic impacts of foot and mouth disease - what are they, how big are they and where do they occur?. Preventive Veterinary Medicine, 112(3-4): 161-173. DOI: https://www.doi.org/10.1016/j.prevetmed.2013.07.013

Mansour KA, Naser HH, and Hussain MH (2018). Clinical, molecular detection and phylogenetic analysis study of local foot-and-mouth disease virus in Al-Qadisiyah province of Iraq. Veterinary World, 11(9): 1210-1213. DOI: https://www.doi.org/10.14202/vetworld.2018.1210-1213

McLachlan I, Marion G, McKendrick IJ, Porphyre T, Handel IG, and Bronsvoort BD (2019). Endemic foot and mouth disease: Pastoral in-herd disease dynamics in sub-Saharan Africa. Scientific Reports, 9(1): 17349. DOI: https://www.doi.org/10.1038/s41598-019-53658-5

Mohebbi MR, Barani SM, and Mahravani H (2017). An uncommon clinical form of foot-and-mouth disease in beef cattle presented

with cornual skin lesions. Iranian Journal of Veterinary Research, 18(4): 291-293. DOI: https://www.doi.org/10.22099/ijvr.2017.4638

Paixão TA, Neta AV, Paiva NO, Reis JR, Barbosa MS, Serra CV, Silva RR, Beckham TR, Martin BM, Clarke NP et al. (2008). Diagnosis of foot-and mouth disease by real time reverse transcription polymerase chain reaction under field conditions in Brazil. BMC Veterinary Research, 4(1): 53. DOI: https://www.doi.org/10.1186/1746-6148-4-53

Ranta MR, Lestari PF, and Budiasa IM (2022). Standardization of Bali male cattle in accelerate genetic quality improvement and increase production to maintain national food security. Agroteksos, 31(3): 171-179. DOI: https://www.doi.org/10.29303/agroteksos.v31i3.706

Rehman S, Ullah S, Abuzahra M, Effendi MH, Budiastuti B, Kholik K, Munawarah M, Zaman A, Rahman AU, Malik MI et al. (2025). Determination of risk factors for foot and mouth disease emergence in East Java, Indonesia. Open Veterinary Journal, 15(5): 2049-2058. DOI: https://www.doi.org/10.5455/ovj.2025.v15.i5.21

Reid SM, Ferris NP, Hutchings GH, Samuel AR, and Knowles NJ (2000). Primary diagnosis of foot-and-mouth disease by reverse transcription polymerase chain reaction. Journal of Virological Methods, 89(1-2): 167-176. DOI: https://www.doi.org/10.1016/s0166-0934(00)00213-5

Reid SM, Grierson SS, Ferris NP, Hutchings GH, Alexandersen S (2023). Evaluation of automated RT-PCR to accelerate the laboratory diagnosis of foot-and-mouth disease virus. Journal of Virological Methods, 107(2): 129-139. DOI: https://www.doi.org/10.1016/s0166-0934(02)00210-0

Saili T (2020). Production and reproduction performances of Bali cattle in Southeast Sulawesi-Indonesia. IOP Conference Series: Earth and Environmental Science, 465(1): 012004. Available at: https://iopscience.iop.org/article/10.1088/1755-1315/465/1/012004

Saeed A, Khan QM, Waheed U, Arshad M, Asif M, and Farooq M (2011). RT-PCR evaluation for identification and sequence analysis of foot-and-mouth disease serotype O from 2006 to 2007 in Punjab, Pakistan. Comparative Immunology, Microbiology and Infectious Diseases, 34(2): 95-101. DOI: https://www.doi.org/10.1016/j.cimid.2009.10.004

Septiani A, Hirzi RH, and Fikriah NU (2023). Analysis spread of foot and mouth diseases (FMD) in cattle in Central Lombok Regency using Moran index in 2022. Variance: Journal of Statistics and Its Applications, 5(2): 159-168. DOI: https://www.doi.org/10.30598/variancevol5iss2page159-168

Sharma GK, Mahajan S, Matura R, Subramaniam S, Ranjan R, Biswal J, Rout M, Mohapatra JK, Dash BB, Sanyal A et al. (2015). Diagnostic assays developed for the control of foot-and-mouth disease in India. World Journal of Virology, 4(3): 295-302. DOI: https://www.doi.org/10.5501/wjv.v4.i3.295

Statistics of Nusa Tenggara Barat Province (BPS) (2020). Nusa Tenggara Barat Province in figure 2020. BPS of Nusa Tenggara Barat., Mataram, pp. 241-242. Available at: https://ntb.bps.go.id/id/publication/2020/04/27/aa55eda38b5104eafb5cf8b5/provinsi-nusa-tenggara-barat-dalam-angka-2020

Statistics of Nusa Tenggara Barat Province (BPS) (2024). Nusa Tenggara Barat Province in figure 2024. BPS of Nusa Tenggara Barat., Mataram, pp. 326-329. Available at: https://ntb.bps.go.id/id/publication/2024/02/28/375b8367273e8c7900e8174e/provinsi-nusa-tenggara-barat-dalam-angka-2024.html

Susila EB, Daulay RS, Hidayati DN, Prasetyowati SR, Wriningati, Andesfha E, Irianingsih SH, Dibia IN, Faisal, Supriyadi A et al. (2023). Detection and identification of foot-and-mouth disease O/ME-SA/Ind-2001 virus lineage, Indonesia, 2022. Journal of Applied Animal Research, 51(1): 487-494. DOI: https://www.doi.org/10.1080/09712119.2023.2229414

Thrusfield MV (2007). Veterinary epidemiology, 3rd Edition. Blackwell Science Ltd., Ames, Iowa, pp. 238-224. Available at: https://download.e-bookshelf.de/download/0003/7722/97/L-X-0003772297-0002180510.XHTML/index.xhtml

World organisation of animal health (WOAH) (2022). Foot and mouth disease (infection with foot and mouth disease virus). WOAH Terrestrial Manual 2022, Paris, France. Chapter 3.1.8, pp. 1-34. Available at: https://www.woah.org/fileadmin/Home/fr/Health_standards/tahm/3.01.08_FMD.pdf

Zainuddin N, Wicaksono A, Widiastuti T, Ekowati RV, Yupiana Y, Suandy I, Pratama ML, Elisadewi Y, Yulianti S, Fleuryantari H et al. (2022). Indonesian veterinary emergency preparedness series on foot and mouth disease (FMD). Directorate General of Animal Husbandry and Animal Health, Directorate of Animal Health. Jakarta, pp. 1-2. Available at: https://repository.pertanian.go.id/items/4bb59d44-2c89-4663-bc8f-12d334089fd97

Publisher's note: Scienceline Publication Ltd. remains neutral with regard to jurisdictional claims in published maps and institutional affiliations.

Open Access: This article is licensed under a Creative Commons Attribution 4.0 International License, which permits use, sharing, adaptation, distribution and reproduction in any medium or format, as long as you give appropriate credit to the original author(s) and the source, provide a link to the Creative Commons licence, and indicate if changes were made. The images or other third party material in this article are included in the article's Creative Commons licence, unless indicated otherwise in a credit line to the material. If material is not included in the article's Creative Commons licence and your intended use is not permitted by statutory regulation or exceeds the permitted use, you will need to obtain permission directly from the copyright holder. To view a copy of this licence, visit https://creativecommons.org/licenses/by/4.0/.
© The Author(s) 2025

2025, Scienceline Publication
World's Veterinary Journal
World Vet J, 15(4): 1120-1129.
ISSN 2322-4568

DOI: https://dx.doi.org/10.54203/scil.2025.wvj115
PII: S232245682500115-15

In Silico Study on Structure Prediction of Apical Membrane Antigen 1 in *Eimeria tenella*

Pham Hoang Son Hung[1]*, Ho Thi Dung[1], Duong Thanh Hai[1], and Tran Nguyen Thao[1]

Faculty of Animal Science and Veterinary Medicine, University of Agriculture and Forestry, Hue University, Hue city, 49000, Vietnam

*Corresponding author's Email: phamhoangsonhung@hueuni.edu.vn

SHORT COMMUTATION
Received: September 29, 2025
Revised: October 27, 2025
Accepted: November 30, 2025
Published: December 31, 2025

ABSTRACT

The micronemal apical membrane antigen 1 (AMA1) has been demonstrated to be critical for host cell invasion by apicomplexan parasites. The present study predicted the structure of *Eimeria tenella* AMA1 (EtAMA1) using AlphaFold3. The structural model ranked first by AlphaFold3 was selected for analysis after removing unreliable regions. Comparative structural analyses were performed between the resulting EtAMA1 model and the well-characterized *Plasmodium falciparum* AMA1 (PfAMA1) using PyMOL. The results indicated that domains I and II of EtAMA1 may adopt the PAN motif (a conserved structural fold consisting of a five-stranded β-sheet and an α-helix) stabilized by five disulfide bonds, similar to PfAMA1. In addition, aromatic residues within the ligand binding pocket of PfAMA1 are conserved in EtAMA1, except for the critical Y251. The Proline-rich DII loop at the corner of the conserved hydrophobic pocket in EtAMA1 is shorter than that of PfAMA1, which possibly makes the hydrophobic pocket wider. Notably, domain III of *Et*AMA1 is predicted to form a three-stranded β-sheet with no disordered loop and α-helix, which is different from *Plasmodium* AMA1 structures. The present study provided preliminary information on structural divergences of EtAMA1, based on AlphaFold3 prediction, underscoring the need for experimental validation and investigation of possible implications for the parasite invasion mechanism.

Keywords: Apical membrane antigen 1, Domain, Hydrophobic pocket, *Eimeria tenella*

INTRODUCTION

Coccidiosis, caused by the apicomplexan parasites of the genus *Eimeria*, is a common and devastating disease in the poultry industry, especially in broiler production (Blake et al., 2020). Seven pathogenic *Eimeria* species in chickens, including *Eimeria acervuline (E. acervuline), E. brunetti, E. praecox, E. mitis, E. necatrix, E. maxima,* and *E. tenella*, invade and damage specific sites in the chicken's gastrointestinal tract (Mathis et al., 2025). For example, *E. tenella* infects the ceca, while *E. maxima* invades the small intestine. Clinical symptoms of coccidiosis include diarrhea, reduced weight gain, and reduced feed conversion (Quiroz-Castaneda, 2018). Severe intestinal lesions leading to hemorrhagic necrosis may occur, ultimately resulting in mortality (Pham et al., 2021).

Eimeria parasites are placed within the phylum *Apicomplexa* with the human malaria parasite Plasmodium and other well-known parasites, including *Toxoplasma*, *Babesia*, *Cryptosporidium*, and *Theileria*. Despite their diverse hosts and life cycles, apicomplexan parasites employ a broadly conserved mechanism to invade host cells. Central to the invasion process is the formation of a moving junction (MJ) that requires the apical membrane antigen 1 (AMA1), which is secreted by micronemes and translocated to the parasite apical surface, to interact with the rhoptry neck protein 2 (RON2), which is secreted by rhoptries and inserted into the host cell membrane (Besteiro et al., 2009; 2011; Lamarque et al., 2011; Srinivasan et al., 2011; Tonkin et al., 2011; Harvey et al., 2014). The direct interaction between AMA1 and RON2 were first confirmed in *Toxoplasma gondii* (Besteiro et al., 2009) and later in *Plasmodium falciparum* (Srinivasan et al., 2011; Lamarque et al., 2011; Tonkin et al., 2011). AMA1 is a type I integral membrane protein, comprising a disordered N-terminal tail, the ectodomain (or extracellular domain), a single-helix transmembrane domain, and finally a C-terminal cytosolic tail. The ectodomain, composed of domain I (DI), domain II (DII), and domain III (DIII), forms the core and most essential structural element of AMA1. On the ectodomain of AMA1, the key binding site of RON2 is located at the hydrophobic pocket defined by residues at the apical surface of DI and a loop from DII (denoted as DII loop; Besteiro et al., 2011; Srinivasan et al., 2011; Tonkin et al., 2011). The base of this hydrophobic pocket contains hydrophobic residues that are conserved across various apicomplexan parasites, while polymorphic residues are located at the margin of the pocket (Bai et al., 2005). Based on its role in host cell invasion, AMA1 has been extensively studied as a potential vaccine candidate against the life-threatening malaria disease. Early clinical trials indicated that immunization with heterogenous AMA1 elicited protective immunity against *Plasmodium falciparum* (Chuang et al., 2013). Antibodies targeted DIII of PfAMA1 have been shown to impair erythrocyte penetration of merozoite

To cite this paper: Hung PHS, Dung HT, Hai DT, and Thao TN (2025). *In Silico* Study on Structure Prediction of Apical Membrane Antigen 1 in *Eimeria tenella. World Vet. J.*, 15(4): 1120-1129. DOI: https://dx.doi.org/10.54203/scil.2025.wvj115

Plasmodium falciparum, demonstrating that DIII contributes to functional epitopes that can be targeted to generate vaccines (Nair et al., 2002). However, the high polymorphism of PfAMA1 reduces its effectiveness as a vaccine (Ouattara et al., 2012). For *Eimeria* parasites that cause coccidiosis in birds, host cell invasion may also require the formation of the AMA1-RON2 complex, which is essential for the host cell invasion, analogous to what is found in *Plasmodium* (Wang et al., 2020). A study revealed that *Eimeria tenella* apical membrane antigen 1 (EtAMA1) is predominantly expressed at the sporozoite stage, during which the parasites invade the chick cecum's epithelial cells (Li et al., 2018). The recombinant *E. maxima* AMA1 (EmAMA1) expressed in *E. tenella*, when used as a vaccine component against *E. maxima*, provided partial protection against coccidiosis in chickens (Pastor-Fernandez et al., 2018). Similarly, inoculation of transgenic Lactic bacteria expressing EtAMA1 induced adaptive immune response (Liu et al., 2020) and mitigated oocyst shedding and cecal lesion severity in chicks challenged with homologous *E. tenella* (Li et al., 2018).

Despite the relevance of *Eimeria* AMA1 as a vaccine target for coccidiosis, the three-dimensional structure of AMA1 from *Eimeria* has not yet been experimentally determined. A search on the Protein Data Bank (PDB) identified no structural entries for *Eimeria* AMA1, confirming a significant gap in current knowledge and underscoring the need for structural prediction and comparative analysis of EtAMA1. In the present study, the 3D structure of *Eimeria tenella* apical membrane antigen 1 (EtAMA1) was predicted by AlphaFold3 and compared with previously characterized *Plasmodium* AMA1 structures to identify possible conserved and divergent features.

MATERIALS AND METHODS

Protein sequences

Protein sequences used for the multiple sequence alignment and structure prediction in the present study were retrieved from NCBI (Table 1).

Table 1. Protein sequences of apical membrane antigen 1 from *Plasmodium faciparum*, and different *Eimeria* species used for the sequence alignment

Protein	Species	NCBI accession number	Sequence length (amino acids)
PfAMA1	*Plasmodium falciparum*	UIH11214.1	622
EtAMA1	*Eimeria tenella*	AEJ33058.1	536
EmAMA1	*Eimeria maxima*	SNT95431.1	539
EiAMA1	*Eimeria intestinalis*	WIW69503.1	549
EbAMA1	*Eimeria brunetti*	BAM16294.1	551

Sequence alignment

Multiple sequence alignment was carried out using Clustal W in MEGAX 10.2.6 with gap-open penalties set to 10 and gap-extension penalties set to 0.2. Results were visualized using ESPript 3 (Robert and Gouet, 2014). The identical percentage was calculated by pairwise alignment between two sequences using MEGAX 10.2.6 with gap-open penalties set to 10 and gap-extension penalties set to 0.2.

Protein structure prediction

The full-length amino acid sequence of EtAMA1 (536 amino acids) was used for structural prediction with AlphaFold3 (AF3) under default settings (Abramson et al., 2024). AF3 outputted five structural models, which were ranked by the ranking _score, which incorporated the predicted template modeling (pTM) to reflect the global reliability of the predicted structure, a penalty for steric clashes, and a small gain for predicted disorder (Jumper et al., 2021; Abramson et al., 2024). The model ranked first by AF3 was chosen for subsequent analysis in this study. The local quality of the selected model was further justified considering the predicted local difference distance test (plDDT). The plDDT metric indicates the accuracy of predicted atomic position, using a 1-100 scale in which higher values indicate greater confidence of protein folding (Mariani et al., 2013; Guo et al., 2022; Abramson et al., 2024).

Structure visualization and analysis

The AF3-predicted structure of EtAMA1 was visualized and superimposed with the crystal structures of PfAMA1 (PDB ID: 1Z40) and *Plasmodium vivax* AMA1 (PvAMA1; PDB ID: 1W8K) using PyMOL (version 2.6, Schrodinger Inc). Root mean square deviation of atomic position (RMSD) values was calculated with the *super* command in PyMOL (Fukutani et al., 2021). As the crystal structure of PfAMA1 represents only residues 108-438, rather than the full-length PfAMA1 protein sequence, the RMSD calculation was performed by superimposing the PfAMA1 crystal structure with the corresponding region in EtAMA1 (residues 60-392). Specifically, five cycles of pairwise alignment and structural superposition between the Cα atoms of EtAMA1 and PfAMA1 were performed by PyMOL, during which outlier atoms (with RMSD > 2 Å) were rejected to eliminate poorly aligned regions. After rejection, the remaining 198 Cα atoms from each structure were superimposed.

RESULTS AND DISCUSSION

Sequence conservation among apical membrane antigen 1 proteins

Multiple sequence alignment of five AMA1 protein sequences from *Eimeria* and *Plasmodium* species revealed a relatively low conservation, with only 82 residues strictly conserved across all sequences (Figure 1). Among the strictly conserved residues, ten cysteine residues that form five disulfide bonds in domains I and II of PfAMA1 are also completely conserved in *Eimeria* AMA1 proteins, suggesting the conservation of these five disulfide linkages in AMA1 structure across two different genera. Protein sequences at the N-terminal region are highly variable between *Plasmodium falciparum* AMA1 (PfAMA1) and *Eimeria* AMA1, and among *Eimeria* AMA1 proteins. In addition, over 150 amino acids near the C-terminal end of PfAMA1 are not conserved in *Eimeria*, although the C-terminal end is highly conserved among the four *Eimeria* AMA1 proteins. The strictly conserved residues mainly locate in the central part of *Eimeria* AMA1, aligned with residues at the well-structured domain I and domain II of PfAMA1. Similar observations have been reported in AMA1 studies of parasites, where structural constraints preserve the fold despite extensive antigenic polymorphism (Bai et al., 2005).

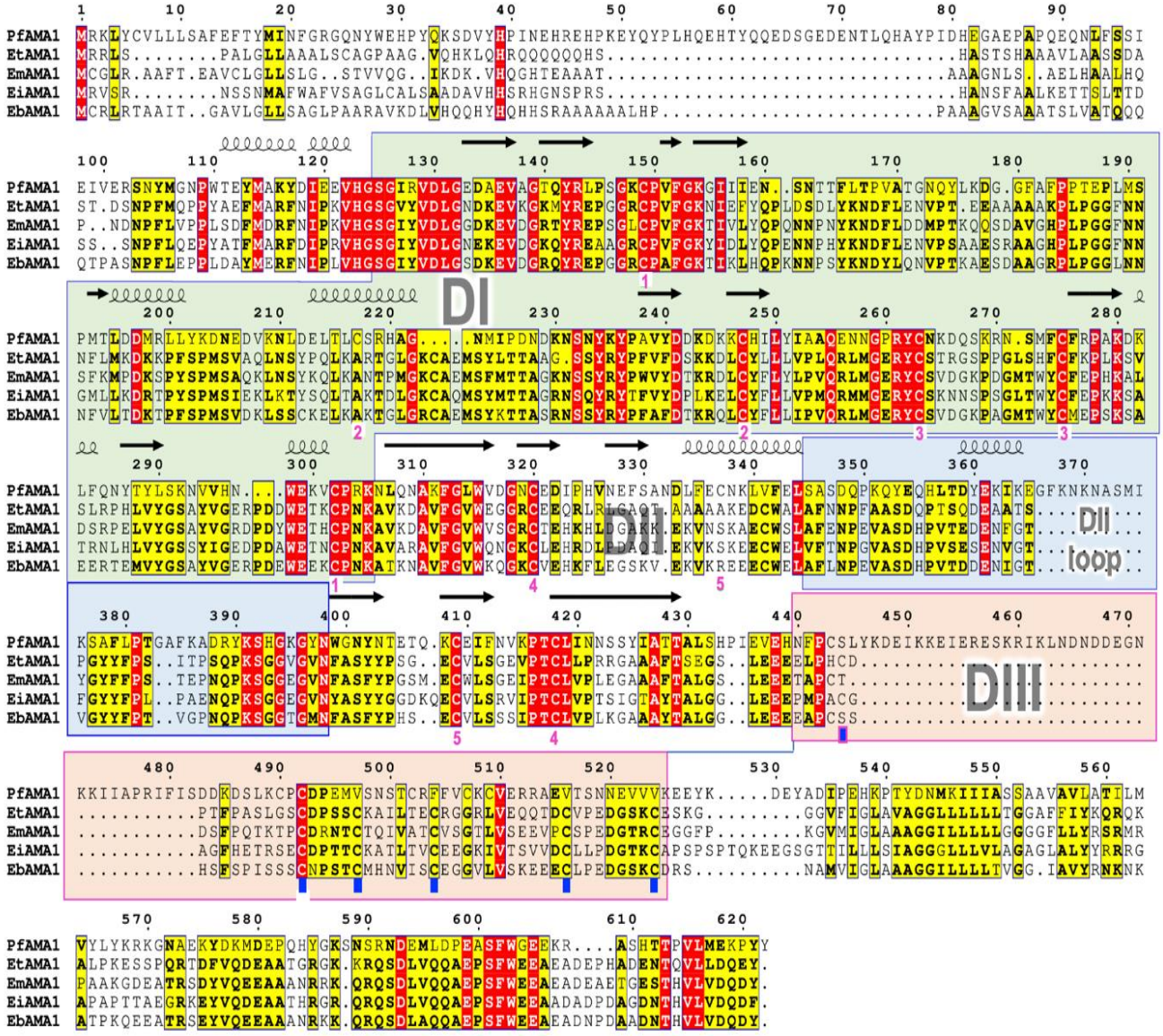


Figure 1. Multiple protein sequence alignment of apical membrane antigen 1 (AMA1) showing relationships between *Eimeria tenella* and *Plasmodium falciparum*. Helices and arrows above the alignment, respectively, represent α-helices and β-strands in the crystal structure of *P. falciparum AMA1* (PfAMA1). Pink numbers below mark cysteine residues forming disulfide bonds in PfAMA1. Blue squares indicate cysteine residues that are predicted to form disulfide bonds in domain III of *E. tenella* AMA1 (EtAMA1). Red shading marks strictly conserved residues; Yellow indicates residues conserved in most sequences. Domains I, II, and III, labelled respectively as DI, DII, and DIII, are marked with light green, transparent, and light peach backgrounds. The loop within Domain II participating in the hydrophobic pocket, labeled as DII loop, is marked with a light blue background.

Structural features of *Eimeria tenella* apical membrane antigen 1

First, the local quality of the AF3-predicted structure of EtAMA1 was assessed by plDDT scores (Figure 2A). Low plDDT scores (plDDT < 70) were observed in the N-terminal segment (residues 1-59), which likely corresponds to the disordered N-terminal tail, and the C-terminal segment (residues 441-536), which may include the transmembrane helix and the C-terminal cytosolic tail. As a low plDDT score indicates intrinsic disorder or structural uncertainty (Guo et al., 2022; Kovalevskiy et al., 2024), the two segments (1-59 and 441-536) were excluded from further structural analysis. The truncated AF3-predicted EtAMA1 model is predominantly high in pLDDT scores (> 90), indicating reliable folding predictions. The EtAMA1 structure was divided into four parts, including an N-terminal α-helix and three domains, denoted as domains I (DI), domain II (DII), and domain III (DIII; Figure 2B). Boundaries for the N-terminal α-helix, DI, and DII were inferred from the sequence alignment in Figure 1, using the domain boundaries defined in the crystal structure of PfAMA1 as a reference. DI and DII in the EtAMA1 model are packed against each other, consistent with the core structure of AMA1 ectodomain from *Plasmodium* and *Toxoplasma* (Bai et al., 2005; Crawford et al., 2010), suggesting that the overall architecture of AMA1 ectodomain may still have been preserved across the phylum despite low sequence identity. Detailed structural comparisons and discussions for each domain were presented in later sections.

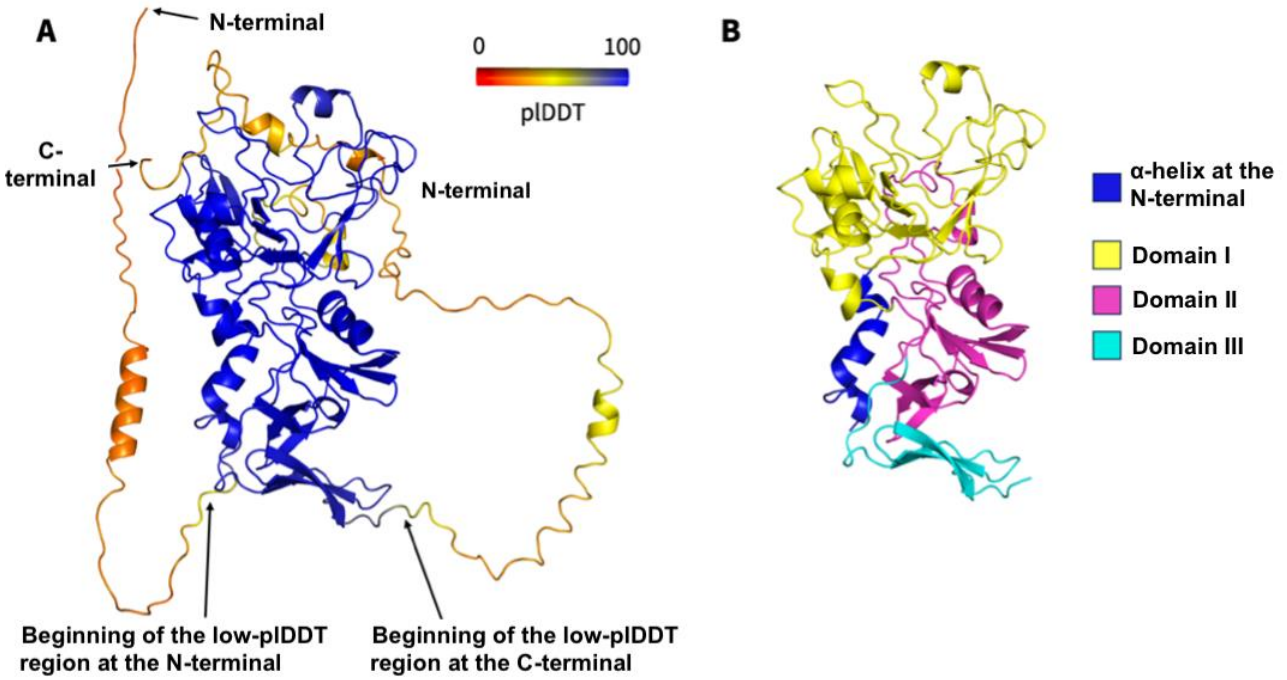


Figure 2. Predicted structure of *Eimeria tenella* apical membrane antigen 1 (EtAMA1) by AlphaFold. **A:** The AlphaFold3-predicted structure of EtAMA1 is colored according to the predicted local distance difference test (pLDDT) score, ranging from red (low confidence, pLDDT = 0) to blue (high confidence, pLDDT = 100). **B:** The AlphaFold3-predicted structure of EtAMA1 was trimmed to remove the N-terminal and C-terminal regions with low pLDDT scores. The final trimmed structure was colored by domain, with the N-terminal helix depicted in blue, domain I in yellow, domain II in pink, and domain III in cyan.

Conservation of the PAN motif in domains I and II

The N-terminal α-helix, DI and DII of EtAMA1 are predicted to closely resemble the corresponding domains in the crystallographic structure of PfAMA1 (PDB ID: 1Z40). The root mean square deviation between the crystal structure of PfAMA1 and the AF3-predicted structure of EtAMA1 (DIII and low plDDT-scoring regions excluded) was calculated to be 0.759 Å over 198 Cα atoms (aligned by PyMOL), suggesting high structural similarity, particularly in the core of DI and DII. Despite only 19% amino acid identity between EtAMA1 and PfAMA1, the folding characteristics of DI and DII may be conserved. DI and DII of EtAMA1 exhibited the classical PAN motif (Figure 3), a conserved structural fold consisting of a five-stranded β-sheet and an α-helix, found in DI and DII of PfAMA1 and *Toxoplasma gondii* AMA1 (TgAMA1; Bai et al., 2005; Pizarro et al., 2005; Crawford et al., 2010). Earlier reports in *Plasmodium* AMA1 indicated that disulfide bonds played a crucial role in maintaining the structural integrity of the AMA1 ectodomain (Bai et al., 2005). Similarly, ten cysteine residues were predicted to form five disulfide bonds in EtAMA1, all conserved across *Eimeria* species, possibly reinforcing the stability of DI and DII. Eight out of the ten cysteines are invariant compared to PfAMA1, while the remaining two cysteines are present but shifted by several residues relative to their positions in PfAMA1. The similarity in structural scaffold and cysteine framework between the EtAMA1 model and PfAMA1, inferred from AF3 prediction, suggested the possibility that EtAMA1 may engage in a function analogous to PfAMA1. Moreover, a low sequence identity between EtAMA1 and PfAMA1, in contrast to the anticipated preservation of their core folding within DI and DII, may suggest an evolutionary strategy that maintains essential functional architecture of DI and DII while allowing substantial polymorphism.

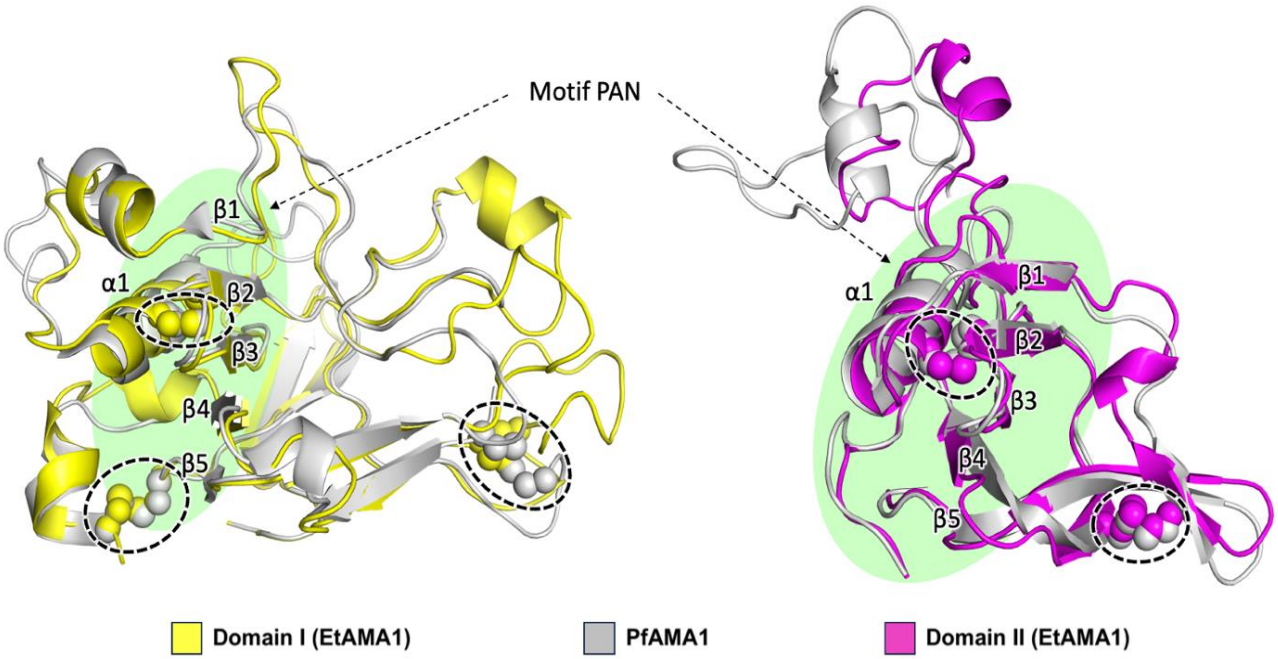


Figure 3. Structural comparison between domain I (left) and domain II (right) of *Eimeria tenella* apical membrane antigen 1 (EtAMA1) with that of *Plasmodium falciparum* apical membrane antigen 1 (PfAMA1). DI or DII of EtAMA1 and PfAMA1 were superimposed by PyMOL. Domain I and II of EtAMA1 are shown respectively in yellow and magenta, and the two domains in PfAMA1 are both colored in grey. Cysteine residues forming disulfides are shown as spheres, and the disulfide bridges are circled with dashed lines. The PAN motif, consisting of one α-helix (α1) and five β-strands (β1-β5), in each structure is highlighted with a light green-filled shape.

Variations of the critical residues from domain I at the conserved hydrophobic pocket for ligand binding

The binding partner of *Eimeria* AMA1 has not yet been identified; however, it is possible that *Eimeria* AMA1 also interacts with a RON2 orthologue, similar to the *Plasmodium* model. Superimposition of the EtAMA1 model into the PfAMA1 crystal structure (PDB ID: 1Z40) revealed that residues F181, Y234, Y236, F281, and F367 at the critical hydrophobic pocket of PfAMA1 for RON2 binding are also found in the AF3-predicted EtAMA1 model, respectively, as F149, Y198, Y200, F239, and F339. Interestingly, Y251 and I252 at the conserved hydrophobic pocket in PfAMA1 are replaced by L215 and V216 in EtAMA1 (Figure 4). Notably, Y251 in PfAMA1 has been recognized as a key residue mediating AMA1-RON2 interaction, and is conserved across AMA1 proteins from species of different genera, including *Plasmodium vivax*, *P. vivax*, *Toxoplasma gondii*, *Babesia bovis*, and *Neospora caninum* (Crawford et al., 2010). A study indicated that a single mutation at Y251 of PfAMA1 resulted in the loss of RON2-binding capacity, highlighting the critical role of this Tyrosine in determining ligand binding affinity (Srinivasan et al., 2011). It is not known why AMA1 in *Eimeria tenella*, *E. intestinalis*, and *E. brunetti*, except *E. maxima*, have a Leucine (L214 in EtAMA1) instead of a Tyrosine as Y251 in PfMATE in its otherwise conserved hydrophobic pocket. Substituting the amphipathic, aromatic Tyrosine residue with the smaller, hydrophobic yet non-aromatic Leucine residue may alter the interactions at the binding site. However, it should be noted that the structure predicted by AlphaFold3 is highly speculative and unverified by experimental data.

Divergence of the domain II loop between *Eimeria tenella* apical membrane antigen 1 and *Plasmodium falciparum* apical membrane antigen 1

Apart from the differences in critical residues from DI at the hydrophobic pocket, there are also differences in the DII loop. From the alignment in the present study, the sequences of the DII loop among *Eimeria* species are mainly well conserved, while they are significantly different from PfAMA1 (Figure 1). In addition, the DII loop in EtAMA1 is 12 residues shorter than that of PfAMA1. Although the majority of the DII loop from EtAMA1 is predicted to have no well-defined secondary structure (Figure 4), there are six Proline residues in the sequence of the DII loop, which could impose certain conformational constraints on the loop (Figure 1). Four out of six Prolines are completely conserved across *Eimeria*, while the number of Proline residues in the entire DII loop of PfAMA1 is only one. While the DII loop of PfAMA1 reaches Y251 on the base of the hydrophobic pocket, the DII loop of EtAMA1 in the predicted structure does not extend over the hydrophobic pocket and remains spatially distant from the Y251 equivalent (L214), seemingly providing more access to the hydrophobic pocket in EtAMA1 compared with PfAMA1 (PDB ID: 1Z40). The

hydrophobic pocket in EtAMA1 appears wider than that in PfAMA1, with the maximum width estimated (PyMOL) at about 17.4 Å for EtAMA1 and 11.1 Å for PfAMA1. Previously, the DII loop has been described as a gatekeeper, shielding the hydrophobic pocket in PfAMA1 and TgAMA1, before being lifted away to allow the formation of the AMA1-RON2 complex (Tonkin et al., 2011; Vulliez-Le Normand et al., 2012). In addition, DII loops also modulate ligand binding affinity, as genetically modifying the DII loop in PfAMA1 to shorten its length significantly hampered the ability of PfAMA1 to bind the cognate RON2 (Delgadillo et al., 2016). The DII loop also affects ligand specificity (Parker and Boulanger, 2015). Replacing the DII loop of TgAMA1 with a shorter linker substantially enhanced the interaction between the genetically modified TgAMA1 and the heterogenous *Eimeria tenella* RON2 (EtRON2), even though TgAMA1 with an intact DII loop only interacted weakly with it (Parker and Boulanger, 2015). In the present study, the differences in DII loop sequence and length between *Eimeria* and *Plasmodium* AMA1 proteins have been given based on structural prediction of EtAMA1, providing preliminary information for future investigations into how possible divergences may influence the functional biology of EtAMA1.

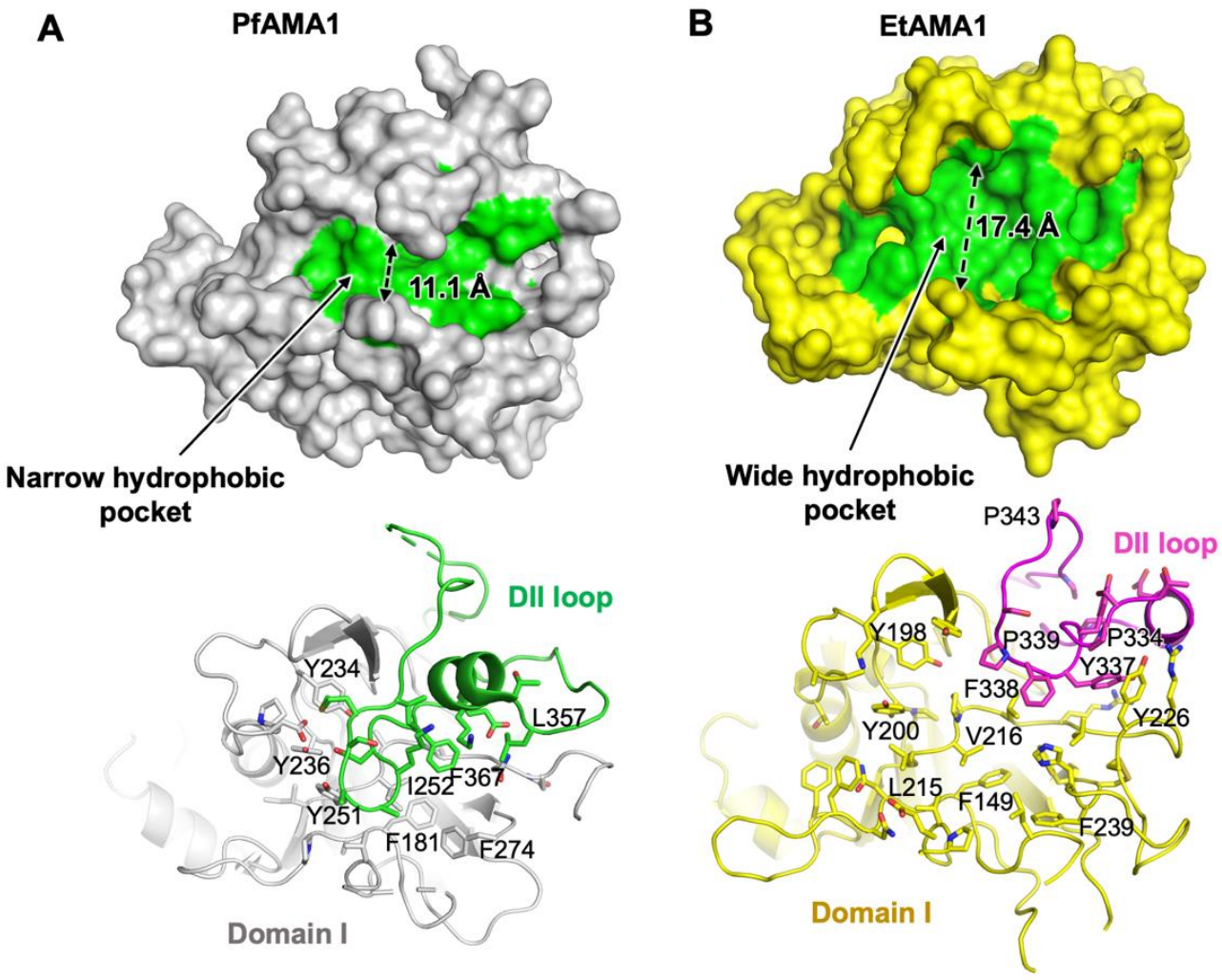


Figure 4. The hydrophobic pocket of apical membrane antigen 1 (AMA1) proteins. **A:** Crystal structure of the *Plasmodium falciparum* AMA1 (PfAMA1), shown in surface representation with the hydrophobic pocket highlighted in green (upper panel), and in cartoon representation with the loop of domain II (DII loop) colored in green (lower panel). **B:** AlphaFold-predicted structure of *Eimeria tenella* AMA1 (EtAMA1), shown in surface representation with the hydrophobic pocket highlighted in green (upper panel), and in cartoon representation with the loop of domain II (DII loop) colored in pink (lower panel). Residues at the hydrophobic pocket are indicated. The two-headed dashed arrows indicate the widths of the hydrophobic pocket, as estimated in angstroms using PyMOL.

Structural characteristics of domain III in *Eimeria tenella* apical membrane antigen 1

The AF3-predicted structure of EtAMA1 possesses a DIII, characterized by three antiparallel β-strands, forming a β-pleated sheet (Figure 5A). Structural elements of DIII in EtAMA1 were also predicted for *Eimeria maxima* AMA1 (EmAMA1; Figure 5B). Sequence alignment confirmed that five of six cysteine residues in DIII are strictly conserved

across *Eimeria*, suggesting that disulfide linkages may be conserved among *Eimeria* species. The NMR structure of DIII from PfAMA1 (PDB ID: 1HN6; Nair et al., 2002) and the crystal structure of DIII from *Plasmodium vivax* AMA1 (PvAMA1; PDB ID: 1W8K; Pizarro et al., 2005) have been previously reported; thus, they are used in the present study for comparative analysis of DIII (Figure 5C and 5D). The DIII structure of PvAMA1 contains a great number of structural elements, beginning with an N-terminal α-helix followed by an unstructured loop, then a β-strand, and a short α-helix packed against a small three-stranded β-sheet, and finally a β-hairpin positioned alongside another α-helix (Figure 5C). On the other hand, DIII of PfAMA1 features a short α-helix preceded by 50-residue-long disordered loop and a short β-hairpin (Figure 5D). The overall topology of the predicted DIII structure of EtAMA1 does not resemble any of the two *Plasmodium* DIII structures, while the local substructure displays certain similarity. In particular, while each *Plasmodium* DIII structure contains an α-helix followed by an extended disordered loop in the N-terminal region of DIII, EtAMA1 lacks all of these. Nevertheless, two β-strands of the three-stranded β-sheet in DIII of EtAMA1 (residues 414-431 in EtAMA1) can be superimposed with the β-hairpin of DIII in PfAMA1 (residues 492-509 in PfAMA1), with an RMSD between Cα atoms of 1.1 Å. Three disulfide bonds (C397-C420, C408-C432, and C413-C440) are present in the DIII model of EtAMA1 (Figure 5A). While the same number of disulfide bonds is present in the *Plasmodium* DIII structures, the sequence alignment revealed that only one out of six Cysteines is invariant in EtAMA1 (corresponding to C408 in EtAMA1; Figure 1). In summary, the structural topology of DIII in EtAMA1 is speculated to differ markedly from that of PvAMA1 and PfAMA1. Notwithstanding, experimental determination of its structure will be necessary to validate these predictions and to reveal the functional implications of possible divergence.

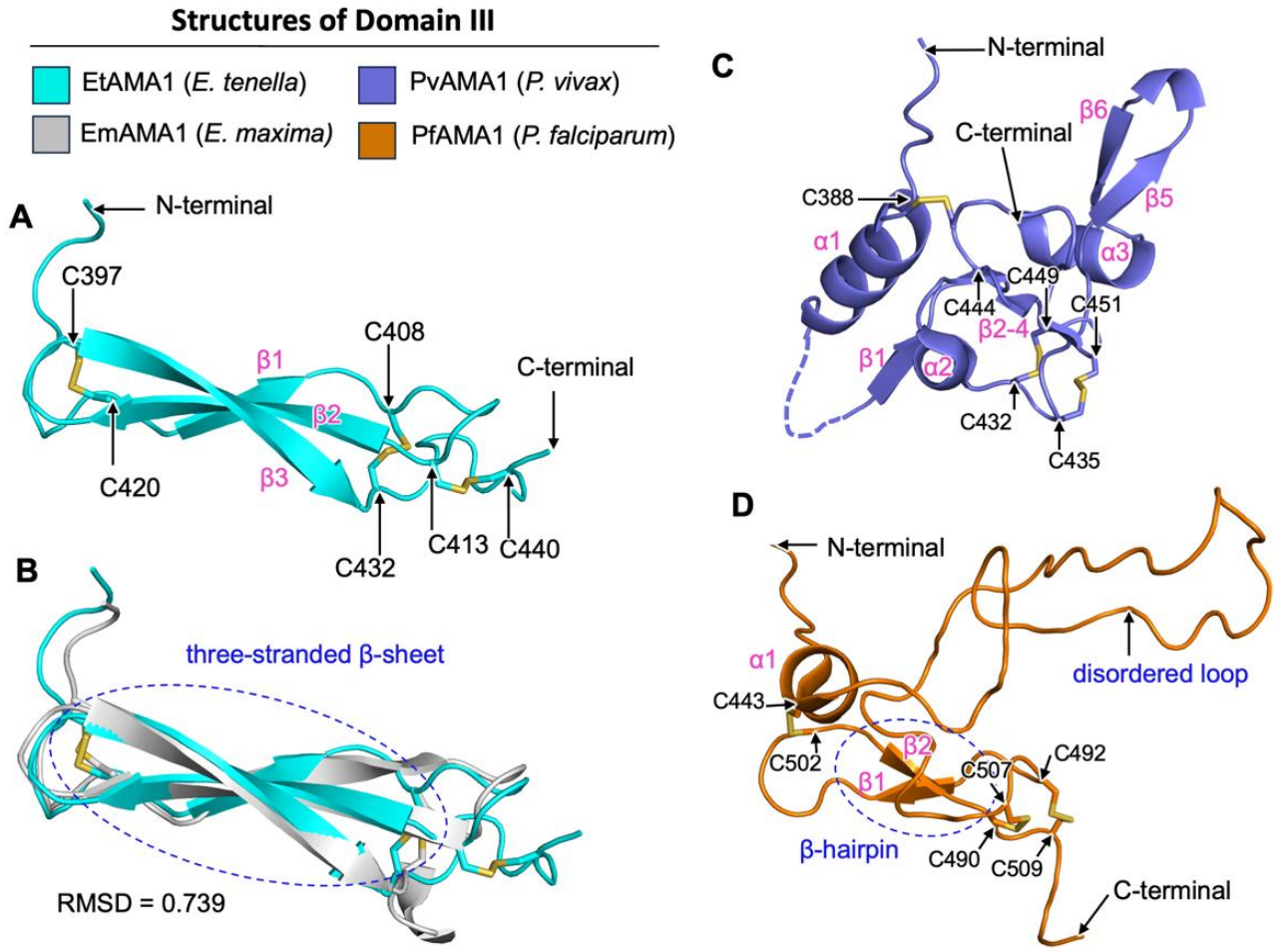


Figure 5. Domain III of apical membrane antigen 1 (AMA1) proteins. The secondary structure elements of domain III are annotated according to standard conventions, with α-helices labeled sequentially as α1, α2, α3, and β-strands labeled sequentially as β1, β2, β3 to β6 following their order along the polypeptide chain. **A:** The predicted domain III structure of *Eimeria tenella* AMA1 **(**EtAMA1) features a three-stranded β-sheet (β1-β3). **B:** Structural superposition of predicted domain III models from EtAMA1 and *Eimeria maxima* AMA1 **(**EmAMA1). The root mean square deviation between the Cα atoms of the two structures is 0.739Å. **C:** The crystal structure of domain III of *Plasmodium vivax* AMA**1** (PvAMA1) features an N-terminal α-helix (α1) followed by an unstructured loop, then a β-strand (β1), and a short α-helix (α2) packed against a small three-stranded β-sheet (β2-β4), and finally a β-hairpin (β5-β6) positioned alongside another α-helix (α3). **D:** The NMR structure of domain III of *Plasmodium falciparum* AMA**1** (PfAMA1) possesses an N-terminal α-helix (α1) followed by a long disordered loop and finally a β-hairpin (β1-β2). Cysteine residues that formed disulfide bonds in domain III are indicated.

CONCLUSION

The present study presents a sequence alignment and a comparative structural analysis of *Eimeria tenella* apical membrane antigen 1 (EtAMA1) based on AlphaFold3 prediction. Although overall sequence identity between EtAMA1 and *Plasmodium falciparum* AMA1 (PfAMA1) is low (19%), the core architecture of domains I and II, including the PAN motif and the disulfide framework, may be preserved. While five aromatic residues forming the hydrophobic pocket for ligand binding in PfAMA1 are conserved in EtAMA1, the substitutions of Y251 and I252 in PfAMA1 with L215 and V216 in EtAMA1 suggest that specific interactions with ligand may differ. The shorter, proline-rich DII loop of EtAMA1 could cover less of the hydrophobic pocket, a difference that could be functionally relevant, although this remains to be experimentally verified. Domain III of EtAMA1 is also predicted to diverge significantly in topology from *Plasmodium* DIII structures, with a three-stranded β-sheet stabilized by three disulfide bonds. Overall, the present study predicted regions of conservation shared between *Plasmodium* and *Eimeria*, as well as potential *Eimeria*-specific structural divergences, based on AlphaFold3. Structural insights into the *Eimeria*-specific hydrophobic pocket and domain III may inform the design of binding peptides to *Eimeria* AMA1 capable of inhibiting host cell invasion, a strategy that has been established in malaria disease. As the interpretations rely on AlphaFold3 prediction, future experimental determination of EtAMA1 structure and ligand-binding characteristics will be essential to validate the results and to clarify their biological significance.

DECLARTIONS

Acknowledgements

The authors would like to thank Hue University for partial support of this study under the Core Research Program.

Author contributions

All authors contributed to the study conception and design. Material preparation, data collection, and analysis were performed by Pham Hoang Son Hung, Ho Thi Dung, Duong Thanh Hai, and Tran Nguyen Thao. The first draft of the manuscript was written by Pham Hoang Son Hung, and all authors commented on previous versions of the manuscript. All authors read and approved the final edition of the manuscript.

Availability of data and materials

Protein sequences and crystal structures used for analysis in this study are provided in the manuscript.

Competing interests

The authors declare that they have no competing interests. The corresponding author takes full responsibility for any conflicts of interest or published content.

Ethical considerations

The authors declare that they did not use artificial intelligence (AI) for the designing the study, writing the manuscript, nor for the creation of images, graphics, tables, or captions. Also authors confirmed that the manuscript was checked for plagiarism and no duplicate publication was done.

Funding

The present study received no funding or financial support.

REFERENCES

Abramson J, Adler J, Dunger J, Evans R, Green T, Pritzel A, Ronneberger O, Willmore L, Ballard AJ, Bambrick J et al. (2024). Accurate structure prediction of biomolecular interactions with AlphaFold 3. Nature, 630(7943): 493-500. DOI: https://www.doi.org/10.1038/s41586-024-07487-w

Bai T, Becker M, Gupta A, Strike P, Murphy VJ, Anders RF, and Batchelor AH (2005). Structure of AMA1 from *Plasmodium falciparum* reveals a clustering of polymorphisms that surround a conserved hydrophobic pocket. Proceedings of the National Academy of Sciences of the United States of America, 102(36): 12736-12741. DOI: https://www.doi.org/10.1073/pnas.0501808102

Besteiro S, Dubremetz JF, and Lebrun M (2011). The moving junction of apicomplexan parasites: A key structure for invasion. Cellular Microbiology, 13(6): 797-805. DOI: https://www.doi.org/10.1111/j.1462-5822.2011.01597.x

Besteiro S, Michelin A, Poncet J, Dubremetz JF, and Lebrun M (2009). Export of a *Toxoplasma gondii* rhoptry neck protein complex at the host cell membrane to form the moving junction during invasion. PLoS Pathogens, 5(2): e1000309. DOI: https://www.doi.org/10.1371/journal.ppat.1000309

Blake DP, Knox J, Dehaeck B, Huntington B, Rathinam T, Ravipati V, Ayoade S, Gilbert W, Adebambo AO, Jatau ID et al. (2020). Re-calculating the cost of coccidiosis in chickens. Veterinary Research, 51(1): 115. DOI: https://www.doi.org/10.1186/s13567-020-00837-2

Chuang I, Sedegah M, Cicatelli S, Spring M, Polhemus M, Tamminga C, Patterson N, Guerrero M, Bennett JW, McGrath S et al. (2013). DNA prime/adenovirus boost malaria vaccine encoding *P. falciparum* CSP and AMA1 induces sterile protection associated with cell-mediated immunity. PLoS ONE, 8(2): e55571. DOI: https://www.doi.org/10.1371/journal.pone.0055571

Crawford J, Tonkin ML, Grujic O, and Boulanger MJ (2010). Structural characterization of apical membrane antigen 1 (AMA1) from *Toxoplasma gondii*. Journal of Biological Chemistry, 285(20): 15644-15652. DOI: https://www.doi.org/10.1074/jbc.M109.092619

Delgadillo RF, Parker ML, Lebrun M, Boulanger MJ, and Douguet D (2016). Stability of the *Plasmodium falciparum* AMA1-RON2 complex is governed by the domain II (DII) loop. PLoS One, 11(1): e0144764. DOI: https://www.doi.org/10.1371/journal.pone.0144764

Fukutani T, Miyazawa K, Iwata S, and Satoh H (2021). G-RMSD: Root mean square deviation based method for three-dimensional molecular similarity determination. Bulletin of the Chemical Society of Japan, 94(2): 655-665. DOI: https://www.doi.org/10.1246/bcsj.20200258

Guo HB, Perminov A, Bekele S, Kedziora G, Farajollahi S, Varaljay V, Hinkle K, Molinero V, Meister K, Hung C et al. (2022). AlphaFold2 models indicate that protein sequence determines both structure and dynamics. Scientific Report, 12: 10696. DOI: https://www.doi.org/10.1038/s41598-022-14382-9

Harvey KL, Yap A, Gilson PR, Cowman AF, and Crabb BS (2014). Insights and controversies into the role of the key apicomplexan invasion ligand, apical membrane antigen 1. International Journal for Parasitology, 44(12): 853-857. DOI: https://www.doi.org/10.1016/j.ijpara.2014.08.001

Jumper J, Evans R, Pritzel A, Green T, Figurnov M, Ronneberger O, Tunyasuvunakool K, Bates R, Zidek A, Potapenko A et al. (2021). Highly accurate protein structure prediction with AlphaFold. Nature, 596(7873): 583-589. DOI: https://www.doi.org/10.1038/s41586-021-03819-2

Kovalevskiy O, Mateos-Garcia J, and Tunyasuvunakool K (2024). AlphaFold two years on: Validation and impact. Proceedings of the National Academy of Sciences of the United States of America, 121(34): e2315002121. DOI: https://www.doi.org/10.1073/pnas.2315002121

Lamarque M, Besteiro S, Papoin J, Roques M, Vulliez-Le Normand B, Morlon-Guyot J, Dubremetz JF, Fauquenoy S, Tomavo S, Faber BW et al. (2011). The RON2-AMA1 interaction is a critical step in moving junction-dependent invasion by apicomplexan parasites. PLoS Pathogens, 7(2): e1001276. DOI: https://www.doi.org/10.1371/journal.ppat.1001276

Li J, Wang F, Ma C, Huang Y, Wang D, and Ma D (2018). Recombinant *Lactococcus lactis* expressing *Eimeria tenella* AMA1 protein and its immunological effects against homologous challenge. Experimental Parasitology, 191: 1-8. DOI: https://www.doi.org/10.1016/j.exppara.2018.05.003

Liu Q, Jiang Y, Yang W, Liu Y, Shi C, Liu J, and Li J (2020). Protective effects of a food-grade recombinant *Lactobacillus plantarum* with surface displayed AMA1 and EtMIC2 proteins of *Eimeria tenella* in broiler chickens. Microbial Cell Factories, 19: 28. DOI: https://www.doi.org/10.1186/s12934-020-1297-4

Mariani V, Biasini M, Barbato A, and Schwede T (2013). lDDT: A local superposition-free score for comparing protein structures and models using distance difference tests. Bioinformatics, 29(21): 2722-2728. DOI: https://www.doi.org/10.1093/bioinformatics/btt473

Mathis GF, Lumpkins B, Cervantes HM, Fitz-Coy SH, Jenkins MC, Jones MK, Price KR, and Dalloul RA (2025). Coccidiosis in poultry: Disease mechanisms, control strategies, and future directions. Poultry Science, 104(5): 104663. DOI: https://www.doi.org/10.1016/j.psj.2024.104663

Nair M, Hinds MG, Coley AM, Hodder AN, Foley M, Anders RF, and Norton RS (2002). Structure of domain III of the blood-stage malaria vaccine candidate, *Plasmodium falciparum* apical membrane antigen 1 (AMA1). Journal of Molecular Biology, 322(4): 741-753. DOI: https://www.doi.org/10.1016/s0022-2836(02)00806-9

Ouattara A, Takala-Harrison S, Thera MA, Coulibaly D, Niangaly A, Saye R, Tolo Y, Dutta S, Heppner DG, Soisson L et al. (2013). Molecular basis of allele-specific efficacy of a blood-stage malaria vaccine: vaccine development implications. The Journal of Infectious Diseases, 207(3): 511-519. DOI: https://www.doi.org/10.1093/infdis/jis709

Parker ML and Boulanger MJ (2015). An extended surface loop on Toxoplasma gondii apical membrane antigen 1 (AMA1) governs ligand binding selectivity. PLoS ONE, 10(5): e0126206. DOI: https://www.doi.org/10.1371/journal.pone.0126206

Pastor-Fernandez I, Kim S, Billington K, Bumstead J, Marugan-Hernández V, Küster T, Ferguson DJP, Vervelde L, Blake DP, and Tomley FM (2018). Development of cross-protective *Eimeria*-vectored vaccines based on apical membrane antigens. International Journal for Parasitology, 48(7): 505-518. DOI: https://www.doi.org/10.1016/j.ijpara.2018.01.003

Pham HHS, Matsubayashi M, Tsuji N, and Hatabu T (2021). Relationship between *Eimeria tenella* associated-early clinical signs and molecular changes in the intestinal barrier function. Veterinary Immunology and Immunopathology, 240: 110321. DOI: https://www.doi.org/10.1016/j.vetimm.2021.110321

Pizarro JC, Vulliez-Le Normand B, Chesne-Seck ML, Collins CR, Withers-Martinez C, Hackett F, Blackman MJ, Faber BW, Remarque EJ, Kocken CH et al. (2005). Crystal structure of the malaria vaccine candidate apical membrane antigen 1. Science, 308(5720): 408-411. DOI: https://www.doi.org/10.1126/science.1107449

Quiroz-Castaneda RE (2018). Avian coccidiosis, new strategies of treatment. avian coccidiosis, new strategies of treatment. Farm animals diseases, recent omic trends and new strategies of treatment. InTech., United Kingdom, pp. 119-133. DOI: https://www.doi.org/10.5772/intechopen.74008

Robert X and Gouet P (2014). Deciphering key features in protein structures with the new ENDscript server. Nucleic Acids Research, 42(W1): W320-W324. DOI: https://www.doi.org/10.1093/nar/gku316

Srinivasan P, Beatty WL, Diouf A, Herrera R, Ambroggio X, Moch JK, Tyler JS, Narum DL, Pierce SK, Boothroyd JC et al. (2011). Binding of *Plasmodium* merozoite proteins RON2 and AMA1 triggers commitment to invasion. Proceedings of the National Academy of Sciences, 108(32): 13275-13280. DOI: https://www.doi.org/10.1073/pnas.1110303108

Tonkin ML, Roques M, Lamarque MH, Pugniere M, Douguet D, Crawford J, Lebrun M, and Boulanger MJ (2011). Host cell invasion by apicomplexan parasites: Insights from the co-structure of AMA1 with a RON2 peptide. Science, 333(6041): 463-467. DOI: https://www.doi.org/10.1126/science.1204988

Tyler JS, Treeck M, and Boothroyd JC (2011). Focus on the ringleader: the role of AMA1 in apicomplexan invasion and replication. Trends in Parasitology, 27(9): 410-420. DOI: https://www.doi.org/10.1016/j.pt.2011.04.002

Vulliez-Le Normand B, Tonkin ML, Lamarque MH, Langer S, Hoos S, Roques M, Saul FA, Faber BW, Bentley GA, Boulanger MJ et al. (2012). Structural and functional insights into the malaria parasite moving junction complex. PLoS Pathogen, 8(6): e1002755. DOI: https://www.doi.org/10.1371/journal.ppat.1002755

Wang G, Drinkwater N, Drew DR, MacRaild CA, Chalmers DK, Mohanty B, Lim SS, Anders RF, Beeson JG, Thompson PE et al. (2016). Structure–activity studies of β-hairpin peptide inhibitors of the *Plasmodium falciparum* AMA1–RON2 interaction. Journal of Molecular Biology, 428(20): 3986-3998. DOI: https://www.doi.org/10.1016/j.jmb.2016.07.001

Wang Q, Zhao Q, Zhu S, Huang B, Yu S, Liang S, Wang H, Zhao H, Han H, and Dong H (2020). Further investigation of the characteristics and biological function of *Eimeria tenella* apical membrane antigen 1. Parasite, 27: 70. DOI: https://www.doi.org/10.1051/parasite/2020068

Publisher's note: Scienceline Publication Ltd. remains neutral with regard to jurisdictional claims in published maps and institutional affiliations.

Open Access: This article is licensed under a Creative Commons Attribution 4.0 International License, which permits use, sharing, adaptation, distribution and reproduction in any medium or format, as long as you give appropriate credit to the original author(s) and the source, provide a link to the Creative Commons licence, and indicate if changes were made. The images or other third party material in this article are included in the article's Creative Commons licence, unless indicated otherwise in a credit line to the material. If material is not included in the article's Creative Commons licence and your intended use is not permitted by statutory regulation or exceeds the permitted use, you will need to obtain permission directly from the copyright holder. To view a copy of this licence, visit https://creativecommons.org/licenses/by/4.0/.
© The Author(s) 2025

2025, Scienceline Publication
World's Veterinary Journal
World Vet J, 15(4): 1130-1137.
ISSN 2322-4568

DOI: https://dx.doi.org/10.54203/scil.2025.wvj116
PII: S232245682500116-15

Effects of Heat Stress on Growth Performance, Egg Production, Egg Quality, and Potential Controlling Strategies in Layer Chicken: A Review

Eyayu Gobezie*, Ashenafi Timotiwos, and Getahun Simeneh

College of Agricultural and Environmental Conservation, Department of Animal Science, Debark University, P.O. Box 90, Debark, Ethiopia

*Corresponding author's Email: gobezieeyayu@gmail.com

REVIEW ARTICLE
Received: September 19, 2025
Revised: October 24, 2025
Accepted: November 21, 2025
Published: December 31, 2025

ABSTRACT

Egg production is a key indicator of laying hens' reproductive efficiency. High ambient temperatures cause heat stress in laying hens, which negatively impacts their health, behavior, blood chemistry, feed intake, egg production, and egg quality. The present study aimed to focus on the effects of heat stress on growth performance, egg production, egg quality, and potential controlling strategies for heat stress in layer chickens. Heat stress reduces body weight, feed efficiency, egg yield, and egg quality. Reduced feed intake is the main reason contributing to its negative impacts on production. The reduced feed intake and decreased nutrient digestibility have adverse effects on egg quality and production performance. Heat stress reduces egg production and impairs the behavior, welfare, and immunity of layer chickens, resulting in significant financial losses. Higher ambient temperatures (above 25°C) can lead to lower egg quality (soft shells or shell-less eggs), weakened skeletal integrity in hens, and fewer eggs. Poor hatchability results from reduced feed intake due to high temperatures, which adversely affects semen fertility and quality. Eggs produced under extreme heat stress had lower Haugh units, egg yolk color, and eggshell thickness and strength. Overcrowding, also known as high stocking density, adversely affects animal health by degrading their habitat and increasing competition for resources such as feed, which can ultimately lead to feather pecking and cannibalism. Due to a quicker metabolic rate, chickens produce more body heat and are more susceptible to heat stress. High stocking density and high ambient temperature increase the risk of heat stress. Reducing stocking density to prevent heat stress may limit the number of hens that can be raised in a given space. Heat stress significantly reduces egg production, egg quality, and egg weight in laying hens under hot conditions. The current findings highlighted the need for improved environmental management and methods to mitigate the harmful effects of heat stress in laying hens.

Keywords: Egg production, Egg quality, Egg weight, Heat stress, Laying chicken

INTRODUCTION

Climate change has become a significant global concern for the livestock industry, resulting from increasing weather patterns that lead to higher ambient temperatures and humidity (Nawab et al., 2018). According to Charles (2002), the ideal temperature range for the thermoneutral zone and performance is 19-22°C for laying hens and 18-22°C for broiler chickens; however, their usual body temperature is 41-42°C (Naga et al., 2018). Heat stress is caused by the interaction of several factors, such as high ambient temperature, high humidity, radiant heat, and airspeed (Lara and Rostagno, 2013). Chickens experience heat stress at any temperature above 25°C (Donkoh, 1989). Chickens have feathers all over their bodies and no sweat glands (Richards, 1970), which makes it more difficult for them to regulate body temperature, so when the outside temperature rises, they should actively dissipate heat via panting. When chickens experience heat stress, their body temperature rises because they are unable to dissipate extra heat into the surrounding environment (Sugiharto, 2020). Heat stress reduces the body weight, feed intake, egg production, fertility, and survivorship in laying hens (Mashaly et al., 2004; Barrett et al., 2019). According to the study conducted by Mashaly et al. (2004), 31-week-old laying hens exposed to heat stress for five weeks experienced a notable decrease in body weight, feed intake, egg production rate, and egg weight. In tropical and temperate nations, high environmental temperature is one of the most significant factors influencing laying hens' production performance (Tesakul et al., 2025). High ambient temperatures and humidity can cause heat stress in laying hens, greatly impacting their egg production, quality, feed intake, blood chemistry, health, and behavior (Tesakul et al., 2025). According to Sahin et al. (2007), the three main reasons for egg losses are reproductive failure (fewer eggs), poor egg quality (soft shells or shell-less eggs), and impaired hen skeletal integrity.

To cite this paper: Gobezie E, Timotiwos A, and Simeneh G (2025). Effects of Heat Stress on Growth Performance, Egg Production, Egg Quality, and Potential Controlling Strategies in Layer Chicken: A Review. *World Vet. J.,* 15(4): 1130-1137. DOI: https://dx.doi.org/10.54203/scil.2025.wvj116

Heat stress in poultry can be classified as acute, characterized by abrupt, short-duration exposures to extreme heat, or chronic, involving sustained exposure to elevated temperatures (Kpomasse et al., 2021). Depending on the length and severity of the stressor, there are two types of heat stress. While chronic heat stress occurs during a prolonged period of high temperature and humidity, acute heat stress is defined as an abrupt increase in temperature and humidity over a brief period. Heat stress in chickens can last 1 to 24 hours (acute), 7 days (moderate), or longer (chronic) at temperatures between 27°C and 38°C (Vandana et al., 2021). Acute or chronic heat stress may reduce egg production (Deng et al. 2012; Ebeid et al., 2012). Extreme weather conditions and chronic heat stress affect hen physiology, leading to lower egg production efficiency, poor health, and increased death rates (Saeed et al., 2019; Attia et al., 2024; Kim et al., 2024). Significant physiological problems, immune suppression, and gut microbial imbalance can result from both acute and chronic heat stress (Wasti et al., 2020). Serious physiological issues (elevated heart rate, increased body core temperature, and sweating), immunological suppression, and an imbalance in gut microbes can result from heat stress (Lara and Rostagno, 2013; Attia et al., 2018). The biggest concern for large economic losses in the poultry sector is stress, stemming from numerous types of stressors; heat stress is a prominent one (Safi et al., 2022). Moreover, reduced egg production directly affects the number of day-old chicks and increases production expenses (Lara and Rostagno, 2013). Thus, one of the most important challenges in raising chicken productivity and profitability during heat stress is increasing egg production (Radwan, 2020). Reduced egg production is a significant problem in the world's food shortage situation and directly impacts farmers' incomes (Pawar et al., 2016). According to a 2021 UN report (FAO, IFAD, UNICEF, WFP, and WHO), the prevalence of hunger in the world increased sharply in 2020. It was estimated that between 9.2% and 10.4% of the global population faced undernourishment that year, with a central estimate of 9.9% (FAO, 2021). In terms of egg quality, meat quality, growth, and egg output, heat stress affects the total performance of both layers and broiler chickens (Safi et al., 2022).

Poultry in the thermoneutral zone (19-22ºC for laying hens and 18-22ºC for growing broilers) do not experience heat stress because their body temperature is kept constant and they dissipate heat through routine behaviors (Charles, 2002). The production of body heat and heat loss cannot be balanced in chickens under heat stress (Lara and Rostagno, 2013). Laying hens exposed to severe heat stress at 33 °C had significantly reduced feed intake and lower egg production (Kim et al., 2024). Additionally, the laying hens' immediate environment contains more etiologically dangerous bacteria as the temperature rises. Climate change affects the emergence and spread of diseases by increasing the prevalence of parasitic and bacterial infections (Ranjan et al., 2019). Certain feeding practices have gained importance and are employed in commercial settings because heat stress negatively impacts the health, welfare, and laying performance of laying hens (Attia et al. 2016; Jahromi et al. 2016; Abdel-Moneim et al. 2021). Heat stress strategies include a variety of treatments, such as supplementing feed or water with natural antioxidants, organic acids, vitamins, minerals, electrolytes, prebiotics, probiotics, and Phytobiotics, rationing, feed restriction, dietary changes, and drinking cold water (Abd El-Ghany and Babazadeh, 2022).

Understanding the basics of heat stress's causes, detrimental effects, and methods for lowering or mitigating heat stress in the chicken industry is essential to resolving global food security challenges. The present study aimed to assess the effects of heat stress on growth performance, egg output, and egg quality, and to identify potential control strategies for heat stress in laying chickens.

GROWTH PERFORMANCE

As shown in Figure 1, heat stress results in a number of physiological alterations, including oxidative stress, acid-base imbalance, and inhibited immunocompetence. These alterations impact the quality of meat and eggs as well as increase mortality and decrease feed efficiency, body weight, feed intake, and egg production (Wasti et al., 2020). High temperatures can also increase panting under heat stress, leading to elevated carbon dioxide levels and higher blood pH (Lara and Rostagno, 2013). In hot weather, chickens use more water and less feed, and poultry perform badly (Saeed et al., 2019; Rahman and Hidayat, 2020). To maintain homeostasis and reduce heat production, chickens decrease their feed intake (Etches et al., 2008). Decreased feed intake is likely the main reason heat stress harms production, leading to losses in body weight, feed efficiency, egg yield, and egg quality (Barrett et al., 2019). Reduced feed intake and nutrient digestibility have negative impacts on production performance, meat, and egg quality (Song and King, 2015; Song et al., 2022). Deng et al. (2012) demonstrated that a 12-day heat stress exposure (34°C) in 60-week-old commercial hens (Hy-Line Brown) reduced egg production by 28.8% (from 79.5% to 50.7%). This was accompanied by a significant reduction in daily feed intake of 28.6 g per chicken. Additionally, in 24-week-old laying hens, exposure to 32°C heat stress for 22 days significantly reduced hen-day egg production by approximately 34% during the first week of exposure and slightly reduced average egg weight (~1%; Star et al. 2009). When ambient temperature increases from 21.1°C to 32.2°C, feed intake decreases by approximately 9.5% per bird per day during the post-hatch period up to 6 weeks of age. This

reduction in feed consumption is associated with poorer feed conversion efficiency and lower daily weight gain in chickens exposed to heat stress (Syafwan et al., 2011). He et al. (2019) demonstrated that cyclic heat stress, exposure to 37 ± 2°C for 8 hours per day, reduces average daily feed intake by 15.8%. Weight loss may have resulted from the heat-stressed chickens eating less feed than the control group (Mashaly et al., 2004). Moreover, Zhang et al. (2017) indicated that in 21-day-old Cobb male broiler chickens, high ambient temperatures (33°C) reduce development rate and meat yield. Due to the reduced nutritional requirements in chickens, protein digestibility may decrease by as much as 9.7%. The growth rates, feed efficiency, immunity, and carcass quality in broiler chickens can decrease due to high ambient temperatures (Dayyani and Bakhtiyari, 2013). Consequently, layer chickens grow more slowly and are more susceptible to illnesses (Nawaz et al., 2021).

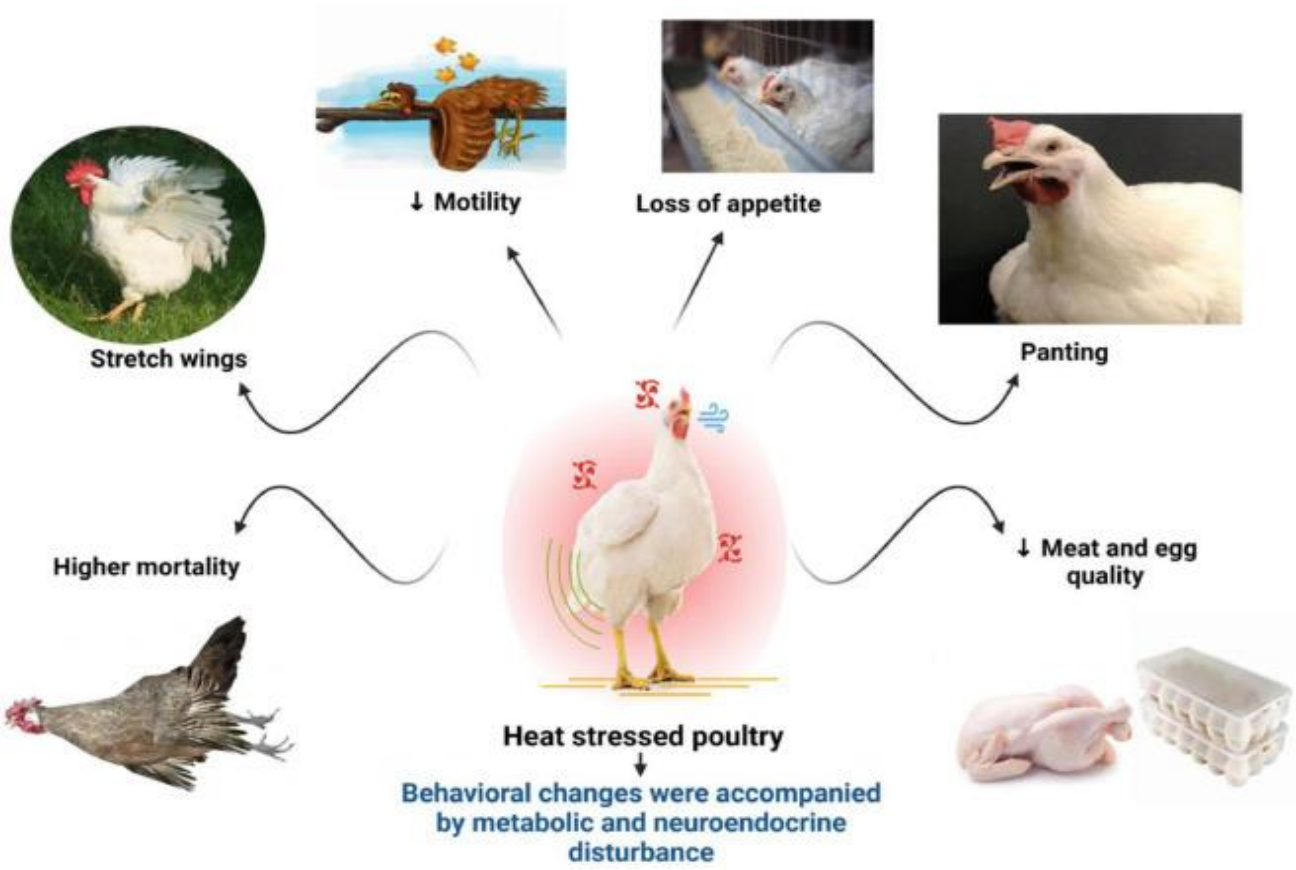


Figure 1. Effect of heat stress on the production performance in layer chickens. Source: Ahmed et al. (2024).

EGG PRODUCTION

Heat stress is the primary reason for the egg weight loss. The weight loss of egg albumen and yolk is likewise predominantly driven by high temperatures above 26°C (Smith, 1974). According to Ugurlu et al. (2001), hens exposed to heat had lower egg weights. Mashaly et al. (2004) found that high temperatures (35°C) can significantly reduce the shell thickness, as measured by a micrometer screw gauge, and specific gravity, in addition to the weights of the egg yolk, egg albumen, and shell.

The number of eggs produced by hens kept in a hot chamber (23.9 to 35 ^{o}C) differed significantly from those kept in regulated chambers (23.9°C), which were maintained for 5 weeks (Mashaly et al., 2004). This implied that egg production and surrounding temperature are inversely related. In a study by Rozenboim et al. (2007), 36 White Leghorn hens (31 weeks old) exposed to 42 ± 3°C for 12 hours daily developed hyperthermia and demonstrated a marked reduction in egg production and egg weight. These effects were accompanied by hormonal changes detectable just two days after heat exposure, compared to controls kept at 24-26°C. Yan et al. (2022) reported that Hy-Line Brown laying hens that were exposed to 32°C (heat stress for 14 days) compared to the hens in the control group (22°C), indicated an 18.75% drop in egg production on day 4 of heat exposure, from 90.63% in the control to 71.88% in the heat group. Additionally, Deng et al. (2012) found that during a 12-day heat stress phase in 96 commercial Hy-Line Brown hens at the age of 60 weeks, egg production decreased by 28.8%. In four genetically distinct strains, including Lohman Brown, Golden Sabathia (23.21%), Fayoumi (15.15%), and White Leghorn (28.57%) in Egypt, it was found that exposure to a

temperature of 35 ± 1°C and 55 ± 5% relative humidity for six hours had detrimental effects on egg quality and production (Ghoname et al., 2022). Kim et al. (2024) indicated that hens exposed to 33°C and 66% relative humidity for 28 days experienced an 11% decrease in egg production rate. Furthermore, eggs produced by laying hens under extreme heat stress result in low-quality output, more broken eggs, and thinner eggshells (Lin et al., 2013). Moreover, heat stress has been shown to reduce eggshell weight (9.93%), thickness (1.2%), percentage (0.66%), and Egg weight (3.24%; Ebeid et al., 2012).

EGGSHELL QUALITY

Hereditary (genetic) factors, environmental factors (management, housing, stress), nutrition, and external components all contribute to eggshell quality flaws, including thin shell, softness, speckles, fractures, and translucency (Cheng and Ning, 2023). Laying hens can produce high-quality eggshells only when they are raised in optimal conditions with all essential components present and functioning in unison (Ketta and Tůmová, 2016). Eggshell development is disrupted by high ambient temperatures (over 32-35°C), which significantly reduces the eggshell's weight, thickness, and strength. A variety of issues, including low feed intake by hens, acid-base and mineral imbalances, physiological disorders in the endocrine system, and other organs involved in eggshell formation, are associated with the negative impact of high ambient temperatures on eggshell quality (Kavtarashvili and Buyarov, 2021). High ambient temperatures (above 32-35°C) disrupt shell formation, leading to lighter, thinner, and weaker shells (Kavtarashvili and Buyarov, 2021). A low-calcium diet significantly decreased hen-day egg production, eggshell weight, strength, and thickness. Calcium deficiency in hens leads to poor shell quality, which may be exacerbated under stressors (Li X et al., 2024). According to Elijah and Adedapo (2006), a drop in feed intake during high ambient temperatures (32.4-33.15 °C) compromised the quality of the eggshell, causing small egg size, low egg production, and eggshell cracking, using climatological data and data from poultry farmers over a period of five years (2000-2004).

SIGNS OF HEAT STRESS IN LAYER CHICKENS

As shown in Figure 1, the signs of heat stress in poultry include open-mouthed panting, lethargy, reduced feed intake, and decreased egg production and quality, as well as a rapid breathing rate, a characteristic posture of standing with wings outstretched, and an increased tendency for cannibalism, which can ultimately lead to prostration and death (Nardone et al., 2010). Additionally, a heat-stressed chicken would pant, spread its wings, hold them slightly apart from its body, stand or lie down, and close its eyes (Dayyani and Bakhtiyari, 2013). Providing cool drinking water to hens under heat stress (33°C) maintained egg production and significantly improved eggshell strength (Kim et al., 2025). Exposure of chickens to severe heat stress (≥ 40-42°C) can cause very high mortality, sometimes approaching 100% during acute heat waves, whereas moderate-to-severe heat stress typically results in mortality rates of about 5-50%, depending on duration, humidity, genotype, age, and management. Annual financial losses from heat stress in the US layer industry were estimated at 61.4 million USD (St-Pierre et al., 2003).

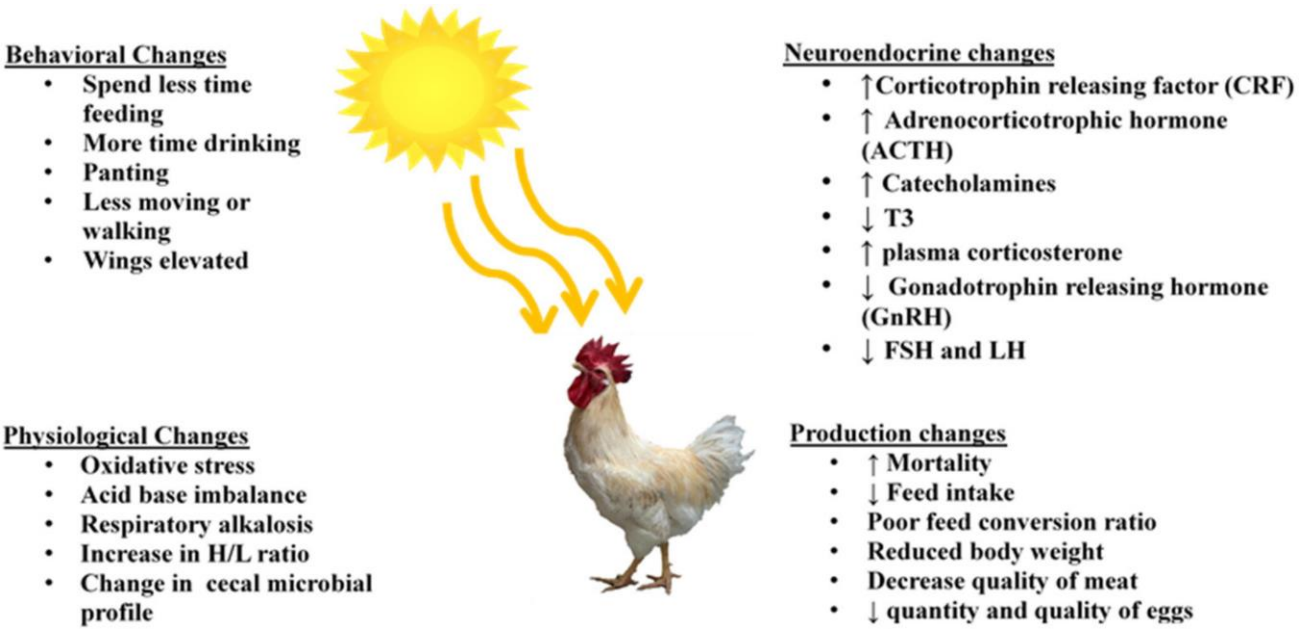


Figure 2. Layer chicken responds to heat stress. Source: Wasti et al. (2020).

To deal with heat stress, chickens try to control their body temperature by changing their normal behaviors (Figure 2). The chickens may rest to dissipate heat from activity, eat less feed, drink more water, lift their wings away from their bodies to reveal any patches of skin without feathers, move into air streams or against cooler surfaces such as brick walls, and move away from other chickens and breathe rapidly (Lara and Rostagno, 2013).

CONTROLLING STRATEGIES

The layout and design of the housing are essential factors in reducing heat stress in hens during hot weather. Therefore, it is necessary to ensure that air flows freely into and out of the layer chicken pens (Pawar et al., 2016; Nawab et al., 2018). Wet feeding, self-selection, diurnal feeding patterns, and coarser meals are all effective ways to combat heat stress (Rahman and Hidayat, 2020). To boost appetite on hot days, more feeders should be available, and the feed should be well-prepared into mash, crumbles, or pellets (Pawar et al., 2016). Open-style homes with adequate ventilation, shade, and water input are essential in hot and muggy climates. It is advised that houses be oriented east-west (Oloyo and Ojerinde, 2020).

When environmental temperatures exceed the thermoneutral zone (16-26°C), chickens should be managed to consume less feed and increase their water intake to aid in cooling (Diarra and Poasa, 2014). Sahin et al. (2002) reported that serum vitamin E levels decreased in poultry under heat stress, while supplemental vitamin E and vitamin A improved broiler performance, increased serum triiodothyronine (T_3), thyroxine (T_4), calcium, and phosphorus, and reduced adrenocorticotropic hormone (ACTH) and specific blood metabolites under heat stress (32°C). Dietary supplementation with vitamin E and organic selenium significantly improved growth performance (body weight gain and feed intake) and reduced heat-related mortality in broiler chickens exposed to heat stress (Çalik et al., 2022). Dehydration, the most intuitive panting-related disadvantage, usually results in higher water requirement and consumption (Wang et al., 2018). Providing chickens with cool drinking water aids cooling by absorbing body heat and helps maintain thermoregulation under high ambient temperatures (Kim et al., 2025), while adding electrolytes to the water helps restore essential minerals and balance blood pH levels disrupted by heat stress (Olayiwola and Adedokun, 2025).

To reduce the negative effects of heat stress on feed intake and utilization, managing feeding time is essential (Farghly et al., 2018). As a result, the hens should be fed a lot in the early morning and late evening when it is cold outside, and the rest of the feed can be provided at any time the layer chickens choose. Since feed-starved chickens produce less heat than fed ones, removing feed on hot days can improve performance traits such as egg production, feed efficiency, egg weight, and growth rate (Daghir, 2009).

Adequate ventilation is crucial because it helps to remove moisture, carbon dioxide, and ammonia that have accumulated in the poultry barns (Pawar et al., 2016; Nawab et al., 2018). Ventilation technology can reduce health issues associated with stress (Pawar et al., 2016; Nawab et al., 2018).

Heat stress is also influenced by stocking density. Excessive stocking density, or overcrowding, has detrimental effects on animal welfare by lowering the general quality of the habitat and making it more difficult for hens to compete for resources. However, lowering stocking density to reduce heat stress can also limit the number of hens that can be raised on a particular farm or in a specific home. Feather pecking and cannibalism are two problems that may arise from overcrowding (Shakeri et al., 2014). Low economic return may result from high stocking density, which generally has negative effects on health, and production performance (Pawar et al., 2016; Nawab et al., 2018).

CONCLUSION

Heat stress has detrimental effects on the health and productivity of hens, posing a major problem for tropical poultry farming. A drop in feed intake during high ambient temperatures compromised the quality of the egg shell, causing small egg size, low egg production, and eggshell cracking. Heat stress has impaired layer production performance by reducing eggshell thickness, increasing egg breakage, and decreasing egg weight and percentage. There are strategies worldwide to mitigate the negative effects of heat stress, including selecting rearing systems with enhanced ventilation, suitable housing conditions, and recommended optimal stocking densities, all of which are critical for enhancing performance at high temperatures. Therefore, exploring other strategies to reduce heat stress while maintaining stocking density without compromising the chickens' performance and well-being is necessary. It is important to conduct further studies on novel approaches that leverage heat-tolerance genes in chickens, as well as on genetic markers to identify chicken genotypes with enhanced heat tolerance.

DECLARATIONS

Acknowledgments

The authors would like to express their gratitude to the reviewers for their constructive criticisms, which have contributed to enhancing the quality of the present manuscript.

Authors' contributions

Eyayu Gobezie conceived and designed the review topic, conducted the comprehensive literature search, synthesized and critically analyzed the published data, and prepared the original draft of the manuscript. Ashenafi Timotiwos contributed to literature collection and organization, assisted in writing specific sections related to growth performance and egg quality, and participated in manuscript revision. Getahun Simeneh contributed to reviewing and editing the manuscript for scientific accuracy and clarity and provided intellectual input on mitigation strategies for heat stress in layer chickens. All authors checked and approved the last edition of the manuscript.

Funding

The current study received no funding.

Competing interests

The authors declared no conflict of interest.

Ethical considerations

The authors declared and confirmed that the manuscript is original, free from misconduct, and has not been previously published in another journal. It is confirmed to be a new contribution to this journal. All authors checked the originality of the data and sentences via a plagiarism checker. No AI tools were used during the writing and preparation of the present study.

Availability of data and materials

No new data were created or analyzed in this study. This article is a review of existing literature, and all referenced materials are cited in the reference list.

REFERENCES

Abd El-Ghany WA and Babazadeh D (2022). Betaine: A potential nutritional metabolite in the poultry industry. Animals, 12(19): 2624. DOI: https://www.doi.org/10.3390/ani12192624

Abdel-Moneim AME, Shehata AM, Mohamed NG, Elbaz AM, and Ibrahim N (2021). Synergistic effect of *Spirulina platensis* and selenium nanoparticles on growth performance, serum metabolites, immune responses, and antioxidant capacity of heat-stressed broiler chickens. Biological Trace Element Research, 200(2): 768-779. DOI: https://www.doi.org/10.1007/s12011-021-02662-w

Ahmed G, Samar T, Khalid M, Shatha G, Asmaa F, Norhan E, Mariusz J, Moustafa M, Alshaharni MO, and Algopish U (2024). Heat shock proteins as a key defense mechanism in poultry production under heat stress conditions. Poultry Science, 103(4): 103537. https://www.doi.org/10.1016/j.psj.2024.103537

Attia YA, Abd El-Hamid AEH, Abedalla AA, Berika MA, Al-Harthi MA, Kucuk O, Sahin K, and Abou-Shehema BM (2016). Laying performance, digestibility and plasma hormones in laying hens exposed to chronic heat stress as affected by betaine, vitamin C, and/or vitamin E supplementation. Springer Plus, 5: 1619. DOI: https://www.doi.org/10.1186/s40064-016-3304-0

Attia YA, Aldhalmi AK, Youssef IM, Bovera F, Tufarelli V, ElHack MEA, ElKholy KH, and Shukry M (2024). Climate change and its effects on poultry industry and sustainability. Discover Sustainability, 5(1): 397. DOI: https://www.doi.org/10.1007/s43621-024-00627-2

Attia YA, Al-Harthi MA, and Elnaggar SH (2018). Productive, physiological and immunological responses of two broiler strains fed different dietary regimens and exposed to heat stress. Italian Journal of Animal Science, 17(3): 686-697. DOI: https://www.doi.org/10.1080/1828051X.2017.1416961

Barrett NW, Rowland K, Schmidt CJ, Lamont SJ, Rothschild MF, and Ashwell CM (2019). Effects of acute and chronic heat stress on the performance, egg quality, body temperature, and blood gas parameters of laying hens. Poultry Science, 98(12): 6684-6692. DOI: https://www.doi.org/10.3382/ps/pez541

Çalik A, Emami N, White M, Walsh M, Romero L, and Dalloul R (2022). Influence of dietary vitamin E and selenium supplementation on broilers subjected to heat stress: Part I — Growth performance, body composition and intestinal nutrient transporters. Poultry Science, 101(6): 101857. https://www.doi.org/10.1016/j.psj.2022.101857

Charles DR (2002). Responses to the thermal environment. Poultry environment problems, a guide to solutions. Nottingham University Press., Nottingham, United Kingdom, pp. 1-16. DOI: https://www.doi.org/10.1093/ps/81.8.1257

Cheng X and Ning Z (2023). Research progress on bird eggshell quality defects: A review. Poultry Science, 102(1): 102283. DOI: https://www.doi.org/10.1016/j.psj.2022.102283

Daghir NJ (2008). Poultry production in hot climates, 2nd Edition. CAB International., Wallingford, Oxfordshire, UK, pp. xiii, 387. DOI: https://www.doi.org/10.1079/9781845932589.0000

Dayyani N and Bakhtiyari H (2013). Heat stress in poultry: Background and affective factors. International Journal of Advanced Biological and Biomedical Research, 1(11): 1409-1413. Available at: http://www.ijabbr.com/article_7968_f56af19891048da54f54040274e4cd73.pdf

Deng W, Dong XF, Tong JM, and Zhang Q (2012). The probiotic *Bacillus licheniformis* ameliorates heat stress-induced impairment of egg production, gut morphology, and intestinal mucosal immunity in laying hens. Poultry Science, 91(3): 575-582. DOI: https://www.doi.org/10.3382/ps.2010-01293

Diarra S and Poasa T (2014). Feeding management of poultry in high environmental temperatures, International Journal of Poultry Science, 13(11): 657-661. DOI: https://www.doi.org/10.3923/ijps.2014.657.661

Donkoh A (1989) Ambient temperature: A factor affecting performance and physiological response of broiler chickens. International Journal of Biometeorology, 33(4): 259-265. DOI. https://www.doi.org/10.1007/BF01051087

Ebeid TA, Suzuki T, and Sugiyama T (2012). High temperature influences eggshell quality and calbindin-D28k localization of eggshell gland and all intestinal segments of laying hens. Poultry Science, 91(9): 2282-2287. DOI: http://www.doi.org/10.3382/ps.2011-01898

Elijah OA and Adedapo A (2006). The effect of climate change on poultry productivity in Ilorin Kwara State, Nigeria. International Journal of Poultry Science, 5(11): 1061-1068. DOI: https://www.doi.org/10.3923/ijps.2006.1061.1068

Etches RJ, John TM, Verrinder, and Gibbins AM (2008). Behavioral, physiological, neuroendocrine and molecular responses to heat stress. In: N. J. Daghir, Editor, Poultry production in hot climates, 2nd Edition. CAB International., Wallingford (UK), pp. 48-79. DOI: https://www.doi.org/10.1079/9781845932589.0048

Farghly MF, Kh M, Mahrose AE, Galal RM, Ali EA, Ahmed M, Rehman Z, Ullah Z, and Ding C (2018). Implementation of different feed withdrawal times and water temperatures in managing turkeys during heat stress. Poultry Science, 97(9): 3076-3084. DOI: http://www.doi.org/10.3382/ps/pey173.

Food and agriculture organization of the United Nations (FAO) (2021). The state of food security and nutrition in the world. Available at: https://openknowledge.fao.org/server/api/core/bitstreams/1c38676f-f5f7-47cf-81b3-f4c9794eba8a/content

Ghoname M, Elnaggar A, Hassan S, and Habashy W (2022). Effect of acute heat stress on production performance and egg quality in four strains of chickens. South Africa Journal of Animal Science, 52(2): 168-176. DOI: https://www.doi.org/10.4314/sajas.v52i2.6

He S, Li S, Arowolo MA, Yu Q, Chen F, Hu R, and He J (2019). Effect of resveratrol on growth performance, rectal temperature, and serum parameters of yellow-feather broilers under heat stress. Animal Science Journal, 90(3): 401-411. DOI: https://www.doi.org/10.1111/asj.13161

Jahromi MF, Altaher YW, Shokryazdan P, Ebrahimi R, Ebrahimi M, Idrus Z, Tufarelli V, and Liang JB (2016). Dietary supplementation of a mixture of lactobacillus strains enhances performance of broiler chickens raised under heat stress conditions. International Journal of Biometeorology, 60(7): 1099- 1110. DOI: https://www.doi.org/10.1007/s00484-015-1103-x

Kavtarashvili A and Buyarov V (2021). The reasons for the deterioration of chicken eggshell quality at high temperatures: A review. E3S Web of Conferences, 247(2): 01015. DOI: https://www.doi.org/10.1051/e3sconf/202124701015

Ketta M and Tůmová E (2016). Eggshell structure, measurements, and quality-affecting factors in laying hens: A review. Czech Journal of Animal Science, 61(7): 299-309. DOI: https://www.doi.org/10.17221/46/2015-CJAS

Kim CH, Lee WD, Lim SJ, Yang KY, and Jeon JH (2025). Effects of cool water supply on laying performance, egg quality, rectal temperature and stress hormones in heat-stressed laying hens in open-type laying houses. Animals, 15(11): 1635. DOI: https://www.doi.org/10.3390/ani15111635

Kim HR, Ryu C, Lee SD, Cho JH, and Kang H (2024). Effects of heat stress on the laying performance, egg quality, and physiological response of laying hens. Animals, 14(7): 1076. DOI: https://www.doi.org/10.3390/ani14071076

Kpomasse CC, Emmanuel Oke O, Frédérick M, and Kokou T (2021). Broiler production challenges in the tropics: A review. Veterinary Medicine and Science, 7(3): 831-842. DOI: https://www.doi.org/10.1002/vms3.435

Lara L and Rostagno M (2013). Impact of heat stress on poultry production. Animals, 3(2): 356-369. DOI: https://www.doi.org/10.3390/ani3020356

Li X, Uyanga VA, Jiao H, Wang X, Zhao J, Zhou Y, Li H, and Lin H (2024). Effects of low dietary calcium and lipopolysaccharide challenges on production performance, eggshell quality, and bone metabolism of laying hens. Frontiers in Physiology, 15: 1396301. DOI: https://www.doi.org/10.3389/fphys.2024.1396301

Lin H, Mertens K, Kemps B, Govaerts T, De Ketelaere B, De Baerdemaeker J, Decuypere E, and Buyse J (2013). New approach of testing the effect of heat stress on eggshell quality: Mechanical and material properties of eggshell and membrane. British Poultry Science, 45(4): 476-482. DOI: https://www.doi.org/10.1080/00071660400001173

Mashaly MM, Hendricks GL, Kalama MA, Gehad AE, Abass AO, and Patterson PH (2004). Effects of heat stress on production parameters and immune response of commercial laying hens. Poultry Science, 83(6): 889-894. DOI: https://www.doi.org/10.1093/ps/83.6.889

Naga R, Kumari K, and Narendra D (2018). Ameliorative measures to counter heat stress in poultry. World's Poultry Science Journal, 74(1): 117-130. DOI: https://www.doi.org/10.1017/S0043933917001003

Nardone A, Ronchi B, Lacetera N, Ranieri MS, and Bernabucci U (2010). Effects of climate changes on animal production and sustainability of livestock systems. Livestock Science, 130(1-3): 57-69. DOI: https://www.doi.org/10.1016/j.livsci.2010.02.011

Nawab A, Ibtisham F, Li G, Kieser B, Wu J, Liu W, Zhao Y, Nawab Y, and Li K Xiao M (2018). Heat stress in poultry production: Mitigation strategies to overcome the future challenges facing the global poultry industry. Journal of Thermal Biology, 78: 131-139. DOI: https://www.doi.org/10.1016/j.jtherbio.2018.08.010

Nawaz AH, Amoah K, Leng QY, Zheng JH, Zhang WL, and Zhang L (2021). Poultry response to heat stress: Its physiological, metabolic, and genetic implications on meat production and quality including strategies to improve broiler production in a warming world. Frontiers in Veterinary Science, 8: 699081. DOI: https://www.doi.org/10.3389/fvets.2021.699081

Olayiwola S and Adedokun S (2025). Heat stress in poultry: The role of nutritional supplements in alleviating heat stress and enhancing gut health in poultry. Frontiers in Veterinary Science, 12: 1691532. DOI: https://www.doi.org/10.3389/fvets.2025.1691532

Oloyo A and Ojerinde A (2020). Poultry housing and management. In: A. A. Kamboh (Editor), Poultry- An advanced learning. Intech Open, pp. 1-17. DOI: https://www.doi.org/10.5772/intechopen.83811

Pawar SS, Sajjanar B, Lonkar VD, Nitin KP, Kadam AS, Nirmale AV, Brahmane MP, and Bal SK (2016). Assessing and mitigating the impact of heat stress in poultry. Advances in Animal and Veterinary Sciences, 4(6): 332-341. DOI: http://www.doi.org/10.14737/journal.aavs/2016/4.6.332.341

Radwan LM (2020). Genetic improvement of egg laying traits in Fayoumi chickens bred under conditions of heat stress through selection and gene expression studies. Journal of Thermal Biology, 89: 102546. DOI: https://www.doi.org/10.1016/j.jtherbio.2020.102546

Rahman and Hidayat C (2020). Reducing the negative effect of heat stress in broiler through nutritional and feeding strategy. IOP Conference Series: Earth Environmental Science, 465(1): 012034. DOI: https://www.doi.org/10.1088/1755-1315/465/1/012034

Ranjan A, Sinha R, Devi I, Rahim A, and Tiwari S (2019). Effect of heat stress on poultry production and their management approaches. International Journal of Current Microbiology and Applied Sciences, 8(2): 1548-1555. DOI: https://www.doi.org/10.20546/ijcmas.2019.802.181

Richards SA (1970). Physiology of thermal panting in birds. Annales de Biologie Animale, Biochimie, Biophysique, 10(Hors-série 2): 151-168. DOI: https://www.doi.org/10.1051/rnd:19700614

Rozenboim I, Tako E, Gal-Garber O, Proudman JA, and Uni Z (2007). The effect of heat stress on ovarian function of laying hens. Poultry Science, 86(8): 1760-1765. DOI: https://www.doi.org/10.1093/ps/86.8.1760

Saeed M, Abbas G, Alagawany M, Kamboh AA, Abd El-Hack ME, Khafaga AF, and Chao S (2019). Heat stress management in poultry farms: A comprehensive overview. Journal of Thermal Biology, 84(2): 414-425. DOI: https://www.doi.org/10.1016/j.jtherbio.2019.07.025

Safi A, Imtiaz M, Ahsan HM T, Riaz A, Ali and S, and Uzair MD (2022). Effect of heat stress in poultry and its mitigation. Current Research in Agriculture and Farming, 3(6): 9-18. DOI: http://www.doi.org/10.18782/2582-7146.179

Sahin K, Küçük O, Miller D, and Sahin N (2002). Effects of vitamin E and vitamin A supplementation on lipid peroxidation and concentrations of some minerals in broilers reared under heat stress (32 °C). Poultry Science, 81(11): 1650-1657. DOI: https://www.doi.org/10.1093/ps/81.11.1650

Sahin N, Onderci M, Balci TA, Cikim G, Sahin K, and Kucuk O (2007). The effect of soy isoflavones on egg quality and bone mineralization during the late laying period of quail. British Poultry Science, 48(3): 363-369. DOI: https://www.doi.org/10.1080/00071660701341971

Shakeri M, Zulkifli I, Soleimani AF, O'Reilly EL, Eckersall PD, Anna AA, Kumari S, and Abdullah FFJ (2014). Response to dietary supplementation of L-glutamine and L-glutamate in broiler chickens reared at different stocking densities under hot, humid tropical conditions. Poultry Science, 93(11): 2700-2708. DOI: https://www.doi.org/10.3382/ps.2014-03910

Smith AJ (1974). Changes in the average weight and shell thickness of eggs produced by hens exposed to high environmental temperatures: A review. Tropical Animal Health and Production, 6(4): 237-244. DOI: https://www.doi.org/10.1007/BF02383283

Song D, Li A, Wang Y, Song G, Wang L, Lin K, Min Y, and Wang W (2022). Effects of symbiotic on growth, digestibility, immune and antioxidant performance in broilers. Animal, 16(4): 100497. DOI: https://www.doi.org/10.1016/j.animal.2022.100497

Song DJ and King AJ (2015). Effects of heat stress on broiler meat quality. World's Poultry Science Journal, 71(4): 701-709. DOI: https://www.doi.org/10.1017/S0043933915002421

Star L, Juul-Madsen, HR, Decuypere E, Nieuwland MGB, de Vries Reilingh G, van den Brand H, Kemp B, and Parmentier HK (2009). Effects of early life thermal conditioning and immune challenge on thermotolerance and humoral immune competence in adult laying hens. Poultry Science, 88(11): 2253-2261. DOI: https://www.doi.org/ 10.3382/ps.2008-00373

St-Pierre B, Cobanov, and Schnitkey G (2003). Economic losses from heat stress by us livestock industries. Journal of Dairy Science, 86(Suppl.): E52-E77. DOI: https://www.doi.org/10.3168/jds.S0022-0302(03)74040-5

Sugiharto S (2020). Alleviation of heat stress in broiler chicken using turmeric. A short review. Journal of Animal Behaviour Biometeorology, 8(3): 215-222. DOI: https://www.doi.org/10.31893/jabb.20028

Syafwan W, Kwakkel R, and Verstegen M (2011). Heat stress and feeding strategies in meat-type chickens. World's Poultry Science Journal, 67(4): 653-674. DOI: https://www.doi.org/10.1017/S0043933911000742

Tesakul S, Mitsuwan W, Morita Y, and Kitpipit W (2025). Effects of heat stress on egg performance in laying hens under hot and humid conditions. Veterinary World, 18(4): 851-858. DOI: DOI: https://www.doi.org/10.14202/vetworld.2025.851-858

Ugurlu N, Acar B, and Topak R (2001). Production performance of caged layers under different environmental temperatures. Archiv fur Geflugelkunde, 66(1): 43-46. Available at: https://acikerisim.selcuk.edu.tr/items/c92fd093-5167-4c6c-b51d-fdee1dcfd951

Vandana GD, Sejian V, Lees AM, Pragna P, Silpa MV, and Maloney SK (2021). Heat stress and poultry production: Impact and amelioration. International Journal of Biometeorology, 65(2): 163-179. DOI: https://www.doi.org/10.1007/s00484-020-02023-7

Wang W, Yan F, Hu J, Amen O, and Cheng H (2018). Supplementation of Bacillus subtilis-based probiotic reduces heat stress-related behaviors and inflammatory response in broiler chickens. Journal of Animal Science, 96(5): 1654-1666. DOI: https://www.doi.org/10.1093/jas/sky092

Wasti S, Sah N, and Mishra B (2020). Impact of heat stress on poultry health and performances, and potential mitigation strategies. Animals, 10(8): 1266. DOI: https://www.doi.org/10.3390/ani10081266

Yan L, Hu M, Gu L, Lei M, Chen Z, Zhu H, and Chen R (2022). Effect of heat stress on egg production, steroid hormone synthesis, and related gene expression in chicken preovulatory follicular granulosa cells. Animals, 12(11): 1467. DOI: https://www.doi.org/10.3390/ani12111467

Zhang C, Zhao XH, Yang L, Chen XY, Jiang RS, Jin SH, and Geng ZY (2017). Resveratrol alleviates heat stress-induced impairment of intestinal morphology, microflora, and barrier integrity in broilers. Poultry Science, 96(12): 4325-4332. DOI: https://www.doi.org/10.3382/ps/pex266

Publisher's note: Scienceline Publication Ltd. remains neutral with regard to jurisdictional claims in published maps and institutional affiliations.

Open Access: This article is licensed under a Creative Commons Attribution 4.0 International License, which permits use, sharing, adaptation, distribution and reproduction in any medium or format, as long as you give appropriate credit to the original author(s) and the source, provide a link to the Creative Commons licence, and indicate if changes were made. The images or other third party material in this article are included in the article's Creative Commons licence, unless indicated otherwise in a credit line to the material. If material is not included in the article's Creative Commons licence and your intended use is not permitted by statutory regulation or exceeds the permitted use, you will need to obtain permission directly from the copyright holder. To view a copy of this licence, visit https://creativecommons.org/licenses/by/4.0/.
© The Author(s) 2025

2025, Scienceline Publication
World's Veterinary Journal
World Vet J, 15(4): 1138-1148.
ISSN 2322-4568

DOI: https://dx.doi.org/10.54203/scil.2025.wvj117
PII: S232245682500117-15

The Role of Chronic Inflammation in the Pathogenesis of Gizzard Erosion in Pipped Poultry Embryos: A Review

Debashis Dutta * and Rajeeb Roy

Research and Development, RR Animal Health Care Ltd., Hyderabad, Telangana, India

*Corresponding author's Email: communications@rrahc.in

REVIEW ARTICLE
Received: October 11, 2025
Revised: November 13, 2025
Accepted: December 13, 2025
Published: December 31, 2025

ABSTRACT

Gizzard erosion remains a recurrent issue in commercial broiler and layer embryos, leading to poor hatchability and early chick mortality, yet the mechanisms linking infectious, nutritional, and toxic factors remain poorly understood. The present review synthesized published pathological, immunological, and toxicological evidence to explore how these diverse factors may contribute to the development of gizzard erosion. A structured evaluation of experimental and field studies was performed to integrate the available findings. On the basis of this synthesis, the review proposed a two-hit inflammatory hypothesis to explain disease onset. In this hypothesis, the first hit involved chronic, low-grade inflammatory priming during embryogenesis driven by maternal mycotoxins, breeder immune stress, or vertically transmitted infections, whereas the second hit consisted of acute oxidative and metabolic stress during pipping and hatching that may precipitate visible epithelial injury in predisposed gizzards. The hypothesis is presented as a conceptual framework derived from existing literature rather than as an established mechanism, emphasizing that current evidence supports a plausible sequential inflammatory process. Understanding gizzard erosion through this exploratory framework underscores the need for preventive control of prenatal inflammatory triggers and identifies clear directions for future experimental validation at the embryonic level.

Keywords: Broiler, Chronic inflammation, Gizzard erosion, Immunology, Layer, Toxicology

INTRODUCTION

Gizzard Erosion and Ulceration (GEU) is a pathological syndrome diagnosed in post-hatch poultry, has emerged as a significant welfare and economic concern for the global poultry industry (Haque et al., 2023). The condition contributes to substantial financial losses, which are attributable to reductions in feed conversion efficiency, impaired growth rates, decreased flock uniformity, and elevated mortality rates (Mirzazadeh et al., 2021). Clinically, the diagnosis of GEU is predicated on the identification of characteristic macroscopic defects on the gizzard's mucosal surface (Das Kumar and Shelke, 2024; Ouchhour et al., 2024). The gizzard lesions range in severity from erosions, defined as defects confined to the protective koilin layer, to ulcerations, which are more severe lesions that penetrate the koilin to involve the underlying glandular epithelium and mucosa (Haque et al., 2023). Gross pathological examination often reveals defects with dark brown, black, or reddish discoloration, indicative of focal to confluent hemorrhage within the tissue (Jones et al., 2023). In severe outbreaks, the entire koilin layer may exhibit extensive necrosis, becoming brittle and easily detachable from the mucosa (Ouchhour et al., 2024). Pathology surveys in commercial broiler complexes have documented the incidence of severe GEU to be as high as 20-32%, underscoring the profound prevalence and economic significance of the syndrome (da Silva et al., 2024). Although GEU is clinically diagnosed in post-hatch birds, growing experimental and field observations indicate that pathological priming may originate during late embryogenesis.

Histopathological analysis provides a more detailed view of the cellular damage and confirmed that a robust inflammatory response is a unifying hallmark of GEU pathogenesis, regardless of the primary etiology (Mirzazadeh et al., 2021; Jones et al., 2023; da Silva et al., 2024). Histologically, the condition is characterized by necrotic changes in the koilin-secreting glandular epithelium, which is coupled with the degradation and shedding of the koilin layer (Mirzazadeh et al., 2021; da Silva et al., 2024; Ouchhour et al., 2024). The most critical and unifying feature is the marked inflammatory cell infiltration into the damaged tissue (Kumar et al., 2021; Jones et al., 2023; Ouchhour et al., 2024). This infiltrate is typically characterized as a lymphoplasmacytic or lymph histiocytic inflammation, composed of heterophils (the avian equivalent of neutrophils), lymphocytes, and plasma cells (da Silva et al., 2024; Ouchhour et al., 2024; Kardoudi et al., 2025). The inflammation is not superficial; it is commonly found within the lamina propria and submucosa (Kumar et al., 2021; Jones et al., 2023). Furthermore, severe cases demonstrate that the infiltrate can

To cite this paper: Dutta D and Roy R (2025). The Role of Chronic Inflammation in the Pathogenesis of Gizzard Erosion in Pipped Poultry Embryos: A Review. *World Vet. J.,* 15(4): 1139-1148. DOI: https://dx.doi.org/10.54203/scil.2025.wvj117

penetrate as deep as the gizzard's muscle wall (Kumar et al., 2021; El-Shall et al., 2022; Kardoudi et al., 2025). The consistent presence of this inflammatory cascade suggests a compelling association between inflammation and the tissue destruction characteristic of GEU, supporting the view that inflammation may represent a leading mechanistic pathway (El-Shall et al., 2022; Haque et al., 2023; Kardoudi et al., 2025). The present review evaluated whether prenatal inflammatory and toxicological influences create a predisposed gizzard that exhibits visible lesions only at hatch. The aim of the present review was to synthesize current pathological, immunological, and toxicological evidence to assess whether late-embryonic inflammatory priming can plausibly explain the perinatal onset of GEU.

METHODOLOGY

The present review is based on a comprehensive literature search to identify studies relevant to the perinatal pathogenesis of Gizzard Erosion and Ulceration (GEU). The search was conducted using the electronic databases PubMed and Google Scholar. The search terms, used individually and in combination, included "Gizzard Erosion and Ulceration (GEU)", "poultry embryo", "chronic inflammation", "perinatal pathology", "Fowl adenovirus-1 (FAdV-1)", "maternally transferred toxins", and "mycotoxins". The inclusion criteria for selecting articles were peer-reviewed original research, review papers, and relevant case studies, provided they were published in English and demonstrated direct relevance to the etiology, pathology, or *in ovo* immune mechanisms associated with GEU. The collected literature was critically synthesized to evaluate the evidence for an embryonic origin of the disease and to support the "two-hit" pathogenic framework presented in the present review.

THE IMMUNOCOMPETENT AVIAN EMBRYO PRIMED FOR INFLAMMATION

Ontogeny of the gut-associated lymphoid tissue

A central principle of the 'two-hit' framework is that the late-stage embryo is not immunologically passive (Sharma et al., 2025). On the contrary, the following section outlines the evidence that the embryo possesses a functional immune system capable of mounting a complex and ultimately damaging inflammatory response before hatching (Ayalew et al., 2025). The biological plausibility of this framework is contingent upon the avian mucosal immune system achieving functional maturity *in ovo* (Gong et al., 2023). Immune development begins early in embryogenesis when hematopoietic stem cells migrate from the yolk sac (Brand et al., 1983). The hematopoietic stem cells then populate the primary lymphoid organs, the thymus, where T-cells mature, and the bursa of Fabricius, which is responsible for B-cell maturation (Bar Shira and Friedman, 2018). While these foundational events occur early, the gut-associated lymphoid tissue (GALT), which constitutes the largest immunological component in the bird, undergoes its most significant organization and functional development during the critical final stages of incubation, from approximately embryonic day (ED) 14 to ED 21 (Janković et al., 1975). During the pre-hatch period, the embryonic gut is systematically populated by waves of lymphocytes that migrate from the primary lymphoid organs, seeding the intestinal lamina propria and epithelium with immunocompetent cells (Da Silva et al., 2019).

The maturation of the GALT and lymphocyte population establishes a state of functional readiness, particularly within the innate immune system (Ayalew et al., 2025). While the embryo's adaptive immune capacity is still developing and relies heavily on the passive protection conferred by maternally derived Immunoglobulin Y (IgY) transferred via the egg yolk, the innate system, comprising physical barriers, phagocytic cells, and humoral components, becomes fully operational to form the first line of defense for the neonate (Sharma et al., 2025). Although the embryonic gut is considered a largely sterile environment, this late-stage maturation is not a passive process (Gong et al., 2023). The maturation is driven by powerful physiological stimuli, including the embryo's swallowing of amniotic fluid and the programmed anticipation of massive microbial colonization at the moment of hatch (Bar Shira and Friedman, 2018). The maturation of the GALT, driven by amniotic fluid ingestion and preparation for microbial colonization, represents a form of immune education, whereby the developing mucosal immune system learns to differentiate between its own organisms and pathogens, a foundational training that begins *in ovo* (Brand et al., 1983). Therefore, by the time of pipping, the embryo possesses a well-organized GALT that provides the essential anatomical and cellular framework required to initiate and orchestrate the complex inflammatory responses central to our hypothesis (Janković et al., 1975; Da Silva et al., 2019).

Functional competence of innate immune cells

The structural development of the GALT happens parallel to the functional maturation of its resident innate immune cell populations (Ayalew et al., 2025). By ED 18, the embryonic intestine is equipped with a diverse and functionally competent array of innate immune cells, which are not merely present but are fully capable of recognizing and

responding to molecular stimuli, specifically pathogen-associated molecular patterns (PAMPs; Schilling et al., 2018). Such a state of readiness is critical, providing the embryo with an immediate defense mechanism upon hatching (Bavananthasivam et al., 2019). The first line of defense is formed by the intestinal epithelial cells (IECs) themselves. Far from being a passive physical barrier, IECs are active participants and sentinels of mucosal immunity. The maturation of intestinal epithelial cells becomes histologically evident from ED 14 onwards, and by ED 19-20, enterocytes display enhanced microvilli density in preparation for their absorptive and defensive roles (Yoshimura et al., 2024). Crucially, the IECs are programmed to produce a range of antimicrobial peptides (AMPs), such as avian β-defensins (AvBDs) and cathelicidins, which provide a formidable chemical barrier against the first wave of microbial colonizers (Zhang and Wong, 2019). The pre-hatch expression of the AMPs demonstrates that the most superficial layer of the gut is already an immunologically active tissue.

Beyond the epithelial barrier, by ED18, the embryonic lamina propria is populated by a network of professional phagocytes essential for surveillance and response (Ayalew et al., 2025). Macrophages, which originate from the yolk sac, are present in embryonic tissues and are deeply involved in both immune surveillance and the extensive tissue remodeling that occurs during late-stage development (approximately ED 14-21; Balic et al., 2014). Dendritic cells (DCs) also establish a functional network within the gut during this same ED 14-21. As the key antigen-presenting cells, DCs are crucial for linking the innate and adaptive immune responses (Kannaki et al., 2015). The maturation of these phagocytic cells is not a random process; rather, it is precisely controlled by local signals from the gut microenvironment (Hincke et al., 2019). Such signals are initiated through the activation of pattern recognition receptors (PRRs), particularly Toll-like Receptors (TLRs), and involve key regulatory molecules like the cytokine Transforming Growth Factor-beta (TGF-β; Terada et al., 2020). The PRR and TGF-β–mediated maturation of phagocytic cells indicates the presence of a sophisticated regulatory system that prepares macrophages and dendritic cells to effectively sample antigens and initiate immune responses upon encountering microbial stimuli at hatch.

The embryonic intestine is also populated by other important specialized innate and innate-like lymphoid cell types that contribute to a multi-layered defense (Ayalew et al., 2025). Natural killer (NK) cells, which provide vital defense against virally infected and transformed host cells, appear within the intestinal intraepithelial lymphocyte population by ED 19 (Alkie et al., 2019). Although NK cells appear within the intestinal intraepithelial lymphocyte population by ED19 (Alkie et al., 2019), direct evidence linking embryonic NK cell activity to defense against FAdV-1 is lacking; however, their early presence suggests a potential role in responding to vertically transmitted viral infections. Furthermore, a unique subset of T-cells, the gamma-delta (γδ) T cells, which function at the interface of innate and adaptive immunity, are functionally mature by ED 13-16 (Ayalew et al., 2025). T-cells are notably abundant in epithelial tissues, including the intestine. These γδ T cells are considered a critical first line of defense in both the late-stage embryo (approximately ED 14-21) and during the first few days post-hatch. The collective presence of this diverse complement of functional immune cells, from AMP-secreting epithelial cells to a network of phagocytes and specialized lymphocytes, definitively establishes the embryo's capacity during the final stages of incubation (approximately ED 14-21) to recognize and mount a robust response to immunological triggers, providing the cellular machinery for the inflammatory events central to GEU pathogenesis (Sun et al., 2025).

The embryonic inflammatory repertoire

The functional competence of the previously described innate immune cells is substantiated by the embryo's demonstrated ability to express a wide and sophisticated repertoire of immune signaling molecules (Sharma et al., 2025). Gene expression studies have confirmed that the embryonic intestine is not merely reactive but is pre-programmed to orchestrate a complex inflammatory response upon stimulation by molecular triggers, such as PAMPs (Cheng et al., 2022). A distinct developmental trajectory for the gene expression of key immune mediators, including both pro-inflammatory and regulatory cytokines, has been identified in the embryonic gut, which is not stochastic but follows a highly coordinated timeline (Cooley et al., 2014). A study revealed that while a baseline level of the expression of these immune-related genes is present at ED 14 and ED 17, a significant upregulation of key immune-related genes occurs at ED 20, particularly within the cecum (Sharma et al., 2025). The significant upregulation of key immune-related genes immediately prior to hatch indicates a deliberate and organized preparation for the imminent immunological challenges of the post-hatch environment, establishing a state of heightened immune readiness (Cheng et al., 2022).

The programmed upregulation of immune genes includes a full spectrum of both pro-inflammatory and regulatory mediators, indicating a sophisticated system capable of both initiating and limiting an inflammatory response (Sharma et al., 2025). The embryo during these final stages of incubation (approximately ED 14-21) is fully capable of expressing potent pro-inflammatory cytokines that are central to antimicrobial defense. For instance, the cecal expression of Interferon-gamma (IFN-ϒ), a critical cytokine for antiviral defense and macrophage activation, and Interleukin-6 (IL-6), a central mediator of the acute phase response, increases significantly at ED 20 compared to earlier time points such as

ED 14 and ED 17 (Sharma et al., 2025). Experimental challenges with pathogens or toxins (like deoxynivalenol) further confirm that embryonic tissues can robustly upregulate other classical inflammatory drivers, including IL-1β, IL-6, and tumor necrosis factor-alpha (TNF-α; Cheng et al., 2022). However, the embryonic immune system is not solely pro-inflammatory; it concurrently establishes regulatory mechanisms to maintain homeostasis. The expression of transforming growth factor-beta (TGF-β), a multifunctional cytokine involved in immune suppression and tissue repair, also indicated a statistically significant increase at ED 20 (Cooley et al., 2014). This is complemented by the documented expression of the anti-inflammatory cytokine IL-10, which serves to counterbalance the pro-inflammatory signals (Sharma et al., 2025). The concurrent expression of both pro-inflammatory and regulatory cytokines highlights a sophisticated system capable of both initiating and controlling an inflammatory response *in-ovo*.

The ability to mount these pro-inflammatory and regulatory responses is predicated on the expression of PRRs that detect danger signals, such as pathogen-associated molecular patterns (PAMPs; Sharma et al., 2025). By late-stage embryogenesis, intestinal tissues express a variety of TLRs, including TLR2, TLR4, TLR15, and TLR21, which are essential for recognizing bacterial and viral components and initiating downstream signaling cascades (MyD88 and NF-κB) that culminate in cytokine production (Kannaki et al., 2015; Terada et al., 2020). The simultaneous upregulation of both PRRs and cytokines at ED 20 is not a random occurrence; it represents a programmed, evolutionarily conserved "immunological priming" in preparation for the massive microbial and antigenic exposure at hatch (Alkie et al., 2019). The coordinated PRR- and cytokine-driven immunological priming at ED20 is a critical developmental milestone, but its very complexity also renders the system vulnerable (Garcia et al., 2021). The potential for a dysregulated, hyper-inflammatory state provides a direct mechanistic framework for the hypothesis that chronic, low-level prenatal insults can establish a primed inflammatory state that manifests as acute pathology, such as GEU, when the physiological stress of hatching further challenges the system (Kogut et al., 2012; Schilling et al., 2018; Neerukonda and Katneni, 2020; Rehman et al., 2021).

A PATHOGENIC MODEL FOR CHRONIC PRIMING AND ACUTE TRIGGERS

Prenatal triggers of sustained inflammatory responses

A sustained, or chronic, inflammatory state can be established in the embryo when it is exposed to persistent immunological triggers that originate either from the breeder hen via vertical transmission or from adverse conditions within the incubation environment (Grafl et al., 2012; Kardoudi et al., 2025). Persistent prenatal immunological triggers disrupt the carefully orchestrated process of immune development, shifting the system from a state of balanced readiness to one of active, low-grade inflammation (Al Amaz and Mishra, 2024; Al-Zghoul et al., 2025). The breeder hen serves as a primary and direct source of these inflammatory stimuli, specifically through the maternal-fetal transfer of infectious pathogens and the deposition of nutritional toxins (Grafl et al., 2012; Kardoudi et al., 2025). The combined maternal pathways of pathogen transfer and nutritional toxin deposition provide a clear and direct mechanism for initiating a chronic inflammatory process in embryonic tissues long before the stress of hatching occurs (Al-Zghoul et al., 2025; Aryal et al., 2025).

FAdV-1 provides a well-documented case of a pathogenic trigger, as the virus is known to pass from an infected breeder flock to its embryos via vertical transmission (Grafl et al., 2012; Kardoudi et al., 2025). The FAdV-1 is capable of establishing a persistent, low-level infection in different embryonic tissues, including the gizzard, well before hatching (Kardoudi et al., 2025). The persistence of low-level infection creates a constant source of viral PAMPs, which leads to the sustained activation of PRRs similar to TLRs in local immune and epithelial cells (Al-Zghoul et al., 2025). The sustained activation of PRRs resulting from persistent low-level FAdV-1 infection, in turn, drives the continuous production of pro-inflammatory cytokines, which may establish a chronic inflammatory state either locally within infected gizzard tissue or systemically through circulating inflammatory mediators (Al-Zghoul et al., 2025). In the context of FAdV-1, priming appears to be local within the gizzard, whereas other prenatal triggers, such as mycotoxins or heat stress, are more likely to induce a remote, cecum-originating inflammatory priming with systemic effects on the gizzard. A parallel non-infectious mechanism exists with the maternal transfer of mycotoxins, particularly trichothecenes such as T-2 toxin and deoxynivalenol (Al Amaz and Mishra, 2024). Contaminated breeder feed allows for the deposition of these mycotoxins into the egg yolk and albumin, exposing the developing embryo to potent immunomodulatory and pro-inflammatory compounds throughout its development (Aryal et al., 2025). Trichothecene mycotoxins such as T-2 toxin and deoxynivalenol can directly damage the integrity of the developing intestinal epithelium, compromising its barrier function, and can directly activate immune cells, triggering a persistent inflammatory response that impairs normal tissue development and function (Al-Zghoul et al., 2025; Aryal et al., 2025).

Beyond vertical transmission, the incubation environment, specifically parameters such as temperature, humidity, and CO_2 levels, itself can act as a powerful modulator of the embryonic immune system, with the potential to program a

long-lasting inflammatory phenotype (Al Amaz and Mishra, 2024; Aryal et al., 2025). Chronic or acute heat stress during incubation is a well-documented inflammatory trigger in avian embryos (Al Amaz and Mishra, 2024). High temperatures trigger the embryo's hypothalamic-pituitary-adrenal (HPA) axis, resulting in the secretion of stress hormones and the subsequent disruption of metabolic homeostasis (Aryal et al., 2025). At the molecular level, thermal stress activates pro-inflammatory signaling pathways, such as the TLR/MyD88/NF-κB pathway, resulting in the upregulation of cytokines like IL-6 and IFN-γ, thereby contributing to the establishment of a pro-inflammatory state *in ovo* (Al-Zghoul et al., 2025). It is likely that epigenetic modifications are the mechanism responsible for the long-lasting effects of such environmental stressors on immune function (Aryal et al., 2025). Such stressors can induce changes in DNA methylation patterns and histone modifications in immune-related genes, effectively pre-programming the embryo for a hyper-responsive or dysregulated inflammatory phenotype that persists into post-hatch life (Al Amaz and Mishra, 2024; Al-Zghoul et al., 2025).

Pathophysiological mechanisms linking inflammation to tissue vulnerability

A state of chronic, sub-clinical inflammation, established by the persistent prenatal triggers previously discussed, fundamentally alters the gizzard's tissue architecture and homeostatic balance, rendering it highly susceptible to subsequent damage (Mirzazadeh et al., 2021; Jones et al., 2023). The increased susceptibility to damage resulting from chronic, sub-clinical inflammation is not a passive condition but is an active ongoing process driven by two primary pathophysiological mechanisms (Jones et al., 2023). The first is direct, cell-mediated tissue damage caused by the continuous infiltration of activated inflammatory cells, such as heterophils and macrophages (Mirzazadeh et al., 2021). The second is a more subtle, but equally destructive, cytokine-mediated disruption of the mucosal epithelial barrier (Jones et al., 2023). Together, these processes progressively weaken the structural and functional integrity of the gizzard, priming it for catastrophic failure when faced with an acute stressor like hatching (Mirzazadeh et al., 2021).

The histopathological hallmark of GEU is the massive infiltration of inflammatory cells into the gizzard wall, and it is the activity of these cells that drives much of the direct tissue damage (Mirzazadeh et al., 2021; Jones et al., 2023). In a state of chronic inflammation, the persistent presence of triggers such as viral antigens or mycotoxins leads to the continuous recruitment and activation of innate immune cells, particularly heterophils and macrophages, into the gizzard's lamina propria and submucosa (Jones et al., 2023). Once activated, these heterophils and macrophages release a range of cytotoxic effector molecules (Mirzazadeh et al., 2021). Activated heterophils undergo degranulation, releasing reactive oxygen species (ROS) and a suite of proteolytic enzymes that are designed to eliminate pathogens (Jones et al., 2023). However, in a chronic and dysregulated setting, these antimicrobial molecules, specifically the ROS and proteolytic enzymes, cause significant collateral damage to the surrounding host tissue (Mirzazadeh et al., 2021). The primary victims of this inflammatory damage are the delicate glandular epithelial cells responsible for secreting and maintaining the protective koilin layer (Jones et al., 2023). This destruction of the glandular epithelium creates a destructive, self-perpetuating cycle in which initial tissue damage leads to the recruitment of more inflammatory cells, which in turn release more cytotoxic mediators, causing further damage and amplifying the pathological process that ultimately leads to widespread necrosis and erosion (Mirzazadeh et al., 2021).

In addition to the direct cellular damage previously described, the local cytokine environment also plays a crucial role in compromising the integrity of the gizzard's epithelial barrier (Mirzazadeh et al., 2021). High local concentrations of pro-inflammatory cytokines, particularly IFN-γ and TNF-α, are known to disrupt this barrier (Liu et al., 2025). The disruption of the epithelial barrier occurs because these cytokines can alter the expression and localization of key tight junction proteins, such as occludin and claudins (Mirzazadeh et al., 2021). As these proteins are responsible for sealing the intercellular space between epithelial cells, their disruption leads to a loss of barrier integrity (Liu et al., 2025). The disruption of tight junction proteins weakens the gizzard's mucosal barrier, making it significantly more susceptible to damage from both the highly acidic environment of the proventriculus and the intense mechanical grinding forces within the gizzard itself (Mirzazadeh et al., 2021; Liu et al., 2025).

Furthermore, the oxidative-inflammatory cascade has been identified as a core pathological process in stress-induced tissue damage (Aryal et al., 2025; Liu et al., 2025). This cascade involves a vicious cycle of mitochondrial dysfunction, redox imbalance (an excess of ROS), and the activation of apoptosis signaling pathways (Mirzazadeh et al., 2021). If this cascade were to be initiated within the gizzard's glandular epithelium as a result of chronic inflammation, it would directly lead to the widespread cell death, necrosis, and subsequent sloughing of epithelial cells that are the defining histological features observed in clinical cases of GEU (Mirzazadeh et al., 2021; Liu et al., 2025).

The “two-hit” hypothesis for perinatal gizzard erosion and ulceration

Based on the synthesis of the available evidence, which confirms the embryonic origin of GEU, the functional immunocompetence of the late-stage embryo, and the various prenatal triggers of inflammation, this review proposes a

"two-hit" hypothesis to explain the pathogenesis of GEU in pipped embryos. This model posits that the development of clinically apparent lesions at hatch is not the result of a single, acute event but is rather the culmination of a chronic priming event that renders the gizzard tissue vulnerable, followed by an acute physiological trigger that precipitates mucosal failure. This 'two-hit' model provides a cohesive explanation that can accommodate the diverse and multifactorial etiology that defines GEU as a syndrome unifying seemingly disparate causes under a common inflammatory pathway.

Hit 1, the chronic priming event, occurs during the final week of embryonic development (approximately ED 14-20), when the embryo is exposed to one or more of the aforementioned prenatal stressors. Prenatal stressors include vertically transmitted pathogens such as FAdV-1, maternally transferred nutritional toxins such as mycotoxins, or adverse incubation conditions such as thermal stress.

Sustained exposure to these prenatal stressors establishes a sub-clinical, chronic inflammatory state within the developing gizzard tissue. Sub-clinical and chronic inflammatory state is characterized by a dysregulated local immune profile, including an imbalance of pro- and anti-inflammatory cytokines, a compromised epithelial barrier function due to altered tight junction integrity, and a heightened sensitivity of local immune cells to further stimulation. The gizzard, therefore, enters the final phase of incubation not in a state of homeostasis, but in a vulnerable condition, effectively primed for an exaggerated and destructive inflammatory response.

Hit 2, the acute triggering event, is hypothesized to occur during the process of hatching. The transition from chorioallantoic membrane respiration to pulmonary respiration, the physical exertion of internal and external pipping, and the associated metabolic and circulatory stress may together create a substantial physiological challenge for the embryo. When such acute systemic stress is superimposed on a gizzard that has already undergone chronic inflammatory priming, it could plausibly trigger the pathological cascade leading to mucosal failure. The acute hatching-associated stress phase may involve inflammatory cell recruitment, oxidative injury, focal hemorrhage, and necrosis of the glandular epithelium, ultimately producing the GEU lesions observed at hatch.

The 'two-hit' framework explains why non-infectious stressors, such as high dietary copper, can produce histopathological lesions with inflammatory infiltrates that are remarkably similar to those seen in infectious cases; both act as initiators of the same core inflammatory priming pathway. It is important to clarify that the prenatal inflammatory priming proposed in this hypothesis may arise through more than one route. Vertically transmitted pathogens such as FAdV-1 can generate a local priming environment within gizzard tissue, whereas nutritional toxins and incubation stressors more likely initiate a remote priming response in the cecum, with systemic cytokines subsequently influencing gizzard vulnerability. The local (gizzard-based) and remote (cecum-originating) priming routes are therefore not contradictory; instead, they represent alternative pathways that converge on the same primed and susceptible gizzard phenotype described in Hit 1. Furthermore, the literature supports that the most significant pre-hatch immunological priming event occurs in the cecum, an organ anatomically distant from the gizzard, which has profound implications. It is plausible that a primary inflammatory dysregulation initiated in the lower gut could have systemic consequences, with circulating pro-inflammatory cytokines or activated immune cells affecting other organs (Hou et al., 2023; Vörösházi et al., 2024; Aryal et al., 2025). The gizzard, being under intense metabolic and physical stress during pipping, may represent a particularly susceptible target for this systemic inflammation (Gong et al., 2023; Liu et al., 2025). The potential systemic connection, where inflammatory dysregulation in the cecum influences gizzard vulnerability, raises the possibility of a gut-gizzard axis in the embryo, where inflammatory events in the lower gut can remotely influence the health and integrity of the upper gastrointestinal tract, a novel and important area for future investigation.

NUTRITIONAL STRATEGIES FOR THE MITIGATION OF PERINATAL GIZZARD EROSION AND ULCERATION

The breeder hen's diet is the primary modulator of embryonic health

An effective strategy for preventing GEU must be predicated on the understanding that the health trajectory of the embryo is profoundly influenced by the physiological and nutritional status of the breeder hen (Gong et al., 2023). The maternal-embryonic axis in avian species is a direct and comprehensive conduit, supplying not only the foundational elements for life but also the programming for post-hatch resilience or vulnerability (Wang et al., 2021). Through the yolk and albumin, the hen provides a complete nutritional package, including lipids, proteins, and vital micronutrients, such as Vitamin E, selenium, and zinc, alongside a foundational immune system in the form of passively transferred maternal antibodies (IgY; Lv et al., 2018; Thanabalan and Kiarie, 2021). This maternal transfer of nutrients and antibodies is designed to support the embryo through the rigors of development and provide crucial protection during the immunologically naive period immediately after hatching (Santos et al., 2022).

However, this maternal-embryonic transfer mechanism also serves as a direct route for the delivery of detrimental, pro-inflammatory triggers from the hen to the embryo (Wang et al., 2021). This dual role establishes the breeder diet as a critical control point (Olariu et al., 2025). As has been established, vertically transmitted pathogens can establish an active infection *in ovo*, but the feed itself can carry potent, non-infectious inflammatory agents (Wang et al., 2021). Mycotoxins present in contaminated breeder rations are a primary example (Olariu et al., 2025). These compounds are not merely inert contaminants (Wang et al., 2021). These mycotoxins are potent immunomodulatory and cytotoxic agents that are readily transferred and deposited into the egg (Olariu et al., 2025). The presence of these toxins in the yolk and albumin creates a toxic embryonic environment, exposing the developing chick to a continuous toxicological burden throughout its development (Wang et al., 2021). This sustained toxicological exposure can directly damage the integrity of the nascent gastrointestinal epithelium and activate a persistent, low-grade inflammatory response long before the embryo faces the stress of hatching (Wang et al., 2021; Olariu et al., 2025).

Therefore, the diet of the breeder hen does more than simply fuel embryonic growth (Lv et al., 2018; Thanabalan and Kiarie, 2021; Gong et al., 2023; Wang et al., 2025). The diet actively programs the embryo's immunological state (Lv et al., 2018; Thanabalan and Kiarie, 2021; Olariu et al., 2025). A hen consuming a diet with a high toxic load or one that promotes systemic inflammation will, in turn, produce an embryo that is already in a pro-inflammatory state and is thus predisposed to mucosal injury (Wang et al., 2021; Hou et al., 2023; Olariu et al., 2025). This recognition of the diet's immunological programming role is crucial, as it highlights that the breeder hen's diet is one of the most critical, modifiable factors in any strategy aimed at preventing perinatal GEU (Lv et al., 2018; Thanabalan and Kiarie, 2021; Verwoolde et al., 2022; Santana et al., 2025). Consequently, any truly effective preventative approach must be multi-generational, targeting the nutritional plane of the breeder flock to mitigate the “first hit” of prenatal inflammatory priming at its ultimate source (Verwoolde et al., 2022; Gong et al., 2023; Wang et al., 2025; Santana et al., 2025).

Key nutritional interventions to combat inflammatory triggers

Given that the breeder hen's diet is a primary conduit for prenatal inflammatory triggers, targeted nutritional interventions represent the most logical and proactive strategy for mitigating the risk of GEU in progeny (Qiu et al., 2021; Abdelli et al., 2021). A comprehensive nutritional strategy should be designed to achieve two primary objectives (Phillips et al., 2023). First, neutralize or significantly reduce the load of compounds with pro-inflammatory and cytotoxic properties within the feed itself; and second, bolster the hen's own physiological, metabolic, and immune resilience through the targeted supplementation discussed in the following sections (Dalia et al., 2018; Phillips et al., 2023). A healthier hen with a lower systemic inflammatory burden will provide a more optimal embryonic environment and transfer a higher quality of passive immunity, directly influencing the hen's ability to withstand the intense metabolic and physical stressors of hatching (Surai, 2000; Qiu et al., 2021).

The management of mycotoxins is a non-negotiable first line of defense in any preventative nutritional program (Abdelli et al., 2021; Phillips et al., 2023). Due to the unavoidable presence of mycotoxin contamination in many raw feed ingredients, a two-pronged approach involving both screening and active mitigation to neutralize these toxins is essential (Qiu et al., 2021). The most effective mitigation strategy is the strategic inclusion of high-efficacy, broad-spectrum mycotoxin-binding agents, such as bentonite clays or yeast cell wall extracts, in the finished breeder ration (Dalia et al., 2018). Mycotoxin-binding agents, such as bentonite clays and yeast cell wall–derived carbohydrates, function by sequestering mycotoxin molecules within the hen's gastrointestinal tract, forming stable complexes that cannot be absorbed into the bloodstream (Abdelli et al., 2021). This sequestration process effectively prevents their subsequent deposition into the egg yolk and albumin (Surai, 2000). By neutralizing mycotoxins at the maternal gut level, this intervention directly blocks the maternal-fetal transfer of a key inflammatory trigger, representing a direct and highly effective method for preventing the first hit of prenatal inflammatory priming in the embryo (Phillips et al., 2023).

Beyond simply neutralizing threats, the breeder diet can be fortified to enhance the hen's systemic health and the quality of the embryonic environment. The fortification strategy involves supplementing the diet with a synergistic blend of immunomodulatory and antioxidant compounds. Essential micronutrients such as Vitamin E, a potent lipid-soluble antioxidant, and trace minerals like selenium and zinc, which serve as critical cofactors for endogenous antioxidant enzymes such as glutathione peroxidase, are vital for protecting the hen from oxidative stress (Surai, 2000; Dalia et al., 2018; Qiu et al., 2021; Abdelli et al., 2021; Phillips et al., 2023).

Furthermore, the inclusion of phytogenic, a class of plant-derived bioactive compounds such as polyphenols, flavonoids, and essential oils, offers significant benefits (Abdelli et al., 2021; Phillips et al., 2023). Plant-derived bioactive compounds often possess powerful direct antioxidant properties and have been shown to exert immunomodulatory effects, helping to maintain a balanced inflammatory state within the hen (Dalia et al., 2018; Phillips et al., 2023). By reducing the hen's systemic inflammatory load, these phytogenic additives ensure that a less pro-inflammatory environment is transferred to the embryo and that the quality and potency of passive immunity via

maternal IgY are maximized (Surai, 2000; Qiu et al., 2021). The multi-faceted approach ensures the embryo is not only protected from toxins but is also endowed with a more robust foundational immunity (Phillips et al., 2023).

Synergistic nutritional strategies to mitigate prenatal inflammatory priming

The multifactorial etiology of the prenatal inflammatory state that precedes GEU logically warrants preventative strategies that are correspondingly multifaceted and synergistic. While interventions with single classes of compounds, such as the sole use of mycotoxin binders or individual antioxidants, are beneficial, the scientific literature suggests that a more robust and comprehensive approach should involve the formulation of integrated nutritional solutions (Dalia et al., 2018; Abdelli et al., 2021; Phillips et al., 2023). This represents a modern paradigm in veterinary preventative medicine, moving beyond addressing individual threats and towards targeting the root pathophysiological state, in this case, the chronic inflammatory priming of the embryo (Gong et al., 2023; Wang et al., 2025; Olariu et al., 2025). Such strategies are designed to proactively modulate the maternal-embryonic environment by simultaneously addressing the key triggers of inflammation (Surai, 2000; Qiu et al., 2021; Abdelli et al., 2021; Phillips et al., 2023).

From a mechanistic standpoint, a multi-functional dietary supplement is therefore precisely targeted at mitigating the "first hit" of the "two-hit" hypothesis. By simultaneously neutralizing toxins, reducing maternal inflammation, and bolstering embryonic tissue integrity, this approach aims to produce progeny that are fundamentally more resilient. The progeny would then face the physiologically demanding hatching period not from a state of pre-existing, sub-clinical inflammation, but from a baseline of sound health, making them far better equipped to withstand the "second hit" of hatching stress. Future research should therefore focus on quantifying the efficacy of these synergistic formulations, specifically measuring their impact on reducing embryonic inflammatory markers (e.g., IL-6, IFN-γ) and optimizing maternal antibody transfer.

CONCLUSION

The present review synthesizes pathological, immunological, and etiological evidence to characterize GEU in pipped poultry embryos as a syndrome of perinatal inflammatory failure, rather than a singular post-hatch disease. The analysis highlights that the late-stage embryo possesses a functionally competent immune system, characterized by a developed gut-associated lymphoid tissue and the ability to mount complex cytokine responses. This immunocompetence allows for the establishment of a chronic, sub-clinical inflammatory state *in ovo* driven by prenatal stressors such as vertically transmitted pathogens and maternally transferred toxins. The synthesis of published evidence supports the proposed 'two-hit' framework presented in this review. In the two-hit model, the chronic inflammatory priming serves as the first hit that renders the gizzard vulnerable, while the acute physiological stress of hatching acts as the second, triggering event that precipitates mucosal necrosis and erosion. The two-hit framework emphasizes the necessity of shifting the focus of control from reactive measures in the hatchery to proactive, multi-generational management centred on the breeder flock. The health, immune status, and nutritional plane of the breeder hen are paramount, as the maternal-embryonic axis represents the primary route for initiating the embryonic inflammatory state. Consequently, sustainable management of GEU should prioritize breeder hen vaccination, rigorous mycotoxin control, and the use of synergistic nutritional supplements to reduce maternal inflammation. Future research strategies directed towards these upstream interventions offer the most promising pathway to producing robust poultry and ensuring a sustainable production system.

DECLARATIONS

Acknowledgements

The authors acknowledge RR Animal Health Care Ltd for providing the essential facilities and support.

Authors' contributions

Debashis Dutta performed the study, carried out data analysis, and contributed to manuscript preparation, while Rajeeb Roy provided supervision, assisted with data interpretation, and revised the manuscript.

Availability of data and materials

The analyzed data during the present study are available from the corresponding author upon reasonable request.

Ethical considerations

Plagiarism, consent to publish, misconduct, data fabrication and/or falsification, double publication and/or submission, and redundancy have been checked by all authors. The authors confirmed that no AI-assisted text generation was used in the preparation of this study and the final manuscript.

Competing interest

The authors declare that they have no competing interests.

REFERENCES

Abdelli N, Solà-Oriol R, and Pérez JF (2021). Phytogenic feed additives in poultry: Achievements, prospective and challenges. Animals, 11(12): 3471. DOI: https://www.doi.org/10.3390/ani11123471

Al Amaz S and Mishra B (2024). Embryonic thermal manipulation: A potential strategy to mitigate heat stress in broiler chickens for sustainable poultry production. Journal of Animal Science and Biotechnology, 15(1): 75. DOI: https://www.doi.org/10.1186/s40104-024-01028-1

Alkie TN, Yitbarek A, Hodgins DC, Kulkarni RR, Taha-Abdelaziz K, and Sharif S (2019). Development of innate immunity in chicken embryos and newly hatched chicks: A disease control perspective. Avian Pathology, 48(4): 288-310. DOI: https://www.doi.org/10.1080/03079457.2019.1607966

Al-Zghoul MB, Hundam S, Mayyas M, Gerrard DE, and Dalloul RA (2025). Impact of thermal manipulation of broiler eggs on growth performance, splenic inflammatory cytokine levels, and heat shock protein responses to post-hatch lipopolysaccharide (LPS) challenge. Animals, 15(12): 1736. DOI: https://www.doi.org/10.3390/ani15121736

Aryal B, Kwakye J, Ariyo OW, Ghareeb AFA, Milfort MC, Fuller AL, Khatiwada S, Rekaya R, and Aggrey SE (2025). Major oxidative and antioxidant mechanisms during heat stress-induced oxidative stress in chickens. Antioxidants, 14(4): 471. DOI: https://www.doi.org/10.3390/antiox14040471

Ayalew H, Xu C, Adane A, Sanchez ALB, Li S, Wang J, Wu S, Qiu K, Qi G, and Zhang H (2025). Ontogeny and function of the intestinal epithelial and innate immune cells during early development of chicks: To explore *in ovo* immunomodulatory nutrition. Poultry Science, 104(1): 104607. DOI: https://www.doi.org/10.1016/j.psj.2024.104607

Balic A, Garcia-Morales C, Vervelde L, Gilhooley H, Sherman A, Garceau V, Gutowska MW, Burt DW, Kaiser P, Hume DA et al. (2014). Visualisation of chicken macrophages using transgenic reporter genes: Insights into the development of the avian macrophage lineage. Development, 141(16): 3255-3265. DOI: https://www.doi.org/10.1242/dev.105593

Bar Shira E and Friedman A (2018). Innate immune functions of avian intestinal epithelial cells: Response to bacterial stimuli and localization of responding cells in the developing avian digestive tract. PLoS One, 13(7): e0200393. DOI: https://www.doi.org/10.1371/journal.pone.0200393

Bavananthasivam J, Alkie TN, Matsuyama-Kato A, Hodgins DC, and Sharif S (2019). Characterization of innate responses induced by in ovo administration of encapsulated and free forms of ligands of Toll-like receptor 4 and 21 in chicken embryos. Research in Veterinary Science, 125: 405-415. DOI: https://www.doi.org/10.1016/j.rvsc.2017.10.002

Brand A, Galton J, and Gilmour DG (1983). Committed precursors of B and T lymphocytes in chick embryo bursa of Fabricius, thymus, and bone marrow. European Journal of Immunology, 13(6): 449-455. DOI: https://www.doi.org/10.1002/eji.1830130604

Cheng S, Liu X, Mu J, Yan W, Wang M, Chai H, Sha Y, Jiang S, Wang S, Ren Y et al. (2022). Intense innate immune responses and severe metabolic disorders in chicken embryonic visceral tissues caused by infection with highly virulent Newcastle disease virus compared to the avirulent virus: A bioinformatics analysis. Viruses, 14(5): 911. DOI: https://www.doi.org/10.3390/v14050911

Cooley JR, Yatskievych TA, and Antin PB (2014). Embryonic expression of the transforming growth factor beta ligand and receptor genes in chicken. Developmental Dynamics, 243(3): 497-508. DOI: https://www.doi.org/10.1002/dvdy.24085

da Silva DHL, Cordeiro LFM, Rios DL, de Freitas Neto OC, Lara LJC, Oliveira JCA, Aburjaile FF, and Ecco R (2024). Pathological and ileal microbiota findings in seven-day-old chicks with gizzard lesions and growth delay. Poultry, 3(4): 409-419. DOI: https://www.doi.org/10.3390/poultry3040031

Da Silva M, Dombre C, Brionne A, Monget P, Chessé M, De Pauw M, Mills M, Combes-Soia L, Labas V, Guyot N et al. (2019). The unique features of proteins depicting the chicken amniotic fluid. Molecular & Cellular Proteomics, 18(Suppl 1): S174-S190. DOI: https://www.doi.org/10.1074/mcp.RA117.000459

Dalia AM, Loh TC, Sazili AQ, Jahromi MF, and Samsudin AA (2018). Effects of vitamin E, inorganic selenium, bacterial organic selenium, and their combinations on immunity response in broiler chickens. BMC Veterinary Research, 14(1): 249. DOI: https://www.doi.org/10.1186/s12917-018-1578-x

Das Kumar A and Shelke MV (2024). Fowl adenovirus induced gizzard erosion in broiler chickens in southern India. Agricultural Science Digest, 44(4): 779-786. DOI: https://www.doi.org/10.18805/AG.D-5890

El-Shall NA, El-Hamid HSA, Elkady MF, Ellakany HF, Elbestawy AR, Gado AR, Geneedy AM, Hasan ME, Jaremko M, Selim S et al. (2022). Epidemiology, pathology, prevention, and control strategies of inclusion body hepatitis and hepatitis-hydropericardium syndrome in poultry: A comprehensive review. Frontiers in Veterinary Science, 9: 963199. DOI: https://www.doi.org/10.3389/fvets.2022.963199

Garcia P, Neo Y, Viallet J, and Macek Jilkova Z (2021). The chicken embryo model: A novel and relevant model for immune-based studies. Frontiers in Immunology, 12: 791081. DOI: https://www.doi.org/10.3389/fimmu.2021.791081

Grafl B, Aigner F, Liebhart D, Marek A, Prokofieva I, Bachmeier J, and Hess M (2012). Vertical transmission and clinical signs in broiler breeders and broilers experiencing adenoviral gizzard erosion. Avian Pathology, 41(6): 599-604. DOI: https://www.doi.org/10.1080/03079457.2012.740614

Haizhou Gong, Taiping Wang, Min Wu, Qianran Chu, Hainan Lan, Wuying Lang, Lingyu Zhu, Yang Song, Yujie Zhou, Qiongyi Wen et al. (2023). Maternal effects drive intestinal development beginning in the embryonic period on the basis of maternal immune and microbial transfer in chickens. Microbiome, 11: 41. DOI: https://www.doi.org/10.1186/s40168-023-01490-5

Haque MA, Zuo Z, and He C (2023). Pathogenesis of gizzard erosion and ulcerations and comprehensive control strategy in poultry. In: R. Z. Abbas, N. M. Saeed, M. Younus, L. Aguilar-Marcelino, and A. Khan (Editors), One health triad, Vol. II. Unique Scientific Publishers., Faisalabad, Pakistan, pp. 129-137. DOI: https://www.doi.org/10.47278/book.oht/2023.52

Hincke MT, Da Silva M, Guyot N, Gautron J, McKee MD, Guabiraba-Brito R, and Réhault-Godbert S (2019). Dynamics of structural barriers and innate immune components during incubation of the avian egg: Critical interplay between autonomous embryonic development and maternal anticipation. Journal of Innate Immunity, 11(2): 111-124. DOI: https://www.doi.org/10.1159/000493719

Hou L, Yuan H, Liu Y, Sun X, Chang J, Zhang H, Zhang J, Sun J, Wang Q, and Chen F (2023). Effect of deoxynivalenol on inflammatory injury on the glandular stomach in chick embryos. Poultry Science, 102(11): 102870. DOI: https://www.doi.org/10.1016/j.psj.2023.102870

Janković BD, Isaković K, Lukić ML, Vujanović NL, Petrović S, and Marković BM (1975). Immunological capacity of the chicken embryo. I. Relationship between the maturation of lymphoid tissues and the occurrence of cell-mediated immunity in the developing chicken embryo. Immunology, 29(3): 497-508. Available at: https://pubmed.ncbi.nlm.nih.gov/1165107/

Jones MK, Hofacre CL, Hoerr FJ, Baxter VA, Berghaus RD, Sellers HS, Ferguson-Noel N, and Smith JA (2023). Investigations into increased incidence of severe gizzard erosions and ulcerations in U.S. commercial broilers. Avian Diseases, 67(4): 349-365. DOI: https://www.doi.org/10.1637/aviandiseases-D-23-00052

Kannaki TR, Reddy MR, Verma PC, and Shanmugam M (2015). Differential Toll-like receptor (TLR) mRNA expression patterns during chicken embryological development. Animal Biotechnology, 26(2): 130-135. DOI: https://www.doi.org/10.1080/10495398.2014.939658

Kardoudi A, Benani A, Allaoui A, Kichou F, Biskri L, Ouchhour I, and Fellahi S (2025). Fowl adenovirus serotype 1: From gizzard erosion to comprehensive insights into genome organization, epidemiology, pathogenesis, diagnosis, and prevention. Veterinary Sciences, 12(4): 378. DOI: https://www.doi.org/10.3390/vetsci12040378

Kogut MH, Chiang HI, Swaggerty CL, Pevzner IY, and Zhou H (2012). Gene expression analysis of Toll-like receptor pathways in heterophils from genetic chicken lines that differ in their susceptibility to Salmonella enteritidis. Frontiers in Genetics, 3: 121. DOI: https://www.doi.org/10.3389/fgene.2012.00121

Kumar R, Sturos M, Porter RE, Singh A, Armién AG, Goyal SM, and Mor SK (2021). An outbreak of fowl aviadenovirus A-associated gizzard erosion and ulceration in captive bobwhite quail (*Colinus virginianus*). Avian Diseases, 65(1): 52-58. DOI: https://www.doi.org/10.1637/aviandiseases-D-20-00064

Liu Q, Ma L, Liu L, Guan D, Zhu Z, and Hu X (2025). Molecular pathogenesis of avian splenic injury under thermal challenge: Integrated mitigation strategies for poultry heat stress. Current Issues in Molecular Biology, 47(6): 410. DOI: https://www.doi.org/10.3390/cimb47060410

Lv Z, Fan H, Zhan B, Xing K, and Guo Y (2018). Dietary genistein supplementation for breeders and their offspring improves the growth performance and immune function of broilers. Scientific Reports, 8: 5161. DOI: https://www.doi.org/10.1038/s41598-018-23530-z

Mirzazadeh A, Grafl B, Abbasnia M, Emadi-Jamali S, Abdi-Hachesoo B, Schachner A, and Hess M (2021). Reduced performance due to adenoviral gizzard erosion in 16-day-old commercial broiler chickens in Iran, confirmed experimentally. Frontiers in Veterinary Science, 8: 635186. DOI: https://www.doi.org/10.3389/fvets.2021.635186

Neerukonda SN and Katneni U (2020). Avian pattern recognition receptor sensing and signaling. Veterinary Sciences, 7(1): 14. DOI: https://www.doi.org/10.3390/vetsci7010014

Olariu RM, Fiţ NI, Bouari CM, and Nadăş GC (2025). Mycotoxins in broiler production: Impacts on growth, immunity, vaccine efficacy, and food safety. Toxins, 17(6): 261. DOI: https://www.doi.org/10.3390/toxins17060261

Ouchhour I, Fellahi S, Arbani O, Mastour M, El Kadmiri AA, Mouahid M, Kardoudi A, Benani A, Allaoui A, and Kichou F (2024). Gizzard erosion and ulceration syndrome in Moroccan poultry flocks and molecular characterization of fowl adenoviruses (FAdV). Avian Diseases, 68(3): 217-224. DOI: https://www.doi.org/10.1637/aviandiseases-D-24-00004

Phillips CJC, Hosseintabar-Ghasemabad B, Gorlov IF, Slozhenkina MI, Mosolov AA, and Seidavi A (2023). Immunomodulatory effects of natural feed additives for meat chickens. Life, 13(6): 1287. DOI: https://www.doi.org/10.3390/life13061287

Qiu K, Zheng JJ, Obianwuna UE, Wang J, Zhang HJ, Qi GH, and Wu SG (2021). Effects of dietary selenium sources on physiological status of laying hens and production of selenium-enriched eggs. Frontiers in Nutrition, 8: 726770. DOI: https://www.doi.org/10.3389/fnut.2021.726770

Rehman MS, Rehman S, Yousaf W, Hassan F, Ahmad W, Liu Q, and Pan H (2021). The potential of Toll-like receptors to modulate avian immune system: Exploring the effects of genetic variants and phytonutrients. Frontiers in Genetics, 12: 671235. DOI: https://www.doi.org/10.3389/fgene.2021.671235

Santana TP, da Silva ACF, Bastos MS, Dos Santos Conceição J, de Souza Khatlab A, Gasparino E, Barbosa LT, Brito CO, and Del Vesco AP (2025). Methionine supplementation of maternal diet improves hatching traits, initial development, and performance in Japanese quail fed different levels of methionine during growth. Animal Science Journal, 96(1): e70044. DOI: https://www.doi.org/10.1111/asj.70044

Santos JS, Araújo ICS, Lacerda MJR, Andrade MA, Café MB, Leandro NSM, and Stringhini JH (2022). Effects of broiler breeder age on immune system development of progeny. Revista Brasileira de Zootecnia, 51: e20210127. DOI: https://www.doi.org/10.37496/rbz5120210127

Schilling MA, Katani R, Memari S, Cavanaugh M, Buza J, Radzio-Basu J, Mpenda FN, Deist MS, Lamont SJ, and Kapur V (2018). Transcriptional innate immune response of the developing chicken embryo to Newcastle disease virus infection. Frontiers in Genetics, 9: 61. DOI: https://www.doi.org/10.3389/fgene.2018.00061

Sharma S, Alizadeh M, Pratt S, Stamatikos A, and Abdelaziz K (2025). Differential expression of key immune markers in the intestinal tract of developing chick embryos. Veterinary Sciences, 12(2): 186. DOI: https://www.doi.org/10.3390/vetsci12020186

Sun J, Borowska D, Furniss JJ, Sutton K, Macqueen DJ, and Vervelde L (2025). Cellular landscape of avian intestinal organoids revealed by single cell transcriptomics. Scientific Reports, 15(1): 11362. DOI: https://www.doi.org/10.1038/s41598-025-95721-4

Surai PF (2000). Effect of selenium and vitamin E content of the maternal diet on the antioxidant system of the yolk and the developing chick. British Poultry Science, 41(2): 235-243. DOI: https://www.doi.org/10.1080/713654909

Terada T, Nii T, Isobe N, and Yoshimura Y (2020). Effects of Toll-like receptor ligands on the expression of proinflammatory cytokines and avian β-defensins in cultured chick intestine. The Journal of Poultry Science, 57(3): 210-222. DOI: https://www.doi.org/10.2141/jpsa.0190086

Thanabalan A and Kiarie EG (2021). Influence of feeding omega-3 polyunsaturated fatty acids to broiler breeders on indices of immunocompetence, gastrointestinal, and skeletal development in broiler chickens. Frontiers in Veterinary Science, 8: 653152. DOI: https://www.doi.org/10.3389/fvets.2021.653152

Verwoolde MB, Arts J, Jansen CA, Parmentier HK, and Lammers A (2022). Transgenerational effects of maternal immune activation on specific antibody responses in layer chickens. Frontiers in Veterinary Science, 9: 832130. DOI: https://www.doi.org/10.3389/fvets.2022.832130

Vörösházi J, Neogrády Z, Mátis G, and Mackei M (2024). Pathological consequences, metabolism and toxic effects of trichothecene T-2 toxin in poultry. Poultry Science, 103(3): 103471. DOI: https://www.doi.org/10.1016/j.psj.2024.103471

Wang Y, Quan H, Li X, Li Q, Haque MA, Shi Q, Fu Q, and He C (2021). Contamination with fumonisin B and deoxynivalenol is a threat to egg safety and contributes to gizzard ulcerations of newborn chickens. Frontiers in Microbiology, 12: 676671. DOI: https://www.doi.org/10.3389/fmicb.2021.676671

Yoshimura Y, Nii T, and Isobe N (2024). Innate immune training in chickens for improved defense against pathogens: A review. The Journal of Poultry Science, 61: 2024008. DOI: https://www.doi.org/10.2141/jpsa.2024008

Zhang H and Wong EA (2019). Expression of avian β-defensin mRNA in the chicken yolk sac. Developmental and Comparative Immunology, 95: 89-95. DOI: https://www.doi.org/10.1016/j.dci.2019.02.006

Publisher's note: Scienceline Publication Ltd. remains neutral with regard to jurisdictional claims in published maps and institutional affiliations.

Open Access: This article is licensed under a Creative Commons Attribution 4.0 International License, which permits use, sharing, adaptation, distribution and reproduction in any medium or format, as long as you give appropriate credit to the original author(s) and the source, provide a link to the Creative Commons licence, and indicate if changes were made. The images or other third party material in this article are included in the article's Creative Commons licence, unless indicated otherwise in a credit line to the material. If material is not included in the article's Creative Commons licence and your intended use is not permitted by statutory regulation or exceeds the permitted use, you will need to obtain permission directly from the copyright holder. To view a copy of this licence, visit https://creativecommons.org/licenses/by/4.0/.
© The Author(s) 2025

Instructions for Authors

Manuscript as Original Research Paper, Short Communication, Case Reports and Review or Mini-Review are invited for rapid peer-review publishing in the *World's Veterinary Journal* (WVJ). Considered subject areas include: Behavior; environment and welfare; animal reproduction and production; parasitology, endocrinology, microbiology, immunology, pathology, pharmacology, epidemiology, molecular biology, immunogenetics, surgery, radiology, ophthalmology, dermatology, chronic disease, anatomy, and non-surgical pathology issues of small to large animals, cardiology and oncology are sub-specialties of veterinary internal medicine. ... view full aims and scope

WVJ EndNote Style
Manuscript Template (.doc)
Sample Articles
Declaration form
Publication Ethics

Submission

The manuscript and other correspondence should be submit online preferentially. Please embed all figures and tables in the manuscript to become one single file for submission. Once submission is complete, the system will generate a manuscript ID and password sent to author's contact emails**:** editor@wvj.science-line.com. All manuscripts must be checked (by English native speaker) and submitted in English for evaluation (in totally confidential and impartial way).

Supplementary information

The online submission form allows supplementary information to be submitted together with the main manuscript file and covering letter. If you have more than one supplementary files, you can submit the extra ones by email after the initial submission. Author guidelines are specific for each journal. Our Word template can assist you by modifying your page layout, text formatting, headings, title page, image placement, and citations/references such that they agree with the guidelines of journal. If you believe your article is fully edited per journal style, please use our Word template before submission.
Supplementary materials may include figures, tables, methods, videos, and other materials. They are available online linked to the original published article. Supplementary tables and figures should be labeled with a "S", e.g. "Table S1" and "Figure S1". The maximum file size for supplementary materials is 10MB each. Please keep the files as small possible to avoid the frustrations experienced by readers with downloading large files.

Submission to the Journal is on the understanding that

1.The article has not been previously published in any other form and is not under consideration for publication elsewhere;
2.All authors have approved the submission and have obtained permission for publish work.
3.Researchers have proper regard for conservation and animal welfare considerations (see IAVE-Author Guidelines on Animal Ethics and Welfare). Attention is drawn to the '*Guidelines for the Treatment of Animals in Research and Teaching*'. Any possible adverse consequences of the work for populations or individual organisms must be weighed against the possible gains in knowledge and its practical applications. If the approval of an ethics committee is required, please provide the name of the committee and the approval number obtained.

Ethics Committee Approval

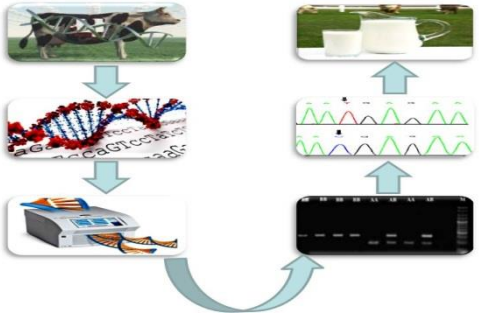
Experimental research involving human or animals should have been approved by author's institutional review board or ethics committee. This information can be mentioned in the manuscript including the name of the board/committee that gave the approval. Investigations involving humans will have been performed in accordance with the principles of *Declaration of Helsinki*. And the use of animals in experiments will have observed the Interdisciplinary Principles and Guidelines for the Use of Animals in Research, Testing, and Education by the New York Academy of Sciences, Ad Hoc Animal Research Committee. If the manuscript contains photos or parts of photos of patients, informed consent from each patient should be obtained. Patient's identities and privacy should be carefully protected in the manuscript.

Competing Interests

Competing interests that might interfere with the objective presentation of the research findings contained in the manuscript should be declared in a paragraph heading "Competing interests" (after Acknowledgment section and before References). Examples of competing interests are ownership of stock in a company, commercial grants, board membership, etc. If there is no competing interest, please use the statement "The authors have declared that no competing interest exists.

Graphical Abstract

Authors should provide a graphical abstract (a beautifully designed feature figure) to represent the paper aiming to catch the attention and interest of readers. Graphical abstract will be published online in the table of content. The graphical abstract should be colored, and kept within an area of 12 cm (width) x 6 cm (height) or with similar format. Image should have a minimum resolution of 300 dpi and line art 1200dpi. **Note:** Height of the image should be no more than the width. Please avoid putting too much information into the graphical abstract as it occupies only a small space. Authors can provide the graphical abstract in the format of PDF, Word, PowerPoint, jpg, or png, after a manuscript is accepted for publication. If you have decided to provide a Professional Graphical Abstract, please click **here**.



Presentation of the article

Main Format

First page of the manuscripts must be properly identified by the title and the name(s) of the author(s). It should be typed in Times New Roman (font sizes: 17pt in capitalization for the title, 10pt for the section headings in the body of the text and the main text, 9pt for References, double spaced, in A4 format with 2cm margins. All pages and lines of the main text should be numbered consecutively throughout the manuscript. The manuscript must be saved in a .doc format, (not .docx files). Abbreviations in the article title are not allowed.

Manuscripts should be arranged in the following order:

a. TITLE (brief, attractive and targeted)
b. Name(s) and Affiliation(s) of author(s) (including post code) and corresponding E-mail
c. ABSTRACT
d. Key words (separate by semicolons; or comma,)
e. Abbreviations (used in the manuscript)
f. INTRODUCTION
g. MATERIALS AND METHODS
h. RESULTS
i. DISCUSSION
j. CONCLUSION
k. DECLARATIONS
1. REFERENCES
m. Tables
n. Figure captions
o. Figures

Results and Discussion can be presented jointly if preferred.
Discussion and Conclusion can be presented jointly if preferred.

Article Sections Format

Title should be a brief phrase describing the contents of the paper. The first letter of each word in title should use upper case. The Title Page should include the author(s)'s full names and affiliations, the name of the corresponding author along with phone and e-mail information. Present address (es) of author(s) should appear as a footnote.

Abstract should be informative and completely self-explanatory, briefly present the topic, state the scope of the experiments, indicate significant data, and point out major findings and conclusions. The abstract should be 150 to 300 words in length. Complete sentences, active verbs, and the third person should be used, and the abstract should be written in the past tense. Standard nomenclature should be used and abbreviations should be avoided. No literature should be cited.
Following the abstract, about 3 to 10 key words that will provide indexing references should be listed.

Introduction should provide a clear statement of the problem, the relevant literature on the subject, and the proposed approach or solution. It should be understandable to colleagues from a broad range of scientific disciplines.

Materials and Methods should be complete enough to allow experiments to be reproduced. However, only truly new procedures should be described in detail; previously published procedures should be cited, and important modifications of published procedures should be mentioned briefly. Capitalize trade names and include the manufacturer's name and address. Subheadings should be used. Methods in general use need not be described in detail.

Results should be presented with clarity and precision. The results should be written in the past tense when describing findings in the author(s)'s experiments. Previously published findings should be written in the present tense. Results should be explained, but largely without referring to the literature. Discussion, speculation and detailed interpretation of data should not be included in the results but should be put into the discussion section.

Discussion should interpret the findings in view of the results obtained in this and in past studies on this topic. State the conclusions in a few sentences at the end of the paper. The Results and Discussion sections can include subheadings, and when appropriate, both sections can be combined.

Conclusion can be presented jointly if preferred.

Declarations section

Tables should be kept to a minimum and be designed to be as simple as possible. Tables are to be typed double-spaced throughout, including headings and footnotes. Each table should be on a separate page, numbered consecutively in Arabic numerals and supplied with a heading and a legend. Tables should be self-explanatory without reference to the text. The details of the methods used in the experiments should preferably be described in the legend instead of in the text. The same data should not be presented in both table and graph forms or repeated in the text.

Figure legends should be typed in numerical order on a separate sheet. Graphics should be prepared using applications capable of generating high resolution GIF, TIFF, JPEG or PowerPoint before pasting in the Microsoft Word manuscript file. Use Arabic numerals to designate figures and upper case letters for their parts (Figure 1). Begin each legend with a title and include sufficient description so that the figure is understandable without reading the text of the manuscript. Information given in legends should not be repeated in the text.

Declarations section - Please include declarations heading

Please ensure that the sections:
-Ethics (and consent to participate)
-Authors' contributions
-Competing interests
-Availability of data and materials
are included at the end of your manuscript in a Declarations section.

Authors' Contributions

For manuscripts with more than one author, WVJ require an Authors' Contributions section to be placed after the Competing Interests section.
An 'author' is generally considered to be someone who has made substantive intellectual contributions to a published study. To qualify as an author one should 1) have made substantial contributions to conception and design, or acquisition of data, or analysis and interpretation of data; 2) have been involved in drafting the manuscript or revising it critically for important intellectual content; and 3) have given final approval of the version to be published. Each author should have participated sufficiently in the work to take public responsibility for appropriate portions of the content. Acquisition of funding, collection of data, or general supervision of the research group, alone, does not justify authorship.
We suggest the following format (please use initials to refer to each author's contribution): AB carried out the molecular genetic studies, participated in the sequence alignment and drafted the manuscript. JY carried out the immunoassays. MT participated in the sequence alignment. ES participated in the design of the study and performed the statistical analysis. FG conceived of the study, and participated in its design and coordination and helped to draft the manuscript. All authors read and approved the final manuscript.
For authors that equally participated in a study please write 'All/Both authors contributed equally to this work.'
Contributors who do not meet the criteria for authorship should be listed in an acknowledgements section.

Competing Interests

Competing interests that might interfere with the objective presentation of the research findings contained in the manuscript should be declared in a paragraph heading "Competing interests" (after Acknowledgment section and before References). Examples of competing interests are ownership of stock in a company, commercial grants, board membership, etc. If there is no competing interest, please use the statement "The authors declare that they have no competing interests.".
World's Veterinary Journal adheres to the definition of authorship set up by The International Committee of Medical Journal Editors (ICMJE). According to the ICMJE authorship criteria should be based on 1) substantial contributions to conception and design of, or acquisition of data or analysis and interpretation of data, 2) drafting the article or revising it critically for important intellectual content and 3) final approval of the version to be published. Authors should meet conditions 1, 2 and 3.
It is a requirement that all authors have been accredited as appropriate upon submission of the manuscript. Contributors who do not qualify as authors should be mentioned under Acknowledgements.

Change in authorship

We do not allow any change in authorship after provisional acceptance. We cannot allow any addition, deletion or change in sequence of author name. We have this policy to prevent the fraud.

Acknowledgements

We strongly encourage you to include an Acknowledgements section between the Authors' contributions section and Reference list. Please acknowledge anyone who contributed towards the study by making substantial contributions to conception, design, acquisition of data, or analysis and interpretation of data, or who was involved in drafting the manuscript or revising it critically for important intellectual content, but who does not meet the criteria for authorship. Please also include their source(s) of funding. Please also acknowledge anyone who contributed materials essential for the study.
Authors should obtain permission to acknowledge from all those mentioned in the Acknowledgements. Please list the source(s) of funding for the study, for each author, and for the manuscript preparation in the acknowledgements section. Authors must describe the role of the funding body, if any, in study design; in the collection, analysis, and interpretation of data; in the writing of the manuscript; and in the decision to submit the manuscript for publication.

Data Deposition

Nucleic acid sequences, protein sequences, and atomic coordinates should be deposited in an appropriate database in time for the accession number to be included in the published article. In computational studies where the sequence information is unacceptable for inclusion in databases because of lack of experimental validation, the sequences must be published as an additional file with the article.

References

1. A WVJ reference style for **EndNote** may be found **here**.
2. All references to publications made in the text should be presented in a list with their full bibliographical description.
3. In the text, a reference identified by means of an author's name should be followed by the date of the reference in parentheses. When there are more than two authors, only the first author's surname should be mentioned, followed by 'et al'. In the event that an author cited has had two or more works published during the same year, the reference, both in the text and in the reference list, should be identified by a lower case letter like 'a' and 'b' after the date to distinguish the works.
4. References in the text should be arranged chronologically (e.g. Kelebeni, 1983; Usman and Smith, 1992 and Agindotan et al., 2003). The list of references should be arranged alphabetically on author's surnames, and chronologically per author. If an author's name in the list is also mentioned with co-authors, the following order should be used: Publications of the single author, arranged according to publication dates - publications of the same author with one co-author - publications of the author with more than one co-author. Publications by the same author(s) in the same year should be listed as 1992a, l992b, etc.
5. Names of authors and title of journals, published in non-latin alphabets should be transliterated in English.
6. A sample of standard reference is "1th Author surname A, 2th Author surname B, 3th Author surname C. 2013. Article title should be regular and 7 pt . *World Vet. J.,* Add No. of Volume (Issue No.): 00-00."
7. The color of references in the text of article is dark blue. Example: (Preziosi et al., 2002; Mills et al., 2015).
8. At least 35% of the references of any submitted manuscript (for all types of article) should include scientific results published in the last five years.

-Examples (at the text- blue highlighted)

Abayomi (2000), Agindotan et al. (2003), (Kelebeni, 1983), (Usman and Smith, 1992), (Chege, 1998; Chukwura, 1987a,b; Tijani, 1993,1995), (Kumasi et al., 2001).

--Examples (at References section)

a) For journal:

Lucy MC (2000). Regulation of ovarian follicular growth by somatotropin and insulin- like growth factors in cattle. Journal of Dairy Science, 83: 1635-1647. DOI: XXX

Kareem SK (2001). Response of albino rats to dietary level of mango cake. Journal of Agricultural Research and Development. pp 31-38. DOI: XXX

Chikere CB, Omoni VT and Chikere BO (2008). Distribution of potential nosocomial pathogens in a hospital environment. African Journal of Biotechnology. 7: 3535-3539. DOI: XX

b) For symposia reports and abstracts:

Cruz EM, Almatar S, Aludul EK and Al-Yaqout A (2000). Preliminary Studies on the Performance and Feeding Behaviour of Silver Pomfret (Pampus argentens euphrasen) Fingerlings fed with Commercial Feed and Reared in Fibreglass Tanks. Asian Fisheries Society Manila, Philippine 13: 191-199. Link

c) For edited symposia, special issues, etc., published in a journal:

Korevaar H (1992). The nitrogen balance on intensive Dutch dairy farms: a review. In: A. A. Jongebreur et al. (Editors), Effects of Cattle and Pig Production Systems on the Environment: Livestock Production Science, 31: 17-27. Link

d) For books:

AOAC (1990). Association of Official Analytical Chemists. Official Methods of Analysis, 15th Edition. Washington D.C. pp. 69-88. Link

Pelczar JR, Harley JP, Klein DA (1993). Microbiology: Concepts and Applications. McGraw-Hill Inc., New York, pp. 591-603. Link

e) Books, containing sections written by different authors:

Kunev M (1979). Pig Fattening. In: A. Alexiev (Editor), Farm Animal Feeding. Vol. III. Feeding of Different Animal Species, Zemizdat, Sofia, p. 233-243 (Bg). Link

In referring to a personal communication the two words are followed by the year, e.g. (Brown, J. M., personal communication, 1982). In this case initials are given in the text.

Nomenclature and Abbreviations

Nomenclature should follow that given in NCBI web page and Chemical Abstracts. Standard abbreviations are preferable. If a new abbreviation is used, it should be defined at its first usage. Abbreviations should be presented in one paragraph, in the format: "term: definition". Please separate the items by ";".

E.g. ANN: artificial neural network; CFS: closed form solution...

Abbreviations of units should conform to those shown below:

Decilitre	dl	**Kilogram**	kg
Milligram	mg	**hours**	h
Micrometer	mm	**Minutes**	min
Molar	mol/L	**Mililitre**	ml
Percent	%		

Other abbreviations and symbols should follow the recommendations on units, symbols and abbreviations: in "A guide for Biological and Medical Editors and Authors (The Royal Society of Medicine London 1977).

Papers that have not been published should be cited as "unpublished". Papers that have been accepted for publication, but not yet specified for an issue should be cited as "to be published". Papers that have been submitted for publication should be cited as "submitted for publication".

Formulae, numbers and symbols

1. Typewritten formulae are preferred. Subscripts and superscripts are important. Check disparities between zero (0) and the letter 0, and between one (1) and the letter I.
2. Describe all symbols immediately after the equation in which they are first used.
3. For simple fractions, use the solidus (/), e.g. 10 /38.
4. Equations should be presented into parentheses on the right-hand side, in tandem.
5. Levels of statistical significance which can be used without further explanations are *P < 0.05, **P < 0.01, and ***P < 0.001
6. In the English articles, a decimal point should be used instead of a decimal comma.
7. In chemical formulae, valence of ions should be given, e.g. Ca2+ and CO32-, not as Ca++ or CO3.
8. Numbers up to 10 should be written in the text by words. Numbers above 1000 are recommended to be given as 10 powered x.
9. Greek letters should be explained in the margins with their names as follows: Aα - alpha, Bβ - beta, Γγ - gamma, Δδ - delta, Eε - epsilon, Zζ - zeta, Hη - eta, Θθ - theta, Iι - iota, Kκ - kappa, Λλ - lambda, Mμ - mu, Nν - nu, Ξξ - xi, Oo - omicron, Ππ - pi, Pρ - rho, Σσ - sigma, Tτ - tau, Yυ - ipsilon, Φφ - phi, Xχ - chi, Ψψ - psi, Ωω - omega.

Review/Decisions/Processing

WVJ uses a double-blind review model for all papers that successfully enter the peer-review process. Each submission is reviewed and edited by an English language editor, a statistical editor, and at least three external reviewers, selected by the section editor. Reviewers are also required to complete a result form to provide their feedback to the authors. Possible editorial decisions include: accept as is, minor revision, major revision/resubmission, or reject. Authors are expected to submit their revised manuscripts within 14 days of receiving the review outcome. A sample evaluation form is available for reference.

To submit a revision please click here, fill out the form, and mark "Revised" attach the revision (MSword) and submit when completed. After review and editing the article, a final formatted proof is sent to the corresponding

author once again to apply all suggested corrections during the article process. The editor who received the final revisions from the corresponding authors shall not be hold responsible for any mistakes shown in the final publication. Manuscripts with significant results are typically reviewed and published at the highest priority.

Plagiarism: There is a zero-tolerance policy towards plagiarism (including self-plagiarism) in our journals. Manuscripts are screened for plagiarism by one of the plagiarism finding tools (iThenticate, PlagScan and or Docol©c), before or during publication, and if found they will be rejected at any stage of processing. See sample of Docol©c-Report.

Declaration

After manuscript accepted for publication, a declaration form will be sent to the corresponding author who that is responsible to coauthors' agreements to publication of submitted work in WVJ after any amendments arising from the peer review.

Date of issue

The journal will be issued on 25th of March, June, September and December, each year.

Publication charges

The publication costs are covered through article processing charges (APCs) and no submission or any other fees are required for the publication of the accepted article. There is a modest APC of 150 Euro(€) editor fee for the processing of each primary accepted paper (1000-4000 words) to encourage high-quality submissions. APCs are only charged for articles that pass the pre-publication checks and are ready to be published. A surcharge will be placed on any article that is over 4000 words in length to cover the considerable additional processing costs. Payment can be made by credit card, bank transfer, money order or check. Instruction for payment is sent during publication process as soon as manuscript is accepted. Meanwhile, this journal encourages the academic institutions in low-income countries to publish high quality scientific results, free of charges.

WORD COUNT	PRICE*
1000-4000 words	€150
over 4000 words	€230
* The prices are valid until 30th June 2026.	

In response to the time-sensitive nature of academic publishing, WVJ recognizes the various deadlines authors often face, such as those related to promotion and tenure, thesis defense, grant proposals, research fund expenditures, subsequent paper publications, and the urgency of disseminating critical findings. To support authors facing such deadlines, WVJ offers a fast-track review process. However, the journal imposes no processing fee for submitted manuscripts in a fast-track review process. In the event of rejection, authors are exempt from any fees in the fast-track review process. Upon acceptance, authors are required to pay the publication fee (calculated based on the total word count) plus an additional 200 Euros when an invoice and the declaration form are sent to them. Authors submitting a manuscript to WVJ will receive an email explaining the conditions for the fast-track review process within a working day of submission. They can initiate the process by confirming the conditions of the fast-track review process and contacting the journal via email. It is essential to emphasize that the request for a fast-track review does not affect the editorial decision-making process, maintaining the integrity and thoroughness of our evaluation standards.

The Waiver policy

The publication fee will be waived for invited authors, authors of hot papers, and corresponding authors who are editorial board members of the *World's Veterinary Journal* (WVJ). The Journal will consider requests to waive the fee for cases of financial hardship (for high quality manuscripts and upon acceptance for publication). Requests for waiver of the submission fee must be submitted via individual cover letter by the corresponding author and cosigned by an appropriate institutional official to verify that no institutional or grant funds are available for the payment of the fee. Letters including the manuscript title and manuscript ID number should be sent to: editor.wvj@gmail.com. It is expected that waiver requests will be processed and authors will be notified within one business day.

Submission Preparation Checklist

- Authors are required to check off their submission's compliance with all of the following items, and submissions may be returned to authors that do not adhere to the following guidelines.
- The submission has not been previously published, nor is it before another journal for consideration (or an explanation has been provided in Comments to the Editor).
- The submission file is in Microsoft Word, RTF, or PDF document file format.
- Where available, URLs for the references have been provided.
- The text is single-spaced; uses a 12-point font; and all illustrations, figures, and tables are placed within the text at the appropriate points, rather than at the end.
- The text adheres to the stylistic and bibliographic requirements outlined in the Author Guidelines.

Scienceline Publication, Ltd.
Editorial Office:
Ömer Nasuhi Bilmen Road, Dönmez Apart., G Block, No:1/6, Yakutiye, Erzurum/25100, Turkey
Homepage: www.science-line.com ; Email: administrator@science-line.com
Phone: +90 538-7708824 (Turkey)

SCIENCELINE PUBLISHING CORPORATION

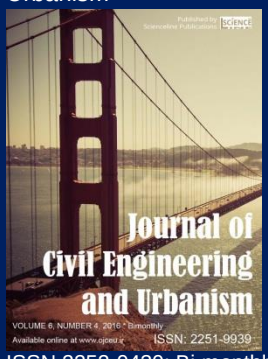
Scienceline Publication Ltd is a limited liability non-profit non-stock corporation incorporated in Turkey (Company No. 0757086921600001). Scienceline journals that concurrently belong to many societies, universities and research institutes, publishes internationally peer-reviewed open access articles and believe in sharing of new scientific knowledge and vital research in the fields of life and natural sciences, animal sciences, engineering, art, linguistic, management, social and economic sciences all over the world. Scienceline journals include:

Online Journal of Animal and Feed Research



ISSN 2228-7701; Bi-monthly
View Journal | Editorial Board
Email: editors@ojafr.ir
Submit Online >>

Journal of Civil Engineering and Urbanism



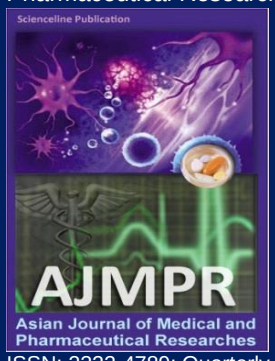
ISSN 2252-0430; Bi-monthly
View Journal | Editorial Board
Email: ojceu@ojceu.ir
Submit Online >>

Journal of Life Sciences and Biomedicine



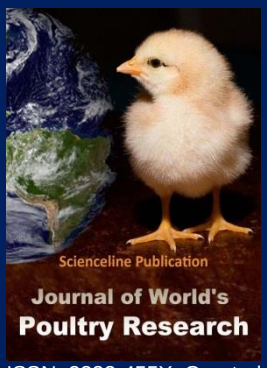
ISSN: 2251-9939; Bi-monthly
View Journal | Editorial Board
Email: editors@jlsb.science-line.com
Submit Online >>

Asian Journal of Medical and Pharmaceutical Researches



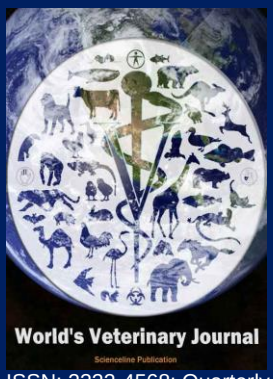
ISSN: 2322-4789; Quarterly
View Journal | Editorial Board
Email: editor@ajmpr.science-line.com
Submit Online >>

Journal of World's Poultry Research



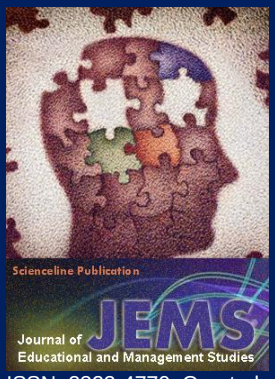
ISSN: 2322-455X; Quarterly
View Journal | Editorial Board
Email: editor@jwpr.science-line.com
Submit Online >>

World's Veterinary Journal



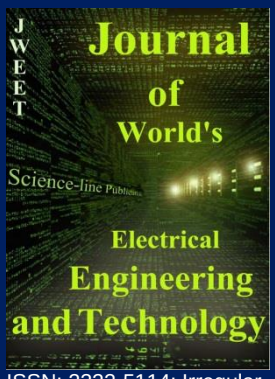
ISSN: 2322-4568; Quarterly
View Journal | Editorial Board
Email: editor@wvj.science-line.com
Submit Online >>

Journal of Educational and Management Studies



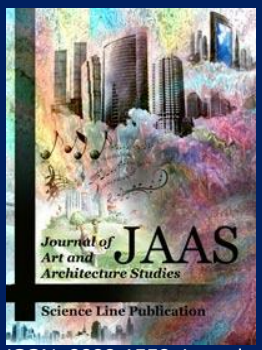
ISSN: 2322-4770; Quarterly
View Journal | Editorial Board
Email: info@jems.science-line.com
Submit Online >>

Journal of World's Electrical Engineering and Technology



ISSN: 2322-5114; Irregular
View Journal | Editorial Board
Email: editor@jweet.science-line.com
Submit Online >>

Journal of Art and Architecture Studies



ISSN: 2383-1553; Irregular
View Journal | Editorial Board
Email: jaas@science-line.com
Submit Online >>

Asian Journal of Social and Economic Sciences



ISSN: 2383-0948; Quarterly
View Journal | Editorial Board
Email: ajses@science-line.com
Submit Online >>

Journal of Applied Business and Finance Researches



ISSN: 2382-9907; Quarterly
View Journal | Editorial Board
Email: jabfr@science-line.com
Submit Online >>

Scientific Journal of Mechanical and Industrial Engineering



ISSN: 2383-0980; Quarterly
View Journal | Editorial Board
Email: sjmie@science-line.com
Submit Online >>

ABOUT
AIMS AND SCOPE
LEADERSHIP TEAM
POLICIES AND PUBLICATION ETHICS
TERMS AND CONDITIONS
CONTACT US

Scienceline is a non-profit organisation inspired by research funders and led by scholars. Our mission is to help researchers accelerate discovery and innovation by operating a platform for research communication that encourages and recognises the most responsible behaviours in science.

Scienceline Publications, Ltd is a limited liability non-profit non-stock corporation registered in the State of Erzurum, Turkey, with company number 0757086921600001, and branch number 18677/25379 at the address: Scienceline Publications, Ltd., Ömer Nasuhi Bilmen Road, Dönmez Apart., G1/6, Yakutiye, Erzurum 25100, Turkey